

Advances in Experimental Medicine and Biology 1357

Henriqueta Louro
Maria João Silva *Editors*

Nanotoxicology in Safety Assessment of Nanomaterials

 Springer

Advances in Experimental Medicine and Biology

Volume 1357

Series Editors

Wim E. Crusio, Institut de Neurosciences Cognitives et Intégratives
d'Aquitaine, CNRS and University of Bordeaux, Pessac Cedex, France
Haidong Dong, Departments of Urology and Immunology, Mayo Clinic,
Rochester, MN, USA

Heinfried H. Radeke, Institute of Pharmacology & Toxicology,
Clinic of the Goethe University Frankfurt Main, Frankfurt am
Main, Hessen, Germany

Nima Rezaei, Research Center for Immunodeficiencies, Children's Medical
Center, Tehran University of Medical Sciences, Tehran, Iran

Ortrud Steinlein, Institute of Human Genetics, LMU University Hospital
Munich, Germany

Junjie Xiao, Cardiac Regeneration and Ageing Lab, Institute of
Cardiovascular Science, School of Life Science, Shanghai University,
Shanghai, China

Advances in Experimental Medicine and Biology provides a platform for scientific contributions in the main disciplines of the biomedicine and the life sciences. This series publishes thematic volumes on contemporary research in the areas of microbiology, immunology, neurosciences, biochemistry, biomedical engineering, genetics, physiology, and cancer research. Covering emerging topics and techniques in basic and clinical science, it brings together clinicians and researchers from various fields.

Advances in Experimental Medicine and Biology has been publishing exceptional works in the field for over 40 years, and is indexed in SCOPUS, Medline (PubMed), Journal Citation Reports/Science Edition, Science Citation Index Expanded (SciSearch, Web of Science), EMBASE, BIOSIS, Reaxys, EMBiology, the Chemical Abstracts Service (CAS), and Pathway Studio.

2020 Impact Factor: 2.622


More information about this series at <https://link.springer.com/bookseries/5584>


Henriqueta Louro • Maria João Silva
Editors

Nanotoxicology in Safety Assessment of Nanomaterials

 Springer

Editors

Henriqueta Louro 
Department of Human Genetics
National Institute of Health Dr. Ricardo
Jorge (INSA)
Lisbon, Portugal

Maria João Silva 
Department of Human Genetics
National Institute of Health Dr. Ricardo
Jorge (INSA)
Lisbon, Portugal

National Institute of Health Dr. Ricardo Jorge

ISSN 0065-2598 ISSN 2214-8019 (electronic)
Advances in Experimental Medicine and Biology
ISBN 978-3-030-88070-5 ISBN 978-3-030-88071-2 (eBook)
<https://doi.org/10.1007/978-3-030-88071-2>

© The Editor(s) (if applicable) and The Author(s), under exclusive license to Springer Nature Switzerland AG 2022, corrected publication 2022
Chapters 10 and 15 are licensed under the terms of the Creative Commons Attribution 4.0 International License (<http://creativecommons.org/licenses/by/4.0/>). For further details see license information in the chapter.

This work is subject to copyright. All rights are solely and exclusively licensed by the Publisher, whether the whole or part of the material is concerned, specifically the rights of translation, reprinting, reuse of illustrations, recitation, broadcasting, reproduction on microfilms or in any other physical way, and transmission or information storage and retrieval, electronic adaptation, computer software, or by similar or dissimilar methodology now known or hereafter developed. The use of general descriptive names, registered names, trademarks, service marks, etc. in this publication does not imply, even in the absence of a specific statement, that such names are exempt from the relevant protective laws and regulations and therefore free for general use.

The publisher, the authors and the editors are safe to assume that the advice and information in this book are believed to be true and accurate at the date of publication. Neither the publisher nor the authors or the editors give a warranty, expressed or implied, with respect to the material contained herein or for any errors or omissions that may have been made. The publisher remains neutral with regard to jurisdictional claims in published maps and institutional affiliations.

This Springer imprint is published by the registered company Springer Nature Switzerland AG
The registered company address is: Gewerbestrasse 11, 6330 Cham, Switzerland

Preface

The idea of this book grew out from the research that we have been developing for more than a decade in the field of nanotoxicology. Indeed, as with many other toxicologists with expertise in the field of human and environmental genotoxicity, we were challenged by the need to assess the safety of nanomaterials (NMs), due to the exponential growth of technologies based on those materials. Nanotechnologies are considered key enabling technologies in several sectors such as agriculture, food industry, medicine, energy, environment, and electronics. Numerous products, already available and marketed contain, for example, silver or titanium dioxide NMs, and others are under development, such as nanocelluloses or nanoformulations of pesticides. In face of this landscape, the European Union Strategic and Action Plan for Nanosciences and Nanotechnologies emphasized the need of ensuring the development of safe, integrated, and responsible nanotechnologies and nanotechnology products. Given our former expertise, it could be assumed that the conventional tests to assess toxicity and, in particular, the genotoxicity of chemical substances, could also be applied to NMs. However, we faced several difficulties and challenges, both in the performance of the tests and in the interpretation of their results. In fact, it has been recognized that the specific physicochemical properties of NM are crucial to define their nano-bio interactions and their toxic potential. Moreover, processes such as translocation to the bloodstream and adsorption of proteins to the nanoparticles surface forming the so-called “corona” or the digestion of NMs may modify their primary physicochemical properties leading to unexpected outcomes in human cells. Such observations stimulated us to the quest of obtaining reliable and conclusive results using those conventional methodologies. Clearly, we were not the pioneers, nor were we alone in this search, and we benefited enormously from being part of interdisciplinary teams in the context of European Projects (NANOGENOTOX Joint Action; NANOREG Project).

In this evolving field of nanotoxicology, we have been engaged in a major scientific effort for linking the (primary and secondary) physicochemical properties of the NMs with their toxic effects. These and other nano-specific issues have been hindering the categorization of NM according to their toxicity and, consequently, their risk assessment and management. Nonetheless, considering the wide array of NMs produced or under development, a case-by-case approach to the risks of each NM seems an unreasonably extensive task. Thus, the development of high-throughput omics-based tools adapted

for the toxicity assessment of NM and, on the other hand, the elucidation of the cellular and molecular mechanisms underlying NM toxicity is of utmost importance to progress faster in the field of nanotoxicology. Such approach and the information generated will allow the development of cost-efficient screening strategies and predictive nanotoxicology approaches, driving the synthesis of safer NMs.

The main purpose of this book is to provide a perspective on recent developments in the synthesis, application, and characterization of nanomaterials and nanotechnologies, focusing on the use of nanotoxicology, including predictive nanotoxicology, for the accurate safety assessment of NMs early in the product development cycle. This mechanistic knowledge has been evidenced as central to aid in grouping and reading across, based on similarities of induced cellular and molecular events, towards the risk assessment and regulation of nanomaterials. Various experts from different organizations and countries discuss the above referred topics in the three parts of this book. The first part is mainly devoted to nanotechnologies advancement and intends to provide a perspective on recent developments in the synthesis, application, and characterization of NMs. Setting the base, the first chapter describes the definition of NMs and related unknowns, which raise questions in their analytical detection and quantification. Other chapters tackle the production and application of NMs in biomedicine, such as the use of innovative nanoparticulate systems for local or systemic drug delivery (e.g., lipid and polymeric nanocarriers), and the relevance of assessing their potential toxicity, as well. The use of nanoparticles for nanotheragnostics targeting, particularly cancer, is also approached. Finally, the versatility of nanocelluloses applications due to their remarkable properties, allowing the production of functional materials with endless applications and an overall low toxicity, is described.

The second part is focused on the assessment of NMs' toxic properties and comprises both reviews and original data on the toxicity of several NMs, spanning from metal-based NMs (e.g., titanium dioxide, cerium oxide, silver, and iron) to nanocelluloses. Also noteworthy are the chapters that address innovative methodological approaches in nanotoxicology. The relevance of using next-generation *in vitro* approaches that are physiologically relevant and, as such, that generate results more comparable to those produced *in vivo* is underlined in several chapters. In addition, the use of omics-based methodologies, for example, transcriptomics, epigenomics, and proteomics, in nanotoxicology is described. While one chapter gives the reader a more global perspective on this topic, another one describes the application of epigenetics/epigenomics to understand the potential effects of NM on gene expression regulation, which are less explored but relevant NMs effects deserving further investigation. Despite the evolution of *in vitro* systems, there is no doubt, however, that *in vivo* studies continue to have relevance because they reflect the complex response of a living organism. In this sense, the application of invertebrate models, for example, *Drosophila*, can be an alternative to murine models that should be considered in the future.

This book would not have been complete without addressing different aspects related to the assessment and management of risks associated with exposure to NMs and their implications in the regulatory framework.

Occupational exposure to nanomaterials is tackled in one chapter, as well as the measures to be implemented to manage the potential associated risks. For closing this book, the reader finds a chapter that addresses predictive nanotoxicology, in a future and innovative perspective of the safety assessment of NMs, based on a strong mechanistic knowledge. This is a chapter that offers an overview of the key effects of NMs (metal-, carbon-, and silicon-based NMs) at the tissue, cellular, and molecular levels and the adverse outcome pathways (AOP) that are or can be derived, highlighting their applications in environmental and human health risk assessment.

Overall, it is our view that an adequate safety assessment early in the development of new NMs, following the safe and sustainable by design (SSbD) principle, will enable nanosafety to keep pace with innovation, with the goal of fostering a sustainable and safe innovation in the field of nanotechnologies. Additionally, and not less important, is the urgent need to further develop human biomonitoring tools applicable to NMs, allowing to assess the human internal exposure to NMs and thereby contributing to predict their long-term consequences, while also contributing to NMs risk assessment.

Since we find nanotoxicology at the crossroad of several disciplines, from chemistry and toxicology to biological, regulatory, and materials sciences, among others, we expect that this book will provide an interdisciplinary and state-of-the-art vision in this field, valuable for scientists, educators, and students. In addition, with this book, we hope to reach out to industrial practitioners, regulators, and policy makers, improving their understanding about the current and next-generation perspectives for the safety assessment of nanomaterials, thereby bridging science and policy.

Lisbon, Portugal

Henriqueta Louro

Lisbon, Portugal

Maria João Silva

Acknowledgments

The editors are grateful to all contributors who accepted the challenge of being part of this book, providing their relevant expertise to the reflection on the safety assessment of nanomaterials.

Our thanks for the support of all colleagues from the genetic toxicology group at the National Institute of Health Dr. Ricardo Jorge, Lisbon, Portugal.

This book has been developed under the scope of the projects INGESTnano (PTDC/SAU-PUB/29481/2017) and ToxApp4NanoCELF (PTDC/SAU-PUB/32587/2017) funded by national funds through the FCT – Foundation for Science and Technology, I.P., Portugal, and TOXOMICS (UIDB/00009/2020; UIDP/00009/2020).

Each of the chapters included in this book has been submitted to a peer-review process, and we thank the experts involved who provided their valuable revisions. The experts involved in the peer-review process are listed below:

Ana F. Bettencourt, Research Institute for Medicines (iMed.U LISBOA), Faculty of Pharmacy, Universidade de Lisboa, Av. Professor Gama Pinto, 1649-003 Lisbon, Portugal

Ana M. Tavares, Department of Human Genetics, National Institute of Health Dr. Ricardo Jorge (INSA), Lisbon, Portugal

Célia Ventura, Department of Human Genetics, National Institute of Health Doutor Ricardo Jorge (INSA), Lisbon, Portugal

Espen Mariussen, NILU - Norwegian Institute for Air Research, Kjeller, Norway

Fátima Pinto, Department of Human Genetics, National Institute of Health Dr. Ricardo Jorge (INSA), Lisbon, Portugal

Francesco Cubadda, Istituto Superiore di Sanità - National Institute of Health, Rome, Italy

Isabel Gaivão, Department of Genetics and Biotechnology and Animal and Veterinary Research Centre (CECAV), University of Trás-os-Montes and Alto Douro (UTAD), 5000 Vila Real, Portugal

João Lavinha, Retired from Department of Human Genetics, National Institute of Health Doutor Ricardo Jorge, Lisbon, Portugal

José Vega-Baudrit, LANOTEC CENAT, San José, Costa Rica

Lídia Gonçalves, Research Institute for Medicines (iMed.U LISBOA), Faculty of Pharmacy, Universidade de Lisboa, Av. Professor Gama Pinto, 1649-003 Lisbon, Portugal

Lola Bajard, Masaryk University, Faculty of Science, RECETOX, Kamenice 5, Brno, Czechia

Nicolaj Bischoff, Department of Toxicogenomics, GROW-School for Oncology and Developmental Biology, Maastricht University Medical Center, P.O. Box 616 6200 MD Maastricht, The Netherlands

Teresa Borges, Directorate-General of Health, Ministry of Health, Lisbon, Portugal

Contents

Part I Nanotechnologies: Synthesis, Application and Characterization of Nanomaterials

- 1 Challenges in Nanomaterial Characterization – From Definition to Analysis** 3
José A. M. Catita
- 2 Trends in the Design and Evaluation of Polymeric Nanocarriers: The *In Vitro* Nano-Bio Interactions** 19
Ana Bettencourt and Lídia M. Gonçalves
- 3 LipNanoCar Technology – A Versatile and Scalable Technology for the Production of Lipid Nanoparticles** 43
Vera L. R. Esgueira, Clara P. A. Lopes, Ana Catarina A. dos Santos, Fátima Pinto, Sílvia A. Sousa, Dragana P. C. de Barros, Jorge H. Leitão, and Luis P. Fonseca
- 4 Dermal Delivery of Lipid Nanoparticles: Effects on Skin and Assessment of Absorption and Safety** 83
Fátima Pinto, Luis P. Fonseca, and Dragana P. C. de Barros
- 5 Targeting Cancer by Using Nanoparticles to Modulate RHO GTPase Signaling** 115
Paulo Matos, Joana F. S. Pereira, and Peter Jordan
- 6 Nanocelluloses: Production, Characterization and Market** 129
Paulo J. T. Ferreira and Ana F. Lourenço

Part II Nanotoxicology: Concepts and Methodologies for Toxicity Evaluation of Nanomaterials

- 7 Nanocelluloses – Nanotoxicology, Safety Aspects and 3D Bioprinting** 155
Gary Chinga-Carrasco, Jennifer Rosendahl, and Julia Catalán
- 8 New “Omics” Approaches as Tools to Explore Mechanistic Nanotoxicology** 179
Célia Ventura, Vukosava Torres, Luís Vieira, Bruno Gomes, António Sebastião Rodrigues, José Rueff, Deborah Penque, and Maria João Silva

9	Epigenetic Mechanisms in Understanding Nanomaterial-Induced Toxicity	195
	Manosij Ghosh, Lode Godderis, and Peter Hoet	
10	Cellular and Molecular Mechanisms of Toxicity of Ingested Titanium Dioxide Nanomaterials	225
	Adriana Vieira, Ana Gramacho, Dora Rolo, Nádía Vital, Maria João Silva, and Henriqueta Louro	
11	Nanomaterial-Induced Extra-Pulmonary Health Effects – the Importance of Next Generation Physiologically Relevant <i>In Vitro</i> Test Systems for the Future of Nanotoxicology	259
	Ali Kermanizadeh and Gwyndaf Roberts	
12	<i>Drosophila</i> as a Suitable <i>In Vivo</i> Model in the Safety Assessment of Nanomaterials	275
	Eşref Demir, Fatma Turna Demir, and Ricard Marcos	
13	Toxicological Aspects of Iron Oxide Nanoparticles	303
	Natalia Fernández-Bertólez, Carla Costa, Fátima Brandão, João Paulo Teixeira, Eduardo Pásaro, Vanessa Valdiglesias, and Blanca Laffon	
14	Hazard Assessment of Benchmark Metal-Based Nanomaterials Through a Set of <i>In Vitro</i> Genotoxicity Assays	351
	Nádía Vital, Mariana Pinhão, Naouale El Yamani, Elise Rundén-Pran, Henriqueta Louro, Maria Dušínská, and Maria João Silva	
Part III Towards the Risk Assessment and Regulation of Nanomaterials		
15	Nanomaterials, a New Challenge in the Workplace	379
	Ana Rita Alberto, Cristina Matos, Gabriel Carmona-Aparicio, and Muriel Iten	
16	Nanomaterials in Foods and Human Digestion: An Important Layer in the Assessment of Potential Toxic Effects	403
	Carla Martins, Paula Alvito, and Ricardo Assunção	
17	Overview of Adverse Outcome Pathways and Current Applications on Nanomaterials	415
	Dora Rolo, Ana Tavares, Nádía Vital, Maria João Silva, and Henriqueta Louro	
	Correction to: Hazard Assessment of Benchmark Metal-Based Nanomaterials Through a Set of <i>In Vitro</i> Genotoxicity Assays	C1

Part I

**Nanotechnologies: Synthesis, Application
and Characterization of Nanomaterials**



Challenges in Nanomaterial Characterization – From Definition to Analysis

1

José A. M. Catita

Abstract

Nanomaterials have outstanding properties and have several applications, ranging from foods, cosmetics, pharmaceuticals to energy, construction, etc. As with all novel products, the benefits of nanomaterials use must be weighed against its health and environmental impact. They have different origins, natural, incidental, or engineered, they are widespread, and they need to be classified and characterized for various purposes, including nanotoxicology studies and risk assessment, workplaces and environment safety evaluation, consumer products evaluation, as well as manufacturing process control. To properly characterize nanomaterials, a consensual definition of nanomaterial is needed, and several analyses using the available characterization techniques must be performed. Various properties are relevant in the characterization process and many of them, namely size, are still a challenge that the research community is facing. The measurement of physical and chemical properties is very important in the case of nanomaterials. In view of this, in this chapter, available ana-

lytical techniques are reviewed based on nanomaterials classification, regulatory demands and toxicology assessment. Additionally, some of the current major challenges and gaps in nanomaterials characterization are identified and listed.

Keywords

Nanomaterial characterization · Nanomaterial classification · Nanomaterial properties

1.1 Introduction

Nanotechnology has been a relevant topic in the scientific community due to the unique properties of materials in the nanoscale, and it has become an enabling technology for numerous applications. Produced science on new nanomaterials (NMs), and their characteristics and applications, has been identified as a key enabling technology and keeps stimulating industrial growth, innovation and development, in the most diverse fields such as medicine, food, cosmetics, electronics, automotive, energy, construction, and other areas. Consequently, studying the exposure to nanomaterials is a critical aspect when assessing their safety and risks, particularly in three scenarios: environment, consumer products and working places [49]. Results from these studies

J. A. M. Catita (✉)
FP-ENAS, Faculty of Health Sciences, University
Fernando Pessoa, Porto, Portugal

Paralab SA, Gondomar, Portugal
e-mail: jcatita@ufp.edu.pt

will contribute to overcome uncertainties about NMs safety for human health and the environment which are still hampering a more widespread exploration of its potentials. Several authorities and official organisms are therefore defining actions for the implementation of a safe, integrated, and responsible approach for nanoscience and nanotechnologies. As an important step in that direction, definitions of nanomaterials have been proposed and are being implemented for regulatory and policy purposes in order to ensure harmonized terminology and definitions across different pieces of documentations and legislation. The difficulty in comparing the toxicity results for available nanomaterials comes from the wide variety of production processes and also from some lack of systematic work regarding physical and chemical characterization of NMs [9]. Measuring nanomaterials properties should be done by using the most appropriate technique(s) and results should be confirmed against a control or reference material, using an orthogonal analytical approach since no single technique is capable of fully characterize a nanomaterial [49]. Additional difficulties may come from the need to characterize NMs in complex and poly-disperse media (e.g. biological) as well as from the fact that many times their concentration in these types of media may be quite low [1].

The toxicity of NMs for living organisms is probably the main factor hampering their use and application. To proper balance between the positiveness of their use and their toxicity is mandatory, and it should be based on adequate experimental models which ultimately depend on the adequate physical and chemical characterization of NMs [50]. However, the reliable detection, characterization, and quantification of nanomaterials is still quite challenging, particularly in complex media, and work has to be done to overcome difficulties inherent to nanoscale materials, to the difficult access to all the available techniques, and to the lack of harmonized procedures and interlaboratory studies [40].

1.2 Types of Nanomaterials

1.2.1 Classification

Nanomaterials (NMs) are basically materials that have one dimension between 1 nm to 999 nm. This would be the expected classification when simply considering the word itself. However, that is not the case and there have been several approaches to group and classify nanomaterials. Initially, in 2007, ISO/TR 27628 appears with the classification of a nanoparticle as a particle with a nominal diameter smaller than 100 nm [17]. One year later, ISO/TS 27687 proposes terminology and definitions for nano-objects which include nanoparticle, nanofiber and nanoplate [19]. A classification tree is proposed for nanoobjects (see Fig. 1.1). In 2010, ISO/TS 80004 harmonizes terminology and definitions, and nanomaterial is defined as a material with any external dimension in the nanoscale or having an internal structure or surface structure in the nanoscale, ranging the nanoscale approximately from 1 nm to 100 nm [21]. At the same time ISO/TR 11360:2010 [20] provided a basic classification system for different types of nanomaterials which accounts for their different

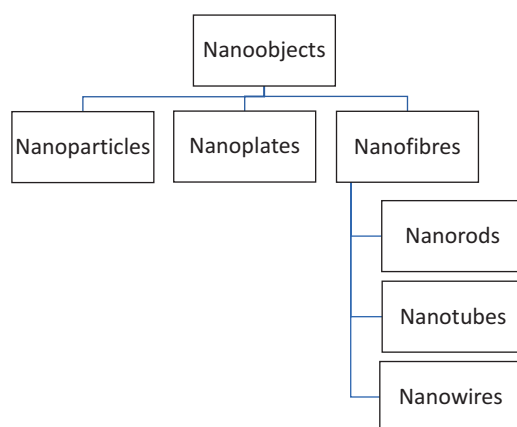


Fig. 1.1 Nanoobjects classification according to ISO/TS 27687:2008

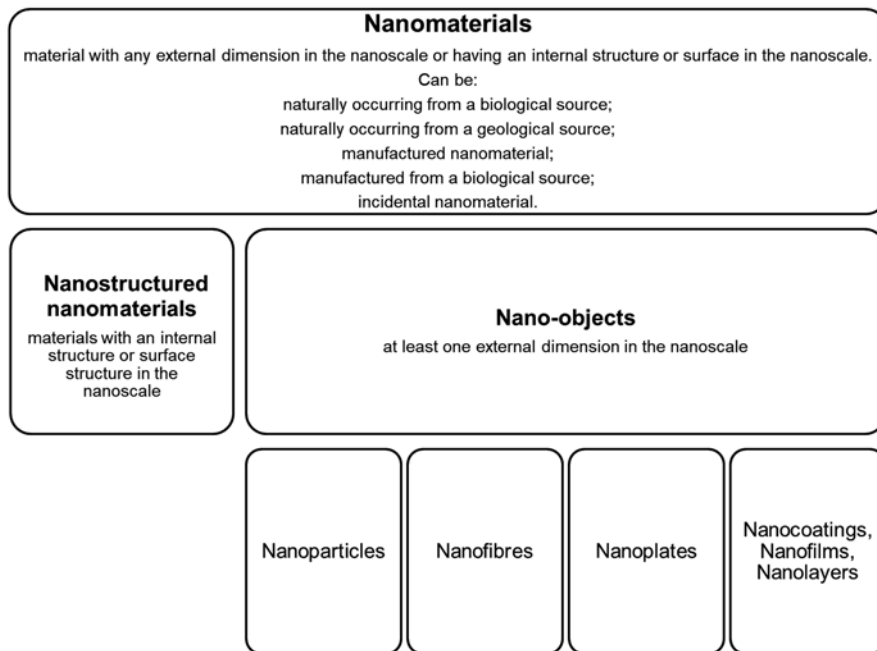


Fig. 1.2 Classification of nanomaterials according to ISO/TR 18401:2017

properties. Following classifications trees, nanomaterials are grouped according to their dimensions, structure, chemical and physical properties and functional behavior.

ISO/TR 18401:2017 [26] revisited the vocabulary and defined a nanoparticle as a nano-object with all external dimensions in the nanoscale where the lengths of the longest and the shortest axes of the nano-object do not differ significantly. These are broad spectrum definitions in which several types of materials can be included and grouped under two major categories: nano-objects and nanostructured materials (see Fig. 1.2). Regarding nanostructured nanomaterials, Hansen et al. [13] have proposed a classification quite relevant since it considers the matrix where nanoparticles may be embedded (Fig. 1.3). This classification helps to predict how challenging must be to separate and characterize nanoparticles depending on where they must be isolated from.

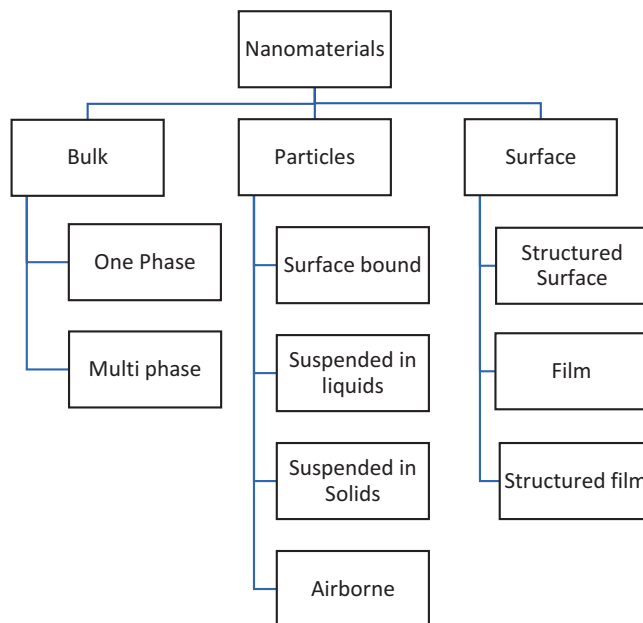
1.2.2 Properties

A systematic approach of classification and categorization of nanomaterials just based on dimension is quite limited. Other properties than size must be considered to properly define a logical hierarchy of classification.

ISO/TR 11360:2010 [20] describes a classifying system, termed “nano-tree” which aims to provide a structured view of nanotechnology and facilitates a common understanding of nanotechnology concepts.

The nano-tree depicts the understanding of the structure and relationships of nanomaterials providing means to classify them. It uses dimension and key functional properties to distinguish nanomaterials from one another and to show its relationships. By this way, nanomaterials are grouped according to their dimensions (1D, 2D and 3D), their chemical nature (eg. ceramic,

Fig. 1.3 The categorization framework for nanomaterials. The nanomaterials are categorized according to the location of the nanostructure in the material. (Adapted from [13])



metallic, organic, inorganic), their physical properties (eg. optical, magnetic, acoustic), their mechanical properties (eg. elastic, plastic), their chemical properties and their biological properties, as well as some combined properties (eg. electro-optical or thermoelectric). This ISO standard, together with other proposals for the classification of nanomaterials, makes possible to harmonize their classification in a rational and systematic manner. However, all these proposals would be cross-cutting if we do not consider the size. In fact, size is the critical property that makes it possible to classify nanomaterials as such.

1.3 Risk Assessment and Regulatory Perspective

Since the begin of the study of nanomaterials, the impact of their use in the various possible areas of application has always been the main concern. In other words, because nano-scale materials have unique properties, there has always been a need to study them in isolation and to understand their impact on ecosystems, and on life in general, and human life in particular. Nanomaterials have therefore been studied from the perspective

of the risk their use poses to human life and the environment in general.

As size of nanoparticles (NPs) gets smaller, the surface area increases exponentially, which make these particles more reactive and potentially more toxic. Also, with decrease in size, their ability to penetrate plant and animal tissues increases, and at such small sizes, even well-known substances behave in uncommon ways. Penetration of NPs through the different barriers of the cells is largely dependent on size. It is a “rule of thumb” that particles with a size less than 100 nm can enter cells by crossing cell membrane. When the size becomes smaller than 40 nm they can enter into nuclei of cells while those with less than 35 nm can penetrate into blood–brain barrier [10, 42]. Larger particles (200–500 nm) can also enter cells [16] but with less probability which makes size specification of 100 nm an acceptable reference value for regulatory purposes.

Given the relevance of size for crossing barriers, more definitions began to emerge where the cut-off value was 100 nm. This was intended to create a well-defined criterion, based on which a certain group of materials was classified as ‘nanomaterial’ and which might deserve specific

considerations in a regulatory context. Nanomaterials are not necessarily hazardous, and size-based definitions are not specifically based on hazard or risk assessment. However, the fact that particles larger than 100 nm cannot easily cross membranes, implies that the risk of use may be much lower. In those circumstances, their risk can be addressed according to their many other properties and in the same way as materials/substances already known before the introduction of the “nanoscale”. This applies when they are used both at a molecular level (liquids, solutions, gas) or as larger particles (solids, suspensions, aerosols).

In 2011, the European Commission proposed a definition for nanomaterials, based on ISO definition [6]. This definition recommendation, that has been revisited but not reviewed so far [47, 48], considers a nanomaterial defined as “a natural, incidental or manufactured material containing particles, in an unbound state or as an aggregate or as an agglomerate and where, for 50% or more of the particles in the number size distribution, one or more external dimensions is in the size range 1 nm–100 nm...”. The European Commission Nano Material (EC NM) definition further specifies that “fullerenes, graphene flakes and single wall carbon nanotubes with one or more external dimensions below 1 nm should be considered as nanomaterials” and that “‘particle’, ‘agglomerate’ and ‘aggregate’ are defined as follows: (a) ‘particle’ means a minute piece of matter with defined physical boundaries; (b) ‘agglomerate’ means a collection of weakly bound particles or aggregates where the resulting external surface area is similar to the sum of the surface areas of the individual components; (c) ‘aggregate’ means a particle comprising of strongly bound or fused particles” [6].

Surface area is directly correlated with particle size and with the reactivity/toxicity of nanomaterials. For that reason, the EC NM defines that “Where technically feasible and requested in specific legislation, compliance with the definition may be determined on the basis of the specific surface area by volume. A material should be considered as falling under the definition where the specific surface area by vol-

ume of the material is greater than $60 \text{ m}^2/\text{cm}^3$. However, a material which, based on its number size distribution, is a nanomaterial should be considered as complying with the definition ... even if the material has a specific surface area lower than $60 \text{ m}^2/\text{cm}^3$.” [6]. The number size distribution should cover for the fact that nanomaterials most typically consist of many particles present in different sizes and in a particular size distribution. Without specifying the number size distribution, it would be difficult to determine if a specific material complies with the definition where some particles are below 100 nm while others are not. [47, 48].

Identification of a material as a nanomaterial according to the EC NM definition is not determined by a certain (chemical) composition, a certain structure, novel properties that are attributable to the particles’ external dimensions, or by the application of the material in a specific field. Exceptions are fullerenes, graphene flakes and single wall carbon nanotubes with one or more external dimensions below 1 nm, which are explicitly considered as nanomaterials. Regarding particles origin, NMs and its possible risks do not depend on whether its particles are natural, produced incidentally, or the result of an engineering process with or without the explicit intention to manufacture a nanomaterial. In that respect, natural materials can exhibit the same properties as those that are manufactured and vice versa. Therefore, EC NM definition does not exclude certain types of materials just because of their origin. However, there is an exception to individual proteins, polymers and macromolecules; which are excluded from the scope of the EC NM definition as they are considered single molecules. Even so, if these macromolecules are assembled into solid objects with clearly defined and stable external boundaries, and if they are stable enough to retain their shape over a longer period and to allow the measurement of their external dimensions, these objects should be considered as particles.

In the same way of the European Commission (EC), many other official organizations across the world have adopted similar definitions. As EC, all of them defined 100 nm as the reference

top range size for the classification, and most of them refer to a characterization based on a number distribution. [3].

Similarly, sector organizations like the Food and Drug Administration (FDA) or the World Health Organization (WHO) have created guidelines with a nanomaterial definition. In fact, FDA has not established regulatory definitions of “nanotechnology,” “nanomaterial,” “nanoscale,” or other related terms. Since they are already commonly used, FDA simply adopted the definition of nanomaterial as a material that have at least one dimension in the size range of approximately 1 nm to 100 nm [12]. Bigger materials in the nanoscale (here defined as sizes up to 1000 nm) were also considered to address products resulting from nanotechnology, but they were grouped in a different category. This decision reflects the fact that materials or end products can be engineered to exhibit properties or phenomena, including physical or chemical properties or biological effects, that are attributable to its dimension(s), even if these dimensions fall outside the typical nanoscale range (1 to 100 nm), up to one micrometer (1000 nm).

In the same way, WHO also adopted the common definition of nanomaterial as materials that have at least one dimension (height, width or length) that is smaller than 100 nm. A nanoparticle is defined as a nano-object with all three external dimensions in the nanoscale (<100 nm diameter) and manufactured nanomaterials are defined as solid, particulate substances intentionally manufactured at the nanoscale, consisting of nano-objects with at least one dimension between 1 and 100 nm, and their aggregates and agglomerates. [51].

The definitions referred above were all very similar and were presented in a context of risk assessment of nanomaterials (NMs) exposure and therefore its toxicological impact. The toxicity of NMs may largely depend on numerous physicochemical properties, including size, shape (i.e. external size in a particular dimension), composition, surface characteristics, charge and rate of dissolution. The introduction of NMs in many different types of products and into the environment, and the human exposure to

both, has raised additional needs in NM characterization in order to understand which core properties besides dimension may be relevant in risk assessment and toxicological impact on humans [28]. A new discipline arose – nanotoxicology, to characterize and categorize the adverse effects induced by NMs and to determine relationships of structure and function between nanoparticles and toxicity [4, 11].

Based on biodegradability and on the fact that biodegradable material in the human body has *a priori* a lower toxicity risk, a nanotoxicological classification system (NCS) has been proposed [30]. This simple system considers size and biodegradability and classifies nanomaterials in four main categories (I to IV) from low/no risk to high risk. However, specific methods to evaluate bioavailability, pharmacokinetic pathways, persistency, degradation by-products, cell uptake, intercellular fate, cell interaction were yet to consider at the time. Regulatory and standardization measures to characterize different nanomaterials like chemicals, biocides, consumer products and food, and to characterize human exposure, biokinetics and toxicity, require appropriate analytical development and capabilities. [32].

Risk assessment and toxicological evaluation of NMs has been always quite challenging since there is an enormous amount of different materials in different contexts of use, with different properties, and different behavior. Considering that, an approach for toxicity prediction without testing every single material and fully characterize it, is to use *in silico* methods such as the (quantitative) structure–activity relationship ((Q) SAR) [8]. To properly apply this approach, a high amount of high-quality experimental data needs to be assessed. The establishment of standard protocols (or operation procedures) is paramount for enabling the generation of this data by means of accurate measurement of the physicochemical and biological properties of ENMs [44]. Also, the set of properties to be characterized (core properties) needs to be defined in advance according to its relevance for the toxicological assessment. The Organization for Economic Cooperation and Development (OECD) Working Group on Manufactured Nanomaterials, the

Table 1.1 List of physicochemical properties that might be relevant to address for nanomaterials characterization [43]

Characterization (as on the shelf)		Characterization (in respective media)
<ul style="list-style-type: none"> – Appearance – Melting point – Density – Size, size distribution – N-octanol–water partition coefficient – Water solubility/dispersibility, hydrophilicity – Solubility/dispersibility in organic solvents, oleophilicity – Auto flammability – Stability in solvents and identity of relevant degradation products – Oxidation reduction potential – Storage stability and reactivity towards container material – Stability towards thermal, sunlight, metals – Catalytic activity – Radical formation potential – Flammability 	<ul style="list-style-type: none"> – Dissociation constant – pH – Agglomeration or aggregation – Crystalline phase – Crystallite and grain size – Aspect ratio, shape – Specific surface area – Zeta potential – Surface chemistry – Stability and homogeneity (on the shelf, in water and organic solvents) – Dustiness – Porosity, pore and pour density – Photocatalytic activity – Explosiveness – Oxidizing properties 	<ul style="list-style-type: none"> – Composition/purity – Size, size distribution – Agglomeration/aggregation – Zeta-potential – Biophysical properties (protein binding/corona characterization, residence times, adsorption enthalpy, conformation changes on binding) – Test item preparation protocol, conditioning, homogeneity and short term stability

OECD WPMN, prepared one of the most comprehensive lists of the important physicochemical characteristics for toxicological studies (see Table 1.1). In the same document, also a list of “endpoints” is presented where stability; biodegradation and toxicity, among others, are suggested [43].

The set of listed properties allows to properly characterize nanomaterials, but not all of them are equally relevant to predict toxicity [44]. In that context, size and size distribution are the most relevant since they allow to classify the material as nano in first place. As previously written in this chapter, size is also related with the ability of NMs to cross cell membranes, penetrate the nucleus or pass through blood barrier membrane. The interaction of NMs with living systems and the uptake and deposition of NMs within the human body are therefore affected by particle size. Also, the surface area increases with decreasing particle size, affecting surface energy and hence the reactivity of the material.

Before addressing toxicological tests, it is needed to understand and identify the most relevant physicochemical properties of NMs. Other properties such as particle shape (external dimensions), crystal structure, surface chemistry, sur-

face charge, and aggregation state have been identified to be paramount to correlate nanomaterials exposure with toxicity [22, 44].

The shape of NMs, and indirectly their external dimensions, is an important property that influences the biological activities of the particles [5, 34, 46]. Several nondimensional shape indexes can be used to quantify the shape characteristics of particles, such as sphericity/circularity, aspect ratio/elongation, convexity, and fractal dimensions [18]. Using quantitative descriptors for external dimensions and shape, rather than the usual qualitative ones (e.g. rod, sphere) highly potentiates the possibility of establishing better correlations between toxicity and shape, meaning a better QSAR.

Nanomaterials with the same chemical composition may affect differently the integrity and fluidity of membranes depending on the crystalline phase. The toxicity mechanism of NPs with different structure or different surface coatings will have different toxicological effects depending on their phase/crystallinity. [41, 53].

Surface chemistry plays an important role in the interaction of NMs with biological systems and subsequently, their toxicity. On the other hand, it is also relevant for the characterization of

NPs since it defines the potential surface interactions and aggregation behavior of NPs in liquid media [15, 50].

Surface charge, and consequently zeta potential is another important characteristic that may affect the toxicity of NMs. The biological interactions of NMs, their fate and hence their biological activities, are highly surface-charge dependent. On the other hand, the electrostatic stability of particles in liquid medium and, in practical terms, the influence it has on the formation of agglomerates may also affect toxicity [33].

Some NPs tend to form large agglomerates either in the dry form or in suspension. When this happens, NPs may behave like larger particles because of their increased global size. Increasing the size of NMs through aggregation may change its nanotoxicity in comparison to the exposure of isolated nanoparticles of the same material. [2, 31].

1.4 Available Techniques to Characterize Nanoparticles Size, Size Distribution and Shape

According to the common classifications in use, a nanomaterial is classified as such when that at least 50% of the particles have one or more external dimensions ('size') between 1 nm and 100 nm. This definition has already been adopted by several European countries as well as by the European Food Safety Authority [7], along with other world countries and international organizations (eg. WHO, FDA and OECD).

It is consensual from all the available definitions of nanomaterial that size, size distribution by number and shape (external dimensions) in the range of 1–100 nm and over, are critical properties to classify a material as nano.

1.4.1 Size

Regardless of the difference in scope and implementation, all definitions of the term "nanomaterial" have a common characteristic as the basic defining element: particle size. Therefore, in any case of deciding whether a material is a nanomaterial, its particle size distribution must always be determined. This involves particle size measurement from a few nanometers to a few microns. Although the particle size can be determined by a variety of analytical techniques, each technique has its scope of application in terms of material type, material properties, and achievable size range, as well as the medium in which the particles are dispersed and are to be isolated from and measured.

The European Commission through the Joint Research Center (JRC) recognizes about thirteen possible techniques and grouped them according to their working range (1–100 nm and 100 nm–100 μ m) and the type of measurement signal weighting regime (light intensity or extinction, particle mass and particle number) [47, 48].

In the past few years, the measurement performance and quality assurance level of common particle size measurement techniques have improved, but these techniques still cannot measure NMs within the entire size range related to their definitions, that is, from 1 nm well into the micrometer region. Among the techniques with a wider analytical range is Analytical Ultra Centrifugation (AUC). This technique is able to separate and measure particles from some nanometers to about 30 μ m. However, particles need to have an optical property distinguishable from other solution components and a density compatible with a reasonable sedimentation rate within the experimental gravitational field [52]. In comparison to other available techniques, AUC is time consuming and therefore with a low throughput [45]. Similar to AUC, is Centrifugal Liquid Sedimentation (CLS), in which particle size is determined by means of centrifugal sedimentation in a liquid and its concentration by means of the transmission of a light beam. The method is applicable to powders that can be dispersed in liquids. In it, all particles are assumed to have the same density

and comparable shapes, and its density must be different from the density of the dispersing liquid. Typical particle size range for analysis is from about 5 nm to more than 10 μm [52].

Laser diffraction (LD) spectroscopy comprises angular light scattering techniques, which are primarily designed to resolve the scattering pattern at small scattering angles. Although its typical analytical range can start at values lower than 100 nm, it is a technique usually devoted to microparticles rather than NPs. LD is prone to underestimate the amount of NPs and, thus, to overestimate the number-weighted sample median. Additionally, the sample typically needs to be diluted and it measures an equivalent sphere diameter not resolving different particle shapes. [27, 35].

Small-angle X-ray scattering (SAXS) is a technique that allows to obtain size information of nanomaterials and it is based on the interaction between X-rays and matter. Its working range is one of the narrower (1 nm to 100 nm) although under certain conditions (narrow size distributions, appropriate instrumental configuration, and idealized shape) this limit of 100 nm could be extended. This characteristic leads to underestimation of the median particle size for broad size distributions that goes beyond 100 nm, which results in a misclassification of NMs. [14].

Most of the techniques are able to measure both size distribution of equivalent spherical particles but a few can distinguish individual particles from aggregates/agglomerates [35]. Another relevant point is that, except for atomic force microscopy (AFM), all the purposed techniques are already supported by an ISO standard. This allows for the different users of each technique to access each technique with a higher level of harmonization, and better compare results obtained from different samples, in different instruments by different operators.

The results of different particle size measurement techniques are usually not in complete agreement because the measurement principles and working range behind each method are different. Accordingly, particle size results should always be reported along with the size range in which the size was measured, as well as the instrumental technique and analytical method.

A descriptor commonly used for evaluating particle size distributions is the $x_{50.0}$ value, also called the median (the size at which 50% of the analyzed particles of a sample have a property of less than this value and for the other 50% of the particles the same property is higher). However, due to the differences in the measuring technique principles, the median can relate to different properties like light intensity, volume, number, mass, or some external dimension. The knowledge of material properties allows the original size distribution to be converted to other distributions, however trueness can be compromised depending on the accuracy of the material information used to do it.

1.4.2 Number-Based Distribution and Shape

Most definitions of nanomaterials refer to the distribution in number. That is, a material will be considered as nano if a part (usually 50%) of its particles (number-based distribution) is below 100 nm. Thus, any technique used has to be able to measure particles with sizes under and above 100 nm, of different shapes and chemical nature, in their isolated state or in aggregates/agglomerates and still be able to count each particle for the number-based distribution. As with any method, it is desired that these measurements are feasible in laboratory reality, *i.e.* fast, accurate and precise, robust and accessible. Nowadays there is no method or technique capable of fulfilling all these objectives, however electronic microscopy techniques have some advantages:

- They operate in the desired measurement range.
- They distinguish particles from aggregate/agglomerates.
- Allow number-based distribution.
- Allow analysis of particles of any chemical nature.
- Allow the measurement of external dimensions and shape
- They are supported by standard procedures (ISOs)
- They may be able to do chemical discrimination

Despite their enormous capabilities, electron microscopy techniques have certain limitations and weaknesses:

The sample preparation can be difficult and is material dependent.

Not applicable to liquid dispersions.

Among electron microscopy techniques, scanning electron microscopy (SEM) is easier to use on a routine basis (less sample preparation, less consumables, lower cost per analysis) but is limited in size range. The best instrument configuration in the best-case scenario does not perform well for sizes lower than 10 nm.

A very good automation is required in terms of image acquisition hardware and image processing software.

To obtain a representative result with statistical relevance, at least 10,000 particles need to be measured [23] which makes it time-consuming.

It is high cost.

There are other techniques available that can measure size and make the distribution in number:

Atomic force microscopy (AFM)

Particle tracking analysis (PTA)

Tunable resistive pulse sensing (TRPS) / electrical sensing zone (ESZ) / nano Coulter counter

Single particle inductively coupled plasma - mass spectrometry (spICP-MS)

Differential electrical mobility analysis (DEMA)

AFM share most of the advantages and disadvantages with electron microscopy. However, it is strongly dependent on sample preparation (immobilized particles on substrate need to be representative of the material), working range is more limited and it is not supported by an ISO standard.

All the other proposed techniques lack the ability to distinguish single particles from aggregates/agglomerates and to provide any shape information or particular external dimension. TRPS does not perform well for sizes under

30 nm and DEMA for sizes above 1 micron. DEMA only analyses samples in the form of aerosols and ICP-MS is not able to detect particles with no metals in their composition (carbon based, organic or biological).

Particle tracking analysis (PTA) is an alternative since it is supported by an ISO standard [24], it can measure particles from about 10 nm (material dependent), is quite simple to use and comparably affordable. Depending on the instrument configuration and material chemistry, it may be able to do chemical discrimination.

The interplay between sample preparation, identification of constituent particles and the accurate determination of the external dimensions of these constituent particles requires complex and often time- and resource-intensive measurement techniques. However, even when it is not possible to determine the exact number-based distribution as such, a decision whether a material needs to be classified as nanomaterial or not is still relevant.

In this context, dynamic light scattering (DLS) is a very good first choice [39, 40]. Although it is a technique with several limitations and that needs extra care and knowledge to interpret the results [25], it has several advantages that can be listed below:

- It is applicable to broad size distributions from 1 nm to more than 1 μm ,
- it allows a relatively inexpensive and fast assessment of particle size,
- it is fast and robust,
- it is applicable to any type of material (carbon based, organic, inorganic, biological or metallic), as long as particles remain in a stable suspension and undergoing Brownian motion.
- a minimum amount of information about the sample is needed to run the analysis
- It is non-destructive (sample may be recovered)
- small amount of sample is needed to run a test

The methods and measurement techniques that can be used to measure particle size distributions and shape can be based on very different

Table 1.2 Comparative evaluation of selected methods for size, shape and size distribution characterization

Measuring principle	Technique	Size range	Liquid dispersion	Solid/powder	Shape	Polydispersity	Size distribution of raw data	Measures constituent particles in aggregated / agglomerated samples
Microscopy	SEM	10 nm to >10 mm	No	Yes	Yes	Yes	Number-based	Yes
	TEM	1 nm to >10 mm	No	Yes	Yes	Yes	Number-based	Yes
	AFM	1 nm to 10 mm	No	Yes	Yes	Yes	Number-based	Yes
Separation	FFF	1 nm to 10 mm	Yes	No	No	Yes	Scattered light intensity based	No
	AC	1 nm to 10 mm	Yes	No	No	Yes	Light extinction-based	No
Scattering	DEMA	2 nm to 1 mm	No (only aerosolized NPs)	No (only aerosolized NPs)	No	Yes	Electrical mobility based	No
	PTA	10 nm to 1 mm	Yes	No	No	Yes	Number-based	No
	DLS	1 nm to 10 mm	Yes	No	No	No	Scattered light intensity based	No
Other	ICP-MS	10 nm to 1 mm	Yes	Yes	No	N/A	Number-based	No
	SAXS	1 nm to 100 nm	Yes	Yes	No	No	Mass based	No

Source: Adapted from [7, 35]

measurement principles, and the level of detail that they provide, and their working range can also differ considerably. For many materials, available methods already allow their classification as nanomaterials according to the accepted definitions, however, there is still a path to make to overcome the cases for which that is still too challenging (Table 1.2).

1.5 Major Challenges in Characterization

In the last two decades a huge effort, work, and investment has been put in place to improve NMs characterization in all perspectives (legal, regulatory, technical, and scientific).

So far, all relevant definitions apply to nanomaterials from 1 to 100 nm and recommend a number-based distribution approach.

Recently, the NanoDefine Methods Manual, parts 1[36], 2[35] and 3[37] have been published. With these manuals, general recommendations have been produced to support the user in the decision whether a material is a nanomaterial according to the EC Recommendation on the Definition of Nanomaterial. Those recommendations refer to the available measurement techniques, which are candidates for performing a reliable analysis of the number-based size distribution of a particulate material; as well as to Standard Operation Procedures (SOPs) for the sample preparation.

Analyzing nanomaterials remains a challenge and the main difficulties have been thoroughly identified and discussed [29, 38].

In general, one may distribute the main difficulties into two main categories: those related exclusively to size characterization and those that apply to all characterization techniques of all physical and chemical properties of nanomaterials.

In the first case one can identify:

- The size range. Many available techniques are not capable of detect and analyze particles

smaller than 50 nm, and many others have a narrow working range.

- The differentiation between isolated particles, aggregates, and agglomerates
- The ability to measure the external dimensions of particles and consequently determine their shape
- The ability to count particles individually with the aim of obtaining a number-based distribution.

The biggest challenges that can be identified for most of the available techniques are also related to the nano scale since the measurement of common properties becomes more difficult within this size range. They can be identified as:

- The preparation of the sample. The sample must be representative and have statistical significance.
- The isolation of nanomaterials included in complex matrices. Media such as soils, food, cosmetics, or pharmaceuticals still represent a major challenge in terms of separation of nanomaterials prior to analysis.
- How to report the results is critical. Linking a number to the technique, analytical method and method of sample preparation is critical.
- International Standardization. It is probably one of the biggest challenges in characterization. Ensuring that the entire community uses the same techniques in the same way allows for a better evolution of knowledge regarding the properties of nanomaterials.
- The establishment of interlaboratory tests that allows a greater degree of confidence in the results obtained in regulatory or quality control laboratories.

The more progress is made in minimizing the difficulties identified, the more and better results will be produced that will enable even better correlations to be established between a given physical-chemical property and the behavior of nanomaterials in a variety of environments, and consequently its toxicological potential. The development of methods that are both more effective and cost-efficient will help in the NMs

safety evaluation through the improvement of the existing regulatory guidelines.

References

1. Abdolapur Monikh F, Chupani L, Vijver MG, Vancová M, Peijnenburg WJGM (2019) Analytical approaches for characterizing and quantifying engineered nanoparticles in biological matrices from an (eco)toxicological perspective: old challenges, new methods and techniques. *Sci Total Environ* 660:1283–1293. <https://doi.org/10.1016/j.scitotenv.2019.01.105>
2. Andreani T, Fernandes PMV, Nogueira V, Pinto VV, Ferreira MJ, Rasteiro MG, Pereira R, Pereira CM (2020) The critical role of the dispersant agents in the preparation and ecotoxicity of nanomaterial suspensions. *Environ Sci Pollut Res* 27(16):19845–19857. <https://doi.org/10.1007/s11356-020-08323-0>
3. Boverhof DR, Bramante CM, Butala JH, Clancy SF, Lafranconi M, West J, Gordon SC (2015) Comparative assessment of nanomaterial definitions and safety evaluation considerations. *Regul Toxicol Pharmacol* 73(1):137–150. <https://doi.org/10.1016/j.yrtph.2015.06.001>
4. Buzea C, Pacheco II, Robbie K (2007) Nanomaterials and nanoparticles: sources and toxicity. *Biointerphases* 2(4):17–71. <https://doi.org/10.1116/1.2815690>
5. Cohignac V, Landry MJ, Ridoux A, Pinault M, Annangi B, Gerdil A, Herlin-Boime N, Mayne M, Haruta M, Codogno P, Boczkowski J, Pairon J-C, Lanone S (2018) Carbon nanotubes, but not spherical nanoparticles, block autophagy by a shape-related targeting of lysosomes in murine macrophages. *Autophagy* 14(8):1323–1334. <https://doi.org/10.1080/15548627.2018.1474993>
6. Commission E (2011) Commission recommendation of 18 October 2011 on the definition of nanomaterial. *Off J Eur Union L* 275
7. Committee ES, Hardy A, Benford D, Halldorsson T, Jeger MJ, Knutsen HK, More S, Naegeli H, Noteborn H, Ockleford C, Ricci A, Rycken G, Schlatter JR, Silano V, Solecki R, Turck D, Younes M, Chaudhry Q, Cubadda F, Gott D, Oomen A, Weigel S, Karamitrou M, Schoonjans R, Mortensen A (2018) Guidance on risk assessment of the application of nanoscience and nanotechnologies in the food and feed chain: part 1, human and animal health. *EFSA J* 16(7):e05327. <https://doi.org/10.2903/j.efsa.2018.5327>
8. Cronin MTD, Jaworska JS, Walker JD, Comber MHI, Watts CD, Worth AP (2003) Use of QSARs in international decision-making frameworks to predict health effects of chemical substances. *Environ Health Perspect* 111(10):1391–1401. <https://doi.org/10.1289/ehp.5760>
9. da Costa GM, Hussain CM (2020) 17-safety risk, ELSI (ethical, legal, social issues), and economics of nanomaterials. In: Mustansar Hussain C (ed) *Handbook of nanomaterials in analytical chemistry*. Elsevier, pp 435–446. <https://doi.org/10.1016/B978-0-12-816699-4.00017-7>
10. Dawson KA, Salvati A, Lynch I (2009) Nanoparticles reconstruct lipids. *Nat Nanotechnol* 4(2):84–85. <https://doi.org/10.1038/nnano.2008.426>
11. Donaldson K, Stone V, Tran CL, Kreyling W, Borm PJ (2004) *Nanotoxicology*. *Occup Environ Med* 61(9):727–728. <https://doi.org/10.1136/oem.2004.013243>
12. FDA (2014) Guidance for industry considering whether an FDA-regulated product involves the application of nanotechnology. Food and Drug Administration - Office of the Commissioner, Office of Policy, Legislation, and International Affairs, Office of Policy, Maryland
13. Foss Hansen S, Larsen BH, Olsen SI, Baun A (2007) Categorization framework to aid hazard identification of nanomaterials. *Nanotoxicology* 1(3):243–250. <https://doi.org/10.1080/17435390701727509>
14. Gaillard C, Mech A, Wohlleben W, Babick F, Hodoroaba V-D, Ghanem A, Weigel S, Rauscher H (2019) A technique-driven materials categorisation scheme to support regulatory identification of nanomaterials. *Nanoscale Adv* 1(2):781–791. <https://doi.org/10.1039/C8NA00175H>
15. Gattoo MA, Naseem S, Arfat MY, Dar AM, Qasim K, Zubair S (2014) Physicochemical properties of nanomaterials: implication in associated toxic manifestations. *Biomed Res Int* 2014:498420–498420. <https://doi.org/10.1155/2014/498420>
16. Hillaireau H, Couvreur P (2009) Nanocarriers' entry into the cell: relevance to drug delivery. *Cell Mol Life Sci* 66:2873–2896. <https://doi.org/10.1007/s00018-009-0053-z>
17. ISO (2007) ISO TR 27628:2007-workplace atmospheres – ultrafine, nanoparticle and nanostructured aerosols – inhalation exposure characterization and assessment. International Organization for Standardization, Geneva
18. ISO (2008a) ISO 9276-6:2008 – representation of results of particle size analysis — part 6: descriptive and quantitative representation of particle shape and morphology. International Organization for Standardization, Geneva
19. ISO (2008b) ISO/TS 27687:2008 – nanotechnologies — terminology and definitions for nano-objects — nanoparticle, nanofibre and nanoplate. International Organization for Standardization, Geneva
20. ISO (2010a) ISO/TR 11360:2010 – methodology for the classification and categorization of nanomaterials. International Organization for Standardization, Geneva
21. ISO (2010b) ISO/TS 80004-1:2010 – nanotechnologies — vocabulary — part 1: Core terms. International Organization for Standardization, Geneva
22. ISO (2012) ISO/TR 13014:2012 - nanotechnologies — guidance on physico-chemical characterization of engineered nanoscale materials for toxicologic

- assessment. International Organization for Standardization, Geneva
23. ISO (2014) ISO 13322-1:2014 – particle size analysis — image analysis methods — part 1: static image analysis methods. International Organization for Standardization, Geneva
 24. ISO (2016) ISO 19430:2016 – particle size analysis — particle tracking analysis (PTA) method. International Organization for Standardization, Geneva
 25. ISO (2017a) ISO 22412:2017 – particle size analysis — dynamic light scattering (DLS). International Organization for Standardization, Geneva
 26. ISO (2017b) ISO/TR 18401:2017 – nanotechnologies — plain language explanation of selected terms from the ISO/IEC 80004 series. International Organization for Standardization, Geneva
 27. ISO (2020) ISO 13320:2020 – particle size analysis — laser diffraction methods. International Organization for Standardization, Geneva
 28. Jeevanandam J, Barhoum A, Chan YS, Dufresne A, Danquah MK (2018) Review on nanoparticles and nanostructured materials: history, sources, toxicity and regulations. *Beilstein J Nanotechnol* 9:1050–1074. <https://doi.org/10.3762/bjnano.9.98>
 29. Johnston LJ, Gonzalez-Rojano N, Wilkinson KJ, Xing B (2020) Key challenges for evaluation of the safety of engineered nanomaterials. *NanoImpact* 18:100219. <https://doi.org/10.1016/j.impact.2020.100219>
 30. Keck CM, Müller RH (2013) Nanotoxicological classification system (NCS) – a guide for the risk-benefit assessment of nanoparticulate drug delivery systems. *Eur J Pharm Biopharm* 84(3):445–448. <https://doi.org/10.1016/j.ejpb.2013.01.001>
 31. Kyzyma OA, Avdeev MV, Bolshakova OI, Melentev P, Sarantseva SV, Ivankov OI, Korobov MV, Mikheev IV, Tropin TV, Kubovcikova M, Kopcansky P, Korolovych VF, Aksenov VL, Bulavin LA (2019) State of aggregation and toxicity of aqueous fullerene solutions. *Appl Surf Sci* 483:69–75. <https://doi.org/10.1016/j.apsusc.2019.03.167>
 32. Laux P, Tentschert J, Riebeling C, Braeuning A, Creutzenberg O, Epp A, Fessard V, Haas K-H, Haase A, Hund-Rinke K, Jakubowski N, Kearns P, Lampen A, Rauscher H, Schoonjans R, Störmer A, Thielmann A, Mühle U, Luch A (2018) Nanomaterials: certain aspects of application, risk assessment and risk communication. *Arch Toxicol* 92(1):121–141. <https://doi.org/10.1007/s00204-017-2144-1>
 33. Lowry GV, Hill RJ, Harper S, Rawle AF, Hendren CO, Klaessig F, Nobbmann U, Sayre P, Rumble J (2016) Guidance to improve the scientific value of zeta-potential measurements in nanoEHS. *Environ Sci Nano* 3(5):953–965. <https://doi.org/10.1039/C6EN00136J>
 34. Lunnoo T, Assawakhajornsak J, Puangmali T (2019) In silico study of gold nanoparticle uptake into a mammalian cell: interplay of size, shape, surface charge, and aggregation. *J Phys Chem C* 123(6):3801–3810. <https://doi.org/10.1021/acs.jpcc.8b07616>
 35. Mech A, Rauscher A, Rasmussen K, Babick F, Hodoroaba V, Ghanem A, Wohlleben W, Marvin H, Brüngel R, Friedrich C (2020a) The nanodefines methods manual. Part 2. Publications Office of the European Union, Luxembourg. <https://doi.org/10.2760/071877>. 10.2760/06428
 36. Mech A, Rauscher H, Babick F, Hodoroaba V, Ghanem A, Wohlleben W, Marvin H, Weigel S, Brüngel R, Friedrich M (2020b) The nanodefines methods manual. Part 1. Publications Office of the European Union, Luxembourg. <https://doi.org/10.2760/55181>. <https://doi.org/10.2760/824352>
 37. Mech A, Rauscher H, Rasmussen K, Babick F, Hodoroaba V, Ghanem A, Wohlleben W, Marvin H, Brüngel R, Friedrich C, Löschner K, Gilliland D (2020c) The nanodefines methods manual. Part 3. Publications Office of the European Union, Luxembourg. <https://doi.org/10.2760/02910>. <https://doi.org/10.2760/778>
 38. Miernicki M, Hofmann T, Eisenberger I, von der Kammer F, Praetorius A (2019) Legal and practical challenges in classifying nanomaterials according to regulatory definitions. *Nat Nanotechnol* 14(3):208–216. <https://doi.org/10.1038/s41565-019-0396-z>
 39. Modena MM, Rühle B, Burg TP, Wuttke S (2019) Nanoparticle characterization: what to measure? *Adv Mater* 31(32):1901556. <https://doi.org/10.1002/adma.201901556>
 40. Mourdikoudis S, Pallares RM, Thanh NTK (2018) Characterization techniques for nanoparticles: comparison and complementarity upon studying nanoparticle properties. *Nanoscale* 10(27):12871–12934. <https://doi.org/10.1039/C8NR02278J>
 41. Nogueira DJ, Vaz VP, Neto OS, Silva MLN, Simioni C, Ouriques LC, Vicentini DS, Matias WG (2020) Crystalline phase-dependent toxicity of aluminum oxide nanoparticles toward *Daphnia magna* and ecological risk assessment. *Environ Res* 182:108987. <https://doi.org/10.1016/j.envres.2019.108987>
 42. Oberdörster G, Sharp Z, Atudorei V, Elder A, Gelein R, Kreyling W, Cox C (2004) Translocation of inhaled ultrafine particles to the brain. *Inhal Toxicol* 16(6–7):437–445. <https://doi.org/10.1080/08958370490439597>
 43. OECD (2010) Guidance manual for the testing of manufactured nanomaterials. Organization for Economic Cooperation and Development,
 44. Oksel C, Ma CY, Liu JJ, Wilkins T, Wang XZ (2015) (Q)SAR modelling of nanomaterial toxicity: a critical review. *Particology* 21:1–19. <https://doi.org/10.1016/j.partic.2014.12.001>
 45. Proulx K, Wilkinson KJ (2014) Separation, detection and characterisation of engineered nanoparticles in natural waters using hydrodynamic chromatography and multi-method detection (light scattering, analytical ultracentrifugation and single particle ICP-MS). *Environ Chem* 11(4):392–401. <https://doi.org/10.1071/EN13232>

46. Ramanathan A (2019) Toxicity of nanoparticles_ challenges and opportunities. *Appl Microscop* 49(1):2. <https://doi.org/10.1007/s42649-019-0004-6>
47. Rauscher H, Roebben G, Mech A, Gibson N, Kestens V, Linsinger T, Sintes JR (2019a) An overview of concepts and terms used in the European Commission’s definition of nanomaterial. Publications Office of the European Union
48. Rauscher HMA, Gibson P, Gilliland D, Held A, Kestens V, Koeber R, Linsinger T, Stefaniak EA (2019b) Identification of nanomaterials through measurements. Publications Office of the European Union. <https://doi.org/10.2760/053982>, <https://doi.org/10.2760/7644>
49. Sayes CM (2020) Nanotoxicology: developing a responsible technology. In: Norris P, Friedersdorf L (eds) *Women in Nanotechnology*. Springer, pp 43–55. https://doi.org/10.1007/978-3-030-19951-7_4
50. Sukhanova A, Bozrova S, Sokolov P, Berestovoy M, Karaulov A, Nabiev I (2018) Dependence of nanoparticle toxicity on their physical and chemical properties. *Nanoscale Res Lett* 13(1):44. <https://doi.org/10.1186/s11671-018-2457-x>
51. WHO (2017) WHO guidelines on protecting workers from potential risks of manufactured nanomaterials. World Health Organization, Geneva
52. Wohlleben W, Coleman VA, Gilliland D (2020) Chapter 3.3.1 – analytical centrifugation. In: Hodoroaba V-D, Unger WES, Shard AG (eds) *Characterization of nanoparticles*. Elsevier, pp 225–247. <https://doi.org/10.1016/B978-0-12-814182-3.00015-8>
53. Zhu B, Wei X, Song J, Zhang Q, Jiang W (2020) Crystalline phase and surface coating of Al₂O₃ nanoparticles and their influence on the integrity and fluidity of model cell membranes. *Chemosphere* 247:125876. <https://doi.org/10.1016/j.chemosphere.2020.125876>



Trends in the Design and Evaluation of Polymeric Nanocarriers: The *In Vitro* Nano-Bio Interactions

Ana Bettencourt and Lídia M. Gonçalves

Abstract

Different types of natural and synthetic polymeric nanocarriers are being tested for diverse biomedical applications ranging from drug/gene delivery vehicles to imaging probes. The development of such innovative nanoparticulate systems (NPs) should include in the very beginning of their conception a comprehensive evaluation of the nano-bio interactions. Specifically, intrinsic physicochemical properties as size, surface charge and shape may have an impact on cellular uptake, intracellular trafficking, exocytosis and cyto- or genocompatibility. Those properties can be tuned for effectiveness purposes such as targeting intracellular organelles, but at the same time inducing unforeseen adverse nanotoxicological effects. Further, those properties may change due to the adsorption of biological components (e.g. proteins) with a tremendous impact on the cellular response. The evaluation of these NPs is highly challenging and has produced some controversial results. Future research work should focus on the standardization of analytical or computational methodologies, aiming the identification of

toxicity trends and the generation of a useful meta-analysis database on polymeric nanocarriers.

This chapter covers all the aforementioned aspects, emphasizing the importance of the *in vitro* cellular studies in the first stages of polymeric nanocarriers development.

Keywords

Polymeric-nanostructures · *In vitro* tests · Physicochemical properties · Safe-by-design · Nanotoxicology

2.1 Introductory Remarks

2.1.1 Nanomedicine

Nanotechnology applied to medicine – usually called “Nanomedicine” is one of the most promising *key enabling technology* to foster human health [1]. Specifically, “Nanomedicine” can be defined as “the science and technology of diagnosing, treating and preventing disease and traumatic injury using nanometre size scale complex systems ranging from 1 to 1000 nm” [2].

An increasing number of these nanomedicine products are being explored for diagnostic and the delivery of drugs, bioactive compounds, or genes as innovative therapeutic tools to tackle difficulty to treat pathologies such as cancer, dia-

A. Bettencourt (✉) · L. M. Gonçalves
Research Institute for Medicines (iMed.U LISBOA),
Faculty of Pharmacy, Universidade de Lisboa,
Lisbon, Portugal
e-mail: asimao@ff.ulisboa.pt

betes, and infections [3–6]. In particular, the employment of appropriately designed nanocarriers for the sustained/controlled and targeted delivery of pharmaceuticals to the site of action aims to offer numerous advantages over plain drug administration, that is, enhancement of drug bioavailability to the targeted site, avoidance of drug degradation and side effects, as well as superior transportation method [7]. In sum, improving drug's therapeutic index while reducing their side effects [8]. Also, different types of fluorescent nanostructures are being extensively used as imaging probes, ranging from fixed to living cells and model organisms [9].

2.1.2 Polymeric Nanocarriers

To date several classes of nanometre sized biomaterials have demonstrated promising properties as probes and therapeutic carriers (drug and gene “delivery vehicles” [10, 11] including but not limited to metals (e.g. titanium oxide [12], gold [11]), ceramics (e.g. calcium phosphate, silica [13]), lipids (lecithins [14]) or polymers.

Among those, polymeric nanocarriers due to their high structural integrity, stability during storage, ease of preparation and functionalization plus their capability of controlled payload release are being intensively explored in the last three decades and have proven to be one of the most successful type of nanocarriers [15, 16].

2.1.3 Classification of the Polymeric Nanocarriers

Polymeric nanocarriers can be classified according to different criteria. A key classification refers to the **chemical composition** and their **origin** (natural or synthetic). Different examples are shown in Fig. 2.1. Also, they can be classified as biodegradable (e.g. chitosan, PLGA) and non-biodegradable (poly(methyl methacrylate), polystyrene) as recently reviewed in [17].

Polymers can be used in different forms (Fig. 2.1) [4, 7]: **cluster of nanocarriers** (polymer–drug conjugates), **nanomicelle** (nanosized colloidal

particles composed of amphiphilic block copolymers which spontaneously self-assemble into micellar structures when dissolved in certain solvents at concentrations exceeding their so-called “critical micelle concentration” [6]), **nanogel** (swollen nano-sized networks composed of hydrophilic or amphiphilic polymer chains [18]), **polymerosome** (self-assembled polymeric vesicles prepared from amphiphilic block-copolymers [19]), **polyplex** (nanosized complexes with DNA or RNA [20]), **dendrimer** (large polymeric structures with nanosized dimensions 1–10 nm [21]) or **nanoparticle** (solid colloid carriers).

2.1.4 The Potential Therapeutic Applications and Toxicity Concerns

The interest in using nanocarriers for biomedical targeting applications as the cellular delivery of DNA, interfering (RNAi)-based molecules, proteins, peptides, and drugs is transversal to various polymeric nanomaterials (natural and synthetic) and have been well documented in several “proof of concept studies” [22, 23] as illustrated in Table 2.1. These approaches can be classified in three main targeting categories: **primary**, defined as the accumulation of the delivery system in the tissue of interest; **secondary**, defined as the accumulation in the cell of interest; and **tertiary**, defined as targeting specific subcellular compartments, which remains the ultimate challenge of nanomedicine [24].

Among different applications, polymeric nanocarriers can be a valuable platform for anti-tumour drugs delivery because they not only can improve the drug pharmacokinetics but also further response to the permeation and retention effect to enhance the accumulation of drugs at the site of the tumour during cancer treatment [36].

Further, the potential for polymeric nanocarriers to enable target therapy can be exemplified by studies exploring the effect of antibiotics loaded into nanoparticles [25, 26, 37, 38]. The rationale is related to the fact that drugs display increased therapeutic activity, given that they reach a higher

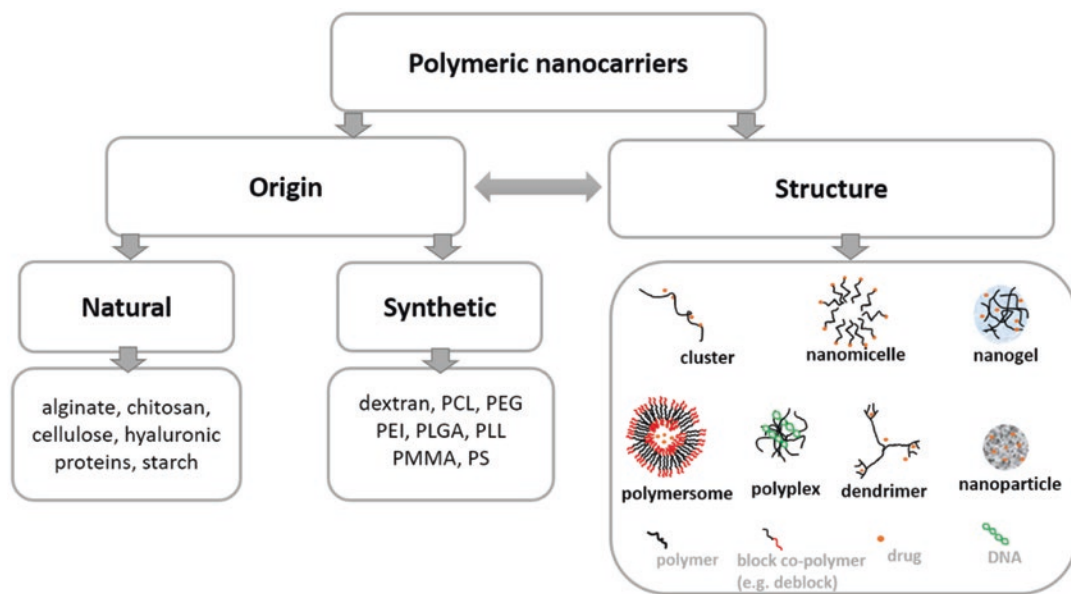


Fig. 2.1 Example of various types of polymeric nanocarriers classified according to their origin (natural and synthetic) and structure. *Note:* PCL poly- ϵ -caprolactone, PEG polyethylene glycol; PEI polyethylenimine, PLGA poly(lactic-co-glycolic acid), PLL poly-D-lysine, PMMA poly(methyl methacrylate), PS polystyrene

Table 2.1 Examples of “proof of concept studies” using polymers as nanocarriers for different targeting strategies (primary, secondary, and tertiary)

Targeting	Polymer	Compound	Application	References
<i>Primary targeting</i>				
Bone	Poly- ϵ -caprolactone	Daptomycin	Infection	[25]
Ocular surface	Chitosan	Ceftazidime	Infection	[26]
Pulmonary	Chitosan	Gene	Genetic disorders	[27]
Tumour tissue	Polyamidoamine dendritic	Folic acid, methotrexate, or tritium	Cancer	[28]
<i>Secondary targeting</i>				
Gingival fibroblast	Chitosan	Minocycline	Periodontal disease	[29]
Lung cancer cell	Hyaluronic acid	Docetaxel	Cancer	[30]
Neuronal cell	Polybutylcyanoacrylate	Protein	Neurodegenerative disease	[31]
Intestinal cells	Hyaluronic acid	Insulin	Diabetes	[32]
<i>Tertiary targeting</i>				
Mitochondria	Oligomeric hyaluronic acid-dithiodipropionic acid-berberine	Vitamin B6	Cancer	[33]
Mitochondria	Poly (lactic-co-glycolic acid)	Mdivi1	Myocardial ischemia	[34]
Nucleus	Polyphosphoester	TAT-Ce6/DOX	Cancer	[35]

Note: Ce6 chlorin e6, DOX doxorubicin, Mdivi1 mitochondrial division inhibitor 1, TAT pHe-sensitive transactivator of transcription

concentration at the target site (infected tissue), which facilitates its binding to bacteria, including resistant strains [39]. Also, several studies report increased efficacy of nano and microencapsulated antibiotics against bacterial biofilms, including against *Staphylococcus aureus* and *S. epidermidis*, often the cause of implant-associated infections [37, 38].

Moreover, the nanoparticles are able to reach intracellular bacteria reservoirs that can be of major therapeutic relevance in pathological situations difficult to treat due to the persistence of the microorganisms inside the cells as periodontal diseases or bone-associated-infections [29, 40].

Finally, the concept of subcellular targeting, holds great promising for targeting organelles, namely the mitochondria or the nucleus [41, 42]. One of the early examples of polymeric nanoparticles for mitochondria targeting was a PCL-PEG polymer loaded with an anti-oxidant (coenzyme Q10) [43]. Natural polymers, such as proteins and oligopeptides and synthetic, including poly-ethylenimine and polyamidoamine, are being explored for nano-gene therapy applications associated with the delivery of drugs (e.g. doxorubicin) [42].

Despite these promising and encouraging study reports, comprehensive understanding of nanostructure systems is highly limited, especially concerning their interactions with cells, and potential toxicity [23, 44].

In fact, regardless of the increasing knowledge on nanoparticulate systems properties and the decreasing side effects, nano-mediated toxicity still exists. The same physicochemical properties of the nanostructures, such as small size, large surface area, and flexible chemical compositions that facilitate their use in nanomedicine, have also been found to contribute to their enhanced toxicological side effects [42].

In view of improving the successful translation of the nanosystems to the clinics, there is a growing awareness that an understanding of the fundamental interactions of nanoscale objects with cells plays a central role [45, 46]. Also, it is perceivable that the physicochemical properties represent key parameters in those fundamental

interactions with consequences not only on targeting strategies but also in the nanotoxicological profile [41].

A large body of *in vitro* studies aiming to unravel these complex interplays has been published providing some clues. The present chapter offers an overview on those studies focusing in the relation between representative physicochemical properties as size, surface charge and shape with impact on nanosystems cellular uptake, intracellular trafficking, exocytosis and/or cytotoxicity as important aspects in the context of efficacy as well as safety evaluation. For simplicity, all types of nanostructures will be generally identified in the next sections as NanoParticulate systems (NPs).

2.2 The Interplay Between Physicochemical Properties and the Cellular Responses

Physicochemical properties represent a central role for nanoparticulate targeting strategies including for intracellular and sub-cellular organelles delivery [41]. In this sense, in the design of efficient therapeutic nanocarriers for targeted delivery, small changes in formulation can impact NPs physicochemical properties such as surface charge, shape or size. These changes will possibly have an effect on nano-bio interactions, with influence not only on the therapeutic effectiveness but also on NPs nanosafety profile [10, 47, 48].

For example, the inclusion of a poloxamer surfactant in the preparation of PLGA-NPs decreased their zeta potential, a measure of surface charge, in comparison to plain PLGA-NPs [49]. Surface charge has a high impact on cellular response, including uptake mechanism and cytotoxicity. Thus, its crucial to evaluate the effect of NPs formulation changing, in particularly, related to nanotoxicity effects. Also, managing NPs particle size can fulfil specific objectives as improving drug intracellular targeting [9], with concomitant possible toxicity cellular effects, namely ROS production and/or genotoxicity [50–52].

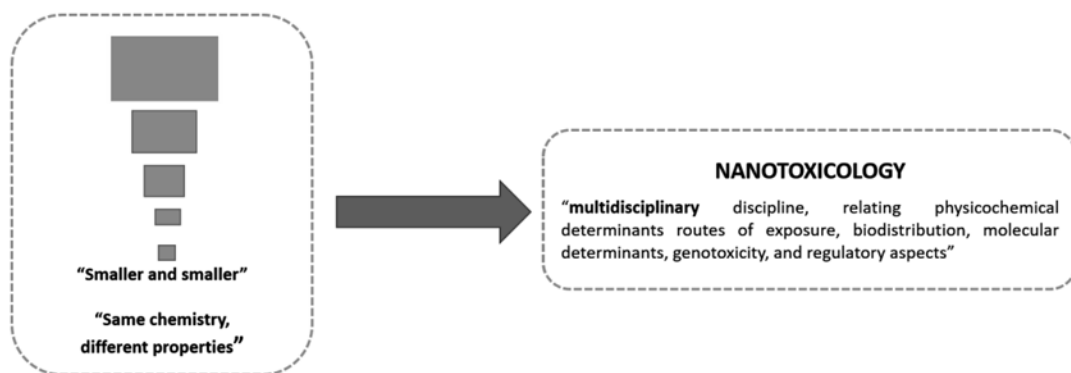


Fig. 2.2 The observation that “smaller” materials have different properties comparing to their macro forms lead to the emerging of a multidisciplinary discipline named “nanotoxicology”

Nanotoxicology: Some Concepts

The importance of polymeric nanocarriers for biomedical applications has grown along with questions and concern about their safety [53]. The simple observation “when bulk materials are made into smaller and smaller pieces of matter their surface chemistry and area changes and chemical reactivity increases” lead to the emerging of a new interdisciplinary subdiscipline of toxicology called “**nanotoxicology**” [54] (Fig. 2.2).

One of the simplest assumptions of nanotoxicology “basic physicochemical properties should be accounted for when interpreting the toxicological data” is a fundamental aspect in the context of NPs risk assessment [51, 52].

In fact, besides the common factors affecting NPs toxicity such as the chemical composition, dosage, administration forms, and exposure routes, contrary to non-nano forms, specific physicochemical properties as size, charge, shape, dispersity, surface chemistry, crystalline forms, and so on will directly influence the nano-bio interactions (Fig. 2.3). These **primary** physicochemical properties may be changed by NPs interaction with the complex biological media and a novel “**secondary**” entity should be considered [55, 56].

Nanotoxicology evaluation of polymeric based nanoproducts should be of concern at the very beginning of their development [57, 58]. The objective is establishing “Safe-by-Design (SbD)” selection rules and synthetic approaches

that can be used for the reduction of nanotechnology associated risks [59]. The implementation of the SbD concept for nanomedicines development is rather new in the context of nanotechnology, aiming the development of functional as well as safe nanomaterials, nanocarriers and nano-enabled products [50, 60].

As quoted by Kraegeloh et al. [60] “The novelty of SbD concept is not due to the fact that current nanomaterials or nanoproducts are regarded as intrinsically unsafe. Rather the application of this concept requires comprehensive knowledge questioning what property makes a nanomaterial or nanoproduct more or less safe”.

In this context, the characterization of polymeric nanocarriers should be sufficiently addressed for the translation of the nanoproducts into a SbD driven approach. However, data on the nanocarrier alone is frequently missing in scientific reports [57].

Presently, the vast majority of “first step/proof of concept studies” are focused on the optimization of the pharmaceutical drug/gene loaded NPs [7]. Studies related to the nanocarrier alone are less frequent becoming difficult to obtain systematic data related only to the carriers.

For example, Xiong et al. [61] pointed to the fact that “Although more than 1,000 articles, on PLGA nanoparticle as drug delivery systems have been published and indexed in the *Web of Science*, the number of papers with that reports on its cytotoxicity are fewer than 10”.

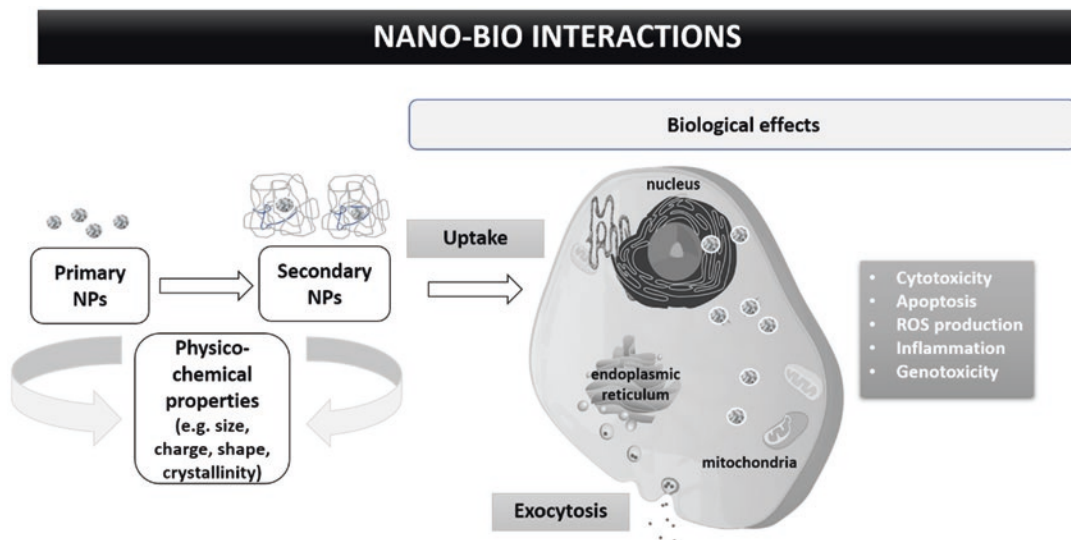


Fig. 2.3 Schematic overview of the interplay between primary and secondary NPs physicochemical properties and cellular uptake, intracellular trafficking, exocytosis and cytocompatibility responses

2.2.1 Physicochemical Properties and Cellular Uptake, Intracellular Trafficking, and Exocytosis

Among the most crucial studies that provide a first glance on the NPs-bio interactions are the *in vitro* **uptake** tests. Outcomes from these studies in the past decade have greatly influenced NPs design [62]. Identifying the mechanisms of interaction of the engineered NPs with cell membranes and the uptake mechanism is the key for understanding potential NPs cytotoxicity, as well as their therapeutic interest.

In some cases, the successful delivery of NPs cargo (drugs or genes) across the cell membrane and enhanced cell uptake is desirable, especially those that have their therapeutic target in the cytoplasm, (e.g. delivery of small interfering (si)-RNA [63], antibiotics against intracellular bacteria [29, 40, 64] or other subcellular compartments (mitochondria, nucleus) [33–35]. On the other hand, the cell membrane binding without uptake is essential for applications like diagnostic imaging and *in vivo* stem cell tracking [65]. Following internalization by different pathways, NPs normally enter early endosomes, which function as sorting compartments to further destinations of

recycling, degradation or **exocytosis** [9]. Also, once inside the cells, NPs may cause cytotoxic and or genotoxic effects that will determine their success or failure [65].

Thus, a detailed understanding of how physicochemical properties influences NPs get “in and out” of cells is important for developing new nanocarriers with improved selectivity and less cytotoxicity [9, 66]. Examples of studies showing how the physicochemical properties (size, surface charge and shape) can regulate the nano-bio interactions are presented in Table 2.2.

Cellular Uptake

In general, NPs can be internalized by cells via different pathways (active or passive) as reviewed in [75–78] and summarized in Table 2.3. Non energy-dependent pathways are only possible for very small NPs. Interestingly, many studies show that NPs experience cellular uptake through more than one internalization process [41].

To assess the cellular uptake, NPs loaded dyes (e.g. FTIC, coumarin-6) and qualitative/quantitative microscopic imaging techniques (e.g. CLSM) have often been used (Table 2.2). To perform those experiments, the selection of NPs dose is critical, because excessively high dose levels cannot show differential cellular

Table 2.2 Examples of *in vitro* cellular tests for the evaluation of NPs uptake, intracellular trafficking, and exocytosis

NPs	Aim	Physicochemical properties/Techniques	Type of cells	Cellular assays	Main conclusions	References
Amphiphilic block copolymers	Effect of shape/size on cellular uptake	Size (TEM): sphere (11 ± 2 nm); short cylindrical (180 ± 120 nm-length- and 20 ± 2 nm-cross-sectional diameter); long cylindrical (970 ± 900 nm-length- and 30 ± 2 nm-cross-sectional diameter) Tested media: NI Morphology (TEM): 1 spherical and 2 cylindrical	Chinese Hamster Ovary (CHO)	CLSM dye: AlexaFluor 594	The smaller, spherical NPs had a higher rate of cell entry into the cells than did the larger, cylindrical NPs The rate of cell exit was dependent on the NPs shape	[67]
Chitosan	Effect of Mw and DD on cellular uptake	Size (DLS): 163–387 nm; (+FTIC): 192–394 nm; PDI: 0.0.33–0.51; +(FTIC) 0.36–0.59 ZP (ELS): +34.6 to +14.3 mV; +(FTIC): +32.2 to +11.4 mV Tested media: NI Morphology (TEM): sphere	Adeno- carcinoma human alveolar basal epithelial (A549)	Fluorometry dye: FTIC	Size and ZP were dependent on Mw and DD FITC-conjugation did not change the ZP but modified the size DD had a greater influence on cellular uptake than Mw	[68]
Malto-dextrin	Endocytosis and exocytosis characterization	Size (DLS): 60 ± 13.1 nm; PDI: 0.22 ZP (ELS): $+25 \pm 1.5$ mV Tested media: 15 mM NaCl Morphology (TEM): Nanosphere Aggregation: Stable for 12 months	Human bronchial epithelial (16HBE14o)	CLSM dye: FTIC	Cationic NPs interact with anionic sites and were quickly endocytosed via the clathrin pathway NPs exocytosis was cholesterol dependent	[69]
PEG	Influence of shape (sphere, rod, cube, disk) on cellular uptake			Large scale dissipative particle dynamics (DPD) simulation	The spherical NPs exhibited the fastest internalization rate, followed by the cubic, then rod- and disk-like NPs	[10]
PS	Effect of surface charge on endocytosis pathways	Size (DLS): (+)113 nm; (-) 121 nm; PDI: (+)0.01; (-)0.017 ZP (ELS): (+) 59 and (-) 60 mV (pH = 7.2). Tested media: NI	HeLa (human)	Inhibitors (drugs) of endocytosis FC CLSM TEM dye: PMI	Macropinocytosis was an important mechanism for (+)NPs Clathrin-coated pits play a minor role in the uptake of (+) NPs , having no effect in endocytosis of (-)NPs	[65]
PLGA	Effect of shape on endocytosis	Size (SEM): spheres (1.8 mm diameter); elliptical Disks (aspect ratio of 5) Tested media: NI	Mouse brain endothelial (bEND.3) Human umbilical vein endothelial (HUVECs)	Fluorescent microscopy SEM dye: FTIC	Elliptical disks were endocytosed at a slower rate compared to spheres Both NPs accumulated near the nucleus	[70]

(continued)

Table 2.2 (continued)

NPs	Aim	Physicochemical properties/Techniques	Type of cells	Cellular assays	Main conclusions	References
PLGA	Characterize endocytosis and exocytosis	Size (TEM): 97 ± 3 nm ZP (ELS): -20 ± 1 mV; 0.5 mg/mL (in water)	Human arterial vascular smooth muscle (VSMCs)	CLSM HPLC dye: coumarin 6	Endocytosis and exocytosis Of NPs were dynamic and energy-dependent processes	[71]
PS and PLGA	Effect of shape (sphere, needles) on intra-cellular delivery	PS (size): 200 nm, 500 nm and 1 μ m; PLGA: NI Tested media: NI	Murine endothelial (C166-GFP)	FC CLSM dye: GFP	Needle-shaped NPs were shown to exhibit higher cytoplasmic delivery of drugs compared to their spherical counterparts	[64]
PS	Effect of size on cellular uptake	Size: 50, 100, 200, 500 and 1000 nm	Human colon adenocarcinoma (Caco 2)	CLSM cryo-SEM TEM dye: coumarin 6	Size affected NPs internalization: 100 nm were the ones uptake more efficiently	[72]
PS	Effect of surface charge on cellular uptake	Size and shape (TEM and SEM): 254-429 nm; sphere ZP (ELS): -41 to $+42$ mV (DW); -42 to -27 mV (RPMI); -47 to -32 mV (DMEM). Tested media: ZP in DW and 2 cell media No endotoxin contamination at 50 mg/mL	Phagocytic differentiated THP-1 Non-phagocytic (A549)	FC Fluorometry CLSM dye: fluorescein amino methyl	The number of internalized NPs showed a good positive correlation with the ZP in both cell lines	[73]
PS	Effect of shape (nanodisk, nanosphere) on cellular uptake	Size (DLS): Disk (225 nm in DW; 40 nm in FBS); sphere (150 nm in DW; 80 nm in FBS) Shape (TEM): Sphere/disk ZP (ELS): Disk (-13.6 mV in DW and -23.4 mV in FBS); sphere (-16.8 mV in DW and -24.3 mV in FBS) Tested media: DW and 10% FBS	Human embryonic kidney (Hek 293) BJ Jurkat (clone E6 - 1) HeLa (human)	FC Fluorometry CLSM Permeation experiments dye: fluorescein	Nanodisk , unlike nanosphere prefer to localize in phospholipids bilayers and have a very low tendency to penetrate cell membranes	[74]
PS (carboxylated)	Effect of size	Size (DLS and TEM): 40 and 150 nm	HeLa (human), MCF-7 (human breast cancer)	Inhibitors (drugs) of endocytosis FC CLSM dye: NI	NPs size influenced endocytosis and exocytosis Particle size is a key factor for the regulation of intracellular trafficking	[9]

Note: CLSM confocal laser scanning microscopy, DD degree of deacetylation, DLS dynamic light scattering, DW distilled water, ELS electrophoretic light scattering, FBS foetal bovine serum, FC Flow cytometry, FITC fluorescein isothiocyanate, GFP green fluorescent protein, HPLC High-performance Liquid Chromatography, Mw molecular weight, NI no information, PEG polyethylene glycol, PLGA poly(lactic-co-glycolic acid), PMI Perylene monoamide, PS polystyrene, Ref References, SEM surface electron microscopy, TEM transmission electron microscopy, ZP zeta potential

Table 2.3 Different examples of pathways for NPs cellular internalization

Pathway	Definition
Passive mechanism (energy non-dependent)	
Direct binding	Plasma penetration across cell membrane
Perforation	Transport using specialized membrane-transport protein channels
Active mechanism (energy-dependent): Endocytosis	
Phagocytosis	Restricted to specialized cells (e.g. macrophages, monocytes, dendritic cells); internalization of foreign materials with size larger than 0.5 μm
Pinocytosis	Subdivided into different categories involving: Extensions of the cell membrane: Macropinocytosis Vesicular transport related or not to different types of protein: Clathrin-mediated, caveolin-mediated, clathrin- and caveolin independent

uptake due to particle overload and/or cell death by the NPs. Likewise, dose levels that are too low might not provide measurable fluorescence intensities [73].

Cellular Uptake and Size

Size-dependent cellular uptake of NPs has been extensively investigated in various cell lines [77] (Table 2.2), being a complex correlation. Reports suggest that ~50 nm is the optimum size for NPs to achieve the highest and efficient cellular uptake [77, 78], but it is not a general rule. For example, in the case of polystyrene-NPs, the ones of 50 nm in size were less uptake by the cells than the larger ones (Table 2.2) [72]. In another study [67], it was shown that nanomicelles-NPs size alone was not the only factor influencing the cellular entry; the smaller spherical particles (on the 10 nm scale) were internalized by the cells faster than were the cylindrical particles with dimensions more close to 50 nm (i.e. 20 or 30 nm diameters and larger than 200 nm in one dimension). Thus, size alone is not the only factor affecting the cellular uptake.

Studies also show that the mechanism of NPs internalization can be controlled by their diameter, as observed by Wang et al. [9] using carboxylated-polystyrene-NPs (Table 2.2). The NPs with a smaller size (40 nm) were internalized mainly through clathrin-dependent pathway while NPs with a larger size (150 nm) preferred caveolae mediated endocytosis.

Cellular Uptake and Surface Charge

Another relevant physicochemical property to understand the interaction between NPs surface and cellular entities is the surface charge. It compromises the uptake mechanism, subcellular localizations and the ability to trigger toxic events [56]. The surface charge of NPs can affect their efficiency and the pathway of cellular uptake because biological systems consist of numerous biomolecules with various charges [77]. Generally, positively charged NPs are uptake more efficiently due to the interaction with the negatively charged cell membrane negative components [73, 79], as observed in a study focusing on maltose-dextrin NPs (Table 2.2), a cationic polysaccharide based nanocarrier [69].

Moreover, the surface charge will be directly associated with NPs surface chemistry that among others depends on the composition of the polymers used for NPs formulation and coating. For instance, Huang et al. [68] found that physicochemical and uptake properties of chitosan-NPs were dependent on its molecular weight (Mw) and degree of deacetylation. Interestingly, the uptake was more influenced by the degree of chitosan deacetylation, which affects surface charge than Mw which influenced NPs size. Thus, changes in NPs formulation that affect their charge may have a significant effect on the uptake. This fact was also demonstrated by Graça et al. [56] linked to the inclusion of a permeable polymer (EUDRAGIT®) into PMMA-NPs to increase drug's release rate. The change in the formulation had a pronounced effect on PMMA-NPs surface charge and consequently their cellular uptake.

Moreover, internalization pathway has also been linked to surface charge, with positively charged NPs tending towards internalization via

clathrin receptors, while negatively charged counterparts are prone for caveolae mediated uptake [73]. However, each NPs must be evaluated by itself. For example, in another study using positively charged fluorescein aminomethyl-polystyrene-NPs, the clathrin-dependent pathway played a minor role [65].

From a nanotechnological point of view, the effect of charge has been often explored to improve NPs efficacy. To give an example, the slight negative surface charge of PLGA-NPs tends to limit their interaction with the negatively charged plasmids and their intracellular uptake. Therefore, attempts have been made to modify the surface of PLGA-NPs using cationic polymers such as chitosan [80].

Cellular Uptake and Shape

Another essential parameter for the design of NPs is shape. Often, spherical NPs had been reported in the literature to exhibit the fastest internalization rate and being the most efficient therapeutic nanocarriers among differently shaped NPs [10, 67, 70, 74]. This has been explained by the different membrane bending energy required for entry of NPs of different shapes. Spherical NPs encounter minimal membrane bending energy during endocytosis, comparing with other differently shaped counterparts [10].

However, other studies have already demonstrated that non-spherical geometry of NPs can provide unique and improved abilities that are difficult to achieve with spherical particles [70]. For example, needle-shaped NPs are shown to exhibit substantially higher cytoplasmic delivery of siRNA in endothelial cells, which allows them to permeabilize the cell membrane compared to their spherical counterparts [64].

It is understandable that due to the complex interplay between size, shape and surface properties, most experimental studies lead to ambiguous/contradictory descriptions of the relevance of shape [10]. Therefore, methodologies based on computational studies as “large scale dissipative particle dynamics simulations” have proven to serve as an efficient and accurate approach to study the internalization density of NPs [10] (Table 2.2). Comparing systems of pegylated-

NPs with identical surface area, ligand–receptor interaction strength, and grafting density of the polyethylene glycol, the authors found that the spherical NPs exhibited the fastest internalization rate, followed by the cubic NPs, then rod- and disk-like NPs. They have concluded that the spherical NPs need to overcome a minimal membrane bending energy barrier, compared with the non-spherical counterparts, while the internalization of disk-like NPs involved a strong membrane deformation, responsible for a large free energy barrier. Authors have also concluded that star-shaped NPs can be quickly wrapped by the cell membrane, like their spherical counterparts, indicating star-shaped NPs can be used for drug delivery with high efficacy. Thus, such precisely defined conditions of computational studies will allow to unambiguously explore the shape effect of NPs during internalization in an attempt to provide guidance on the design and fabrication of NPs to achieve better therapeutic efficacy.

Intracellular Trafficking and Organelle Targeting

After cellular internalization, NPs can be engaged into a centripetal pathway from the membrane region to other intracellular locations, being shuttled from **early endosomes** to **late endosomes**, finally reaching **lysosomes** [81] as shown in Fig. 2.4, describing the intracellular trafficking of chitosan-NPs [29]. Further, in this specific study, the NPs after being internalized by macropinocytosis or clathrin-based endocytosis, were found to induce cell autophagic activity, suggested by the existence of **amphisomes**, resulting from the fusion of autophagosomes with endosomes. Amphisomes and endosomes were found to fuse with lysosomes contributing to the degradation of endocytic and sequestered cargo (Fig. 2.4).

Thus, for intracellular targeting, NPs effectiveness hinges upon their ability to escape from the endosomes or lysosomes [45, 64]. Several strategies, including NPs physicochemical properties changes by the use of cationic or hydrophobic moieties on the polymers, which destabilize the endosomes membranes by electrostatic interactions and facilitating endosomal escape are under evaluation [45].

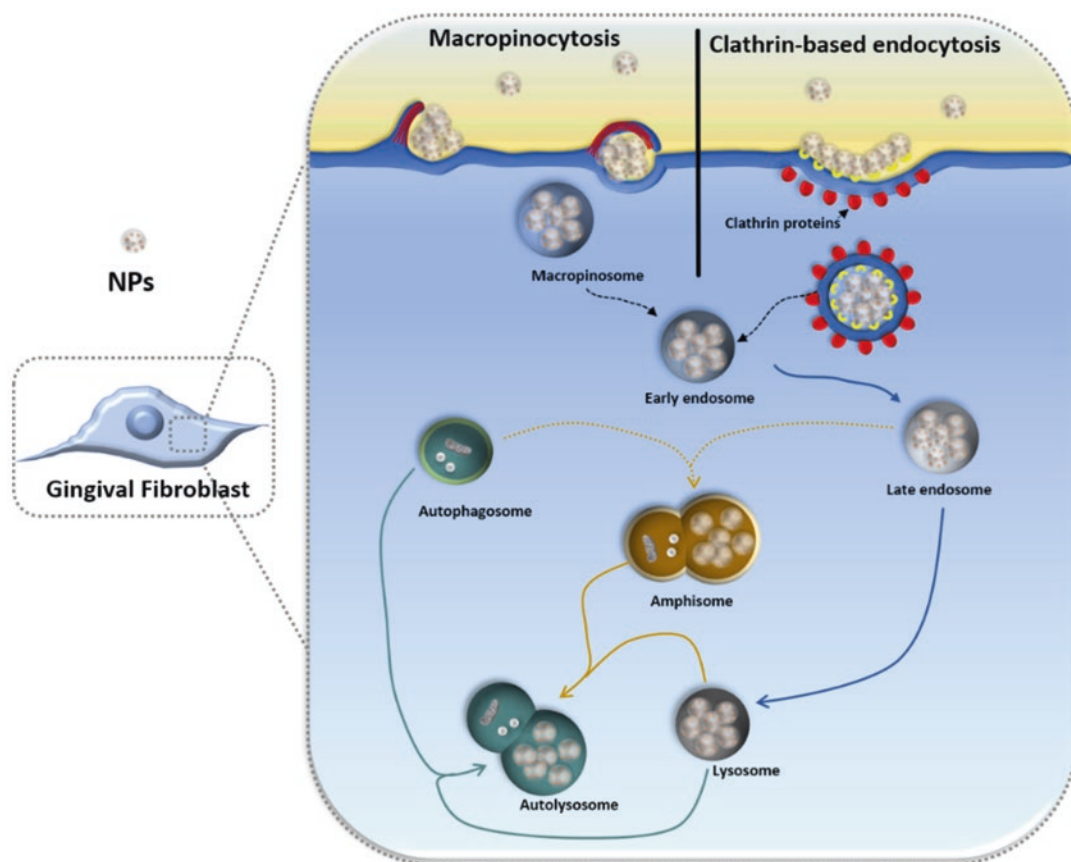


Fig. 2.4 Schematic representation of human gingival fibroblast uptake mechanisms (macropinocytosis and clathrin-based endocytosis) and intracellular trafficking of

chitosan-NPs. Adapted with permission from [29]. Copyright © 2019 Elsevier

Moreover, for each subcellular compartment, studies specifically reporting the effect of size and charge have been published. For example, in the case of mitochondrial targeting, size of nanocarriers should be as small as possible [82]. Cations are generally known to target the mitochondria, primarily because of its high membrane potential (negative inside) compared to the plasma membrane [41]. Marrache and Dhar found that an optimum size of less than 100 nm and a positive zeta potential of greater than $\sim +22$ mV is needed for efficient mitochondrial uptake [83].

With respect to nucleus, keeping in mind that only small molecules (< 39 nm) are able to pass through the nuclear pore channels (NPC) via passive diffusion, whereas larger ones must possess

a nuclear localization signal (NLS), a comprehensive evaluation of the size range of NPs that can translocate across the NPC channels is necessary for designing optimum nuclear targeted NPs [41]. Till present, it is still a rather complex problem. Tamana et al. [84] formulated chitosan-NPs of different sizes (S-NPs ≈ 25 nm; L-NP ≈ 150 nm) that were modified with different densities of the octapeptide NLS in order to compare their efficiency in nuclear delivery of protein cargo. Authors hypothesized that, even if the nuclear localization is generally reduced for L-NPs, the overall amount of delivered proteins might be higher than with S-NPs. Researchers found that S-NPs were capable of localizing in the nucleus without the help of an NLS; on the

contrary, modification with NLS reduces nuclear localization. L-NPs were also able of nuclear entry, however, with the help of NLS. Results indicated that a higher NLS density does not result in maximum protein nuclear localization and that a universal optimal density for NPs of different sizes does not exist [84].

Exocytosis

Finally, the duration of the NPs within the cells will depend on the way/rate they “leave the cell” that is “**exocytosis**”. In contrast to endocytosis, investigations regarding exocytosis of NPs are rather rare (Table 2.2). Relatively little effort has been made to investigate the exocytosis of NPs that may be responsible for their systemic elimination and toxicity [41]. In most studies, exocytosis was assumed to be negligible [71] or reports were focused on the description of the process itself. For example, Panyam and Labhasetwar [71] found that the exocytosis of PLGA-NPs coated with albumin was a dynamic and energy-dependent process (Table 2.2). Furthermore, authors demonstrated that the exocytosis pattern of the NPs was dependent on the proteins in the medium, that were uptake into the cells along with the NPs [71]. Also, the exocytosis of polysaccharide cationic NPs (approximate size of 60 nm) was found to be cholesterol dependent [69].

Few studies report the influence of specific properties as size or shape on the exocytosis process. For example, Wang et al. [9] demonstrated that in contrast to smaller polystyrene-NPs, which accumulated intracellularly after internalization, larger polystyrene-NPs were targeted to exosomes and transported towards the cell membrane. The observed selective extracellular exportation of larger NPs implied that cellular retention of drug nanocarriers might be regulated by particle size. Also, Zhang et al. [67] found that shape influenced NPs exocytosis.

These new findings on the exocytosis process not only shed light on the interaction between cells and NPs but will assist in the engineering of NPs with improved selectivity and safety [9].

2.2.2 Physicochemical Properties and Cytotoxicity

The expression “biocompatible polymer” has often been used in the nanotechnology and nanomaterial fields as synonym of “recognized as safe polymer”. However, the word “biocompatible” has a broader scope meaning not only safe but also suitable for the desired function [85]. Thus, to classify polymeric nanocarriers as biocompatible, if the intended final therapeutic target is a sub-cellular organelle, not only they should not exert deleterious side effects as also must deliver the cargo at the desired target.

Consequently, the term “biocompatible” can be misleading if the polymer is not evaluated in relation not only to its structural parameters, its dosage form, the route of administration, toxicity but also the intended use. Also, it is erroneous to generalize the term “biocompatible” for a certain type of polymer. For example, in the case of chitosan, a polymer repeatedly tested as a nanocarrier due to its “biocompatible profile”, studies show that molecular weight and the degree of deacetylation influence the cytotoxicity profile [44]. Moreover, there is evidence that certain chitosan samples are hemolytic and should not be classified as inert carriers [68, 86].

Additionally, compounds used in small amounts in NPs preparation (e.g. surfactants, organic solvents) may be present in the final formulation and impact toxicity. For example, accentuated toxicity profile presented by PLAA-NPs could be related to the use of a high concentration of a surfactant (Pluronic F68) during their production [86]. Residual organic solvents such as dichloromethane, frequently used in emulsion/evaporation methods to dissolve the polymers, should be conveniently eliminated preventing deleterious effects in the final formulations [87, 88].

Moreover, any change in the NPs formulation will affect the physicochemical properties of the nanocarrier with unknown consequences on their nanotoxicity profile.

A vast body of literature has been published trying to establish correlations between specific NPs physicochemical parameters and *in vitro* cellular responses as illustrated in Table 2.4.

Cytotoxicity and Size

In general, smaller NPs tend to have higher cytotoxicity, due to the high number of molecules available on the surface of the particles to interact with surrounding biomolecules such as proteins [61]. Even small changes in the physicochemical characteristics of similar NPs can originate different sizes and cytotoxicity profiles. However, size can have different effects depending on the evaluated cellular endpoint (Table 2.4). For example, this fact was observed with PLA-NPs [22]. Authors found that smaller NPs were able to induce higher cellular toxicity, mediated by ROS production. Interestingly other tested endpoints (inflammatory potential and immunotoxicity) were not influenced by the size of the NPs. Also, Xiong et al. [61] reported no apparent cytotoxicity for PLGA-NPs regardless of the size (60, 100, 200 nm) when using a metabolic assay. However, small NPs triggered increase in intracellular calcium influx which may be linked to ROS production. Further, this study highlighted the importance of the concentration range to draw conclusions on nanocarriers safety. It was observed, in respect to immunotoxicity, that the smaller NPs (60 and 100 nm) started to show statistical difference when compared with control from 10 to 100 $\mu\text{g/mL}$, respectively. The larger NPs (200 nm) did not trigger significant release of TNF- α up to 300 $\mu\text{g/mL}$.

Other factors that may influence the size-cytotoxicity effects are the cell lineage [89] and polymers molecular weight and branching degree [20] (Table 2.4).

Cytotoxicity and Surface Charge

The surface charge is another key parameter which decides NPs biological impact. Generally, a positive charge on NPs can promote increased cytotoxicity and genotoxicity compared to that of their neutral or negatively charged counterparts

(reviewed in Louro et al. [50]). This relation can be found in tests using different cell lines as reported by Platel et al. [88] with respect to PLGA-NPs with the same size but different surface charges. The positive ones were cytotoxic and genotoxic for the three tested cell lines. As plasma membrane and the intracellular environment is negatively charged, positively charged NPs may be rapidly endocytosed and thus exert their intracellular toxic effects. Also, a strong interaction of positively charged PHBHHx-NPs with negatively charged cellular membranes, due to the presence of negative phospholipids and/or proteins was suggested by Shao et al. [23], applying AFM to quantify the interactions between the cells and NPs. Moreover, as DNA is negatively charged, cationic NPs may be more likely to interact with the genetic material leading to chromosomal aberrations [88, 91].

The described works further emphasize the importance of controlling zeta potential, as a measure of surface charge, in developing polymeric-based NPs in the future.

Cytotoxicity and Shape

Only recently shape has been recognized as an important factor determining the behaviour of particles in a biological context [92]. Relevant work included the toxicity study of PLGA-PEG NPs (spherical- or needle-shaped) [90]. Experimental evidence showed that, only the needle-shaped NPs induced lysosomal membrane disruption, caused lysosome enlargement, and subsequently the activation of caspase-3 and DNA damage, both of which eventually led to cell apoptosis.

Till the moment, the question whether NPs size, charge, shape, chemistry, and other physicochemical properties as hydrophobicity [56] or a specific combination of all possible characteristic contributes to cytotoxicity or genotoxicity remains open [67]. Moreover, different aspects as those next described complicate the task for obtaining systematic data that effectively links physicochemical properties with specific cellular effects.

Table 2.4 Examples of *in vitro* cytocompatibility tests for evaluating the effect of physicochemical NPs properties

NPs	Aim	Physicochemical Properties/ Techniques	Type of Cells	Cytocompatibility endpoints	Main conclusions	References
CS	Effect of concentration (31.25-1000 µg/mL), time (24, 48, 72 h) and size	Size (DLS): 200 to 700 nm Aggregation: PDI < 0.5 ZP (ELS): +72-74 mV Morphology (TEM): spherical-shaped Tested media: NI	Mouse bone marrow-derived hemato-poietic stem Progenitor cells	Uptake (FTIC dye; fluorescent microscopy) Viability (MTT, live/dead) ROS (flow cytometry)	Viability effects were time/concentration and size dependent Cytotoxicity was observed for a high concentration of small NPs No effect on ROS production	[89]
PLA	Effect of size on cytotoxicity, hemo- and immune-toxicity	Size (DLS, TEM): 187.9 ± 36.9 nm and 109.1 ± 10.4 nm. In RPMI, similar size (≈ 100 nm). In DMEM, 75.3 ± 9.8 nm and 161.9 ± 8.2 nm. Aggregation: PDI < 0.5 ZP (ELS): -24.0 ± 4.7 mV and -6.6 ± 11.2 mV; neutral charge in DMEM and RPMI Morphology (TEM): Spherical-shaped Tested media: Pyrogen free water and cell culture media (RPMI and DMEM)	Peripheral blood mononuclear cells (PBMCs) Murine macrophage (RAW 264.7)	PBMCs: Immunotoxicity (MTT and PI); Hemotoxicity (haemolysis test) Raw 264.7: Viability (MTT) ROS (DCFH-DA, fluorometry); NO production (Griess reagent, colorimetry)	Small size: Higher dose-dependent ROS production Irrespective of size differences, none of the PLA NPs presented an inflammatory potential (NO production) or a haemolytic activity in human blood	[22]
PLGA	Effect of size on cytotoxicity	Size (TEM, SEM): 60, 100 and 200 nm (DLS): 101 to 207 nm (DW); 120 to 196 nm (CDMEM); 158 to 536 nm (BEGM) Zeta potential (ELS): -17.0 to -21.4 mV (DW); -2 to -13 mV (cell media) Morphology (TEM, SEM): Sphere Tested media: Water, CDMEM, BEGM	Human bronchial epithelial (BEAS-2B) Murine macrophage (RAW264.7)	Metabolic activity (MTS) Cytokine release (TNF-α, ELISA) Multiparametric assay Endotoxin (PYROGENT) NP-protein adsorption study (Pierce 660 nm protein assay)	Measuring technique influenced size Different-sized NPs, different results in the multiparametric assay Size and concentration-dependent inflammation response Protein adsorption was size-dependent	[61]

PLGA	Effect of surface charge on cytotoxicity and genotoxicity	Size (DLS): Similar size (\cong 80 nm) ZP (ELS): -25 mV for (-) NPs, -1 mV for (neutral) NPs and + 15 mV for (+) NPs Tested media: 15 mM NaCl (DLS); DW (ELS)	Mouse lymphoma (L5178Y) Human B-lymphoblast-oid (TK6) Human bronchial epithelial (16HBE14o)	Uptake (endocytosis) Cytotoxicity (MTT) ROS (DCFDA) Genotoxicity (micronucleus and comet assay)	(+) NPs: High endocytosis; cytotoxic (ROS induction); Chromosomal aberrations 16HBE14o- more suitable for the <i>in vitro</i> screening than the regulatory L5178Y and TK6	[88]
PLGA-PEG	Effect of shape (spherical and needle-shaped)	Size and morphology (TEM, SEM): Sphere (90 nm); disk (30 nm, aspect ratio ~ 18) ZP (ELS, PBS): ~ - 23 mV	Human liver cancer (HepG2)	Uptake (CLSM, dye: Neutral red) Viability (MTT, LDH) Apoptosis (caspase-3 activity)	Needle-shaped , but not the spherical-shaped were found to induce cytotoxicity The cytotoxicity of needle-shaped NPs was induced through lysosome disruption	[90]
PHBHHx	Effect of surface charge	Size (DLS): 220–245 nm ZP (ELS): -30 to +40 mV Morphology (SEM): sphere Colloidal stability (DLS and transmittance, at 0, 6, 24, 48, 72 h; 37 °C) Tested media: ZP (DW)	Mouse fibroblast (L929)	Viability (MTT); dead/alive (Calcein-AM and PI, fluorescent microscopy) Cell interaction (AFM)	(+) NPs were more toxic Than (-)NPs (+) NPs offered higher interaction force with cells	[23]
PEI/DNA complex	Effect of polyplex Size, Mw, and branching degree	Size (DLS): 80.94–548.56 nm (in HBG) and 602.7–2785 nm (in HBS) Tested media: HBS and HBG	Murine neuro-blastoma (Neuro2)	Viability (MTT) Apoptosis (PI and flow cytometry, G1 population)	Cytotoxicity increased with decreasing size Linear 250 KDa PEI was non-toxic whereas branched PEIs with lower MWs showed toxicity Concentration -dependent effects Polyplexes in HBG with higher Mw and branched had smaller sizes which result to higher cell toxicity and DNA damage	[20]

Note: AFM atomic force microscopy, *BEGM* bronchial epithelial growth medium, *Calcein-AM* calcein-acetyloxy/methoxy, *CLSM* confocal laser scanning microscopy, *CS* chitosan, *DCFDA-DA* dichloro-dihydro-fluorescein diacetate, *DLS* dynamic light scattering, *ELS* electrophoretic light scattering, *HBG* HEPES-buffered glucose, *HBS* HEPES-buffered; saline, *MTT* 3-(4,5-dimethylthiazol-2-yl)-2,5-diphenyltetrazolium bromide, *LDH* lactate dehydrogenase, *Mw* molecular weight, *NI* no information, *NR* neutral red, *NO* nitric oxide, *PDI* polydispersity index, *PEG* polyethylene glycol, *PEI* polyethylenimine, *PHBHHx* poly-3-hydroxybutyrate-co-3-hydroxyhexanoate, *PI* propidium iodide, *PLA* polylactic acid, *PLGA* poly(lactic-co-glycolic acid), *ROS* reactive oxygen species, *SEM* surface electron microscopy, *Ref.* References, *TEM* transmission electron microscopy, *ZP* zeta potential

2.2.3 *In Vitro* Cellular Effects Screening Remains a Difficult Task

In vitro cellular studies can provide useful information but clearly does not mimic the complex biological environment. Moreover, nano-objects require specific considerations with respect to the *in vitro* toxicity assays because their behaviour is distinct from water soluble chemicals [93]. Thus, many challenges, transversal to all types of nano-carriers, are faced including the choice of relevant tests and suitable cellular models [88].

A first key aspect refers to the plethora of cellular lines, exposure times, concentration range, tested endpoints, and protocols data that can be found in the literature, that prevent in most cases the comparison between different studies and may result in different conclusions (Tables 2.2 and 2.4). Having those aspects in mind it is becoming recognized that more than one cell line and endpoint should always be tested, in a suitable concentration range and for different exposure times, following standardized procedures preferentially included in harmonized guidelines [44].

Primary and Secondary Properties

In vitro cellular experiments need the dispersion of the NPs in a suitable cellular media enabling their effect on the cells. However, repeatedly only the NPs primary properties (usually assessed in water) are evaluated (Tables 2.2 and 2.4). That is, the interference of the cellular media components (e.g. ions composition, presence or concentration of serum, pH, etc.) is not assessed. This aspect is critical due to the possible influence of the cellular media on NPs primary properties. For example, different cellular media (RPMI and DMEM) affected distinctively the PLA nanocarriers size, justifying the higher toxicity against RAW 264.7 when the nanocarriers were suspended in DMEM [22]. Also, Graça et al. [56] showed that positive charged NPs (composed of PMMA-EUDRAGIT®) became neutral in cell culture media; this fact explained NPs unpredictable low cytotoxic and genotoxic effects. Further,

a slight shift in the pH of the culture medium to the acidic side increased the positive surface charge of PLGA/chitosan-NPs inducing membrane damage [94]. Thus, there is an undeniable impact of cell type medium, presence/absence of serum on NPs physicochemical properties that consequently influence their interaction with the cells [94]. Those effects must be always addressed enabling the correct evaluation of the results.

Agglomeration/Aggregation

Another important aspect to consider refers to stability aspects of colloidal NPs once dispersed in the cellular media. NPs due to their very high surface energy as a result of their extremely small particle size once inserted in a biological environment can adsorb biomolecules and proteins and as a consequence they tend to agglomerate/aggregate to reduce energy spread, resulting in thermodynamic instability, increased size and often change in their surface charge [23, 56] (Fig. 2.5). These phenomena have a high impact on the physicochemical properties and cellular effects of the NPs. Still, in most of the published studies these aspects are not taken in consideration [56, 94].

Experimental Technical Challenges

At present, the majority of the *in vitro* nanotoxicity assays are the same as those primarily used to investigate the generic cytotoxicity or genotoxicity of chemicals [93]. However, there are specific challenges associated with the characterization of nanostructured materials that must be considered and methodologies have to be carefully validated for each type of nanocarrier (reviewed in [95]). For example, in the case of the frequently used MTT test (Table 2.4), the adsorption of the dye to the NPs may interfere with the quantification of the mitochondrial activity, leading to erroneous conclusions on cell viability [93]. Also, it is not clear in the majority of studies if the dye itself changes NPs properties as size and charge or if it leaks during the experiments [96, 97].

Regarding microscopic imaging techniques, commonly used to evaluate cellular interactions as uptake and intracellular trafficking, most

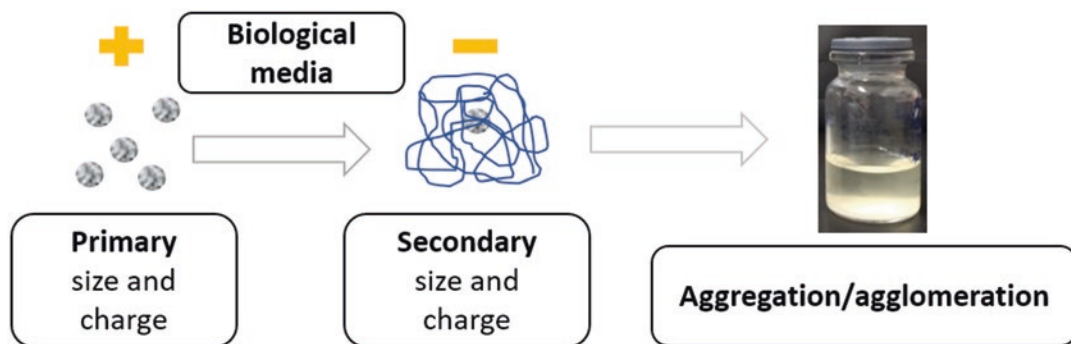


Fig. 2.5 Changes in size and surface charge of NPs in biological media may result in aggregation/agglomeration phenomena

studies do not distinguish between internalized and adsorbed NPs and often not consider the autofluorescence of cells. Specifically, for confocal microscopy it is relevant to conduct z-stacking; the orthogonal views can clearly demonstrate that the NPs are inside the cells instead of sitting on the cell membrane as illustrated in Fig. 2.6.

Another underestimated aspect is the detection of endotoxin contamination in the NPs, often an overlooked feature. However, the presence of endotoxin may significantly alter the results of *in vitro* tests. In particularly, when discussing cytokine stimulation or oxidative stress, endotoxin contamination should not be neglected [61].

Finally, the determination of the physicochemical properties themselves faces multiple difficulties (as reviewed in [98]), including the fact that NPs size and size distributions may differ depending on the used technique. For example, the primary size of PLGA-NPs (assessed by TEM and SEM) was different from the hydrodynamic size measured by DLS [61].

2.3 Concluding Remarks, Gaps and Future Trends

Based on the papers presented in the previous sections, describing the link between physicochemical properties of different polymeric NPs

and their cellular effects, it is possible to draw some general conclusions, gaps and future trends summarized in Table 2.5.

Overall, the polymeric nanocarriers present exciting opportunities in Nanomedicines. Although the raw materials are generally recognized as safe, the question regarding their toxicity in the nano-form remains open. Understanding how changes in formulations may impact physicochemical properties is essential in the first steps of NPs development in a context of “Safe-by-Design” approach.

Similarly, to other classes of biomaterial based-nanostructures, the nano-bio interactions of polymeric nanocarriers are one of the most critical issues that need to be addressed for nano-product development in the first stage of their development. Presently, the *in vitro* effects of physicochemical properties are tested in a “case by case approach” as they depend on a combination of different variables, including the type of cell, cellular endpoints, exposure time and concentration range [44, 77]. Unsolved hurdles, and specificities of these *in vitro* tests, common to all types of nanomaterials, still produce questionable data preventing the establishment of a robust data of the correlation between the physicochemical properties of polymeric nanocarriers and their biological effects [95]. An effort for establishing clear regulatory guideline(s) on the *in vitro* testing/evaluation of NPs should be considered, including the “blank” nanocarriers.

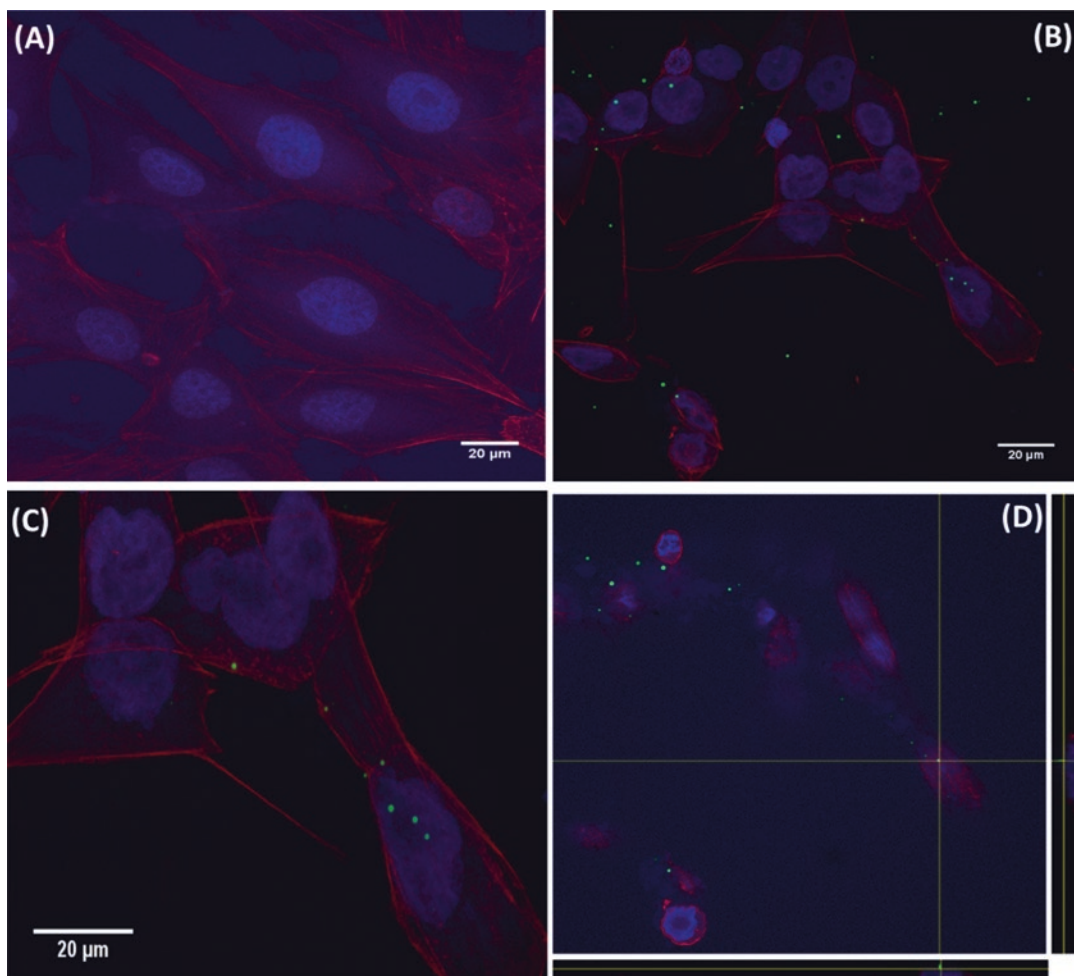


Fig. 2.6 Confocal microscopy analysis of polymeric NPs internalized by human osteoblast MG-63 cells. (a) Control cells which were not exposed to NPs; (b) Intracellular distribution of 6-coumarin loaded NPs after 24 h exposure to cells; (c) Enlarged region of (b); (d) Orthogonal views

from different planes (x/y , x/z or y/z) of the (c) image. Note – in red: actin cytoskeleton of cells, in blue: nucleus of cells, and in green: NPs. Scale bars = 20 μm. Reprinted with permission from [40]. Copyright © 2018 Elsevier

Despite the gaps and challenges to face, fundamental knowledge of how physical-chemical properties impact cellular interactions of engineered polymeric nanostructures is critical to their future success in healthcare and key criteria that should be considered in a nanotechnology, nanotoxicology and regulatory context.

Acknowledgements This work was supported by the Fundação para a Ciência e Tecnologia (Portugal) FCT/MCTES, through national funds (PIDDAC), PTDC/SAU-PUB/29481/2017 and co-funded by iMed. ULisboa (Pest-UID/DTP/04138/2019).

Table 2.5 Summary of the main conclusions, gaps to be addressed and future trends for the *in vitro* evaluation of the interactions between polymeric NPs and cells

Conclusions	Gaps	Future trends
<p>Polymeric NPs offer enormous opportunities in nanomedicine (diagnostic and therapeutic). The <i>in vitro</i> nano-bio interactions testing, including nanotoxicity evaluation, should be the starting point for the NPs development in a SbD context.</p> <p>Evaluation of the nanocarrier alone should always be performed.</p> <p>NPs p-c properties affects their biological fate.</p> <p>The impact of p-c properties is often multifactorial.</p> <p>A plethora of different methodologies (e.g. cell lines, endpoints, concentration range, exposure times, data reporting, statistics) are described.</p> <p>Closely related NPs reveal distinct properties. Primary properties of the NPs may differ substantially from those in the biological environment.</p> <p>Protein adsorption and agglomeration/aggregation are key parameters affecting NPs properties.</p> <p>“Case by case analysis” should be considered.</p>	<p>Data related to polymeric NPs drug delivery, intracellular targeting and nanotoxicity is scarce and poorly harmonized.</p> <p>The question whether NPs size, shape, chemistry, charge, or a specific combination of all possible characteristics contributes to nano-bio interactions remains open.</p> <p>Lacking: Complete characterization of NPs p-c properties under the <i>in vitro</i> experimental conditions.</p> <p>It remains challenging to reliably correlate a cellular response with a specific p-c property.</p> <p>Aggregation and agglomeration effects as well as the role of protein corona needs further clarification.</p> <p>Validation of proper techniques for the NPs evaluation is missing.</p> <p>Accurate knowledge of the NPs interactions is limited delaying their application in clinics.</p> <p>No systematic safety evaluation has been established.</p> <p>Still, there is not enough interdisciplinarity.</p>	<p>Increased efficacy of NPs for targeting intracellular organelles.</p> <p>Collect data will contribute to organize a bank to elucidate about the nanotoxicity of polymeric NPs.</p> <p>Computational studies will help to build a body of evidence assisting regulatory agencies.</p> <p>Standardization of methodologies fitting NPs specificities.</p> <p>Understanding the principles governing the formation of the protein corona (e.g. connection between NPs p-c properties and corona composition) will set new directions for bio nanoscience.</p> <p>Build data on multiparametric evaluation.</p> <p>Harmonized guidelines for reporting the results from a combination of different methods and cell lines will facilitate meta-analysis of NPs related studies, across different types of polymeric nanocarriers.</p> <p>Merge of nanotoxicology with nanotechnology to increase the interdisciplinarity and assist the regulatory agencies.</p>

Note: p-c physicochemical, SbD safe-by-design

References

- H2020-EU.2.1.2. – Industrial leadership – leadership in enabling and industrial technologies – Nanotechnologies [Internet]. 2020 [Cited 2020 Jul 21]. Available from: <https://cordis.europa.eu/programme/id/H2020-EU.2.1.2>
- European Science Foundation (2005) ESF Forward look on nanomedicine 2005 [Internet]. Cited 2020 Jul 21. Available from: http://archives.esf.org/fileadmin/Public_documents/Publications/Nanomedicine_01.pdf
- Santos-Ferreira I, Bettencourt A, Almeida AJ (2015) Nanoparticulate platforms for targeting bone infections: meeting a major therapeutic challenge. *Nanomedicine* 10(20):3131–3145
- Grossen P, Witzigmann D, Sieber S, Huwylar J (2017) PEG-PCL-based nanomedicines: a biodegradable drug delivery system and its application. *J Control Release* 260(April):46–60
- Altay Y, Cao S, Che H, Abdelmohsen LKEA, Van Hest JCM (2019) Adaptive polymeric assemblies for applications in biomimicry and nanomedicine. *Biomacromolecules* 20(11):4053–4064
- Prasad M, Lambe UP, Brar B, Shah IJM, Ranjan K et al (2018) Nanotherapeutics: an insight into healthcare and multi-dimensional applications in medical sector of the modern world. *Biomed Pharmacother* 97(October 2017):1521–1537
- Jain AK, Thareja S (2019) In vitro and in vivo characterization of pharmaceutical nanocarriers used for drug delivery. *Artif Cells Nanomed Biotechnol* 47(1):524–539
- Sarmento B (2019) Have nanomedicines progressed as much as we'd hoped for in drug discovery and development? *Expert Opin Drug Discov* 14(8):723–725
- Wang T, Wang L, Li X, Hu X, Han Y, Luo Y et al (2017) Size-dependent regulation of intracellular trafficking of polystyrene nanoparticle-based drug-delivery systems. *ACS Appl Mater Interfaces* 9(22):18619–18625
- Li Y, Kröger M, Liu WK (2015) Shape effect in cellular uptake of PEGylated nanoparticles: comparison between sphere, rod, cube and disk. *Nanoscale* 7(40):16631–16646
- Wang E, Wang A (2014) Nanoparticles and their applications in cell and molecular biology. *Integr Biol* 6(1):9–26
- Hasanzadeh Kafshgari M, Goldmann W (2020) Insights into theranostic properties of titanium dioxide for nanomedicine, *Nano-Micro Letters*, vol 12. Springer, Singapore
- Yang L, Sheldon BW, Webster TJ (2010) Nanophase ceramics for improved drug delivery: current opportunities and challenges. *Am Ceram Soc Bull* 89(2):24–32
- Puri A, Loomis K, Smith B, Lee JH, Yavlovich A, Heldman E et al (2009) Lipid-based nanoparticles as pharmaceutical drug carriers: from concepts to clinic. *Crit Rev Ther Drug Carrier Syst* 26(6):523–580
- Singh R, Lillard JW (2009) Nanoparticle-based targeted drug delivery. *Exp Mol Pathol* 86(3):215–223
- Duncan R (2017) Polymer therapeutics at a crossroads? Finding the path for improved translation in the twenty-first century. *J Drug Target* 25(9–10):759–780
- Li Y, Wang S, Ju D (2020) Toxicity of polymeric nanomaterials. In: *Nanotoxicity*, pp 167–191
- Kabanov A, Vinogradov S (2010) Nanogels as pharmaceutical carriers: finite networks of infinite capabilities. *Angew Chem Int Ed Engl* 48(30):5418–5429
- Rideau E, Dimova R, Schwille P, Wurm FR, Landfester K (2018) Liposomes and polymersomes: a comparative review towards cell mimicking. *Chem Soc Rev* 47(23):8572–8610
- Kazemi Oskuee R, Dabbaghi M, Gholami L, Taheri-Bojd S, Balali-Mood M, Mousavi SH et al (2018) Investigating the influence of polyplex size on toxicity properties of polyethylenimine mediated gene delivery. *Life Sci* 197(December 2017):101–108
- Kalomiraki M, Thermos K, Chaniotakis NA (2015) Dendrimers as tunable vectors of drug delivery systems and biomedical and ocular applications. *Int J Nanomedicine* 11:1–12
- da Silva J, Jesus S, Bernardi N, Colaço M, Borges O (2019) Poly(D, L-lactic Acid) nanoparticle size reduction increases its immunotoxicity. *Front Bioeng Biotechnol* 7(June):1–10
- Shao XR, Wei XQ, Song X, Hao LY, Cai XX, Zhang ZR et al (2015) Independent effect of polymeric nanoparticle zeta potential/surface charge, on their cytotoxicity and affinity to cells. *Cell Prolif* 48(4):465–474
- Parodi A, Corbo C, Cevenini A, Molinaro R, Palomba R, Pandolfi L et al (2015) Enabling cytoplasmic delivery and organelle targeting by surface modification of nanocarriers. *Nanomedicine* 10(12):1923–1940
- Santos Ferreira I, Bettencourt A, Kasper S, Bétrisey B, Kikhney J, Moter A et al (2015) Activity of daptomycin- and vancomycin-loaded poly-epsilon-caprolactone microparticles against mature staphylococcal biofilms. *Int J Nanomedicine* 10:4351–4366
- Silva MM, Calado R, Marto J, Bettencourt A, Almeida AJ, Gonçalves LMD (2017) Chitosan nanoparticles as a mucoadhesive drug delivery system for ocular administration. *Mar Drugs* 15(12):1–16
- Gaspar DP, Vital J, Leiva MC, Gonçalves LMD, Taboada P, Remuñán-López C et al (2019) Transfection of pulmonary cells by stable pDNA-polycationic hybrid nanostructured particles. *Nanomedicine* 14(4):407–429
- Kukowska-Latallo JF, Candido KA, Cao Z, Nigavekar SS, Majoros IJ, Thomas TP et al (2005) Nanoparticle targeting of anticancer drug improves therapeutic response in animal model of human epithelial cancer. *Cancer Res* 65(12):5317–5324
- Martin V, Ribeiro IAC, Alves MM, Gonçalves L, Almeida AJ, Grenho L et al (2019) Understanding intracellular trafficking and anti-inflammatory effects of minocycline chitosan-nanoparticles in human gin-

- gival fibroblasts for periodontal disease treatment. *Int J Pharm* 572(October)
30. Cadete A, Olivera A, Besev M, Dhal PK, Gonçalves L, Almeida AJ et al (2019) Self-assembled hyaluronan nanocapsules for the intracellular delivery of anti-cancer drugs. *Sci Rep* 9(1):1–11
 31. Hasadsri L, Kreuter J, Hattori H, Iwasaki T, George JM (2009) Functional protein delivery into neurons using polymeric nanoparticles. *J Biol Chem* 284(11):6972–6981
 32. Han L, Zhao Y, Yin L, Li R, Liang Y, Huang H et al (2012) Insulin-loaded pH-sensitive hyaluronic acid nanoparticles enhance transcellular delivery. *AAPS PharmSciTech* 13(3):836–845
 33. Fang L, Fan H, Guo C, Cui L, Zhang P, Mu H et al (2019) Novel mitochondrial targeting multifunctional surface charge-reversal polymeric nanoparticles for cancer treatment. *J Biomed Nanotechnol* 15(11):2151–2163
 34. Ishikita A, Matoba T, Ikeda G, Koga JI, Mao Y, Nakano K et al (2016) Nanoparticle-mediated delivery of mitochondrial division inhibitor 1 to the myocardium protects the heart from ischemia-reperfusion injury through inhibition of mitochondria outer membrane permeabilization: a new therapeutic modality for acute myocardial. *J Am Heart Assoc* 5(7):1–17
 35. Cao Z, Li D, Wang J, Xiong M, Yang X (2019) Direct nucleus-targeted drug delivery using Cascade pH/photo dual-sensitive polymeric Nanocarrier for cancer therapy. *Small* 15(36):1–13
 36. Li B, Li Q, Mo J, Dai H (2017) Drug-loaded polymeric nanoparticles for cancer stem cell targeting. *Front Pharmacol*, February 8:1–12
 37. Ferreira IS, Bettencourt A, Bétrisey B, Gonçalves LMD, Trampuz A, Almeida AJ (2015) Improvement of the antibacterial activity of daptomycin-loaded polymeric microparticles by Eudragit RL 100: an assessment by isothermal microcalorimetry. *Int J Pharm* 485(1–2):171–182
 38. Santos Ferreira I, Kikhney J, Kursawe L, Kasper S, Gonçalves LMD, Trampuz A et al (2018) Encapsulation in polymeric microparticles improves Daptomycin activity against mature staphylococci biofilms—a thermal and imaging study. *AAPS PharmSciTech* 19(4):1625–1636
 39. Simões NG, Bettencourt AF, Monge N, Ribeiro IAC (2016) Novel antibacterial agents: an emergent need to win the battle against infections. *Mini Rev Med Chem* 17(14)
 40. Woischnig AK, Gonçalves LM, Ferreira M, Kuehl R, Kikhney J, Moter A et al (2018) Acrylic microparticles increase daptomycin intracellular and in vivo anti-biofilm activity against *Staphylococcus aureus*. *Int J Pharm* 550(1–2):372–379
 41. Yameen B, Choi WIL, Vilos C, Swami A, Shi J, Farokhzad OC (2014) Insight into nanoparticle cellular uptake and intracellular targeting. *J Control Release* 190:485–499
 42. Xiao Y, Shi K, Qu Y, Chu B, Qian Z (2019) Engineering nanoparticles for targeted delivery of nucleic acid therapeutics in tumor. *Mol Ther Methods Clin Dev* 12(March):1–18
 43. Sharma A, Soliman GM, Al-Hajaj N, Sharma R, Maysinger D, Kakkur A (2012) Design and evaluation of multifunctional nanocarriers for selective delivery of coenzyme Q10 to mitochondria. *Biomacromolecules* 13:239–252
 44. Jesus S, Schmutz M, Som C, Borchard G, Wick P, Borges O (2019) Hazard assessment of polymeric nanobiomaterials for drug delivery: what can we learn from literature so far. *Front Bioeng Biotechnol* 7(October)
 45. Zha Z, Li J, Ge Z (2015) Endosomal-escape polymers based on multicomponent reaction-synthesized monomers integrating alkyl and Imidazolyl moieties for efficient gene delivery. *ACS Macro Lett* 4(10):1123–1127
 46. Lundqvist M, Stigler J, Elia G, Lynch I, Cedervall T, Dawson KA (2008) Nanoparticle size and surface properties determine the protein corona with possible implications for biological impacts. *Proc Natl Acad Sci USA* 105(38):14265–14270
 47. Shin SW, Song IH, Um SH (2015) Role of physicochemical properties in nanoparticle toxicity. *Nano* 5(3):1351–1365
 48. Patra JK, Das G, Fraceto LF, Campos EVR, Rodriguez-Torres MDP, Acosta-Torres LS et al (2018) Nano based drug delivery systems: recent developments and future prospects 10 technology 1007 nanotechnology 03 chemical sciences 0306 physical chemistry (incl. Structural) 03 chemical sciences 0303 macromolecular and materials chemistry 11 medical and he. *J Nanobiotechnol* 16(1):1–33
 49. Santander-Ortega MJ, Jódar-Reyes AB, Csaba N, Bastos-González D, Ortega-Vinuesa JL (2006) Colloidal stability of Pluronic F68-coated PLGA nanoparticles: a variety of stabilisation mechanisms. *J Colloid Interface Sci* 302(2):522–529
 50. Louro H, Bettencourt A, Gonçalves LM, Almeida AJ, João SM (2015) Role of Nanogenotoxicology studies in safety evaluation of nanomaterials. *Nanotechnol Appl Tissue Eng*:263–287
 51. Oomen AG, Steinhäuser KG, Bleeker EAJ, van Broekhuizen F, Sips A, Dekkers S et al (2018) Risk assessment frameworks for nanomaterials: scope, link to regulations, applicability, and outline for future directions in view of needed increase in efficiency. *NanoImpact* 9(September 2017):1–13
 52. Prasad M, Lambe UP, Brar B, Shah IJM, Ranjan K et al (2018) Nanotherapeutics: an insight into healthcare and multi-dimensional applications in medical sector of the modern world. *Biomed Pharmacother* 97(November 2017):1521–1537
 53. Arora S, Rajwade JM, Paknikar KM (2012) Nanotoxicology and in vitro studies: the need of the hour. *Toxicol Appl Pharmacol* 258(2):151–165
 54. Fischer HC, Chan WC (2007) Nanotoxicity: the growing need for in vivo study. *Curr Opin Biotechnol* 18(6):565–571

55. Elsaesser A, Howard CV (2012) Toxicology of nanoparticles. *Adv Drug Deliv Rev* 64(2):129–137
56. Graça D, Louro H, Santos J, Dias K, Almeida AJ, Gonçalves L et al (2017) Toxicity screening of a novel poly(methylmethacrylate)-Eudragit nanocarrier on L929 fibroblasts. *Toxicol Lett* 276(November 2016):129–137
57. Marques C, Som C, Schmutz M, Borges O, Borchard G (2020) How the lack of Chitosan characterization precludes implementation of the safe-by-design concept. *Front Bioeng Biotechnol* 8(March)
58. Schmutz M, Borges O, Jesus S, Borchard G, Perale G, Zinn M et al (2020) A methodological safe-by-design approach for the development of nanomedicines. *Front Bioeng Biotechnol* 8(April):1–7
59. Cobaleda-Siles M, Guillamon AP, Delpivo C, Vázquez-Campos S, Puentes VF (2017) Safer by design strategies. *J Phys Conf Ser* 838(1)
60. Kraegeloh A, Suarez-Merino B, Sluijters T, Micheletti C (2018) Implementation of safe-by-design for nanomaterial development and safe innovation: why we need a comprehensive approach. *Nanomaterials* 8(4)
61. Xiong S, Yu H, Damoiseaux R, France B, Woei K, Chye Loo JS (2013) Size influences the cytotoxicity of poly (lactic-co-glycolic acid) (PLGA) and titanium dioxide (TiO₂) nanoparticles. *Arch Toxicol* 87(6):1075–1086
62. Albanese A, Tang PS, Chan WCW (2012) The effect of nanoparticle size, shape, and surface chemistry on biological systems. *Annu Rev Biomed Eng* 14(1):1–16
63. Tiemann K, Rossi JJ (2009) RNAi-based therapeutics-current status, challenges and prospects. *EMBO Mol Med* 1(3):142–151
64. Kolhar P, Doshi N, Mitragotri S (2011) Polymer nanoneedle-mediated intracellular drug delivery. *Small* 7(14):2094–2100
65. Dausend J, Musyanovych A, Dass M, Walther P, Schrezenmeier H, Landfester K et al (2008) Uptake mechanism of oppositely charged fluorescent nanoparticles in HeLa cells. *Macromol Biosci* 8(12):1135–1143
66. Zhao B, Wang XQ, Wang XY, Zhang H, Dai WB, Wang J et al (2013) Nanotoxicity comparison of four amphiphilic polymeric micelles with similar hydrophilic or hydrophobic structure. *Part Fibre Toxicol* 10(1):1–16
67. Zhang K, Fang H, Chen Z, Taylor JSA, Wooley KL (2008) Shape effects of nanoparticles conjugated with cell-penetrating peptides (HIV Tat PTD) on CHO cell uptake. *Bioconjug Chem* 19(9):1880–1887
68. Huang M, Khor E, Lim LY (2004) Uptake and cytotoxicity of chitosan molecules and nanoparticles: effects of molecular weight and degree of deacetylation. *Pharm Res* 21(2):344–353
69. Dombu CY, Kroubi M, Zibouche R, Matran R, Betbeder D (2010) Characterization of endocytosis and exocytosis of cationic nanoparticles in airway epithelium cells. *Nanotechnology* 21(35)
70. Yoo JW, Doshi N, Mitragotri S (2010) Endocytosis and intracellular distribution of PLGA particles in endothelial cells: effect of particle geometry. *Macromol Rapid Commun* 31(2):142–148
71. Panyam J, Labhsetwar V (2003) Dynamics of endocytosis and exocytosis of poly(D,L-lactide-co-glycolide) nanoparticles in vascular smooth muscle cells. *Pharm Res* 20(2):212–220
72. Yin Win K, Feng SS (2005) Effects of particle size and surface coating on cellular uptake of polymeric nanoparticles for oral delivery of anticancer drugs. *Biomaterials* 26(15):2713–2722
73. Jeon S, Clavadetscher J, Lee DK, Chankeshwara SV, Bradley M, Cho WS (2018) Surface charge-dependent cellular uptake of polystyrene nanoparticles. *Nano* 8(12):1–11
74. Zhang Y, Tekobo S, Tu Y, Zhou Q, Jin X, Dergunov SA et al (2012) Permission to enter cell by shape: Nanodisk vs Nanosphere. *ACS Appl Mater Interfaces* 4(8):4099–4105
75. Salatin S, Yari KA (2017) Overviews on the cellular uptake mechanism of polysaccharide colloidal nanoparticles. *J Cell Mol Med* 21(9):1668–1686
76. Foroozandeh P, Aziz AA (2018) Insight into cellular uptake and intracellular trafficking of nanoparticles. *Nanoscale Res Lett* 13
77. Oh N, Park JH (2014) Endocytosis and exocytosis of nanoparticles in mammalian cells. *Int J Nanomedicine* 9(Suppl 1):51–63
78. Behzadia S, Serpooshanb V, Taa W, Hamalyc M, Alkawareekd M, Dreadene E et al (2017) Cellular uptake of nanoparticles: journey inside the cell. *Chem Soc Rev* 46(14):4218–4244
79. Fröhlich E (2012) The role of surface charge in cellular uptake and cytotoxicity of medical nanoparticles. *Int J Nanomedicine* 7:5577–5591
80. El Hady WEA, Mohamed EA, El-Aazeem Soliman OA, El-Sabbagh HM (2019) In vitro-in vivo evaluation of chitosan-PLGA nanoparticles for potentiated gastric retention and anti-ulcer activity of diosmin. *Int J Nanomedicine* 14:7191–7213
81. Duncan R, Richardson SCW (2012) Endocytosis and intracellular trafficking as gateways for nanomedicine delivery: opportunities and challenges. *Mol Pharm* 9(9):2380–2402
82. Battogtokh G, Cho YY, Lee JY, Lee HS, Kang HC (2018) Mitochondrial-targeting anticancer agent conjugates and nanocarrier systems for cancer treatment. *Front Pharmacol* 9(August):1–20
83. Marrache S, Dhar S (2012) Engineering of blended nanoparticle platform for delivery of mitochondria-acting therapeutics. *Proc Natl Acad Sci USA* 109(40):16288–16293
84. Tammam SN, Azzazy HME, Breitingner HG, Lamprecht A (2015) Chitosan nanoparticles for nuclear targeting: the effect of nanoparticle size and nuclear localization sequence density. *Mol Pharm* 12(12):4277–4289
85. Williams DF (2008) On the mechanisms of biocompatibility. *Biomaterials* 29(20):2941–2953

86. Lee KY, Ha WS, Park WH (1995) Blood compatibility and biodegradability of partially IV-acylated chitosan derivatives. *Biomaterials* 16(16):1211–1216
87. Bettencourt A, Florindo HF, Ferreira IFS, Matos A, Monteiro J, Neves C et al (2010) Incorporation of tocopherol acetate-containing particles in acrylic bone cement. *J Microencapsul* 27(6):533–541
88. Platel A, Carpentier R, Becart E, Mordacq G, Betbeder D, Nesslany F (2016) Influence of the surface charge of PLGA nanoparticles on their *in vitro* genotoxicity, cytotoxicity, ROS production and endocytosis. *J Appl Toxicol* 36(3):434–444
89. Omar Zaki SS, Katas H, Hamid ZA (2015) Lineage-related and particle size-dependent cytotoxicity of chitosan nanoparticles on mouse bone marrow-derived hematopoietic stem and progenitor cells. *Food Chem Toxicol* 85:31–44
90. Zhang B, Sai Lung P, Zhao S, Chu Z, Chrzanowski W, Li Q (2017) Shape dependent cytotoxicity of PLGA-PEG nanoparticles on human cells. *Sci Rep* 7(1):1–8
91. Singh N, Manshian B, Jenkins GJS, Griffiths SM, Williams PM, Maffei TGG et al (2009) NanoGenotoxicology: the DNA damaging potential of engineered nanomaterials. *Biomaterials* 30(23–24):3891–3914
92. Ridolfo R, Williams DS, Van Hest JCM (2020) Influence of surface charge on the formulation of elongated PEG-: B -PDLLA nanoparticles. *Polym Chem* 11(16):2775–2780
93. Kroll A, Pillukat MH, Hahn D, Schnekenburger J (2012) Interference of engineered nanoparticles with *in vitro* toxicity assays. *Arch Toxicol* 86(7):1123–1136
94. Nafee N, Schneider M, Schaefer UF, Lehr CM (2009) Relevance of the colloidal stability of chitosan/PLGA nanoparticles on their cytotoxicity profile. *Int J Pharm* 381(2):130–139
95. Kroll A, Pillukat MH, Hahn D, Schnekenburger J (2009) Current *in vitro* methods in nanoparticle risk assessment: limitations and challenges. *Eur J Pharm Biopharm* 72(2):370–377
96. Mura S, Hillaireau H, Nicolas J, Le Droumaguet B, Gueutin C, Zanna S et al (2011) Influence of surface charge on the potential toxicity of PLGA nanoparticles towards Calu-3 cells. *Int J Nanomedicine* 6:2591–2605
97. Snipstad S, Hak S, Baghirov H, Sulheim E, Mørch Y, Lélou S et al (2017) Labeling nanoparticles: dye leakage and altered cellular uptake. *Cytom Part A* 91(8):760–766
98. Modena MM, Rühle B, Burg TP, Wuttke S (2019) Nanoparticle characterization: what to measure? *Adv Mater* 31(32):1–26



LipNanoCar Technology – A Versatile and Scalable Technology for the Production of Lipid Nanoparticles

Vera L. R. Esgueira, Clara P. A. Lopes,
Ana Catarina A. dos Santos, Fátima Pinto,
Sílvia A. Sousa, Dragana P. C. de Barros,
Jorge H. Leitão, and Luis P. Fonseca

Abstract

The extensive knowledge in the miniemulsion technique used in biocatalysis applications by the authors allowed the development of drug delivery systems that constitutes the LipNanoCar technology core for the production of lipid nanoemulsions and solid lipid nanoparticles. The LipNanoCar technology, together with adequate formulations of different oils, fatty acids, surfactants, and temperature, allows the entrapment of several bioactive and therapeutic compounds in lipid nanoparticles for cosmetic, nutrition, and pharmaceutical applications.

The LipNanoCar technology allowed lipid nanoparticles production with average sizes ranging from 100 to 300 nm and Zeta Potentials between -55 and -20 mV. Concomitantly, high entrapment or encapsulation

efficiencies (%EE) were achieved, as illustrated in this work for β -carotene and vitamins derivatives ($>85\%$) for cosmetic application, and for antibiotics currently used in chemotherapy, like rifampicin (69–85%) and pyrazinamide (14–29%) against *Mycobacterium tuberculosis* (TB), and ciprofloxacin ($>65\%$) and tobramycin ($\sim 100\%$) in Cystic Fibrosis (CF) respiratory infections therapy. Ciprofloxacin presented, for example, a quick-release from the lipid nanoparticles using a dialysis tubing (96% in the first 7 h), but slower than the free antibiotic (95% in the first 3 h). This result suggests that ciprofloxacin is loaded near the external surface of the lipid nanoparticles.

The toxicity and validation of entrapment of antibiotics in lipid nanoparticles for Cystic Fibrosis therapy were assessed using *Caenorhabditis elegans* as an animal model of bacterial infection. Fluorescence microscopy of an entrapped fluorescent dye (DiOC) confirmed the uptake of the lipid nanoparticles by ingestion, and their efficacy was successfully tested in *C. elegans*. *Burkholderia contaminans* IST408 and *Burkholderia cenocepacia* K56–2 infections were tested as model bacterial pathogens difficult to eradicate in Cystic Fibrosis respiratory diseases.

V. L. R. Esgueira · C. P. A. Lopes
A. C. A. dos Santos · F. Pinto
D. P. C. de Barros · L. P. Fonseca (✉)
Bioengineering Department, Instituto Superior
Técnico, University of Lisbon, Institute for
Bioengineering and Biosciences, Lisbon, Portugal
e-mail: luis.fonseca@tecnico.ulisboa.pt

S. A. Sousa · J. H. Leitão · L. P. Fonseca
Associate Laboratory, i4HB—Institute for Health and
Bioeconomy at Instituto Superior Técnico University
of Lisbon, Brisbane, Australia
e-mail: natasha.montesalvo@earthcheck.org

Keywords

Lipid nanoparticles · Miniemulsion · Entrapment · Encapsulation · Antibiotics · Chemotherapy · Tuberculosis · Cystic fibrosis · *Caenorhabditis elegans* · Health benefits

3.1 Introduction

The failure and main problems raised presently by some new current clinical therapies include: inadequate drug concentration due to low absorption; rapid metabolism and consequent elimination of the active principle (*e.g.*, drugs, antibiotics, peptides, and proteins); the distribution of highly toxic drugs to non-target tissues (*e.g.*, cancer drugs) and; the low water solubility of some drugs. Drugs often have an optimum concentration range. Concentrations above or below this optimum can either be toxic or ineffective. A rapid drug absorption can lead to a concentration plasma peak reaching toxic levels in the body. Suitable drug carrier systems need to be developed to overcome some of the concerns and drawbacks mentioned above [1].

Nanomedicine is presently responsible for accelerated growth in R&D and clinical trial registration for new therapeutic applications in the fields of new drug therapies and new drug delivery systems (DDSs). The new DDS should be characterized by the absence of toxicity such as cytotoxicity, provide chemical and physical stability for the entrapped or encapsulated drug, have a sufficient drug loading capacity, and offer the possibility of drug targeting and controlled release characteristics. The feasibility of scaling up with reasonable overall costs to ensure the product's reliability on a large scale is another critical factor.

Since the 1960s until today, several nanostructures such as liposomes, nanoemulsions, reversed micelles, polymeric nanoparticles, nanocapsules, lipid nanoparticles, dendrimers, drug nanocrystals, nanosuspensions, and soluble polymer-drug conjugates, among others, are examples of colloidal nanocarriers developed and tested as drug delivery systems [2]. However, liposomes and liquid nano-

emulsions have been characterized by limited physical stability, drug leakage, low specific cell targeting, and upscaling problems. Additionally, dendrimers and polymeric nanoparticles have shown some problems of cytotoxicity and the implementation of large-scale production. In contrast, lipid nanoparticles (LNPs) have shown to be more stable and present various advantages, including controlled drug release, reliable protection of incorporated labile drugs from degradation, excellent tolerability, easy scale-up, and allowing multiple administration routes [3].

A successful process to engineer a drug delivery system includes the following steps: encapsulation or entrapment of a therapeutic substance or drug in an adequate DDS for a specific route administration, the release of the active ingredients, and the subsequent transport of the active principle or drug across the biological membrane to the specific location for therapeutic action. The most suitable DDS choice depends on the desired route of administration, namely dermal, oral, intravenous, parenteral, ocular, or nasal. According to the administration route of the DDS, different size ranges are demanded from a few nanometers (colloidal systems) to the micrometer range (microparticles) [4].

The LNPs target multiple of these goals, which make them superior to conventional DDS, including; their ability to travel through the bloodstream undetected (when below 200 nanometers), to exhibit *in vivo* high drug stability, to control drug pharmacokinetic and pharmacodynamic profiles, and to deliver the drug to, and only to, the target location [5].

3.2 Lipid Nanoparticles (LNPs)

The DDSs based on lipid nanoparticles have a typical structural matrix consisting mainly of lipids, considered physiologically acceptable and biodegradable with a GRAS (Generally Recognized as Safe) *status*, which decreases the associated toxicity. From different lipid DDSs developed, we can highlight the fat lipids, liposomes, reversed micelles, liquid nanoemulsions, and lipid nanoparticles (LNPs), namely solid

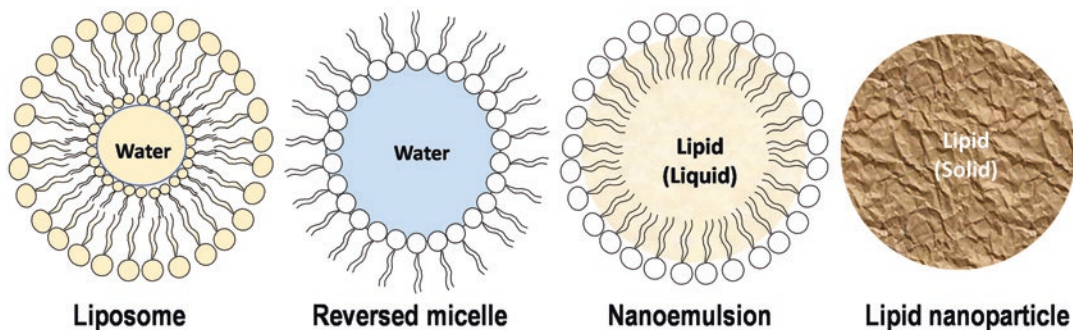
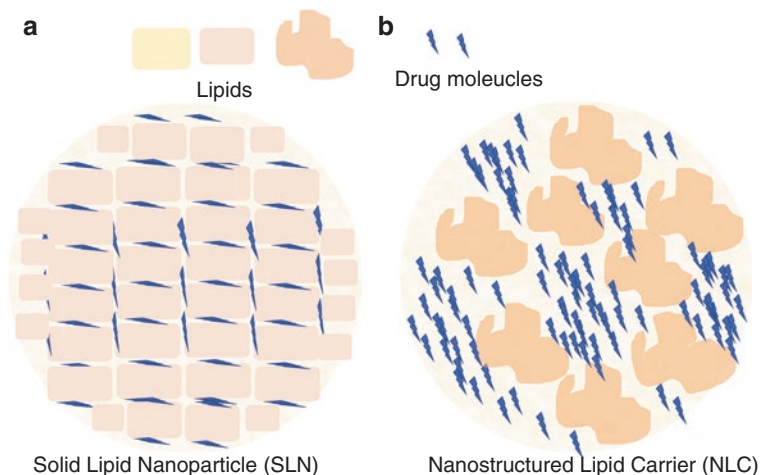


Fig. 3.1 Structure of liposomes, reversed micelles, nanoemulsions, and lipid nanoparticles

Fig. 3.2 Schematic structure of Solid Lipid Nanoparticles (a) and Nanostructured Lipid Carriers (b)



lipid nanoparticles and nanostructured lipid carriers (Fig. 3.1).

Solid lipid nanoparticles (SLNs), compared to liposomes and nanoemulsions, have advantages of physical stability, protection of the entrapped drug from degradation, and controlled release. Additionally, SLNs have low-cost excipients and production processes, and their manufacture on a large-scale is easily implemented [6].

SLNs can be used in various administration routes [7]. However, conventional SLNs presented several limitations, such as limited drug loading capacity due to the crystalline structure of solid lipid and drug release due to low storage stability. A second-generation of LNPs named Nanostructured Lipid Carriers (NLCs) was developed to overcome some of those limitations [8]. SLNs and NLCs differ in their inner solid lipid

structure and, consequently, physicochemical properties and characteristics. Commonly, the structure of SLNs is compared to a “symmetric brick wall,” and the NLCs as a “Welsh natural stone wall” (Fig. 3.2).

Three different models can describe the incorporation of drugs in SLNs with particle size ranges between 50 and 1000 nm [9]. These models include the homogenous matrix solid solution model (in which drug is either molecularly dispersed or present as amorphous clusters in the lipid matrix); the drug-enriched shell model (outer lipid shell containing drug with lipid core), and the drug-enriched core model (drug core surrounded by lipid layer or reservoir type system) (Fig. 3.3) [10, 11].

Therefore, despite SLNs being interesting drug delivery systems, their relatively low drug loading

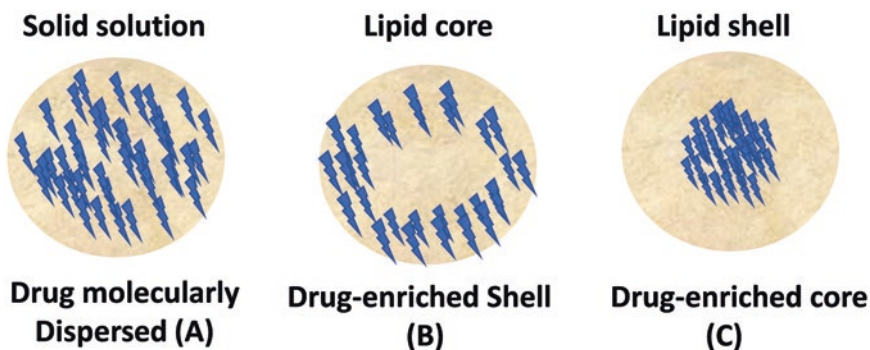


Fig. 3.3 Three drug incorporation models in SLNs: (a) Homogenous matrix of Solid Solution; (b) Drug-enriched shell; (c) Drug-enriched core

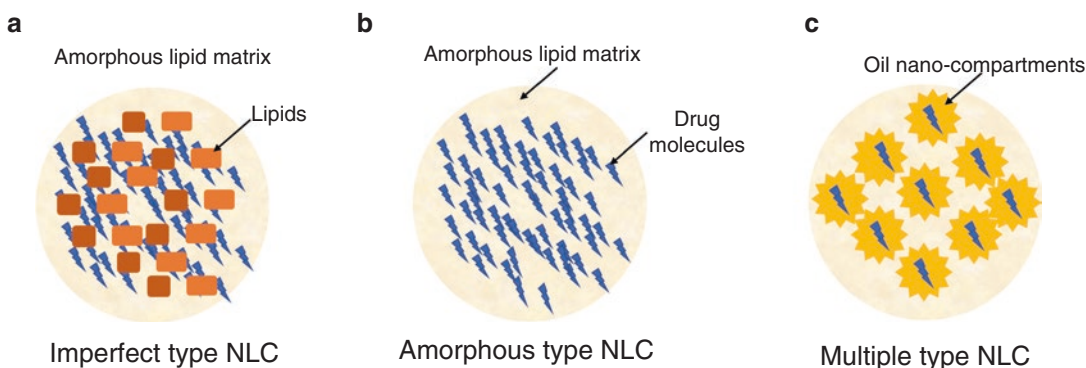


Fig. 3.4 Models of drug incorporation in Nanostructured Lipid Carriers

capacity and potential expulsion of the drug during storage led scientists to think about new strategies. These alternatives start by observing that mixtures of more complex lipids lead to a less perfect matrix and, consequently, a higher drug loading [9, 12].

A second-generation of lipid nanocarriers, identified as Nanostructured Lipid Carriers (NLCs), was developed at the turn of the twenty-first century. NLCs matrices consist of a less ordered lipid matrix with imperfections due to the mixtures or blend of solid and liquid lipids (e.g., oils) (Fig. 3.2b). The resulting LNPs show a lower melting point than SLNs. However, they are still solid at body temperature and increase entrapment or encapsulation efficiency (%EE), drug loading capacity, physical stability, and the feasibility of incorporating drugs in their final dosage forms such as tablets and capsules [13]. NLCs can

be of three types: the imperfect type, the amorphous type, and the multiple type (Fig. 3.4) [14].

Within the last decade, several advances were achieved in the application of LNPs as carriers for the delivery of poorly water-soluble drugs such as antineoplastic agents. Many other drugs included in the Biopharmaceutics Classification System (BCS) II or IV have been gaining interest. Additionally, these colloidal delivery systems can overcome and minimize the drawbacks and concerns mentioned above [13, 15]. Although SLNs and NLCs can incorporate hydrophilic molecules, their loading capacity is relatively low. Thus, synthetic lipid-drug-conjugates (LDCs) in the form of salts between hydrophilic molecules and fatty acids, or, as an alternative, the hydrophilic molecule covalently bound to a lipodic structure [10, 16].

To synthesize LDCs, the drugs should have a functional amino or hydroxyl group conjugated with the carboxylic group present in the fatty acid. In the covalent linking, the drug reacts with a fatty acid or alcohol in the presence of a catalyst. Then, in the form of ester or ether, the resulting product is then purified by recrystallization. The obtained bulk LDCs, in the form of a salt or a covalent linking, are then processed with an aqueous surfactant solution in the oil-in-water emulsion for lipid nanoparticle formulation [16].

The SLNs, NLCs, and the synthetic LDCs are prepared similarly to an oil-in-water (O/w) emulsion, and several techniques have been developed for their production.

3.2.1 Techniques for Production of LNPs

Several techniques have been developed for the LNPs production, resulting in different particle sizes, shapes, stability, and drug loading capacity, but some parameters must be considered when choosing the suitable formulation technique. The size, drug loading, stability of nanoparticles, and toxicological issues, are fundamental parameters that can influence the pharmacological properties of the LNPs. GRAS materials and their biocompatibility and biodegradability are not the unique parameters for a successful DDS. For instance, traces of organic solvents in the final product can be a significant drawback. The use of expensive and sophisticated machines and processes can hamper the production from the lab-scale to a large scale as they can preclude the possibility to scale-up. Finally, more and more complex molecules are being entrapped within LNPs, and it is crucial to obtain high drug loading, thus avoiding the use of a high amount of matrix of biodegradable lipids. These new drug molecules have different physical and chemical properties (solubility, hydrophobicity, others) and stability issues (temperature, pH, others). For this reason, there are multiple factors to choose the formulation technique. Nevertheless, the most appropriate LNP production technique should enhance

drug loading and %EE without damaging the drug molecule's chemical stability.

Different technique approaches are available for LNP production, such as:

- **High-pressure of the hot and cold homogenization** started with melted lipid aqueous solution [17]. For both techniques, lipid contents range from 5–10% in the aqueous solution, but a higher concentration (up to 40% of lipid) can be homogenized to obtain nanodispersion [18]. Either medium scale or large scale production is possible for LNPs by hot homogenization, and it is the most extensively used technique for the preparation of SLNs. The cold homogenization is used for the entrapment of thermolabile drugs in LNPs [11].
- **Microemulsion** is obtained by the mixture of a heated aqueous phase containing the emulsifier with the lipid phase in appropriate ratios, stirring above their melting point, and then diluted with cold water (2–8 °C) to produce LNPs like SNLs. The ratio of hot microemulsion to cold water is usually in the range of 1:10 to 1:50, and therefore, no external energy is required to achieve the small particle size [19]. Nanoparticle concentration in the suspension is below 1%, and excess water can be removed either by ultrafiltration or lyophilization.
- **Ultrasounds** use high-energy sonication for nanoemulsion formulation. The solid lipids are heated at 5–10 °C above their melting point before drug dissolution or dispersion. Then, a hot aqueous surfactant solution (preheated at the same temperature) is added to the drug-lipid melt and homogeneously dispersed by a high shear mixing device. Finally, lipid nanoemulsion is cool down to room temperature, obtaining the LNPs [20, 21].
- **Phase inversion temperature (PIT)** uses some surfactants (e.g., polyethoxylated) to change their partition for water and oil phases according to the temperature [22]. In this technique, an oil phase, constituted by solid lipids and nonionic surfactant, and an aqueous phase containing a specific ionic strength (e.g.,

NaCl) are separately prepared, both heated above the PIT, and then mixed. The mixture constituting the W/O emulsion is then cooled to room temperature under slow and continuous stirring [23].

- **Solvent-based techniques** are based mainly on two distinct methodologies, the solvent emulsification-evaporation and solvent emulsification-diffusion used for entrapment of temperature-sensitive drugs (e.g., protein, peptides). However, trace amounts of the organic solvent remains in the final product can potentially create toxicity problems. The drug is added into a water-immiscible organic solvent (e.g., cyclohexane, dichloromethane, tetrahydrofuran, toluene, chloroform, others), and then emulsified in an aqueous surfactant solution by mechanical agitation in both methodologies. In the solvent emulsification-evaporation technique, the lipid phase precipitation forms the LNP dispersion in the aqueous surfactant medium during the solvent evaporation process [24]. In the solvent emulsification-diffusion, the O/W emulsion is then diluted with an excess of water, in typical ratios ranging from 1:5 to 1:10, causing the solvent's dissolution in water and subsequent precipitation of the LNPs [19].
- **Other techniques** such as coacervation [13], membrane contactor [25], supercritical fluid-based [26], microfluidic system [19], or combinations of those above have been tested and reviewed recently on the for LNPs production [27].

3.2.2 LipNanocar Technology: LNPs Production Based on a Miniemulsion Technique

A particular emulsions class consists of colloidal dispersions with a droplet size between 20 and 500 nm, known as miniemulsions, nanoemulsions, or ultrafine emulsions, resulting from liquid lipid nanodispersions at high temperatures. The cold nanoemulsion appearance is transparent or bluish for the smallest droplet sizes between 20 and 100 nm, or milky for sizes up to 500 nm [28].

Luis Fonseca's team has widely used an O/w miniemulsion methodology on biocatalysis applications that showed a high loading capacity 20–50% (w/w) of several hydrophobic compounds (e.g., short/medium/long fatty acids, aldehydes, ketones, alcohols, esters, chiral compounds, others) [29–32]. The extensive knowledge allowed the development of a new DDS based on miniemulsion methodology that constitutes the LipNanoCar technology core for LNPs production. This technology is focused on the LNPs production with entrapment or encapsulation of several bioactive and hydrophobic compounds, antibiotics, and drugs for cosmetic, nutrition, and pharmaceutical applications.

LNPs can be prepared according to the LipNanoCar technology by vigorous mechanical agitation or high-energy emulsification methods like ultrasonication or high-pressure homogenization.

In all cases, the aqueous and lipid phases are previously and separately prepared and heated above the lipid melt temperature before mixing with magnetic stirring, and different temperature conditions were commonly tested (50–70 °C). When the fatty acids (e.g., lauric acid) or the fatty acids and oils combination (e.g., lauric acid/coconut oil) are fully melted, a hot aqueous solution containing a surfactant or a tension-active agent (e.g., Lutensol AT 50, Tween 80, Span 80, others) and, eventually, a co-surfactant (e.g., hexadecane) preheated at the same temperature are mixed. For LNPs loaded, the active biological compound is mixed with the lipid phase for at least 15 min before adding the aqueous solution at the same temperature. Then, a hot O/w miniemulsion is obtained when submitted to ultrasonication using a sonication probe (MS72) in a sonicator (Bandelin, Germany) for 5 min (25%; 5 s-on; 5 s-off) without temperature control. Alternatively, a hot O/w miniemulsion is obtained by vigorous mechanical agitation using a standard Teflon impeller for a few minutes (Fig. 3.5).

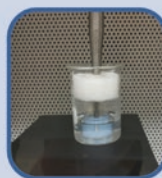
In both cases, the transparent hot O/w emulsion is then cooled to room temperature under stirring, resulting in a milky or bluish LNP suspension. After cooling, the samples from each

Ultrasonication

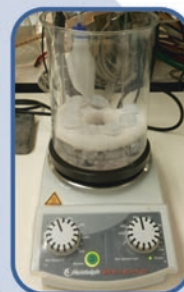
Simple, reproducible, without the need of organic solvents!



750 rpm, 50-70°C



Sonication, 5min
(25% ; 5s-on / 5s-off)



room temperature,
750 rpm, 2h

Mechanical agitation

Simple, reproducible, without the need of organic solvents!



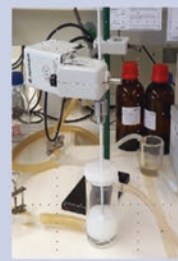
250 rpm, 50-70°C



PTFE Impeller



Mechanical agitation 250rpm, 1h, 70°C,



room temperature,
250 rpm, 2h

Fig. 3.5 Lipid nanoparticle production by LipNanoCar technology. **Ultrasonication:** first step, Lipid phase and aqueous phase warmed separately at 70 °C; second step, Mixing and sonication of hot pre-emulsion; third step, Cooling down to room temperature. **Mechanical**

agitation: first step, Lipid phase and aqueous phase warmed separately at 70 °C; second step, Mixing and vigorous mechanical agitation of hot pre-emulsion; third step, Cooling down to room temperature

formulation are stored in a refrigerator at 4 °C or left at room temperature.

LipNanoCar technology produces GRAS *status* nanocarriers like O/w Liquid Lipid Nanoemulsions and LNPs (e.g., SLNs or NLCs) incorporating in their composition lipids that are solid at room temperature to carry and deliver bioactive compounds and drugs. Furthermore, the LNPs did not show any toxicity issues, in contrast with synthetic polymers like poly (lactide-co-glycolide) (PLGA) due to the acidic by-products formed during their degradation, rendering them inappropriate for extended use in some health applications. LipNanoCar technology shows enormous potential as a valuable technological platform for nanocarriers development for pharmaceutical, dermatological, and nutritional applications that can improve health and well-being.

LNPs produced by LipNanoCar technology are cost-effective. Additionally, LipNanoCar technology shows to be a feasible and attractive methodology for large scale production of GRAS lipid nanocarriers containing medium and long lipid and solid fatty acids, natural oils, and using GRAS tension-active agents or surfactants. The optimized delivery nanocarriers allowed the entrapment of several bioactive compounds. These include a wide range of compounds: omega-3 unsaturated fatty acids (DHA/EPA); esters based in lipid conjugation (e.g., DHA-nicotinol) [32]; pure mono-, di- and triglycerides; several oils (e.g., olive, coconut, soybean, among others) [33]; antioxidants (e.g., α -tocopherol and derivatives) [33]; vitamins (e.g., retinoids, retinyl palmitate) [34]; β -carotene [35]; antibiotics and drugs (e.g., rifampicin [35], pyrazinamide [35], lidocaine [36], tobramycin [37], ciprofloxacin [37]); and fluorescent molecules (e.g., DiOC) that allow their optical detection [37, 38].

The projects developed in the last years based on LipNanoCar technology in the field of DDSs were namely:

- Antibiotics for Tuberculosis treatment [35],
- Bioactive compounds for incorporation in lubricant-anesthetic-disinfectant intraurethral gels [36],
- Antibiotics for Cystic Fibrosis treatment and validation of non-cytotoxicity of unloaded and

loaded-lipid nanoparticles using *Caenorhabditis elegans* as an animal model of bacterial infection [37],

- Antioxidant and vitamins incorporated in topical administration for skin healing and protective effects [38],
- Permeation of tocopherol through a 3D model of the reconstructed human epidermis (RHE) and cytotoxicity studies using MTT with Human epidermal keratinocytes [38],
- More recently, the entrapment of bioactive extracts from Amazonian plant seeds, which is in development.

3.3 Fate and Toxicological Concerns of Drug Delivery Using LNPs

Macrophages, specialized cells of the human immune system, recognize all external nanoparticles as antagonistic matter and quickly phagocyte and eliminate them from the body. Nonetheless, these specialized immunological cells are present in the human body's limited areas (e.g., lungs). Furthermore, nanoparticles with sizes below 100 nm can be internalized by all body cells [9, 39]. Regarding the typical LNPs sizes of 100–300 nm (size above 100 nm), as their cellular uptake is not expected, the risks of interference with the oral administration of the DDS are reduced, and, consequently, they do not present significant toxicological concerns [40].

3.3.1 LNPs Fate When Used in Oral Administration Route

Oral administration of LNPs (e.g., SLNs, NLCs, or LDCs) is possible as aqueous dispersion [41] or transformed into traditional dosage forms such as tablets, pellets, capsules, or powders in sachets [42]. However, aqueous dispersions of LNPs might not be suitable to be administered as a dosage form due to the stomach acidic environment and high ionic strength that favor particle aggregation. Besides, the presence of food will also have a high impact on their performance [26].

The packing of LNPs in sachets for redispersion in water or juice before oral administration will allow individual dosing by volume of the reconstituted LNPs. The aqueous lipid nanoparticle dispersions can be used for tablet production instead of a granulation fluid in the granulation process. Alternatively, LNPs can be transformed previously to a powder (by spray-drying or lyophilization) and then added and mixed with other powder ingredients to form a tablet. However, it is beneficial to have higher solid content to avoid removing excess of water. Due to cost reasons, spray drying might be the preferred method for transforming lipid nanoparticle dispersions into powders, in general, by the previous addition of a protectant agent [43]. The lipid nanoparticle dispersions can also be used as a wetting agent in the extrusion process for pellets production. Lipid nanoparticle powders can also be incorporated to fill hard gelatine capsules.

Several drugs (hydrophobic and hydrophilic) have been incorporated in LNPs, being examples of the potential benefits of lipid nanoparticle carriers for application in oral administration and recently reviewed [13, 44, 45].

Concerning the typical lipid nanoparticle triglyceride-based composition, it is expected that after oral administration, they undergo similar mechanisms of food-ingested lipids. The lipid matrix degradation occurs mostly by lipases, whereas non-enzymatic hydrolytic processes degrade only a minor part. A regular healthy adult gastrointestinal (GI) tract can daily hydrolyze about 100–140 g of dietary lipids (mainly in the form of triglycerides). Lipids digestion generally begins in the stomach, where triglycerides are hydrolyzed into diglycerides and fatty acids by the acid-stable lipases such as the lingual and the gastric lipases. Afterward, gastric contents reach the duodenum, the first section of the small intestine, where lipid's presence stimulates the production of both lipase/co-lipase enzymes by the pancreas and bile salts (phospholipids and cholesterol) by the gall bladder. Bile salts adhere to emulsion droplets' surface, promoting the lipase/co-lipase action and originating free fatty acids and colloidal species like micelles, mixed micelles, and vesicles. The absorption of fatty

acids and entrapped drugs occurs mostly in the small intestine, where substances move directly into the systemic circulation, or firstly into lymphatic circulation and subsequently to blood [42, 46].

The nanoparticle size is an essential factor for uptake into the GI epithelia. Intestinal cells cannot absorb nanoparticles larger than 400 nm [47]. Furthermore, LNPs have adhesive properties, allowing their adherence to the enterocytes (intestinal epithelial cells) surface. Therefore, drug release from the nanoparticles is immediately followed by direct absorption within the enterocytes. In parallel, the presence of LNPs in the duodenum promotes lipase/co-lipase activities and bile salts secretion. The former hydrolyzes the triglycerides into monoglycerides and fatty acids, forming micelles, which undertake (i.e., re-solubilize) the drug; meanwhile, the drug is released with the degradation of the nanoparticles. Additionally, the bile salts interact with micelles and form mixed micelles. Subsequently, the drug is absorbed, together with these colloidal species, by one or more of the transport mechanisms depicted in Fig. 3.6.

Even for the biodegradable nanoparticles, the use of high concentrations of the carriers can lead to toxicological concerns. Therefore, the fate of the carriers in the body should be clarified. LNPs are easily eliminated through physiologic and metabolic pathways, relatively fast as non-toxic compounds, decreasing acute and chronic toxicity risk as they are generally produced from natural and GRAS excipients.

3.3.2 *In Vitro* Toxicological Studies of LNPs

Depending on the administration route, the NPSs' toxicity requirements can change, being the requirements lower for dermal, moderate for oral, and higher for intravenous administration [9].

Toxicological studies should be first performed *in vitro*, using cell models that mimic the body conditions to minimize the number of animal studies and to have an idea of the cytotoxicity of the DDSs in an early stage. The

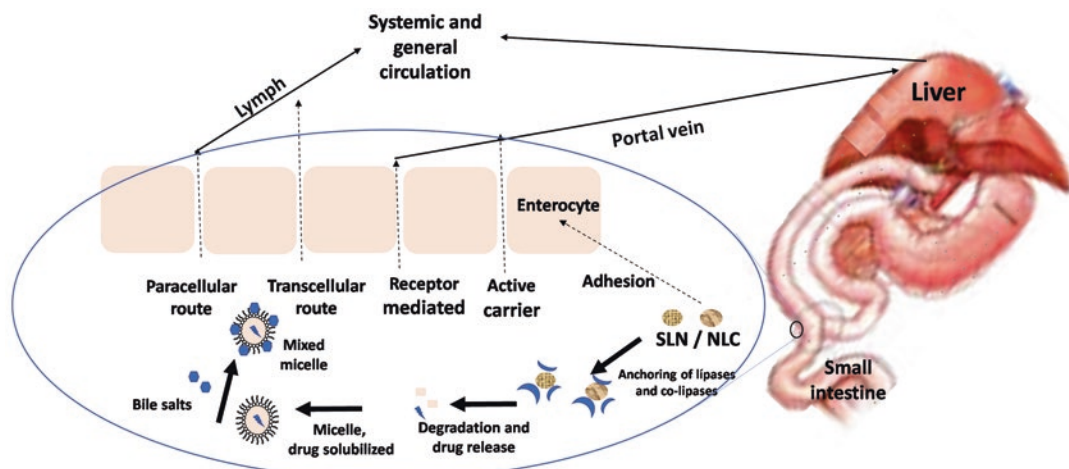


Fig. 3.6 Transport mechanisms enhancing drug bioavailability in the presence of lipids

Caco-2 cell line is often used as an *in vitro* model since it mimics the Gastrointestinal (GI) tract conditions [48, 49], and the viability of human granulocytes have also been studied for toxicological and pharmacological studies [50, 51]. Several studies have reported and confirmed that LNPs show high biocompatibility, being well-tolerated, and exhibiting low cytotoxicity, compared with other conventional drug nanocarriers, which increases their attractiveness for drug-delivery applications [50]. For example, SLNs prepared with lipids concentrations up to 2.5% do not exhibit any cytotoxic effects *in vitro* [50, 51]. Even for lipids concentrations higher than 10%, these LNPs led to a viability of 80% in cultures of human granulocytes [51]. In contrast, some polymeric nanoparticles led to complete cell death at concentrations of 0.5%. In a few cases, the SLN's cytotoxicity can be mainly attributed to emulsifiers or preservative compounds used to produce these DDSs [9].

From the data obtained until now, the lipid nanoparticle formulations appear to fulfill the essential prerequisite to the clinical use of an oral colloidal lipid carrier with low cytotoxicity. However, *in vitro* studies sometimes use short periods and small concentration ranges, which do not allow realistic conclusions about the nanocarrier cytotoxicity. For this reason, *in vivo* studies

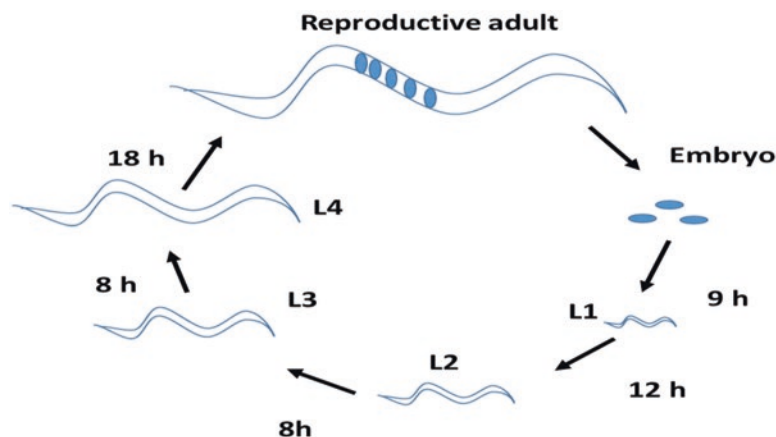
must always be performed before the move to human clinical trials [52].

3.3.3 *In Vivo* Toxicological Studies Using *C. elegans* and as an Animal Model of Bacterial Infection for Assay Drug Delivery Efficiency of LNPs

Caenorhabditis elegans is a small, free-living soil hermaphroditic nematode that feeds on microbes, particularly *E. coli* strains. The nematode is an important model system for many biological research fields such as genetics, genomics, cell biology, neuroscience, and aging. *C. elegans* genome is approximately 72% similar to the human genome, and each worm gene has a counterpart in the human genome. The life cycle of the animal comprises the embryonic stage, four larval stages (L1-L4), and adulthood (Fig. 3.7) [53, 54].

C. elegans feeding involves food ingestion, digestion, nutrient absorption, and defecation. The digestive system of *C. elegans* is also the main path of uptake of nanoparticles as the worms ingest them actively during feeding [53]. The particle size smaller than 1000 nm can come in through the nematode mouth and then be

Fig. 3.7 Representative stages of the *C. elegans* life cycle (L1 through L4). L4 larvae molt into young adults, developing into reproductive adults that survive for approximately 3 weeks under standard laboratory conditions



ingested. The ingestion of nanoparticles can occur through two different mechanisms: voluntary ingestion or non-voluntary ingestion. The nanoparticle ingestion can coincide with the ingestion of *E. coli* OP50 bacteria due to the pharynx's continuous pumping action [55].

C. elegans have been studied as a model of infection for several pathogenic bacteria that replace the *E. coli* food source and then, following the disease progress, evaluated by the survival of a population or other parameters such as reproduction. The mortality of *C. elegans* is due to some lethal toxins produced by the pathogens. Other pathogens are also virulent by provoking intestinal infections and signs of illness such as locomotion defects, distended intestine, paralysis, or erratic movement. The nematode has been used to study Gram-positive human pathogens such as *Staphylococcus aureus* and Gram-negative isolates from Cystic Fibrosis belonging to species *Pseudomonas aeruginosa* and the *Burkholderia cepacia* complex (Bcc) [54, 56].

Burkholderia contaminans IST408 and *Burkholderia cenocepacia* K56–2 belong to the Bcc group pathogens. They can induce an infection-like in the *C. elegans* nematode, providing a useful model to evaluate LNPs' efficacy with encapsulated antibiotics (e.g., ciprofloxacin, tobramycin) to rescue infected *C. elegans* populations.

3.4 LNPs Loaded with Antibiotics Produced by LipNanoCar Technology for Oral Administration Against Tuberculosis

Tuberculosis (TB) is an infectious disease produced by bacilli belonging to the *Mycobacterium tuberculosis* complex [57]. Currently, available chemotherapy includes first-line drugs such as isoniazid (INH), rifampicin (RIF), ethambutol (EMB), and pyrazinamide (PYZ) [58]. The actual short-course treatment guideline aims for the complete elimination of active and dormant bacilli and involves two phases. During the initial phase, four drugs (usually isoniazid, rifampicin, pyrazinamide, and ethambutol) are administered daily for 2 months. The continuation phase is based on an additional administration for 4 months, either daily or 3 times per week. Fewer drugs (usually isoniazid and rifampicin) are administered, targeting and killing off any remaining or dormant bacilli to prevent reversion [57].

The search for new anti-TB drugs is an essential key in this fight, but searching for new drug delivery strategies may also play an important role. The alternative delivery systems, such as nanocarriers for anti-TB drugs, may reduce administration frequency and shorten treatment periods, improving patient compliance and

efficacy of treatment, reducing drug-related toxicity. For example, isoniazid, rifampicin, and pyrazinamide chemotherapy in conventional DDSs have shown hepatotoxicity [59], a side effect due to its action on hepatocytes rather than macrophages, the primary host cells that harbor *M. tuberculosis*. Thus, a delivery mechanism that introduces these antibiotics selectively into macrophages would significantly increase their therapeutic efficacy by achieving higher concentrations of the antibiotics in the infection site without exposing the patient to high and toxic systemic concentrations.

Since *M. tuberculosis* resides and multiplies intracellularly in host mononuclear phagocytes and because they internalize particles more efficiently than other host cells, encapsulation of anti-TB drugs in nanoparticles offers a mechanism for specific targeting of *M. tuberculosis*-infected cells. Indeed, because nanoparticles are uptake by macrophages of the reticuloendothelial system and accumulate in the liver, spleen, and lung [60–62], they are ideal for treating *M. tuberculosis*, which infects macrophages in these organs.

As macrophages exhibit several receptors, it is also possible to modify these nanocarriers' surfaces to achieve macrophages' active targeting. Particle size is also a vital characteristic in the passive targeting of macrophages since they affect these cells' internalization success. In this regard, particles with diameters of about 500 nm have been reported as ideal to undergo phagocytosis by alveolar macrophages [63].

Different nanocarriers have been produced as delivery platforms of anti-TB drugs in this work, for example, entrapment of rifampicin and pyrazinamide in LNPs.

3.4.1 Preparation of SLNs and NLCs by LipNanoCar Technology

The identification and composition formulation used to produce the LNPs against Tuberculosis is presented in Table 3.1 [35].

Table 3.1 Identification and formulation composition (%w/w) of LNPs produced. The remaining % is Milli Q water

ID	Formulation			
	Lauric acid (%)	Oil ^a (%)	Co-surfactant Hexadecane (%)	Surfactant Lutensol A15 (%)
SLN_1	10.0	–	3.0	7.1
SLN_2	5.6	–	3.2	7.4
SLN_3	2.9	–	3.2	7.6
SLN_4	6.9	–	3.1	7.3
SLN_5	8.2	–	3.1	7.2
SLN_6	4.3	–	3.2	7.5
NLC_1	5.5	1.4	3.1	7.3
3.0 β -SLN	6.9	–	3.1	7.3
3.0 β -NLC	5.5	1.4		
1.1RIF-SLN	7.1	–	3.2	7.5
1.1RIF-NLC	5.7	1.4		
2.0RIF-SLN	7.1	–	3.2	7.5
2.0RIF-NLC	5.7	1.4		
1.1PYZ-SLN	7.1	–	3.2	7.5
1.1PYZ-NLC	5.7	1.4		

3.0 β , 1.1RIF, 2.0RIF, and 1.1PYZ corresponds to the amount (mg) of bioactive compound added per 1 g of the miniemulsion system to produce LNPs

^aOil is Coconut oil

3.4.1.1 Influence of Sonication, Lauric Acid (LA) Content, and Temperature on the Production of LNPs

The non-sonicated SLNs dispersions produced by LipNanoCar technology in these conditions exhibit a milky aspect, while sonicated SLNs dispersions are clearer and bluish (Fig. 3.8).

As expected, the sonicated SLNs samples are characterized by a decrease in mean particle size (Z-Ave) according to the DLS results (Fig. 3.9). Usually, from literature, colloidal dispersions with droplet sizes between 20 and 100 nm are transparent or bluish, while colloidal dispersions with larger droplets sized up to 500 nm exhibit a milky aspect [20].

Fig. 3.8 Macroscopic aspect of empty SLNs: (left) – non-sonicated formulation; (right) – sonicated formulation

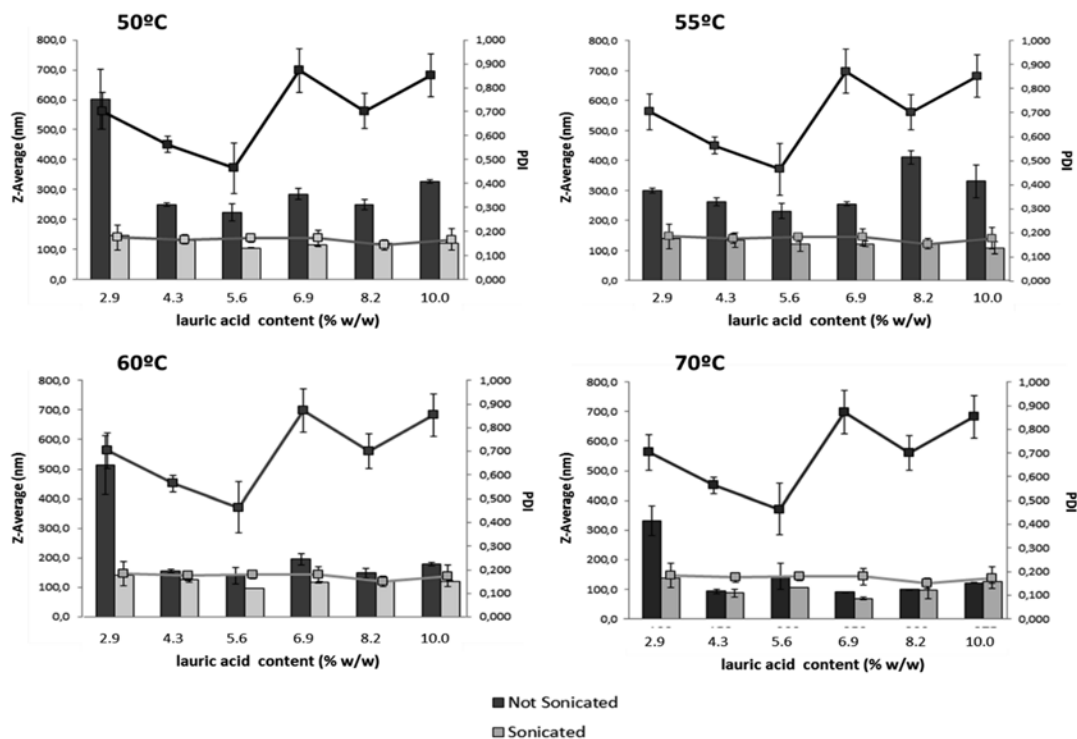
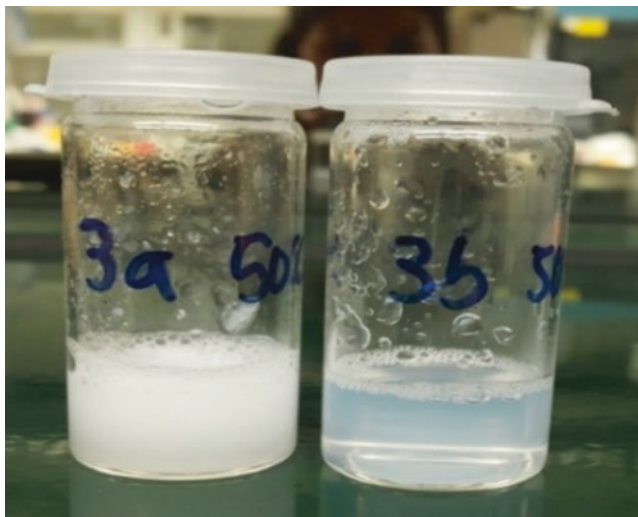


Fig. 3.9 Z-average and PDI of empty SLNs with different lauric acid content and for the temperatures of 50 °C, 55 °C, 60 °C, and 70 °C

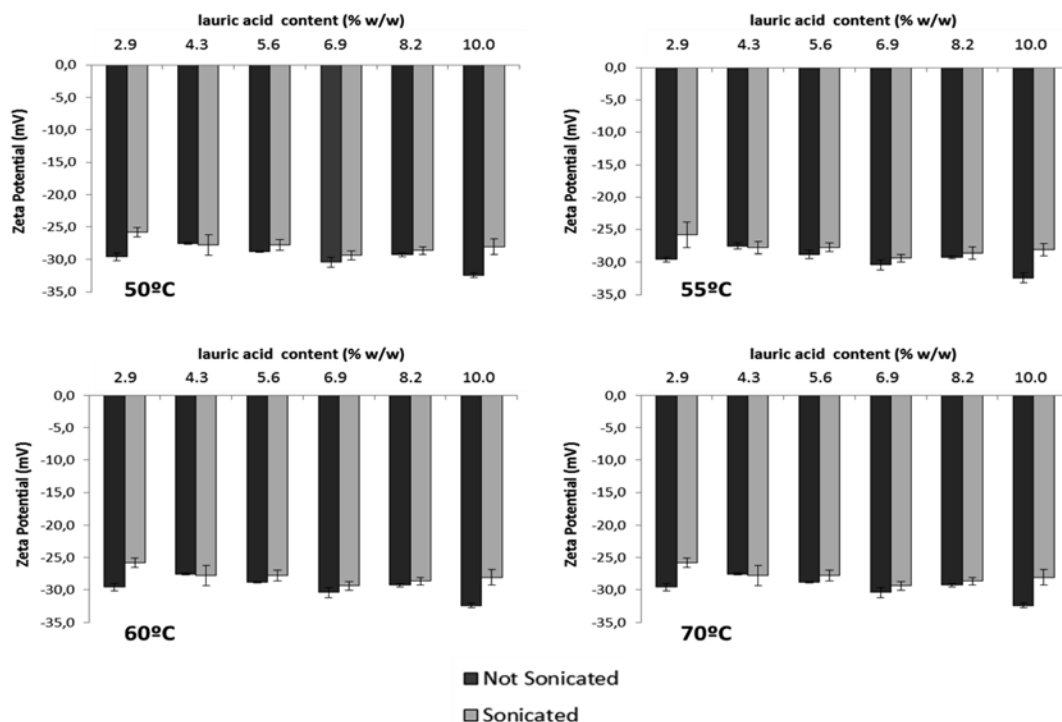


Fig. 3.10 Zeta Potential of empty SLNs with different lauric acid content and for the temperatures of 50 °C, 55 °C, 60 °C, and 70 °C

All SLNs obtained using sonicated formulations show a mean Z_{ave} lower than 150 nm (Fig. 3.9). This smaller size is due to shear stress resulting from the application of ultrasound energy that promotes a shear on lauric acid molecules, impairing aggregation, and avoiding the formation of larger lipid particles. Despite this significant effect on particle size, ultrasonication does not appear to play an essential role in the physical stability of SLNs, since ZP is very similar between non-sonicated and sonicated SLNs (Fig. 3.10).

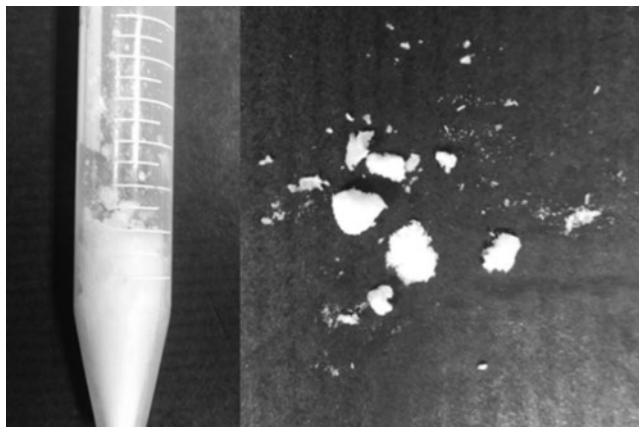
The application of ultrasound energy seems to decrease the mean particle size of SLNs and homogenize the miniemulsion suspension significantly since PDI values decreased when sonication was used in the formulations tested.

The effect of temperature on the pre-emulsion preparation in the formulations used in this study was also investigated. Four different temperatures, 50 °C, 55 °C, 60 °C, and 70 °C, were tested. The primary influence of temperature was

observed on non-sonicated formulations as there was a notorious size reduction of non-sonicated particles (Z_{ave}) with the increase of temperature. At the same time, no significant variation of the PDI and ZP values was observed (Fig. 3.9 and 3.10). The increase of temperature usually decreases the lipid and aqueous phases viscosity and hence the mixture efficiency by magnetic or mechanical stirring. In other words, increasing the temperature favors lipids fusion and decreases the viscosity, resulting in smaller emulsion droplets and lipid particle sizes [19].

The influence of lauric acid content on SLNs properties was also investigated (Fig. 3.9 and 3.10). The non-sonicated formulations analysis revealed that particle sizes of SLNs prepared with the lowest concentration of lauric acid at 50 °C, 60 °C, and 70 °C were larger when compared with other SLNs. This result is probably due to the Ostwald ripening effects or the aggregation of clusters of smaller LNPs, in both cases minimizing the energy of Gibbs of the system.

Fig. 3.11 Powder resulting from lyophilization of SLN_1 obtained with formulation 60 °C; 10.0% LA; sonicated



The clustering of small LNPs can be so perfect that the DSC software interprets it as a larger lipid nanoparticle, with a size ranging from 300 to 600 nm. The literature suggests increasing the lipid content, over 10%, leads to larger particles (including microparticles) and broader particle size distributions due to particle agglomeration [64]. However, in this work, this was not observed for the percentage of lauric acid used. Nevertheless, the PDI values of the non-sonicated SLNs produced with the different lauric acid formulations were also high.

The different percentage of lauric acid in the formulations tested also seems not to affect the ZP and all features considered for LNPs obtained using sonication. Furthermore, 5.6% of lauric acid improved the system homogenization, in particular, for non-sonicated SLNs. The temperature of 60 °C was chosen for forwarding studies on lipid nanoparticle preparation with or without sonication, as the values of Z-ave obtained were similar.

3.4.1.2 Lyophilization of LNPs

Lyophilization (or freeze-drying) was the final step used in the SLNs production process. The lyophilization promotes water removal from a frozen sample by sublimation and desorption under a high vacuum. Many pharmaceutical products, mainly heat-sensitive compounds, are dried using this technique since it improves the long-term physic-chemical stability and prevents

degradation reactions such as hydrolysis. Lyophilization is also used with nanoparticles to prevent nanoparticle aggregation and enhance the stability of SNLs in powder form.

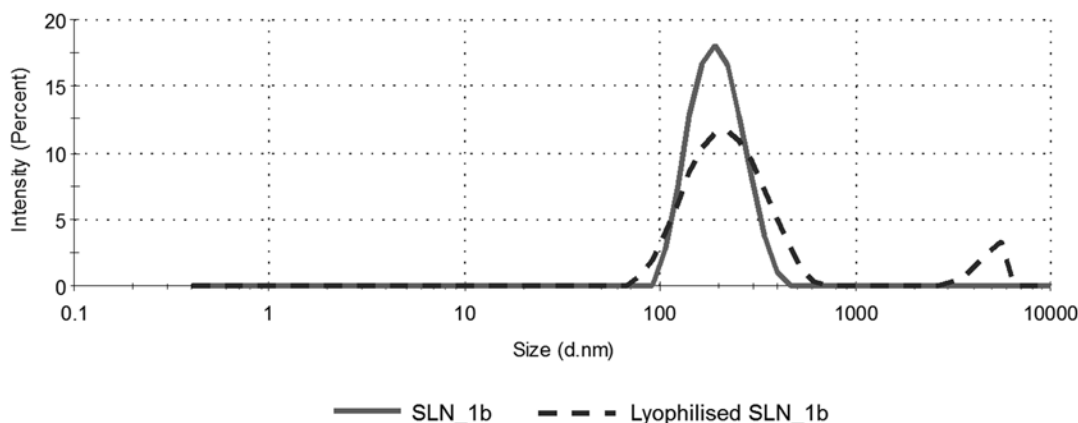
The aqueous suspension of lipid nanoparticles (SNLs) was fast frozen at $-80\text{ }^{\circ}\text{C}$ for 5 h in an ultra-low refrigerator. Then, the frozen samples were moved into the chamber of a freeze-drier (Christ Alpha 1–2 LD) for lyophilization for 48 h in order to get in the end a powder of LNPs (Fig. 3.11).

The values of Z-ave, PDI, and ZP of the SLN_1 (formulation 60 °C; 10.0% LA; sonicated) before and after lyophilization shows a slight increase of particle size from $153 \pm 31\text{ nm}$ to $191 \pm 4\text{ nm}$, while the PDI of lyophilized SLNs increased from 0.13 ± 0.04 to 0.49 ± 0.10 , respectively (Table 3.2). Before and after lyophilization, the particle size distribution comparison showed a second particle population larger than $1\text{ }\mu\text{m}$ in reconstituted lyophilized powder in Milli Q water (Fig. 3.12).

This population with larger particle size most probably results from an aggregation phenomenon that explains the increase of PDI. However, unexpectedly, the absolute ZP value increased from 30 ± 2 to $35 \pm 2\text{ mV}$, meaning an increase in particle stability. An explanation for these results could be an insufficient magnetic stirring force or time applied to the resuspension of lyophilized SLNs in Milli-Q water. If the attractive forces holding the aggregate of powder LNPs together

Table 3.2 Physicochemical properties of the SLN_1b obtained with formulation 60 °C; 10.0% LA; sonicated. Values are mean \pm SD, n = 3

Formulation	Z-Ave (nm)	PDI	ZP (mV)
Before lyophilization (SLN_1b)	153 \pm 32	0.13 \pm 0.04	-30 \pm 2
After lyophilization (SLN_1b)	191 \pm 4.0	0.49 \pm 0.10	-35 \pm 2

**Fig. 3.12** Particle Size Distribution by Intensity of the SLN_1b obtained with formulation 60 °C; 10.0% LA; sonicated before and after lyophilization

are very large compared with the conventional forces used in stirring, the system is regarded as permanently aggregated. To minimize this result, the addition of a cryoprotective agent before lyophilization could preserve the physicochemical properties of original SLNs and decrease SLNs aggregation. Typical cryoprotective agents are sorbitol, mannose, trehalose, glucose, and polyvinylpyrrolidone, and the best results occurred in the concentration range 10–15% [65].

3.4.1.3 Long-Term Stability of LNPs

Aqueous SLNs suspensions were stored at room temperature (25 °C) and in the refrigerator (4 °C), without agitation, for 7 months. The long-term stability of SLNs suspensions was assessed through particle size (Z-ave and PDI) and ZP measurements, macroscopic observation, and TEM analysis. The samples stored at room temperature remained with a milky-like appearance, although some of the aqueous SLNs suspensions presented particle sedimentation. Additionally, during storage at 4 °C after more than 1 week, some unpredictable gelation occurred in some aqueous SLNs suspensions.

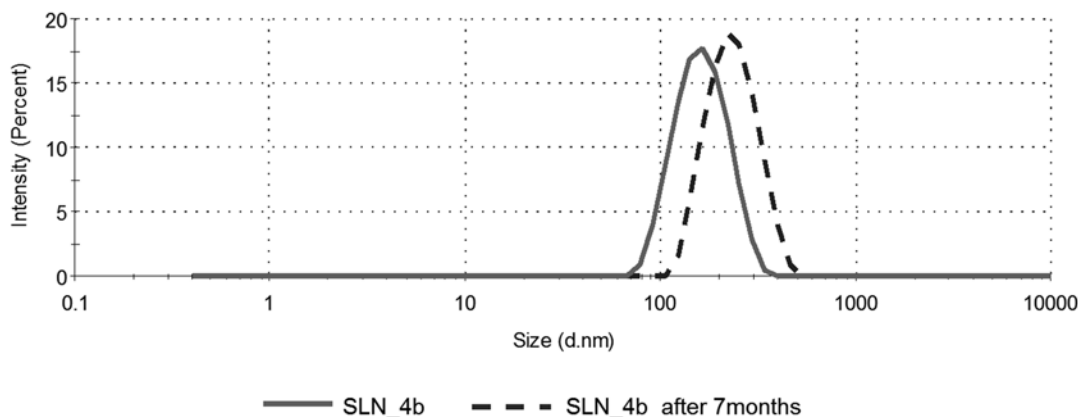
Gels are more structured than liquids. SLNs can organize themselves in superstructures. The change in morphology of LNPs from spheres to platelets is responsible for the gelation of SLN dispersions [66]. Depending on the composition, especially of the emulsifier(s) and the amount of lipid matrix, the liquid dispersions gelation can be observed during storage [66].

The values of Z-ave, PDI, and ZP for aqueous SNL_4 suspensions (obtained with formulation 60 °C; 6.9% LA; sonicated) before and after storage at room temperature for 7 months are present in Table 3.3. The absolute ZP value decreased from 29.1 \pm 0.9 to 28.3 \pm 0.6 mV, indicating slight particle structure changes. Additionally, the DLS measurements also confirmed a slight increase of particle size from 154 \pm 25 to 223 \pm 54 nm, but the mean particle size remained lower than 400 nm (Fig. 3.13). Since PDI and particle size remain relatively low, homogeneously sized SLNs displayed good long-term stability.

The shape and surface morphology of empty SLN_4b after storage for 7 months were analyzed by TEM, and the observed size agrees with

Table 3.3 Physicochemical properties of the SLN_4 obtained with formulation 60 °C; 6.9% LA; sonicated. Values are mean \pm SD, n = 3

Formulation	Z-ave (nm)	PDI	ZP (mV)
SLN_4 before storage	154 \pm 25	0.07 \pm 0.03	-29.1 \pm 0.9
SLN_4 after 7 months	223 \pm 54	0.05 \pm 0.02	-28.3 \pm 0.6

**Fig. 3.13** Particle Size Distribution by Intensity of the SLN_4b obtained with formulation 60 °C; 6.9% LA; sonicated, after 1 day and 7 months after production

the DLS analysis (Fig. 3.14). All the particles showed to be smoothly spherical or oval with a well-defined periphery and size estimated by particle observation exactly top-on and edge-on. No visible aggregation of the SLN_4b formulation was observed.

3.4.1.4 Comparison of Bioactive Compounds Entrapment in SLNs and NLCs

For NLCs production, the SLNs obtained with formulation 60 °C; 6.9% LA; sonicated, was changed slightly by keeping the same lipid composition in weight percentage, but part of the lauric acid in weight substituted by coconut oil (NLC_1). The experimental procedure was similar to the SLNs production, as described previously.

The values of Z-ave, PDI, and ZP of the NLC_1 formulation were slightly different compared to SLN_4b (Table 3.4). Since both LNPs have an identical percentage of lipid content and were produced under the same conditions, the increase of particle size from 154 \pm 25 nm to

282 \pm 56 nm was attributed to the use of coconut oil (Table 3.4). The combination of different chain fatty acid triglycerides promotes changes in the structure of LNPs. These changes were also observed for particle surface electrical charge supported by the slight reduction of absolute ZP value from -29.1 \pm 0.9 to -26.4 \pm 0.7 mV.

The size of the produced LNPs is in the range of 150–300 nm with an increase of particle size of NLCs, but both LNPs size remains lower than 400 nm, as required for oral administration and easy cross of intestinal cells. Particles smaller than 200 nm usually remain invisible to the reticulum-endothelial system (RES) and remain on the circulation system over a prolonged period [67].

The entrapment or encapsulation efficiency of some bioactive compounds in lipid nanoparticles (SLN_4b and NLC_1) based on lauric acid was investigated. In this comparative study, the temperature was kept at 60 °C, followed by 5 minutes of sonication (25%, 5 s-on, 5 s-off). The anti-TB drugs rifampicin and pyrazinamide were chosen for entrapment within these LNPs. The

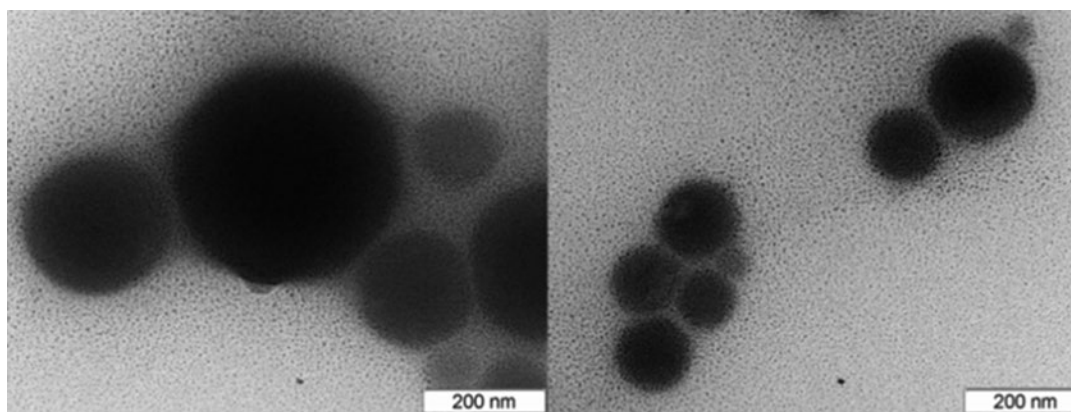


Fig. 3.14 TEM image of SLN_4b obtained with formulation 60 °C; 6.9% LA; sonicated, after storage for 7 months

Table 3.4 Physicochemical characteristics of the empty NLC_1 (60 °C; 6.9% LA; sonicated). Values are mean \pm SD, n = 3

Formulation	Z-Average (nm)	PDI	ZP (mV)
NLC_1	282 \pm 56	0.43 \pm 0.09	-26.4 \pm 0.7
SLN_4b	154 \pm 25	0.07 \pm 0.03	-29.1 \pm 0.9

β -carotene entrapment was also tested as a lipophilic compound model.

The macroscopic appearance of empty and loaded NLC_1 was distinct, but all the nanoemulsions were significantly more transparent after sonication (Fig. 3.15).

β -carotene (β) was incorporated in LNPs with formulation 60 °C, 6.9% LA ((3.0 β -SLN) or 5.7% LA + 1.4 Oil (3.0 β -NLC), sonicated, 3 mg β -carotene added per 1 g of the miniemulsion system. The values of Z-ave, PDI, and ZP of loaded LNPs were measured 1 day after production (Table 3.5). The entrapment or encapsulation efficiency (%EE) is defined as the percentage of drug incorporated into the LNPs relative to the total drug added to the system. The %EE of these LNPs was determined indirectly by calculating the amount of free bioactive compound (e.g., β -carotene) that was not entrapped and present in the aqueous phase of nanoemulsion dispersions. As expected, SLN_4b and NLC_1 loaded with β -carotene were larger than empty LNPs, respectively (Table 3.5). Nevertheless, the particle size of loaded LNPs remained lower than 400 nm, as

required for oral administration. No significant changes seemed to occur on the stability of both loaded SLN_4b and NLC_1 since ZP values remained similar to those obtained for empty LNPs. Besides, since β -carotene is less soluble in oil than in fat, the %EE of 3.0 β -SLN is higher than 3.0 β -NLC. Morphological analysis of 3.0 β -NLCs by TEM images showed that the LNPs size was in agreement with DLS results. Besides, TEM analysis also revealed nanoparticles with almost spherical shapes and a rough surface (results not shown).

The values of Z-ave, PDI, ZP, and %EE of rifampicin loaded in the LNPs (with formulation 60 °C; 6.9% LA or 5.5% LA + 1.4% Oil; sonicated, 1.1 or 2.00 mg of RIF added per 1 g of the miniemulsion system) showed as expected that RIF-NLCs were larger than RIF-SLNs (Table 3.6). Besides, LNPs loaded with RIF also reduced the electrical charge at the surface to mean values below the absolute ZP of 20 mV compared with empty SLNs and NLCs. Furthermore, the RIF was entrapped in the lipid matrix of LNPs due to the high RIF solubility in

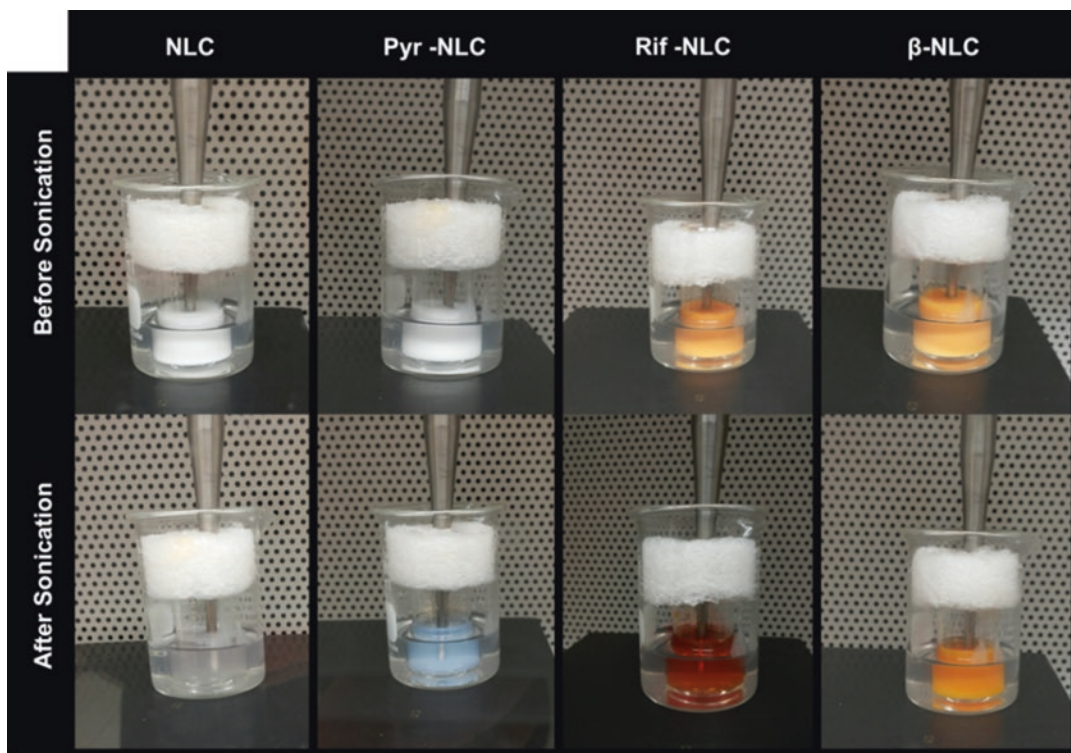


Fig. 3.15 Macroscopic differences exhibited by empty and loaded NLC₄ immediately before and after sonication

Table 3.5 Physicochemical characteristics of the β -carotene incorporated in LNPs (with formulation 60°C, 6.9% La or 5.5% LA + 1.4 oil, sonicated, 3mg β -carotene added per 1 g of the miniemulsion system). Values are mean \pm SD, n = 3

Formulation	Z-Ave (nm)	PDI	ZP (mV)	EE (%)
3.0 β -SLN	281 \pm 19	0.34 \pm 0.03	-29 \pm 5	95 \pm 5
3.0 β -NLC	328 \pm 65	0.28 \pm 0.06	-25 \pm 3	83 \pm 6

Table 3.6 Physicochemical properties of the LNPs loaded with RIF (70 °C; 7.1% LA or 5.7% LA + 1.4 Oil; sonicated, 1.1 and 2.0 mg of RIF added per 1 g of miniemulsion system). Values are mean \pm SD, n = 3

Formulation	Z-Ave (nm)	PDI	ZP (mV)	EE (%)
1.1RIF_SLN	84 \pm 1.0	0.23 \pm 0.01	-17.8 \pm 0.7	69 \pm 1
1.1RIF_NLC	180 \pm 90	0.36 \pm 0.08	-19.5 \pm 0.9	69 \pm 1
2.0RIF_SLN	181 \pm 31	0.34 \pm 0.03	-19.2 \pm 1.3	79 \pm 7
2.0RIF_NLC	215 \pm 5.0	0.28 \pm 0.03	-18.8 \pm 0.6	85 \pm 5

the lipid core, resulting in high entrapment efficiencies for all the formulations, ranging between 69 \pm 1 and 85 \pm 5%. The RIF-NLC entrapped a slightly higher amount of RIF than RIF-SLN when both loaded with 1.1 mg antibiotic per 1 g

of the miniemulsion system. However, no significant differences in %EE were found between RIF-SLNs and RIF-NLCs when testing a RIF concentration of 1.1 mg RIF per 1 g of the miniemulsion system.

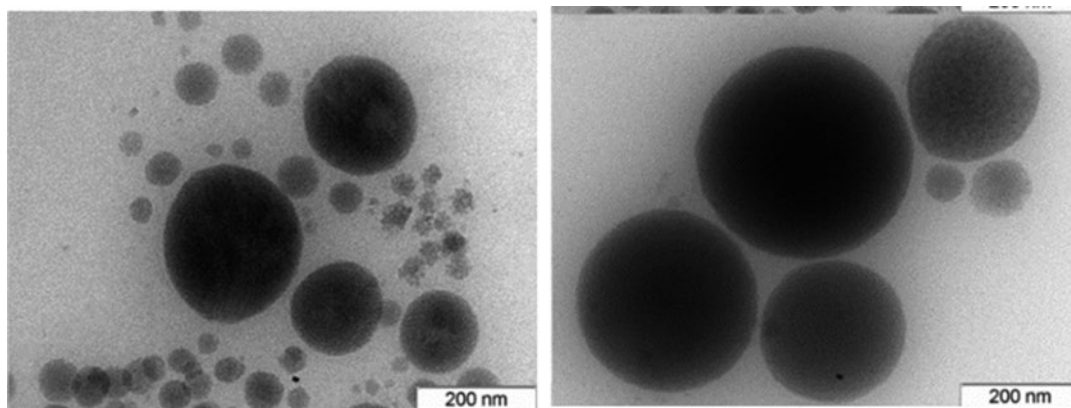


Fig. 3.16 TEM images of rifampicin loaded lipid nanoparticles (RIF-NLCs)

The RIF-NLCs also exhibited spherical shapes as revealed by TEM analysis, indicating that drug loading did not lead to morphological changes. In addition, observed particle sizes agreed with particle size data obtained from dynamic light scattering-analysis (Fig. 3.16).

Two studies in the literature reported the encapsulation of RIF in LNPs. In one study, RIF was loaded into Compritol ATO 888 SLNs, fabricated by a modified microemulsion technique. The particle sizes obtained were 141 ± 13 nm, the ZP value was -3.5 ± 0.8 mV, and the %EE was $65 \pm 3\%$ [68]. In the second study, RIF was encapsulated together with pyrazinamide and isoniazid in a stearic acid SLNs produced by solvent emulsification-diffusion technique with a %EE $51 \pm 5\%$ [69]. The lower %EE of RIF encapsulated was probably due to the fact that RIF was combined with other anti-TB drugs, resulting in a lower % of EE compared to the results here reported. In general, results obtained in this project with the LipNanoCar technology seem to be very good compared with reported results found in the literature. Other advantages include higher entrapment efficiencies, and the organic solvent-free production technology, with lower toxicity levels of the produced LNPs.

The %EE of pyrazinamide (PYZ) loaded in both LNPs ranged from $14 \pm 8\%$ for PYZ-SLN to $29 \pm 15\%$ for PYZ-NLC (Table 3.7).

The low entrapment values are due to the high pyrazinamide hydrophilicity used in the current

chemotherapy against Tuberculosis. The pyrazinamide partitioned between the melted lipid and aqueous phase, and the low encapsulation result is due to the higher solubility of this antibiotic in water (15 mg/mL). This value of %EE is low, especially compared with the value published in the literature of $41 \pm 7\%$ for pyrazinamide encapsulated in SLNs based in stearic acid and entrapment combined with isoniazid and rifampicin [69]. According to the LipNanoCar technology, the cooling process to room temperature can be optimized to control the crystallization process and enhance the entrapment efficiency. However, the best strategy to increase the %EE is the previous synthesis of lipid drug-conjugate of the pyrazinamide with a fatty acid, according to the authors' biocatalysis expertise in miniemulsion systems [30–32].

The TEM analysis of LNPs loaded with PYZ was in good agreement with size measurements by DLS. However, the nanoparticles presented poor spherical shape, with irregular shapes and some aggregates, indicating significant alterations on lipid nanoparticle structure when loaded with PYZ.

The comparison of the encapsulation of rifampicin (Table 3.6), pyrazinamide (Table 3.7), and β -carotene (Table 3.5) shows that the highest percentage of entrapment efficiency was obtained for β -carotene, as it is the most lipophilic of these three active compounds. In contrast, a lower percentage of encapsulation was obtained for pyrazinamide, the more hydrophilic one.

Table 3.7 Physicochemical characteristics of the LNPs loaded with pyrazinamide (60 °C; 7.1% LA or 5.7% LA + 1.4 Oil; sonicated, 1.1 PYZ added per 1 g of the miniemulsion system). Values are mean ± SD, n = 3

Formulation	Z-Ave (nm)	PDI	ZP (mV)	EE (%)
1.1PYZ-SLN	217 ± 87	0.31 ± 0.08	-21.0 ± 0.7	14 ± 8
1.1PYZ-NLC	313 ± 214	0.34 ± 0.17	-22.7 ± 2.4	29 ± 15

3.5 LNPs Loaded with Antibiotics Produced by LipNanoCar Technology for Oral Administration Against Cystic Fibrosis Pathogens

Cystic fibrosis (CF) is an autosomal recessive disorder that affects approximately 70,000 individuals worldwide [89]. CF individuals have viscous secretions in the airways of the lungs and the pancreas vessels. These viscous secretions cause obstruction and inflammation, tissue damage, and later organ destruction. Other organ systems containing epithelia like sweat glands, biliary ducts of the liver, male reproductive tract, and intestine, can also be affected. The loss of pancreatic exocrine function results in malnutrition and weak growth, and diet supplements are usually prescribed to the CF patient [70].

CF airways are prone to infection by bacterial opportunists entering the upper and lower respiratory tract by inhalation or aspiration. These bacteria grow and establish themselves in the lungs, leading to local inflammation and establishing a chronic inflammatory response. The chronic obstruction, infection, and inflammation leads to a lifelong degradation of the lung anatomy and respiratory failure, contributing to premature death and about 80% of CF patients' mortality [71, 72].

The bacteria most commonly found in CF patients' lungs include *Pseudomonas aeruginosa*, *Staphylococcus aureus*, *Haemophilus influenzae*, *Stenotrophomonas maltophilia*, *Achromobacter xylosoxidans*, and bacteria of the *Burkholderia cepacia* complex [72].

The *Burkholderia cepacia* complex (Bcc) comprises at least 24 genetically related Gram-negative bacterial species initially identified in the 1950s as *Pseudomonas cepacia* [73–75]. These bacteria are opportunistic pathogens, espe-

cially in CF patients, and are associated with a worse prognosis and decreased life expectancy. One of Bcc infection's most striking features is the unpredictable clinical outcome, ranging from asymptomatic carriage to the cepacia syndrome, a fatal necrotizing pneumonia often associated with septicemia. The majority of CF patients infected with Bcc develop a chronic infection that can last for years, leading to the progressive loss of lung function [76]. Several Bcc species, in particular, *B. cenocepacia* and *B. multivorans*, are highly transmissible and can quickly spread among CF patients [74, 77].

CF patients are highly susceptible to bacterial respiratory infections. Thus, intensive antibiotic therapy is used to maintain lung function and reduce inflammation in infected patients [72]. The infection eradication caused by bacteria is often unpredictable due to their intrinsic resistance to the vast majority of clinically available antimicrobials [77, 78]. The characterization of bacterial susceptibility profiles can lead to the correct choice of antimicrobial therapy. Current chemotherapies use combinations of two or three antibiotics [76, 78].

The treatment of chronic *P. aeruginosa* with aerosolized antibiotics have emerged, such as tobramycin inhalation solution (TIS) as Bramitob® or inhalation dry powder (TOBI® Podhaler®). Aztreonam lysine (Cayston®) and colistin (Colobreathe®) are also other aerosolized antibiotics. Liposomal amikacin, ciprofloxacin dry powder, levofloxacin inhalation solution, and new combinations of antibiotics and other antimicrobial therapies are in development [72].

For the *Burkholderia cepacia* complex, the current antibiotic treatments include Doxycyclin for oral administration and Meropenem and Tobramycin for intravenous administration [72].

Multiple bacterial barriers decrease antibiotics efficacy. Some of those barriers include bacte-

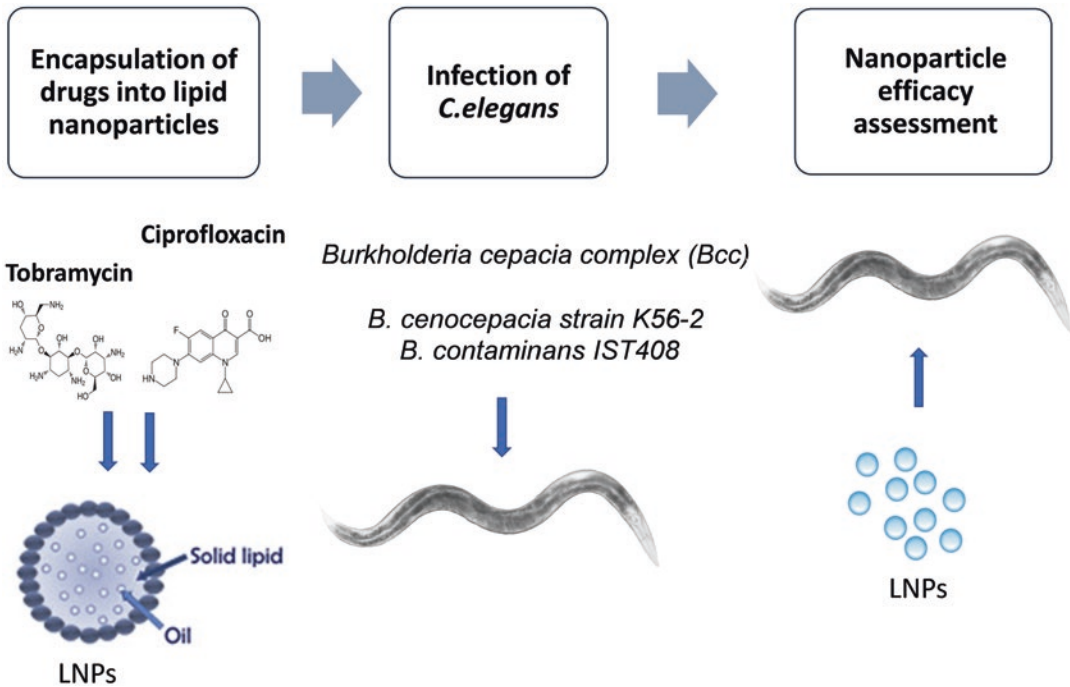


Fig. 3.17 Scheme of antibiotics encapsulation in LNPs and assess their efficacy in bacterial infected *C. elegans*

rial biofilms, impermeable cell walls, and destructive enzymes, and the antibiotics inability to cross the biofilm matrix. In CF, the viscous mucus clogging the airways comprises glycolipids, proteins, glycoproteins, polysaccharides, and DNA. The bacterial cell wall, negatively charged in both Gram-negative and Gram-positive bacteria, is another obstacle. The destructive enzymatic barrier comprises several enzymes produced by bacteria that can modify the antibiotics, rendering their inactivation [79]. These problems can be overcome or minimized through the use of nanoparticles. Nanoparticles can bypass bacterial drug resistance, acting on the alteration of bacteria efflux pump activity, antibiofilm activity, enhanced penetration through biofilms, protection against enzymatic degradation, specific targeting, and sustained-release. Factors that can affect the nanoparticle advantages are the size, surface hydrophobicity, and zeta potential of nanoparticles [79].

The *C. elegans* was used in this work as an animal model of bacterial infection, particularly with

pathogens belonging to the Bcc group (*Burkholderia contaminans* IST408 and *Burkholderia cenocepacia* K56-2). Thus, the LNPs with encapsulated antibiotics (e.g., ciprofloxacin, tobramycin) were fed to infected *C. elegans*, and the efficacy of encapsulated antibiotics into nanoparticles could be assessed (Fig. 3.17).

3.5.1 Preparation of NLCs

The identification and composition formulation used to produce the LNPs to be used against Cystic Fibrosis infections is present in Table 3.8 [37].

3.5.1.1 Differential Scanning Calorimetry (DSC) Analysis of NLCs

NLCs were prepared from a mixture of fatty acids and oil at 70 °C (formulation NLC_1 constituted by 0.5% MA, 0.9% LA, 1.4% CO, 4.9% Tween 80) without the sonication step. No solidi-

Table 3.8 Identification and composition (%w/w) formulation of lipid nanoparticles. The remaining % is Milli Q water

ID	Formulation		
	FA ^a (0.8%)	Oil ^b (1.2%)	Surfactant (4.9%)
NLC_2	SA	CO	Span 80
NLC_3	SA	SFO	Tween 80
NLC_4	SA	SFO	Span 80
NLC_5	LA	SFO	Span 80
NLC_6	MA	SFO	Span 80
NLC_7	PA	SFO	Span 80
NLC_ TOB0.25	SA	SFO	Span 80
NLC_ CIP0.25	SA	SFO	Span 80

TOB0.25 and CIP0.25 corresponding to the amount (0.25 mg) of bioactive compound added per 1 mL of miniemulsion system to produce LNPs

^aFatty acids (FA): SA stearic acid, LA lauric acid, MA myristic acid, PA palmitic acid

^bOil: CO Coconut oil, SFO sunflower oil

fication was detected in this lipid nanoparticle formulation as the melting temperature dropped significantly to 33.0 °C, and this NLC is not solid at body temperature compared to the melting point of 56.3 °C and 46.5 °C of pure myristic acid and lauric acid, respectively (Fig. 3.18).

Based on differential scanning calorimetry, Keles et al. [80] reported that lauric acid and myristic acid are phase change materials with a high melting point. However, their melting point can change and decrease to 37.2 °C when mixed, forming a eutectic mixture [80]. This phenomenon was also observed for other mixtures of fatty acids, such as lauric acid and palmitic acid [81], stearic acid, and lauric acid [82]. Thus, the NLC_1 formulation is better classified as a liquid nanoemulsion than a solid nanostructured lipid carrier.

Empty LNPs prepared using a step of sonication (formulations NLC_2 to NLC_7) were also analyzed by differential scanning calorimetry (DSC). The mean particle size (Z-ave), PDI, ZP, and melting point were obtained for the empty NLCs (formulations NLC_2 to NLC_7) and loaded NLCs (NLC_TOB0.25 and NLC_CIP0.25) and summarized in Table 3.9.

LNPs of formulations NLC_5 and NLC_6 are also not solid at body temperature, but the melting point of these NLCs can be enhanced by increasing the solid lipid amount in the formulation and/or decreasing the oil content.

No significant differences in the melting points were observed for LNPs prepared with different surfactants (NLC_3 with Tween 80 and NLC_4 with Span 80) and different oils (NLC_2 with coconut oil and NLC_4 with sunflower oil). LNPs containing different fatty acids exhibited increasing melting temperatures related to the fatty acid chain's length, as expected.

LNPs loaded with ciprofloxacin (NLC_CIP0.25), and tobramycin (NLC_TOB0.25) were also analyzed by DSC, presenting, respectively, melting points of 59.5 °C and 56.9 °C. These results confirm that these LNPs are solid at body temperature and similar to the corresponding empty nanoparticles (NLC_4) (Fig. 3.19) (Table 3.9).

The shape and morphology of these LNPs were investigated with TEM. Formulation NLC_1 exhibited aggregation of nanoparticles with an average size of 20 nm (Fig. 3.20a) and spherical nanoparticles with approximately 200 nm (Fig. 3.20b). DLS analysis did not detect the small nanoparticle aggregation as a significant population, and a Z-ave of 219 ± 11.0 nm with a PDI of 0.4 ± 0.04 for this formulation was estimated. Those aggregates could correspond to some contamination, or the DLS analysis considered these aggregates as single particles with approximately 200 nm. The formulation corresponding to NLC_4 with 225.9 ± 40.8 nm, PDI of 0.342 ± 0.06, ZP of -56.9 ± 3.72 mV, and a melting point of 58.9 ± 3.72 °C, was selected for further studies.

The first TEM visualization of LNPs prepared with formulations NLC_4, NLC_CIP0.25, or NLC_TOB0.25 was not clear, as a film masked the image, and nanoparticles could not be observed. This film was presumed to be due to the high lipophilicity of Span 80. Therefore, these LNPs were filtered, allowing more explicit TEM images. Empty LNPs with formulation NLC_4 (Fig. 3.21a) and nanoparticles loaded

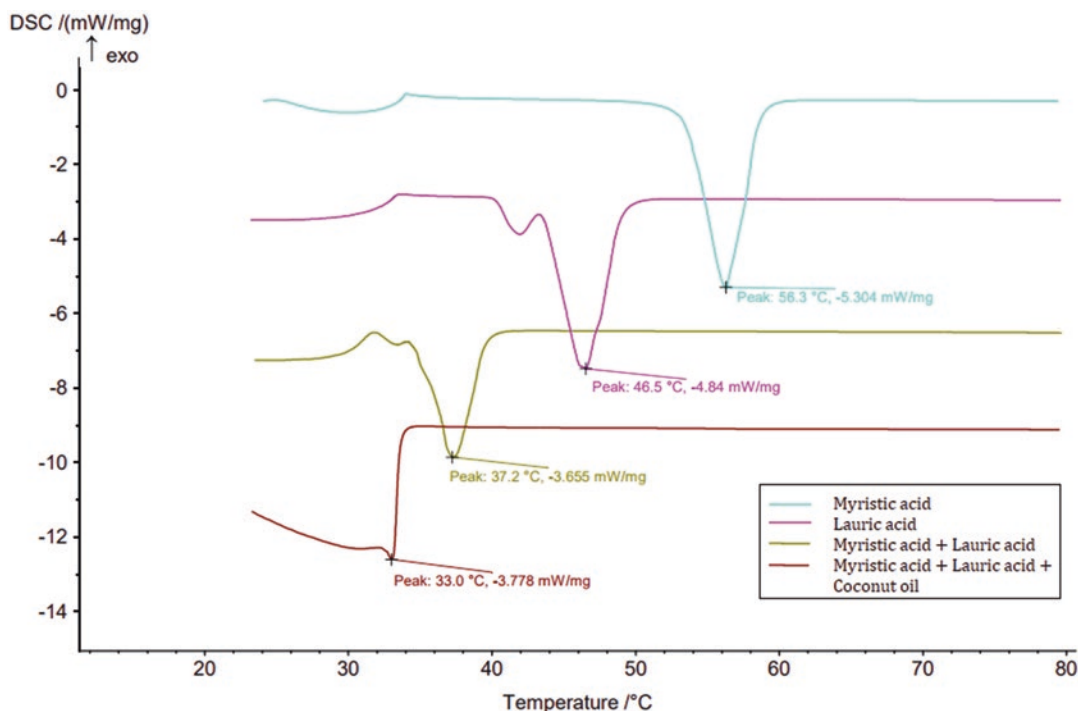


Fig. 3.18 DSC analysis of pure lauric acid (LA) or myristic acid (MA) and a mixture of fatty acids (LA and MA) and different lipids (LA, MA, and coconut oil)

Table 3.9 Melting point of nanoparticles in the formulations NLC_2 to NLC_7

Formulation	Size (nm)	PDI	ZP (mV)	Melting point (°C)
NLC_1	219.0 ± 11.0	0.400 ± 0.04	-20.3 ± 0.52	33.0 ± 1.00
NLC_2	273.8 ± 55.0	0.345 ± 0.08	-52.6 ± 3.42	58.1 ± 0.95
NLC_3	668.1 ± 232.6	0.840 ± 0.08	-24.1 ± 0.65	59.9 ± 0.50
NLC_4	255.9 ± 40.8	0.342 ± 0.06	-56.9 ± 3.72	58.9 ± 2.25
NLC_5	205.6 ± 17.9	0.196 ± 0.07	-54.8 ± 7.30	32.2 ± 1.30
NLC_6	202.4 ± 2.7	0.208 ± 0.03	-47.5 ± 0.90	36.5 ± 1.00
NLC_7	246.3 ± 1.6	0.350 ± 0.02	-50.8 ± 5.05	55.3 ± 0.60
NLC_CIP0.25	258.5 ± 50.7	0.399 ± 0.08	-48.9 ± 4.09	59.5 ± 0.85
NLC_TOB0.25	255.3 ± 63.5	0.325 ± 0.09	-22.0 ± 3.62	56.9 ± 0.30

with tobramycin (Fig. 3.21b) presented a spherical shape and a size of around 200 nm, results similar to those obtained by dynamic light scattering analysis (255.9 ± 40.8 nm and 255.3 ± 63.5 nm, respectively). LNPs loaded with ciprofloxacin were also filtered. However, this procedure did not yield sharp and clear images, although it was possible to observe the nanoparticles (dark spots) with sizes ranging from 100 to 200 nm, similar to DLS analysis (258 ± 50.7 nm) (Fig. 3.21c).

3.5.1.2 Filtration of NLCs Suspension

Antibiotic entrapment efficiency was calculated by quantifying ciprofloxacin and tobramycin in the filtrate obtained after centrifugation of the lipid nanoparticle suspension using a Spin-X® UF centrifugal filter device (Corning, USA). A known concentration of each antibiotic was previously filtrated and then analyzed before and after the centrifugation step. These controls show a filtration efficiency of 99.8% and 88.8% for ciprofloxacin and tobramycin, respectively. The lower

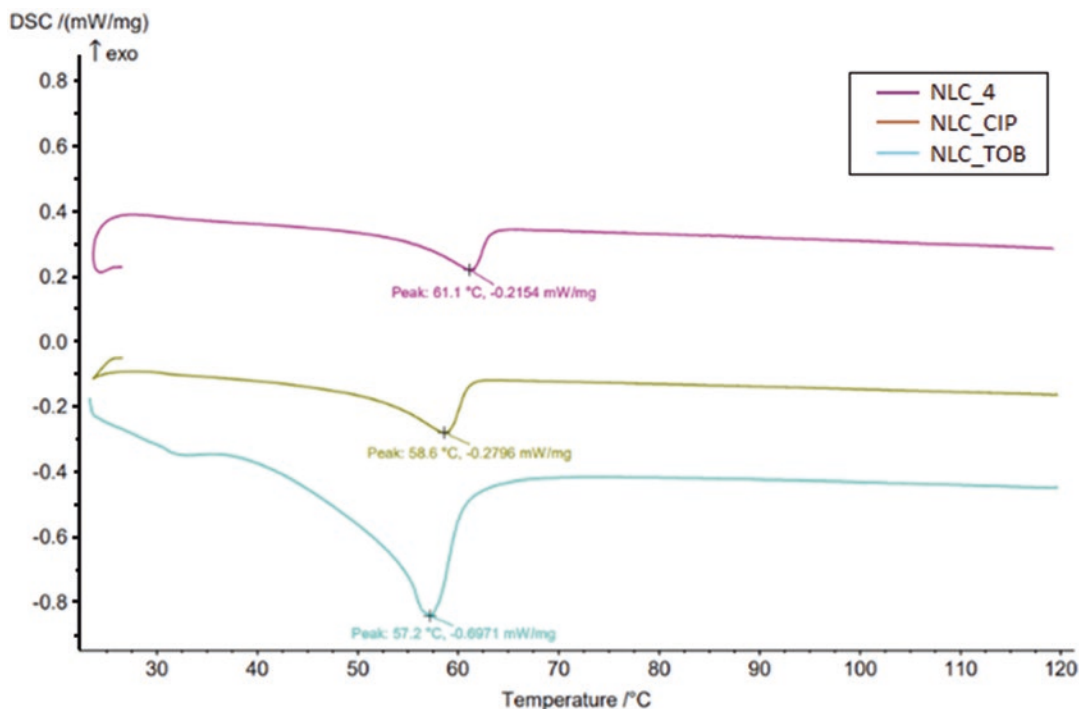


Fig. 3.19 Melting points of empty nanoparticles (NLC_4) and loaded with ciprofloxacin (NLC_CIP0.25) or tobramycin (NLC_TOB0.25)

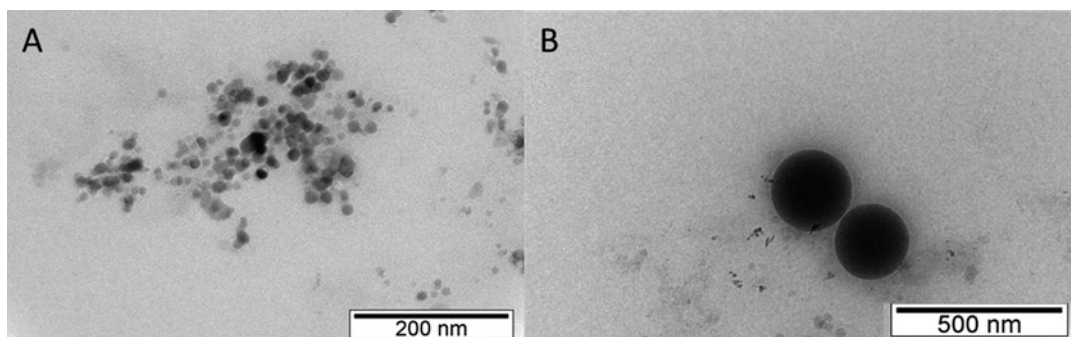


Fig. 3.20 Transmission electron microscopy images of nanoparticles obtained with formulation NLC_1

filtration efficiency for tobramycin is probably due to its high ionic character promoting its absorption on the membrane surface (polyethersulfone - PES).

The integrity of LNPs after the centrifugation step was evaluated by analysis of Z-ave, PDI, and ZP of the two loaded antibiotics before and after the centrifugation step. After centrifugation, nanoparticle size decreased, suggesting that

larger lipid nanoparticles were retained by the smaller size of the pore membrane (cut-off of 10,000 Da) from Corning, USA. The decrease variation of nanoparticle size was 16% to 20%, while ZP values decreased 13 to 18% (Table 3.10).

Additionally, the resulting filtrates from the centrifugation were treated with fluorescamine that can react intensively with amine groups of tobramycin. However, those filtrates did not

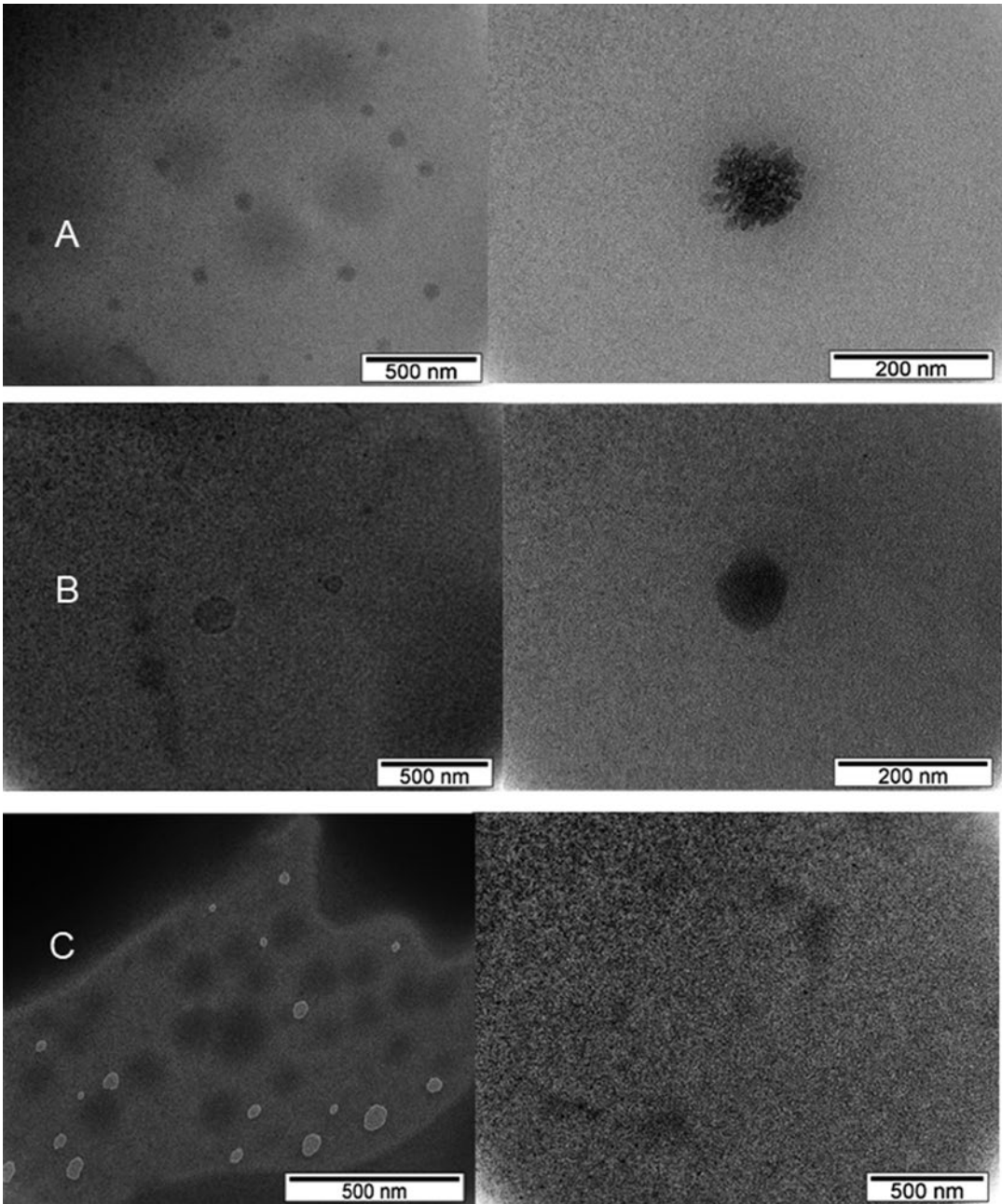


Fig. 3.21 TEM images of empty nanoparticles (a), nanoparticles loaded with tobramycin (b), and nanoparticles loaded with ciprofloxacin (c)

present fluorescence compared to a blank composed of water + fluorescamine, neither with a blank composed of phosphate buffer + fluorescamine, indicating that tobramycin was not present in the filtrate. Consequently, tobramycin

encapsulation efficiency was close to 100%. Furthermore, to check if the tobramycin encapsulation could be quantified by fluorescence analysis, the effect of the temperature or sonication on the antibiotic degradation was assessed. The fluo-

Table 3.10 Average size, PDI, and ZP of nanoparticles loaded with ciprofloxacin (NLC_CIP0.25) or tobramycin (NLC_TOB0.25) before and after filtration

	Z-ave (nm)	Variation (%)	PDI	ZP (mV)	Variation (%)
NLC_CIP0.25 before filtration	253.4 ± 13.9	20	0.384 ± 0.006	-52.8 ± 2.687	13
NLC_CIP0.25 after filtration	202.1 ± 28.2		0.260 ± 0.073	-46.10 ± 2.969	
NLC_TOB0.25 before filtration	316.3 ± 78.6	16	0.405 ± 0.031	-26.70 ± 0.565	18
NLC_TOB0.25 after filtration	264.3 ± 56.9		0.334 ± 0.021	-21.95 ± 0.353	

rescence intensity was measure before and after the heating step. After the heating and sonication steps, the fluorescence intensity of tobramycin remained unchanged.

These results seem to show an unexpectedly high encapsulation efficiency of 100% for tobramycin. This result may be possible due to the 5 primary amino groups that this antibiotic presents that can conjugate to the carboxylic group of the stearic acid, improving the entrapment or encapsulation yield. However, more studies should be performed to determine what occurred with this antibiotic and its quantification directly from the LNPs.

3.5.1.3 Loading the NLCs with Tobramycin, Ciprofloxacin, and Fluorescent Dye (DiOC)

The antibiotics ciprofloxacin and tobramycin were entrapped in LNPs prepared from 0.25 mg of CIP per mL of the miniemulsion system based on the formulation NLC_4. The Z-ave, PDI, and ZP values obtained for these nanoparticles show that the particle size and the polydispersity index (PDI) of these LNPs containing the antibiotics ciprofloxacin (258.5 ± 50.7 nm; 0.399 ± 0.08) and tobramycin (255.2 ± 63.5 nm; 0.324 ± 0.09) were similar to those determined for empty nanoparticles (255.9 ± 40.8 nm; 0.342 ± 0.06) (Table 3.9).

The pH of the lipid nanoparticle suspensions loaded with tobramycin increased (7.58 ± 0.13) compared with empty nanoparticles (5.53 ± 0.34) due to the strong basicity character of tobramycin associated with the 5 primary amino groups in its chemical structure. At that pH (7.58 ± 0.13), the amines are positively charged, leading to an increase of the solution pH. Furthermore, the values of ZP of loaded LNPs slightly decreased for cipro-

floxacin (-48.9 ± 4.09 mV) compared to empty nanoparticles (-56.9 ± 3.72 mV), while nanoparticles loaded with tobramycin exhibited a significant decrease of the ZP (-22.0 ± 3.62 mV) (Table 3.9).

The decrease of the absolute value of ZP of LNPs loaded with tobramycin is due to the more positive charge of this antibiotic at pH 7.5, as tobramycin may be binding to the particle surface or conjugated with the carboxylic group of fatty acid like stearic acid. Stearic acid is negatively charged at this pH value, thus decreasing the ZP of the loaded LNPs.

Different concentrations of each antibiotic (0.25, 0.5, and 1 mg/mL of the miniemulsion system) were also incorporated in the LNPs. The Z-ave, PDI, and ZP values of the loaded LNPs change a little, except for the significant increase of the size of nanoparticles with 1 mg/mL of ciprofloxacin (Fig. 3.22).

LNPs prepared from formulations NLC_4 and respective loaded particles NLC_CIP0.25 and NLC_TOB0.25 were stored at room temperature for 2 months, and their size, PDI, and ZP after one and 2 months after preparation were assessed. Those results showed that loaded nanoparticles with CIP are stable for at least 60 days. In contrast, phase separation occurred in the suspension of nanoparticles loaded with TOB after 1 month (Fig. 3.23). Therefore, we conclude that the LNPs loaded with TOB are not long-term stable, which agrees with the low absolute value of ZP previously obtained (Fig. 3.22).

The LNPs loaded with CIP presented a slight increase of Z-ave, and the absolute value of ZP decreased with storage time compared with empty LNPs with the same formulation (Fig. 3.24).

In order to investigate if the nematode *C. elegans* ingested or not the LNPs, the

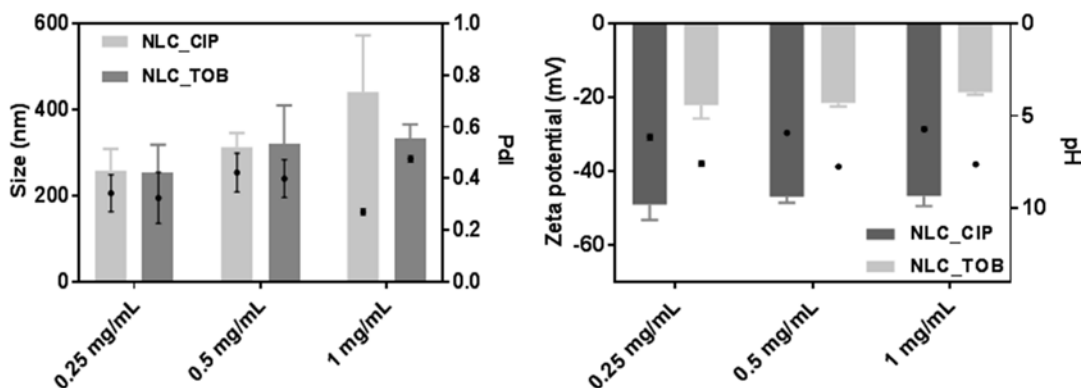


Fig. 3.22 Average size (vertical bars), PDI (black dots), zeta potential (vertical bars), and pH (black dots) of nanoparticles loaded with ciprofloxacin (formulation

NLC_CIP) or tobramycin (formulation NLC_TOB) loaded with 0.25, 0.5, or 1 mg of each antibiotic per mL of the miniemulsion system

Fig. 3.23 Photograph showing the visual aspect of vials containing empty nanoparticles (left) or loaded nanoparticles with tobramycin after 1 month (right)



DiO18(3), a fluorescent dye (Thermo Fisher Scientific), was also entrapped in formulation NLC_4, together with ciprofloxacin or tobramycin. The values of Z-Ave, PDI, and ZP of these LNPs exhibited an increase in the size and a higher polydispersity index than the empty LNPs (Table 3.11).

3.5.1.4 Optimization of Ciprofloxacin Loading in NLCs

Different ciprofloxacin concentrations (0.25, 0.5, and 1 mg per mL of the miniemulsion system) were tested into lipid nanoparticle formulations. Entrapment efficiency was calculated by the

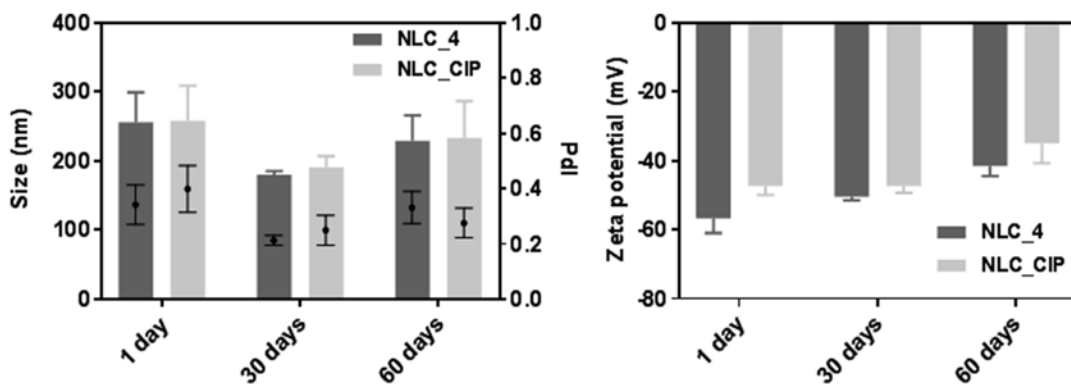


Fig. 3.24 Size, PDI, and Zeta potential of nanoparticles obtained with empty formulation (NLC_4) and loaded formulations (NLC_CIP0.25) measured after 1, 30, and 60 days after production

Table 3.11 Average size, PDI, and ZP of nanoparticles prepared with formulations NLC_4, NLC_CIP0.25, or NLC_TOB0.25 together with a fluorescent dye (DiOC)

	Size (nm)	PDI	ZP (mV)
NLC_4	255.9 ± 40.8	0.342 ± 0.06	-56.9 ± 3.72
NLC_Dio	334.9 ± 5.2	0.608 ± 0.05	-50.3 ± 1.80
NLC_DioCIP0.25	309.0 ± 11.2	0.552 ± 0.09	-52.8 ± 0.78
NLC_DioTOB0.250	321.7 ± 6.9	0.405 ± 0.03	-22.9 ± 0.45

HPLC quantification ciprofloxacin present in filtrates resulting from the centrifugation step of loaded lipid nanoparticle suspensions. Encapsulation efficiencies of nanoparticles loaded with 0.25, 0.5, and 1 mg of ciprofloxacin per mL of the miniemulsion system (formulation NLC_CIP) were, respectively, $68.16 \pm 4.9\%$, $67.26 \pm 8.27\%$, and $64.11 \pm 9.99\%$ (Fig. 3.25).

Drug loading capacity is defined as the percentage of drugs incorporated into the lipid nanoparticles relative to the total weight of the lipid phase. The drug loading capacities of nanoparticles loaded with 0.25, 0.5, and 1 mg of ciprofloxacin per mL of miniemulsion system (formulation NLC_CIP) were, respectively, $0.79 \pm 0.10\%$, $1.84 \pm 0.03\%$, and $4.46 \pm 0.44\%$ (Fig. 3.25). The amount of ciprofloxacin added into the formulation was between 5 and 20 mg of antibiotic for 400 mg nanoparticle carriers.

Jain and Banerjee [83] obtained an %EE ranging from $8.66\% \pm 1.64\%$ to $38.71\% \pm 2.38\%$ for SLN formulations prepared by the microemul-

sion technique, while Ghaffari et al. [84] obtained an %EE of $88 \pm 4.5\%$ using the emulsification-sonication method. Shazly [85] obtained an %EE of 73.94% for SLNs with stearic acid prepared by the emulsification-sonication method.

The nature of the lipid used to prepare LNPs significantly impacts the different formulations' entrapment efficiency and drug loading capacity. Different lipids with distinct chemical properties can be used to optimize the maximum percentage of drug encapsulation. Additional studies should be performed to determine the maximum drug loading capacity of these NLCs formulations.

3.5.1.5 Ciprofloxacin Release Profile from NLCs

Studies of ciprofloxacin release from the LNPs were performed with dialysis tubing, a semi-permeable membrane that facilitates the exchange of molecules in solution. Lipid nanoparticle suspension was poured into the dialysis tubing, with an external medium com-

Fig. 3.25 Encapsulation efficiency (vertical bars) and drug loading capacity (black dots) of nanoparticles loaded with different amounts of ciprofloxacin (0.25, 0.5, and 1 mg of CIP per mL of the miniemulsion system)

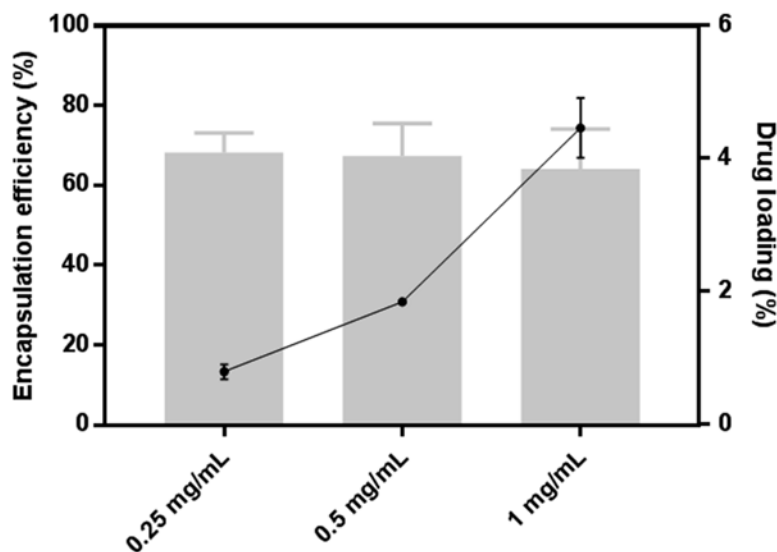
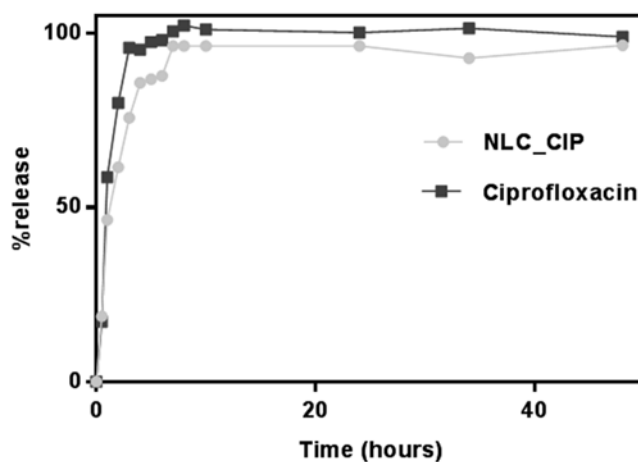


Fig. 3.26 Release ciprofloxacin profile from nanoparticles (Formulation NLC_CIP0.25) and free ciprofloxacin over 48 h



posed of phosphate buffer pH = 7.4. Phosphate buffer samples were taken at different times, and ciprofloxacin was quantified by HPLC. The diffusion through the dialysis tubing of free ciprofloxacin was also analyzed and measured as a control.

The release profile of ciprofloxacin from LNPs and free ciprofloxacin is shown in Fig. 3.26. The release profile shows a burst release, with the drug being released within the first 7 h (96% release at $t = 7$ h). Ciprofloxacin encapsulated in the LNPs had a slightly slower release than free antibiotics (95% release at $t = 3$ h).

Table 3.12 Characterization of lipid nanoparticles (NLC_CIP0.25) before and after the release profile studies

	Z-Ave (nm)	PDI
Initial NLC	230.4 ± 1.6	0.363 ± 0.028
Final NLC	777.1 ± 732.3	0.678 ± 0.288

Before and after the release studies, the Z-ave and PDI analysis suggest that most LNPs have disrupted due to the higher average size (777.15 ± 732.3 nm) and the polydispersity index of the final suspension (Table 3.12).

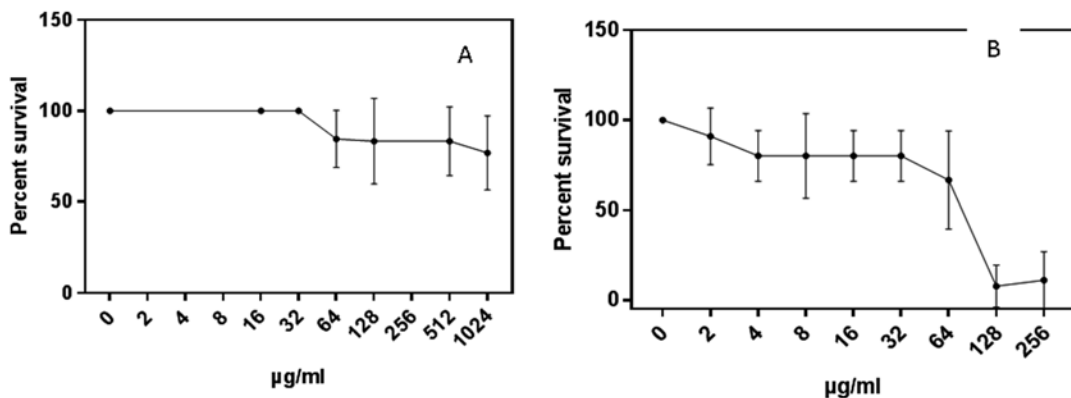


Fig. 3.27 Percentage of *C. elegans* survival when cultivated in the presence of the indicated concentrations of ciprofloxacin (a) and tobramycin (b)

These results suggest that ciprofloxacin is close to the lipid nanoparticle surface described by an imperfect type of structure at the nanoparticle surface, as the antibiotic quickly diffuses when in contact with the release medium (phosphate buffer). The early phase of release corresponds to ciprofloxacin at the nanoparticles' surface, while the delayed phase is due to entrapped antibiotic that diffuses from the solid lipid matrix structure [83].

Jain and Banerjee [83] produced five different types of nanoparticles of albumin, gelatin, chitosan, and SLNs with ciprofloxacin. Chitosan and gelatin nanoparticles released the antibiotic for 96 h, whereas drug release from SLNs occurred for up to 80 h. On the other hand, free ciprofloxacin hydrochloride showed a burst release with almost 50% free drug released in 30 min and more than 90% drug diffusing in 70 min [83]. Their results suggest SLNs as promising carriers for sustained ciprofloxacin release. Shazly [85] produced SLNs with different lipids and nanoparticles formulated with only stearic acid that displayed a burst release profile and faster release. These authors proposed that this could be due to the fast dissolution of ciprofloxacin molecules present at the surface layer of the SLNs. Ghaffari et al. [84] also obtained a similar release profile for ciprofloxacin encapsulated into SNLs with a significant burst effect.

3.5.2 *In Vivo C. Elegans* Toxicity Assay of Tobramycin and Ciprofloxacin

The percentage of *C. elegans* survival in a liquid medium containing different tobramycin and ciprofloxacin concentrations was evaluated. Our results indicate that tobramycin has a higher toxic effect on the nematode when compared to ciprofloxacin. Exposure to tobramycin concentrations ranging from 2 to 256 µg/mL led to a decreased survival of the nematodes from, respectively, 80% to only 11% (Fig. 3.27b). Kaplan et al. [86] presented a study where *C. elegans* infected with pathogens (e.g., *S. aureus*) were exposed to tobramycin with a concentration equally low (1.25 µg/mL).

In this work, *C. elegans* exposed to ciprofloxacin presented a maximum survival percentage for antibiotic concentrations up to 32 µg/mL, and even for the highest concentration tested (1024 µg/mL), a survival percentage close to 80% was registered (Fig. 3.27a).

The Minimal Inhibitory Concentration (MIC) values of ciprofloxacin determined for the exponentially growing bacterial strains *B. contaminans* IST408 (0.54 µg/mL) and *B. cenocepacia* K56-2 (2.66 µg/mL) are lower than the ciprofloxacin concentrations with high survival of *C. elegans*.

However, the tobramycin MIC value for *B. contaminans* IST 408 was 5300 µg/mL, while for strain

B. cenocepacia K56–2 this antibiotic showed no efficacy for the concentrations tested. These values are high above the 256 µg/mL concentration that caused about 80% of the mortality of *C. elegans*.

The visual inspection of the nematodes morphology carried out with a stereoscope's aid revealed that *C. elegans* were smaller in medium supplemented with antibiotics compared to controls without antibiotics (results not shown).

3.5.3 *In Vivo C. elegans* Toxicity Assay of LNPs

In this work, the first LNPs tested for toxicity in *C. elegans* were prepared with formulation (NLC_1). This formulation showed to be extremely toxic to the nematodes as the worms died and formed agglomerates after contact with these lipid nanoparticles (Fig. 3.28).

Similar results were observed when using nanoparticles prepared with formulation NLC_5. These formulations had in common lauric acid. Based on these results, we hypothesized that this fatty acid caused high and almost instantaneous nematodes mortality. Another possibility is some trace impurity in the fatty acid composition that negatively affects the worm's survival. In 1994, Stadler et al. [87] investigated fatty acids and other compounds with nematocidal activity towards

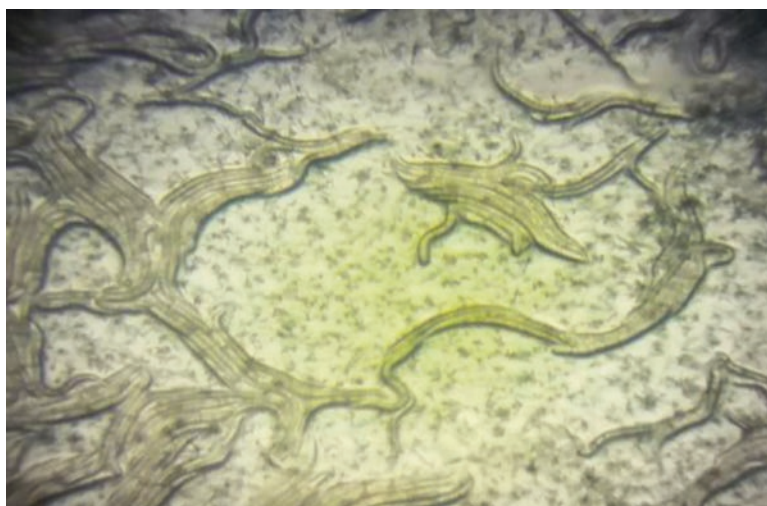
C. elegans at the L4 larval stage after 18 h of exposure. Fatty acids were found to exhibit low values of LD₅₀ (dose required to kill half of the members of a tested population) for *C. elegans*. Reported values include: lauric acid LD₅₀ = 25 µg/mL, myristic acid LD₅₀ = 5 µg/mL, palmitic acid LD₅₀ = 25 µg/mL, and stearic acid LD₅₀ = 50 µg/mL [87].

3.5.4 Ingestion of LNPs Loaded with DiOC Fluorescent Dye by *C. elegans*

The fluorescent dye DiOC was incorporated into the emulsion formulation to confirm that the worms ingested the LNPs. The fluorescent dye was encapsulated together with each antibiotic, ciprofloxacin, or tobramycin. After 3 h of exposure to LNPs loaded with DiOC, *C. elegans* were observed by fluorescence microscopy. Images obtained show green fluorescence along with the worms' digestive system, indicating that they ingested the LNPs (Fig. 3.29).

Remarkably, we observed that only a few worms were fluorescent after exposure to LNPs loaded with tobramycin, in contrast with the more significant number of fluorescent worms detected upon exposure to LNPs loaded with ciprofloxacin and the dye.

Fig. 3.28 Image of *C. elegans* after exposure of nanoparticles prepared with formulation NLC_1. All worms were dead after 2 min



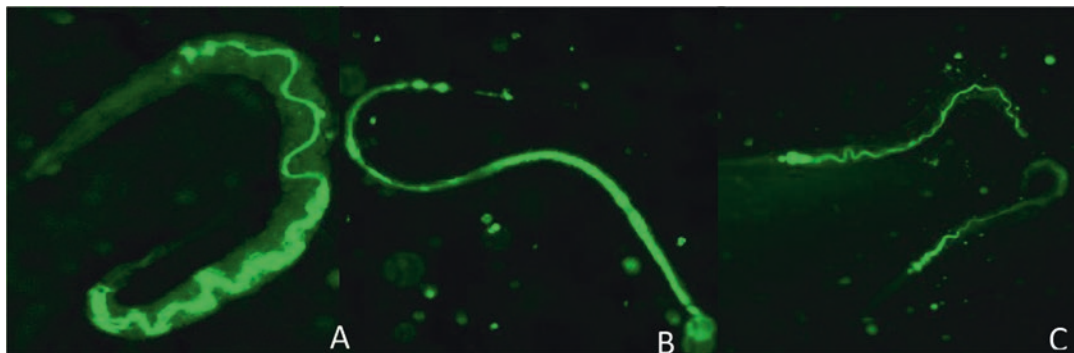


Fig. 3.29 Microscopy images of *C. elegans* fed with nanoparticles containing fluorescent dye and the antibiotics ciprofloxacin or tobramycin. (a) nanoparticles loaded

with DiOC; (b) nanoparticles loaded with ciprofloxacin and DiOC; (c) nanoparticles loaded with tobramycin and DiOC

3.5.5 *C. elegans* as an Animal Model of Bacterial Infection to Assess Antibiotic Delivery Efficiency Using LNPs

To evaluate the efficacy of LNPs loaded with ciprofloxacin or tobramycin against pathogenic bacteria, we have first compared the survival percentages of worms feeding on the non-pathogenic *E.coli* OP50 in the absence and presence of empty or ciprofloxacin-loaded lipid nanoparticles. Control experiments with no nanoparticles were also carried out. About 29.7% of mortality occurred among the worms exposed to empty nanoparticles, while 28.92% of mortality was observed for worms exposed to nanoparticles loaded with ciprofloxacin (Fig. 3.30).

Therefore, the mortality of worms exposed to empty LNPs or nanoparticles containing ciprofloxacin is not significantly distinct ($P = 0.9074$). However, results obtained with each formulation tested is significantly different for those obtained with no nanoparticles ($P < 0.0001$). Altogether these results indicate that these LNPs present some toxicity to the worms, nevertheless lower than demonstrated with LNPs with formulation NLC_1.

Next, we assessed the survival percentage of infected worms with *B. contaminans* IST408 or *B. cenocepacia* K56–2, using the same conditions as those described above for *E. coli* OP50.

Worms infected with *B. cenocepacia* strain K56–2 presented a mortality rate of 45.24% for

the control with no nanoparticles, 38.71% for empty nanoparticles, and 36.87% in the presence of nanoparticles loaded with ciprofloxacin (Fig. 3.31).

The small difference observed in the survival of infected worms exposed or not to empty or ciprofloxacin-loaded nanoparticles is not statistically significant, according to the Mantel-Cox statistical model using the log-rank. In a study published by Cardona et al. [88], the survival rate percentage of worms infected with *B. cenocepacia* K56–2 was 22% on day 2. The difference of percentage compared with this assay is possibly due to different developmental stages of the *C. elegans* used (L2 larval stage worms used in this study, while Cardona et al. [88] used L4 larval stage worms). After 3 days, the *C. elegans* infected with *B. cenocepacia* K56–2 were visibly smaller than those feeding only on *E. coli* OP50 and laid eggs after this period.

C. elegans infected with *B. contaminans* IST408 for 3 days presented mortality rates of 84.5% for the control without nanoparticles, 87.8% for the control with empty nanoparticles, and 77.5% when nanoparticles loaded with the antibiotic ciprofloxacin (Fig. 3.32). The difference observed in worm mortality in the presence of empty nanoparticles or nanoparticles loaded with ciprofloxacin had a p-value of 0.0061, indicating that survival curves were statistically significant. Worms infected in the 3 conditions exhibited the typical morphological aspect of

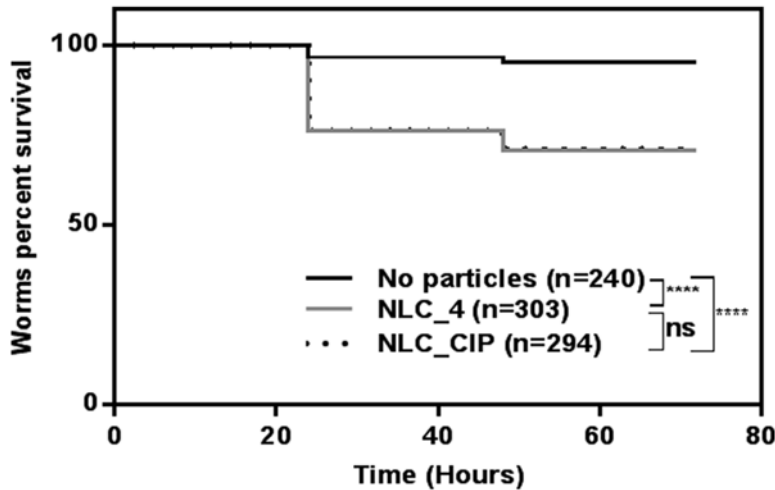
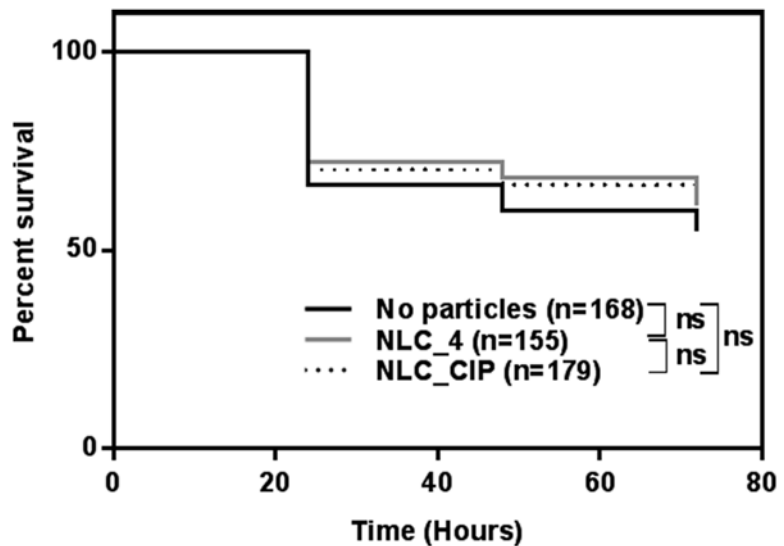


Fig. 3.30 Survival (%) of worms in the absence of nanoparticles, empty nanoparticles (formulation NLC_4), and nanoparticles loaded with ciprofloxacin (formulation NLC_CIP0.25) when feeding on the non-pathogenic *E. coli*

OP50. The survival curves compared using the log-rank (Mantel-Cox) test, and the p-value is represented by * when $P < 0.05$, **when $P < 0.01$ *** when $P < 0.001$, **** when $P < 0.0001$ or ns (not significant), n, number of worms

Fig. 3.31 Percentage survival of worms infected with *B. cenocepacia* K56-2 in the absence of nanoparticles, empty nanoparticles (NLC_4), or nanoparticles with ciprofloxacin (NLC_CIP0.25). The survival curves compared using the log-rank (Mantel-Cox) test, ns (not significant), n, number of worms



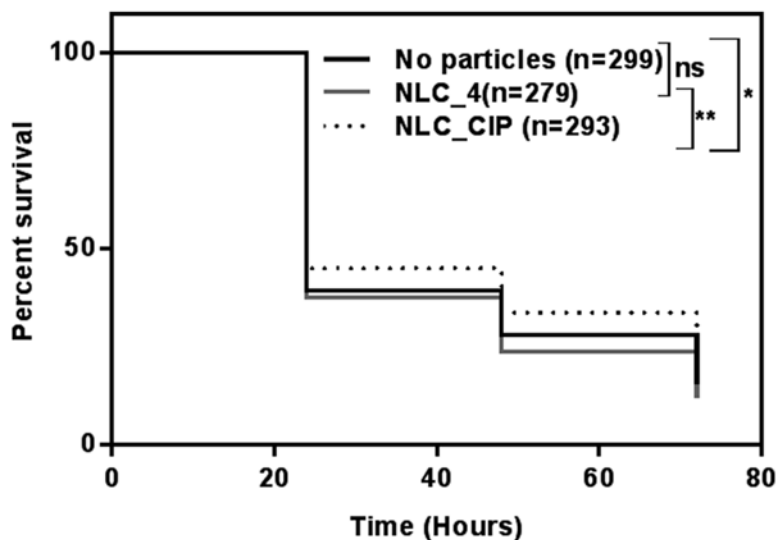
infected *C. elegans*: smaller size and distended intestine.

Sousa et al. [89] reported that 80% of the mortality of *C. elegans* after 3 days of infection by *B. contaminans* IST408. The slight differences in the reported survival rate compared to the present work might be due to using distinct

C. elegans strains, DH2 in Sousa et al. [89], and BN2 in this study.

C. elegans presents many advantages as a biological model to study bacterial pathogens and antimicrobial therapies, including the use of nanoparticles loaded with antibiotics. Among these advantages, it is worth to mention oral

Fig. 3.32 Percentage survival of *B. contaminans* IST408-infected worms in the absence of nanoparticles or the presence of empty nanoparticles (formulation NLC_4) and nanoparticles loaded, ns (not significant), n, number of worms



absorption as the main route of drug administration. In this study, worms were used as an *in vivo* animal model to evaluate the oral absorption and efficacy of LNPs and their toxicity. Even though LNPs presented some toxicity for *C. elegans*, the fatty acid tested in this work are natural food substances and recognized generally as safe, according to FDA. Span 80 and Tween 80 are considered as food additives allowed for direct addition to food products for human consumption [90].

The amount of ciprofloxacin loaded in the LNPs used in rescue experiments with infected *C. elegans* was 32 $\mu\text{g}/\text{mL}$. Our results indicate that ciprofloxacin is more effective against *B. contaminans* IST408 compared to *B. cenocepacia* K56–2, in good agreement with the results of rescue experiments with infected *C. elegans*. However, for the 32 $\mu\text{g}/\text{mL}$ concentration used, differences in the *B. cenocepacia* K56–2 survival were expected, as the MIC value for this strain was only 2.66 $\mu\text{g}/\text{mL}$. However, the effective antibiotic concentration in the worm's intestine should be lower than the MIC value when applied at the surface of the culture plates because it depends on the ingestion of the lipid nanoparticles by the nematode.

For future studies, different pathogens have to be chosen to assess the efficacy of LNPs loaded with tobramycin, since tobramycin is not effec-

tive against the tested strains *B. cenocepacia* K56–2 and *B. contaminans* IST408.

3.6 Conclusions and Perspectives

The formulations of lipid nanoparticles (e.g., SLNs and NLCs) tested and produced according to the LipNanoCar technology, with particle size below 400 nm, are ideal for oral administration as they cross the intestinal cells easily. Inclusive, some formulations led to a particle size below 200 nm, which is an even better result since these particles will remain invisible to the reticuloendothelial system (RES) and kept in the circulation system over a prolonged time. Transmission electron microscopy images of these nanoparticles showed their spherical shape and confirmed the particle size of approximately 200 nm. Thermal analysis (DSC) also showed that these lipid nanoparticles are solid at body temperature for an adequate formulation.

The Zeta Potential of lipid nanoparticles was negative enough to ensure their excellent physical stability, indicating Lutensol AT 50, Tween 80, and mainly Span 80 as suitable surfactants for lipid nanoparticle production. However, the zeta potential of lipid nanoparticles with tobramycin was much lower, as this antibiotic with 5 amino

groups interferes with the composition and surfactant aggregation in the emulsion interface. The low ZP of the lipid nanoparticle suspensions loaded with tobramycin led to phase separation in less than 1 month compared with the several months of long-term stability of lipid nanoparticles loaded with the other antibiotics tested in this work.

Filtration of lipid nanoparticle suspensions was a successful process to remove the excess of water. Nevertheless, lyophilization seems to be a better alternative by simultaneously removing the excess of water and enhancing the particles' stability during storage. Besides, the resulting powders can be used to produce classic solid dosage forms that can be redispersed in water or juice before administration or used to filling hard gelatine capsules.

Rifampicin, ciprofloxacin, tobramycin, and β -carotene were successfully loaded into the lipid nanoparticles with entrapment and encapsulation efficiencies higher than 85%. Rifampicin encapsulation efficiencies (69 to 85%) obtained in this work were higher than those reported in the literature. Contrastingly, low encapsulation efficiencies were achieved for Pyrazinamide, most probably due to its high hydrophilicity, leading to a low partition into the lipid phase than in the aqueous phase.

Ciprofloxacin presented a quick-release from the lipid nanoparticle using a dialysis tubing (96% in the first 7 h), but slower than the free antibiotic (95% in the first 3 h). This result suggests that ciprofloxacin is loaded near the external surface of the lipid nanoparticle.

C. elegans was used as an animal model of bacterial infection, and strains belonging to the Bcc group were used as models of difficult to eradicate Cystic Fibrosis pathogens such as *B. contaminans* IST408 and *B. cenocepacia* K56–2. For the first strain, significant differences were observed between nanoparticles with ciprofloxacin and the control without nanoparticles (p -value<0.05) and between empty nanoparticles and loaded nanoparticles with the antibiotic (p -value<0.01). In the case of *B. cenocepacia*

K56–2, no significant difference was observed in rescue experiments without nanoparticles or with nanoparticles loaded with the antibiotic.

Fluorescence microscopy confirmed the uptake of the lipid nanoparticles, and their efficacy was successfully tested in *C. elegans*. This nematode was used as an alternative model to mimic the GI tract conditions for drug delivery systems for oral route administration. These studies are usually performed with the Caco-2 cell line to evaluate the cytotoxicity and uptake of lipid nanoparticles.

LipNanoCar technology was revealed to be simple, reproducible, allowing the preparation of lipid nanoparticles without the need for organic solvents or any sophisticated instruments. The technology has the potential of easy scale-up for industrial production. The nanocarriers produced by the LipNanoCar technology are based on the *GRAS status* Oil in Water (O/w) Liquid Lipid Nano-emulsions and Solid Lipid Nanoparticles characterized by:

- Water used as a solvent in the range of 50–90% (w/w),
- No use of organic solvents, toxic compounds, or endocrine-disrupting chemicals,
- The nanocarriers formulations are all based on materials (e.g., oils, glycerides, emulsifiers, medium/long fatty acids, hydrophobic compounds, among others) with *GRAS status*,
- The liquid lipid and solid lipid nanocarriers contain fatty acids that are liquid and solid at room temperature, respectively,
- These nanocarriers have an average size ranging from 50 to 350 nm, with a low polydispersity index (PDI),
- The average size of the nanocarriers allows their sterilization by simple microfiltration (0.45 μ m),
- The nanocarriers can be formulated to have zeta potentials in the range of –50 to –25 mV, avoiding liquid nano-droplet coalescence and lipid nanoparticles aggregation,
- The right formulation and the zeta potential values contribute to the production of lipid

nanoemulsions and lipid nanoparticles stable in water/aqueous solution for several months.

- The nanocarriers have high loading capacities at least 10–50% (w/w) for hydrophobic bioactive compounds and low for hydrophilic compounds (e.g., pyrazinamide), which can be easily improved by previous lipid conjugation strategy.

Acknowledgments The authors thank Fundação para a Ciência e a Tecnologia (FCT) and IBB – Institute for Bioengineering and Biosciences for funding through project UIDB/04565/2020.

References

- Fahr A, Liu X (2007) Drug delivery strategies for poorly water-soluble drugs. *Expert Opin Drug Deliv* 4:403–416
- Jaiswal P, Gidwani B, Vyas A (2016) Nanostructured lipid carriers and their current application in targeted drug delivery. *Artif Cell Nanomed B* 44(1):27–40
- Weissig V, Petting TK, Murdock A (2014) Nanopharmaceuticals (part 1): products on the market. *Int J Nanomedicine* 9:4357–4373
- Beloqui A, Solinís MA, Rodríguez-Gascón A, Almeida AJ, Prêat V (2016) Nanostructured lipid carriers: promising drug delivery systems for future clinics. *Nanomed-Nanotechnol* 12(1):143–161
- Attama AA, Momoh MA, Builders PF (2012) Lipid nanoparticulate drug delivery systems : a revolution in dosage form design and development. In: *Recent advances in novel drug carrier systems*. <https://doi.org/10.5772/50486>
- Chauhan I, Yasir M, Verma M, Singh AP (2020) Nanostructured lipid carriers: a groundbreaking approach for transdermal drug delivery. *Adv Pharm Bull* 10(2):150–165
- Weber S, Zimmer A, Pardeike J (2014) Solid lipid nanoparticles (SLN) and nanostructured lipid carriers (NLC) for pulmonary application: a review of the state of the art. *Eur J Pharm Biopharm* 86(1):7–22
- Subramaniam B, Siddik ZH, Nagoor NH (2020) Optimization of nanostructured lipid carriers: understanding the types, designs, and parameters in the process of formulations. *J Nanopart Res* 22:141. <https://doi.org/10.1007/s11051-020-04848-0>
- Gordillo-Galeano A, Mora-Huertas CE (2018) Solid lipid nanoparticles and nanostructured lipid carriers: a review emphasizing on particle structure and drug release. *Eur J Pharm Biopharm* 133:285–308
- Muchow M, Maincent P, Muller RH (2008) Lipid nanoparticles with a solid matrix (SLN®, NLC®, LDC®) for oral drug delivery. *Drug Dev Ind Pharm* 34(12):1394–1405
- Müller RH, Mäder K, Gohla S (2000) Solid lipid nanoparticles (SLN) for controlled drug delivery – a review of the state of the art. *Eur J Pharm Biopharm* 50:161–177
- Garud A, Singh D, Garud N (2012) Solid lipid nanoparticles (SLN): method, characterization and applications. *Int Curr Pharm J* 1:384–393
- Das S, Chaudhury A (2011) Recent advances in lipid nanoparticle formulations with solid matrix for oral drug delivery. *AAPS Pharm Sci Tech* 12(1):62–76
- Haider M, Abdin SA, Kamal L, Orive G (2020) Nanostructured lipid carriers for delivery of chemotherapeutics: a review. *Pharmaceutics* 12(3):288
- Van de Waterbeemd H (1998) The fundamental variables of the biopharmaceutics classification system (BCS): a commentary. *Eur J Pharm Sci* 7:1–3
- Neupane YR, Sabir MD, Ahmad N, Ali M, Kohli K (2013) Lipid drug conjugate nanoparticle as a novel lipid nanocarrier for the oral delivery of decitabine: ex vivo gut permeation studies. *Nanotechnology* 24:1–11
- Lucks S, Müller R (1999) Medication vehicles made of solid lipid particles (solid lipid nanospheres-SLN). *EP Patent* 0,605,497
- Lippacher A, Müller R, Mader K (2000) Investigation on the viscoelastic properties of lipid based colloidal drug carriers. *Int J Pharm* 196:227–230
- Parhi R, Suresh P (2012) Preparation and characterization of solid lipid nanoparticles – a review. *Curr Drug Discov Technol* 9:2–16
- Kentish S, Wooster TJ, Ashokkumar M, Balachandran S, Mawson R, Simons L (2008) The use of ultrasonics for nanoemulsion preparation. *Innov Food Sci Emerg Technol* 9:170–175
- Kim B-D, Na K, Choi H-K (2005) Preparation and characterization of solid lipid nanoparticles (SLN) made of cacao butter and curdlan. *Eur J Pharm Sci* 24:199–205
- Shinoda K, Saito H (1969) The stability of O/W type emulsions as a function of temperature and the HLB of emulsifiers: the emulsification by PIT-method. *J Colloid Interface Sci* 30(2):258–263
- Montenegro L, Campisi A, Sarpietro MG, Carbone C, Acquaviva R, Raciti G, Puglisi G (2011) In vitro evaluation of idebenone-loaded solid lipid nanoparticles for drug delivery to the brain. *Drug Dev Ind Pharm* 37:737–746
- Sjöstrom B, Kronberg B, Carlfors J (1993) A method for the preparation of submicron particles of sparingly water-soluble drugs by precipitation in oil-in-water emulsions. I: influence of emulsification and surfactant concentration. *J Pharm Sci* 82:579–583
- Battaglia L, Gallarate M, Panciani PP, Ugazio E, Sapino S, Peira E, Chirio D (2014) Techniques for the preparation of solid lipid nano and microparticles. *Appl Nanotechnol Drug Deliv*:51–75

26. Mehnert W, Mäder K (2001) Solid lipid nanoparticles: production, characterization and applications. *Adv Drug Deliv Rev* 47:165–196
27. Ganesan P, Naruyanasamy D (2017) Lipid nanoparticles: different preparation techniques, characterization, hurdles, and strategies for the production of solid nanoparticles and nanostructured lipid carriers for oral drugs delivery. *Sustain Chem Pharm* 6:37–56
28. Solans C, Esquena J, Forgiarini AM, Uson N, Morales D, Izquierdo P (2002) Nanoemulsions: formation and properties. In: Mittal KL, Shah DO (eds) *Surfactants in solution: fundamentals and applications*. Springer, New York
29. Lourenço NMT, Matias SC, Altas MC, Fonseca LP (2015) Low-temperature enzymatic hydrolysis resolution in mini-emulsion media. *Chem Pap* 69(6):810–816
30. de Barros DPC, Pinto F, Pfluck ACD, Dias ASA, Fernandes P, Fonseca LP (2018) Improvement of enzyme stability for alkyl esters synthesis in miniemulsion systems by using media engineering. *J Chem Technol Biotechnol* 93(5):1338–1346
31. Birolli WG, Porto ALM, Fonseca LP (2020) Miniemulsion in biocatalysis, a new approach employing a solid reagent and an easy protocol for product isolation applied to the aldol reaction by *Rhizopus niveus* lipase. *Bioresour Technol* 297:122441
32. Lourenço JMP (2016) Synthesis of nutraceuticals (DHA and/or EPA – nicotinol esters) by enzymatic esterification, Fonseca LP, Supervisor, Master thesis in biological engineering, Instituto Superior Técnico, University of Lisbon, Portugal. <https://fenix.tecnico.ulisboa.pt/cursos/mebiol/dissertacao/283828618789726>
33. Pinto F, de Barros DPC, Fonseca LP (2018) Design of multifunctional nanostructured lipid carriers enriched with α -tocopherol using vegetable oils. *Ind Crop Prod* 118:149–159
34. Pinto F, de Barros DPC, Reis C, Fonseca LP (2019) Optimization of nanostructured lipid carriers loaded with retinoids by central composite design. *J Mol Liq* 293:111468
35. Lopes CPA (2014) Development and characterization of lipid nanoparticles prepared by miniemulsion technique, Fonseca LP Supervisor, Master thesis in biotechnology, Instituto Superior Técnico, University of Lisbon, Portugal. <https://bibliotecas.utl.pt/cgi-bin/koha/opac-detail.pl?biblionumber=519643>
36. dos Santos ACA (2016) Development, optimization and characterization of lipid nanoparticles: Encapsulation of lidocaine in nanostructured lipid carriers. Fonseca LP Supervisor, Master thesis in biological engineering, Instituto Superior Técnico, University of Lisbon, Portugal. <https://fenix.tecnico.ulisboa.pt/cursos/mebiol/dissertacao/283828618789685>
37. Esgueira VLR (2017) Nanostructured lipid carriers as a delivery system of tobramycin and ciprofloxacin. Fonseca LP and Leitão HJ Supervisors, Master thesis in biotechnology, Instituto Superior Técnico, University of Lisbon, Portugal. <https://bibliotecas.utl.pt/cgi-bin/koha/opac-detail.pl?biblionumber=526417>
38. Pinto FCRV (2018) Design and characterization of lipid nanoparticles for an effective topical administration of active compounds. Fonseca LP and de Barros DPC Supervisors, PhD thesis in bioengineering, MIT-Portugal programme at Instituto Superior Técnico, University of Lisbon, Portugal. <https://bibliotecas.utl.pt/cgi-bin/koha/opac-detail.pl?biblionumber=527326>
39. Vega-Villa KR, Takemoto JK, Yáñez JA, Remsberg CM, Forrest ML, Davies NM (2008) Clinical toxicities of nanocarrier systems. *Adv Drug Deliv Rev* 60:929–938
40. Müller RH, Gohla S, Keck CM (2011) State of the art of nanocrystals – special features, production, nanotoxicology aspects and intracellular delivery. *Eur J Pharm Biopharm* 78:1–9
41. Liu C, Liu D, Bai F, Zhang J, Zhang N (2010) In vitro and in vivo studies of lipid-based nanocarriers for oral N3-o-toluy-l-fluorouracil delivery. *Drug Deliv* 17:352–363
42. Chakraborty S, Shukla D, Mishra B, Singh S (2009) Lipid-an emerging platform for oral delivery of drugs with poor bioavailability. *Eur J Pharm Biopharm* 73:1–15
43. Jenning V, Thünemann AF, Gohla SH (2000) Characterisation of a novel solid lipid nanoparticle carrier system based on binary mixtures of liquid and solid lipids. *Int J Pharm* 199:167–177
44. Lin C-H, Chen CH, Lin Z-C, Fang J-Y (2017) Recent advances in oral delivery of drugs and bioactive natural products using solid lipid nanoparticles as the carriers. *J Food Drug Anal* 25(2):219–234
45. Poonia N, Kharb R, Lather V, Pandita D (2016) Nanostructured lipid carriers: versatile oral delivery vehicle. *Future Sci OA* 2(3). <https://doi.org/10.4155/foa-2016-0030>
46. Trevaskis NL, Charman WN, Porter CJH (2008) Lipid-based delivery systems and intestinal lymphatic drug transport: a mechanistic update. *Adv Drug Deliv Rev* 60:702–716
47. Hyuk Suh W, Suslick S, Stucky D, Suh Y-H (2009) Nanotechnology, nanotoxicology, and neuroscience. *Prog Neurobiol* 87:133–170
48. Ferruzza S, Rossi C, Scarino ML, Sambuy Y (2012) A protocol for differentiation of human intestinal Caco-2 cells in asymmetric serum-containing medium. *Toxicol In Vitro* 26:1252–1255
49. Silva C, González-Mira E, García ML, Egea M, Fonseca J, Silva R, Santos D, Souto EB, Ferreira D (2011) Preparation, characterization and biocompatibility studies on risperidone-loaded solid lipid nanoparticles (SLN): high pressure homogenization versus ultrasound. *Colloids Surf B Biointerfaces* 86:158–165
50. Serpe L, Catalano MG, Cavalli R, Ugazio E, Bosco O, Canaparo R, Muntoni E, Frairia R, Gasco MR, Eandi M, Zara GP (2004) Cytotoxicity of anticancer drugs incorporated in solid lipid nanoparticles on HT-29

- colorectal cancer cell line. *Eur J Pharm Biopharm* 58:673–680
51. Schubert MA, Müller-Goymann CC (2005) Characterisation of surface-modified solid lipid nanoparticles (SLN): influence of lecithin and non-ionic emulsifier. *Eur J Pharm Biopharm* 61:77–86
 52. Souto EB, Martins-Lopes P, Lopes CM, Gaivao I, Silva AM, Guedes-Pinto H (2009) A note on regulatory concerns and toxicity assessment in lipid-based delivery systems (LDS). *J Biomed Nanotechnol* 5:317–322
 53. Gonzalez-Moragas L, Roig A, Laromaine A (2015) *C. elegans* as a tool for in vivo nanoparticle assessment. *Adv Colloid Interf Sci* 219:10–26
 54. Ramos CG, Leitão JH (2011) *Caenorhabditis elegans* as a research tool to unveil bacterial virulence determinants: lessons from the *Burkholderia cepacia* complex. In: Boeri F, Chung JA (eds) *Nematodes: morphology, functions and management strategies*. Nova Science Publishers
 55. Colmenares D, Sun Q, Shen P, Yue Y, McClements DJ, Park Y (2016) Delivery of dietary triglycerides to *Caenorhabditis elegans* using lipid nanoparticles: Nanoemulsion-based delivery systems. *Food Chem* 202:451–457
 56. Ewbank JJ (2002) Tackling both sides of the host – pathogen equation with *Caenorhabditis elegans*. *Microbes Infect* 4:247–256
 57. World Health Organization (WHO), Global tuberculosis report 2013. WHO library cataloging-in-Publicati data, World Health Organization. ISBN: 9789241564656
 58. Grange JM, Zumla A (2002) The global emergency of tuberculosis: what is the cause? *J R Soc Promot Heal* 122:78–81
 59. Van Hest R, Baars H, Kik S, van Gerven P, Trompenaars M-C, Kalisvaart N, Keizer S, Borgdorff M, Mensen M, Cobelens F (2004) Hepatotoxicity of Rifampin-pyrazinamide and isoniazid preventive therapy and tuberculosis treatment. *Clin Infect Dis* 39:488–496
 60. He Q, Zhang Z, Gao F, Li Y, Shi J (2011) In vivo biodistribution and urinary excretion of mesoporous silica nanoparticles: effects of particle size and PEGylation. *Small* 7:271–280
 61. Lee JE, Lee N, Kim H, Kim J, Choi SH, Kim JH, Kim T, Song IC, Park SP, Moon WK, Hyeon T (2009) Uniform mesoporous dye-doped silica nanoparticles decorated with multiple magnetite nanocrystals for simultaneous enhanced magnetic resonance imaging, fluorescence imaging, and drug delivery. *J Am Chem Soc* 132:552–557
 62. Chen H, Wang L, Yeh J, Wu X, Cao Z, Wang YA, Zhang M, Yang L, Mao H (2010) Reducing non-specific binding and uptake of nanoparticles and improving cell targeting with an antifouling PEO-b-PyMPS copolymer coating. *Biomaterials* 31:5397–5407
 63. Mutil P, Wang C, Hickey A (2009) Inhaled drug delivery for tuberculosis therapy. *Pharm Res* 26:2401–2416
 64. Siekmann B, Westesen K (1994) Melt-homogenized solid lipid nanoparticles stabilized by the nonionic surfactant tyloxapol. I. Preparation and particle size determination. *Pharm Pharmacol* 3:194–197
 65. Schwarz C, Mehnert W (1997) Freeze-drying of drug-free and drug-loaded solid lipid nanoparticles. *Int J Pharm* 157:171–179
 66. Westesen K, Siekmann B (1997) Investigation of the gel formation of phospholipid stabilized solid lipid nanoparticles. *Int J Pharm* 151:35–45
 67. Bhandari R, Kaur IP (2013) Pharmacokinetics, tissue distribution and relative bioavailability of isoniazid-solid lipid nanoparticles. *Int J Pharm* 441:202–212
 68. Singh H, Bhandari R, Kaur IP (2013) Encapsulation of rifampicin in a solid lipid nanoparticulate system to limit its degradation and interaction with isoniazid at acidic pH. *Int J Pharm* 446:106–111
 69. Pandey R, Sharma S, Khuller GK (2005) Oral solid lipid nanoparticle-based antitubercular chemotherapy. *Tuberculosis (Edinb)* 85:415–420
 70. Cutting GR (2015) Cystic fibrosis genetics: from molecular understanding to clinical application. *Nat Rev Genet* 16:45–56
 71. Flume PA, Van Devanter DR (2012) State of progress in treating cystic fibrosis respiratory disease. *BMC Med* 10:88
 72. Döring G, Flume P, Heijerman H, Elborn JS (2012) Treatment of lung infection in patients with cystic fibrosis: current and future strategies. *J Cyst Fibros* 11:461–479
 73. Mahenthalingam E, Urban TA, Goldberg JB (2005) The multifarious, multireplicon *Burkholderia cepacia* complex. *Nat Rev Microbiol* 3:144–156
 74. Drevinek P, Mahenthalingam E (2010) *Burkholderia cenocepacia* in cystic fibrosis: epidemiology and molecular mechanisms of virulence. *Clin Microbiol Infect* 16:821–830
 75. Martina P, Leguizamon M, Prieto CI, Sousa SA, Montanaro P, Draghi WO, Stämmli M, Bettiol M, de Carvalho CCCR, Palau J, Figoli C, Alvarez F, Benetti S, Lejona S, Vescina C, Ferreras J, Lasch P, Lagares A, Zorreguieta A, Leitão JH, Yantorno OM, Bosch A (2018) *Burkholderia puraquae* sp. nov., a novel species of the *Burkholderia cepacia* complex isolated from hospital settings and agricultural soils. *Int J Syst Evol Microbiol* 68:14–20
 76. Coutinho CP, Barreto C, Pereira L, Cristino JM, Sá-Correia I (2015) Incidence of *Burkholderia* contaminants at a cystic fibrosis Centre with an unusually high representation of *Burkholderia cepacia* during 15 years of epidemiological surveillance. *J Med Microbiol* 64:927–935
 77. Sousa SA, Feliciano JR, Pita T, Guerreiro SI, Leitão JH (2017) *Burkholderia cepacia* complex regulation of virulence gene expression: a review. *Genes* 8(1):43
 78. Leitão JH, Sousa SA, Ferreira AS, Ramos CG, Silva IN, Moreira LM (2010) Pathogenicity, virulence factors, and strategies to fight against *Burkholderia cepacia* complex pathogens and related species. *Appl Microbiol Biotechnol* 87(1):31–40

79. Diab R, Khameneh B, Joubert O, Duval R (2015) Insights in nanoparticle-bacterium interactions: new frontiers to bypass bacterial resistance to antibiotics. *Curr Pharm Des* 21:4095–4105
80. Keles S, Kaygusuz K, Sari A (2005) Lauric and myristic acids eutectic mixture as phase change material for low-temperature heating applications. *Int J Energy Res* 29:857–870
81. Tunc K, Sari A, Tarhan S, Ergu G, Kaygusuz K (2005) Lauric and palmitic acids eutectic mixture as latent heat storage material for low temperature heating applications. *Energy* 30:677–692
82. Sari A, Kaygusuz K (2002) Thermal performance of a eutectic mixture of lauric acid and stearic acids as PCM encapsulated in the annulus of two concentric pipes. *Solar Energy* 72(6):493–504
83. Jain D, Banerjee R (2008) Comparison of ciprofloxacin hydrochloride-loaded protein, lipid, and chitosan nanoparticles for drug delivery. *J Biomed Mater Res B Appl Biomater* 86:105–112
84. Ghaffari S, Varshosaz J, Haririan I, Khorhayand MR (2011) Ciprofloxacin loaded alginate/chitosan and solid lipid nanoparticles, preparation, and characterization. *J Dispers Sci Technol* 33(5):685–689
85. Shazly GA (2017) Ciprofloxacin controlled-solid lipid nanoparticles: characterization, in vitro release, and antibacterial activity assessment. *Biomed Res Int*. <https://doi.org/10.1155/2017/2120734>
86. Kaplan JB, LoVetri K, Cardona ST, Madhyastha S, Sadovskaya I, Jabbouri S, Izano EA (2012) Recombinant human DNase I decreases biofilm and increases antimicrobial susceptibility in staphylococci. *J Antibiot* 65:73–77
87. Stadler M, Mayer A, Anke H, Sterner O (1993) Fatty acids and other compounds with Nematicidal activity from cultures of basidiomycetes. *Planta Med* 60:128–132
88. Cardona ST, Wopperer J, Eberl L, Valvano MA (2005) Diverse pathogenicity of *Burkholderia cepacia* complex strains in the *Caenorhabditis elegans* host model. *Microbiol Lett* 250:97–104
89. Sousa SA, Ramos CG, Moreira LM, Leitão JH (2019) The *hfq* gene is required for stress resistance and full virulence of *Burkholderia cepacia* to the nematode *Caenorhabditis elegans*. *Microbiology* 156:896–908
90. FDA U.S Food and Drug Administration. Available at: <https://www.fda.gov/default.htm>. Accessed 5 Oct 2017



Dermal Delivery of Lipid Nanoparticles: Effects on Skin and Assessment of Absorption and Safety

Fátima Pinto, Luis P. Fonseca,
and Dragana P. C. de Barros

Abstract

During the recent decades, dermal delivery has achieved visible popularity mainly due to the increase of chronic skin diseases and the demand for targeted delivery and patient compliance. Dermal delivery provides an attractive alternative to oral drug delivery, promoting the drug application directly at the site of action, resulting in higher localized drug concentration with reduced systemic drug exposure. Among several types of drug delivery systems used in dermal delivery are the lipid nanoparticles, which include solid lipid nanoparticles (SLNs) and nanostruc-

tured lipid carriers (NLCs). These lipid nano-carriers have attracted great interest and have been intensively studied for their use in dermal applications. Lipid nanoparticles increase the transport of active compounds through the skin by improving drug solubilization in the formulation, drug partitioning into the skin, and fluidizing skin lipids. Moreover, these nanocarriers are composed of biologically active and biodegradable lipids that show less toxicity and offer many favorable attributes such as adhesiveness, occlusion, skin hydration, lubrication, smoothness, skin penetration enhancement, modified release, improvement of formulation appearance providing a whitening effect, and offering protection of actives against degradation.

This chapter focuses on the effects of lipid nanoparticles in dermal delivery, on the types of active compounds that are used in their formulation and application, some aspects related to their possible toxicity, and a description of the most commonly used techniques for the evaluation of drug absorption on the skin.

F. Pinto (✉)

Department of Human Genetics, Instituto Nacional de Saúde Dr. Ricardo Jorge, Lisbon, Portugal
e-mail: fatima.pinto@insa.min-saude.pt

L. P. Fonseca

Institute for Bioengineering and Biosciences (iBB), Bioengineering Department, Instituto Superior Técnico (IST), Universidade de Lisboa, Lisboa, Portugal

D. P. C. de Barros

Instituto de Tecnologia Química e Biológica António Xavier (ITQB), Universidade Nova de Lisboa, Oeiras, Portugal

Keywords

Dermal delivery · Solid lipid nanoparticles · Nanostructured lipid carriers · Occlusion · Vegetable oils · Retinoids · Dermal absorption

4.1 Introduction

Nanotechnology is a fundamental science that has been consolidated during the twenty-first century in designing, characterizing, and using materials, devices, and systems in the nanometre size range [1–3]. There are several innovative applications of nanotechnology in the cosmetic and dermal pharmaceutical industries which have transformed the administration of active compounds and represent outstanding opportunities for both academic and industrial fields [4, 5].

Dermal formulations of nanocarriers have been used for improved delivery of active substances inside and through the skin mostly due to their several advantages over conventional passive delivery systems as skin hydration, increased surface area, smoothness, softness, adhesiveness, occlusion, higher solubility, site-targeted delivery, improved stability, controlled release, reduced skin irritancy, protection from degradation and increased drug loading [6–8]. Several approaches addressing nano-enabled technologies have been developed to increase drug bioavailability and to enhance its absorption or permeation in the skin [2]. The size of these nanocarriers is the characteristic that confers them more efficiently than currently available formulations and also determines their effectiveness and targeted delivery [5]. The application of nanocarriers into cosmetic and pharmaceutical products offers several advantages as the possibility to protect active substances from degradation, to encapsulate poorly water-soluble compounds, and to confer a controlled release that avoids repeated administrations and promotes patient compliance [9, 10]. The types of nanocarriers that are being studied for topical administration are liposomes [11], lipid nanoparticles [12–15], nanoemulsions [16], polymeric nanoparticles [17], hydrogels [18], and microneedles [19].

The history of lipid nanoparticles started around the '90s, and at the beginning, different names were used as lipid nanospheres [20] and even lipid microparticles or microspheres [21, 22] to designate solid lipid nanoparticles (SLNs) which was then the name assigned by the

inventors to describe a type of nanocarriers structurally similar to nanoemulsions but containing a solid matrix composed by a solid lipid [23]. These nanocarrier systems were first developed as an efficient alternative to traditional carriers as emulsions, liposomes, and polymeric nanoparticles and explored to avoid some of their issues in biological media [2].

SLNs are described in the literature as the first generation of lipid nanoparticles and are defined as colloidal spherical particles with sizes ranging from 40 to 1000 nm, composed of solid lipids, dispersed in an aqueous phase, and stabilized by surfactants [6, 23–25]. SLNs are produced using one crystalline solid lipid or a mixture of solid lipids, as glycerides or waxes in concentrations typically varying from 0.1% to 30% w/w and surfactants in contents ranging from 0.5% to 5% w/w [6, 25]. An important prerequisite of the lipids is that they should be solid at 37 °C that is considered as the body temperature [26], and more than one surfactant can be used to prevent aggregation of particles in the dispersions [25]. Similar to nanoemulsions, SLNs are produced by substituting the oil phase of the emulsion (O/W) with one solid lipid or a mixture of solid lipids. The incorporation of drugs occurs by melting the solid lipid and suspending or dissolving the active substance in the melted lipid. Then, the droplets of melted lipid recrystallize and self-assemble, typically yielding a mixture of high-energy crystallized form (α and β'), and low-energy form (β') lipid modifications. However, the lipids incline to increase their order during storage and be converted from α/β' to β modifications which can lead to a subsequent decrease in imperfections of the lipid matrix lattice and consequently occurs the loss or leakage of the active substance from the nanocarrier [6, 26]. The main advantages of SLNs are their physicochemical stability, providing higher protection for incorporated active substances from chemical and physical degradation, and the controlled release and transport of drugs to target sites, consequently increasing its bioavailability and efficacy [27]. Also, the use of biocompatible solid lipids is a great benefit which allows encapsulating generally lipophilic drugs on SLNs crystal-

line matrix lattice, on its lipid layers, and or between the chains of fatty acids [2]. Moreover, the release profile of the encapsulated drugs can be adjusted for a specific application through the selection of a specific combination of lipids and fatty acids [2, 28].

The second generation of lipid nanoparticles, or nanostructured lipid carriers (NLCs), was introduced to overcome the main limitations of SLNs related to low drug capacity and its loss or leakage from the nanocarrier during storage [5, 6, 28]. NLCs are composed of an unstructured solid lipid matrix consisting of a mixture of solid and liquid lipids that are dispersed in an aqueous phase containing one surfactant or a mixture of surfactants [29]. Generally, the solid lipids are blended with the liquid lipids in ratios from 70:30 up to 99.9:0.1, while the surfactant concentration usually varies from 1.5% to 5% (w/v) [30]. The incorporation of liquid lipids in the solid matrix results in a decrease of the melting point when compared to exclusively the solid lipid. Also, the addition of oils leads to a substantial crystal order disturbance producing several imperfections in the crystalline lattice, which provides more space to loading active compounds, increase the drug loading capacity, and avoids or reduces the drug expulsion during storage due to a higher drug incorporation capacity, in comparison with previous developed SLNs [5, 26, 31]. To achieve a high degree of imperfections on the lipid crystal lattice, the lipid blends should comprise structurally different molecules as e.g. oils with a lower chain of fatty acids and solid lipids with a higher chain of fatty acids. Nevertheless, when choosing the composition of the lipid blends it is necessary to have into consideration that its melting point still needs to be above the body or skin temperature at 32 °C [26].

Lipid nanoparticles are very effective carriers of active compounds used in cosmetics to moisturize the skin due to their occlusive properties, to improve skin elasticity due to their ability to increase skin hydration, reduce wrinkles, and be used as antioxidant agents in anti-aging formulations [25, 26, 30, 32, 33]. These nanoparticles are also excellent carriers of perfumes and insect repellent thanks to their adhesive properties and

the possibilities of sustained-release [1, 34, 35] and are commonly used in physical and chemical sunscreens since they can reflect radiation and produce a synergistic effect of protection, thus reducing the amount of incorporated UV filter which limits the possibility of irritation and also reduces the associated production costs [25]. The incorporation of lipid nanoparticles in cosmetics holds several advantages over traditional personal care products including enhancing the product aesthetics, improving the stability of active substances, targeting active ingredients to the wanted locations, controlling the release of active ingredients to achieve continued effects, and conferring skin protection due to their occlusion property [36, 37]. This type of nanocarriers is mainly proposed in cosmetics used in anti-aging products, sunscreens, moisturizers to preserve skin hydration, as well as personal care products to maintain daily hygiene and look, and also other innovative uses such as the release of fragrances [38, 39].

The absorption of active compounds into the different skin layers has been widely assessed and one crucial issue in current dermatological research. Scientists have established different techniques to estimate the amount of drug delivery to the skin. General guidelines for dermal absorption studies published by different organizations from Europe and the United States present documents with descriptions and rules of how to implement dermal absorption assays [40–47]. However, the measurements are not properly regulated. Samples from skin biopsy can be used to directly measure the absorption of topical drugs, however, biopsies are invasive and not suitable for obtaining kinetic data. There are alternative techniques that are used to evaluate the bioavailability of topical drugs, as *in vivo* assays including tape stripping/dermatopharmacokinetics, microdialysis, and vasoconstrictor assay, *in vitro* assays performed in Franz diffusion cells, and *ex vivo* assays that use isolated perfused skin models [40]. The bioavailability of topical drugs may be assessed by several techniques, which can be used in complement taking advantage of each technique's resources [48, 49].

This chapter, focus on the effects of lipid nanoparticles in dermal delivery, on the types of active compounds that are used in their formulation and application, which physicochemical properties are determinant for their efficiency and some aspects related to their possible toxicity and description of the most commonly used techniques for the evaluation of drug absorption on the skin.

4.2 Skin Morphology and Barrier Function

The skin is the largest organ of the human body and comprehends a surface area of about 2 m², corresponding to 15% of the total body weight in an adult [50, 51]. The skin has an integrated complex structure, and it serves as a very effective barrier to the entry of exogenous substances [6, 52]. The whole dimension of human skin is composed of three strata: the epidermis, dermis, and hypodermis (Fig. 4.1).

The hypodermis is the most inner, which is rich in triglycerides and performs as an insulator. Sweat and pilosebaceous glands emerge from the hypodermis to the surface of the epidermis [6]. Hair follicles in humans are low in number compared to furry animals [53, 54].

The dermis layer that is highly vascularised lies beneath the epidermis, is rich in collagen and elastin, and is embedded in a ground substance surrounding fibroblasts which represent the highest number of cells in the dermis. This stratum is primarily constituted of connective tissue, is more hydrophilic in nature, and provides oxygen and nutrients to the skin [51, 55].

The epidermis is the most external layer of the skin, include five different layers detectable by cellular differentiation, which form the viable epidermis: the *stratum lucidum*, *stratum granulosum*, *stratum spinosum*, *stratum germinativum*, and the non-viable but chemically active *stratum corneum* (SC) which is the extreme layer in contact with the environment consisting in about 15 layers of corneocytes [6, 51, 54, 56]. Keratinocytes containing high quantities of keratin filaments and water are flat dead cells that migrate toward

the skin surface and undergo maturation to differentiate in corneocytes. The SC is commonly illustrated by the “bricks and mortar” model, in which the corneocytes are illustrated as bricks embedded in a mortar that consists of a hydrophobic matrix mainly constituted of cholesterol, cholesterol esters, ceramides, keratin, and fatty acids [6, 51, 57]. Due to the great complexity of the SC, this layer represents the main barrier for the passage of active compounds through the skin. The other layers of the dermis do not significantly contribute to the probable percutaneous absorption. However, a very lipophilic active compound that hypothetically can overcome the SC barrier will face serious obstacles to absorption through the subsequent aqueous interface [56].

The strong skin barrier can limit the drug uptake, slows drug absorption rates, and promotes the lack of dosing precision [59]. The final absorption potential of an active compound can be increased or limited by choice of a suitable carrier/vehicle for transdermal or dermal delivery, respectively. The interactions between the carrier/vehicle and the active substance are of great importance in formulation development [56]. Therefore, the characteristics of an active such as its exposure at the skin surface and partitioning into the skin are identified as major properties contributing to absorption. The carrier can improve the active limitations and directly affect the mentioned characteristics [56, 60].

4.3 Skin Absorption Pathways

Many factors affect the absorption through the skin as skin age and environment, state of the skin (normal or diseased), differences between species, skin temperature, area of application, physical characteristics of the penetrant, contact time, and degree of hydration of the skin. The mechanism of skin absorption is diffusion which is concentration-dependent [50, 61]. Dermal delivery may be considered topical and transdermal; it is topical when the active compound acts locally or transdermal when the active compound is delivered in the systemic route. The main advantages

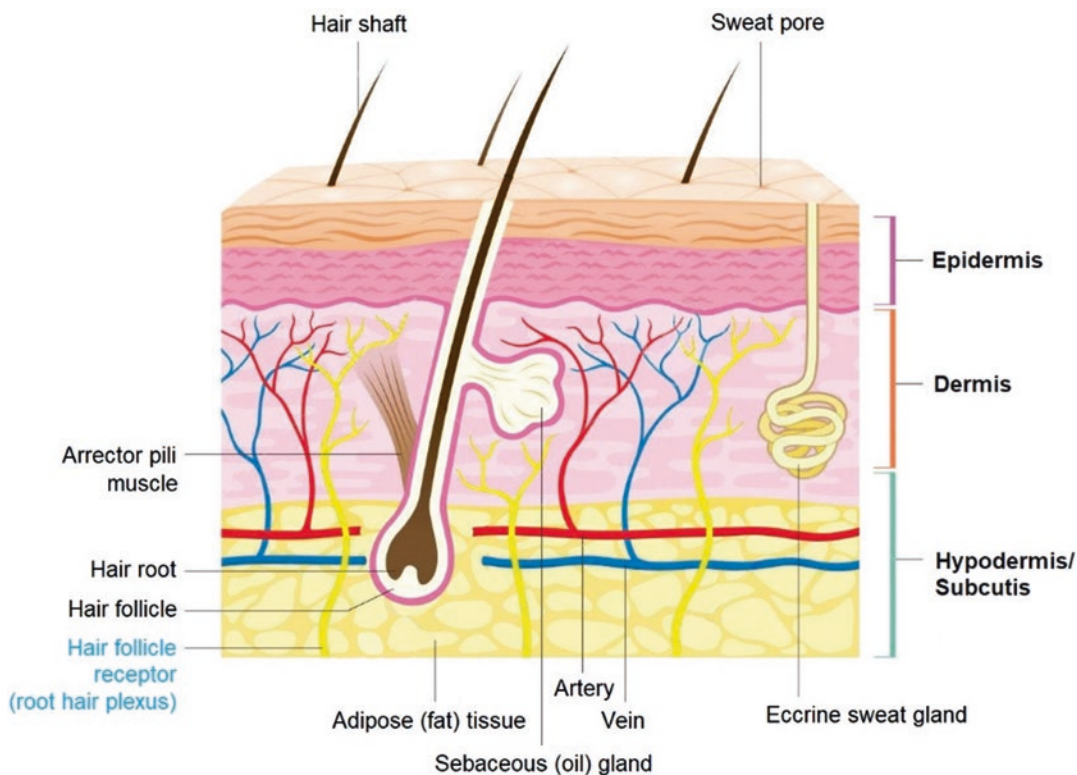


Fig. 4.1 Morphology of human skin. (Adapted from [58] Public domain)

of skin delivery consist of a sustained release of drugs, the avoidance of side effects connected with oral delivery of drugs, easy clearance of medication in case of overdose, bypassing hepatic metabolism, and patient compliance [6, 62].

The SC is commonly considered the main barrier to the absorption of topically applied substances and confers primary protection from external pollutants in the epidermis, contributing to the limitation of the therapeutic efficiency of topically applied compounds. It is well acknowledged that a molecule will permeate across the SC through one of the three possible pathways, i.e., transcellular (intracellular), intercellular, and the appendageal (follicular) [6, 51, 63].

The passage of active compounds through the lipid matrix consists in the intercellular route, while the passage via keratinocytes consists in the transcellular route. The appendageal route of drugs occurs across sweat glands, hair follicles, and sebaceous glands [6, 62]. The physicochemical properties of the permeating molecules dic-

tate by which pathways they may cross the barrier, with most substances possibly permeating the skin by more than one pathway [64].

The permeation of active compounds includes several events starting with the release of the permeant from the formulation, then occurs the diffusion into and through the SC, followed by the partitioning to the more aqueous epidermal environment, ending up by the passage into the cutaneous circulation or the diffusion to deeper tissues. These events are highly dependent on the diffusivity and solubility of the permeant substance within each environment. The diffusion coefficient of an active substance relies on its physicochemical properties as the melting point, molecular size, potential for binding within the environment, ionization, solubility and may be also affected by its viscosity and tortuosity or diffusional path length that are factors linked with the environment [6, 64].

The transcellular route has been considered as a polar route through the SC. This is mainly due to

the intracellular keratin matrix of corneocytes, which is relatively hydrated and consequently polar in nature, which conditions the permeation requiring a repeated partitioning between this polar environment and the lipophilic domains surrounding the corneocytes [64]. Nevertheless, it is usually admitted that the transport through the SC occurs principally by the intercellular route. Within the intercellular lipid domains, transport can take place via both lipids (diffusion via the lipid core) and polar (diffusion via the polar head groups) pathways. The diffusional rate-limiting region of very polar permeants is the polar pathway of the SC, which is fairly independent of their partition coefficient, while less polar permeants probably diffuse via the lipid pathway, and their permeation increases with an increase in lipophilicity [64]. The appendageal route is considered to be more appropriate for molecules with a high molecular weight that diffuses slowly through the skin and also for nanoparticles [65]. Hair follicles represent around 0.1% of the skin surface which makes them a potential pathway for drug permeation. Indeed, the SC layer in the deeper parts of hair follicles is thinner than other regions in the epidermis. Moreover, the profound invagination facilitates access to the capillary network, making hair follicles the pathway of choice for transdermal delivery [66].

4.4 Properties of Lipid Nanoparticles and Their Effects on Skin

Lipid nanoparticles, both SLNs and NLCs can be produced relatively easily, providing an improved absorption of active substances on skin and are highly effective carriers based on physical and chemical principles. Their effects on skin rely on these principles: physical adhesion to the skin, mainly due to the small size of the nanoparticles and consequently high surface area; occlusion through the formation of a superficial film; physical occlusion stimulating the absorption of active substances and chemical interaction between the lipids from the skin and the lipids from the nanoparticles [6].

4.4.1 Mechanisms of Skin Absorption from Lipid Nanoparticles

The topical administration of lipid nanoparticles (SLNs and NLCs) on the skin results in a monolayer film due to their adhesiveness property. This film formation is even more pronounced when the quantity of nanoparticles in the dispersion is higher and sufficient to cover the skin surface. NLCs were consequently also called the “invisible dermal patch” [26, 67]. This film is hydrophobic, and its resistance and effects are dependent on the size of the particles that constitute it. In addition, due to its hydrophobicity, it has an occlusive effect. Moreover, the lipids of the nanoparticles may also interact with the skin lipids, which affects the delivery of the active compound between the lipid structures of the skin and disturbs its absorption rate. However, there is currently little knowledge about this mechanism, and the composition of an ideal lipid matrix to reach this interaction with the skin lipids has to be found empirically [26, 68].

A proposed mechanism for the interaction between lipid nanoparticles and skin lipids demonstrates that the nanoparticles primarily remain on the skin without interaction with the skin lipids if the particle matrix possesses a very high melting point or if their lipids matrix are not miscible with SC lipids. In this case, the particles might only be slightly flattened by the existing pressure. On the other hand, it can occur an interaction between lipids when the melting point of the nanoparticles' lipids is below the skin temperature or in the case of good miscibility of the lipids. This leads to the integration of the lipid nanoparticles in the lipid phase on SC due to the desegregation of the nanoparticle matrix and the occurrence of an inter-diffusion of lipids between particles and SC lipids [26].

Zhai and Zhai, 2014 [69] demonstrated that NLCs could disrupt the intercellular environment surrounding the corneocytes and keratinocytes, particularly by acting on its lipids composition. The tight anomalies junctions in SC would lead to imperfections in the barrier function and would stimulate the skin permeation of drugs [51].

In a mechanism for the skin absorption of SLNs proposed by Jensen et al. 2011 [70], the nanoparticles persist in the SC at the skin surface and accumulate, forming a drug reservoir from where they release the encapsulated active compounds, depending on the degree of lipophilicity of the active substance and consequent capacity to reach the target cells in the lower strata of the skin. The SLNs would release the active molecules in a biphasic way, with an initial burst release from the surface of the nanoparticles followed by a reservoir effect at the skin surface and SC [51, 70]. SLNs interact with the skin lipids depending on the drug partitioning in the lipid nanoparticle, by the drug lipophilicity, by the type of interacting skin lipid, and the composition of the lipid matrix. Both SLNs and NLCs could cross the appendageal pathway since they promote follicular deposition due to their high lipophilicity [51].

4.4.2 Occlusion

The SC constitutes a barrier for lipid and water-soluble substances represented by the “brick-mortar” model consisting of a continuous lipid layer [26, 71]. The lipid nanoparticles adhere to the skin leading to a film formation and subsequently to an occlusion effect with an increased hydration effect [1, 68, 72]. This hydration effect contributes to the skin’s healthy appearance and directly influences the percutaneous absorption of active substances. For topical administrations, it is important that the active is not systemically absorbed but instead is crucial that a certain absorption occurs in the skin to the desired effect take place [1, 73].

The occlusion effect resultant from a mono-layered hydrophobic film formation increases the hydration of the SC by reducing the water evaporation from the skin surface, which usually has about 10–15 % water content. This effect promotes the formation of spaces between the corneocytes and the increase in the inter-corneocyte gaps, promoting an increase in the SC’s permeability and, consequently, the penetration of active compounds [26, 71]. It was reported that approximately 4% of lipid nanoparticles with a diameter

of about 200 nm should hypothetically form a mono-layered hydrophobic film when c. 4 mg of the formulation is applied per cm² [68, 74]. This occlusion factor is directly dependent on several factors: (i) lipid content, (ii) degree of crystallinity of the re-crystallized lipid, and also (iii) particle size [1]. Therefore, different occlusion effects can be obtained by manipulating the particle size of lipid nanoparticles [68]. When the particle size decreases, at a certain lipid concentration, the occlusion effect can be increased or instead when the concentration of lipid (number of nanoparticles at a given particle size) increase the occlusion effect is more pronounced at a given particle size by increasing the number of particles (concentration of lipid) and consequently, a “controlled occlusion effect” can occur (Fig. 4.2) [7, 72].

It was reported that the particle size has to be less than 260 nm [75] to accomplish a higher occlusion and a more significant interaction with the skin surface. Moreover, it was also reported that an increase in the liquid content might reduce the occlusive effect, which is higher for lipid nanoparticles possessing the highest crystallinity, thus indicating that SLNs had a higher occlusive effect than NLCs [26, 76, 77]. Lombardi Borgia et al. 2005 [78] reported that after SLNs application on the skin, its water content evaporates, resulting in a recrystallization phenomenon inducing the partial release of the active and its skin penetration [51].

The occlusion effect induced by typical ointment formulations does not ensure rapid hydration. Thus, it is preferable to use a preparation that can supply water, which lipid nanoparticle suspensions are suitable to offer. Moreover, due to their hydration properties, it can be assumed that lipid nanoparticles may enhance skin elasticity [79] and that these particles can be further used to formulate anti-aging products [68].

4.4.3 Enhanced Stabilization of Actives and Skin Bioavailability

The solid matrix of both SLNs and NLCs represents one of their most important features. It enables the advantage of stabilizing active ingre-

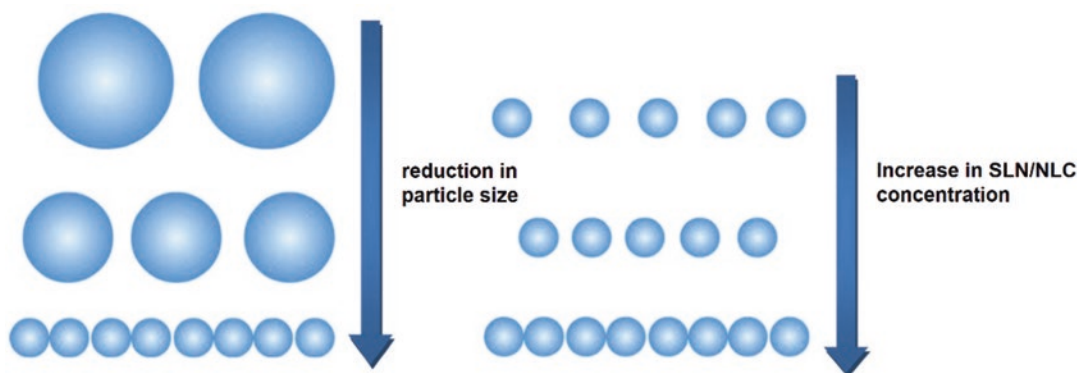


Fig. 4.2 The controlled occlusion effect of lipid nanoparticles in function of the particle size. Left: At a given identical lipid content, reducing the particle size leads to an increase in particles number which results in a denser film.

Right: At a given particle size, increasing the lipid concentration leads to an increase in particle number and density of the film which also result in a higher occlusion effect. (Adapted from [7, 72]. Published with permission)

dients that are chemically labile against degradation by light, oxidation and hydrolysis [1, 68]. The selection of an appropriate lipid is a major factor to be considered as the active compound must be totally solubilized/retained within the lipid matrix during the storage time [68, 72].

The effect of chemical stability of actives after their incorporation into lipid nanocarriers was already proven for, e.g., coenzyme Q10 [80, 81], ascorbyl palmitate [82, 83], and retinoids [1, 68, 84–86].

The lipids composition of lipid nanoparticles will also determine their skin bioavailability and targeting in two possible ways: (1) the differences in lipid composition might lead to different interactions with the lipids of the SC and consequently to a different localization of the active compound; (2) the lipid composition will determine the localization of the active compound inside the particle, modulating its bioavailability and release [72, 87].

4.4.4 Modulation of Actives Release and Supersaturation Effects

Before the incorporated active ingredient on SLN and NLC may exercise their function into the skin, it is prime necessary its release [68, 88]. The release profile of lipid nanoparticles depends

on the interaction of numerous factors, thus being a multifactorial event [89]. It is dependent on the preparation method, the composition of the formulation (i.e., composition and concentration of surfactant), the solubilizing properties of the surfactant for the incorporated active compound, and the solubility of the active compound in the lipid matrix (oil/water partition coefficient) [68, 89]. These factors influence the inner structure of the lipid nanoparticles and, therefore, the rate of release of incorporated ingredients [86, 90, 91]. Depending on the matrix structure, the release profiles can vary from very fast release, medium, or extremely prolonged release [68, 92]. Moreover, the release of actives can also be stimulated by enzymatic lipid degradation due to the microbial flora existing on skin or electrolyte changes in the SC [71]. The lipid structure of the particles may be influenced by the electrolytes, which can present a more polymorphic form promoting drug expulsion [26, 89].

Most active dermal substances are not intended for deeper skin absorption having only a superficial action in local effect and avoiding the undesired absorption into the systemic blood circulation [68]. Moreover, it seems clear that a release profile over weeks is not interesting for *in vivo* topical delivery. Although, dispersions of lipid nanoparticles demonstrate the capacity to control the rate of actives penetration into the

skin and modulate the drug release, i.e., adapting it accordingly to the therapeutic needs [89]. Modulation of drug release into specific layers of the skin and, therefore, drug absorption across skin membranes can also be achieved due to the creation of a supersaturated system [93]. These systems can be created by the incorporation of lipid nanoparticles into topical formulations (creams, ointments, emulsions, and gels). The increase in saturation solubility will lead to an increased diffusion pressure of the drug into the skin [68, 89]. During storage, the active compounds continue entrapped into the matrix of the lipid nanoparticles since it preserves its polymorphic form. With the application of a supersaturated cream into the skin and an increase in temperature and water evaporation, the lipid nanoparticles' lipid matrix transforms from a more unstable polymorph to a more ordered polymorph leading to drug expulsion. Consequently, the active is expelled from the lipid matrix into the emulsion already saturated with the same active, thus creating a supersaturation effect. This phenomenon increases thermoactivity and leads to active absorption into the skin [68, 89].

4.5 Active Compounds Used in Dermal Formulations

Essential properties of galenic and cosmetic formulations as efficacy and tolerability, are determined by the active and the vehicle's nature. Thus, a well-formulated base of empty lipid nanoparticles may have numerous positive effects on the skin, as occlusion and stabilization of the epidermal barrier. Moreover, the effects of many active compounds are dependent from the overall formulation and preparation as it may confer them more stability and protection, increasing their bioavailability. The interactions between the carrier, active ingredient and the skin greatly influence their effects in the formulation and the release profile of the active substance [133]. The categories in which the active substances used in dermal formulations belong will be presented and further discussed.

4.5.1 Vegetable Oils and Fatty Acids

Current research on dermal formulation has been directed towards using vegetable ingredients by very good results of scientific research on the properties of natural origin raw materials and motivated by consumers' preferences [94]. Vegetable oils are abundant renewable and readily available sources exhibiting great interest as raw materials to develop natural and eco-friendly dermal products [95, 96]. These vegetable fats remain in the liquid form at room temperature and are most frequently extracted from seeds, fruits, or plant seedlings. Oils are composed of a mixture of higher saturated and unsaturated fatty acids with triglycerides [97]. These compounds result from a combination of higher fatty acids presenting long aliphatic carbon chains (low C14:0) with esters of glycerol and in small amounts they may contain phospholipids, free sterols, tocopherols (tocopherols and tocotrienols), triterpene alcohols, hydrocarbon and fat soluble vitamins [95, 97, 98].

Depending upon the individual percentages of fatty acids in their molecules, vegetable oils exhibit multiple skin benefits and therapeutic activities as antioxidant properties, providing skin protection against reactive oxygen species (ROS) [99, 100], and also anti-carcinogenic and anti-inflammatory activities [95, 101]. In dermal formulations, vegetable oils are used as moisturizers and emollients by increasing hydration and preventing water loss from the skin, primarily by forming a protective layer on the epidermis [97, 102]. Moreover, the beneficial effects of vegetable oils are well-recognized in the biological synthesis of components of cell membranes and in the transport and oxidation of cholesterol, thus playing a critical role in the proper functioning of the human body [97].

There are some research works reporting the use of vegetable oils in the formulation of lipid nanoparticles. For instance, Badea et al. [95] described a study involving the selection of seven vegetable oils, namely pomegranate seed oil, blackcurrant seed oil, sesame seed oil, raspberry seed oil, carrot root oil, wheat germ oil and rice bran oil to design and produce NLCs as nanocar-

riers for the encapsulation of diethylamino hydroxybenzoyl hexyl benzoate (DHHB) which is a synthetic sunscreen by hot high-pressure homogenization. They obtained appropriate sized NLCs, having mean particle sizes ranging between 100 nm and 145 nm, and showed that vegetable oils and especially their combinations have a great potential to be used to development antioxidant nanostructured lipid carriers loaded with a UVA to boost their photo-protective action. Lacatusu et al. [103] investigated the possibility of grape seed oil (GSO) and squalene (Sq) to formulate biocompatible NLCs with antioxidant properties as a protective and safety formula for b-carotene by a melt high-shear homogenization process and obtained nanoparticles with average diameters of about 85 nm for GSO and 89 nm for Sq and excellent antioxidant properties mainly attributed to the presence of Sq and GSO. Also, Lacatusu et al. [104] successfully synthesized by a combination of high shear and high pressure homogenization techniques, soft and functional nanocarriers based on pumpkin and amaranth oils able to co-encapsulate and co-deliver avobenzone and octocrylen, two UV-A and UV-B filters with mean diameters of 100 and 160 nm, good antioxidant activity and strong anti-UV properties.

4.5.2 Retinoids

Retinoids are poorly water-soluble compounds, chemically related natural and synthetic vitamin A derivatives that in part present different biological activities [31, 105]. This group includes various substances or derivatives of retinol, as retinaldehyde, retinoic acid (tretinoin) or retinyl esters as retinyl palmitate [105]. In this context, it is possible to differentiate two major retinoids families of acids, including isotretinoin and tretinoin, and non-acids. Furthermore, due to the lipophilic characteristic of retinoids, they can diffuse through cellular and phospholipid membranes [106].

In the skin, retinoids play a crucial regulatory role in epidermal growth and differentiation. They increase skin elasticity, decrease skin

roughness and prevent the peroxidation of skin lipids [31, 107]. Research studies have demonstrated that retinoids present several therapeutic benefits such as preventing oxidative stress; they can act as UV filters; help to renew epidermal cells; improve skin aging and photo-aging, and control cutaneous bacterial flora [105]. Retinoids demonstrate some other biological effects, including the decrease in skin roughness, the reduction of actinic keratoses and, hyperpigmentation and the improvement of fine wrinkles and acne vulgaris [31]. Moreover, topical retinoids act as antioxidants, preventing tissue atrophy and the loss of collagen that is generally a result of aging [108] and show antimicrobial activity against the bacteria typically involved in acne [109, 110].

Some retinoids as retinol (vitamin A), retinyl palmitate, beta carotene, tretinoin, isotretinoin, adapalene (ADA), and tazarotene have a great impact in topical administration [106]. Retinol is the most commonly used substance in modern antiaging preparations. Compared with tretinoin presents less irritant effects to the skin and is generally well-tolerated in topical administrations [111]. Retinol and their derivative retinyl esters are currently considered the “gold standard” of antiaging agents. They can be applied at a maximal concentration of up to 0.3% as the clinical efficacy of these compounds has been scientifically well studied and proven [106, 111]. Tretinoin has been commonly used in dermatology since the early 1960s, but it was only in the 1980s that its importance in treating aging skin was discovered [106]. Isotretinoin is a neo-collagenous substance that inhibits the functioning of metalloproteinases and is more tolerable than tretinoin. Although, it is typically recommended for the acne treatment, it is also viewed as an alternative approach to photo-aging [112, 113].

Despite the numerous beneficial effects of retinoids in the previously mentioned skin, the development of topical systems containing these compounds also presents some drawbacks as poor water solubility, high chemical instability, and photo-instability and potential irritation upon administration [31, 114]. Thus, retinoid-loaded

lipid nanoparticles have been pointed to help in decrease the adverse effects of these molecules and protect them against degradation [31, 109, 115, 116].

Jain et al. [117] investigated the possibility of co-administration of encapsulated ADA, which is a drug that demonstrates efficacy in the treatment of minor to moderate acne in humans and vitamin C, which is an important complementary active compound because of its antioxidant activity, within carbopol hydrogel to obtain a delivery system having in simultaneous prolonged anti-acne activity and anti-oxidative potential. The NLCs were prepared by high-pressure homogenization (HPH) method followed by incorporation into vitamin C loaded gel. All NLCs-ADA formulations presented an average size of 268.3 ± 2.5 nm with a narrow size distribution (PDI- 0.218 ± 0.0012) and zeta potential of 16.35 ± 0.21 mV, which gives it an improved permeability across bio-membranes and a beneficial effect while accumulating in skin layers. Furthermore, in contrast to that seen with free ADA, NLCs-ADA presented higher skin-targeting potential, and the adjuvant antioxidant helped to exacerbate the potential of ADA during chronic therapy, thus demonstrating the potential of NLCs as an efficient carrier for the dermal delivery of ADA and also the synergistic effect of vitamin C in topical therapeutics.

Lee et al. [118] developed a topical formulation of retinyl retinoate (RR) NLCs composed of canola oil as vegetable oil, Precirol or Compritol as solid lipids, and Tween 80 as a surfactant. RR is a newly synthesized anti-aging and anti-wrinkle agent synthesized from a reaction between retinoic acid and retinol and demonstrates higher chemical stability and improved skin regeneration effect than other retinoids that have been extensively used for the treatment of acne vulgaris and psoriasis. The method of HPH was efficiently employed in the NLC production. It yielded homogenous nanodispersions with a size range of 230–300 nm and PDI values of 0.2, regardless of the solid lipid selected. Precirol-based NLC

(P-NLC) showed an improved entrapment of RR with encapsulation efficiencies of 97.8% and a drug loading capacity (mg RR/g lipid) of 89.6 mg/g. In release studies using Franz diffusion cells, P-NLCs showed a controlled release pattern, being thus considered an appropriate system for topical drug delivery of the heat-labile ingredient RR.

Liu et al. [119] developed an isotretinoin-loaded SLN (IT-SLN) formulation with skin targeting for topical delivery of isotretinoin, commonly used to treat severe acne and other dermatological diseases. The hot homogenization method was performed to prepare the drug-loaded SLN using PRECIROL ATO 5 as solid lipid and the surfactants Tween 80 and soybean lecithin. SLN formulations showed a small average size between 30 and 50 nm, Transmission electron microscopy (TEM) images presented IT-SLN particles with a spherical shape, and the zeta potentials of all the formulations are about -15 mV. IT-SLN formulations showed high entrapment efficiency ranging from 80% to 100%. The penetration of isotretinoin from the IT-SLN formulations through skins and into skins was evaluated *in vitro* using Franz diffusion cells fitted with rat skins. The *in vitro* permeation data showed that all the IT-SLN formulations could avoid the systemic uptake of isotretinoin in skins. Furthermore, IT-SLN consisting of 3.0% PRECIROL ATO 5, 4.0% soybean lecithin, and 4.5% Tween 80 significantly increased the accumulative uptake of isotretinoin in the skin and showed a significantly enhanced skin targeting effect.

4.5.3 Antioxidants

Antioxidants are a heterogeneous group of substances that prevent oxidative stress from tissues of the body and offer protection to cell membranes by reducing or neutralizing the concentration of toxic oxygen molecules and free radicals [120, 121]. During the aging process, antioxidants are significantly reduced by extrinsic and intrinsic factors of human body. Among the various factors contributing to the skin aging are

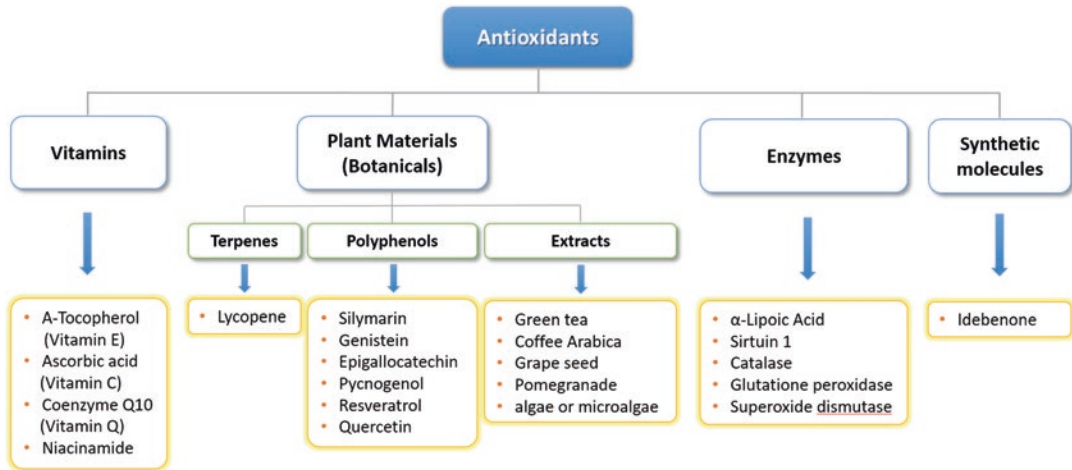


Fig. 4.3 Diagram of some antioxidants most commonly used in dermal formulations. (Adapted from [122]. Published with permission)

photo-damage, free radicals and oxidation, smoking, hormones, heredity and life style [120].

Topical antioxidants are considered a powerful strategy to reduce skin damage produced by reactive oxygen species (ROS) and restore or improve its antioxidant defense mechanisms [122]. This has driven the design of several pharmaceutical and cosmetic formulations to prevent or correct the injuries related to skin aging, thus improving skin healthiness and appearance [120, 123]. Some of the most commonly employed antioxidants in skincare formulations, claiming anti-aging effects, are based on exogenous antioxidants such as vitamins, enzymes, plant-derived active ingredients as polyphenols, and synthetic compounds that humans cannot synthesize in the body (Fig. 4.3) [120, 122].

Many skincare products are based on botanical active ingredients and extracts due to its potent antioxidant activity that plants produce to counteract the effect of UV radiation to which they are regularly exposed [121]. However, besides the important antioxidant characteristic, many topical products based on plant-derived active ingredients show other biologic properties such as anti-inflammatory and anti-carcinogenic activities [122]. An example of such a cases is resveratrol which belongs to the polyphenolic phytoalexins family and is found in grapes, nuts,

fruits (coloured berries), and many red wines. Resveratrol has pronounced antioxidant activity with strong anti-inflammatory, anti-proliferative, and sirtuin-activating properties [120, 122].

Vitamins as vitamin C (l-ascorbic acid), vitamin E (α -tocopherol), and vitamin B3 (niacinamide) are at present the most common active ingredients in cosmetic formulations to treat premature skin aging [124, 125]. α -Tocopherol is a lipid-soluble antioxidant found in concentrations of 2–20% in countless skin care products, in various foods such as vegetables, seeds, in meat, and in the skin [120]. It has demonstrated good tolerability on the skin with very positive effects and it can also be used against oxidation in dermal and food formulations. Besides its physiologic anti-inflammatory, immunostimulatory, and anti-proliferative effects, α -tocopherol prevent the epidermis to dry by creating a moisture barrier, protects the skin from harmful bacteria and helps skin repair itself [106, 126]. Moreover, this vitamin also showed antiaging effects, it accelerates the epithelialization of the skin, increases enzyme effects, and has photoprotective effects [120].

The main drawback of most compounds with proven antioxidant activity is that they do not show suitable properties to achieve adequate concentrations in the skin layers where they should exert their action. Thus, the rationale design of

skin delivery systems based on lipid nanocarriers could promote the delivery and bio-distribution of these compounds more efficiently and represent an undeniable benefit for many anti-aging skin care products [122].

Guo et al. [127] developed quercetin-loaded nanostructured lipid carriers (QT-NLCs) and evaluated their potential as a topical delivery system. Quercetin (QT) is a natural flavonoid that presents various biological activities. Besides its antioxidant potential, it also presents anti-cancer, anti-inflammation, anti-platelet aggregation, anti-anemic action, and anti-anaphylaxis effects. The method of emulsion evaporation-solidification was used to prepare QT-NLCs at low temperature, which presented an average particle size of 215.2 nm, with zeta potential values of -20.10 ± 1.22 mV and spherically shaped. The drug loading and average entrapment efficiency of the optimized QT-NLCs were $3.05 \pm 0.01\%$ and $89.95 \pm 0.16\%$, respectively. *In vitro* and *in vivo* skin permeation studies showed that QT-NLCs could increase drug retention in the epidermis and dermis compared to QT propylene glycol solution. Studies on effect of QT-NLCs on skin surface confirmed that QT-NLCs could weaken the barrier function of SC and facilitate drug permeation in skin, thus indicating that NLCs have a targeting and prolonged release effect and could be a promising vehicle for topical delivery of QT.

Soldati et al. [128] developed SLNs formulations containing natural seed butter from an Amazon tree, *Theobroma grandiflorum*, for the topical release of resveratrol. This compound is a non-flavonoid polyphenolic and unstable molecule with a broad range of biological activities such as antioxidant, anti-inflammatory, and cardio-protective properties. SLN loaded with resveratrol (R-SLN) was prepared by modified high shear homogenization technique and presented a homogenous size distribution with particle diameter equal to $195.30 \text{ nm} \pm 12.19 \text{ nm}$ and PdI of 0.16 ± 0.09 while the zeta potential revealed negative surface charge (-19.54 ± 1.89 mV). The obtained drug loading capacity and encapsulation efficiency were $3.36 \pm 0.11\%$ and $74.12 \pm 2.17\%$, respectively. A drug release study was performed using Franz Diffusion cells con-

taining artificial human sweat for 24h, and the kinetics revealed a burst release followed by a sustained drug release from R-SLNs. It was also verified an increased antioxidant activity in 20% and increased permeation and retention of resveratrol in the human skin, raising the amount of resveratrol over than 2-fold in stratum corneum compared to the resveratrol solution itself.

Dzulhi et al. [129] formulated SLN loaded with green tea leaves extract (GT-SLN) and evaluated their potential for skin penetration. The green tea leaves extract has a potent antioxidant activity due to polyphenols, which is known to be even higher compared with vitamin C and vitamin E. GT-SLN was prepared by solvent emulsification-evaporation method and presented a zeta potential of -30.967 ± 1.29 , with an average particle size of 155.6 ± 10.04 nm; polydispersity index of 0.409 ± 0.05 ; entrapment efficiency of $81.124 \pm 0.443\%$ and a spherical shape. *In vitro* penetration study performed in Franz diffusion cell was analyzed for 12 hours at 12 point intervals and showed flux value for GT of $0.261 \pm 0.005 \mu\text{g}/\text{cm}^2\cdot\text{hour}$ and from GT-SLN of $1.965 \pm 0.025 \mu\text{g}/\text{cm}^2\cdot\text{hour}$. The results indicated that GT-SLN formulations had a better penetration rate than the extract itself without being incorporated in SLN.

4.5.4 Moisturizers

Moisturizing creams aim at maintaining skin integrity and well-being by providing a healthy appearance for the individual. The products can be regarded as cosmetics but may also be regulated as medicinal products if they are marketed against dry skin diseases, such as atopic dermatitis and ichthyosis [130]. Moisturizers smooth a rough skin surface and protect it from dryness, containing emollients, occlusive agents, and moisture-retaining substances [120]. Thus, they are classified according to the mechanism of action of their compounds as occlusive, emollients, and humectants [106].

Most frequently, commercially available products use compounds of each of these classes in their formulations. Moisturizers not only serve as lipid-

replenishing and rehydrating skin care of dry skin, but also help maintain the aging skin health [130].

4.5.5 Polypeptides

At the molecular and functional level, polypeptides are capable of increasing collagen regeneration and preventing their degradation. Polypeptides with improved anti-aging activity are divided into signalers, neurotransmitter inhibitors, enzyme carriers, and inhibitors and are classified according to their main functional effects [106].

There is evidence that amino acids and peptides may enhance the texture and consistency of skin surface with impressive anti-aging results without undesirable effects [106]. It became possible to produce peptide sequences that imitate body's molecules, such as collagen or elastin, thus influencing metabolic processes such as collagen synthesis [120].

4.6 Toxicological Concerns

Applicable toxicity studies of lipid nanoparticles can be planned based on their intended use, exposure levels, and the ingredients present in the formulations [131]. The importance of toxicity studies lies in assuring the safety of new nanoparticles before any pre-clinical and clinical studies and they are recorded for common use in the pharmaceutical industry or in cosmetics. In this regard, it is of great importance to estimate the toxicology of lipid nanoparticles and perform standard toxicological experiments for a better assessment of these nanomaterials and their effects [132].

After the dermal exposure of a new substance, its dermal toxicity is evaluated through studies of local and systemic effects. The compounds that permeate the skin and induce systemic toxicity are identified through these dermal toxicity studies, however, it is not possible to quantify the total absorbed substance [133].

The SC, as the outmost layer of the skin, and its bi-lipid layers, regulate the degree of dermal permeation, which commonly occurs through

passive diffusion. Nevertheless, the biotransformation of test nanomaterial can occur prior to its systemic absorption in the deeper viable areas of the skin [134]. Certain biological factors mainly influence the dermal absorption process of nanoparticles as skin localization, SC integrity, and thickness of the epidermis [132]. Lipid nanoparticles are known to be stable in aqueous dispersion and allow the encapsulation of hydrophilic and lipophilic drugs, acting as drug reservoirs in various skin layers, accumulating between corneocytes, and intermixing with skin lipids, or by disintegrating and merging with lipidic layers [135].

Depending on ingredients to prepare lipid nanoparticles, it is possible to modify the release profile of active compounds and avoid their adverse effects. For instance, SLNs prepared with a drug-enriched shell show burst release characteristics, whereas SLNs with a drug-enriched core lead to a sustained release. Despite their composition, the physicochemical properties, impurity, and purity may also influence the toxic profiles of lipid nanoparticles. Given the above, an important advantage of SLNs is their biodegradability. Generally, SLN and NLC are well-tolerated in living organism, lipids easily undergo natural decomposition, for example, under the effect of enzymes. There is a risk that nanoparticles can be cytotoxic, if they adhere to the cell membrane and then gradually release the products of cytotoxic degradation. In the case when lipid matrix materials are made of fatty acids, the products of biodegradation are compounds naturally present in human organisms [25]. The components used to formulate SLNs are safe as compared to polymeric nano and microparticles, which may cause systemic toxicity by impairment of the reticuloendothelial system due to slow degradation of its components up to 4 weeks [136]. However, it is worth emphasizing that surfactants that are part of lipid nanoparticles can have the most significant impact on their toxicity since these agents interact with cell membranes composed of phospholipids. A prerequisite to being safe is the GRAS (generally recognized as safe) status of the excipients of lipid nanoparticles, but additional nanotoxicological studies

are needed to allow the understanding of the effect of nanoparticles in the body [137, 138]. There is an established relationship between the size of nanoparticles and their toxicity, as the lower the size, the higher the surface area and the higher the reactivity.

Due to the rigidity and dimensions of the SC barrier layer, it is established that nanoparticles with sizes greater than 100 nm do not perfuse this skin layer. However, particles of ≈ 200 nm size provide an occlusive protective effect on skin surface that in turn enhances penetration of the skin [136].

A major concern in evaluating skin absorption and toxicity of nanomaterials is how to conduct the experiments. Both *in vivo* and *in vitro* methods are used to determine the skin penetration of lipid nanoparticles because selecting either of these techniques may result in distinct types of results and information [139]. The Franz diffusion cell is a well-established model for dermal and transdermal delivery, and it has been used as an important method for transdermal drug research [140]. The *in vitro* dermal penetration techniques using donated human skin are preferred to *in vivo* tests in animals. *In vitro* studies have shown that SLNs are acceptable at concentrations <1 mg/mL (total lipids), and with particle diameter >500 nm can be less tolerated, which can be explained by their aggregation. It was also shown that the stabilized formulations composed of several surfactants are less biocompatible than those based on one surfactant only. For polysorbate 80 and poloxamer 188, two surfactants mostly used in SLNs formulations, enough evidence has been found to determine their safety [141].

In vivo studies, which evaluate the organism as a whole, with the skin of rat or pig produce better results since these animals are anatomically, physiologically and biochemically similar to humans, but are strictly restrained by legislation. Therefore, *in vivo* studies are important to define the concentration and location of the active compound in the tissues and systemic toxicity [142]. Systems produced with large quantities of surfactants present a higher risk of exhibiting cytotoxicity.

It seems evident that the knowledge of the toxicological profile of any active compound and the biocompatibility of the delivery systems are

critical for implementing new therapies, but the currently available information of lipid nanoparticle dermal toxicity is still very limited [143].

4.7 Experimental Assessment of Dermal Absorption

Dermal absorption is the way how different compounds pass through skin into the systemic circulation [144]. The interaction of a compound from the skin's external surface with the epidermis but not with the circulatory system is a dermal penetration. Dermal permeation is the penetration through functionally and structurally different layers. Moreover, dermal resorption is the uptake of a substance into the dermal blood or lymph capillaries, thus entering directly or indirectly the systemic circulation [145].

The most effective way to transport bioactive compounds to the skin for topical and transdermal applications is through different nanocarriers formulations. The bioavailability of topical drugs evaluation requires different methodologies due to the type of drug, disease to treat, and product application [146]. Therefore, using the right methodology to study penetration and permeation through the skin phenomena is a multifaceted issue.

The characteristics of the drug carrier system strongly influence how the system can be most successfully examined [40, 145]. Different methods have been defined for the cutaneous drug release and penetration profile studies using nanocarriers. General rules for dermal absorption studies are given by the regulations from Europe and the United States. However, ethical issues and non uniform methodologies require replacing animal use in the cosmetic, pharmacological, and toxicological sciences to replace trustworthy and reproducible alternative methods. The European Union legislation forbade the use of animals for cosmetic products tests. Since 2004 and 2009, the use of animal models for commercial product testing has been banned. Besides, to substitute the use of animal *in vivo* studies, the European Centre for the Validation of Alternative Methods (ECVAM) presented a document with the list of authorized

in vitro cell models for the safety assessment of cosmetic products [146–148]. These documents give some norms on conducting dermal absorption assay, but the detailed experimental details are not properly regulated. However, for the study of carcinogenicity, repeat dose toxicity and reproductive toxicity assays, for which there is no alternative in vitro methods development of in vitro models, are urgently needed.

The Guidance Notes on Dermal Absorption (No.156) [44], Test Guidelines 427 (*in vivo* methods) [43] and 428 (*in vitro* methods) [42], and the Guidance Document for the Conduct of Skin Absorption Studies [41] were published about this subject by Organization for Economic Cooperation and Development (OECD). The OECD has given guidelines, but those are not fixed and specified protocols, so a detailed pre-experimental optimization of the particular experimental conditions such as characteristics of the test compound, protocol conditions, and the purposes of the study are necessary to be done. The OECD 428 determines detailed rules of obligatory experimental details, and the test system needs to be justified [41].

Interested in more information about this regulation can found the information in the World Health Organization International Program on Chemical Safety (WHO/IPCS) Environmental Health Criteria 235 [45], the European Centre for Ecotoxicology and Toxicology of Chemicals (ECETOC) Monograph 20 [149], the United States Environmental Protection Agency (USEPA) report on dermal exposure assessment [150], and the European Food Safety Agency (EFSA) Guidance on dermal absorption for plant protection products [47]. The standard technique by which the bioavailability of all topical drugs can be assessed does not exist. Based on research discussion between pharmaceutical scientists and dermatologists from academia, industry, and regulatory agencies, the outcome emphasized a need for greater attention to quality, probably, via a Quality-By-Design (QBD) approach. In addition, it has been suggested that multiple techniques be used in complement to take advantage of each technique's assets [48, 49].

Concerning the chemical composition and the skin morphology and characteristics, lipid

nanoparticles showed immense potential as vehicles for cutaneous administration of bioactive compounds, mainly due to the targeting effect and controlled release in different skin strata. Looking into the literature, it is perceivable that lipid nanoparticles have been used to a much superior level for topical and dermal drug delivery compared to transdermal application. Since the epidermis is rich in lipids, lipid carriers for drugs can promote absorption into the outermost layer of the skin, the SC. However, local and systemic toxic effects are major issues in skin absorption [151].

Techniques for modeling absorption through human skin are divided in two main group: quantitative techniques (Diffusion cells) and qualitative or semi-quantitative techniques which include different microscopic and spectroscopic methods such as Fluorescence microscopy, Two-Photon microscopy (2-PFM), Confocal Laser Scanning microscopy (CLSM), and the Raman microscopic methods.

The most commonly utilized methodologies are 1) *in vitro* (Diffusion cells), 2) *ex vivo* (extracted from organism's skin models), 3) *in vivo* (vasoconstrictor assay, tape stripping, and microdialysis).

In vitro and *ex vivo* techniques are usually used in the early stages of drug development to optimize drug delivery. *In vivo* techniques are used in the later stages to consider additional local and systemic effects.

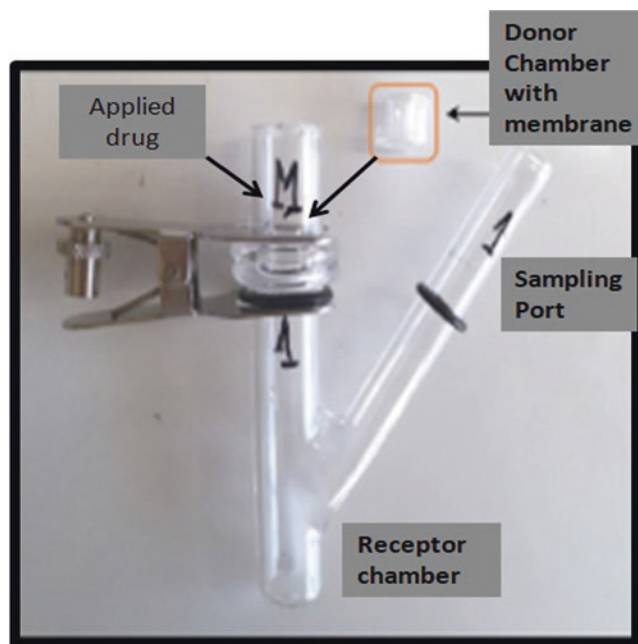
4.7.1 In Vitro Methods to Evaluate Skin Penetration

4.7.1.1 Diffusion Cells and Diffusion Tests

Diffusion cells are typically made of glass and can be categorized into three primary classes [152–154]:

1. Franz diffusion cell (vertical) (Fig. 4.4)
2. Two – chambered Side-by-side cell (horizontal)
3. One – chambered flow – through cell (vertical)

Fig. 4.4 Example of a Franz diffusion cell



The Franz diffusion cell divides into two sections (Fig. 4.4): the donor compartment and the receptor compartment, which can be open, semi-open, or closed. The two compartments are divided by an artificial membrane or a skin model horizontally oriented, with the drug being applied to the donor chamber. A receptor medium with sink conditions is regularly sampled for drug/metabolite and replaced [40, 152, 153].

Side-by-side water jacketed diffusion cells housed both the receptor and donor cells for permeability testing separated by membrane.

Side-by-side water-jacketed diffusion cells for permeability study permit liquid circulation through the vertical membrane, separating the receptor and donor compartment.

Another type of diffusion cell approach is the “one-chamber flow-through” type described by Bronaugh and Stewart [154]. The goal is to mimic *in vivo* conditions by automating sampling where the receptor fluid is continually pumping through the dermal chamber, and sample gathering is in a fraction collector. Related results have been described for all types of cells.

Depending on objectives, two types of diffusion protocols exist: *in vitro* release tests (IVRT) and *in vitro* skin permeation studies (IVPT) [155]. The IVRT study shows the release rate, and the IVPT study shows the flux profile. The IVRT incorporates the use of artificial membranes (lipid or non-lipid-based model), and the sample dose must be blocked and infinite. Usually should be used in the early phase of the study. The IVPT should be used for promising formulations as this protocol include the use of the human skin. The sample dose should be un-occluded and finite [152, 155].

Artificial Polymeric Membranes

The non-lipid silicone membranes are most effective for studying the skin permeability of lipophilic compounds though their use for hydrophilic compounds has not been suggested [156, 157]. The poly(dimethylsiloxane) (PDMS) membranes have been used as a model to study the mechanism of methyl paraben and salicylic acid transport across human skin [158]. The solvent membrane, composed of 70% silicone oil and 30% isopropyl myristate compared with human skin permeability coef-

ficients, was shown to be a suitable model to determine SC/water partition coefficients using Parallel Artificial Membrane Permeability Assay (skin-PAMPA model) for a variety of model drugs in agreement to the existing literature values [159]. High human skin permeability correlation for different drug systems was achieved with another synthetic membrane, namely the Strat-M™ membrane. This membrane creates a morphology similar to human skin, characterized by a very tight surface layer with a porous structure. The membrane is composed of multiple layers of polyether sulfone, which could be impregnated with a specific blend of synthetic lipids, mimicking the additional skin-like properties of the artificial membrane [160].

Lipid based model membranes, using the skin-PAMPA protocol, developed by Sinkó et al. [161], showed a good permeability correlation of a selected drug model tested with the different human skin databases. The membrane model composition reproduces simplified composition of the skin lipid matrix, which includes free fatty acids, cholesterol, and a synthetic ceramide-analog. In the standard skin-PAMPA procedure, a huge quantity of samples is requested for the donor plate, which does not meet the concept of a limited dose. A poor correlation was obtained between the skin-PAMPA and the epidermis, while between the skin-PAMPA and the full-thickness skin was obtained a good correlation [161]. For more details on the skin-PAMPA applications, the reader is referred to look at Sinkó et al., 2015 [162].

The Phospholipid vesicle-based permeation (PVPA) model is based on tightly fused liposomes on a polymeric membrane filter to mimic the human SC. The PVPA model provides a tool to perform a high-throughput permeability screening. By tuning liposome compositions to mimic thigh SC barriers, it is possible to obtain different PVAP absorption barrier models that can cover drugs with different lipophilic characteristics and penetration ability [163–165].

Reconstructed Human Skin Equivalents (RHSEs)

Another test systems such as reconstructed skin models have been developed due to limited availability of human skin, ethical issues, and interspecies variability regarding the use of animal skin for cosmetic applications. These models are already commercially available (e.g., EpiDerm®, MatTek; EpiSkin®, SkinEthic, Lyon, France) [164, 166–175]. Reconstructed skin models try to imitate the structure and physiology of human skin. These models have already been validated for phototoxicity, acute skin irritation, skin corrosion testing, and drug permeability studies [166, 170, 176]. They are usually classified in two groups [166, 170, 174]:

1. Reconstructed Human Epidermis (RHEs) models with SC and viable epidermis (e.g., EpiSkin®, SkinEthic®, EpiDerm®). EpiSkin® was developed by L'Oréal (France), and commercially supplied by SkinEthics Laboratories (France), involve the epidermal layers of native skin. [167]. Also, the Epiderm™ model (MatTek Corporation, Massachusetts, USA) was successfully used for in vitro toxicology assessment, such as dermal corrosivity, skin irritation, and phototoxicity of several cosmetic ingredients [167, 169, 176].
2. Full-Thickness skin models (FTMs) consist of SC, viable epidermis, and dermal analogous (GraftSkin®, EpiDermFT®, Phenion®). Commercially available models such as Graftskin TMLSETM (Organogenesis, MA, USA) and Phenion® (Henkel Corp, Düsseldorf, Germany) showed good reproducibility of the permeation profile.) The Full-Thickness skin models contain keratinocytes grown on a dermal substrate populated with fibroblasts to form epidermal and dermal compartments.

The major limitation of RHSEs is the overpredicted permeability parameters compared to those from human or animal skin, probably due to different lipid composition and organization of SC. Also, there is no available RHSEs model

with appendages as hair follicles, pilosebaceous units, and sweat glands to study the drug permeation mechanisms. Thus, RHSEs are considerably more permeable but more uniform in permeability than *ex vivo* human skin models, which are more inconsistent. Nevertheless, RHSEs could provide an adequate tool for quality control of cosmetic products [173, 175].

Skin-on-a-Chip

Technological advance in microfluidics has provided an opportunity to integrate three-dimensional (3D) tissue engineered models to develop ‘organ-on-chip’ systems to create human skin analogs that better mimic the morphology and functionalities of human skin, compared to conventional static culture systems (Fig. 4.5). Overcoming the lack of vascularization and incapability for long-term culture of RHSEs models, microfluidic-based platforms have been developed and incorporate previously engineered skin models to better simulate the *in vitro* skin function [177–179]. “Skin-on-a-chip” model culture skin tissue inside of a microfluidic system to develop the 3D microdomains of the natural human skin, and also to control skin model surroundings. A microfluidic and biosensor technology is used to create the “skin-on-a-chip” model with different skin culture models [178, 179]. Identifying a suitable cell source that resembles the natural skin and is widely accessible, reproducible, and cost-effective is of enormous importance for developing a skin-on-chip platform. For example, Wufuer et al. developed a skin-on-a-

chip model that simulated inflammation and edema [180].

Skin-on-a-chip platforms include continuous, pulsatile, and gravity flows [181]. Contrary to liquid-liquid interface tissues (LLI), the epidermis belongs to air-liquid interface (ALI) tissues. A majority of studies applied LLI for *in vitro* research, while some studies modeled ALI. *In vitro* immune-competent model was developed by Ramadan and Ting evaluate the protection impact of the keratinocytes layer and toxicity of different hazards [182]. Though it shows potential for capturing the aspects of drug transport and distribution, skin-on-a-chip still faces challenges such as scalability issues, analytical detection limitation, and different requirements of media supplementation for each tissue [177, 181].

3D Three-Dimensional Bioprinted Skin Equivalent

Bioprinting or direct cell printing is a very useful addition to tissue engineering technology. This relatively new technology aims to create *de novo* organs with precisely controlled structural design, high reproducibility, and repeatability. A computer-aided bioadditive manufacturing process has emerged to deposit living cells together with hydrogel-based scaffolds for 3-D tissue and organ fabrication through a layer-by-layer building process [184, 185].

Development of high-throughput, reproducible, three-dimensional (3D) bioprinted skin equivalents (BPSEs) that have structure and func-

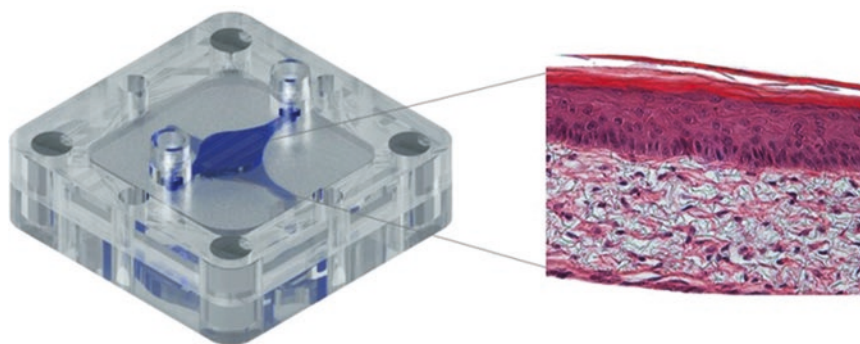


Fig. 4.5 Schematic layout of a microfabricated 3D-skin-on-a-chip. (Reproduced with permission from authors [183])

tionally similar to native skin tissue have a considerable interest, as well for the skin related diseases and regenerative medicine issues, as for the industrial application in cosmetics [186]. Regarding bioink admission, bioprinting modalities are divided into three types: droplet-, extrusion-, and laser-based bioprinting [187, 188]. Concerning the inherent multilayered, multicellular composition of human skin, bioprinting is an advantageous production method to create skin models for pharmaceutical and dermatological testing.

Tseng et al. [211] use magnetic 3D bioprinting and fibroblasts as the cellular component for performed toxicity assay of five different drugs [189].

4.7.2 Ex vivo Models to Evaluate Skin Penetration

The use of *ex vivo* models of either human or animal origin for dermal absorption studies is extensively reported in the literature. Various types of skin are proposed for this studies such as human cadaver skin and excised skin from different animals (e.g., rodents, pigs, guinea pigs, snakes) [163, 172, 175, 190, 191]. Excised human skin is acknowledged as the best surrogate for *in vivo* humans compared to other skin [190]. However, the choice of an appropriate *ex vivo* model for the drug permeability depends on different factors such as precise experimental conditions, storage, sample treatment, and preparation [191]. The region from breast or abdominal skin should be used for the experimental outcome and excised skin barrier properties stay stable for six months at -20°C [175].

With characteristics closely similar to human skin, regard to similar skin layer thicknesses, follicular structures, skin lipids composition, and dermal anatomy, porcine skin has been widely used in skin-permeation studies (usually skins of the flanks and/or the pig ears) [192, 193]. Mainly used animal skin models are from primates such as a mouse, rat, guinea pig, rabbit, bovine (udder). The snake models are also

used. As the primate research has very controlled rules and ethical considerations, the rodent skin, regarding its relative facility to obtain (small size of rodents, uncomplicated handling, and relatively low cost), is mostly used as a model in *in vitro* and *in vivo* (trans) dermal studies [191].

The topical bioavailability of drugs in isolated perfused skin models is assessed similarly to the Franz diffusion cell. The comparison of *in vitro* and *ex vivo* studies on the percutaneous permeation of various topical formulations containing ibuprofen using both the isolated bovine udder and Franz diffusion cell shows visible differences in the permeation of ibuprofen occurred *in vitro* (udder skin) and *ex vivo* (isolated perfused bovine udder). However, in the cellophane membrane, it was not observed [194]. Yet, authors suggested the use of Franz diffusion cells when work costs are essential, and they propose the use of isolated skin/organs to study mechanisms of cell-cell interactions or to study the metabolism of the drug in the skin [194].

4.7.3 In Vivo Models

In vivo absorption methodologies are influenced by ethical, economic, and experimental issues [171]. The main instructions and suggestions can be found in OECD documents about this subject, for example, the Guidance Notes on Dermal Absorption (No. 156) and Test Guidelines 427 (*in vivo* methods) [43, 44].

In vivo techniques are used in the advanced phases to study possible additional local and systemic effects and define the final product [40]. We will briefly present the most used *in vivo* techniques and indicate the literature for more detailed explanations.

1. The human skin blanching assay (Vasoconstrictor assay)

This protocol uses the blanching effects to determine the bioequivalence (BE) of topical

corticosteroids. This bioassay may apply in various test modes (e.g., ointments, creams, and gels, and for the comparison of generic formulations) for several purposes, such as evaluation of the drug delivery system impact on the skin, topical efficiency of new corticosteroid molecules, and study the efficacy of penetration enhancers. The methodology is also helpful to determine the effectiveness of viable formulations for clinical applications. However, the various authors presented diverse experimental methods, which difficult comparison of results [195, 196].

2. Tape stripping/dermatopharmacokinetics (DKP)

The tape stripping method is used to measure the penetration of topically applied drugs on the SC layer of human skin. The assumption of the DPK method is that (i) the SC is the rate-limiting barrier to appropriate permeabilization of the stratum corneum, and (ii) the amount of drug in the SC is directly related to drug quantity in the epidermis [197, 198]. During the specific absorption time, the drug is applied to several sites on the skin. Then in this minimally invasive method, layers of the SC are detached by an adhesive tape, and the skin sample from the adhesive tape is analyzed. Additionally, the impact of the compounds on skin hydration effect on skin SC structure can be analyzed [199, 200]. The method may be quantitative or semiquantitative depending on the analysis (High-Pressure Liquid Chromatography analysis (HPLC) or Attenuated Total Reflectance Fourier transform infrared spectroscopy (ATR-FTIR) [201].

3. Microdialysis (MD)

Microdialysis in the skin is a technique for *in vivo* sampling in dermal and transdermal drug delivery. MD as a research method has proved to be a safe and important tool for phar-

macokinetic and pharmacodynamic studies. It allows direct, continuous observing of the extracellular concentration of drugs in the dermis. Microdialysis is a low invasive method that uses a probe with an implanted semipermeable membrane. The probe is taken by the small skin punctures, which provokes low tissue trauma that generally disappear after 60–90 minutes [202–204].

4.7.4 Microscopic Techniques

Qualitative or semi-quantitative techniques for modeling absorption through human skin include diverse microscopic and spectroscopic methods [152]. The central objective of these techniques is usually to follow the administration of the drug between the diverse skin layers and clarification of the penetration mechanism. The relative quantity of the active compound through different skin layers can be followed and evaluated [205–208].

By fluorescence microscopy is possible to detect the position of fluorophore molecules in the sample (e.g., drug vehicle cellular uptake) and confocal microscopy as a specific type of fluorescence microscopy allows obtaining 3D images of the analyzed system. The most used confocal techniques are Two-photon microscopy (2-PFM), Confocal Laser Scanning Microscopy (CLSM), and lately, laser-based microscopy used to perform Raman spectroscopy.

Visualization of lipid domains in human skin SC in a broad temperature range [209], imaging of all layers of the porcine cornea [210], images of pigskin structure and transdermal delivery of liposomes [211], two-photon fluorescence lifetime imaging of the skin SC pH Gradient [212] are some of the examples where 2-PFM has been successfully used.

Confocal laser scanning microscopy (CLSM) is a fluorescence technique frequently used to imagine the position/movement of observed fluorescent compounds in the skin. CLSM can be used to observe the skin morphology without tissue fixation and/or mechanical sectioning [173].

CLSM can be applied to clarify the transport mechanism of the drug delivery system through the skin [213–218]. The CLSM may identify the penetration profiles of fluorescent markers incorporated in nanostructured carriers by encapsulation [152].

Transport mechanism through the SC of native and *in vitro* reconstructed epidermis [217], liposome–skin interaction [213–215], the penetration of fluorescent probes into fibroblasts and nude mice skin [216], and the uniform permeation into the SC of reconstructed human epidermis model of TOC-DiO-NLC (Fig. 4.6) [218], are some of the examples of CLSM efficiency for permeation studies.

Raman spectroscopy is a highly selective, noninvasive spectroscopic method that uses a laser ray for molecule excitation those producing the distinctive vibrational energy levels of a

molecule that allows clear molecular identification. Using Raman spectroscopy dismisses the use of fluorescent probes. Raman microscopy allows understanding percutaneous drug delivery of bioactive compounds and skin structure [219, 220]. It can be used *in vitro* as well as *in vivo* permeation studies [221–223]. Bakonyi et al. [224] used Raman spectroscopy to study the spatial distribution of lidocaine in the skin for four types of formulation: hydrogel, oleogel, lyotropic liquid crystal, and NLCs. Nakagawa et al. perform *in vivo* determination of the water amount in the dermis using confocal Raman spectroscopy [225]. Also, the impact of permeation enhancers for drug distribution in *ex vivo* human skin were explained by this methodology [222].

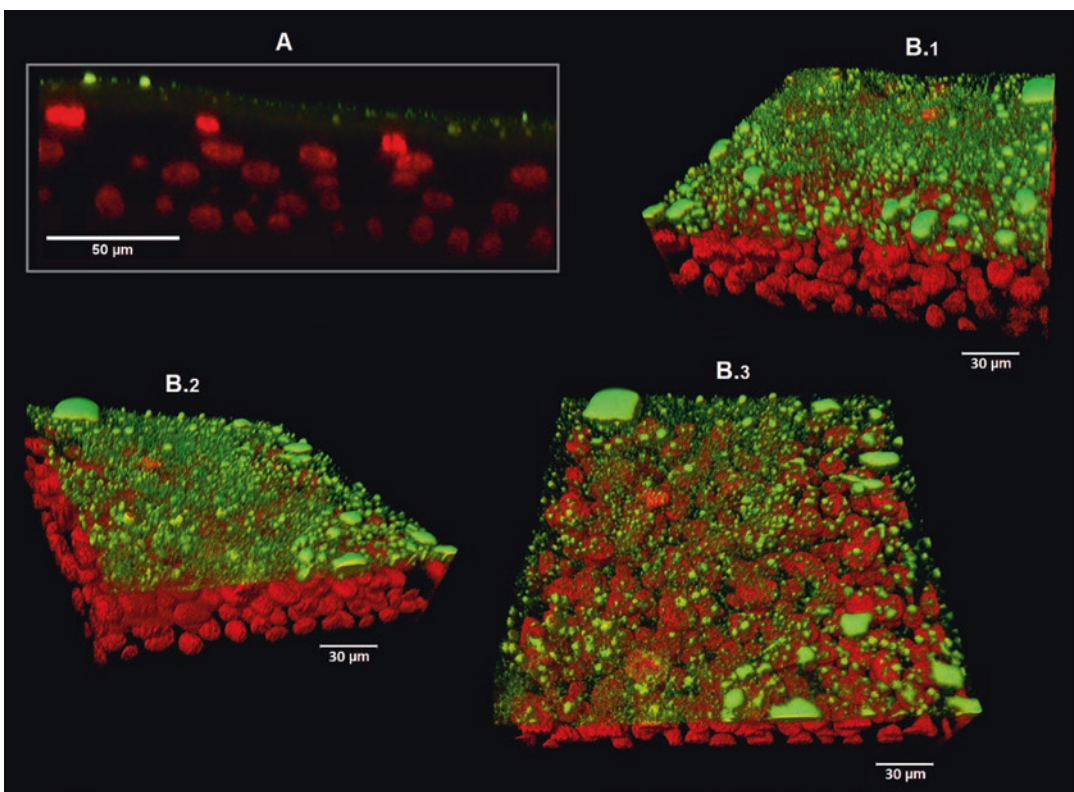


Fig. 4.6 Images of skin cross-sections from qualitative *in vitro* adsorption studies of TOC-DiO-NLCs by CLSM. (Reproduced with permission from authors [218])

4.7.5 Skin Permeation Studies of Lipid Nanoparticles

The composition and characteristics of lipid nanocarriers made them most studied systems for topical application. Solid lipid nanoparticles and nanostructured lipid carriers belong to the group of matrix nanoparticles. Table 4.1 show examples of methodologies explained in previous chapters used for the skin permeation/penetration studies performed with lipid nanoparticles [173].

4.8 Conclusions

Dermal delivery provides a successful alternative to the oral route which major limitation is the mostly impermeable *SC* that limits the entry of active compounds through the skin. However, in the last decades, researchers have been dedicated to developing lipid nanoparticles for skin delivery that offer advantages in terms of better drug loading and encapsulation efficiency, colloidal stability, adhesion, film formation, and occlusion in contrast to liposomes and polymeric nanoparticles. SLNs and NLCs are the most studied lipid-based drug delivery systems, which can deliver drugs and also nutrients for several administration routes due to their biocompatibility, low toxicity, high loading capacity, slow-release rate, and high stability. Moreover, lipid nanoparticles can protect the active compounds against chemical degradation and achieve controlled drug release, once the drug is entrapped the lipid core surrounded by a surfactant at the outer surface. These systems are being developed as drug carriers for administration by various routes, including dermal, ocular, and oral, with the dermal route being the safest. SLNs and NLCs have additional advantages in terms of drug encapsulation efficiency and colloidal stability. Regarding the mechanism of skin interactions, these deliv-

ery systems enable the formation of a hydrophobic film on the skin resulting in an occlusive effect leading to *SC* rearrangement, promoting skin penetration. Lipid nanoparticles have physicochemical properties that give them exceptional biological activity, with their toxicological profile being dependent on these properties, mainly the particle size and size distribution, as well as zeta potential. Thus, site-specific targeting can be achieved by tailoring their composition in terms of lipids and surfactants, and consequently, their properties, optimized by factorial design approach with important therapeutic outcomes. However, there is still limited knowledge about the ability of these nanocarrier systems to permeate biological membranes, distribute the active compounds in the skin strata, and deposit themselves in the body's tissues, giving information about skin penetration.

The success of topical therapy using lipid nanoparticles is associated with the techniques used to evaluate the preparations, which facilitate the optimization of the skin penetration of bioactive compounds. The selection of the most suitable techniques is essential and should be based on availability, facility of use, cost, and particular restrictions. The models and testing protocols are standardized and validated by regulatory authorities and industry to ensure reproducibility and similarity to *in vivo* scenarios. While being valuable for an early testing phase *in vitro* and *ex vivo* techniques are usually used in the early stages of drug development to optimize drug delivery, while *in vivo* techniques are used in the later stages to consider additional local and systemic effects, as well as finalize development. Additionally, localization and penetration/permeation complexity measurements, investigation of penetration mechanism into skin facilitated by nanocarriers have also been addressed by various microscopic, spectroscopic, and structural methods.

Table 4.1 Overview of methodologies used in dermal absorption studies applying on lipid nanoparticles

Lipid nanoparticle	Active compound	Formulation	Methodology	References
NLC	tocopherol	Vegetable oil, myristic acid	<i>In vitro</i> , Reconstructed human epidermis, Franz-type diffusion cell, confocal microscopy	[218]
Lipid nanospheres	Vitamin A or E	Lecinol, soybean oil	<i>In vitro</i> , full-thickness rat skin, Franz diffusion cell	[226]
SLN	Vitamin A	Compritol® 888 ATO	<i>In vitro</i> , full-thickness pig skin, diffusion cell	[227]
SLN	Oxybenzone	Cetyl palmitate, Tego Care 450®	<i>In vivo</i> , human skin, tape stripping technique	[228]
SLN	Triptolide	Tristearin glyceride, stearic acid	<i>In vitro</i> , full-thickness rat skin, Franz diffusion cell	[229]
SLN, NLC, nanoemulsion	-	Compritol®, Precirol®, Oleic acid, Miglyol® 812	<i>In vitro</i> , full-thickness pig skin, Franz diffusion cell, fluorescence microscopy	[78]
NLC	Indomethacin	Compritol® 888 ATO, Miglyol® 812	<i>In vitro</i> , human skin, Franz-type diffusion cell	[230]
SLN, NLC	Ascorbyl palmitate	Witepsol® E85, Mygliol® 812	<i>In vitro</i> , full-thickness human skin, Franz diffusion cell	[231]
SLN	Triptolide	Tristearin glyceride, stearic acid	<i>In vitro</i> , full-thickness rat skin, Franz diffusion cell	[232]
SLN	RU58841-myristate	Compritol®, Precirol®	<i>In vitro</i> , reconstructed epidermis (SkinEthic), Franz diffusion cell, Fluorescence microscopy	[233]
SLN	Podophyllotoxin	Tripalmitin	<i>In vitro</i> , full-thickness porcine skin, Franz diffusion cell	[234]
SLN	Vitamin A palmita	Compritol® 888 ATO	<i>In vitro</i> , full-thickness human skin, Keshary Chien cells	[107]
NLC	Ketorolac	Compritol® 888 ATO, Miglyol®812	<i>In vitro</i> , epidermal human membranes, Franz-type diffusion cell	[235]
SLN	<i>Artemisia arborescens</i> essential oil	Compritol® 888 ATO	<i>In vitro</i> , full-thickness pig skin, Franz diffusion cell	[236]
Lipid nanoparticles	Hinokitiol	Stearic acid	<i>In vitro</i> , full-thickness hairless mouse skin, Franz diffusion cell	[237]
SLN	Isotretinoin	Precirol® ATO 5	<i>In vitro</i> , full-thickness rat skin, Franz diffusion cell	[85]
NLC	-	Sabowax CP®, Miglyol® 821	<i>In vitro</i> , full-thickness human skin, Franz diffusion cells, confocal microscopy	[77]

(continued)

Table 4.1 (continued)

Lipid nanoparticle	Active compound	Formulation	Methodology	References
Lipid nanoparticles	Corticosterone	Medium-chain triglycerides, tripalmitate, cholesteryl myristate, cholesteryl nonanoate, glycerol monooleate	<i>In vitro</i> , human heat-separated epidermis trypsin isolated stratum corneum, Franz diffusion cell, Fluorescence light microscopy	[238]
Lipid nanoparticles	Ketoprofen and naproxen	Compritol® 888 ATO, Miglyol®812	<i>In vitro</i> , human epidermal membranes, Franz diffusion cell	[239]
SLN	Tretinoin	Fruit kernel fats	<i>In vitro</i> , full-thickness rat skin, Franz diffusion cell	[240]
SLN	Miconazole nitrate	Compritol® 888 ATO	<i>In vitro</i> , full-thickness human skin, Franz diffusion cell	[241]
SLN	Econazole nitrate	Precirol® ATO 5	<i>In vitro</i> , porcine epidermal membrane, Franz diffusion cell	[242]

Source: Adapted from Contri et al. [206]

References

- Guimarães KL, Ré MI (2011) Lipid nanoparticles as carriers for cosmetic ingredients: the first (SLN) and the second generation (NLC), in *Nanocosmetics and nanomedicines*. Springer, pp 101–122
- Severino P et al (2016) Advances in nanobiomaterials for topical administrations: new galenic and cosmetic formulations, in *Nanobiomaterials in Galenic Formulations and Cosmetics*. Elsevier, pp 1–23
- Yan L et al (2014) Advanced materials and nanotechnology for drug delivery. *Adv Mater* **26**(31):5533–5540
- Jain KK (2008) Nanomedicine: application of nanobiotechnology in medical practice. *Med Princ Pract* **17**(2):89–101
- Montenegro L et al (2016) From nanoemulsions to nanostructured lipid carriers: a relevant development in dermal delivery of drugs and cosmetics. *Journal of Drug Delivery Science and Technology* **32**:100–112
- Abla MJ, Singh ND, Banga AK (2016) Role of nanotechnology in skin delivery of drugs. In: *Percutaneous penetration enhancers chemical methods in penetration enhancement*. Springer, pp 1–13
- Escobar-Chávez JJ et al (2012) Nanocarrier systems for transdermal drug delivery. In: *Recent advances in novel drug carrier systems*. Intech
- Mihiryan A, Ferraz N, Strømme M (2012) Current status and future prospects of nanotechnology in cosmetics. *Prog Mater Sci* **57**(5):875–910
- Garcês A et al (2017) Formulations based on solid lipid nanoparticles (SLN) and nanostructured lipid carriers (NLC) for cutaneous use: a review. *Eur J Pharm Sci*
- Souto E, Almeida A, Müller R (2007) Lipid nanoparticles (SLN®, NLC®) for cutaneous drug delivery: structure, protection and skin effects. *J Biomed Nanotechnol* **3**(4):317–331
- Jose A et al (2018) Effective skin cancer treatment by topical co-delivery of curcumin and STAT3 siRNA using cationic liposomes. *AAPS PharmSciTech* **19**(1):166–175
- Alvarez-Trabado J, Diebold Y, Sanchez A (2017) Designing lipid nanoparticles for topical ocular drug delivery. *Int J Pharm*
- Pathan IB et al (2018) Curcumin loaded ethosomes for transdermal application: formulation, optimization, in-vitro and in-vivo study. *Journal of Drug Delivery Science and Technology* **44**:49–57
- Puglia C et al (2017) Nanostructured lipid carriers (NLC) as vehicles for topical administration of sesamol: in vitro percutaneous absorption study and evaluation of antioxidant activity. *Planta Med* **83**(05):398–404
- Teeranachaideekul V, Chantaburaran T, Junyaprasert VB (2017) Influence of state and crystallinity of lipid matrix on physicochemical properties and permeation of capsaicin-loaded lipid nanoparticles for topical delivery. *Journal of Drug Delivery Science and Technology* **39**:300–307
- Tamayo I et al (2017) Topical immunization using a nanoemulsion containing bacterial membrane antigens. *Journal of Drug Delivery Science and Technology* **42**:207–214
- Sahle FF et al (2017) Formulation and comparative in vitro evaluation of various dexamethasone-loaded pH-sensitive polymeric nanoparticles intended for dermal applications. *Int J Pharm* **516**(1-2):21–31
- Paolicelli P et al (2017) Design and characterization of a biocompatible physical hydrogel based on

- scleroglucan for topical drug delivery. *Carbohydr Polym* **174**:960–969
19. Arya J et al (2017) Tolerability, usability and acceptability of dissolving microneedle patch administration in human subjects. *Biomaterials* **128**:1–7
 20. Müller SLAR (1991) Medication vehicles made of solid lipid particles (solid lipid nanospheres – SLN). In: mbH MGfKS (ed) Google patents. Germany
 21. Gasco MR (1993) Method for producing solid lipid microspheres having a narrow size distribution. Google Patents
 22. Gasco MR (2002) Microparticles for drug delivery across mucosa and the blood-brain barrier. Google Patents
 23. Müller RH, Shegokar R, Keck CM (2011) 20 years of lipid nanoparticles (SLN and NLC): present state of development and industrial applications. *Curr Drug Discov Technol* **8**(3):207–227
 24. Keck CM et al (2014) Formulation of solid lipid nanoparticles (SLN): the value of different alkyl polyglucoside surfactants. *Int J Pharm* **474**(1-2):33–41
 25. Zielińska A, Nowak I (2016) Solid lipid nanoparticles and nanostructured lipid carriers as novel carriers for cosmetic ingredients. In: *Nanobiomaterials in Galenic Formulations and Cosmetics*. Elsevier, pp 231–255
 26. Müller RH et al (2016) Nanostructured lipid carriers (NLC): the second generation of solid lipid nanoparticles. In: *Percutaneous penetration enhancers chemical methods in penetration enhancement*. Springer, pp 161–185
 27. Souto EB, Fangueiro JF, Müller RH (2013) Solid lipid nanoparticles (SLNTM). In: *Fundamentals of pharmaceutical nanoscience*. Springer, pp 91–116
 28. Müller RH, Radtke M, Wissing SA (2002) Nanostructured lipid matrices for improved microencapsulation of drugs. *Int J Pharm* **242**(1):121–128
 29. Beloqui A et al (2016) Nanostructured lipid carriers: Promising drug delivery systems for future clinics. *Nanomedicine* **12**(1):143–161
 30. Pardeike J, Hommoss A, Müller RH (2009) Lipid nanoparticles (SLN, NLC) in cosmetic and pharmaceutical dermal products. *Int J Pharm* **366**(1):170–184
 31. Morales JO et al (2015) Lipid nanoparticles for the topical delivery of retinoids and derivatives. *Nanomedicine (Lond)* **10**(2):253–269
 32. Mitrea E, Ott C, Meghea A (2014) New approaches on the synthesis of effective nanostructured lipid carriers. *Rev Chim* **65**:50–55
 33. Souto EB, Müller RH (2007) Lipid nanoparticles (SLN and NLC) for drug delivery. 103–122.
 34. Mitri K et al (2011) Lipid nanocarriers for dermal delivery of lutein: preparation, characterization, stability and performance. *Int J Pharm* **414**(1-2):267–275
 35. Puglia C, Bonina F (2012) Lipid nanoparticles as novel delivery systems for cosmetics and dermal pharmaceuticals. *Expert Opin Drug Deliv* **9**(4):429–441
 36. Mu L, Sprando RL (2010) Application of nanotechnology in cosmetics. *Pharm Res* **27**(8):1746–1749
 37. Padamwar MN, Pokharkar VB (2006) Development of vitamin loaded topical liposomal formulation using factorial design approach: drug deposition and stability. *Int J Pharm* **320**(1-2):37–44
 38. Hosseinkhani B et al (2015) Novel biocompatible nanocapsules for slow release of fragrances on the human skin. *N Biotechnol* **32**(1):40–46
 39. Poland CA, Larsen PB, Read SAK, Varet J, Hankin SM, Lam HR (2016) Assessment if nano-enabled technologies in cosmetics. The Danish Environmental Protection Agency, Copenhagen, p 142
 40. Patel P, Schmieder S, Krishnamurthy K (2016) Research techniques made simple: drug delivery techniques, part 2: commonly used techniques to assess topical drug bioavailability. *J Invest Dermatol* **136**(5):e43–e49
 41. OECD, Guidance document for the conduct of skin absorption studies, in OECD series on testing and assessment. 2004: Paris, France.
 42. OECD, Test Guideline 428: Skin absorption: In Vitro Method. 2004: Paris, France.
 43. OECD, Test Guideline 427: Skin absorption: In Vivo Method. 2004: Paris, France.
 44. OECD, Series on Testing and Assessment No. 28: Guidance document for the conduct of skin absorption studies. 2004.
 45. Janet Kielhorn SM, Mangelsdorf I (2006) Dermal absorption, in environmental health criteria. World Health Organization
 46. Finnin B, Walters KA, Franz TJ (2012) In vitro skin permeation methodology. In: Benson HAE, Watkinson AC (eds) *Transdermal and topical drug delivery: principles and practice*. John Wiley & Sons, p 24
 47. Authority EFS et al (2017) Guidance on dermal absorption. *EFSA J* **15**(6):e04873
 48. Yacobi A et al (2014) Current challenges in bioequivalence, quality, and novel assessment technologies for topical products. *Pharm Res* **31**(4):837–846
 49. Dumont C et al (2015) Review of the availability of in vitro and in silico methods for assessing dermal bioavailability. *Appl In Vitro Toxicol* **1**(2):147–164
 50. Alexander A et al (2012) Approaches for breaking the barriers of drug permeation through transdermal drug delivery. *J Control Release* **164**(1):26–40
 51. Sala M et al (2018) Lipid nanocarriers as skin drug delivery systems: properties, mechanisms of skin interactions and medical applications. *Int J Pharm* **535**(1):1–17
 52. Jain A et al (2014) Novel strategies for effective transdermal drug delivery: a review. *Crit Rev Ther Drug Carrier Syst* **31**(3):219–272
 53. Jacobi U et al (2005) Gender-related differences in the physiology of the stratum corneum. *Dermatology* **211**(4):312–317

54. Korting HC, Schafer-Korting M (2010) Carriers in the topical treatment of skin disease. *Handb Exp Pharmacol* 197:435–468
55. El Maghraby GM, Barry BW, Williams AC (2008) Liposomes and skin: From drug delivery to model membranes. *Eur J Pharm Sci* 34(4):203–222
56. Flaten GE et al (2015) In vitro skin models as a tool in optimization of drug formulation. *Eur J Pharm Sci* 75:10–24
57. Riviere JE, Papich MG (2001) Potential and problems of developing transdermal patches for veterinary applications. *Adv Drug Deliv Rev* 50(3):175–203
58. 123rf.com, Vector - Human skin. Layered epidermis with hair follicle, sweat and sebaceous glands. Healthy skin anatomy medical vector illustration. Dermis and epidermis skin, hypodermis. 2018. <https://www.123rf.com>.
59. Lam PL, Gambari R (2014) Advanced progress of microencapsulation technologies: in vivo and in vitro models for studying oral and transdermal drug deliveries. *J Control Release* 178:25–45
60. Chittenden JT, Brooks JD, Riviere JE (2014) Development of a mixed-effect pharmacokinetic model for vehicle modulated in vitro transdermal flux of topically applied penetrants. *J Pharm Sci* 103(3):1002–1012
61. Bhojar N et al (2012) Recent advances in novel drug delivery system through gels: review. *J Pharm Allied Health Sci* 2:21–39
62. Banga AK (2011) Transdermal and intradermal delivery of therapeutic agents: application of physical technologies. CRC Press
63. Lane ME (2013) Skin penetration enhancers. *Int J Pharm* 447(1–2):12–21
64. Benson HA (2012) Skin structure, function, and permeation. *Topical and Transdermal Drug Delivery: Principles and Practice*, pp 1–22
65. Lademann J et al (2015) Hair follicles as a target structure for nanoparticles. *J Innov Opt Health Sci* 8(04):1530004
66. Knorr F et al (2009) Follicular transport route – research progress and future perspectives. *Eur J Pharm Biopharm* 71(2):173–180
67. Müller RM, Sinambela P, Keck C (2013) NLC - The invisible dermal patch for moisturizing & skin protection. 6:20–22
68. Souto EB, Muller RH (2008) Cosmetic features and applications of lipid nanoparticles (SLN, NLC). *Int J Cosmet Sci* 30(3):157–165
69. Zhai Y, Zhai G (2014) Advances in lipid-based colloid systems as drug carrier for topic delivery. *J Control Release* 193:90–99
70. Jensen LB, Petersson K, Nielsen HM (2011) In vitro penetration properties of solid lipid nanoparticles in intact and barrier-impaired skin. *Eur J Pharm Biopharm* 79(1):68–75
71. Schäfer-Korting M, Mehnert W, Korting H-C (2007) Lipid nanoparticles for improved topical application of drugs for skin diseases. *Adv Drug Deliv Rev* 59(6):427–443
72. Müller RH et al (2007) Nanostructured lipid carriers (NLC) in cosmetic dermal products. *Adv Drug Deliv Rev* 59(6):522–530
73. Cevc G, Vierl U (2010) Nanotechnology and the transdermal route: a state of the art review and critical appraisal. *J Control Release* 141(3):277–299
74. Wissing SA, Lippacher A, Müller RH (2001) Investigations on the occlusive properties of solid lipid nanoparticles (SLN). 52:313–324
75. Mardhiah Adib Z et al (2016) The effect of particle size on the deposition of solid lipid nanoparticles in different skin layers: a histological study. *Adv Pharm Bull* 6(1):31–36
76. Souto EB et al (2004) Development of a controlled release formulation based on SLN and NLC for topical clotrimazole delivery. *Int J Pharm* 278(1):71–77
77. Teeranachaideekul V et al (2008) Influence of oil content on physicochemical properties and skin distribution of Nile red-loaded NLC. *J Control Release* 128(2):134–141
78. Lombardi Borgia S et al (2005) Lipid nanoparticles for skin penetration enhancement—correlation to drug localization within the particle matrix as determined by fluorescence and piezoelectric spectroscopy. *J Control Release* 110(1):151–163
79. Wissing S, Müller R (2003) The influence of solid lipid nanoparticles on skin hydration and viscoelasticity – in vivo study, vol 56, pp 67–72
80. Teeranachaideekul V et al (2007) Cetyl palmitate-based NLC for topical delivery of Coenzyme Q(10) - Development, physicochemical characterization and in vitro release studies. 67:141–148
81. Wissing S et al (2004) Structural characterization of Q10-loaded solid lipid nanoparticles by NMR spectroscopy. 21:400–405
82. Teeranachaideekul V, Helmut Müller R, Buraphacheep Junyaprasert V (2007) Encapsulation of ascorbyl palmitate in nanostructured lipid carriers (NLC) - Effects of formulation parameters on physicochemical stability. 340:198–206
83. Üner M et al (2005) Skin moisturizing effect and skin penetration of ascorbyl palmitate entrapped in Solid Lipid Nanoparticles (SLN) and Nanostructured Lipid Carriers (NLC) incorporated into hydrogel. 60:751–755
84. Jee J-P et al (2006) Stabilization of all-trans retinol by loading lipophilic antioxidants in solid lipid nanoparticles. 63:134–139
85. Liu J et al (2007) Isotretinoin-loaded solid lipid nanoparticles with skin targeting for topical delivery. 328:191–195
86. Pople P, Singh K (2006) Development and evaluation of topical formulation containing solid lipid nanoparticles of vitamin A. 7:91
87. Sivaramakrishnan R et al (2004) Glucocorticoid entrapment into lipid carriers—characterisation by piezoelectric spectroscopy and influence on dermal uptake. *J Control Release* 97(3):493–502

88. Castro G et al (2007) Development of a new solid lipid nanoparticle formulation containing retinoic acid for topical treatment of acne. *24*:395–407
89. Muller RH, Souto E, Mehnert W (2005) Solid lipid nanoparticles (SLN) and nanostructured lipid carriers (NLC) for dermal delivery. In: Robert HIM, Bronaugh L (eds) *Percutaneous absorption: drugs - cosmetics - mechanisms - methodology*. Taylor & Francis Group, p 916
90. Bunjes H, Steiniger F, Richter W (2007) Visualizing the structure of triglyceride nanoparticles in different crystal modifications. *23*:4005–4011
91. Souto EB et al (2004) Development of a controlled release formulation based on SLN and NLC for topical clotrimazole delivery. *278*:71–77
92. Müller RH, Radtke M, Wissing SA (2002) Solid Lipid Nanoparticles (SLN) and Nanostructured Lipid Carriers (NLC) in Cosmetic and Dermatological Preparations. *54*(Suppl 1):S131–S155
93. De Vringer T (1997) Topical preparation containing a suspension of solid lipid particles. Google Patents
94. Rigano I, Giammarrusti G, Rastrelli F (2006) Vegetable oils – the base of new active principles. *SÖFW-Journal* **132**:8
95. Badea G et al (2015) Use of various vegetable oils in designing photoprotective nanostructured formulations for UV protection and antioxidant activity. *Ind Crop Prod* **67**:18–24
96. Balboa EM et al (2014) Potential of antioxidant extracts produced by aqueous processing of renewable resources for the formulation of cosmetics. *Ind Crop Prod* **58**:104–110
97. Zielińska A, Nowak I (2014) Fatty acids in vegetable oils and their importance in cosmetic industry. *68*:103–110
98. Karak N (2012) 3 - Vegetable oils and their derivatives, in *Vegetable Oil-Based Polymers*. Woodhead Publishing, pp 54–95
99. Dhavamani S, Rao YPC, Lokesh BR (2014) Total antioxidant activity of selected vegetable oils and their influence on total antioxidant values in vivo: a photochemiluminescence based analysis. *Food Chem* **164**:551–555
100. Tehranifar A et al (2011) High potential of agro-industrial by-products of pomegranate (*Punica granatum L.*) as the powerful antifungal and antioxidant substances. *Ind Crop Prod* **34**(3):1523–1527
101. Cicerale S, Lucas LJ, Keast RS (2012) Antimicrobial, antioxidant and anti-inflammatory phenolic activities in extra virgin olive oil. *Curr Opin Biotechnol* **23**(2):129–135
102. Saraf S et al (2010) Comparative measurement of hydration effects of herbal moisturizers. *Pharm Res* **2**(3):146–151
103. Lacatusu I et al (2012) Highly antioxidant carotene-lipid nanocarriers: synthesis and antibacterial activity. *J Nanopart Res* **14**(6):902
104. Lacatusu I et al (2014) Design of soft lipid nanocarriers based on bioactive vegetable oils with multiple health benefits. *Chem Eng J* **246**:311–321
105. Sorg O et al (2006) Retinoids in cosmeceuticals. *Dermatol Ther* **19**(5):289–296
106. de Nóvoa EG et al (2015) Menopause and cosmeceuticals. In: *Skin, mucosa and menopause*. Springer, pp 455–478
107. Pople PV, Singh KK (2006) Development and evaluation of topical formulation containing solid lipid nanoparticles of vitamin A. *AAPS PharmSciTech* **7**(4):91
108. Thomas JR, Dixon TK, Bhattacharyya TK (2013) Effects of topicals on the aging skin process. *Facial Plastic Surgery Clinics* **21**(1):55–60
109. Raza K et al (2013) Nanocolloidal carriers of isotretinoin: antimicrobial activity against *Propionibacterium acnes* and dermatokinetic modeling. *Mol Pharm* **10**(5):1958–1963
110. Ridolfi DM et al (2012) Chitosan-solid lipid nanoparticles as carriers for topical delivery of tretinoin. *Colloids Surf B Biointerfaces* **93**:36–40
111. Kerscher M, Buntrock H (2016) 9. Cosmetics and cosmeceuticals. 77-88.
112. Kligman AM et al (1986) Topical tretinoin for photoaged skin. *J Am Acad Dermatol* **15**(4 Pt 2):836–859
113. Mukherjee S et al (2006) Retinoids in the treatment of skin aging: an overview of clinical efficacy and safety. *Clin Interv Aging* **1**(4):327
114. Brisaert M, Plaizier-Vercammen J (2000) Investigation on the photostability of a tretinoin lotion and stabilization with additives. *Int J Pharm* **199**(1):49–57
115. Prasad S et al (2012) Efficacy and safety of a nano-emulsion gel formulation of adapalene 0.1% and clindamycin 1% combination in acne vulgaris: a randomized, open label, active-controlled, multicentric, phase IV clinical trial. *Indian J Dermatol Venereol Leprol* **78**(4):459–467
116. Raza K et al (2013) Systematically optimized biocompatible isotretinoin-loaded solid lipid nanoparticles (SLNs) for topical treatment of acne. *Colloids Surf B Biointerfaces* **105**:67–74
117. Jain A et al (2016) A synergistic approach of adapalene-loaded nanostructured lipid carriers, and vitamin C co-administration for treating acne. *Drug Dev Ind Pharm* **42**(6):897–905
118. Lee S et al (2012) Topical formulation of retinyl retinoate employing nanostructured lipid carriers. *J Pharm Investig* **42**
119. Liu J et al (2007) Isotretinoin-loaded solid lipid nanoparticles with skin targeting for topical delivery. *Int J Pharm* **328**(2):191–195
120. Kerscher M, Buntrock H (2016) Cosmetics and cosmeceuticals, pp 77–88
121. Salavkar S, Tamanekar R, Athawale R (2011) Antioxidants in skin ageing-Future of dermatology. *Int J Green Pharmacy* **5**(3):161

122. Montenegro L (2014) Nanocarriers for skin delivery of cosmetic antioxidants. *J Pharm Pharmacogn Res* **2**(4)
123. Vinardell MP, Mitjans M (2015) Nanocarriers for delivery of antioxidants on the skin. *Cosmetics* **2**(4):342–354
124. Bissett DL, Oblong JE, Berge CA (2005) Niacinamide: A B vitamin that improves aging facial skin appearance. *Dermatol Surg* **31**(7 Pt 2):860–865. discussion 865
125. Friedland JA, Buchel EW (2000) Skin care and the topical treatment of aging skin. *Clin Plast Surg* **27**(4):501–506
126. Kullavanijaya P, Lim HW (2005) Photoprotection. *J Am Acad Dermatol* **52**(6):937–958. quiz 959–62
127. Chen-yu G et al (2012) Development of a quercetin-loaded nanostructured lipid carrier formulation for topical delivery. *Int J Pharm* **430**(1-2):292–298
128. Soldati PP et al (2018) Controlled release of resveratrol from lipid nanoparticles improves antioxidant effect. *IFAC-PapersOnLine* **51**(27):16–21
129. Dzulhi S, Anwar E, Nurhayati T (2018) Formulation, characterization and in vitro skin penetration of green tea (*Camellia sinensis* L.) leaves extract-loaded solid lipid nanoparticles. *J App Pharm Sci* **8**:057–062
130. Lodén M (2005) The clinical benefit of moisturizers. *J Eur Acad Dermatol Venereol* **19**(6):672–688
131. Newton AMJ, Kaur S (2019) Chapter 9 - Solid lipid nanoparticles for skin and drug delivery: Methods of preparation and characterization techniques and applications. In: Grumezescu AM (ed) *Nanoarchitectonics in biomedicine*. William Andrew Publishing, pp 295–334
132. Hashempour S et al (2019) Skin toxicity of topically applied nanoparticles. *Ther Deliv* **10**(6):383–396
133. OECD, Guidelines for the testing of chemicals - In vitro skin irritation: reconstructed human epidermis test method. 2015.
134. Abo-Elfadl MT et al (2016) Photothermal therapeutic effect of PEGylated gold nano-semicubes in chemically-induced skin cancer in mice. *J Photochem Photobiol B* **164**:21–29
135. Bseiso EA et al (2015) Recent advances in topical formulation carriers of antifungal agents. *Indian J Dermatol Venereol Leprol* **81**(5):457–463
136. Kaur IP et al (2020) Chapter one - Solid lipid nanoparticles in dermaticals. In: Pippa N, Demetzos C (eds) *Nanomaterials for clinical applications*. Elsevier, pp 1–27
137. Monteiro-Riviere, N. and Tran CL, *Nanotoxicology: characterization, dosing and health effects*. 2007.
138. Dhawan A, Sharma V (2010) Toxicity assessment of nanomaterials: methods and challenges. *Anal Bioanal Chem* **398**(2):589–605
139. Diembeck W et al (2005) Skin absorption and penetration. *Altern Lab Anim* **33**(Suppl 1):105–107
140. Berkó S et al (2014) Monitoring of skin penetration and absorption with a new in vivo experimental model. *Farmacia* **62**:1157–1163
141. Doktorovova S et al (2016) Preclinical safety of solid lipid nanoparticles and nanostructured lipid carriers: Current evidence from in vitro and in vivo evaluation. *Eur J Pharm Biopharm* **108**:235–252
142. Marquis BJ et al (2009) Analytical methods to assess nanoparticle toxicity. *Analyst* **134**(3):425–439
143. Campos JR et al (2020) Chapter 1 - Solid lipid nanoparticles (SLN): prediction of toxicity, metabolism, fate and physicochemical properties. In: Shegokar R (ed) *Nanopharmaceuticals*. Elsevier, pp 1–15
144. Shah VP et al (2015) A science based approach to topical drug classification system (TCS). *Int J Pharm* **491**(1-2):21–25
145. Finnin B, Walters KA, Franz TJ In vitro skin permeation methodology. In: *Topical and transdermal drug delivery*, pp 85–108
146. Comission, E., Directive 2003/15/EC of the European Parliament and of the Council. 2003: Official Journal of the European Union p. 26-35.
147. Comission, E., EURL ECVAM progress report on the development, validation and regulatory acceptance of alternative methods (2010-2013). 2013, European Comission, Luxembourg: Prepared in the framework of Directive 76/768/EEC and Regulation (EC) No 1223/2009 on cosmetic products (Ed.).
148. Comission, E., ESAC Statement on the scientific validity of an iEURL ECVAM progress report on the development, validation and regulatory acceptance of alternative methods (2010-2013) in-vitro test method for skin corrosivity testing. 2013, European Union, Luxembourg: European Commissio - Institute for Health and Consumer Protection (Ed.). Publications Office of the European Union.
149. Chemicals, E.C.f.E.a.T.o (1993) Percutaneous absorption, monograph. European Centre for Ecotoxicology and Toxicology of Chemicals, Bruxelles
150. (EPA), E.S.E.P.A. Dermal exposure assessment: a summary of EPA approaches. [cited 1 April 2019].
151. Nafisi S, Maibach HI (2018) Chapter 3 - Skin penetration of nanoparticles. In: Shegokar R, Souto EB (eds) *Emerging nanotechnologies in immunology*. Elsevier, Boston, pp 47–88
152. Zsikó S et al (2019) Methods to evaluate skin penetration in vitro. *Scientia Pharmaceutica* **87**:19
153. Franz TJ (1978) The finite dose technique as a valid in vitro model for the study of percutaneous absorption in man. *Curr Probl Dermatol* **7**:58–68
154. Bronaugh RL, Stewart RF, Simon M (1986) Methods for in vitro percutaneous absorption studies. VII: Use of excised human skin. *J Pharm Sci* **75**(11):1094–1097
155. Agency EM (2018) FDA draft guideline on quality and equivalence of topical products EMA/CHMP/QWP/708282/2018. European Medicines Agency: Amsterdam, The Netherlands.
156. Oliveira G et al (2010) Alcohol enhanced permeation in model membranes. Part I. Thermodynamic

- and kinetic analyses of membrane permeation. *Int J Pharm* **393**(1-2):61–67
157. Nakano M, Patel NK (1970) Release, uptake, and permeation behavior of salicylic acid in ointment bases. *J Pharm Sci* **59**(7):985–988
 158. Miki R et al (2015) Development of a membrane impregnated with a poly(dimethylsiloxane)/poly(ethylene glycol) copolymer for a high-throughput screening of the permeability of drugs, cosmetics, and other chemicals across the human skin. *Eur J Pharm Sci* **66**:41–49
 159. Ottaviani G, Martel S, Carrupt PA (2006) Parallel artificial membrane permeability assay: a new membrane for the fast prediction of passive human skin permeability. *J Med Chem* **49**(13):3948–3954
 160. Karadzovska D, Riviere JE (2013) Assessing vehicle effects on skin absorption using artificial membrane assays. *Eur J Pharm Sci* **50**(5):569–576
 161. Sinkó B et al (2012) Skin-PAMPA: a new method for fast prediction of skin penetration. *Eur J Pharm Sci* **45**(5):698–707
 162. Sinkó B, Vizserálek G, Krisztina T-N (2015) Skin PAMPA: Application in practice. *ADMET & DMPK* **2**
 163. Tsai P-C et al (2020) Selection considerations for membranes and models for in vitro/ex vivo permeation studies. In: Ghosh TK (ed) *Dermal drug delivery: from innovation to production*. Boca Raton
 164. Flaten G et al (2009) The phospholipid vesicle-based drug permeability assay: 5. Development toward an automated procedure for high-throughput permeability screening. *J Assoc Lab Autom* **14**:12–21
 165. Engesland A et al (2013) New applications of phospholipid vesicle-based permeation assay: permeation model mimicking skin barrier. *J Pharm Sci* **102**
 166. Van Gele M et al (2011) Three-dimensional skin models as tools for transdermal drug delivery: challenges and limitations. *Expert Opin Drug Deliv* **8**(6):705–720
 167. Ponec M et al (2000) Lipid and ultrastructural characterization of reconstructed skin models. *Int J Pharm* **203**(1-2):211–225
 168. Ponec M et al (2002) Characterization of reconstructed skin models. *Skin Pharmacol Appl Skin Physiol* **15**(Suppl 1):4–17
 169. OECD, Test guideline for the testing of chemicals, No. 431, In vitro skin corrosion; human skin model test. 2004: Paris, France.
 170. Netzlaff F et al (2005) The human epidermis models EpiSkin, SkinEthic and EpiDerm: an evaluation of morphology and their suitability for testing phototoxicity, irritancy, corrosivity, and substance transport. *Eur J Pharm Biopharm* **60**(2):167–178
 171. Küchler S, Strüver K, Friess W (2013) Reconstructed skin models as emerging tools for drug absorption studies. *Expert Opin Drug Metab Toxicol* **9**(10):1255–1263
 172. Flaten GE et al (2015) In vitro skin models as a tool in optimization of drug formulation. *Eur J Pharm Sci* **75**:10–24
 173. Contri R, et al (2011) Transport of substances and nanoparticles across the skin and in vitro models to evaluate skin permeation and/or penetration, p. 3–35.
 174. Auxenfans C et al (2009) Evolution of three dimensional skin equivalent models reconstructed in vitro by tissue engineering. *Eur J Dermatol* **19**(2):107–113
 175. Schreiber S et al (2005) Reconstructed epidermis versus human and animal skin in skin absorption studies. *Toxicol In Vitro* **19**(6):813–822
 176. Almeida A, Sarmiento B, Rodrigues F (2017) Insights on in vitro models for safety and toxicity assessment of cosmetic ingredients. *Int J Pharm* **519**(1-2):178–185
 177. Zhang Q et al (2018) Current advances in skin-on-a-chip models for drug testing. *Microphysiol Syst* **2**:4–4
 178. Sriram G et al (2018) Full-thickness human skin-on-chip with enhanced epidermal morphogenesis and barrier function. *Mater Today* **21**(4):326–340
 179. Biedermann T et al (2015) Long-term expression pattern of melanocyte markers in light- and dark-pigmented dermo-epidermal cultured human skin substitutes. *Pediatr Surg Int* **31**(1):69–76
 180. Wufuer M et al (2016) Skin-on-a-chip model simulating inflammation, edema and drug-based treatment. *Sci Rep* **6**:37471
 181. Ahadian S et al (2018) Organ-on-a-chip platforms: a convergence of advanced materials, cells, and microscale technologies. *Adv Healthc Mater*:7(2)
 182. Ramadan Q, Ting FCW (2016) In vitro microphysiological immune-competent model of the human skin. *Lab Chip* **16**(10):1899–1908
 183. Zoio PA, Oliva AG, Conde JP (2019) Fully-humanized skin-on-a-chip for medical applications: combining microtechnology with 3D tissue engineering to develop human skin. Poster Session presented at the European Commission JRC, Ispra
 184. Ozbolat I, Yu Y (2013) Bioprinting toward organ fabrication: challenges and future trends. *IEEE Transactions on Biomedical Engineering*
 185. Barron JA et al (2004) Biological laser printing: a novel technique for creating heterogeneous 3-dimensional cell patterns. *Biomed Microdevices* **6**(2):139–147
 186. Satpathy A et al (2018) Developments with 3D bioprinting for novel drug discovery. *Expert Opin Drug Discovery* **13**(12):1115–1129
 187. Koch L et al (2012) Skin tissue generation by laser cell printing. *Biotechnol Bioeng* **109**:1855–1863
 188. Derr K et al (2019) Fully three-dimensional bioprinted skin equivalent constructs with validated morphology and barrier function. *Tissue Eng Part C Methods* **25**(6):334–343
 189. Tseng H et al (2015) A spheroid toxicity assay using magnetic 3D bioprinting and real-time mobile device-based imaging. *Sci Rep* **5**:13987
 190. Huong SP et al (2009) Use of various models for in vitro percutaneous absorption studies of ultraviolet filters. *Skin Res Technol* **15**(3):253–261

191. Abd E et al (2016) Skin models for the testing of transdermal drugs. *Clin Pharmacol: Adv Appl* **8**:163–176
192. Jacobi U et al (2007) Porcine ear skin: an in vitro model for human skin. *Skin Res Technol* **13**(1):19–24
193. Gray GM, Yardley HJ (1975) Lipid compositions of cells isolated from pig, human, and rat epidermis. *J Lipid Res* **16**(6):434–440
194. Stahl J et al (2012) The comparability of in vitro and ex vivo studies on the percutaneous permeation of topical formulations containing Ibuprofen. *Altern Lab Anim* **40**(2):91–98
195. Smith EW et al (1991) The human skin-blanching assay for comparing topical corticosteroid availability. *J Dermatol Treat* **2**
196. Schäfer U (2003) Topical absorption of dermatological products. *Eur J Pharm Biopharm* **55**:139–140
197. Herkenne C et al (2008) In vivo methods for the assessment of topical drug bioavailability. *Pharm Res* **25**(1):87–103
198. Escobar-Chávez JJ et al (2008) The tape-stripping technique as a method for drug quantification in skin. *J Pharm Pharm Sci* **11**(1):104–130
199. Klang V et al (2012) In vitro vs. in vivo tape stripping: validation of the porcine ear model and penetration assessment of novel sucrose stearate emulsions. *Eur J Pharm Biopharm* **80**(3):604–614
200. Herkenne C et al (2007) Dermatopharmacokinetic prediction of topical drug bioavailability in vivo. *J Invest Dermatol* **127**(4):887–894
201. European Commission, J.R.C., EURL ECVAM dataset on alternative methods to animal experimentation (DB-ALM). 2019.: <http://data.europa.eu/89h/b7597ada-148d-4560-9079-ab0a5539cad3>.
202. Holmgaard R, Nielsen JB, Benfeldt E (2010) Microdialysis sampling for investigations of bioavailability and bioequivalence of topically administered drugs: current state and future perspectives. *Skin Pharmacol Physiol* **23**(5):225–243
203. Hammarlund-Udenaes M (2017) Microdialysis as an Important Technique in Systems Pharmacology—a Historical and Methodological Review. *AAPS J* **19**(5):1294–1303
204. Ault JM et al (1992) Microdialysis sampling for the investigation of dermal drug transport. *Pharm Res* **9**(10):1256–1261
205. Zhang LW, Monteiro-Riviere NA (2013) Use of confocal microscopy for nanoparticle drug delivery through skin. *J Biomed Opt* **18**(6):061214
206. Schreiner V et al (2000) Barrier characteristics of different human skin types investigated with X-ray diffraction, lipid analysis, and electron microscopy imaging. *J Invest Dermatol* **114**(4):654–660
207. Hofland HE et al (1995) Interactions between liposomes and human stratum corneum in vitro: freeze fracture electron microscopical visualization and small angle X-ray scattering studies. *Br J Dermatol* **132**(6):853–866
208. Förster M et al (2011) Confocal Raman microspectroscopy of the skin. *Eur J Dermatol* **21**(6):851–863
209. Plasencia I, Norlén L, Bagatolli LA (2007) Direct visualization of lipid domains in human skin stratum corneum's lipid membranes: effect of pH and temperature. *Biophys J* **93**(9):3142–3155
210. Batista A et al (2016) Two-photon spectral fluorescence lifetime and second-harmonic generation imaging of the porcine cornea with a 12-femtosecond laser microscope. *J Biomed Opt* **21**(3):36002
211. Carrer DC, Vermehren C, Bagatolli LA (2008) Pig skin structure and transdermal delivery of liposomes: a two photon microscopy study. *J Control Release* **132**(1):12–20
212. Hanson KM et al (2002) Two-photon fluorescence lifetime imaging of the skin stratum corneum pH gradient. *Biophys J* **83**(3):1682–1690
213. Zellmer S, Reissig D, Lasch J (1998) Reconstructed human skin as model for liposome-skin interaction. *J Control Release* **55**(2-3):271–279
214. van Kuijk-Meuwissen MEMJ, Junginger HE, Bouwstra JA (1998) Interactions between liposomes and human skin in vitro, a confocal laser scanning microscopy study. *Biochim Biophys Acta (BBA) - Biomembrane* **1371**(1):31–39
215. van Kuijk-Meuwissen ME et al (1998) Application of vesicles to rat skin in vivo: a confocal laser scanning microscopy study. *J Control Release* **56**(1-3):189–196
216. Touitou E et al (2001) Intracellular delivery mediated by an ethosomal carrier. *Biomaterials* **22**(22):3053–3059
217. Simonetti O et al (1995) Visualization of diffusion pathways across the stratum corneum of native and in-vitro-reconstructed epidermis by confocal laser scanning microscopy. *Arch Dermatol Res* **287**(5):465–473
218. Pinto F et al (2020) Topical distribution and efficiency of nanostructured lipid carriers on a 3D reconstructed human epidermis model. *J Drug Delivery Sci Technol* **57**:101616
219. Caspers PJ et al (2001) In vivo confocal Raman microspectroscopy of the skin: noninvasive determination of molecular concentration profiles. *J Invest Dermatol* **116**(3):434–442
220. Ashtikar M et al (2013) Non-invasive depth profile imaging of the stratum corneum using confocal Raman microscopy: first insights into the method. *Eur J Pharm Sci* **50**(5):601–608
221. Smith GP et al (2015) Raman imaging of drug delivery systems. *Adv Drug Deliv Rev* **89**:21–41
222. Pyatski Y et al (2016) Effects of permeation enhancers on flufenamic acid delivery in Ex vivo human skin by confocal Raman microscopy. *Int J Pharm* **505**(1-2):319–328
223. dos Santos L et al (2017) In vivo confocal Raman spectroscopy and molecular dynamics analysis of penetration of retinyl acetate into stratum corneum. *Spectrochim Acta A Mol Biomol Spectrosc* **174**:279–285
224. Bakonyi M et al (2018) Following-up skin penetration of lidocaine from different vehicles by Raman

- spectroscopic mapping. *J Pharm Biomed Anal* **154**:1–6
225. Nakagawa N, Matsumoto M, Sakai S (2010) In vivo measurement of the water content in the dermis by confocal Raman spectroscopy. *Skin Res Technol* **16**(2):137–141
226. Yeon L, Young M (1999) Lipid nanospheres containing vitamin A or vitamin E: Evaluation of their stabilities and In Vitro skin permeability. *J Ind Eng Chem* **5**(4) (01.12.1999):306–313
227. Jenning V et al (2000) Vitamin A loaded solid lipid nanoparticles for topical use: occlusive properties and drug targeting to the upper skin. *Eur J Pharm Biopharm* **49**(3):211–218
228. Wissing SA, Müller RH (2002) Solid lipid nanoparticles as carrier for sunscreens: in vitro release and in vivo skin penetration. *J Control Release* **81**(3):225–233
229. Mei Z et al (2003) Solid lipid nanoparticle and microemulsion for topical delivery of triptolide. *Eur J Pharm Biopharm* **56**(2):189–196
230. Ricci M et al (2005) Evaluation of indomethacin percutaneous absorption from nanostructured lipid carriers (NLC): in vitro and in vivo studies. *J Pharm Sci* **94**(5):1149–1159
231. Uner M et al (2005) Skin moisturizing effect and skin penetration of ascorbyl palmitate entrapped in solid lipid nanoparticles (SLN) and nanostructured lipid carriers (NLC) incorporated into hydrogel. *Pharmazie* **60**(10):751–755
232. Mei Z et al (2005) Triptolide loaded solid lipid nanoparticle hydrogel for topical application. *Drug Dev Ind Pharm* **31**(2):161–168
233. Münster U et al (2005) RU 58841-myristate--pro-drug development for topical treatment of acne and androgenetic alopecia. *Pharmazie* **60**(1):8–12
234. Chen H et al (2006) Podophyllotoxin-loaded solid lipid nanoparticles for epidermal targeting. *J Control Release* **110**(2):296–306
235. Puglia C et al (2006) Evaluation of alternative strategies to optimize ketorolac transdermal delivery. *AAPS PharmSciTech* **7**(3):E61–E69
236. Lai F et al (2007) SLN as a topical delivery system for *Artemisia arborescens* essential oil: in vitro antiviral activity and skin permeation study. *Int J Nanomedicine* **2**(3):419–425
237. Jo S-M, Lee H, Kim J-C (2007) Characterization and In-vitro Permeation Study of Stearic Acid Nanoparticles containing Hinokitiol. *JAOCS* **84**:859–863
238. Kuntsche J et al (2008) Interaction of lipid nanoparticles with human epidermis and an organotypic cell culture model. *Int J Pharm* **354**(1-2):180–195
239. Puglia C et al (2008) Lipid nanoparticles for prolonged topical delivery: an in vitro and in vivo investigation. *Int J Pharm* **357**(1-2):295–304
240. Mandawgade SD, Patravale VB (2008) Development of SLNs from natural lipids: application to topical delivery of tretinoin. *Int J Pharm* **363**(1-2):132–138
241. Bhalekar MR et al (2009) Preparation and evaluation of miconazole nitrate-loaded solid lipid nanoparticles for topical delivery. *AAPS PharmSciTech* **10**(1):289–296
242. Passerini N et al (2009) Evaluation of solid lipid microparticles produced by spray congealing for topical application of econazole nitrate. *J Pharm Pharmacol* **61**(5):559–567



Targeting Cancer by Using Nanoparticles to Modulate RHO GTPase Signaling

Paulo Matos, Joana F. S. Pereira, and Peter Jordan

Abstract

Functionalized nanomaterials have recently been introduced as efficient vehicles for targeted delivery of drugs and other tailored molecules to cancer cells. They emerge as new opportunities for addressing particular challenging targets such as RHO guanosine triphosphatases (GTPases), a group of signaling molecules involved in the progression of a variety of tumor types. RHO GTPases comprise a subfamily of the Ras superfamily of small GTPases. They are best known for their role in cell migration through the remodeling of the actin cytoskeleton. However, they are also key regulators of a broad number of cellular functions, ranging from proliferation to cell adhesion and differentiation. Not surprisingly, their dysregulation has been implicated in the development and progression of many types of cancer. The RHO GTPase subfamily includes 20 members that can be further separated into typical and atypical RHO GTPases. The typical RHO family members include the

classical RHOA, RAC1 and CDC42 proteins, which cycle between an active GTP-bound and inactive GDP-bound conformation, under the coordinated action of three types of regulators: GEFs, GAPs and GDIs. Atypical RHO family members have small changes in key residues that alter their regulatory mechanisms. Nevertheless, both typical and atypical RHO GTPases contribute to cancer progression but, in contrast to Ras proteins, very few mutations have been found in tumors. In most cancers, it is the expression level and/or activity of RHO GTPases that is dysregulated. RHO GTPase signaling has thus long been seen as an attractive target for cancer treatment but their ubiquity and the lack of isoform-specific drugs have posed significant obstacles to the development of viable therapeutic strategies. Based on the success of recent nanomedicine approaches, this chapter reviews representative studies of how functionalized nanoparticles can be designed to target tumor-specific molecules and directly or indirectly modulate the expression and/or activity of particular RHO GTPases in cancer cells.

P. Matos (✉) · J. F. S. Pereira · P. Jordan
Department of Human Genetics, Instituto Nacional
de Saúde Doutor Ricardo Jorge,
Lisbon, Portugal

BioISI – Instituto de Biosistemas e Ciências
Integrativas, Faculdade de Ciências, Universidade de
Lisboa, Lisbon, Portugal
e-mail: paulo.matos@insa.min-saude.pt

Keywords

Tumorigenic signaling targeting · RHO
GTPase inhibition · “Smart” nanoparticle
carriers

5.1 Introduction

RHO GTPases are low molecular weight proteins that belong to the large RAS superfamily of small GTPases. The more than 20 members of the RHO GTPase family have been grouped into eight sub-families based on their structure and sequence homology: RHO, RAC, CDC42, RHOD/RHOF, RHOH, RHOU/RHOV, Rnd, and RHOBTB [1]. RHOA, RAC1, and CDC42 are, by far, the best-studied members of this family. First identified for their role in regulating actin cytoskeleton organization and dynamics [2], they were subsequently recognized as key regulators of signaling pathways involved in a plethora of cellular processes, including gene expression, cell-cycle progression, cell polarity, and cell survival [3]. Like most RAS superfamily proteins, most RHO GTPases cycle between a cytoplasmic inactive state, where the proteins are bound to guanosine diphosphate (GDP), and a cell membrane-associated active state, in which the proteins are bound to guanosine triphosphate (GTP). To be able to interact with cellular membranes, where they become activated, most RHO GTPases are prenylated at a C-terminal CAAX motif, most often by the addition of a geranylgeranyl group [1]. Once at the membrane, three families of regulatory proteins tightly regulate their activation/inactivation cycles: guanine-nucleotide exchange factors (GEFs), GTPase-activating proteins (GAPs), and guanine-nucleotide dissociation inhibitors (GDIs) (Fig. 5.1). GEFs promote the exchange of GDP for GTP to activate RHO GTPases [4], while GAPs accelerate the intrinsic GTPase activity of RHO GTPases, which inactivates them [5].

RHOGDIs bind to GDP-bound RHO GTPases and regulate their activity, both spatially and temporally [6, 7]. They form a hydrophobic pocket through which they bind to the prenylated tails of RHO GTPases allowing their extraction from the membrane upon inactivation by GAPs. Then, RHOGDIs interact with the so-called switch domains of RHO GTPases and prevent the dissociation of GDP and interaction with GEFs and effector proteins in the cytoplasm. Following appropriate stimuli, RHO GTPases release from

RHOGDIs, which allows their integration into the membrane via their C-terminal prenyl groups, where they can be activated by GEF proteins [1, 6, 7].

Upon activation, for example downstream of many membrane receptors, RHO GTPases undergo conformational changes and can interact with a large number of effector proteins, including enzymes and scaffolding proteins, to mediate diverse yet specific and spatially and temporally regulated cellular responses [8]. In many cases, the downstream signaling feeds back to RHO GTPases, further modulating their activity through post-translational modifications, including phosphorylation, ubiquitination, sumoylation, and lipid modification [1, 7, 9].

5.2 Dysregulation of RHO GTPases in Cancer

Given their involvement in various cellular functions, it is not unexpected that the dysregulation of RHO GTPases, their regulators or effectors has been associated with nearly all stages of cancer development and progression, including the dysregulation of cell proliferation, cellular transformation, resistance to apoptosis, tissue invasion, angiogenesis, metastasis, and resistance to chemotherapy [9]. Unlike Ras proteins, which are mutated in approximately 20–30% of human cancers, mutations in RHO GTPases are much less frequent. Indeed, despite recent cancer genome-sequencing data identifying rare mutations in various RHO proteins in multiple cancer types [10], the main body of experimental evidence indicates that the dysregulation of RHO GTPase activities in cancer occurs mainly through changes in the expression levels or activation status of RHO proteins, their regulators or effectors, via epigenetic and post-translational events [9]. Upregulation of several RHO GTPase family members with tumor-promoting properties and downregulation of other members with tumor-suppressing activity are often observed in human cancers, and are known to participate in several steps of cancerigenesis [9, 11]. For instance, a study by Zhou et al. [12] described

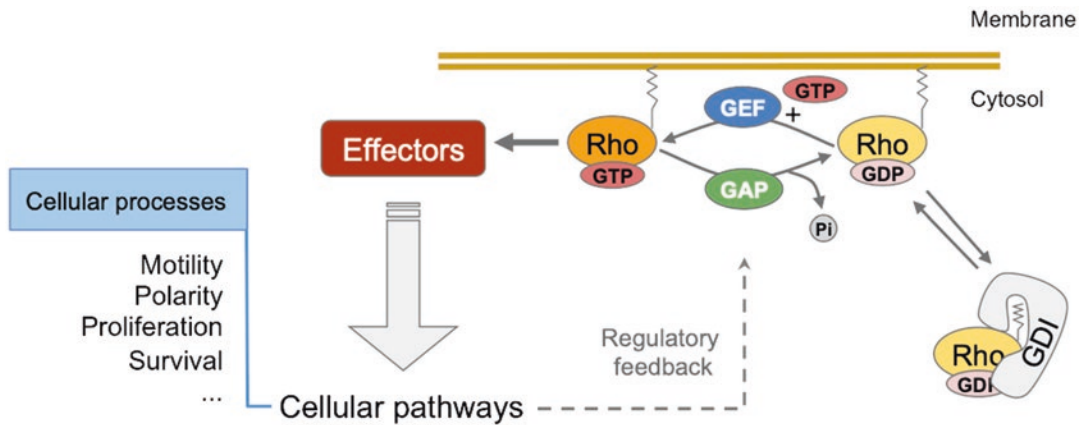


Fig. 5.1 The regulatory cycle of RHO-GTPases. RHO-family GTPases are membrane-anchored via prenylated tails and become activated by guanine-nucleotide exchange factors (GEFs), which promote the exchange of bound GDP with GTP present in the cytosol. GTP binding alters RHO-GTPase conformation so that interaction can occur with effector proteins, which then trigger downstream signaling. Through the action of GTPase-activating proteins (GAPs), which accelerate the intrinsic GTPase

activity of RHO GTPases, GTP is hydrolysed and the protein returns to its inactive conformation. Additional regulatory factors of RHO-GTPases are guanine-nucleotide dissociation inhibitors (GDIs) that contain a hydrophobic pocket allowing binding to the prenylated tails of RHO GTPases with subsequent extraction from the membrane. This prevents further activation cycles until suitable stimuli lead to the release from RHOGDIs and re-integration of RHO-GTPases into the membrane

that whereas RHOA and RHOC expression is elevated in gastric cancer tissues, RHOB expression is downregulated or even absent, in comparison to normal gastric tissues. Moreover, the overexpression of RHOA in human gastric cancer cell lines promoted cell proliferation, whereas RHOC overexpression enhanced motility and invasiveness. In contrast, RHOB overexpression suppresses these malignant phenotypes in the same cell lines [12]. The tumor suppressor role of RHOB extends to several other malignancies, including breast, colon, and neurologic cancers such as the highly aggressive glioblastoma [13, 14]. In another example, the canonical RHO GTPases RHOA, RAC1 and CDC42 are frequently found overexpressed in breast cancers [11]; however, the atypical RHO GTPase RHOBTB2 is often silenced by promoter methylation in these tumors and has thus been described as a tumor suppressor gene in breast cancer development [15]. As a final example, the expression of RHO GTPase RHOE (also known as RND3) is frequently downregulated in hepatocellular carcinomas, which correlates with cancer progression and poor prognosis [16]. However, RHOE expression is often upregulated in gastric

cancers, and has been implicated in the promotion of epithelial-to-mesenchymal transition and multidrug resistance in these tumors [17, 18]. Thus, the roles of the various RHO family members in cancer progression are complex and depend on a multitude of factors, including tumor cell type, tumor stage and likely the individual tumor context, both intracellular and extracellular. Nevertheless, their common abnormal expression and aberrant signaling in virtually all types of cancers make them attractive targets for cancer therapy.

5.3 Targeting RHO GTPases in Cancer

The Ras superfamily of small GTPases, including RHO GTPases, have long been viewed as attractive targets for therapeutic interventions in cancer. However, their structure and functional properties have deemed them “undruggable” or, at least, “hard-to-target” molecules [19]. Given the micromolar GTP concentration in cells and the sub-nanomolar binding affinity of RHO GTPases for GTP or GDP, it is difficult to drug

RHO GTPases using nucleotide analogs like those used to inhibit many protein kinases. Moreover, except for the nucleotide-binding pocket, the globular structure of RHO GTPases provides limited tractable cavities for small-molecule binding. In addition, the complexity and pleiotropy of RHO GTPase downstream signaling pathways further confounds the challenging requirement of targeting a particular cell type or cellular process. Notwithstanding, several bacterial toxins have been long known to modulate the activity of RHO GTPases [20]. For instance, C3 transferase, an ADP-ribosyltransferase from *Clostridium botulinum*, inactivates RHOA, RHOB, and RHOC but not RAC1 or CDC42, while *Clostridium difficile* toxin A and B inactivate multiple RHO GTPase subfamilies. In contrast, RHO proteins can be activated by the cytotoxic necrotizing factors CNF1 and CNF2 from *Escherichia coli* and by the dermonecrotizing toxin DNT from *Bacillus bronchiseptica*. These toxins are small proteins that bind RHO GTPases and block their intrinsic and GAP-stimulated GTP hydrolysis, thereby rendering them constitutively active. However, while these toxins have been powerful tools in dissecting several cellular functions of RHO GTPases, they are large molecules, have low specificity, and most introduce irreversible modifications to their targets, making them clinically unusable [19]. Therefore, significant effort has been dedicated in the last decades to develop small molecule inhibitors that can selectively modulate RHO GTPase activity. A few molecules have been identified, but their translation into the clinical setting has been limited.

As mentioned earlier, most RHO GTPases are post-translationally modified by the addition of a geranylgeranyl moiety in their C-terminus, and this is a crucial step to allow their interaction with intracellular membranes and subsequent activation. GGTI-2418 is a peptidomimetic small-molecule inhibitor of geranylgeranyl-transferase I that prevents the prenylation of RHO GTPases leading to the inhibition of their functions [21]. This inhibitor has recently entered phase I clinical trials but, while well-tolerated at all tested doses, no objective patient responses were observed

[22]. Other isoprenyl transferase inhibitors are available and currently on clinical trials. However, given their low selectivity, it has been suggested that the major targets for these inhibitors are likely proteins other than RHO GTPases [23].

As discussed above, RHO GTPases require specific GEFs to become activated in response to distinct stimuli, and several small-molecules have been identified that specifically target RHO GTPase/GEF interactions. For example, Rhosin, a molecule identified through a structure-based design coupled to a virtual-binding screening strategy, inhibits the interaction of RHOA and RHOC with many of their specific GEFs, and its administration suppresses the invasiveness of breast cancer cells in vitro [24]. NSC23766 and EHT 1864 are RAC1-specific inhibitors that, in vitro, suppress the proliferation, migration and invasion of cancer cells of multiple origins [25]. NSC23766, also identified using a structural-based virtual compound screen, inhibits RAC1 interaction with a subset of Rac-specific GEFs, such as Tiam1 and Trio [26], whereas EHT 1864 acts by promoting the loss of bound nucleotide, inhibiting both GEF-stimulated nucleotide exchange and nucleotide association [27]. However, critical off target effects in mouse platelets, as well as their high IC₅₀ (~50 μM) make these compounds pharmacologically ineffective [28]. EHop-016 was identified during the optimization of NSC23766, and suppresses cancer cell migration by interfering with the binding of RAC1 to Vav2 [29]. Importantly, EHop-016 reduced mammary tumor growth by ~80% in nude mice and inhibited angiogenesis and metastasis [30]. However, the drug's effective concentrations are high due to its relatively low bioavailability, which hinders its potential translation to the clinic [25]. As a final example, CDC42 Activity Specific Inhibitor (CASIN), a compound identified in cell-based assays, disrupts APC-stimulated exchanging factor (ArhGEF4)-mediated CDC42 activation with a low IC₅₀ (~2 μM). Suggestively, CDC42 inhibition via CASIN treatment reduced tumorigenicity in colorectal cancer xenograft models and prevented progression of mouse and human tumor organoids [31].

5.4 Modulating RHO GTPases Through Functionalized Nanoparticles

As discussed above, RHO GTPases are considered highly promising but very “hard-to-target” molecules, despite numerous efforts to develop GTPase inhibitors [19]. Recently, targeting mRNA instead of protein by use of RNA interference (RNAi) with antisense oligonucleotides has become an alternative strategy to target GTPase for cancer treatment [32, 33]. This technology uses synthetic small interfering RNAs (siRNAs), generally from 21 to 25 base-pairs (bp), or short hairpin RNAs (shRNAs), delivered through viral or bacterial vectors to activate the RNA-induced silencing complex (RISC). This complex has ribonuclease activity and uses these synthetic short RNAs to recognize (by sequence complementarity) and cleave specific mRNA molecules in the cell’s cytoplasm, thus reducing de expression of the corresponding proteins [33]. However, oligonucleotides are polyanionic biomacromolecules that are subtract to serum nucleases and do not pass easily across cell membranes. Therefore, specific delivery vehicles are required to facilitate the cytosolic oligonucleotide delivery [34]. In recent years, nanoparticles (NPs) have been proven as powerful tools for systemic delivery of antisense oligonucleotides and several RNAi-NP platforms have entered into early phase clinical trials for the treatment of various diseases including cancer [35]. Several recent studies suggest that this could be a viable therapeutic strategy to selectively target RHO GTPases in cancer.

5.4.1 Nanoparticle-Mediated Anti-RHO RNAi

RHOA activity is dysregulated in various human cancers, and has been implicated in almost every stage of cancer progression. In breast cancer, for instance, RHOA overexpression correlates with increased proliferation, invasion, and angiogenesis [9]. Consistently, the knockdown of RHOA by siRNA inhibits the growth and angiogenesis of xenografted breast cancer cell lines [36, 37]. In a

seminal study, Pillé and co-workers [38] increased the efficacy of anti-RHOA siRNA delivery by encapsulating the antisense oligonucleotides in polyisohexylcyanoacrylate (PIHCA) nanoparticles coated with chitosan. Chitosan is a deacylated derivative of chitin, which is one of the most abundant mucopolysaccharides in crustaceans and insects. Besides being cost effective, the use of chitosan in nonviral delivery systems increases bioavailability without significant immunogenicity, enabling repeated clinical administration [39]. Intravenous administration of anti-RHOA siRNA in chitosan-coated nanoparticles to athymic nude mice carrying xenografts of aggressive MDA-MB-231 breast cancer cells resulted in over 90% tumor growth inhibition without any apparent physiological or histological toxicity to other tissues [38].

Nevertheless, given the pleiotropic functions of RHO GTPases, the non-targeted systemic delivery of RHO GTPase downregulating molecules through nanopatforms may produce unforeseen adverse effects. One way to circumvent these issues is to develop functionalized “smart” nanoparticle carriers that selectively target cancer cells. Promising carriers include NPs functionalized with activatable cell-penetrating peptides (dtACPPs). These explore the lower pH and the presence of elevated levels of active matrix metalloproteinases (MMPs) in the tumor microenvironment to selectively expose cell-penetrating peptides that coat the drug/nucleic acid-containing nanoparticles, thus driving their internalization, along with the therapeutic molecules, into the tumor cells [40]. Bao et al. [41] used this strategy to functionalize nanoparticles carrying RAC1-specific shRNAs. Upregulation of RAC1 expression has been found in hepatic metastases of colorectal cancers and associates with decreased patient survival [41, 42]. Liver metastases are very common in patients with advanced colon cancer and, when detected at diagnosis, the prognosis is so poor that the benefit of treating the primary cancer is uncertain [43]. Importantly, RAC1 downregulation through RNA interference significantly inhibits migration and invasion of colorectal cancer cells [41, 44]. To translate these findings into an effec-

tive therapeutic approach Bao et al. functionalized dtACPP-PEG-DGL (dtACPPD) nanoparticles with an EGFP-labeled, RAC1-specific shRNA. In this system, the authors used R-maleimidyl- ω -N-hydroxysuccinimidyl polyethyleneglycol (MAL-PEG-NHS) to conjugate dtACPP to the surface of poly-L-lysine (DGL), which has the ability to encapsulate DNA, forming low pH/MMP-sensitive nanoparticles [41]. Upon intravenous administration of the functionalized nanoparticles into a HCT116 colorectal cancer cell xenograft model, the authors further observed a very high accumulation of EGFP signal in the tumors, indicative of highly efficient dtACPPD-mediated delivery of the shRNAs into the tumor cells. Moreover, this led to a significant decrease of RAC1 expression in the tumors and a significant reduction in tumor metastasis to the liver, suggesting that the use of dtACPPD/shRAC1 nanoparticles may constitute an innovative strategy to address hepatic metastasis in colon cancer [41].

5.4.2 Efficient Cytosolic Delivery of Anti-RHO siRNAs

Another, important aspect in the design of siRNA carriers is an efficient cytosolic delivery, i.e., once internalized by the target cells, the NP platform needs to respond to endosomal pH and allow the siRNA molecules to efficiently escape from endosomes to improve gene silencing efficacy [34].

Li and coworkers [45] have recently developed endosomal pH-responsive nanoparticles to enhance the delivery of RAC1-targeting siRNA together with cisplatin to xenografts of chemoresistant breast cancers.

In breast cancers, overexpression of RAC1 has also been associated with multi-drug resistance to neoadjuvant chemotherapy, especially in triple-negative breast cancers [45, 46]. RAC1 stimulates the pentose phosphate pathway by upregulating glycolysis and this leads to increased nucleotide metabolism, which protects breast cancer cells from chemotherapeutic-induced DNA damage. By using an endosomal pH-

responsive methoxyl-poly (ethylene glycol)-b-poly(2-(diisopropylamino) ethyl methacrylate) (Meo-PEG-b-PDPA) polymer with a pKa (~6.24) close to the endosomal pH (6.0–6.5), Li et al. achieved a highly efficient cytosolic siRAC1 delivery that effectively depleted RAC1 expression and reversed the resistance to chemotherapeutic drugs in breast cancer cell lines. Importantly, similar results were obtained in triple-negative breast cancer patient-derived xenografts, when the Meo-PEG-b-PDPA/siRAC1 NPs were administered intravenously [45].

5.4.3 Combining Selective Targeting with Efficient Cytosolic Delivery of Anti-RHO siRNAs

The overexpression of another RHO family member, RHOC, has been linked to increased invasion, migration, and metastases of breast cancers [47]. In addition, downregulation of RHOC expression using siRNA inhibited the metastatic spread of aggressive breast cancer cells [48]. These observations prompted the development of another type of innovative “smart” nanoparticles to selectively deliver anti-RHOC siRNA molecules to metastatic breast cancer cells [49, 50]. A degradable, pH-sensitive, β -cyclodextrin (β CD)-based polymeric carrier that condenses anti-RHOC siRNA was used to form the “smart” particles. These smart anti-RHOC particles were efficiently internalized, successfully escaped the endosome, and delivered the RNA cargo into the cytoplasm of highly invasive SUM149 and MDA-MB-231 breast cancer cells. Their incorporation suppressed RHOC protein levels by >90% and drastically inhibited the motility, migration and invasion of SUM149 and MDA-MB-231 cells [49]. In a subsequent study by the same group, the tumor-cell selectivity of these “smart” particles was further optimized by the asymmetrical functionalization of the β CD core to display a “brush” of hydrophilic polyethylene glycol (PEG) chains on the primary face, and amphiphilic cationic/hydrophobic grafts that complex the anti-RHOC siRNA cargo

on the secondary face [50]. The free tips of the PEG chains were then further functionalized to display EPPT1 targeting peptides. EPPT1 are antibody-derived peptides that bind with high affinity to the peptide backbone of MUC1 receptors that become exposed in >90% of metastatic breast cancer cells due to underglycosylation (uMUC1) [51]. Functionalization of with EPPT1 peptides allowed selective recognition and binding of the nanoparticles to the uMUC1 receptors present on the surface of aggressive breast cancer cells followed by particles internalization via endocytosis and intracellular delivery of anti-RHOC siRNA, which resulted in a dose-dependent inhibition of breast cancer cell migration and invasion [50].

5.5 Indirect Targeting of RHO GTPases Through Functionalized NPs

The discovery that the abnormal expression of certain micro RNAs (miRNAs – endogenous small non-coding RNA molecules of similar size and function to the above-described synthetic siRNAs), plays an important role in different steps of tumorigenesis and in tumor resistance to therapy opened the possibility for developing selective miRNA-based therapeutic approaches to target cancer [52]. An example of this is miR-21 that was found highly overexpressed in glioblastoma (GBM) [53–55], a neuroepithelial tumor of the central nervous system, characterized by an extremely aggressive clinical phenotype with very poor prognosis (only 3–5% of patients survive for more than 5 years) [56]. MiR-21 directly targets the RHO-family GTPase RHOB [57], whose expression decreases with increasing glioma grade [58] and has a tumor repressive activity [59], namely by inhibition of PKC α -driven GBM cell motility and invasion [14]. Thus, targeting the upregulation of miR-21 would constitute an attractive strategy to indirectly restore RHOB expression and decrease the aggressiveness of GBM tumors. However, the successful *in vivo* delivery of anti-miRNA oligo-

nucleotides (AMOs) to brain tumors requires the use of carriers able to overcome the blood–brain barrier, allowing their uptake by target tumor cells. In this regard, Costa et al. [60] reported the development of a stable nucleic acid lipid particles (SNALPs)-based miRNA delivery system, designed to target GBMs. This was achieved by coupling of chlorotoxin (CTX), a scorpion-derived peptide that was reported as a reliable and specific marker for gliomas [61], to the surface of stabilized DSPE-PEG-Maleimide liposomes [60]. These were then used to encapsulate anti-miR-21 AMOs and tested in an orthotopic mouse model of GBM. The authors observed that intravenous administration of SNALP-CTX nanoparticle-formulated anti-miR-21 AMOs to GBM-bearing mice resulted in a tumor-selective increase in RHOB mRNA and protein levels, which promoted decreased tumor cell proliferation and increased tumor cell apoptosis leading to tumor size reduction and improved animal survival upon co-exposure to the tyrosine kinase inhibitor sunitinib [60].

Another example of how RHO GTPase dysregulation can be indirectly used to target cancer cells was reported by Liu et al. [62]. These authors functionalized ultrafine gold-iodine (Au@I) nanoparticles (AIRA NPs) with a specific anti-RHOJ antibody to be used as radiosensitizers, enhancing the killing efficacy of radiation therapy by potentiating the susceptibility of tumor tissue to low-dosage radiation while reducing the injury to the surrounding normal tissues [62]. RHOJ is a member of the CDC42 subfamily of RHO GTPases that is mainly expressed on the surface of endothelial cells (ECs) and upregulated in the peri- and intratumoral vasculature of several human cancers [63, 64]. Once injected into mouse models with orthotopic breast tumor xenografts, these anti-RHOJ functionalized AIRA NPs bound specifically to both newly formed tumor vessels in peri- and intratumoral regions and pre-existing tumor vessels. AIRA NPs administration remarkably enhanced the efficacy of radiation therapy *in vivo*, when compared to radiation alone or even to anti-angiogenesis chemotherapy [62].

5.6 Potential Adverse Effects of Carrier NPs on Endogenous RHO GTPases

A cautionary note should be made here regarding the potential effects of carrier NP composition on endogenous cellular levels and activity of RHO GTPases. It has been observed that the uptake of NP can affect cell behavior including cell proliferation, apoptosis, invasion, and migration [65]. For instance, a study that analysed the effects on cancer cell migration of PCL-PEG nano-micelles observed that exposure to nano-micelles of different PCL and PEG chain sizes resulted in different patterns of cell migration and matrix adhesion. Importantly, these variations in cellular behavior reflected differences in endogenous RHOA and RAC1 expression and activity [66]. In another example, treatment of endothelial cells with non-functionalized zinc oxide nanoparticles (ZnO-NPs) caused the activation of RAC1 and CDC42, leading to the overexpression of intercellular adhesion molecule-1 (ICAM-1) that potentiates vascular inflammation through stimulation of leukocyte adherence [67]. Also of note, exposure of mice during pregnancy/lactation to titanium dioxide NPs (Nano-TiO₂), a nanomaterial broadly applied in food packaging systems and food additives, increased RAC1 and CDC42 expression and decreased RHOA levels in offspring mice neurons, resulting in brain and cognitive impairment [68].

Thus, while NP carriers are potentially extremely powerful tools to therapeutically modulate the activity of RHO GTPases in cancer and other human diseases, great care has to be taken, as with any other bioactive agent, in controlling their toxicity while maximizing their bioavailability, enhancing target cell uptake and minimizing potential adverse effects.

5.7 Concluding Remarks and Perspectives

In recent years, nanotechnology has revolutionized the field of biomedicine with the development of powerful tools and “smart” carriers for

the targeted delivery of bioactive molecules. This has opened the possibility of designing innovative approaches to tackle the therapeutic modulation of “hard-to-target” molecules such as RHO GTPases. As discussed above, most modulation strategies developed so far explored the use of the antisense oligonucleotides to either deplete upregulated RHO proteins or to target endogenous downregulators, such as miRNAs, in the case of pathologically downregulated GTPases (Fig. 5.2). An interesting approach that may be explored in the future is the use of “smart” NPs to selectively deliver the few available RHO GTPase small molecule inhibitors to cancer cells, thus avoiding the reported toxicity and adverse effect caused by their systemic delivery. This principle has been recently applied in the development of innovative tools to treat osteoporosis. Protein–DNA hybrid hydrogels were engineered to selectively target osteoclasts and allow the spatiotemporally controlled release of C3 toxin to inhibit RHOA signaling. Notably, the application of these C3 toxin-loaded hydrogels effectively reduced osteoclast formation and bone resorption activity [69].

Another stimulating possibility is the use of NPs to improve the delivery of modified antisense oligonucleotides (ASOs) to suppress the splicing of tumor-associated RHO GTPase isoforms. Certain RHO GTPase isoforms have been associated with cancer progression. For instance, two CDC42 variants, CDC42-v1 and CDC42-v2, can be generated through alternative splicing, and it was shown that the downregulation of CDC42-v2 isoform in ovarian cancer leads to increased proliferation and invasion of tumor cells [70]. Another example is RAC1B, a splice variant of RAC1 GTPase that is overexpressed in various cancers, including colorectal [71], breast [72], lung [73], and thyroid carcinomas [74]. RAC1B results from the inclusion of an additional exon that adds 19 amino acids to the conventional RAC1 protein, increasing its GDP/GTP exchange and channeling its signaling towards pro-proliferative and pro-survival pathways [75]. These tumor-associated splicing events could be targeted using ASOs such as phosphorodiamidate Morpholino oligomers (PMOs) that instead of promoting mRNA degradation rather modify

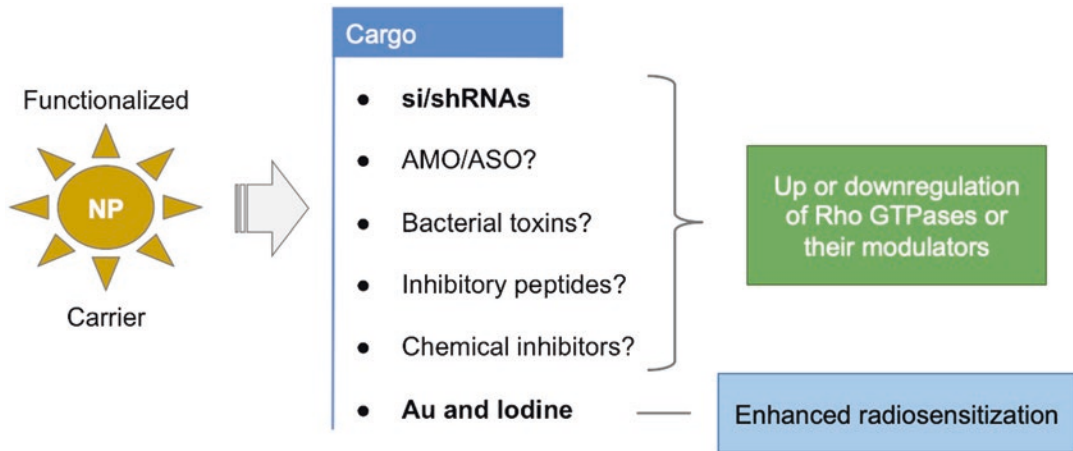


Fig. 5.2 Overview of nanoparticle-deliverable cargo molecules to inhibit RHO-GTPase activity. Nanoparticles have been developed as new tools for carrying pharmacological inhibitors (cargo). The scheme summarizes the possible cargo molecules to tackle the therapeutic modulation of RHO GTPases, as detailed in the text. For the

compounds shown in bold experimental proof has been provided; however, the remaining compounds represent potential strategies that can be explored in the future, in particular when combined with “smart” carriers allowing targeted or tissue-specific delivery, e.g., to cancer cells

gene expression by blocking specific regulatory elements, namely those required for exon inclusion/skipping during splicing [76]. This strategy has already been proven successful in the clinic for the treatment of spinal muscular atrophy (SMA), an autosomal recessive disorder characterized by loss of motor neurons and muscle atrophy, with symptoms manifesting in early childhood [77]. SMA is caused by mutations in the survival motor neuron (SMN1) gene that abrogate its expression. A second duplicated gene, SMN2, produces very little functional protein due to the abnormal splicing of exon 7. The recently approved drug Nusinersen is an ASO that binds SMN2 and prevents exon 7 skipping, increasing SMN protein levels and improving patient motor function [78]. Importantly, this drug has to be delivered intrathecally since ASOs cannot cross the blood-brain barrier (BBB), but it was shown recently that this may be overcome using ASO-functionalized nanoparticles based on modified BBB-crossing peptides [79]. Thus, equivalent ASO-NP-based strategies could be used in the future to specifically target splicing events leading to the abnormal expression of

tumor-associated RHO GTPase isoforms in different cancer types.

A third strategy worth future investigation is the use of functionalized NPs to enhance the bioavailability of short peptide inhibitors of RHO GTPase activation and signaling. Several RHO inhibiting peptides have been developed in the last decades [80]. For example, using random peptide T7 phage display technology, Sakamoto et al. [81] identified a short peptide capable of inhibiting the interaction between RAC1 and its GEF DOCK2. When delivered to intracellular compartments by combination with cell-penetrating peptide CPP, this inhibitory peptide significantly reduced endogenous RAC1 activation in B-lymphocytes and strongly impaired of B-cell migration. In another study, Nur-E-Kamal et al. [82] developed a short peptide, derived from the CDC42-binding domain of the activated Cdc42-associated kinase 1 (ACK-1), that inhibits CDC42 downstream signaling by blocking the interactions of CDC42-GTP with effectors, such as ACKs, p21-activated kinases (PAKs) and Wiskott–Aldrich syndrome protein (N-WASP). Recently, another group developed a 16-mer

cyclic peptide with similar CDC42 inhibitory properties that, upon addition of a cell-penetrating sequence, was able to suppress proliferation, migration and invasion in RAS-driven cancer cell models [83]. The problem with peptide drugs is that they usually have low bioavailability, poor specific bio-distribution, and a high risk of immunogenicity [84], and in the case of RHO proteins an added risk of systemic adverse effects, as described above for chemical inhibitors. Therefore, the design of NP carriers, functionalized to enhance the bioavailability and targeted distribution of RHO peptide inhibitors, would certainly improve their pharmacological applicability.

Despite the exciting therapeutic possibilities brought up by NP-carrier technology, it must be stressed here that most of the studies reviewed in this chapter report *in vitro* investigational findings, which do not address important questions such as the biological fate of the NP carriers after delivering their cargo, their biopersistence in target organs and other tissues, and related physiological consequences, namely regarding potentially toxic side effects. Indeed, recent evidence on the interaction of metal and metal oxide NPs, such as the Au-, ZnO-, and TiO₂-carriers described in this chapter, has been reported to disturb the natural functions of cells and their components, with potentially significant health consequences (recently reviewed in [85]). These deleterious effects range from cell membrane perforation and cytoskeleton abnormalities, to reactive oxygen species (ROS) production, genomic damage and epigenetic alterations, and relate not only to the size and physicochemical properties of NPs but also to their concentration in biological systems. Thus, it is of paramount importance that the design of novel NP-based therapeutic strategies is accompanied by robust nanotoxicological *in vitro* and *in vivo* research, so that the clear potential benefits of their use are not hampered by unforeseen adverse health effects.

Acknowledgements The authors' work is supported by Fundação para a Ciência e a Tecnologia (FCT), Portugal, through grant UID/MULTI/04046/2019 to the BioISI Research Unit and a research fellowship to J.F.S.P. from project grant PTDC/SAU-PUB/29481/2017.

References

- Hodge RG, Ridley AJ (2016) Regulating Rho GTPases and their regulators. *Nat Rev Mol Cell Biol* 17:496–510
- Nobes CD, Hall A (1995) Rho, Rac, and Cdc42 GTPases regulate the assembly of multimolecular focal complexes associated with actin stress fibers, lamellipodia, and filopodia. *Cell* 81:53–62
- Phuyal S, Farhan H (2019) Multifaceted Rho GTPase signaling at the endomembranes. *Front Cell Dev Biol* 7:127
- Schmidt A (2002) Guanine nucleotide exchange factors for Rho GTPases: turning on the switch. *Genes Dev* 16:1587–1609
- Tcherkezian J, Lamarche-Vane N (2007) Current knowledge of the large RhoGAP family of proteins. *Biol Cell* 99:67–86
- Golding AE, Visco I, Bieling P, Bement WM (2019) Extraction of active RhoGTPases by RhoGDI regulates spatiotemporal patterning of RhoGTPases. *Elife* 8:e50471
- Cho, Kim, Baek, Kim, Lee (2019) Regulation of Rho GTPases by RhoGDIs in human cancers. *Cell* 8:1037
- Etienne-Manneville S, Hall A (2002) Rho GTPases in cell biology. *Nature* 420:629–635
- Jung H, Yoon SR, Lim J, Cho HJ, Lee HG (2020) Dysregulation of Rho GTPases in human cancers. *Cancer* 12:1179
- Svensmark JH, Brakebusch C (2019) Rho GTPases in cancer: friend or foe? *Oncogene* 38:7447–7456
- Haga RB, Ridley AJ (2016) Rho GTPases: regulation and roles in cancer cell biology. *Small GTPases* 7:207–221
- Zhou J, Zhu Y, Zhang G, Liu N, Sun L, Liu M et al (2011) A distinct role of RhoB in gastric cancer suppression: suppressive effect of RhoB on gastric cancer cells. *Int J Cancer* 128:1057–1068
- Ju J, Gilkes D (2018) RhoB: team oncogene or team tumor suppressor? *Genes* 9:67
- Baldwin RM, Parolin DAE, Lorimer IAJ (2008) Regulation of glioblastoma cell invasion by PKC α and RhoB. *Oncogene* 27:3587–3595
- Beder LB, Gunduz M, Ouchida M, Gunduz E, Sakai A, Fukushima K et al (2006) Identification of a candidate tumor suppressor gene RHOBTB1 located at a novel allelic loss region 10q21 in head and neck cancer. *J Cancer Res Clin Oncol* 132:19–27
- Grise F, Sena S, Bidaud-Meynard A, Baud J, Hiriart J-B, Makki K et al (2012) Rnd3/RhoE is down-regulated in hepatocellular carcinoma and controls cellular invasion. *Hepatology* 55:1766–1775
- Li K, Lu Y, Liang J, Luo G, Ren G, Wang X et al (2009) RhoE enhances multidrug resistance of gastric cancer cells by suppressing Bax. *Biochem Biophys Res Commun* 379:212–216
- Zhou J, Li K, Gu Y, Feng B, Ren G, Zhang L et al (2011) Transcriptional up-regulation of RhoE by hypoxia-inducible factor (HIF)-1 promotes epithelial to mesenchymal transition of gastric cancer cells

- during hypoxia. *Biochem Biophys Res Commun* 415:348–354
19. Lin Y, Zheng Y (2015) Approaches of targeting rho GTPases in cancer drug discovery. *Expert Opin Drug Discov* 10:991–1010
 20. Aktories K, Schmidt G, Just I (2000) Rho GTPases as targets of bacterial protein toxins. *Biol Chem* 381:421–426
 21. Kazi A, Carie A, Blaskovich MA, Bucher C, Thai V, Moulder S et al (2009) Blockade of protein geranylgeranylation inhibits Cdk2-dependent p27Kip1 phosphorylation on Thr187 and accumulates p27Kip1 in the nucleus: implications for breast cancer therapy. *MCB* 29:2254–2263
 22. Karasic TB, Chiorean EG, Sebti SM, O'Dwyer PJ (2019) A phase I study of GGTI-2418 (geranylgeranyl transferase I inhibitor) in patients with advanced solid tumors. *Target Oncol* 14:613–618
 23. Haluska P, Dy GK, Adjei AA (2002) Farnesyl transferase inhibitors as anticancer agents. *Eur J Cancer* 38:1685–1700
 24. Shang X, Marchioni F, Sipes N, Evelyn CR, Jerabek-Willemsen M, Duhr S et al (2012) Rational design of small molecule inhibitors targeting RhoA subfamily rho GTPases. *Chem Biol* 19:699–710
 25. Maldonado M d M, Dharmawardhane S (2018) Targeting Rac and Cdc42 GTPases in cancer. *Cancer Res. canres*;0008–5472.CAN-18-0619v1
 26. Gao Y, Dickerson JB, Guo F, Zheng J, Zheng Y (2004) Rational design and characterization of a Rac GTPase-specific small molecule inhibitor. *Proc Natl Acad Sci* 101:7618–7623
 27. Shutes A, Onesto C, Picard V, Leblond B, Schweighoffer F, Der CJ (2007) Specificity and mechanism of action of EHT 1864, a novel small molecule inhibitor of Rac family small GTPases. *J Biol Chem* 282:35666–35678
 28. Dütting S, Heidenreich J, Cherpokova D, Amin E, Zhang S-C, Ahmadian MR et al (2015) Critical off-target effects of the widely used Rac1 inhibitors NSC23766 and EHT1864 in mouse platelets. *J Thromb Haemost* 13:827–838
 29. Montalvo-Ortiz BL, Castillo-Pichardo L, Hernández E, Humphries-Bickley T, De La Mota-Peynado A, Cubano LA et al (2012) Characterization of EHOp-016, novel small molecule inhibitor of Rac GTPase. *J Biol Chem* 287:13228–13238
 30. Castillo-Pichardo L, Humphries-Bickley T, De La Parra C, Forestier-Roman I, Martínez-Ferrer M, Hernandez E et al (2014) The Rac inhibitor EHOp-016 inhibits mammary tumor growth and metastasis in a nude mouse model. *Transl Oncol* 7:546–555
 31. Sakamori R, Yu S, Zhang X, Hoffman A, Sun J, Das S et al (2014) CDC42 inhibition suppresses progression of incipient intestinal Tumors. *Cancer Res* 74:5480–5492
 32. Whitehead KA, Langer R, Anderson DG (2009) Knocking down barriers: advances in siRNA delivery. *Nat Rev Drug Discov* 8:129–138
 33. Chakraborty C, Sharma AR, Sharma G, Doss CGP, Lee S-S (2017) Therapeutic miRNA and siRNA: moving from bench to clinic as next generation medicine. *Mol Therap – Nucleic Acid* 8:132–143
 34. Shi J, Kantoff PW, Wooster R, Farokhzad OC (2017) Cancer nanomedicine: progress, challenges and opportunities. *Nat Rev Cancer* 17:20–37
 35. Zuckerman JE, Davis ME (2015) Clinical experiences with systemically administered siRNA-based therapeutics in cancer. *Nat Rev Drug Discov* 14:843–856
 36. Fritz G, Just I, Kaina B (1999) Rho GTPases are overexpressed in human tumors. *Int J Cancer* 81:682–687
 37. Pillé J-Y, Denoyelle C, Varet J, Bertrand J-R, Soria J, Opolon P et al (2005) Anti-RhoA and anti-RhoC siRNAs inhibit the proliferation and invasiveness of MDA-MB-231 breast cancer cells in vitro and in vivo. *Mol Ther* 11:267–274
 38. Pillé J-Y, Li H, Blot E, Bertrand J-R, Pritchard L-L, Opolon P et al (2006) Intravenous delivery of anti-RhoA small interfering RNA loaded in nanoparticles of chitosan in mice: safety and efficacy in Xenografted aggressive breast cancer. *Hum Gene Ther* 17:1019–1026
 39. Pouton CW, Seymour LW (2001) Key issues in non-viral gene delivery. *Adv Drug Deliv Rev* 46:187–203
 40. Huang S, Shao K, Liu Y, Kuang Y, Li J, An S et al (2013) Tumor-targeting and microenvironment-responsive smart nanoparticles for combination therapy of antiangiogenesis and apoptosis. *ACS Nano* 7:2860–2871
 41. Bao Y, Guo H, Lu Y, Feng W, Sun X, Tang C et al (2016) Blocking hepatic metastases of colon cancer cells using an shRNA against Rac1 delivered by activatable cell-penetrating peptide. *Oncotarget* 7:77183–77195
 42. Kotelevets L, Chastre E (2020) Rac1 signaling: from intestinal homeostasis to colorectal cancer metastasis. *Cancer* 12:665
 43. Sheth KR, Clary BM (2005) Management of hepatic metastases from colorectal cancer. *Clin Colon Rectal Surg* 18:215–223
 44. Zhao S-Y, Sun Y, Lai Z-S, Nan Q-Z, Li K, Zhang Z-S (2009) Inhibition of migration and invasion of colorectal cancer cells via deletion of Rac1 with RNA interference. *Mol Cell Biochem* 322:179–184
 45. Li Q, Qin T, Bi Z, Hong H, Ding L, Chen J et al (2020) Rac1 activates non-oxidative pentose phosphate pathway to induce chemoresistance of breast cancer. *Nat Commun* 11:1456
 46. McAndrew N, DeMichele A (2018) Neoadjuvant chemotherapy considerations in triple-negative breast cancer. *J Target Ther Cancer* 7:52–69
 47. Rosenthal DT, Zhang J, Bao L, Zhu L, Wu Z, Toy K et al (2012) RhoC impacts the metastatic potential and abundance of breast cancer stem cells. Anderson KI, editor. *PLoS One* 7:e40979
 48. Wu M, Wu Z, Rosenthal DT, Rhee EM, Merajver SD (2010) Characterization of the roles of RHOC and RHOA GTPases in invasion, motility, and matrix

- adhesion in inflammatory and aggressive breast cancers. *Cancer* 116:2768–2782
49. Kaushal N, Durmaz YY, Bao L, Merajver SD, ElSayed MEH (2015) “Smart” nanoparticles enhance the cytoplasmic delivery of anti-RhoC silencing RNA and inhibit the migration and invasion of aggressive breast. *Cancer Cells Mol Pharmaceutic* 12:2406–2417
 50. Kaushal N, Tiruchinapally G, Durmaz YY, Bao L, Gilani R, Merajver SD et al (2018) Synergistic inhibition of aggressive breast cancer cell migration and invasion by cytoplasmic delivery of anti-RhoC silencing RNA and presentation of EPPT1 peptide on “smart” particles. *J Control Release* 289:79–93
 51. Brockhausen I, Yang J-M, Burchell J, Whitehouse C, Taylor-Papadimitriou J (1995) Mechanisms underlying aberrant glycosylation of MUC1 mucin in breast cancer cells. *Eur J Biochem* 233:607–617
 52. Hayes J, Peruzzi PP, Lawler S (2014) MicroRNAs in cancer: biomarkers, functions and therapy. *Trends Mol Med* 20:460–469
 53. Shea A, Harish V, Afzal Z, Chijioke J, Kedir H, Dusmatova S et al (2016) MicroRNAs in glioblastoma multiforme pathogenesis and therapeutics. *Cancer Med* 5:1917–1946
 54. Novakova J, Slaby O, Vyzula R, Michalek J (2009) MicroRNA involvement in glioblastoma pathogenesis. *Biochem Biophys Res Commun* 386:1–5
 55. Banelli B, Forlani A, Allemanni G, Morabito A, Pistillo MP, Romani M (2017) MicroRNA in glioblastoma: an overview. *Int J Genomic* 2017:1–16
 56. Szopa W, Burley TA, Kramer-Marek G, Kaspera W (2017) Diagnostic and therapeutic biomarkers in glioblastoma: current status and future perspectives. *Biomed Res Int* 2017:1–13
 57. Liu M, Tang Q, Qiu M, Lang N, Li M, Zheng Y et al (2011) miR-21 targets the tumor suppressor RhoB and regulates proliferation, invasion and apoptosis in colorectal cancer cells. *FEBS Lett* 585:2998–3005
 58. Forget M-A, Desrosiers RR, Del M, Moudjian R, Shedid D, Berthelet F et al (2002) The expression of rho proteins decreases with human brain tumor progression: potential tumor markers. *Clin Exp Metastasis* 19:9–15
 59. Karlsson R, Pedersen ED, Wang Z, Brakebusch C (2009) Rho GTPase function in tumorigenesis. *Biochimica et Biophysica Acta (BBA)*. *Rev Cancer* 1796:91–98
 60. Costa PM, Cardoso AL, Custódia C, Cunha P, Pereira de Almeida L, Pedrosa de Lima MC (2015) MiRNA-21 silencing mediated by tumor-targeted nanoparticles combined with sunitinib: a new multimodal gene therapy approach for glioblastoma. *J Control Release* 207:31–39
 61. Mamelak AN, Jacoby DB (2007) Targeted delivery of antitumoral therapy to glioma and other malignancies with synthetic chlorotoxin (TM-601). *Expert Opin Drug Deliv* 4:175–186
 62. Liu S, Li H, Xia L, Xu P, Ding Y, Huo D et al (2017) Anti-RhoJ antibody functionalized Au@I nanoparticles as CT-guided tumor vessel-targeting radiosensitizers in patient-derived tumor xenograft model. *Biomaterials* 141:1–12
 63. Yuan L, Sacharidou A, Stratman AN, Le Bras A, Zwiers PJ, Spokes K et al (2011) RhoJ is an endothelial cell-restricted Rho GTPase that mediates vascular morphogenesis and is regulated by the transcription factor ERG. *Blood* 118:1145–1153
 64. Shi T-T, Li G, Xiao H-T (2016) The role of RhoJ in endothelial cell biology and tumor pathology. *Biomed Res Int* 2016:1–9
 65. Rivolta I, Panariti, Miserocchi (2012) The effect of nanoparticle uptake on cellular behavior: disrupting or enabling functions? *NSA* 87
 66. Shen Y, Leng M, Yu H, Zhang Q, Luo X, Gregersen H et al (2015) Effect of amphiphilic PCL-PEG nanomicelles on HepG2 cell migration: amphiphilic PCL-PEG regulates cell migration. *Macromol Biosci* 15:372–384
 67. Li C-H, Liao P-L, Shyu M-K, Liu C-W, Kao C-C, Huang S-H et al (2012) Zinc oxide nanoparticles-induced intercellular adhesion molecule 1 expression requires Rac1/Cdc42, mixed lineage kinase 3, and c-Jun N-terminal kinase activation in endothelial cells. *Toxicol Sci* 126:162–172
 68. Hong F, Zhou Y, Ji J, Zhuang J, Sheng L, Wang L (2018) Nano-TiO₂ inhibits development of the central nervous system and its mechanism in offspring mice. *J Agric Food Chem* 66:11767–11774
 69. Gačanin J, Kovtun A, Fischer S, Schwager V, Quambusch J, Kuan SL et al (2017) Spatiotemporally controlled release of rho-inhibiting C3 toxin from a protein-DNA hybrid hydrogel for targeted inhibition of osteoclast formation and activity. *Adv Healthc Mater* 6:1700392
 70. He X, Yuan C, Yang J (2015) Regulation and functional significance of CDC42 alternative splicing in ovarian cancer. *Oncotarget* 6:29651–29663
 71. Matos P, Oliveira C, Velho S, Gonçalves V, da Costa LT, Moyer MP et al (2008) B-Raf(V600E) cooperates with alternative spliced Rac1b to sustain colorectal cancer cell survival. *Gastroenterology* 135:899–906
 72. Schnelzer A, Prectel D, Knaus U, Dehne K, Gerhard M, Graeff H et al (2000) Rac1 in human breast cancer: overexpression, mutation analysis, and characterization of a new isoform, Rac1b. *Oncogene* 19:3013–3020
 73. Liu J, Lee W, Jiang Z, Chen Z, Jhunjunhwal S, Haverty PM et al (2012) Genome and transcriptome sequencing of lung cancers reveal diverse mutational and splicing events. *Genome Res* 22:2315–2327
 74. Faria M, Félix D, Domingues R, Bugalho MJ, Matos P, Silva AL (2019) Antagonistic effects of RAC1 and tumor-related RAC1b on NIS expression in thyroid. *J Mol Endocrinol* 63:309–320
 75. Matos P, Collard JG, Jordan P (2003) Tumor-related alternatively spliced Rac1b is not regulated by Rho-GDP dissociation inhibitors and exhibits selective downstream signaling. *J Biol Chem* 278:50442–50448

76. Singh NN, Luo D, Singh RN (1828) Pre-mRNA splicing modulation by antisense oligonucleotides. *Methods Mol Biol* 2018:415–437
77. Bowerman M, Becker CG, Yáñez-Muñoz RJ, Ning K, Wood MJA, Gillingwater TH et al (2017) Therapeutic strategies for spinal muscular atrophy: SMN and beyond. *Dis Model Mech* 10:943–954
78. Chiriboga CA (2017) Nusinersen for the treatment of spinal muscular atrophy. *Expert Rev Neurother* 17:955–962
79. Shabanpoor F, Hammond SM, Abendroth F, Hazell G, Wood MJA, Gait MJ (2017) Identification of a peptide for systemic brain delivery of a morpholino oligonucleotide in mouse models of spinal muscular atrophy. *Nucleic Acid Therapeutic* 27:130–143
80. Hurd CA, Mott HR, Owen D (2020) Therapeutic peptides targeting the Ras superfamily. *Peptide Sci*:e24165
81. Sakamoto K, Adachi Y, Komoike Y, Kamada Y, Koyama R, Fukuda Y et al (2017) Novel DOCK2-selective inhibitory peptide that suppresses B-cell line migration. *Biochem Biophys Res Commun* 483:183–190
82. Nur-E-Kamal MSA, Kamal JM, Qureshi MM, Maruta H (1999) The CDC42-specific inhibitor derived from ACK-1 blocks v-Ha-Ras-induced transformation. *Oncogene* 18:7787–7793
83. Tetley GJN, Murphy NP, Bonetto S, Ivanova-Berndt G, Revell J, Mott HR et al (2020) The discovery and maturation of peptide biologics targeting the small G-protein Cdc42: a bioblockade for Ras-driven signaling. *J Biol Chem* 295:2866–2884
84. Haggag YA (2018) Peptides as drug candidates: limitations and recent development perspectives. *BJSTR* 8:6659–6662. <https://doi.org/10.26717/BJSTR.2018.08.001694>
85. Attarilar S, Yang J, Ebrahimi M, Wang Q, Liu J, Tang Y et al (2020) The toxicity phenomenon and the related occurrence in metal and metal oxide nanoparticles: a brief review from the biomedical perspective. *Front Bioeng Biotechnol* 8:822



Nanocelluloses: Production, Characterization and Market

6

Paulo J. T. Ferreira and Ana F. Lourenço

Abstract

Nanocelluloses are a very promising material that has been widely explored for the most diverse applications. The pursuit for sustainable and environmentally friendly materials is in line with the nature of nanocelluloses and therefore they have emerged as the perfect candidate for plastics substitution, food additive, rheology controller, 3D printing of diverse structures, among many other possibilities. This derives from their interesting characteristics, such as reduced size and high specific surface area, high tensile strength, crystallinity and transparency, and from the fact that, such as cellulose, they are obtained from renewable sources, with relative ease for functionalization in order to obtain desired specificities. Thus, the industry is trying to react and effectively respond to the exponential growth of published research in the last years, and therefore new facilities (not only lab and pilot plants but already industrial sites) have been producing nanocelluloses. This new fibrous materials can be obtained from different raw-materials by dif-

ferent methodologies, leading to different types of nanocelluloses with, obviously, different characteristics. Nonetheless, technical and economical constraints have been addressed, such as the high energy demand or the clogging of homogenizers/microfluidizers.

This chapter intends to present a review addressing the main features related to the production, characterization and market of nanocelluloses and providing additional information regarding the vast literature published in these domains.

Keywords

Nanocelluloses · Production · Characterization · Market

6.1 Introduction

Nanocelluloses are defined as cellulosic materials with, at least, one dimension at the nanometer scale [1, 41, 66, 112, 138]. The interest in this material has increased exponentially due to its peculiar characteristics like high aspect ratio (AR), specific surface area (SSA), mechanical strength, low coefficient of thermal expansion and good optical properties [1, 16, 41, 112].

The number of publications regarding the production, characterization and/or utilization of

P. J. T. Ferreira (✉)
University of Coimbra, CIEPQPF, Department of
Chemical Engineering, PT, Coimbra, Portugal
e-mail: paulo@eq.uc.pt

A. F. Lourenço
RAIZ – Forest and Paper Research Institute,
Quinta de S. Francisco, Apartado 15, PT, Portugal

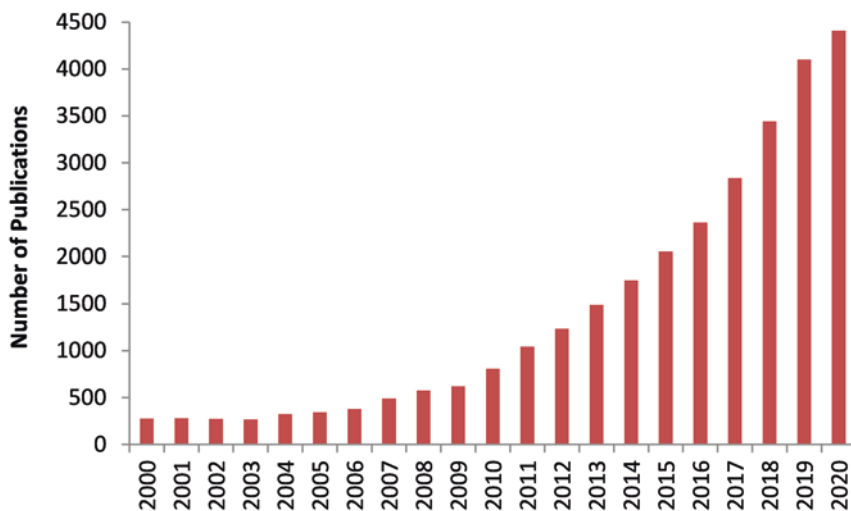


Fig. 6.1 Publications including journal articles and patents about the theme nanocellulose, using the Web of Science database

nanocelluloses has increased exponentially (Fig. 6.1¹).

In the last years several terms have arisen for the classification of nanocelluloses. According to ISO standard TS 20477 [65] and standard proposal TAPPI WI 3021 [141], terms like cellulose nanofibrils (CNF), cellulose microfibrils (CMF), cellulose nanocrystals (CNC), cellulose microcrystals and bacterial nanocellulose (BNC) can be found, depending on the production process (raw material used and process conditions) and on the final dimensions. The process of production may be top-down, in which the nanocelluloses are obtained through fibrillation of lignocellulosic biomass, such as wood (types CNF, CMF, CNC) or bottom-up, in which they are created from glucose monomer units, using for example cellulose-producing bacteria (type BNC). Figure 6.2 presents the hierarchical structure of cellulose and the isolation of the cellulose nanomaterials from wood (top-down method).

¹The following keywords were used for the search in the Web of Science database: “nanocellulose” OR “cellul*” NEAR/1 (“microfib*” OR “nanofib*” OR “bact*” OR “microb*” OR “nanocryst*” OR “microcryst*” OR “whisk*”).

6.2 Nanocelluloses – Sources and Types

6.2.1 Cellulose Nanofibrils (CNF) and Cellulose Microfibrils (CMF)

Cellulose nanofibrils (also called nanofibrillar cellulose or cellulose nanofibers) and microfibrils (or cellulose microfibrils) are a type of nanocellulose that possesses amorphous and crystalline parts (Fig. 6.2). With aspect ratio usually greater than 10, their lengths are found to be up to 100 μm and, in the case of CNF, the width is usually 3–100 nm. CMF have a size distribution with not only cellulose fibrils at the nanoscale but also a significant amount of fibrils with non-nanometric dimensions, being sometimes difficult to distinguish between CNF and CMF. The dimensions referred to above are specified in ISO standard TS 20477 [65]. Nonetheless, it must be taken into account that many other dimensions can be found in the literature: e.g. distinction between CNF and CMF by the cross sections of 3–20 nm and 10–30 nm, respectively [36] or even more specific, distinguishing also the length between CNF (diameter 2–10 nm, length > 10 μm , aspect-

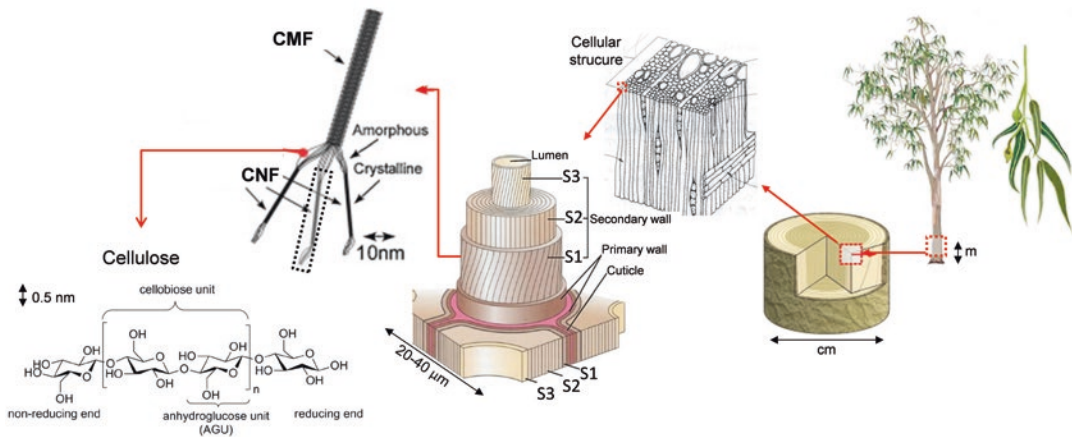


Fig. 6.2 Schematic illustration of the hierarchical structure of cellulose and of the isolation of cellulose nanomaterials from wood

ratio > 1000) and CMF (diameter 10–100 nm, length 0.5–10 μm , aspect-ratio 50–100) [132]. Cellulose filaments (CF) can be considered as a variant of CMF with a greater aspect ratio than the latter, i.e., 1000 or more, with diameter of 80 to 300 nm and length of 100 to 2000 μm [77].

CNF consist in a bundle of stretched cellulose molecules chains, very flexible and long, and thus tend to become entangled, which is one of the reasons why they are so valued as they are good for strength, reinforcement, and rheology modification [1, 66, 74]. The typical sources for their production are wood, hemp, flax, sugar beet, potato tuber, among others (Table 6.1).

In recent years, considerable research has arisen on lignocellulosic nanofibers (LCNF), in order to value residual biomass, reduce raw material costs and environmental impact [40]. The raw materials studied by various authors include residues of the primary industrialization of wood and straw wastes [39, 43, 122, 143, 144]. Some authors have even drawn attention to the best production performance of LCNF when compared to CNF [60, 131].

6.2.2 Cellulose Nanocrystals (CNC) and Cellulose Microcrystals

CNC (also known as nanowhiskers or nanorods) have an elongated rod-like shape and are highly

crystalline, presenting low flexibility and an aspect ratio smaller than that of CNF (CNC AR = 5–50, according to ISO standard TS 20477 [65]), usually with diameters of 3–50 nm and lengths as low as 100 nm. In its turn, cellulose microcrystals (also known as microcrystalline cellulose) contain 90% of the material with diameters superior to 5 nm and aspect ratio higher than 2. They exhibit a high degree of crystallinity (50–90%) [18, 166] with limited flexibility compared to CNFs. The degree of crystallinity and their morphology depend on the cellulosic material used for their production (usually wood, cotton, wheat and rice straw, tunicin, bacteria and algae), as well as on the preparation conditions and on the techniques used. Besides being good for strength, reinforcement and rheology modification, CNC are also good for the enhancement of optical, electrical, and chemical properties.

6.2.3 Bacterial Nanocellulose (BNC)

Finally, BNC (also called biocellulose or microbial cellulose) are produced from the glucose units of a genus of bacteria: *Gluconacetobacter* [1, 41, 54]. The bacteria are cultivated in common aqueous nutrient media and the BNC are excreted to the air resulting in a highly swollen network (diameters between 10 and 40 nm) with a distinct tunnel and pore structure [73]. This

Table 6.1 Types of nanocelluloses and their sources and representative references and dimensions

Type	Sources	References	dimension ^a
Cellulose nano and microfibrils (CNF/CMF)	Wood, hemp, flax, sugar beet, potato tuber, wheat straw, bagasse	CNF: [17, 120, 167] CMF: [19, 34, 37, 38, 105, 156]	Diameter: 3–100 nm AR: >10
Cellulose nano and microcrystals (CNC)	Wood, cotton, tunicin	[90, 84, 97]	Diameter: 3–50 nm AR: >5
Bacterial nanocellulose (BNC)	Low-molecular weight sugars and alcohols	[83, 111]	Diameter: 10–40 nm AR: 100–150

^athe dimensions are based on ISO standard TS 20477 [65] (except for BNC). AR = length/diameter

type of nanocellulose possesses high molecular weight, crystallinity and good mechanical stability. Besides, it is free of lignin, hemicellulose and pectin, being a source of very pure cellulose ($\geq 98\%$) [131].

6.3 Production

For ease of understanding, the available state of the art on the nanocellulose production will be divided into the top-down and bottom-up methodologies. A recent report produced by TAPPI (Technical Association of the Pulp and Paper Industry), summarized the state of the industry regarding the production of cellulose nanomaterials, and the numbers revealed that a) nanocelluloses are produced not only in laboratory and pilot facilities, but already at industrial scale and that b) CMF is produced in greater quantities when compared to CNF and CNC [93]. These nanomaterials are being produced worldwide, and therefore a topic related to their commercialization will be addressed in sect. 4.

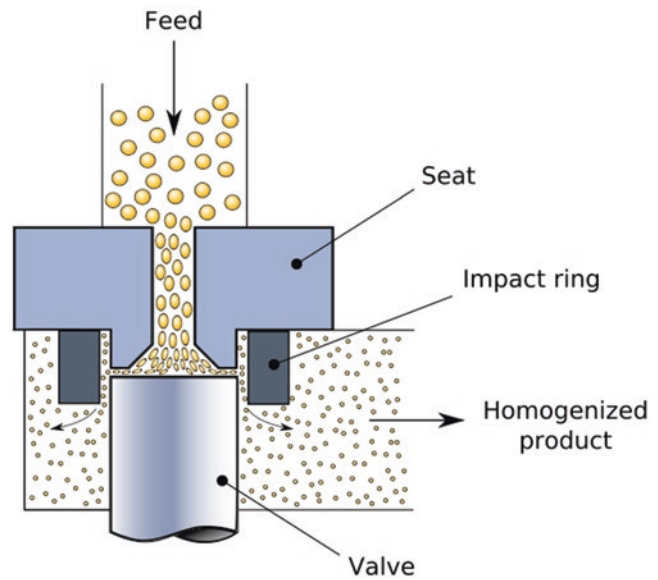
6.3.1 Mechanical Treatments

CNF and CMF can be produced by mechanical, chemical or enzymatic treatments or by a combination of the aforementioned. The defibrillation of the fibers involves an intensive mechanical treatment and for that refining, homogenization, microfluidization, high inten-

sity ultrasonication, milling or cryocrushing can be used. The most common mechanical treatments used to produce CNF are refining and high pressure homogenization (HPH), being commonly used together. In the first, the fibres are forced through a gap between two surfaces fitted (one or both) with bars and grooves, which damages the microfibril structure promoting external fibrillation by gradually peeling off the external cell wall layers (primary and secondary S1) and exposing the secondary S2 layer (Fig. 6.2). In this way, the fibers are ready for treatment in the homogenizer in which the fiber suspension is submitted to high pressures in order to pass through a small nozzle at high velocity so that the impact and shear rates suffered by the suspension result in the reduction of the fibers size to the nanoscale (Fig. 6.3). This process, although very efficient and simple, presents some drawbacks, namely the frequent obstruction of the small nozzle and the high energy consumption [1]. The microfluidization process is very similar to the HPH: the fiber undergoes high-pressure treatments as the slurry is accelerated and sent out of the equipment, passing through a chamber with a Z-shape structure that promotes an intense collision between particles so that the high impact splits the fibers into fibrils. In this equipment, the smaller the Z-shape constriction, the higher is the pressure and therefore the higher the fibrillation degree [104].

In the high intensity ultrasonication (HIU) the fibrils are isolated by ultrasound hydrodynamic forces created by a powerful mechanical

Fig. 6.3 Scheme of the valve of a high-pressure homogenizer (reproduced entirely from Wikimedia https://commons.wikimedia.org/wiki/File:Homogenizing_valve.svg)



oscillation that promotes intense waves [155]. According to Wang and Cheng [155] several factors (temperature, power, time) may affect the efficiency of fibrillation and a mixture of micro and nanofibrillar material is obtained and therefore the authors claimed that by combining HIU and HPH a more uniform fibrillar suspension is obtained. The grinding treatment is based on a static and a rotating grind stones system generating shear forces that individualize the nanofibers from the pulp wall structure. However, in this process, the pulp fibers can become highly degraded which may affect their reinforcing potential [129, 158]. Both in HPH and grinding, it is common to repeat the process several times, by increasing the number of cycles, in order to increase the degree of fibrillation. Another alternative to produce nanocellulose is cryocrushing. In this method the water swollen cellulosic fibers are immersed in liquid nitrogen and submitted to high shear forces, which leads to the rupture of the cell wall by the pressure exerted by the ice crystals. The grinding and cryocrushing processes are usually accompanied by high pressure treatments [56, 68, 156].

As expected, the average particle size decreases with increasing energy consumption

[42]. This is most important when considering the potential of nanocelluloses to be used at an industrial scale. Despite the many efforts to reduce the energy consumption while producing nanocelluloses with controlled sizes, it is legitimate to say that the process is still not economically feasible for smaller added-value applications, such as paper and paperboard products [104]. In fact, large amounts of energy were reported with values exceeding 30.000 kW h/t [85].

6.3.2 Chemical and Enzymatic Treatments

Since the aforementioned treatments are not 100% efficient in producing nanofibrils and the energy costs necessary to perform them are high, it has become usual to pre-treat the fibers, before the mechanical step. In fact, it is stated that, for cellulosic fibers, the pre-treatment helps reducing the energy consumption by 91–98% [11, 129].

The pre-treatments can be of enzymatic or chemical nature. In the first, the enzyme is used to modify or degrade the lignin and the hemicellulose, besides helping to hydrolyze cellulosic

fiber specific components [1, 59]. The most conventional enzyme applied for the modification of pulp fibers in order to produce CNF is endo-1,4- β -D-glucanase, which requires some disordered structure in cellulose to disrupt it [1]. Pääkko et al. [105] and Henriksson et al. [58] applied a mild enzymatic hydrolysis (using endoglucanase) combined with refining and passes in a HPH to produce a CMF gel with diameters in the nanometer range and high aspect ratio. In these studies they also compared the enzymatic treatment with a chemical one (acid hydrolysis), concluding that the CMF produced by the former method possessed a more favorable structure with a more homogeneous distribution of nanofiber geometries and higher aspect ratio than the CMF produced by the latter method. The enzymatic hydrolysis is already being studied as a cost-effective approach to produce CMF to be used as a paper reinforcement: in a quite recent article Tarrés et al. [142] concluded that the pulp consistency, pH of the suspension, the treatment time and enzyme dosage have a key role during the production of CMF with high specific surface. In this article the authors used an enzyme cocktail which contains endo- β -1,4-glucanases but the same authors also produced CNF with a commercial enzyme obtained from genetically modified *Trichoderma reesei* [55]. Since cellulosic fibers contain different organic compounds it is usual to apply a cocktail of cellulase enzymes in order to disrupt the fibers, which is hardly done by a single enzyme [113].

Another approach for the nanocellulose production is by chemical treatment. The most commonly used process for the extraction of CNCs from native cellulose is based on a strong acid hydrolysis under strictly controlled conditions of temperature, agitation, and time. Hydrochloric and sulfuric acid have been mostly used in the extraction process [115, 161]. An acidic attack dissolves the amorphous portions of cellulose, resulting in the formation of a nanocrystal structure [72]. During this process, negatively charged sulfate groups are introduced on the cellulose chain, leading to intermolecular repulsive forces that confer electrostatic stability to CNCs in polar aqueous suspensions [30, 90, 115].

For the cellulose nanofibrils production there are several possibilities, such as the use of ionic liquids to dissolve cellulose or the introduction of carboxyl groups on the fibers to facilitate the fiber wall delamination. Li et al. [80] pretreated sugarcane bagasse with an ionic liquid in order to dissolve the cellulose and stated that this facilitated the mechanical treatment in a HPH. Besides, other chemical pre-treatments such as acetylation, silylation, or treatments with isocyanate have been used to generate CNF hydrophobic surfaces in order to reduce the agglomeration of these materials. Nonetheless the most effective and used pre-treatments are based on the modification of the fibers in order to introduce ionic groups. One approach that fits this purpose is carboxymethylation that negatively charges the cellulosic fibers surface and increases the breakup of lignocellulosic fibers to nanosize by adding carboxymethyl groups to the cellulose chains of the fibers. The most cited author regarding this pre-treatment is J. A. Walecka [153] and his work is based on the etherification of the cellulose hydroxyl groups with monochloroacetic acid (MCA) in its sodium salt form, in the presence of sodium hydroxide (Fig. 6.4). Wagberg et al. [152] used this method followed by HPH to produce carboxymethylated CNF with cross section diameters of 5–15 nm. In this study it was shown that very high concentrations of the salt or too low pH would cause agglomeration of the fibers. The same authors studied the accessibility of polyelectrolytes to carboxymethylated cellulose microfibrils and found that high molecular weight polyelectrolytes were accessible to all carboxyl groups [151], which can be very important when considering the additives used in papermaking. Carboxymethylated CNF are known to increase the water retention value [22], reducing hornification during drying [44], and to limit aggregation of particles [130].

Another common approach is oxidation. The most reliable method is based on the use of TEMPO (2,2,6,6-Tetramethylpiperidine-1-oxyl) to mediate the oxidation, in which carboxylic groups are introduced at the C6 position of the glucose unit [66, 117–120]. Figure 6.5 shows the scheme of the oxidation in which the primary

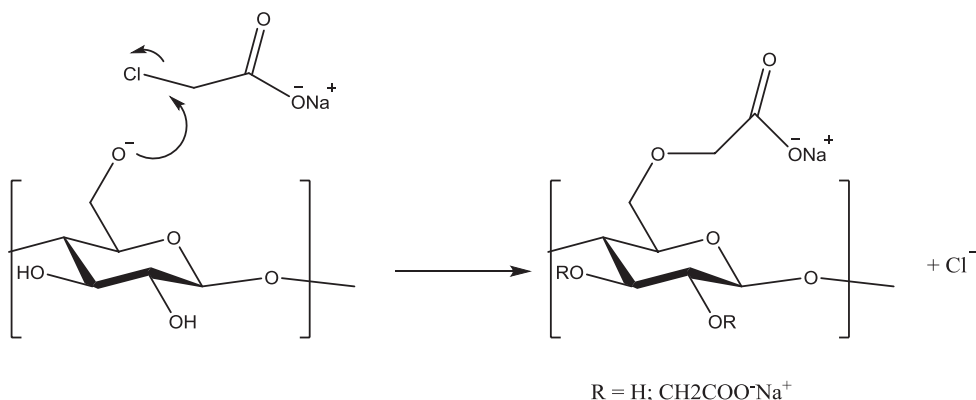


Fig. 6.4 Carboxymethylation reaction with sodium monochloroacetate. R depends on the progress of the reaction [88]

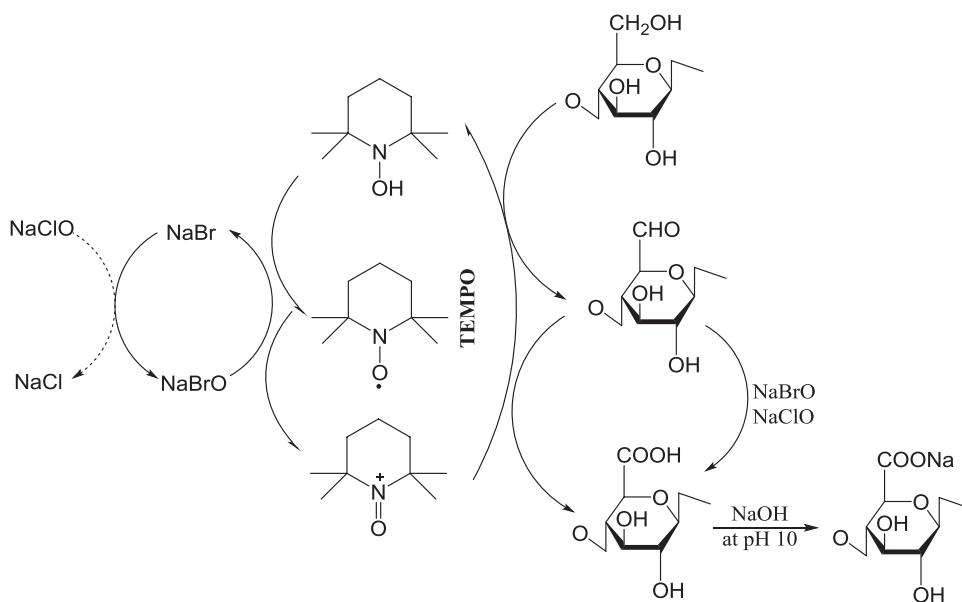


Fig. 6.5 Scheme of TEMPO-mediated oxidation of cellulose

oxidant (NaClO) is added to a cellulose suspension in the presence of catalytic amounts of TEMPO and NaBr at pH 9–11. In this reaction, the C6 primary hydroxyl groups of cellulose are converted to carboxylic groups via C6 aldehyde groups, at the expense of NaClO and NaOH consumption as the oxidation proceeds [118].

Some side reactions can occur in this reaction under alkaline conditions, such as the depolymerization or discoloration of the oxidized cellulose due to the presence of residual aldehyde groups and therefore some authors applied a different system consisting of TEMPO/NaClO/NaClO₂

under neutral or slightly acidic conditions [121, 140, 163]. Several studies have proven that, by pre-treating the cellulosic fibers with TEMPO, it is possible to reduce the number of passes in the homogenizer required to produce CNF [16, 17, 31]. Other oxidation pre-treatment commonly used is periodate-chlorite oxidation since it improves the fibrillation efficiency of CNF. In this pre-treatment a sequential oxidation of the cellulose fibers with periodate and chlorite occurs, in which firstly the vicinal hydroxyl groups of cellulose at C2 and C3 positions are oxidized to the corresponding aldehyde groups,

and then these aldehyde groups are further oxidized to carboxyl. Liimatainen et al. [82] stated that, by using this pre-treatment, oxidized celluloses with carboxyl contents ranging from 0.38 to 1.75 mmol/g could nanofibrillate to highly viscous and transparent gels with yields of 85–100% without clogging the homogenizer.

6.3.3 Biosynthesis of Bacterial Cellulose

As stated, bacterial nanocellulose is manufactured by a bottom-up method, contrary to the processes aforementioned. The most studied species of bacteria for production of cellulose is *Glunoacetobacter xylinus*. These bacteria produce an extracellular, chemically pure-glucan, supporting their survival in the natural environment since the cells are kept at the surface of culture media, being entrapped inside gelatinous, skin-like membranes, consisting of entangled cellulose fibers [50]. The advantage of bacterial derived cellulose microfibrils is that it is possible to adjust culturing conditions to alter the microfibril formation and crystallization [96].

The *G. xylinus* species are usually cultivated at 30 °C for 7–14 days in a Hestrin-Schramm medium (composed of a carbon source, enriched nitrogen source and a small amount of citric acid) with pH adjusted to 5.7. Several authors have modified the composition of this medium in order to optimize BNC production [95, 159, 164]. Besides, and according to Gama et al. [50], there is the need to optimize separately the conditions of cellulose biosynthesis from diverse carbon sources for each BNC producer. In most cases glucose, glycerol, sucrose, and mannitol were found to be the most suitable carbon sources for cellulose production (here mentioned in the order from the most to the least efficient source).

The culture can be performed under static or agitated conditions. In the static culture, the microbiological medium is placed in shallow trays and inoculated with bacteria, being therefore a more expensive method and characterized by low productivity [50, 95]. As for the agitated culture, a higher power supply is needed, but it

has the main advantage of high cell concentration and productivity [168].

Since several authors have considered that the industrial scale production of BNC is still not efficient or cost effective in static cultures, some research has been carried out to produce BNC in a large scale at a low cost by using culture medium composed of agroindustrial sources or wastes [10].

6.4 Properties and Characterization

The production methods abovementioned usually generate an aqueous suspension/dispersion with low amounts of solids (CNC 1–2 wt% and CMF 0.5–3 wt%). Besides, the pre-treatments including functionalization of the cellulose structure can also give rise to a gel (Fig. 6.6), which is stable and transparent, also at very low solids concentration (such as 1–2 wt% for oxidized CNF) [45]. For their characterization, but mainly for their commercialization, there may be the need to dry them, and therefore nanocelluloses can be manipulated as a film, an aerogel or a foam. The mechanisms for drying will be discussed in Sect. 3.7.

As stated, nanocelluloses have many unique properties that make them attractive for several applications. According to a previous review, the main points that should be addressed are the amount of produced nanomaterial, the rheology of the dispersion, the average particle size and size distribution, crystallinity, specific surface area, surface chemistry, and mechanical properties [71]. Obviously, taking into account the foreseen applications, some properties can have more importance than others. An accurate, consistent and reliable characterization of the nanocelluloses is essential, not only for their application, but also to evaluate the interaction with the local environment, which is fundamental for their commercialization. With this regard, mention is due to the following publications: i) the review article by Foster et al. [45] which establishes the details of the best practices, methods and techniques for characterizing CNC and CNF and ii)

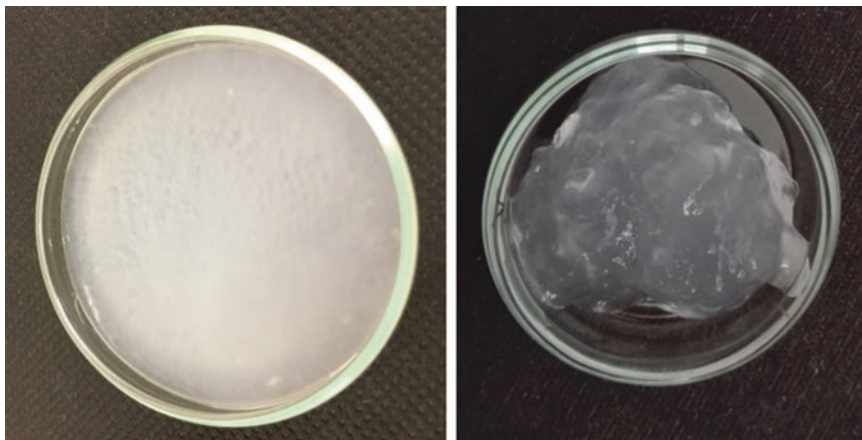


Fig. 6.6 Examples of a CMF suspension (left) and a CNF gel (right), both at *ca.* 1 wt% solids

the ISO standard TS 21346 [64] that defines the characterization techniques to be used in elementary fibrils, or individualized cellulose nanofibrils.

In the present text the state of the art of the nanocelluloses characterization is divided by the properties considered as more important and will be focused mainly in CNF, CMF and BNC. Other types of nanocelluloses or even other methods for their production will remain out of scope.

6.4.1 Amount of Nanomaterial

As stated in sect. 1, there are several types of nanocelluloses with different characteristics and the amount of nanomaterial is an important property to be determined since the samples are not usually entirely composed of nano-sized material. The most common technique used for the estimation of this property is ultracentrifugation. By this method the nanofibrils are separated from the large size particles that remain concentrated at the bottom of the sample holder and, by weight difference, the nano-sized material content is determined. The centrifugation conditions to be used are much dependent on the type of sample and on the degree of fibrillation: Ahola et al. [4] applied 10,400 rpm to nanocellulose dispersions for 2 h while Taipale et al. [138] used only 45 min with the same speed and Gamelas et al. [51] used only 9000 rpm for 30 min (*ca.* 9000 g) since the

nanofibers were more fibrillated. ISO standard TS 21346 [64] states that the suspensions should be at 0.1% consistency and the centrifugal separation performed at more than 12,000 g for longer than 20 min.

6.4.2 Morphology and Fibril Dimensions

The assessment of the fibrils appearance, morphology, shape and size has been performed using different techniques, being the most common those based in microscopy, although some indirect methods, such as turbidimetry or light scattering, are becoming common [45].

Among the microscopic methods, it is usual to start by performing optical microscopy (OM) to get an overview of the sample and of its homogeneity. After, higher resolutions are needed in order to analyze the fibrils details and for that field emission scanning electron microscopy (FE-SEM), transmission electron microscopy (TEM) and atomic force microscopy (AFM) are used. These techniques have the advantage of allowing the visualization of the nanocelluloses and, when combined with image analysis, measuring their dimensions [4, 24, 27, 59]. However, typically, the size distribution is limited to the width distribution since the aspect-ratio is too high to obtain the length-distribution values. Figure 6.7 shows an example of FE-SEM and

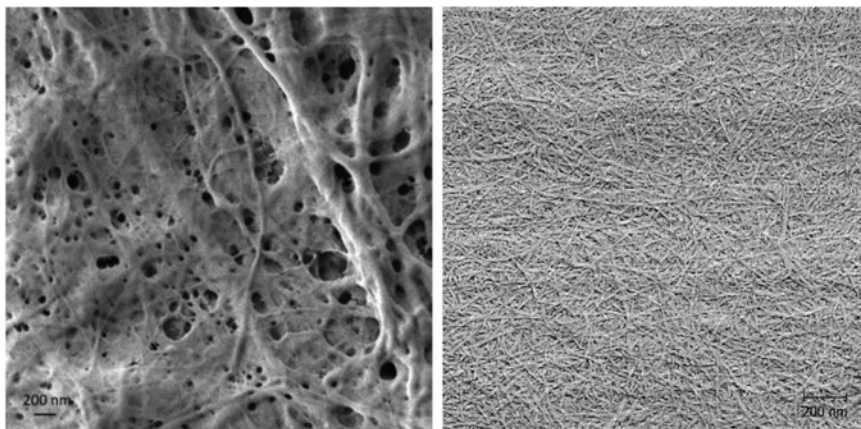


Fig. 6.7 FE-SEM image of a mechanically-produced CMF (left) and AFM image of TEMPO-oxidized nanocellulose from wood (right) [87]

AFM images taken on nanocelluloses. Nonetheless, it is worth mention that these techniques may require a careful preparation of the samples (particularly TEM) and are laborious, time consuming and very user-dependent. Besides, the observation field is limited and therefore the results are not always representative of the entire sample. The shape of the nanofibers may appear different depending on the method used: e.g., when using AFM, tip-broadening effects make it difficult to understand if the morphology observed is due to individual particles or to agglomerates. Therefore, the techniques mentioned provide different but complementary information about the morphology and dimensions of the nanocellulose fibrils and, in order to obtain a good and accurate analysis, one must use a combination of the microscopic methods [24].

Indirect measurements such as turbidimetry have also been used. For suspensions of TEMPO-oxidized CNF, the visible spectra in the transmittance mode evidenced higher transmittance for more fibrillated samples, corresponding to a clearer suspension with higher amount of nano-sized material [51, 119]. On the other hand, techniques based on light scattering and diffraction, such as dynamic light scattering (DLS) or laser diffraction spectrometry (LDS), can overcome some of the drawbacks mentioned for the microscopy-based techniques [97, 112]. However, the particles should be spherical, and

since cellulose nanofibrils are a fibrillar-like material with high aspect ratio, the values obtained from DLS cannot be directly linked to the particle length or cross-section dimensions and cannot be directly correlated with particle size distributions. It should therefore be taken as a hydrodynamic “apparent particle size” that can be used as an internally consistent method to assess the dispersion quality or state of aggregation. Notwithstanding, it was reported for cellulose nanocrystals that the equivalent hydrodynamic radius, measured by DLS, did not differ much from the theoretical hydrodynamic radius, calculated for cylinder-shaped particles based on the dimensions of length and width assessed by FE-SEM [46, 51]. Thus, microscopy and light scattering methods are considered complementary. In fact, Gamelas et al. [51] analyzed different CNF obtained by NaClO/NaBr/TEMPO pre-oxidation and mechanical treatment and calculated the nanofibrils length based on the width measured by AFM and the hydrodynamic diameter assessed by DLS.

6.4.3 Physical Properties

Some important physical properties to consider when characterizing nanocelluloses are the crystallinity, specific surface area (SSA) and the degree of polymerization (DP). The crystallinity can be

determined by X-ray diffraction (XRD), Raman spectroscopy, infrared spectroscopy (FT-IR) and ^{13}C nuclear magnetic resonance (NMR) but it strongly depends on the source and processes used to produce the nanocelluloses. Alemdar and Sain [6] determined by XRD the crystallinity of wheat straw and of soy hull nanofibers produced by a chemical-mechanical technique and concluded that an increase of the crystallinity of 35% and of 16%, respectively, occurred because the treatment removed non-cellulosic components such as lignin and hemicelluloses. The same conclusions were stated by Jonoobi et al. [70] with nanofibers extracted from kenaf core. However, it is difficult to compare results from the literature since they depend on the calculation methods used to obtain the values (peak height/intensity, peak area/deconvolution, amorphous subtraction) [71].

Regarding the specific surface area determination, different methods have been used. One of the most common is the Brunauer–Emmett–Teller (BET) method by N_2 adsorption for nanopapers or freeze-dried nanocelluloses. The drawback of this technique is the sample preparation (drying) that highly affects the surface area due to aggregation. According to Sehaqui et al. [125], after direct water evaporation, the specific surface area can be as low as $10^{-2} \text{ m}^2\text{g}^{-1}$ corresponding to a nanopaper with *ca.* 20% porosity. However, if a water exchange to methanol or acetone prior to drying is performed, the porosity increases to 28% and 40%, respectively [59]. Sehaqui et al. [125] produced a CNF nanopaper by supercritical CO_2 drying with exceptionally high specific surface area (up to $480 \text{ m}^2 \text{ g}^{-1}$). Other method often used to determine the specific surface area is the Congo red adsorption. Spence et al. [132] determined the specific surface area of freeze-dried bleached and unbleached fibers/microfibrils and concluded that the unbleached samples adsorbed about 1.8 times more Congo red per unit of BET surface area than the bleached samples since, contrary to the BET method, the Congo red adsorption method is considered to depend on the chemical composition of the fibers. Specifically, there is more rapid adsorption of the dye to hydrophobic lignin than to hydrophilic cellulose.

The degree of polymerization has been reported to strongly depend on the aspect ratio of the nanofibers [79]. Shinoda et al. [126] found a linear relation between DP and length of TEMPO-oxidized CNF. It is common to apply the ISO standard 5351 [63] that calculates the average DP by applying the Staudinger–Mark–Houwink equation through the determination of the limiting viscosity number with a solution of cupriethylenediamine (CED) [59, 167]. When considering TEMPO-oxidized CNF, Shinoda et al. [126] stated that only CED could completely dissolve this type of nanofibrils consisting of both partially oxidized and unoxidized cellulose molecules. According to Zimmerman et al. [167], the production of CMF from softwood sulfite pulp led to a decrease in viscosities/DPs between 15% and 63%. The authors also referred that the strength properties of films or composites containing CMF decreased with the decrease of the DP which makes it a valuable tool for evaluation of the CMF performance.

6.4.4 Chemical Properties

Concerning the chemical properties of nanocelluloses, perhaps the most important issue to consider is their surface chemistry. As stated, nanocelluloses can be modified by different methods which, in consequence, will inevitably modify their surface chemistry. In this matter, it is usual to measure the surface charge, for example by the identification of the functional groups present at the surface. Stenstad et al. [135] and Taipale et al. [138] analyzed the charge of CMF samples by zeta potential measurements. In the first study, the authors produced CMF by homogenization and modified its surface with different chemicals, changing the surface charge from negative to positive, while in the second study, CMF produced by carboxymethylation revealed to possess twice the surface charge than CMF produced by only mechanical treatments. Gamelas et al. [51, 52] also determined the zeta potential of TEMPO-oxidized CNF by measuring the electrophoretic mobility concluding that this treatment leads to strongly negatively

charged fibers, in accordance with other authors [15, 97, 165]. The production of CMF from the same source, but with enzymatic treatments, did not alter the charge of the initial fibers [89].

To determine the content of functional groups at the surface of nanofibers it is common to use titrimetric methods. For CNF produced by TEMPO-mediated oxidation several authors determined the content of aldehyde and carboxylic groups using conductometric titrations [12, 87, 117]. For instance, Saito and Isogai [117] determined carboxyl and aldehyde contents of 0.67 and 0.21 mmol/g, respectively, for nanocellulose produced from cotton linter. Other related methods such as potentiometric or polyelectrolyte titrations can be used. Syverud et al. [137] used both the conductometric and potentiometric titrations and obtained similar results for the carboxyl's content of TEMPO-oxidized cellulose (0.52 and 0.51 mmol/g, respectively).

Characterization techniques such as FT-IR to determine the oxidation level during the TEMPO-mediated oxidation (through the measurement of the intensity of the band at 1738 cm^{-1} due to the carbonyl stretching [119]), or X-ray photoelectron spectroscopy (XPS) to determine the surface chemical composition regarding the surface modification of nanofibers are also usually applied to nanocellulose.

6.4.5 Rheology

As abovementioned, nanocelluloses can form a gel even at very low concentrations in water – usually 1 to 5%, but for values as low as 0.125% a gel can also be found [105]. This is one of the reasons why they are a suitable material for diverse applications. CNF suspensions also appear as a rheology modifier to be applied in cosmetics, paints, food, as mineral suspending agent, among other applications [9]. Therefore, it becomes essential to assess the rheological behavior of this gel, e.g., for paper surface treatments in which the dosage and coating must be well controlled. Several authors have studied the rheological behavior of nanocelluloses. Hubbe et al. [62] dedicated a 100 pages review article to

the subject, containing issues such as flow, fluid layers, entanglement of cellulose fibrils and effect of pH or salt addition, among others.

Most publications evidence their pseudoplastic behavior [16, 78, 99, 105], meaning that the increase of the shear stress or of the shear strain leads to a decrease of the viscosity. However, these authors also claim that this behavior is noticed above the critical concentration – e.g., for Lasseguette et al. [78] this value is of 0.23% – while below this the behavior can be similar to that of a Newtonian fluid. According to Kangas et al. [71] this is due to the fact that, at this concentration, the fibrils form a strong entangled network. Also, the gel point – the lowest fibrous volume at which all the flocs are interconnected forming a self-supporting network [81] – is claimed to be reduced with the addition of cationic polymers [147]. This is related to the compressive yield stress of the flocs, which is affected by the strength of the interparticle bridging forces. In papermaking, it is important that the nanocellulose sample possesses a low gel point in order to improve drainage [81]. Alves et al. [9] also studied the fibrils aggregation as a major factor in the suspensions rheology, stating that as the pH is decreased and carboxylic groups is protonated, the suspensions viscosity increases.

Thixotropy, *i.e.* reversible shear-thinning behavior, is also referred to as a property of nanocelluloses [32, 62], with recovery times depending on the type of material assessed – e.g., higher fibrillation reduces the recovery time [33]. Regarding temperature, it was found that heating a cellulose nanofibrils suspension did not affect significantly its viscosity, since the nanocellulose had a dominant effect over the aqueous medium [3, 57]. Finally, it was also demonstrated that the introduction of charged groups to the nanocellulose structure is responsible for the decrease of viscosity, due to strong repulsive forces between surfaces, which act as kind of lubricant [62]. In this sense, several authors have introduced salts, dispersants or surfactants to the nanocellulose suspension in order to control the dispersion stability and reduce the viscosity [9]. Sodium chloride and carboxymethylcellulose are the most reported additives when studying rheology of nanocellulose [32, 100].

In papermaking, nanocelluloses have been found to be a great rheology-controller for coating formulations, as not only viscosity is enhanced but also water-binding [32, 62].

6.4.6 Toxicity

The production of nanocellulose at an industrial scale and its application in a multiplicity of products and biomedical devices can represent a potential hazard to workers along the lifecycle as well as to consumers [149]. Vartiainen et al. [148] concluded that workers' exposure to particles in the air during grinding and spray drying of birch cellulose was low or non-existent with the implementation of appropriate protection equipment and proper handling. However, the high aspect ratio of CNF and its biodurability in the human lungs [133] resembles the fiber paradigm that has been associated to the adverse effects of other fibrous nanomaterials (e.g., carbon nanotubes). Therefore, to ensure the safety of CNF to humans prior to their largescale commercialization, it is of utmost importance to investigate their potential toxicological properties, particularly their genotoxicity that is closely associated to carcinogenicity. Cytotoxicity deals with the effect of the CNF on cell viability, while immunotoxicity regards the effects on the functioning of local and systemic immune systems and finally, the genotoxicity is related with the direct or indirect damaging effects on DNA or chromosomes. Most toxicological studies have focused on nanocellulose types with morphological and surface chemical characteristics different from the above-mentioned CNF. These include BNC [69, 83, 98, 108, 123, 124] and CNC [20, 28, 35, 76, 127, 160]. These nanocellulose types are generally considered as nontoxic, although CNC could induce low cytotoxicity and immunotoxicity *in vitro* and *in vivo* [28, 160]. Regarding CNF, the few published studies mainly indicate no relevant cytotoxic, genotoxic or immunotoxic effects [7, 29, 103, 109, 148]. Nevertheless, a recent study by Catalán et al. [21] showed that mice exposure by pharyngeal aspiration to CNF produced through TEMPO oxidation led to an acute lung inflammatory response

and induced DNA damage in lung cells. Moreover, Lopes et al. [86] reported that an unmodified CNF induced a pro-inflammatory effect in THP-1 macrophages that could be moderated by the introduction of surface modifications.

6.4.7 CNF/CMF Drying and Films

Nanocelluloses are usually processed in their aqueous suspension form because of their hydrophilic nature and of the propensity to agglomerate during drying. In fact, the hydrogen bonds between water and the cellulose particles enable the system to remain thermally and kinetically stable even at different moisture contents [107]. However, if properly dried, nanocellulose can be used to produce composites or form films and aerogels with excellent properties. Films made entirely of nanocelluloses are usually called "nanopapers" and reported to be transparent rigid films with high strength, flexibility, low thermal expansion coefficient and good barrier properties [1, 41, 79, 158], which make them excellent materials to be used as substrates in several applications. However, removing water from the CNF suspensions can be a delicate process and some authors tried to propose viable solutions to the problem, being already in operation some pilot plants to the production of nanopaper [139]. Peng et al. [107] studied the effect of several techniques to dry cellulose nanocrystals and nanofibrillated cellulose: oven drying, freeze-drying, supercritical drying and spray-drying. The authors concluded that spray-drying was the most suitable technique to dry CNF without affecting the particles nano-scale, while the other techniques created a highly networked structure with cellulose agglomerates. Pääkkö et al. [105] produced aerogels with strong mechanical properties by applying two different freeze-drying techniques (cryogenic and vacuum) to a CNF suspension, stating that these are advantageous and cheaper than the usual technique: supercritical drying. Fig. 6.8a shows a freeze-dried TEMPO-nanocellulose.

Regarding the formation of nanopapers, several techniques can be used, namely vacuum fil-

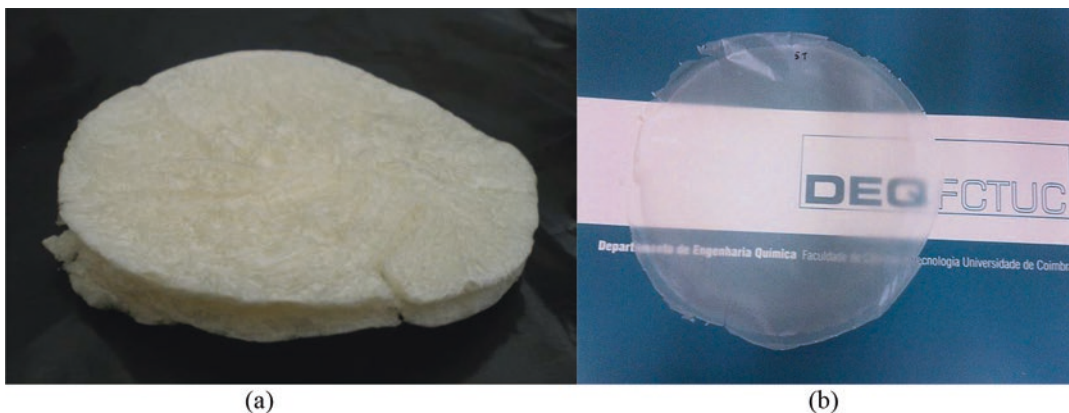


Fig. 6.8 Examples of TEMPO-oxidized nanocelluloses obtained by (a) freeze-drying and (b) solvent casting

tration, spraying, solvent casting, solvent exchange, spin-coating, among others [27, 45, 59, 91]. The fastest method to produce nanopapers is vacuum filtration by using a dynamic sheet former. Some authors stated that with the use of an appropriate wire, usually membranes or polyamide cloths, it is possible to obtain transparent and strong nanopapers [47, 59, 114]. The main objective of the production of nanopapers has been the study of their mechanical properties, but also, in a minor degree, the analysis of the optical and barrier properties. Syverud and Stenius [136] produced nanopapers with thickness values of 20–33 μm that possessed strength properties comparable to, or higher than, those of cellophane. Besides, they stated that the dense structure formed by the fibrils gave superior barrier properties and the films were comparable, in terms of oxygen transmission, to the best synthetic polymers used for packaging, like polyvinylidene chloride or polyester. It must be stressed out that the properties of the films strongly depend on the raw material used for their production and values of tensile strength around 130 MPa for nanopapers produced from sulfite pulp [59] or as high as 233 MPa with TEMPO-oxidized softwood pulps [47] can be found. The classical method to produce nanopapers is solvent casting in which the solvent is evaporated with controlled temperature, relative humidity and time. However, it is a time consuming method that can take up to five days if, for example, room temperature is used [13, 24, 132]. Figure 6.8b

shows a nanopaper made by solvent casting of a TEMPO-oxidized BEKP. Other processes such as solvent exchange are commonly found in the literature. With these methods it is also possible to produce porous films. According to Sehaqui et al. [125] a water exchange to methanol or acetone prior to drying increases the porosity from 20% to 28% and 40%, respectively, which is due to the less hydrophilic character of the solvents that reduce the capillary effects during the drying process. In this work, the authors produced nanopapers using three different methods, namely liquid CO_2 evaporation, supercritical CO_2 drying and tert-butanol freeze-drying, obtaining nanopapers with high specific surface area and with mechanical properties comparable to those of typical commodity thermoplastics but with much lower density (640 kg m^{-3}). Finally, Ahola et al. [5] produced a thin and smooth film by another strategy: the authors spin-coated cellulose nanofibril dispersions on silica substrates. This method differs from the previous in the sense that the nanopaper is formed directly on a suitable substrate.

Chinga-Carrasco et al. [24–27] have researched thoroughly the micro-structure of nanopapers surfaces by the use of image analysis techniques. In their works, novel microscopy techniques and automatic computerized image analysis have shown to be preferable to the common visual and subjective evaluations. The effect of residual fibers in the roughness of nanopapers was studied in detail, concluding that without a

proper treatment, such as fractionation, the nanopapers had an extreme rough surface structure, which to some applications such as printing, is very detrimental [27]. By using laser profilometry topography, it was possible to distinguish size differences in the top and bottom sides of a TEMPO-oxidized nanopaper, and therefore a quantification of the amount of nanofibrils present in different samples was performed [51].

Regarding the optical properties, it is well known that films made entirely of nanocellulose are transparent since the size of the nanofibrils is much inferior to the wavelength of visible light [61, 129]. Indeed, Fukuzumi et al. [47] produced TEMPO-oxidized nanopapers with 20 μm thickness and stated that at 600 nm a 90% transmittance, when using softwood, and a 78% transmittance, when using hardwood, was found. Similar values were obtained by Wang et al. [158], with nanopapers derived from waste corrugated paper, and by Nogi et al. [102], that evaluated the influence of the surface roughness in transmittance, concluding that the light transmittance could be increased to *ca.* 90% if the films were polished or impregnated with an optical transparent polymer layer (acrylic resin).

As already stated, nanopapers have unique properties that make them an outstanding material for diverse applications: transparent films for food packaging [92], antimicrobial films [116], water treatment [91], electronic devices [145], conductive papers [61], coating technologies, among others. However, some problems remain associated with the nanopapers production/use that still need a solution, such as their hydrophilic nature, preservation and the fact that nanocelluloses do not redisperse, among others.

6.5 Market

6.5.1 Commercialization

In order to effectively commercialize the nanocellulose products, several aspects have to be taken into account. A report from Miller [93] identifies the main producers at large scale (Table 6.2). It must be taken into account that

Table 6.2 Nanocellulose main producers (tonnes per year, dry basis) [93]

Producer	Material	Capacity
FiberLean technologies, UK	CMF	8800
Kruger, Canada	CF(CMF)	6000
Borregaard, Norway	CMF	1100
Nippon paper, Japan	CNF	560
CelluForce, Canada	CNC	300
Norske Skog, Norway	CMF	260
University of Maine, U.S.A	CNF	260
Daicel, Japan	CMF	200
RISE, transportable container factory	CMF	200
American process, U.S.A	CNC	130
American process, U.S.A	CNF	130
CelluComp, UK	CNF	100
Chuetsu pulp and paper, Japan	CNF	100

FiberLean Technologies produces a hybrid material as CMF are mixed with mineral fillers at a 1:1 ratio [53]. *International Paper* and *Stora Enso* companies are also reported to be producing CMF, largely for use in their own paper and paperboard products [94].

Some technical challenges, related to the aforementioned specific characteristics of the nanomaterials, are identified within this topic [2, 93, 146] and can be synthesized as follows:

- Drying and dispersion
- Compatibilization
- Cost
- Consistent quality from batch to batch
- Safety and regulatory issues

If by the one hand the cost of production is the bottleneck of nanocellulose usage at industrial scale, by the other hand, drying is considering one of the most important issues. Due to the high hydrophilic character, and to the tendency to irreversibly aggregate while drying, one significant challenge is to produce dry CNF powder with a preserved nanoscale structure and re-dispersion capacity, which would provide advantages in CNFs storage and transportation. However,

according to Miller [94], when considering the papermaking industry, 75% of all nanocellulose is produced by mills and used in their own production, which minimizes the challenges identified. Overall, there is the need to select the best material for a given application, define the optimal loading, and consider a learning curve for the end-user. Besides, the development of applications to use the product, with the research and development associated, and the scale up necessary, are still assumed to be a challenge for commercialization [94].

A variety of market reports and guides for end users have been published forecasting the nanocellulose market, including companies such as Future Markets Inc., RISI, Market Intel, LLC and TAPPI [75]. A report from Future Markets Inc. predicted the global market for nanocellulose until 2030, stating that, overall, the production costs of these nanomaterials should be reduced (as example, TEMPO-CNF should decrease from 50 USD/kg to ≈ 2 USD/kg) [48]. The cost of producing nanocellulose is primarily dependent on the type of pre-treatment applied, with the cheapest process being probably the enzymatic pre-treatment, where the cost for making CMF from the pulp integrated in a pulp mill is 0.4 €/kg, which today is in operation in large-scale papermaking applications [75]. For non-integrated use of CNF/CMF in papermaking applications, the cost including pulp cost and profits should be lower than 2.5 €/kg [75].

6.5.2 Applications

Due to the amazing properties presented by nanocelluloses, and considering the opportunity to produce a functional material with specific characteristics directed to the desired requests, several applications have been arising and the nanocellulose use is almost endless. In this sense nanocelluloses have been applied, as said, in the most diverse fields such as papermaking, textiles, medicine, cosmetics, pharmaceuticals, food industry and technology. Table 6.3 presents the applications with higher potential volume for nanocelluloses, as depicted by BioBased Markets

Table 6.3 Applications and potential volume of nanocelluloses, in tonnes [93]

	Market size	Potential loading	Nanocellulose potential
Paper and paperboard	400,000	5.0%	20,000
Textiles	50,000	2.0%	1000
Paints and coatings	40,000	2.0%	800
Carbon black	15,000	2.0%	300
Films and barriers	9670	2.0%	200
Composites	9000	2.0%	180
Oil and gas	17,500	1.0%	180
Nonwovens	7000	2.0%	140
Water treatment	4650	2.0%	90
Excipients	4600	2.0%	90
Cement	15,000	0.5%	75
Adhesives	500	2.0%	10
Cosmetics	300	1.0%	3
Battery separator	60	2.0%	1
TOTAL			23,063

in their 2018 annual report. Examples of applications are the water treatment [91, 150, 154], printed electronics [145, 162], tissue engineering and drug delivery [14, 83, 110].

According to Klemm et al. [75], there is an agreement that high value and/or high volume applications should be pursued in order to reduce the nanocellulose production cost. Considering the aforementioned, the major potential use of nanocelluloses is in papermaking.

Nonetheless, despite the high potential of use in papermaking, textiles or coatings, these are low-value products, and it is noticed that the research available has been primarily focused on high-value products, especially in composite materials. According to Siró and Plackett [129] nanocomposites are two-phase materials in which one of the phases has at least one dimension in the nanometer range (1–100 nm). Besides their excellent mechanical properties, nanocelluloses present many advantages in the production of composites, such as biocompatibility, transparency and high reactivity due to the presence of hydroxyl groups within a high surface area. Composites with nanocelluloses have been pro-

duced with petroleum-derived non-biodegradable polymers such as polyethylene (PE) or polypropylene (PP) and also with biodegradable polymers such as polylactic acid (PLA), polyvinyl alcohol (PVOH) and starch [129], and several works have arisen with inorganic fillers [8, 145]. The main purpose of the works published in this field is to improve the strength properties of the composites [49, 101, 106]. Besides, exceptionally smooth surfaces are reported under specific conditions, which make these composites a promising material for printed electronics. However, it is noteworthy that all of the research performed strongly depends on the nature and preparation method of the nanocelluloses used [167]. Some disadvantages of using nanocelluloses in composites for reinforcement applications should also be referred to, namely the high moisture absorption and the incompatibility with most of the polymeric matrices and of course the temperature limitation because lignocellulosic materials start to degrade near 220 °C [128], which can restrict the type of composite that can be produced. Examples of applications are the CNC composite filter papers for rapid removal of bacteria from aqueous solutions [23], the electrically conductive composites (Zhang et al. 2019) or even the CMF films with acetic anhydride that possess barrier properties similar to the common packaging materials [114], among several others.

6.6 Final Remarks

Nanocelluloses, in their varied denominations, shapes and properties, have been widely explored in the last decades. The state of the art regarding these interesting and promising materials is very extensive and covers the research and development based on the possible sources, production, properties and characterization but also on the proposed usages.

In this sense, nanocelluloses can have very distinct characteristics, depending on the raw material used, as well as on the treatments applied for their production. The different characteristics will have distinct impacts on their final applications, which make it very important to always

perform a complete analysis of the intrinsic properties of these new materials.

Their use in the most diverse applications has been widely explored, as nanocelluloses may be used for plastics substitution, as food additive, rheology controller, 3D printing of diverse structures, among many other possibilities, which reinforces the idea that the behavior of nanocelluloses in the presence of other components should be carefully studied, with all of its specificities.

Acknowledgments The authors acknowledge FCT Project ToxApp4NanoCELF (PTDC/SAU-PUB/32587/2017), cofunded by ToxOmics – Center for Toxicogenomics and Human Health (UIDB/00009/2020; UIDP/00009/2020), CIEPQPF – Strategic Research Centre Project (UIDB/00102/2020), FCT PhD. Grant SFRH/BDE/108095/2015.

References

1. Abdul Khalil HPS, Davoudpour Y, Nazrul Islam M, Mustapha A, Sudesh K, Dungani R, Jawaid M (2014) Production and modification of nanofibrillated cellulose using various mechanical processes: a review. *Carbohydr Polym* 99:649–665
2. Agenda 2020 Technology Alliance (2016) Cellulose nanomaterials – research roadmap
3. Agoda-Tandjawa G, Durand S, Berot S, Blassel C, Gaillard C, Garnier C, Doublier J-L (2010) Rheological characterization of microfibrillated cellulose suspensions after freezing. *Carbohydr Polym* 80(3):677–686
4. Ahola S, Österberg M, Laine J (2008a) Cellulose nanofibrils – adsorption with poly(amidamine) epichlorohydrin studied by QCM-D and application as a paper strength additive. *Cellulose* 15(2):303–314
5. Ahola S, Salmi J, Johansson L, Laine J, Österberg M (2008b) Model films from native cellulose Nanofibrils. Preparation, swelling, and surface interactions. *Biomacromolecules* 9:1273–1282
6. Alemdar A, Sain M (2008) Isolation and characterization of nanofibers from agricultural residues-wheat straw and soy hulls. *Bioresour Technol* 99:1664–1671
7. Alexandrescu L, Syverud K, Gatti A, Chingacarrasco G (2013) Cytotoxicity tests of cellulose nanofibril-based structures. *Cellulose* 20:1765–1775
8. Alves L, Ferraz E, Gamelas JAF (2019) Composites of nanofibrillated cellulose with clay minerals: a review. *Adv Colloid Interf Sci* 272:101994
9. Alves L, Ferraz E, Lourenço AF, Ferreira PJ, Rasteiro MG, Gamelas JAF (2020) Tuning rheology

- and aggregation behaviour of TEMPO oxidized cellulose nanofibrils aqueous suspensions by addition of different acids. *Carbohydr Polym* 237:116109. <https://doi.org/10.1016/j.carbpol.2020.116109>
10. Andrade FK, Morais JPS, Muniz CR, Nascimento JHO, Vieira RS, Gama FMP, Rosa MF (2019) Stable microfluidized bacterial cellulose suspension. *Cellulose* 26:5851–5864
 11. Ankerfors M (2012) Microfibrillated cellulose: Energy-efficient preparation techniques and key properties. Litentiate thesis presented to Innventia AB and KTH Royal Institute of Technology
 12. Araki J, Wada M, Kuga S (2001) Steric stabilization of a cellulose microcrystal suspension by poly(ethylene glycol) grafting. *Langmuir* 17:21–27
 13. Aulin C, Gällstedt M, Lindström T (2010) Oxygen and oil barrier properties of microfibrillated cellulose films and coatings. *Cellulose* 17:559–574
 14. Bacakova L, Pajorova J, Bacakova M, Skogberg A, Kallio P, Kolarova K, Svorcik V (2019) Versatile application of Nanocellulose: from industry to skin tissue engineering and wound healing. *Nano* 9(2):164
 15. Benhamou K, Dufresne A, Magnin A, Mortha G, Kaddami H (2014) Control of size and viscoelastic properties of nanofibrillated cellulose from palm tree by varying the TEMPO-mediated oxidation time. *Carbohydr Polym* 99:74–83
 16. Besbes I, Alila S, Boufi S (2011a) Nanofibrillated cellulose from TEMPO-oxidized eucalyptus fibres: effect of the carboxyl content. *Carbohydr Polym* 84:975–983
 17. Besbes I, Vilar MR, Boufi S (2011b) Nanofibrillated cellulose from alfa, eucalyptus and pine fibres: preparation, characteristics and reinforcing potential. *Carbohydr Polym* 86:1198–1206
 18. Bras J, Viet D, Bruzzese C, Dufresne A (2011) Correlation between stiffness of sheets prepared from cellulose whisks and nanoparticles dimensions. *Carbohydr Polym* 84:211–215
 19. Brodin F, Eriksen Ø (2015) Preparation of individualised lignocellulose microfibrils based on thermo-mechanical pulp and their effect on paper properties. *Nordic Pulp Paper Res J* 30:443–451
 20. Catalán J, Ilves M, Järventaus H, Hannukainen KS, Kontturi E, Vanhala E, Alenius H, Savolainen KM, Norppa H (2015) Genotoxic and immunotoxic effects of cellulose nanocrystals in vitro. *Environ Molecular Mutagenesis* 56:171–182
 21. Catalán J, Rydman E, Aimonen K, Hannukainen KS, Suhonen S, Vanhala E, Moreno C, Meyer V, Perez DD, Sneek A, Forsström U, Højgaard C, Willemoes M, Winther JR, Vogel U, Wolff H, Alenius H, Savolainen KM, Norppa H (2017) Genotoxic and inflammatory effects of nanofibrillated cellulose in murine lungs. *Mutagenesis* 32(1):23–31
 22. Chen Y, Wan J, Dong X, Ma Y (2013) Fiber properties of eucalyptus Kraft pulp with different carboxyl group contents. *Cellulose* 20:2839–2846
 23. Chen W, Chen F, Zhang G, Liu X, Kong S, Cai W, Wang J, Du L, Wu C (2019) Fabrication of cellulose nanocrystal composite filter papers for rapid and highly efficient removal of bacteria from aqueous solutions. *Cellulose* 26:7027–7035
 24. Chinga-Carrasco G, Yu Y, Diserud O (2011a) Quantitative electron microscopy of cellulose nanofibril structures from eucalyptus and Pinus radiata Kraft pulp fibers. *Microsc Microanal* 17:563–571
 25. Chinga-Carrasco G, Miettinen A, Hendriks CLL, Gamstedt EK, Kataja M (2011b) Structural characterisation of Kraft pulp Fibres and their Nanofibrillated materials for biodegradable composite applications. In *nanocomposites and polymers with analytical methods* (ed J Cuppoletti). INTECH:243–260
 26. Chinga-Carrasco G, Tobjörk D, Österbacka R (2012) Inkjet-printed silver nanoparticles on nano-engineered cellulose films for electrically conducting structures and organic transistors: concept and challenges. *J Nanopart Res* 14:1213
 27. Chinga-Carrasco G, Averianova N, Kondalenko O, Garaeva M, Petrov V, Leinsvang B, Karlsen T (2014) The effect of residual fibres on the micro-topography of cellulose nanopaper. *Micron* 56:80–84
 28. Clift MJ, Foster EJ, Vanhecke D, Studer D, Wick P, Gehr P, Rothen-Rutishauser B, Weder C (2011) Investigating the interaction of cellulose nanofibers derived from cotton with a sophisticated 3D human lung cell coculture. *Biomacromolecules* 12:3666–3673
 29. Colić M, Mihajlovic D, Mathew A, Naseri N, Kokol V (2015) Cytocompatibility and immunomodulatory properties of wood based nanofibrillated cellulose. *Cellulose* 22:763–778
 30. Das K, Ray D, Bandyopadhyay NR, Ghosh T, Mohanty AK, Misra M (2009) A study of the mechanical, thermal and morphological properties of microcrystalline cellulose particles prepared from cotton slivers using different acid concentrations. *Cellulose* 16:783–793
 31. Delgado-Aguilar M, González I, Tarrés Q, Alcalà M, Pèlach MÀ (2015) Approaching a low-cost production of cellulose nanofibers for papermaking applications. *Bioresources* 10:5345–5355
 32. Dimic-Misic K, Salo T, Paltakari J, Gane P (2014) Comparing the rheological properties of novel nanofibrillar cellulose-formulated pigment coating colours with those using traditional thickener. *Nordic Pulp Paper Res J* 29(2):253–270
 33. Dimic-Misic K, Vanhatalo K, Dahl O, Gane P (2018) Rheological properties comparison of aqueous dispersed nanocellulose derived from a novel pathway-produced microcrystalline cellulose or by conventional methods. *Appl Rheol* 28:64474
 34. Dinand E, Chanzy H, Vignon M. R. (1999) Suspensions of cellulose microfibrils from sugar beet pulp. *Food Hydrocol* 13: 275–283
 35. Dong S, Hirani AA, Colacino KR, Lee YW, Roman M (2012) Cytotoxicity and cellular uptake of cellulose nanocrystals. *Nano Life* 2(3):1241006

36. Dufresne A (2012) Nanocellulose – from nature to high performance tailored materials. De Gruyter, Germany. ISBN 978-3-11-025456-3
37. Dufresne A, Cavaille J, Vignon MR (1997) Mechanical behavior of sheets prepared from sugar beet cellulose microfibrils. *J Appl Polym Sci* 64:1185–1194
38. Dufresne A, Dupeyre D, Vignon MR (2000) Cellulose microfibrils from potato tuber cells : processing and characterization of starch – cellulose microfibril composites. *J Appl Polym Sci* 76:2080–2092
39. Ehman N, Tarrés Q, Delgado Aguilar M, Vallejos ME, Felissia F, Area MC, Mutjé P (2016) From pine sawdust to cellulose nanofibres. *Cellul Chem Technol* 50(3–4):361–367
40. Ehman NV, Lourenço AF, McDonagh BH, Vallejos ME, Felissia FE, Ferreira PJT, Chinga-Carrasco G, Area MC (2020) Influence of initial chemical composition and characteristics of pulps on the production and properties of lignocellulosic nanofibers. *Int J Biol Macromol* 143:453–461
41. Eichhorn SJ, Dufresne A, Aranguren M, Marcovich NE, Capadona JR, Rowan SJ, Weder C, Thielemans W, Roman M, Renneckar S, Gindl W, Veigel S, Keckes J, Yano H, Abe K, Nogi M, Nakagaito AN, Mangalam A, Simonsen J, Benight AS, Bismarck A, Berglund LA, Peijs T (2010) Review: current international research into cellulose nanofibres and nanocomposites. *J Mater Sci* 45:1–33
42. Eriksen Ø, Syverud K, Gregersen Ø (2008) The use of microfibrillated cellulose produced from Kraft pulp as strength enhancer in TMP paper. *Nordic Pulp Paper Res J* 23:299–304
43. Espinosa E, Tarrés Q, Delgado-Aguilar M, González I, Mutjé P, Rodríguez A (2016) Suitability of wheat straw semichemical pulp for the fabrication of lignocellulosic nanofibres and their application to paper-making slurries. *Cellulose* 23:837–852
44. Eycholzer C, Bordeanu N, Lopez-Suevos F, Rentsch D, Zimmermann T, Oksman K (2010) Preparation and characterization of water-redispersible microfibrillated cellulose in powder form. *Cellulose* 17:19–30
45. Foster EJ, Moon RJ, Agarwal UP, Bortner MJ, Bras J, Camarero-Espinosa S, Chan KJ, Clift MJD, Cranston ED, Eichhorn SJ, Fox DM, Hamad WY, Heux L, Jean B, Korey M, Nieh W, Ong KJ, Reid MS, Renneckar S, Roberts R, Shatkin JA, Simonsen J, Stinson-Bagby K, Wanasekara N, Youngblood J (2018) Current characterization methods for cellulose nanomaterials. *Chem Soc Rev* 47(8):2609–2679
46. Fraschini C, Chauve G, Le Berre J-F, Ellis S, Méthot M, Connor BO, Bouchard J (2014) Critical discussion of light scattering and microscopy techniques for CNC particle sizing. *Nordic Pulp Paper Res J* 29:31–40
47. Fukuzumi H, Saito T, Iwata T, Kumamoto Y, Isogai A (2009) Transparent and high gas barrier films of cellulose nanofibers prepared by TEMPO-mediated oxidation transparent and high gas barrier films of cellulose nanofibers prepared by TEMPO-mediated oxidation. *Biomacromolecules* 10:162–165
48. Future Markets Inc (2014) The global market for nanocellulose
49. Gabr MH, Phong NT, Abdelkareem MA, Okubo K, Uzawa K, Kimpara I, Fujii T (2013) Mechanical, thermal, and moisture absorption properties of nano-clay reinforced nano-cellulose biocomposites. *Cellulose* 20:819–826
50. Gama M, Dourado F, Bielecki S (2016) Bacterial Nanocellulose: From Biotechnology to Bio-Economy. Elsevier ISBN: 978–0–444-63458-0
51. Gamelas JAF, Pedrosa J, Lourenço AF, Mutjé P, González I, Chinga-Carrasco G, Singh G, Erreira PJT (2015a) On the morphology of cellulose nanofibrils obtained by TEMPO-mediated oxidation and mechanical treatment. *Micron* 72:28–33
52. Gamelas JAF, Pedrosa J, Lourenço AF, Ferreira PJ (2015b) Surface properties of distinct nanofibrillated celluloses assessed by inverse gas chromatography. *Colloids Surf A Physicochem Eng Asp* 469:36–41
53. Gane PAC, Schenker M, Subramanian R, Schoelkopf J (2018) Process for the production of gel-based composite materials. Patent EP 3:266–931
54. Gardner DJ, Oporto GS, Mills R, Azizi Samir MAS (2008) Adhesion and surface issues in cellulose and nanocellulose. *J Adhes Sci Technol* 22:545–567
55. González I, Vilaseca F, Alcalá M, Pèlach MA, Boufi S, Mutjé P (2013) Effect of the combination of biobearing and NFC on the physico-mechanical properties of paper. *Cellulose* 20:1425–1435
56. Hassan ML, Mathew AP, Hassan EA, El-wakil NA, Oksman K (2012) Nanofibers from bagasse and rice straw: process optimization and properties. *Wood Sci Technol* 46:193–205
57. Hegset EB, Chinga-Carrasco G, Syverud K (2017) Temperature stability of nanocellulose dispersions. *Carbohydr Polym* 157:114–121
58. Henriksson M, Henriksson G, Berglund LA, Lindström T (2007) An environmentally friendly method for enzyme-assisted preparation of microfibrillated cellulose (MFC) nanofibers. *Eur Polym J* 43:3434–3441
59. Henriksson M, Berglund LA, Isaksson P, Lindstro T, Nishino T (2008) Cellulose Nanopaper structures of high toughness. *Biomacromolecules* 9:1579–1585
60. Horseman T, Tajvidi M, Diop CIK, Gardner DJ (2017) Preparation and property assessment of neat lignocellulose nanofibrils (LCNF) and their composite films. *Cellulose* 24(6):2455–2468
61. Hu L, Zheng G, Yao J, Liu N, Weil B, Eskilsson M, Karabulut E, Ruan Z, Fan S, Bloking JT, McGehee MD, Wågberg L, Cui Y (2013) Transparent and conductive paper from nanocellulose fibers. *Energy Environ Sci* 6:513
62. Hubbe MA, Tayeb P, Joyce M, Tyagi P, Kehoe M, Dimic-Misic K, Pal L (2017) Rheology of nanocellulose-rich aqueous suspensions: a review. *Bioresources* 12(4):9556–9661

63. ISO 5351:2010 Pulps — Determination of limiting viscosity number in cupri-ethylenediamine (CED) solution
64. ISO/TS 21346:2021 Nanotechnologies – Characterization of individualized cellulose nanofibril samples
65. ISO/TS 20477:2017 Nanotechnologies — Standard terms and their definition for cellulose nanomaterial
66. Isogai A (2013) Wood nanocelluloses: fundamentals and applications as new bio-based nanomaterials. *J Wood Sci* 59:449–459
67. Isogai A, Saito T, Fukuzumi H (2011) TEMPO-oxidized cellulose nanofibers. *Nanoscale* 3:71–85
68. Iwamoto S, Nakagaito AN, Yano H, Nogi M (2005) Optically transparent composites reinforced with plant fiber-based nanofibers. *Appl Phys A Mater Sci Process* 81:1109–1112
69. Jeong SI, Lee SE, Yang H, Jin YH, Park CS, Park YS (2010) Toxicologic evaluation of bacterial synthesized cellulose in endothelial cells and animals. *Mol Cellular Toxicol* 6:373–380
70. Jonoobi M, Harun J, Tahir PM, Zaini LH, Azry SS, Makinejad MD (2010) Characteristics of nanofibers extracted from kenaf core. *Bioresources* 5:2556–2566
71. Kangas H, Lahtinen P, Sneek A, Saariaho A-M, Laitinen O, Hellén E (2014) Characterization of fibrillated celluloses. A short review and evaluation of characteristics with a combination of methods. *Nordic Pulp Paper Res J* 29:129–143
72. Kargarzadeh H, Mariano M, Gopakumar D, Ahmad I, Thomas S, Dufresne A, Huang J, Lin N (2018) Advances in cellulose nanomaterials. *Cellulose* 25:2151–2189
73. Klemm D, Schumann D, Kramer F, Heßler N, Hornung M, Schmauder HP, Marsch S (2006) Nanocelluloses as innovative polymers in research and application. *Polysaccharides II in Adv Polymer Sci* 205:49–96
74. Klemm D, Kramer F, Moritz S, Lindström T, Ankerfors M, Gray D, Dorris A (2011) Nanocelluloses: a new family of nature-based materials. *Angew Chem Int Ed* 50:5438–5466
75. Klemm D, Cranston ED, Fischer D, Gama FM, Kedzior SA, Kralisch D, Kramer F, Kondo T, Lindström T, Nietzsche S, Petzold-Welcke K, Rauchfuß F (2018) Nanocellulose as a natural source for groundbreaking applications in materials science: today's state. *Mater Today* 21(7):720–748
76. Kovacs T, Naish V, O'Connor B, Blaise C, Gagné F, Hall L, Trudeau V, Martel P (2010) An ecotoxicological characterization of nanocrystalline cellulose (NCC). *Nanotoxicology* 4:255–270
77. Kruger Inc (2019) The FiloCell Advantage. Available at <https://biomaterials.kruger.com/products/the-filocell-advantage/> [consulted 12.2019]
78. Lasseguette E, Roux D, Nishiyama Y (2008) Rheological properties of nanofibrillar suspension of TEMPO-oxidized pulp. *Cellulose* 15:425–433
79. Lavoine N, Desloges I, Dufresne A, Bras J (2012) Microfibrillated cellulose – its barrier properties and applications in cellulosic materials: a review. *Carbohydr Polym* 90:735–764
80. Li J, Wei X, Wang Q, Chen J, Chang G, Kong L, Su J (2012) Homogeneous isolation of nanocellulose from sugarcane bagasse by high pressure homogenization. *Carbohydr Polym* 90:1609–1613
81. Li Q, Raj P, Abbas Husain F, Varanasi S, Rainey T, Garnier G, Batchelor W (2016) Engineering cellulose nanofibre suspensions to control filtration resistance and sheet permeability. *Cellulose* 23:391–402
82. Liimatainen H, Visanko M, Sirviö JA, Hormi OEO, Niinimäki J (2012) Enhancement of the nanofibrillation of wood cellulose through sequential periodate-chlorite oxidation. *Biomacromolecules* 13:1592–1597
83. Lin N, Dufresne A (2014) Nanocellulose in biomedicine: current status and future prospect. *Eur Polym J* 59:302–325
84. Lin N, Huang J, Chang PR, Feng J, Yu J (2011) Surface acetylation of cellulose nanocrystal and its reinforcing function in poly (lactic acid). *Carbohydr Polym* 83:1834–1842
85. Lindström T, Naderi A, Wiberg A (2015) Large scale applications of Nanocellulosic materials – a comprehensive review. *J Korea TAPPI* 47:5–21
86. Lopes VR, Sanchez-Martine C, Strømme M, Ferraz N (2018) In vitro biological responses to nanofibrillated cellulose by human dermal, lung and immune cells: surface chemistry aspect. *Part Fibre Toxicol* 14:1
87. Lourenço AF, Gamelas JAF, Nunes T, Amaral J, Mutjé P, Ferreira PJ (2017) Influence of TEMPO-oxidised cellulose nanofibrils on the properties of filler-containing papers. *Cellulose* 24(1):349–362
88. Lourenço AF, Godinho D, Gamelas JAF, Sarmiento P, Ferreira PJ (2019a) Carboxymethylated cellulose nanofibrils in papermaking: influence on filler retention and paper properties. *Cellulose* 26:3489–3502
89. Lourenço AF, Gamelas JAF, Sarmiento P, Ferreira PJ (2019b) Enzymatic nanocellulose in papermaking – the key role as filler flocculant and strengthening agent. *Carbohydr Polym* 224:115200
90. Lu P, Hsieh Y (2010) Preparation and properties of cellulose nanocrystals: rods, spheres, and network. *Carbohydr Polym* 82:329–336
91. Mautner A, Maples HA, Sehaqui H, Zimmermann T, de Larraya UP, Mathew AP, Lai C, Li K, Bismarck A (2016) Nitrate removal from water using a nanopaper ion-exchanger. *Environ Sci Water Res Technol* 2:117–124
92. Mikkonen KS, Tenkanen M (2012) Sustainable food-packaging materials based on future biorefinery products: Xylans and mannans. *Trends Food Sci Technol* 28:90–102
93. Miller J (2018) Nanocellulose: producers, products, and applications. A Guide for End Users, Biobased Markets

94. Miller J (2019) Nanocellulose: Packaging Applications and Commercial Development. Presentation at International Conference on Nanotechnology for Renewable Materials, Chiba, Japan
95. Mohammadkazemi F, Azin M, Ashori A (2015) Production of bacterial cellulose using different carbon sources and culture media. *Carbohydr Polym* 117:518–523
96. Moon RJ, Martini A, Nairn J, Simonsen J, Youngblood J (2011) Cellulose nanomaterials review: structure, properties and nanocomposites. *Chem Soc Rev* 40:3941–3994
97. Morais JPS, Rosa MDF, Filho MDSM, Nascimento LD, do Nascimento DM, Cassales AR (2013) Extraction and characterization of nanocellulose structures from raw cotton linter. *Carbohydr Polym* 91:229–235
98. Moreira S, Silva NB, Almeida-Lima J, Rocha HA, Medeiros SR, Alves C Jr, Gama FM (2009) BC nanofibres: in vitro study of genotoxicity and cell proliferation. *Toxicol Lett* 189:235–241
99. Naderi A, Lindström T (2016) A comparative study of the rheological properties of three different nanofibrillated cellulose systems. *Nordic Pulp Paper Res J* 31(3):354–363
100. Naderi A, Lindström T, Torbjörn T (2014) The state of carboxymethylated nanofibrils after homogenization-aided dilution from concentrated suspensions: a rheological perspective. *Cellulose* 21:2357–2368
101. Nakagaito AN, Fujimura A, Sakai T, Hama Y, Yano H (2009) Production of microfibrillated cellulose (MFC)-reinforced polylactic acid (PLA) nanocomposites from sheets obtained by a papermaking-like process. *Compos Sci Technol* 69:1293–1297
102. Nogi BM, Iwamoto S, Nakagaito AN (2009) Optically transparent nanofiber paper. *Adv Mater* 21:1595–1598
103. Nordli HR, Chinga-Carrasco G, Rokstad AM, Pukstad B (2016) Producing ultrapure wood cellulose nanofibrils and evaluating the cytotoxicity using human skin cells. *Carbohydr Polym* 150:65–73
104. Osong SH, Norgren S, Engstrand P (2016) Processing of wood-based microfibrillated cellulose and nanofibrillated cellulose, and applications relating to papermaking: a review. *Cellulose* 23:93–123
105. Pääkko M, Ankerfors M, Kosonen H, Nykänen A, Ahola S, Österberg M, Ruokolainen J, Laine J, Larsson PT, Ikkala O, Lindström T (2007) Enzymatic hydrolysis combined with mechanical shearing and high-pressure homogenization for nanoscale cellulose fibrils and strong gels. *Biomacromolecules* 8:1934–1941
106. Pahimanolis N, Salminen A, Penttilä PA, Korhonen JT, Johansson LS, Ruokolainen J, Serimaa R, Seppälä J (2013) Nanofibrillated cellulose/carboxymethyl cellulose composite with improved wet strength. *Cellulose* 20:1459–1468
107. Peng Y, Gardner DJ, Han Y (2012) Drying cellulose nanofibrils: in search of a suitable method. *Cellulose* 19:91–102
108. Pertile RAN, Moreira S, da Costa RMG, Correia A, Guardao L, Gartner F, Vilanova M, Gama M (2012) Bacterial cellulose: long-term biocompatibility studies. *J Biomat Sci* 23:1339–1354
109. Pitkänen M, Kangas H, Laitinen O, Sneek A, Lahtinen P, Peresin MS, Niinimäki J (2014) Characteristics and safety of nano-sized cellulose fibrils. *Cellulose* 21:3871–3886
110. Plackett D. V., Letchford K., Jackso, J. K., Burt H. M. (2014) A review of nanocellulose as a novel vehicle for drug delivery. *Nordic Pulp and Paper Research Journal* 29: 105–118
111. Pommert M, Juntaro J, Heng JYY, Mantalaris A, Lee AF, Wilson K, Kalinka G, Shaffer MSP, Bismarck A (2008) Surface modification of natural fibers using bacteria: depositing bacterial cellulose onto natural fibers to create hierarchical fiber reinforced nanocomposites. *Biomacromolecules* 9:1643–1651
112. Qua EH, Hornsby PR, Sharma HSS, Lyons G (2011) Preparation and characterisation of cellulose nanofibres. *J Mater Sci* 46:6029–6045
113. Ribeiro RSA, Pohlmann BC, Calado V, Bojorge N, Pereira N (2019) Production of nanocellulose by enzymatic hydrolysis: trends and challenges. *Eng Life Sci* 19:279–291
114. Rodionova G, Lenes M, Eriksen Ø, Gregersen Ø (2011) Surface chemical modification of microfibrillated cellulose: improvement of barrier properties for packaging applications. *Cellulose* 18:127–134
115. Roman M, Winter WT (2004) Effect of sulfate groups from sulfuric acid hydrolysis 1194 on the thermal degradation behavior of bacterial cellulose. *Biomacromolecules* 5:1671–1677
116. Saini S, Falco CY, Belgacem MN, Bras J (2016) Surface cationized cellulose nanofibrils for the production of contact active antimicrobial surfaces. *Carbohydr Polym* 135:239–247
117. Saito T, Isogai A (2004) TEMPO-mediated oxidation of native cellulose. The effect of oxidation conditions on chemical and crystal structures of the water-insoluble fractions. *Biomacromolecules* 5:1983–1989
118. Saito T, Isogai A (2005) Ion-exchange behavior of carboxylate groups in fibrous cellulose oxidized by the TEMPO-mediated system. *Carbohydr Polym* 61:183–190
119. Saito T, Isogai A (2006) Introduction of aldehyde groups on surfaces of native cellulose fibers by TEMPO-mediated oxidation. *Colloids Surfaces A Physicochem Eng Asp* 289:219–225
120. Saito T, Isogai A (2007) Wet strength improvement of TEMPO-oxidized cellulose sheets prepared with cationic polymers. *Ind Eng Chem Res* 46:773–780
121. Saito T, Hirota M, Tamura N, Kimura S, Fukuzumi H, Heux L, Isogai A (2009) Individualization of nano-sized plant cellulose fibrils by direct surface

- carboxylation using TEMPO catalyst under neutral conditions. *Biomacromolecules* 10:1992–1996
122. Sánchez R, Espinosa E, Domínguez-Robles J, Mauricio Loaiza J, Rodríguez A (2016) Isolation and characterization of lignocellulose nanofibers from different wheat straw pulps. *Int J Biol Macromol* 92:102–1033
 123. Saska S, Scarel-Caminaga RM, Teixeira LN, Franchi LP, dos Santos RA, Gaspar AM, de Oliveira PT, Rosa AL, Takahashi CS, Messaddeq Y, Ribeiro SJ, Marchetto R (2012) Characterization and in vitro evaluation of bacterial cellulose membranes functionalized with osteogenic growth peptide for bone tissue engineering. *J Mater Sci Mater Med* 23:2253–2266
 124. Scarel-Caminaga RM, Saska S, Franchi LP, Santos RA, Gaspar AM, Capote TSO, Ribeiro SJL, Messaddeq Y, Marchetto R, Takahashi CS (2014) Nanocomposites based on bacterial cellulose in combination with osteogenic growth peptide for bone repair: cytotoxic, genotoxic and mutagenic evaluations. *J Appl Biol Biotechnol* 2:1–8
 125. Sehaqui H, Zhou Q, Ikkala O, Berglund LA (2011) Strong and tough cellulose nanopaper with high specific surface area and porosity. *Biomacromolecules* 12:3638–3644
 126. Shinoda R, Saito T, Okita Y, Isogai A (2012) Relationship between length and degree of polymerization of TEMPO-oxidized cellulose Nanofibrils. *Biomacromolecules* 13:842–849
 127. Shvedova AA, Kisin ER, Yanamala N, Farcas MT, Menas AL, Williams A, Fournier PM, Reynolds JS, Gutkin DW, Star A, Reiner RS, Halappanavar S, Kagan VE (2016) Gender differences in murine pulmonary responses elicited by cellulose nanocrystals. *Part Fibre Toxicol* 13:28
 128. Siqueira G, Bras J, Dufresne A (2010) Cellulosic bionanocomposites: a review of preparation, properties and applications. *Polymers (Basel)* 2:728–765
 129. Siró I, Plackett D (2010) Microfibrillated cellulose and new nanocomposite materials: a review. *Cellulose* 17:459–494
 130. Siró I, Plackett D, Hedenqvist M, Ankerfors M, Lindström T (2011) Highly transparent films from Carboxymethylated microfibrillated cellulose – the effect of multiple homogenization steps on key properties. *J Appl Polym Sci* 119:2652–2660
 131. Skočaj M (2019) Bacterial nanocellulose in papermaking. *Cellulose* 26:6477–6488
 132. Spence KL, Venditti RA, Rojas OJ, Habibi Y, Pawlak JJ (2011) A comparative study of energy consumption and physical properties of microfibrillated cellulose produced by different processing methods. *Cellulose* 18:1097–1111
 133. Stefaniak AB, Seehra MS, Fix NR, Leonard SS (2014) Lung biodurability and free radical production of cellulose nanomaterials. *Inhal Toxicol* 26(12):733–749
 134. Stenius P (2014) Nanocellulose technology – conclusions and perspectives. In: *Proc. Recent advances in cellulose nanotechnology research – Production, characterization and applications*. Seminar, PFI, Trondheim (Norway)
 135. Stenstad P, Andresen M, Tanem BS, Stenius P (2008) Chemical surface modifications of microfibrillated cellulose. *Cellulose* 15:35–45
 136. Syverud K, Stenius P (2009) Strength and barrier properties of MFC films. *Cellulose* 16:75–85
 137. Syverud K, Xhanari K, Chinga-Carrasco G, Yu Y, Stenius P (2011) Films made of cellulose nanofibrils: surface modification by adsorption of a cationic surfactant and characterization by computer-assisted electron microscopy. *J Nanoparticle Res* 13:773–782
 138. Taipale T, Österberg M, Nykänen A, Ruokolainen J, Laine J (2010) Effect of microfibrillated cellulose and fines on the drainage of Kraft pulp suspension and paper strength. *Cellulose* 17:1005–1020
 139. Tammelin T., Hippo U., Salminen A. (2013) Method for the preparation of nfc films on supports. WO patent 2013/060934 A2
 140. Tanaka R, Saito T, Isogai A (2012) Cellulose nanofibrils prepared from softwood cellulose by TEMPO/NaClO/NaClO₂ systems in water at pH 4.8 or 6.8. *Int J Biol Macromol* 51:228–234
 141. TAPPI standard proposal WI 3021. Standard terms and their definition for cellulose nanomaterials, draft. Available at: <http://www.tappi.org/content/hidden/draft3.pdf>
 142. Tarrés Q, Saguer E, Pèlach MA, Alcalà M, Delgado-Aguilar M, Mutjé P (2016) The feasibility of incorporating cellulose micro / nanofibers in papermaking processes : the relevance of enzymatic hydrolysis. *Cellulose* 23:1433–1445
 143. Tarrés Q, Pellicer N, Balea A, Merayo N, Negro C, Blanco A, Delgado-Aguilar M, Mutjé P (2017a) Lignocellulosic micro/nanofibers from wood sawdust applied to recycled fibers for the production of paper bags. *Int J Biol Macromol* 105:664–670
 144. Tarrés Q, Ehman NV, Vallejos ME, Area MC, Delgado-Aguilar M, Mutjé P (2017b) Lignocellulosic nanofibers from triticale straw: the influence of hemicelluloses and lignin in their production and properties. *Carbohydr Polym* 163:20–27
 145. Torvinen K, Sievänen J, Hjelt T, Hellén E (2012) Smooth and flexible filler-nanocellulose composite structure for printed electronics applications. *Cellulose* 19:821–829
 146. USDA (2014) Cellulose nanomaterials — a path towards commercialization. Workshop Report, USDA Forest Service, Washington D.C., USA
 147. Varanasi S, Batchelor W (2014) Superior non-woven sheet forming characteristics of low-density cationic polymer-cellulose nanofibre colloids. *Cellulose* 21:3541–3550
 148. Vartiainen J, Pöhler T, Sirola K, Pylkkänen L, Alenius H, Hokkinen J, Tapper U, Lahtinen P, Kapanen A, Putkisto K, Hiekkataipale P, Eronen P, Ruokolainen J, Laukkanen A (2011) Health and environmental safety aspects of friction grinding and spray drying of microfibrillated cellulose. *Cellulose* 18:775–786

149. Ventura C, Lourenço AF, Sousa-Uva A, Ferreira PJT, Silva MJ (2018) Evaluating the genotoxicity of cellulose Nanofibrils in a co-culture of human lung epithelial cells and monocyte-derived macrophages. *Toxicol Lett* 291:173–183
150. Voisin H, Bergström L, Liu P, Mathew A (2017) Nanocellulose-based materials for water purification. *Nano* 7(3):57
151. Wågberg L, Winter L, Ödberg L, Lindström T (1987) On the charge stoichiometry upon adsorption of a cationic polyelectrolyte on cellulosic materials. *Colloids Surf* 27:163–173
152. Wågberg L, Decher G, Norgren M, Lindström T, Ankerfors M, Axnäs K (2008) The build-up of polyelectrolyte multilayers of microfibrillated cellulose and cationic polyelectrolytes. *Langmuir* 24:784–795
153. Walecka JA (1956) An Investigation of Low Degree of Substitution Carboxymethylcelluloses. Doctor's Dissertation presented to The Institute of Paper Chemistry, Wisconsin
154. Wang D (2019) A critical review of cellulose-based nanomaterials for water purification in industrial processes. *Cellulose* 26(2):687–701
155. Wang S, Cheng Q (2009) A novel process to isolate fibrils from cellulose fibers by high-intensity Ultrasonication , part 1 : process optimization. *J Appl Polym Sci* 113:1270–1275
156. Wang B, Sain M (2007) Dispersion of soybean stock-based nanofiber in a plastic matrix. *Polym Int* 56:538–546
157. Wang B, Sain M, Oksman K (2007) Study of structural morphology of hemp fiber from the micro to the nanoscale. *Appl Compos Mater* 14:89–103
158. Wang H, Li D, Zhang R (2013) Preparation of ultralong cellulose nanofibers and optically transparent nanopapers derived from waste corrugated paper pulp. *Bioresources* 8:1374–1384
159. Yamanaka S, Watanabe K, Kitamura N, Iguchi M, Mitsuhashi S, Nishi Y, Uryu M (1989) The structure and mechanical properties of sheets prepared from bacterial cellulose. *J Mater Sci* 24:3141–3145
160. Yanamala N, Farcas MT, Hatfield MK, Kisin ER, Kagan VE, Geraci CL, Shvedova AA (2014) In vivo evaluation of the pulmonary toxicity of cellulose nanocrystals: a renewable and sustainable nanomaterial of the future. *ACS Sustain Chem Eng* 2:1691–1698
161. Yu H, Qin Z, Liang B, Liu N, Zhou Z, Chen L (2013) Facile extraction 1305 of thermally stable cellulose nanocrystals with a high yield of 93% through hydrochloric acid hydrolysis under hydrothermal conditions. *J Mater Chem A* 1:3938–3944
162. Zhang H., Dou C., Pal L., Hubbe M. A. (2019) Review of Electrically Conductive Composites and Films. *BioResources* 14: 1–49.
163. Zhao M, Li J, Mano E, Song Z, Tschäen DM, Gravowski EJJ, Reider PJ (1999) Oxidation of primary alcohols to carboxylic acids with sodium chlorite catalyzed by TEMPO and bleach. *J Org Chem* 64:2564–2566
164. Zhou L, Sun D, Hu L, Li Y, Yang J (2007) Effect of addition of sodium alginate on bacterial cellulose production by *Acetobacter xylinum*. *J Ind Microbiol Biotechnol* 34:483–489
165. Zhou YM, Fu SY, Zheng LM, Zhan HY (2012) Effect of nanocellulose isolation techniques on the formation of reinforced poly(vinyl alcohol) nanocomposite films. *Express Polym Lett* 6:794–804
166. Zhu H, Luo W, Ciesielki PN, Fang Z, Zhu JY, Henriksson G, Himmel ME, Hu L (2016) Wood-derived materials for green electronics, biological devices, and energy applications. *Chem Rev* 116:9305–9374
167. Zimmermann T, Bordeanu N, Strub E (2010) Properties of nanofibrillated cellulose from different raw materials and its reinforcement potential. *Carbohydr Polym* 79:1086–1093
168. Zywicka A, Peitler D, Rakoczy R, Konopacki M, Kordas M, Fijałkowski K (2015) The effect of different agitation modes on bacterial cellulose synthesis by *Gluconacetobacter Xylinus* strains. *Acta Scientiarum Polonorum Zootechnica* 14(1):137–150

Part II

**Nanotoxicology: Concepts
and Methodologies for Toxicity Evaluation
of Nanomaterials**



Nanocelluloses – Nanotoxicology, Safety Aspects and 3D Bioprinting

7

Gary Chinga-Carrasco, Jennifer Rosendahl,
and Julia Catalán

Abstract

Nanocelluloses have good rheological properties that facilitate the extrusion of nanocellulose gels in micro-extrusion systems. It is considered a highly relevant characteristic that makes it possible to use nanocellulose as an ink component for 3D bioprinting purposes. The nanocelluloses assessed in this book chapter include wood nanocellulose (WNC), bacterial nanocellulose (BNC), and tunicate nanocellulose (TNC), which are often assumed to be non-toxic. Depending on various chemical and mechanical processes, both cellulose nanofibrils (CNF) and cellulose nanocrystals (CNC) can be obtained from the three mentioned nanocelluloses (WNC, BNC, and TNC). Pre/post-treatment processes (chemical and mechanical) cause modifications regarding surface chemistry and nano-

morphology. Hence, it is essential to understand whether physicochemical properties may affect the toxicological profile of nanocelluloses. In this book chapter, we provide an overview of nanotoxicology and safety aspects associated with nanocelluloses. Relevant regulatory requirements are considered. We also discuss hazard assessment strategies based on tiered approaches for safety testing, which can be applied in the early stages of the innovation process. Ensuring the safe development of nanocellulose-based 3D bioprinting products will enable full market use of these sustainable resources throughout their life cycle.

Keywords

Nanocellulose · 3D printing · Bioprinting · Toxicology · Medical devices · Regulatory frameworks

G. Chinga-Carrasco (✉)
RISE PFI, Trondheim, Norway
e-mail: gary.chinga.carrasco@rise-pfi.no

J. Rosendahl
RISE, Division Materials and Production,
Department Chemistry, Biomaterials and Textiles,
Section Biological Function, Borås, Sweden

J. Catalán
Occupational Safety, Finnish Institute of
Occupational Health, Helsinki, Finland

Department of Anatomy, Embryology and Genetics,
University of Zaragoza, Zaragoza, Spain

7.1 Introduction

Several types of nanocelluloses can be obtained from different raw materials, including wood, annual plants, agro-industrial side streams, bacteria, and marine resources. The most common nanocelluloses are obtained from hard- and soft-wood chemical pulp fibers, *e.g.* kraft and sulfite pulp fibers and will be referred to as wood nano-

celluloses (WNC) in this chapter. Wood pulp fibers are roughly 1–5 mm in length and 15–50 μm in width.

Wood pulp fibers are processed with chemical and enzymatic pre-treatments to facilitate the structural deconstruction of the fibers into two main types of WNCs, i.e., cellulose nanofibrils (CNF) and cellulose nanocrystals (CNC). Depending on the pre-treatments, wood CNFs have dimensions of roughly $>1 \mu\text{m}$ in length and $<100 \text{ nm}$ in width, while wood CNC are shorter nano-objects with lengths of $<200 \text{ nm}$ and widths $<50 \text{ nm}$ (Table 7.1). For simplicity, in this book chapter, we will apply the term CNF in general, including cellulose nanofibrils, cellulose nanofibers, microfibrillated cellulose, and nanofibrillated cellulose.

Compared to wood-derived nanocelluloses, bacterial nanocellulose (BNC) is obtained from bacterial biosynthesis and is commonly composed of longer and nano-sized fibrils (diameters $<100 \text{ nm}$). Also, tunicate nanocellulose (TNC) is another type of nanomaterial obtained from marine animals (Tunicates). BNC and TNC are composed mainly of cellulose, while WNC may contain hemicellulose and residual lignin due to the plant origin.

Various types of nanocelluloses have been assessed from a biomedical perspective. Applications include wound dressings, scaffolds for tissue engineering, neural guidelines, to name a few [1–5]. These applications would benefit from a controlled deposition of nanocellulose and additional components to form specific and personalized constructs. It would make it possible to fabricate biomedical devices that are tailor-made for particular patients and situations. Such technology is also most valuable for constructing tissue models that mimic tissues such as skin, tumors, and human organs. Here is where three-dimensional (3D) printing will play a significant role, i.e., the development of tailor-made model constructs for testing drugs, medicines and, in the long run, for replacing malfunctioning body organs with fully functioning vascularized 3D printed constructs.

3D printing is an additive manufacturing process to create a 3D object layer-by-layer, aided

by a pre-defined computer model. There exist various types of 3D printing processes applied to the fabrication of biomedical devices and tissue models, e.g., fused deposition modeling (FDM), stereolithography, inkjet printing, and micro-extrusion (also called direct-ink-writing) [6–8]. The fabrication of tissue models or organoids can comprise the 3D printing with biomaterial inks (e.g., nanocelluloses, collagen, and alginates) to construct scaffolds and then load the scaffolds with cells to form a tissue model that is matured in a bioreactor. A more direct approach is to utilize a biomaterial ink directly loaded with cells (defined as bioink) and deposit the bioink layer-by-layer following a pre-defined design, also termed as 3D bioprinting [9].

This book chapter will describe various nanocelluloses intended for biomedical applications, focusing on physicochemical properties that may determine the toxicological profile. More attention to 3D bioprinting of nanocellulose-based bioinks and the requirements necessary to fulfill from a regulatory point of view will be given.

7.2 Overview of Nanocelluloses

Good overviews have been recently published about several types of nanocelluloses for biomedical applications and 3D bioprinting [8, 10, 11]. The various studies are mostly based on wood nanocelluloses with different physicochemical characteristics that may affect the toxicological profile and the 3D printability. Note that the nanocelluloses WNC, BNC, and TNC differ on the source of cellulose (wood, bacterial biosynthesis, and tunicate, respectively). Depending on the raw materials pre-treatment, the nanocelluloses may have different structural and surface chemical characteristics (Table 7.1 and Fig. 7.1).

WNCs are probably the most common type of cellulose nanomaterial proposed for biomedical applications. Wood CNF is one type of WNC and is characterized by being high aspect ratio nano-objects with diameters in the nanoscale ($<100 \text{ nm}$) and lengths in the micrometer-scale (roughly $>1 \mu\text{m}$) [12–14]. CNF is composed of amorphous and crystalline domains [15]. CNF for bio-

Table 7.1 Some characteristics of nanocellulose produced from woody biomass. Reprinted and adapted with permission from [8]. Copyright (2018) American Chemical Society

Sample	Carboxyl (mol/g)	Carboxy-methyl (mol/g)	Aldehyde (mol/g)	Sulphate half ester (mol/g)	DP	Nanofibril diameter (nm)	Nanofibril length (µm)	References
M-CNF	100				890	<100	>1	[16, 24, 25]
E-CNF	24				913	~20	>1	[19, 26]
T-CNF	765–1800		211		250–620	<20	0.2–1.1	[5, 14, 24, 27, 28]
C-CNF	58	346–515				<20	<1	[5, 13, 16, 24]
C-P-CNF		393	1202		<80	<20	<0.2	[21]
CNC				300	90	<20	<0.2	[20, 27]

^aThe CNF materials were produced without pre-treatment (M-CNF) and with enzymatic (E-CNF), 2,2,6,6-tetramethylpiperidyl-1-oxyl (TEMPO)-mediated oxidation (T-CNF), carboxymethylation (C-CNF), and carboxymethylation/periodate oxidation (C-P-CNF) pre-treatments, respectively. DP is the degree of polymerization

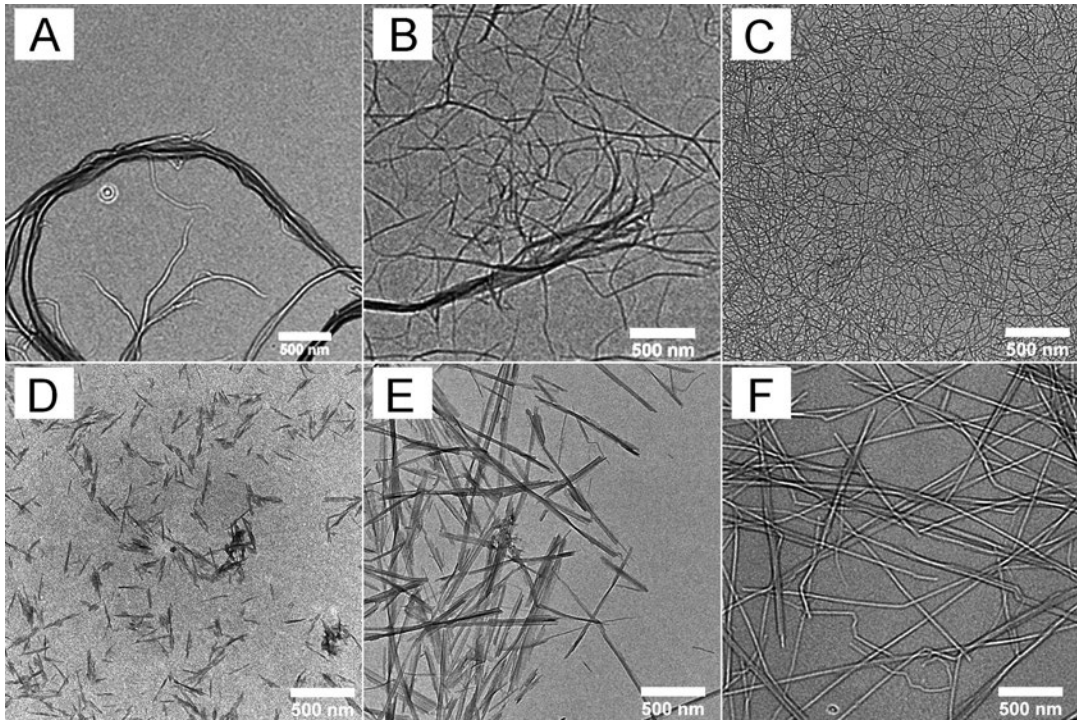


Fig. 7.1 Transmission electron microscopy images of wood CNFs: (a) mechanical grade, (b) enzymatic pre-treated, and (c) TEMPO mediated oxidized. (d) wood

CNC, (e) BNC, and (f) TNC have been treated with H_2SO_4 . Reproduced and modified with permission from [29]. Copyright (2014) American Chemical Society

medical applications and testing have been obtained by mechanical nanofibrillation by using, *e.g.*, homogenizers, fluidizers, and grinders [16–18]. Before the mechanical nanofibrillation, various chemical and enzymatic pre-treatments can be applied to ease the fibrillation of fibers into homogeneous nanofibril dispersions. Such pre-treatments affect not only the physical characteristics of the nanofibrils but also the surface chemistry. Contrary to enzymatic pre-treatments [19], chemical pre-treatments introduce *e.g.* carboxyl, carboxymethyl and aldehyde groups [12, 13, 20, 21]. Phosphorylation has also been applied to introduce phosphoryl side groups on the surface of CNF [22].

Wood CNCs are another type of WNC and are low aspect ratio nano-objects prepared by chemical hydrolysis (through HCl and H_2SO_4) of the amorphous parts of the nanofibrils (Fig. 7.1d). Although the mechanical strength (Young modulus) of CNC has been reported to be high, this may vary considerably depending on the source

of cellulose, methodology, and direction of measurement, *e.g.*, transversal or longitudinal [23].

BNC consists of only glucose monomers, which are biologically extruded into cellulose nanofibrils by Gram-Negative acetic acid bacteria, resulting in extracellular cellulose pellicles [30]. Various carbon sources are utilized and fermented in the acidic-neutral pH range by the bacteria [31]. The BNC materials have a series of advantageous characteristics: high water holding capacity, a large degree of polymerization, high crystallinity, and excellent mechanical properties. Compared to WNC, BNC has a low production yield, being thus an expensive biomaterial. However, based on its purity (only cellulose chains), BNC has been proposed for a series of high-value applications within the biomedical sector [10]. BNC *per se* is not 3D printable as the material is produced as cellulose pellicles. Hence, additional post-processing of BNC has been applied to produce nanocrystals through acid hydrolysis [32] and mechanical disintegration

and homogenization to make a 3D printable BNC dispersion [33].

TNC is derived from tunicate animals, which contain cellulose in the tunic tissues, i.e., on the surface of the epidermis of the tunicate marine animals. The cellulose nanofibrils are synthesized by enzyme complexes involved in the synthesis of glucan chains [34]. TNC is obtained by processing the tunicate material with alkali process, similar to kraft pulping of woody material [35], is composed almost entirely of cellulose, and the nanofibrils are highly crystalline and with a high aspect ratio (Fig. 7.1f).

7.3 Nanotoxicology and Safety Aspects

Due to their natural origin, cellulosic materials (*e.g.*, WNC, BNC, and TNC) are often assumed not to be toxic. However, the induction of lung diseases by cellulose fiber-containing dust in textile workers and the pulp and paper-producing industry has been well recognized since the last century [36], leading to several studies investigating the possible health risks associated with cellulosic materials. Although the toxicological findings were contradictory among studies, all of them agreed on the high biopersistence of cellulose fibers. According to the fiber pathogenicity and frustrated phagocytosis paradigms, biopersistent long ($>10\ \mu\text{m}$) fibers may have the potential to be carcinogenic [37, 38], leading to lung cancer [39]. Although it is expected that long and stiff fibers (*e.g.*, carbon nanotubes) may negatively affect phagocytosis, CNFs are considered softer and flexible, which may facilitate the phagocytosis by macrophages. However, features, such as nanoscale sizes (at least one dimension less than 100 nm), larger surface area, and modified surface chemistry, may impart novel material properties and biological behavior compared with conventional materials [40]. Therefore, it is necessary to address the human health and environmental safety aspects of nanocelluloses before scaling up their production [41].

Various studies and reviews have addressed the potential toxicity of nanocelluloses. According to Stoudmann et al. [42], the studies revealed variations and some contradictory findings attributed to several factors, *e.g.*, cellulose source, pre-treatments, and incomplete material characterization. It seems that compared to CNC, various grades of CNFs have caused the most variable results when it comes to endpoints such as cytotoxicity, genotoxicity, and inflammation. It is important to emphasize that CNFs vary considerably depending not only on the source but also on the pre-treatment (*e.g.*, enzymatic and chemical) and mechanical nanofibrillation (Table 7.1). It is thus essential to be specific when the toxicological profile of CNF materials is assessed and describe the physicochemical aspects in detail, including, *e.g.*, the size (width and length), the nanofibrillation yield (fraction of nanofibrils concerning the total mass), and the surface chemistry (which depends on the pre-treatment) (Table 7.1).

Keep in mind that nanocelluloses include a wide range of CNC and CNF materials, and most studies are based on lab-scale production of nanocelluloses, which may raise concerns about the reproducibility of the assessed materials. Hence, an appropriate comparison of the toxicological findings of different studies may be difficult. Also, samples of wood CNFs may contain micrometer-sized residual fibers [43], depending on the pre-treatments and mechanical equipment (grinders, homogenizers, and fluidizers) been applied during production. Hence, it is also essential to quantify the nanofibrillation yield [44].

Unfortunately, in some previous studies concerning toxicology, CNFs have mostly been grouped and generalized as one nano-object, and no adequate characterization or description of the CNF materials has been provided. This may lead to confusion and misleading conclusions that have to be taken with care. Hence, this observation raises a significant concern previously emphasized, i.e., “proper characterization of structural, chemical and biological aspects should be a requirement in scientific publications in

order to document the characteristics of nanocelluloses and their biological impacts” [8].

Hence, in this section, to the best of our knowledge and depending on the information provided by the specific reviewed studies, we have tried to identify the various specific CNF grades according to the terminology used in Table 7.1 to provide more insight into the physicochemical effects on the corresponding toxicological profile.

7.3.1 Routes of Exposure

The route of exposure may determine the toxicological responses to nanocelluloses. The main portals of entry to the human body include the gastrointestinal tract, skin, systemic circulation, and the lung, through inhalation [36]. The latter is considered the primary route of exposure for humans for any nanoparticle released into the environment, especially in occupational settings [45]. A life cycle risk assessment of nanocelluloses identified inhalation of dry nanocellulose powders or, in the case of wet slurry, airborne wet nanocellulose-containing particles during the production and manufacturing of nanocelluloses as the most relevant exposure scenarios [46]. Also, nanocelluloses seem to have long pulmonary biopersistence, as supported by *in vitro* experiments with artificial lung airway lining and macrophage phagolysosomal fluids [47], and by *in vivo* evidence [48–53]. As previously mentioned, the biopersistence of fibers has been identified as a critical feature governing the toxicological response following chronic inhalation exposures. Therefore, the release and inhalation of cellulose/polymer particles during processing steps, such as drilling, cutting, and sanding of polymer nanocomposites, in addition to possible liquid aerosols in wet operations, might be a concern [41].

Although inhalation has been pointed out as the main route for human exposure to nanomaterials, there is little information about exposure concentrations. When M-CNF were properly handled, no significant increases of particles in the air, compared to background levels, were

observed during friction, grinding and spray drying [54]. Dustiness measurements were used in another study to simulate occupational exposure to spray-dried CNC [55]. The authors estimated that the mass fractions of inhalable, thoracic, and respirable particles were moderate. The National Institute for Occupational Safety and Health (NIOSH, USA) conducted an exposure characterization study of the production of CNC that had been tagged with cesium [56]. The analyses of filter-based air samples for elemental cesium indicated that CNCs were aerosolized during centrifugation and manipulation of the dry product without exceeding the occupational exposure limit (OEL) values for cellulose dust. There is not enough data on occupational exposure or inhalation toxicity for nanocelluloses to determine material-specific OEL values for airborne dust [56, 57]. As for other nanomaterials, lower exposure levels may be expected to be harmful for nano-sized fibers, compared to bulk forms.

Exposure to nanocelluloses may also happen by the oral route, as nanocelluloses are intended to be incorporated into food (*e.g.*, as a rheological agent), as well as in food packaging [18, 58, 59]. No clear demonstration of release from packages has been shown to date [46]. Recently, fluorescently labeled E-CNFs were used for monitoring leaching in laboratory papers (100% E-CNFs and E-CNF-fiber blended papers). The results showed loss values below 3 wt% E-CNFs, as fibrillation of E-CNF increased, improving paper stability, and reducing overall cellulose nanofibril loss [59].

Most of the potential 3D printed applications involving nanocelluloses are meant to be biomedical applications [8, 11]. Dermal exposure is the potential route for wound dressings—assuming that nanocelluloses are released from the dressings—especially as the absorption may be higher through the damaged skin barrier (*e.g.*, burn skin). In the case of constructs for tissue engineering and drug delivery systems, nanocellulose-based products are expected to be directly delivered into the human body. Hence, the toxicity of the nanocelluloses will be determined by their potential release from the products, translocation through different

body compartments, and clearance rate from the body [60].

7.3.2 Human Toxicological Studies

Knowledge of the potential adverse biological impact of nanocelluloses is still scarce, despite the increasing number of studies addressing the toxic effects of these materials in the last few years. The excellent reviews of Roman [60], Endes et al. [36] and Seabra et al. [61], followed by the more recent ones of Ventura et al. [62], Čolić et al. [63] and Stoudmann et al. [42], summarize the existing studies, showing that conflicting conclusions are reached.

Most toxicological studies on nanocelluloses have been performed *in vitro*, using mammalian cell cultures. These studies (summarized in the previously reported reviews) indicated absence or low cytotoxicity for CNCs, whereas more contradictory responses seemed to be reported for CNFs. As mentioned above, this is most probably due to the complex physicochemical characteristics of different CNFs (Table 7.1). Regarding genotoxic effects, the existing studies are too scarce to allow clear conclusions. Although *in vitro* models are appropriate for identifying acute effects and elucidating mechanisms of action, they cannot provide information on the behavior of the materials in complex systems, such as whole organisms [62]. *In vitro* methods are neither well-suited for studying long-term effects. Hence, *in vivo* studies using animal models are still needed to get full understanding of the toxic effects of nanocelluloses.

Most of the few existing *in vivo* studies have been performed by administering the nanocelluloses through the respiratory tract, mainly by intratracheal instillation [52] or (oro)pharyngeal aspiration [48–51, 64–66]. Regarding CNC, they elicited an acute inflammatory response in mice 24 h after a single administration [64]. Pulmonary exposure to repeated doses of CNC resulted in reprotoxic effects in male mice three months after the last administration [65]. Some CNFs appear to be highly inflammogenic 24 h following pulmonary exposure, but the inflammatory

response subsides within a month [51, 52]. Interestingly, different inflammatory pathways seem to be involved in response to CNC or CNF exposures [66]. On the other hand, some CNFs seem to show a genotoxic potential [49, 50, 52], which raises concerns about their possible carcinogenicity. Only one study has assessed the toxicity of CNC by inhalation [55]. Rats were exposed to aerosolized CNCs at a maximum concentration of 0.26 mg/L for 4 hours. After monitoring the animals for mortality, gross toxicity, and behavioral changes for a period of 14 d, they were euthanized and subjected to autopsy. No adverse effects were observed.

In all previous studies, the maximum post-treatment period analyzed was up to one month. Shvedova et al. [48] investigated the effects of repeated doses of CNC (resulting in an accumulated dose of 240 µg/mouse) after three months post-exposure, showing an inflammatory response more pronounced in female than male mice. More recently, one study investigated the pulmonary toxicity exerted by BNC nanofibrils after a total period of 6 months [53]. C57BL/6 mice were intratracheally instilled with repeated doses (for three consecutive weeks) of 100 µg/mouse of BNC nanofibrils. Histological analyses revealed a chronic bronchoalveolar inflammation together with alterations in the lung tissue after six months.

As concerns, animal experiments performed by other routes, no skin sensitization, corrosion, or irritation was demonstrated for CNC using standardized Organization for Economic Co-operation and Development (OECD) Test Guidelines [55]. The same authors did not find acute or sub-chronic toxic effects after oral administration of CNC. Although still very limited in number, the available studies suggest that CNCs are non-toxic upon ingestion or contact with the skin [60]. On the other hand, rats administered with M-CNF (produced by grinding) by gavage showed no significant differences in hematological and serum markers and histopathological analyses than control animals [18]. In another study, no adverse effects were observed in rats fed with CNF for 90 consecutive days [67]. The CNF was produced by mechanical

homogenization, i.e., apparently a type of M-CNF (Table 7.1).

To date, no human biomonitoring studies specifically dealing with nanocellulose exposure have been performed. The few toxicological studies on nanocellulose-based products in humans are clinical trials for some specific biomedical applications. For instance, CNF (homogenized and without pre-treatment reported by the authors, M-CNF) was applied to develop a wound dressing assessed in a clinical trial on burn patients. No allergic reaction or inflammatory response was observed [17]. On the other hand, a BNC-containing wound dressing incorporating sericin and polyhexamethylene biguanide was assessed by applying it on the skin of healthy volunteers. No signs of irritation were shown on the skin of any of the individuals [68].

7.3.3 The Effect of Physicochemical Properties

It is well-recognized that physicochemical features of nanomaterials may affect their toxicity [40, 69, 70]. CNC and CNF are produced using different techniques, which dramatically affect their physicochemical characteristics (see Table 7.1). Hence, they also show different hazard features. CNC, which is internalized by macrophages and lung epithelial cells, triggers an inflammatory response. On the other hand, some types of CNFs, which may not be so efficiently phagocytized or taken up, elicit none or milder inflammatory reaction [62, 71]. Furthermore, both CNC and CNF show less hazardous effects than those produced by other nanofibres that also display a high aspect ratio and show long pulmonary biopersistence, such as multiwalled carbon nanotubes (MWCNTs) [51, 72]. E-CNF appeared to be more potent than MWCNTs in inducing systemic acute phase response in one *in vivo* study [52]. Therefore, differences in other physicochemical properties, such as rigidity or metal impurities, may explain the more severe effects of MWCNTs [66].

Differences in some physicochemical properties are also affecting the biological behavior of nanocelluloses belonging to a similar category (e.g., CNC vs. CNF). For instance, the interaction of CNF with dendritic cells depended on the thickness and length of the material [73]. On the other hand, the magnitude of the immune response triggered by three different CNCs in the human lung alveolar epithelial cell line A549 was directly related to their effective particle sizes [71]. Moreover, surface functionalization is indeed one of the key features [60]. Surface functionalized nanocelluloses are increasingly proposed for several applications, such as healthcare products and food packaging, due to the new beneficial properties imparted by the surface modifications [58]. The abundance of hydroxyl and carboxyl groups on the surface of nanocellulose, allowing subsequent modification with polymers, has made this material attractive for drug delivery applications [74, 75]. However, different functionalization will determine differences in the agglomeration rate, hydrophobicity, surface charge, and surface chemistry of nanocelluloses, affecting their cellular uptake, interaction with subcellular organelles and downstream biological responses [62]. Surface functionalization, which affects the material surface chemistry and the size (width) and morphology, has been reported to drive the inflammatory response to CNF [16]. A pro-inflammatory response, measured by cytokine secretion, was detected in THP-1 macrophages treated with an E-CNF. However, such an effect was not observed when the surface charge groups carboxymethyl (C-CNF) and hydroxypropyltrimethylammonium were introduced into CNF [16]. On the other hand, the same group has recently assessed the effects of CNFs with different surface modifications (carboxymethylation, hydroxypropyltrimethylammonium substitution, phosphorylation, and sulfoethylation) on the intestinal cell line Caco-2 [58]. In this case, CNF surface functionalization did not have an impact on the cell metabolic activity and cell membrane integrity. The effect of surface charge on the immunological response evoked by two differentially functionalized CNCs has been investigated

in a mouse macrophage-like cell line (J774A.1) and human THP-1 macrophages [76]. The cationic CNCs-poly (aminopropylmethacrylamide, APMA) showed a more robust secretion of inflammatory cytokines in the murine cell line, while the anionic CNCs-poly (N-isopropylacrylamide, NIPAAm) showed a significant NLRP3 inflammasome-dependent and independent immunological response in human macrophages. Furthermore, mitochondrial function was differentially affected by both types of CNCs. Differential induction of cell morphology changes was previously reported for the same CNCs, with CNCs-poly (NIPAAm) causing cell enlargement and elongation [77]. In another study, the capacity of one type of unmodified CNC and four cationic derivatives of it to stimulate NLRP3-inflammasome-dependent immunological response and enhance the production of mitochondrial reactive oxygen species (ROS) was analyzed in the J774A.1 cell line [78]. Only one of the cationic derivatives activated the inflammatory response, being the presence of amide linkage and fewer cationic polymer brushes the potential modulating factors. On the opposite, nanocellulose (denominated as CNC by the authors) bearing negatively charged carboxylic groups (introduced through TEMPO mediated oxidation), which were used as precursors to obtain hydrogel patches by cation-induced gelation, did not show cytotoxic effects on a human melanoma cell line [79]. A short-term repeated oral toxicity study revealed hepatotoxicity of a CNC modified with oxalate ester in the exposed rats [75]. As pointed out by the authors, the introduction of this functional group at the surface of CNC might increase its hydrophobicity, a surface characteristic that has been associated with increased cytotoxicity and inflammatory response. Unfortunately, the unmodified CNC was not included in the study of Otuechere et al. [75], which precludes raising conclusions on whether the observed deleterious effects were exclusively due to the modification.

Hadrup et al. [52] studied the adverse effects induced in mice exposed to E-CNF and carboxylated CNF, provided by different manufacturers, by intratracheal instillation. They concluded that

carboxylation of CNF was associated with reduced pulmonary and systemic toxicity, and suggested the involvement of hydroxy groups in the inflammatory and acute phase responses. This conclusion has to take into account that carboxylation (probably through TEMPO mediated oxidation, T-CNF, Table 7.1) causes a higher nanofibrillation of pulp fibers, compared to enzymatically pre-treated CNF (E-CNF), i.e., E-CNF may have a larger fraction of residual fibers, lower nanofibrillation yield and thicker and longer nanofibrils. Hence, conclusions about toxicity and considering only the surface modifications and chemistry of CNFs have to be taken with caution as in most cases, the effect of the surface modification cannot be decoupled from the CNF morphology and physical properties (e.g., width, length, nanofibrillation yield, and residual fibers). This is a crucial point, usually not considered in toxicological studies.

Similar results were found in other studies where the same materials and C-CNF were administrated to mice by (oro)pharyngeal aspiration [50, 51]. CNFs (apparently M-CNF and E-CNF based on the data provided by the authors and producers) were more prone to trigger inflammation [51] and to induce DNA strand breaks in the lungs [50] than those modified by carboxymethylation (C-CNF). Interestingly, when tested *in vitro*, E-CNF was the only material showing high cytotoxicity and significant increased production of the pro-inflammatory cytokines IL-1 β and TNF- α in exposed THP-1 macrophages [51]. But none of the materials induced cytotoxicity or genetic damage in human bronchial epithelial BEAS-2B cells, suggesting that the mechanisms involved in the genotoxic effects detected *in vivo* are not present in the *in vitro* model [50]. Alternatively, the increase of pro-inflammatory cytokines caused by E-CNF in this particular study may have been triggered by the relatively high endotoxin levels (1.27 endotoxin units/ml) reported by the authors [51].

Far from being an obstacle, the possibility of moderating biological responses by modifying the properties of the materials opens up the option of designing them safer [40, 80]. As concerns biomedical applications, the consideration at

early stages of the design of those attributes linked to the safety and efficacy of the product are the pillar of current quality-by-design approaches [81]. In that sense, the characterization needs, which are addressed in currently available regulatory documents for nanotechnology-enabled health products, have been extracted and categorized by the REFINE project [82]. Hence, requirements for characterization were suggested as endpoints for quality and safety assessments. Most of the extracted parameters refer to the nanoscale properties specific for or associated with the materials, such as size, shape, morphology, or surface properties [82]. However, the success of those strategies requires the existence of validated characterization methods for nanomaterials [70], which are still lacking for a reliable characterization of nanocelluloses, both in complex liquid media used in *in vitro* cellular models [69] and real occupational settings [46, 83].

7.3.4 Regulatory Frameworks

Nanomaterials are explicitly or implicitly covered by the European Union's (EU) regulatory framework, which consists of several pieces of horizontal and sector-specific legislation, each of them with a defined purpose and scope. For each regulation, specific provisions for the safety assessment and authorization of nanomaterials are applied [84].

As concerns the production of nanocelluloses, they are exempted from the Registration, Evaluation, Authorization, and Restriction of Chemical (REACH) regulation (1907/2006/EC). Cellulose is a natural polymer, and natural polymers (including nanofoms) are exempted from the REACH registration.

Worker protection is regulated in the EU through the directive on safety and health at work (89/391/EEC), the directive on risks related to chemical agents at work (98/24/EC), and their related national legislations. OEL values are set to any chemical agent relevant to the work environment, except for carcinogen (regulated by the carcinogens and mutagens directive, 2004/37/

EC). As mentioned above, no specific OEL values exist for nanocelluloses. The Permissible Exposure Limit allowable by the Occupational Safety and Health Administration (OSHA, USA) for cellulose dust is 5 mg/m³ for the respirable fraction, expressed as 8-h time-weighted average, TWA [57]. No OEL values for cellulose dust are available at the EU. Instead, several countries (*e.g.*, Finland) use the OEL value for unspecific organic dust as inhalable fraction (5 mg/m³, TWA). On the other hand, an OEL value of 0.01 fibers/cm³ has been recommended for nanocelluloses [85], which is the same value suggested for other biopersistent fibrous nanomaterials, *e.g.*, carbon nanofibers. However, the same authors recommended minimizing the exposure as far as reliable methods for quantitative measurement of air sample concentrations, which would allow comparison with the suggested OEL value, are available.

Although polymers are exempted from the REACH registration, they should comply with food-related regulations. Both cellulose fibers (millimetric scale) and micro-cellulose (micrometric scale) have been evaluated by the European Food and Safety Agency (EFSA) [86]. As neither intestinal absorption nor toxicity was observed, both materials were considered as safe. A similar statement applies to the chemically modified celluloses that were included in the same assessment. However, other types of modified celluloses should be considered as a different material than those authorized, and a new process to obtain the pre-marketing authorization must start. In the case of nanocelluloses, their nano features may affect the interaction with biological systems. Hence, a specific assessment is required during their safety evaluation, as described by the EFSA Guidance on Nanomaterials [86], which is currently under revision.

To date, no specific regulatory framework exists for nanomaterial-based medical products and devices. Instead, nanotechnology-enabled health products follow current regulatory frameworks for medicinal products or medical devices. However, they may require additional quality and safety assessments triggered by the nanomaterial's unique characteristics [82]. Furthermore, the clas-

sification of a product into a medicinal product or a medical device depends on the primary mode of action. Such classification may not always be clearly defined for nanotechnology-enabled health products due to their increasing complexity and high diversity. A product's components may have different modes of action, which are governed by different regulations [82]. Recently, a draft guideline on the quality requirements for drug-device combinations has been released [87].

Most of the 3D printing applications involving nanocelluloses are related to medical devices, which are regulated by the Medical Devices Regulation (EU) 2017/745 (MDR), and the In Vitro Diagnostic Medical Devices Regulation (EU) 2017/746 (IVDR). Both Regulations entered into force in May 2017 and have a staggered transitional period of 4 and 5 years, respectively. The latter does not contain specific requirements regarding nanomaterials, whereas several provisions on nanomaterials are included in the former [82]. The MDR requires special attention when devices have or consist of nanomaterials that can be released into the patient's or user's body unless they only come into contact with intact skin [82, 84]. An indication informing on the presence of nanomaterials on the device should be included on the device's label. Nanomaterials also require an independent safety assessment, even if the corresponding non-nano sized substance is already authorized. The biological evaluation -included in the safety assessment- can be performed according to the ISO/TC 194 (2012) [88]. The MDR also specifies that medical devices incorporating or consisting of a nanomaterial belong to class III, i.e., the highest risk class, unless the nanomaterial is encapsulated or bound in such a manner that it cannot be released into the patient's or user's body when the device is used within its intended purpose [84]. The guidance adopted by the Scientific Committee on Emerging and Newly Identified Health Risks (SCENIHR) on the Determination of Potential Health Effects of Nanomaterials Used in Medical Devices [89] can help to clarify how the MDR should be applied in practice. A summary of it can be found in Annex B of the REFINE white paper [82].

7.3.5 Safety Assessment and Testing Strategies

Safety assessment is required in all the above-described regulations, most of which agree on the human health and environmental effects that should be addressed [90]. Hazard assessment generally relies on several toxicological endpoints that are assessed using validated test guidelines or guidance documents, most of them still requiring animal experiments. However, new alternative methods, in agreement with the 3R principles, may replace them in the future [91]. 3R means that all animal tests should be replaced by alternative methods when this is possible (Replace), reduce the number of animals used as much as possible without compromising the quality of the data (Reduce), and that all experimental procedures are performed in a way that minimizes suffering, stress and pain of the animals (Refine). Besides, nanotechnology-enabled health products always require clinical trials before their use in clinical practice can be approved [82]. Therefore, the production and commercialization of nanocelluloses and nanocellulose-based products will have to comply with the corresponding regulatory requirements, depending on the products' intended final use. Nevertheless, it is highly advised to screen the toxic potential of the nanocelluloses, based on *in vitro* assays, at the pre-commercialization or pre-clinical stages, which allows supporting safe-by-design and quality-by-design strategies [41]. Figure 7.2 summarizes the different steps of the testing strategies that have been proposed, which would allow a safety assessment of nanocelluloses before their regulatory approval for medical applications.

One of the challenges in testing nanomaterials is that the observed toxic effects may change from one nanoform to another similar one that shows a slight variation in any of its physicochemical features [92]. Hence, a thorough characterization of the tested nanomaterials is required [70, 92]. Although protocols for characterizing nanocelluloses have recently been proposed [93], not well-validated methods are still

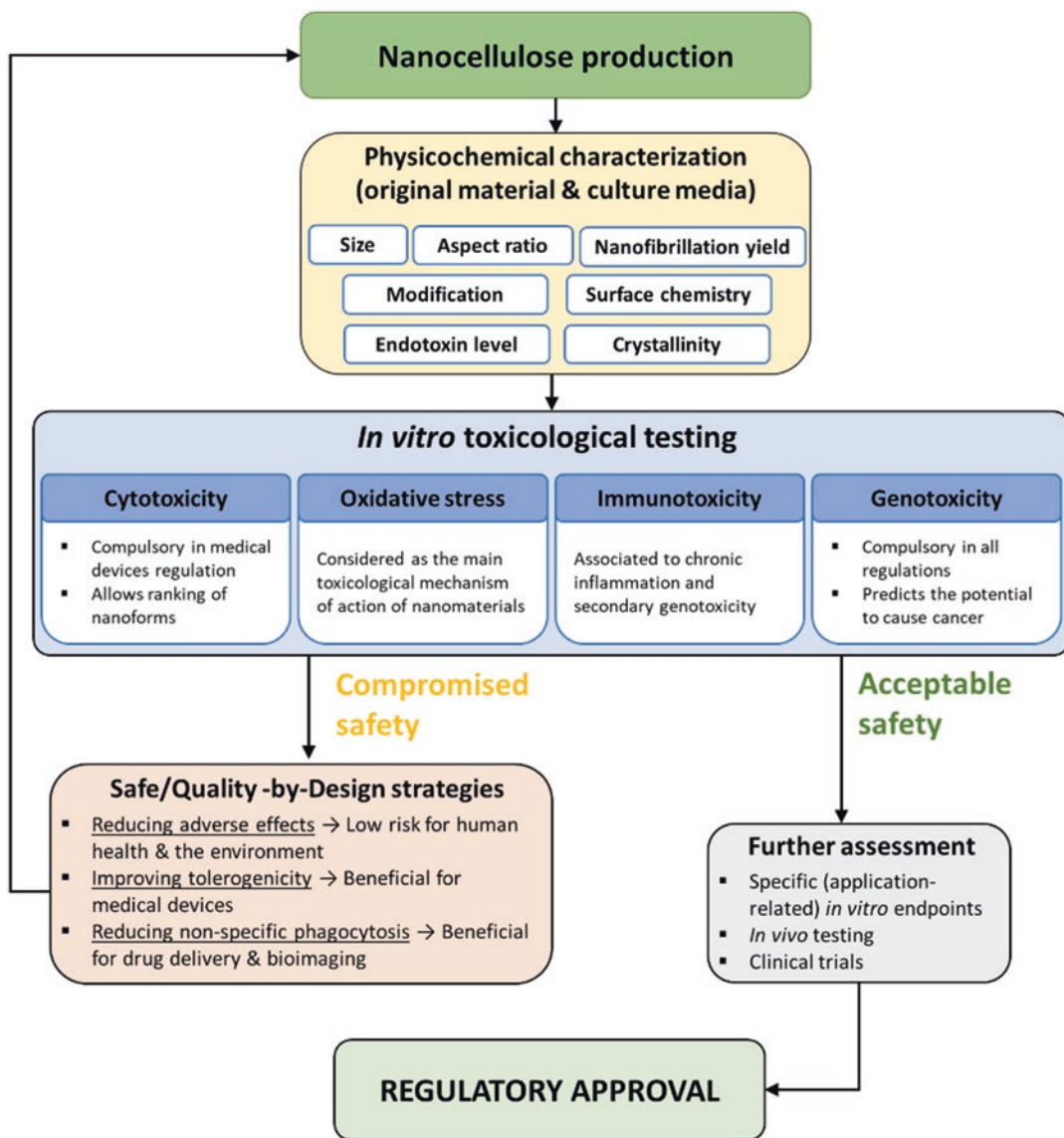


Fig. 7.2 A testing strategy for the safety assessment of nanocelluloses used in medical applications (based on Ventura et al. [62] and Čolić et al. [63])

available, especially concerning characterization in culture media [69].

Bacterial endotoxins are lipopolysaccharides originating from the outer wall of Gram-negative bacteria. Endotoxins are known to trigger inflammation, and they may induce oxidative stress and, subsequently, other toxic effects (*e.g.*, DNA damage) [94]. Therefore, demonstration of a level of endotoxins sufficiently low in the material is recommended when investigating the tox-

icity of nanomaterials [95], especially for immunotoxicity testing, and is required for biomedical applications [3, 94]. As bacterial endotoxins are common contaminants of naturally derived materials, endotoxin testing is especially relevant in the case of nanocelluloses [3]. However, endotoxin testing is challenging as nanomaterials may interfere with the endotoxin assays [94]. Polymyxin B has sometimes been used in parallel immunotoxicity experiments to

inhibit the potential effects of any endotoxin present in the CNF samples [16]. However, it is more desired to produce and handle the nanocelluloses in an environment as much endotoxin-free as possible. An illustrative example is the method that Nordli et al. [3] developed to obtain ultrapure T-CNF suitable for wound dressings.

Several testing strategies suitable for nanomaterials have been proposed in the last years [96–98]. All of them suggest a battery of assays to assess key endpoints involved in nanomaterials-induced adverse cellular effects [91]. Nanomaterials can induce cells to produce ROS, which may lead to pro-inflammatory effects. Increased ROS levels produced directly by the nanomaterial or as a consequence of the inflammatory response can result in DNA or chromosome damage [62, 91]. Each of these endpoints can be assessed using methods already existing for conventional chemicals. However, many of the methods need to be modified when applied to nanomaterials, mainly due to the materials' interference with the assays [84].

Cytotoxicity is usually the first step in assessing the toxicity of nanomaterials. It is one of the endpoints requested for testing of medical devices to obtain regulatory approval [Medical Devices Regulation (EU) 2017/745 (MDR)], and it is also required as a pre-test for establishing the range of doses to be evaluated in the genotoxicity assays [96]. However, although cytotoxicity assays are useful for the early screening and ranking of nanomaterials, they do not provide information on the type of hazardous event and the possible mechanism of action. Furthermore, the lack of cytotoxicity does not mean lack of hazardous effects [41]. For instance, Lopes et al. [16] reported inflammatory effects induced by E-CNFs (Table 7.1) in macrophages at doses that did not impair the cells' viability.

Generation of ROS is a normal mechanism in maintaining cellular metabolism, but when produced in excess (oxidative stress) results in adverse effects [75]. As oxidative stress is the prevailing paradigm in explaining how nanomaterials induce adverse cellular effects [91], this endpoint is included in most of the testing strategies proposed for nanomaterials, including the one suggested by

Endes et al. [99] to mimic the inhalation of high aspect ratio nanoparticles in a 3D lung model. Endes et al.'s and other strategies also recommend assessing immunotoxicity [97, 99], as inflammation is one of the initial steps that may give rise to lung fibrosis, secondary genotoxic effects, and carcinogenesis after inhaling biopersistent nanofibers [41]. Furthermore, immunotoxicity testing is part of the regulatory assessment of nanotechnology-enabled health products [82]. Finally, genotoxicity is a critical endpoint in the toxicity testing of nanomaterials [96, 97], as it is a hazard endpoint required in all the regulations previously described. It is because of the critical consequences of mutations on human health, as they play a crucial role in the initiation and progression of carcinogenesis, and reproductive and developmental abnormalities [41].

Current *in vitro* toxicological testing of nanomaterials is limited by the ability of the present assays to deal with secondary toxic mechanisms and organ specificity that are fully present only in a whole organism *in vivo* [41]. Co-culture of, *e.g.*, inflammatory and target cells and 3D tissue models may help in detecting secondary effects of nanomaterials, although the number of studies utilizing these techniques is scarce. In the case of nanocelluloses, an *in vitro* multicellular model of lung epithelium using an air-liquid interface cell exposure system was used to assess the specific fibre-cell interactions of two types of CNCs [100]. On the other hand, Ventura et al. [44] used a co-culture of A549 and THP-1 cells to assess the toxicity of T-CNFs. More recently, an advanced intestinal co-culture model consisting of Raji B, Caco-2, and HT29-MTX cells has been used for toxicological testing of CNFs [101]. Furthermore, omics approaches can present a supporting tool in elucidating the prevailing mechanisms of nanomaterials' toxicity. To date, only one study has assessed gene expression changes in the lung tissue of mice three months post-exposure to CNC using a high-throughput mRNA microarray [48]. However, more data is needed to validate these methods before making a clear conclusion and recommendations about their applicability [91].

7.4 3D Bioprinting of Biomaterials and Model Tissue Constructs

Significant advances have been made regarding 3D printing of biomaterials, and 3D bioprinting, including cell-laden bioinks, as well as supporting components into complex 3D functional scaffolds [102]. Hence, 3D bioprinting, which involves additional complexities, should consider the technical printing and the interaction of the biomaterial with the cells. However, there is still a lack of knowledge concerning the materials for bioprinting [103].

3D bioprinting implies requirements regarding the biomaterial preferences: the material must be dispensable in the technologies used for deposition and patterning, it needs to quickly solidify after material dispersing, maintain volume during and after 3D printing (not swell or shrink). A biomaterial to be tested for 3D bioprinting of, *e.g.*, tissue models, medical devices, and vehicles for drug delivery, should be biocompatible and safe, and this should be ensured as described in the previous sections. During 3D bioprinting, each layer should be joined together to keep the structure, mechanical characteristics should be similar to the *in vivo* situation, and it should be stable in a growth environment for cells, often 37 °C. Further, the material must allow cells to attach, migrate and proliferate; it should not be cytotoxic (as explained in the previous sections), and depending on the application, it should be degradable [102, 104].

Materials for 3D printing fall under two main categories, distinguished by their components and means of production, *i.e.* naturally derived and principally synthetic. Examples of naturally derived biomaterials for 3D printing are nanocellulose, collagen hydrogels, gelatin, agarose, hyaluronic acid-based hydrogels, alginate, and chitosan-alginate composite scaffolds [105]. Synthetic inks often consist of poly(ethylene glycol) (PEG), Polyvinylpyrrolidone (PVP), poly(lactic-co-glycolic acid) (PLGA) or Polycaprolactone (PLC).

Biomaterials are often combined to optimize a bioink; for example, nanocellulose has been

mixed with alginate to obtain better shear thinning, cell survival, cellular differentiation, and to keep a stable construct during culturing [26, 106]. This exemplifies an essential aspect of biomaterials, *i.e.*, that a single biomaterial cannot meet all the criteria necessary to fabricate a functional bioink for bioprinting [107].

Bioinks are utilized to fabricate scaffolds with specific shapes, sizes, and geometrical complexities to create 3D tissue constructs that may mimic the human body [108]. 3D structures enable different cell responses, compared to the corresponding 2D structures, *e.g.*, integrin expression, cell migration, cell mechanics, proliferation, differentiation, stemness [109–113]. The possibility to bioprint scaffolds to mimic the human microenvironment as *in vitro* models makes it possible for various applications, such as tissue engineering, regenerative medicine, drug screening with high-throughput assays, wound dressing, transplantation, and clinical application [108]. Different tissue constructs that mimic native tissues and organs have been successfully bioprinted utilizing several 3D printing approaches, for example; skin [114], cardiac [115], bone [116], cartilage [117], liver [118], and lung [119]. However, the fabrication of fully functional tissue models and organs is still demanding due to limitations regarding, *e.g.*, vascularization [120].

3D bioprinting has been an alternative for tissue engineering and regenerative medicine and a robust drug screening tool and discovery tool. 3D bioprinting will facilitate these *in vitro* models that potentially represent the specific pathological environment of patients. Remember that the lack of relevant human mimicking pre-clinical models is a primary reason for drug candidates failing in clinical trials [121, 122]. Additionally, multiple cancer cell lines have exhibited more drug resistance when cultured in 3D than 2D [123–125], and drug resistance in the 3D cultures has also been shown more similar to *in vivo* models [126–130]. It is also important to emphasize that there are increasing legal requirements and public opinions for the use of alternative, non-animal models in the regulatory safety assessment of chemicals, drugs, and medical devices [131]. It is considered one of the significant driv-

ing forces regarding the research community's efforts to develop fully functional tissue models by 3D bioprinting technologies. It is important to emphasize that the research community, pharmaceutical companies, and regulatory instances are striving to work according to 3R (Replace, Reduce, Refine).

7.4.1 Nanocellulose-Based Inks for 3D Printing

Specifically, nanocelluloses have demonstrated a considerable potential to be utilized in 3D printing of several medical devices and tissue models, including wound dressings, tissue engineering models, and drug delivery. The performance of nanocellulose inks on 3D printing operations depends on various factors, including i) the concentration, ii) the rheology, iii) surface chemistry, and iv) the cellulose nanofibril and cellulose nanocrystal physical characteristics.

The research and development of nanocelluloses have advanced, and this is exemplified by various companies that are presently offering nanocelluloses that can be used for 3D printing applications. Companies were requested to provide information about their corresponding (semi)commercial products, and the information provided by the companies that kindly responded to this request is listed in Table 7.2.

The commercial nanocelluloses are obtained from different sources from woody biomass (soft- and hardwood) and marine animals (Tunicates), applying various pre-treatments and consequently have different characteristics (Table 7.2). It is crucial to provide such specifications relevant to the 3D printing process and understand the application of nanocellulose-based inks for specific 3D bioprinting purposes and the corresponding biological effects.

Various types of nanocelluloses can be applied for 3D bioprinting processes [26, 132–135]. The concentration of nanocellulose inks can also be tuned, which may affect the structure of the scaffolds. The porosity and pore connectivity in scaffolds are essential for the diffusion of nutrients during the maturing of tissue models. The struc-

tures of the 3D printed scaffolds are observed in Fig. 7.3. Note the differences regarding the porosity and pore wall roughness, which are most probably caused by the nanofibril morphology.

Compared to BNC, which has been extensively developed for wound dressings [136], T-CNF has been proposed as a good alternative as it can form translucent structures, with good liquid absorption, adequate mechanical strength in wet conditions [137], some antimicrobial properties [138, 139] and particular immunogenic properties [140, 141]. Also, nanocelluloses are in general 3D printable (Fig. 7.3), which opens the possibility to 3D bioprint skin constructs, *e.g.*, for testing wound dressings or for medical use in wound healing situations.

As mentioned above, one of the potential and promising applications of nanocellulose-based inks is the fabrication of tissue models for, *e.g.*, cancer research (Figs. 7.4 and 7.5). Scaffolds can be 3D printed, freeze-dried, and seeded with cancer cells. The scaffolds are incubated for a limited time, and laboratory testing can be performed, *e.g.*, gene expression analysis, western blot, flow cytometry, and functional testing (Fig. 7.4).

In Fig. 7.5, breast cancer cells have been grown on T-CNF and imaged using scanning electron microscopy (SEM). It clearly shows that cells are attaching to the surface, and there are many different phenotypes of cells. Note the different shapes such as elongated and rounded up. Further, it also shows that cell interconnection exists between adjacent cancer cells and cells that are far from each other. It is considered a promising observation as cancer cells can be grown on T-CNF scaffolds. The next steps currently being explored are the maturation of such constructs and the cancer cells' corresponding characterization through gene expression analysis. This approach will potentially facilitate cancer tissue models that can be applied for drug screening and, thus, developing personalized medicine for cancer treatment.

It is important to note that nanocelluloses used for 3D printing of tissue models, *e.g.*, drug screening, could be easier to commercialize than nanocelluloses that will be applied for, *e.g.*, tissue engineering and medical devices that will be in

Table 7.2 Characteristics of some (semi)commercial nanocelluloses. All the values in this table has been kindly provided by the corresponding companies

Commercial name	Raw material	Pre-treatment/ Type of nanocellulose	Concentration (wt%)	Purity (%)	Crystallinity (%)	Degree of polymerization	Nanofibril morphology (nm)	Endotoxin content (EU/ml)	Commercial/ Semi-commercial	Company
TUNICELL ETC	Tunicates	Enzymatic	2.5	Glucose 99.2 ± 0.3	89.07 ± 1.6	3900–4200	Width: 8.5 Length: 2519	≤0.5	Commercial	Ocean TuniCell, Norway
Exilva	Softwood sulfite pulp	Not stated	2–10	Hemicellulose <10 Lignin <1	Not stated	800–2000	Diameter range: 5–1000 nm	Not stated	Commercial	Borregaard, Norway
Corbiocel	Hardwood Kraft bleached pulp	TEMPO mediated oxidation	1–2	Extractives: 0.4 Lignin: 0.3 Glucan: 73.7 Xylan: 19.5 Ashes: 0.7	Not stated	250–270	Width: 2–3 Length: 400–600	Not stated	Semi-commercial	Regemat3D, Spain
GrowInk™	Hardwood Kraft pulp	“Native” nanofibrillar cellulose and anionic nanofibrillar cellulose	< 3 wt%	Contains hemicellulose	~70	500–1800	Width: 4–20 length: 1000–20,000 (depending obviously somewhat on grade)	<5	Commercial product, potential for use in clinical environment.* manufactured according to ISO13485 standard.	UPM, Finland

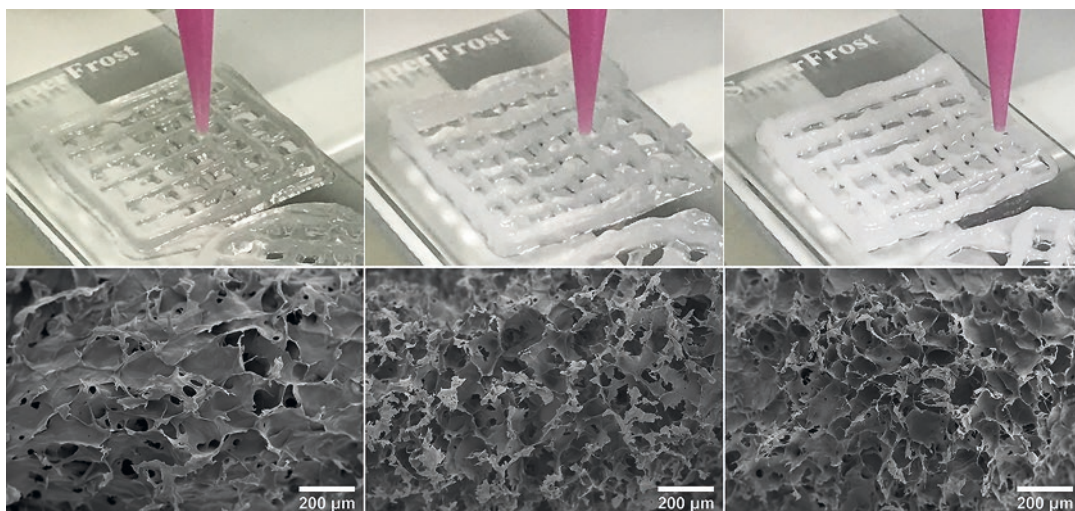


Fig. 7.3 3D printing of different CNFs and the corresponding pore structures of the printed and freeze-dried structures. Left) T-CNF (2.5 wt%, produced by RISE PFI). Middle) TUNICELL ETC CNF (2.5 wt produced by Ocean TuniCell AS). Right) Exilva CNF (5 wt%, pro-

duced by Borregaard). All the scaffolds were 3D printed with a Regemat3D printing unit, utilizing a nozzle of 0.41 mm and a speed of 3 mm/s. The same settings were used in all the printing operations, and no attempt was made to improve the 3D print quality

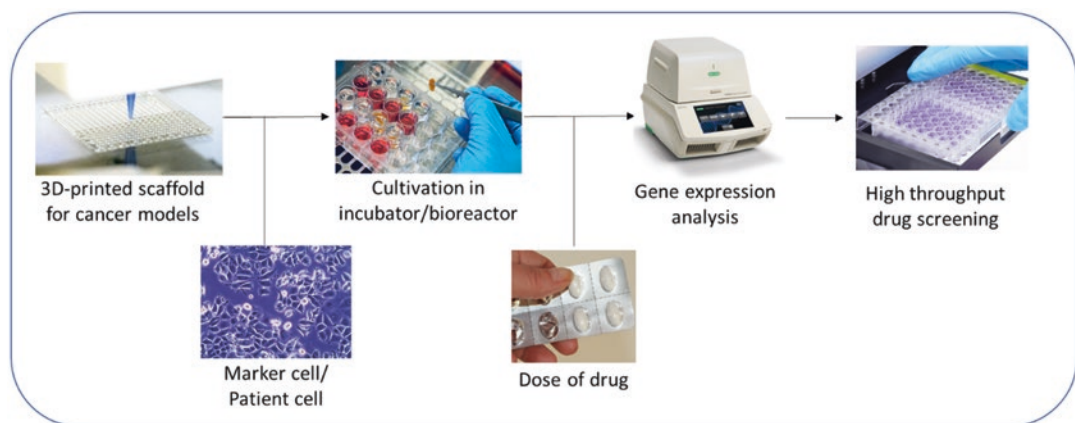


Fig. 7.4 Workflow of drug screening using 3D printed tissue scaffold and gene expression analysis

direct contact with human tissue. This is due to the extensive regulations applied to nanomaterials (Regulation (EU) 2017/745) that can be released into the patient's or user's body. However, the development of nanocellulose for 3D printing of tissue models should follow the Regulation (EU) 2017/746 on In-Vitro Diagnostic Devices.

7.5 Concluding Remarks

This book chapter has provided an overview of nanotoxicology and safety aspects associated with different types of nanocelluloses, including CNC and CNF. Although the assessed nanocelluloses are mainly obtained from woody biomass, different kinds of nanocelluloses can be produced

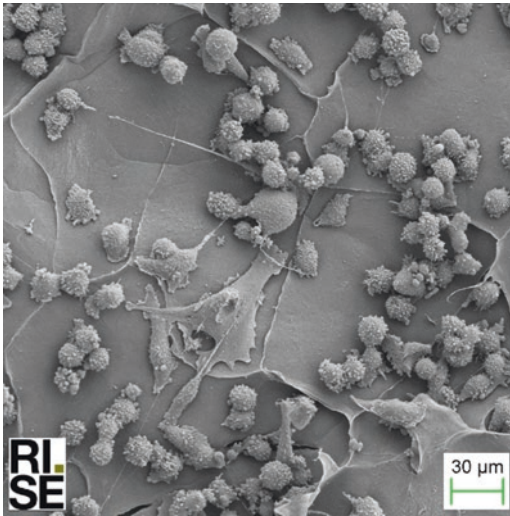


Fig. 7.5 Cancer cells grown on T-CNF 3D printed scaffolds. The concentration of the T-CNF was 1%, and the scaffolds were freeze-dried

from tunicates or bacterial biosynthesis. Relevant regulatory requirements were considered. Finally, a short overview was provided of (semi)commercial nanocelluloses that are or can be used as ink components for 3D bioprinting, and a specific example towards bioprinting of cancer tissue model was exemplified. This demonstrates the potential of nanocellulose as a natural biopolymer for biomedical applications, also considering aspects related to regulatory approval before commercialization.

Acknowledgments The authors would like to thank Dr. Piia Taxell (Finnish Institute of Occupational Health) and the European Chemicals Agency (ECHA) for providing information on the workers' regulations and the current status of nanocelluloses under the REACH regulation, respectively. Sarunas Petronis (RISE) is acknowledged for acquiring the SEM image with cancer cells. This paper was funded by the Finnish Work Environment Fund (grant no. 117146), Swedish foundation for strategic research and by the OxyPol project, Nano2021 program, Research Council of Norway (grant no. 309178).

References

1. Mertaniemi H et al (2016) Human stem cell decorated nanocellulose threads for biomedical applications. *Biomaterials* 82:208–220

2. Lou YR et al (2014) The use of Nanofibrillar cellulose hydrogel as a flexible three-dimensional model to culture human pluripotent stem cells. *Stem Cells Dev* 23(4):380–392
3. Nordli HRC-C, Rokstad AM, Pukstad B (2016) Producing ultrapure wood cellulose nanofibrils and evaluating the cytotoxicity using human skin cells. *Carbohydr Polym* 150:65–73
4. Kuzmenko V et al (2018) Tailor-made conductive inks from cellulose nanofibrils for 3D printing of neural guidelines. *Carbohydr Polym* 189:22–30
5. Rashad A et al (2017) Cytocompatibility of wood-derived cellulose Nanofibril hydrogels with different surface chemistry. *Biomacromolecules* 18(4):1238–1248
6. Chimene D, Kaunas R, Gaharwar AK (2020) Hydrogel bioink reinforcement for additive manufacturing: a focused review of emerging strategies. *Adv Mater* 32(1):e1902026
7. Chiulan I et al (2017) Recent advances in 3D printing of aliphatic polyesters. *Bioengineering (Basel)* 5(1)
8. Chinga-Carrasco G (2018) Potential and limitations of Nanocelluloses as components in biocomposite inks for three-dimensional bioprinting and for biomedical devices. *Biomacromolecules* 19(3):701–711
9. Marga F et al (2012) Toward engineering functional organ modules by additive manufacturing. *Biofabrication* 4(2):022001
10. Wang X, Wang Q, Xu C (2020) Nanocellulose-based inks for 3D bioprinting: key aspects in research development and challenging perspectives in applications—a mini review. *Bioengineering (Basel)* 7(2)
11. Xu W et al (2018) Three-dimensional printing of wood-derived biopolymers: a review focused on biomedical applications. *ACS Sustain Chem Eng* 6(5):5663–5680
12. Saito T et al (2006) Homogeneous suspensions of individualized microfibrils from TEMPO-catalyzed oxidation of native cellulose. *Biomacromolecules* 7(6):1687–1691
13. Wagberg L et al (2008) The build-up of polyelectrolyte multilayers of microfibrillated cellulose and cationic polyelectrolytes. *Langmuir* 24(3):784–795
14. Fukuzumi H, Saito T, Isogai A (2013) Influence of TEMPO-oxidized cellulose nanofibril length on film properties. *Carbohydr Polym* 93(1):172–177
15. Habibi Y, Lucia LA, Rojas OJ (2010) Cellulose nanocrystals: chemistry, self-assembly, and applications. *Chem Rev* 110(6):3479–3500
16. Lopes VRS-M, Strømme M, Ferraz N (2017) In vitro biological responses to nanofibrillated cellulose by human dermal, lung and immune cells: surface chemistry aspect. *Part Fibre Toxicol* 14(1):1
17. Hakkarainen T et al (2016) Nanofibrillar cellulose wound dressing in skin graft donor site treatment. *J Control Release* 244(Pt B):292–301
18. DeLoid GMC, Molina RM, Silva DI, Bhattacharya K, Ng KW, Loo SCJ, Brain JD, Demokritou P (2019) Toxicological effects of ingested nanocellu-

- lose in in vitro intestinal epithelium and in vivo rat models. *Environ Sci. Nano* 6(7):2105–2115
19. Fall AB, Burman A, Wagberg L (2014) Cellulosic nanofibrils from eucalyptus, acacia and pine fibers. *Nordic Pulp Paper Res J* 29(1):176–184
 20. Liimatainen H et al (2012) Enhancement of the Nanofibrillation of wood cellulose through sequential Periodate-chlorite oxidation. *Biomacromolecules* 13(5):1592–1597
 21. Chinga-Carrasco G, Syverud K (2014) Pretreatment-dependent surface chemistry of wood nanocellulose for pH-sensitive hydrogels. *J Biomater Appl* 29(3):423–432
 22. Kokol V et al (2015) Characterisation and properties of homo- and heterogeneously phosphorylated nanocellulose. *Carbohydr Polym* 125:301–313
 23. Dri FLHJ, Moon RJ, Zavattieri PD (2013) Anisotropy of the elastic properties of crystalline cellulose I β from first principles density functional theory with Van der Waals interactions. *Cellulose* 20:2703–2718
 24. Heggset EB, Chinga-Carrasco G, Syverud K (2017) Temperature stability of nanocellulose dispersions. *Carbohydr Polym* 157:114–121
 25. Le Van H (2017) Properties of nano-fibrillated cellulose and its length-width ratio determined by a new method. *Cellul Chem Technol* 51(7–8):649–653
 26. Markstedt K et al (2015) 3D bioprinting human chondrocytes with Nanocellulose-alginate bio-ink for cartilage tissue engineering applications. *Biomacromolecules* 16(5):1489–1496
 27. Moberg T et al (2017) Rheological properties of nanocellulose suspensions: effects of fibril/particle dimensions and surface characteristics. *Cellulose* 24(6):2499–2510
 28. Tanaka R et al (2014) Determination of nanocellulose fibril length by shear viscosity measurement. *Cellulose* 21(3):1581–1589
 29. Sacui IA et al (2014) Comparison of the properties of cellulose nanocrystals and cellulose Nanofibrils isolated from bacteria, tunicate, and wood processed using acid, enzymatic, mechanical, and oxidative methods. *ACS Appl Mater Interfaces* 6(9):6127–6138
 30. Gorgieva, S. and J. Trcek, Bacterial cellulose: production, modification and perspectives in biomedical applications. *Nanomaterials* (Basel), 2019. 9(10)
 31. Molina-Ramirez C et al (2017) Effect of different carbon sources on bacterial Nanocellulose production and structure using the low pH resistant strain *Komagataeibacter Medelinensis*. *Materials* 10(6)
 32. Choi SM, Shin EJ (2020) The Nanofication and functionalization of bacterial cellulose and its applications. *Nanomaterials* (Basel) 10(3)
 33. Gutierrez E et al (2019) 3D printing of antimicrobial alginate/bacterial-cellulose composite hydrogels by incorporating copper nanostructures. *ACS Biomater Sci Eng* 5(11):6290–6299
 34. Kimura SI (1996) New cellulose synthesizing complexes (terminal complexes) involved in animal cellulose bio, synthesis in the tunicate *Metandrocarpa uedai*. *Protoplasma* 194:151–163
 35. Zhao Y et al (2017) Cellulose nanofibers from softwood, hardwood, and tunicate: preparation-structure-film performance interrelation. *ACS Appl Mater Interfaces* 9(15):13508–13519
 36. Endes CC-E, Mueller S, Foster EJ, Petri-Fink A, Rothen-Rutishauser B, Weder C, Clift MJ (2016) A critical review of the current knowledge regarding the biological impact of nanocellulose. *J Nanobiotechnology* 14(1):78
 37. Donaldson KM, Duffin R, Poland CA (2010) Asbestos, carbon nanotubes and the pleural mesothelium: a review of the hypothesis regarding the role of long fibre retention in the parietal pleura, inflammation and mesothelioma. Part *Fibre Toxicol* 7(5):1–17
 38. Stanton MF (1973) Some etiologic considerations of fibre carcinogenesis., 289–294. In: ‘Biological effects of asbestos’ WHO IARC. Lyon Bogovski P, Gilson JC, Timbrell V, Wagner JC
 39. Donaldson K, Poland CA (2009) Nanotoxicology: new insights into nanotubes. *Nat Nanotechnol* 4(11):708–710
 40. Lynch I, Weiss C, Valsami-Jones E (2014) A strategy for grouping of nanomaterials based on key physico-chemical descriptors as a basis for safer-by-design NMs. *Nano Today* 9(3):266–270
 41. Catalán J, Norppa H (2017) Safety aspects of bio-based nanomaterials. *Bioengineering* (Basel) 4:4
 42. Stoudmann N et al (2020) Human hazard potential of nanocellulose: quantitative insights from the literature. *Nanotoxicology*:1–17
 43. Chinga-Carrasco G (2011) Cellulose fibres, nanofibrils and microfibrils: the morphological sequence of MFC components from a plant physiology and fibre technology point of view. *Nanoscale Res Lett* 6(1):417
 44. Ventura CL, Sousa-Uva A, Ferreira PJT, Silva MJ (2018) Evaluating the genotoxicity of cellulose nanofibrils in a co-culture of human lung epithelial cells and monocyte-derived macrophages. *Toxicol Lett* 291:173–183
 45. Ede JD et al (2019) Risk analysis of cellulose nanomaterials by inhalation: current state of science. *Nanomaterials* (Basel) 9(3)
 46. Shatkin JA, Kim B (2015) Cellulose nanomaterials: life cycle risk assessment, and environmental health and safety roadmap. *Environ Sci Nano* 2(5):477–499
 47. Stefaniak AB et al (2014) Lung biodurability and free radical production of cellulose nanomaterials. *Inhal Toxicol* 26(12):733–749
 48. Shvedova AAK, Yanamala N, Farcas MT, Menas AL, Williams A, Fournier PM, Reynolds JS, Gutkin DW, Star A, Reiner RS, Halappanavar S, Kagan VE (2016) Gender differences in murine pulmonary responses elicited by cellulose nanocrystals. Part *Fibre Toxicol* 13(1):28
 49. Catalán JR, Aimonen K, Hannukainen KS, Suhonen S, Vanhala E, Moreno C, Meyer V, Perez DD, Sneek A, Forsström U, Højgaard C, Willemoes M, Winther JR, Vogel U, Wolff H, Alenius H, Savolainen KM, Norppa H (2017) Genotoxic and inflammatory

- effects of nanofibrillated cellulose in murine lungs. *Mutagenesis* 32(1):23–31
50. Lindberg HKC, Aimonen KJ, Wolff H, Wedin I, Nuopponen M, Savolainen KM, Norppa H (2017) Evaluation of the genotoxic potential of different types of nanofibrillated celluloses. *TechConnect Briefs*:229–232
 51. Ilves MV, Aimonen K, Lindberg HK, Pesonen S, Wedin I, Nuopponen M, Vanhala E, Højgaard C, Winther JR, Willemoës M, Vogel U, Wolff H, Norppa H, Savolainen K, Alenius H (2018) Nanofibrillated cellulose causes acute pulmonary inflammation that subsides within a month. *Nanotoxicology* 12(7):729–746
 52. Hadrup NK, Berthing T, Wolff H, Bengtson S, Kofoed C, Espersen R, Højgaard C, Winther JR, Willemoës M, Wedin I, Nuopponen M, Alenius H, Norppa H, Wallin H, Vogel U (2019) Pulmonary effects of nanofibrillated celluloses in mice suggest that carboxylation lowers the inflammatory and acute phase responses. *Environ Toxicol Pharmacol* 66:116–125
 53. Silva-Carvalho RS, Ferreirinha P, Leitão AF, Andrade FK, Gil da Costa RM, Cristelo C, Rosa MF, Vilanova M, Gama FM (2019) Inhalation of bacterial cellulose Nanofibrils triggers an inflammatory response and changes lung tissue morphology of mice. *Toxicol Res* 35(1):45–63
 54. Vartiainen JP, Sirola K, Pylkkänen L, Alenius H, Hokkinen J, Tapper U, Lahtinen P, Kapanen A, Putkisto K, Hiekkataipale P, Eronen P, Ruokolainen J, Laukkanen A (2011) Health and environmental safety aspects of friction grinding and spray drying of microfibrillated cellulose. *Cellulose* 18(3):775–786
 55. O'Connor, B.B., R.; Goguen, R. , Commercialization of cellulose nanocrystal (NCC™) production: a business case focusing on the importance of proactive EHS management, in *Nanotechnology environmental health and safety*, M. Hull, Bowman, D., Editor. 2014, Elsevier Inc Oxford. p. 225–246
 56. Martinez KF, Rudie A, Geraci C (2014) Occupational exposure characterization during the manufacture of cellulose nanomaterials. In: *Production and applications of cellulose nanomaterials*. TAPPI Press, pp 61–64
 57. Shatkin JAO, Comment on Shvedova et al (2016) Gender differences in murine pulmonary responses elicited by cellulose nanocrystals. *Part Fibre Toxicol* 13(1):59
 58. Lopes VRS, Ferraz N (2020) In vitro biological impact of nanocellulose fibers on human gut bacteria and gastrointestinal cells. *Nano* 10(6)
 59. Reid MS, Karlsson M, Abitbol T (2020) Fluorescently labeled cellulose nanofibrils for detection and loss analysis. *Carbohydr Polym* 250:116943
 60. Roman M (2015) Toxicity of cellulose nanocrystals: a review. *Ind Biotechnol* 11(1):25–33
 61. Seabra ABB, Fávaro WJ, Paula AJ, Durán N (2018) Cellulose nanocrystals as carriers in medicine and their toxicities: a review. *Carbohydr Polym* 181:514–527
 62. Ventura CP, Lourenço AF, Ferreira PJT, Louro H, Silva MJ (2020) On the toxicity of cellulose nanocrystals and nanofibrils in animal and cellular models. *Cellulose* 27(10):5509–5544
 63. Čolić MT, Bekić M (2020) Immunological aspects of nanocellulose. *Immunol Lett* 222:80–89
 64. Yanamala NF, Hatfield MK, Kisin ER, Kagan VE, Geraci CL, Shvedova AA (2014) In vivo evaluation of the pulmonary toxicity of cellulose nanocrystals: a renewable and sustainable nanomaterial of the future. *ACS Sustainable Chemistry and Engineering* 2(7):1691–1698
 65. Farcas MTK, Menas AL, Gutkin DW, Star A, Reiner RS, Yanamala N, Savolainen K, Shvedova AA (2016) Pulmonary exposure to cellulose nanocrystals caused deleterious effects to reproductive system in male mice. *J Toxicol Environ Health A* 79(21):984–997
 66. Park EJ et al (2018) Fibrous nanocellulose, crystalline nanocellulose, carbon nanotubes, and crocidolite asbestos elicit disparate immune responses upon pharyngeal aspiration in mice. *J Immunotoxicol* 15(1):12–23
 67. Ong KJ et al (2020) A 90-day dietary study with fibrillated cellulose in Sprague-Dawley rats. *Toxicol Rep* 7:174–182
 68. Napavichayanun S, Yamdech R, Aramwit P (2016) The safety and efficacy of bacterial nanocellulose wound dressing incorporating sericin and polyhexamethylene biguanide: in vitro, in vivo and clinical studies. *Arch Dermatol Res* 308(2):123–132
 69. Bitounis D et al (2019) Dispersion preparation, characterization, and dosimetric analysis of cellulose nano-fibrils and nano-crystals: implications for cellular toxicological studies. *NanoImpact* 15
 70. OECD (2019) Physical-chemical decision framework to inform decisions for risk assessment of manufactured nanomaterials. *ENV/JM/MONO(2019)12*, Series on the Safety of Manufactured Nanomaterials, 2019. 90
 71. Menas ALY, Farcas MT, Russo M, Friend S, Fournier PM, Star A, Iavicoli I, Shurin GV, Vogel UB, Fadeel B, Beezhold D, Kisin ER, Shvedova AA (2017) Fibrillar vs crystalline nanocellulose pulmonary epithelial cell responses: cytotoxicity or inflammation? *Chemosphere* 171:671–680
 72. Clift MJDF, Vanhecke D, Studer D, Wick P, Gehr P, Rothen-Rutishauser B, Weder C (2011) Investigating the interaction of cellulose nanofibers derived from cotton with a sophisticated 3D human lung cell coculture. *Biomacromolecules* 12(10):3666–3673
 73. Tomić S et al (2016) Native cellulose nanofibrils induce immune tolerance in vitro by acting on dendritic cells. *Sci Rep* 6(1):31618
 74. Khine YYB, Raveendran R, Stenzel MH (2020) Photo-induced modification of Nanocellulose: the Design of Self-Fluorescent Drug Carriers. *Macromol Rapid Commun* 41(1):e1900499
 75. Otuechere CAA, Adebayo OL, Ebigwei IA (2020) In vivo hepatotoxicity of chemically modified nanocellulose in rats. *Hum Exp Toxicol* 39(2):212–223


76. Despres HWS, Anderson P, Hemraz UD, Boluk Y, Sunasee R, Ckless K (2019) Mechanisms of the immune response cause by cationic and anionic surface functionalized cellulose nanocrystals using cell-based assays. *Toxicol In Vitro* 55:124–133
77. Jimenez AS et al (2017) Effect of surface organic coatings of cellulose nanocrystals on the viability of mammalian cell lines. *Nanotechnol Sci Appl* 10:123–136
78. Sunasee RA, Pyram D, Hemraz UD, Boluk Y, Ckless K (2015) Cellulose nanocrystal cationic derivative induces NLRP3 inflammasome-dependent IL-1 β secretion associated with mitochondrial ROS production. *Biochem Biophys Rep* 4:1–9
79. Meschini SP, Maestri CA, Condello M, Bettotti P, Condello G, Scarpa M (2020) In vitro toxicity assessment of hydrogel patches obtained by cation-induced cross-linking of rod-like cellulose nanocrystals. *J Biomed Mater Res B Appl Biomater* 108(3):687–697
80. Kraegeloh A et al (2018) Implementation of safe-by-Design for Nanomaterial Development and Safe Innovation: why we need a comprehensive approach. *Nanomaterials (Basel)* 8(4)
81. Bastogne T (2017) Quality-by-design of nanopharmaceuticals – a state of the art. *Nanomedicine* 13(7):2151–2157
82. Halamoda Kenzaoui B, Box H, Van Elk M, Gaitan S, Geertsma R, Gainza Lafuente E, Owen A, Del Pozo A, Roesslein M, Bremer S (2019) Anticipation of regulatory needs for nanotechnology-enabled health products. EUR 29919 EN: Publications Office of the European Union, Luxembourg
83. Roberts RG, Stebounova LV, Anne Shatkin J, Peters T, Johan Foster E (2019) Collection of airborne ultrafine cellulose nanocrystals by impinger with an efficiency mimicking deposition in the human respiratory system. *J Occup Environ Hyg* 16(2):141–150
84. Rauscher H, Rasmussen K, Sokull-Klüttgen B (2017) Regulatory aspects of nanomaterials in the EU. *Chemie Ingenieur Technik* 89(3):224–231
85. Stockmann-Juvala HT, Santonen T (2014) Formulating Occupational Exposure Limits Values (OELs) (Inhalation & Dermal). Helsinki, Finland: Finnish Institute of Occupational Health
86. Additives EPOF et al (2018) Re-evaluation of celluloses E 460(i), E 460(ii), E 461, E 462, E 463, E 464, E 465, E 466, E 468 and E 469 as food additives. *EFSA J* 16(1):e05047
87. EMA (2019) Guideline on the quality requirements for drug-device combinations https://www.ema.europa.eu/en/documents/scientific-guideline/draft-guideline-quality-requirements-drug-device-combinations_en.pdf, 2019
88. 194., I.T. (2012) Biological evaluation of medical devices- Part 22: Guidance on nanomaterials. . ISO / TR 10993–22
89. SCENIHR (2015) Opinion on the guidance on the determination of potential health effects of nanomaterials used in medical devices. Final Opinion January:1–77
90. Ong KJS, Nelson K, Ede JD, Retsina T (2017) Establishing the safety of novel bio-based cellulose nanomaterials for commercialization. *NanoImpact* 6:19–29
91. Drasler B et al (2017) In vitro approaches to assess the hazard of nanomaterials. *NanoImpact* 8:99–116
92. Gao X, Lowry GV (2018) Progress towards standardized and validated characterizations for measuring physicochemical properties of manufactured nanomaterials relevant to nano health and safety risks. *NanoImpact* 9:14–30
93. Foster EJ et al (2018) Current characterization methods for cellulose nanomaterials. *Chem Soc Rev* 47(8):2609–2679
94. Giannakou C et al (2019) Sensitive method for endotoxin determination in nanomedicinal product samples. *Nanomedicine (Lond)* 14(10):1231–1246
95. Agency EC (2017) Guidance on information requirements and chemical safety assessment. Appendix R7–1 for nanomaterials applicable to Chapter R7a, Version 2.0
96. Dusinska M et al (2015) Towards an alternative testing strategy for nanomaterials used in nanomedicine: lessons from NanoTEST. *Nanotoxicology* 9(Suppl 1):118–132
97. Dusinska M et al (2017) Immunotoxicity, genotoxicity and epigenetic toxicity of nanomaterials: new strategies for toxicity testing? *Food Chem Toxicol* 109(Pt 1):797–811
98. EFSA Scientific Committee, Benford D, Halldorsson T, Jeger MJ, Knutsen HK, More S, Naegeli H, Noteborn H, Ockleford C, Ricci A, Rychen G, Schlatter JR, Silano V, Solecki R, Turck D, Younes M, Chaudhry Q, Cubadda F, Gott D, Oomen A, Weigel S, Karamitrou M, Schoonjans R, Mortensen A (2018) Guidance on risk assessment of the application of nanoscience and nanotechnologies in the food and feed chain: part 1, human and animal health. *EFSA J* 16(7):95
99. Endes C et al (2014) An in vitro testing strategy towards mimicking the inhalation of high aspect ratio nanoparticles. *Part Fibre Toxicol* 11:40
100. Endes C et al (2015) Fate of cellulose nanocrystal aerosols deposited on the lung cell surface in vitro. *Biomacromolecules* 16(4):1267–1275
101. Pradhan SH et al (2020) Physical, chemical, and toxicological characterization of fibrillated forms of cellulose using an in vitro gastrointestinal digestion and co-culture model. *Toxicol Res (Camb)* 9(3):290–301
102. Murphy SV, Atala A (2014) 3D bioprinting of tissues and organs. *Nat Biotechnol* 32(8):773–785
103. Gungor-Ozkerim PS et al (2018) Bioinks for 3D bioprinting: an overview. *Biomater Sci* 6(5):915–946
104. Hölzl KL, Tytgat L, Van Vlierberghhe S, Gu L, Ovsianikov A (2016) Bioink properties before, during and after 3D bioprinting. *Biofabrication* 8(3):032002

105. Rijal G, Li W (2016) 3D scaffolds in breast cancer research. *Biomaterials* 81:135–156
106. Jessop ZM et al (2019) Printability of pulp derived crystal, fibril and blend nanocellulose-alginate bioinks for extrusion 3D bioprinting. *Biofabrication* 11(4):045006
107. Ojansivu M et al (2019) Wood-based nanocellulose and bioactive glass modified gelatin-alginate bioinks for 3D bioprinting of bone cells. *Biofabrication* 11(3):035010
108. Matai I et al (2020) Progress in 3D bioprinting technology for tissue/organ regenerative engineering. *Biomaterials* 226:119536
109. Birgersdotter A, Sandberg R, Ernberg I (2005) Gene expression perturbation in vitro—a growing case for three-dimensional (3D) culture systems. *Semin Cancer Biol* 15(5):405–412
110. Kleinman HK, Martin GR (2005) Matrigel: basement membrane matrix with biological activity. *Semin Cancer Biol* 15(5):378–386
111. Kim JB (2005) Three-dimensional tissue culture models in cancer biology. *Semin Cancer Biol* 15(5):365–377
112. Bissel MJK, Radisky DC (2005) Microenvironmental regulators of tissue structure and function also regulate tumor induction and progression: the role of extracellular matrix and its degrading enzymes. *Cold Spring Harb Symp Quant Biol* 70:343–356
113. Landberg G et al (2020) Patient-derived scaffolds uncover breast cancer promoting properties of the microenvironment. *Biomaterials* 235:119705
114. Cubo N et al (2016) 3D bioprinting of functional human skin: production and in vivo analysis. *Biofabrication* 9(1):015006
115. Duan B (2017) State-of-the-art review of 3D bioprinting for cardiovascular tissue engineering. *Ann Biomed Eng* 45(1):195–209
116. Singh YP et al (2018) Hierarchically structured seamless silk scaffolds for osteochondral interface tissue engineering. *J Mater Chem B* 6(36):5671–5688
117. Lee CH et al (2009) Tissue formation and vascularization in anatomically shaped human joint condyle ectopically in vivo. *Tissue Eng Part A* 15(12):3923–3930
118. Faulkner-Jones AF, Cornelissen D-J, Gardner J, King J, Courtney A, Shu W (2015) Bioprinting of human pluripotent stem cells and their directed differentiation into hepatocyte-like cells for the generation of mini-livers in 3D. *Biofabrication* 7(4):044102
119. Horvath L et al (2015) Engineering an in vitro air-blood barrier by 3D bioprinting. *Sci Rep* 5:7974
120. Tomasina C et al (2019) Bioprinting vasculature: materials, cells and emergent techniques. *Materials (Basel)* 12(17)
121. Perrin S (2014) Preclinical research: make mouse studies work. *Nature* 507(7493):423–425
122. Hutchinson LK (2011) High drug attrition rates—where are we going wrong? . *Nature reviews. Clin Oncol* 8:189
123. Ma HLJ, Han S, Wu Y, Tomshine JC, Wang D, Gan Y, Zou G, Liang X-J (2012) Multicellular tumor spheroids as an in vivo-like tumor model for three-dimensional imaging of chemotherapeutic and Nano material cellular penetration. *Mol Imaging* 11(6):7290
124. Abuelba H et al (2015) In vitro evaluation of curcumin effects on breast adenocarcinoma 2D and 3D cell cultures. *Romanian J Morphol Embryol* 56(1):71–76
125. Lovitt CJ, Shelper TB, Avery VM (2015) Evaluation of chemotherapeutics in a three-dimensional breast cancer model. *J Cancer Res Clin Oncol* 141(5):951–959
126. David L et al (2008) Hyaluronan hydrogel: an appropriate three-dimensional model for evaluation of anticancer drug sensitivity. *Acta Biomater* 4(2):256–263
127. Chitcholtan K, Sykes PH, Evans JJ (2012) The resistance of intracellular mediators to doxorubicin and cisplatin are distinct in 3D and 2D endometrial cancer. *J Transl Med* 10:38
128. Karlsson H et al (2012) Loss of cancer drug activity in colon cancer HCT-116 cells during spheroid formation in a new 3-D spheroid cell culture system. *Exp Cell Res* 318(13):1577–1585
129. Masuda S, Izipisua Belmonte JC (2013) The microenvironment and resistance to personalized cancer therapy. *Nat Rev Clin Oncol* 10(2)
130. Iseri OD et al (2011) Drug resistant MCF-7 cells exhibit epithelial-mesenchymal transition gene expression pattern. *Biomed Pharmacother* 65(1):40–45
131. Mostrag-Szlichtyng AZC, Worth AP (2010) Computational toxicology at the European commission's joint research Centre. *Expert Opin Drug Metab Toxicol* 6(7):785–792
132. Heggset EBS, Sundby KW, Simon S, Chinga-Carrasco G, Syverud K (2018) Viscoelastic properties of nanocellulose based inks for 3D printing and mechanical properties of CNF/alginate biocomposite gels. *Cellulose* 26(1):581–595
133. Xu W et al (2019) On low-concentration inks formulated by Nanocellulose assisted with gelatin methacrylate (GelMA) for 3D printing toward wound healing application. *ACS Appl Mater Interfaces* 11(9):8838–8848
134. Chinga-Carrasco GE, Pettersson J, Vallejos ME, Brodin MW, Felissia FE, Håkansson J, Area MC (2018) Pulping and pretreatment affect the characteristics of bagasse inks for three-dimensional printing. *ACS sustainable. Chem Eng* 6(3):4068–4075
135. Martinez Avila HS, Rotter N, Gatenholm P (2016) 3D bioprinting of human chondrocyte-laden nanocellulose hydrogels for patient-specific auricular cartilage regeneration. *Bioprinting* 1-2:22–35

136. Czaja W et al (2006) Microbial cellulose—the natural power to heal wounds. *Biomaterials* 27(2):145–151
137. Sun F et al (2017) Mechanical characteristics of nanocellulose-PEG bionanocomposite wound dressings in wet conditions. *J Mech Behav Biomed Mater* 69:377–384
138. Powell LC et al (2016) An investigation of *Pseudomonas aeruginosa* biofilm growth on novel nanocellulose fibre dressings. *Carbohydr Polym* 137:191–197
139. Jack AA et al (2017) The interaction of wood nanocellulose dressings and the wound pathogen *P. aeruginosa*. *Carbohydr Polym* 157:1955–1962
140. Nordli HRP, Chinga-Carrasco G, Rokstad AM (2019) Ultrapure wood Nanocellulose—assessments of coagulation and initial inflammation potential. *ACS Appl Bio Mater* 2(3):1107–1118
141. Basu AH, Ferraz N (2017) Hemocompatibility of Ca²⁺-crosslinked Nanocellulose hydrogels: toward efficient management of hemostasis. *Macromol Biosci* 17(11):1700236



New “Omics” Approaches as Tools to Explore Mechanistic Nanotoxicology

Célia Ventura, Vukosava Torres, Luís Vieira, Bruno Gomes, António Sebastião Rodrigues, José Rueff, Deborah Penque, and Maria João Silva 

Abstract

In the last years, “omics” approaches have been applied to study the toxicity of nanomaterials (NM) with the aim of obtaining insightful information on their biological effects. One of the most developed “omics” field, transcriptomics, expects to find unique profiles of differentially-expressed genes after exposure to NM that, besides providing evidence of their mechanistic mode of action, may also be used as biomarkers for biomonitoring purposes. Moreover, several NM have been associated with epigenetic alterations, i.e., changes in the regulation of gene expression caused by differential DNA methyl-

ation, histone tail modification and microRNA expression. Epigenomics research focusing on DNA methylation is increasingly common and the role of microRNAs is being better understood, either promoting or suppressing biological pathways. Moreover, the proteome is a highly dynamic system that changes constantly in response to a stimulus. Therefore, proteomics can identify changes in protein abundance and/or variability that lead to a better understanding of the underlying mechanisms of action of NM while discovering biomarkers. As to genomics, it is still not well developed in nanotoxicology. Nevertheless, the individual susceptibility to NM mediated by constitutive or acquired genomic variants represents an important component in understanding the variations in the biological response to NM exposure and, consequently, a key factor to evaluate possible adverse effects in exposed individuals. By elucidating the molecular changes that are involved NM toxicity, the new “omics” studies are expected to contribute to exclude or reduce the handling of hazardous NM in the workplace and support the implementation of regulation to protect human health.

C. Ventura (✉) · L. Vieira · D. Penque · M. J. Silva
Department of Human Genetics, National Institute of Health Doutor Ricardo Jorge (INSA), Lisbon, Portugal

Center for Toxicogenomics and Human Health (ToxOmics), NOVA Medical School-FCM, UNL, Lisbon, Portugal
e-mail: celia.ventura@insa.min-saude.pt

V. Torres
Faculty of Sciences, DQB—Department of Chemistry and Biochemistry, University of Lisbon, Lisbon, Portugal

BioISI—Biosystems & Integrative Sciences Institute, University of Lisbon, Lisbon, Portugal

B. Gomes · A. S. Rodrigues · J. Rueff
Center for Toxicogenomics and Human Health (ToxOmics), NOVA Medical School-FCM, UNL, Lisbon, Portugal

Keywords

Toxicogenomics · Epigenomics · Transcriptomics · microRNAs · Proteomics · Nanomaterials

8.1 Introduction

In recent years, we have been witnessing a new way of approaching genetic toxicology with the use of methodologies increasingly based on molecular and cellular biology, applied either *in vitro* or *in vivo*. This innovative trend in toxicity assessment became particularly evident with the development of laboratory methodologies that could offer high-throughput data, as is the case with hybridization-based technologies (microarrays), next-generation sequencing (NGS) or mass spectrometry. The National Research Council of USA defined “toxicogenomics” as the application of genomic technologies (for example, genetics, genome sequence analysis, gene expression profiling, proteomics, metabolomics, and related approaches) to study the adverse effects of environmental and pharmaceutical chemicals on human health and the environment [63]. In a single experiment, and in a short time, these technologies can gather much more biological information than conventional assays, ultimately allowing a global overview of all molecular pathways that are modified in the cell, tissue or organism in response to a toxic insult. For instance, the comet assay, one of the most common assays in toxicology [71], indicates if a nanomaterial (NM) induces genotoxic effects by causing DNA strand breaks. However, when molecular methodologies are used, the molecules involved in this process can be identified, from mitochondrial anti-oxidative enzymes to DNA repair enzymes, among several others. This greater insight at the molecular level, coupled with a wide range of biological findings, has resulted in a deeper understanding of the mechanism of action of NM and the cellular functional pathways affected by exposure. This knowledge allows building comprehensive adverse outcome pathways (AOPs) [5, 65] from the molecular initiating event to the final adverse outcome [29, 36]. Further efforts are underway to develop NM-relevant AOPs [20, 29, 36]. Thus, although the classical *in vivo* bioassays, clinical chemistry, and histopathological endpoints are still considered the “gold standard” for detecting substance-induced toxicity in animal models, the use of data derived from alterna-

tive toxicogenomics tools is gaining acceptance by the regulatory community for hazard identification and for understanding the underlying mode-of-action (MOA) of NM. Following the landmark report *Toxicity Testing in the 21st Century: A Vision and a Strategy* of the U.S. National Academy of Sciences in 2007, various reports have identified toxicogenomics as key in the next generation of risk science, including national regulatory agencies [46, 47, 55]. For example, it is possible to screen for carcinogenicity and to discern the potential MOA of a chemical based on analysis of gene expression [91]. However, it is often necessary to have specialized bioinformatics skills and expertise in order to treat, analyze and interpret the massive amounts of complex data that are obtained. Genomics, i.e., the study of the whole genome of an organism, is an approach that is still not developed in toxicology. The Environmental Genome Project (<https://egp.gs.washington.edu/>) is one of the few initiatives that has evolved from a candidate gene approach to exome sequencing in order to develop a database of single-nucleotide polymorphisms (SNPs) to examine the relationships between environmental exposures, inter-individual sequence variation in human genes and disease risk in U.S. populations. Most toxicological studies continue to focus on studying genetic variations in a predefined set of genes of interest, and still do not apply high-throughput methodologies.

In this sense, the genomic sequence (i.e., genotype) of an individual can significantly affect the pharmacokinetics and pharmacodynamics for a particular chemical, thereby determining the individual’s susceptibility to toxicity via changes in the target tissue dose [84]. It is the case of SNPs in the *CYP*, *NAT* and *GST* genes, encoding for biotransformation phase I and II metabolic enzymes, which are used as toxicological susceptibility markers in exposure to industrial and environmental carcinogens [83]. Besides genes encoding enzymes involved in the biotransformation of xenobiotics, also genes involved in the cellular defense against toxicant-induced cell damage or coding for the receptors or transcription factors which regulate

the expression of these enzymes are of particular interest [83]. Nevertheless, few genetic studies exist in nanotoxicology, and even fewer at the genomics level. Two of these studies have used collections of mutant organisms in order to find out which mutants triggered a different response to the NM exposure [60, 92]. Wu et al. [92] studied titanium dioxide nanoparticles (nano-TiO₂) toxicity in *Caenorhabditis elegans* mutants and found that *sod-2*, *sod-3*, *mtl-2*, and *hsp-16.48* genes were susceptibility genes for toxicity, probably by enhancing the uptake of nano-TiO₂ into the nematodes' body. Marmioli et al. [60], using deletion mutants of *Saccharomyces cerevisiae*, identified 112 and 114 strains associated to increased sensitivity or tolerance to cadmium sulphide quantum dots exposure, respectively (Marmioli et al. [60]). A genome-wide association (GWA) study was performed to identify potential candidate susceptibility genes associated with nano-Ag-induced neutrophil influx into the lung [73]. Mice from 25 different inbred strains were exposed to 0.25 mg/kg of 20-nm citrate-coated nano-Ag by oropharyngeal aspiration. The mouse genetic background contributed to inflammatory response variations, highlighting the role of individual genotypes in susceptibility to exposure. GWA mapping identified 10 significant SNPs on mouse chromosomes 1, 4, 15, and 18, and identified 3 promising candidate susceptibility genes, *Nedd4l* (neural precursor cell expressed developmentally downregulated gene 4-like; chromosome 18), *Rnf220* (Ring finger protein 220; chromosome 4), and *Ano6* (anocatmin 6; chromosome 15), for which mRNA levels were inversely correlated with nano-Ag-induced lung inflammation [73].

Much more common in nanotoxicology than genomics are other “omics” approaches, namely, transcriptomics, epigenomics and proteomics, and, for that reason, we will now further develop each of these “omics” separately, towards the discovery of biomarkers having risk/safety or mechanistic assessment utility in nanotoxicology.

8.2 Transcriptomics

Many biological effects of NM on a living system are reflected upstream in gene expression in a way that is necessary for the cell to adapt to their new stimulus. Therefore, the major focus of toxicogenomics has been on identifying changes in gene expression triggered by exposure to NM, through the identification and/or quantification of coding transcripts, i.e., the messenger RNAs (mRNAs) that exist in the cell. This can be restricted to studying the expression of a small group of genes, for example, by reverse transcription-quantitative real-time PCR (RT-qPCR), or by studying global gene expression using microarrays or RNA-Sequencing (RNA-Seq). These genomics methods, in combination with bioinformatics tools for ontology and pathway analyses, have been used to identify molecular MOAs of toxicants [37, 38]. Signatures of cancer-relevant genes can discriminate between direct vs. indirect genotoxic carcinogens vs. non-genotoxic and non-carcinogens [22–24].

To date, several studies have identified gene expression profiles associated with exposure to NM that were suggested as biomarkers of effect in human biomonitoring. Many of these studies have been performed in rodents exposed by inhalation, pharyngeal aspiration or intratracheal instillation. Carbon nanotubes (CNT), either single-walled (SWCNT) or multi-walled (MWCNT), are one of the most studied NM. In the case of MWCNT, it was suggested that *Ccdc99*, *Msx2*, *NOS2* and *Wif1* genes are of possible utility for medical surveillance in occupational settings [66], whereas larger sets of differentially expressed genes were suggested to be potentially useful to predict lung cancer risk [34] or were linked to pulmonary fibrosis [68]. Gene expression profiles from lungs of mice exposed to three different MWCNT were used to identify the altered pathways underlying key biological events linking MWCNT exposure to lung fibrosis. Then, for each perturbed pathway, benchmark doses were calculated and associated

with the gene expression changes in order to derive transcriptional benchmark doses for MWCNT-induced lung fibrosis. Their use was suggested to establish acceptable levels of exposure applicable to human health risk assessment [49].

Nevertheless, many of those studies have analysed global lung tissue collected from euthanized rodents. Therefore, considering that a less invasive sampling process is needed for human biomonitoring, it must be investigated not only if these gene expression profiles are similar in humans, but also if they are similar on other surrogate tissues, such as peripheral blood. A study that compared gene expression changes in the lungs and blood of mice exposed by pharyngeal aspiration to a MWCNT reported that only 9 of the 38 differentially expressed genes on the lungs were similarly altered in blood, and 6 genes were only found to have increased expression in the systemic circulation [25]. Therefore, different tissues other than the target tissue, i.e., the tissue affected by exposure, must be carefully evaluated, before genomic profiles can be used as biomarkers of effect.

As already mentioned, besides their utility as possible biomarkers of effect, the under- or over-expressed mRNAs can be linked into functional networks using bioinformatics tools to reveal MOAs through activating or inhibitory events. A network of differentially expressed genes in MWCNT-7 exposed mice is presented in Fig. 8.1, which links related genes in functional nodules, allowing an immediate global view of the consistency of the findings and their impact in cellular functions.

Some types of MWCNT, such as MWCNT-7 (Mitsui-7), have been frequently compared to asbestos due to their shared fibrous-shape and biopersistence, and transcriptional studies have confirmed a frequent association between MWCNT exposure and expression changes of lung cancer-related genes [13, 44, 64, 79]. Apart from cancer-related pathways, CNT exposure has been associated with disturbances in a multiplicity of other cellular pathways, such as apoptosis, inflammation, oxidative stress, fibrosis, cell cycle and proliferation [4, 13, 14, 19, 21, 34, 41, 44, 64, 66–68, 77–79].

Toxicogenomics studies of other commonly used NM, such as nano-TiO₂, revealed that the pulmonary injuries observed in mice following long-term exposure to nano-TiO₂ suspensions by nasal instillation were also associated with expression changes in genes involved in immune/inflammatory responses, apoptosis, oxidative stress, cell cycle, stress responses, cell proliferation, the cytoskeleton, signal transduction, and metabolic processes [52]. Intratracheal instillation of rutile nano-TiO₂ in mice revealed dose- and time-dependent changes in genes associated with inflammation, ion homeostasis and muscle function, and suggested that retention of nano-TiO₂ without long-term inflammation may perturb calcium, ion, and lipid homeostasis, and affect pulmonary smooth muscle contraction, potentially contributing to the development of lung diseases [43]. In the case of mice exposed to anatase nano-TiO₂ by intraperitoneal injection, whole genome analysis found that this form of nano-TiO₂ triggered lipid and glucose metabolic changes and deregulated xenobiotic metabolism in the liver [53]. Moreover, it induced oxidative stress related to mitochondrial dysfunction, inflammatory responses and apoptosis in the lungs, which could be related to lung-specific carcinogenesis [53]. Nano-TiO₂ also induced changes in global gene expression of ovaries from mice treated by intragastric administration, supporting the hypothesis that this NM directly affects ovarian function. For instance, upregulation of Cyp17a1 and Akr1c18 genes could explain the increase in estradiol biosynthesis and the decrease in progesterone, respectively [28]. Other differentially expressed genes in mice ovaries were related to apoptosis, oxidative stress, immune and inflammatory responses, transcription, ion transport, regulation of cell proliferation, and oxidoreductase activity of ovary [28]. Changes in genes related to DNA damage or repair, oxidative stress, and apoptosis were also identified in human airway epithelial cell cultures [8].

Several other metallic NM have been the focus of toxicogenomics studies. *In vitro* exposure to a sub-lethal dose of zinc oxide nanoparticle (nano-ZnO) increased the expression of 4 genes

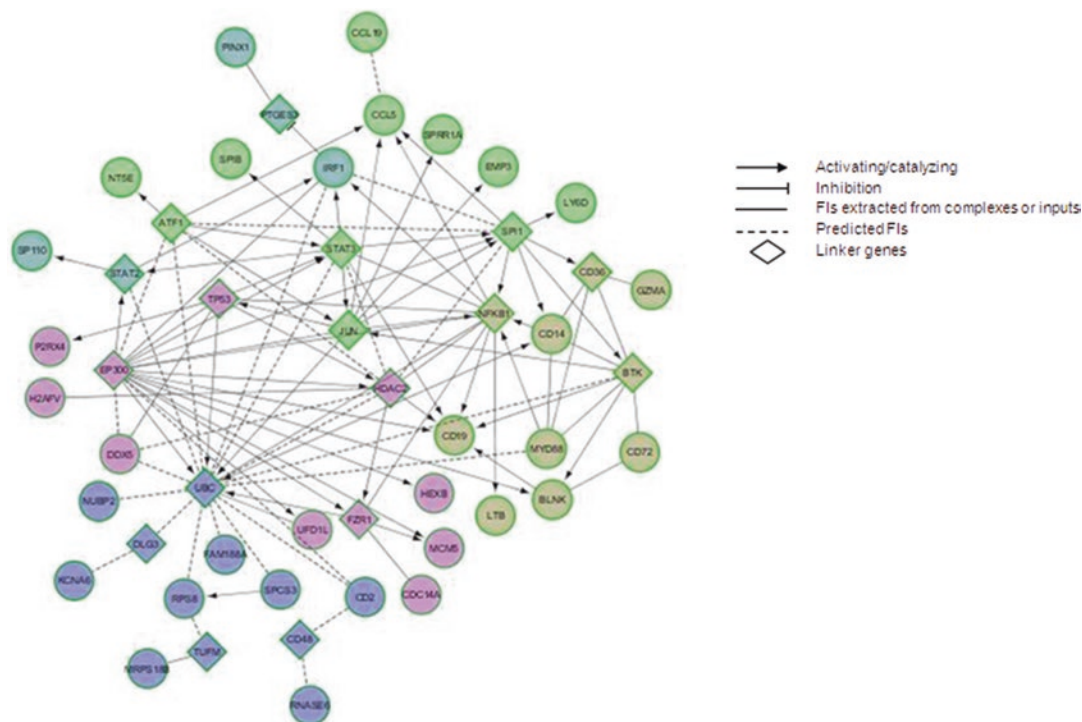


Fig. 8.1 Functional interaction network analysis of 41 differentially expressed genes identified in mice exposed to MWCNT-7. Different colors indicate sub-networks of

functionally related genes involved in common molecular pathways [88]

involved in apoptosis and oxidative stress (*BNIP*, *PRDX3*, *PRNP*, and *TXRND1*) [42]. In addition, microarray analyses of global gene expression in lung tissues from rats following a short-term inhalation exposure to copper oxide nanoparticles (nano-CuO), showed several differentially expressed genes, with much less impact after a 22-day recovery period, and cell proliferation/survival and inflammation were again the main processes triggered by exposure, but with no significant changes of oxidative stress-related pathways. Up-regulation of the oncogene epithelial cell transforming protein 2 (Ect2) and chemokine CCL2 were observed [15]. Macrophages exposed to welding-related metal oxide NM previously identified in welders' lungs (Fe_2O_3 , Fe_3O_4 , MnFe_2O_4 and CrOOH NP) induced a profound modification of differential gene expression in response to the different NM, among which MnFe_2O_4 NP was the most potent to induce THP-1 macrophage activation [7].

Overall, these results suggest that oxidative stress is a major mechanism of action of metallic NM, leading to inflammation, DNA damage and apoptosis.

Whole genome expression analysis in RAW 264.7 macrophages using RNA-seq showed several deregulated genes after exposure to non-cytotoxic doses of mesoporous silica nanoparticles (nano-Si), but not after exposure to nonporous nano-Si. Gene ontology and functional pathway analyses revealed lysosome pathway up-regulation, probably caused by damaged organelles due to the presence of nano-Si, which activates autophagosome formation that subsequently merge with lysosomes [94]. Only the smaller sized amorphous nano-Si induced significant gene expression changes in another *in vitro* study, where lysosomal-related pathways were again the most significantly affected, appearing to be associated with higher nano-Si internalization and subsequent lysosomal overload in the cytoplasm

[18]. Other significantly affected pathways included oxidative phosphorylation, steroid biosynthesis, terpenoid backbone biosynthesis and cytokine–cytokine receptor interaction, among others [18]. Whole genome microarray analysis of the early gene expression changes induced by 10 and 500 nm amorphous silica nanoparticles, performed by Waters et al. [90] revealed that the most important transcriptional change was an induction of the Cxcl2 chemokine (MIP-2a), also implicated in crystalline silica-induced lung neutrophil recruitment. The magnitude of change for the majority of genes affected correlated more tightly with particle surface area than with either particle mass or number, and was particle size-specific. The overall biological processes affected by all gene expression changes were nearly identical, irrespective of particle diameter. Interestingly, these data indicate that common biological MOAs are expected for nano- and supranano-sized silica particles [90].

One issue that needs further elucidation is the concordance of *in vitro* and *in vivo* studies. It should be highlighted that *in vivo* and *in vitro* systems may identify similar altered biological pathways, but with different underlying gene expression changes [67]. Improving the existing *in vitro* models can allow a better resemblance with the *in vivo*. For instance, Snyder-Talkington et al. [78] compared global MWCNT-induced gene expression from human lung epithelial cells (SAEC) and microvascular endothelial cells (HMVEC) in monoculture and co-culture, with gene expression obtained from mouse lungs exposed to MWCNT. Their data indicated that genes involved in inflammation and fibrosis, which are known outcomes of *in vivo* MWCNT exposure, were more concordant with the gene expression in the co-culture system [78]. Nevertheless, although differences still exist, *in vitro* exposures seem to efficiently recapitulate the significantly altered molecular functions *in vivo* [45].

At least one transcriptomics study was performed in humans. Shvedova et al. [75] com-

pared global mRNA and non-coding RNA expression profiles in the blood of workers exposed to a MWCNT aerosol and non-exposed workers from the same manufacturing facility. Microarray studies revealed 785 differentially expressed genes involved in cell cycle, apoptosis and proliferation. The related pathways and signaling networks were mostly associated with pulmonary outcomes, mainly pulmonary inflammation and fibrosis (including cytokines such as IL6, CSF2 and CXCL2, and growth factors such as VEGFA and PDGFA), cardiovascular outcomes and, exclusively in the highly exposed group, carcinogenic outcomes, namely, bronchoalveolar adenoma and adenocarcinoma, and goblet cell metaplasia and hyperplasia [75]. These findings are similar to those described in rodents exposed to MWCNT.

Although toxicogenomics is increasingly becoming integrated in toxicology studies, finding a profile of significant differentially-expressed genes for each mechanism of toxicity, starting from an initial set of thousands of genes that are under- or up-expressed as compared to a non-exposed control, can be bioinformatically cumbersome. Furthermore, the lack of standardization in the experimental designs has hindered their consistency and the generation of more reliable, unbiased and accurate predictive toxicological models. For instance, the comparison between 4 different transcriptomics studies that shared the same *in vivo* model (C57BL/6 mice) exposed to the same NM (MWCNT-7), has shown that there was not a single gene in common [88]. The lack of standard guidelines for preprocessing the large transcriptomics data sets, such as criteria for quality control, filtering, and normalization, may be a major contributor to these discrepancies. In addition, different tools used for differential expression analysis may have variable impact in the detection of true positive results [95]. A review of current standards, available resources and good practices for the bioinformatics analysis of transcriptomics data in toxicogenomics is available elsewhere [26].

8.3 Epigenomics

Another layer of understanding the way a NM can affect gene expression is through epigenomics, i.e., the study of regulation of gene expression that is attained by modifying histone tails (e.g., by methylation, phosphorylation, acetylation), or altering DNA methylation and microRNA (miRNA) expression [56, 81]. These are all fine-tuned cellular mechanisms that work in synchronization to regulate gene expression in order to achieve cellular homeostasis. Here, we will focus on the last two.

Regulating the levels of methylated cytosines (5-methylcytosine, 5-mC) in CpG dinucleotides and its oxidized derivative 5-hydroxymethylcytosines (5-hmC) plays a fundamental role in the regulation of the transcriptional activity of the genome [33]. There is still very limited data on this subject regarding NM exposure.

It was suggested that blood DNA methylation levels could be a biomarker for lung inflammation and disease following MWCNT exposure, since C57BL/6 mice exposed via oropharyngeal instillation showed global genomic hypomethylation in lungs and blood at 7 days post-exposure, coinciding with disease development. Moreover, in whole lung tissue, promoter hypomethylation of the pro-inflammatory genes *IFN- γ* and *TNF- α* matched cytokine production, and promoter hypomethylation of *Thy-1*, a gene involved in tissue fibrosis, matched collagen deposition [10]. Laser printer-emitted engineered NM released from nano-enabled toners during consumer use also caused alterations in the global methylation of DNA and transposable elements *in vivo* and *in vitro*, although with differences between both models that suggested more hypomethylation *in vitro*, and hypermethylation *in vivo* [57]. Nano-SiO₂ also induced global genomic hypomethylation in HaCaT cells [31] and, in another study by the same author using the same cellular model, decreased mRNA expression and protein levels of poly(ADP-ribose) polymerase-1 (PARP-1), a pivotal repair enzyme, through increased site specific methylation in the *PARP-1* gene promoter mediated at least in part, by DNA methyltransferase 1 (DNMT1) [32].

Accordingly, most studies have shown an association between NM exposure and DNA hypomethylation. By contrast, Brzóska et al. [11] found no changes in promoter methylation of 44 genes related to inflammation and apoptosis in HepG2 cells exposed to low cytotoxic doses of nano-Ag, nano-Au, and superparamagnetic iron oxide nanoparticles. Nevertheless, nine miRNAs related to these processes were differentially expressed, mostly related to cell proliferation inhibition and tumorigenesis [11].

Changing miRNA expression is another mechanism of gene regulation. miRNAs are small 19 to 25 nucleotides-long non-coding RNAs usually acting as endogenous repressors of gene activity via post-transcriptional binding to a "seed" sequence in the 3' untranslated region (3'-UTR) of mRNA [35]. Extracellular circulating miRNAs have shown to be remarkably stable in plasma and serum, resistant to RNase activity and extreme pH, as well as to multiple freeze-thaw cycles [12, 30, 72]. Moreover, they are tissue specific, and for these reasons they have attracted much interest as potential biomarkers of disease [70, 74, 93], particularly in malignant diseases [3, 69, 79].

The utility of miRNAs as biomarkers of NM exposure has been first investigated by Nagano et al. [62] that compared the effectiveness of serum levels of liver-specific miRNAs with that of conventional hepatic biomarkers for liver damage after exposure to nano-Si (nSP70) in mice, concluding that the sensitivity of miR-122 was at least as good as those of the conventional markers of hepatic function, alanine aminotransferase (ALT) and aspartate aminotransferase (AST).

When studying gene expression changes associated with mitochondrial dysfunction in human bronchial epithelial cells exposed to MWCNT-7, Nymark et al. [64] also studied miRNA expression changes and found four miRNAs associated with decreased mitochondrial membrane potential [64]. Global lung mRNA/miRNA regulatory relationships associated with inflammation and fibrosis after exposure to MWCNT-7 were also studied using microarrays [19], and the correlation between mRNA/miRNA changes and health outcomes was investigated by Snyder-Talkington et al. [79] in whole

blood of rodents exposed to MWCNT. The results showed an association between FCRL5/miR-122-5p and hyperplasia, MTHFD2/miR-206-3p and fibrosis, FAM178A/miR-130a-3p and bronchiolo-alveolar adenoma, and IL7R/miR-210-3p and bronchiolo-alveolar adenocarcinoma, among others. A high-throughput deep sequencing method was used by Li et al. [51] in mouse embryo-derived NIH/3 T3 cells exposed to MWCNT for identifying the altered miRNAs and the corresponding functional pathways. NGS was also used to identify differentially expressed miRNAs in A549 epithelial alveolar cells exposed to MWCNT-7 or crocidolite asbestos for 24 hours, their target genes and the deregulated cellular pathways [89]. In Fig. 8.2 we can see the profile of differentially expressed miRNAs in A549 cells after exposure to MWCNT-7, and the functional pathways enriched with genes post-transcriptionally regulated by these miRNAs. Most of these genes are cancer-related, highlighting the carcinogenic potential of MWCNT-7.

Other NM, as nano-TiO₂, have been also shown to change the expression of several miRNAs *in vitro*, up-regulating a large number of

genes involved in the KEGG categories “metabolism” (thiamine metabolism, purine metabolism, glycosaminoglycan biosynthesis-chondroitin sulfate/dermatan sulfate, glycosaminoglycan biosynthesis-heparan sulfate/heparin, metabolic pathways, lysine degradation, retinol metabolism), “human diseases cancers” (transcriptional misregulation in cancer, microRNAs in cancer, N-Glycan biosynthesis), “environmental information processing” (Notch signaling pathway, ECM-receptor interaction, Hedgehog signaling pathway, mTOR signaling Pathway, phosphatidylinositol signaling system), and “cellular processes” (gap junction, endocytosis, signaling pathways regulating pluripotency of stem cells). Moreover, it was suggested that miRNAs 378b and 378 g may play an important role in TiO₂-NPs-mediated colonic cytotoxicity [54].

All these studies suggest that NM can cause subtle epigenetic changes, highlighting the need to investigate these types of alterations when analyzing the health risks of NM exposure. These alterations can be used as biomarkers of effect in biomonitoring exposure to NM and also provide a mean to uncover their mechanistic adverse effects on human health.

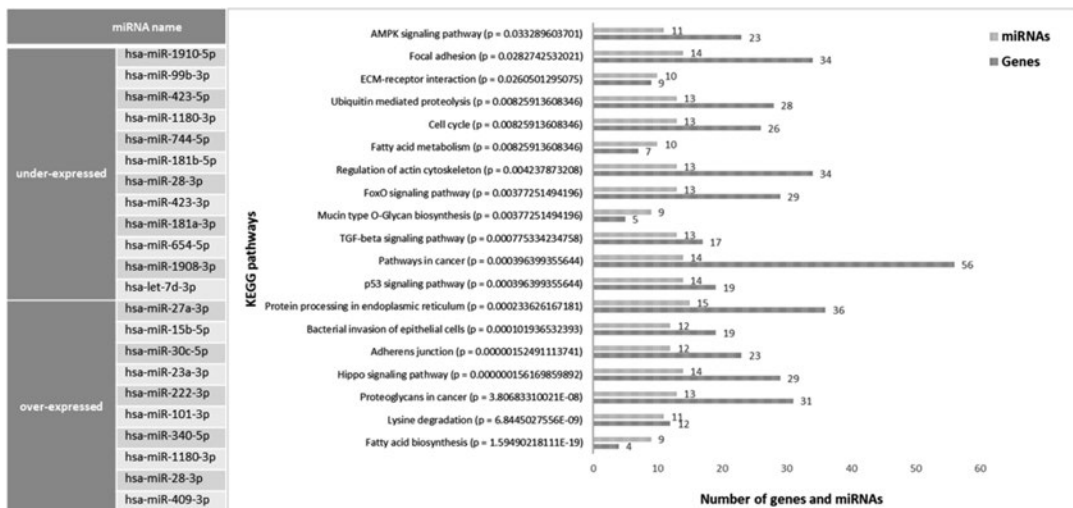


Fig. 8.2 Differentially expressed miRNAs in A549 cells after 24 hours exposure to MWCNT-7 comparatively to non-exposed cells, and KEGG pathways enriched with

genes targeted by these miRNAs, ordered by decreasing p-value [89]

8.4 Proteomics

Information derived from genomic and transcriptomic studies about NM fate and MOA in biological systems are often inconclusive, because DNA provides the blueprint how to build an organism, but proteins execute the hard work [2, 86]. According to the central molecular biology dogma, one gene codes one protein. However, if we take into account the products of alternative splicing, single amino acid polymorphisms arising from non-synonymous single nucleotide polymorphism and covalent posttranslational modifications at one or more sites of proteins, it is speculated that as much as 100 protein variants (proteoforms) can be derived from a single gene [76]. Of about 25,000 genes in the human body, nearly 20,000 are encoding proteins, which means theoretically nearly one million protein/proteoforms possibly constitute the human proteome [1]! The proteome is a highly dynamic system that changes constantly in response to exo- and endogenous stimuli. Changes in protein abundance and/or in protein variability are key aspects influencing the body response and adaptation to environmental exposures. Proteomics, the science of the proteome, offers the great opportunity to identify and quantify the proteins/proteoforms associated with these processes, leading to a better understanding of the underlying mechanisms while discovering biomarkers.

Knowing that protein quantities cannot be amplified prior to measurement, as in the case of DNA, ultrasensitive techniques are needed to analyze and measure protein changes that occur at the subcellular level and/or under a wide dynamic range of protein concentrations. Advances in mass spectrometry-based proteomics technology, coupled with bioinformatics tools, added evidence to the information offered by genomics and transcriptomics.

Mass spectrometry (MS) is the most powerful approach to identify and elucidate the structure of complex molecules like peptides and/or proteins, including protein post-translation modifications (PTMs) [6]. Global proteome profiling using MS coupled with liquid chromatography and dedicated software systems, known as shot-

gun MS, is the method of choice in discovery proteomics as it offers the possibility to explore the complete protein plethora of a given cell/organism [87]. Several MS analytical platforms have been developed and proven to be robust and straightforward in proteomics [87].

In NM-toxicoproteomics, shotgun proteomics is used to investigate changes in physiological processes triggered by NM, or to encounter putative biomarkers for quantitative evaluation of NM toxicity. The number of the yearly publications in this field is continuously growing (according to PubMed), especially since 2010, which confirms the involvement of proteomics in mechanistic nanotoxicology.

Several extensive reviews were published about the toxicoproteomics of carbon based NM (e.g., CNT, fullerenes, graphene, graphite and carbon black) [9, 39, 59]. Their common conclusions about cellular protein alterations upon exposure involves changes in oxidative stress, cell differentiation, metabolic processes, cytoskeleton formation and apoptosis. It was shown that chemical modifications and different functionalizations of carbon NM can ameliorate toxicity when compared to pristine NM. Acute toxicity of PEGylated and Tween functionalized SWCNTs was tested *in vivo* in BALB/c mice. While standard toxicity assays assumed SWCNT as safe, proteomics analysis showed statistically significant alterations in expression of proteins with antioxidative and detoxifying properties such as peroxiredoxin-6 (Prdx6), electron transport flavoprotein (Etf-a) and thioredoxin peroxidase (TPx). Unlike biochemical and pathohistological tests, proteomics revealed, not only which metabolic processes were involved in toxicity, but also the impact of functionalization, where SWCNT-Tween provoked a stronger cell response when compared to PEGylated SWCNT [2]. Moreover, gold standard *in vitro* toxicity tests assumed a low carbon NM concentration as safe, while proteomics revealed changes of protein expression to have a toxic action before it was detectable at the cellular and biochemical level [85]. Interesting work was performed by Hilton et al. [40] that compared the results of conventional submerged and air-liquid interface

(ALI) exposures using a co-culture model consisting of macrophages, epithelial cells (A549) and fibroblasts (MRC-5) exposed for 5 days to a sub-chronic dose of CNT. Discovery proteomics identified 3500 proteins of which ATP5PO, NDUFS3, UQCR10 and UQCRFS1 were found to be up-regulated in the ALI model, but not in the submerged model. These proteins are generally associated with oxidative phosphorylation and mitochondrial dysfunction. These results are of great importance, since they may serve as a guideline in future nanotoxicity method development [40].

Zhang et al. showed that cytotoxic metal NM impacted metabolic pathways such as antioxidant response, TCA cycle, oxidative stress, endoplasmic reticulum stress, and immune response. Bioinformatics analysis uncovers that changes in expression of proteins involved in oxidative stress (HMOX1), chaperone functions (HS71B, DNJB1) and autophagy (SQSTM) were able to distinguish different classes of metal-containing NM, hence identifying them as putative biomarkers for the evaluation of the NM toxic effect [96].

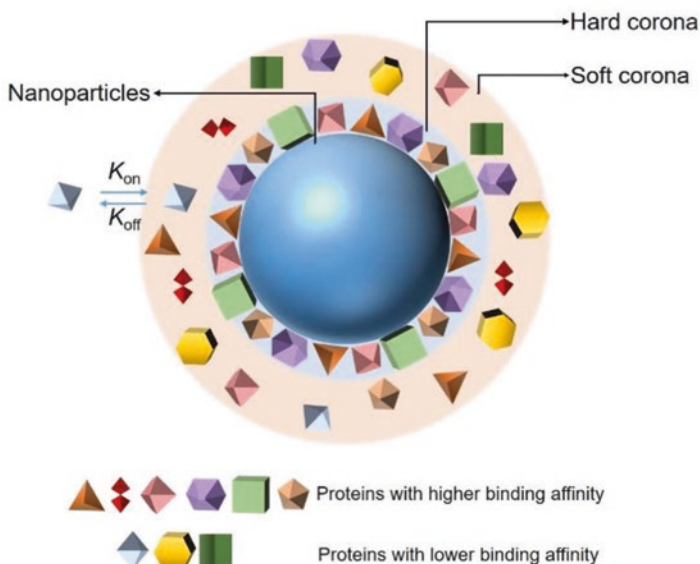
The concern that the presence of silver containing NM (widely used as effective antimicrobial agents) in the environment, particularly in water and soil, could significantly change the natural microflora, motivated the proteomics

study of the influence of nano-Ag on the soil-dwelling bacterium *Bacillus thuringiensis*. The results disclosed 34 differentially-expressed proteins upon exposure, involved in oxidative stress, protein degradation, apoptosis, metal detoxification, cytoskeleton remodeling and transcription/elongation processes [61].

Dalzon et al. [17] reported selective toxicity of nano-Si toward macrophages with changes in cytoskeleton, phagocytic capacity, and increased DNA sensitivity toward alkylating reagents. AMP-activated protein kinase (AMPK pathway) and myeloid differentiation primary response protein 88 (myd88) pathways were the main affected metabolic routes [17].

Moreover, proteomics can give us deep information about the NM fate once they enter a biological system. The NM protein corona represents their biological identity and defines the physical interaction between NM and target cells. Therefore, it is of great importance to unveil and understand the processes that occur in the NM surface, as well as corona composition. Protein corona is a dynamic system, since, at first, proteins with high concentration and high association rate occupy the NM surface, and lately, proteins with lower concentration, but higher affinity, will exchange and replace the initially associated proteins (Fig. 8.3) [16, 50, 58].

Fig. 8.3 Protein corona composition. (Adapted from [50])



Tenzer et al. [82] investigated the kinetics of corona formation on nano-Si and polystyrene nanoparticles (nano-Ps) in the human blood, and applied label-free proteomics to obtain quantitative information on the protein corona fingerprint. Surprisingly, they discover that corona is formed in less than 30 s, independently of the NM type, and identified 166 proteins. A longer incubation time caused a more heterogeneous and complex corona with more than 300 identified proteins. Corona composition changed over time in terms of amount, but not in composition. It was found that early formed corona mediates haemolysis, thrombocyte activation, NM uptake and cell death [82]. Proteomics analysis of single-layered graphene oxide (SLGO) and multi-layered graphene oxide (MLGO) incubated in standard cell medium (DMEM+FBS) identified an average of 300 proteins, of which 115 were unique for SLGO, and 11 for MLGO in concordance with previous findings [27]. Moreover, surface chemistry, size and porosity were responsible for corona composition and, subsequently, NM physiological activity [27]. In fact, data obtained by proteomics show that cellular immune response depends on the corona composition. The complex nano-ZnO-corona, formed upon incubation of nano-ZnO in serum, is enriched with opsonin protein, which interacts with immune effector cells, triggering rapid clearance and toxicity. Surface modification of nano-ZnO with polyacrylamide-grafted guar gum (PAm-g-GG) polymer changes corona toward improved biocompatibility with decreased toxicity [80]. A team of scientists went one step further in investigating NM biocompatibility introducing a method for studying the ultimate line between NM and the cell – SURface proteomics, Safety, Targeting and Uptake (SUSTU). The rationale for this method relies on the fact that proteins from corona can determine the selection of the receptors on the target cells. This method relies on a classical strategy for analysing cell surface by proteomics. Briefly, corona was biotin-labelled, followed by *in situ* trypsin digestion, and tryptic digests were recovered and analysed by label free quantitative mass spectrometry. Using SUSTU it will be possible to rapidly char-

acterize the surface of engineered NM, toward improved targeting, uptake, function and safety [48]. Hence, the ability to identify active sites that trigger undesirable reactions make proteomics a necessary tool for the design of new, biocompatible, and more effective formulations of NM.

8.5 Conclusions

The safety of NM has to be assessed to ensure consumer, occupational, and environmental health. “Omics” approaches studying gene expression, epigenetic modifications and proteomics allow deepening the knowledge on the molecular effects of NM pointing towards possible future targets for mechanistic research on the toxicity of these materials. Advances in “omics” technologies have improved our understanding of the gene and protein expression changes that are linked to biological key events triggered by NM exposure. This knowledge allows the construction of NM-relevant AOPs, from the molecular initiating event to the final adverse outcome. Since “omics” methodologies are capable of detecting subtle cellular changes, the adoption of *in vitro* models that better mimic the *in vivo* than the conventional monocultures of immortalized cell lines, can provide more reliable toxicological information. Moreover, proteomics of corona became an emerging scientific domain that complements genomics and transcriptomics to better understand the NM metabolic fate and interaction with the biological environment. Furthermore, the discovery and development of appropriate sensitive and specific accessible biomarkers, suitable for occupational and environmental biomonitoring programs, is critical. Here, “omics” can also be a tool to identify novel effect biomarkers, either through differentially expressed genes, miRNAs or proteins. Individual susceptibility to NM mediated by constitutive or acquired genomic variants is still a poorly explored issue, but would represent an important component in understanding the variations in the biological response to NM exposure and, consequently, for evaluating possible adverse effects in exposed individuals.

Acknowledgments This work was funded by FCT/MCTES, project PTDC/SAU-PUB/32587/2017 and project PTDC/BTM-TEC/28554/2017 through national funds (PIDDAC), ToxOmics (UIDB/00009/2020; UIDP/00009/2020) and BioISI—Biosystems & Integrative Sciences Institute, Faculty of Sciences University of Lisbon, Lisbon, Portugal. It is also a result of the GenomePT project (POCI-01-0145-FEDER-022184), supported by COMPETE 2020 - Operational Programme for Competitiveness and Internationalisation (POCI), Lisboa Portugal Regional Operational Programme (Lisboa2020), Algarve Portugal Regional Operational Programme (CRESC Algarve2020), under the PORTUGAL 2020 Partnership Agreement, through the European Regional Development Fund (ERDF), and by FCT, and the National Mass Spectrometry Network (RNEM)-FCT Infrastructure Program, Portugal.

References

1. Aebersold R, Agar JN, Amster IJ, Baker MS, Bertozzi CR, Boja ES, Costello CE, Cravatt BF, Fenselau C, Garcia BA, Ge Y, Gunawardena J, Hendrickson RC, Hergenrother PJ, Huber CG, Ivanov AR, Jensen ON, Jewett MC, Kelleher NL, Kiessling LL, Krogan NJ, Larsen MR, Loo JA, Ogorzalek Loo RR, Lundberg E, MacCoss MJ, Mallick P, Mootha VK, Mrksich M, Muir TW, Patrie SM, Pesavento JJ, Pitteri SJ, Rodriguez H, Saghatelian A, Sandoval W, Schlüter H, Sechi S, Slavoff SA, Smith LM, Snyder MP, Thomas PM, Uhlén M, Van Eyk JE, Vidal M, Walt DR, White FM, Williams ER, Wohlschläger T, Wysocki VH, Yates NA, Young NL, Zhang B. (2018) How many human proteoforms are there? *Nat Chem Biol* 14(3):206–214. <https://doi.org/10.1038/nchem-bio.2576>. 29443976
2. Ahmadi H, Ramezani M, Yazdian-Robati R, Behnam B, Razavi Azarkhiavi K, Hashem Nia A et al (2017 Sep 25) Acute toxicity of functionalized single wall carbon nanotubes: a biochemical, histopathologic and proteomics approach. *Chem Biol Interact* 275:196–209
3. Ak G, Tomaszek SC, Kosari F, Metintas M, Jett JR, Metintas S, Yildirim H et al (2015) microRNA and mRNA features of malignant pleural mesothelioma and benign asbestos-related pleural effusion. *Biomed Res Int* 635748:1–8
4. Alazzam A, Mfoumou E, Stiharu I, Kassab A, Darnel A, Yasmeeen A, Sivakumar N, Bhat R, Al MA (2010) Identification of deregulated genes by single wall carbon-nanotubes in human normal bronchial epithelial cells. *Nanomedicine* 6:563–569
5. Ankley GT, Bennett RS, Erickson RJ, Hoff DJ, Hornung MW, Johnson RD et al (2010) Adverse outcome pathways: a conceptual framework to support ecotoxicology research and risk assessment. *Environ Toxicol Chem* 29(3):730–741. <https://doi.org/10.1002/etc.34>
6. Arevalo R Jr, Ni Z, Danell RM (2020 Jan) Mass spectrometry and planetary exploration: a brief review and future projection. *J Mass Spectrom* 55(1):e4454. <https://doi.org/10.1002/jms.4454>
7. Audureau É, Simon-Deckers A, Franco-Montoya ML, Annangi B, Kermanizadeh A, Boczkowski J, Lanone S (2018) Substantial modification of the gene expression profile following exposure of macrophages to welding-related nanoparticles. *Sci Rep* 8(1):8554. <https://doi.org/10.1038/s41598-018-26988-z>
8. Aydın E, Türkez H, Hacımuftüoğlu F, Tatar A, Geyikoğlu F (2017) Molecular genetic and biochemical responses in human airway epithelial cell cultures exposed to titanium nanoparticles in vitro. *J Biomed Mater Res Part A* 105:2056–2064. <https://doi.org/10.1002/jbm.a.35994>
9. Basak SC, Vracko M, Witzmann FA (2016) Mathematical Nanotoxicoproteomics: quantitative characterization of effects of multi-walled carbon nanotubes (MWCNT) and TiO₂ Nanobelts (TiO₂-NB) on protein expression patterns in human intestinal cells. *Curr Comput Aided Drug Des* 12(4):259–264. <https://doi.org/10.2174/1573409912666160824145722>
10. Brown TA, Lee JW, Holian A, Porter V, Fredriksen H, Kim M, Cho YH (2016) Alterations in DNA methylation corresponding with lung inflammation and as a biomarker for disease development after MWCNT exposure. *Nanotoxicology* 10(4):453–461. <https://doi.org/10.3109/17435390.2015.1078852>
11. Brzóska K, Gradzka I, Kruszewski M (2019) Silver, gold, and iron oxide nanoparticles alter miRNA expression but do not affect DNA methylation in HepG2 cells. *Materials* 12:1038. <https://doi.org/10.3390/ma12071038>
12. Chen X, Ba Y, Ma L, Cai X, Yin Y, Wang K, Guo J, Zhang Y, Chen J, Guo X, Li Q, Li X, Wang W, Zhang Y, Wang J, Jiang X, Xiang Y, Xu C, Zheng P, Zhang J, Li R, Zhang H, Shang X, Gong T, Ning G, Wang J, Zen K, Zhang J, Zhang CY (2008) Characterization of microRNAs in serum: a novel class of biomarkers for diagnosis of cancer and other diseases. *Cell Res* 18(10):997–1006. <https://doi.org/10.1038/cr.2008.282>
13. Chen D, Stueckle TA, Luanpitpong S, Rojanasakul Y, Lu Y, Wang L (2015) Gene expression profile of human lung epithelial cells chronically exposed to single-walled carbon nanotubes. *Nanoscale Res Lett* 10:12
14. Chou C-C, Hsiao H-Y, Hong Q-S, Chen C-H, Peng Y-W, Chen H-W, Yang P-C (2008) Single-walled carbon nanotubes can induce pulmonary injury in mouse model. *Nano Lett* 8(2):437–445. <https://doi.org/10.1021/nl0723634>
15. Costa PM, Gosens I, Williams A, Farcial L, Pantano D, Brown DM, Stone V, Cassee FR, Halappanavar S, Fadeel B (2018) Transcriptional profiling reveals gene expression changes associated with inflammation and cell proliferation following short-term inhalation exposure to copper oxide nanoparticles. *J Appl Toxicol* 38:385–397. <https://doi.org/10.1002/jat.3548>

16. Cuervo AM, Wong ES, Martinez-Vicente M (2010) Protein degradation, aggregation, and misfolding. *Mov Disord* 25(Suppl 1):S49–S54. <https://doi.org/10.1002/mds.22718>
17. Dalzon B, Aude-Garcia C, Collin-Faure V, Diemer H, Béal D, Dussert F, Fenel D, Schoehn G, Cianféran S, Carrière M, Rabilloud T (2017 Jul 13) Differential proteomics highlights macrophage-specific responses to amorphous silica nanoparticles. *Nanoscale* 9(27):9641–9658. <https://doi.org/10.1039/c7nr02140b>
18. Decan N, Wu D, Williams A, Bernatchez S, Johnston M, Hill M, Halappanavar S (2016) Characterization of in vitro genotoxic, cytotoxic and transcriptomic responses following exposures to amorphous silica of different sizes. *Mutat Res Genet Toxicol Environ Mutagen* 796:8–22. <https://doi.org/10.1016/j.mrgentox.2015.11.011>
19. Dymacek J, Snyder-Talkington BN, Porter DW, Mercer RR, Wolfarth MG, Castranova V, Qian Y, Guo NL, Virginia W (2015) mRNA and miRNA regulatory networks reflective of multi-walled carbon nanotube-induced lung inflammatory and fibrotic pathologies in mice. *Toxicol Sci* 144:51–64
20. Ede JD, Lobaskin V, Vogel U, Lynch I, Halappanavar S, Doak SH, Roberts M, Shatkin JA (2020) Translating scientific advances in the AOP framework to decision making for nanomaterials. *Nano* 10(6):1–22. <https://doi.org/10.3390/nano10061229>
21. Ellinger-Ziegelbauer H, Pauluhn J (2009) Pulmonary toxicity of multi-walled carbon nanotubes (Baytubes) relative to alpha-quartz following a single 6h inhalation exposure of rats and a 3 months post-exposure period. *Toxicology* 266:16–29. <https://doi.org/10.1016/j.tox.2009.10.007>
22. Ellinger-Ziegelbauer H, Stuart B, Wahle B, Bomann W, Ahr HJ (2005 Aug 4) Comparison of the expression profiles induced by genotoxic and nongenotoxic carcinogens in rat liver. *Mutat Res* 575(1-2):61–84. <https://doi.org/10.1016/j.mrfmmm.2005.02.004>
23. Ellinger-Ziegelbauer H, Gmuender H, Bandenburg A, Ahr HJ (2008 Jan 1) Prediction of a carcinogenic potential of rat hepatocarcinogens using toxicogenomics analysis of short-term in vivo studies. *Mutat Res* 637(1-2):23–39. <https://doi.org/10.1016/j.mrfmmm.2007.06.010>
24. Ellinger-Ziegelbauer H, Aubrecht J, Kleinjans JC, Ahr HJ (2009 Apr 10) Application of toxicogenomics to study mechanisms of genotoxicity and carcinogenicity. *Toxicol Lett* 186(1):36–44. <https://doi.org/10.1016/j.toxlet.2008.08.017>
25. Erdely A, Hulderman T, Salmen R, Liston A, Zeidler-Erdely PC, Schwegler-Berry D, Castranova V, Koyama S, Kim YA, Endo M, Simeonova PP (2009) Cross-talk between lung and systemic circulation during carbon nanotube respiratory exposure. Potential Biomarkers *Nano Lett* 9(1):36–43
26. Federico A, Serra A, Ha MK, Kohonen P, Choi J-S, Liampa I, Nymark P, Sanabria N, Cattelani L, Fratello M, Kinaret PAS, Jagiello K, Puzyn T, Melagraki G, Gulumian M, Afantitis A, Sarimveis H, Yoon T-H, Grafström R, Dario GD (2020) Transcriptomics in toxicogenomics, Part II: preprocessing and differential expression analysis for high quality data. *Nanomaterials* 10:903. <https://doi.org/10.3390/nano10050903>
27. Franqui LS, De Farias MA, Portugal RV, Costa CAR, Domingues RR, Souza Filho AG, Coluci VR, Leme AFP, Martinez DST (2019 Jul) Interaction of graphene oxide with cell culture medium: evaluating the fetal bovine serum protein corona formation towards in vitro nanotoxicity assessment and nanobiointeractions. *Mater Sci Eng C Mater Biol Appl* 100:363–377. <https://doi.org/10.1016/j.msec.2019.02.066>
28. Gao G, Ze Y, Li B, Zhao X, Zhang T, Sheng L, Hu R, Gui S, Sang X, Sun Q, Cheng J, Cheng Z, Wang L, Tang M, Hong F (2012) Ovarian dysfunction and gene-expressed characteristics of female mice caused by long-term exposure to titanium dioxide nanoparticles. *J Hazard Mater* 243:19–27. <https://doi.org/10.1016/j.jhazmat.2012.08.049>
29. Gerloff K, Landesmann B, Worth A, Munn S, Palosaari T, Whelan M (2017) The adverse outcome pathway approach in nanotoxicology. *Comput Toxicol* 1:3–11. <https://doi.org/10.1016/j.comtox.2016.07.001>
30. Glinge C, Clauss S, Boddum K, Jabbari R, Jabbari J, Risgaard B, Tomsits P, Hildebrand B, Kääh S, Wakili R, Jespersen T, Tfelt-Hansen J (2017 Feb 2) Stability of circulating blood-based MicroRNAs - pre-analytic methodological considerations. *PLoS One* 12(2):e0167969. <https://doi.org/10.1371/journal.pone.0167969>
31. Gong C, Tao G, Yang L, Liu J, Liu Q, Zhuang Z (2010) SiO₂ nanoparticles induce global genomic hypomethylation in HaCaT cells. *Biochem Biophys Res Commun* 397:397–400
32. Gong C, Tao G, Yang L, Liu J, Liu Q, Li W, Zhuang Z (2012) Methylation of PARP-1 promoter involved in the regulation of nano-SiO₂-induced decrease of PARP-1 mRNA expression. *Toxicol Lett* 209:264–269
33. Greenberg MVC, Bour'his D (2019) The diverse roles of DNA methylation in mammalian development and disease. *Nat Rev Mol Cell Biol* 20:590–607. <https://doi.org/10.1038/s41580-019-0159-6>
34. Guo NL, Wan Y, Denvir J, Porter DW, Pacurari M, Wolfarth MG, Castranova V, Qian Y (2012) Multiwalled carbon nanotube-induced gene signatures in the mouse lung: potential predictive value for human lung cancer risk and prognosis. *J Toxicol Environ Heal A* 75:1129–1153
35. Ha M, Kim VN (2014) Regulation of microRNA biogenesis. *Nat Rev Mol Cell Biol* 15:509–552
36. Halappanavar S, Ede JD, Shatkin JA, Krug HF (2019) A systematic process for identifying key events for advancing the development of nanomaterial relevant adverse outcome pathways. *NanoImpact* 15:100178. <https://doi.org/10.1016/j.impact.2019.100178>
37. Hamadeh HK, Bushel PR, Jayadev S, DiSorbo O, Bennett L, Li L, Tennant R, Stoll R, Barrett JC, Paules RS, Blanchard K, Afshari CA (2002a) Prediction of

- compound signature using high density gene expression profiling. *Toxicol Sci* 67(2):232–240. <https://doi.org/10.1093/toxsci/67.2.232>
38. Hamadeh HK, Bushel PR, Jayadev S, Martin K, DiSorbo O, Sieber S et al (2002b) Gene expression analysis reveals chemical-specific profiles. *Toxicol Sci*. <https://doi.org/10.1093/toxsci/67.2.219>
 39. Haniu H, Matsuda Y, Usui Y, Aoki K, Shimizu M, Ogihara N, Hara K, Okamoto M, Takanashi S, Ishigaki N, Nakamura K, Kato H, Saito N (2011) Toxicoproteomic evaluation of carbon nanomaterials in vitro. *J Proteome* 74(12):2703–2712. ISSN 1874-3919. <https://doi.org/10.1016/j.jprot.2011.03.004>
 40. Hilton G, Barosova H, Petri-Fink A, Rothen-Rutishauser B, Bereman M (2019 Feb 1) Leveraging proteomics to compare submerged versus air-liquid interface carbon nanotube exposure to a 3D lung cell model. *Toxicol In Vitro* 54:58–66
 41. Hsieh WY, Chou CC, Ho CC, Yu SL, Chen HY, Chou HY, Chou HY, Chen J, Chen HW, Yang PC (2012) Single-walled carbon nanotubes induce airway hyper-reactivity and parenchymal injury in mice. *Am J Respir Cell Mol Biol* 46:257–267
 42. Huang CC, Aronstam RS, Chen DR, Huang YW (2010 Feb) Oxidative stress, calcium homeostasis, and altered gene expression in human lung epithelial cells exposed to ZnO nanoparticles. *Toxicol In Vitro* 24(1):45–55. <https://doi.org/10.1016/j.tiv.2009.09.007>
 43. Husain M, Saber AT, Guo C, Jacobsen NR, Jensen KA, Yauk CL, Williams A, Vogel U, Wallin H, Halappanavar S (2013) Pulmonary instillation of low doses of titanium dioxide nanoparticles in mice leads to particle retention and gene expression changes in the absence of inflammation. *Toxicol Appl Pharmacol* 269:250–262. <https://doi.org/10.1016/j.taap.2013.03.018>
 44. Kim JS, Choi YC, Yu IJ, Song KS, Bang IS, Lee JK, Kang CS (2012) Toxicogenomic comparison of multi-wall carbon nanotubes (MWCNTs) and asbestos. *Arch Toxicol* 86:553–562
 45. Kinaret P, Marwah V, Fortino V, Ilves M, Wolff H, Ruokolainen L, Auvinen P, Savolainen K, Alenius H, Greco D (2017) Network analysis reveals similar transcriptomic responses to intrinsic properties of carbon nanomaterials in vitro and in vivo. *ACS Nano* 11(4):3786–3796
 46. Krewski D, Andersen ME, Mantus E, Zeise L (2009 Apr) Toxicity testing in the 21st century: implications for human health risk assessment. *Risk Anal* 29(4):474–479. <https://doi.org/10.1111/j.1539-6924.2008.01150.x>
 47. Krewski D, Westphal M, Andersen ME, Paoli GM, Chiu WA, Al-Zoughool M et al (2014) A framework for the next generation of risk science. *Environ Health Perspect* 122(8):796–805. <https://doi.org/10.1289/ehp.1307260>
 48. Kuruvilla J, Farinha AP, Bayat N, Cristobal S (2017) Surface proteomics on nanoparticles: a step to simplify the rapid prototyping of nanoparticles. 2:55
 49. Labib S, Williams A, Yauk CL, Nikota JK, Wallin H, Vogel U, Halappanavar S (2016) Nano-risk science: application of toxicogenomics in an adverse outcome pathway framework for risk assessment of multi-walled carbon nanotubes. *Part Fibre Toxicol* 13(1):15. <https://doi.org/10.1186/s12989-016-0125-9>
 50. Li Y, Lee JS (2020) Insights into characterization methods and biomedical applications of nanoparticle-protein corona. *Materials (Basel)* 13:14
 51. Li S, Wang H, Qi Y, Tu J, Bai Y, Tian T, Huang N et al (2011) Biomaterials assessment of nanomaterial cytotoxicity with SOLiD sequencing-based microRNA expression profiling. *Biomaterials* 32(34):9021–9030
 52. Li B, Ze Y, Sun Q, Zhang T, Sang X, Cui Y, Wang X, Gui S, Tan D, Zhu M, Zhao X, Sheng L, Wang L, Hong F, Tang M (2013) Molecular mechanisms of nanosized titanium dioxide-induced pulmonary injury in mice. *PLoS One* 8:e55563. <https://doi.org/10.1371/journal.pone.0055563>
 53. Li Y, Yan J, Ding W, Chen Y, Pack LM, Chen T (2017) Genotoxicity and gene expression analyses of liver and lung tissues of mice treated with titanium dioxide nanoparticles. *Mutagenesis* 32:33–46. <https://doi.org/10.1093/mutage/gew065>
 54. Li W, Jia MX, Deng J, Wang JH, Zuberi Z, Yang S, Ba J, Chen Z (2020) MicroRNA response and toxicity of potential pathways in human colon cancer cells exposed to titanium dioxide nanoparticles. *Cancers* 12:1236. <https://doi.org/10.3390/cancers12051236>
 55. Liu Z, Huang R, Roberts R, Tong W (2019) Toxicogenomics: a 2020 vision. *Trends Pharmacol Sci* 40(2):92–103. <https://doi.org/10.1016/j.tips.2018.12.001>
 56. Lu X, Miousse IR, Pirela SV, Melnyk S, Koturbash I, Demokritou P (2016a) Short-term exposure to engineered nanomaterials affects cellular epigenome. *Nanotoxicology* 10(2):140–150. <https://doi.org/10.3109/17435390.2015.1025115>
 57. Lu X, Miousse IR, Pirela SV, Moore JK, Melnyk S, Koturbash I, Demokritou P (2016b) In vivo epigenetic effects induced by engineered nanomaterials: a case study of copper oxide and laser printer-emitted engineered nanoparticles. *Nanotoxicology* 10(5):629–639. <https://doi.org/10.3109/17435390.2015.1108473>
 58. Lynch I, Cedervall T, Lundqvist M, Cabaleiro-Lago C, Linse S, Dawson KA (2007 Oct) The nanoparticle-protein complex as a biological entity; a complex fluids and surface science challenge for the 21st century. *Adv Colloid Interf Sci* 134-135:167–174. <https://doi.org/10.1016/j.cis.2007.04.021>
 59. Madannejad R, Shoaie N, Jahanpeyma F, Darvishi MH, Azimzadeh M, Javadi H (2019 Jul 1) Toxicity of carbon-based nanomaterials: reviewing recent reports in medical and biological systems. *Chem Biol Interact* 307:206–222. <https://doi.org/10.1016/j.cbi.2019.04.036>
 60. Marmiroli M, Pagano L, Pasquali F, Zappettini A, Tosato V, Bruschi CV, Marmiroli N (2016) A genome-wide nanotoxicology screen of *Saccharomyces cere-*

- visiae mutants reveals the basis for cadmium sulphide quantum dot tolerance and sensitivity. *Nanotoxicology* 10(1):84–93. <https://doi.org/10.3109/17435390.2015.1019586>
61. Mirzajani F, Askari H, Hamzelou S, Schober Y, Römpp A, Ghassempour A, Spengler B (2014 Feb) Proteomics study of silver nanoparticles toxicity on bacillus thuringiensis. *Ecotoxicol Environ Saf* 100:122–130. <https://doi.org/10.1016/j.ecoenv.2013.10.009>
62. Nagano T, Higashisaka K, Kunieda A, Iwahara Y, Tanaka K, Nagano K, Abe Y, Kamada H, Tsunoda S, Nabeshi H, Yoshikawa T, Yoshioka Y, Tsutsumi Y (2013) Liver-specific microRNAs as biomarkers of nanomaterial-induced liver damage. *Nanotechnology* 24:405102. (7pp)
63. National Research Council (US) Committee on Applications of Toxicogenomic Technologies to Predictive Toxicology. *Applications of Toxicogenomic Technologies to Predictive Toxicology and Risk Assessment*. Washington (DC): National Academies Press (US); 2007. 1, Introduction. Available from: <https://www.ncbi.nlm.nih.gov/books/NBK10209/>
64. Nymark P, Wijshoff P, Cavill R, van Herwijnen M, Coonen MLJ, Claessen S, Catalán J, Norppa H, Kleinjans JCS, Briedé JJ (2015) Extensive temporal transcriptome and microRNA analysis identify molecular mechanisms underlying mitochondrial dysfunction induced by multi-walled carbon nanotubes in human lung cells. *Nanotoxicology* 9(5):624–635
65. OECD (2017) Guidance document on developing and assessing adverse outcome pathways. OECD Environment, Health and Safety Publications Series on Testing and Assessment. No 184. ENV/JM/MONO(2013)6, Paris, France
66. Pacurari M, Qian Y, Porter DW, Wolfarth M, Wan Y, Luo D, Ding M, Castranova V, Guo NL (2011) Multi-walled carbon nanotube-induced gene expression in the mouse lung: association with lung pathology. *Toxicol Appl Pharmacol* 255:18–31. <https://doi.org/10.1016/j.taap.2011.05.012>
67. Poulsen SS, Jacobsen NR, Labib S, Wu D, Husain M, Bøgelund JP, Andersen O, Købler C, Møhlhave K, Kyjovska ZO et al (2013) Transcriptomic analysis reveals novel mechanistic insight into murine biological responses to multi-walled carbon nanotubes in lungs and cultured lung epithelial cells. *PLoS One* 8:1–25. <https://doi.org/10.1371/journal.pone.0080452>
68. Poulsen SS, Saber AT, Williams A, Andersen O, Købler C, Atluri R, Pozzebon ME, Mucelli SP, Simion M, Rickerby D, Vogel U (2015) MWCNTs of different physicochemical properties cause similar inflammatory responses, but differences in transcriptional and histological markers of fibrosis in mouse lungs. *Toxicol Appl Pharm* 284:16–32. <https://doi.org/10.1016/j.taap.2014.12.011>
69. Pu Q, Huang Y, Lu Y, Peng Y, Zhang J, Feng G (2016) Tissue-specific and plasma microRNA profiles could be promising biomarkers of histological classification and TNM stage in non-small cell lung cancer. *Thorac Cancer* 7:348–354
70. Rupani H, Sanchez-elsner T, Howarth P (2013) MicroRNAs and respiratory diseases. *Eur Respir J* 41:695–705
71. Sabine L, Amaya A, Collins A (2015) The comet assay: past, present, and future. *Front Genet* 6:266. <https://doi.org/10.3389/fgene.2015.00266>
72. Schwarzenbach H, Nishida N, Calin GA, Pantel K (2014) Clinical relevance of circulating cell-free microRNAs in cancer. *Nat Rev Clin Oncol* 11(3):145–156. <https://doi.org/10.1038/nrclinonc.2014.5>
73. Scoville DK, Botta D, Galdanes K, Schmuck SC, White CC, Stapleton PL, Bammler TK, MacDonald JW, Altemeier WA, Hernandez M, Kleeburger SR, Chen LC, Gordon T, Kavanagh TJ (2017 Oct) Genetic determinants of susceptibility to silver nanoparticle-induced acute lung inflammation in mice. *FASEB J* 31(10):4600–4611. <https://doi.org/10.1096/fj.201700187R>
74. Sessa R, Hata A (2013) Role of microRNAs in lung development and pulmonary diseases. *Pulm Circ* 3(2):315–328
75. Shvedova AA, Yamamala N, Kisin ER, Khailullin TO, Birch ME, Fatkhutdinova LM (2016) Integrated analysis of dysregulated ncRNA and mRNA expression profiles in humans exposed to carbon nanotubes. *PLoS One* 11(3):1–32
76. Smith LM, Kelleher NL (2013 Mar) Proteoform: a single term describing protein complexity. *Nat Methods* 10(3):186–187
77. Snyder-Talkington BN, Dymacek J, Porter DW, Wolfarth MG, Mercer RR, Pacurari M, Denvir J, Castranova V, Qiana Y, Guo NL (2013) System-based identification of toxicity pathways associated with multi-walled carbon nanotube-induced pathological responses. *Toxicol Appl Pharm* 272(2):476–489. <https://doi.org/10.1016/j.taap.2013.06.026>
78. Snyder-Talkington BN, Dong C, Zhao X, Dymacek J, Porter DW, Wolfarth MG, Castranova V, Qian Y, Guo NL (2015) Multi-walled carbon nanotube-induced gene expression in vitro: concordance with in vivo studies. *Toxicology* 328:66–74. <https://doi.org/10.1016/j.tox.2014.12.012>
79. Snyder-Talkington BN, Dong C, Porter DW, Ducatman B, Wolfarth MG, Andrew M, Battelli L, Raese R, Castranova V, Guo NL, Qian Y (2016) Multiwalled carbon nanotube-induced pulmonary inflammatory and fibrotic responses and genomic changes following aspiration exposure in mice: a 1-year postexposure study. *J Toxicol Environ Health A* 79:352–366
80. Srivastav AK, Dhiman N, Khan H, Srivastav AK, Yadav SK, Prakash J et al (2019) Impact of surface-engineered ZnO nanoparticles on protein corona configuration and their interactions with biological system. *J Pharm Sci* 108(5):1872–1889
81. Stocco A, Karlsson HL, Coppède F, Migliore L (2013) Epigenetic effects of nano-sized materials. *Toxicology* 313:3–14
82. Tenzer S, Docter D, Kuharev J, Musyanovych A, Fetz V, Hecht R, Schlenk F, Fischer D, Kiouptsi K, Reinhardt C, Landfester K, Schild H, Maskos M, Knauer SK, Stauber RH (2013 Oct) Rapid formation

- of plasma protein corona critically affects nanoparticle pathophysiology. *Nat Nanotechnol* 8(10):772–781. <https://doi.org/10.1038/nnano.2013.181>
83. Thier R, Brüning T, Roos PH, Rihs HP, Golka K, Ko Y, Bolt HM (2003 Jun) Markers of genetic susceptibility in human environmental hygiene and toxicology: the role of selected CYP, NAT and GST genes. *Int J Hyg Environ Health* 206(3):149–171. <https://doi.org/10.1078/1438-4639-00209>
 84. Thomas RS, Rank DR, Penn SG, Zastrow GM, Hayes KR, Hu T, Pande K, Lewis M, Jovanovich SB, Bradfield CA (2002 Dec) Application of genomics to toxicology research. *Environ Health Perspect* 110(Suppl 6):919–923. <https://doi.org/10.1289/ehp.02110s6919>
 85. Titz B, Elamin A, Martin F, Schneider T, Dijon S, Ivanov NV et al (2014) Proteomics for systems toxicology. *Comput Struct Biotechnol J*:73–90
 86. Tyers M, Mann M (2003) From genomics to proteomics. *Nature* 422:193–197
 87. Van Gool A, Corrales F, Čolović M, Krstić D, Oliver-Martos B, Martínez-Cáceres E, Jakasa I, Gajski G, Brun V, Kyriacou K, Burzyska-Pedziwiatr I, Wozniak LA, Nierkens S, Pascual García C, Katrlík J, Bojic-Trbojevic Z, Vacek J, Llorente A, Antohe F, Suica V, Suarez G, t'Kindt R, Martin P, Penque D, Martins IL, Bodoki E, Iacob BC, Aydindogan E, Timur S, Allinson J, Sutton C, Luidert T, Wittfooth S, Sammar M (2020 Apr) Analytical techniques for multiplex analysis of protein biomarkers. *Expert Rev Proteomics* 17(4):257–273. <https://doi.org/10.1080/14789450.2020.1763174>
 88. Ventura C, Sousa Uva A, Lavinha J, Silva MJ (2018) Conventional and novel “omics”-based approaches to the study of carbon nanotubes pulmonary toxicity. *Environ Mol Mut* 59(4):334–362. <https://doi.org/10.1002/em.22177>
 89. Ventura C, Vieira L, Silva C, Sousa Uva A, Silva MJ (2020) Functional effects of differentially expressed microRNAs in A549 cells exposed to MWCNT-7 or crocidolite. *Toxicol Lett* 328:7–18. <https://doi.org/10.1016/j.toxlet.2020.04.002>
 90. Waters KM, Masiello LM, Zangar RC, Tarasevich BJ, Karin NJ, Quesenberry RD et al (2009) Macrophage responses to silica nanoparticles are highly conserved across particle sizes. *Toxicol Sci* 107(2):553–569. <https://doi.org/10.1093/toxsci/kfn250>
 91. Waters MD, Jackson M, Lea I (2010 Dec) Characterizing and predicting carcinogenicity and mode of action using conventional and toxicogenomics methods. *Mutat Res* 705(3):184–200. <https://doi.org/10.1016/j.mrrev.2010.04.005>
 92. Wu Q, Zhao Y, Li Y, Wang D (2014 Aug) Susceptible genes regulate the adverse effects of TiO₂-NPs at predicted environmental relevant concentrations on nematode *Caenorhabditis elegans*. *Nanomedicine* 10(6):1263–1271. <https://doi.org/10.1016/j.nano.2014.03.010>
 93. Yanaihara N, Caplen N, Bowman E, Seike M, Kumamoto K, Yi M, Stephens RM et al (2006) Unique microRNA molecular profiles in lung cancer diagnosis and prognosis. *Cancer Cell* 9(3):189–198
 94. Yazdimamaghani M, Moos PJ, Ghandehari H (2017) Global gene expression analysis of macrophage response induced by nonporous and porous silica nanoparticles. *Nanomedicine* 14:533–545. <https://doi.org/10.1016/j.nano.2017.11.021>
 95. Zhang ZH, Jhaveri DJ, Marshall VM, Bauer DC, Edson J, Narayanan RK, Robinson GJ, Lundberg AE, Bartlett PF, Wray NR, Zhao QY (2014) A comparative study of techniques for differential expression analysis on RNA-Seq data. *PLoS One* 9(8):e103207. <https://doi.org/10.1371/journal.pone.0103207>
 96. Zhang T, Gaffrey MJ, Thomas DG, Weber TJ, Hess BM, Weitz KK, Piehowski PD, Petyuk VA, Moore RJ, Qian WJ, Thrall BD (2020) A proteome-wide assessment of the oxidative stress paradigm for metal and metal-oxide nanomaterials in human macrophages. *NanoImpact* 17. <https://doi.org/10.1016/j.impact.2019.100194>



Epigenetic Mechanisms in Understanding Nanomaterial-Induced Toxicity

9

Manosij Ghosh, Lode Godderis, and Peter Hoet

Abstract

The toxic effects of different forms of nanomaterials comprise a series of biological effects such as oxidative stress; DNA damage; inflammatory response; activation of nuclear transcription factors. Some of these are key characteristics of human carcinogens and have been considered for hazard identification of nanomaterials. In addition, epigenetic changes also play a key role in the multi-step sequential process of carcinogenesis. Epigenetic modifications may constitute changes in DNA methylation, histone modifications (methylation, acetylation etc), and changes in non-coding RNA, leading to an altered gene expression profile. In this chapter, we describe the state-of-the-art of epigenetic modifications induced by different nanomaterials, from a limited number of *in vitro*- *in vivo* and human studies, a majority of which is primarily focused on DNA methylation. We also highlight the potential challenges and future directions in the field of epigenetics research in nanomaterial toxicology.

Keywords

Nanotoxicology · Epigenetics · DNA methylation · Histone modification

9.1 Introduction

Different aspects of nanotoxicology has been discussed in the previous chapters, and it has become abundantly clear that nanoparticles (NPs) can induce oxidative stress [30, 53, 60, 75], DNA damage [30, 59, 76], alter DNA repair efficiency [11, 91], induce an inflammatory response [75, 76], can potentially be immunomodulatory/immunosuppressive [13, 42, 62, 66] and can affect cell death/cell proliferation [1, 21, 48, 72, 79, 95]. While, it is also clear that the field of nanotoxicology research is quickly emerging and there are significant knowledge gaps, some of the observed effects reported for one or more nanoparticle align with the “*Key Characteristics of Carcinogens as a Basis for Organizing Data on Mechanisms of Carcinogenesis*” described by Smith et al. [92]. In addition, the “*10 key characteristics*” identified by Smith et al. [92] towards organization of mechanistic data, also included epigenetic alterations.

Epigenetic alterations are defined (by NCI) as changes “in the chemical structure of DNA that does not change the DNA coding sequence” [19]. In other words, epigenetic alterations are broadly considered heritable changes that do not

M. Ghosh (✉) · L. Godderis · P. Hoet
Department of Public Health and Primary Care,
Centre Environment & Health, KU Leuven, Leuven,
Belgium
e-mail: manosij.ghosh@kuleuven.be

involve a change in the DNA sequence itself. Epigenetic alterations, such as DNA/RNA methylation, histone modifications (methylation, acetylation), non-coding RNA regulate gene expression by regulating chromatin structure and accessibility. Such alterations/signatures play a crucial role in proper cellular function, differentiation, development and are influenced by a wide range of endogenous and exogenous factors. One of the most studied epigenetic alteration is DNA methylation (and demethylation), where a methyl-group (CH_3) is covalently added to position 5 of the cytosine pyrimidine ring, and a family of DNA methyltransferase (DNMT) and ten-eleven translocation (TET) enzymes play important role in the maintenance of methylation pattern [40, 46, 100]. It is generally accepted that CpG islands (regions with a high frequency of CpG sites) in promoter regions of genes are predominantly unmethylated which activate gene transcription [4, 5]. Besides, DNA methylation, histone modifications play crucial role in maintaining chromatin conformation, and these processes are tightly coupled [12, 27, 40]. These post-translational covalent modifications of histone mainly studied in the tail domains of H3 and H4, include modifications such as acetylation and methylation of lysine and arginine among other [12, 27, 40]; and are regulated by enzyme families such as histone acetyl transferase (HAT), histone deacetylase (HDAC), Histone methyltransferase (HMT). Another group of key regulators are the non-coding RNAs and regulate gene expression at the transcriptional and post-transcriptional levels [26, 99], and closely interact with the DNA methylation and histone modification machinery [41, 102].

From the standpoint of environmental and occupational diseases and that of chemical induced carcinogenesis, it is considerably well established that epigenetic modifications play a crucial role. Epigenetic changes induced by genotoxic environmental carcinogens have been systematically reviewed by Chappell et al. [14]. While epigenetic changes can be used as biomarker of exposure, or as marker of disease and disease progression [52] they can also be used as potential therapeutic targets [50]. This

is particularly relevant for NP toxicology, where rate of NP production far exceeds the hazard identification and risk assessment, while an increasing number of workers and consumers are being exposed to these diverse group of materials [8, 38].

Despite considerable progress in the field of epigenetics and disease biology and cancer epigenetics, major gaps remain in understanding of chemical induced epigenetic alterations. This is also true for the field of nanotoxicology. This chapter will therefore summarize the state-of-the-art and developments in understanding NP induced epigenetic changes and comment briefly on future direction. While the NPs discussed in the chapter is not exhaustive, it is representative of some of the most produced and studied particles in relation to toxicology. We have identified studies that have evaluated one or more epigenetic endpoints, however no mechanistic conclusion for individual particle or NP as a group has been made in the chapter due to the limited number of comparable studies (differences in particle properties, experimental design, test system and cell types).

9.2 Epigenetic Changes Induced by Metal and Metal Oxide Nanoparticles

While the evidence stream on epigenetic changes induced by metal and metal oxide nanoparticle are relatively scarce, some studies have observed epigenetic modifications induced by TiO_2 -NPs, ZnO -NPs, CuO -NPs, SiO_2 NPs, silver and gold nanoparticles among others. In this section we discuss briefly, the distinct mechanistic evidence exhibited by each of these NPs and at the same time try to identify the commonality exhibited by these particles.

9.2.1 TiO_2 Nanoparticles

TiO_2 -NPs are one of the most abundantly produced nanomaterials, with considerable evidence regarding oxidative stress, cyto-genotoxicity, impaired DNA repair efficiency and limited evi-

dence on immunotoxicity, in vitro and in vivo [20, 39, 74, 88, 10, 63]. While limited by number, in this section (Table 9.1), we discuss the growing number of studies that have identified some of the underlying epigenetic mechanism.

Pogribna et al. [80], studied global (5-mC) and gene specific (EpiTect array) changes in DNA methylation, induced by TiO₂-NP (Aeroxide TiO₂ P25; 100 µg/mL) in Caco-2, HepG2, NL20 and A-431 cell lines. The authors observed global hypomethylation after 72 h of exposure, for A-431, HepG2 and Caco-2 cells and promoter specific methylation changes in several genes associated with apoptosis and cell cycle modulatory effects. Changes were observed in all cell line for *CDKN1A* and *SCARA3*, while genes like *GADD45A*, *DNAJC15*, *TP53* were also differentially methylated in one or more of the cell lines [80]. In the same study, while the expression of the epigenetic regulators (*DNMT1*, *DNMT3A*, *DNMT3B*, *MBD2*, *UHRF1*) were altered, it was not consistent among the cell types. Given that there is epigenetic heterogeneity among tissues and cell types, such studies using multiple cell line (of relevance to the exposure route, and target) can be very important.

Despite evidences of the influence of TiO₂ crystal phase on toxicity, the effect of crystal phase on epigenetic changes is not well studied. In our study we reported significant global DNA hypomethylation (5-mC), and a decrease in global hydroxymethylation (5-hmC) induced by different crystal phase of TiO₂-NP (NM-102/Anatase, NM-104/Rutile, and NM-105/Anatase-rutile) at sub cytotoxic concentrations in 16-HBE cells [32] however such changes were not mechanistically linked to other toxicity endpoints. In another study the authors used surfaced coated TiO₂-NP, to study the effect on DNA methylation, in A549 cells, in addition to other cytogenotoxic endpoints [93]. The authors observed significant decrease in Long Interspersed Nuclear Element-1 (LINE-1) methylation after 72 h of exposure to silica and citrate coated TiO₂-NP, while no significant changes were observed after 48 h of exposure.

Patil et al. [77] also reported global DNA (5-mC) hypomethylation, in MRC-5 cells after 24 and 48 h exposure to TiO₂-NP (<100 nm, mixture of rutile and anatase, 1 and 8 µg/mL). They also observed reduced mRNA expression of DNA methyltransferases *DNMT1*, *DNMT3A*, and *DNMT3B* [77]. These changes in DNA methylation were associated with induction of oxidative stress. The influence of TiO₂-NP (<25 nm, 24 h) induced oxidative stress on DNA methylation was also reported by Bai et al. [2], in A549 cells, where they observed significant DNA hypermethylation in the promoter region of *PARP-1* (encoding poly (ADP-ribose) polymerase 1, involved in DNA repair). Based on the other endpoints (cyto-genotoxic and oxidative stress), Stocco et al. [93] suggested that oxidative stress could be a primary event in inducing genotoxicity and epigenotoxicity. While most studies have evaluated DNA methylation as a primary epigenetic endpoint, Jayaram and Payne [45], studied the effect of TiO₂-NP induced intracellular superoxide on *HDAC9* (histone deacetylase 9) expression, they used SOD-TiO₂-NPs (SOD corona), and passivated TiO₂-NP. Both passivated and SOD particles did not result in intracellular ROS production. SOD-TiO₂-NPs were able to scavenge superoxide and the expression of *HDAC9* were comparable to control. Similar results were observed for the passivated TiO₂-NPs [45]. In a study by the same group, a decrease in *HDAC9* expression, and an increase in *HDAC10* expression was observed; induced by food-grade TiO₂ particles [44]. While food grade TiO₂ particle, more specifically E171 may not be primarily a nanoparticle, electron microscopy analysis shows that at least 36% of the particles (by number) are below 100 nm [29, 97]. In another study [57], in addition to oxidative stress, the authors observed significant global DNA hypomethylation in A549 and 16HBE cells at different concentrations (0.1–100 µg mL⁻¹, 48 h) of TiO₂-N25 and TiO₂-A60. Both TiO₂-N25 and TiO₂-A60 exposure resulted in significant changes in the mRNA and protein expression levels of methylation related genes (*DNMT3B*, *TET1*, *TET2* and *TET3*) in A549 and 16HBE

Table 9.1 Summary table of studies reporting epigenetic changes induced by TiO₂ nanoparticles

Nanoparticle properties	Experiment ^a		Condition	Epigenetic (and associated) endpoint studied ^b	Result	References
	Type	System				
JRC TiO ₂ ; NM-102 (~21 nm, Anatase; BET surface area 60.227 m ² /g), NM-104; (~26 nm, rutile, BET surface area 41.216 m ² /g), NM-105 (~261 m, Anatase-rutile, BET surface area 37.345 m ² /g);	In vitro	Human Bronchial Epithelial cell line (16HBE)	3, 12.5, 12.5 and 25 µg/ml; 1, 3 and 24 h	Global DNA methylation and hydroxymethylation (LC-MS/MS)	Significant global DNA (5-mC) hypomethylation, decrease in hydroxymethylation	[31]
TiO ₂ -NP (NM101; 20.99 ± 6.4 nm)	In vitro	Human bronchial epithelial cells (BEAS-2B cells)	11 and 20 mg/mL for up to 4 weeks; exposure media changed every 3 days, sample collected at 2 and 4 weeks	Genome wide methylation- human methylation450 BeadChip	DNA methylation changes of 21 CpG sites- corresponding to 22 genes	[90]
Aeroxide P25 (21 nm)	In vitro	Human colorectal adenocarcinoma cells (Caco-2), human hepatocyte carcinoma (HepG2), human bronchial transformed epithelial cells (NL20), human epidermoid carcinoma cells (A-431)	100 µg/mL (non-cytotoxic) TiO ₂ for 24 or 72 h	Global DNA methylation (5-mC), gene specific methylation-EpiTect methylation array, expression of <i>DNMT1</i> , <i>DNMT3a</i> , <i>DNMT3b</i> , <i>MBD2</i> , <i>UHRF1</i>	Global DNA (5-mC) hypomethylation, promoter specific hypermethylation of <i>CDKN1A</i> and <i>SCARA3</i>	[80]
TiO ₂ (634662)- Sigma Aldrich; <100 nm; mixture of rutile and anatase	In vitro	Human fetal fibroblasts (MRC5)	1 and 8 µg/mL, 24 and 48 h	Immunohistochemical staining and ELISA based detection of DNA methylation (5-mC); DNMT expression (<i>DNMT1</i> , <i>DNMT3a</i> , <i>DNMT3b</i>)	Global DNA (5-mC) hypomethylation, reduced DNMT activity, oxidative stress	[77]
22.1 nm- Sigma-Aldrich; surface area of 45–55 m ² /g	In vitro	Human lung adenocarcinoma cell line (A549)	6.25, 12.5, 25, 50, 100 µg/mL; 24 h	Methylation-specific PCR	Oxidative stress associated hypermethylation of PARP-1 promoter region	[2]
Pristine TiO ₂ (5 nm), citrate coated TiO ₂ and silica coated TiO ₂ , Aeroxide® P25 (21 nm)	In vitro	Human lung adenocarcinoma cell line (A549)	8.3–266.6 µg/ml (1.25 to 80 µg/cm ²); 40 µg/cm ² used for DNA methylation study	ELISA method to detect LINE-1 methylation	Global methylation (of LINE-1) not affected at 48 h, significant hypomethylation at 72 h	[93]

TiO ₂ -NPs (21 nm, #718467, Sigma-Aldrich); P-TiO ₂ -NPs (passivated TiO ₂ -NPs- sodium aluminate, #11138491, Sigma-Aldrich; and silica #1056212500, Sigma-Aldrich); SOD-TiO ₂ -NPs (TiO ₂ -NP with SOD corona)	Human lung adenocarcinoma cell line (A549)	800 µg/mL in T25 flask, 994 µg/mL in 35 mm optical dishes; 24 h	HDAC9 expression (western blot)	Decrease in HDAC9 expression; the SOD corona inhibits the production of intracellular ROS- partially restoring HDAC9 expression, similar results were observed for passivated TiO ₂ -NP	[45]
Food-grade TiO ₂ particles (E171), 148 ± 44 nm; up to 32% particles <100 nm (information from literature)	Human lung adenocarcinoma cell line (A549)	994 µg/mL	HDAC9, HDAC10 expression (western blot)	HDAC9, HDAC10	[44]
TiO ₂ -N25 nanotubes (25 nm average diameter, Sigma-Aldrich); TiO ₂ (TiO ₂ -A60; Anatase, 60 nm average diameter, Aladdin-Shanghai, China)	Human lung adenocarcinoma cell line (A549), human bronchial epithelial cell line (16HBE)	Stock further diluted in cell culture media to 0.1, 1, 10 and 100 µg mL ⁻¹ and sonicated within 5 min before the treatment; 48 h	Global DNA methylation (5-mC)	Global DNA hypomethylation, significant changes in the mRNA and protein expression (<i>DNMT3b</i> , <i>TET1</i> , <i>TET2</i> and <i>TET3</i>)	[57]
TiO ₂ (EVONIK-Parsippany, NJ), 21 nm; specific surface area 50 m ² /g	Human monocyte (THP1), primary small airway epithelial cells (SAEC), murine macrophage cells (RAW264.7)	The cells were in the respective cell culture media at two doses (0.5 and 30 µg/mL) for 24h	Global DNA methylation (5-mC) and hydroxymethylation (5-hmC), LINE1 and Alu/SINE methylation specific PCR	No significant difference in global of sequence specific DNA methylation	[55]

(continued)

Table 9.1 (continued)

Nanoparticle properties	Experiment ^a		Condition	Epigenetic (and associated) endpoint studied ^b	Result	References
	Type	System				
TiO ₂ -NPs (25 nm; anatase, Aladdin-Shanghai, China)	In vivo	Healthy male NIH mice	5-week (young group) 10-week (adult group); housed in controlled conditions (20 ± 2 °C; 50–70% humidity; 12 h light/dark cycle), fed commercial pellet diet and deionized water ad libitum. 4 groups (6 mice/ group): Young control, young TiO ₂ -NP, adult control, adult TiO ₂ -NP; intranasal instillation (20 mg/kg body weight), left naris, once/ day for 30 days	Global DNA methylation (5-mC) and DNA hydroxymethylation (5-hmC) (ELISA); Pyrosequencing (<i>IFN-γ</i> , <i>TNF-α</i> and <i>Thy-1</i>) in lung tissue; <i>DNMT3B</i> or <i>MBD2</i> expression (western blot); RNA sequencing (Illumina HiSeq 4000)	Increased inflammation; global hypomethylation, decreased DNA hydroxymethylation; significant changes in promoter methylation of <i>TNF-α</i> and <i>Thy-1</i> ; altered mRNA expression-pathways in cancer	[58]
TiO ₂ -NP	Human population	DNA from leucocyte	Non exposed (n = 43, age: 37.95 ± 8.94) TiO ₂ -NP exposed (n = 26, age: 34.65 ± 7.99, exposure duration: 2.33 ± 2.49 years)	Global DNA methylation (5-mC; HPLC)	No significant change in DNA methylation, increased oxidative stress	[54]

^aLimited exposure information provided here, for additional information refer to full text

^bFor other endpoints refer to full text

cells. While, most studies have observed oxidative stress and changes in DNA methylation induced by TiO₂-NP, in one study [56] the authors did not observe significant changes in global DNA methylation/hydroxymethylation or LINE1 methylation in TiO₂-NP (21 nm) exposed THP-1, SAEC, RAW264.7 cells at subtoxic concentrations (0.5 and 30 µg/mL for 24 h). Studies reporting the effect of long-term exposure to TiO₂-NP on epigenetic changes are limited. Sierra et al. [90] observed changes in DNA methylation (21 CpG sites- corresponding to 22 genes), in TiO₂-NP (NM-101; 20.99 ± 6.4 nm) exposed BEAS-2B cells after a period of up to 4 weeks. Since the number of differentially methylated genes were few, further enrichment analysis was not performed on the set.

In an in vivo study [58], the effect of anatase TiO₂-NP (25 nm), after 30 day-intranasal instillations in young (5-week) and adult (10-week) mice was investigated and observed that the lung of young mice were more susceptible, compared to the adult mice. While, inflammatory markers were upregulated in both young and adult mice, significant global DNA hypomethylation and decrease in DNA hydroxymethylation were observed in young mice. Significant changes in sequence specific methylation of *TNF-α* promoter (2 positions) and *Thy-1* (cell surface antigen) were also observed. Expression of DNMT mRNAs (*DNMT1*, *DNMT3A* and *DNMT3B*) were significantly upregulated in the young mice as well. Changes in DNA methylation, DNMT expression, and changes in expression of genes associated with pathways in cancer indicated the importance of epigenetic regulation and the potential to be used as biomarker for exposure and disease [58]. Additionally, in a cross-sectional study, Liou et al. [54], investigated the effect of TiO₂ exposure in workers handling (n = 26) TiO₂-NP and observed an increase in oxidative stress, but no changes in global DNA methylation were observed.

Overall, the studies reporting epigenetic alterations induced by TiO₂-NP, primarily investigated DNA methylation changes. Despite the heterogeneity in particle and cell types used in such studies, evidence indicate towards disrup-

tion of DNA methyltransferase (DNMT) activity and DNA hypomethylation, often associated with increased oxidative stress. Since oxidative stress and oxidative DNA damage has been shown to interfere with the ability of DNMTs to efficiently interact with DNA [104], resulting in DNA hypomethylation and genomic instability, oxidative stress induced epigenetic mechanisms warrant further investigation.

9.2.2 Zinc and ZnO Nanoparticles

Previous studies have identified ZnO-NP induced cyto-genotoxicity and oxidative stress, in vitro and in vivo, and a major attribute of ZnO-NP toxicity is ionization/dissolution [96, 101]. However, only a handful of studies have investigated epigenetic alteration. In a study (Table 9.2) which also evaluated epigenetic effect of TiO₂-NP, Patil et al. [77] reported DNA hypomethylation and changes in mRNA expression of *DNMT1*, *DNMT3A*, and *DNMT3B*, in MRC-5 cells for ZnO-NP (<100 nm, 1 and 8 µg/mL, 24 and 48 h exposure). Choudhury et al. [84] investigated the effect of ZnO-NP (90 ± 2 nm) in human embryonic kidney cells (HEK-293) on several key endpoints and observed a significant increase in oxidative stress and apoptosis. The authors observed a significant DNA hypomethylation, sequence specific demethylation of LINE1 and an increase in DNA hydroxymethylation, and a significant increase in expression of Ten-Eleven Translocation (TET) [84]. Another in vitro study in HaCaT cells, exposed to ZnO-NP revealed significant increase in H3K9 methylation and a decrease in H4K5 acetylation [28]. These changes were associated with an increase in expression of pro-apoptotic genes and increased oxidative stress and DNA damage and G2/M cell cycle arrest. While, the limited number of studies provide some evidence regarding oxidative stress induced epigenetic alteration, further studies (both in vitro and in vivo) are required to evaluate the epigenetic changes induced by ZnO-NP taking into account physicochemical attributes such as dissolution.

Table 9.2 Summary table of studies reporting epigenetic changes induced by Zinc nanoparticles

Nanoparticle properties		Experiment ^a		Epigenetic (and associated) endpoint studied ^b	Result	References
Type	System	Condition				
ZnO-NP (544906)- Sigma Aldrich, <100 nm	Human fetal fibroblasts (MRC5)	In vitro 1 and 8 µg/mL, 24 and 48 h		Immunochemical staining and ELISA based detection of DNA methylation (5-mC); DNMT expression (<i>DNMT1</i> , <i>DNMT3a</i> , <i>DNMT3b</i>)	Global DNA (5-mC) hypomethylation, reduced DNMT activity, oxidative stress	[31, 32]
ZnO-NP (90 ± 2 nm), synthesized from 0.5 M zinc nitrate hexahydrate [Zn(NO ₃)-6H ₂ O] and NaOH	Human embryonic kidney cells (HEK-293)	In vitro 25 and 50 µg/ml, 48 h		Global DNA methylation (5-mC) and DNA hydroxymethylation (5-hmC); expression of TET (<i>TET1</i> , <i>TET2</i> , and <i>TET3</i>) and DNMT (<i>DNMT1</i> , <i>DNMT3A</i> , and <i>DNMT3B</i>); sequence specific DNA methylation (pyrosequencing)- <i>LINE-1</i> , <i>NBL2</i> and <i>D4Z4</i>	Significant global DNA (5-mC) hypomethylation, significant increase in hydroxymethylation (5-hmC), reduced DNMT activity, significant increase in TET expression, hypomethylation of <i>LINE1</i> , oxidative stress	[84]
ZnO-NP(<100 nm; 99.7% metal basis; specific surface area, 15–25 m ² /g, sigma-Aldrich co. St Louis, MO, USA)	Human epidermal keratinocyte cell line (HaCaT)	In vitro 20, 50 µg/mL, 24 h		Histone modification (H4K5ac, H3K9me2; western blot)	Decreased H4K5ac levels and increased H3K9me2	[28]

^aLimited exposure information provided here, for additional information refer to full text

^bFor other endpoints refer to full text

9.2.3 Silica Nanoparticles

Only few studies have reported epigenetic alterations induced by silica nanoparticles (Table 9.3). One such evidence comes from the study by Seidel et al. [86] in Bhas 42 cell, exposed to Min-U-Sil® 5 (crystalline silica, 15 and 25 $\mu\text{g}/\text{cm}^2$) or NM-203 (pyrogenic amorphous silica, 2 and 5 $\mu\text{g}/\text{cm}^2$). The authors observed significant global DNA hypomethylation and significant changes in the DNMT expression (increased *DNMT3A* and *DNMT3B*) [86] and an increase in Histone H4 acetylation and significant changes in HDAC expression by Min-U-Sil® 5, but not for NM-203. For Min-U-Sil® 5, the authors also observed increased acetylated histone H3 lysine 4 (H3K4Ac), histone H3 lysine 9 (H3K9Ac) and acetylated histone H3 lysine 27 (H3K27Ac) on c-Myc promoter, which plays important role in cellular metabolism and proliferation and in cell transformation [86]. Epigenetic alterations were also studied in HaCaT cells, exposed to SiO₂ NP (15 nm) [36]; where the authors observed significant increase in promoter methylation of Poly [ADP-ribose] polymerase 1 (*PARP-1*), which plays key role in chromatin remodelling and multiple DNA damage repair pathways [82]. Using a *DNMT1* knockdown, the authors confirmed the role of *DNMT1* in the observed SiO₂ NP mediated effect. SiO₂ NP exposure (5 $\mu\text{g}/\text{mL}$, 30 passage) in BEAS-2B cells also induced significant changes in DNA methylation including *PI3K-Akt* and sequence specific hypermethylation of *CREB3L1* and *Bcl-2* promoters indicating the role of mitochondria mediated apoptosis [105]. In a cross-sectional study Liou et al. [54], observed an increase in oxidative stress markers in a group of workers handling SiO₂ (n = 31), but changes in DNA methylation was not observed. Based on these studies, it can be suggested that SiO₂ NP can induce epigenetic changes to the DNA and histone, and these changes are primarily associated with cell cycle regulation and proliferation. However, important aspect of SiO₂ NP toxicity such as the crystal structure and surface silanols have not been addressed by these studies.

9.2.4 Copper and Copper Oxide Nanoparticles

In an in vitro study [56], the authors evaluated effect of CuO NP (58.7 nm, 0.5 and 30 $\mu\text{g}/\text{m}$, 24 h) in different cell lines (THP-1, SAEC, RAW264.7) and observed small but significant changes in LINE 1 methylation, while no changes in global DNA methylation/hydroxymethylation were observed (Table 9.4). In a study aimed at identifying anticancer effect of green synthesized CuO NP, the authors observed significant inhibition of HDAC family [47] in A549 cells, however description of exposure was not very well defined for further interpretation. Most evidence regarding epigenetic changes induced by copper and copper oxide nanoparticles come from in vivo studies. While several key endpoints were evaluated, here we discuss the epigenetic endpoints of interest. In an in vivo study [55] on BALB/c male mice, using the same CuO NP (58.7 nm) particle as mentioned above [56], the authors observed an Increase in 5-mC levels and 5-hmC levels in lung tissue, hypermethylation of SINE B1 elements in the alveolar macrophages; and methylation of LINE-1 remained unchanged. In their study on female ICR (Institute of Cancer Research) mice, Rosner et al. [83] observed no significant change in global DNA methylation upon whole-body inhalation exposure to CuO NPs (3 days, 6 weeks, and 3 months). Enriched pathways, based on results of miRNA -mRNA expression changes were associated with lysosomal function, adherens and tight junction, pathways in cancer among others. In another study, Ognik et al. [67] observed an increase in oxidative stress markers (lipid peroxides, MDA), a decrease in catalase, total glutathione and global DNA hypomethylation for animals receiving Cu, CuNP through their diet. Through their results the authors suggested that Cu deficiency could impair oxidative defence, and that CuNP supplementation in the diet reduces protein oxidation, nitration, DNA oxidation and methylation [67].

Table 9.3 Summary table of studies reporting epigenetic changes induced by Silica nanoparticles

Nanoparticle properties	Experiment ^a		Condition	Epigenetic (and associated) endpoint studied ^b	Result	References
	Type	System				
SiNP	In vitro	Human bronchial epithelial cells (BEAS-2B cells)	5 µg/mL, 30 passages	Genome wide methylation-human methylation450 BeadChip; pyrosequencing	223 CpG hypomethylated, 1973 CpG hypermethylated; PI3K/Akt signaling pathway altered, sequence specific hypermethylation of CREB3L1 and Bcl-2 gene	[105]
SiO ₂ -NP (15 nm; Wan Jing New Material Co. Ltd. Hangzhou, Zhejiang, China)	In vitro	Human epidermal keratinocyte cell line (HaCaT)	HaCaT cell with or without DNMT1 knock down; cells exposed to 2.5, 5, 10 µg/mL SiO ₂ NP, 48 h	Methylation specific PCR and bisulfite sequencing of <i>PARP1</i> promoter	Increase in the level of <i>PARP-1</i> methylation, decrease of <i>PARP1</i> expression on mRNA and protein level; expression and promoter methylation of <i>PARP1</i> restored following DNMT1 knock down	[36]
Min-U-Sil® 5 (crystalline silica particle), NM-203 (pyrogenic amorphous silica nanoparticle); particles dispersed in sterile water, sonicated for 5 min at 10% amplitude (Branson Sonifier S-450 D, Branson Ultrasonics corp., Danbury, CT);	In vitro	Bhas 42 cell	Min-U-Sil® 5 (15 and 25 µg/cm ²), NM-203 (2 and 5 µg/cm ²); cell in experiment for upto 29 days, cell pellets collected on day 6, and cell pellets were collected on day 29.	Global DNA methylation (5-mC); DNMT (<i>DNMT1</i> , <i>DNMT3A</i> , <i>DNMT3B</i>) and HDAC (<i>HDAC1</i> , <i>HDAC2</i> , <i>HDAC3</i> , <i>HDAC6</i>) expression, H3/ H4 acetylation, c-Myc expression and histone modification on c-Myc promoter	Global DNA hypomethylation (Min-U-Sil® 5), increased <i>DNMT3A</i> and <i>DNMT3B</i> protein levels for Min-U-Sil® 5, no changes observed for NM-203; increase in histone H4 acetylation and significant changes in HDAC expression by Min-U-Sil® 5 and no changes observed for NM-203; Min-U-Sil® 5 increased acetylated histone H3 lysine 4 (H3K4Ac), histone H3 lysine 9 (H3K9Ac) and acetylated histone H3 lysine 27 (H3K27Ac) on c-Myc promoter	[86]
SiO ₂ -NP	Human population	DNA from leucocyte	Non exposed (n = 43, age: 37.95 ± 8.94) SiO ₂ -NP exposed (n = 31, age: 35.52 ± 9.89, exposure duration: 2.49 ± 2.40 years)	Global DNA methylation (5-mC; HPLC)	No significant change in DNA methylation, increased oxidative stress	[54]

^aLimited exposure information provided here, for additional information refer to full text^bFor other endpoints refer to full text

Table 9.4 Summary table of studies reporting epigenetic changes induced by copper nanoparticles

Nanoparticle properties	Experiment ^a		Condition	Epigenetic (and associated) endpoint studied ^b	Result	References
	Type	System				
CuO, 58.7 nm; specific surface area 16.2 m ² /g	In vitro	Human monocyte (THP1), primary small airway epithelial cells (SAEC), murine macrophage cells (RAW264.7)	The cells were in the respective cell culture media at two doses (0.5 and 30 µg/mL) for 24 h	Global DNA methylation (5-mC) and hydroxymethylation (5-hmC), LINE1 and Alu/SINE methylation specific PCR	No significant difference in global DNA methylation; small hypermethylation observed in 5'-UTR, ORF1 and ORF2 of SAEC, ORF2 of THP-1	[56]
Green synthesized CuO NP; FE-SEM- 40 nm; DLS- 577 nm; zeta potential - 25.4 mV	In vitro	Human lung adenocarcinoma cell line (A549)		HDACs mRNA expression	Inhibition against total HDAC and different classes of HDACs.	[47]
CuO NPs (generated by using the thermal decomposition of metal organic precursor copper (II) acetylacetonate); 7.64–229.6 nm (inhalation chamber)	In vivo	Female ICR mice (8 animals/group)	Whole-body inhalation chamber to 8 × 10 ⁻⁵ CuO NP/cm ³ (geometric mean diameter 29.4 nm) for 3 days, 2 weeks, 6 weeks, and 3 months	Lung; Global DNA methylation (5-mC); miRNA expression; whole genome transcriptome analysis	No significant effect on global DNA methylation; mRNA expression changes (cell adhesion, migration, and cytokine production)	[83]
CuNP, 40–60 nm; purity 99.9%, spherical; specific surface area 12 m ² /g, bulk density 0.2 g/cm ³	In vivo	Male albino Wistar rats (Han IGS rat [CrI:WI(Han)]), 5 weeks, body weight- 135 ± 10 g; housed randomly and individually in stainless steel cages at a stable temperature (21–22 °C), relative humidity 50% ± 10%, a 12-hr light-dark cycle, and a ventilation rate of 20 air changes per hour;	Five experimental groups: CuD (control without cu in mineral mixture); Diet with MX without cu (n = 8); CuS-H: Diet containing 6.5 mg/kg cu from CuCO ₃ (n = 8); CuS-L: Diet containing 3.25 mg/kg cu from CuCO ₃ (n = 8); CuNP-H: Diet containing 6.5 mg/kg cu from preparation of cu nanoparticles (n = 8); CuNP-L: Diet containing 3.25 mg/kg cu from preparation of cu nanoparticles (n = 8)	Global DNA methylation, oxidative stress markers	Cu supplementation reduces protein oxidation, nitration, DNA oxidation and methylation	[67]

(continued)

Table 9.4 (continued)

Nanoparticle properties	Experiment ^a		Condition	Epigenetic (and associated) endpoint studied ^b	Result	References
	Type	System				
CuO, 58.7 nm; specific surface area 16.2 m ² /g	In vivo	Eight-week-old BALB/c male mice, mice housed environmentally controlled room at 25 ± 1 °C with a relative humidity of 50 ± 10% under a 12-h light/dark cycle, food and water were provided ad libitum;	CuO at 2.5 mg/kg body weight; Intratracheally instilled with these treatments and sacrificed 24 h after administration with an intraperitoneal injection of fatal-plus; macrophages, lung tissue and blood collected	Global DNA methylation (5-mC) and hydroxymethylation (5-hmC), LINE1 and Alu/SINE methylation specific PCR; expression of <i>DNMT1</i> , <i>DNMT3a</i> and <i>DNMT3b</i>	Increase in 5-mC levels and 5-hmC levels in lung tissue, methylation of LINE-1 not changed, SINE B1 elements hypermethylated in the alveolar macrophages	[55]

^aLimited exposure information provided here, for additional information refer to full text

^bFor other endpoints refer to full text

9.2.5 Silver Nanoparticles

While silver nanoparticles are one of the most studied, both for its biomedical application and to identify its toxicity, the studies reporting epigenetic alterations are limited (Table 9.5). Gonzalez-Palomo et al. [37] in a study on EA.hy926 endothelial cells, observed global hypermethylation, downregulation of some miRNAs (miRNA -126, -155, and -146) and increase in some inflammatory markers and levels of vascular cell adhesion molecule 1 (*VCAM-1*). Very few changes in DNA methylation were observed in BEAS-2B cells, exposed for a period of up to 6 weeks to Ag-NP (1 µg/mL), while significant changes in the transcriptome was observed [35]. Brzóška et al. [9] reported changes in miRNA expression (miR-499a, miR-1-3p), however DNA methylation were not altered in HepG2 cells, exposed to Ag-NP (20 nm, 10 µg/mL) for 24 h. In mouse hippocampal neuronal cell line (HT22), Mytych et al. [64] observed a significant increase in DNMT activity and global DNA methylation after 48 h of Ag-NP exposure and also after a recovery period of 96 h. In another study the authors observed significant H3 deacetylation and global DNA hypermethylation in A549 cells, exposed to higher concentration of PVP-coated Ag-NP [7]. While only a small percentage of PVP was part of particle preparation (99.9% Ag, 0.3% PVP), like in most epigenetic studies the influence of surface coating was not very clear [7]. Another study addressed the effect of Ag-NP on phosphorylation of histone H3 [103] in different cell lines (HaCaT, A549, MCF-7), where significant p-H3S10 (phosphorylation of histone H3 at serine 10) was observed, and was associated with cellular uptake of the particles. In contrast to other metal (oxide) nanoparticles, most studies on Ag-NP reported DNA hypermethylation, either at a global or sequence specific levels. However, the mechanistic explanation behind such changes have not been reported. Additionally, toxicologically relevant properties for silver nanoparticles such as effect of shape/size and ionization have also not been reported.

9.2.6 Gold Nanoparticles

Among metal nanoparticles, gold (Au-NP) has been studied rather extensively for epigenetic mechanism (Table 9.6), however with a focus, primarily on therapeutic properties for biomedical application. Majority of the particles used in such studies are biosynthesized, and are surface coated with citrate, PLGA etc. for specific application. In this section, we try to discuss the evidence on such epigenetic changes, focusing on the toxicological aspect where possible. However, it would be important to remember that surface coating of particle has an influence on uptake and thereby on the observed effects. Therefore, these results cannot be generalized for Au-NP as a group. Patil et al. [78] reported DNA methylation changes in human normal skin fibroblast (hypermethylation after 24 h, hypomethylation after 48 h) and A375 cells (hypomethylation after 24 and 48 h) and aberrant DNMT expression (*DNMT1*, *DNMT3A* and *DNMT3B*) exposed to biosynthesized Au-NP [78]. In another study the authors reported the reduction of cell cycle related protein expression and histone deacetylase activity in HepG2 cells treated with “gold-quercetin loaded into poly(DL-lactide-co-glycolide)” nanoparticles, however due to presence of multiple chemicals [6] such effect cannot be directly attributed to Au-NP. In another in vitro study, in human embryonic stem cells (hESCs), the authors investigated several cytotoxicity and epigenetic endpoints for coated Au-NPs of different size (mercaptosuccinic acid coated-1.5, 4 nm, and citrate coated 14 nm) [87]. These nanoparticles exhibited global DNA hypomethylation (5-mC) and an increase in DNA hydroxymethylation (5-hmC) at sublethal concentrations. This effect was most prominent for Au-NP (4 nm) with 31,000 CpG sites showing demethylation [87]. However, no further interpretation on pathways were provided. In HepG2 cells, exposed to citrate coated Au-NP (10 µg/mL) for 24 h, Brzóška et al. reported changes in miRNA expression (miR-499a, miR-491-5p etc) however DNA methylation were not altered [9]. In a separate study, Ng et al. [65] reported that Au-Np (21 nm, citrate reduction) downregulated

Table 9.5 Summary table of studies reporting epigenetic changes induced by Silver nanoparticles

Nanoparticle properties		Experiment ^a		Epigenetic (and associated) endpoint studied ^b		Result	References
Type	System	Condition					
Ag-NP (<100 nm; sigma-Aldrich, cat. No. 758329)	Mouse hippocampal neuronal cell line (HT22)	Freshly prepared stock solution of Ag-NPs (10 mg/ml in sterile PBS); 1 to 20 µg/ml, 48 h and 144 h (96 h after Ag-NP removal)	In vitro	Mouse hippocampal neuronal cell line (HT22)	Global DNA methylation (5-mC); <i>DNMT1</i> , <i>DNMT3A</i> and <i>DNMT3B</i> expression	Global DNA hypermethylation and increase in DNMT expression	[64]
Ag-NP (1.8 ± 0.3 nm in diameter)	Human endothelial cells (EA.hy926)	Ag-NP (0.1, 0.5, 1 µM), 24 h	In vitro	Human endothelial cells (EA.hy926)	Global DNA methylation (5-mC, flow cytometry- immunolabelling)	Global DNA hypermethylation	[37]
Ag-NP (10, 75 nm)	Human bronchial epithelial cells (BEAS-2B cells)	1 µg/mL; cells were split (trypsinization), counted, re-seeded twice a week and re-exposed to the Ag-NPs for a total of 6 weeks.	In vitro	Human bronchial epithelial cells (BEAS-2B cells)	Genome wide DNA methylation (Infinium human Methylation450 bead chip) and RNA-sequencing (RNA-Seq)	Small effect on DNA methylation, significant changes in transcriptome of 1717 genes, some of which were associated with fibrosis, epithelial-mesenchymal transition	[35]
Polyvinyl pyrrolidone (PVP)-coated Ag-NPs (99.9% Ag, 0.3% PVP, 20 nm; NanoAmor, Houston, USA)	Human lung adenocarcinoma cell line (A549)	0–200 µg/mL of Ag-NPs for 48 and 72 h	In vitro	Human lung adenocarcinoma cell line (A549)	Global DNA methylation (5-mC, ELISA), H3 acetylation (Western blot)	Significant deacetylation of H3, global DNA hypermethylation	[7]
Ag-NP, 20 nm, Plasmachem GmbH, Berlin, Germany	Human hepatocyte carcinoma (HepG2)	10 µg/mL, 24 h	In vitro	Human hepatocyte carcinoma (HepG2)	Gene specific methylation-EpiTest methylation array and miScript miRNA PCR Array- Human Inflammatory Response & Autoimmunity Signature Panel and human apoptosis signature panel	miRNA expression (miR-499a, miR-1-3p etc) significantly altered, no change in DNA methylation	[9]
Ag-NP (<100 nm; Sigma-Aldrich, cat. No. 576832, St. Louis, MO, USA)	Human skin keratinocytes (HaCaT), human lung adenocarcinoma cell line (A549), human lung adenocarcinoma cell line (MCF-7)	0.1, 0.3, 0.5 and 1 mg/mL for 24 h	In vitro	Human skin keratinocytes (HaCaT), human lung adenocarcinoma cell line (A549), human lung adenocarcinoma cell line (MCF-7)	p-H3S10- phosphorylation of histone H3 at serine 10 (Western blot)	Increase in p-H3S10, in all 3 cell lines, and associated with uptake	[103]

^aLimited exposure information provided here, for additional information refer to full text

^bFor other endpoints refer to full text

Table 9.6 Summary table of studies reporting epigenetic changes induced by Gold nanoparticles

Nanoparticle properties	Experiment ^a		Condition	Epigenetic (and associated) endpoint studied ^b	Result	References
	Type	System				
Au-NP synthesized by Pseudoalteromonas, 23–30 nm; aliphatic compounds, aromatic ring and aromatic phosphates identified on surface	In vitro	Human normal skin fibroblast cell line, human skin melanoma cancer (A375)	AuNP concentrations (1000, 500, 250, 125, 62.5, 31.25, 15.625 µg/mL), 24 and 48 h	Immunohistochemical staining of DNA methylation (5-mC); DNMT expression (<i>DNMT1</i> , <i>DNMT3a</i> , <i>DNMT3b</i>)	Human normal skin fibroblast: Hypermethylation after 24 h, hypomethylation after 48 h; A375 cells: Hypomethylation after 24 and 48 h; aberrant DNMT expression (<i>DNMT1</i> , <i>DNMT3A</i> and <i>DNMT3B</i>)	[78]
Au-Np (1.5, 4, and 14 nm); Au-NP (1.05 nm and 4 nm) capped with mercaptosuccinic acid (MSA); Au-NP (14 nm) citrate coated	In vitro	Human embryonic stem cells (hESCs)	Sublethal dosage Au-NP 1.5 nm (1 µg mL ⁻¹), Au-NP 4 nm (10 µg mL ⁻¹), Au-NP 14 nm (10 µg mL ⁻¹); 24 h	5-mC immunoprecipitation-based colorimetric assay; HM450K array	Global hypomethylation for all particles, highest for Au-NP 4 nm; increase in hydroxymethyl cytosine (5-hmC), DNA hypomethylations in 31,000 CpG sites for Au-NP 4 nm	[87]
Au-NP, 20 nm; synthesized by citrate reduction of gold salts	In vitro	Human fetal fibroblasts (MRC5), primary small airway epithelial cells (SAEC)	1 nM, 48 and 72 h	Bisulfite sequencing of PROS1	No change in DNA methylation of the PROS1	[65]
Au-NP (20 nm), NanoComposix, San Diego, CA, USA; Sodium-citrate-coated	In vitro	Human hepatocyte carcinoma (HepG2)	10 µg/mL, 24 h	Gene specific methylation-EpiTect methylation array and miScript miRNA PCR Array-Human Inflammatory Response & Autoimmunity Signature Panel and human apoptosis signature panel	miRNA expression (miR-499a, miR-491-5p etc) significantly altered, no change in DNA methylation	[9]
Au-NP (5, 60 and 250 nm); Citrate-coated colloidal AuNPs	In vivo	Male BALB/c mice (~20 g, 7 weeks old), housed in a conventional animal house at controlled temperature (21 ± 1 °C) and humidity (50 ± 10%) with 12-h dark/light cycles	Vehicle control (n = 8); AuNPs (n = 5/group): 5 nm, low dose (0.25 mg/kg) and high dose (2.5 mg/kg); 60 nm, low dose (0.25 mg/kg) and high dose (2.5 mg/kg); 250 nm, low dose (0.25 mg/kg) and high dose (2.5 mg/kg); by single intra-tracheal instillation, 48-h post exposure animal sacrificed	Global DNA methylation and hydroxymethylation (LC-MS/MS), sequence specific DNA methylation	No changes in global methylation (5-mC) and hydroxymethylation (5-hmC) levels in mouse lungs; AuNP 60 nm induced CpG hypermethylation in <i>ATM</i> , <i>CDK</i> and <i>GSR</i> genes and hypomethylation in <i>GPX</i> ; <i>GSR</i> and <i>Trp53</i>	[94]

(continued)

Table 9.6 (continued)

Nanoparticle properties	Experiment ^a		Epigenetic (and associated) endpoint studied ^b	Result	References
	Type	System			
Au-NP, colloidal suspension (40 and 100 nm), BB international (Cardiff, UK)	In vivo	Female Swiss albino mice (H strain), weighing 28–30 g and aged 2.5–3 months; mated with males of the same cross, mating ratio- 1:3	Pregnant mice divided into 3 groups-untreated controls (2 dams); au-NP; 40 nm (3 dams); and au-NP; 100 nm (2 dams). Additional animals used for clastogenicity study. Pregnant mice were treated on days 10, 12, 14 and 17 of gestation with 1 ml/mouse of AuNP suspensions (either 40 nm or 100 nm), injected intraperitoneally (i.p), delivering an average dose of 3.3 mg/kg body weight.	Changes associated with cell proliferation, apoptosis, inflammation	[3]

^aLimited exposure information provided here, for additional information refer to full text

^bFor other endpoints refer to full text

the expression of *PROS1* (Vitamin K-dependent protein S) gene, mediated by the up-regulation of microRNA-155 (miR-155) but no change in methylation was observed for *PROS1*.

From the limited in vivo evidence, it is also clear that Au-NPs can induce epigenetic alterations in different tissue/cell types. In a study by our group [94], in BALB/c mice exposed to different sizes of citrate coated Au-NP (5, 60, 250 nm), while no changes were observed on the level of global DNA methylation (5-mC) and hydroxymethylation (5-hmC), Au-NP (60 nm) induced CpG hypermethylation in *ATM*, *CDK* and *GSR* genes and hypomethylation in *GPX*, *GSR* and *TRP53*. These changes were also associated with deregulations in immune markers. In another study, transplacental miRNA expression changes associated with cell proliferation, apoptosis, inflammation etc. were also observed in liver and lung of mice foetus, for Au-NP (40, 100 nm) administered intraperitoneally (3.3 mg/Kg) [3].

9.3 Epigenetic Changes Induced by Carbon Nanotubes

Due to the growing evidence of toxicity induced by carbon nanotubes (CNTs), and the increasing emphasis on high aspect ratio, and the asbestos analogy [49, 81], there has been considerable research on epigenetic changes compared to other NPs. Classification of “MWCNT-7” as “Possibly carcinogenic to humans” (International Agency for Research on Cancer- IARC Group 2B) [43] and growing emphasis on mechanistic evidence for potential carcinogenicity, has also highlighted the need of epigenetic study. In this section we discuss the studies (Table 9.7) that have used different types of CNTs (MWCNT-Multi wall, SWCNT- Single wall) to evaluate epigenetic alterations, and where possible try to draw parallels with that of evidence available for asbestos.

From our study, in human bronchial epithelial cells (16HBE), we observed significant changes in DNA methylation induced by MWCNTs (JRC NM400; diameter 11 nm, length 846 nm) and

SWCNTs (NIST SRM:2483; diameter 0.8 nm, length 8000 nm) [69]. While we did not observe global DNA methylation changes [33, 69] and sequence specific changes in LINE1 methylation [33], we observed significant changes in individual CpG sites for MWCNT (2398 genes were hypomethylated at gene promoters), and SWCNTs (589 CpG sites hypo- or hypermethylated), associated with pathways such as p53 signaling, DNA damage repair and cell cycle. We also were able to identify sequence specific changes in DNA methylation of several important genes such as *NPAT/ATM*, *PIK3R2*, *DNMT1*, *HDAC4*, *SKI* and *GSTP1* [33, 69]. We did not observe significant changes in miRNA expression, which could however be due to the smaller number of replicates [33]. In a subsequent study we compared the epigenetic alterations observed for CNTs to that induced by asbestos in 16 HBE cells (Esra [24]), and mostly observed no significant changes in global DNA, however sequence specific methylation was altered for *ATM* (chrysotile, SWCNT, and MWCNT), *CDKN1A* (SWCNT, MWCNT, and amosite) and *TRAF2* (only SWCNT) (Esra [24]) all of which play important role in pathways associated with DNA damage and apoptosis. In our study we also did not observed significant changes in global RNA methylation, which is a post-translational modification with important role in gene regulatory processes. Our analysis of genome wide methylation changes induced by asbestos fibers (amosite, crocidolite and chrysotile) in 16HBE cells [70] also revealed significant changes in methylation pattern (associated with MAPK signaling pathway, pathways in cancer, WNT gene family and homeobox group) and some of the altered pathways were similar to that observed for CNTs. Differentially methylated regions including HOX genes have also been reported by Kettunen et al. [51] for asbestos-exposed patients. In a recent study, we reported the effect of long-term CNT and amosite exposure and recovery on DNA methylation, and we found that SWCNTs/amosite induced hypermethylation at CpG sites and MWCNT induced hypomethylation at CpG sites [71]. Moreover, spontaneous DNA methylation changes were observed during the recovery period [71].

Table 9.7 Summary table of studies reporting epigenetic changes induced by carbon nanotubes

Nanoparticle properties		Experiment ^a		Epigenetic (and associated) endpoint studied ^b	Result	References
Type	System	Condition	System			
MWCNT (NM-400, JRC)- diameters 11 nm, length 846 nm; SWCNT (NISTS, RM:2483)- diameters 0.8 nm, length 8000 nm	Human Bronchial Epithelial cell line (16HBE)	25 and 100 µg/ml, 24 h	In vitro	Global DNA methylation (5-mC; LC-MS/MS); genome-wide (Infinium HumanMethylation450 BeadChip Array); gene- specific DNA methylation (pyrosequencing) and RNA-expression analyses (RNA sequencing)	No global DNA methylation alteration on 5-methylcytosine (5-mC); MWCNTs: 2398 genes were hypomethylated (at gene promoters), SWCNTs: 589 CpG sites (located on 501 genes) were either hypo- (N = 493 CpG sites) or hypermethylated (N = 96 CpG sites); SWCNT exposure showed hypermethylation of SKI proto-oncogene (<i>SKI</i>), glutathione S-transferase pi 1 (<i>GTSP1</i>), SHROOM family member 2 (<i>SHROOM2</i>)	[69]
MWCNT (NM-400, JRC)- diameters 11 nm, length 846 nm; SWCNT (NISTS, RM:2483)- diameters 0.8 nm, length 8000 nm	Human Bronchial Epithelial cell line (16HBE)	2.5, 5 and 25 µg/ml, 24 h	In vitro	Global DNA methylation (5-mC; LC-MS/MS); gene-specific DNA methylation (pyrosequencing) and miRNA-expression analyses (TaqMan® Array human MicroRNA)	No global DNA methylation alteration on 5-methylcytosine (5-mC) or LINE 1 elements; sequence specific changes in <i>DNMT1</i> , <i>HDAC4</i> , <i>MAP3K10</i> , <i>NPAT</i> / <i>ATM</i> genes; no significant changes in miRNA expression	[33]

<p>MWCNT (NM-400, JRC)- diameters 11 nm, length 846 nm; SWCNT (NISTs, RM:2483)- diameters 0.8 nm, length 8000 nm</p>	<p>In vitro</p>	<p>Human monocyte (THP1)</p>	<p>MWCNT/SWCNT (25 and 100 µg/ml); 24 h</p>	<p>Global DNA methylation (5-mC; LC-MS/MS); genome-wide (Infinium HumanMethylation450 BeadChip Array)</p>	<p>No global methylation or hydroxymethylation, significant gene specific methylation, collectively CNTs induced gene promoter-specific hypomethylation in 1127 different genes- associated with platelet activation, VEGF receptor signaling pathway, chromatin organization, pathways in cancer, MAPK signaling pathway, PI3K-Akt signaling pathway</p>	<p>[68]</p>
<p>MWCNT (NM-400, JRC)- diameters 11 nm, length 846 nm; SWCNT (NISTs, RM:2483)- diameters 0.8 nm, length 8000 nm; Amosite (South African, NB #4173-111- 4), Crocidolite (South African, NB #4173-111-3) and Chrysotile ("A" Rhodesian, NB #4173-111-2)</p>	<p>In vitro</p>	<p>Human Bronchial Epithelial cell line (16HBE)</p>	<p>MWCNT/ SWCNT (25 and 100 µg/ml), Asbestos (2.5 µg/ ml); 24 h</p>	<p>Global DNA and RNA (hydroxy)methylation (LC-MS/MS); m6A-RNA methylation (ELISA); gene-specific DNA methylation (pyrosequencing)</p>	<p>MWCNT-significant global DNA hypomethylation of cytosine and global RNA hypomethylation of adenosine; ATM methylation was affected by chrysotile, SWCNT, and MWCNT; decreased DNA methylation of CDKN1A for SWCNT, MWCNT, and amosite.</p>	<p>[24]</p>
<p>MWCNT (NM-400, JRC)- diameters 11 nm, length 846 nm; SWCNT (NISTs, RM:2483)- diameters 0.8 nm, length 8000 nm; Amosite (South African, NB #4173-111-4)</p>	<p>In vitro</p>	<p>Human Bronchial Epithelial cell line (16HBE)</p>	<p>MWCNT/ SWCNT (0.25 µg/ ml), Asbestos (0.05 µg/ml); total of 4 weeks +2 weeks of recovery</p>	<p>Genome-wide (Infinium MethylationEPIC BeadChip Kit-EPIC array)</p>	<p>Hippocalcinlike 1 (HPCAL1), protease serine 3 (PRSS3), kallikrein-related peptidase 3 (KLK3), kruppel like factor 3 (KLF3) genes were hypermethylated at different time points in either SWCNT-exposed or amosite-exposed cells. Spontaneous DNA methylation alterations were noted even after the recovery period.</p>	<p>[71]</p>

(continued)

Table 9.7 (continued)

MWCNT (Cheaptubes Inc., Cambridgeport, VT): LW- long length and wide diameter (length: 10–30 µm, diameter: 20–30 nm), LN- long length and narrow diameter (length: 10–30 µm, diameter: 8–15 nm), SN- short length and narrow diameter (length: 0.5–2.0 µm, diameter: 8–15 nm)	In vitro	Human bronchial epithelial cells (BEAS-2B cells), human hepatocyte carcinoma (HepG2)	EC20 (mg/L)- HepG2 cells (LW- 45.28, LN- 38.52, SN- 8.37), BEAS-2B (LW- 25.19, LN- 9.68, SN- 6.34); 24 h	Global DNA methylation (5-mC); DNMT1, DNMT3A and DNMT3B activity	Global DNA hypermethylation in HepG2 cells, global DNA hypomethylation in BEAS-2B cells	[15]
MWCNT (NM401; length- 6012.09 ± 4091.45 NM, diameter- 64.2 ± 34.5 nm)	In vitro	Human bronchial epithelial cells (BEAS-2B cells)	10 and 20 mg/mL for up to 4 weeks; exposure media changed every 3 days, sample collected at 2 and 4 weeks	Genome wide methylation- human methylation450 BeadChip	DNA methylation changes of 755 CpG sites- corresponding to 453 genes; mostly hypomethylated	[90]
Rigid MWCNT (Mitsui, diameter-22 nm; length- 13,000 nm)	In vitro	Human monocyte (THP1)	THP1 were and differentiated for 48 h with 50 nM PMA; 5, 10, and 20 µg of rCNT/mL, for 24, 48 or 72 h	Genome wide methylation- human methylation BeadChip	Significant changes in DNA methylation, and transcriptomic changes in pathways associated with cell cycle regulation, immune system, signal transduction, metabolism	[85]
MWCNTs (Cheaptubes Inc., Cambridgeport, VT) NS- narrow diameter and short length (10–20 nm, 0.5–2 µm), WS- wide diameter and short length (30–50 nm, 0.5–2 µm), NL- narrow diameter and long length (10–20 nm, 10–30 µm)	In vivo	Male and female C57BL/6 mice (2 month), maintained in specific pathogen-free conditions (22 ± 2 °C, 30–40% humidity, 12 h light/12 h dark cycles)	Mice were exposed to MWCNTs by oropharyngeal aspiration; after 24 h or 7 days, mice were euthanized; lung lavage fluid and lung tissues were harvested	Luminometric methylation assay and sequence specific methylation (pyrosequencing)- IL-1β, IL-6, and TNF-α	Significant global hypomethylation (NL > WS > NS); significant sequence specific promoter hypomethylation of <i>IL-1β</i> , <i>IL-6</i> , and <i>TNF-α</i> at 24 h followed by a reversal of the trend at 7 days post exposure	[18]

MWCNT (NM-400, JRC)- diameters 11 nm, length 846 nm; SWCNT (NISTS, RM:2483)- diameters 0.8 nm, length 8000 nm	In vivo	Male BALB/c mice (~20 g, 7 weeks old), housed in a conventional animal house at controlled temperature (21 ± 1 °C) and humidity (50 ± 10%) with 12-h dark/light cycles	Vehicle control (n = 8); CNTs (n = 5/group); single-walled CNTs (SWCNTs), low dose (0.25 mg/kg) and high dose (2.5 mg/kg) and multi-walled CNTs (MWCNTs) low dose (0.25 mg/kg) and high dose (2.5 mg/kg); by single intra- tracheal instillation, 48-h post exposure animal sacrificed	Global DNA methylation and hydroxymethylation (LC-MS/MS), sequence specific DNA methylation	No changes in global methylation (5-mC) and hydroxymethylation (5-hmC) levels in mouse lungs; SWCNTs and MWCNTs had shape effects on promoter methylation of ATM	[94]
CNT (long and short), amosite (long and short), characterization reported elsewhere.	In vivo	C57BL/6 strain mice (eight-week- old female, Charles River laboratories, UK), maintained on a normal 12 hr. light and dark cycle.	Intraperitoneal injection; vehicle control (VC), SFA, LFA, SNT or LNT. For 1- and 12-weeks exposure, CNT (5 mg/mouse, n = 4). For 6 months and 1-year exposure: VC, LFA and LNT, with n = 4, dose of 2.5 mg/ mouse (100 mL) of LNT. For prolonged (up to 20 months) exposure, mice were injected with 1 mg/mouse of LNT (n = 4), 0.5 mg/mouse of LNT (n = 5) or 0.2 mg/mouse of LNT (n = 12). Asbestos fiber samples were administered at a dose of 25 mg/mouse (100 mL) (n = 4) for short-term studies and n = 16, prolonged exposure) or at 50 mg/mouse (n = 16, prolonged exposure).	Bisulphite sequencing	Hypermethylation of p16/ Ink4a and p19/Arf for long CNT and Asbestos, preceded mesothelioma induction	[16]

(continued)

Table 9.7 (continued)

MWCNT (200 nm–100 µm agglomerates)	Human population	DNA extracted from whole blood	Control (n = 43, age: 34.64 ± 8.57), exposed (n = 24, age: 35.87 ± 6.90, average duration of exposure: 4.25 ± 2.40 years); based on levels of EC in workplace was determined to be between 4.6 and 42.6 µg/m ³ —three categories of exposed workers: ‘lab-low’ (n = 9; 1 µg/m ³ EC), ‘lab-high’ (n = 6; 7 µg/m ³ EC), and ‘operators’ (n = 7; 45 µg/m ³ EC);	Global DNA methylation (5-mC, 5-hmC; LC-MS/MS); gene-specific DNA methylation (pyrosequencing)	No significant difference in global methylation (5-mC), hydroxymethylation (5-hmC) and LINE1 methylation; significant change in methylation for <i>DNMT1</i> , <i>ATM</i> , <i>SKI</i> , and <i>HDAC4</i> promoter CpGs in MWCNT-exposed workers	[31]
MWCNT	Human population	RNA was extracted from whole blood	Control (n = 7, 20–30 years), MWCNT (n = 8, 23–60 years, 6–24 months working, average inhalable EC concentration: 14.42 ± 3.8 µg/m ³)	miRNA, ncRNA and mRNA expression	529 lncRNAs were upregulated and 448 lncRNAs were downregulated. A total of 29 miRNAs, 2404 lncRNAs and 2655 mRNAs dysregulated by high MWCNT exposure; inflammation, fibrosis, tumor progression and cancer	[89]

^aLimited exposure information provided here, for additional information refer to full text

^bFor other endpoints refer to full text

However, the induction of DNA methylation changes for the chronic exposure period was less pronounced compared to our acute exposure experiment and such difference could be due to both the lower concentration of exposure for the chronic phase and possibly due to tolerance and adaptation. While in our study we observed fewer DNA methylation changes, in a long-term study in BEAS-2B cells, with MWCNT (NM401) exposure period of up to 4 weeks, Sierra et al. [90] observed a significant hypomethylation of 697 CpG, primarily associated with functions such as cell adhesion. The difference between the two long terms studies could primarily be due to the difference in lower exposure concentration (0.25 µg/ml) used in our study [71] compared to that reported by Sierra et al. [90] (20 µg/ml), but also due to the difference in cell lines used.

From one of our study, in BALB/c mice, intra-tracheal administration of MWCNT and SWCNT resulted in a sequence specific DNA methylation in ATM [94]. Such changes have been observed in other cell types as well. For instance, in one of our studies in THP1 monocytes, while we observed no changes in global methylation or hydroxymethylation, significant gene specific methylation associated with pathways such as platelet activation, VEGF receptor signaling pathway, chromatin organization, pathways in cancer, MAPK signaling pathway, PI3K-Akt signaling pathway were observed [68]. In another study, Saarimäki et al. [85] reported significant changes in transcriptome and epigenome (DNA methylation) associated with pathways related to immune system, cell cycle and signal transduction, in differentiated THP1 monocyte exposed to rigid MWCNT.

In an in vitro study, Chatterjee et al. [15] critically evaluated the effect of MWCNT diameter and length in BEAS-2B and HepG2 cells. In the study, the authors observed a global DNA hypermethylation in HepG2 cells while a global DNA hypomethylation was observed for BEAS-2B cells [15]. These changes were in line with DNMT1 and DNMT3B expression in both cell lines. Of the different forms of MWCNT studied, long-narrow and short-narrow forms induced the

most significant epigenetic changes, associated with other oxidative stress and inflammatory markers. In another study, significant global hypomethylation was observed in lung tissue of C57BL/6 mice, exposed to MWCNTs of different length and diameter by oropharyngeal aspiration [18]. In the study narrow diameter and long length MWCNT induced the most significant effect [18], in line with the observation made by Chatterjee et al. [15]. The authors also reported significant sequence specific promoter hypomethylation of IL-1 β , IL-6, and TNF- α at 24 h, associated with increase in the inflammatory markers, followed by a reversal of the trend 7 days post exposure [18]. These two studies [15, 18] taken together, provide significant evidence regarding the influence of diameter and aspect ratio on CNT induced toxicity and epigenotoxicity. Another evidence in support of the asbestos analogy and high aspect ratio fiber toxicity comes from the in vivo study of Chernova et al. [16], where the authors used long and short forms of Amosite and carbon nanotubes. In the study the authors observed induction of mesothelioma, by pleural injection of long CNT and long amosite asbestos fibers, preceded by hypermethylation of overlapping genes p16/Ink4a and p19/Arf [16], which are often inactivated in different forms of cancer.

In addition, studies have identified considerable evidence of occupational exposure to CNTs, and has been presented in a recent review by Canu et al. [38]. In a study by our group [31], while we did not observe any significant difference in global methylation (5-mC), hydroxymethylation (5-hmC) and LINE1 methylation; we observed significant changes in CpG methylation for *DNMT1*, *ATM*, *SKI*, and *HDAC4* in MWCNT exposed workers. These sequence specific methylation changes were also observed in our in vitro studies as discussed above. In another cross-sectional study, Shvedova et al. [89] observed significant enrichment of miRNA-lncRNA-mRNA changes in inflammation, fibrosis, tumor promotion and cancer progression pathways in MWCNT exposed workers. While these studies do not allow for a definitive inter-

pretation regarding the cause or dose response relationship, some other cross-sectional studies have shown significant changes in inflammation and effect on cardiovascular and lung health [25, 34, 98]. These studies provided the first set of evidence of epigenetic alterations induced by occupational exposure to CNTs, but larger longitudinal population studies are needed to provide more detailed inside.

9.4 Summary and Perspectives

From the studies presented above, it is clear that NPs can induce epigenetic changes both at toxic and sub-cytotoxic concentrations. In the studies discussed above, with the exception of Ag-NP, most of the particles induced global DNA hypomethylation. DNA hypomethylation is observed in carcinogenesis and is highly correlated with methylation of DNA repeat elements [22]. Methylation of repeat elements such as LINE 1 and Alu represent approximately 50% of global methylation levels and hypomethylation has been associated with genomic instability and therefore can be used to study epigenetic alterations induced by NPs. Additionally, it has been established that global DNA methylation levels are modulated by oxidative stress [61, 73], and these mechanisms share one-carbon metabolism as the common denominator. This was observed for several of the NPs, but mostly for TiO₂-NP, as discussed above. In a relatively small number of studies and primarily in case of Ag-NP DNA hypermethylation has been observed as well. DNA hypermethylation at global level and at specific loci has been implicated in large number of diseases including cancer [23]. Sequence specific DNA hypermethylation of *GSTP1*, *TP53*, *p16*, *p21*, *ATM* among other important genes, increased phosphorylation of H3 and concurrent mRNA dysregulation has been observed for the nanoparticles, similar to that observed for other genotoxic carcinogens such as formaldehyde, benzene [14]. While these findings are extremely interesting, it limits further mechanistic interpretation due to certain study limitations discussed further. While most epigenetic changes have been observed at a sub cyto-

toxic concentration, the observed results are representative of a single time window. Given that epigenetic changes are highly dynamic, and most of the nanoparticles were studied for shorter duration of exposure, the results cannot provide information of a chronic exposure scenario or that resulting from a change in exposure conditions. Therefore, to understand the dynamic nature of such changes, studies need to be designed taking into account- **chronic low exposure**, different time windows and an inclusion of recovery period. Another important aspect of a study design, aimed at understanding epigenetic effect should be the selection of appropriate **cell type**, representative of the exposure and elimination route. Despite the limited evidence, this is something that has been observed for NPs [80] and is extremely important as epigenetic changes are cell type specific. Additional experimental conditions, relevant for nanotoxicological experiments in general, such as **physico-chemical properties**, dispersion condition, shape of material, aspect ratio of fibres, surface coating and functionalization are equally important in the interpretation of epigenetic changes. Furthermore, these changes observed in mostly in vitro studies must be validated in vivo and if possible, in exposed human population. Epigenetic alterations can be valuable in providing key mechanistic insight which can play important role in risk assessment, regulation, and classification based on mechanistic evidences by agencies such as the IARC [17, 92].

References

1. Asweto CO et al (2017) Cellular pathways involved in silica nanoparticles induced apoptosis: a systematic review of in vitro studies. *Environ Toxicol Pharmacol*:191–197. <https://doi.org/10.1016/j.etap.2017.09.012>
2. Bai W, Chen Y, Gao A (2015) Cross talk between poly(ADP-ribose) polymerase 1 methylation and oxidative stress involved in the toxic effect of anatase titanium dioxide nanoparticles. *Int J Nanomedicine* 10:5561–5569. <https://doi.org/10.2147/IJN.S88059>
3. Balansky R et al (2013) Transplacental clastogenic and epigenetic effects of gold nanoparticles in mice. *Mutat Res* 751–752(1):42–48. <https://doi.org/10.1016/j.mrfmmm.2013.08.006>

4. Baylin SB (2005) DNA methylation and gene silencing in cancer. *Nat Clin Pract Oncol*:S4–S11. <https://doi.org/10.1038/nponc0354>
5. Baylin SB et al (2001) Aberrant patterns of DNA methylation, chromatin formation and gene expression in cancer. *Hum Mol Genet* 10(7):687–692. <https://doi.org/10.1093/hmg/10.7.687>
6. Bishayee K, Khuda-Bukhsh AR, Huh SO (2015) PLGA-loaded gold-nanoparticles precipitated with quercetin downregulate HDAC-Akt activities controlling proliferation and activate p53-ROS cross-talk to induce apoptosis in hepatocarcinoma cells. *Mol Cells* 38(6):518–528. <https://doi.org/10.14348/molcells.2015.2339>
7. Blanco J et al (2017) Polyvinyl pyrrolidone-coated silver nanoparticles in a human lung cancer cells: time- and dose-dependent influence over p53 and caspase-3 protein expression and epigenetic effects. *Arch Toxicol* 91(2):651–666. <https://doi.org/10.1007/s00204-016-1773-0>
8. Bocconi F et al (2020) Occupational exposure to graphene and silica nanoparticles. Part I: workplace measurements and samplings. *Nanotoxicology* 14(9):1280–1300. <https://doi.org/10.1080/17435390.2020.1834634>
9. Brzóska K, Grądzka I, Kruszewski M (2019) Silver, gold, and iron oxide nanoparticles Alter miRNA expression but do not affect DNA methylation in HepG2 cells. *Materials* 12(7):1038. <https://doi.org/10.3390/ma12071038>
10. Carmo TLL et al (2019) Overview of the toxic effects of titanium dioxide nanoparticles in blood, liver, muscles, and brain of a Neotropical detritivorous fish. *Environ Toxicol* 34(4): 457–468. <https://doi.org/10.1002/tox.22699> LK - <http://limo.libis.be/resolver?&sid=EMBASE&issn=15227278&id=doi:10.1002%2Ftox.22699&atitle=Overview+of+the+toxic+effects+of+titanium+dioxide+nanoparticles+in+blood%2C+liver%2C+muscles%2C+and+brain+of+a+Neotropical+detritivorous+fish&stitle=Environ.+Toxicol.&title=Environmental+Toxicology&volume=34&issue=4&spage=457&epage=468&au last=Carmo&au first=Talita+L.+L.&au init=T.L.L.&au full=Carmo+T.L.L.&coden=ETOXF&isbn=&pages=457-468&date=2019&au init1=T&au initm=L.L>
11. Carriere M et al (2017) Impact of nanoparticles on DNA repair processes: current knowledge and working hypotheses. *Mutagenesis* 32(1):203–213. <https://doi.org/10.1093/mutage/gew052>
12. Cedar H, Bergman Y (2009) Linking DNA methylation and histone modification: patterns and paradigms. *Nat Rev Genet* 10(5):295–304. <https://doi.org/10.1038/nrg2540>
13. Chakraborty B et al (2016) Immunomodulatory properties of silver nanoparticles contribute to anti-cancer strategy for murine fibrosarcoma. *Cell Mol Immunol* 13(2):191–205. <https://doi.org/10.1038/cmi.2015.05>
14. Chappell G et al (2016) Epigenetic alterations induced by genotoxic occupational and environmental human chemical carcinogens: a systematic literature review. Elsevier. <https://doi.org/10.1016/j.mrrev.2016.03.004>
15. Chatterjee N et al (2016) Diameter size and aspect ratio as critical determinants of uptake, stress response, global metabolomics and epigenetic alterations in multi-wall carbon nanotubes. *Carbon* 108:529–540
16. Chernova T et al (2017) Long-fiber carbon nanotubes replicate asbestos-induced mesothelioma with disruption of the tumor suppressor gene *Cdkn2a* (*Ink4a/Arf*). *Curr Biol* 27(21): 3302–3314.e6. <https://doi.org/10.1016/j.cub.2017.09.007>
17. Coglianò VJ et al (2008) Use of mechanistic data in IARC evaluations. *Environ Mol Mutagen*:100–109. <https://doi.org/10.1002/em.20370>
18. Cole E et al (2019) Multiwalled carbon nanotubes of varying size lead to dna methylation changes that correspond to lung inflammation and injury in a mouse model. *Chem Res Toxicol* 32(8):1545–1553. <https://doi.org/10.1021/acs.chemrestox.9b00075>
19. Definition of epigenetic alteration – NCI Dictionary of Cancer Terms – National Cancer Institute (n.d.). Available at: <https://www.cancer.gov/publications/dictionaries/cancer-terms/def/epigenetic-alteration>. Accessed 4 Feb 2021
20. Dhupal M et al (2018) Immunotoxicity of titanium dioxide nanoparticles via simultaneous induction of apoptosis and multiple toll-like receptors signaling through ROS-dependent SAPK/JNK and p38 MAPK activation. *Int J Nanomedicine* 13:6735–6750. <https://doi.org/10.2147/IJN.S176087>
21. Dinicola S et al (2015) Multiwalled carbon nanotube buckypaper induces cell cycle arrest and apoptosis in human leukemia cell lines through modulation of AKT and MAPK signaling pathways. *Toxicol In Vitro* 29(7):1298–1308. <https://doi.org/10.1016/j.tiv.2015.05.006>
22. Ehrlich M (2009) DNA hypomethylation in cancer cells. *Epigenomics*:239–259. <https://doi.org/10.2217/EPI.09.33>
23. Ehrlich M (2019) DNA hypermethylation in disease: mechanisms and clinical relevance. *Epigenetics*:1141–1163. <https://doi.org/10.1080/15592294.2019.1638701>
24. Emerce E et al (2019) Carbon nanotube- and Asbestos-induced DNA and RNA methylation changes in bronchial epithelial cells. *Chem Res Toxicol* 32(5). <https://doi.org/10.1021/acs.chemrestox.8b00406>
25. Fatkhutdinova LM et al (2016) Fibrosis biomarkers in workers exposed to MWCNTs. *Toxicol Appl Pharmacol* 299:125–131. <https://doi.org/10.1016/j.taap.2016.02.016>
26. Ferreira HJ, Esteller M (2018) Non-coding RNAs, epigenetics, and cancer: tying it all together. *Cancer Metastasis Rev* 37(1):55–73. <https://doi.org/10.1007/s10555-017-9715-8>
27. Fuks F (2005) DNA methylation and histone modifications: teaming up to silence genes. *Curr Opin*

- Genet Dev:490–495. <https://doi.org/10.1016/j.gde.2005.08.002>
28. Gao F et al (2016) Zinc oxide nanoparticles-induced epigenetic change and G2/M arrest are associated with apoptosis in human epidermal keratinocytes. *Int J Nanomedicine* 11:3859–3874. <https://doi.org/10.2147/IJN.S107021>
 29. Geiss O et al (2020) Characterisation of food grade titania with respect to nanoparticle content in pristine additives and in their related food products. *Food Addit Contam Part A* 37(2):239–253. <https://doi.org/10.1080/19440049.2019.1695067>
 30. Ghosh M et al (2012) In vitro and in vivo genotoxicity of silver nanoparticles. *Mutat Res* 749(1–2). <https://doi.org/10.1016/j.mrgentox.2012.08.007>
 31. Ghosh M, Öner D, Poels K, Tabish AM et al (2017a) Changes in DNA methylation induced by multi-walled carbon nanotube exposure in the workplace. *Nanotoxicology* 11(9–10). <https://doi.org/10.1080/17435390.2017.1406169>
 32. Ghosh M, Öner D, Duca RC et al (2017b) Cytogenotoxic and DNA methylation changes induced by different crystal phases of TiO₂-np in bronchial epithelial (16-HBE) cells. *Mutat Res* 796:1–12. <https://doi.org/10.1016/j.mrfmmm.2017.01.003>
 33. Ghosh M et al (2018) Single-walled and multi-walled carbon nanotubes induce sequence-specific epigenetic alterations in 16 HBE cells. *Oncotarget* 9(29):20351–20365. <https://doi.org/10.18632/oncotarget.24866>
 34. Ghosh M et al (2020) Increased telomere length and mtDNA copy number induced by multi-walled carbon nanotube exposure in the workplace. *J Hazard Mater* 394:122569. <https://doi.org/10.1016/j.jhazmat.2020.122569>
 35. Gliga AR et al (2018) RNA-sequencing reveals long-term effects of silver nanoparticles on human lung cells. *Sci Rep* 8(1):1–14. <https://doi.org/10.1038/s41598-018-25085-5>
 36. Gong C et al (2012) Methylation of PARP-1 promoter involved in the regulation of nano-SiO₂-induced decrease of PARP-1 mRNA expression. *Toxicol Lett* 209(3):264–269. <https://doi.org/10.1016/j.toxlet.2012.01.007>
 37. González-Palomo AK et al (2021) Effect of silver nanoparticles (AgNPs) exposure on microRNA expression and global DNA methylation in endothelial cells EA.hy926. *Environ Toxicol Pharmacol* 81:103543. <https://doi.org/10.1016/j.etap.2020.103543>
 38. Guseva Canu I et al (2020) State of knowledge on the occupational exposure to carbon nanotube. *Int J Hyg Environ Health* 225:113472. <https://doi.org/10.1016/j.ijheh.2020.113472>
 39. Halappanavar S et al (2011) Pulmonary response to surface-coated nanotitanium dioxide particles includes induction of acute phase response genes, inflammatory cascades, and changes in microRNAs: a toxicogenomic study. *Environ Mol Mutagen*:425–439. <https://doi.org/10.1002/em.20639>
 40. Handy DE, Castro R, Loscalzo J (2011) Epigenetic modifications: basic mechanisms and role in cardiovascular disease. *Circulation* 123(19):2145–2156. <https://doi.org/10.1161/CIRCULATIONAHA.110.956839>
 41. Hanly DJ, Esteller M, Berdasco M (2018) Interplay between long non-coding RNAs and epigenetic machinery: emerging targets in cancer? *Philos Trans R Soc B Biol Sci*. <https://doi.org/10.1098/rstb.2017.0074>
 42. Huaux F et al (n.d.) Mesothelioma response to carbon nanotubes is associated with an early and selective accumulation of immunosuppressive monocytic cells. *Part Fibre Toxicol* 13(1):46. <https://doi.org/10.1186/s12989-016-0158-0>
 43. IARC Working Group on the Evaluation of Carcinogenic Risks to Humans (2017) Carbon nanotubes. IARC Monogr 111
 44. Jayaram DT, Payne CK (2020a) Food-grade TiO₂Particles generate intracellular superoxide and Alter epigenetic modifiers in human lung cells. *Chem Res Toxicol* 33(11):2872–2879. <https://doi.org/10.1021/acs.chemrestox.0c00331>
 45. Jayaram DT, Payne CK (2020b) Intracellular generation of superoxide by TiO₂Nanoparticles decreases histone deacetylase 9 (HDAC9), an epigenetic modifier. *Bioconjug Chem* 31(5):1354–1361. <https://doi.org/10.1021/acs.bioconjchem.0c00091>
 46. Jin B, Robertson KD (2013) DNA methyltransferases, DNA damage repair, and cancer. *Adv Exp Med Biol*:3–29. https://doi.org/10.1007/978-1-4419-9967-2_1
 47. Kalaiarasi A et al (2018) Copper oxide nanoparticles induce anticancer activity in A549 lung cancer cells by inhibition of histone deacetylase. *Biotechnol Lett* 40(2):249–256. <https://doi.org/10.1007/s10529-017-2463-6>
 48. Kalishwaralal K et al (2009) Silver nanoparticles inhibit VEGF induced cell proliferation and migration in bovine retinal endothelial cells. *Colloids Surf B Biointerfaces* 73(1):51–57. <https://doi.org/10.1016/j.colsurf.2009.04.025>
 49. Kane AB, Hurt RH, Gao H (2018) The asbestos-carbon nanotube analogy: an update. *Toxicol Appl Pharmacol* 361:68–80
 50. Kelly TK, De Carvalho DD, Jones PA (2010) Epigenetic modifications as therapeutic targets. *Nat Biotechnol*:1069–1078. <https://doi.org/10.1038/nbt.1678>
 51. Kettunen E et al (2017) Asbestos-associated genome-wide DNA methylation changes in lung cancer. *Int J Cancer* 141(10):2014–2029. <https://doi.org/10.1002/ijc.30897>
 52. Ladd-Acosta C (2015) Epigenetic signatures as biomarkers of exposure. *Curr Environ Health Rep* 2(2):117–125. <https://doi.org/10.1007/s40572-015-0051-2>

53. Li JJ et al (2010) Autophagy and oxidative stress associated with gold nanoparticles. *Biomaterials* 31(23):5996–6003. <https://doi.org/10.1016/j.biomaterials.2010.04.014>
54. Liou S-HH et al (2017) Global DNA methylation and oxidative stress biomarkers in workers exposed to metal oxide nanoparticles. *J Hazard Mater* 331:329–335. <https://doi.org/10.1016/j.jhazmat.2017.02.042>
55. Lu X, Mioussé IR, Pirela SV, Moore JK et al (2016a) In vivo epigenetic effects induced by engineered nanomaterials: a case study of copper oxide and laser printer-emitted engineered nanoparticles. *Nanotoxicology* 10(5):629–639. <https://doi.org/10.3109/17435390.2015.1108473>
56. Lu X, Mioussé IR, Pirela SV, Melnyk S et al (2016b) Short-term exposure to engineered nanomaterials affects cellular epigenome. *Nanotoxicology* 10(2):140–150. <https://doi.org/10.3109/17435390.2015.1025115>
57. Ma Y et al (2017) Titanium dioxide nanoparticles induce size-dependent cytotoxicity and genomic DNA hypomethylation in human respiratory cells. *RSC Adv* 7(38):23560–23572. <https://doi.org/10.1039/C6RA28272E>
58. Ma Y et al (2019) Different effects of titanium dioxide nanoparticles instillation in young and adult mice on DNA methylation related with lung inflammation and fibrosis. *Ecotoxicol Environ Saf* 176:1–10. <https://doi.org/10.1016/j.ecoenv.2019.03.055>
59. Magdolenova Z et al (2014) Mechanisms of genotoxicity. A review of *in vitro* and *in vivo* studies with engineered nanoparticles. *Nanotoxicology* 8(3):233–278. <https://doi.org/10.3109/17435390.2013.773464>
60. Manke A, Wang L, Rojanasakul Y (2013) Mechanisms of nanoparticle-induced oxidative stress and toxicity. *Biomed Res Int*. <https://doi.org/10.1155/2013/942916>
61. Menezo YJR et al (2016) Oxidative stress and alterations in DNA methylation: two sides of the same coin in reproduction. *Reprod Biomed Online*:668–683. <https://doi.org/10.1016/j.rbmo.2016.09.006>
62. Mitchell LA et al (2009) Mechanisms for how inhaled multiwalled carbon nanotubes suppress systemic immune function in mice. *Nat Nanotechnol* 4(7):451–456. <https://doi.org/10.1038/nnano.2009.151>
63. Murugadoss S et al (2020) Agglomeration of titanium dioxide nanoparticles increases toxicological responses in vitro and in vivo. *Part Fibre Toxicol* 17(1):10. <https://doi.org/10.1186/s12989-020-00341-7>
64. Mytych J et al (2017) Prolonged effects of silver nanoparticles on p53/p21 pathway-mediated proliferation, DNA damage response, and methylation parameters in HT22 hippocampal neuronal cells. *Mol Neurobiol* 54(2):1285–1300. <https://doi.org/10.1007/s12035-016-9688-6>
65. Ng CT et al (2011) The induction of epigenetic regulation of PROS1 gene in lung fibroblasts by gold nanoparticles and implications for potential lung injury. *Biomaterials* 32(30):7609–7615. <https://doi.org/10.1016/j.biomaterials.2011.06.038>
66. Ngobili TA, Daniele MA (2016) Nanoparticles and direct immunosuppression. *Exp Biol Med*:1064–1073. <https://doi.org/10.1177/1535370216650053>
67. Ognik K et al (2019) The effect of copper nanoparticles and copper (II) salt on redox reactions and epigenetic changes in a rat model. *J Anim Physiol Anim Nutr* 103(2):675–686. <https://doi.org/10.1111/jpn.13025>
68. Öner D et al (2017) Epigenetic effects of carbon nanotubes in human monocytic cells. *Mutagenesis* 32(1):181–191. <https://doi.org/10.1093/mutage/gew053>
69. Öner D, Ghosh M, Bové H et al (2018a) Differences in MWCNT- and SWCNT-induced DNA methylation alterations in association with the nuclear deposition. *Part Fibre Toxicol* 15(1):11. <https://doi.org/10.1186/s12989-018-0244-6>
70. Öner D, Ghosh M, Moisse M et al (2018b) Global and gene-specific DNA methylation effects of different asbestos fibres on human bronchial epithelial cells. *Environ Int* 115:301–311. <https://doi.org/10.1016/j.envint.2018.03.031>
71. Öner D et al (2020) Induction and recovery of CpG site specific methylation changes in human bronchial cells after long-term exposure to carbon nanotubes and asbestos. *Environ Int* 137:105530. <https://doi.org/10.1016/j.envint.2020.105530>
72. Ou L et al (2017) The mechanisms of graphene-based materials-induced programmed cell death: a review of apoptosis, autophagy, and programmed necrosis. *Int J Nanomedicine*:6633–6646. <https://doi.org/10.2147/IJN.S140526>
73. Oxidative stress alters global histone modification and DNA methylation (2015) *Free Radic Biol Med* 82:22–28. <https://doi.org/10.1016/j.freeradbiomed.2015.01.028>
74. Pakrashi S et al (2014) In vivo genotoxicity assessment of titanium dioxide nanoparticles by Allium cepa root tip assay at high exposure concentrations. *PLoS One* 9(2):e87789. <https://doi.org/10.1371/journal.pone.0087789>
75. Park EJ, Park K (2009) Oxidative stress and pro-inflammatory responses induced by silica nanoparticles in vivo and in vitro. *Toxicol Lett* 184(1):18–25. <https://doi.org/10.1016/j.toxlet.2008.10.012>
76. Park MVDZ et al (2011) The effect of particle size on the cytotoxicity, inflammation, developmental toxicity and genotoxicity of silver nanoparticles. *Biomaterials* 32(36):9810–9817. <https://doi.org/10.1016/j.biomaterials.2011.08.085>
77. Patil NA, Gade WN, Deobagkar DD (2016) Epigenetic modulation upon exposure of lung fibroblasts to TiO₂ and ZnO nanoparticles: alterations



- in DNA methylation. *Int J Nanomedicine* 11:4509–4519. <https://doi.org/10.2147/IJN.S110390>
78. Patil YM, Rajpathak SN, Deobagkar DD (2019) Characterization and DNA methylation modulatory activity of gold nanoparticles synthesized by *Pseudoalteromonas* strain. *J Biosci* 44(1):1–13. <https://doi.org/10.1007/s12038-018-9842-6>
 79. Patlolla A, Patlolla B, Tchounwou P (2010) Evaluation of cell viability, DNA damage, and cell death in normal human dermal fibroblast cells induced by functionalized multiwalled carbon nanotube. *Mol Cell Biochem* 338(1–2):225–232. <https://doi.org/10.1007/s11010-009-0356-2>
 80. Pogribna M et al (2020) Effect of titanium dioxide nanoparticles on DNA methylation in multiple human cell lines. *Nanotoxicology* 14(4):534–553. <https://doi.org/10.1080/17435390.2020.1723730>
 81. Poland CA et al (2008) Carbon nanotubes introduced into the abdominal cavity of mice show asbestos-like pathogenicity in a pilot study. *Nat Nanotechnol* 3(7):423–428. <https://doi.org/10.1038/nnano.2008.111>
 82. Ray Chaudhuri A, Nussenzweig A (2017) The multifaceted roles of PARP1 in DNA repair and chromatin remodelling. *Nat Rev Mol Cell Biol*:610–621. <https://doi.org/10.1038/nrm.2017.53>
 83. Rossner P et al (2020) Gene expression and epigenetic changes in mice following inhalation of copper(II) oxide nanoparticles. *Nano* 10(3):550. <https://doi.org/10.3390/nano10030550>
 84. Roy Choudhury S et al (2017) ZnO nanoparticles induced reactive oxygen species promotes multimodal cyto- and epigenetic toxicity. *Toxicol Sci* 156(1):kfw252. <https://doi.org/10.1093/toxsci/kfw252>
 85. Saarimäki LA et al (2020) Toxicogenomics analysis of dynamic dose-response in macrophages highlights molecular alterations relevant for multi-walled carbon nanotube-induced lung fibrosis. *NanoImpact* 20:100274. <https://doi.org/10.1016/j.impact.2020.100274>
 86. Seidel C et al (2017) Epigenetic changes in the early stage of silica-induced cell transformation. *Nanotoxicology* 11(7):923–935. <https://doi.org/10.1080/17435390.2017.1382599>
 87. Senut M-C et al (2016) Size-dependent toxicity of gold nanoparticles on human embryonic stem cells and their neural derivatives. *Small* 12(5):631–646. <https://doi.org/10.1002/sml.201502346>
 88. Shukla RK et al (2011) ROS-mediated genotoxicity induced by titanium dioxide nanoparticles in human epidermal cells. *Toxicol In Vitro* 25(1):231–241. <https://doi.org/10.1016/j.tiv.2010.11.008>
 89. Shvedova AA et al (2016) Integrated analysis of dysregulated ncRNA and mRNA expression profiles in humans exposed to carbon nanotubes. *PLoS One* 11(3):e0150628. <https://doi.org/10.1371/journal.pone.0150628>
 90. Sierra MI et al (2017) DNA methylation changes in human lung epithelia cells exposed to multi-walled carbon nanotubes. *Nanotoxicology* 11(7):857–870. <https://doi.org/10.1080/17435390.2017.1371350>
 91. Singh N et al (2017) Exposure to engineered nanomaterials: impact on DNA repair pathways. *Int J Mol Sci*. <https://doi.org/10.3390/ijms18071515>
 92. Smith MT et al (2016) Key characteristics of carcinogens as a basis for organizing data on mechanisms of carcinogenesis
 93. Stoccoro A et al (2017) Multiple endpoints to evaluate pristine and remediated titanium dioxide nanoparticles genotoxicity in lung epithelial A549 cells. *Toxicol Lett* 276:48–61. <https://doi.org/10.1016/j.toxlet.2017.05.016>
 94. Tabish AM et al (2017) Changes in DNA methylation in mouse lungs after a single intra-tracheal Administration of Nanomaterials. *PLoS One* 12(1):e0169886. <https://doi.org/10.1371/journal.pone.0169886>
 95. Unfried K et al (2008) Carbon nanoparticle-induced lung epithelial cell proliferation is mediated by receptor-dependent Akt activation. *Am J Phys Lung Cell Mol Phys* 294(2):L358–L367. <https://doi.org/10.1152/ajplung.00323.2007>
 96. Vandebriel RJ, De Jong WH (2012) A review of mammalian toxicity of ZnO nanoparticles. *Nanotechnol Sci Appl*:61–71. <https://doi.org/10.2147/NSA.S23932>
 97. Verleysen E et al (2020) Physicochemical characterization of the pristine E171 food additive by standardized and validated methods. *Nano* 10(3):592. <https://doi.org/10.3390/nano10030592>
 98. Vlaanderen J et al (2017) A cross-sectional study of changes in markers of immunological effects and lung health due to exposure to multi-walled carbon nanotubes. *Nanotoxicology* 11(3):395–404. <https://doi.org/10.1080/17435390.2017.1308031>
 99. Wei JW et al (2017) Non-coding RNAs as regulators in epigenetics (review). *Oncol Rep* 37(1):3–9. <https://doi.org/10.3892/or.2016.5236>
 100. Williams K, Christensen J, Helin K (2012) DNA methylation: TET proteins – guardians of CpG islands? *EMBO Rep* 13(1):28–35. <https://doi.org/10.1038/embor.2011.233>
 101. Yu KN et al (2013) Zinc oxide nanoparticle induced autophagic cell death and mitochondrial damage via reactive oxygen species generation. *Toxicol In Vitro* 27(4):1187–1195. <https://doi.org/10.1016/j.tiv.2013.02.010>
 102. Zhao Y, Sun H, Wang H (2016) Long noncoding RNAs in DNA methylation: new players stepping into the old game. *Cell Biosci*:45. <https://doi.org/10.1186/s13578-016-0109-3>
 103. Zhao X, Toyooka T, Ibuki Y (2017) Silver nanoparticle-induced phosphorylation of histone H3 at serine 10 is due to dynamic changes in actin filaments and the activation of Aurora kinases.

- Toxicol Lett 276:39–47. <https://doi.org/10.1016/j.toxlet.2017.05.009>
104. Ziech D et al (2011) Reactive oxygen species (ROS) – induced genetic and epigenetic alterations in human carcinogenesis. *Mutat Res*:167–173. <https://doi.org/10.1016/j.mrfmmm.2011.02.015>
105. Zou Y et al (2016) DNA Hypermethylation of CREB3L1 and Bcl-2 associated with the mitochondrial-mediated apoptosis via PI3K/Akt pathway in human BEAS-2B cells exposure to silica nanoparticles. *PLoS One* 11(6):e0158475. <https://doi.org/10.1371/journal.pone.0158475>



Cellular and Molecular Mechanisms of Toxicity of Ingested Titanium Dioxide Nanomaterials

10

Adriana Vieira, Ana Gramacho, Dora Rolo,
Nádia Vital, Maria João Silva ,
and Henriqueta Louro 

Abstract

An exponential increase in products containing titanium dioxide nanomaterials (TiO₂), in agriculture, food and feed industry, lead to increased oral exposure to these nanomaterials (NMs). Thus, the gastrointestinal tract (GIT) emerges as a possible route of exposure that may drive systemic exposure, if the intestinal barrier is surpassed. NMs have been suggested to produce adverse outcomes, such as genotoxic effects, that are associated with increased risk of cancer, leading to a concern for public health. However, to date, the differences in the physicochemical characteristics of the NMs studied and other variables in the test systems have generated contradictory results in the literature. Processes like human digestion may change the NMs characteristics, inducing unexpected toxic effects in the intestine. Using TiO₂ as case-study, this chapter provides a review of the works addressing the interactions

of NMs with biological systems in the context of intestinal tract and digestion processes, at cellular and molecular level. The knowledge gaps identified suggest that the incorporation of a simulated digestion process for *in vitro* studies has the potential to improve the model for elucidating key events elicited by these NMs, advancing the nanosafety studies towards the development of an adverse outcome pathway for intestinal effects.

Keywords

Titanium dioxide · Nanomaterials · Ingestion · Nanotoxicology · Intestinal cells

10.1 Nanomaterials in Food and Feed

Nanomaterials (NMs) and nanoparticles (NPs) show specific physicochemical properties (e.g., dimension, surface area area and functionalization) that provide advantageous mechanical, optical and electrical characteristics [1]. Nanotechnology is one of the recognized key enabling technologies due to its potential to improve the quality and performance of many types of products and processes, thus being widely applied in several industries, namely in the food industry, including food processing and packaging, and animal feed [2, 3] (Fig. 10.1).

A. Vieira · A. Gramacho · D. Rolo · N. Vital
Department of Human Genetics, National Institute of Health Dr. Ricardo Jorge (INSA), Lisbon, Portugal

M. J. Silva · H. Louro (✉)
Department of Human Genetics, National Institute of Health Dr. Ricardo Jorge (INSA), Lisbon, Portugal

ToxOmics – Centre for Toxicogenomics and Human Health, NOVA Medical School, Universidade NOVA de Lisboa, Lisbon, Portugal
e-mail: henriqueta.louro@insa.min-saude.pt

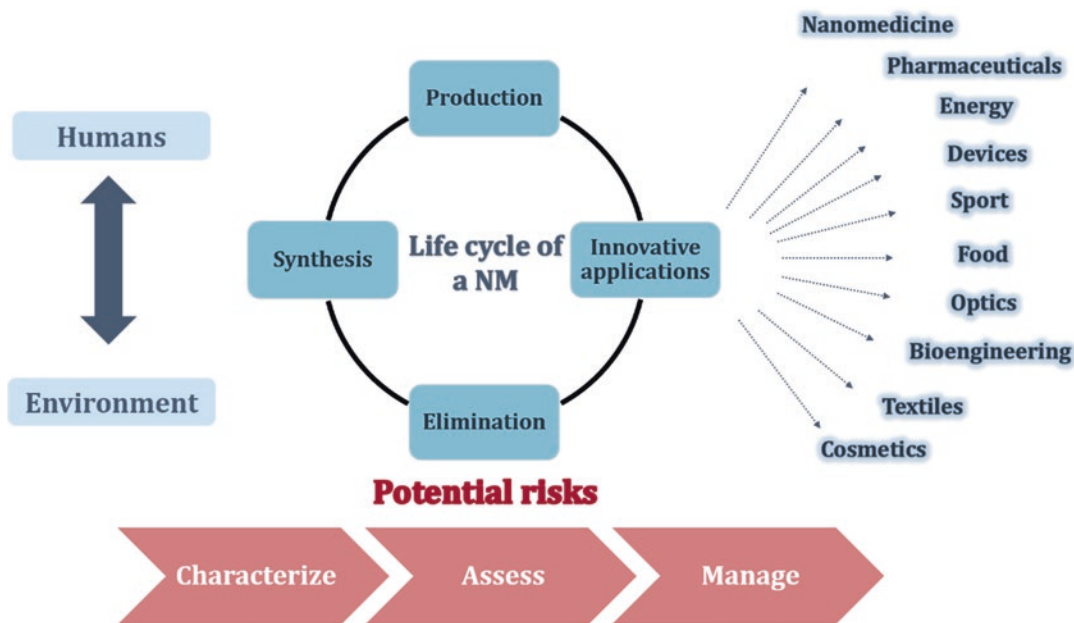


Fig. 10.1 Human and environmental exposure in the manufactured nanomaterials life cycle context

However, the exponential development of NMs contrasts with lacking conclusive risk assessment regarding the human health and the environment, causing concerns for public health [1].

In the food sector, NMs can be used as food additive to enhance product characteristics (e.g., texture, flavour and colour), improve the food stability during processing and storage or increasing nutritional value of food products [3, 4]. Several food additives have been recently identified to be NMs or as having a substantial fraction of the constituting particles in the nano range, with TiO_2 being one of the most applied in food products [3]. TiO_2 is used as food additive to augment the white colour of some products, such as dairy products, pastries, candies, sweets and chewing gums. In addition to being used as pigment, TiO_2 can also be used to improve the flavor of non-white foods like vegetables, nuts, soups, sauces (e.g., mustard) and to clear beverages (beer, cider and wine) [5, 6]. Another important NM applied in food as an additive is silicon dioxide (SiO_2 , E551). This NM is used to clear beer and wines (prevent the turbidity of beverages) and as an anticaking and anticlumping agent [7].

Both NMs (TiO_2 and SiO_2), as well as nano-sized magnesium oxide (MgO , E530) can be used in edible coatings to provide moisture or oxygen barrier and/or enhance sensory perceptions (e.g., flavor), thereby improving the product shelf life [4].

Furthermore, some NMs can improve the nutritional value of food, including animal feed products, via nanoencapsulation and nanoemulsions of supplements. Encapsulation of a compound (e.g., vitamins and flavonoids) in a nano sized vehicle confers protection against degradation and improves stability and solubility, thus leading to an increased bioavailability and a more efficient delivery to cells and tissues [3, 8]). As a component of numerous enzymes and hormones, zinc is essential for vital physiological functions in humans and, therefore, is common to add zinc oxide (ZnO) NMs as a source of in food supplements [9]. In the animal feed sector, the size reduction of selenium to nano range can increase the nutrient absorption in sheep, improving feed digestion [10]. Also, it is claimed that the addition of silver NPs (AgNPs) to drinking water can replace the use of antibiotics in chickens and pigs, improve digestion of feed and reduce the

aflatoxin toxicity, which is very important since mycotoxins represent a worldwide problem for farmers [11–13]. In fact, Ag NPs are widely used for the disinfection of water, as well as TiO₂ to decompose organic and inorganic contaminants in water [14].

NMs may also be applied in food contact materials (FCM), i.e., materials that directly contact with food products during manufacturing, transportation and storage [2]. Some examples are food packaging, cooking materials equipment, storing boxes, crockery and coatings of machines and surfaces [3]. Conversely, the application of NMs in FCM appears to have a promising future, since their incorporation can prevent microbial growth, reduce weight, increase heat resistance, increase mechanical strength and improve barrier against gases, UV radiation and moisture of the packaging. All of these features contribute positively to maintain the quality and safety of the food, increasing its shelf life [15].

Due to their antimicrobial properties against a broad range of microorganisms (e.g., viruses, bacteria, fungi), AgNPs are the most common NMs added to food packaging [3, 16]. In Europe (EU), these particles are not approved for use in plastic materials, since they can migrate to the food [17]. Chitosan, zinc oxide (ZnO), magnesium oxide (MgO) are candidates also to be used in FCM to prevent the appearance of pathogens in food [18, 19], however they are not allowed yet in EU. The incorporation of NMs, such as nanocellulose in FCM might improve the mechanical and thermal properties of the materials, namely the ones consisting in biodegradable polymers, since due to their natural origin these polymers tend to present poor barriers [20]. A summary of present, as well as future, applications of nanomaterials in food production, that may cause either direct or indirect consumer exposure, can be found in [21].

More recently, the utilization of (nano)biosensors in FCM has become a popular trend that is commonly known as “active packaging” and/or “smart packaging” [2]. The incorporation of nanobiosensors allows the detection of pesticides, pathogens, toxins and the monitoring of

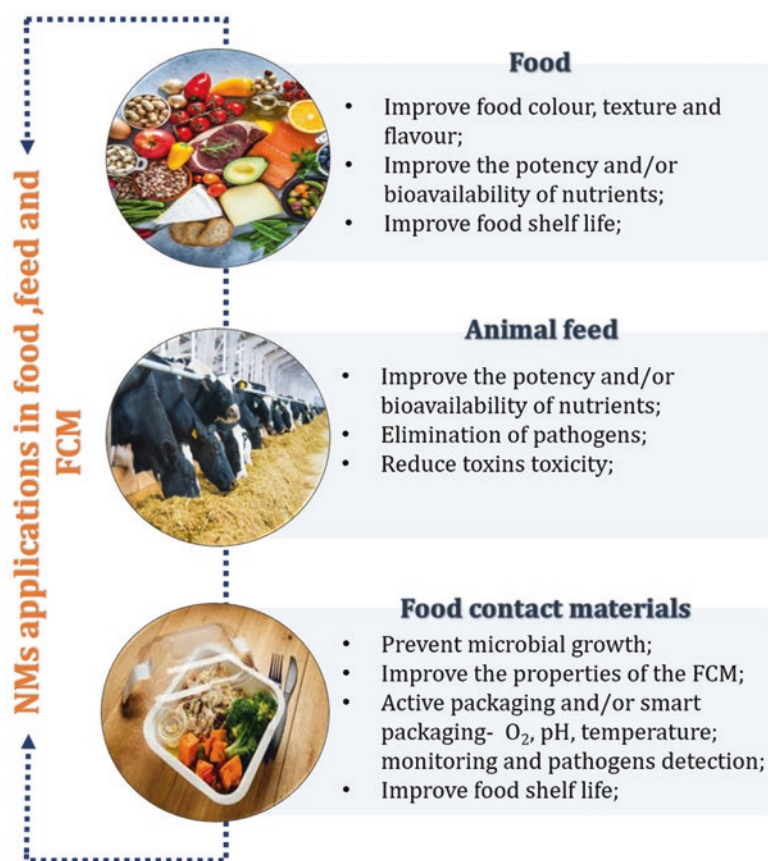
pH, oxygen (O₂) and temperature, thereby delivering information of food quality in real time [2, 22–24]. Recently, Sahoo et al. [22] work reported that ZnO quantum dots (QDs) could detect several pesticides due to their high affinity for the Cl groups present in the pesticides. At the same time, ZnO QDs could photocatalyze the pesticides during the interaction [22]. Through color change, nanobiosensors based on TiO₂ or nanocrystalline tin(IV) oxide (SnO₂) can indicate O₂, gases and pH changes or even the metabolites formation upon microbiological growth [3].

Currently, many of these applications in food and feed are already being commercialized and other are in development expecting to reach the market in a near future (summarized in Fig. 10.2). In this context, the human exposure to NMs may occur directly via ingestion of products containing NMs [21]. Conversely, it can occur indirectly, after the ingestion of foods contaminated with NMs that had been released from food-contact materials (FCM), or used as feed additives or nanopesticides. These different cases are addressed in the EFSA guideline for nanospecific risk assessment [25]. Although nanotechnology offers a broad range of promising and innovative applications, it also presents new risks. Therefore, it is becoming increasingly important to assess the potential risks of NMs in human health.

10.2 Human Exposure to Titanium Dioxide Nanomaterials (TiO₂) in Food and Food Chain

Since TiO₂ can improve the color, texture, flavor and stability of many food products, nutritional supplements and pharmaceutical formulations, it is one of the most used NMs in the food sector. E171, the European designation for food-grade TiO₂, is a food additive and colorant approved by the European Union in 1969 [26, 27], in which, “approximately, 30% of its particles are less than 100 nm in diameter” [28]. The size range where most particles lie is ca. 40–250 nm [29]. The percentage by number of constituent particles smaller than 30 nm has been determined to be ≤1% in samples of E171, either pristine or

Fig. 10.2 Applications of nanomaterials in the food and feed sectors, including food contact materials (FCM)



extracted from foods [28]. It might be applied as a pigment/food colorant to whiten and improve the opacity of skim milk, ice creams, coffee creams, sauces, pastries and candies, while also being capable of enhancing the flavor of processed food items and to clear distinct beverages [5, 6, 30, 31]. TiO_2 can also be utilized as an anti-caking agent in granular and powdered foods [5, 32]. Sweets and candies (e.g. chewing gum, chocolate and products with white icing) contain the largest content of TiO_2 in their composition amongst the available food products: 0.01–1 mg per serving [5]. This led to the estimation of consumption of 0.2–1 mg/kg/day of TiO_2 by the average adult [5]. Some of the lesser relevant examples of its oral intake are mainly associated with the accidental ingestion of toothpaste and lipstick [6, 33]. In this sense, others estimate that most humans follow a West European diet and used toothpaste, that may imply an oral intake of

0.06–5.5 mg TiO_2 /kg body weight/day [33–35]. In a very recent report, EFSA Panel estimated, for several population groups (infants, toddlers, children, adolescents, adults and the elderly), the chronic dietary exposure to E171. It was concluded that in the scenario assessment of maximum level exposure, the mean exposure to E171 varied from 0.06 mg/kg bw/day in infants to 12.8 mg/kg bw/day in toddlers [28].

Nanosized TiO_2 also exhibits increased UV-blocking properties, in a different form associated to a transparent appearance, with particles entirely <100 nm, and this form is used in UV filters, which are advantageous for its incorporation in food packaging and storage [32]. Due to the emerging number of applications of TiO_2 in the food sector, there is a higher potential of oral intake of food products. In addition, the use of TiO_2 in pharmaceutical sector, or cosmetics such as toothpaste and lipstick, can also result in the

ingestion of nanosized TiO₂, although these are outside the regulation of the food sector.

As a matter of fact, in a study using human volunteers with a normal intestinal permeability, it was shown that a fraction of pharmaceutical or food-grade TiO₂ can be directly absorbed into the bloodstream in its particulate form, after its oral administration (100 mg, in this case) [36]. The same authors also suggested that there are, probably, two distinct particle uptake pathways in the human gut, one in the proximal small intestine and another in the distal small intestine [36]. To quantify the human exposure and uptake of TiO₂ and to unravel the responsible mechanisms, further quantitative measurements were suggested to be needed [36]. Also, Böckmann et al. [37] reported the absorption of capsules or anatase powder containing TiO₂ from the gastrointestinal tract (GIT) into the bloodstream, following oral administration. More recently, it was reported the accumulation of both titanium (Ti) and TiO₂ in the human liver and spleen analyzed *post-mortem*, in which more than 24% of the particles were at the nanoscale (< 100 nm) [38]. This means that the daily oral exposure to TiO₂ particles found in consumer and food products can lead to bioaccumulation upon human oral intake [38].

As a consequence, the oral ingestion/intake of TiO₂ might constitute an emerging risk for human health, which implies a need to perform the safety assessment of these NMs in order to understand the biological effects and toxicity regarding their consumption. Despite TiO₂ is one of the most commonly applied NMs in food sector, the majority of the (nano)toxicological studies focus on non-oral routes of exposure (i.e. inhalation and dermal contact). The available data regarding toxicokinetics upon oral exposure is still very limited and, therefore, it's crucial to study the possible toxic effects of these NMs [30, 31, 39, 40]. A key study demonstrated the absorption and deposition of E171 in rodents upon repeated oral exposure, where the accumulation of E171 in the liver and intestine of mice was observed, at a dose comparable to human exposure levels [41]. The inflammation in the intestine and stomach of the exposed mice, as well as increased superox-

ide production upon E171 treatment, highlighted the need for considering human health risks as a result of dietary exposure to the food-grade TiO₂ [41].

10.3 Safety Assessment of Ingested TiO₂ – The View from a Regulatory Perspective

TiO₂ have been classified as possibly carcinogenic to humans (IARC, group 2B) [42], based on studies on animals exposed by inhalation, and also as a potential occupational carcinogen (NIOSH, 2011). As for cosmetics, the Scientific Commission for Consumer Health (SCCS) has declared that its use does not harbour increased health risks, as long as the TiO₂ containing products are applied on intact skin [43]. In 2019, the European Parliament and the Council on cosmetic products published an amendment to the Regulation (EC) No 1223/2009 in accordance with the opinion of the Standing Committee on Cosmetic Products, warning that it must not to be used on the lips (Official Journal of the European Union, 2019).

Up to date, no consensus exist on the use of TiO₂ as a food additive. The Food and Drug Administration (FDA) categorizes TiO₂ as “Generally Recognized as Safe” (GRAS) and allows products not to exceed more than 1% TiO₂ in weight (<https://www.accessdata.fda.gov/scripts/cdrh/cfdocs/cfCFR/CFRSearch.cfm?fr=73.575>, accessed 24/09/2020). In spite the European Union (EU) had approved the use of food-grade TiO₂ or E171 as a Group II food color at *quantum satis*, that is, it can be applied to products “*at a level not higher than is necessary to achieve the intended purpose*”. (European Commission, 2008), very recently this risk assessment has been revisited by EFSA. As of 6th May 2021, EFSA updated its safety assessment concerning E171, concluding that it can no longer be considered as safe when used as a food additive [28]. This is line with decisions from other regulatory bodies such as the French Agency for Food, Environmental and

Occupational Health and Safety (ANSES), that imposed in France the ban of its use in food, since January 2020 [44], highlighting the need of further studies to characterize the potential health effects related to ingestion of E171. The latest EFSA report, describes the re-assessment of the toxicological data according to the requirements specified in the 2018 EFSA Guidance on nanotechnology [28]. The Panel concluded that the available data did not suggest adverse effects with either E171 up to a dose of 1000 mg/kg bw per day or with TiO₂ (<30 nm) up to 100 mg/kg bw per day. Furthermore, it was considered that studies found in the literature on reproductive and developmental toxicity of E171 or neurotoxicity were not reliable and that the studies on immunotoxicity and inflammation were inconsistent. A new reproduction toxicity one-generation study was performed and did not reveal general toxicity, nor effect on thyroid or sex hormone levels, reproductive function and fertility nor pre- and postnatal development. A slight effect was observed in immunotoxicity, with no dose-response, while the effect of E171 in producing aberrant crypt foci described in Bettini et al. [45] was not replicated in other studies. Noteworthy, the Panel concluded that “TiO₂ particles have the potential to induce DNA strand breaks and chromosomal damage, but not gene mutations, and a concern for genotoxicity of TiO₂ particles cannot be ruled out” [28]. The up to date evidence, along with all the uncertainties, further highlight the need for accurate risk assessment of TiO₂ that can be ingested and affect human health.

10.4 Nano-Bio Interactions of Ingested Nanoparticles

The mechanisms of toxicity of NMs following oral exposure and ingestion have been poorly characterized, although changes in the secondary properties of NMs may occur in view of their dynamic behavior under physiological conditions, and a global network of cellular and molecular pathways are likely to be impacted upon such exposure. The reports concerning the toxicity of NMs are often contradictory as a result of

poorly characterized formulations and exposure conditions. Our previous work has suggested that the primary physicochemical descriptors of NMs may not be the most adequate to foresee their toxicological behavior [46]. In fact, changes in cellular environment, such as the culture medium, may affect the outcome of toxicity assays [46, 47]. It was shown *in vitro* that the same TiO₂ test material, prepared with standardized dispersion protocols, yields different outcomes in blood or respiratory cells, alongside with the use of distinct cell culture conditions, that have different effects in secondary characteristics of the NMs, leading to discrepant observations [46].

When ingested, the interaction between TiO₂ and the organic biomolecules in food and in the gastrointestinal fluids is unavoidable. Under these circumstances, the physicochemical properties of the particles may change, as well as the experimental outcome [48]. NMs may agglomerate/aggregate, react or bind to other components of food/feed, solubilize upon reaction with digestion fluids, or can even be excreted from the body [49]. Due to the plethora of possible transformations, NMs may not be available in free particulate forms, and their translocation across the GIT may be influenced as well as their cytotoxic and genotoxic outcomes [50]. For example, very recently, Zhang et al. [49] reported that the potential toxicity of TiO₂ can be reduced by the presence of a food matrix. Another study investigated the dissolution behavior of NMs under the influence of the GIT context, by using simple acidic and neutral solutions, showing that an important characteristic that influences TiO₂ solubility is the crystal form [51]. In that work, all the TiO₂ forms dissolved very slowly at both pHs, but a greater solubility was observed for nano-anatase compared to nano-rutile at neutral pH [51].

In vivo studies may provide more realistic approaches concerning the modifications that NMs may suffer in the digestion process. In spite some *in vivo* studies in rats addressed the biodistribution, elimination and toxicity of ingested NMs [52–54], the impact on the GIT should be re-considered in view of the major differences that exist between humans and rats, regarding the physiology and nutrient uptake of the GIT [55].

Considering these limitations, simulated digestion models that are available can provide an interesting tool for investigating the digestion of food contaminants [56] and eventually NMs [30], thus providing an *in vitro* improved alternative to animal models. One of such models has undergone international harmonization, particularly the standardized INFOGEST *in vitro* digestion method [57, 58]. This method simulates the physiological conditions, including the pH, time duration, enzymes activity, and composition of simulated digestive fluids of the upper GIT, including the several digestion stages: oral, gastric and small intestinal [57]. Briefly, the process involves three successive digestive phases: oral, gastric and intestinal. The oral phase includes exposure of the compound to simulated salivary fluid and amylase enzyme, followed by the addition of simulated gastric fluid and gastric enzymes (pepsin and gastric lipase). In the intestinal phase, simulated intestinal fluid, bile salts and pancreatin enzyme are added and, after incubation, an enzyme inhibitor, such as 4-(2-aminoethyl) benzenesulfonyl fluoride hydrochloride (Pefabloc) is used to stop enzymatic reactions). Our previous results using this model showed that one anatase/rutile TiO₂ mixture submitted to simulated *in vitro* digestion (NM-105), toxicity occurred after exposure of HT29-MTX-E12 intestinal cells, and was more pronounced as compared to undigested NMs, together with subtle decreases in the hydrodynamic size of the NM in cell moiety [59].

Other simulated digestion models have been described in the literature, but are not usually applied to NMs. The dissolution, biodurability and persistence of several NMs in individual simulated gastrointestinal fluids (saliva, gastric and intestinal) were recently studied in a physiologically relevant digestion cascade (including saliva -gastric - intestinal), and TiO₂ was found to be the most biodurable and persistent NM [55]. The biopersistence and lack of dissolution during digestion is consistent with the TiO₂ observed in the final product of digestion performed using standardized INFOGEST *in vitro* digestion method, detected in nano form and agglomerated nanoclusters [59]. In other work, a detailed characterization of size, size distribution, morphol-

ogy and the pH and their changes with the digestive medium showed increasing agglomerate size over time and during the gastrointestinal tract cascade [55]. Using different TiO₂, our recent work did not show major differences in agglomerates' size for two TiO₂ (NM-102, NM-103 provided by the Joint Research Centre, Ispra, Italy) in the end of the standardized INFOGEST *in vitro* digestion method, but found smaller agglomerate's size for one TiO₂ (NM-105) [59]. This finding may favor the view of an influence of the NM crystal phase and properties in their biopersistence, previously referred [50]. It is therefore foreseen that the addition to the test system of a diversity of individual factors/components during treatment, the exposure approach, and the selected cell model may lead to *in vivo*-like conditions, better representing intestine for nanosafety research [60].

10.5 Cellular Effects and Underlying Mechanisms of Action of TiO₂ in the Intestine

Following ingestion, NMs may move through the upper GIT, reaching the colon. The potentially adverse effects of ingested TiO₂ may therefore occur within the site of NMs absorption (intestine), as well as in other organs in the body after absorption like the liver and spleen, the sites of NM metabolism and detoxification [61]. Upon reaching the intestinal cells, TiO₂ can exert a direct damage on the GIT structures. Recent *in vitro* and *in vivo* studies have shown that TiO₂ can damage intestinal microvilli and tight junctions and interact with the epithelium of the small intestine, disturbing digestion/absorption of food, eventually leading to deficiencies of macro- and microelements in the organism [62–65]. The disruption of the brush border in human intestinal Caco-2 cells exposed to food grade TiO₂ was already described *in vitro* [62]. In a model of Caco-2/HT29-MTX cells, TiO₂ NMs decreased the number of microvilli, reducing the surface area available for absorption of nutrients, Fe and Zn, capture of fatty acids and inhibitor of apopto-

sis protein activity [63]. In the same cell model, in the presence of TiO₂ there were alterations in glucose uptake/transport, caused by intestinal microvilli damage, [65]. As suggested by ICP-MS data, the TiO₂ penetrated intestinal mucosa and, in male rats, one dose increased height and width of villi, while there was dose-related increase in density of goblet cells, not seen on female rats [66]. Brun et al. showed that the agglomerates of TiO₂ crossed the regular epithelium of the ileum, altered its permeability and persisted in gut cells, where they could induce chronic damage [67]. A higher accumulation of TiO₂ was seen in Goblet cells and M-cells, as compared to enterocytes, and tight junction remodelling was promoted through deregulation of genes encoding for proteins involved in epithelial structure maintenance [67]. In Caco-2 cells, Koeneman et al. showed that uncoated TiO₂ can translocate through epithelial lining (at low levels) by transcytosis and lead to sub-lethal effects as microvilli reorganization and changes on the apical surface of the epithelium and calcium level, without disrupting junctional complexes [64]. Further recent evidence shows that the *in vitro* exposure of Caco-2 cells to TiO₂, disturbed the tight junctions-permeability barrier with an effect detectable after 4 h of incubation and extensive effects on barrier integrity at 24 h, indicating that nano-sized TiO₂ particles exert harmful effects on the intestinal epithelium layer [68]. On the contrary, an *in vitro* study using a co-culture of human enterocytes (Caco-2 cells) and M-cells, provided evidence for the lack of translocation of TiO₂ across the gut epithelium model, and the results from the same authors after oral administration in rats did not suggest any significant internal exposure of the consumer to the NP by oral ingestion of nano- or larger particles of TiO₂ via food [53]. In spite, the accumulation of both titanium (Ti) and TiO₂ in the human liver and in the spleen analysed *post-mortem* that was reported recently suggests that the daily oral exposure to TiO₂ can lead to bioaccumulation [38]. In fact, only recently, studies on uptake and translocation of ingested TiO₂ across the GIT are starting to emerge. Following ingestion, uptake of NPs across the GIT can occur via different pathways.

In the case of poorly soluble nano TiO₂, active uptake by endocytosis-related pathways at the mucosal membrane are probably the most accepted uptake mechanisms [69]. Whether or not crystal structure and size influences the rate of uptake of Ti from TiO₂ by gut cells, was investigated by Gitrowski et al. [69]. The authors found that cells accumulate Ti from TiO₂ exposure possibly explained by an active uptake of Ti-containing particles in physiologically competent cells, suggesting the probable relevance of crystal structure-effect, being the anatase form of TiO₂ absorbed faster than the rutile [69]. The TiO₂ uptake in GIT, via the Peyer patches, was also proposed to take place, due to the elevated presence of TiO₂ in the lymphoid tissues [67].

Information on cellular uptake of NMs gives a first indication on its possible mechanisms of action. For example, the interaction of NM directly with DNA can only occur if the NM is taken up by the cell and is able to enter the nucleus to reach the DNA [70]. Thus far, the mechanisms of NM tissue and/or cell damage is unclear, and the molecular changes involved in these processes are unclear [71], but it has been considered that ROS formation could contribute to the induction of cell damage [27]. An elevated level of reactive oxygen species (ROS) and expression of inflammatory transcripts with increasing NMs concentration, as well as the binding of TiO₂ to the cellular membrane and its passage into the cells, has been reported. ROS formation have been implicated in both indirect primary genotoxicity and secondary genotoxicity mechanisms following exposure to NMs [72]. A comprehensive review of *in vitro* mammalian studies of effects of TiO₂ by Iavicoli et al. [73] revealed that most papers report induction of ROS by TiO₂, followed by different types of cellular effects [73]. In most of the studies, TiO₂ induced ROS generation following exposure to TiO₂. In undifferentiated Caco-2 cells, exposure to different types of TiO₂ particles (anatase, 50 nm; rutile, 50 nm; anatase, 100 nm; rutile, 250 nm; and P25, 21 nm) at 25 and 50 µg/mL, significantly increased ROS levels in undifferentiated Caco-2 cells, following 3 h exposure, and an increase of IL-8 expression at the highest dose

tested [74]. Exposure to different sizes of 80% anatase and 20% rutile TiO₂ TNP 18 (5.84 ± 6.59 nm), TNP 30 (24.59 ± 8.60 nm) and TNP 87 (81.80 ± 5.27 nm) for 4 h was also showed to induced a 10–18 fold increase of ROS levels at higher doses (60 µg/mL and 100 µg/mL) compared to control for 48 h post exposure [75]. TiO₂ A12 (95% anatase, 5% rutile; 12 nm) and R20 (90% rutile; 10% anatase; 22 nm) were seen to accumulate in undifferentiated Caco-2 cell cultures exposed to 50 µg/mL, with no alterations in cell viability or DNA damage despite increased ROS generation, after 6 and 48 h [76]. A high-level increase of ROS in a dose-dependent manner was also seen after exposure to 1, 2.5, 5, 10, 20 µg/cm² (corresponding to 6.4–128.0 µg/ml) of TiO₂ (anatase <25 nm, 99.7% purity, BET surface area 45–55 m²/g), after 6 h, but not after 24 h, with no induction of cytotoxicity, or IL-8 release [77]. Later, the same group, found that exposure to 1 and 2.5 µg/cm² (corresponding to 6.4 and 16.0 µg/ml) of the same NM significantly increased the basal level of DNA 8-oxodG in comparison to the control at 6 and 24 h of treatment, which was more evident at 6 h exposure [78]. Using a different model of non-mucus-producing phenotype of colorectal adenocarcinoma (HT-29) cells, an increase in ROS was observed after short exposures to 4.5, 9 and 36 µg/ml TiO₂ (anatase, <25 nm, surface area 45–55 m²/g), for 6 and 24 h [66], more evident after 6 h exposure. In the human colon cancer cell line (HCT116) and normal colon cell line (NCM460), TiO₂ (25 nm, anatase) promoted a dose-dependent increase of ROS production, after exposure to 15 µg/mL, 30 and 60 µg/mL for 24 h [71, 79]. The intracellular ROS formation was markedly elevated by TiO₂ in a dose-dependent manner in Caco-2 and HepG2 cells treated with rutile 30 nm TiO₂ (100–300 µg/mL) for 24 h [61]. Also, in HepG2 cells, ROS levels dramatically increased from 6th to 24th hours exposed to 10 µg/mL TiO₂ [80, 81]. Positive findings on ROS generation have also been found in co-culture of Caco-2 and HT29-MTX cells. Guo et al. [63] assessed the formation of ROS, following 4 h and 5 days exposure to TiO₂ (30 nm), showing an increase in ROS production.

Following acute and chronic exposure to three different types of TiO₂, particularly, E171 (> 95% anatase; 118 ± 53 nm), P25 (86% anatase/14% rutile; 24 ± 6 nm) and A12 (> 95% anatase; 12 ± 3 nm) induced ROS formation was observed after at all three timepoints (6 h, 24 h and 48 h), following acute exposure to 50 µg /mL P25 and E171 (the latter also induced ROS at 10 and 100 µg/mL concentrations), while A12 induced ROS after 6 and 24 h exposure, but not at 48 exposure [82]. Similarly, intracellular ROS levels were higher in repeatedly-exposed cells (along 21 days), following exposure to P25 (at 50 µg / mL) and E171 (at 50–100 µg/mL) when compared to untreated cells.. DNA strand breaks, alkali-labile sites and oxidative purine lesions were observed only when cells were exposed to the highest concentration, 50 µg/mL, of E171 using the comet assay and FPG-modified comet assay [82]. Later, the same group showed an induction of ROS generation after exposure for 6 h, 24 h or 48 h to 50 µg/mL to A12 (95% anatase, 5% rutile; 12 nm), NM-105 (86% anatase, 24 nm), or E171 (>95% anatase, 118 nm) or to 10, 50 and 100 µg/mL of E171, independently of exposure time or type of TiO₂. Increased ROS level in cells exposed to E171, was concentration-dependent, with significantly higher ROS levels in cells exposed to 50 or 100 µg/mL of E171 [83]. After 24 h of exposure of NPs decrease in intracellular GSH levels of Caco-2 and HepG2 cells was observed at 100, 150, 200, and 300 µg/mL.

In vivo, after TiO₂ treatment, the ROS levels of liver and kidney cells in ICR mice were significantly increased, in dose-dependent manners [80, 81]. After intragastric administration of TiO₂ to mice during 30 days, an increase in the accumulation of ROS (e.g. OH⁻) was observed in the spleen of mice, involving p38-Nrf-2 signalling pathway, due to lipid peroxidation [84].

Negative results concerning oxidative stress were also reported in literature. In Caco-2 cells, TiO₂ with a diameter ranging from 3.94–25.20 nm was induced cell mortality, but no oxidative stress or DNA damage [85]. Gerloff et al. [85] found that TiO₂ containing anatase-rutile, in contrast to the pure anatase, induced cell death or mild DNA damage, suggesting that both surface area and

crystallinity are critical determinants of TiO₂ toxicity. Nevertheless, they did not find any signs of oxidative stress and ROS production, following exposure to 20 a 80 µg/cm² for 24 h, suggesting that other mechanisms that require further studies might have led to the toxic responses reported [85]. Abbott Chalew and Schwab [86] also did not report increased ROS generation in undifferentiated Caco-2 and SW480 cells following 4 or 24 h exposure to 0, 0.1, 1, 10, or 100 µg/mL TiO₂ Aeroxide P25 NM105 (80% rutile:20% anatase; 21 nm), as measured by DCFH-DA fluorescence assay [86]. In fact, they found an overall reduction of ROS, which was more prominent after 24 h exposure. ROS generation was also inhibited in medium comprising 0.05% BSA in two human colon cancer cells lines (Caco-2 and/or HCT116), as measured by electron spin resonance (ESR)/paramagnetic resonance spectroscopy, following 24 exposure to 0.143 and 1.43 µg/cm² (which equivalents to 1 and 10 µg/mL, respectively) of E171, and TiO₂ (10–30 nm), in Caco-2 cells, which was only increased following exposure to micro-sized TiO₂ particles (average size 535 nm) [27]. The authors suggested a scavenging or inhibitory effect by the protein corona which may prevent ROS formation by inhibiting the contact between particle surface and ROS precursors. Also, no intracellular ROS generation was found in undifferentiated Caco-2 cells following exposure to 0.125–125 µg/ml E171, for 3 h [87]. In differentiated Caco-2 cells, no significant increase in ROS formation, cytotoxicity and DNA damage was observed following a 3 h or 24 h exposure to 0–256 µg/mL of TiO₂ rutile hydrophobic form (JRC benchmark NM-103, 25 nm) and rutile hydrophilic (JRC benchmark NM-104, 25 nm), using the CellROX assay [88].

The use of digestion simulation fluids for TiO₂ before undifferentiated Caco-2 cell cultures exposure, induced a slight decrease in cell viability and membrane integrity and an increase in ROS generation, following exposure to 100 µg/mL and 200 µg/mL of two anatases T1 (99 ± 30 nm) and T2 (26 ± 12 nm) for 24 h [89]. However, it had no effect on differentiated Caco-2 cells [89].

The inconsistency of the results observed in the literature may be due to the physicochemical properties of the NM itself, NM dispersion method, difference in NMs' size and dispersion stability or to the specific protocol conditions, as previously described in a literature review [90], such as the time of exposure or the different cell models used.

The ability of NMs to affect the immune system has been discussed in several *in vitro* and *in vivo* studies. NMs were identified in recent reports as potential stimulants of immune responses that may lead to immunotoxicity, being this endpoint relevant for addressing nanosafety [91]. *In vitro*, Tada-Oikawa et al. [74] reported that the exposure to anatase (50 nm) TiO₂ during 72 h, decreased the cell viability of Caco-2 cells in a dose-dependent way and also induced proinflammatory response, seen by increased levels of IL-1β and IL-8. In addition, TiO₂ particles triggered an inflammatory response in co-culture of Caco-2/HT29-MTX cells, showing increased release of IL-1β, IL-8, IL-17A, eotaxin, and RANTES and moderate increase in the expression of some efflux pumps [83]. In other work, the exposure of cocultures to TiO₂ caused increases in IL-8 release, but had no effect on IL-8 release in monocultures [63]. *In vivo*, Trouiller et al. [92] an elevated expression of inflammatory cytokines such as TNF-α, interferon-γ and IL-8 in the blood of mice was shown after oral intake of 100 mg/kg bw TiO₂ for 5 days. In rats exposed for 7 and 100 days to ingestion of 10 mg/kg bw of E171, was observed a decreased frequency of immunoregulatory Tregs and CD4 + CD25+ Thelpers, as well as the induction of inflammatory markers such as TNF-α, IL-8 and IL-10, in aberrant crypts after 100 days of exposure [45]. A potent Th1/Th17 immune response was detected via an increased production of IFN-γ in Peyer's Patches and IFN-γ and IL-17 in the spleen after 7 days of exposure [45]. More recently, increased concentration of IL-6 in the serum of rats treated with 50 mg/kg TiO₂ for 30 days was observed [93]. Long-term oral exposure to TiO₂ also impaired immune functions in rats [94]. Also, the molecular nature of TiO₂-induced immunotoxicity in RAW 264.7

macrophage which shown to occur via induction of apoptosis and simultaneous multiple toll-like receptors signalling through ROS-dependent SAPK/JNK and p38 MAPK activation [95]. Using livers from mice exposed intragastrically to 10 mg/kg bw for 90 days, Cui et al. [96] observed the generation of inflammation and a reduction in immune capacity by the downregulation of genes involved in the complement system through whole genome microarray analysis. Liver Inflammation and fibrosis were described after long-term exposure to TiO₂ in mice fed for 9 months [97]. In primary bone marrow derived macrophages, TiO₂ activated the inflammasome in macrophages [98].

In a co-culture of Caco-2/HT29-MTX intestinal cells, although ROS production was detected, only minor changes were observed in mRNA expression of genes involved in ROS regulation, DNA repair via base-excision repair, and endoplasmic reticulum stress [83]. The consequences of epigenetic changes induced by exposure to NMs are still poorly understood [99]. It is recognized the potential of NMs to change global DNA methylation, as well as gene-specific methylation patterns, including tumour suppressor genes, inflammatory genes, DNA repair genes, and impaired expression of genes involved in DNA methylation reactions, are all potentially relevant to cancer development [100]. For example, in bronchial cells, hypomethylation was observed for anatase, rutile and anatase: rutile mixture forms of TiO₂ [101], suggesting that epigenetic studies should be performed along with conventional toxicity testing methods.

TiO₂ appears to have impact on the microbiome, as seen as bacterial ratio of the human intestinal community *in vitro* which can affect the immune response [102]. *In vitro* bacterial growth inhibition and morphological and structural damage was observed following exposure to E171 [103]. However, these studies were conducted *in vitro* and therefore do not reflect the complexity of gut microbiome. Pinget et al. [104] investigated the impact of E171 on gut microbiota using male mice orally exposed via drinking water [104]. They observed that TiO₂ had minimal impact on the composition of the microbiota in

the small intestine and colon, but it changed the release of bacterial metabolites *in vivo* and affected the spatial distribution of commensal bacteria *in vitro* promoting biofilm formation. The same authors also reported, in mice exposed via intragastric to 150 mg/kg TiO₂ (21 nm) for 30 days, reduced expression of a key component of the intestinal mucus layer, the colonic mucin-2 gene, and increased expression of the beta defensin gene, events associated with colonic inflammation [104, 105]. Furthermore, it was shown that, although unapparent pathological changes were observed in small intestine, gut microbiota was remarkably decreased, and gut microbial community compositions was significantly changed. Chen et al. [93] also found changes in the gut microbiota and faeces metabolomics, in Sprague-Dawley rats orally exposed to 0, 2, 10, 50 mg/kg TiO₂ (29 nm, anatase), daily for 30 days [93]. Pathological inflammatory infiltration and mitochondrial abnormalities were observed also in rats after TiO₂ [93].

Events such as immunotoxicity, inflammation and DNA damage are recognized in general to increase the risk of developing cancer. In distal colon of mice, after intragastric exposure to E171, Proquin et al. [106] observed induced oxidative stress and immune response pathways, activation of DNA repair genes and gene expression changes in genes related to cancer development, together with epithelium in colonic crypts, 14 and 21 days after E171 ingestion. The results are consistent with previous studies conducted by the same authors, with an identical colitis associated mouse model, in which hyperplastic alterations in the colon of mice were observed from 4 weeks of E171 ingestion accompanied by a decrease in the number of goblet cells in animals exposed by oral gavage to 5 mg/kg bw per day, 5 days a week, for 10 weeks, [107]. Besides, in an Adult male Wistar rat model exposed to 10 mg/kg bw/day for 7 days of E171, by intragastric gavage, led to the promotion of microinflammation, as well as initiation of preneoplastic lesions [45].

Overall, no clear picture has emerged yet between the key events (KE) and the adverse outcomes (AO) that have been reported upon GIT

exposure to NMs, hindering the development of an adverse outcome pathway (AOP), as defined by OECD [108]. Results from multiple studies here presented, although often contradictory, suggest a potentially harmful effects of TiO₂ in *in vitro* and *in vivo* intestinal tissue, liver and spleen after oral exposure, which is apparently related to generate ROS, induced oxidative stress and inflammation [109], but it is unknown whether these events subsequently result in irreversible adverse effects in humans [109]. Also, a great number of studies did not use food-grade NMs, such as E171, in their experiments, which might hinder conclusions on its relevance for human safety. It was suggested in a recent assessment of the current evidence that key cellular and molecular effects of TiO₂ particles can occur in human liver, intestinal tissue, spleen and kidney after oral exposure, but it is unknown whether these events subsequently result in irreversible adverse outcomes (AO) in humans [109]. Further research is necessary to clarify whether TiO₂ leads to AOs, and under which conditions this may occur, in order to guarantee the safe use of TiO₂ as a food additive.

10.6 Ingested TiO₂ Cytotoxic and Genotoxic Effects – Potential Implications in Cancer

Genotoxicity can be defined as the process in which a test agent is responsible for inducing damaging effects on DNA (single and double strand breaks, loss of excision repairs, cross-links, alkali labile sites), RNA or chromosomes (structural and numerical chromosomal aberrations), affecting the integrity or function of those structures [110, 111]. Furthermore, genotoxicity and carcinogenicity are correlated since many carcinogenic agents might act through genotoxic mechanisms [112, 113].

The genotoxic effects after the exposure to an agent, such as NMs, can be assessed by specific genotoxicity assays. According to the Food and Drug Administration (FDA), they can be defined as “*in vitro and in vivo tests designed to detect*

compounds that induce genetic damage by various mechanisms” [114], that have the potential to replace long-term carcinogenicity studies. A positive result can indicate that a certain compound has the potential to be a human carcinogen [114]. For an adequate assessment of genotoxicity, the Organization for Economic Co-operation and Development (OECD) has defined Genetic Toxicology Test Guidelines (TGs) for the usage of these assays [115]. Methodologies such as the *in vitro* chromosome aberration, the *in vitro* or *in vivo* micronucleus test and the *in vivo* comet assay are included in those guidelines with specific orientations. Whenever possible, *in vivo* testing should be replaced by *in vitro* assays, in order to avoid using animal models [116]. It was necessary to adapt some of the previously described assays to NMs’ genotoxicity testing since some of their physicochemical properties interfere with the outcome [115, 117].

Since genotoxic effects can be often masked by cytotoxic effects, it is imperative to carry out a preliminary cytotoxicity assessment of a compound in order to find the proper range of concentrations to perform the following genotoxic assays. Cytotoxicity assays can detect the number of viable cells in a determined cell population and in this way, enable the assessment of the cytotoxic potential of a test agent. There are many assays to evaluate cytotoxicity, being one of the most important based on the mitochondrial activity and metabolic cell proliferation [118]. This includes the MTT (3-[4,5-dimethylthiazol-2-yl]-2,5 diphenyl tetrazolium bromide) assay, in which mitochondrial enzymes released only by living cells can convert tetrazolium salts (MTT) into insoluble formazan crystals. Accordingly, the amount of purple formazan crystals produced is dependent on the number of viable cells, which is reflected by an increase in the optical density (OD) [118, 119].

As previously described, nanosized TiO₂ is one of the most used NMs with applications in consumer and industrial products and the trend for its use is increasing exponentially [120]. Bearing this in mind, the study of cytotoxicity and genotoxicity that may arise from the use of products containing these NMs has also triggered

interest, namely in the food and feed sector. In this sense, the study of the adverse biological effects that may derive from the ingestion and subsequent digestion of TiO₂ and its possible absorption into the GIT are of extreme importance.

Human intestinal epithelial cells (namely, Caco-2 and HT29-MTX cell lines) can be used as *in vitro* models to study the cytotoxic and genotoxic effects of TiO₂ following its ingestion or a simulated digestion procedure [121]. These are less expensive, have an increased reproducibility and their outcome is more rapidly achieved in comparison with *in vivo* models [122]. Both referred cell lines are derived from a human epithelial colorectal adenocarcinoma. Caco-2 cell line is considered as the best characterized *in vitro* model for the intestinal barrier, since it mimics the most abundant cell type found in the small intestine - the absorptive enterocytes. It's widely used in many (nano)toxicological and pharmacological studies, including drug transport and NM absorption/uptake [123–125]. On the other hand, HT29-MTX cells present a mucus-secreting phenotype that resembles Goblet cells, also found in the intestine [126]. The presence of a mucus layer is considered as a thick and dense physical barrier that might influence the diffusion of TiO₂ in the intestine, which can be retained and consequently, reduce the possible translocation/internalization of these NMs [123].

The Caco-2 and HT29-MTX cell co-culture model can be advantageous compared to monocultures in *in vitro* absorption studies, since it allows to better mimic the intrinsic structure of the intestine epithelium and its physiological conditions, also increasing the robustness and reproducibility of the obtained results [124].

More complex representative models include *in vivo* testing in animals or human volunteer studies. The first, besides being time consuming and expensive, display significant differences in the physiology and nutrient uptake of the GIT of humans and rats, as pointed by some authors [127]. Volunteer studies may have ethical constraints and the results can be influenced by the characteristics of individuals, generally in small number [128].

Currently, there are already some studies reporting the cyto- and genotoxicity of TiO₂ after a digestion process or after ingestion, upon exposure of intestinal cells, that are described in the next sections. Some recent projects addressing this issue are also underway, such as the nationally funded project INGESTnano (PTDC/SAU-PUB/29481/2017, Foundation for Science and Technology, Portugal).

10.6.1 Cytotoxicity of TiO₂ and Ingested TiO₂ *In Vitro*

A summary of the *in vitro* cytotoxicity studies related to TiO₂ exposure in GIT is presented in Table 10.1, displaying 12 studies.

Regarding TiO₂ cytotoxicity in intestinal cells, the majority of the studies in the Caco-2 cell line indicated absence of effects [82, 86, 88, 129]. TiO₂ anatase with 215 nm was unable to produce a cytotoxic outcome on Caco-2 cells using the LDH assay (20 and 80 µg/cm²), after 4 h or 24 h exposure [129]. Also, Abbott Chalew and Schwab [86] reported no cytotoxicity in Caco-2 cells after 24 h and 48 h of exposure to P25 (80% rutile/20% anatase; 21 nm) (0–100 µg/mL) through the MTT assay. The same outcome was verified in Dorier et al. [82], after 24 h of exposure to P25 (86% anatase/14% rutile; 24 ± 6 nm), using the WST-1 assay (0–200 µg/mL). Additionally, after 24 h of exposure to rutile hydrophobic NM-103 and rutile hydrophilic NM-104 (0–256 µg/mL), Jalili et al. [88] reported no cytotoxic effects in Caco-2 differentiated monolayer cells using neutral red uptake assay. Likewise, Dorier et al. [76] reported an absence of cytotoxicity in Caco-2 cells upon 24 h exposure to A12 (95% anatase/5% rutile; 12 ± 3 nm) and R20 (90% rutile/10% anatase; 22 ± 4 nm). Conversely, using the Trypan Blue Viability test, E171 (316 ± 284.4 nm) and TiO₂ (99.5% anatase; 10.25 nm) (0–143 µg/cm²) induced both a decrease in Caco-2 cell viability after 24 h of exposure to 143 µg/cm² concentration, and to the 14.3 µg/cm² concentration of E171 [27]. In the same experimental conditions, HCT116 cells (another human colon cancer cell

Table 10.1 *In vitro* cytotoxicity reports regarding exposure of a monoculture of cells (Caco-2, C2BBE1, HT29 and HCT116), a co-culture of Caco-2/HT29-MTX cells or a tri-culture of Caco-2/HT29-MTX/Raji B cells to TiO₂

Cell Type	Assay Used	Tested TiO ₂	Concentration	Time of Exposure	Result (Positive/Negative)	Reference
Caco-2	LDH	Anatase (215 nm)	20 and 80 µg/cm ²	4 h and 24 h	Negative	[129]
Caco-2	MTT	P25 (80% rutile/20% Anatase; 21 nm)	0–100 µg/mL	24 h and 48 h	Negative	[86]
C2BBE1	MTT	Digested anatase/rutile mixture (21 nm)	10 µg/cm ²	24 h	Positive	[130]
Caco-2	MTT	A12 (95% Anatase/5% rutile; 12 ± 3 nm) R20 (90% rutile/10% Anatase; 22 ± 4 nm)	0–200 µg/mL	24 h	Negative	[76]
Caco-2	Trypan blue viability	E171 (316 ± 282.4 nm)	0–143 µg/cm ²	24 h	Positive for 14.3 and 143 µg/cm ² concentrations	[27]
		99.5% Anatase (10.25 nm)			Positive for 143 µg/cm ² concentration	
HCT116		E171 (316 ± 282.4 nm)	5–100 µg/cm ²		Negative	
HT29	MTT	Anatase (< 25 nm)	1–20 µg/cm ²	6 h, 24 h and 48 h	Negative	[66]
Caco-2	WST-1	P25 (86% rutile/14% Anatase; 24 ± 6 nm)	0–200 µg/mL	24 h	Negative	[82]
Co-culture Caco-2/HT29-MTX		E171 (> 95% Anatase; 118 ± 53 nm)		6 h, 24 h and 48 h		
		P25 (86% rutile/14% Anatase; 24 ± 6 nm)				
		A12 (> 95% Anatase; 12 ± 3 nm)				
HT29	MTT	Anatase/rutile (27.38 ± 5.90)	2–10 µg/mL	24 h	Negative	[131]
	Trypan blue exclusion				Positive (decrease of the membrane integrity and an increased percentage of apoptotic cells)	
Caco-2 differentiated monolayer	Neutral red uptake	NM-103 (rutile hydrophobic; 25 nm)	0–256 µg/mL	24 h	Negative	[88]
		NM-104 (rutile hydrophilic; 25 nm)				
HT29	MTT	< 20 nm	50, 100, 200 and 400 µg/mL	48 h	Positive for 50 and 400 µg/mL concentration	[132]

(continued)

Table 10.1 (continued)

Cell Type	Assay Used	Tested TiO ₂	Concentration	Time of Exposure	Result (Positive/Negative)	Reference
Co-culture Caco-2/ HT29-MTX	MTT	A12 (> 95% Anatase; 12 ± 3 nm)	0–200 µg/mL	6 h and 48 h	Negative	[83]
		E171 (> 95% Anatase; 118 ± 53 nm)				
		NM-105 (Anatase/rutile; 24 ± 6 nm)				
Tri-culture Caco-2/ HT29-MTX/ Raji B	LDH	Digested E171 (370 nm)	1% w/w	24 h	Positive for 150 ppm boscalide pesticide with 1% w/w E171 using the fasting food model (FFM)	[133]
Tri-culture Caco-2/ HT29-MTX/ Raji B	LDH	Digested E171 (370 nm)	0.75% and 1.5% w/w	24 h	Positive for both concentrations using the FFM	[134]

line), did not show signs of cytotoxicity up to the concentration of 100 µg/cm² [27].

There are some cytotoxicity studies performed using the HT29 cell model (i.e. non-producing mucus phenotype), following exposure to TiO₂. However, studies using mucus-producing Goblet cells (HT29-MTX) are not widely used in this context, and no reports were found regarding cytotoxicity assessment upon TiO₂ treatment. No cytotoxic effects were reported after 6, 24 and 48 h exposure of HT29 cells to 1–20 µg/cm² TiO₂ (anatase; < 25 nm) or to 2–10 µg/mL (anatase/rutile; 27.38 ± 5.90 nm) through the MTT assay [66, 131]. On the contrary, a 20–30% decrease in cell viability was observed after 48 h exposure of HT29 cells to higher concentrations (50 and 400 µg/mL) of TiO₂ (< 20 nm), using the same assay [132]. Regarding the trypan blue exclusion test, it was also possible to detect a significant decrease of the membrane integrity and an abnormal increased percentage of apoptotic HT29 cells, after 24 h treatment to 2–10 µg/mL TiO₂ [131]. This outcome can be a result of apoptotic processes activated by the uptaken or absorbed NMs [131].

More recently, Dorier et al. [82], using the WST-1 assay, verified that, after 6, 24 and 48 h of exposure, E171 (> 95% anatase; 118 ± 53 nm), P25 (86% anatase/14% rutile; 24 ± 6 nm) and

A12 (> 95% anatase; 12 ± 3 nm) (0–200 µg/mL) did not induce cytotoxic effects in a co-culture system of Caco-2 and HT29-MTX intestinal cells. Later, Dorier et al. [83] described the same conclusions regarding the co-culture exposed for 24 h to the >95% anatase A12 (12 ± 3 nm), E171 (> 95% anatase; 118 ± 53 nm) and anatase-rutile mixture NM-105 (0–200 µg/mL), using the MTT assay.

As mentioned before, an important point to consider regarding the potential risk of TiO₂ in food/feed is the variety of transformations that are likely to undergo when in the GIT. In this regard, some authors started to study the effects of ingested TiO₂ in intestinal cell lines, following an *in vitro* simulated digestion process. Through the MTT assay, a slight reduction in C2BBel cell (a cell clone of Caco-2) viability was observed after 24 h of exposure to 10 µg/cm² (app. 40 µg/mL) of digested anatase-rutile mixture (21 nm) [130]. Still, the authors point out that the minor cytotoxicity observed may be due to the bile salts that were adsorbed to the NMs' surface. The digestion model used by McCracken et al. [130] had some differences compared to the most recent *in vitro* digestion process described by Brodkorb et al. [57]. For example, it did not include oral phase and it used other enzymes, bile salts concentrations and timepoints. Between

steps, the NPs were recovered by centrifugation [130], a procedure not used in the INFOGEST 2.0 protocol.

In a distinct report by Cao et al. [134], E171 (110 nm) was submitted to two different types of *in vitro* simulated digestion procedure, namely the fasting food model (FFM) and the standardized food model (SFM), which was based on the American dietary. In both, it was used a GIT simulator in which the three phases of a digestion cycle are present: oral, gastric and small intestinal. More specifically, in the oral phase, E171 was mixed with simulated salivary fluid at 37 °C and inverted for only 10 seconds; on the gastric phase, the resulting product was combined with simulated gastric fluid and incubated for 2 h at 37 °C with agitation. Finally, in the small intestinal phase, the digested product was mixed with salts, bile extract and lipase that mimic the intestinal fluid and additionally incubated for 2 h at 37 °C. The obtained results showed a significant dose-dependent cytotoxicity (using the LDH assay) in a tri-culture of Caco-2/HT29-MTX/Raji B cells when exposed for 24 h to digested E171 (0.75% and 1.5% w/w), through the FFM. No significant reduction on the cell viability upon treatment with both concentrations of E171 was observed for the SFM. The authors concluded that the presence of E171 in a fasting type diet can result in cytotoxic effects [134]. Using the FFM, the LDH assay and the same tri-cellular model, Cao et al. [133] also assessed the potential combined effects of TiO₂ (E171) and the pesticide boscalid in food. Exposure to digested E171 alone (1% w/w) and boscalid at 10 ppm, with or without E171 (1% w/w), only led to the induction of a slight cytotoxicity after 24 h. By contrast, 150 ppm boscalid in the presence of 1% w/w E171 digesta caused a reduction on the cell viability (22.6% cytotoxicity) level and was significantly more cytotoxic ($p < 0.01$) than digesta from FFM with 150 ppm boscalid alone [133]. Also, under the nationally funded project INGESTnano (PTDC/SAU-PUB/29481/2017, Foundation for Science and Technology, Portugal), the cytotoxicity of TiO₂ was analyzed in Caco-2 cells, after a harmonized *in vitro* simulated digestion process. The TiO₂ selected for this

study was NM-102 (provided by Joint Research Center, Ispra, Italy; anatase; 22 nm). Preliminary studies using the MTT assay in Caco-2 cells exposed for 24 h to NM concentrations ranging from 0–48 µg/mL revealed a marked cytotoxicity at the highest concentrations (Fig. 10.3). This cytotoxicity was observed also in the negative controls of the digestion, where only solvent without NM was applied (cell culture medium with sterile-filtered 0.05 wt % BSA-water with 0.5% absolute ethanol, in the same proportion as in the NM samples).

The results revealed that digestion products without the NM induced cytotoxic effects above the concentration equivalent to 20 µg/mL (>12.5% of digestion product) in cell culture medium, challenging the applicability of the digestion product in further biological assays. Conversely, no cytotoxicity was observed when cells were exposed to NM-102, without the simulated digestion process. It was thus concluded that the digestion product *per se* was cytotoxic and that the enzyme inhibitor pefabloc, added in the final step of simulated digestion, was not the source of this toxicity (Fig. 10.3). Likewise, changes in pH and/or osmolality were discarded as cause of DIG toxicity (results not shown).

When performing a digestion without adding bile salts (DIG0-mod), the results suggested that the addition of bile salts accounted for most of the toxicity observed (Fig. 10.4). This was verified when comparing the cytotoxic effects of digestion product without bile salts (DIG0-mod) with normal digestion procedure, DIG0 (Fig. 10.4), where a significant difference was observed in cytotoxicity ($p < 0.05$, Student's t-test).

The fact that the *in vitro* human simulated digestion by Brodtkorb et al. [57] requires a concentration of bile salts 166-fold higher than the concentration used by McCracken et al. [130] can justify the different toxicity observed for the same concentration tested in intestinal cells (40 µg/mL). This increased concentration of bile salts is based on the normal physiological values found in a human adult intestine [57, 58]. In addition, McCracken et al. [130] used purification by centrifugation, possibly further reducing the bile

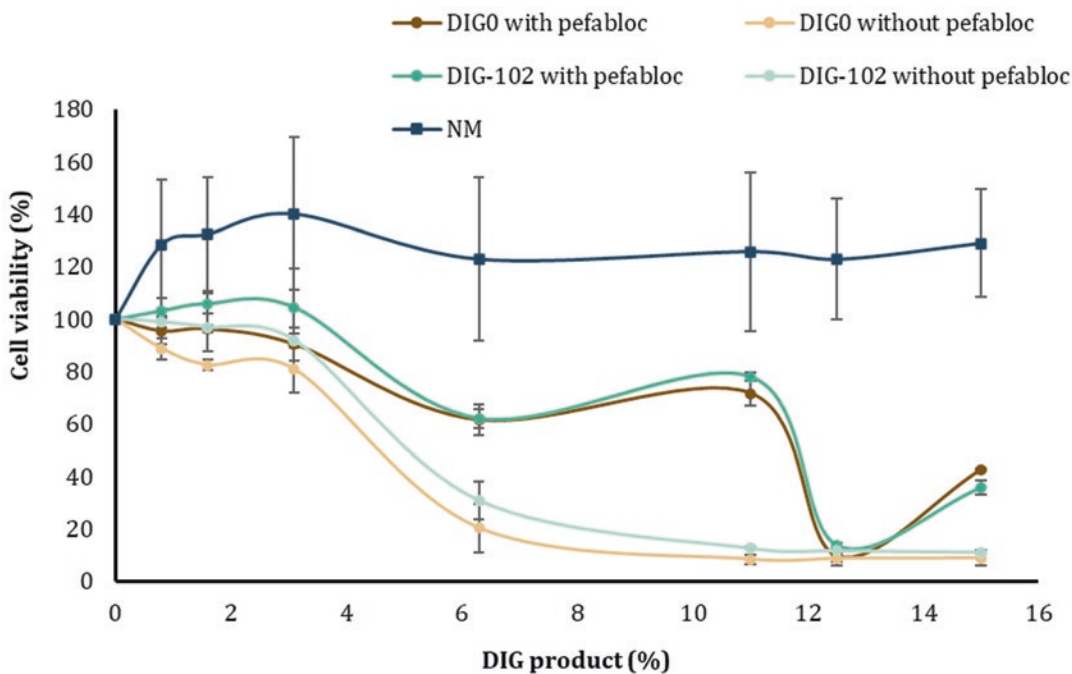


Fig. 10.3 Results of the cell viability assay in Caco-2 cells, showing cytotoxic effects as a function of the concentration of the digestion product (DIG product, %) without NM (DIG0), both with or without pefabloc, and comparison with the digestion product with NM (DIG-102) or the undigested NM (NM-102). Pefabloc is a reagent included in the last steps of the *in vitro* digestion process to inhibit enzymatic activity of the digestion mixture reagents

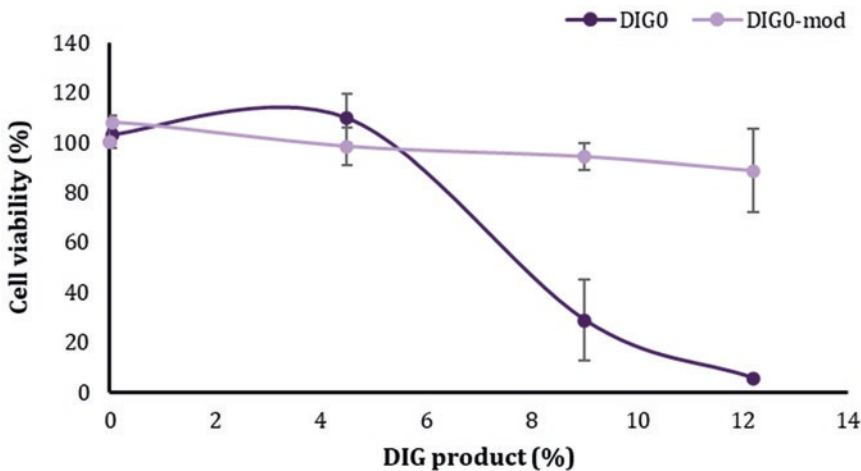


Fig. 10.4 Results of the cell viability assay in Caco-2 cells, showing high cytotoxic effects of the digestion product without NM (DIG0) and lower cytotoxicity without bile salts use (DIG0-mod)

salts content before adding it to cells. Indeed, other authors also pointed out that bile salts present in digestion product could be considered

cytotoxic [50, 135]. However, the introduction of a purification step in the digestion protocol used may lead to the loss of NM in the digestion prod-

uct, as well to further modifications in the NMs' properties that do not reflect a realistic situation.

It was concluded that, at a concentration range below 12.5% of digestion product (corresponding to 28 µg/mL of NM), even using bile salts, the harmonized digestion method could be used for addressing the toxicity of ingested NMs. In addition, the literature suggests that concentrations of 0.14 µg/mL of TiO₂ are physiologically relevant for intestinal cells [65], so such levels of concentration was used for further experiments without concerns of cytotoxic effects due to interference of the digestion reagents. Having these findings in consideration, further studies of the toxic effects of three different TiO₂ (NM-103, NM-103 and NM-105) on the gastrointestinal tract cells, Caco-2 and HT29-MTX-E12, were investigated, with the application of the standardized static INFOGEST 2.0 *in vitro* digestion method to mimic human digestion of TiO₂. The most recent results showed that, among these three NMs, the digested NM-105 (anatase-rutile) showed an increased toxicity in HT29-MTX-E12 cells, compared to undigested NM. This difference was accompanied with subtle changes in secondary characteristics of this NM [59].

10.6.2 Cytotoxicity of Ingested TiO₂ *In Vivo*

Few studies related to the study of the *in vivo* cytotoxicity of ingested or orally administered TiO₂ using animal models have been reported and are summarized in Table 10.2.

In the Sycheva et al. [136] work, nanosized TiO₂ (33.2 ± 16.7 nm) was administered daily for 7 days (40, 200 and 1000 mg/kg bw) to male mice. No cytogenetic effects were induced in the forestomach, colon and testis cells after exposure; on the contrary, upon treatment with the 40 mg/kg bw dose, a significant increase in the mitotic index was observed in forestomach and colon epithelia. Furthermore, an augmented mitotic activity in the colon at the 200 mg/kg bw and an increased apoptotic level at the highest concentration were detected [136].

An induction of the apoptosis pathway (assessed through the Bax and p53 gene expression) in the intestine and liver cells was observed in rats treated orally to 10, 50 and 100 mg/kg bw TiO₂ following a 30-day exposure. Nonetheless, an activity of other biochemical parameters such as alanine aminotransferase (ALT), aspartate

Table 10.2 *In vivo* cytotoxicity reports regarding exposure of animal models to ingested TiO₂

Animal Model	Assay Used	Tested TiO ₂	Concentration	Time of Exposure	Result	Reference
Male mice	Poly-organ Karyological	Nanosized TiO ₂ (33.2 ± 16.7 nm)	40, 200 and 1000 mg/kg bw	Daily for 7 days	No cytogenetic effects; increased mitotic index in forestomach and colon cells at a 40 mg/kg bw dose; increased apoptotic level in colon after exposure to 1000 mg/kg bw	[136]
<i>Drosophila melanogaster</i>	Trypan blue dye exclusion	Anatase (< 25 nm)	0.8 and 1.60 mg/mL	24 h and 48 h	Cytotoxic effects on midgut and imaginal disc tissues	[137]
Rat	Biochemical tests + Caspase-3 activity and TUNEL	TiO ₂	10, 50 and 100 mg/kg bw	Daily for 30 days	Induction of the apoptosis pathway in the intestine and liver cells	[61]
Wister rats	Lymphocyte proliferation assay + LDH	E171	20 and 40 µg/mL	Daily for 90 days	Decrease in the lymphocyte proliferation; increase of the LDH release	[94]

aminotransferase (ASP), lactate dehydrogenase (LDH) and alkaline phosphatase (ALP) were increased in all previous concentrations [61].

More recently, through oral gavage, Wister rats were exposed to 20 and 40 $\mu\text{g}/\text{mL}$ bw of E171 daily for 90 consecutive days [94]. Two cytotoxic parameters were assessed, more specifically, the lymphocyte transformation and the determination of the LDH activity. A significant decrease in the lymphocyte proliferation was reported when compared to the control untreated group. Nevertheless, an increase of the LDH release was detected for both concentrations, following a linear and a quadratic increment [94].

In other animal model, namely *Drosophila melanogaster*, an induction of cytotoxic effects on midgut and imaginal disc tissues of larvae was detected *in vivo* after an 24 and 48 h oral exposure to 0.8 or 1.60 mg/mL TiO_2 (anatase; < 25 nm), through the trypan blue dye exclusion test [137].

10.6.3 Genotoxicity of TiO_2 and Ingested TiO_2 *In Vitro*

As previously mentioned, the *in vitro* comet and the cytokinesis-blocked micronucleus (CBMN) assays are frequently used in the genotoxicity assessment of intestinal epithelial cells exposed to TiO_2 , but other assays such as mutation assays or chromosomal aberration tests, or even oxidative DNA damage assays can be used. Concerning the *in vitro* methods referred, different results have been reported after TiO_2 exposure, mainly due to the distinct concentrations and primary sizes of the tested TiO_2 or related to the exposure conditions. A review on genotoxic effects of TiO_2 that includes other cell types and routes of administration not related to GIT, can be found in the recent EFSA report [28]. In the next sections, we focus on the effects related to GIT.

Table 10.3 synthesizes the reports in the literature corresponding to the *in vitro* genotoxicity assessment following exposure of intestinal epithelial cells to TiO_2 . No significant genotoxic effects were induced in the Caco-2 cell line exposed for 4 h to 20 $\mu\text{g}/\text{cm}^2$ TiO_2 (anatase,

6.7 ± 1.3 nm; anatase, 3.94 ± 0.05 nm; 90% anatase/10% rutile; 21.90 ± 0.30 nm), using the conventional and FPG-modified comet assays [129]. With the same assay, Dorier et al. [76] did not report increased DNA strand breaks after 6 h, 24 h and 48 h exposure of Caco-2 cells to 50 $\mu\text{g}/\text{mL}$ of an anatase TiO_2 (particle size of 12 ± 3 nm) or to a rutile TiO_2 (22 ± 4 nm). In these two studies, the reports of the exposure in different units ($\mu\text{g}/\text{mL}$ or $\mu\text{g}/\text{cm}^2$) hamper the comparison between the different results mentioned, although in this case it is evident that the particle size did not induce differences in terms of genotoxicity. Furthermore, no genotoxic effects were reported in the conventional alkaline comet assay by Dorier et al. [82] after an acute 6 h, 24 h or 48 h exposure to 10 and 50 $\mu\text{g}/\text{mL}$ P25 (86% anatase/14% rutile; 24 ± 6 nm), A12 (95% anatase/5% rutile; 12 ± 3 nm) and E171 (>95% anatase; 118 ± 53 nm). Likewise, a 21-day repeated exposure to the same TiO_2 did not induce significant DNA damage in Caco-2 cells [82, 83].

Contradictory results were obtained for Caco-2 cells exposed for 21-days to E171 (10 and 50 $\mu\text{g}/\text{mL}$), in which a moderate genotoxicity was observed, using the FPG-modified comet assay [82]. Furthermore, through the conventional alkaline comet assay, the NanoGenotox Joint action reported that three TiO_2 produced by the JRC repository, namely NM-102 (anatase; 22 nm), NM-103 (rutile hydrophobic; 25 nm) and NM-105 (81.5% anatase/19.5% rutile; 30 nm) induced genotoxic damage in Caco-2 cells (0–256 $\mu\text{g}/\text{mL}$ concentration range), after 24 h exposure; conversely, treatment of the same cell type with the rutile hydrophilic NM-104 (25 nm) did not induce a significant level of DNA damage [138]. These results suggest that the hydrophobic or hydrophilic nature of NMs with the same primary size can greatly influence the genotoxicity outcome; besides, NMs with the same size but with distinct crystalline phases can lead to distinct outcomes regarding genotoxic damage. In the same work, no significant increased DNA strand break level was observed after just 3 h of exposure to any of the NMs referred to [138]. Zijno et al. [78] also reported an increase of the

Table 10.3 *In vitro* genotoxicity reports regarding exposure of monocultures (Caco-2 and HT29) and co-cultures of Caco-2/HT29-MTX cells to TiO₂. CBMN – Cytokinesis-Block Micronucleus Assay

Cell Type	Assay Used	Tested TiO ₂	Concentration	Time of Exposure	Result (Positive/Negative)	Reference
Caco-2	Conventional alkaline and FPG-modified comet	TUF _A I (Anatase; 6.7 ± 1.3 nm)	20 µg/cm ²	4 h	Negative	[129]
		TUF _A II (Anatase; 3.94 ± 0.05 nm)			Negative	
		TUF _{A/R} I (77% Anatase/23% rutile; 25.20 ± 0.20 nm)			Positive for the conventional comet assay	
		TUF _{A/R} II (90% Anatase/10% rutile; 21.90 ± 0.30 nm)			Negative	
Caco-2	Conventional alkaline comet	NM-102 (Anatase; 22 nm)	0–256 µg/mL	3 h and 24 h	Positive for 24 h exposure; negative for 3 h exposure	[138]
		NM-103 (rutile hydrophobic; 25 nm)			Positive for 24 h exposure; negative for 3 h exposure	
		NM-104 (rutile hydrophilic; 25 nm)			Negative for 3 and 24 h exposure	
		NM-105 (81.5% Anatase/18.5% rutile; 30 nm)			Positive for 24 h exposure; negative for 3 h exposure	
		Same TiO ₂			Negative (for all tested TiO ₂)	
					Negative	
Caco-2	CBMN assay	A12 (95% Anatase/5% rutile; 12 ± 3 nm)	50 µg/mL	52 h	Negative	[76]
		R20 (90% rutile/10% Anatase; 22 ± 4 nm)			Negative	
		Anatase (< 25 nm)			Negative	
Caco-2	Conventional alkaline comet	Anatase (< 25 nm)	1 and 2.5 µg/cm ²	2 h, 4 h, 6 h and 24 h	Positive for 1 µg/cm ² at 4 h exposure	[78]
					Positive for 1 µg/cm ² at 4 h exposure and 2.5 µg/cm ² at 2 h exposure	
					Positive for 1 µg/cm ² at 2 h and 24 h exposure	
					Negative	
Caco-2	FPG-modified comet		1–20 µg/cm ²	6 h and 24 h	Negative	
					EndoIII-modified comet	
					CBMN	

Caco-2	Conventional alkaline comet	P25 (86% Anatase/14% rutile; 24 ± 6 nm) A12 (95% Anatase/5% rutile; 12 ± 3 nm) E171 (> 95% Anatase; 118 ± 53 nm)	10 and 50 µg/mL	6 h, 24 h and 48 h or chronic exposure for 21 days (three times a week for 3 weeks)	Negative	[82]
	FPG-modified comet				Positive for both concentrations of E171 at 21-day exposure Negative	
Co-culture Caco-2/ HT29-MTX	Conventional alkaline comet				Positive for the 50 µg/mL concentration of E171 at 21-day exposure	[131]
	FPG-modified comet				Negative	
HT29	Conventional alkaline comet	Anatase/rutile (27.38 ± 5.90 nm)	2–10 µg/mL	24 h	Negative	[131]
	FPG-modified comet				Positive for the 8 and 10 µg/mL concentrations	
Caco-2 differentiated monolayer	Conventional alkaline and FPG-modified comet	NM103 (rutile hydrophobic; 25 NM)	0–256 µg/mL	24 h	Negative	[88]
	CBMN	NM-104 (rutile hydrophilic; 25 nm)				
		NM-100 (104.01 ± 39.49 nm)				
Caco-2 differentiated monolayer	Conventional alkaline comet	NIM-105 (86% Anatase/14% rutile; 24 ± 6 nm) A12 (95% Anatase/5% rutile; 12 ± 3 nm) E171 (> 95% Anatase; 118 ± 53 nm)	10, 25 and 100 µg/mL	24 h	Positive for the 10 µg/mL concentration	[139]
	FPG-modified comet		50 µg/mL	24 h	Negative	
Co-culture Caco-2/ HT29-MTX	Conventional alkaline and FPG-modified comet				Negative	[83]

DNA damage concerning Caco-2 cells exposed to 1 and 2.5 $\mu\text{g}/\text{cm}^2$ of anatase TiO_2 (< 25 nm) with the conventional comet assay and its combination with the FPG and EndoIII enzymes. Despite experiments with four different exposure hours – 2, 4, 6 and 24 h - most of the genotoxicity outcomes were obtained at shorter exposure times and only one positive result was verified at the time of 24 h. In this sense, the author suggests that after 24 h of exposure to TiO_2 , Caco-2 cells can repair the DNA and oxidative lesions [78]. Consequently, the time of exposure can interfere tremendously with the final genotoxic result.

In a monolayer of differentiated Caco-2 cells model, Vila et al. [139] did not observe the induction of oxidative damage through the FPG version of the comet assay upon treatment with 10, 25 and 100 $\mu\text{g}/\text{mL}$ of JRC NM-100 (104.01 \pm 39.49 nm) for 24 h. Nonetheless, exposure to 10 $\mu\text{g}/\text{mL}$ showed a slight genotoxicity DNA damage (increased DNA strand break level) through the conventional alkaline comet assay. This can be explained as the higher the concentration of TiO_2 , the greater their tendency to form aggregates in the cell culture medium. Then, TiO_2 may remain attached to the extracellular membrane of Caco-2 cells, not being able to be internalized and to have contact with the cell nucleus, preventing the possibility of causing DNA damage at higher concentrations [140]. Likewise, Jalili et al. [88] reported no significant increase in DNA damage in a Caco-2 differentiated monolayer following a 24 h exposure to higher concentrations (0–256 $\mu\text{g}/\text{mL}$) of JRC benchmark NM-103 (rutile hydrophobic; 25 nm) and NM-104 (rutile hydrophilic; 25 nm), using the conventional and FPG-modified comet assays.

Regarding the CBMN assay, the majority of the reports show no genotoxic effects after exposure to TiO_2 . No significant chromosome damage effects were observed in Caco-2 cells after 52 h of treatment to 0–256 $\mu\text{g}/\text{mL}$ NM-102, NM-103, NM-104 and NM-105 (all obtained from JRC), assessed by the CBMN assay [138]. Following a 6 and 24 h exposure to 1–20 $\mu\text{g}/\text{cm}^2$ of anatase TiO_2 (< 25 nm), no increase in the fre-

quency of micronucleated cells was detected in Caco-2 cells [78]. Furthermore, Jalili et al. [88] observed also no clastogenic or aneugenic effects, evaluated through the CBMN assay, following a 24 h exposure to NM-103 (rutile hydrophobic; 25 nm) and NM-104 (rutile hydrophilic; 25 nm) (0–256 $\mu\text{g}/\text{mL}$) considering a Caco-2 differentiated monolayer. It is therefore possible to conclude that all mentioned studies did not report an increase in the frequency of micronuclei in Caco-2 cells following exposure to nano-sized TiO_2 . Nevertheless, there are still few studies related to this assay performed with intestinal epithelial cell lines, namely Caco-2, that allow definitive conclusions to be drawn regarding the capacity of TiO_2 to induce chromosomal damage in the GIT. More experimental tests should then be performed in order to predict the behavior of these NMs in the GIT and to be able to draw a safe conclusion about their possible DNA or chromosomal damage ability in intestinal cells.

As with cytotoxicity assays, no studies on genotoxicity in HT29-MTX cells were found in the literature, but only in its non-mucus-producing phenotype (HT29 colorectal adenocarcinoma cells). Nevertheless, only one study was found regarding genotoxicity assessment (more specifically, the conventional and FPG-modified comet assay) in HT29 cells. This may be due to the fact that the Caco-2 cell line is currently the most applied *in vitro* model of the intestinal barrier for toxicological studies, since it resembles the most common type of cells in the small intestine, namely the absorptive enterocytes. After 24 h exposure of HT29 cells to an anatase/rutile mixture of TiO_2 (27.38 \pm 5.90 nm) (2–10 $\mu\text{g}/\text{mL}$), no significant increase in the DNA strand break level was observed evaluated by the conventional comet assay; conversely, an increase of the oxidative damage level was reported upon treatment with the 8 and 10 $\mu\text{g}/\text{mL}$ concentrations. [131].

As already mentioned, the presence of a co-culture model comprising Caco-2 and HT29-MTX cells enable to better mimic the structure and physiological properties of the intestinal bar-

rier. This allows it to be a more reliable and reproducible *in vitro* model in toxicological assessment studies as it is closer to the physiological condition of the human intestine. A co-culture of Caco-2 and HT29-MTX cells was exposed for 6 h, 24 h and 48 h or chronically for 21 days (three times a week for 3 weeks) to three different types of TiO₂ (P25, A12 and E171) in two different concentrations – 10 and 50 µg/mL [82]. The conventional and FPG-modified comet assays were used and showed that only the highest concentration of E171 (50 µg/mL), induced a significant increase in oxidative purine lesions and alkali-labile sites, but not the DNA strand break level, following a chronic exposure [82]. Using the same assay and the same benchmark NMs at a concentration of 50 µg/mL, no DNA damage was detected in a co-culture of Caco-2 and HT29-MTX cells following only 24 h of exposure [83].

Through the mouse lymphoma gene mutation assay and using L5178Y cells, no increase of the mutation frequency was verified after 4 h and 24 h exposure to 40 nm TiO₂ (0.0312–2 µg/mL) [141]. On the contrary, a linear increase in the mutation frequency was observed in WIL2-NS cells following incubation with 0, 25, 65 and 130 g/mL TiO₂ (< 100 nm) for 6, 24 and 48 h, using the hypoxanthine-guanine phosphoribosyl-transferase (HPRT) gene mutation assay [142].

As can be seen, inconsistent results are found in the literature concerning the *in vitro* genotoxicity assessment of TiO₂. The conflicting results can be explained by the different crystalline phase, size, exposure time and concentration used in each genotoxicity assay. Besides that, the different methods applied, the NMs dispersion procedure or even the exposure units referred to in reports (µg/mL or µg/cm²) might influence critically the toxicological outcome. Due to the lack of harmonization in these procedures, a more detailed and in-depth investigation is needed in order to infer whether the ingested TiO₂ are genotoxic. No reports were found regarding the genotoxicity testing of nanosized TiO₂ following *in vitro* simulated digestion, that could provide an advancement for a more realistic approach.

10.6.4 Genotoxicity of Ingested TiO₂ *In Vivo*

Although *in vivo* tests should be avoided, *in vitro* genotoxicity positive outcomes require confirmation by an appropriate follow-up *in vivo*. This is needed since this type of tests offers a more realistic approach, thus allowing a better prediction of biological responses of organisms to test agents like TiO₂, in spite of species-specific differences already mentioned. Table 10.4 summarizes the reports found in the literature regarding the *in vivo* genotoxic effects of ingested TiO₂.

Mice treated orally with TiO₂ (anatase, 20–50 nm), for 14 days in a range of concentrations of 10–100 mg/kg bw, led to a statistically significant dose-dependent increase in the % of DNA in tail in the liver cells, evaluated through the comet assay. In the same study, using the CBMN assay, an increase of micronuclei frequency in bone marrow cells was observed only after treatment with the highest concentration – 100 mg/kg bw [145]. Conversely, the exposure of rats by oral gavage during 45 days to 0.5 mg/kg/day TiO₂ (41.99 ± 1.63 nm) did not show DNA damage in blood or liver cells [148]. The exposure to 500 mg/kg bw of P25 (75% anatase/25% rutile; 21 nm) for 5 days, led to an increase in the frequency of micronucleated binucleated cells in peripheral blood cells of mice [92]. Furthermore, Manivannan et al. [149] reported genotoxic and clastogenic effects in multiple organs of Swiss albino male mice treated orally with sub-acute concentrations (0.2, 0.4 and 0.8 mg/kg bw) of rutile TiO₂ (25 nm) over a period of 28 days. Long-term exposure to low concentrations of rutile TiO₂ induced DNA damage in organs such as liver, spleen, and thymus. Chromosomal aberration test in bone marrow cells revealed the clastogenicity of TiO₂ at sub-chronic low concentrations [149]. In fact, Wang et al. [54, 142] already had verified that TiO₂ accumulate in the liver of rats after 2 weeks of oral exposure to a dose of 5 g/kg bw. This suggests that after ingested and internalized by the GIT, TiO₂ might be transported to other tissues and organs, being the liver a possible target organ for the digested TiO₂. This idea is reinforced by Heringa et al.

Table 10.4 *In vivo* genotoxicity reports regarding exposure of animal models to oral/ingested TiO₂

Animal Model	Assay Used	Tested TiO ₂	Dose	Duration of Exposure	Result (Positive/Negative)	Reference
Wistar rats	Comet	E 171 (118 nm), Anatase (20–340 nm) and NM-105 (15–24 nm)	10 mg/kg bw/day	7 days	Negative in Peyer's patch cells	[45]
Zucker (obese) rats	Comet	E171	50 or 500 mg/kg/week	10 weeks	Negative liver, lung	[87]
Rats	Comet Karyological assay (micronuclei, nuclear protrusions, etc.)	Anatase, TDM (160 nm) and TDN (33 nm)	40, 200 and 1000 mg/kg bw per day	7 days	TDM induced DNA-damage and micronuclei in bone-marrow cells and TDN induced DNA-damage in the cells of bone marrow and liver brain, liver and bone marrow	[136]
Mice	Comet	Anatase (117 nm and 17 nm)	10, 50, 250 µg/mouse	3 days after treatment	Positive in blood leucocytes	[143]
Mice	Comet	Anatase (10–25 nm)	500, 1000, 2000 mg/kg bw per day	7 days	Positive liver and kidney	([80]; [81])
Rat	Comet Micronucleus	Anatase (5–12 nm)	50, 100, 200 mg/kg bw per day	60 days	Positive in leucocytes Positive in rat bone marrow at 100 and 200 mg/kg bw	[144]
Mice	Comet Micronucleus	Anatase (20–50 nm)	10–100 mg/kg bw	14 days	Positive in liver cells (dose-dependent increase in the % of DNA in tail) Positive in bone marrow cells for the 100 mg/kg bw concentration	[145]
Mice	Micronucleus	P25 (75% Anatase/25% rutile; 21 nm)	500 mg/kg bw	5 days	Positive in peripheral blood cells	[92]
Mice	Comet Micronucleus and chromosomal aberration	TiO ₂ (58 nm)	200 and 500 mg/kg per bw	90 days	Positive in liver and kidney Positive in bone marrow	[146]
Rats	Micronucleus	Anatase (75 nm)	10–200 mg/kg per bw	30 days	Negative in bone marrow	[147]
Wistar rats	Comet	TEM size: 41.99 ± 1.63 nm; hydrodynamic diameter: 447.67 ± 6.43 nm	0.5 mg/kg/day	45 days	Negative in blood and liver cells	[148]
Swiss albino male mice	Comet Chromosomal aberration	Rutile (25 nm)	0.2, 0.4 and 0.8 mg/kg bw	28 days	Positive in liver, spleen and thymus cells Positive for bone marrow cells	[149]

[38] work, where both Ti and TiO₂ were found in the human liver and the spleen analyzed *post-mortem* and, wherein at least 24% of the particles found ($\geq 24\%$) were nanometric (< 100 nm), as already mentioned in this chapter.

Biopersistence of TiO₂ in gut cells can possibly induce damage associated to cancer events. We take the example of Urrutia-Ortega et al. [107] and Bettini et al. [45] works, where the exposure to E171 induced tumor formation in the distal colon, as well as preneoplastic lesions and growth of aberrant crypt foci in rats [45, 107]. In spite Bettini reports were not replicated in subsequent studies Blevins et al. [150], the uncertainty of the consequences of the genotoxicity observed in most studies raise major concerns. The recent report by EFSA clearly states that, on balance TiO₂ have the potential to induce chromosomal and DNA damage, and considering the fact that “genotoxicity concern could not be ruled out”, the Panel concluded that “E171 can no longer be considered as safe when used as a food additive” [28]. Furthermore, it is evident that physicochemical properties of NMs might influence the cytotoxic and genotoxic outcome, and other uses of TiO₂ aside from E171, should be reconsidered. These observations show that it is essential to continue studying the possible genotoxic and cytotoxic effects, in order to verify if their oral consumption/intake is safe for human health.

10.7 Final Remarks/Perspectives

In this chapter, we showed the extensive work that has been reported worldwide for assessing the cellular and molecular mechanisms of toxicity of TiO₂, with the purpose of assuring its safety for use in promising applications. In spite many of these applications rely on food and feed products, the risk analysis often disregards the impact of the ingestion process in the TiO₂ toxicological outcomes. To this regard, knowledge gaps have been identified, concerning: (i) the modifications of the TiO₂ throughout the GIT, upon interaction with digestion fluids; (ii) how these modifications can facilitate/block the systemic absorption of the TiO₂; (iii) conclusive evidence of key

molecular events that may lead to adverse outcomes; (iv) adverse outcomes such as genotoxicity and cancer, that can be most relevant after long term exposure to low doses.

In this context, the application of an *in vitro* digestion process for TiO₂ can be considered a valuable tool. This is an innovative approach and currently there are no reports in literature related to the genotoxic potential of digested TiO₂ in intestinal cells. To better integrate the modifications that NMs suffer in the organism, the addition of a simulated digestion process in the safety evaluation of ingested NMs used *in vitro* bioassays can provide a significant improvement on existing approaches [59], that may decrease uncertainties in the hazard assessment of ingested NMs. The added value of *in vitro* simulated GIT models has been highlighted in EFSA nanoguidance [25], but this outlook also emphasizes the need for a comprehensive *in vitro-in vivo* integrated approach associated to the use of documented dispersion protocols, concomitantly with a comprehensive physicochemical characterization of the test material in each case. Furthermore, the use of advanced multidimensional cellular models, such as co-cultures and 3D-cell cultures, with the inclusion of a multitude of individual factors that approximates *in vivo* conditions [60], as well as molecular screening and epigenetic endpoints, may provide additional information and a relevant alternative to animal experiments, at an early stage of safety assessment of NMs and in product development of NMs intended for human ingestion. By providing a screening tool for industry, a safe-by-design approach to the development of innovative NMs is foreseen in the near future.

Acknowledgements This work was funded by national funds through the FCT - Foundation for Science and Technology, I.P., under the project INGESTnano- PTDC/SAU-PUB/29481/2017. Research co-funded by European Union Seventh Framework Programme (FP7/2007e2013) under the project NANoREG (A common European approach to the regulatory testing of nanomaterials), grant agreement 310584 and by UIDB/00009/2020; UIDP/00009/2020 (Centre for Toxicogenomics and Human Health – ToxOmics, Foundation for Science and Technology). NV holds a FCT PhD Scholarship grant (2020.07168.BD).

The authors thank all the support from the colleagues Paula Alvito, Carla Martins and Ricardo Assunção (Food Safety Department, INSA, Lisbon, Portugal) and from Ana F. Bettencourt and Lídia Gonçalves (FarmID, Lisbon University, Portugal), as well from all INGESTnano team members.

References

- Louro H, Borges T, Silva MJ (2013) Nanomateriais manufacturados: novos desafios para a saúde pública. *Rev Portuguesa de Saude Pub* 31. <https://doi.org/10.1016/j.rpsp.2012.12.004>
- He X, Deng H, Hwang H, min. (2019) The current application of nanotechnology in food and agriculture. *J Food Drug Anal* 27(1):1–21. <https://doi.org/10.1016/j.jfda.2018.12.002>
- Peters RJB, Bouwmeester H, Gottardo S, Amenta V, Arena M, Brandhoff P et al (2016) Nanomaterials for products and application in agriculture, feed and food. *Trends Food Sci Technol* 54:155–164. <https://doi.org/10.1016/j.tifs.2016.06.008>
- Chaudhry Q, Scotter M, Blackburn J, Ross B, Boxall A, Castle L et al (2008) Applications and implications of nanotechnologies for the food sector. *Food Addit Contaminants* 25(3):241–258. <https://doi.org/10.1080/02652030701744538>
- Weir A, Westerhoff P, Fabricius L, Hristovski K, Von Goetz N (2012) Titanium dioxide nanoparticles in food and personal care products. *Environ Sci Technol* 46(4):2242–2250. <https://doi.org/10.1021/es204168d>
- Winkler HC, Notter T, Meyer U, Naegeli H (2018) Critical review of the safety assessment of titanium dioxide additives in food. *J Nanobiotechnol* 16. <https://doi.org/10.1186/s12951-018-0376-8>
- Athinarayanan J, Periasamy VS, Alsaif MA, Al-Warthan AA, Alshatwi AA (2014) Presence of nanosilica (E551) in commercial food products: TNF-mediated oxidative stress and altered cell cycle progression in human lung fibroblast cells. *Cell Biol Toxicol* 30(2):89–100. <https://doi.org/10.1007/s10565-014-9271-8>
- Jampilek J, Kos J, Kralova K (2019) Potential of nanomaterial applications in dietary supplements and foods for special medical purposes. *Nano* 9(2). <https://doi.org/10.3390/nano9020296>
- Cao Y (2017) Toxicity of ingested nanomaterials. In: A. A. Press (ed) *Food toxicology current advances and future challenges*, pp 348–355. <https://doi.org/10.1201/b13390-38>
- Xun W, Shi L, Yue W, Zhang C, Ren Y, Liu Q (2012) Effect of high-dose nano-selenium and selenium-yeast on feed digestibility, rumen fermentation, and purine derivatives in sheep. *Biol Trace Elem Res* 150:130–136. <https://doi.org/10.1007/s12011-012-9452-3>
- Fondevila M, Herrer R, Casallas MC, Abecia L, Duchá JJ (2009) Silver nanoparticles as a potential antimicrobial additive for weaned pigs. *Anim Feed Sci Technol* 150(3–4):259–269. <https://doi.org/10.1016/j.anifeedsci.2008.09.003>
- Gholami-Ahangaran M, Zia-Jahromi N (2013) Nanosilver effects on growth parameters in experimental aflatoxicosis in broiler chickens. *Toxicol Ind Health* 29(2):121–125. <https://doi.org/10.1177/0748233711425078>
- Pineda L, Chwalibog A, Sawosz E, Lauridsen C, Engberg R, Elnif J et al (2012) Effect of silver nanoparticles on growth performance, metabolism and microbial profile of broiler chickens. *Arch Anim Nutr* 66(5):416–429. <https://doi.org/10.1080/1745039X.2012.710081>
- Khin MM, Nair AS, Babu VJ, Murugan R, Ramakrishna S (2012) A review on nanomaterials for environmental remediation. *Energy Environ Sci* 5(8):8075–8109. <https://doi.org/10.1039/c2ee21818f>
- Amenta V, Aschberger K, Arena M, Bouwmeester H, Botelho Moniz F, Brandhoff P et al (2015) Regulatory aspects of nanotechnology in the Agri/feed/food sector in EU and non-EU countries. *Regul Toxicol Pharmacol* 73(1):463–476. <https://doi.org/10.1016/j.yrtph.2015.06.016>
- Peters R, Kramer E, Oomen AG, Herrera Rivera ZE, Oegema G, Tromp PC et al (2012) Presence of nano-sized silica during in vitro digestion of foods containing silica as a food additive. *ACS Nano* 6(3):2441–2451. <https://doi.org/10.1021/nn204728k>
- European Commission (2011) Commission Regulation (EU) No 10/2011 of 14 January 2011 on plastic materials and articles intended to come into contact with food. *Official Journal of the European Union*
- Dizaj SM, Lotfipour F, Barzegar-Jalali M, Zarrintan MH, Adibkia K (2014) Antimicrobial activity of the metals and metal oxide nanoparticles. *Mater Sci Eng C* 44:278–284. <https://doi.org/10.1016/j.msec.2014.08.031>
- Li W, Li X, Zhang P, Xing Y (2011) Development of nano-ZnO coated food packaging film and its inhibitory effect on *Escherichia coli* in vitro and in actual tests. *Adv Mater Res* 152–153:489–492. <https://doi.org/10.4028/www.scientific.net/AMR.152-153.489>
- Honarvar Z, Hadian Z, Mashayekh M (2016) Nanocomposites in food packaging applications and their risk assessment for health. *Electron Physician* 8(6):2531–2538. <https://doi.org/10.19082/5212>
- Cubadda F (2019) Chapter 4: Exposure to substances via food consumption: nanoparticles in food. In: Heinemeyer G, Jantunen M, Hakkinen P (eds) *The practice of consumer exposure assessment*. Springer, pp 323–359
- Sahoo D, Mandal A, Mitra T, Chakraborty K, Bardhan M, Dasgupta AK (2018) Nanosensing of pesticides by zinc oxide quantum dot: an optical and

- electrochemical approach for the detection of pesticides in water. *J Agric Food Chem* 66(2):414–423. <https://doi.org/10.1021/acs.jafc.7b04188>
23. Sun Y, Fang L, Wan Y, Gu Z (2018) Pathogenic detection and phenotype using magnetic nanoparticle-urease nanosensor. *Sensors Actuators B Chem* 259:428–432. <https://doi.org/10.1016/j.snb.2017.12.095>
 24. Zhang W, Han Y, Chen X, Luo X, Wang J, Yue T, Li Z (2017) Surface molecularly imprinted polymer capped Mn-doped ZnS quantum dots as a phosphorescent nanosensor for detecting patulin in apple juice. *Food Chem* 232:145–154. <https://doi.org/10.1016/j.foodchem.2017.03.156>
 25. EFSA Scientific Committee, Hardy A, Benford D, Halldorsson T, Jeger MJ, Knutsen HK, More S, Naegeli H, Noteborn H, Ockleford C, Ricci A, Rychen G, Schlatter JR, Silano V, Solecki R, Turck D, Younes M, Chaudhry Q, Cubadda F, Gott D, Oomen A, Weigel S, Karamitrou M, Schoonjans R, Mortensen A (2018) Guidance on risk assessment of the application of nanoscience and nanotechnologies in the food and feed chain: part 1, human and animal health. *EFSA J* 16(7):5327. <https://doi.org/10.2903/j.efsa.2018.5327>
 26. European Commission (2012) Commission Regulation (EU) No 231/2012 of 9 March 2012 laying down specifications for food additives listed in Annexes II and III to Regulation (EC) No 1333/2008 of the European Parliament and of the Council. *Official Journal of the European Union* (vol. 83). <https://doi.org/10.1201/9781315152752>
 27. Proquin H, Rodríguez-Ibarra C, Moonen CGJ, Urrutia Ortega IM, Briedé JJ, de Kok TM et al (2016) Titanium dioxide food additive (E171) induces ROS formation and genotoxicity: contribution of micro and nano-sized fractions. *Mutagenesis* 32(1):139–149. <https://doi.org/10.1093/mutage/gew051>
 28. EFSA Panel on Food Additives and Flavourings, Younes M, Aquilina G, Castle L, Engel K-H, Fowler P, Frutos Fernandez MJ, Furst P, Gundert-Remy U, Gurtler R, Husøy T, Manco M, Mennes W, Moldeus P, Passamonti S, Shah R, Waalkens-Berendsen I, Wolffe D, Corsini E, Cubadda F, De Groot D, FitzGerald R, Gunnare S, Gutleb AC, Mast J, Mortensen A, Oomen A, Piersma A, Plichta V, Ulbrich B, Van Loveren H, Benford D, Bignami M, Bolognesi C, Crebelli R, Dusinska M, Marcon F, Nielsen E, Schlatter J, Vleminckx C, Barmaz S, Carfi M, Civitella C, Giarola A, Rincon AM, Serafimova R, Smeraldi C, Tarazona J, Tard A, Wright M (2021) Scientific opinion on the safety assessment of titanium dioxide (E171) as a food additive. *EFSA J* 19(5):6585. <https://doi.org/10.2903/j.efsa.2021.6585>
 29. Verleysen E, Waegeneers N, Brassinne F, De Vos S, Jimenez IO, Mathioudaki S, Mast J (2020) Physicochemical characterization of the pristine E171 food additive by standardized and validated methods. *Nano* 10(3):592. <https://doi.org/10.3390/nano10030592>
 30. DeLoid GM, Cohen JM, Pyrgiotakis G, Demokritou P (2017a) An integrated dispersion preparation, characterization and in vitro dosimetry methodology for engineered nanomaterials. *Nat Protoc* 12(2):335–371. <https://doi.org/10.1038/nprot.2016.172>
 31. Shi H, Magaye R, Castranova V, Zhao J (2013) Titanium dioxide nanoparticles: a review of current toxicological data. *Part Fibre Toxicol* 10(15):1–33
 32. Martirosyan A, Schneider YJ (2014) Engineered nanomaterials in food: implications for food safety and consumer health. *Int J Environ Res Public Health* 11(6):5720–5750. <https://doi.org/10.3390/ijerph110605720>
 33. EFSA (2016) Re-evaluation of titanium dioxide (E 171) as a food additive. *EFSA J* 14(9):1–83. <https://doi.org/10.2903/j.efsa.2016.4545>
 34. Rempelberg C, Heringa MB, van Donkersgoed G, Drijvers J, Roos A, Westenbrink S et al (2016) Oral intake of added titanium dioxide and its nanofraction from food products, food supplements and toothpaste by the Dutch population. *Nanotoxicology* 10(10):1404–1414. <https://doi.org/10.1080/17435390.2016.1222457>
 35. Sprong C, Bakker M, Niekerk M, Vennemann F (2015) Exposure assessment of the food additive titanium dioxide (E 171) based on use levels provided by the industry. National Institute for Public Health and the Environment, Bilthoven
 36. Pele LC, Thoree V, Bruggraber SFA, Koller D, Thompson RPH, Lomer MC, Powell JJ (2015) Pharmaceutical/food grade titanium dioxide particles are absorbed into the bloodstream of human volunteers. *Part Fibre Toxicol* 12(1):1–6. <https://doi.org/10.1186/s12989-015-0101-9>
 37. Böckmann J, Lahl H, Eckert T, Unterhalt B (2000) Blood titanium levels before and after oral administration titanium dioxide. *Pharmazie* 55(2):140–143
 38. Heringa MB, Peters RJB, Bleys RLAW, van der Lee MK, Tromp PC, van Kesteren PCE et al (2018) Detection of titanium particles in human liver and spleen and possible health implications. *Part Fibre Toxicol* 15(1):15. <https://doi.org/10.1186/s12989-018-0251-7>
 39. Bettini S, Houdeau E (2014) Exposition orale aux nanoparticules de dioxyde de titane (TiO₂): du franchissement de l'épithélium buccal et intestinal au devenir et aux effets dans l'organisme. *Biol Aujourd'hui* 208(2):167–175. <https://doi.org/10.1051/jbio/20140022>
 40. Skocaj M, Filipic M, Petkovic J, Novak S (2011) Titanium dioxide in our everyday life; is it safe? *Radiol Oncol* 45(4):227–247. <https://doi.org/10.2478/v10019-011-0037-0>
 41. Talamini L, Gimondi S, Violatto MB, Fiordaliso F, Pedica F, Tran NL, Sitia G, Aureli F, Raggi A, Nelissen I, Cubadda F, Bigini P, Diomedea L (2019) Repeated administration of the food additive E171 to mice results in accumulation in intestine and liver and promotes an inflammatory status.

- Nanotoxicology 13(8):1087–1101. <https://doi.org/10.1080/17435390.2019.1640910>
42. Lyon F (2010) IARC monographs on the evaluation of carcinogenic risks to humans VOLUME 93 carbon black, titanium dioxide, and talc
 43. Bernauer U, Chaudhry Q, Dusinska M, Liliensblum W, Platzeck T, van Benthem J et al (2015) Opinion of the Scientific Committee on Consumer safety (SCCS) - revision of the opinion on the safety of the use of titanium dioxide, nano form, in cosmetic products. *Regul Toxicol Pharmacol* 73. <https://doi.org/10.1016/j.yrtph.2015.09.005>
 44. ANSES (2019) AVIS de l'Agence nationale de sécurité sanitaire de l'alimentation, de l'environnement et du travail relatif aux risques liés à l'ingestion de l'additif alimentaire E171, Maisons-Alfort
 45. Bettini S, Boutet-Robinet E, Cartier C, Coméra C, Gaultier E, Dupuy J et al (2017) Food-grade TiO₂ impairs intestinal and systemic immune homeostasis, initiates preneoplastic lesions and promotes aberrant crypt development in the rat colon. *Sci Rep* 7. <https://doi.org/10.1038/srep40373>
 46. Louro H (2018) Relevance of physicochemical characterization of nanomaterials for understanding nano-cellular interactions. *Adv Exp Med Biol* 1048. https://doi.org/10.1007/978-3-319-72041-8_8
 47. Louro H, Saruga A, Santos J, Pinhão M, Silva MJ (2019) Biological impact of metal nanomaterials in relation to their physicochemical characteristics. *Toxicol In Vitro* 56. <https://doi.org/10.1016/J.TIV.2019.01.018>
 48. Yusoff R, Kathawala MH, Nguyen LTH, Setyawati MI, Chiew P, Wu Y et al (2018) Biomolecular interaction and kinematics differences between P25 and E171 TiO₂ nanoparticles. *NanoImpact* 12(August):51–57. <https://doi.org/10.1016/j.impact.2018.10.001>
 49. Zhang Z, Zhang R, Xiao H, Bhattacharya K, Bitounis D, Demokritou P, McClements DJ (2019) Development of a standardized food model for studying the impact of food matrix effects on the gastrointestinal fate and toxicity of ingested nanomaterials. *NanoImpact* 13–25. <https://doi.org/10.1016/j.impact.2018.11.002>
 50. DeLoid GM, Wang Y, Kapronezai K, Lorente LR, Zhang R, Pyrgiotakis G et al (2017b) An integrated methodology for assessing the impact of food matrix and gastrointestinal effects on the biokinetics and cellular toxicity of ingested engineered nanomaterials. *Part Fibre Toxicol* 14. <https://doi.org/10.1186/s12989-017-0221-5>
 51. Avramescu M-L, Rasmussen PE, Chénier M, Gardner HD (2017) Influence of pH, particle size and crystal form on dissolution behaviour of engineered nanomaterials. *Environ Sci Pollut Res* 24:1553–1564. <https://doi.org/10.1007/s11356-016-7932-2>
 52. Kreyling WG, Holzwarth U, Schleh C, Kozempel J, Wenk A, Haberl N et al (2017) Quantitative biokinetics of titanium dioxide nanoparticles after oral application in rats: part 2. *Nanotoxicology* 11. <https://doi.org/10.1080/17435390.2017.1306893>
 53. MacNicol A, Kelly M, Aksoy H, Kramer E, Bouwmeester H, Chaudhry Q (2015) A study of the uptake and biodistribution of nano-titanium dioxide using in vitro and in vivo models of oral intake. *J Nanopart Res* 17(2):1–20. <https://doi.org/10.1007/s11051-015-2862-3>
 54. Wang J, Zhou G, Chen C, Yu H, Wang T, Ma Y et al (2007b) Acute toxicity and biodistribution of different sized titanium dioxide particles in mice after oral administration. *Toxicol Lett* 168(2):176–185. <https://doi.org/10.1016/j.toxlet.2006.12.001>
 55. Sohal IS, Cho YK, O'Fallon KS, Gaines P, Demokritou P, Bello D (2018a) Dissolution behavior and biodegradability of ingested engineered nanomaterials in the gastrointestinal environment. *ACS Nano* 12(8):8115–8128. <https://doi.org/10.1021/acsnano.8b02978>
 56. Tan Y, Li R, Liu C, Muriel Mundo J, Zhou H, Liu J, McClements DJ (2020) Chitosan reduces vitamin D bioaccessibility in food emulsions by binding to mixed micelles. In: *Food and function*, vol 11. Royal Society of Chemistry, pp 187–199. <https://doi.org/10.1039/c9fo02164g>
 57. Brodkorb A, Egger L, Alminger M, Alvito P, Assunção R, Ballance S et al (2019) INFOGEST static in vitro simulation of gastrointestinal food digestion. *Nat Protoc* 14. <https://doi.org/10.1038/s41596-018-0119-1>
 58. Minekus M, Alminger M, Alvito P, Ballance S, Bohn T, Bourlieu C et al (2014) A standardised static in vitro digestion method suitable for food-an international consensus. *Food Function* 5:1113–1124. <https://doi.org/10.1039/c3fo60702j>
 59. Bettencourt A, Gonçalves LM, Gramacho AC, Vieira A, Rolo D, Martins C et al (2020) Analysis of the characteristics and cytotoxicity of titanium dioxide nanomaterials following simulated in vitro digestion. *Nano* 10(8):1516. <https://doi.org/10.3390/nano10081516>
 60. Kämpfer AAM, Busch M, Schins RPF (2020) Advanced in vitro testing strategies and models of the intestine for Nanosafety research. *Chem Res Toxicol* 33. <https://doi.org/10.1021/acs.chemrestox.0c00079>
 61. Abbasi-Oshaghi E, Mirzaei F, Pourjafar M (2019) NLRP3 inflammasome, oxidative stress, and apoptosis induced in the intestine and liver of rats treated with titanium dioxide nanoparticles: in vivo and in vitro study. *Int J Nanomedicine* 14:1919–1936. <https://doi.org/10.2147/IJN.S192382>
 62. Faust JJ, Doudrick K, Yang Y, Westerhoff P, Capco DG (2014) Food grade titanium dioxide disrupts intestinal brush border microvilli in vitro independent of sedimentation. *Cell Biol Toxicol* 30(3):169–188. <https://doi.org/10.1007/s10565-014-9278-1>
 63. Guo Z, Martucci NJ, Moreno-Olivas F, Tako E, Mahler GJ (2017) Titanium dioxide nanoparticle ingestion alters nutrient absorption in an in vitro

- model of the small intestine. *NanoImpact* 5:70–82. <https://doi.org/10.1016/j.impact.2017.01.002>
64. Koeneman BA, Zhang Y, Westerhoff P, Chen Y, Crittenden JC, Capco DG (2010) Toxicity and cellular responses of intestinal cells exposed to titanium dioxide. *Cell Biol Toxicol* 26(3):225–238. <https://doi.org/10.1007/s10565-009-9132-z>
65. Richter JW, Shull GM, Fountain JH, Guo Z, Musselman LP, Fiumera AC, Mahler GJ (2018) Titanium dioxide nanoparticle exposure alters metabolic homeostasis in a cell culture model of the intestinal epithelium and *drosophila melanogaster*. *Nanotoxicology* 12(5):390–406. <https://doi.org/10.1080/17435390.2018.1457189>
66. Ammendolia MG, Iosi F, Maranghi F, Tassinari R, Cubadda F, Aureli F et al (2017) Short-term oral exposure to low doses of nano-sized TiO₂ and potential modulatory effects on intestinal cells. *Food Chem Toxicol* 102:63–75. <https://doi.org/10.1016/j.fct.2017.01.031>
67. Brun E, Barreau F, Veronesi G, Fayard B, Sorieul S, Chanéac C, ..., Carrière M (2014) Titanium dioxide nanoparticle impact and translocation through ex vivo, in vivo and in vitro gut epithelia
68. Pedata P, Ricci G, Malorni L, Venezia A, Cammarota M, Volpe MG et al (2019) In vitro intestinal epithelium responses to titanium dioxide nanoparticles. *Food Res Int* 119:634–642. <https://doi.org/10.1016/j.foodres.2018.10.041>
69. Gitrowski C, Al-Jubory AR, Handy RD (2014) Uptake of different crystal structures of TiO₂ nanoparticles by Caco-2 intestinal cells. *Toxicol Lett* 226(3):264–276. <https://doi.org/10.1016/j.toxlet.2014.02.014>
70. Dekkers S, Wijnhoven SWP, Braakhuis HM, Soeteman-Hernandez LG, Sips AJAM, Tavernaro I et al (2020) Safe-by-design part I: proposal for nano-specific human health safety aspects needed along the innovation process. *NanoImpact* 18(May):100227. <https://doi.org/10.1016/j.impact.2020.100227>
71. Li W, Jia MX, Deng J, Wang JH, Zuberi Z, Yang S et al (2020) MicroRNA response and toxicity of potential pathways in human colon cancer cells exposed to titanium dioxide nanoparticles. *Cancers* 12(5). <https://doi.org/10.3390/cancers12051236>
72. Magdolenova Z, Collins A, Kumar A, Dhawan A, Stone V, Dusinska M (2014) Mechanisms of genotoxicity. A review of in vitro and in vivo studies with engineered nanoparticles. *Nanotoxicology* 8(3):233–278. <https://doi.org/10.3109/17435390.2013.773464>
73. Iavicoli I, Leso V, Fontana L, Bergamaschi A (2011) Toxicological effects of titanium dioxide nanoparticles: A review of in vitro mammalian studies. *Eur Rev Med Pharmacol Sci* 15. <https://doi.org/10.1155/2012/964381>
74. Tada-Oikawa S, Ichihara G, Fukatsu H, Shimanuki Y, Tanaka N, Watanabe E et al (2016) Titanium dioxide particle type and concentration influence the inflammatory response in Caco-2 cells. *Int J Mol Sci* 17(4). <https://doi.org/10.3390/ijms17040576>
75. Gandamalla D, Lingabathula H, Yellu N (2019) Nano titanium exposure induces dose- and size-dependent cytotoxicity on human epithelial lung and colon cells. *Drug Chem Toxicol* 42(1):24–34. <https://doi.org/10.1080/01480545.2018.1452930>
76. Dorier M, Brun E, Veronesi G, Barreau F, Pernet-Gallay K, Desvergne C et al (2015) Impact of anatase and rutile titanium dioxide nanoparticles on uptake carriers and efflux pumps in Caco-2 gut epithelial cells. *Nanoscale* 7(16):7352–7360. <https://doi.org/10.1039/c5nr00505a>
77. De Angelis I, Barone F, Zijno A, Bizzarri L, Russo MT, Pozzi R et al (2013) Comparative study of ZnO and TiO₂ nanoparticles: physicochemical characterisation and toxicological effects on human colon carcinoma cells. *Nanotoxicology* 7(8):1361–1372. <https://doi.org/10.3109/17435390.2012.741724>
78. Zijno A, De Angelis I, De Berardis B, Andreoli C, Russo MT, Pietraforte D et al (2015) Different mechanisms are involved in oxidative DNA damage and genotoxicity induction by ZnO and TiO₂ nanoparticles in human colon carcinoma cells. *Toxicol In Vitro* 29(7):1503–1512. <https://doi.org/10.1016/j.tiv.2015.06.009>
79. Li N, Ma L, Wang J, Zheng L, Liu J, Duan Y et al (2009) Interaction between Nano-Anatase TiO₂ and liver DNA from mice in vivo. *Nanoscale Res Lett* 5(1):108–115. <https://doi.org/10.1007/s11671-009-9451-2>
80. Shi Z, Niu Y, Wang Q, Shi L, Guo H, Liu Y et al (2015a) Reduction of DNA damage induced by titanium dioxide nanoparticles through Nrf2 in vitro and in vivo. *J Hazard Mater* 298:310–319. <https://doi.org/10.1016/j.jhazmat.2015.05.043>
81. Shi Z, Niu Y, Wang Q, Shi L, Guo H, Liu Y, Zhu Y, Liu S, Liu C, Chen X, Zhang R (2015b) Reduction of DNA damage induced by titanium dioxide nanoparticles through Nrf2 in vitro and in vivo. *J Hazard Mater* 298:310–319. <https://doi.org/10.1016/j.jhazmat.2015.05.043>
82. Dorier M, Béal D, Marie-Desvergne C, Dubosson M, Barreau F, Houdeau E et al (2017) Continuous in vitro exposure of intestinal epithelial cells to E171 food additive causes oxidative stress, inducing oxidation of DNA bases but no endoplasmic reticulum stress. *Nanotoxicology* 11. <https://doi.org/10.1080/17435390.2017.1349203>
83. Dorier M, Tisseyre C, Dussert F, Béal D, Arnal ME, Douki T et al (2019) Toxicological impact of acute exposure to E171 food additive and TiO₂ nanoparticles on a co-culture of Caco-2 and HT29-MTX intestinal cells. *Mutat Res Genet Toxicol Environ Mutagenesis* 845(July 2018):402980. <https://doi.org/10.1016/j.mrgentox.2018.11.004>
84. Wang J, Li N, Zheng L, Wang S, Wang Y, Zhao X et al (2011) P38-Nrf-2 signaling pathway of oxidative stress in mice caused by nanoparticulate TiO₂.

- Biol Trace Elem Res 140(2):186–197. <https://doi.org/10.1007/s12011-010-8687-0>
85. Gerloff K, Albrecht C, Boots AW, Frster I, Schins RPF (2009) Cytotoxicity and oxidative DNA damage by nanoparticles in human intestinal Caco-2 cells. *Nanotoxicology* 3(4):355–364. <https://doi.org/10.3109/17435390903276933>
 86. Abbott Chalew TE, Schwab KJ (2013) Toxicity of commercially available engineered nanoparticles to Caco-2 and SW480 human intestinal epithelial cells. *Cell Biol Toxicol* 29(2):101–116. <https://doi.org/10.1007/s10565-013-9241-6>
 87. Jensen DM, Løhr M, Sheykhzade M, Lykkesfeldt J, Wils RS, Loft S, Møller P (2019) Telomere length and genotoxicity in the lung of rats following intra-gastric exposure to food-grade titanium dioxide and vegetable carbon particles. *Mutagenesis* 34(2):203–214. <https://doi.org/10.1093/mutage/gez003>
 88. Jalili P, Gueniche N, Lanceleur R, Burel A, Lavault M-T, Sieg H et al (2018) Investigation of the in vitro genotoxicity of two rutile TiO₂ nanomaterials in human intestinal and hepatic cells and evaluation of their interference with toxicity assays. *NanoImpact* 11:69–81. <https://doi.org/10.1016/J.IMPACT.2018.02.004>
 89. Song ZM, Chen N, Liu JH, Tang H, Deng X, Xi WS et al (2015) Biological effect of food additive titanium dioxide nanoparticles on intestine: an in vitro study. *J Appl Toxicol* 35(10):1169–1178. <https://doi.org/10.1002/jat.3171>
 90. Charles S, Jomini S, Fessard V, Bigorgne-Vizade E, Rousselle C, Michel C (2018) Assessment of the in vitro genotoxicity of TiO₂ nanoparticles in a regulatory context. *Nanotoxicology* 12(4):357–374. <https://doi.org/10.1080/17435390.2018.1451567>
 91. IPCS (2019) Principles and methods to assess the risk of immunotoxicity associated with exposure to nanomaterials. *Environmental Health Criteria*: n. 244. Geneva
 92. Trouiller B, Reliene R, Westbrook A, Solaimani P, Schiestl RH (2009) Titanium dioxide nanoparticles induce DNA damage and genetic instability in vivo in mice. *Cancer Res* 69(22):8784–8789. <https://doi.org/10.1158/0008-5472.CAN-09-2496>
 93. Chen Z, Han S, Zhou D, Zhou S, Jia G (2019) Effects of oral exposure to titanium dioxide nanoparticles on gut microbiota and gut-associated metabolism: in vivo. *Nanoscale* 11(46):22398–22412. <https://doi.org/10.1039/c9nr07580a>
 94. Hashem MM, Abo-EL-Sooud K, Abd-Elhakim YM, Badr YAH, El-Metwally AE, Bahy-El-Dien A (2020) The long-term oral exposure to titanium dioxide impaired immune functions and triggered cytotoxic and genotoxic impacts in rats. *J Trace Elem Med Biol* 60(February):126473. <https://doi.org/10.1016/j.jtemb.2020.126473>
 95. Dhupal M, Oh JM, Tripathy DR, Kim SK, Koh SB, Park KS (2018) Immunotoxicity of titanium dioxide nanoparticles via simultaneous induction of apoptosis and multiple toll-like receptors signaling through ROS-dependent SAPK/JNK and p38 MAPK activation. *Int J Nanomedicine* 13:6735–6750. <https://doi.org/10.2147/IJN.S176087>
 96. Cui Y, Liu H, Ze Y, Zhang Z, Hu Y, Cheng Z, Cheng J, Hu R, Gao G, Wang L, Tang M, Hong F (2015) Corrigendum: gene expression in liver injury caused by long-term exposure to titanium dioxide nanoparticles in mice. *Toxicol Sci* 146(1):202. <https://doi.org/10.1093/toxsci/kfv097>. Erratum for: *Toxicol Sci*. 2012 Jul;128(1):171–85. PMID: 26101236
 97. Hong F, Ji J, Ze X, Zhou Y, Ze Y (2020) Liver inflammation and fibrosis induced by long-term exposure to Nano titanium dioxide (TiO₂) nanoparticles in mice and its molecular mechanism. *J Biomed Nanotechnol* 16(5):616–625. <https://doi.org/10.1166/jbn.2020.2921>
 98. Kolling J, Tigges J, Hellack B, Albrecht C, Schins RPF (2020) Evaluation of the nlrp3 inflammasome activating effects of a large panel of tio2 nanomaterials in macrophages. *Nano* 10(9):1–18. <https://doi.org/10.3390/nano10091876>
 99. Smolkova B, El Yamani N, Collins AR, Gutleb AC, Dusinska M (2015) Nanoparticles in food. Epigenetic changes induced by nanomaterials and possible impact on health. *Food Chem Toxicol* 77:64–73. <https://doi.org/10.1016/j.fct.2014.12.015>
 100. Stoccoro A, Karlsson HL, Coppedè F, Migliore L (2013) Epigenetic effects of nano-sized materials. *Toxicology* 313. <https://doi.org/10.1016/j.tox.2012.12.002>
 101. Ghosh M, Öner D, Duca RC, Cokic SM, Seys S, Kerkhofs S et al (2017) Cyto-genotoxic and DNA methylation changes induced by different crystal phases of TiO₂-np in bronchial epithelial (16-HBE) cells. *Mutat Res* 796:1–12. <https://doi.org/10.1016/j.mrfmmm.2017.01.003>
 102. Dufeoi W, Moniz K, Allen-Vercoe E, Ropers MH, Walker VK (2017) Impact of food grade and nano-TiO₂ particles on a human intestinal community. *Food Chem Toxicol* 106(Pt A):242–249. <https://doi.org/10.1016/j.fct.2017.05.050>
 103. Radziwill-Bienkowska JM, Talbot P, Kamphuis JBJ, Robert V, Cartier C, Fourquaux I, Lentzen E, Audinot JN, Jamme F, Réfrégiers M, Bardowski JK, Langella P, Kowalczyk M, Houdeau E, Thomas M, Mercier-Bonin M (2018) Toxicity of food-grade TiO₂ to commensal intestinal and transient food-borne bacteria: new insights using Nano-SIMS and synchrotron UV fluorescence imaging. *Front Microbiol* 9:794. <https://doi.org/10.3389/fmicb.2018.00794>
 104. Pinget G, Tan J, Janac B, Kaakoush NO, Angelatos AS, O'Sullivan J et al (2019) Impact of the food additive titanium dioxide (e171) on gut microbiota-host interaction. *Frontiers. Nutrition* 6(May). <https://doi.org/10.3389/fnut.2019.00057>
 105. Zhang S, Jiang X, Cheng S, Fan J, Qin X, Wang T et al (2020) Titanium dioxide nanoparticles via oral exposure leads to adverse disturbance of gut microecology and locomotor activity in adult mice. *Arch*

- Toxicol 94(4):1173–1190. <https://doi.org/10.1007/s00204-020-02698-2>
106. Proquin H, Jetten MJ, Jonkhout MCM, Garduño-Balderas LG, Briedé JJ, de Kok TM, van Loveren H, Chirino YI (2018) Transcriptomics analysis reveals new insights in E171-induced molecular alterations in a mouse model of colon cancer. *Sci Rep* 8(1):9738. <https://doi.org/10.1038/s41598-018-28063-z>
107. Urrutia-Ortega IM, Garduño-Balderas LG, Delgado-Buenrostro NL, Freyre-Fonseca V, Flores-Flores JO, González-Robles A et al (2016) Food-grade titanium dioxide exposure exacerbates tumor formation in colitis associated cancer model. *Food Chem Toxicol* 93:20–31. <https://doi.org/10.1016/j.fct.2016.04.014>
108. OECD (2016) Users' handbook supplement to the guidance document for developing and assessing adverse outcome pathways. ENV/JM/MONO(2016)12. Paris. <https://doi.org/10.1787/5f1m9d1g32-en>
109. Brand W, Peters RJB, Braakhuis HM, Maślankiewicz L, Oomen AG (2020) Possible effects of titanium dioxide particles on human liver, intestinal tissue, spleen and kidney after oral exposure. *Nanotoxicology* 14(7):985–1007. <https://doi.org/10.1080/17435390.2020.1778809>
110. Louro H, Bettencourt A, Gonçalves LM, Almeida AJ, Silva MJ (2015) Nanotechnology applications for tissue engineering. In: Thomas S, Grohens Y, Ninan N (eds) Nanotechnology applications for tissue engineering. Elsevier, pp 263–287. <https://doi.org/10.1016/B978-0-323-32889-0.00009-1>
111. Shah SU (2012) Importance of genotoxicity & S2A guidelines for genotoxicity testing for pharmaceuticals. *IOSR J Pharm Biol Sci* 1(2):43–54. <https://doi.org/10.1103/PhysRevB.84.064423>
112. Nohmi T (2018) Thresholds of genotoxic and non-genotoxic carcinogens. *Toxicol Res* 34(4):281–290. <https://doi.org/10.5487/TR.2018.34.4.281>
113. Singh N, Manshian B, Jenkins GJS, Griffiths SM, Williams PM, Maffei TGG et al (2009) NanoGenotoxicology: the DNA damaging potential of engineered nanomaterials. *Biomaterials* 30(23–24):3891–3914. <https://doi.org/10.1016/j.biomaterials.2009.04.009>
114. Food and Drug Administration (FDA) (2012) S2(R1) genotoxicity testing and data interpretation for pharmaceuticals intended for human use. <https://doi.org/10.1246/bcsj.79.1054>
115. OECD (2017) Overview of the set of OECD Genetic Toxicology Test Guidelines and updates performed in 2014–2015. Series on Testing & Assessment, No. 238 (2nd edn), ENV/JM/MONO(2016)33/REV1. Retrieved from [https://www.oecd.org/officialdocuments/publicdisplaydocumentpdf/?cote=ENV-JM-MONO\(2016\)33/rev1&doclanguage=en](https://www.oecd.org/officialdocuments/publicdisplaydocumentpdf/?cote=ENV-JM-MONO(2016)33/rev1&doclanguage=en)
116. ICH (1995) Guideline on the need for Carcinogenicity Studies on Pharmaceuticals (S1A)
117. Dusinska M, Mariussen E, Pran ER, Hudcová AM, Elje E, Kazimirova A et al (2019) In vitro approaches for assessing the genotoxicity of nanomaterials. In: Zhang Q (ed) *Nanotoxicity: methods and protocols, methods in molecular biology*. Springer, pp 83–122
118. Adan A, Kiraz Y, Baran Y (2016) Cell proliferation and cytotoxicity assays. *Curr Biotechnol Pharm* 17(14):1873–4316. <https://doi.org/10.2174/13892010176661608081605>
119. van Meerloo J, Kaspers GJL, Cloos J (2011) Cell sensitivity assays: the MTT assay. In: Cree IA (ed) *Cancer cell culture. Methods in molecular biology (methods and protocols)*, vol 731. Humana Press, pp 237–246. <https://doi.org/10.1007/978-1-61779-080-5>
120. Landsiedel R, Ma-Hock L, Kroll A, Hahn D, Schneckeburger J, Wiench K, Wohlleben W (2010) Testing metal-oxide nanomaterials for human safety. *Adv Mater* 22(24):2601–2627. <https://doi.org/10.1002/adma.200902658>
121. McCracken C, Dutta PK, Waldman WJ (2016) Critical assessment of toxicological effects of ingested nanoparticles. *Environ Sci Nano* 3(2):256–282. <https://doi.org/10.31729/jnma.1240>
122. Laloux L, Polet M, Schneider Y-J (2017) Interaction between ingested-engineered nanomaterials and the gastrointestinal tract: in vitro toxicology aspects. In: Axelos MAV, Vande Voorde M (eds) *Nanotechnology in agriculture and food science*. Wiley, pp 311–332. <https://doi.org/10.1002/9783527697724.ch18>
123. Braakhuis HM, Kloet SK, Kezic S, Kuper F, Park MVDZ, Bellmann S, Bouwmeester H (2015) Progress and future of in vitro models to study translocation of nanoparticles. *Arch Toxicol* 89(9):1469–1495. <https://doi.org/10.1007/s00204-015-1518-5>
124. Hilgendorf C, Spahn-Langguth H, Regårdh CG, Lipka E, Amidon GL, Langguth P (2000) Caco-2 versus Caco-2/HT29-MTX co-cultured cell lines: Permeabilities via diffusion, inside- and outside-directed carrier-mediated transport. *J Pharm Sci* 89(1):63–75. [https://doi.org/10.1002/\(SICI\)1520-6017\(200001\)89:1<63::AID-JPS7>3.0.CO;2-6](https://doi.org/10.1002/(SICI)1520-6017(200001)89:1<63::AID-JPS7>3.0.CO;2-6)
125. Natoli M, Leoni BD, D'Agnano I, Zucco F, Felsani A (2012) Good Caco-2 cell culture practices. *Toxicol In Vitro* 26. <https://doi.org/10.1016/j.tiv.2012.03.009>
126. Lesuffleur T, Barbat A, Dussaulx E, Zweibaum A (1990) Growth adaptation to methotrexate of HT-29 human colon carcinoma cells is associated with their ability to differentiate into columnar absorptive and mucus-secreting cells. *Cancer Res* 50(19):6334–6343
127. Sohal IS, O'Fallon KS, Gaines P, Demokritou P, Bello D (2018b) Ingested engineered nanomaterials: state of science in nanotoxicity testing and future research needs. *Part Fibre Toxicol* 15(1):29. <https://doi.org/10.1186/s12989-018-0265-1>
128. Hur SJ, Lim BO, Decker EA, McClements DJ (2011) In vitro human digestion models for food applications. *Food Chem* 125(1):1–12. <https://doi.org/10.1016/j.foodchem.2010.08.036>
129. Gerloff K, Fenoglio I, Carella E, Kolling J, Albrecht C, Boots AW et al (2012) Distinctive toxicity of

- TiO₂ rutile/anatase mixed phase nanoparticles on Caco-2 cells. *Chem Res Toxicol* 25. <https://doi.org/10.1021/tx200334k>
130. McCracken C, Zane A, Knight DA, Dutta PK, Waldman WJ (2013) Minimal intestinal epithelial cell toxicity in response to short- and long-term food-relevant inorganic nanoparticle exposure. *Chem Res Toxicol* 26(10):1514–1525. <https://doi.org/10.1021/tx400231u>
 131. Schneider T, Westermann M, Gleis M (2017) In vitro uptake and toxicity studies of metal nanoparticles and metal oxide nanoparticles in human HT29 cells. *Arch Toxicol* 91(11):3517–3527. <https://doi.org/10.1007/s00204-017-1976-z>
 132. Kukia NR, Rasmi Y, Abbasi A, Koshoridze N, Shirpoor A, Burjanadze G, Saboory E (2018) Bio-effects of TiO₂ nanoparticles on human colorectal cancer and umbilical vein endothelial cell lines. *Asian Pacific J Cancer Prevent* 19(10):2821–2829. <https://doi.org/10.22034/APJCP.2018.19.10.2821>
 133. Cao X, Deloid GM, Bitounis D, La Torre-Roche RD, White C, Zhang Z et al (2019) Co-exposure to the food additives SiO₂ (E551) or TiO₂ (E171) and the pesticide boscalid increases cytotoxicity and bioavailability of the pesticide in a tri-culture small intestinal epithelium model: potential health implications. *Environ Sci Nano* 6(9):2786–2800. <https://doi.org/10.1039/c9en00676a>
 134. Cao X, Zhang T, DeLoid GM, Gaffrey MJ, Weitz KK, Thrall BD et al (2020) Evaluation of the cytotoxic and cellular proteome impacts of food-grade TiO₂ (E171) using simulated gastrointestinal digestions and a tri-culture small intestinal epithelial model. *NanoImpact* 17(August 2019). <https://doi.org/10.1016/j.nano.2019.100202>
 135. Barrasa JJ, Olmo N, Lizarbe MA, Turnay J (2013) Bile acids in the colon, from healthy to cytotoxic molecules. *Toxicol In Vitro* 27(2):964–977. <https://doi.org/10.1016/j.tiv.2012.12.020>
 136. Sycheva LP, Zhurkov VS, Iurchenko VV, Dauge-Dauge NO, Kovalenko MA, Krivtsova EK, Durnev AD (2011) Investigation of genotoxic and cytotoxic effects of micro- and nanosized titanium dioxide in six organs of mice in vivo. *Mutat Res* 726(1):8–14. <https://doi.org/10.1016/j.mrgentox.2011.07.010>
 137. Carmona ER, Escobar B, Vales G, Marcos R (2015) Genotoxic testing of titanium dioxide anatase nanoparticles using the wing-spot test and the comet assay in *Drosophila*. *Mutat Res Genet Toxicol Environ Mutagenesis* 778:12–21. <https://doi.org/10.1016/j.mrgentox.2014.12.004>
 138. NanoGenoTox Joint Action (2013) NANOGENOTOX final report. Facilitating the safety evaluation of manufactured nanomaterials by characterising their potential genotoxic hazard. Retrieved from http://www.nanogenotox.eu/index.php?option=com_content&view=article&id=136&Itemid=158
 139. Vila L, García-Rodríguez A, Marcos R, Hernández A (2018b) Titanium dioxide nanoparticles translocate through differentiated Caco-2 cell monolayers, without disrupting the barrier functionality or inducing genotoxic damage. *J Appl Toxicol* 38(9):1195–1205. <https://doi.org/10.1002/jat.3630>
 140. Vila L, García-Rodríguez A, Cortés C, Marcos R, Hernández A (2018a) Assessing the effects of silver nanoparticles on monolayers of differentiated Caco-2 cells, as a model of intestinal barrier. *Food Chem Toxicol* 116. <https://doi.org/10.1016/j.fct.2018.04.008>
 141. Du X, Gao S, Hong L, Zheng X, Zhou Q, Wu J (2019) Genotoxicity evaluation of titanium dioxide nanoparticles using the mouse lymphoma assay and the Ames test. *Mutat Res Genet Toxicol Environ Mutagenesis* 838(November 2018):22–27. <https://doi.org/10.1016/j.mrgentox.2018.11.015>
 142. Wang JJ, Sanderson BJS, Wang H (2007a) Cytotoxicity and genotoxicity of ultrafine TiO₂ particles in cultured human lymphoblastoid cells. *Mutat Res* 628(2):99–106. <https://doi.org/10.1016/j.mrgentox.2006.12.003>
 143. Murugadoss S, Brassinne F, Sebaihi N, Petry J, Cokic SM, Van Landuyt KL, Godderis L, Mast J, Lison D, Hoet PH, van den Brule S (2020) Agglomeration of titanium dioxide nanoparticles increases toxicological responses in vitro and in vivo. *Part Fibre Toxicol* 17(1):10. <https://doi.org/10.1186/s12989-020-00341-7>
 144. Grissa I, Elghoul J, Ezzi L, Chakroun S, Kerkeni E, Hassine M, El Mir L, Mehdi M, Ben CH, Haouas Z (2015) Anemia and genotoxicity induced by sub-chronic intragastric treatment of rats with titanium dioxide nanoparticles. *Mutat Res Genet Toxicol Environ Mutagen* 794:25–31. <https://doi.org/10.1016/j.mrgentox.2015.09.005>
 145. Shukla RK, Kumar A, Vallabani NVS, Pandey AK, Dhawan A (2014) Titanium dioxide nanoparticle-induced oxidative stress triggers DNA damage and hepatic injury in mice. *Nanomedicine* 9(9):1423–1434. <https://doi.org/10.2217/nmm.13.100>
 146. Chakrabarti S, Goyary D, Karmakar S, Chattopadhyay P (2019) Exploration of cytotoxic and genotoxic endpoints following sub-chronic oral exposure to titanium dioxide nanoparticles. *Toxicol Ind Health* 35(9):577–592. <https://doi.org/10.1177/0748233719879611>
 147. Chen Z, Wang Y, Ba T, Li Y, Pu J, Chen T, Song Y, Gu Y, Qian Q, Yang J, Jia G (2014) Genotoxic evaluation of titanium dioxide nanoparticles in vivo and in vitro. *Toxicol Lett* 226(3):314–319. <https://doi.org/10.1016/j.toxlet.2014.02.020>
 148. Martins ADC Jr, Azevedo LF, de Souza Rocha CC, Carneiro MFH, Venancio VP, de Almeida MR, Antunes LMG, de Carvalho Hott R, Rodrigues JL, Ogunjimi AT, Adeyemi JA, Barbosa F Jr (2017) Evaluation of distribution, redox parameters, and genotoxicity in Wistar rats co-exposed to silver and titanium dioxide nanoparticles. *J Toxicol Environ Health A* 80(19–21):1156–1165. <https://doi.org/10.1080/15287394.2017.1357376>

149. Manivannan J, Banerjee R, Mukherjee A (2019) Genotoxicity analysis of rutile titanium dioxide nanoparticles in mice after 28 days of repeated oral administration. *Nucleus* 63(1):17–24. <https://doi.org/10.1007/s13237-019-00277-0>
150. Blevins LK, Crawford RB, Bach A, Rizzo MD, Zhou J, Henriquez JE, Khan DMIO, Sermet S, Arnold LL, Pennington KL, Souza NP, Cohen SM, Kaminski NE (2019) Evaluation of immunologic and intestinal effects in rats administered an E 171-containing diet, a food grade titanium dioxide (TiO₂). *Food Chem Toxicol* 133:110793. <https://doi.org/10.1016/j.fct.2019.110793>

Open Access This chapter is licensed under the terms of the Creative Commons Attribution 4.0 International License (<http://creativecommons.org/licenses/by/4.0/>), which permits use, sharing, adaptation, distribution and reproduction in any medium or format, as long as you give appropriate credit to the original author(s) and the source, provide a link to the Creative Commons license and indicate if changes were made.

The images or other third party material in this chapter are included in the chapter's Creative Commons license, unless indicated otherwise in a credit line to the material. If material is not included in the chapter's Creative Commons license and your intended use is not permitted by statutory regulation or exceeds the permitted use, you will need to obtain permission directly from the copyright holder.





Nanomaterial-Induced Extra-Pulmonary Health Effects – the Importance of Next Generation Physiologically Relevant *In Vitro* Test Systems for the Future of Nanotoxicology

Ali Kermanizadeh and Gwyndaf Roberts

Abstract

Manufactured nanomaterials (NMs) offer incredible scientific and societal benefits but their potential hazard to human health is not yet fully comprehended. In the last decade, a significant body of evidence indicates that certain NMs are capable of translocating from the primary exposure site (skin, lungs and gastrointestinal tract) to a number of secondary organs which includes the liver. Moreover, recent advances in the field of nanomedicine has resulted in increasing direct intravenous injection of NMs with the liver being a particularly important organ with regards to potential toxic effects and accumulation of said materials. It is generally acknowledged that it is not always possible to make direct or meaningful comparisons between *in vitro* and *in vivo* xenobiotic-induced toxicological responses. One of the main reasons for the lack of comparability between the testing strategies is that biological responses are not

often alike which can in part be attributed to the numerous limitations of traditional mono-cellular *in vitro* test systems which are acting as a surrogate for a whole organ. In an attempt to address and highlight this important issue, this chapter will discuss the progress made in the production and validation of next generation more physiologically relevant multi-cellular *in vitro* models of skin, GIT and the liver utilised for the assessment of the NM-induced toxicological effects.

Keywords

Nanotoxicology · Nanomaterials ·
Biologically relevant *in vitro* test systems ·
Liver · GIT · Skin · Human health · Hazard ·
In vitro and *in vivo* comparisons · Exposure
routes

A. Kermanizadeh (✉)
University of Derby, Human Sciences Research
Centre, Derby, UK
e-mail: A.Kermanizadeh@derby.ac.uk

G. Roberts
Bangor University, School of Medical Sciences,
Bangor, UK

11.1 Introduction

The ever-increasing interest in the commercialization of nano sized materials has led to significant growth in the disciplines of nanotechnology and nanomedicine [79, 80]. As a consequence of this however, the same nano specific characteristics which make NMs desirable might also influence their toxicity [44, 49]. As public and

occupational exposure increases there is a real need to evaluate the possibility of detrimental health consequences of exposure to engineered NMs.

The skin, lungs and the gastrointestinal tract (GIT) are continually exposed to the external environment, hence they are the primary exposure sites for NMs [7]. However, it is now understood that certain materials can translocate from these primary exposure sites [48, 95]. As a secondary exposure tissue, the liver is very important, as it has been shown to accumulate NMs at higher quantities compared to other target organs [48, 95]. In addition, the recent advancements in the development of nanomedicine will result in direct injection of NMs into the circulatory system. Once in the blood materials can quickly reach the reach the liver [33, 58, 99].

The potential toxicity of a substance is determined not only by the dose and route of exposure, but also via a set of parameters referred to as “toxicokinetics,” which combined describe the uptake, metabolism and transport and elimination of the substance from the organism. These considerations are crucial, since the toxicity of a substance is dependent on which organs or cell type/s it meets, the exact form the xenobiotic and the time-span the substance persists at a specific location within an organism.

NMs must be distributed in the organism and pass organ barriers before entering tissues and reaching cells. It is believed that inhaled materials deposit in the respiratory tract via different mechanisms including one or combination of interception, impaction, sedimentation and diffusion [19, 32, 77, 83]. It is also important to note macrophages are important in the distribution of NMs in and out of the lungs [60, 103]. These mechanisms all contribute to the release of a proportion NMs into the blood at which point they are transported to secondary organs [6, 70, 88, 107].

As a complete overview of the current status of the field of nanotoxicology is not possible within the remit of one chapter, the focus here will be on NM-induced extra-pulmonary health effects with particular attention being paid to the next generation more physiologically relevant

multi-cellular *in vitro* models of the liver, GIT and the skin utilised for the assessment of the toxicological effects associated with NM exposure. Due to space constraints only a selected number of investigations are highlighted in the main text, but the conclusions and discussions are on a based much larger literature search. As an important consideration, short-comings in *in vitro* nanotoxicology for these specific systems are highlighted and discussed with a number of suggestions made that might improve experimental design in the future.

11.2 Dermal NM Exposure and *In Vitro* Test Systems of the Skin

The human skin is composed of three layers being the subcutaneous tissue, the dermis and the epidermis. The superficial epidermis provides a protective barrier against foreign antigens and xenobiotics, regulates release of water from the body and forms a physical barrier from harm. Keratinocytes are the major cell type of the epidermis accounting for approximately 90% of the cell population. These cells originate in the deepest layer of the epidermis, the stratum basale and migrate to the third and final layer of the skin, the stratum corneum. Dermal absorption is described as the transport of a substance from the outer surface of the skin into the organ, resulting in the xenobiotic becoming systemically available. Importantly, absorption is not the same as permeation, which is simply the diffusion of a compound into a layer of skin. In particular, the stratum corneum is one of the most important barriers against external compounds due to its physical structure and its hydrophobicity. However, specific features such as hair follicles and sweat glands might potentially offer routes of entry for NMs [63].

NMs are extensively utilised in cosmetics as a means of protecting the skin from exposure to UV sunlight notably by the incorporation of ZnO and TiO₂ NMs as inorganic UV filters in sunscreens [100]. Generally speaking, both NMs are considered safe for their use in sunscreens although concerns have been raised for

TiO₂ NMs in some products due to the potential for photocatalytic activity and phototoxicity [90–92, 100].

In particular two important aspects need to be fully considered for evaluation of potential hazards for the exposure of NM to the skin. Firstly, there is the possibility for “local” toxicity in terms of potential for irritation and sensitization (additional genotoxicity/mutagenicity cannot be excluded either), and secondly there is the possibility for penetration of the skin resulting in systemic exposure to the NMs. Dermal exposure can occur due to accidental spillage or low hygienic occupational settings or due to purpose made consumer products for skin application such as sunscreens as touched upon above. Currently, the sensitization potential of NMs is still fairly unknown. One of the fundamental reasons for this is the difficulty and uncertainty in how testing for sensitizing for NMs should be performed. The use of intradermal injection at the base of the ear in mice described as an alternative for the local lymph node assay (LLNA), is one such option [43]. The injection of TiO₂ NMs in acetone-olive-oil-treated control mice did not effect lymph node (LN) proliferation as an indicator for immune stimulation [43]. 2,4-Dinitrochlorobenzene (DNCB) sensitization on the other hand resulted in LN proliferation, which was further increased by the injection of TiO₂ NMs. In a follow-up study topical exposure of TiO₂, Ag or SiO₂ NMs did not induce an immune response in the draining local lymph node when applied on the skin [98]. In both studies no immune stimulation in the draining lymph node was noted as an indication for sensitization potential, however, in combination with the well-known model sensitizer DNCB enhancement of the DNCB response was observed indicating adjuvant activity for the NMs.

Furthermore and importantly to this chapter, several studies have shown that NMs such as ZnO, Ag, TiO₂, and CeO₂ do not show local irritation activity [57, 73, 102]. In a reconstructed human epidermis (RhE) model the NMs can be applied in a water or lipid based solution on top of the epidermal construct that has similar tissue

layers as normal human skin. To date a number of RhE models have been validated and accepted for determination of the irritant activity of chemicals in OECD TG 439. These include:

1. EpiSkin™ – *in vitro* reconstructed human epidermis from normal human keratinocytes cultured on a collagen matrix at the air-liquid interface. This model is histologically similar to the *in vivo* human epidermis.
2. EpiDerm™ – highly differentiated 3D tissue model consisting of normal, human-derived epidermal keratinocytes cultured on tissue culture inserts.
3. SkinEthic™ – an *in vitro* reconstructed human epidermis from normal human keratinocytes cultured on an inert polycarbonate filter at the air-liquid interface
4. epiCS® skin – stratified squamous epithelium. Proliferating cells of the basal layer undergo a series of morphological and biochemical changes that culminate in the production of dead, flattened, enucleated squames.
5. Skin +™ model – reconstructed epidermis model

At this juncture it is important to note the prohibition of animal testing of cosmetic products and ingredients on animals enforced in the EU in 2013 which clearly highlights the absolute necessity for the above *in vitro* testing models.

Whether NMs penetrate through intact skin is a controversial topic mainly due to huge knowledge gaps in the available literature [48, 76]. One area of research that is clearly lacking is long-term NM skin exposure studies. That being said, it is currently generally believed that following exposure local penetration of low-solubility NMs in the skin is mainly limited to the first superficial layers of the stratum corneum [15, 89], with accumulation in hair follicles also possible [17]. In contrast, after dermal exposure to ZnO NMs (20 nm) (Zn administrated as sunscreens) could be detected in the blood of treated volunteers [36]. In these studies, ⁶⁸Zn natural isotopes were utilised to allow for assessment of biodistribution throughout the body.

Another important factor influencing NM skin penetration and systemic distribution is whether the skin is healthy or damaged. Recent data has demonstrated that skin damage like abrasions and sunburns can influence dermal penetration and uptake [42, 75]. As an example, Ag NMs were shown to penetrate damaged (burnt skin) down to the dermis layer, whereas, this was not the case in healthy skin [42].

From the scrutiny of the literature, there are a number of considerations that seem to govern the dermal absorption of NMs. Specifically, NM size and surface chemistry appear to be important, whereas the composition and shape seem to have less significance. Generally speaking; materials larger than 50 nm do not seem to penetrate through the stratum corneum (exemplified by size dependent penetration of NMs – ≤ 4 nm penetrating intact skin, NMs with sizes between 4 and 20 nm able to penetrate intact and damaged skin, and 21 and 45 nm NMs only capable of entering damaged skin (reviewed by [64])). This being said, an understanding of materials aggregate/agglomerate during and at the end of an experiment could be vital in the quantities of NMs penetrating the skin and the translocation thereafter. Moreover, the solubility of the NM in question will influence the toxicokinetics and distribution of the material. The literature seems to indicate that exposure to positively charged materials will result in greater penetration through the skin although there is also some confliction whether or not this is the case. The role and importance of impaired barrier function on dermal penetration of NMs appears minimal and somehow divisive with some studies providing data which is in contradiction of the above statement. Another important consideration in study design is whether hair is shaved from the skin as this could be an important parameter influencing the organ barrier function. In summary, the skin seems to be a relatively impermeable barrier to NM entry into circulation [93], however NM translocation following dermal exposure is not entirely impossible. Overall, from the available data it appears that the risk of NM-induced damage to secondary organs following dermal exposure of intact healthy skin is low.

11.3 Oral NM Exposure and *In Vitro* Test Systems of the GIT

NM ingestion can occur directly from eating food, drinking water or via oral medication [16, 51]. In addition, mucociliary clearance of NMs may result in the transfer and accumulation of materials to the GIT. It is believed that the vast quantity of ingested NMs are rapidly passed through the GIT and excreted via the faeces [18, 37, 83]. Very similar to the skin, the surface properties of NMs play an important role in their translocation from the GIT (this will be expanded upon below). Once in sub-mucosal tissue, NMs are capable of entering the lymphatics and the blood [74]. The stability of NMs in the GIT is complex and not fully understood due to a number of factors including changes in the pH through the different regions of GI tract, the protective mucus layer and presence of powerful destructive digestive enzymes [69]. After oral administration, NMs are absorbed in the small intestine. With enterocytes, mucus secreting goblet cells and the immune sampling M cells of the Peyer's patches all important in the process [61, 69]. Of particular importance to nanotoxicology, the M cells are associated with the immune cells within the GIT and might be involved in NM-mediated immunotoxicity in GIT [74] (expanded upon below).

The adult GIT provides a large complex interface around five metres in length along which NMs can interact [35, 38]. The primary area of absorption is the small intestine and, with its three distinct regions called the duodenum, jejunum, and ileum, it accounts for two thirds of this length. Its villi and microvilli increase the surface absorption area 60–120 times, contributing to a mean mucosal surface within the GI tract of around 35 m² [38]. The GI epithelium is the main barrier that regulates the movement of material from the lumen into the lamina propria and its blood vessels and lymphatics [35]. It is composed of a community of cooperating cell types. Up to a quarter are mucus-secreting Goblet cells dispersed within a lawn of enterocytes which are responsible for the absorption of nutrients [9, 40]. The follicle-associated epithelium (FAE)

characterises the Peyer's patches at the distal end of the ileum and consist of enterocytes, fewer Goblet cells (leading to a thinner mucosal layer), and microfold cells (M-cells) which sample microbes and particulates before transferring them to underlying immune cells via transepithelial transport [25, 62]. The complexity of the GI tract is further increased by the physiological conditions found within the lumen. The low pH of the stomach and the high ionic strength in both the stomach and small intestine expose NMs to a harsh environment that can fundamentally alter their properties [5, 78]. There are further pH changes in the small intestine to accompany the barrier posed by the lining of mucus, and as well as the influence of the local microbiota [21].

Enterocytes are columnar epithelial cells with a dense microvillus brush border, held together by tight junctions that limit the passive paracellular movement of substances to materials less than 2 nm [27, 30]. Molecules can instead cross the epithelial barrier by diffusion, or by receptor-mediated endocytosis followed by transcytosis [27]. However, a complex glycocalyx extends along the apical membrane functioning as a size-selective barrier. The ability of NMs to navigate across is dependent on its thickness, density, negative charge, and renewal characteristics [20, 26]. The properties of NMs determine the extent to which they can penetrate the covering layer of mucus provided by the Goblet cells, for example, smaller materials are able to penetrate more, while positively charged particulates are mucoadhesive [10]. There is some data indicating that once in contact with NMs mature enterocytes can take up the material by endocytosis, however, their ability to absorb particles >100 nm by endocytosis is limited due to the presence of the microvilli that hinder invagination of the apical membrane [14, 45]. Instead M-cells are predominantly responsible for the uptake of both microparticles and NMs using their established mechanism for the translocation of antigens from the GI tract [31, 45]. It has also been proposed that NMs can translocate across the epithelia barrier through damaged cells or through the gap left by the normal shedding of enterocytes in a process known as persorption, although the signifi-

cance of these routes have been largely discounted [41, 86].

The most common NMs to which we are exposed to orally are TiO₂, SiO₂, Ag and ZnO [28, 85]. Survey data on food and fluid consumption combined with published estimates on nanoparticle daily ingestion suggest concentrations in the GI tract of 0.12–12.6 µg/ml TiO₂, 9.2–50.4 µg/ml for SiO₂ and 0.008–0.032 µg/ml for Ag. Further estimation indicates 0.23 µg/cm² TiO₂ and SiO₂ NMs can be expected along the GIT [28]. Equivalent estimates for ZnO are harder to establish because in addition to food it can be taken in through nutritional supplements and is widely used in healthcare products which can lead to accidental ingestion [28].

The use of *in vivo* models is the benchmark used to establish toxicity and preclinical efficacy of substances but such experimentations are costly and the ethical implications of any *in vivo* study must be fully considered. The biochemical, physiological and anatomical characteristics of the section of the human GIT that is under consideration will dictate the most appropriate substitute. For example, the dog stomach is the most similar to the human, whereas the passage of material through the human small intestine is more analogous to that of the rat [23, 28]. Even so, there are disparities in the transit time through the differing lengths of the GI tracts, and variations in the villi morphology and mucin composition. In addition, interspecies comparisons of gut microbiota reveal potentially significant differences in bacterial strains and their distribution [27]. While the presence of an intact anatomy and physiology is an advantage for animal models, the common experimental techniques have inevitable shortcomings. Gavage is often used in studies to determine systemic absorption, excretion, and persistence, but this approach doesn't accurately recapitulate the realistic exposure to a material. In situ perfusion involves a region of GI tract being exposed to the passage of a solution by afferent and efferent cannulas allowing analysis of the perfusate, but again the extent to which this mirrors normal human exposure is limited [66].

Ex vivo tissue samples have been used for high throughput studies of mucoadhesive properties,

the uptake and transport of NMs, and drug delivery. The viability time of the tissue samples is limited and on occasions predictive inaccuracies, when compared to *in vivo* observations, have been thought to be due to the absence of digestive juices in the extracellular environment [20, 66]. However, *ex vivo* and *in vivo* murine models have provided comparable data, for example, about the paracellular transepithelial passage of TiO₂ NMs through disrupted tight junctions [14].

In an attempt to replace, reduce or refine animal studies, *in vitro* investigations of NM-induced GIT health effects have gained significant momentum over the last decade. There has also been a change in emphasis from descriptive toxicological analyses of what happens to those explaining the biological mechanisms behind the observations [79, 80]. There are various cell lines available for such studies but the most common and best known are the Caco-2 enterocytes derived from human intestinal carcinoma. These form an adherent monolayer with many features typical of GI tract physiology and morphology including the microvilli brush border, polarisation, tight junctions and the expression of metabolic enzymes [66, 94]. Caco-2 cells are often grown and differentiated in a Transwell® on a porous membrane insert which allows for the basolateral chamber to be sampled for signs of translocated NMs previously layered upon the

Caco-2 apical surface. Changes caused by NMs to an alternative cell line seeded in the basolateral chamber can also be analysed [29].

While such monocultures are an easier option to allow for the generation of more physiologically relevant toxicological and uptake data, cocultures of various cell types (more histologically accurate model systems) are now being used in nanotoxicological studies. The differentiated Caco-2 monolayer has been successfully combined with mucus secreting HT29 goblet-like cells to produce a model system that combines the enterocyte monolayer with an adhesive mucus barrier [94]. Recently it was proposed that a seeding proportion between the two cell types of 9:1 (Caco-2:HT29) showed the best simulation of the GIT epithelia based on tight junction characteristics (as determined by transepithelial electrical resistance), histological analysis and gene expression [82]. Furthermore, a triple culture model has been developed to incorporate the M-cell into the model. As such an example, in European funded project PATROLS [84], a triple cell model has been established and validated with differentiated Caco-2 and HT29 cells co-cultured in the apical side Transwell® filter inserts with Raji B lymphocytes in the basolateral compartment stimulating the differentiation of Caco-2 cells into M-cells (Fig. 11.1). The data provided from this model provided evidence of the importance of

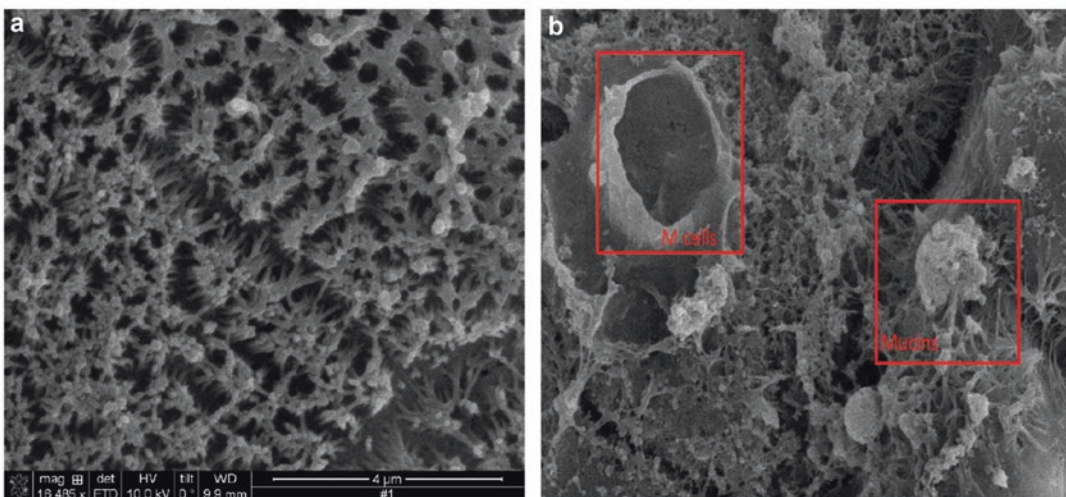


Fig. 11.1 Scanning electron microscopy of (a) differentiated Caco-2 cells and (b) Triple cell culture intestinal model with highlighted M cells and mucins (unpublished data)

the mucus layer and M cells in governing the uptake and immune modulation following NM exposure (manuscript in preparation and standard operating protocols in development as part of the deliverables for the PATROLS project).

Other *in vitro* nanotoxicological considerations have involved the development of various non-cellular fluid models mimic the physical, chemical, enzymic and microbial characteristics of the GIT that show some promise for the evaluation of NM bio accessibility, stability, dissolution and aggregation [79, 80]. These models have been designed to mimic different physiological micro-environments sections within of the GIT i.e. the lumen of the stomach, the lumen of the large intestine, and the epithelial barrier such as the mucus layer. Artificial membrane systems have also allowed the analysis of the effect of pH on passive epithelial translocation of substances [66]. However, all these models require further adaption and standardisation. Finally as an additional consideration, recent *in vitro* data has suggested that simulation of the digestion processes for NMs may add value to physiologically relevant NM toxicological data [12, 22].

The combination of experimental data from *in vivo*, *ex vivo* and *in vitro* systems with complex computational algorithms is driving the development of *in silico* high-throughput models for primary analysis of chemical dissolution and bioavailability. Evidence suggests that they can predict drug bioavailability as accurately as *in vivo* rat, *in vitro* cell culture and artificial membrane models [68]. The usefulness of *in silico* model nanotoxicology with data gathered from such projects as PATROLS is being used to inform the algorithms [66].

The recent progress in microfabrication techniques and microfluidics have allowed the manufacture of the so-called gut-on-a-chip: an experimental system that more closely resembles the three-dimensional physiological environment of the GIT lumen. The optically transparent and gas permeable chip contains two chambers separated by a porous and flexible membrane: one representing the GI lumen seeded with epithelial cells; and the other a blood vessel seeded with vascular endothelial cells. The chip can be inte-

grated with analytic sensors to allow synchronous monitoring of events at a cellular or tissue level [4]. The chamber representing the GI lumen is coated with an extracellular matrix on which cells can attach to mimic the three-dimensional structure of the mucosa. In a recent study, Caco-2 cells were seeded on a collagen scaffold which were exposed mechanical forces to simulate peristalsis and induced to differentiate into a range of gut epithelial cells such as goblet cells, enteroendocrine cells and Paneth cells [55]. This model system can also be used to investigate the gut microbiota and the role it plays within the GIT and its impact on human health [56]. Despite the great potential with the gut-on-a-chip models, concerns have been raised with regards to the physical interferences of NMs in such systems as well as the limitations in the toxicological endpoints that can be measured with the available technologies. Additionally, these models are currently extremely expensive which for the most part makes them unattainable for academic research.

The models described so far have many appropriate applications and have each helped to advance the understanding of the interactions between micro/nanomaterials with the GIT. However, inevitably there are limitations in these models as with all *in vitro* test systems. The physiological conditions within the GIT lumen, which many of these model systems struggle to replicate, can have a profound influence on the properties of NMs, for example salt content and pH can influence agglomeration and charge and thereby alter their rate of translocation across the epithelia [27, 66]. The close relationship between human health and gut microbiota would suggest that the interaction of NMs with up to 1000 bacterial species resident in the GIT needs closer consideration but this is often overlooked [28]. The movement and digestion of substances within the GIT is a dynamic process that takes place over a complex three-dimensional landscape which is impossible to recapitulate with the two-dimensional cell culture models [4].

From the scrutiny of the literature, in the majority of nanotoxicological investigations relating to GIT the toxicity was assessed via bio-

chemistry, without any corresponding clinical findings making it difficult to determine the relevance and extent of these findings. Of great importance, the assessment of uptake across a range of NMs indicates that the translocation from the GIT to secondary organs is very small (\leq % of the administered dose). As an addition, in recent years there is growing body of literature suggesting that there is very translocation of NMs in a healthy gut (this data generated predominately in rodent models). From the available data, it appears that NM adsorption in the GIT decreases with increasing size of the material. Therefore, in all reality NM agglomeration might affect the bio-availability of the original NM [71]. To summarise, despite great advancements in the field in particular with regards to more physiologically relevant *in vitro* test systems it is still very difficult to determine the relevance of NM-induced adverse effects in the GIT and following oral exposure.

11.4 Hepatic Nanotoxicology and *In Vitro* Models of the Liver

The liver is the bodies' principal and most effective detoxification centre [58, 81]. The organ is highly structured and organised and composed of its main cell population of hepatocytes as well as numerous non-parenchymal cell populations including the Kupffer cells (KCs – resident macrophages), hepatic stellate cells and sinusoidal endothelial cells [33, 46, 53]. As touched upon above, in addition to accidental and consumer exposure to NMs, the advancements in the field of nanomedicines will result in intentional intravenous administration of materials into the bloodstream and the resulting subsequent accumulation in the liver [8, 51]. Very importantly in hepatic nanotoxicology is the fact that the KCs and sinusoidal endothelial cells line the liver sinusoids (natural fenestrations in the organ which allow quick contact of xenobiotics with hepatic cell populations). These openings allow for continuous cell contact with gut-originated antigens and could include materials reaching the

organ from the blood via the portal vein. Due to the location of the KCs and endothelial cells in the sinusoids these cells might in all reality act as a barrier to the non-soluble NMs, preventing them from physically coming into contact with the hepatocytes. Moreover, the location of KCs in the sinusoids is one the reasons for these macrophages controlling the hepatic immune response following a particulate challenge (demonstrated *in vitro* (comparisons made between 3D primary human liver MT composed of hepatocytes only or co-cultures of hepatocytes and KCs) [53] and *in vivo* (mice with depleted KC cell population) [46]). KCs are one of the most important hepatic cells in the modulation and governance of hepatic immunity as well as being heavily involved in the initiation and progression of disease in the organ [13, 46, 99, 108]. In a healthy liver, KCs are pivotal in the maintenance of immune tolerance with the cells residing in a semi-activated state due to constant low-level exposure to gut-derived. However, in disease and or under stress, these macrophages can fully activate and differentiate into M1-like or M2 phenotypes [11]. For all these reasons, it is highly beneficial that KCs are incorporated in all next generation *in vitro* hepatic models intended for hazard assessment of NMs (an example of few such test systems and studies are reproduced from a review by [54] and highlighted below). The inclusion of KCs in *in vitro* test systems is even more valuable if the models are designed to be used as a replacement for animal testing [52, 53].

The use of *in vitro* hepatocyte only test systems has been extremely useful over the last 30 years. Historically, hepatocytes were regarded as the most important cell population in the liver for drugs and chemical toxicity screening. This is explicable as drugs and chemical are predominantly metabolised and it is often the metabolic intermediates that are hepatotoxic. However, since low solubility NMs are not metabolised, but rather interact and are internalised by KCs [1, 97], the use of hepatocyte only mono-cultures is questionable for particle hepatic toxicity screening. It is important to state that the field of hepatic toxicology as a whole is recognising the importance of the inclusion of KCs in test systems with

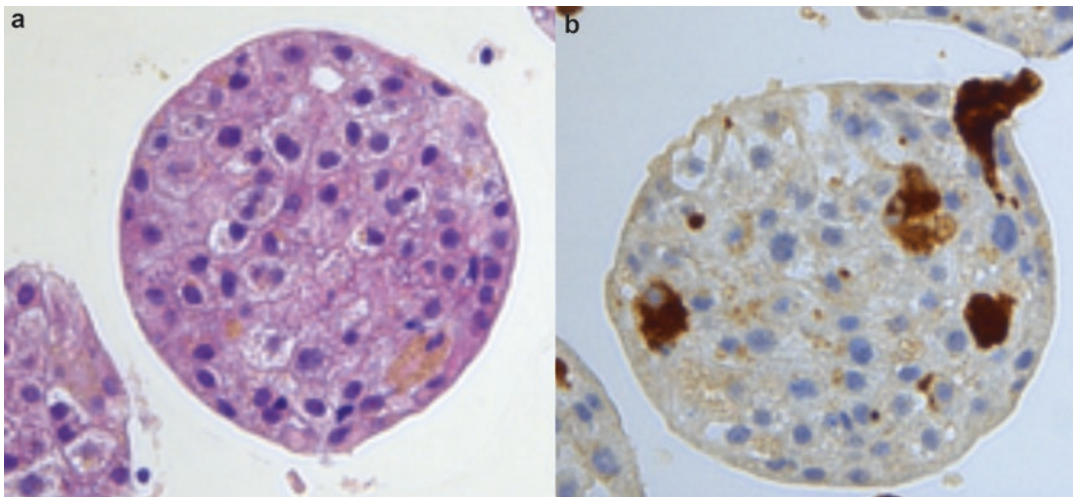


FIG. 11.2 Histological and immunological staining of 3D primary human liver spheroid model comprising of primary human hepatocytes, KCs and hepatic endothelial

cells (a) HE staining (b) CD68 staining – KCs (unpublished data)

more and more drug induced liver injury (DILI) screening being conducted in more physiologically relevant systems.

In a unique and novel collection of *in vitro* studies, a 3D primary human liver spheroid model composed of primary human hepatocytes, KCs and hepatic endothelial cells (Fig. 11.2) were exposed via either a single or repeated multiple exposure (up to 13 exposures every other day) regimes to a wide selection of NMs including Ag, ZnO, MWCNT, TiO₂, and CeO₂ for up to 3 weeks. These experiments also benefited from recovery periods of up to 2 weeks. The data demonstrated that very low dose repeated exposures more than sufficient for a comprehensive toxicological profiling of NMs with adverse effects being more profound for the Ag and ZnO NMs (cytotoxicity, inflammation, liver function and oxidative stress). Unsurprisingly as stated above the authors showed that the KCs are crucial in dictating the overall NM-mediated hepatic toxicity. Finally, exposure to low solubility NM-treated showed a clear penetration of materials into the core of the microtissue [47, 52, 53].

In another important *in vitro* study, a co-culture model of hepatocytes and KCs were utilised for a comparative analysis of the toxicity of 29 metal oxide NMs (i.e. cobalt oxide, CuO, Fe₃O₄, antimony oxide, TiO₂, tungsten trioxide,

gadolinium oxide and ZnO). In this study, KUP5 (immortalized mice KCs) and Hepa-1-6 cells (mice hepatocyte cell line) were exposed to the NMs for 24 hr. at a concentrations of up to 50 µg/ml. The authors showed differences in the toxicity of different metals with the transition-metal oxides inducing caspases 3 and 7 activity. Moreover, the exposure to the rare-earth oxide NMs resulted in lysosomal damage, NLRP3 inflammasome activation, caspase 1 activation, IL-1β secretion and pyroptosis in KCs [72]. As a final example in a 2014 study, buffalo rat hepatocytes and primary rat KC were exposed to a 90 nm SiO₂ NM for 24 hr. (up to 1000 µg/ml). The data showed a concentration dependant decrease in cell viability and increased mitochondrial damage accompanied with a secretion of TNF-α and nitric oxide [104].

The potential for NMs to translocate to secondary organs via different routes of exposure is very real, with the liver demonstrated to accumulate a large proportion of the total translocated dose [2, 3, 67]. Therefore, it is essential that the impact of NM exposure to normal liver function and health was comprehensively investigated. Despite the impressive research carried out on the topic there are still major knowledge gaps (some of which are discussed below) that require attention to allow for meaningful progress and a

better understanding of “real” hazard of NMs to the liver.

It is generally acknowledged that it is not always possible to make direct or meaningful comparisons between *in vitro* and *in vivo* hepatic toxicological responses. One of the key reasons for the lack of comparability between *in vitro* and *in vivo* is that biological responses are rarely like for like which can be partially attributable to the use of traditional mono-cellular *in vitro* test systems as a representative of a whole organ [54]. As an example, cytotoxicity measurements *in vitro* in a hepatocyte cell line will never compare to AST/ALT *in vivo* alterations (this is even more apparent for NMs as compared to drugs or chemicals). Unique for the liver and fundamentally important, is the requirement for consideration and understanding that currently *in vitro* models cannot emulate the liver’s unparalleled and incredible regeneration capability. The liver’s ability to regenerate is essential in damage/disease recovery in everyday life. Since acute liver failure is not possible for NMs it is extremely important that the organ’s ability to regenerate is considered in future *in vitro/in vivo* NM hazard assessment strategies. Based on the advancements in hepatic nanotoxicology and data generated, it is reasonable to speculate that for the majority of materials reaching the organ, any meaningful NM-mediated adverse effects in the liver observed at acute time points will be quickly reversed (i.e. [50, 105]), and real hazard would only occur after long-term exposure in the general population. As an extension to this and as an important consideration, *in vitro* acute cytotoxicity assessment alone are in all reality not that meaningful for hazard assessment of NMs in the liver, as this end-point has little to no *in vivo* relevance. Therefore, it is important to identify and investigate organ specific sub-lethal toxicological end-points that are might prove more valuable in predicating “real” NM related hazard.

A comprehensive review of the literature [54] clearly indicates that the route of exposure is key in the bio-accumulation of material within the organ and subsequent severity of adverse effects

observed in the liver. Unsurprisingly, IV exposure results in the most significant quantities of administered NMs reaching the organ (over 80% of injected dose at 24 hr. after injection i.e. [65]). This rapid accumulation in the liver is not surprising as there is no barrier for materials entering the bloodstream. The liver is at the forefront of filtering blood, hence the rapid and direct transport of the full dose to the liver sinusoids. As mentioned previously, it is also abundantly clear that NMs can translocate to extra-pulmonary organs following inhalation and oral exposure (i.e. [98, 106]). The extent of uptake of insoluble NMs is material and size dependant but believed to be in the region of ~1–5% of the total dose (summarised in [48]) and can be detected in the liver as early as 24 hr. post exposure (i.e. [34, 87, 101]). Generally speaking, few studies have looked at the long-term bio-distribution and toxicity of NMs, however in extra-pulmonary organs. However, interestingly and crucially, data has demonstrated that low solubility materials accumulated predominately in the KCs for up to one year post initial exposure [59, 96]. These experiments clearly indicate that the long-term effects of NM exposure in the liver are very important and cannot be ignored for bio-persistent NMs.

Importantly, a few selected *in vivo* studies have indicated that pre-existing liver disease is vital not only in the augmentation of acute NM associated damage (manifested as pathological and biochemical alterations to the norm) and perhaps more importantly in impeding the organ’s ability to regenerate after the NM challenge [24, 50]. With ever increasing global body mass index it is now estimated that 40–45% of global adult population might suffer from a wide array of undiagnosed sub-clinical liver injury (in most cases steatosis). Therefore, it is imperative that liver disease is considered for future hazard assessment strategies for all xenobiotics including NMs. Finally, from the scrutinization of the published data (reviewed in [54]), it is clear that there are almost no (with the exception of [39]) epidemiological studies that have investigated the potential adverse effects of NMs on the

human liver. Therefore, despite thousands of *in vitro* and *in vivo* publications on the subject we are still not that well informed on how NMs actually affect the human liver over the course of a life-time.

11.5 Concluding Remarks

In order to carry out an informed, evidence-based risk assessment, a comprehensive apprehension of all aspects of NM risk is needed and one very important component to achieving this is the design and validation of physiologically relevant *in vitro* test systems. In addition, for a critical risk assessment information on levels of NM exposure, route of exposure, bio-persistence in the organism and inherent toxicity and physicochemical properties of the material being tested is required. It is important to acknowledge that the field of nanotoxicology is no longer in its infancy. Therefore, the utilisation of physiologically relevant test systems are the only option to advance the field of nanotoxicology beyond the initial screening and dose finding experiments. The selection of cost effective and easy experiments may no longer be all that useful for hazard assessment purposes, and experiments must be designed to try to mimic “real” *in vivo* exposure scenario and biological responses. That being said a full understanding of the limitations of test system is key – even the “best” *in vitro* test system will not be suitable for everything. It is absolutely essential that there is a clear effort in the development and validation of standardized operating protocols for more consistent assessment of NM-induced toxicity to strengthen legislation and just as importantly to keep up with the rapid pace of the research in this area. Ideally, these protocols should include the use of reference materials that could allow interlaboratory comparisons. Finally, even though toxicological analysis in individual organs of interest is extremely important, for NMs the coexistence of toxic effects in all major organs indicates that the toxicological profiling of NMs might be required on an organism level.

Acknowledgements The authors are grateful to colleagues at University of Derby and Bangor University. The corresponding author was an advisor on EU funded project PATROLS.

References

1. Aalapati S, Ganapathy S, Manapuram S, Anumolu G, Prakya BM (2014) Toxicity and bio-accumulation of inhaled cerium oxide nanoparticles in CD1 mice. *Nanotoxicology* 8:786–798
2. Antunes AF, Pereira P, Reis C, Rijo P, Reis C (2017) Nanosystems for skin delivery: from drugs to cosmetics. *Curr Drug Metab* 18:412–425
3. Argueta-Figueroa L, Martinez-Alvarez O, Santos-Cruz J, Garcia-Contreras R, Acosta-Torres LS, de la Fuente-Hernandez J, Arenas-Arrocena MC (2017) Nanomaterials made of non-toxic metallic sulfides: a systematic review of their potential biomedical applications. *Mat Sci Eng C Mat Biol Appl* 76:1305–1315
4. Ashammakhi N, Nasiri R, Barros N, Tebon P, Thakor J, Goudie M, Shamloo A, Martin M, Khademhosseini A (2020) Gut-on-a-chip: current progress and future opportunities. *Biomaterials* 255:120196
5. Axson J, Stark D, Bondy A, Capracotta S, Maynard A, Philbert M, Bergin I, Ault A (2015) Rapid kinetics of size and pH-dependent dissolution and aggregation of silver nanoparticles in simulated gastric fluid. *J Phys Chem C* 119:20632–20641
6. Bai R, Zhang L, Liu Y, Li B, Wang L, Wang P, Autrup H, Beer C, Chen C (2014) Integrated analytical techniques with high sensitivity for studying brain translocation and potential impairment induced by intranasally instilled copper nanoparticles. *Toxicol Lett* 226:70–80
7. Bakand S, Hayes A, Dechsakulthorn F (2012) Nanoparticles: a review of particle toxicology following inhalation exposure. *Inhal Toxicol* 24:125–135
8. Balasubramanian SK, Jittiwat J, Manikandan J, Ong CN, Yu LE, Ong WY (2010) Biodistribution of gold nanoparticles and gene expression changes in the liver and spleen after intravenous administration in rats. *Biomaterials* 13:2034–2042
9. Baumgart D, Dignass A (2002) Intestinal barrier function. *Curr Opin Clin Nutr Metab Care* 5:685–694
10. Behrens I, Pena A, Alonso M, Kissel T (2002) Comparative uptake studies of bioadhesive and non-bioadhesive nanoparticles in human intestinal cell lines and rats: the effect of mucus on particle adsorption and transport. *Pharm Res* 19:1185–1193
11. Beljaars L, Schippers M, Reker-Smit C, Martinez FO, Helming L, Poelstra K, Melgert BN (2014) Hepatic localization of macrophage phenotypes dur-

- ing fibrogenesis and resolution of fibrosis in mice and humans. *Front Immunol* 5:30
12. Bettencourt A, Goncalves LM, Gramacho AC, Vieira A, Rolo D, Martins C, Assuncao R, Alvito P, Silva MJ, Louro H (2020) Analysis of the characteristics and cytotoxicity of titanium dioxide nanomaterials following simulated in vitro digestion. *Nano* 10:1516
 13. Bottcher JP, Knolle PA, Stabenow D (2011) Mechanisms balancing tolerance and immunity in the liver. *Dig Dis* 29:384–390
 14. Brun E, Barreau F, Veronesi G, Fayard B, Sorieul S, Chanéac C, Carapito C, Rabilloud T, Mabondzo A, Herlin-Boime N, Carrière M (2020) Titanium dioxide nanoparticle impact and translocation through ex vivo, in vivo and in vitro gut epithelia. *Part Fibre Toxicol* 11:13
 15. Butz T, Reinert T, Pinheiro T, Moretto P, Pallon J, Kiss AZ, Stachura J, Dabro SW, Stachura Z, Lekki J, Lekka M, Hunyadi J, Bro T, Sticherling M, Van Vaecck L, Van Royen P, Surlève-Bazeille JE. (2007) NANODERM, Quality of Skin as a Barrier to ultra-fine Particles, QLK4-CT-2002-02678 Final Report
 16. Card JW, Jonaitis TS, Tafazoli S, Magnuson BA (2011) An appraisal of the published literature on the safety and toxicity of food-related nanomaterials. *Crit Rev Toxicol* 41:22–49
 17. Chaudhry Q (2015) Opinion of the Scientific Committee on Consumer safety (SCCS) – revision of the opinion on the safety of the use of titanium dioxide, nano form, in cosmetic products. *Regulatory Toxicol Pharmacol* 73:669–670
 18. Cho WS, Kang BC, Lee JK, Jeong J, Che JH, Seok SH (2013) Comparative absorption, distribution, and excretion of titanium dioxide and zinc oxide nanoparticles after repeated oral administration. *Part Fibre Toxicol* 10:9
 19. Chuang HC, Juan HT, Chang CN, Yan YH, Yuan TH, Wang JS, Chen HC, Hwang YH, Lee CH, Cheng TJ (2014) Cardiopulmonary toxicity of pulmonary exposure to occupationally relevant zinc oxide nanoparticles. *Nanotoxicology* 8:593–604
 20. Cone R (2009) Barrier properties of mucus. *Adv Drug Deliv Rev* 61:75–85
 21. D’Argenio V, Salvatore F (2015) The role of the gut microbiome in the healthy adult status. *Clin Chim Acta* 451:97–102
 22. DeLoid GM, Cao X, Molina RM, Silva DI, Bhattacharya K, Ng KW, Loo SCJ, Brain JD, Demokritou P (2019) Toxicological effects of ingested nanocellulose in in vitro intestinal epithelium and in vivo rat models. *Environ Sci Nano* 6:2105–2115
 23. DeSesso J, Jacobson C (2001) Anatomical and physiological parameters affecting gastrointestinal absorption in humans and rats. *Food Chem Toxicol* 39:209–228
 24. Du LJ, Xiang K, Liu JH, Song ZM, Liu Y, Cao A, Wang H (2018) Intestinal injury alters tissue distribution and toxicity of ZnO nanoparticles in mice. *Toxicol Lett* 295:74–85
 25. Ermund A, Gustafsson J, Hansson G, Keita Å (2013) Mucus properties and goblet cell quantification in mouse, rat and human ileal peyer’s patches. *PLoS One* 8:e83688
 26. Frey A, Giannasca K, Weltzin R, Giannasca P, Reggio H, Lencer W, Neutra M (1996) Role of the glycocalyx in regulating access of microparticles to apical plasma membranes of intestinal epithelial cells: implications for microbial attachment and oral vaccine targeting. *J Exp Med* 184:1045–1059
 27. Fröhlich E, Fröhlich E (2016) Cytotoxicity of nanoparticles contained in food on intestinal cells and the gut microbiota. *Int J Mol Sci* 17:509
 28. Fröhlich E, Roblegg E (2016) Oral uptake of nanoparticles: human relevance and the role of in vitro systems. *Arch Toxicol* 90:2297–2314
 29. Gamboa J, Leong K (2013) In vitro and in vivo models for the study of oral delivery of nanoparticles. *Adv Drug Deliv Rev* 65:800–810
 30. Garnett M, Kallinteri P (2006) Nanomedicines and nanotoxicology: some physiological principles. *Occup Med* 56:307–311
 31. Gebert A, Rothkötter H, Pabst R (1996) M cells in Peyer’s patches of the intestine. *Int Rev Cytol* 167:91–159
 32. Geiser M, Kreyling WG (2010) Deposition and biokinetics of inhaled nanoparticles. *Part Fibre Toxicol* 7:2
 33. Godoy P, Hewitt NJ, Albrecht U, Andersen ME, Ansari N, Bhattacharya S, Bode JH, Bolleyn J, Borner C, Bottger J et al (2014) Recent advances in 2D and 3D in vitro systems using primary hepatocytes, alternative hepatocyte sources and non-parenchymal liver cells and their use in investigating mechanisms of hepatotoxicity, cell signalling and ADME. *Arch Toxicol* 87:1315–1530
 34. Gosens I, Kermanizadeh A, Jacobsen NR, Lenz AG, Bokkers B, de Jong WH, Krystek P, Tran L, Stone V, Wallin H, Stoeger T, Cassee FR (2015) Comparative hazard identification by a single dose lung exposure of zinc oxide and silver nanomaterials in mice. *PLoS One* 10:e0126934
 35. Gray H, Standring S, Ellis H, Berkovitz B (2005) *The anatomical basis of clinical practice*, 39th edn. Elsevier Churchill Livingstone, Edinburgh, pp 1157–1172
 36. Gulson B, Mccall M, Korsch M, Gomez L, Casey P, Oytam Y, Taylor A, Mcculloch M, Trotter J, Kinsley L, Greenoak G (2010) Small amounts of zinc from zinc oxide particles in sunscreens applied outdoors are absorbed through human skin. *Toxicol Sci* 118:140–149
 37. He X, Zhang H, Ma Y, Bai W, Zhang Z, Lu K, Ding Y, Zhao Y, Chai Z (2010) Lung deposition and extrapulmonary translocation of nano-ceria after intratracheal instillation. *Nanotechnology* 21:285103
 38. Helander H, Fändriks L (2014) Surface area of the digestive tract – revisited. *Scand J Gastroenterol* 49:681–689

39. Heringa MB, Peters RJB, Bleys RLAW, van der Lee MK, Tromp PC, van Kesteren PCE, van Eijkeren JCH, Undas AK, Oomen AG, Bouwmeester H (2018) Detection of titanium particles in human liver and spleen and possible health implications. *Part Fibre Toxicol* 15:15
40. Hilgendorf C, Spahn-Langguth H, Regårdh C, Lipka E, Amidon G, Langguth P (2000) Caco-2 versus Caco-2/HT29-MTX co-cultured cell lines: Permeabilities via diffusion, inside- and outside-directed carrier-mediated transport. *J Pharm Sci* 89:63–75
41. Hillyer J, Albrecht R (2001) Gastrointestinal per-sorption and tissue distribution of differently sized colloidal gold nanoparticles. *J Pharm Sci* 90:1927–1936
42. Holmes AM, Lim J, Studier H, Roberts MS (2016) Varying the morphology of silver nanoparticles results in differential toxicity against micro-organisms, HaCaT keratinocytes and affects skin deposition. *Nanotoxicology* 10:1503–1514
43. Hussain S, Smulders S, De Vooght V, Ectors B, Boland S, Marano F, Van Landuyt KL, Nemery B, Hoet PH, Vanoirbeek JA (2012) Nano-titanium dioxide modulates the dermal sensitization potency of DNCB. *Part Fibre Toxicol* 9:15
44. Johnston H, Brown D, Kermanizadeh A, Gubbins E, Stone V (2012) Investigating the relationship between nanomaterial hazard and physicochemical properties: informing the exploitation of nanomaterials with therapeutic and diagnosis applications. *J Control Release* 164:307–313
45. Kalgaonkar S, Lönnerdal B (2009) Receptor-mediated uptake of ferritin-bound iron by human intestinal Caco-2 cells. *J Nutr Biochem* 20:304–311
46. Kermanizadeh A, Chauche C, Balharry D, Brown DM, Kinase N, Boczkowski J, Lanone S, Stone V (2014a) The role of Kupffer cells in the hepatic response to silver nanoparticles. *Nanotoxicology* 8:149–154
47. Kermanizadeh A, Løhr M, Roursgaard M, Messner S, Gunness P, Kelm JM, Møller P, Stone V, Loft S (2014b) Hepatic toxicology following single and multiple exposure of engineered nanomaterials utilising a novel primary human 3D liver microtissue model. *Part Fibre Toxicol* 11:56
48. Kermanizadeh A, Balharry D, Wallin H, Loft S, Møller P (2015) Nanomaterial translocation – the biokinetics, tissue accumulation, toxicity and fate of materials in secondary organs – a review. *Critical Rev Toxicol* 45:837–872
49. Kermanizadeh A, Gosens I, MacCalman L, Johnston H, Danielsen PH, Jacobsen NR, Lenz AG, Fernandes T, Schins RPF, Cassee FR, Wallin H, Kreyling W, Stoeger T, Loft S, Møller P, Tran L, Stone V (2016) A multilaboratory toxicological assessment of a panel of 10 engineered nanomaterials to human health – ENPRA project – the highlights, limitations, and the current and future challenges. *J Toxicol Environ Health – Part B* 19:1–28
50. Kermanizadeh A, Jacobsen NR, Roursgaard M, Loft S, Møller P (2017) Hepatic hazard assessment of silver nanoparticle exposure in healthy and chronically alcohol fed mice. *Toxicol Sci* 158:176–187
51. Kermanizadeh A, Powell L, Stone V, Møller P (2018) Nano delivery systems and stabilized solid drug nanoparticles for orally administered medicine – current landscape. *Int J Nanomedicine* 13:7575–7605
52. Kermanizadeh A, Berthing T, Guzniczak E, Wheelon M, Whyte G, Vogel U, Moritz W, Stone V (2019a) Assessment of nanoparticle-induced hepatotoxicity using a 3D human primary multi-cellular microtissue exposed repeatedly over 21 days – suitability of the in vitro test system as an in vivo surrogate. *Part Fibre Toxicol* 16:42
53. Kermanizadeh A, Brown DM, Moritz W, Stone V (2019b) The importance of inter-individual Kupffer cell variability in the governance of hepatic toxicity in a 3D primary human liver microtissue model. *Nat Sci Rep* 9:7295
54. Kermanizadeh A, Powell LG, Stone V (2020) A review of hepatic nanotoxicology – summation of recent findings and considerations for the next generation of study designs. *J Toxicol Environ Health B Crit Rev* 23:137–176
55. Kim H, Ingber D (2013) Gut-on-a-chip microenvironment induces human intestinal cells to undergo villus differentiation. *Integr Biol* 5:1130
56. Kim J, Hegde M, Jayaraman A (2010) Co-culture of epithelial cells and bacteria for investigating host-pathogen interactions. *Lab Chip* 10:43–50
57. Kim H, Choi J, Lee H, Park J, Yoon BI, Jin SM, Park K (2016) Skin corrosion and irritation test of nanoparticles using reconstructed three-dimensional human skin model, EpiDerm[®]. *Toxicol Res* 32:311–316
58. Kmiec Z (2001) Co-operation of liver cells in health and disease. *Adv Anat Embryol Cell Biol* 161:1–151
59. Kolosnjaj-Tabi J, Javed Y, Lartigue L, Volatron J, Elgrabli D, Marangon I, Pugliese G, Caron B, Figuerola A, Luciani N, Pellegrino T, Alloyeau D, Gazeau F (2015) The one year fate of iron oxide coated gold nanoparticles in mice. *ACS Nano* 9:7925–7939
60. Konduru N, Murdaugh K, Sotiriou G, Donaghey T, Demokritou P, Brain J, Molina R (2014) Bioavailability, distribution and clearance of tracheally-instilled and gavaged uncoated or silica-coated zinc oxide nanoparticles. *Part Fibre Toxicol* 11:44
61. Kraehenbuhl JP, Neutra MR (2000) Epithelial M cells: differentiation and function. *Annu Rev Cell Dev Biol* 16:301–332
62. Kucharzik T, Lugerling N, Rautenberg K, Lugerling A, Schmidt M, Stoll R, Domschke W (2006) Role of M cells in intestinal barrier function. *Ann N Y Acad Sci* 915:171–183

63. Kulvietis V, Zurauskas E, Rotomskis R (2013) Distribution of polyethylene glycol coated quantum dots in mice skin. *Exp Dermatol* 22:157–159
64. Larese Filon F, Mauro M, Adami G, Bovenzi M, Crosera M (2015) Nanoparticles skin absorption: new aspects for a safety profile evaluation. *Regul Toxicol Pharmacol* 72:310–322
65. Lee JH, Sung JH, Ryu HR, Song KS, Song NW, Park HM, Shin BS, Ahn K, Gulumian M, Faustman EM, Yu IJ (2018) Tissue distribution of gold and silver after subacute intravenous injection of co-administered gold and silver nanoparticles of similar sizes. *Arch Toxicol* 92:1393–1405
66. Lefebvre D, Venema K, Gombau L, Valerio L, Raju J, Bondy G, Bouwmeester H, Singh R, Clippinger A, Collnot E, Mehta R, Stone V (2014) Utility of models of the gastrointestinal tract for assessment of the digestion and absorption of engineered nanomaterials released from food matrices. *Nanotoxicology* 9:523–542
67. Lim JP, Baeg GH, Srinivasan DK, Dheen ST, Bay BH (2017) Potential adverse effects of engineered nanomaterials commonly used in food on the miRNome. *Food Chem Toxicol* 109:771–779
68. Linnankoski J, Ranta V, Yliperttula M, Urtti A (2008) Passive oral drug absorption can be predicted more reliably by experimental than computational models – fact or myth. *Eur J Pharm Sci* 34:129–139
69. Ma T, Wang L, Yang T, Ma G, Wang S (2014) M-cell targeted polymeric lipid nanoparticles containing a toll-like receptor agonist to boost oral immunity. *Int J Pharm* 473:296–303
70. Marasani N, Skwarczynski M, Toth I (2014) Oral delivery of nanoparticle-based vaccines. *Expert Rev Vaccines* 13:1361–1376
71. Mirshafiee V, Sun B, Chang CH, Liao YP, Jiang W, Jiang J, Liu X, Wang X, Xia T, Nel AE (2018) Toxicological profiling of metal oxide nanoparticles in liver context reveals pyroptosis in Kupffer cells and macrophages versus apoptosis in hepatocytes. *ACS Nano* 12:3836–3852
72. Miyani VA, Huges MF (2017) Assessment of the in vitro dermal irritation potential of cerium, silver, and titanium nanoparticles in a human skin equivalent model. *Cutan Ocul Toxicol* 36:145–151
73. Møller P, Folkmann JK, Danielsen PH, Jantzen K, Loft S (2012) Oxidative stress generated damage to DNA by gastrointestinal exposure to insoluble particles. *Curr Mol Med* 12:732–745
74. Monteiro-Riviere NA, Larese FF (2012) *Skin*. In: *Adverse effects of engineered nanomaterials*, 1st edn. Elsevier, NY, pp 185–207
75. Monteiro-Riviere NA, Larese FF (2017) Effects of engineered nanomaterials on skin. In: *Adverse effects of engineered nanomaterials. Exposure, toxicology, and impact on human health*, 2nd edn. Elsevier/Academic Press, London, pp 357–380
76. Mailander V, Landfester K (2009) Interaction of nanoparticles with cells. *Biomacromolecules* 10:2379–2400
77. Murphy FA, Schinwald A, Poland CA, Donaldson K (2012) The mechanism of pleural inflammation by long carbon nanotubes: interaction of long fibres with macrophages stimulates them to amplify pro-inflammatory responses in mesothelial cells. *Part Fibre Toxicol* 9:8
78. Mwilu S, El Badawy A, Bradham K, Nelson C, Thomas D, Scheckel K, Tolaymat T, Ma L, Rogers K (2013) Changes in silver nanoparticles exposed to human synthetic stomach fluid: effects of particle size and surface chemistry. *Sci Total Environ* 447:90–98
79. Nel A, Nasser E, Godwin H, Avery D, Bahadori T, Bergeson L, Beryt E, Bonner J, Boverhof D, Carter J, Castranova V, DeShazo J, Hussain S, Kane A, Klaessig F, Kuempel E, Lafranconi M, Landsiedel R, Malloy T, Miller M, Morris J, Moss K, Oberdorster G, Pinkerton K, Pleus R, Shatkin J, Thomas R, Tolaymat T, Wang A, Wong J (2013a) A multi-stakeholder perspective on the use of alternative test strategies for nanomaterial Safety assessment. *ACS Nano* 7:6422–6433
80. Nel A, Xia T, Meng H, Wang X, Lin S, Ji Z, Zhang H (2013b) Nanomaterial toxicity testing in the 21st century: use of a predictive toxicological approach and high-throughput screening. *Acc Chem Res* 46:607–621
81. Nguyen KC, Zhang Y, Todd J, Kittle K, Patry D, Caldwell D, Lalonde M, Smith S, Parks D, Navarro M, Massarsky A, Moon TW, Willmore WG, Tayabali AF (2019) Biodistribution and systemic effects in mice following intravenous administration of cadmium telluride quantum dot nanoparticles. *Chem Res Toxicol* 32:1491–1503
82. Pan F, Han L, Zhang Y, Yu Y, Liu J (2015) Optimization of Caco-2 and HT29 co-culture in vitro cell models for permeability studies. *Int J Food Sci Nutr* 66:680–685
83. Papp T, Schiffmann D, Weiss D, Castranova V, Vallyathan V, Rahman Q (2008) Human health implications of nanomaterial exposure. *Nanotoxicology* 2:9–27
84. PATROLS (2020) <https://www.patrols-h2020.eu/>. Accessed 24 Apr 2019
85. Piccinno F, Gottschalk F, Seeger S, Nowack B (2012) Industrial production quantities and uses of ten engineered nanomaterials in Europe and the world. *J Nanoparticle Res* 14
86. Powell J, Faria N, Thomas-McKay E, Pele L (2010) Origin and fate of dietary nanoparticles and microparticles in the gastrointestinal tract. *J Autoimmun* 34:226–233
87. Saber AT, Mortensen A, Szarek J, Kalevi Koponen I, Levin M, Jacobsen NR, Pozzebon ME, Mucelli SP, Rickerby DG, Kling K, Atluri R, Madsen AM, Jackson P, Kyjovska ZO, Vogel U, Jensen KA, Wallin H (2016) Epoxy composite dusts with and without carbon nanotubes cause similar pulmonary responses,

- but differences in liver histology in mice following pulmonary deposition. *Part Fibre Toxicol* 13:37
88. Sadauskas E, Jacobson NR, Danscher G, Soltenberg M, Larsen A, Kreyling W, Wallin H (2009) Bio-disruption of gold nanoparticles in mouse lung following intratracheal instillation. *Chem Cent J* 3:16–23
 89. Samberg ME, Oldenburg SJ, Monteiro-Riviere NA (2010) Evaluation of silver nanoparticle toxicity in skin in vivo and keratinocytes in vitro. *Environ Health Perspect* 118:401–413
 90. SCCS (Scientific Committee on Consumer Safety), Opinion on ZnO (nano form) (2012) European Commission, Brussels, Belgium
 91. SCCS (Scientific Committee on Consumer Safety), ADDENDUM to the Opinion SCCS/1489/12 on Zinc oxide (nano form) (2014a) European Commission, Brussels, Belgium
 92. SCCS (Scientific Committee on Consumer Safety), Opinion on titanium dioxide (nano form) (2014b) European Commission, Brussels, Belgium
 93. SCCS (Scientific Committee on Consumer Safety), Opinion on titanium dioxide (TiO₂) used in cosmetic products that lead to exposure to inhalation (2020). European Commission, Brussels, Belgium
 94. Schimpel C, Teubl B, Absenger M, Meindl C, Fröhlich E, Leitinger G, Zimmer A, Roblegg E (2014) Development of an advanced intestinal in vitro triple culture permeability model to study transport of nanoparticles. *Mol Pharm* 11:808–818
 95. Semmler-Behnke M, Kreyling W, Lipka J, Fertsch S, Wenk A, Takenaka S, Schmid G, Brandau W (2008) Bio-distribution of 1.4 and 18 nm gold particles in rats. *Small* 12:2108–2111
 96. Sepehri M, Sejersen T, Qvortrup K, Lerche CM, Serup J (2017) Tattoo pigments are observed in the Kupffer cells of the liver indicating blood-borne distribution of tattoo ink. *Dermatology* 233:86–93
 97. Shrivastava R, Raza S, Yadav A, Kushwaha P, Flora SJS (2014) Effects of sub-acute exposure to TiO₂, ZnO and Al₂O₃ nanoparticles on oxidative stress and histological changes in mouse liver and brain. *Drug Chem Toxicol* 37:336–347
 98. Smulders S, Luyts K, Brabants G, Van Landuyt K, Kirschhock C, Smolders E, Golanski L, Vanoirbeek J, Hoet PHM (2014) Toxicity of nanoparticles embedded in paints compared with pristine nanoparticles in mice. *Toxicol Sci* 141:132–140
 99. Teigs G, Lohse AW (2009) Immune tolerance: what is unique about the liver. *J Autoimmun* 34:1–6
 100. TGA (Therapeutic Goods Administration). (2016) Literature review on the safety of titanium dioxide and zinc dioxide nanoparticles in sunscreens. Scientific Review Report. TGA, Department of Health, Australian Government. https://www.tga.gov.au/sites/default/files/nanoparticles-sunscreens-review-_2016_1.pdf
 101. Thakur M, Gupta H, Singh D, Mohanty IR, Maheswari U, Vanage G, Joshi DS (2014) Histopathological and ultra structural effects of nanoparticles on rat testis following 90 days (chronic study) of repeated oral administration. *J Nanobiotechnol* 12:42
 102. Vinardell MP, Mitjans M (2017) Alternative methods to animal testing for the Safety evaluation of cosmetic ingredients: an overview. *Cosmetics* 4:30
 103. Wang YX, Wang DW, Zhu XM, Zhao F, Leung KC (2012) Carbon coated superparamagnetic iron oxide nanoparticles for sentinel lymph nodes mapping. *Quant Imaging Med Surg* 2:53–56
 104. Xue Y, Chen O, Ding T, Sun J (2014) SiO₂ nanoparticle-induced impairment of mitochondrial energy metabolism in hepatocytes directly and through a Kupffer cell-mediated pathway in vitro. *Int J Nanomedicine* 9:2891–2903
 105. Yang L, Kuang H, Zhang W, Wei H, Xu H (2018) Quantum dots cause acute systemic toxicity in lactating rats and growth restriction of offspring. *Nanoscale* 10:11564–11577
 106. Zane A, McCracken C, Knight DA, Young T, Lutton AD, Olesik JW, Waldman WJ, Dutta PK (2015) Uptake of bright fluorophore core-silica shell nanoparticles by biological systems. *Int J Nanomedicine* 10:1547–1567
 107. Zhang X, Yin J, Kang C, Li J, Zhu Y, Li W, Huang Q, Zhu Z (2010) Biodistribution and toxicity of nanodiamonds in mice after intratracheal instillation. *Toxicol Lett* 198:237–243
 108. Zhu S, Zhang J, Zhang L, Ma W, Man N, Liu Y, Zhou W, Lin J, Wei P, Jin P, Zhang Y, Hu Y, Gu E, Lu X, Yang Z, Liu X, Bai L, Wen L (2017) Inhibition of Kupffer cell autophagy abrogates nanoparticle-induced liver injury. *Adv Healthc Mater* 6:1601252



Drosophila as a Suitable *In Vivo* Model in the Safety Assessment of Nanomaterials

Eşref Demir, Fatma Turna Demir,
and Ricard Marcos

Abstract

Nanotechnology is often praised as the future technology that will revolutionize the world as we know it, because nanomaterials (NMs) offer numerous practical applications for a wide range of fields such as medicine, cosmetics, food preservation, paintings, and industry. Produced by nanotechnology, NMs are in the front line of this innovative applied science, while nanoparticles (NPs) refer to materials existing in the natural world and measuring 1–100 nanometers in at least one dimension. The recent surge in the number of endeavors to utilize NMs makes it imperative to identify hazards and risk factors involved as we have yet to know harmful effects of this uncharted territory on the environment and public health. While researchers generally choose to carry out *in vitro* experiments in an effort to assess toxicity of NMs, *in vivo* approaches seem to yield better evidence that is more relevant to

risk assessment. In that context, *Drosophila melanogaster* stands out as the most dynamic model organism for biological experiments, since 75% of the genes responsible for human diseases are known to have homologs in *D. melanogaster*, which facilitates research into various pathologies. This book chapter aims to present the full picture of studies on separate NMs that employed *in vivo* approaches (toxicity, genotoxicity, internalization, cell uptake, tissue distribution, etc.) using *D. melanogaster*, attempting to offer an in-depth analysis of risks involved in exposure to NMs, as well as many advantages of other animal models used by nanogenotoxicology studies.

Keywords

Drosophila · Nanomaterials · Nanogenotoxicity · Larvae uptake · Hemocytes · SMART assay

E. Demir · F. T. Demir

Vocational School of Health Services, Department of Medical Services and Techniques, Medical Laboratory Techniques Programme, Antalya Bilim University, Antalya, Turkey

R. Marcos (✉)

Group of Mutagenesis, Department of Genetics and Microbiology, Universitat Autònoma de Barcelona, Barcelona, Spain

e-mail: ricard.marcos@uab.es

12.1 Background

Nanotechnology is a novel field of applied science that has been thriving with huge strides as it affords us ways to manipulate and fine-tune existing matter at extremely small scale. It encompasses every technology and science operating on the nanoscale, along with recently discovered scientific principles and properties during research involving such

small scales [188]. Nanoparticles (NPs) are commonly described as ultrafine or submicron particles that measure less than 100 nm in at least one dimension. Common examples of nanoparticles are silver, gold, nickel, and copper nanowires, nanorods, along with silica, metal oxides, carbon nanotubes, and nanocrystals. Bulk materials often display specific physical properties no matter what their size and dimension would measure, whereas at the nanoscale many of such properties are dependent on size and shape of the particle. Thus, nanomaterials may show significant variations not only in their chemical or physical qualities but also in their surface-to-volume ratio. This phenomenon is particularly more evident in metal oxide NPs that are characterized by large surface area, and this feature plays a pivotal role in their extraordinary physicochemical properties [82]. Owing to the unprecedented characteristics of such particles, nanotechnology is now called “the next big thing” [81], since it offers numerous practical applications across a range of fields such as medicine, electronics, cosmetics, agriculture, and food preservation. It was estimated that the amount of global nanomaterial production would reach 21,713 tons by 2020, while nanotech products generated a revenue totaling \$731 billion [123]. For this reason, the increasing presence of NMs at an accelerating rate demands meticulous research into their potential toxicity and genotoxicity, as well as identification of their interactions with biological systems [7, 87, 106].

We can now engineer NMs to render certain functions and qualities such as enhanced conductivity and strength or to create particles with high surface-area-to-volume ratio [175, 179]. However, these new qualities could lead to higher biological and chemical reactivity, which is likely to magnify the toxicity of NMs. When it comes to the toxicity of NPs, several key factors like particle shape and size, surface area coating are known to regulate their cytotoxicity [124]. To illustrate, smaller particles, as compared to large ones, have been found to exert higher toxicity to living cells [80]. It could therefore be argued that such increased toxicity might be associated with greater surface-to-volume ratio of NPs. Another concern is fiber-like NMs, whose length, shape, purity, and chemical composition may further

their toxic effects, as indicated by the WHO standards related to toxic potency of asbestos fiber exposure [120]. We can cultivate an in-depth understanding of NP-living cell interaction only by exploring and assessing the factors influencing biocompatibility and toxicity of NPs. Meanwhile, there are several reports suggesting that nanowires (NWs) might have toxic potency comparable to that of asbestos, and their crystal structure and greater aspect ratio may facilitate such toxicity [69]. Hence, research into engineered NMs over the past decades has focused on detecting the impact of exposure to these materials on living organisms [190]. One of the general mechanisms underlying toxicity, oxidative stress has been found to play a crucial role in NM cytotoxicity and genotoxicity [106]. Since DNA damage has been demonstrated to play a role in the initial steps of genetic mutations and cancer development, we may suggest that particles with a potential damaging effect on DNA might be involved in carcinogenesis [102]. In fact, research has revealed toxic potency of NMs on living cells through generation of reactive oxygen species (ROS) and DNA damage [109, 126, 145, 209].

Given the increased availability of NMs across the globe, it seems imperative to conduct full-scale and detailed investigation of nanomaterial toxicity and genotoxicity to humans and animals. Indeed, scientists from diverse fields have recently been looking into toxicity of NMs using *in vitro* and *in vivo* experiments. *In vitro* testing, though it may yield some valuable data, often fails to demonstrate what actually happens within a whole living organism, as it usually involves a prescreening method that utilizes various cell types and culture conditions [113]. On the other hand, factors like high costs and ethical concerns over the use of vertebrates in experiments have been severely limiting conventional *in vivo* testing. For that reason, researchers and international associations encourage to carry out toxicological studies with much simpler experimental models such as roundworms [41, 42, 56, 93, 132], zebrafish [61, 89], and a species of fruit fly known as *Drosophila melanogaster* [7]. Among these models, *D. melanogaster* appears to be the most dynamic and practical model organism in testing potential genotoxicity and cytotoxicity of NMs [62–64].

12.2 *Drosophila* in Exploring Potential Hazards of Nanomaterials

D. melanogaster has been gaining substantial attention from a wide range of fields of research, such as physiology, biology, genetics, microbial pathogenesis, and ecology. This species has afforded us invaluable insight into our physiology. As of today, six Nobel prizes have been awarded to scientists who made use of *D. melanogaster* in their studies as a testing model. Given that it is a most frequently tested species during the past years by biologists, geneticists, and toxicologists, *D. melanogaster* may well be the best-known eukaryotic organism across the globe.

The recent surge in the interest in using *D. melanogaster* as a model and its integration into various fields have not simply occurred by chance; the species owes this attention to its advantages over mammalian models, as it features a rapid life cycle [146], large offspring production per generation, substantially lower culturing costs, high fertility and fecundity [192], and its simple genetics featuring four pairs of chromosomes, which enable analysis of several generations within relatively short periods of time. Indeed, the culturing of *D. melanogaster* is so simple and easy that several space missions have bred and housed them on the space shuttle in an attempt to investigate the effects of zero gravity. Despite its relatively simpler nervous system, *D. melanogaster* exhibits complex motor behaviors, and can even be trained through fear conditioning to test memory and learning [14]. DNA sequence of the entire human genome was first mapped in 2003, after which comparative genetic research showed that humans share a large portion of their genes with many other animals, including *D. melanogaster*. Such analyses calculated that around 60% of *Drosophila* genome is identical to human genome, and about 75% of genetic material responsible for diseases in humans, including diabetes, autism, and cancer, has a functional homolog in fruit flies [122]. It can be used as an ideal model in the studies investigating underlying mechanisms of aging, immunity, neurodegenerative disorders, and oxi-

dativ stress [30], Alzheimer's disease [137], and spinocerebellar ataxia [111].

D. melanogaster also shares a range of basic biological mechanisms and molecular pathways with mammals [149, 208], and this makes it a dynamic testing model for neurotoxicity screening [169], as well as pharmacological and genotoxicity research [149]. Most importantly, using *D. melanogaster* allows academic researchers to bypass today's desperately familiar ethical issues regarding the use of vertebrates, or relatively large mammals, in animal experiments [97]. The advantages of this species in toxicity and genotoxicity studies could be summarized as follows:

- It has a remarkable fecundity and reproductive capacity. Under ideal conditions, a female fruit fly can produce 615 offspring on average throughout her life [51].
- Culturing and housing procedures require little care, space, and readily available inexpensive equipment.
- Anesthetizing can be done through simple and cheap material such as ether, carbon dioxide or through cooling.
- *Drosophila* has a rapid and short life cycle (9–10 d at 25 °C) (Fig. 12.1).
- It has 4 pairs of chromosomes, which contribute greatly to our understanding of heredity.
- *D. melanogaster* males do not show meiotic recombination, such as crossing over, which is a trait that facilitates genotoxicity research.
- Like humans, they are classified as eukaryotes, with a well-established DNA arrangement that can be used as a genetic model for higher eukaryotes.
- Abundant knowledge exists regarding the techniques employed for transforming *Drosophila* cell lines.
- Extensive literature affords huge amounts of data on *D. melanogaster* life cycle consisting of embryogenesis, larval, pupal, and adult stages.
- Gynandromorphs, or sexual mosaics with both male and female tissues, can be easily produced, which provide additional tools to investigate developmental processes and genetic mutations.

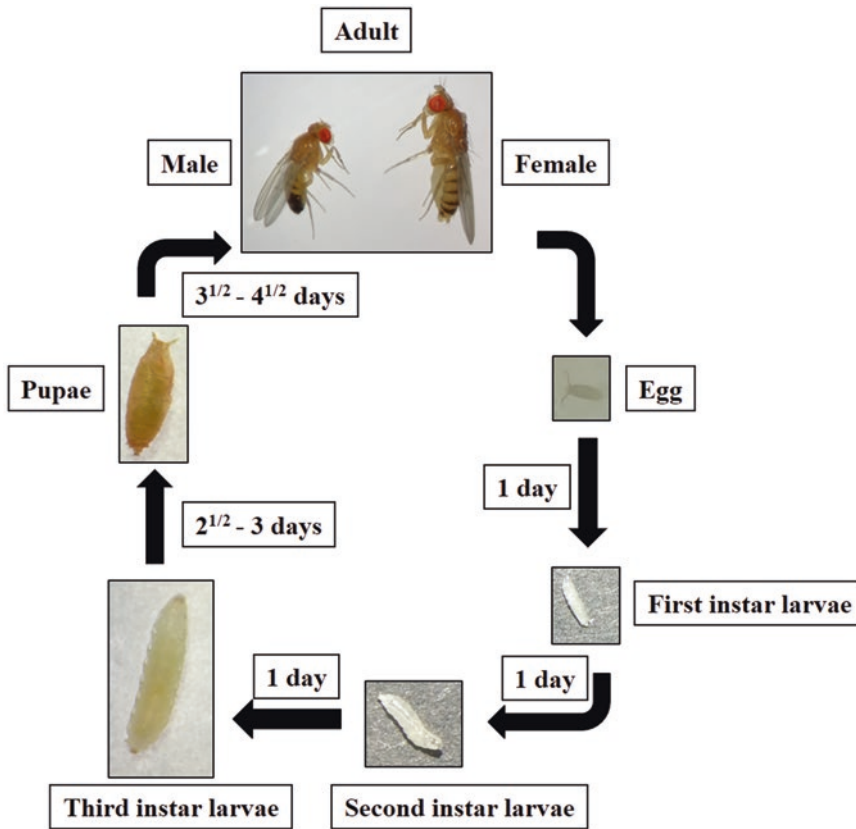


Fig. 12.1 The life cycle of fruit flies is characterized by four key stages: embryo, larva, pupa, and adult. The eggs hatch to give first-instar larvae after 6 to 8 hours, which

grow into second and third instar larvae. On around the fifth day, the larvae become pupae. In the final stage, the adult fruit fly emerges on the ninth or tenth day

The above-mentioned advantages have motivated researchers to employ *D. melanogaster* as a go-to model in assessing toxicity of NMs. The first study to examine the impacts of exposure to NMs on *D. melanogaster* was performed by Strawn et al. [193], and after that study a large amount of research has used this species as an experimental organism to assess the cytotoxicity, genotoxicity, internalization, generation of reactive oxygen species (ROS), morphological deformations, and changes in gene expression occurring upon exposure to various NMs.

D. melanogaster has been employed in toxicity research so frequently that a new research field known as ‘drosophotoxicology’ has recently emerged [169], and it utilizes several methodological approaches on *D. melanogaster* [48]. *In vivo* toxicity assays designed to test nanoparticle exposure in *D. melanogaster*

include mode of delivery to the organism and certain endpoints to detect toxic effects. Thus, mode of delivery plays a particularly important role in exposing *Drosophila* cells or organ systems to NPs, and such modes include embryonic exposure by means of maternal feeding, direct injection into embryos, and direct incubation of embryos. Adult flies are easily exposed to various NP concentrations through ingestion, direct injection, and aerosol in test settings. Acute or chronic toxicity caused by nanoparticles can then be assessed by task-specific assays to characterize survival, fertility, DNA damage, neurological health, and morphological defects [12, 62, 66, 170, 200]. The interest in employing this model in NM toxicity studies is growing every year, as shown in Fig. 12.2, while the total number of studies is shown in Fig. 12.3.

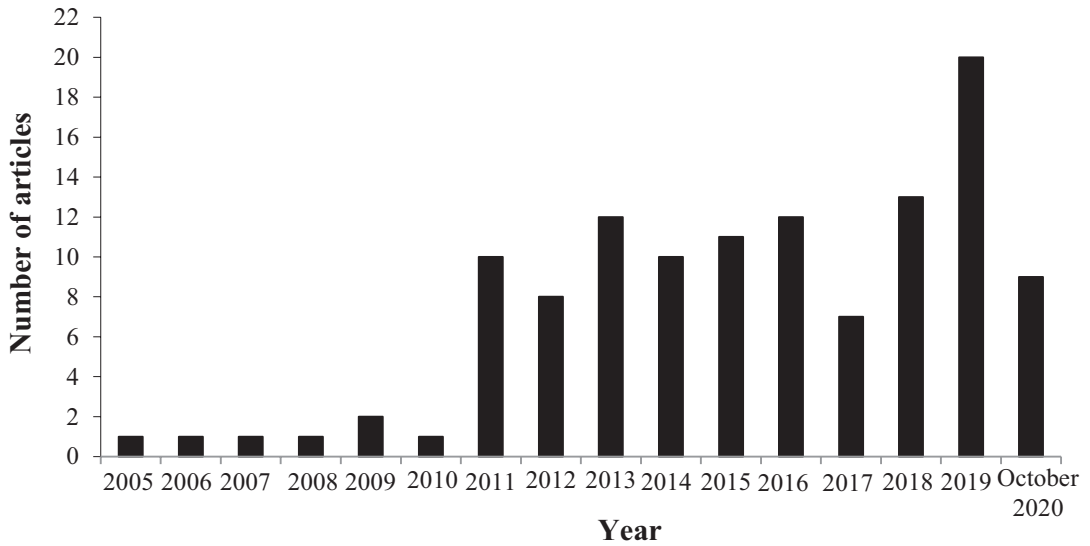


Fig. 12.2 The bar chart illustrates the annual number of research articles featuring *Drosophila* as testing model to explore the effects of nanomaterials. It covers a time interval from the first *Drosophila* study (2005) to October 2020

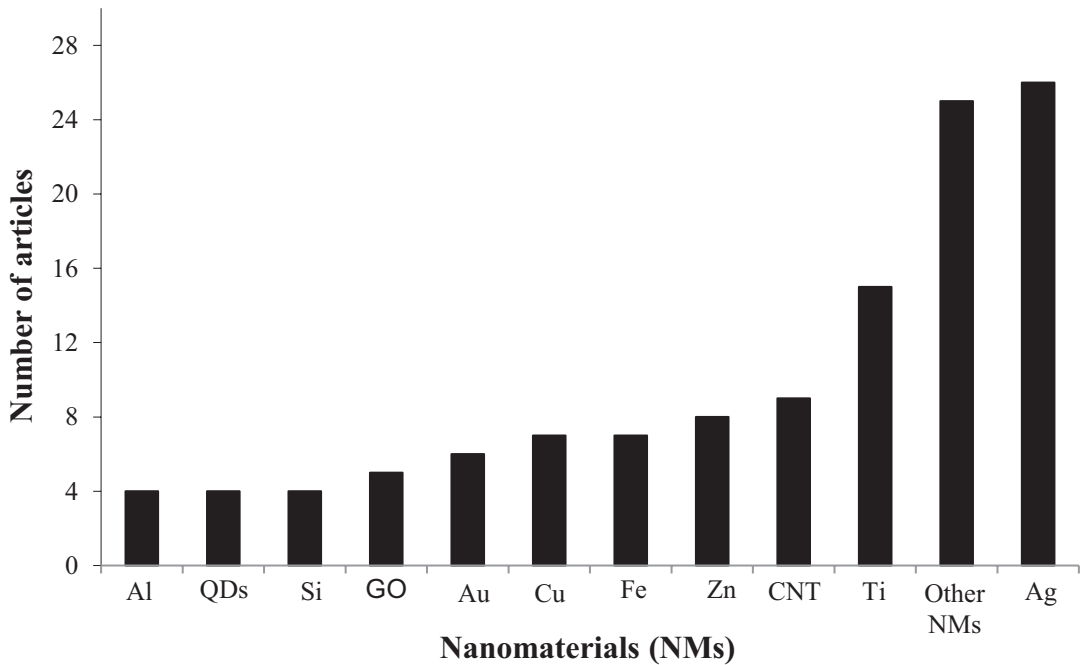


Fig. 12.3 The bar chart illustrates the number of different types of NMs exposed to *Drosophila* in toxicity studies and the number of articles featuring such materials

12.3 Research on Gold Nanoparticles

Gold is a precious metal used for minting coins, making jewelry, and in several arts and crafts throughout human history. It remains solid under standard conditions and is among the least reactive elements. The larger gold particles are inert and solid and they appear yellow, whereas gold nanoparticles (AuNPs) are different in both appearance and reactivity, as AuNPs appear as a red compound once dispersed in water. In recent years, AuNPs have been attracting a great deal of interest thanks to their chemical stability, convenience for synthesis, along with excellent optical qualities [13].

In medical science, AuNPs have traditionally been used for treating rheumatoid arthritis, and are an integral part of certain medical applications. They also exhibit strong electric fields in places close to their surface area, which considerably improves the absorption and scattering of electromagnetic radiation, so these particles have been employed in light-based cancer therapy. However, we have limited evidence on their intracellular activity – further research is needed to detect any potential toxicity [20, 49, 79].

Potential harmful impact of AuNPs on *Drosophila* was first explored by Pompa et al. [161], who observed that they caused a significant reduction in fertility and life span. They also examined several other biological and developmental aspects of *D. melanogaster*, reporting serious impacts on reproductive capacity, DNA damage, and apoptotic/necrotic events. Their study showed that genotoxicity from exposure to AuNPs was associated with increased ROS production and p53 protein. Another study by Vecchio et al. [203] examined toxicity of AuNPs in *D. melanogaster* and found significant genotoxicity, implying a disturbing long-term effect after exposure to AuNPs, since they observed phenotypic alterations in the subsequent generations. Furthermore, they tested potential toxic effects of AuNPs in different sizes and a broad dose range [204]. Their results showed that concentration of AuNPs played a key role in determining toxicity, whereas surface area was not a

critical parameter. They observed some detrimental effects including shorter life span, lower fertility, and damage to DNA. Concentration-dependent toxicity of AuNPs was evidenced by the overexpression of stress genes (*hsp70* and *hsp83*), DNA damage (*p53*), and apoptotic (*Dronc*) biomarkers, all of which suggested that the toxicity of AuNPs could be associated with ROS induction [204].

Besides, AuNPs have been tested to investigate their toxic potency on living organism's metabolism. For example, Wang et al. [208] reported that exposing *D. melanogaster* larvae to AuNPs caused accumulation in key metabolic tissues. Even if the increase in lipid levels leads to non-cellular stress responses, PI3K/Akt/mTOR signaling pathway and fatty acid metabolism were observed to increase. Their study revealed a new function of AuNPs in animal metabolism, suggesting novel therapeutic uses in the fight against metabolic disorders. The impact of AuNPs on *D. melanogaster* embryos were examined through direct microtransfer of NMs to embryos at predicted environmental concentrations [205]. These authors found that AuNPs smaller than 150 nm in diameter showed statistically admissible effects on the viability of *D. melanogaster* embryo, with reduced overall mortality. More recently, the potential genotoxic effects of 30 nm AuNPs were evaluated in the somatic mutation and recombination test (SMART), indicating that such exposure induced no mutagenic or recombinogenic activity [22]. From the foregoing discussion, we can gather that despite the promising future of AuNPs in medical and biological applications, its exposure may potentially induce harmful effects, thus precautions should be taken before and during the use of nanoscale gold particles.

12.4 Research on Silver Nanoparticles

With the development of nanotechnology, silver nanoparticles (AgNPs) have for some time been included in the ingredient lists of several products besides bulk and microparticle forms of sil-

ver. AgNPs possess outstanding electrical, optical, thermal properties, and promising antimicrobial activity [71, 108, 114]. Silver NPs are commonly utilized in products designed for therapeutic purposes, particularly for the treatment of burns [39], thanks to their remarkable antimicrobial activity [139]. This widespread use also raised some concerns over their potential side effects, so an appreciable amount of research has been performed to assess the extent of their toxicity. Research into toxicity of AgNPs shows that ionic silver (Ag^+) leakage and silver oxidation are what causes AgNPs to be toxic [147]. Such toxicity has been associated with the induced ROS. The roles of endocrine disruption mechanisms and ion release have not been explained completely [129].

D. melanogaster has been used as a model to demonstrate the extent of cytotoxic, genotoxic effects, physiological, developmental and fertility alterations and induction of oxidative stress caused by AgNPs [2, 18, 21, 40, 66, 83, 85, 88, 107, 148, 158, 162, 163, 198, 199, 205]. Furthermore, Phatak et al. [157] carried out a study on *D. melanogaster* where they compared nano and micro silver particles to explore the influence of particle size in pigmentation. Their results showed that both nano and micro silver particles mediated leucism, or partial loss of pigmentation, confirmed by the absence of PO activity, lower melanin and tyrosine values. Another study conducted by Ong et al. [146] looked into the toxicity induced by different concentrations of AgNPs on spermatogenesis in *D. melanogaster*. They reported that exposure to AgNPs reduced the fly's viability and caused developmental delays at certain doses. Upon exposure to AgNPs, the testes showed a marked increase in levels of ROS and prematurely developed GSC differentiation, suggesting that AgNP exposure could ultimately lead to a decline in the number of GSC.

On the other side, Raj et al. [165] examined dose-dependent effects of AgNPs by ingestion in adult flies for short and long periods. They found significantly affected egg laying capability and growth of ovaries. Furthermore, dietary exposure to AgNPs in the larval stage was reported to pro-

duce strong effects on decreased longevity, survival, and egg laying capability. Another study published by Raj et al. [166] in the same year reported that dietary exposure to AgNPs during the early larval phase caused behavioral abnormalities. Higher doses of AgNPs caused significant changes in metabolic activity of adult flies such as carbohydrate, lipid, and protein levels. Based on the increased production of ROS in larval tissues, they concluded that exposure to high amounts of AgNPs was detrimental and raised concerns over the use of AgNPs in products for personal or home use. The potential acute and chronic toxicity of AgNPs was tested in *D. melanogaster* through the analysis of parameters including fecundity, hatchability, viability, larva to adult development, and pigmentation upon exposure to AgNPs at different concentrations, and no acute and chronic toxicity was observed in the first generation of *D. melanogaster*, with all the flies completing their full developmental cycle [197]. On the other hand, Mao et al. [128] explored possible adverse effects of dietary AgNPs on *D. melanogaster*, observing that lethal amounts of dietary AgNPs caused delays in development of flies and significant mortality in young adult flies. Contrarily, exposure to sublethal doses caused reductions in the adult lifespan and affected the fly's tolerance to oxidative stress. Notably, dietary exposure to AgNPs induced a diverse range of stress responses, such as DNA damage, apoptosis, and autophagy. The genotoxic effects of AgNPs have recently been studied in specific larval cells of *D. melanogaster* playing crucial roles in immune response and development. The controlled study showed that AgNPs hampered the metamorphosis and reduced the number of pupae and young adults in a dose-dependent manner, as compared to controls. Each concentration of AgNPs (25, 50, 100, 200, and 300 mg/L) suppressed the conversion of pupae into adult flies, with an enormous decrease at doses of 100 mg/L and above [27]. On the other side, Meng et al. [131] explored the possible underlying mechanisms for the toxicity of AgNPs using SDS-PAGE and mass spectrometry analysis, revealing that the expression levels of proteins such as ATP kinase, heat shock protein,

and glucose metabolism related enzymes increased with higher concentrations of AgNPs, which in turn reduced the survival rate of *D. melanogaster* and promoted apoptosis, providing a theoretical basis for toxic mechanism of AgNPs. Finally, by exposing larvae it was demonstrated that AgNPs had the capacity to pass through the intestinal barrier and induce DNA damage by oxidative stress in hemocytes [11].

12.5 Research on Iron Oxide Nanoparticles

Iron oxide NPs (FeONPs) are markedly biocompatible and biodegradable, inducing little or no toxicity. Accordingly, these particles are employed in iron supplements for anemia, and also in biomedical procedures such as drug delivery, vascular imaging, gene therapy, and cleaning up the environment [84, 116, 215]. Research into their possible toxicity or genotoxicity has shown that particle size, surface charge, morphology, and coating could regulate the extent of their impact [17]. In the past decade, several *in vivo* studies investigated the toxicity of FeONPs on *D. melanogaster* [46, 205]. In their study, Vega-Alvarez et al. [205] directly introduced FeONPs into the embryonic cells via microinjection and observed substantial increase in cell mortality, confirming the lethality of FeONPs during the embryonic stage. Furthermore, Chen et al. [46] concluded that exposure to high doses of magnetite NPs could cause a reduction in survival and fecundity among young female flies.

Contrarily, a more recent study involving the *in vivo* toxicity assessment of FeNPs at varying doses in *D. melanogaster*, reported that there was no statistical difference in viability and reproductive ability between the controls and exposed flies. Their wing-spot assay showed lack of toxicity at the tested doses, and analyses confirmed that this remained intact in the exposed larvae, hence the lack of toxicity of FeNPs. Thus, they concluded that FeNPs was neither genotoxic nor mutagenic at the defined concentrations [154]. Furthermore, dietary FeONPs administration suggested to delay aging

and mitigate neurodegeneration in *D. melanogaster*. Thus, the experiments carried out by Zhang et al. [217] demonstrated that FeONPs had high biocompatibility with *D. melanogaster*, intracellular FeONPs levels protecting cells from H₂O₂ induced oxidative stress and apoptosis. More significantly, dietary FeONPs were found to reduce ROS in adult flies, enhancing their climbing ability, and prolonging their life span. Furthermore, their results suggested that FeONPs could display catalase-like activity, reducing intracellular oxidative stress, protecting against neurodegeneration, and delaying the aging process [217]. Regarding the potential genotoxicity of Fe₂O₃NPs, the study of Kaygisiz and Cigerci [105] demonstrated the lack of genotoxicity in fruit flies through the use of SMART assay. Finally, a recent study has looked into the capability of FeONPs to cross the blood-brain barrier and localize in the brain by exposing *D. melanogaster* to super-paramagnetic FeONPs. Upon examination of the brains of third-instar larvae, they detected particles in the optic lobes of larval brains, which confirmed that these particles passed through the blood-brain barrier. However, they reported that there was no apparent systemic toxicity impairing viability in the exposed flies [213]. More recently, low toxic effects of Fe₃O₄NPs (uncoated, and citric acid-coated) in *D. melanogaster* have been reported [133]

12.6 Research on Titanium Dioxide Nanoparticles

Since the FDA granted approval for their use in foods, drugs, and cosmetics [52], titanium dioxide (TiO₂) has been commonly utilized across a range of sectors. TiO₂ nanoparticles exhibit photocatalytic and anticorrosive properties, and excellent stability, thus are regarded as reliable versatile material [167]. These NPs could be found in consumer products, pharmaceuticals, paints, and medical substances. TiO₂NP exposure has been reported to trigger inflammatory responses, oxidative stress, and damage to DNA [44, 45, 94, 119, 189].

TiO₂ is utilized to provide brightness and white opacity in several products, such as toothpaste, inks, plastics, paints, and it represents around 70 percent of pigment production across the globe [43]. Nanoparticle forms of TiO₂ are now employed in cosmetic products combined with zinc oxide (ZnO) particles to afford more protection from UV radiation. However, in its recent report, the International Agency for Research on Cancer (IARC) classified the raw powder form of TiO₂ as a Group 2B carcinogen, stating that it is “possibly carcinogenic to humans by means of inhalation” [95]. Furthermore, several studies suggest that nanoparticles of TiO₂ have the capacity to cause greater toxicity than that of microparticles [103, 180, 196, 212].

Possible detrimental effects of TiO₂NPs have been tested *in vivo* on *D. melanogaster*. For instance, *Drosophila* larvae were exposed to varying doses of TiO₂NPs with no serious impact on survival rate or healthy development [163], but they observed notable changes in gene expression levels of SOD activity. Such findings seem to contradict those indicating that exposure to 50 nm TiO₂NPs caused considerable progeny loss in *D. melanogaster*, corresponding to a marked decline in productivity [158]. Besides, it has recently been reported that larval exposure to TiO₂NPs induced no reduction in survival but caused prolonged pupal stage. Although TiO₂NPs were translocated into *Drosophila* larvae, this presence was not observed in adult flies following metamorphosis course [100]. Another study reported cytotoxic effects of TiO₂NPs (<25 nm) in mid-gut and imaginal disc tissues of *Drosophila* larvae [35]. Using a new method of microinjection during the embryo stage, Vega-Alvarez et al. [205] detected that environmentally applicable amounts of TiO₂NPs induced marked changes during embryonic development. Exposing *Drosophila* larvae to TiO₂NPs measuring 2.3 nm during all developmental stages, did not induce mutagenic effects when the wing-spot assay was used [67]. Relatively comparable results obtained through wing-spot assay were also reported by Carmona et al. [35]. Examination of primary DNA damage in hemocytes revealed significant genotoxic effects. Such results appear to be asso-

ciated with certain characteristics of nanoparticle forms, because no genotoxic response has been observed after exposure to the bulk forms of TiO₂ [35]. Similarly, Reis et al. [171] evaluated the genotoxic effects of titanium dioxide nanocrystals (TiO₂NCs) through the wing-spot test observing that only the smallest particles might induce mutagenic effects, while larger particles (only 2.8 nm larger) caused no DNA damage.

The toxicity of TiO₂NPs was examined by exposing *D. melanogaster* to nanoparticles via oral route, life cycle, their survivability, and behavior upon mechanical stimulus. Results indicate that TiO₂NPs exposure increases ROS generation, which could modify multiple signaling pathways, altering the developmental and behavioral patterns of the fly [174]. Another dietary exposure experiment involving E171, an inactive food ingredient containing TiO₂NPs nanoparticles, using the equivalent to the estimated daily human consumption dose, was carried out for 20 generations. Substantial changes were noted in healthy developmental and reproductive processes, lower fecundity, higher genotoxicity, aberrant morphology and phenotypes. These findings appear to be particularly alarming, because children, as compared to adults, often consume greater amounts of E171 on a daily basis [101]. Food additives containing sugar, surfactants, sodium chloride, as well as metal oxide nanoparticles have been associated with increased prevalence of diseases related to increased intestinal barrier permeability. Recent research into the impact of food additives on gut barrier has been performed on *D. melanogaster* to investigate the mechanisms underlying the role of diet in gut function and permeability. In this context, it has been reported that TiO₂NPs in food additives had insignificant effects on survival and intestinal permeability in *D. melanogaster* [156]. Another study investigated whether TiO₂NPs could damage intestinal function, epithelial tissues, metabolic homeostasis, observing that TiO₂ ingestion caused a reduction in size, and glucose content, thus suggesting that TiO₂NPs altered glucose transport through the intestinal epithelium and ingestion of TiO₂NPs may lead to certain physiological consequences [172]. Regarding

the potential genotoxicity of TiO₂NPs it has been found to increase significantly the frequency of somatic recombination in the wing-spot SMART assay [141], as well as in the eye-spot SMART assay, but negative in the comet assay using neuroblasts [178]. The genotoxic evaluation (comet assay) of TiO₂NPs in different shapes (i.e. nanowires, nanorods, and nanospheres) in hemocytes from *D. melanogaster* larvae, indicate that ROS and DNA damage occurred at the highest concentration tested (10 mM) [62]. Finally, a recent study has examined the impact of a constant exposure to low concentrations of TiO₂NPs, similar to normal human dietary consumption. The study reported that although TiO₂NPs induced certain changes in the wing morphology, these changes fall within the normal allowed wing variation [57].

12.7 Research on Zinc Oxide Nanoparticles

Zinc is an essential element to regulate a range of biological functions, including cell growth, gene expression, and immunity [181, 202]. ZnONPs display high tissue compatibility [219], manufacturability, and producibility [207], so they are employed in a wide range of applications, including biomedical imaging [91], drug delivery in chemotherapy [136], and immunotherapy for cancer [3]. However, ZnONPs may also lead to some detrimental biological responses, since they dissolve once they are internalized by cells under certain physical conditions (a pH value below 6.7 at normal body temperature) [75].

Like other engineered NMs, ZnONPs are often employed in various commercial products, including paints, antibacterial agents, coating solutions, and textiles [55, 118, 138]. Whether exposure to ZnONPs causes cellular responses through direct impact of such particles [140] or through the release of Zn²⁺ ions [33] is not certain yet. There is research that suggests ZnONPs could be causing damage to biomolecules due to elevated ROS [182], which might also hinder

several vital mechanisms for the integrity of DNA [68]. Other factors like particle shape and size have been suggested to play some role in their interaction with living tissue [177]. Surface coating can also be influencing bioreactivity of nanoparticles, or their interactions with cells, through adsorbed proteins on the nanoparticle surface, a process known as corona formation.

In their study, Siddique et al. [185] used *D. melanogaster* to assess the potential toxicity of graphene ZnO nanocomposites (GZnONCs), and found a dose-dependent rise in the number of apoptotic cells, genotoxic effects, and in the levels of oxidative stress. These findings seem to contradict a relatively recent study that reported no apparent toxicity or oxidative stress, nor any significant changes in the frequency of mutant clones or DNA breaks [4]. A paper by Siddique et al. [186] found that Cu-doped ZnONPs have no toxicity, because climbing ability and activity patterns of flies were observed to remain normal. Furthermore, Carmona et al. [36] reported no genotoxicity after exposure to amorphous ZnO and ZnONPs, but both amorphous compounds were found to induce oxidative stress and DNA damage in the comet assay, as measured by the malondialdehyde levels. In the study of Ng et al. [142] the toxicological profile of ZnONPs was determined evaluating the uptake, cytotoxicity, gene expression profiling, generation of ROS, and genotoxicity caused by exposure to ZnONPs. The obtained results indicate a decline in egg-to-adult viability. In addition to this decline in viability, exposure to ZnONPs brought about notable delay in normal development of flies. Chronic exposure to ZnONPs (<50 nm) was reported to cause distinctive phenotypic changes, such as deformed segmented thorax and single or deformed wings, and such changes were transferred from one generation to the next [15]. In an attempt to determine the toxicity profiles of ZnONPs, a dramatic increase in ROS levels were observed [143], while homologous recombination was the primary mechanism to give rise to loss of heterozygosity in fly somatic cells [34].

12.8 Research on Quantum Dots

Quantum dots (QDs) are engineered nanoscale crystals with a capacity to transport electrons. These semiconductor nanoparticles can emit light of various colors under ultraviolet light, so they have been used in applications such as solar cells and fluorescent biological labels. They possess promising photochemical properties useful in diagnostic imaging methods, electronics, and biosensors [218]. Quantum dots are characterized by extremely small size (1–10 nm) and an internal core surrounded by one or two shell layers [98]. Potential health risks of exposure to quantum dots are brought about by their shape and chemical nature, as they often incorporate high-risk heavy metals like cadmium (Cd), mercury (Hg), lead (Pb), or arsenic (As) [201]. So far, several *in vivo* studies have examined the potential effects of QDs on *D. melanogaster*. For instance, Posgai et al. [162] devised a new system for exposing flies to QDs through inhalation that effectively aerosolized QDs at varying sizes. They successfully delivered red fluorescent CdSe/ZnS NPs to the respiratory system of *Drosophila* and visualized the particles in the fly's tracheal system by means of fluorescent microscopy.

Several strategies like utilization of biocompatible coatings were proposed to minimize QD-induced toxicity. The role of coatings as a possible mediator of toxicity has been examined on *D. melanogaster*. Galeone et al. [77] compared the impact of several surface coatings on diminishing leaking of metal ions from CdSe-based QDs, which include mercaptoundecanoic acid, polyethylene glycol coating, polymer coating with polymaleic anhydride octadecene. However, all such coatings failed to prevent survival distress caused by CdSe-based QDs. Interestingly, the decline observed in the life span of *D. melanogaster* was depending on the type of coating. We should underscore that the toxicity induced by Cd-based QD exposure was associated with the release of Cd²⁺ [194] or increased ROS generation [50, 76]. Likewise, in the study of Galeone et al. [77] the authors detected that coating-related ROS generation was linked to

time-dependent degradation observed in all QDs, with significant release of Cd²⁺ ions, which could account for the reduced longevity of flies exposed to ODs.

In their study, Brunetti et al. [32] detected expression of genes *Hsp70*, *Hsp 83*, *p53*, and *Dredd* in *D. melanogaster* after exposure to 100 and 500 pM InP-QDs or Cd-QDs, along with necrosis and induction of apoptosis. Cd-QDs were found to cause changes in expression of all analyzed genes, besides greater apoptotic rate. Such results suggest that *D. melanogaster* is prone to spot subtle effects. Another study employed *D. melanogaster* to test potential effects of CdSe QDs on biodegradation [5]. The researchers detected potential release of Cd²⁺ from QDs by comparing it to a free source of Cd ions (CdCl₂). CdSe QDs were found to pass through the intestinal barrier of *Drosophila* larvae, interacting with hemocytes, reaching the hemolymph, and causing serious genotoxic effects. Besides elevated levels of ROS, they observed significant disruption in *Hsp*, antioxidant and *p53* genes and QD-induced biodegradation. Despite certain detrimental effects of CdSe QDs, such instances were still considered milder than those caused by CdCl₂. The described studies highlight the limitations of QD composition relevant to toxicity. It has been suggested that cytotoxicity and genotoxicity of QDs depend on their surface chemistry in different systems. Despite the association of genotoxicity with oxidative stress, this can partially explain the cytotoxicity and genotoxicity induced by QDs, therefore other mechanisms of action that have yet to be found must be in operation [127].

12.9 Research on Silica Nanoparticles

Silicon (Si), one of the most commonly found elements in the world, has ushered in what is known as the Silicon Age. With its high chemical affinity to oxygen, it has several oxide forms including silicate (SiO₄) and silica, or silicon dioxide, (SiO₂). Silicates naturally occur in a large number of minerals that comprise about

90% of the Earth's crust. Silicon is often used in electronic components of daily life like computers and smartphones, whereas its oxide forms are often utilized in biomedical applications. Silica nanoparticles (SiNPs) exhibit a wide range of unique properties such as modifiable surface and inert chemical composition and are favorable materials, due to their thermal stability and low production costs, that can be modified to create porous carriers for targeted drug delivery [25]. They are also extensively employed in cosmetics, foods, drugs, and chemical-mechanical planarization [115]. Furthermore, SiNPs offer great promise in gene therapy applications, as contrast agents for diagnostic imaging, and hyperthermia to improve the efficacy of cancer treatment [24, 28, 155].

As for *in vivo* toxicity of SiNPs, a number of studies have used *D. melanogaster* to determine whether SiO₂NP exposure carries toxic or genotoxic risks [26, 68, 150]. In the study by Barandeh et al. [26] authors tested SiO₂NPs on *D. melanogaster* and reported the exposure caused no significant impact on neuronal cell bodies and axonal projections. However, when the larvae were exposed to SiO₂NPs, a significant uptake was observed in the midgut cells of larvae. Subsequently, internalization of SiO₂NPs led to a significant elevation of oxidative stress levels. In another study, exposure to SiO₂NPs was also found to significantly increase expression of *hsp70* and *hsp22* genes, along with membrane destabilization, caspase activation, and potential loss of mitochondrial membrane [150]. Such seemingly conflicting findings might be explained by the use of different types of SiO₂NPs, and also by the experimental exposure adopted. In order to explore the potential role of particle size in toxicity and genotoxicity, Demir et al. [68] utilized four different sizes (6, 15, 30, and 55 nm) of SiO₂NPs. When third-instar *D. melanogaster* larvae were exposed to all sizes of SiO₂NPs, no significant changes occurred in the frequency of mutant clones. All tested SiO₂NPs, particularly at high doses, caused a significant increase in primary DNA damage. The complementation of the comet assay with formamidopyrimidine DNA glycosylase (FPG) and endonuclease III (EndoIII)

enzymes demonstrated that such primary DNA damage was, to a large extent, linked to oxidative damage to DNA. Higher levels of DNA damage were observed upon exposure to larger SiO₂NPs (55 nm), which highlights the importance of including different sizes of particles when it comes to testing the potential effects of NMs. Finally, a more recent study conducted by Sapre et al. [176] used adult *D. melanogaster* to investigate pH-responsive cargo release from the widely used mesoporous silica nanoparticles (MSNPs) coated with pH-sensitive polydopamine (PDA) and polyethylene glycol (PEG) polymers. The researchers found that both types of MSNPs ruptured around the acidic midgut of the flies. This study suggests that the *Drosophila* gut can be utilized to test pH-responsive biocompatible materials.

12.10 Research on Copper Nanoparticles

Copper is regarded as an essential element for human health as we need it for many biological functions and plays a crucial role in cellular processes like signal transduction and neuronal activity [73]. Copper-based NPs (CuNPs) have recently been attracting attention with their great promise in biomedical and industrial applications. The increased presence of copper oxide NPs (CuONPs) in the environment resulting from their widespread use in consumer products has raised concerns over their possible adverse risks to humans [173]. As in other NPs, the debate over the main causative factors underlying CuONP-mediated risks still prevails, since we still have inadequate evidence to reach a conclusion about the underlying mechanisms of their toxicity. Several studies have looked into the toxicity of CuONPs using *D. melanogaster* as a testing model. One study reported that CuONPs could penetrate into midgut cells and subsequently localize in internal hemolymph, reducing larval growth, decreasing viability, and delaying egg hatching at higher doses [8]. Exposure to low doses of graphene copper nanocomposites (GCuNCs) had previously yielded similar out-

comes with no considerable toxic effects after exposures for 24 and 48 hours. However, analysis of several parameters such as *hsp70* expression, β -galactosidase activity, oxidative stress, total protein, and apoptotic rate and DNA damage at higher doses of GCuNCs revealed serious hazardous impacts [184]. Conversely, exposure to CuNPs failed to cause any adverse effects during developmental stages of *D. melanogaster* [85]. Carmona et al. [37] reported that exposure to CuONPs caused DNA strand breaks, along with higher frequency of somatic mutations and recombination events, partially explaining oxidative stress generation. These genotoxic effects are close to the threshold, and the deviation of such values might explain the lack of impact reported by Alaraby et al. [8], where CuONPs showed no genotoxic potential, probably thanks to their inability to elevate generation of ROS. Detrimental genotoxic effects of CuONPs were observed only at high doses (10 mM), whereas significant down-regulation of *Hsp70* and ROS induction in the hemocytes of third-instar larvae were detected at all doses.

CuONPs have also been proposed as promising antitumor agents. A study by Alaraby et al. [9] tested whether CuONPs could induce anti-genotoxic effects by using *D. melanogaster* as an experimental model. They used wing-spot assay and comet assay as biomarkers of genotoxicity. The impact of CuONP exposure was compared with that of copper sulfate (CS) exposure. CuONPs and CS failed to reduce the genotoxic effects of EMS exposure, however they managed to decrease the effects induced by potassium dichromate, diminishing the frequency of mutant twin-spots resulting from mitotic recombination. Similar qualitative anti-genotoxic effects were observed in both Cu compounds [9]. Possible mechanisms underlying CuONP-induced toxicity were also investigated by Baeg et al. [23]. Thus, oral administration of CuONPs was found to accumulate throughout the body, causing a decrease in egg-to-adult survival and a developmental delay. CuONPs were also detected inside the intestinal epithelial cells and lumen, while a dramatic increase in apoptosis and reactive oxygen species was observed in the gut. Authors

found that inhibition of the transcription factor Nrf2 further enhanced the toxicity, suggesting that CuONPs disrupt the gut homeostasis and that oxidative stress serves as one of the primary causes of CuONP-induced toxicity in *Drosophila*. Lastly, Carmona et al. [38] used the wing-spot assay to compare the genotoxic activity of CuNPs and nickel NPs to those obtained with their microparticle (MPs) forms. Their results showed that both CuNPs and CuMPs failed to induce an increase in the frequency of mutant spots formation in the wings of the adults, suggesting a lack of genotoxicity in somatic cells of *D. melanogaster*. However, NiNPs at the highest dose caused a significant increase in small single spots and total mutant spots. It was concluded that the genotoxicity of NPs could be related to their nanoscale size, because no genotoxic effects were observed in their microparticles and ions, supporting the view that the nanoparticulate form of copper is responsible for most of the observed harmful effects.

12.11 Research on Aluminum Oxide Nanoparticles

Aluminum (Al) is the most abundant metal in the world, as it makes up approximately 8% of the Earth's crust, and the third most common element after oxygen and silicon. Al is one of the key engineering materials of our time thanks to its unique qualities such as lightness, durability, and functionality. However, there have been serious concerns over aluminum-induced toxicity, and the fibrous form of aluminum oxide (Al_2O_3) is currently listed as toxic under the Toxics Release Inventory of Environmental Protection Agency [16]. With the development of nanotechnology, the nanoparticle form of Al_2O_3 offers a wide range of applications that might cause exposure to humans, thus calling for urgent insight into its biological interactions. In a recent study, the risks of chronic exposure to Al_2O_3 NPs via ingestion, throughout their lifespan, were investigated by screening the progeny flies for behavioral and phenotypic abnormalities. Chronic exposure to Al_2O_3 NPs resulted in the

loss of appendages, absence of halter, deformities like malformed or shortened legs, wing blisters, and segmented thorax, as well as renal failure. These NPs could cause severe health effects such as birth deformities and kidney failure in humans [16]. Research carried out with Al_2O_3 NPs often report a lower toxic and genotoxic potential compared with other metal NPs [168], which seems to be concordant with the genotoxicity results obtained by Demir et al. [67], who found no significant changes in frequency of mutant spots on the wings of flies, suggesting that Al_2O_3 NPs induced no genotoxic responses in *D. melanogaster*. However, they observed some negative effects when they tested a micrometer-sized Al_2O_3 form. On the other hand, some researchers observed significantly decreased spontaneous rhythmic activity in the antennal lobe of *D. melanogaster* brains after 15 min of application of AINPs, indicating a neurotoxic manifestation [92].

12.12 Research on Graphene Oxide Nanoparticles

As its low-cost production has become recently possible, graphene is considered a new wonder material that is now available for a wide range of applications. Graphene oxide (GO) has attracted attention thanks to its unique properties and potential medical applications; however, its long-term effects on organisms remain to be identified. To that end, researchers have been conducting studies to discover possible effects of GONPs using model organisms [47]. One of these studies evaluated *in vivo* toxicity of GONPs in *D. melanogaster* after oral administration, finding that these NPs can induce developmental delay and reduce adult hatching, and that the toxicity of GO could be associated with production of oxidative stress. Their longevity assay results suggested that GONPs caused little adverse effects in the longevity of flies [220]. Another study examined the effects of various concentrations of dietary GO nanosheets on the development of *D. melanogaster*. They found that the exposure led to significant changes in the crawling speed and trailing

path during the larval stage of development, as well as generation of oxygen radicals within the larval hemolymph, DNA damage within the gut cell, and defective phototaxis and geotaxis behavior in adult flies. Besides, phenotypic defects were observed in the wing, eye, and thorax bristles, and mouth parts [164]. 3D nanocomposites produced from two-dimensional GO nanoplatelets and oxide materials have been reported to exhibit improved mechanical and biological properties, with favorable cell viability when tested in *D. melanogaster* [110]. Another recent study compared the *in vivo* toxicity of GONPs and ZnONPs using different assays such as mortality rate, MTT assay, larval crawling and climbing assay, and total protein content analysis. GONPs were found to induce less cytotoxicity, and as for neurotoxicity, ZnONPs affected the neuromuscular coordination the most, whereas GONPs were found to induce less serious effects [191].

12.13 Research on Carbon Nanotubes

Carbon nanotubes (CNTs) are cylinders consisting of single-walled (SWCNT) or multi-walled (MWCNT) graphene layers with diameters measured in nanometers and lengths in micrometers [96]. They have remarkable physical, chemical, electrical, and mechanical properties, thermal and chemical stability, and excellent semi-conductive quality [70]. CNTs are widely used in a range of industrial applications such as electronics, aerospace, construction, drug delivery and gene therapy [19, 29, 90, 216].

Several studies have evaluated potential risks of CNT exposure in *Drosophila* (both SWCNTs and MWCNTs) but only two studies have dealt with their potential genotoxicity so far. In the first study, the larvae were exposed to SWCNTs, and their biodistribution in the different larval compartments was examined. No serious effects on larval viability suggested that the amount of CNTs deposited in different compartments was too low to produce detectable effects [112]. MWCNTs failed to adhere strongly and to reduce

locomotor function or survival [117]. The lack of toxic effects by SWCNT was also observed in another study, where no effects on larval viability and growth were observed [159]. A different exposure approach has also been used where CNTs were not delivered through food media but injected into *Drosophila* embryos. Such conditions of exposure to MWCNTs had no observable effects on cell motility, tissue and organ formation, cell communication, phagocytosis or embryos' general viability [121]. On the other hand, different results have been reported after the use of this exposure approach, where both SWCNTs and MWCNTs produced significant mortality, but SWCNTs caused equivalent effects at lower doses, demonstrating higher toxic effects [205]. Overall, these toxicity results in *Drosophila* appear to support the general view that SWCNTs tend to pose higher risk than do MWCNTs [99].

As for *in vivo* genotoxic effects of CNTs, two studies have carried out wing spot assays on *Drosophila*, detecting both somatic mutation and recombination events. These studies reported negative results for MWCNTs supporting the view that MWCNTs induced no genotoxicity, either in fly strains with high metabolic efficiency [125] or standard strains of the fly [59]. Lastly, a recent study examined the toxicity of candle soot derived CNTs through an *in vivo* assay using *D. melanogaster* and found no toxic effects [151].

12.14 Research on Other Nanoparticles

On top of the above-mentioned research, a few studies employed *D. melanogaster* to identify potential effects of other nanoparticles. For instance, a wide range of doses of cobalt-based NPs (CoNPs) was found to induce no significant effect on the frequency of mutant clones in 72-hour-old *D. melanogaster* larvae. The genotoxic impacts of CoNPs were higher than those caused by cobalt chloride particles, suggesting that Co ions do not pose a major health risk after exposure to CoNPs [200]. The genotoxicity of CoNPs has also been investigated through comet assay in hemocytes and the wing-spot SMART

assay to explore mutant effects on the wings [72]. This study reported that high concentrations (1 and 10 mM) of CoNPs induced genotoxic effects on flies. Recently, detrimental effects of CoNPs on *Drosophila*, including toxicity, internalization, intracellular oxidative stress, gene mutation, and DNA damage have been reported [12].

Both nano and micro sized particles of zirconium (Zr) are often utilized in biosensors, cancer therapy, and implants. ZrNPs have been claimed to have no apparent toxic effects but they are known for their great antioxidant potential. The antioxidant effects of ZrNPs were reported to be more pronounced than those observed in microparticles [104]. As for their genotoxic risk, the lack of significant alterations in the frequency of mutant spots in the wing-spot assay indicates that neither ZrO₂ nanoparticles nor microparticles induced genotoxicity in *D. melanogaster* [67]. Another study explored potential effects of oral administration of various doses of ZrO₂NPs (10 to 12 nm) on *D. melanogaster* physiology and behavior. Authors reported that ZrO₂NPs deposited in the gut in and generated ROS only at doses of 2.5 and 5.0 mg/L. The ROS toxicity altered the larval gut structure, and affected the developmental process by distressing the number of pupae and causing phenotypic changes in sensory organs [134].

More recently, *in vivo* toxicity of novel composites combining hexagonal boron nitride (h-BN) and ZrO₂NPs has been examined in *D. melanogaster*. Results indicate that the composite synthesized by 10 wt% h-BN + 90 wt% ZrO₂NPs caused less cytotoxicity, while the composite combining 90 wt% h-BN + 10 wt% ZrO₂NPs induced higher toxicity as confirmed by disrupted organ development as well as internal damage to the gut, particularly at the lower doses [78]. The first *in vivo* research to provide evidence on the genotoxic and antigeno-toxic potency of boron nitride nanotubes was carried out by Demir and Marcos [65], where they explored toxicity of boron nitride nanotubes (BNNTs) with considerable changes in genetic material involved in antioxidant defense (*CAT* and *SOD*) and integrity of the intestinal barrier (*Duox*, *Hml*, *Muc68D*, and *PPO2*). They also

detected that BNNTs caused significant reduction in intracellular levels of ROS and genotoxicity of potassium dichromate. Such effects can be explained by the material's antioxidant properties, further encouraging the view that BNNTs may offer a substantial pharmacological promise thanks to their antioxidant capacity.

The toxic and genotoxic effects of nickel (Ni)-based nanoparticles have been recently evaluated. Using the wing SMART assay it was observed that all tested concentrations of NiONPs were genotoxic in the standard cross although only the highest concentration (21 mg/mL) was genotoxic in the high bioactivation cross. Somatic recombination was the preferential mechanism inducing genotoxicity in *D. melanogaster* [60]. In addition, a systematic study of NiO₂ nanowires (NWs) and nanospheres (NSs) was carried out to examine the mechanisms of degradation, internalization, and interaction with various biological targets. Distinct shape of NWs has been observed to undergo a series of changes upon oral administration until they reach the intestinal lumen, where their diameter shows a significant reduction. Besides, NiO₂NPs induced DNA damage and molecular changes at the gene expression level, as well as a notable rise in oxidative stress. Regardless of their form, Ni compounds have been found to induce no toxic or mutagenic effects [10].

The testing of cerium oxide nanoparticles (CeO₂NPs) in *Drosophila* showed that its exposure increased longevity in female flies by 18 days and maximum life span by 19 days, along with greater activity in adult female flies [53]. Furthermore, no significant toxic and genotoxic effect of CeO₂NPs or Ce-sulfate was observed after exposure to doses up to 10 mM in the wing-spot assay [6]. The effect of the surface charge has also been evaluated in CeO₂NPs administered to *D. melanogaster* through dietary intake. Positively charged NPs had no effect on the development of the third instar larvae, whereas negatively charged ones caused a delayed growth by around 7 days. TEM images of the larvae gut revealed shrinkage of positively charged, but negatively charged ones showed no changes in size. Such biodegradability can be the reason

underlying the delayed larval growth. Authors concluded that positively charged CeO₂NPs could be used as drug delivery carriers while negatively charged CeO₂NPs might prove detrimental to living organisms [153]. A last study into the toxicity of CeO₂NPs on wild-type third instar larvae and adult males revealed that dietary administration caused no developmental or behavioral defects regardless of dose. Furthermore, no significant alterations were observed in key biochemical parameters like generation of ROS, carbohydrate and protein levels, superoxide dismutase activity, and acetylcholinesterase activity, suggesting that CeO₂ NPs may offer good antioxidant promise and can be used as effective drug carriers [195].

Gallium phosphide (GaP) nanowires (NWs) have been tested for their *in vivo* detrimental effects [1]. Exposing GaPNWs to *Drosophila* larvae or adults via food medium was reported to cause no NW residence in fly tissues, eliciting no significant changes in gene expression, nor any impact on somatic mutation rate or life span of flies. It could be suggested the intestinal tract of *Drosophila* was to some extent insensitive to exposure to NWs.

Hydroxyapatite nanoparticles (HApNPs) have also been investigated in *Drosophila* evaluating the impact of oral intake on growth, development, and behavior. Results indicated that exposure to HApNPs at lower concentrations (5 mg/L) induced more oxidative stress as compared to the highest concentration (80 mg/L), which reflected greater ROS production and cell damage within the larval gut. Furthermore, the studies report that HApNPs interfere with phosphorus and calcium absorption pathways. Findings suggest that HApNPs can cause damaging effects to the bodies of fruit flies depending on the intensity of exposure [152]. Contrarily to these results, HApNPs administered via the oral route, reported no signs of behavioral changes or any signs of toxicity at both lowest and highest doses [58].

Among the carbon structures, in addition to the already cited graphene and nanotubes, stand up the fullerenes. Although fullerenes have been widely studied, only two papers to evaluate its detrimental effects on *Drosophila* have been pub-

lished. The first study examined three different fullerenols (C-60, C-70, and C120) evaluating their effects on lifespan or in behavior abnormalities. The results showed that exposure to such materials did not result in any type of effect on the tested biomarkers [31]. The second study evaluated the effects of buckminsterfullerene (C₆₀) at three levels: DNA, tissue, and organism. Although the exposure activated the *mus209* gene in the salivary glands of larvae, as a potential indicator of induced DNA damage, no effects were observed on cell and organism levels. Authors suggested the potential activation of the repair systems or elimination of disrupted cells to explain the lack of harmful effects [214].

From other nanomaterials, only one report per case has been found. A study looking into the use of chitosan NPs in the field of agriculture to transport agrochemicals observed that at the higher concentration (100 µg/mL) chitosan nanoparticles affect survivability, climbing ability, and larval crawling [183]. Wood-based cellulose nanofibrils (CNFs) has also be considered as a possible drug-delivery alternative. The toxicity and biocompatibility of CNFs were tested by a series of experiments in *D. melanogaster*, measuring larval crawling, thermal sensitivity, larval light preference, and climbing behavior. Although certain abnormalities in larval development and behavior were observed, no cytotoxic effect of CNFs could be confirmed by the gut staining and level of ROS. Overall, CNFs were found to have no significant cytotoxic effects [135]. Lignin nanoparticles are another example of proposed nanocarriers. Their potential cytotoxic and genotoxic impact was evaluated in *D. melanogaster* observing a significant increase in neuronal defects, but no effects in nuclei fragmentation and gut cell damage [187]. Lastly, the potential genotoxic effects of calcium molybdenum NPs have been evaluated in *Drosophila*. Exposing larvae to these NPs does not produce toxic effects as measured by the relative survival rates. In addition, no genotoxic effects were observed as measured by the wing-spot assay [144].

12.15 Discussion and General Conclusion

It is clear from the foregoing review that *D. melanogaster* can be employed as an ideal testing model in exploring the potential toxicity of NMs. As mentioned before, the advantages of using this species of fruit fly include easy and low-cost culturing, as well as mounting evidence on *Drosophila* accumulated over the years. A negative factor that needs to be taken into consideration seems to be the phylogenetic differences existing between fruit flies and humans in terms of interpolation of effects, which poses a risk to extrapolating relevant data on flies to the human body. However, many studies have used *D. melanogaster* as a model to study various human diseases [74, 130, 160, 206]. *D. melanogaster* allows effective *in vivo* testing of exposure to a wide range of nanomaterials at different levels to explore their effects on behavior, locomotion, and physiology. Besides, *D. melanogaster* can serve as a dynamic sensitive biomonitor to detect ions shedding from NPs with the outcome of their physical interactions with living organisms. Some nanoparticles are known to release ions according to the different matrix types [86]. *Drosophila* flies are usually exposed to NMs in testing settings via food medium, which is a complex matrix that might involve release of ions from nanoparticles. In order to prevent misinterpretation of study data, researchers are recommended to combine nanomaterials with their relevant ionic forms during testing [4].

D. melanogaster may prove a most valuable model to satisfy modern nano-toxicity research's demands as it offers optimized pathway-specific screening, accelerates testing of samples at cellular or molecular levels, while allowing rapid detection of genes playing a role in interactions with nanomaterials. In addition, *D. melanogaster* is also an ideal candidate for high throughput screening, because the fly's short generation time allows processing of thousands of flies for screening. *Drosophila*'s capacity to reflect true interac-

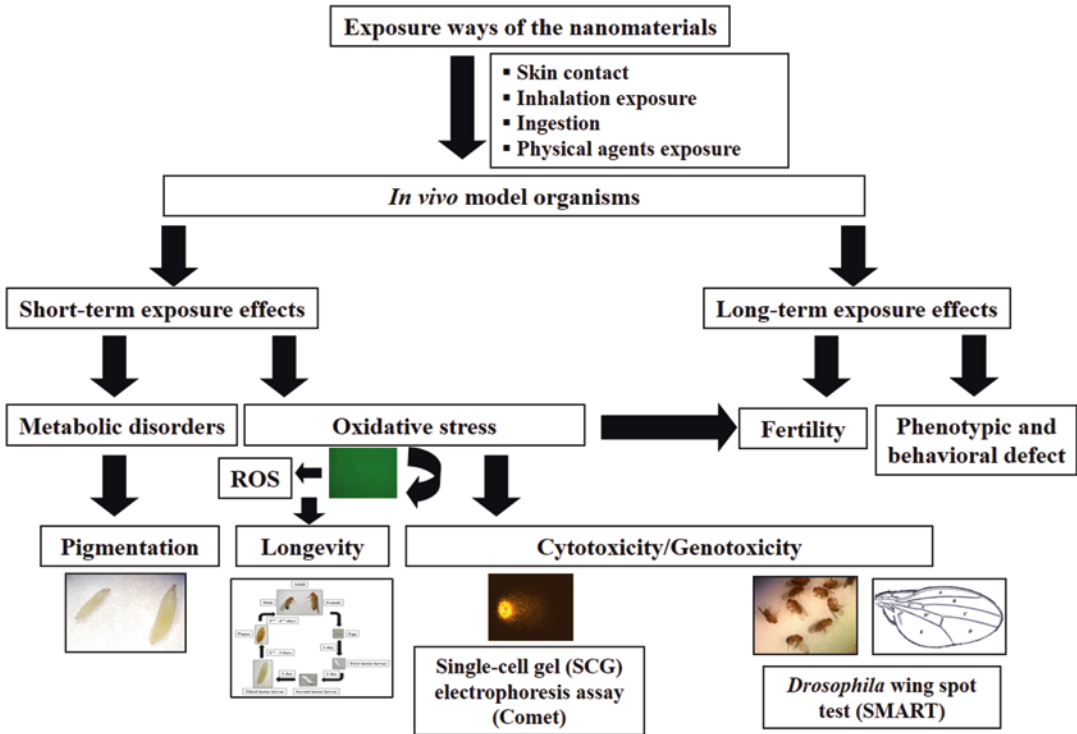


Fig. 12.4 The figure illustrates the testing of nanotoxicity and nanogenotoxicity through *in vivo* models, which are exposed to different types of nanomaterials by inges-

tion, skin contact, or inhalation, leading to a series of short-term and long-term effects

tions between environment and DNA can give us valuable insight into the mechanisms of toxicity in humans. Such prospects led to Collins et al. [54] to propose a novel approach where *D. melanogaster* could bring about a paradigm shift in toxicology research. While some argue that toxicity experiments with alternative testing models such as zebrafish can mimic vertebrate response, *D. melanogaster* stands out as a superior model, as it allows researchers to process a large number of specimens, to identify genes regulating certain pathways at significantly lower costs, giving easy access to important data about key parameters, such as population, survival, longevity, mortality, as well as mutagenic and recombinogenic activity of nanomaterials [12, 62–64, 210, 211]. Many studies have attempted to explore the effects of

NMs on *in vivo* models by examining survival rates, autophagy, oxidative stress, fecundity, and genotoxicity, and such models have so far provided invaluable data for research into toxic potential of nanomaterials (Fig. 12.4).

In conclusion, *D. melanogaster* has become an ideal testing model in research involving assessment of risks from exposure to nanoparticles and toxicological classification. We hope that the newly established research field ‘drosophotoxicology’ will help further our knowledge about potential effects of NPs on humans and other organisms. Our ongoing collaboration with *Drosophila* fruit fly is certain to decipher the underlying mechanisms of seemingly complicated biological and ecological processes associated with exposure to nanoparticles.

References

1. Adolffson K, Schneider M, Hammarin G et al (2013) Ingestion of gallium phosphide nanowires has no adverse effect on *Drosophila* tissue function. *Nanotechnology* 24(28):285101. <https://doi.org/10.1088/0957-4484/24/28/285101>
2. Ahamed M, Posgai R, Gorey TJ et al (2010) Silver nanoparticles induced heat shock protein 70, oxidative stress and apoptosis in *Drosophila melanogaster*. *Toxicol Appl Pharm* 242:263–269. <https://doi.org/10.1016/j.taap.2009.10.016>
3. Akhtar M, Ahamed M, Kumar S et al (2012) Zinc oxide nanoparticles selectively induce apoptosis in human cancer cells through reactive oxygen species. *Int J Nanomedicine* 7:845–857. <https://doi.org/10.2147/IJN.S29129>
4. Alaraby M, Annangi B, Hernández A et al (2015a) A comprehensive study of the harmful effects of ZnO nanoparticles using *Drosophila melanogaster* as an *in vivo* model. *J Hazard Mater* 296:166–174. <https://doi.org/10.1016/j.jhazmat.2015.04.053>
5. Alaraby M, Demir E, Hernández A et al (2015b) Assessing potential harmful effects of CdSe quantum dots by using *Drosophila melanogaster* as *in vivo* model. *Sci Total Environ* 530–531:66–75. <https://doi.org/10.1016/j.scitotenv.2015.05.069>
6. Alaraby M, Hernández A, Annangi B et al (2015c) Antioxidant and antigenotoxic properties of CeO₂ NPs and cerium sulphate: studies with *Drosophila melanogaster* as a promising *in vivo* model. *Nanotoxicology* 9:749–759. <https://doi.org/10.3109/17435390.2014.976284>
7. Alaraby M, Annangi B, Marcos R et al (2016a) *Drosophila melanogaster* as a suitable *in vivo* model to determine potential side effects of nanomaterials: a review. *J Toxicol Environ Health B Crit Rev* 19(2):65–104. <https://doi.org/10.1080/10937404.2016.1166466>
8. Alaraby M, Hernández A, Marcos R (2016b) New insights in the acute toxic/genotoxic effects of CuO nanoparticles in the *in vivo Drosophila* model. *Nanotoxicology* 10(6):749–760. <https://doi.org/10.3109/17435390.2015.1121413>
9. Alaraby M, Hernández A, Marcos R (2017) Copper oxide nanoparticles and copper sulphate act as antigenotoxic agents in *Drosophila melanogaster*. *Environ Mol Mutagen* 58(1):46–55. <https://doi.org/10.1002/em.22068>
10. Alaraby M, Hernández A, Marcos R (2018) Systematic *in vivo* study of NiO nanowires and nanospheres: biodegradation, uptake and biological impacts. *Nanotoxicology* 12(9):1027–1044. <https://doi.org/10.1080/17435390.2018.1513091>
11. Alaraby M, Romero S, Hernández A et al (2019) Toxic and genotoxic effects of silver nanoparticles in *Drosophila*. *Environ Mol Mutagen* 60(3):277–285. <https://doi.org/10.1002/em.22262>
12. Alaraby M, Demir E, Domenech J et al (2020) *In vivo* evaluation of the toxic and genotoxic effects of exposure to cobalt nanoparticles in *Drosophila melanogaster*. *Environ Sci Nano* 7:610–622
13. Alkilany AM, Murphy CJ (2010) Toxicity and cold nanoparticles: what we have learned so far? *J Nanopart Res* 12:2313–2333. <https://doi.org/10.1007/s11051-010-9911-8>
14. Ambegaokar SS, Roy B, Jackson GR (2010) Neurodegenerative models in *Drosophila*: Polyglutamine disorders, Parkinson disease, and amyotrophic lateral sclerosis. *Neurobiol Dis* 40:29–39. <https://doi.org/10.1016/j.nbd.2010.05.026>
15. Anand AS, Prasad DN, Singh SB et al (2017) Chronic exposure of zinc oxide nanoparticles causes deviant phenotype in *Drosophila melanogaster*. *J Hazard Mater* 327:180–186. <https://doi.org/10.1016/j.jhazmat.2016.12.040>
16. Anand AS, Gahlot U, Prasad DN et al (2019) Aluminum oxide nanoparticles mediated toxicity, loss of appendages in progeny of *Drosophila melanogaster* on chronic exposure. *Nanotoxicology* 13(7):977–989. <https://doi.org/10.1080/17435390.2019.1602680>
17. Arami H, Khandhar A, Liggitt D et al (2015) *In vivo* delivery, pharmacokinetics, biodistribution and toxicity of iron oxide nanoparticles. *Chem Soc Rev* 44:8576–8607. <https://doi.org/10.1039/C5CS00541H>
18. Armstrong N, Ramamoorthy M, Lyon D et al (2013) Mechanism of silver nanoparticles action on insect pigmentation reveals intervention of copper homeostasis. *PLoS One* 8:e53186. <https://doi.org/10.1371/journal.pone.0053186>
19. Asakura M, Sasaki T, Sugiyama T et al (2010) Genotoxicity and cytotoxicity of multi-wall carbon nanotubes in cultured Chinese hamster lung cells in comparison with chrysotile a fibers. *J Occup Health* 52:155–166. <https://doi.org/10.1539/joh.L9150>
20. Austin LA, Mackey MA, Dreaden EC et al (2014) The optical, photothermal, and facile surface chemical properties of gold and silver nanoparticles in biodiagnostics, therapy, and drug delivery. *Arch Toxicol* 88:1391–1417. <https://doi.org/10.1007/s00204-014-1245-3>
21. Ávalos A, Haza AI, Drosopoulou E et al (2015) *In vivo* genotoxicity assessment of silver nanoparticles of different sizes by the somatic mutation and recombination test (SMART) on *Drosophila*. *Food Chem Toxicol* 85:114–119. <https://doi.org/10.1016/j.fct.2015.06.024>
22. Ávalos A, Haza AI, Mateo D et al (2018) *In vitro* and *in vivo* genotoxicity assessment of gold nanoparticles of different sizes by comet and SMART assays. *Food Chem Toxicol* 120:81–88. <https://doi.org/10.1016/j.fct.2018.06.061>
23. Baeg E, Sooklert K, Sereemasun A (2018) Copper oxide nanoparticles cause a dose-dependent toxicity via inducing reactive oxygen species in *Drosophila*.

- Nanomaterials (Basel) 8(10):824. <https://doi.org/10.3390/nano8100824>
24. Baeza A, Vallet-Regí M (2015) Smart mesoporous silica nanocarriers for antitumoral therapy. *Curr Top Med Chem* 15:2306–2315. <https://doi.org/10.2174/1568026615666150605114826>
 25. Balakrishnan V, Ab Wab HA, Razak KA et al (2013) In vitro evaluation of cytotoxicity of colloidal amorphous silica nanoparticles designed for drug delivery on human cell lines. *J Nanomater* 2013:8. <https://doi.org/10.1155/2013/729306>
 26. Barandeh F, Nguyen PL, Kumar R et al (2012) Organically modified silica nanoparticles are biocompatible and can be targeted to neurons *in vivo*. *PLoS One* 7:e29424. <https://doi.org/10.1371/journal.pone.0029424>
 27. Basak AK, Chatterjee T, Chakravarty A et al (2019) Silver nanoparticle-induced developmental inhibition of *Drosophila melanogaster* accompanies disruption of genetic material of larval neural stem cells and non-neuronal cells. *Environ Monit Assess* 191:497. <https://doi.org/10.1007/s10661-019-7630-x>
 28. Bharali DJ, Klejbor I, Stachowiak EK et al (2005) Organically modified silica nanoparticles: a nonviral vector for *in vivo* gene delivery and expression in the brain. *PNAS* 102:11539–11544. <https://doi.org/10.1073/pnas.0504926102>
 29. Bianco A, Kostarelos K, Prato M (2005) Applications of carbon nanotubes in drug delivery. *Curr Opin Chem Biol* 9:674–679. <https://doi.org/10.1016/j.cbpa.2005.10.005>
 30. Bier E (2005) *Drosophila*, the golden bug, emerges as a tool for human genetics. *Nat Rev Genet* 6:9–23. <https://doi.org/10.1038/nrg1503>
 31. Bolshakova O, Borisenkova A, Suyasova M et al (2019) In vitro and in vivo study of the toxicity of fullerenols C60, C70 and C120O obtained by an original two step method. *Mater Sci Eng C* 104:109945. <https://doi.org/10.1016/j.msec.2019.109945>
 32. Brunetti V, Chibli H, Fiammengio R et al (2013) InP/ZnS as a safer alternative to CdSe/ZnS core/shell quantum dots: *in vitro* and *in vivo* toxicity assessment. *Nanoscale* 5(1):307–317. <https://doi.org/10.1039/c2nr33024e>
 33. Buerki-Thurnherr T, Xiao L, Diener L et al (2013) In vitro mechanistic study towards a better understanding of ZnO nanoparticle toxicity. *Nanotoxicology* 7:402–416. <https://doi.org/10.3109/17435390.2012.666575>
 34. Cardozo TR, De Carli RF, Seeber A et al (2019) Genotoxicity of zinc oxide nanoparticles: an *in vivo* and *in silico* study. *Toxicol Res (Camb)* 8(2):277–286. <https://doi.org/10.1039/c8tx00255j>
 35. Carmona ER, Escobar B, Vales G et al (2015a) Genotoxic testing of titanium dioxide anatase nanoparticles using the wing-spot test and the comet assay in *Drosophila*. *Mutat Res Genet Toxicol Environ Mutagen* 778:12–21. <https://doi.org/10.1016/j.mrgentox.2014.12.004>
 36. Carmona ER, Inostroza-Blancheteau C, Rubio L et al (2015b) Genotoxic and oxidative stress potential of nanosized and bulk zinc oxide particles in *Drosophila melanogaster*. *Toxicol Ind Health* 32(12):1987–2001. <https://doi.org/10.1177/0748233715599472>
 37. Carmona ER, Inostroza-Blancheteau C, Rubio L et al (2015c) Genotoxic effects of copper oxide nanoparticles in *Drosophila melanogaster*. *Mutat Res* 791:1–11. <https://doi.org/10.1016/j.mrgentox.2015.07.006>
 38. Carmona ER, García-Rodríguez A, Marcos R (2018) Genotoxicity of copper and nickel nanoparticles in somatic cells of *Drosophila melanogaster*. *J Toxicol* 2018:7278036. <https://doi.org/10.1155/2018/7278036>
 39. Chaloupka K, Malam Y, Seifalian AM (2010) Nanosilver as a new generation of nanoparticle in biomedical applications. *Trends Biotechnol* 28(11):580–588. <https://doi.org/10.1016/j.tibtech.2010.07.006>
 40. Charroux B, Royet J (2012) Gut-microbiota interactions in non-mammals: what can we learn from *Drosophila*? *Semin Immunol* 24:17–24. <https://doi.org/10.1016/j.smim.2011.11.003>
 41. Chatterjee N, Yang J, Kim HM (2014a) Potential toxicity of differential functionalized multiwalled carbon nanotubes (MWCNT) in human cell line (BEAS2B) and *Caenorhabditis elegans*. *J Toxicol Environ Health A* 77(22–24):1399–1408. <https://doi.org/10.1080/15287394.2014.951756>
 42. Chatterjee N, Eom HJ, Choi J (2014b) Effects of silver nanoparticles on oxidative DNA damage-repair as a function of p38 MAPK status: a comparative approach using human Jurkat T cells and the nematode *Caenorhabditis elegans*. *Environ Mol Mutagen* 55:122–133. <https://doi.org/10.1002/em.v55.2>
 43. Chen X, Mao SS (2007) Titanium dioxide nanomaterials: synthesis, properties, modifications, and applications. *Chem Rev* 107:2891–2959
 44. Chen J, Dong X, Zhao J et al (2009) In vivo acute toxicity of titanium dioxide nanoparticles to mice after intraperitoneal injection. *J Appl Toxicol* 29:330–337. <https://doi.org/10.1002/jat.v29:4>
 45. Chen T, Yan J, Li Y (2014) Genotoxicity of titanium dioxide nanoparticles. *J Food Drug Anal* 22:95–104. <https://doi.org/10.1016/j.jfda.2014.01.008>
 46. Chen H, Wang B, Feng W et al (2015) Oral magnetite nanoparticles disturb the development of *Drosophila melanogaster* from oogenesis to adult emergence. *Nanotoxicology* 9:302–312. <https://doi.org/10.3109/17435390.2014.929189>
 47. Chen L, Li J, Chen Z et al (2020) Toxicological evaluation of graphene-family nanomaterials. *J Nanosci Nanotechnol* 20(4):1993–2006. <https://doi.org/10.1166/jnn.2020.17364>
 48. Chifiriuc MC, Ratiu AC, Popa M et al (2016) Drosophotoxigenicity: an emerging research area for assessing nanoparticles interaction with living organisms. *Int J Mol Sci* 17(2):36. <https://doi.org/10.3390/ijms17020036>

49. Chin CD, Laksanasopin T, Cheung YK et al (2011) Microfluidics-based diagnostics of infectious diseases in the developing world. *Nat Med* 17:1015–1019. <https://doi.org/10.1038/nm.2408>
50. Clift MJD, Boyles MSP, Brown DM et al (2010) An investigation into the potential for different surface-coated quantum dots to cause oxidative stress and affect macrophage cell signaling *in vitro*. *Nanotoxicology* 4:139–149. <https://doi.org/10.3109/17435390903276925>
51. Clutton-Brock TH (1988) Reproductive success: studies of individual variation in contrasting breeding systems. University of Chicago Press. <https://doi.org/10.1046/j.1420-9101.1990.3050478.x>
52. Code of Federal Regulations (2016) Title 21, updated April 1, 2016. <https://www.accessdata.fda.gov/scripts/cdrh/cfdocs/cfcfr/CFRSearch.cfm>
53. Cohen CA, Karfakis JA, Kurnick MD et al (2008) Cerium oxide nanoparticles reduce free radical-mediated toxicity in *Drosophila melanogaster*. *FASEB J* 22:624. https://doi.org/10.1096/fasebj.22.1_supplement.624.1
54. Collins FS, Gray GM, Bucher JR (2008) Transforming environmental health protection. *Science* 319(5865):906–907. <https://doi.org/10.1126/science.1154619>
55. Contado C (2015) Nanomaterials in consumer products: a challenging analytical problem. *Front Chem* 3:48. <https://doi.org/10.3389/fchem.2015.00048>
56. Contreras EQ, Cho M, Zhu H et al (2012) Toxicity of quantum dots and cadmium salt to *Caenorhabditis elegans* after multigenerational exposure. *Environ Sci Technol* 47:1148–1154. <https://doi.org/10.1021/es3036785>
57. Cvetković VJ, Jovanović B, Lazarević M et al (2020) Changes in the wing shape and size in *Drosophila melanogaster* treated with food grade titanium dioxide nanoparticles (E171)-a multigenerational study. *Chemosphere* 261:127787. <https://doi.org/10.1016/j.chemosphere.2020.127787>
58. Dan P, Sundararajan V, Ganeshkumar H et al (2019) Evaluation of hydroxyapatite nanoparticles - induced *in vivo* toxicity in *Drosophila melanogaster*. *Appl Surf Sci* 484:568–577. <https://doi.org/10.1016/j.apsusc.2019.04.120>
59. de Andrade LR, Brito AS, Melero AM et al (2014) Absence of mutagenic and recombinogenic activity of multi-walled carbon nanotubes in the *Drosophila* wing-spot test and *Allium cepa* test. *Ecotoxicol Environ Saf* 99:92–97. <https://doi.org/10.1016/j.ecoenv.2013.10.013>
60. De Carli RF, Chaves DDS, Cardozo TR et al (2018) Evaluation of the genotoxic properties of nickel oxide nanoparticles *in vitro* and *in vivo*. *Mutat Res Genet Toxicol Environ Mutagen* 836:47–53. <https://doi.org/10.1016/j.mrgentox.2018.06.003>
61. Dedeh A, Ciutat A, Treguer-Delapierre M et al (2015) Impact of gold nanoparticles on zebrafish exposed to a spiked sediment. *Nanotoxicology* 9:71–80. <https://doi.org/10.3109/17435390.2014.889238>
62. Demir E (2020a) An *in vivo* study of nanorod, nanosphere, and nanowire forms of titanium dioxide using *Drosophila melanogaster*: toxicity, cellular uptake, oxidative stress, and DNA damage. *J Toxicol Environ Health A* 83(11–12):456–469. <https://doi.org/10.1080/15287394.2020.1777236>
63. Demir E (2020b) A review on nanotoxicity and nanogenotoxicity of different shapes of nanomaterials. *J Appl Toxicol*. <https://doi.org/10.1002/jat.4061>
64. Demir E (2020c) *Drosophila* as a model for assessing nanopesticide toxicity. *Nanotoxicology*. <https://doi.org/10.1080/17435390.2020.1815886>
65. Demir E, Marcos R (2018) Antigenotoxic potential of boron nitride nanotubes. *Nanotoxicology* 12(8):868–884. <https://doi.org/10.1080/17435390.2018.1482379>
66. Demir E, Vales G, Kaya B et al (2011) Genotoxic analysis of silver nanoparticles in *Drosophila*. *Nanotoxicology* 5:417–424. <https://doi.org/10.3109/17435390.2010.529176>
67. Demir E, Turna F, Vales G et al (2013) *In vivo* genotoxicity assessment of titanium, zirconium and aluminium nanoparticles, and their microparticulated forms, in *Drosophila*. *Chemosphere* 93:2304–2310. <https://doi.org/10.1016/j.chemosphere.2013.08.022>
68. Demir E, Aksakal S, Turna F et al (2015) *In vivo* genotoxic effects of four different nanosizes forms of silica nanoparticles in *Drosophila melanogaster*. *J Hazard Mater* 283:260–266. <https://doi.org/10.1016/j.jhazmat.2014.09.029>
69. Donaldson K, Murphy F, Schinwald A et al (2011) Identifying the pulmonary hazard of high aspect ratio nanoparticles to enable their safety-by-design. *Nanomedicine* 6(1):143–156. <https://doi.org/10.2217/nmm.10.139>
70. Dresselhaus MS, Dresselhaus G, Jorio A (2004) Unusual properties and structure of carbon nanotubes. *Annu Rev Mater Res* 34:247–278. <https://doi.org/10.1146/annurev.matsci.34.040203.114607>
71. Ema M, Okuda H, Gamo M et al (2017) A review of reproductive and developmental toxicity of silver nanoparticles in laboratory animals. *Reprod Toxicol* 67:149–164. <https://doi.org/10.1016/j.reprotox.2017.01.005>
72. Ertuğrul H, Yalçın B, Güneş M et al (2020) Ameliorative effects of melatonin against nano and ionic cobalt induced genotoxicity in two *in vivo* *Drosophila* assays. *Drug Chem Toxicol* 43(3):279–286. <https://doi.org/10.1080/01480545.2019.1585444>
73. Festa RA, Thiele DJ (2011) Copper: an essential metal in biology. *Curr Biol* 21:R877–R883. <https://doi.org/10.1016/j.cub.2011.09.040>
74. Foriel S, Willems P, Smeitink J et al (2015) Mitochondrial diseases: *Drosophila melanogaster* as a model to evaluate potential therapeutics. *Int J Biochem Cell Biol* 63:60–65. <https://doi.org/10.1016/j.biocel.2015.01.024>

75. Franklin NM, Rogers NJ, Apte SC et al (2007) Comparative toxicity of nanoparticulate ZnO, bulk ZnO, and ZnCl₂ to a freshwater microalga (*Pseudokirchneriella subcapitata*): the importance of particle solubility. *Environ Sci Technol* 41(24):8484–8490. <https://doi.org/10.1021/es071445r>
76. Gagné F, Auclair J, Turcotte P et al (2008) Ecotoxicity of CdTe quantum dots to freshwater mussels: impacts on immune system, oxidative stress and genotoxicity. *Aquat Toxicol* 86:333–340. <https://doi.org/10.1016/j.aquatox.2007.11.013>
77. Galeone A, Vecchio G, Malvindi MA et al (2012) In vivo assessment of CdSe–ZnS quantum dots: coating dependent bioaccumulation and genotoxicity. *Nanoscale* 4:6401–6407. <https://doi.org/10.1039/c2nr31826a>
78. Gautam A, Gautam C, Mishra M et al (2019) Enhanced mechanical properties of hBN–ZrO₂ composites and their biological activities on *Drosophila melanogaster*: synthesis and characterization. *RSC Adv* 9:40977–40996
79. Giljohann DA, Seferos DS, Daniel WL et al (2010) Gold nanoparticles for biology and medicine. *Angew Chem Int Ed Engl* 49:3280–3294. <https://doi.org/10.1002/anie.200904359>
80. Gliga AR, Skoglund S, OdnevallWallinder I et al (2014) Size-dependent cytotoxicity of silver nanoparticles in human lung cells: the role of cellular uptake, agglomeration and Ag release. *Part Fibre Toxicol* 11(1):11. <https://doi.org/10.1186/1743-8977-11-11>
81. Godwin H, Nameth C, Avery D et al (2015) Nanomaterial categorization for assessing risk potential to facilitate regulatory decision-making. *ACS Nano* 9:3409–3417. <https://doi.org/10.1021/acsnano.5b00941>
82. Golbamaki N, Rasulev B, Cassano A et al (2015) Genotoxicity of metal oxide nanomaterials: review of recent data and discussion of possible mechanisms. *Nanoscale* 7:2154–2198. <https://doi.org/10.1039/C4NR06670G>
83. Gorth DJ, Rand DM, Webster TJ (2011) Silver nanoparticle toxicity in *Drosophila*: size does matter. *Int J Nanomedicine* 6:343–350. <https://doi.org/10.2147/IJN.S16881>
84. Gupta AK, Gupta M (2005) Synthesis and surface engineering of iron oxide nanoparticles for biomedical applications. *Biomaterials* 26(18):3995–4021. <https://doi.org/10.1016/j.biomaterials.2004.10.012>
85. Han X, Geller B, Moniz K et al (2014) Monitoring the developmental impact of copper and silver nanoparticle exposure in *Drosophila* and their microbiomes. *Sci Total Environ* 487:822–829. <https://doi.org/10.1016/j.scitotenv.2013.12.129>
86. Handy RD, Van Den Brink N, Chappell M et al (2012) Practical considerations for conducting ecotoxicity test methods with manufactured nanomaterials: what have we learnt so far? *Ecotoxicology* 21:933–972. <https://doi.org/10.1007/s10646-012-0862-y>
87. Hawkins AD, Thornton C, Kennedy AJ et al (2015) Gill histopathologies following exposure to nanosilver or silver nitrate. *J Toxicol Environ Health A* 78(5):301–315. <https://doi.org/10.1080/15287394.2014.971386>
88. Hayashi Y, Engelmann P, Foldbjerg R et al (2012) Earthworms and humans *in vitro*: characterizing evolutionarily conserved stress and immune responses to silver nanoparticles. *Environ Sci Technol* 46:4166–4173. <https://doi.org/10.1021/es3000905>
89. He X, Aker WG, Hwang H-M (2014) An *in vivo* study on the photo-enhanced toxicities of S-doped TiO₂ nanoparticles to zebrafish embryos (*Danio rerio*) in terms of malformation, mortality, rheotaxis dysfunction, and DNA damage. *Nanotoxicology* 8:185–195. <https://doi.org/10.3109/17435390.2013.874050>
90. Hirsch A (2002) Functionalization of single-walled carbon nanotubes. *Angew Chem Int Ed* 41:1853–1859. [https://doi.org/10.1002/1521-3773\(20020603\)41:11:1-3](https://doi.org/10.1002/1521-3773(20020603)41:11:1-3)
91. Hong H, Shi J, Yang Y et al (2011) Cancer-targeted optical imaging with fluorescent zinc oxide nanowires. *Nano Lett* 11(9):3744–3750. <https://doi.org/10.1021/nl201782m>
92. Huang N, Yan Y, Xu Y et al (2013) Alumina nanoparticles alter rhythmic activities of local interneurons in the antennal lobe of *Drosophila*. *Nanotoxicology* 7:212–220. <https://doi.org/10.3109/17435390.2011.648668>
93. Hunt PR, Marquis BJ, Tyner KM et al (2013) Nanosilver suppresses growth and induces oxidative damage to DNA in *Caenorhabditis elegans*. *J Appl Toxicol* 33:1131–1142. <https://doi.org/10.1002/jat.v33.10>
94. Hussain SM, Hess KL, Gearhart JM et al (2005) In vitro toxicity of nanoparticles in BRL 3A rat liver cells. *Toxicol In Vitro* 19:975–983. <https://doi.org/10.1016/j.tiv.2005.06.034>
95. IARC (2010) Carbon black, titanium dioxide, and talc. IARC monographs on the evaluation of carcinogenic risks to humans, vol 93. World Health Organization, Lyon, p 275
96. Iijima S (1991) Helical microtubules of graphitic carbon. *Nature* 354:56–58. <https://doi.org/10.1038/354056a0>
97. Jennings BH (2011) *Drosophila* - a versatile model in biology & medicine. *Mater Today* 14(5):190–195
98. Ji X, Peng F, Zhong Y et al (2014) Fluorescent quantum dots: synthesis, biomedical optical imaging, and biosafety assessment. *Colloids Surf B Biointerfaces* 124:132–139. <https://doi.org/10.1016/j.colsurfb.2014.08.036>
99. Jia G, Wang H, Yan L et al (2005) Cytotoxicity of carbon nanomaterials: single-wall nanotube, multi-wall nanotube, and fullerene. *Environ Sci Technol* 39:1378–1383. <https://doi.org/10.1021/es0487291>
100. Jovanović B, Cvetković VJ, Mitrović TL (2015) Effects of human food grade titanium dioxide nanoparticle dietary exposure on *Drosophila mela-*

- nogaster* survival, fecundity, pupation and expression of antioxidant genes. *Chemosphere* 144:43–49. <https://doi.org/10.1016/j.chemosphere.2015.08.054>
101. Jovanović B, Jovanović N, Cvetković VJ et al (2018) The effects of a human food additive, titanium dioxide nanoparticles E171, on *Drosophila melanogaster* -a 20 generation dietary exposure experiment. *Sci Rep* 8(1):17922. <https://doi.org/10.1038/s41598-018-36174-w>
 102. Karlsson HL, Cronholm P, Gustafsson J et al (2008) Copper oxide nanoparticles are highly toxic: a comparison between metal oxide nanoparticles and carbon nanotubes. *Chem Res Toxicol* 21:1726–1732. <https://doi.org/10.1021/tx800064j>
 103. Karlsson HL, Gustafsson J, Cronholm P et al (2009) Size dependent toxicity of metal oxide particles-a comparison between nano- and micrometer size. *Toxicol Lett* 188:112–118. <https://doi.org/10.1016/j.toxlet.2009.03.014>
 104. Karunakaran G, Suriyaprabha R, Manivasakan P et al (2013) Screening of *in vitro* cytotoxicity, antioxidant potential and bioactivity of nano- and micro-ZrO₂ and -TiO₂ particles. *Ecotoxicol Environ Safe* 93:191–197. <https://doi.org/10.1016/j.ecoenv.2013.04.004>
 105. Kaygisiz ŞY, Çiğerci İH (2017) Genotoxic evaluation of different sizes of iron oxide nanoparticles and ionic form by SMART, *allium* and comet assay. *Toxicol Ind Health* 33(10):802–809. <https://doi.org/10.1177/0748233717722907>
 106. Keramanzadeh A, Gosens I, MacCalman L et al (2016) A multi-laboratory toxicological assessment of a panel of 10 engineered nanomaterials to human health-ENPRA project-the highlights, limitations and current and future challenges. *J Toxicol Environ Health B Crit Rev* 19:1–28. <https://doi.org/10.1080/10937404.2015.1126210>
 107. Key SCS, Reaves D, Turner F et al (2011) Impacts of silver nanoparticle ingestion on pigmentation and developmental progression in *Drosophila*. *Atlas J Biol* 1:52–61. <https://doi.org/10.5147/ajb.2011.0048>
 108. Kim JS, Kuk E, Yu KN et al (2007) Antimicrobial effects of silver nanoparticles. *Nanomedicine* 3:95–101. <https://doi.org/10.1016/j.nano.2006.12.001>
 109. Kim JS, Song KS, Yu IJ (2016) Multiwall carbon nanotube-induced DNA damage and cytotoxicity in male human peripheral blood lymphocytes. *Int J Toxicol* 35(1):27–37. <https://doi.org/10.1177/1091581815598749>
 110. Kumar S, Gautam C, Mishra VK et al (2019) Fabrication of graphene nanoplatelet-incorporated porous hydroxyapatite composites: improved mechanical and *in vivo* imaging performances for emerging biomedical applications. *ACS Omega* 4(4):7448–7458. <https://doi.org/10.1021/acsomega.8b03473>
 111. Latouche M, Lasbleiz C, Martin E et al (2007) A conditional pan-neuronal *Drosophila* model of spinocerebellar ataxia 7 with a reversible adult phenotype suitable for identifying modifier genes. *J Neurosci* 27:2483–2492. <https://doi.org/10.1523/JNEUROSCI.5453-06.2007>
 112. Leeuw TK, Reith RM, Simonette RA et al (2007) Single-walled carbon nanotubes in the intact organism: near-IR imaging and biocompatibility studies in *Drosophila*. *Nano Lett* 7:2650–2654. <https://doi.org/10.1021/nl0710452>
 113. Lewinski N, Colvin V, Drezek R (2008) Cytotoxicity of nanoparticles. *Small* 4:26–49. [https://doi.org/10.1002/\(ISSN\)16136829](https://doi.org/10.1002/(ISSN)16136829)
 114. Li WR, Xie XB, Shi QS et al (2010) Antibacterial activity and mechanism of silver nanoparticles on *Escherichia coli*. *Appl Microbiol Biot* 85:1115–1122. <https://doi.org/10.1007/s00253-009-2159-5>
 115. Lin W, Huang YW, Zhou XD et al (2006) In vitro toxicity of silica nanoparticles in human lung cancer cells. *Toxicol Appl Pharmacol* 217:252–259. <https://doi.org/10.1016/j.taap.2006.10.004>
 116. Liong M, Lu J, Kovochich M et al (2008) Multifunctional inorganic nanoparticles for imaging, targeting, and drug delivery. *ACS Nano* 2(5):889–896. <https://doi.org/10.1021/nm800072t>
 117. Liu X, Vinson D, Abd D et al (2009a) Differential toxicity of carbon nanomaterials in *Drosophila*: larval dietary uptake is benign, but adult exposure causes locomotor impairment and mortality. *Environ Sci Technol* 43:6357–6363. <https://doi.org/10.1021/es901079z>
 118. Liu Y, He L, Mustapha A et al (2009b) Antibacterial activities of zinc oxide nanoparticles against *Escherichia coli* O157: H7. *J Appl Microbiol* 107:1193–1201. <https://doi.org/10.1111/j.1365-2672.2009.04303.x>
 119. Liu S, Xu L, Zhang T et al (2010) Oxidative stress and apoptosis induced by nanosized titanium dioxide in PC12 cells. *Toxicology* 267:172–177. <https://doi.org/10.1016/j.tox.2009.11.012>
 120. Liu Y, Zhao Y, Sun B et al (2013) Understanding the toxicity of carbon nanotubes. *Acc Chem Res* 46(3):702–713. <https://doi.org/10.1021/ar300028m>
 121. Liu B, Campo EM, Bossing T (2014) *Drosophila* embryos as model to assess cellular and developmental toxicity of multi-walled carbon nanotubes (MWCNT) in living organisms. *PLoS One* 9:e88681. <https://doi.org/10.1371/journal.pone.0088681>
 122. Lloyd TE, Taylor JP (2010) Flightless flies: *Drosophila* models of neuromuscular disease. *Ann N Y Acad Sci* 1184:1–20. <https://doi.org/10.1111/j.17496632.2010.05432.x>
 123. Lux Research (2014) Nanotechnology update: Corporations up their spending as revenues for nano-enabled products increase. https://portal.luxresearchinc.com/research/report_excerpt/16215
 124. Macaroff PP, Simioni AR, Lacava et al (2006) Studies of cell toxicity and binding of magnetic nanoparticles with blood stream macromolecules. *J Appl Phys* 99(8):08S102. <https://doi.org/10.1063/1.2165923>
 125. Machado NM, Lopes JC, Saturnino RS et al (2013) Lack of mutagenic effect by multiwalled functionalized carbon nanotubes in the somatic

- cells of *Drosophila melanogaster*. Food Chem Toxicol 62:355–360. <https://doi.org/10.1016/j.fct.2013.08.051>
126. Magdolenova Z, Collins A, Kumar A et al (2014) Mechanisms of genotoxicity. A review of *in vitro* and *in vivo* studies with engineered nanoparticles. Nanotoxicology 8:233–278. <https://doi.org/10.3109/17435390.2013.773464>
127. Manshian BB, Soenen SJ, Brown A et al (2016) Genotoxic capacity of Cd/Se semiconductor quantum dots with differing surface chemistries. Mutagenesis 31:97–106. <https://doi.org/10.1093/mutage/gev061>
128. Mao B, Chen Z, Wang Y et al (2018) Silver nanoparticles have lethal and sublethal adverse effects on development and longevity by inducing ROS-mediated stress responses. Sci Rep 8:2445. <https://doi.org/10.1038/s41598-018-20728-z>
129. Massarsky A, Trudeau VL, Moon TW (2014) Predicting the environmental impact of nanosilver. Environ Toxicol Pharmacol 38:861–873. <https://doi.org/10.1016/j.etap.2014.10.006>
130. Maximino C, Silva RX, Da Silva SN et al (2015) Non-mammalian models in behavioral neuroscience: consequences for biological psychiatry. Front Behav Neurosci 9:233. <https://doi.org/10.3389/fnbeh.2015.00233>
131. Meng SS, Wang B, Lin XD et al (2019) Effects of silver nanoparticles on pupation, eclosion, life span, apoptosis and protein expression in *Drosophila melanogaster*. Ying Yong Sheng Tai Xue Bao 30(10):3579–3588. <https://doi.org/10.13287/j.1001-9332.201910.036>
132. Meyer D, Williams PL (2014) Toxicity testing of neurotoxic pesticides in *Caenorhabditis elegans*. J Toxicol Environ Health B Crit Rev 17:284–306. <https://doi.org/10.1080/10937404.2014.933722>
133. Mikhaylov VI, Kryuchkova AV, Sitnikov PA et al (2020) Magnetite hydrosols with positive and negative surface charge of nanoparticles: stability and effect on the lifespan of *Drosophila melanogaster*. Langmuir 36(16):4405–4415. <https://doi.org/10.1021/acs.langmuir.0c00605>
134. Mishra M, Sabat D, Ekka B et al (2017) Oral intake of zirconia nanoparticle alters neuronal development and behaviour of *Drosophila melanogaster*. J Nanopart Res 19:282. <https://doi.org/10.1007/s11051-017-3971-y>
135. Mishra PK, Ekielski A, Mukherjee S et al (2019) Wood-based cellulose nanofibrils: Haemocompatibility and impact on the development and behaviour of *Drosophila melanogaster*. Biomol Ther 9(8):363. <https://doi.org/10.3390/biom9080363>
136. Mitra S, Patra P, Chandra S et al (2012) Porous ZnO nanorod for targeted delivery of doxorubicin: *in vitro* and *in vivo* response for therapeutic applications. J Mater Chem 22(45):24145–24154. <https://doi.org/10.1039/C2JM35013K>
137. Moloney A, Sattelle DB, Lomas DA et al (2010) Alzheimer's disease: insights from *Drosophila melanogaster* models. Trends Biochem Sci 35:228–235. <https://doi.org/10.1016/j.tibs.2009.11.004>
138. Montazer M, Maali Amiri M (2014) ZnO nano reactor on textiles and polymers: *Ex situ* and *in situ* synthesis, application, and characterization. J Phys Chem B 118:1453–1470. <https://doi.org/10.1021/jp408532r>
139. Morones JR, Elechiguerra J, Camacho A et al (2005) The bactericidal effect of silver nanoparticles. Nanotechnology 16:2346–2353. <https://doi.org/10.1088/0957-4484/16/10/059>
140. Mu Q, David CA, Galceran J et al (2014) Systematic investigation of the physicochemical factors that contribute to the toxicity of ZnO nanoparticles. Chem Res Toxicol 27:558–567. <https://doi.org/10.1021/tx4004243>
141. Naves MPC, de Moraes CR, Silva ACA et al (2018) Assessment of mutagenic, recombinogenic and carcinogenic potential of titanium dioxide nanocrystals in somatic cells of *Drosophila melanogaster*. Food Chem Toxicol 112:273–281. <https://doi.org/10.1016/j.fct.2017.12.040>
142. Ng CT, Yong LQ, Hande MP et al (2017) Zinc oxide nanoparticles exhibit cytotoxicity and genotoxicity through oxidative stress responses in human lung fibroblasts and *Drosophila melanogaster*. Int J Nanomedicine 12:1621–1637. <https://doi.org/10.2147/IJN.S124403>
143. Ng CT, Ong CN, Yu LE et al (2019) Toxicity study of zinc oxide nanoparticles in cell culture and in *Drosophila melanogaster*. J Vis Exp 151. <https://doi.org/10.3791/59510>
144. Nobre FX, Muniz R, Martins F et al (2020) Calcium molybdate: toxicity and genotoxicity assay in *Drosophila melanogaster* by SMART test. J Mol Struct 1200:127096. <https://doi.org/10.1016/j.molstruc.2019.127096>
145. Oesch F, Landsiedel R (2012) Genotoxicity investigations on nanomaterials. Arch Toxicol 86:985–994. <https://doi.org/10.1007/s00204-012-0838-y>
146. Ong C, Lee QY, Cai Y et al (2016) Silver nanoparticles disrupt germline stem cell maintenance in the *Drosophila* testis. Sci Rep 6:20632. <https://doi.org/10.1038/srep20632>
147. Osborne OJ, Johnston BD, Moger J et al (2013) Effects of particle size and coating on nanoscale Ag and TiO₂ exposure in zebrafish (*Danio rerio*) embryos. Nanotoxicology 7(8):1315–1324. <https://doi.org/10.3109/17435390.2012.737484>
148. Panacek A, Prucek R, Safarova D et al (2011) Acute and chronic toxicity effects of silver nanoparticles (NPs) on *Drosophila melanogaster*. Environ Sci Technol 45:4974–4979. <https://doi.org/10.1021/es104216b>
149. Pandey UB, Nichols CD (2011) Human disease models in *Drosophila melanogaster* and the role of

- the fly in therapeutic drug discovery. *Pharmacol Rev* 63:411–436. <https://doi.org/10.1124/pr.110.003293>
150. Pandey A, Chandra SL, Chauhan KS et al (2013) Cellular internalization and stress response of ingested amorphous silica nanoparticles in the midgut of *Drosophila melanogaster*. *BBA-Gen Subjects* 1830:2256–2266. <https://doi.org/10.1016/j.bbagen.2012.10.001>
151. Pandey H, Saini S, Singh SP et al (2019) Candle soot derived carbon nanoparticles: an assessment of cellular and progressive toxicity using *Drosophila melanogaster* model. *Comp Biochem Physiol C Toxicol Pharmacol* 228:108646. <https://doi.org/10.1016/j.cbpc.2019.108646>
152. Pappus SA, Ekka B, Sahu S et al (2017) A toxicity assessment of hydroxyapatite nanoparticles on development and behaviour of *Drosophila melanogaster*. *J Nanopart Res* 19:136. <https://doi.org/10.1007/s11051-017-3824-8>
153. Parimi D, Sundararajan V, Sadak O et al (2019) Synthesis of positively and negatively charged CeO₂ nanoparticles: investigation of the role of surface charge on growth and development of *Drosophila melanogaster*. *ACS Omega* 4(1):104–113. <https://doi.org/10.1021/acsomega.8b02747>
154. Parvathi VD, Rajagopal K, Sumitha R (2016) Standardization of alternative methods for nanogenotoxicity testing in *Drosophila melanogaster* using iron nanoparticles: a promising link to nanodosimetry. *J Nanotechnol* 2016:1–10. <https://doi.org/10.1155/2016/2547467>
155. Peng F, Su Y, Wei X et al (2013) Silicon-nanowire-based nanocarriers with ultrahigh drug-loading capacity for *in vitro* and *in vivo* cancer therapy. *Angew Chem* 125(5):1497–1501. <https://doi.org/10.1002/ange.201206737>
156. Pereira MT, Malik M, Nostro JA et al (2018) Effect of dietary additives on intestinal permeability in both *Drosophila* and a human cell co-culture. *Dis Model Mech* 11(12):dmm034520. <https://doi.org/10.1242/dmm.034520>
157. Phatak KA, Khanna PK, Nath BB (2016) Particle size-independent induction of leucism in *Drosophila melanogaster* by silver: nano vs. micro. *Metallomics* 8(12):1243–1254. <https://doi.org/10.1039/c6mt00152a>
158. Philbrook NA, Winn LM, Afrooz AN et al (2011a) The effect of TiO₂ and Ag nanoparticles on reproduction and development of *Drosophila melanogaster* and CD-1 mice. *Toxicol Appl Pharmacol* 257:429–436. <https://doi.org/10.1016/j.taap.2011.09.027>
159. Philbrook NA, Walker VK, Afrooz AN et al (2011b) Investigating the effects of functionalized carbon nanotubes on reproduction and development in *Drosophila melanogaster* and CD-1 mice. *Reprod Toxicol* 32:442–448. <https://doi.org/10.1016/j.reprotox.2011.09.002>
160. Plantié E, Migocka-Patrzałek M, Daczewska M et al (2015) Model organisms in the fight against muscular dystrophy: lessons from *Drosophila* and zebrafish. *Molecules* 20:6237–6253. <https://doi.org/10.3390/molecules20046237>
161. Pompa PP, Vecchio G, Galeone A et al (2011) *In vivo* toxicity assessment of gold nanoparticles in *Drosophila melanogaster*. *Nano Res* 4:405–413. <https://doi.org/10.1007/s12274-011-0095-z>
162. Posgai R, Ahamed M, Hussain SM et al (2009) Inhalation method for delivery of nanoparticles to the *Drosophila* respiratory system for toxicity testing. *Sci Total Environ* 408:439–443. <https://doi.org/10.1016/j.scitotenv.2009.10.008>
163. Posgai R, Cipolla-McCulloch CB, Murphy KR et al (2011) Differential toxicity of silver and titanium dioxide nanoparticles on *Drosophila melanogaster* development, reproductive effort, and viability: size, coatings and antioxidants matter. *Chemosphere* 85:34–42. <https://doi.org/10.1016/j.chemosphere.2011.06.040>
164. Priyadarsini S, Sahoo SK, Sahu S et al (2019) Oral administration of graphene oxide nano-sheets induces oxidative stress, genotoxicity, and behavioral teratogenicity in *Drosophila melanogaster*. *Environ Sci Pollut Res Int* 26(19):19560–19574. <https://doi.org/10.1007/s11356-019-05357-x>
165. Raj A, Shah P, Agrawal N (2017a) Dose-dependent effect of silver nanoparticles (AgNPs) on fertility and survival of *Drosophila*: an in-vivo study. *PLoS One* 12(5):e0178051. <https://doi.org/10.1371/journal.pone.0178051>
166. Raj A, Shah P, Agrawal N (2017b) Sedentary behavior and altered metabolic activity by AgNPs ingestion in *Drosophila melanogaster*. *Sci Rep* 7(1):15617. <https://doi.org/10.1038/s41598-017-15645-6>
167. Rajh T, Dimitrijevic NM, Bissonnette M et al (2014) Titanium dioxide in the service of the biomedical revolution. *Chem Rev* 114:10177–10216. <https://doi.org/10.1021/cr500029g>
168. Rajiv S, Jerobin J, Saranya V et al (2016) Comparative cytotoxicity and genotoxicity of cobalt(II, III) oxide, iron(III) oxide, silicon dioxide, and aluminum oxide nanoparticles on human lymphocytes *in vitro*. *Hum Exp Toxicol* 35:170–183. <https://doi.org/10.1177/0960327115579208>
169. Rand MD (2010) *Drosophila* neurotoxicology: the growing potential for *Drosophila* in neurotoxicology. *Neurotoxicol Teratol* 32:74–83. <https://doi.org/10.1016/j.ntt.2009.06.004>
170. Rand MD, Dao JC, Clason TA (2009) Methylmercury disruption of embryonic neural development in *Drosophila*. *Neurotoxicology* 30(5):794–802. <https://doi.org/10.1016/j.neuro.2009.04.006>
171. Reis Éde M, Rezende AA, Oliveira PF et al (2016) Evaluation of titanium dioxide nanocrystal-induced genotoxicity by the cytokinesis-block micronucleus assay and the *Drosophila* wing spot test. *Food Chem Toxicol* 96:309–319. <https://doi.org/10.1016/j.fct.2016.08.023>
172. Richter JW, Shull GM, Fountain JH et al (2018) Titanium dioxide nanoparticle exposure alters metabolic homeostasis in a cell culture model of the

- intestinal epithelium and *Drosophila melanogaster*. *Nanotoxicology* 12(5):390–406. <https://doi.org/10.1080/17435390.2018.1457189>
173. Rubilar O, Rai M, Tortella G et al (2013) Biogenic nanoparticles: copper, copper oxides, copper sulphides, complex copper nanostructures and their applications. *Biotechnol Lett* 35:1365–1375. <https://doi.org/10.1007/s10529-013-1239-x>
 174. Sabat D, Patnaik A, Ekka B et al (2016) Investigation of titania nanoparticles on behaviour and mechanosensory organ of *Drosophila melanogaster*. *Physiol Behav* 167:76–85. <https://doi.org/10.1016/j.physbeh.2016.08.032>
 175. Sanvicens N, Marco MP (2008) Multifunctional nanoparticles – properties and prospects for their use in human medicine. *Trends Biotechnol* 26(8):425–433. <https://doi.org/10.1016/j.tibtech.2008.04.005>
 176. Sapre N, Chakraborty R, Purohit P et al (2020) Enteric pH responsive cargo release from PDA and PEG coated mesoporous silica nanoparticles: a comparative study in *Drosophila melanogaster*. *RSC Adv* 20(10):11716–11722. <https://doi.org/10.1039/C9RA11019D>
 177. Saptarshi SR, Duschl A, Lopata AL (2015) Biological reactivity of zinc oxide nanoparticles with mammalian test systems: an overview. *Nanomedicine (London)* 10:2075–2092. <https://doi.org/10.2217/nmm.15.44>
 178. Sario S, Silva AM, Gaivão I (2018) Titanium dioxide nanoparticles: toxicity and genotoxicity in *Drosophila melanogaster* (SMART eye-spot test and comet assay in neuroblasts). *Mutat Res Genet Toxicol Environ Mutagen* 831:19–23. <https://doi.org/10.1016/j.mrgentox.2018.05.001>
 179. Sau TK, Rogach AL, Jäckel F et al (2010) Properties and applications of colloidal nonspherical noble metal nanoparticles. *Adv Mater* 22(16):1805–1825. <https://doi.org/10.1002/adma.200902557>
 180. Schanen BC, Karakoti AS, Seal S et al (2009) Exposure to titanium dioxide nanomaterials provokes inflammation of an *in vitro* human immune construct. *ACS Nano* 3:2523–2532. <https://doi.org/10.1021/nn900403h>
 181. Shankar AH, Prasad AS (1998) Zinc and immune function: the biological basis of altered resistance to infection. *Am J Clin Nutr* 68(2):447S–463S. <https://doi.org/10.1093/ajcn/68.2.447S>
 182. Sharma V, Anderson D, Dhawan A (2012) Zinc oxide nanoparticles induce oxidative DNA damage and ROS triggered mitochondria mediated apoptosis in human liver cells (HepG2). *Apoptosis* 17:852–870. <https://doi.org/10.1007/s10495-012-0705-6>
 183. Sharma A, Sood K, Kaur J et al (2019) Agrochemical loaded biocompatible chitosan nanoparticles for insect pest management. *Biocatal Agric Biotechnol* 18:101079. <https://doi.org/10.1016/j.bcab.2019.101079>
 184. Siddique YH, Fatima A, Jyoti S et al (2013) Evaluation of the toxic potential of graphene copper nanocomposite (GCNC) in the third instar larvae of transgenic *Drosophila melanogaster* (hsp70-lacZ) Bg9. *PLoS One* 8:e80944. <https://doi.org/10.1371/journal.pone.0080944>
 185. Siddique YH, Khan W, Khanam S et al (2014) Toxic potential of synthesized graphene zinc oxide nanocomposite in the third instar larvae of transgenic *Drosophila melanogaster* (hsp70-lacZ) Bg 9. *Biomed Res Int* 2014:1–10. <https://doi.org/10.1155/2014/382124>
 186. Siddique YH, Haidari M, Khan W et al (2015) Toxic potential of copper-doped ZnO nanoparticles in *Drosophila melanogaster* (Oregon R). *Toxicol Mech Methods* 25:425–432. <https://doi.org/10.3109/15376516.2015.1045653>
 187. Siddiqui L, Bag J, Seetha et al (2020) Assessing the potential of lignin nanoparticles as drug carrier: synthesis, cytotoxicity and genotoxicity studies. *Int J Biol Macromol* 152:786–802. doi:<https://doi.org/10.1016/j.ijbiomac.2020.02.311>
 188. Siegrist M, Wiek A, Helland A et al (2007) Risks and nanotechnology: the public is more concerned than experts and industry. *Nature Nanotechnol* 2:67. <https://doi.org/10.1038/nnano.2007.10>
 189. Silva RM, Teesy C, Franzi L et al (2013) Biological response to nano-scale titanium dioxide (TiO₂): role of particle dose, shape, and retention. *J Toxicol Environ Health A* 76:953–972. <https://doi.org/10.1080/15287394.2013.826567>
 190. Snyder-Talkington BN, Qian Y, Castranova V et al (2012) New perspectives for *in vitro* risk assessment of multiwalled carbon nanotubes: application of coculture and bioinformatics. *J Toxicol Environ Health B Crit Rev* 15:468–492. <https://doi.org/10.1080/10937404.2012.736856>
 191. Sood K, Kaur J, Singh H et al (2019) Comparative toxicity evaluation of graphene oxide (GO) and zinc oxide (ZnO) nanoparticles on *Drosophila melanogaster*. *Toxicol Rep* 6:768–781. <https://doi.org/10.1016/j.toxrep.2019.07.009>
 192. Stocker H, Gallant P (2008) Getting started: an overview on raising and handling *Drosophila*. *Methods Mol Biol* 420:27–44
 193. Strawn ET, Courtney AC, Beverly AR (2006) Cerium oxide nanoparticles increase lifespan and protect against free radical-mediated toxicity. *FASEB J* A1356-A1356. <https://doi.org/10.1096/fasebj.20.5.A1356-c>
 194. Su Y, He Y, Lu H et al (2009) The cytotoxicity of cadmium based, aqueous phase-synthesized, quantum dots and its modulation by surface coating. *Biomaterials* 30:19–25. <https://doi.org/10.1016/j.biomaterials.2008.09.029>
 195. Sundararajan V, Dan P, Kumar A et al (2019) *Drosophila melanogaster* as an *in vivo* model to study the potential toxicity of cerium oxide nanoparticles. *Appl Surf Sci* 490:70–80. <https://doi.org/10.1016/j.apsusc.2019.06.017>
 196. Teow Y, Asharani PV, Hande MP et al (2011) Health impact and safety of engineered nanomaterials.

- Chem Commun 47(25):7025–7038. <https://doi.org/10.1039/C0CC05271J>
197. Thiyagarajan K, Bharti VK, Tyagi S et al (2018) Synthesis of non-toxic, biocompatible, and colloidal stable silver nanoparticle using egg-white protein as capping and reducing agents for sustainable anti-bacterial application. RSC Adv 41(8):23213–23229. <https://doi.org/10.1039/C8RA03649G>
198. Tian H, Eom HJ, Moon S et al (2013) Development of biomarker for detecting silver nanoparticles exposure using a GAL4 enhancer trap screening in *Drosophila*. Environ Toxicol Pharmacol 36:548–556. doi:<https://doi.org/10.1016/j.etap.2013.05.013>
199. Tsyusko OV, Hardas SS, Shoultz-Wilson WA et al (2012) Short-term molecular-level effects of silver nanoparticle exposure on the earthworm, *Eisenia fetida*. Environ Pollut 171:249–255. <https://doi.org/10.1016/j.envpol.2012.08.003>
200. Vales G, Demir E, Kaya B et al (2013) Genotoxicity of cobalt nanoparticles and ions in *Drosophila*. Nanotoxicology 7:462–468. <https://doi.org/10.3109/17435390.2012.689882>
201. Valizadeh A, Mikaeili H, Samiei M et al (2012) Quantum dots: synthesis, bioapplications, and toxicity. Nanoscale Res Lett 7:480. <https://doi.org/10.1186/1556276X-7-480>
202. Vallee BL, Falchuk KH (1993) The biochemical basis of zinc physiology. Physiol Rev 73(1):79–118. <https://doi.org/10.1152/physrev.1993.73.1.79>
203. Vecchio G, Galeone A, Brunetti V et al (2012a) Mutagenic effects of gold nanoparticles induce aberrant phenotypes in *Drosophila melanogaster*. Nanomedicine 8:1–7
204. Vecchio G, Galeone A, Brunetti V et al (2012b) Concentration-dependent, size-independent toxicity of citrate capped AuNPs in *Drosophila melanogaster*. PLoS One 7:e29980. <https://doi.org/10.1371/journal.pone.0029980>
205. Vega-Alvarez S, Herrera A, Rinaldi C et al (2014) Tissue-specific direct microtransfer of nanomaterials into *Drosophila* embryos as a versatile *in vivo* test bed for nanomaterial toxicity assessment. Int J Nanomedicine 9:2031–2041
206. Venken KJ, Sarrion-Perdigones A, Vandeventer PJ et al (2016) Genome engineering: *Drosophila melanogaster* and beyond. Wiley Interdiscip Rev Dev Biol 5:233–267. <https://doi.org/10.1002/wdev.2016.5.issue-2>
207. Wang ZL (2004) Zinc oxide nanostructures: growth, properties and applications. J Condens Matter Phys 16(25):R829. <https://doi.org/10.1088/0953-8984/16/25/R01>
208. Wang B, Chen N, Wei Y et al (2012) Akt signaling-associated metabolic effects of dietary gold nanoparticles in *Drosophila*. Sci Rep 2:563. <https://doi.org/10.1038/srep00563>
209. Willhite CC, Karyakina NA, Yokel RA et al (2014) Systematic review of potential health risks posed by pharmaceutical, occupational and consumer exposures to metallic and nanoscale aluminum, aluminum oxides, aluminum hydroxide and its soluble salts. Crit Rev Toxicol 44(4):1–8. <https://doi.org/10.3109/10408444.2014.934439>
210. Wu VM, Uskoković V (2017) Population effects of calcium phosphate nanoparticles in *Drosophila melanogaster*: the effects of phase composition, crystallinity, and the pathway of formation. ACS Biomater Sci Eng 3(10):2348–2357. <https://doi.org/10.1021/acsbiomaterials.7b00540>
211. Wu VM, Uskoković V (2020) Fruit fly as a model organism for blood-brain barrier penetration and infectious disease in the nanomedical niche. J Bionic Eng 17:553–569. <https://doi.org/10.1007/s42235-020-0044-1>
212. Wu J, Sun J, Xue Y (2010) Involvement of JNK and p53 activation in G2/M cell cycle arrest and apoptosis induced by titanium dioxide nanoparticles in neuron cells. Toxicol Lett 199:269–276
213. Wu VM, Huynh E, Tang S et al (2019) Brain and bone cancer targeting by a ferrofluid composed of superparamagnetic iron-oxide/silica/carbon nanoparticles (earthicles). Acta Biomater 88:422–447. <https://doi.org/10.1016/j.actbio.2019.01.064>
214. Yasinskyi Y, Protsenko O, Maistrenko O et al (2019) Reconciling the controversial data on the effects of C60 fullerene at the organismal and molecular levels using as a model *Drosophila melanogaster*. Toxicol Lett 310:92–98. <https://doi.org/10.1016/j.toxlet.2019.03.006>
215. Zhang XX, Wen GH, Huang S et al (2001) Magnetic properties of Fe nanoparticles trapped at the tips of the aligned carbon nanotubes. J Magn Magn Mater 231(1):9–12. [https://doi.org/10.1016/S0304-8853\(01\)00134-2](https://doi.org/10.1016/S0304-8853(01)00134-2)
216. Zhang WD, Jiang LC, Yu YX et al (2014) Electrodeposition of polyaniline onto TiO₂ nanoparticles/ multiwalled carbon nanotubes for visible light photoelectrocatalysis. J Nanosci Nanotechnol 14:7032–7037. <https://doi.org/10.1166/jnn.2014.8980>
217. Zhang Y, Wang Z, Li X et al (2016) Dietary iron oxide nanoparticles delay aging and ameliorate neurodegeneration in *Drosophila*. Adv Mater 28(7):1387–1393. <https://doi.org/10.1002/adma.201503893>
218. Zhao MX, Zeng EZ (2015) Application of functional quantum dot nanoparticles as fluorescence probes in cell labeling and tumor diagnostic imaging. Nanoscale Res Lett 10:171. <https://doi.org/10.1186/s11671-015-0873-8>
219. Zhou J, Xu NS, Wang ZL (2006) Dissolving behavior and stability of ZnO wires in biofluids: a study on biodegradability and biocompatibility of ZnO nanostructures. Adv Mater 18(18):2432–2435. <https://doi.org/10.1002/adma.200600200>
220. Zou HY, Zhao F, Zhu WF et al (2016) *In vivo* toxicity evaluation of graphene oxide in *Drosophila melanogaster* after oral administration. J Nanosci Nanotechnol 6(7):7472–7478. <https://doi.org/10.1166/jnn.2016.11126>



Toxicological Aspects of Iron Oxide Nanoparticles

13

Natalia Fernández-Bertólez, Carla Costa,
Fátima Brandão, João Paulo Teixeira,
Eduardo Pásaro, Vanessa Valdiglesias,
and Blanca Laffon

Abstract

Iron oxide nanoparticles (ION), with unique magnetic properties, have attracted huge scientific attention for a wide variety of uses, mostly in the biomedical field, due to their high biocompatibility, ability to cross biological membranes, appropriate surface architecture and easy conjugation with targeting ligands. Their current applications include diagnostic imaging, cell labelling,

site-directed drug delivery and anticancer hyperthermia therapy. The ION surface may be modified by coating with different materials, aiming to stabilize the nanoparticles in different environments, to allow biomolecule binding favouring surface attachments with several molecules, and to prolong the recognition time by the immune system. Although the potential benefits of ION are considerable, and more and more ION are being manufactured to meet the demands of the rapidly proliferating field of nanomedicine, there is an urgent need to define their toxicological profile in order to avoid any potential health risks associated with their exposure and to reach optimal benefits of their use. The purpose of this chapter is to describe the current knowledge on the ION toxicological features, addressing their structure and physico-chemical characteristics, main exposure pathways and toxicokinetic aspects, interaction with cells, and their toxic effects, with special attention to those at the cellular and molecular level.

N. Fernández-Bertólez · E. Pásaro · B. Laffon
Grupo DICOMOSA, Centro de Investigaciones Científicas Avanzadas (CICA), Departamento de Psicología, Facultad de Ciencias de la Educación, Universidade da Coruña, A Coruña, Spain

Instituto de Investigación Biomédica de A Coruña (INIBIC), AE CICA-INIBIC, A Coruña, Spain

C. Costa · F. Brandão · J. P. Teixeira
Department of Environmental Health, National Institute of Health Dr- Ricardo Jorge, Porto, Portugal

ISPUP-EPIUnit, Universidade do Porto, Rua das Taipas, Porto, Portugal

V. Valdiglesias (✉)
Instituto de Investigación Biomédica de A Coruña (INIBIC), AE CICA-INIBIC, A Coruña, Spain

Grupo NanoToxGen, Centro de Investigaciones Científicas Avanzadas (CICA), Departamento de Biología, Facultad de Ciencias, Universidade da Coruña, A Coruña, Spain
e-mail: vanessa.valdiglesias@udc.es

Keywords

Iron oxide nanoparticles · Physicochemical properties · Cellular uptake · Cytotoxicity · Genotoxicity

13.1 Introduction

Iron is one of the most abundant of all metals, comprising nearly 5.6% of the earth crust and nearly all of the earth core [198]. Metallic iron is rarely found on the earth surface because it tends to oxidize. Iron forms compounds mainly in the +2 and + 3 oxidation states. Traditionally, iron (II) compounds are called ferrous and iron (III) compounds ferric. There are also iron oxides with six different crystal structures composed of ferrous or ferric iron centres and oxygen: hematite (α -Fe₂O₃), magnetite (Fe₃O₄), maghemite (γ -Fe₂O₃), β -Fe₂O₃, ϵ -Fe₂O₃ and wüstite (FeO) [22, 179].

Iron is essential for the functioning of many biochemical processes, including electron transfer reactions, gene regulation, binding and transport of oxygen, and regulation of cell growth and differentiation [98, 238, 320]. Thus, iron plays an important role in biology, forming complexes with molecular oxygen in haemoglobin and myoglobin; iron compounds are common oxygen transport proteins in vertebrates [12, 81, 98, 214].

Iron is both an essential nutrient and a potential toxicant to cells; it requires a highly sophisticated and complex set of regulatory approaches to meet the demands of cells as well as prevent excessive accumulation [81, 137]. Iron is also the

metal present at the active site of many important redox enzymes dealing with cellular respiration, oxidation, and reduction in plants and animals [226]. Its ability to both donate and accept electrons also means that it can be harmful when present at high enough concentrations. When not bound to functional proteins, free iron can participate in the Fenton reaction that leads to the production of ‘free radicals’, unwanted by-products of the reaction between free iron and hydrogen peroxide [98]. This, in turn, can lead to the detrimental oxidation of molecules, including DNA, lipids and carbohydrates, which causes damage to cells and tissues [81, 98].

In the last decades, scientists have shown noteworthy interest in the properties of magnetic materials such iron, cobalt, or nickel oxides in the nanometer scale. The unique physical and chemical characteristics of these magnetic nanomaterials have enabled a wide range of new applications [111]. Among all of them, iron oxide nanoparticles (ION) offer significant promise due to their chemical stability, easy production, surface tunability, cost-effectiveness and biocompatibility [25, 369]. This is demonstrated by the growing number of scientific works found in the literature in the last two decades addressing the design, study and applications of ION in a variety of fields (Fig. 13.1).

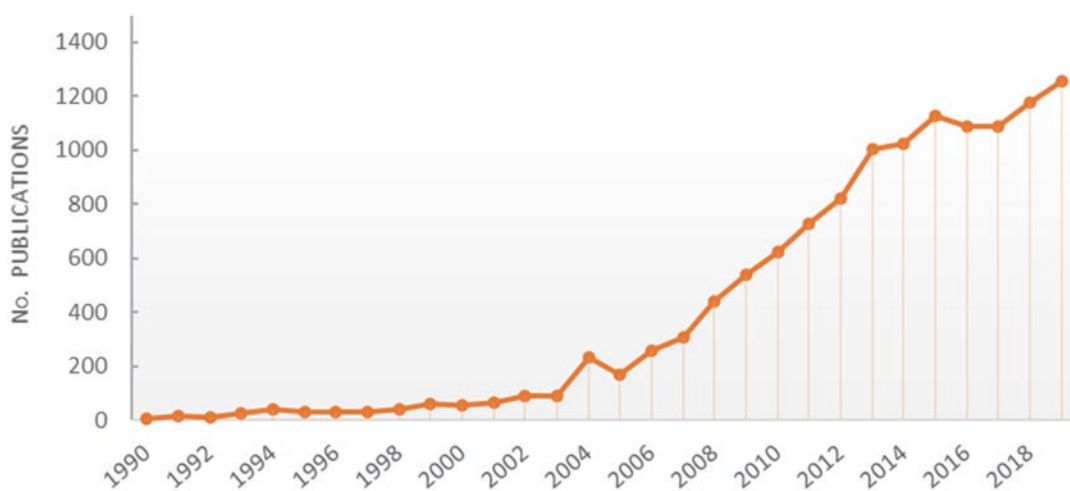


Fig. 13.1 Number of scientific published papers on ION up to the end of 2019 (Source: PubMed). Search term: “iron oxide nanoparticles”

Magnetic properties of nanoparticles depend strongly on their size, surface and shape, in addition to their intrinsic magnetic characteristics [281]. Particularly, ION can exhibit a unique form of magnetism called superparamagnetism. This property is size-dependent and generally arises when the size of nanoparticles is as low as 10–20 nm. On application of an external magnetic field, superparamagnetic particles magnetized up to their saturation magnetization, and on removal of the magnetic field, they no longer exhibit any residual magnetic interaction [318]. In comparison with other nanomaterials, superparamagnetism makes ferromagnets useful for clinical diagnostic and therapeutic applications (theranostics), since they can be addressed to the target sites by controlling/switching an external magnetic field [111]. Moreover, their intrinsic biocompatibility, their high colloidal stability, and their unique biochemical and catalytic properties make ION, by far, the most commonly employed nanoparticles for biomedical applications [7, 35, 105, 252].

Given their biocompatibility and useful physicochemical properties, the design, manufacture, and nanotechnological development of ION has comprised diverse industrial sectors.

According to the report carried out by RIVM (National Institute for Public Health and the Environment of Netherlands) [332] the global market for ION (mainly ferric oxide nanoparticles and ferrofluids) was about €20–40 million, which corresponds roughly to 100 tonnes of nanomaterials used in consumer products, employed for example in automotive industry, electronic components, cosmetics, or other emerging applications as in medicine. In another report by Grand View Research, Inc. [109], the global magnetite nanoparticles market size was world valued at USD 58.4 million in 2019, and is expected to reach USD 87.4 million by 2025, growing at a compound annual growth rate (CAGR) of 10.1% from 2019 to 2025. Their increased demand in industrial applications such as biomedical, electronics, energy, and wastewater treatment (ranked by production importance per application in USD millions) is expected to notably boost the market. Specifically, uses

nanomagnetite-based consumer products in the healthcare technology industry are expected to accumulate the highest growth rate in the market, exceeding 1000 tonnes of production in the corresponding period.

ION are widely utilized in energy field (in photovoltaic film coatings, fuel production and consumption, fuel cells and batteries, thermoelectric materials, and prototype solar panels); in defence and aerospace (as nanocomposites, nanocoatings, sensors and electronics, fuel additives and energy devices); in automotive field (as additives in catalysts and lubricants, nanocoatings, fuel cells, and composite fillers); and in electronics (for high-density information storage media, nanoscale memory, and other electronic and optical devices) [10]. Also, ION can be found being part of building materials (coatings, nanocomposites, nanoscale sensors, and additives to concrete, brick, tile, etc.), and durable pigments (coatings, paints, and coloured concretes) [204]. Furthermore, they are employed in environmental remediation and waste water treatment (permeable reactive barriers, membrane filtration, adsorption), and pollution prevention (pollutant sensors – detection and monitoring) [347], as well as in agriculture ION-based fertilizers (decreasing dose requirement as compared to chemical fertilizers) [267], and as a food additive or pigment, and in food packing composites [40, 317].

However, the most promising uses of ION are in the nanomedicine field. Nanomedicine is an emerging field that combines nanotechnology with pharmaceutical and biomedical sciences, with the goal of developing drugs and imaging agents with higher efficacy and improved safety and toxicological profiles [37]. One of the main biomedical applications of ION consists of using them like a proficient contrast agent in magnetic resonance imaging (MRI), as potential substitute for the commonly used contrast agent gadolinium [164, 290]. To this aim, ultrasmall superparamagnetic coated ION (inorganic core/hydrophilic shell) with particles size smaller than 50 nm are used, since they exhibit low long-term toxicity [63, 201, 329]. In this sense, the US Food and Drug Administration (FDA) approved several

drug formulations for clinical diagnostic, namely ferumoxtran [Combidex® (USA), Sinerem® (EU)] for labeling of cancer cells in contrast-enhanced MRI [289]; and ferucarbotran/ferrixan [Resovist® (USA, EU)], and ferumoxides [Feridex I.V.® (USA), Endorem® (EU)] as cell labeling agents and MRI contrast media [63]. The magnetic and biocompatible properties of ION make them also a mighty therapeutic and/or diagnostic tool for advanced magnetically-guided drug delivery systems [313], since they can be guided toward targeted locations *in vivo* using an external magnetic field to remotely control the distribution of drug molecules in their site of action [76]. Besides, surface of ION can be functionalized, conditioning the drug release to different stimulus, for example, temperature, redox state or pH [218, 313].

Other interesting biomedical applications of ION include the magnetic fluid hyperthermia, in what ION are exposed to an alternating external magnetic field that triggers particle vibration and local heating, leading to cell death in tumour therapy [76, 345]. NanoTherm™ is a colloidal suspension of aminosilane-coated ION, approved in 2010 by the European Medicines Agency (EMA) for local tissue hyperthermia therapy of recurrent glioblastoma, and in 2018 by the USA FDA, for clinical testing in humans to treat prostate cancer [37, 289]. Also, ION are being used in imaging-based diagnostic protocols for magnetically activated cell sorting, a standard separation method for isolating certain cell populations from biological suspensions (*e.g.*, quantification of shifts in monocyte subtype distribution in inflammatory atherosclerosis in humans) [63]. Another therapeutic application is for the clinical treatment of anaemia in chronic kidney disease patients, with the FDA-approved carbohydrate-coated superparamagnetic ION ferumoxytol [(Feraheme® (USA), Rienso® (EU))] [76, 203, 289]. And they can be also used for monitoring the *in vivo* fate of implanted or injected stem cells, offering novel approaches to fight diseases like cancer, neurodegenerative and musculoskeletal disorders, or immunological pathologies [92, 210].

Gene therapy, cell imaging and tissue regeneration are among the most challenging biomed-

ical applications of ION [182]. Indeed, ION can be applied in tissue engineering and regenerative medicine, to visualize scaffold materials or implants, to get information on positioning, proper functionality, or degradation over time [63, 305], and in gene delivery and gene therapy [182, 193].

More specifically, in the last decade, ION have shown to be highly useful for a variety of applications in the central nervous system (CNS), mainly related to imaging, diagnosis, and drug delivery in neurooncological processes, and in neurodegenerative, neurovascular or neuroinflammatory diseases, since ION can surpass the blood-brain barrier (BBB) [103, 178, 263, 291, 353].

For all these clinical applications, ION are introduced into the human body, primarily intravenously, because it is the most efficient way to reach target tissues or organs through the bloodstream. However, in fewer cases, ION can also be administered by intragastric, intraperitoneal, subcutaneous, intratumoral, intrapulmonary, or oral (low doses) routes [193]. For this reason, the intensive study of the possible impact on human health and the toxicological profile of these novel ION has a pivotal importance.

ION generally consists of an iron oxide crystalline core and a coating derived from inorganic, organic or polymeric compounds [76]. Due to their low toxicity, superparamagnetic properties, and catalytic and biochemical properties, magnetite, maghemite or hematite, are by far the most frequent crystalline iron oxide structures used to be part of the ION core for industrial and biomedical applications. However, their critical properties are very different [7].

Magnetite and maghemite are well-known and promising candidates, due to their proved biocompatibility [182]. Both ION show a single crystalline structure and are made of a magnetic domain. Consequently, they show superparamagnetic behaviour and only keep the magnetic moment up in the presence of an external magnetic field. When magnetic field disappear, these ION immediately turn to their non-magnetic states [10]. Magnetite (Fe₃O₄) contains Fe²⁺ and Fe³⁺ ions in a 1:2 ratio. This is a significant matter, as Fe²⁺ triggers the Fenton reaction resulting

in reactive oxygen species (ROS) production in the cells [71]. Magnetite reveals strong magnetism when compared to other transition metal oxides; diameter required for Fe_3O_4 crystals to show superparamagnetism is 50 nm or less (core/coating) [210]. Maghemite ($\gamma\text{-Fe}_2\text{O}_3$) and hematite ($\alpha\text{-Fe}_2\text{O}_3$) contain Fe^{3+} ions and, despite the fact that in bulk they have different magnetic properties, they both turn superparamagnetic after forming sufficiently small crystals [76]. Hematite ($\alpha\text{-Fe}_2\text{O}_3$) is widely used in catalysts, gas sensors, and like pigment compound due to its high corrosion resistance and cost effectiveness. Furthermore, it is also commonly used as a starting material for the synthesis of magnetite and maghemite [210]. The major factors that greatly affect behaviour, toxicity and biocompatibility of these ION include, mostly, the nature of the magnetic core, the methods of synthesis and crystallization, and the final size, shape, and coating composition [10].

At the present, there are a huge number of studies in the literature reporting several efficient synthesis methods to manufacture shape controlled, stable, biocompatible, and monodispersed ION [10, 58, 203]. About 90% of the ION

synthesis approaches adopted are by chemical methods, *i.e.*, co-precipitation, hydrothermal synthesis, microemulsion, thermal and electrochemical decomposition, and sonochemical synthesis. In addition, ION can also be produced by physical methods (8%), such as gas-phase deposition, aerosol, or laser induced pyrolysis, and by biological techniques (2%), *i.e.*, protein, bacterial, fungi, or plant mediated [63, 111]. The surface of ION is, either during or after synthetization, commonly modified with a biocompatible coating. This is done to stabilize them in biological media, to prevent particles from agglomeration and oxidation, to improve their cellular uptake efficiency and biocompatibility, and/or to attach functional molecules required for specifically desired medical applications [10, 63] (Fig. 13.2). Technically speaking, superparamagnetic iron oxide nanoparticles with a particle size greater than 50 nm (core/coating) are called SPION, while those ultra-small superparamagnetic nanoparticles with sizes lower than 50 nm are classified as USPIO [84]. However, in the literature, the term ION is often used interchangeably to refer to both. Therefore, the term ION will be used throughout this chapter for the two types of magnetic nanoparticles.

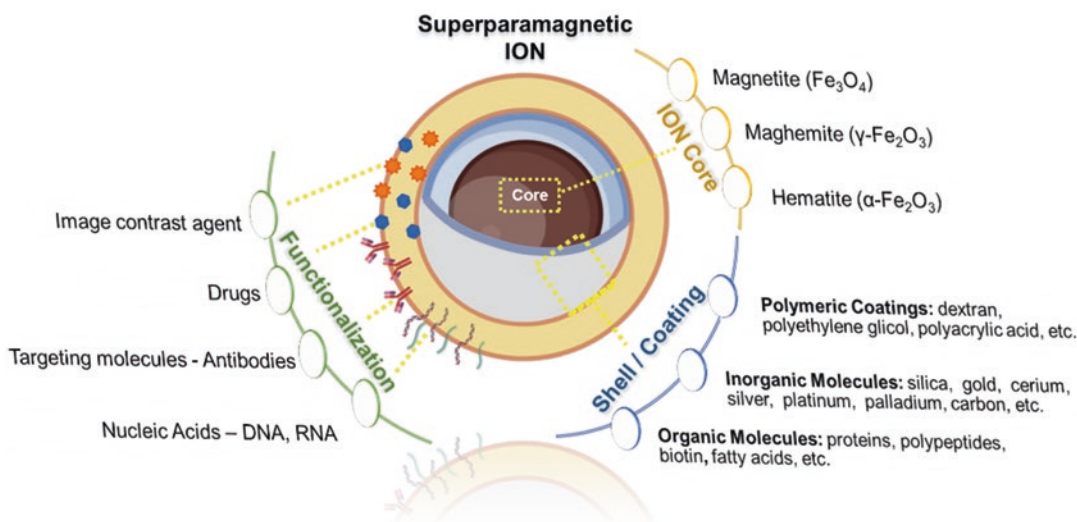


Fig. 13.2 Schematic illustration of core-shell structure of superparamagnetic iron oxide nanoparticles (ION), showing the main iron polymorphic structures employed on core composition – *IRON Core*; the most common shell

molecules used for coating – *Shell/Coating*; and some potential anchor ligands to tailor the ION surface for specific functions required by the target biomedical application – *Functionalization*

13.2 Surface Modification of Iron Oxide Nanoparticles

Chemically, the bare iron or ION experience two major problems in the biological and physiological environment, namely rapid agglomeration (intrinsic instability over long periods of time) and easy oxidation (especially magnetite), due to their large surface area, chemical reactivity, and high surface energy, which can result in loss of colloidal stability and magnetism [371]. Thus, it is important to keep the stability of magnetic ION by developing some effective protection strategies and providing proper surface coatings (or graftings) with organic molecules, polymers, surfactants, biomolecules, or inorganic layers such as metal, metal sulphide, metal oxide, or non-metal elementary substances [290]. The suitable modification of the ION surface can improve their physicochemical properties, to make them more stable in physiological media and biocompatible [8, 10]. In addition, it offers the possibility of a specific subsequent functionalization depending on the biomedical application they have been designed for, allowing a propitious anchor surface between ION and functional biomolecules like antibodies, drugs, proteins, hormones or nucleic acids [371]. The choice of coating is mainly determined by the desired application concerning functionalization, stability or size, since every material has advantages and drawbacks [335].

Moreover, naked nanoparticles introduced into the body can be easily trapped by the immune system as foreign materials, which means that they cannot reach their desired target [262]. In addition to surface coatings, functionalization of the ION surface by incorporating highly specific targeting agents and other functional ligands, such as fluorophores, antibodies and permeation enhancers, can allow monitoring and probing biological, physical and mechanical changes on a molecular scale, which can greatly contribute to improve the applicability and efficacy of these nanoparticles [292]. For this purpose, ION are required to be magnetically targeted to a tissue/organ in order to benefit a therapeutic or diagnostic application. Moreover, in a study using a

number of cell lines, cellular uptake efficiency of ION was demonstrated to be dependent on surface coating of the nanoparticles, irrespective of the cell line used [370]. Hence, a strategy to adjust the cellular uptake efficiency and precision of ION is to modify their surface coating.

Some widespread examples of different materials used to coat the surface of ION and minimize undesirable effects include: natural (such as dextran, alginate, chitosan, starch, pullulan, etc.) or synthetic (such as polyethylene glycol [PEG], polyacrylic acid, polyvinyl pyrrolidone [PVP], polyvinyl alcohol [PVA], polydopamine, polylactic-co-glycolic acid [PLGA], etc.) polymers; fatty acids (such as oleic acid, stearic acid and lauric acid); amino acids (such as phenyl alanine, tyrosine, arginine, lysine and cysteine); metals (such as gold, platinum, palladium, carbon, gadolinium and silver); metal oxides (such as silica and TiO_2); and many biological molecules (such as polypeptides, albumin, casein, antibodies, biotin, etc.) (reviewed in Dadfar et al. [63]). Together with this primary coating, targeting efficiency of ION can be further improved by employing conjugation biomarkers on their surface such as peptides, antibodies or small molecules [216]. Thus, ION coating has frequently been modified with fluorescent dyes for imaging [45, 300], targeting molecules [3, 152], drugs or nucleic acids [278, 339, 369].

However, although this primary coating generally improves ION properties and increases their biocompatibility, it can also modify their toxicological behaviour (reviewed in Valdiglesias et al. [311]). The use of ION in biomedical research is becoming more and more significant, leading to the rapid development of new types of coatings, and therefore of ION. This high diversification of designed ION makes the control of certain characteristics – such as, chemical composition of coating, final hydrodynamic size of the core/shell structure, or presence/type of functionalization elements – extremely important, since they are directly related to the potential mechanisms of action and toxicokinetic profile of ION [180, 371]. Consequently, an increasing number of toxicological studies have been carried out for a wide variety of ION, cell types,

experimental conditions, etc. However, it is not clear yet whether their use is in general safe, or they should be used with caution.

13.2.1 Polymeric Coating

Among all potential materials, polymers, both natural and synthetic, are likely the most popular coating substances, due to their widespread applications in various research areas including nanomedicine [76]. Polymeric nanoparticles attracted the interest of the scientific community because of their structural versatility. Indeed, they can be easily modified with functional groups, such as terminal amine or carboxyl moieties, for further conjugation with bioactive molecules, to anchor ligands at the nanoparticle surface [210, 290]. This allows, for example, to set multifunctional ION up to load different active substances, to deliver their cargo to the targeted site, and to respond to specific external or physiological stimuli [182]. Although this polymeric coating can significantly increase the ION overall size, it can also improve the colloidal stability of the ferrofluid by adjusting the surface charges, which may also modify the toxicokinetic behaviour of the particles, since it may influence their absorption, tissue distribution, and excretion [34, 210, 321].

To date, the most commonly used polymers for surface modification of biomedical ION include natural substances like dextran (for *in vivo* cancer drug carriers or MRI contrast agents) and chitosan (for hyperthermia and tissue engineering) [80, 100, 229, 251, 304], and synthetic molecules like PEG (as MRI contrast agents for *in vivo* cancer imaging, and biosensors), PVA (for *in vivo* imaging, drug delivery, and biosensing) [126, 210, 212, 260], polyethylene imine (for cell separation, gene/drug delivery vehicle, and hyperthermia treatment) due to its high cellular uptake [75, 341], PVP (for targeted killing of breast cancer cells, and MRI contrast agents), and polyacrylic acids (in anticancer drug delivery systems) [371], among others. For MRI applications, ION are generally coated with PEG, or dextran and modified chitosan, due to the long

circulation time of these systems. Some trials also spread gold and gadolinium ions on their surface to enhance the contrasting potential [76].

Dextran is a polysaccharide known for its excellent biocompatibility, good water solubility, bioactivity, biodegradability, and low cytotoxicity [76]. It is one of the mostly used natural polymers for ION coating, a low cost and simple addition substance, with effects on the ION physicochemical properties (such as size, stability, crystallinity, and magnetism) [339]. Due to its general biosafety, dextran-coated ION are rising candidates for biomedical applications [210]. Some authors suggested that dextran-coated ION were cytotoxic at concentrations higher than 50 $\mu\text{g/ml}$ [282]; however, others have clearly shown that dextran-coated ION are non-toxic even at concentrations of 400 $\mu\text{g/ml}$ [307]. These discrepancies found may be due to the lack of stability of the dextran shell, its degradation during the cell membrane interactions or by lysosomal digestion, or also the composition and size of the polymer and the method employed to attach it to the particle surface. Therefore, it is important to carefully monitor the influence of the surface modifications on ION toxicity [76, 180, 218].

PEG is another frequently-used water-soluble synthetic polymer, known for its good compatibility as it carries no potentially toxic groups, favourable chemical properties, and solubility in physiological conditions [168, 356]. Hydroxyl groups at their chain ends, allow the attachment of antibodies and other agents to ION surface [339, 369]. PEG was also recognized to improve circulation half-life time of nanoparticles – due to its hydrophilic surfaces and steric repulsion of PEG chains – and to reduce the cellular uptake of ION; this makes PEG-coated ION very useful as MRI contrast agents, for *in vivo* cancer imaging, and as biosensors [210, 371]. The *in vitro* and *in vivo* experiments carried out by Liu et al. [168] indicated that PEG-coated ION show no cytotoxicity and high resistance to phagocytosis by RAW 264.7 macrophages *in vitro*, as well as low uptake by liver and spleen *in vivo* at a relatively low dose of ION, due to a shielding effect of the dense PEG coating and their net neutral surface.

Similarly, Lee et al. [161] observed that PEGylated ION uptake by macrophage cells was significantly lower in comparison to that of the popular contrast agent, Feridex I.V., suggesting a higher half-life circulation in plasma, due to their high stability and their resistance to uptake by the reticular endothelial system as well. Moreover, it is also reported that PEG coating of magnetite nanoparticles can prevent the reduction of cytochrome C [371].

13.2.2 Inorganic Coating: Nonmetal Oxides

Silica is among the most common and widely employed agents for surface modification of ION, largely used for bioimaging and biosensing purposes [11, 203]. Silica coating has several advantages: it is very stable at wide range of pH and easily dispersible in solution, prevents nanoparticle agglomeration, is inert and biocompatible without affecting magnetism [163], is simply to attach to several active ligands (fluorophores, dyes, quantum dots, drugs, etc.), improves the ION suspension stability [210], and shows low cytotoxic effects [87, 142, 218]. Silica possesses a well-defined and easily tuneable surface chemistry, which can be modified with different functionalities and linked to different biomolecules, allowing an accurate control of the ION interaction with biological structures [13, 218]. Thus, it has demonstrated good biocompatibility, hydrophilicity and stability [371]. Malvindi et al. [191] studied the toxicity in A549 and HeLa cell lines exposed to bare and silica-coated ION (magnetite). They observed that naked ION exhibit higher toxicity due to their stronger *in situ* degradation. Later on, Uribe Madrid et al. [308] reported that different mesoporous silica-coated nanoparticles ($\text{Fe}_3\text{O}_4@m\text{SiO}_2$) show excellent drug release yield, making this core-shell structure ideal for *in vivo* targeted drug delivery. Mesoporous particles made of silicon or silica, characterized by pore sizes ranging from 2 to 50 nm, are excellent options in pharmaceutical nanotechnology. The mesoporous structure allows the control of drug loading and the control

of release kinetics, enhancing drug therapeutic efficacy and reducing toxicity [182]. Besides, their biodegradability can be controlled by modifying a few physicochemical parameters, which enables tailoring these materials for specific biomedical applications and preventing their long-term bioaccumulation [218].

ION surface modification with silica often serves multiple purposes [13, 286]. On one hand, it stabilizes ION in a slightly alkaline pH or high salt concentration environment. For example, silica isoelectric point is close to pH 2, indicating that at $\text{pH} > 2$ the surface will be negatively charged and functionalized with Si-O^- groups, avoiding ION agglomeration in biological fluids [197, 339]. On the other hand, coating the nanoparticle surface with monolayers, such as silica shell or silica mesoporous structures, allows the application of core materials that would be toxic otherwise [218, 257].

13.2.3 Organic Coating: Fatty Acids

For *in vivo* purposes, nanoparticles are required to be biocompatible, stable in biological media, and uniform in size to maintain the suitable magnetic properties [8]. Lipophilic substances such as oleic acid, have gained raising interest for researchers to design lipophilic ION with promising behaviour in non- or weakly polar biological environments [36, 306]. Oleic acid is a monounsaturated fatty acid, widely used as a surfactant agent, and often as a coating substance in the synthesis of highly uniform and monodispersed ION, decreasing interactions between particles and stabilizing them in organic solvents [258, 274]. Additionally, oleic acid can form a dense protective hydrophobic bilayer that binds firmly (through the carboxylic acid) to the ION surface; it can increase ION biocompatibility without affecting too much the magnetic properties [287, 306]. However, the poor water dispersibility of these nanoparticles may sometimes compromise their effectiveness at specific hydrophilic conditions. For this reason, hydrophobic ION can be transferred to the aqueous phase, by simply modifying the oxidation process of oleic

acid-capped ION, to improve the reaction efficiency and their water dispersibility for particular biomedical applications [46].

So far, many research groups have reported the high degree of monodispersity [185, 274, 360], excellent biocompatibility [291, 371], low toxicity [87–90, 142, 181, 309], high colloidal stability and hydrophobicity [36, 222] of different types of oleic acid-coated ION. Specifically, hydrophobicity and non-polar properties of oleic acid capping, make these ION particularly suitable for applications focused on neurological disorders (for drug delivery therapy or hyperthermia), since oleic acid coating improves ION capacity to cross the BBB and reach the brain [70, 139, 291, 339].

13.3 Physicochemical Characteristics of Iron Oxide Nanoparticles

The biocompatibility, biodegradability and toxicological profile of every engineered ION are in tight relation to their physicochemical features, including particle size, surface properties, shape and chemical structure, since these characteristics determine the way and mechanism nanoparticles interact with biological structures [344], the magnetic properties, and all the pharmacokinetic parameters, including uptake or absorption, distribution, metabolism, and excretion. As previously mentioned, ION have a huge future prospective for industrial and biomedical applications, mainly linked to their novel physical and chemical properties [211]. ION interactions with the complex microenvironment of physiological fluids will be determined by: (1) the nanoparticle physical properties, including core composition, crystallinity, surface coating, shape, and size; (2) the chemical characteristics, such as surface chemistry, surface charge, surface coating chemistry, reactivity, solubility, etc.; and (3) the ION biological identity, related to the interplay ION surface-surrounding environment, which triggers the formation of a “corona” composed by different biomolecules, so changes in the agglomeration/aggregation state, nanoparti-

cle size, cellular uptake, and retention time in body fluids may occur [206, 259, 294].

The potential effects of ION on the environment or their impact on the biological response of living organisms have raised great concern in the scientific community [236]. However, it is highly difficult to correlate the biological response observed (overall potential toxicity) with their intricate physicochemical characteristics. Hence, an exhaustive physicochemical characterization is crucial for a proper interpretation of the potential ION toxic effects [240].

Among all physicochemical characteristics that make nanoparticles of the same bulk material different from one another, the nanometric size is one of the most significant. The particle size in the nanoscale modifies availability in the biological environment, since mobility and potential transport through cell membranes is increased with decreasing size, offering the possibility of crossing various biological barriers within the body (*e.g.*, the BBB) [9]. Besides, reduction in nanoparticle size is accompanied by an increase in surface area and, therefore, in surface reactivity, which can lead to an increased grade of biological interaction. This may be one of the reasons why ION are generally considered more toxic than larger particles of the same material [96]. Also, decrease in particle size can be the basis for changes in other parameters such as crystalline structure, optical and electrical properties, or oxidation state, entailing a significant part of the altered toxicological behaviour. For example, for soluble nanoparticles, where the ions themselves can be toxic (*e.g.*, $\text{Fe}^{2+}/\text{Fe}^{3+}$), increased toxicity may result from an increase in particle dissolution with decreasing size and increasing specific surface area [236]. Therefore, size can be a good indicator of the possible toxic effect of ION, since it determines the different mode of action of the particles, it is responsible for changes in other physicochemical characteristics and, consequently, influences toxicity, persistence and bioavailability. Theoretically, particle size is likely to contribute to cytotoxicity, since smaller nanoparticles have a greater specific surface area and, therefore, a greater capacity for interaction with cellular organelles or

molecules such as proteins, carbohydrates, nucleic acids and fatty acids [236]. Moreover, the smaller size likely enhances the ability to cross membranes, enter the cell, and cause cellular damage [125]. Indeed, several works on ION size-dependent distribution showed that nanoparticles with sizes smaller than 10–20 nm have wider distribution levels in the organism. Also, these studies concluded that large sized ION were cleared sooner as compared to smaller ones [9].

Besides size, shape has a significant role in nanoparticle behaviour, since it also affects their chemical reactivity, mechanical, optical, and electric properties, as well as is reported to affect their cellular uptake and pharmacokinetics, which ultimately impact the biological effect or the desired biomedical application [9, 44]. There are many different shapes and structures of nanomaterials based on their morphological characteristics (sphericity or aspect ratio), including cubic, prism, spherical, oval, helical, tube, needle-shaped, platelet, etc. [57, 254]. Nanomaterial shape may have effects on the deposition kinetics and cellular uptake mechanisms [1, 157]. Generally, spherical ION with a low aspect ratio (length-width), have shown shorter blood circulation times over their one-dimensional counterparts, *e.g.*, nanowires, nanotubes or nanorods; this seems to be due to their slower uptake by macrophages by phagocytosis [16]. However, it was demonstrated that the higher the aspect ratio, the more toxic the particle is [44, 254]. Historically, research on nanomaterials for biomedical applications has focused on the spherical-shaped ones, such as quantum dots, and magnetic nanoparticles [94]. Particularly, ION usually present spherical shapes, which involve a significant increase of their cellular uptake efficiency with regard to rod- or tube-shaped particles of similar size [316, 344]. Although not as important as in the case of size, particle shape can also present a distribution based on the dispersion state of the system, and the interactions with the different molecules of the surrounding environment, that can contribute to the behaviour and biological responses of ION [211, 254].

There are a number of techniques to measure particle net size, size distribution, hydrodynamic size, zeta potential, or shape. Some examples include laser diffraction, dynamic light scattering, differential mobility analysis, impaction methods, electron microscopy, time of flight techniques, and surface area measurements. Microscopy is one of the most mighty methods, and often used exclusively to provide information regarding size, shape, morphology, and state of agglomeration/aggregation of nanoparticles [243].

Surface characteristics such as hydrophobicity, surface charge, and charge distribution also have a significant influence on the fate and behaviour of ION in the body [299, 344]. The state of dispersion of nanoparticle systems is another important factor derived from surface properties which refers to the comparison between the relative number of single particles and agglomerates/aggregates in a suspending medium [242]. These nanoparticle agglomerates/aggregates can be established by mild attractive forces (*e.g.*, Van der Waals and hydrophobic interactions) or by binding of surrounding molecules in the medium (*e.g.*, proteins, polysaccharides, etc.) [211, 243]. The smaller the nanoparticle, the stronger the forces between particles. Therefore, the state of agglomeration/aggregation could set up a wide distribution of different shapes and sizes, which can also profoundly affect the dynamics and properties of nanoparticles and thus the resulting potential hazards [195, 277].

Despite the fact that most metallic nanoparticles are poorly soluble and persistent, their solubility can be increased in some biological fluids or culture media, affecting their cellular uptake, subcellular location and toxic effects as well [1, 157]. Particularly, dissolved and undissolved ION have been observed to modify cellular uptake pathways and induce different cytotoxic effects as a function of their ability to release toxic ions [230, 340]. Under aqueous conditions, dissolved ION are known to show a higher release of ions and to induce higher cytotoxicity and apoptosis in mammalian cells than the non-dissolved counterparts, which triggers an increased ROS production and oxidative stress

[215, 224, 340]. Furthermore, as we have seen previously, surface characteristics of ION, along with their size and shape, are the key properties that determine their internalization into cells [344].

As mentioned above, high circulation time of ION in the body is necessary to reach the specific target in some biomedical applications. The absorption of various biomolecules like plasma proteins to the hydrophobic surface of ION can trigger the immune response cascade, immune cell stimulation, phagocytic internalization and clearance of ION, decreasing their circulation time in the organism [72, 79, 219, 244]. Hence, the lower the recognition of ION by the reticulo-endothelial system, and therefore by the immune system, the greater the probability of ION internalization by the target cells. That is why most of the current research is aimed at modifying the hydrophobic surface of ION with different hydrophilic coatings to increase steric repulsive interactions with plasma proteins, and therefore, to increase the half-life of specific nanocarriers in the blood circulation [172].

Surface chemistry consists of a wide variety of properties that lead the way ION interact with biomolecules and biological systems through their chemical composition. In presence of surface modification, results obtained on surface chemical composition analysis reflect the effectiveness of coating to avoid nanoparticle core dissolution [48]. There are extensively used methods for characterizing nanoparticle surface chemistry (*e.g.*, X-ray photoelectron spectroscopy [XPS], electron spectroscopy, and secondary ion mass spectroscopy), as well as to correlate the surface properties with the final physiological effects [248]. Among all ION surface chemical characteristics, surface charge is an extremely important factor, since it influences the particle dispersion, the adsorption of ions and biomolecules to the nanoparticle nucleus (corona formation), and the induction of biological effects [23, 48, 242]. The estimation of the surface charge (assessed by the dynamic light scattering method) is carried out by measuring the zeta potential. The zeta potential is a function between the surface charge of the particle, and the nature and

composition of the surrounding medium where it is scattered [361]. It is a measure of the total electrical potential – ions and nanoparticles – in solution, and thus is affected by changes in pH or ionic strength. Zeta potential measurements range from 0 to ± 60 mV. High values ($> \pm 30$ mV) suggest greater stability due to increased electrostatic repulsion, while low values ($< \pm 30$ mV) indicate a trend of the particles to agglomerate and precipitate [299]. Particle surface charge may affect their cellular uptake as well as how the particles interact with organelles and biomolecules. Consequently, particle surface charge influences cytotoxicity [73]. The toxicity of nanoparticles increased with an increase in surface charge. This suggests that the higher nanoparticle surface charge, the greater electrostatic interactions with the cell and, thus, the greater endocytic uptake [125]. Several studies have reported that similarly sized ION with different surface charge were show different toxic effects [333].

In conclusion, the varied ION physicochemical properties will define their biocompatibility, biodistribution after their entry the body, behaviour, the type of cellular interactions, and their effects [254]. Thus, the exhaustive and in-depth characterization of the ION physicochemical properties (particle size and size distribution, agglomeration/aggregation state, shape, crystalline structure, chemical composition, surface area, surface chemistry and surface charge) plays a key role to understand their possible toxic effects observed in cells [344, 349].

13.4 Iron ion Release

As previously mentioned, iron is an essential trace element that stably interconvert between its most common oxidative forms, ferrous (Fe^{2+}) and ferric (Fe^{3+}), through reduction-oxidation reactions [12]. Iron is indispensable for most life forms and constitutes a wide number of proteins that carry out many metabolic and physiological functions, including formation of heme group of haemoglobin and myoglobin; formation of iron-sulphur clusters in proteins like cytochromes, fer-

rodoxins, reductases and dehydrogenases as mediator in redox and electron transfer reactions; in mitochondrial oxidative phosphorylation; DNA synthesis; or energy production [81, 137]. However, free iron (ionic form) is problematic for biological systems since it is largely insoluble and toxic, due to its capacity to trigger the Fenton reaction, where transition metal ion (ferrous iron, Fe^{2+}) reacts with hydrogen peroxide (H_2O_2) to yield hydroxyl radical ($\bullet\text{HO}$) and ferric iron, Fe^{3+} ; and Haber-Weiss reaction, where oxidized metal ions (ferric iron, Fe^{3+}) and H_2O_2 or superoxide radical ($\bullet\text{O}_2^-$) react to produce $\bullet\text{HO}$ [206, 230]. Once lysosomal specific proteins degrade surface coatings, the ION core is rapidly degraded in the highly acidic lysosome medium, and the free iron (in Fe^{2+} and Fe^{3+} form) is released from the endocytic compartment to cytoplasm, mediated by iron storage or transporter proteins, such as transferrin, DMT1, ferritin, ferroportin, and hemosiderin [81, 262]. Iron is then accumulated into a labile iron pool, process tightly regulated to maintain iron homeostasis, since an excess of this metal can be very toxic for cells [12, 98, 166]. In aqueous media, especially in complex solutions of neutral pH, Fe^{2+} (highly unstable and reactive) is spontaneously oxidized by molecular oxygen to Fe^{3+} . At pH 7.0, the maximum solubility of Fe^{3+} is very low ($\approx 10^{-19}$ M), while the solubility of Fe^{2+} is much higher ($\approx 10^{-2}$ M). On the other hand, the free Fe^{2+} and Fe^{3+} ions in the cytoplasm are capable of catalysing reactions producing harmful free radicals as mentioned above [64]. To maintain iron homeostasis and to avoid the potential toxic effect of free iron ions, organisms have been forced to bind Fe^{3+} to specific proteins (e.g., ferritin, transferrin) that hold their stable form but, simultaneously, keep small quantities of redox-active Fe^{2+} available for biological processes [353]. This is convenient considering that the intracellular ferrous ion is more accessible and a little more toxic [81, 215]. As iron readily shuttles between the reduced ferrous and the oxidized ferric forms, disruption of the cellular redox equilibrium requires only catalytic amounts of the metal [320]. Therefore, overload of intracellular free iron ions derived from ION degradation, leads to excessive ROS production, which

has been shown to induce cytotoxic effects through different mechanisms such as: (i) lipid peroxidation, that induce cellular membrane dysfunction or mitochondrial impairment; (ii) oxidation of key proteins involved in cell cycle or DNA repair processes; or (iii) other cellular effects, *i.e.*, mitochondrial membrane depolarization, actin cytoskeleton dysfunction, altered cell proliferation or cell death induction. On the other hand, genotoxic effects included oxidative DNA damage, impairment of DNA repair systems, or changes in gene transcription.

Exposure to ION concentrations around 100–200 $\mu\text{g}/\text{ml}$ and over causes, in general, dose-dependent increases in intracellular iron in a variety of cells [97, 102, 209, 217, 256, 353], with the consequent increased amount of ROS, and the resulting cytotoxicity through oxidative stress generation [282]. Exposure to high ION concentrations can also overwhelm antioxidant systems and results in enhanced cytotoxicity/genotoxicity and inflammation [64, 103, 319]. Therefore, the normal body capacity to manage iron should be taken into account when considering administration of high or frequently repeated doses of ION [155, 254].

Certain physicochemical properties of ION, such as the iron oxidation state, size, surface charge, or surface coating, are the key factors that determine the ability of ION to generate oxidative stress through the production of ROS and, therefore, to influence the intracellular availability of iron and its cellular toxic effects [224]. The oxidation state of the iron (Fe^{2+} or Fe^{3+}) composing the ION nucleus is an important factor that determines their toxicity by ROS generation [184, 215, 230]. Several recent studies have shown that maghemite nanoparticles (with lower $\text{Fe}^{2+}/\text{Fe}^{3+}$ ratio) induce increased cytotoxicity than magnetite nanoparticles (with higher $\text{Fe}^{2+}/\text{Fe}^{3+}$ ratio) (reviewed in Yarjanli et al. [353]). However, dextran-coated maghemite showed significant genotoxicity correlated with cellular uptake, compared with dextran-coated magnetite, showing that Fe^{3+} ions are more genotoxic than Fe^{2+} ions [282]. In fact, magnetite (major potential to undergo oxidation) has been shown to cause higher levels of oxidative DNA damage

than maghemite in the human lung epithelial cells (A549), without showing a significant decrease in cell viability [131]. As already mentioned, the size of ION may affect their cellular uptake and the iron-mediated cytotoxicity as well. After ION internalization, small nanoparticles degrade sooner since they present more reactive surface area than the larger ones, therefore inducing higher amount of ROS [127, 356]. Surface coating and chemistry also take important part in the persistence and degradation rate of ION, *i.e.*, in the stability of nanoparticle core and its capacity to release free iron ions (either Fe^{2+} or Fe^{3+}). In this regard, Yu et al. [356] demonstrated that bare ION significantly increased ROS and cellular death, but dextran- or PEG-coating reduced ROS formation, blocked their redundant interaction with ION surface hindering ion release from the core and, hence, decreased cytotoxicity. In the same way, ION with various surface modifications and different sizes induced slight, but significant, differences in the amount of accumulated intracellular ROS and, consequently, in observed cytotoxic and genotoxic effects [112].

In addition to the physicochemical properties and the nanoparticle exposure conditions (dosage and duration), it has been found that the management and effects of ION degradation are closely related to the cell type involved, since their uptake and metabolic rate differ [101, 102, 256]. There are conflicting data related to the effects of iron coming from ION in different cells. Thus, Imam et al. [127] observed a viability reduction of the dopaminergic neurons by oxidative stress in the striatum of rats after *in vivo* ION exposure, while Zhang et al. [368] conversely reported that daily intake of 200 $\mu\text{g}/\text{ml}$ magnetite decreased cytotoxic effects of ROS in *Drosophila* Parkinson's disease model cells, showing neuroprotective effects. On the other hand, oxidative stress induced by ION degradation has been shown to have especially significant effects in those organs with high mitochondrial activity, such as the heart or liver, making these cell types more sensitive to iron-mediated toxicity [81]. In fact, under pathological conditions (such as cancer, atherosclerosis, hypertension, or arthritis)

iron may effectively be released from ferritin leading to increased oxidative damage and causing cellular toxicity [312].

Particularly, iron overloading within the brain can be more dangerous than in other tissues. Accordingly, Imam et al. [127] reported that ION, by producing ROS, caused damage to the membrane of rat's brain endothelial cells, due to slower nanoparticle uptake by these cells or by destroying cellular membranes during crossing BBB. Iron is essential for many metabolic processes of the CNS and for proper function of neurons [353]. Nevertheless, excess of iron can be toxic to the brain. Most of the intracellular iron pool is composed of inactive Fe^{3+} bound to ferritin to annul the high toxicity associated with free iron [120, 343], but there is always a small redox-active amount of Fe^{2+} ions that normal metabolism needs [118, 119, 353]. In this regard, an efficient ION uptake and metabolism of extracellular iron (slowly released from ION), as well as strong up-regulation of ferritin expression, may contribute to the high resistance of cells like astrocytes [117], even neurons, to acute iron-mediated toxicity in the brain. This is likely due to slower transfer of internalized nanoparticles to the lysosomes, where major iron ion release occurs [235]. Hence, lysosome storage likely contributes to high cell resistance to iron toxicity, and is especially relevant in the nervous tissue, since even the prolonged presence of large amounts of accumulated ION does not harm these cells [206]. For these reasons, all mechanisms involving transportation and homeostasis of iron in the CNS must be strongly regulated to prevent excess iron and its toxic effects as seen in neurodegenerative diseases [328, 330].

13.5 Exposure and Kinetics

The growing commercialization of nanomaterials in the last years, and particularly the successful application of ION in medicine and clinics, has significantly increased the potential human exposure to these materials. For this reason, carrying out complete and systematic toxicological analyses is of paramount importance, since the poten-

tial negative effects of ION are directly related to their effective dose, duration of exposure, or their persistence in the body [39, 355].

Accidental or intentional exposure routes to nanomaterials may include inhalation [91, 149, 156, 264], ingestion [317, 324], or dermal uptake [175, 207]. In addition, for medical purposes, parenteral, systemic or local administration must be considered [53, 143] (Fig. 13.3). Examples for unintentional exposures to ION include emissions from anthropogenic sources into air (power plants, incineration, internal combustion engines, occupational settings), water and soil (households, effluents from manufacturing sites) or consumer goods (textiles, cosmetics). Intentional exposures occur also from biomedical applications, food additives, etc. [67, 149, 213]. End-product users, occupationally exposed subjects, medical patients and the general public may be at risk of adverse effects due to the direct contact with the organism [44, 125, 194]. The presence of nanoparticles in many consumer products such as drugs, skin care products, cosmetics, food additives, etc., cause both intentional and accidental exposures. In fact, it has been estimated that in developed countries, approximately 10^{12} – 10^{14} nanoparticles/day are ingested per person [186].

Depending on the desired biomedical application, ION are administered primarily through intravenous injection, and to a lesser extent by oral or respiratory pathways [16]. Thus, intravenous administration of ION is the most suitable approach for their use as image contrast agent in MRI, computed tomography (CT), positron emission tomography (PET), or surface plasmon resonance (SPR); for targeted drug/gene delivery systems; or for magnetic hyperthermia therapy [53]. The blood half-life values of different ION (1–24 h in humans) is highly dependent on the dosage and properties of the ION (*i.e.*, size, shape, surface properties, etc.), the characteristics of the individual exposed, and the exposure medium [16]. In this case, the first consideration to take into account for the desired application is that, in blood, ION will come into contact with plasma proteins that will probably lead to the formation of protein corona, which may change the pharmacological properties of the nanoparticles. The pharmacokinetics of ION involves aspects of the rate and extent of their absorption, distribution, metabolism, and excretion (ADME processes) in the body [53].

Due to their small size and tendency to remain airborne for long time periods, the most common accidental route of nanoparticles exposure is via

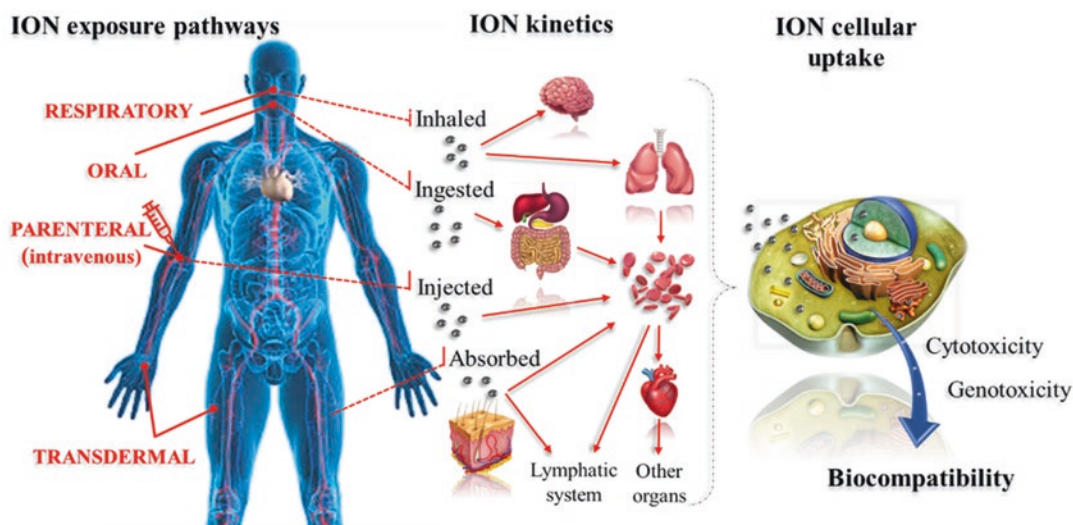


Fig. 13.3 Schematic of human body showing the main routes of exposure, the biodistribution and potential target organs, and the cellular internalization of ION

inhalation from combustion-derived particles, atmospheric airborne nanoparticles, occupational settings, or during production, processing, and handling of iron containing products. Therefore, the main absorption pathway of ION is the respiratory system [27, 149]. ION size determines where they will be deposited along the respiratory tract. Nanoparticles smaller than 55 nm in diameter have higher penetration potential than NP with sizes of 200 nm or more. Approximately 50% of the inhaled ION (≤ 20 nm) are deposited in the alveolar region of lungs, where they are absorbed through the epithelium and enter the vascular or lymphatic system. Another portion of the inhaled ION (biggest particles) are trapped by mucociliary epithelium of the bronchi where they are cleared (phagocytosis), or they go up into the trachea, where they are finally swallowed and translocated to the gastrointestinal tract [149].

Once ION circulate in blood and lymph, they can accumulate in the cells of the bone marrow or lymph nodes, or reach different organs such as the liver, the heart, or the brain, among others [39]. There is also evidence of absorption of ION via the olfactory nerve following inhalation exposure; particles may then enter the brain without crossing the BBB [99, 134, 322]. Once the ION have been introduced into the body, they are rapidly detected by macrophages distributed in the tissues, which engulf them by phagocytosis for their metabolization and degradation. Therefore, there must be a balance between the absorption and distribution of nanoparticles necessary to carry out their functions in the established target organ, and their active clearance by the immune system [16]. For this reason, it is extremely important to know the ADME properties of ION used in biomedical applications, since they allow to establish optimal designs in terms of functionality, as well as to minimize the possible derived undesirable side effects [315].

Regardless the route of absorption, distribution of nanoparticles in the body is strongly dependent on characteristics like chemical composition, size, shape, surface coating or surface charge [116]. ION size gives them the ability to easily access the blood capillaries; they can even

cross different biological barriers, from where they can be internalized by cells through several mechanisms and interact with cellular molecules and organelles [16]. ION-based products are a powerful non-invasive tool in biomedical imaging, clinical diagnosis, and therapy. The successful delivery of drugs is limited and being challenged by these biological barriers including the gastrointestinal tract, brain, skin, lungs, and immune system, among others. Phagocytic sequestration by the macrophages limits ION localization at the target site, leading to non-specific internalization by healthy tissues [54]. There are several studies addressing the biodistribution of oral-administered, inhaled, or injected ION, showing direct evidence of translocation of the administrated nanoparticles across the lung epithelial cell, gastrointestinal tract epithelial cell, kidney endothelial cell, or blood–testis barriers, accumulating in the corresponding organs with mainly low toxic effects [108]. Besides, Di Bona et al. [69] informed that intra-peritoneally injected ION can easily cross the placental barrier in pregnant mice and increase the risk of foetal death due to excessive accumulation of the ION in the foetal liver.

Specifically, due to the general world population aging, CNS pathologies such as neurodegenerative diseases are increasingly becoming a relevant medical, economic, and social issue. Current pharmacological treatments are mainly based on systemic delivery of diagnostic/therapeutic drugs into the CNS, and their effectiveness is seriously limited due to the presence of the most restrictive biological barrier, the BBB. Hence, treatment of this disorders remains a daunting challenge due to the limited access across this barrier [15]. ION provide multifunctional abilities for solving these biomedical and pharmacological issues, along with their confirmed ability to cross the BBB [205, 291]. The improvement of effective drug delivery by magnetic driving of ION is considered one of the most ambitious and versatile systems for inaccessible regions like the brain, being able to provide protection to therapeutic agents while efficiently delivering them into the target areas [263]. These abilities have been strongly exploited in recent

years in the diagnosis and therapy of diseases that affect the CNS, since some ION (*e.g.*, oleic acid- or PVA-coated) showed a great ability to cross the BBB and a low neurotoxicity [76], opening up a new non-invasive way of treating, for instance, difficult-to-approach brain tumours such as glioblastoma [189].

13.5.1 Blood-Brain Barrier (BBB)

Although translocation of nanoparticles to the brain is possible and well-studied in the literature under different experimental conditions [52, 196, 225, 276, 354], the relevance for real-life situations is far from clear. Therefore, evaluation of the potential toxic effects of ION on cells from neural origin is required, as specific mechanisms and pathways through which nanoparticles may exert their toxic effects remain largely unknown. The brain is probably the best protected organ in the human body. The epithelial cells of choroid plexus (CP), situated in the four ventricles of the brain, form an important barrier between the blood and the cerebrospinal fluid (CSF), called BBB [342]. The BBB is a dynamic but solid neuroprotective shield in the cerebral microvascular system. It plays a pivotal role in maintaining CNS homeostasis by regulating the CSF secretion, signalling, selective passive exchange of essential metabolites – such as glucose, water and amino acids – between the blood and the brain, and protects the neural tissue from neurotoxic external and internal chemicals as well as pathogens [205, 342]. Several complex interactions between different nervous cell types – such as the endothelial cells, neurons, astrocytes, pericytes, microglia, and the extracellular matrix of the brain – are important contributors to the structure and function of the [32]. Endothelial cells together shape a highly dense cellular network with tight junctions that restrict CNS entry of xenobiotics and therapeutics from the bloodstream [171]. Besides, astrocytes and pericytes surround the endothelial cells of the BBB providing biochemical support to those cells [220]. Important proteins for the barrier function include tight junction proteins, numerous transporters

and enzymes [151]. The BBB exhibits a high transendothelial electrical resistance, along with a low rate of transcytosis and greatly restricted paracellular permeability [62]. Although tight junction protein complexes are principal contributors to physical barrier properties, they are highly dynamic structures, where expression and/or localization of individual constituent proteins can be modified in response to pathophysiological stressors [171].

Among all nervous cells, astrocytes are particularly interesting since they are the most plentiful cell type in the CNS. Astrocytes are strategically dispensed between the blood vessels and neurons, and in deep contact with the brain capillary endothelial cells through their end-feet, being one of the first cellular type that interact with ION after internalization [102, 349]. Their functions include regulation of neurotransmitter delivery, homeostasis of ions, pH and water, balancing the extracellular potassium concentration, excretion of growth factors, and metabolic support to neurons, among other homeostasis maintaining functions in the brain [228, 342]. During the past two decades, astrocytes emerged also as increasingly important regulators of neuronal functions including the generation of new nerve cells and structural as well as functional synapse remodelling. Moreover, they interact with neurons and modulate their signal transmission [65, 123]. Besides, they seem to play a key role in the aetiology of neurodegenerative disorders and, consequently, have been proposed as new targets for the diagnosis and treatment of important neuropathologies such as Alzheimer's disease, amyotrophic lateral sclerosis, and Parkinson's disease.

Pericytes are important contributors to the structure and function of the neurovascular unit as well, being actively involved in both CNS homeostasis and pathology of neurological disorders, including Alzheimer's disease, multiple sclerosis, or spinal cord injury, among others. These cells are found encased within the basement membrane. They are basic for maintaining the BBB integrity, and promoting neuroinflammation and neurorepair. Some roles of pericytes include: acting as immune system promoters

with their ability to clear up cellular debris, transmigration of immune cells through BBB, boosting the activities of CNS glia, regulating tight junction formation and endothelial transcytosis, or contributing to maturation of oligodendrocytes. Inversely, they can propagate neuroinflammation and promote injury, impairing regenerative processes [32].

On the other hand, neurons are the core constituent of the brain and are crucial for the maintenance of its function. In general, neurons have the specific function to transmit electrochemical signals, and can differ according to their morphology, location, function (motor, sensory), or effect (excitatory, inhibitory) [359]. Neuronal alterations, such as loss of structure or function, are considered to play a key role in the aetiology of certain neurodegenerative diseases as well [337].

Due to their special physicochemical properties, such as small size and large surface area, ION can cross the BBB and accumulate within the brain, and may cause neurotoxicity after reaching the nervous system [173, 176, 333]. Once ION have crossed the BBB, they can interact with neurons, astrocytes and microglial cells, which can induce or trigger a succession of disruptions in the neurological system (oxidative stress, DNA and/or mitochondrial damage, and inflammation), thus increasing the potential risks of neurotoxicity [49, 62]. Neurotoxicity of ION has raised special concern in the last decade because their uses in the diagnosis, monitoring and treatment of CNS disorders may be a promising, although unexplored via for new therapies for neurodegenerative diseases [135].

The raising concern about the effects on human brain cells derived from ION exposure makes *in vitro* studies crucial to initially evaluate their potential risk for the CNS cells, from neurons to glial cells [77, 200]. Nevertheless, nowadays the studies collected in the literature addressing their possible toxic effects in the CNS are still scarce and, in many cases, contradictory [41]. The use of primary human cell culture models, although more representative, is limited, as differentiated nervous cells are difficult to obtain, have a limited proliferating capacity in culture,

and present ethical constraints. The use of standardized cell line stocks have the advantages of the proliferative potential of an immortal cancer cell line and its high efficiency in culture, combined with ability to be differentiated to cells that can then be used in functional assays [333].

13.6 Cellular Uptake

The actual entry of nanoparticles into the cells should be verified prior to toxicity evaluation. The extent of cellular toxicity of any nanoparticle depends on its cellular internalization efficiency. The compatibility of ION relies on their interaction with healthy cells, in such a way that ION will accelerate or retard the growth phase of the cells under living conditions [239]. As it is represented in Fig. 13.4, nanoparticles may be incorporated by cells mainly via passive diffusion, or actively by clathrin-mediated endocytosis, caveolae-mediated endocytosis, phagocytosis, or micropinocytosis [167]. After nanoparticles pass through the cell membrane by active absorption, they are generally encapsulated in intracellular vesicles/early endosomes, and then are located in the early or late lysosomes as the vesicles mature [167]. Sometimes, they might be endocytosed upon pinocytosis. Alternatively, they may also be transported through the cytosol to the endoplasmic reticulum via caveosomes, or by means of transcytotic processes. Besides active uptake, smaller nanoparticles may also cross the plasma membrane by passive diffusion [208]. From the cytosol they may then gain access to subcellular compartments or organelles, *e.g.*, nucleus and mitochondria [348].

Cellular uptake of ION, speed and the endocytic mechanisms associated, are highly dependent on the nanoparticle size, surface coating, charge, shape, or other factors like cell type, cell surface status, differentiation state, external forces, protein or lipidic binding (corona), temperature, and biological medium [48, 51]. All these physicochemical interactions, kinetics, and thermodynamic exchanges that occur between nanoparticle surface and the biological environment (for example binding to proteins, mem-

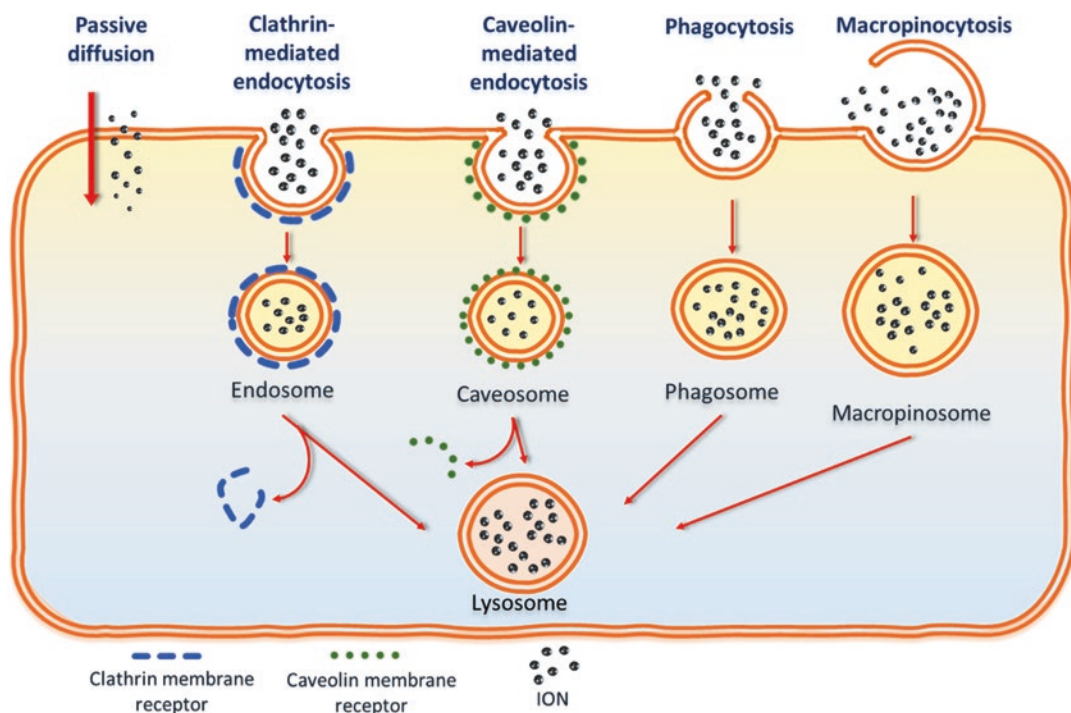


Fig. 13.4 Schematic representation of possible mechanisms by which nanoparticles may enter the cell and cellular compartments. From left to right, nanoparticles may

be taken up by cells by passive diffusion, clathrin-mediated endocytosis, caveolin-mediated endocytosis, phagocytosis, or micropinocytosis

branes, phospholipids, endocytic vesicles, organelles, DNA, and biological fluids) lead to the formation of a corona, a dynamic interface which significantly influences the fate and behaviour of the ION in the body [48, 129]. The efficient cell uptake of ION in different tissues makes them especially appropriate tools for theranostic applications such as MRI, induced magnetic hyperthermia, or drug delivery systems, but it also predisposes target organs (for example, the CNS) to its possible adverse outcomes.

Almost every type of nanoparticle has a specific mechanism of entry into the cell, as a result of its specific physicochemical properties, the adsorption of serum proteins on the surface, the cell type involved, etc. [6, 48]. To date, there is no standardized and validated method for evaluating the internalization of ION, since the choice of a certain method depends mainly on the parameter to be measured, the analytical devices available and their limitations, the type of ION employed, and the biological milieu where it is analysed.

Therefore, although it is not possible to recommend a specific technique for all cases, it is necessary to consider the limitations of the selected system to correctly interpret the results obtained [51]. As evidenced by studies found in the literature, physicochemical properties of nanoparticles, such as size, shape, core composition, and surface coating and/or functionalization, play a key role in the way they interact with cells, including internalization, intracellular fate, and induction of cellular response, questions that may also require different analytical methods [73].

A commonly used method for studying ION cellular uptake and its presence within cells is to directly quantify intracellular iron using the ferrozine method. By means of this technique, it has been shown that the cellular uptake of positively charged ION was increased as compared to the anionic ones, and absorption was even 40-fold higher than for neutrally charged ION [51]. Other analytical techniques for ION uptake quantification are diverse and may include spec-

Microscopic and imaging methods. For instance, inductively coupled plasma (ICP)-based spectroscopic techniques, including optical emission spectrometry (ICP-OES) or mass spectrometry (ICP-MS), can provide elemental composition quantification [73]. Also, high resolution analytical methods widely used for nanoparticle uptake assessment, which can provide an adequate quantification of absolute nanoparticle number into the cell, include electron microscopy (EM) techniques [*e.g.*, transmission (TEM), scanning (SEM), or focused ion beam (FIB-SEM)]. An EM micrograph provides the signal of electron dense nanoparticles and the biological context which requires interpretation prior to quantification [51]. Therefore, computer-assisted counting is often not an option. With increased human intervention in the interpretation, observer expectancy effects may affect the accuracy [73].

On the other hand, fluorescence-based quantitative techniques are highly sensitive methods. They require an intrinsic fluorescence signal from the ION or artificial fluorescence tags, allowing ION detection and quantification by fluorescence spectroscopy, fluorescence imaging techniques, or flow cytometry [73]. Among them, one of the most sensitive and rapid methods to determine cellular uptake of nanoparticles, is flow cytometry (FCM) [51], and fluorescence detection is not necessary. In FCM, individualized cells pass through a flow-cell where a laser irradiate them; then a detection unit collects the signals emitted by each cell in the appropriate detectors. Forward scatter (FSC) light is used to determine cell size or volume, while side scatter (SSC) is a measure of complexity [268]. Integration of all FSC and SSC signals analysed allows to interpret whether the cells contain nanoparticles (Fig. 13.5). In the FCM analysis,

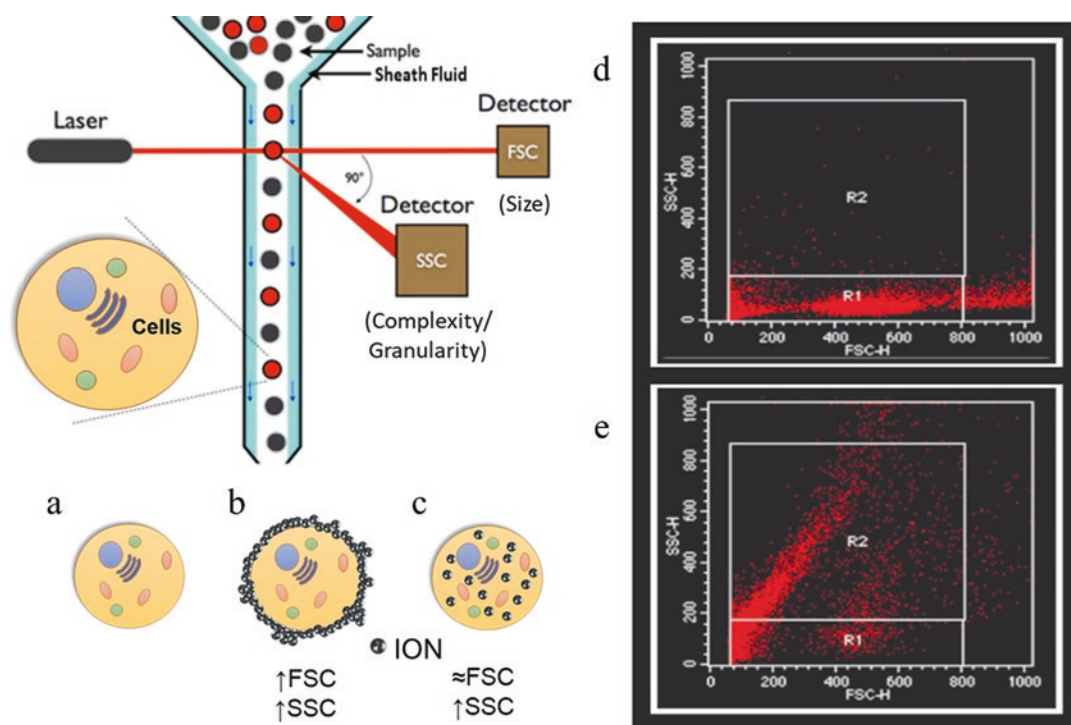


Fig. 13.5 Flow cytometry analysis of cellular nanoparticle uptake. (a) light scattering by a cell in the absence of nanoparticles, (b) nanoparticles adhere to the cell surface, leading to an increase in forward scatter (FSC) and side scatter (SSC), (c) nanoparticle internalization by the cell,

leading to an increase in SSC but not in FSC, (d) FSC/SSC dot plot from flow cytometry analysis of cells not exposed to ION, (e) FSC/SSC dot plot from flow cytometry analysis showing a high proportion of cells with internalized nanoparticles (R2)

ION which are only adhered to the cellular membrane but are unable to be internalized, lead to an increase in both FSC and SSC; while ION uptake by the cells leads to an increase in SSC but not in FSC. Signal integration increases sensitivity as compared with fluorescence imaging methods, but it is not possible to establish the relative location of the nanoparticles in the cell [295].

13.7 Toxic Effects of Iron Oxide Nanoparticles

Nanotoxicity is not only about evaluating the safety of exposure to nanoparticles for the health and the environment. There are many other factors that must be considered in an experimental design to achieve valuable and reproducible data, regarding to instrumentation, analytics and measuring the response of complex biological matrices to nanoparticles [285]. Due to the high variability in ION design and their physicochemical properties, they have become exciting tools for many biomedical applications. This increased handling of ION makes it essential to study their potential adverse consequences to cells. Moreover, toxicity evaluation is a critical point in the development of nanoformulations and, therefore, draws considerable attention [93, 122]. The biomedical use of ION (*e.g.*, for drug delivery) requires to find a balance between optimal bene-

fits of ION application and their potential toxic effect [83, 302]. Although information about the toxicity of ION continues to increase, a knowledge gap exists due to the lack of a complete toxicological profile of these promising nanoparticles for safe use [97] (Fig. 13.6). In general, ION are the most preferable nanomaterials in medical sciences, due to their excellent physicochemical properties and features of minimal toxicity, mostly based on negative results obtained in cytotoxicity studies [190, 223]. However, these results are not always comparable or validated (different dose range, different cell lines, variable culture conditions, method/protocol, tissue susceptibility), and they do not ensure that a slight cytotoxicity may not entail additional risks from ION exposure [309]. For *in vivo* uses, ION must not be toxic to the cells at doses suitable for magnetic targeting or other biomedical applications. Previous studies described excellent biocompatibility and biodegradability of ION, together with low or no toxicity when doses remain below 100 $\mu\text{g/ml}$ [159]. However, physiological significance of the doses tested *in vitro* need to be carefully considered, since several *in vivo* studies revealed that ION, both naked and differently coated, may induce adverse effects through different mechanisms, even at low concentrations (reviewed in Revia and Zhang [252]). For instance, the dose range of ION (ferucarbotran, Resovist[®]) required for clinical MRI (0.2–0.8 mg

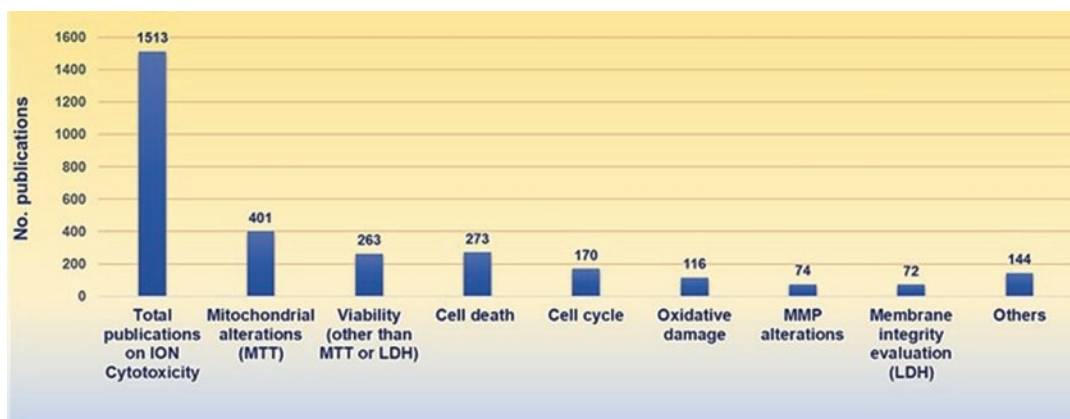


Fig. 13.6 Literature review on ION studies evaluating different cytotoxicity outcomes up to the end of 2019. MTT: 3-(4,5-dimethylthiazol-2-yl)-2,5-diphenyltetrazolium

bromide assay; LDH lactate dehydrogenase assay, MMP mitochondrial membrane potential. (Source: PubMed)

Fe/kg body weight) [250] is roughly equivalent to a range of ION concentrations between 2.5 and 10 $\mu\text{g}/\text{ml}$, which correspond to low concentrations commonly evaluated in most *in vitro* studies reviewed in this chapter. Moreover, standards to determine the toxicity of nanoparticles must be clearly defined [124], and it has been suggested that terms like “biocompatibility” should be reappraised [282]. Several studies carried out so far indicate that ION exposure can induce different harmful cellular effects that include: decreased mitochondrial activity, actin cytoskeleton modulation, ROS-mediated increase of oxidative stress, inflammation, disturbance in iron homeostasis, alteration of signalling pathways activation, cell cycle regulation impairment, indirect and direct DNA damage, and dysregulation of gene expression profiles of living systems [190, 224, 309].

13.7.1 Cytotoxicity

Cell membrane, a bilayer of phospholipids, physical delimits and isolates the cell from the extracellular environment, and its integrity determines cell viability. Additionally, membranes separate different intracellular functional compartments (*i.e.*, mitochondria, reticular endothelial system, lysosomes, nucleus, etc.). Membrane permeability facilitates the selective exchange of molecules, ions or nanoparticles between cells and/or intracellular organelles [314]. Model lipid bilayers are commonly used in nanotoxicology to investigate the nanoparticle interactions with biological membranes [160]. Membrane stability or metabolic activity can be affected by nanoparticles either directly (*i.e.*, physical damage) or indirectly (*e.g.*, by oxidation) which can lead to cell death. One could say that the generation of ROS may indeed be one of the main causes of ION-related cytotoxicity [224], so physicochemical properties of nanoparticles seem to play a key role as inductor of changes in membrane morphology and stability [82]. ROS can damage cell and/or organelle membrane. Membrane dysfunction facilitates the release of Ca^{2+} and cytochrome c from mitochondria, inducing apoptosis.

The damage of organelle membrane allows iron release, coming from lysosomes and mitochondria, and it accumulates in the cytosol, leading to iron-mediated cytotoxicity [93]. The selective permeability of membranes and their transport mechanisms enable, on one hand, to control cellular homeostasis but, on the other hand, it makes them a vulnerable objective for the possible damage caused by ION. Surface properties of nanoparticles (*e.g.*, charge, surface coating and morphology) notably influence the way ION interact with membranes and thus the uptake efficiency and the final fate of ION within the cells [309]. For example, positively charged nanoparticles increased interactions with primarily negatively charged biological surfaces and molecules; or anisotropic morphology or rod-shaped nanoparticles were shown to be taken up less efficiently, but once internalized, they exhibit significant cellular effects [285]. Nanoparticle size plays also a significant role, since it affects the surface pressure and the adhesion forces [227]. Generally, decreasing the particle size increases the amount of cellular uptake and consequently the associated cytotoxicity [285]. Research has shown that different nanomaterials (between 1 and 22 nm diameter), can damage membranes by various processes leading to a compromise of membrane integrity and stability, as well as to the formation of nanosized holes, which bring about loss of cellular viability [104, 255].

Once ION enter the cell, they can potentially cause leakage of cellular components or blockage of cell membranes, leading to adverse cell proliferation, viability and metabolic alterations, and it might also affect nuclear activities [190].

Most *in vitro* studies evaluating cytotoxicity were performed on different cell lines exposed to ION in a wide diversity of experimental conditions. Commonly used toxicological assays for evaluating cytotoxicity include: cell viability tests such as the 3-[4,5-dimethylthiazol-2-yl]-2,5 diphenyl tetrazolium bromide (MTT) assay based on mitochondrial functionality; the lactate dehydrogenase (LDH) assay, indicative of cell membrane integrity; cytoskeleton alterations testing; oxidative stress evaluation (quantification of total

ROS and superoxide anion production); mitochondrial membrane potential (MMP) assay, or cellular oxygen consumption assessment to test mitochondrial impairment; spectrophotometric iron ion release quantification; cell death induction (apoptosis and necrosis); FCM analysis of cell cycle alterations, etc. [223, 224] (Fig. 13.7).

Currently, ION with both magnetite and maghemite cores have already been approved for clinical use as MRI contrast agents [8, 37, 63].

After reviewing the available literature, some contradictions have been found in a large number of studies regarding the cytotoxic effects of ION, since interpretation of outcomes and drawing conclusions strongly depend on surface properties of ION and experimental conditions, such as ION dosage tested, exposure time and/or cell type evaluated [154, 206]. For example, a study using the MTT assay showed that biotinylated ultra-small superparamagnetic ION (5 mg/ml)

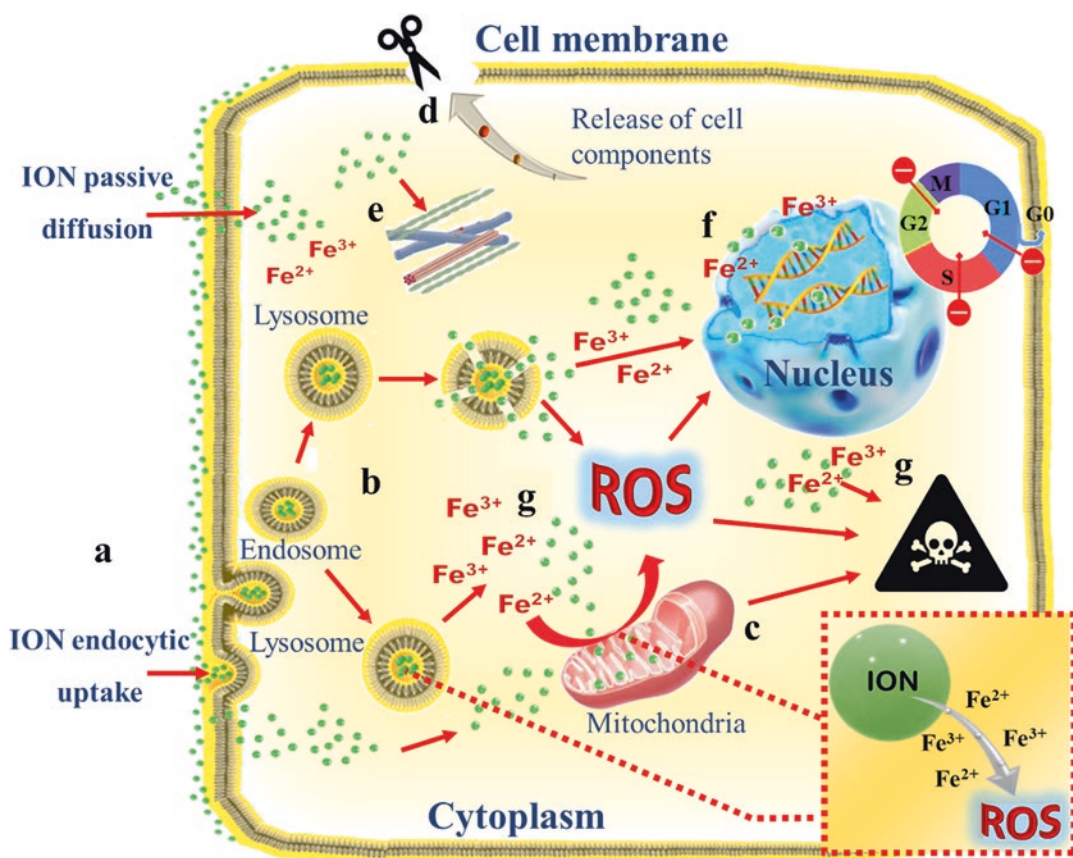


Fig. 13.7 Schematic diagram describing the main ION-mediated cellular toxic effects. (a) Cells take ION up mainly by endocytic processes, although passive diffusion of ultrasmall nanoparticles through cell membrane may occur. Once inside the cell, ION may lead to different cellular toxic effects, including (b) lysosomal damage/dysfunction, high nanoparticle degradation, and iron ion release in the acidic lysosomal environment; however, free ION in the cytoplasm can also produce low quantities of iron ions, (c) impaired mitochondrial function leading to cell death by apoptosis, (d) cell membrane disruption (leading to cell death by necrosis) and release of cellular

components, (e) cytoskeleton alteration, and (f) DNA damage and cell cycle arrest. Accumulation of high amounts of ION and iron ions in the cytoplasm can produce (g) direct damage that leads (in fewer cases) to cell death by autophagy or ferroptosis, but also indirectly through generation of ROS, catalysing Fenton reactions mainly in mitochondria. Increased ROS levels would lead to protein denaturation, lipid peroxidation, enzyme depletion/inactivation, altered gene and protein expression, genetic damage, or iron imbalance, among others, and might eventually result in cell death. ION iron oxide nanoparticles, ROS reactive oxygen species

induced higher concentration-dependent cytotoxicity in mouse brain cells (GL261) than bare ION [249]. Other authors observed that J774 murine cells exposed for 3 h to 25–200 µg/ml of Tween 80-coated ION did not present any toxic effect, but their viability (by MTT) was drastically reduced (55–65%) after 6 h of exposure to 300–500 µg/ml of nanoparticles [209]. Also, cell viability of glial and breast cancer cells was found to be reduced after exposure to 100 µg/ml of uncoated Fe₃O₄ nanoparticles [14]. MCF7 cells exposed for 24 h to 0.1–1 mg/ml of γ-Fe₂O₃ nanoparticles coated with bis(p-sulfonatophenyl) phenylphosphine)-methoxy polyethylene glycol-thiol (mPEG) showed higher viability than cells exposed to bare γ-Fe₂O₃ nanoparticles [303], and the viability of CHO-K1 cells exposed for 72 h to differently sized (50 and 100 nm) PEG-coated ION was found to be higher than the one observed with aminated-coated ION treatment (1–1000 µg Fe/ml) [114].

Other works reported moderate or slight time- and concentration-dependent decreases in viability of L-929 fibroblast after 100–400 mM PVA-coated ION exposure [187]; of human alveolar epithelial A549 cells treated with 40 µg/cm² maghemite but not for magnetite nanoparticles [132]; or of Vero cells after exposure to concentrations greater than 2500 µg/ml of Fe₂O₃ and Fe₃O₄ during 24 h [296]. However, in most cases ION exposure did not lead to any significant cytotoxicity, *e.g.*, 0.5–50 µg/ml silica-coated ION for human monocyte-derived primary macrophages, in terms of mitochondrial dysfunction or cell death induction [155]; or in terms of cell viability (by MTT) for exposure up to 400 µg/ml of PEG-coated ION for human mammary cells [366]; up to 6 µM of Fe₃O₄ nanoparticles for HepG2 cells [24]; or positively and negatively charged ION coated with aminosilane for bEnd.3 nervous cells at concentrations up to 200 µg/ml [293]. In addition, no toxic effects were observed in L-929 mouse fibroblasts treated with doses between 400 and 1600 mM of ION coated with poly(ethylene glycol)-co-fumarate [188], and exposed to 0.1–2 mg/ml of ION coated with acrypol [272], with chitosan [273] or with oleic acid [221].

Han et al. [112] suggested that ION concentration influences cytotoxicity more strongly than any nanoparticle physicochemical property like size or surface coating, since they observed a dose-dependent reduction in L-929 fibroblasts viability (by water-soluble tetrazolium salt proliferation assay, WST-8) after exposure to 100–1000 ppm of different size and surface-modified ION. However, other authors have found evidence of the contrary; therefore, the impact of size and surface coating agents on the overall toxicity of ION, whether through their intrinsic cytotoxicity or through their synergetic or antagonistic activity with nanoparticles, must be carefully considered [1, 115, 122, 146, 209, 253]. For example, Zhang et al. [364] observed dose-, time- and cell type-dependent cytotoxic effects in ION coated (3–100 µM) with six of the 11 agents tested in human epidermal keratinocyte cells (HaCaT) and pulmonary fibroblast cells (CRL-1490); whereas cationic substances (ammonium/ amino compounds) with long aliphatic chains were especially cytotoxic, the neutral and anionic coating agents (sulphur, phosphorous or carboxylic compounds) showed little or no toxicity under the tested conditions. In the same way, Magdolenova et al. [181] observed that increasing doses (30–75 µg/cm² ≈ 144–360 µg/ml) of oleate-coated magnetite ION induced significant cytotoxicity (trypan blue exclusion assay) in human lymphoblastoid TK6 cells (ruling out intrinsic toxicity of sodium oleate), while bare magnetite ION were not cytotoxic. Furthermore, a comparative study in human cervical cancer cells (HeLa) and immortalized human retinal pigment epithelial cells (RPE) exposed to uncoated Fe₃O₄ nanoparticles indicated that, while high concentrations of bare ION (0.40 mg/ml) decreased viability in both cells (measuring intracellular enzymatic activity with calcein-acetyoxymethyl assay and membrane disruption with ethidium homodimer-1), cytotoxicity observed at low concentrations (≤0.20 mg/ml) was cell-type dependent [165]. Investigations aimed at using 1.5–50 µg/ml ION-labelled stem cells in regenerative therapies reported no or low cytotoxicity for these nanoparticles [280, 352, 358]. In addition, no significant cytotoxic effects

were found in viability and proliferation of stem cells incubated with 1–100 $\mu\text{g Fe/ml}$ of MRI contrast agent ferucarbotran (Resovist[®]), clinically approved carboxydextran-coated ION [33, 350], or in neural stem cells treated with 0.01–0.2 mg/ml poly(L-lysine)-coated Fe_2O_3 ION, compared with the commercially available dextran-coated ION (nanomag[®]-D-SPIO) [241]. However, numerous studies have shown that ION can actually trigger multiple effects that would compromise the cellular homeostasis (reviewed in Patil et al. [223] and Valdíglesias et al. [310]). Several reports have evaluated cytotoxicity caused by bare and differently coated ION (maghemite and magnetite) exposure, linking this effect to mitochondrial dysfunction due to membrane physical damage or membrane depolarization [31, 56, 128, 132, 141, 261, 279]; to dose- and time-dependent ROS production [31, 97, 114, 121, 141, 162, 209, 269, 279, 356]; or to inactivation of antioxidant enzymatic systems, glutathione depletion, and oxidative stress generation [4, 26, 78, 89, 97, 125, 169, 326, 363]. Other forms of cytotoxicity reported after ION exposure include cell cycle alterations [20, 158, 231, 334], cytoskeleton alterations [61, 335, 336], disruption of mitochondrial membrane potential [78, 140, 261, 279], plasmatic membrane impairment [245, 327], apoptosis/necrosis [5, 28, 145], autophagy [74, 265, 275], and decreases in cell integrity or viability [18, 59].

13.7.1.1 Cell Cycle

As a consequence of much of the cellular damage previously described in different cells exposed to ION, an adaptation of cellular responses can occur, such as the activation of signalling pathways that regulate cell growth, proliferation and survival (mainly phosphatidylinositol 3-kinase (PI3K)/AKT pathway, and mitogen-activated protein kinase (MAPK)/extracellular signal-regulated kinase (ERK) pathway) [47], leading to an alteration of cell cycle progression [223]. The type and phase of cell cycle arrest seem to be dose-dependent: the higher ION concentration ($\approx 40 \mu\text{g/ml}$), the greater induced cellular damage, which leads to arrests in both S and G_2/M phases, while low concentrations ($\leq 20 \mu\text{g/ml}$) of

nanoparticles generally lead to a G_0/G_1 phase arrest [136]. Particularly, 60 $\mu\text{g/ml}$ dimercaptosuccinic acid modified ION (DMSA- Fe_3O_4) induced G_2/M phase cell cycle arrest and apoptosis in human RPMI-8226 cells, indicative of the presence of hardly repairable DNA damage [50]. The same was observed in human colon HT29 cells treated with concentrations between 0.2 and 0.4 μM of ION conjugated with doxorubicin [20], in leukaemia cells exposed to 100 $\mu\text{g/ml}$ amino-functionalized ION [174], and in rat pheochromocytoma cell line (PC12) treated with 25–200 $\mu\text{g/ml}$ magnetite nanoparticles [334]. Similarly, dose- and time-dependent S phase arrest was found in cell cycle FCM analysis of human A172 glial cells exposed to 5–100 $\mu\text{g/ml}$ oleic acid-coated and silica-coated magnetite [87, 90]; pronounced amount of cells in G_0/G_1 peak was obtained in A549 lung cells treated with 80–320 $\mu\text{g/ml}$ magnetite [147], and in human mesenchymal stem cells exposed to 50 and 200 $\mu\text{g/ml}$ Fe_3O_4 nanoparticles [231], both associated with a significant increase of cells in sub- G_1 phase as well. Moreover, dose- and time-dependent cell cycle arrest and apoptosis-mediated cell death was reported by Tan et al. [297] in human colorectal cancer (HT-29) cell line treated with phytic acid-chitosan-iron oxide nanocomposite (22.5, 45, and 90 $\mu\text{g/ml}$), and by Královec et al. [150] in human HK-2 renal cells exposed to Fe_3O_4 coated with silica (25 and 100 $\mu\text{g/ml}$). However, high doses ($\geq 100 \mu\text{g/ml}$) of oleic acid-coated ION caused dose-dependent increase in G_0/G_1 phase and decrease in G_2/M phase of SH-SY5Y neuronal cells only after 24 h of exposure [88]. Just slight alterations, at high doses (200 $\mu\text{g/ml}$) and long exposure time (24 h), were found in SH-SY5Y cells exposed to silica-coated ION [142], and at the highest dose tested (400 mM) of PVA-coated ION in mouse fibroblast cells [187]. Besides, no cell cycle alteration was observed at any condition tested after exposure of lung epithelial cells to 5 and 10 $\mu\text{g/ml}$ uncoated maghemite nanoparticles [158], of human peripheral blood lymphocytes exposed up to 100 $\mu\text{g/ml}$ of PAA-coated ION [60], or of L929 fibroblast cells to moderate concentrations, *i.e.*, 200 mM, of PVA-ION [187].

13.7.1.2 Cell Death

Different types of cell death, including apoptosis, necrosis and autophagy, were also found to be caused by ION [202]. Previous studies have reported ION-induced time- and concentration-dependent apoptosis (25–500 µg/ml), for example, in murine macrophage cells [209]. The treatment with targeted gold-ION (3.0×10^9 particles/ml) produced time-dependent autophagy and apoptosis of human HCC827 lung cancer cells [247]. Similarly, 24 h exposure to magnetite nanoparticles (1 to 20 µg/ml) caused a dose-dependent cell death by apoptosis, with corresponding increased levels of DNA fragmentation, in rat lung epithelial cells [246]. Cell death by apoptosis was also observed in human fibroblasts [28] and in hepatic HepG2 cells [5], after exposure to 0.05 mg/ml of bare and dextran-coated, and 100 µg/ml of cobalt ION respectively. Synergistic effect of non-toxic quantities of chemotherapeutic agents combined with 60 µg/ml dimercaptosuccinic acid-coated ION (DMSA-Fe₃O₄) have been found to induce apoptotic and necrotic processes in multiple myeloma RPMI-8226 cells [50]. Moreover, long-term (24–72 h) exposure to 10 µg/ml maghemite nanoparticles promoted dose-dependent oxidative stress and necrosis in human endothelial cells [113], and both apoptosis and necrosis in myocardial cells after recurrent exposure of mice to 50 mg/kg Fe₂O₃ nanoparticles [192]. Besides, necrosis was reported in human embryonic kidney cells and in mouse macrophage cells treated both with doses above 50 µg/ml of graphitic carbon-coated ION [145], and Fe₂O₃ nanoparticles [162], respectively.

Autophagy was reported in breast cancer cells [367], in osteosarcoma cells [74], in human A549 lung cells [141], and in human blood cells [275] treated with Fe₃O₄ nanoparticles doses from 100 µg/ml or higher. The results obtained in some studies suggest that the induction of cell death by autophagy after exposure to ION could precede apoptosis [219], which would subsequently occur as a consequence of an excessive intracellular accumulation of nanoparticles [74].

Knowledge on the kinetics of ION degradation has been essential in the frame of recent

discovery of an iron-dependent cell death mechanism termed ferroptosis [42, 98]. The iron-catalysed ROS production through the Fenton reaction, and consequent oxidative stress generation, may play a key role in this iron-induced cell death [81, 254]. Therefore, ferroptosis as a novel and different form of ROS-mediated programmed cellular death, might be involved in metabolism and redox signalling, but also in diverse pathological conditions, such as neurodegeneration, immunity, ischemia injury, and cancer [98]. For instance, after injected mice 5 mg/kg of gadolinium oxide-magnetite hybrid nanoparticles evaluated for brain tumour therapy, they were found able to cross the BBB and release Fe²⁺ and Fe³⁺ from the magnetite after endocytosis, that can directly accelerate Fenton reaction, leading to death of cancer cells by ferroptosis [271].

13.7.2 Genotoxicity

Several *in vitro* research works assessed the toxic effect on genetic material derived from ION exposure [71, 149, 311]. Upon internalization, ION can induce genotoxicity directly, through their binding to DNA structure or whole chromosomes, or indirectly, through the generation of ROS and/or the release of iron ions from their surface to the cytoplasm, inducing oxidative damage and DNA breaks [97]. Moreover, indirect primary genotoxicity can be the consequence of interactions between ION and proteins involved in the cell cycle progression, DNA repair, replication and correct chromosome segregation [107, 285]. Some of the ION genotoxic effects reported in different cell systems included DNA strand breaks, both single and/or double [30, 103, 115, 142, 150, 181, 319], and micronuclei (MN) induction [283] (Fig. 13.8). The most commonly used methods for evaluating genetic damage are the single-cell gel electrophoresis (SCGE) or comet assay (which detects single- and double-strand breaks, alkali-labile sites, crosslinks and incomplete excision repair sites) [133]; the cytokinesis block micronucleus (CBMN) assay [86] and the MN test by FCM (frequency of micronucleated cells) [21, 43]; the

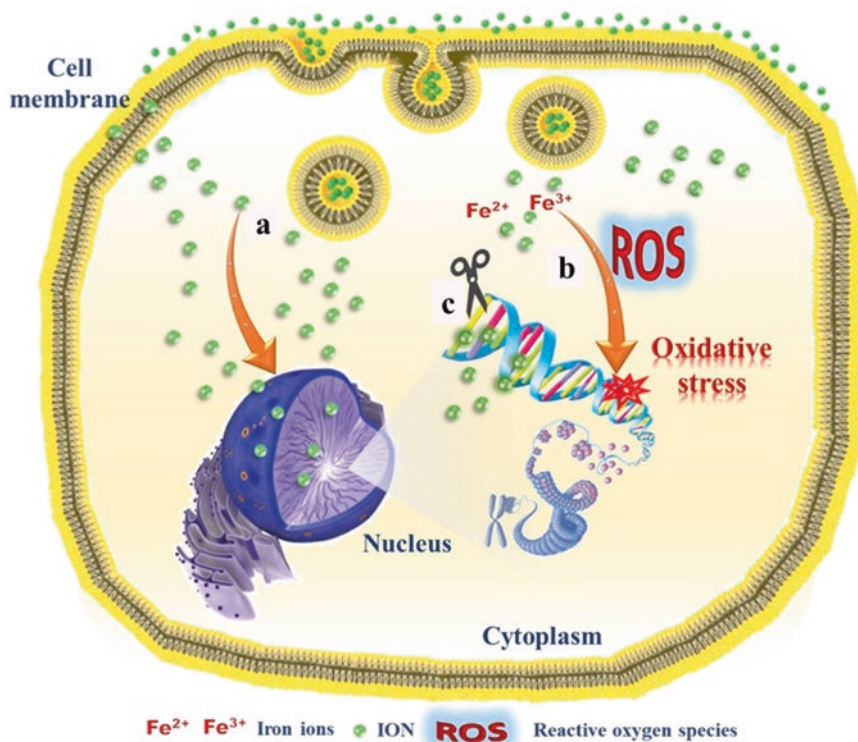


Fig. 13.8 Reported ION-induced genotoxic effects. ION may cause DNA damage through (a) direct interaction with the DNA structure, or (b) by triggering the oxidative radical generation that in turn have the potential to indirectly cause DNA damage, mainly through base oxidation

(mostly 8-hydroxydeoxyguanosine). Consequently, ION exposure may induce (c) either clastogenic or aneugenic effects such as single-strand breaks, double-strand breaks, DNA adducts, gene mutations, chromosome aberrations, or micronuclei formation

H2AX phosphorylation assay (which detects double-strand breaks) evaluated either by FCM or by immunochemistry [183], the chromosomal aberration test (for structural chromosomal abnormalities) [170], and the bacterial reverse mutation test or Ames test (for mutagenic potential) [106].

For example, in two studies using 20–200 $\mu\text{g}/\text{ml}$ of naked or differently coated (D-mannose or poly-L-lysine) ION, dose-dependent induction of DNA breaks (analysed by the comet assay) was reported in murine neural stem cells, regardless of surface coating [241]. Also, 10–100 $\mu\text{g}/\text{ml}$ of uncoated maghemite induced DNA damage and chromosomal aberrations in human lymphocytes in a dose dependent manner [245]. In agreement with these studies, Cicha et al. [55] found a significant increase of phosphorylated H2AX levels

in human primary tubular epithelial cells treated with 0.1 $\mu\text{g}/\text{ml}$ lauric acid-coated ION functionalized with mitoxantrone. Moreover, some other studies reported significant genotoxic outcomes (comet assay) induced by 200–1000 ppm of (3-aminopropyl) trimethoxysilane (APTMS)-, tetraethyl orthosilicate (TEOS)-APTMS, or citrate-coated magnetite nanoparticles in murine L-929 fibroblast cells [112]; by 25–100 $\mu\text{g}/\text{ml}$ of polygonal shaped nanomagnetite in both lung epithelial A549 and skin epithelial A431 cells [4]; and by 10 and 50 $\mu\text{g}/\text{cm}^2$ of $\alpha\text{Fe}_2\text{O}_3$ (hematite) nanoparticles in IMR-90 lung fibroblasts and BEAS-2B bronchial epithelial cells as well [29]. Similarly, significantly increased DNA damage and MN frequency were found in A549 alveolar cells exposed to doses above 50 $\mu\text{g}/\text{cm}^2$ of uncoated Fe_3O_4 nanoparticles [146], and in doses

between 5 and 10 $\mu\text{g/ml}$ of dextran-ION exposed human hepatoma (HepG2) cells [266]. Raises in primary and oxidative DNA damage, measured by comet and enzyme-modified comet assays, were obtained in human lymphoblastoid TK6 cells and primary human leukocytes exposed to concentrations above 140 and 56 $\mu\text{g/ml}$ respectively of oleate-coated nanomagnetite [181], and also in liver and kidney tissues after exposing mice to 20 and 40 mg/kg magnetite nanoparticles [351]. Fe_3O_4 nanoparticles (0.1–0.4 mM), regardless of the different coatings, were able to induce significantly increased levels of DNA breakage in A549 cells but not oxidative damage [199]. Dextran-coated $\gamma\text{Fe}_2\text{O}_3$ nanoparticles (4–100 $\mu\text{g/ml}$) were observed to induce dose-dependent increases in MN frequency of human MCL5 lymphoblastoid cells [283]. CuFe_2O_3 nanoparticles only at the highest concentration tested (100 $\mu\text{g/ml}$), also caused an increase in MN rate in HepG2 cells [2].

Opposite to these findings, studies showing negative results for ION genotoxicity are more frequent. Magdolenova et al. [181] demonstrated absence of negative effects on the DNA of human lymphoblastoid TK6 cells treated with doses up to 135 $\mu\text{g/ml}$ of uncoated nanomagnetite, and Paolini et al. [217] reported no genotoxicity or carcinogenicity on mouse fibroblast Balb/c-3 T3 cells exposed 7 weeks to doses up to 300 $\mu\text{g/ml}$ of rhamnose-coated magnetite nanoparticles. Similarly, no significant chromosome aberrations were described in human T-lymphocytes after treatment with up to 100 $\mu\text{g/ml}$ of polyacrylic acid-coated and uncoated nanomagnetite [60]. Some other works showed negative genotoxicity results (*i.e.* no induction of primary DNA damage and/or no increase in MN frequency) in many cell types exposed to different ION [19, 110, 131, 132, 283, 284, 362]. Two independent studies also evaluated the *in vivo* mutagenic potential of ION in animals [up to 3000 $\mu\text{mol Fe/kg}$ of AMI-25 ION, 150-fold the dose proposed for MRI of the liver [331], and very high-dose levels (17.9 mg Fe/kg/day), more than 150-fold the human dose of ferumoxtran-10 [38]] by means of the Ames test, obtaining negative results as well.

Due to the relatively recent development of nanotechnology, *in vivo* and epidemiological studies on potential genotoxic effects of ION are scarce nowadays. The existing information on ION-mediated genetic damage is largely based on *in vitro* studies with (human) cell lines [237]. The results obtained in genotoxicity *in vitro* studies are usually not easy to extrapolate to *in vivo* conditions, since their limited and specific experimental conditions, tend to overestimate the effects that occur *in vivo*. However, they are useful for screening purposes and mechanistic studies [57]. Although *in vivo* genotoxicity studies are pricey, time-consuming and involve ethical issues and complex methods (for example, toxicokinetics assessment), they have the advantage over *in vitro* tests of giving a more realistic estimation of the nanoparticle effect in the body [107]. Although there are few *in vivo* studies in the literature on the genotoxic effects of ION, those available provide important information on their biological applicability and on their potential *in vivo* genotoxicity. Specifically, Yang et al. [351] exposed Kunming mice to Fe_3O_4 nanoparticles (5–40 mg/kg/day) through intraperitoneal injection, in order to determine the safe dose range for medical use. Results showed that ION are easily able to cross the intestinal barrier and, although they mainly accumulate in kidneys, liver, spleen, heart and bone marrow, exposure did not cause genotoxicity in leucocytes (analysed by the comet assay), chromosomal aberrations in bone marrow cells, or MN in any of the cell types mentioned. Several studies evaluating the MN frequency in bone marrow cells from mice *in vivo* exposed to ION also showed contradictory results; while some authors obtained positive results for doses about 1.6×10^{16} particle/ml ($\approx 5 \times 10^{17}$ particles/kg) [95, 257], other reported no genotoxic effects for doses up to 2.3×10^{17} particles/ml (≈ 5 g ION/kg) [38, 85, 336].

Hence, given the general lack of consistence in the available results from *in vitro* and *in vivo* studies on ION genotoxicity, even at similar doses, additional research is necessary to define the specific mechanisms and conditions underlying their effects on the genetic material.

13.7.3 Neurotoxicity

In recent years, ION are awakening special interest, due to their ability to cross the BBB and thus access the nervous tissue [291]. For this reason, they have been proposed as solid candidates for a wide variety of biomedical applications in the CNS, such as the study, diagnosis and treatment of various neurological disorders, for example, brain cancer, Parkinson's, Alzheimer's, and Huntington's disease, multiple sclerosis, amyotrophic lateral sclerosis, epilepsy and ischemic stroke [205, 263, 298]. Once ION bypassed the BBB, nanoparticles can interact with neurons and glial cells and induce or trigger a series of disruptions (inflammation, oxidative stress, DNA and/or mitochondrial damage and cell death), thereby increasing the potential risks of neurotoxicity [49]. The main pathways ION can use to access the nervous system are by oral [130, 284, 357], pulmonary [156, 270, 323], intravenous [62, 148, 263, 301, 365], and intraperitoneal [53, 143] administration. In addition to the systemic pathways, ION can directly translocate to the brain through olfactory nerves after intranasal instillation [325, 338, 343]. ION administered as a contrast or therapeutic agent (intravenously or intraperitoneally), can be magnetically targeted to the specific site of action, leading to improved absorption of the agent into the target nerve tissue. This means an improvement in the treatment efficacy with the minimum dose and, therefore, to the reduction of ION possible adverse effects on CNS [135, 291]. Therefore, the accessibility that makes ION especially useful for the aforementioned medical purposes, also poses a potential risk to the wellbeing and safety of the nervous system. Consequently, in animal *in vivo* studies, issues such as the exposure effects on nervous tissue physiology or behaviour are key parameters to pay particular attention to [333]. Recent studies reported that neurotoxicity of ION is dose-dependent, due in part to the release of iron ions, leading to the generation of ROS and increased oxidative stress. Given the high vulnerability of the CNS to oxidative stress, imbalance of iron homeostasis in the brain often leads to brain neurodegeneration, and this is precisely the main

mechanism known for ION toxicity induction [353].

To date, most studies on the potential neurotoxicity induced by ION, both naked and differently coated, have been carried out mainly in nerve cells of animal origin, *e.g.*, mouse c17.2 neural progenitor cells [288], chick cortical neurons [253], primary rat cerebellar granule neurons [233], primary cultured brain microglial cells [177, 235], primary and secondary rat astrocytes [232], rat oligodendroglial OLN-93 cells [234], and PC12 rat cells [68, 334, 338]. Although to a lesser extent, human cells have been also tested for that aim, *i.e.*, SH-SY5Y neuroblastoma cells [88, 127, 142], brain-derived endothelial cells [138, 139], and A172 astrocytes [87, 90].

Hence, despite the considerable amount of studies addressing the *in vitro* neurotoxicity of ION in animal cells, there is scarce research on the potential risk of human nerve cell exposure to these nanoparticles. For instance, in a comprehensive *in vitro* comparative study using human SH-SY5Y neurons and A172 astrocytes exposed to magnetite nanoparticles coated with silica and oleic acid (doses from 10–200 µg/ml for neurons, and 5–100 µg/ml for astrocytes), Fernández-Bertólez and colleagues demonstrated that the silica-coated ION showed less cytotoxicity (in terms of viability, membrane integrity, cell cycle alterations and cell death induction), and slightly lower genotoxic effects (mainly primary DNA damage assessed by comet assay) than the oleic acid-coated counterpart, unrelated to double-strand breaks or chromosomal alterations (by MN test). None of the observed toxic effects of oleic acid-coated ION was related to the release of iron ions from the nanoparticle surface. Therefore, silica-coated ION appear to be more biocompatible than oleic acid-coated ones for the nervous system cell lines evaluated. Furthermore, although astrocytes were shown to be more sensitive than neurons to the ION-induced toxic effects, regardless of surface coating, there were no alterations in their DNA repair capacity in the presence of any of the nanoparticles (analysed by DNA repair competence assay) [59, 87, 88, 90, 142]. In addition, it was shown that exposure to these ION generated dose-dependent intracellu-

lar ROS production, which consequently led to a parallel induction of oxidative DNA damage (measured by enzyme-modified comet assay) in both cell types [89]. Another recent study showed that short and long-term exposure of D384 astrocytes (≥ 25 $\mu\text{g/ml}$ after 4 h and 1 $\mu\text{g/ml}$ after 48 h), and SH-SY5Y neurons (10 $\mu\text{g/ml}$ after 48 h only) to Fe_3O_4 nanoparticles affects cellular proliferation and generates cytotoxicity, lower in the later cell type. A dose- and time-dependent accumulation of ION in D384 astrocytes affected mitochondrial function but not membrane integrity [56]. Similarly, Imam et al. [127] reported that exposure of SH-SY5Y human neuroblastoma cells to differently sized Fe_2O_3 nanoparticles (2.5–40 $\mu\text{g/ml}$) caused cell-proliferation inhibition, a significant reduction of mitochondrial activity, and a dose-dependent increase in ROS. Confirming these results, the study carried out by Askri et al. [17] with the same ION and cell type observed that the differently sized maghemites (12.5–200 $\mu\text{g/ml}$) induced size- and concentration-dependent uptake, detachment and cell morphological changes (determined by cytoskeletal affectation), and decreased cell viability. Doses higher than 50 $\mu\text{g/ml}$ of Fe_2O_3 nanoparticles also produced slight genotoxic damage (analysed by modified comet assay) without increasing ROS generation.

On the other hand, the amount of *in vivo* studies on potential neurotoxicity of these nanoparticles is quite restricted. In the review performed by D'Agata et al. [62], the authors observed that the *in vivo* exposure of different types of nerve cells – human, mice and rats – to uncoated and differently coated maghemite or magnetite nanoparticles (dose range tested between 17 and 140 $\mu\text{g/ml}$), did not produce relevant toxic effects, maintaining a high or invariable viability, normal mitochondrial activity, reduced cell death, unaltered BBB permeability, and absence of brain immune response. Most *in vivo* studies on ION neurotoxicity employed rats as experimental model. For instance, Kumari et al. [153] observed irritation and dullness in Wistar rats after 28 days of 30–1000 mg Fe/kg oral daily administration of ION (maghemite). Besides, ION exposure could affect synaptic transmission and nerve conduction

in exposed animals, since a significant dose-dependent inhibition of total ATPases in the brain, and acetylcholinesterase in brain and in red blood cells, was obtained. Also, Wu et al. [336] detected a regional distribution of magnetite in the brain of rats intranasally instilled with 1.25–5 g Fe/kg for 7 days, with a significant induced oxidative damage in striatum but not in hippocampus, despite the presence of nanoparticles in both regions resulted particularly high. Similarly, different physiological responses, including signs of polypnea, exophthalmos and mydriasis were observed in Sprague-Dawley rats after intravenous treatment of 2.6–13 mg ION/kg (ferumoxtran-10), although no psychotropic, neurovegetative, or neurobehavioral effects were detected [38]. However, in the same animals exposed by intraneural injection (sciatic nerve) to maghemite and magnetite nanoparticles with different coatings (10–35 mg ION/ml \approx 0.5–15 mM Fe injected), neural inflammation and apoptosis, infiltration of immune cells and a neural antioxidant response were observed [144]. The nanocomposite for drug delivery of oleic acid-coated magnetite functionalized with the anticancer drug daunorubicin (about 15 mg $\text{Fe}_3\text{O}_4/\text{kg}$ injected), can reduce the neurotoxicity of this drug in the brain of rats *in vivo*, suggesting their possible application to reduce side effects of cancer therapies [346].

Agreeing with these studies in rats, neurotoxicity of ION has been also reported in mice and fish. Intranasal administration of 300–1200 mg/kg of maghemite nanoparticles induced microglial proliferation, cytokine production, T-lymphocyte activation and recruitment, and pathological alterations in the olfactory bulb, hippocampus and striatum of mice brain [325]. Moreover, mice treated by intragastric administration of 600 mg/kg of Fe_3O_4 nanoparticles showed less activity and a slight loss of appetite [324]. In zebrafish, intraperitoneal administration of 200 mg/kg of magnetite nanoparticles coated with dextran caused ION accumulation in the brain, leading to apoptosis-mediated cell death and acetylcholinesterase inhibition in this tissue. Although no alterations in inflammation-related gene expression were observed, increased levels

of Fe³⁺ iron and enhanced mRNA levels of caspase 8, caspase 9 and transcriptional factor AP-1 in the brain of exposed animals were also detected [66].

13.8 Conclusions and Future Perspectives

Among all nanomaterials, ION are particularly interesting mainly in the biomedical field, due to their special physicochemical characteristics, their apparent biocompatibility, and because they exhibit a unique form of magnetism called superparamagnetism. The most promising applications of ION are as a contrast agent in MRI, in targeted drug delivery, gene therapy, cell labelling, tissue repair, and for hyperthermic treatment of tumours. Specifically, in recent years, ION have been shown as powerful tools for the diagnosis and treatment of neurodegenerative diseases or neoplastic processes of the CNS, due to their ability to cross the BBB, thus being able to access the nervous tissue. Although translocation of ION to the brain has been studied under different experimental conditions, it is not yet clear whether they are generally safe or should be used with caution.

ION are generally composed of an iron core with different polymorphic structures, among which magnetite, maghemite and hematite stand out. A common problem associated with ION is their intrinsic instability over long periods of time, as they tend to agglomerate, are highly chemically reactive, and are easily oxidized, generally resulting in a loss of magnetism and dispersibility. To minimize these effects, the surface of the ION can be modified by coating them with different materials, to stabilize them in physiological media, increase their biocompatibility, modify their cellular uptake efficiency, and enhance their properties in the desired biomedical application, although it can also alter their toxicological behaviour. In addition, the great potential of ION is mainly due to their particular physical and chemical properties, which show a complex dependence and interrelation of several factors, such as size, shape, core structure, surface

composition and charge, absence/presence of coating substances, and chemical stability (*e.g.*, solubility and agglomeration/aggregation). These properties of nanoparticles play a crucial role in the induction of biological effects, as they determine their dispersion state and also influence the adsorption of ions and biomolecules onto their surface (biomolecular corona), which can change the way cells interact with ION.

The growing commercialization of ION-containing products in the last years, and particularly their successful application in medicine and clinics, has significantly increased the potential human exposure to these materials. To ensure the safety of the diagnostic or therapeutic use of ION, they must not be toxic to cells at concentrations suitable for magnetic orientation or other biomedical applications. Although most of reports in the literature demonstrate that a range of ION mainly show low toxicity at doses over 100 µg/ml or higher, it has been shown in several *in vitro* and *in vivo* studies that ION, naked or coated with different substances, can induce adverse effects, even at low doses, such as decreased cell viability, cytoskeletal alterations, iron ion release, induction of oxidative stress or mitochondrial dysfunction, among others. Furthermore, their possible effect on other different cellular functions, on genetic material, or on DNA repair capacity, cannot be ruled out either, since to date they have been hardly addressed in human cells. The lack of complete and standardized toxicological evaluations makes the interpretation of the results obtained so far difficult, especially in the case of neurotoxicity. This is due, at least in part, to the fact that the available results on the toxic effects induced by ION are contradictory, and they are not always comparable as they are influenced by a number of factors, including the ION type, their physicochemical properties, the cell type analysed, or the experimental conditions tested (mainly dose and time). Therefore, it is mandatory to evaluate the potential toxic effects that ION can cause in the human cellular systems.

In summary, this chapter provides a comprehensive review of the toxicological features of ION, addressing their structure and physico-

chemical characteristics, influence of coating, main exposure pathways and toxicokinetic aspects, interaction with cells, and their toxic effects, with special attention to those at the cellular and molecular level. Nanotoxicological evaluation of ION is essential to increase the knowledge about their impact on human health, to fully understand their mechanisms of action, and to guarantee their safe use with an adequate benefit/cost ratio. The information obtained in this evaluation will help to define the safety margins and the conditions of use of these nanomaterials to avoid or minimize risks, especially those related to their exponentially growing applications in the biomedical field.

Acknowledgments The present work was supported by Xunta de Galicia (reference ED431B 2019/02), Ministerio de Ciencia e Innovación (PID2020-114908GA-I00), TOXI-NANO (SEM2021-A1), NeuroINPact (SEM2021-B2), NanoBioBarriers (PTDC/MED-TOX/31162/2017) funded by Operational Program for Competitiveness and Internationalisation through European Regional Development Funds (FEDER/FNR) and through national funds by the Portuguese Foundation for Science and Technology (FCT), and NanoLegaTox (PTDC/SAU-PUB/29651/2017) project co-financed by COMPETE 2020, Portugal 2020 and European Union, through FEDER. Vanessa Valdíglesias was supported by Ministerio de Educación, Cultura y Deporte (reference BEAGAL18/00142), and Fátima Brandão by the Portuguese Foundation for Science and Technology (SFRH/BD101060/2014). Authors would also like to acknowledge COST Action CA17140 “Cancer nanomedicine – from the bench to the bedside (NANO2CLINIC)”.

References

1. Abakumov MA, Semkina AS, Skorikov AS, Vishnevskiy DA, Ivanova AV, Mironova E, Davydova GA, Majouga AG, Chekhonin VP (2018) Toxicity of iron oxide nanoparticles: size and coating effects. *J Biochem Mol Toxicol* 32:e22225. <https://doi.org/10.1002/jbt.22225>
2. Adeyemi JA, Machado ART, Ogunjimi AT, Alberici LC, Antunes LMG, Barbosa F (2020) Cytotoxicity, mutagenicity, oxidative stress and mitochondrial impairment in human hepatoma (HepG2) cells exposed to copper oxide, copper-iron oxide and carbon nanoparticles. *Ecotoxicol Environ Saf* 189:109982. <https://doi.org/10.1016/j.ecoenv.2019.109982>
3. Agemy L, Friedmann-Morvinski D, Kotamraju VR, Roth L, Sugahara KN, Girard OM, Mattrey RF, Verma IM, Ruoslahti E (2011) Targeted nanoparticle enhanced proapoptotic peptide as potential therapy for glioblastoma. *Proc Natl Acad Sci U S A* 108:17450–17455. <https://doi.org/10.1073/pnas.1114518108>
4. Ahamed M, Alhadlaq HA, Alam J, Majeed Khan MAA, Ali D, Alarafi S (2013) Iron oxide nanoparticle-induced oxidative stress and genotoxicity in human skin epithelial and lung epithelial cell lines. *Curr Pharm Des* 19:6681–6690. <https://doi.org/10.2174/1381612811319370011>
5. Ahamed M, Akhtar MJ, Khan MAM, Alhadlaq HA, Alshamsan A (2016) Cobalt iron oxide nanoparticles induce cytotoxicity and regulate the apoptotic genes through ROS in human liver cells (HepG2). *Colloids Surf B Biointerfaces* 148:665–673. <https://doi.org/10.1016/j.colsurfb.2016.09.047>
6. Ahmad F, Ashraf N, Ashraf T, Zhou RB, Yin DC (2019) Biological synthesis of metallic nanoparticles (MNPs) by plants and microbes: their cellular uptake, biocompatibility, and biomedical applications. *Appl Microbiol Biotechnol* 103:2913–2935. <https://doi.org/10.1007/s00253-019-09675-5>
7. Akbarzadeh A, Samiei M, Joo SW, Anzaby M, Hanifehpour Y, Nasrabadi HT, Davaran S (2012) Synthesis, characterization and in vitro studies of doxorubicin-loaded magnetic nanoparticles grafted to smart copolymers on A549 lung cancer cell line. *J Nanobiotechnol* 10:46. <https://doi.org/10.1186/1477-3155-10-46>
8. Al Faraj A, Shaik AP, Shaik AS (2015) Effect of surface coating on the biocompatibility and in vivo MRI detection of iron oxide nanoparticles after intrapulmonary administration. *Nanotoxicology* 9:825–834. <https://doi.org/10.3109/17435390.2014.980450>
9. Alalaiwe A (2019) The clinical pharmacokinetics impact of medical nanometals on drug delivery system. *Nanommed Nanotechnol Biol Med* 17:47–61. <https://doi.org/10.1016/j.nano.2019.01.004>
10. Ali A, Zafar H, Zia M, ul Haq I, Phull AR, Ali JS, Hussain A (2016) Synthesis, characterization, applications, and challenges of iron oxide nanoparticles. *Nanotechnol Sci Appl* 9:49–67. <https://doi.org/10.2147/NSA.S99986>
11. Alwi R, Telenkov S, Mandelis A, Leshuk T, Gu F, Oladepo S, Michaelian K (2012) Silica-coated superparamagnetic iron oxide nanoparticles (SPION) as biocompatible contrast agent in biomedical photoacoustics. *Biomed Opt Express* 3:2500–2509. <https://doi.org/10.1364/BOE.3.002500>
12. Anderson GJ, Frazer DM (2017) Current understanding of iron homeostasis. *Am J Clin Nutr* 106:1559S–1566S. <https://doi.org/10.3945/ajcn.117.155804>
13. Andrade AL, Souza DM, Pereira MC, Fabris JD, Domingues RZ (2009) Synthesis and characteriza-

- tion of magnetic nanoparticles coated with silica through a sol-gel approach. *Cerâmica* 55:420–424. <https://doi.org/10.1590/S0366-69132009000400013>
14. Ankamwar B, Lai TC, Huang JH, Liu RS, Hsiao M, Chen CH, Hwu YK (2010) Biocompatibility of Fe₃O₄ nanoparticles evaluated by in vitro cytotoxicity assays using normal, glia and breast cancer cells. *Nanotechnology* 21:75102. <https://doi.org/10.1088/0957-4484/21/7/075102>
 15. Ansari SAMK, Ficiarà E, Ruffinatti FA, Stura I, Argenziano M, Abollino O, Cavalli R, Guiot C, D'Agata F, D'Agata F (2019) Magnetic iron oxide nanoparticles: synthesis, characterization and functionalization for biomedical applications in the central nervous system. *Materials (Basel)* 12:465. <https://doi.org/10.3390/ma12030465>
 16. Arami H, Khandhar A, Liggitt D, Krishnan KM (2015) In vivo delivery, pharmacokinetics, biodistribution and toxicity of iron oxide nanoparticles. *Chem Soc Rev* 44:8576–8607. <https://doi.org/10.1039/C5CS00541H>
 17. Askri D, Cunin V, Béal D, Berthier S, Chovelon B, Arnaud J, Rachidi W, Sakly M, Amara S, Sève M, Lehmann SG (2019) Investigating the toxic effects induced by iron oxide nanoparticles on neuroblastoma cell line: an integrative study combining cytotoxic, genotoxic and proteomic tools. *Nanotoxicology* 13:1021–1040. <https://doi.org/10.1080/17435390.2019.1621399>
 18. Astanina K, Simon Y, Cavalius C, Petry S, Kraegeloh A, Kiemer AK (2014) Superparamagnetic iron oxide nanoparticles impair endothelial integrity and inhibit nitric oxide production. *Acta Biomater* 10:4896–4911. <https://doi.org/10.1016/j.actbio.2014.07.027>
 19. Auffan M, Decome L, Rose J, Orsiere T, De Meo M, Brioso V, Chaneac C, Olivi L, Berge-lefranc J, Botta A, Wiesner MR, Bottero J (2006) In vitro interactions between DMSA-coated maghemite nanoparticles and human fibroblasts: a physicochemical and cyto-genotoxic study. *Environ Sci Technol* 40:4367–4373. <https://doi.org/10.1021/es060691k>
 20. Augustin E, Czubek B, Nowicka AM, Kowalczyk A, Stojek Z, Mazerska Z (2016) Improved cytotoxicity and preserved level of cell death induced in colon cancer cells by doxorubicin after its conjugation with iron-oxide magnetic nanoparticles. *Toxicol Vitro* 33:45–53. <https://doi.org/10.1016/j.tiv.2016.02.009>
 21. Avlasevich SL, Bryce SM, Cairns SE, Dertinger SD (2006) In vitro micronucleus scoring by flow cytometry: differential staining of micronuclei versus apoptotic and necrotic chromatin enhances assay reliability. *Environ Mol Mutagen* 47:56–66. <https://doi.org/10.1002/em.20170>
 22. Babay S, Mhiri T, Toumi M (2015) Synthesis, structural and spectroscopic characterizations of maghemite γ -Fe₂O₃ prepared by one-step coprecipitation route. *J Mol Struct* 1085:286–293. <https://doi.org/10.1016/j.molstruc.2014.12.067>
 23. Baber O, Jang M, Barber D, Powers K (2011) Amorphous silica coatings on magnetic nanoparticles enhance stability and reduce toxicity to in vitro BEAS-2B cells. *Inhal Toxicol* 23:532–543. <https://doi.org/10.3109/08958378.2011.592869>
 24. Banerji B, Pramanik SK, Mandal S, Maiti NC, Chaudhuri K (2012) Synthesis, characterization and cytotoxicity study of magnetic (Fe₃O₄) nanoparticles and their drug conjugate. *RSC Adv* 2:2493. <https://doi.org/10.1039/c2ra01118b>
 25. Bao Y, Wen T, Samia ACS, Khandhar A, Krishnan KM (2015) Magnetic nanoparticles: material engineering and emerging applications in lithography and biomedicine. *J Mater Sci* 51:513–553. <https://doi.org/10.1007/s10853-015-9324-2>
 26. Barker RA, Cicchetti F (2014) Neurodegenerative disorders: the glia way forward. *Front Pharmacol* 5:157. <https://doi.org/10.3389/fphar.2014.00157>
 27. Basinas I, Jiménez AS, Galea KS, Van Tongeren M, Hurley F, van Tongeren M, Hurley F (2018) A systematic review of the routes and forms of exposure to engineered nanomaterials. *Ann Work Expo Health* 62:639–662. <https://doi.org/10.1093/annweh/wxy048>
 28. Berry CC, Wells S, Charles S, Aitchison G, Curtis ASG (2004) Cell response to dextran-derivatized iron oxide nanoparticles post internalisation. *Biomaterials* 25:5405–5413. <https://doi.org/10.1016/j.biomaterials.2003.12.046>
 29. Bhattacharya K, Davoren M, Boertz J, Schins RP, Hoffmann E, Dopp E (2009) Titanium dioxide nanoparticles induce oxidative stress and DNA-adduct formation but not DNA-breakage in human lung cells. *Part Fibre Toxicol* 6:17. <https://doi.org/10.1186/1743-8977-6-17>
 30. Bhattacharya D, Das M, Mishra D, Banerjee I, Sahu SK, Maiti TK, Pramanik P (2011) Folate receptor targeted, carboxymethyl chitosan functionalized iron oxide nanoparticles: a novel ultradispersed nanoconjugates for bimodal imaging. *Nanoscale* 3:1653–1662. <https://doi.org/10.1039/c0nr00821d>
 31. Bhattacharya K, Hoffmann E, Schins RFP, Boertz J, Prantl EM, Alink GM, Byrne HJ, Kuhlbusch TAJ, Rahman Q, Wiggers H, Schulz C, Dopp E (2012) Comparison of micro- and nanoscale Fe+3-containing (hematite) particles for their toxicological properties in human lung cells in vitro. *Toxicol Sci* 126:173–182. <https://doi.org/10.1093/toxsci/kfs014>
 32. Bhattacharya A, Kaushik DK, Lozinski BM, Yong VW (2020) Beyond barrier functions: roles of pericytes in homeostasis and regulation of neuroinflammation. *J Neurosci Res* 98:jnr.24715. <https://doi.org/10.1002/jnr.24715>
 33. Bigini P, Diana V, Barbera S, Fumagalli E, Micotti E, Sitia L, Paladini A, Bisighini C, De Grada L, Coloca L, Colombo L, Manca P, Bossolasco P, Malvestiti F, Fiordaliso F, Forloni G, Morbidelli M, Salmona M, Giardino D, Mennini T, Moscatelli D, Silani V, Cova L (2012) Longitudinal tracking of human fetal cells labeled with super paramagnetic iron oxide nanoparticles in the brain of mice with motor neuron dis-

- ease. *PLoS One* 7:e32326. <https://doi.org/10.1371/journal.pone.0032326>
34. Bjørnerud A, Johansson L (2004) The utility of superparamagnetic contrast agents in MRI: theoretical consideration and applications in the cardiovascular system. *NMR Biomed* 17:465–477. <https://doi.org/10.1002/nbm.904>
35. Blanco-Andujar C, Walter A, Cotin G, Bordeianu C, Mertz D, Felder-Flesch D, Begin-Colin S (2016) Design of iron oxide-based nanoparticles for MRI and magnetic hyperthermia. *Nanomedicine* 11:1889–1910. <https://doi.org/10.2217/nmm-2016-5001>
36. Bloemen M, Brullot W, Luong TT, Geukens N, Gils A, Verbiest T (2012) Improved functionalization of oleic acid-coated iron oxide nanoparticles for biomedical applications. *J Nanopart Res* 14:1100. <https://doi.org/10.1007/s11051-012-1100-5>
37. Bobo D, Robinson KJ, Islam J, Thurecht KJ, Corrie SR (2016) Nanoparticle-based medicines: a review of FDA-approved materials and clinical trials to date. *Pharm Res* 33:2373–2387. <https://doi.org/10.1007/s11095-016-1958-5>
38. Bourrinet P, Bengel HH, Bonnemain B, Dencausse A, Idee J-M, Jacobs PM, Lewis JM (2006) Preclinical safety and pharmacokinetic profile of Ferumoxtran-10, an ultrasmall superparamagnetic iron oxide magnetic resonance contrast agent. *Investig Radiol* 41:313–324. <https://doi.org/10.1097/01.rli.0000197669.80475.dd>
39. Boyes WK, Thornton BLM, Al-Abed SR, Andersen CP, Bouchard DC, Burgess RM, Hubal EAC, Ho KT, Hughes MF, Kitchin K, Reichman JR, Rogers KR, Ross JA, Rygiel PT, Scheckel KG, Thai S-F, Zepp RG, Zucker RM (2017) A comprehensive framework for evaluating the environmental health and safety implications of engineered nanomaterials. *Crit Rev Toxicol* 47:771–814. <https://doi.org/10.1080/01040844.2017.1328400>
40. Bradley EL, Castle L, Chaudhry Q (2011) Applications of nanomaterials in food packaging with a consideration of opportunities for developing countries. *Trends Food Sci Technol* 22:604–610. <https://doi.org/10.1016/j.tifs.2011.01.002>
41. Braeuer AU, Neubert J, Wagner S, Kiwit J, Glumm J (2015) New findings about iron oxide nanoparticles and their different effects on murine primary brain cells. *Int J Nanomedicine* 10:2033. <https://doi.org/10.2147/IJN.S74404>
42. Briceño S, Hernandez AC, Sojo J, Lascano L, Gonzalez G (2017) Degradation of magnetite nanoparticles in biomimetic media. *J Nanopart Res* 19:140. <https://doi.org/10.1007/s11051-017-3800-3>
43. Bryce SM, Bemis JC, Avlasevich SL, Dertinger SD (2007) In vitro micronucleus assay scored by flow cytometry provides a comprehensive evaluation of cytogenetic damage and cytotoxicity. *Mutat Res Genet Toxicol Environ Mutagen* 630:78–91. <https://doi.org/10.1016/j.mrgentox.2007.03.002>
44. Buzea C, Pacheco II, Robbie K (2007) Nanomaterials and nanoparticles: sources and toxicity. *Biointerphases* 2:MR17–MR71. <https://doi.org/10.1116/1.2815690>
45. Cabrera-García A, Checa-Chavarria E, Pacheco-Torres J, Bernabeu-Sanz Á, Vidal-Moya A, Rivero-Buceta E, Sastre G, Fernández E, Botella P (2018) Engineered contrast agents in a single structure for: T1-T2 dual magnetic resonance imaging. *Nanoscale* 10:6349–6360. <https://doi.org/10.1039/c7nr07948f>
46. Cai J, Miao YQ, Yu BZ, Ma P, Li L, Fan HM (2017) Large-scale, facile transfer of oleic acid-stabilized iron oxide nanoparticles to the aqueous phase for biological applications. *Langmuir* 33:1662–1669. <https://doi.org/10.1021/acs.langmuir.6b03360>
47. Cao Z, Liao Q, Su M, Huang K, Jin J, Cao D (2019) AKT and ERK dual inhibitors: the way forward? *Cancer Lett* 459:30–40. <https://doi.org/10.1016/j.canlet.2019.05.025>
48. Capjak I, Goreta SŠ, Jurašin DD, Vrčec IV (2017) How protein coronas determine the fate of engineered nanoparticles in biological environment. *Arh Hig Rada Toksikol* 68:245–253. <https://doi.org/10.1515/aiht-2017-68-3054>
49. Chang X, Li J, Niu S, Xue Y, Tang M (2020) Neurotoxicity of metal-containing nanoparticles and implications in glial cells. *J Appl Toxicol* 40:37:1–17. <https://doi.org/10.1002/jat.4037>
50. Chen B, Wang F, Zhang W, Wang X, Senthilkumar R, Qiao L (2015) Inducing cell cycle arrest and apoptosis by dimercaptosuccinic acid modified Fe₃O₄ magnetic nanoparticles combined with nontoxic concentration of bortezomib and gambogic acid in RPMI-8226 cells. *Int J Nanomedicine* 10:3275. <https://doi.org/10.2147/IJN.S80795>
51. Chen D, Monteiro-Riviere NA, Zhang LW (2017) Intracellular imaging of quantum dots, gold, and iron oxide nanoparticles with associated endocytic pathways. *Wiley Interdiscip Rev Nanomed Nanobiotechnol* 9:1–19. <https://doi.org/10.1002/wnan.1419>
52. Cheng Z, Zhang J, Liu H, Li Y, Zhao Y, Yang E (2010) Central nervous system penetration for small molecule therapeutic agents does not increase in multiple sclerosis- and Alzheimer's disease-related animal models despite reported blood-brain barrier disruption. *Drug Metab Dispos* 38:1355–1361. <https://doi.org/10.1124/dmd.110.033324>
53. Chenthamara D, Subramaniam S, Ramakrishnan SG, Krishnaswamy S, Essa MM, Lin F-H, Qoronfleh MW (2019) Therapeutic efficacy of nanoparticles and routes of administration. *Biomater Res* 23:20. <https://doi.org/10.1186/s40824-019-0166-x>
54. Choudhury H, Gorain B, Pandey M, Khurana RK, Kesharwani P (2019) Strategizing biodegradable polymeric nanoparticles to cross the biological barriers for cancer targeting. *Int J Pharm* 565:509–522. <https://doi.org/10.1016/j.ijpharm.2019.05.042>
55. Cicha I, Scheffler L, Ebenau A, Lyer S, Alexiou C, Goppelt-Struebe M (2015) Mitoxantrone-loaded superparamagnetic iron oxide nanoparticles as drug carriers for cancer therapy: uptake and toxicity in pri-

- mary human tubular epithelial cells. *Nanotoxicology* 5390:1–10. <https://doi.org/10.3109/17435390.2015.1095364>
56. Coccini T, Caloni F, Ramírez Cando LJ, De Simone U (2017) Cytotoxicity and proliferative capacity impairment induced on human brain cell cultures after short- and long-term exposure to magnetite nanoparticles. *J Appl Toxicol* 37:361–373. <https://doi.org/10.1002/jat.3367>
57. Colognato R, Park MVDZ, Wick P, De Jong WH (2012) Interactions with the human body. In: *Adverse effects of engineered nanomaterials*. Elsevier, pp 3–24. <https://doi.org/10.1016/B978-0-12-386940-1.00001-5>
58. Coricovac D-E, Moacă E-A, Pinzaru I, Cîtu C, Soica C, Mihali C-V, Păcurariu C, Tutelyan VA, Tsatsakis A, Dehelean C-A (2017) Biocompatible colloidal suspensions based on magnetic iron oxide nanoparticles: synthesis, characterization and toxicological profile. *Front Pharmacol* 8:154. <https://doi.org/10.3389/fphar.2017.00154>
59. Costa C, Brandão F, Bessa MJMJ, Costa S, Valdiglesias V, Kiliç G, Fernández-Bertólez N, Quaresma P, Pereira E, Pásaro E, Laffon B, Teixeira JPJP (2016) In vitro cytotoxicity of superparamagnetic iron oxide nanoparticles on neuronal and glial cells. Evaluation of nanoparticle interference with viability tests. *J Appl Toxicol* 36:361–372. <https://doi.org/10.1002/jat.3213>
60. Couto D, Sousa R, Andrade L, Leander M, Lopez-Quintela MA, Rivas J, Freitas P, Lima M, Porto G, Porto B, Carvalho F, Fernandes E (2015) Polyacrylic acid coated and non-coated iron oxide nanoparticles are not genotoxic to human T lymphocytes. *Toxicol Lett* 234:67–73. <https://doi.org/10.1016/j.toxlet.2015.02.010>
61. Cromer Berman SM, Kshitiz CJ, Wang CJ, Orukari I, Levchenko A, Bulte JWM, Walczak P (2013) Cell motility of neural stem cells is reduced after SPIO-labeling, which is mitigated after exocytosis. *Magn Reson Med* 69:255–262. <https://doi.org/10.1002/mrm.24216>
62. D'Agata F, Ruffinatti FA, Boschi S, Stura I, Rainero I, Abollino O, Cavalli R, Guiot C (2018) Magnetic nanoparticles in the central nervous system: targeting principles, applications and safety issues. *Molecules* 23:1–25. <https://doi.org/10.3390/molecules23010009>
63. Dadfar SM, Roemhild K, Drude NI, von Stillfried S, Knüchel R, Kiessling F, Lammers T (2019) Iron oxide nanoparticles: diagnostic, therapeutic and theranostic applications. *Adv Drug Deliv Rev* 138:302–325. <https://doi.org/10.1016/j.addr.2019.01.005>
64. Dayem AA, Hossain MK, Lee SB, Kim K, Saha SK, Yang GM, Choi HY, Cho SG (2017) The role of reactive oxygen species (ROS) in the biological activities of metallic nanoparticles. *Int J Mol Sci* 18:1–21. <https://doi.org/10.3390/ijms18010120>
65. De Bock M, Decrock E, Wang N, Bol M, Vinken M, Bultynck G, Leybaert L (2014) The dual face of connexin-based astroglial Ca²⁺-communication: a key player in brain physiology and a prime target in pathology. *Biochim Biophys Acta, Mol Cell Res* 1843:2211–2232. <https://doi.org/10.1016/j.bbamcr.2014.04.016>
66. de Oliveira GMT, Kist LW, Pereira TCB, Bortolotto JW, Paquete FL, de Oliveira EMN, Leite CE, Bonan CD, de Souza Basso NR, Papaleo RM, Bogo MR (2014) Transient modulation of acetylcholinesterase activity caused by exposure to dextran-coated iron oxide nanoparticles in brain of adult zebrafish. *Comp Biochem Physiol C Toxicol Pharmacol* 162:77–84. <https://doi.org/10.1016/j.cbpc.2014.03.010>
67. Debia M, Bakhiyi B, Ostiguy C, Verbeek JH, Brouwer DH, Murashov V (2016) A systematic review of reported exposure to engineered nanomaterials. *Ann Occup Hyg* 60:916–935. <https://doi.org/10.1093/annhyg/mew041>
68. Deng M, Huang Z, Zou Y, Yin G, Liu J, Gu J (2014) Fabrication and neuron cytocompatibility of iron oxide nanoparticles coated with silk-fibroin peptides. *Colloids Surf B Biointerfaces* 116:465–471. <https://doi.org/10.1016/j.colsurfb.2014.01.021>
69. Di Bona K, Xu Y, Gray M, Fair D, Hayles H, Milad L, Montes A, Sherwood J, Bao Y, Rasco J (2015) Short- and long-term effects of prenatal exposure to iron oxide nanoparticles: influence of surface charge and dose on developmental and reproductive toxicity. *Int J Mol Sci* 16:30251–30268. <https://doi.org/10.3390/ijms161226231>
70. Dilnawaz F, Sahoo SK (2015) Therapeutic approaches of magnetic nanoparticles for the central nervous system. *Drug Discov Today* 20:1256–1264. <https://doi.org/10.1016/j.drudis.2015.06.008>
71. Dissanayake NM, Current KM, Obare SO (2015) Mutagenic effects of iron oxide nanoparticles on biological cells. *Int J Mol Sci* 16:23482–23516. <https://doi.org/10.3390/ijms161023482>
72. Dobrovolskaia MA, Shurin M, Shvedova AA (2016) Current understanding of interactions between nanoparticles and the immune system. *Toxicol Appl Pharmacol* 299:78–89. <https://doi.org/10.1016/j.taap.2015.12.022>
73. Drasler B, Vanhecke D, Rodriguez-Lorenzo L, Petri-Fink A, Rothen-Rutishauser B (2017) Quantifying nanoparticle cellular uptake: which method is best? *Nanomedicine* 12:1095–1099. <https://doi.org/10.2217/nnm-2017-0071>
74. Du S, Li J, Du C, Huang Z, Chen G, Yan W (2017) Overendocytosis of superparamagnetic iron oxide particles increases apoptosis and triggers autophagic cell death in human osteosarcoma cell under a spinning magnetic field. *Oncotarget* 8:9410–9424. <https://doi.org/10.18632/oncotarget.14114>
75. Duan J, Dong J, Zhang T, Su Z, Ding J, Zhang Y, Mao X (2014) Polyethyleneimine-functionalized

- iron oxide nanoparticles for systemic siRNA delivery in experimental arthritis. *Nanomedicine* 9:789–801. <https://doi.org/10.2217/nmm.13.217>
76. Dulińska-Litewka J, Łazarczyk A, Hałubiec P, Szafranski O, Karnas K, Karewicz A (2019) Superparamagnetic iron oxide nanoparticles—current and prospective medical applications. *Materials (Basel)* 12:617. <https://doi.org/10.3390/ma12040617>
77. Dwane S, Durack E, Kiely PA (2013) Optimising parameters for the differentiation of SH-SY5Y cells to study cell adhesion and cell migration. *BMC Res Notes* 6:366. <https://doi.org/10.1186/1756-0500-6-366>
78. Dwivedi S, Siddiqui MA, Farshori NN, Ahamed M, Musarrat J, Al-Khedhairi AA (2014) Synthesis, characterization and toxicological evaluation of iron oxide nanoparticles in human lung alveolar epithelial cells. *Colloids Surf B Biointerfaces* 122:209–215. <https://doi.org/10.1016/j.colsurfb.2014.06.064>
79. Easo SL, Mohanan PV (2015) In vitro hematological and in vivo immunotoxicity assessment of dextran stabilized iron oxide nanoparticles. *Colloids Surf B Biointerfaces* 134:122–130. <https://doi.org/10.1016/j.colsurfb.2015.06.046>
80. Easo SL, Mohanan PV (2016) Toxicological evaluation of dextran stabilized iron oxide nanoparticles in human peripheral blood lymphocytes. *Biointerphases* 11:04B302. <https://doi.org/10.1116/1.4962268>
81. Eid R, Arab NTT, Greenwood MT (2017) Iron mediated toxicity and programmed cell death: a review and a re-examination of existing paradigms. *Biochim Biophys Acta, Mol Cell Res* 1864:399–430. <https://doi.org/10.1016/j.bbamcr.2016.12.002>
82. Elsaesser A, Howard CV (2012) Toxicology of nanoparticles. *Adv Drug Deliv Rev* 64:129–137. <https://doi.org/10.1016/j.addr.2011.09.001>
83. Elzoghby AO, Hemasa AL, Freag MS (2016) Hybrid protein-inorganic nanoparticles: from tumor-targeted drug delivery to cancer imaging. *J Control Release* 243:303–322. <https://doi.org/10.1016/j.jconrel.2016.10.023>
84. Estelrich J, Escribano E, Queral J, Busquets MA (2015) Iron oxide nanoparticles for magnetically-guided and magnetically-responsive drug delivery. *Int J Mol Sci* 16:8070–8101. <https://doi.org/10.3390/ijms16048070>
85. Estevanato L, Cintra D, Baldini N, Portilho F, Barbosa L, Martins O, Lacava B, Miranda-Vilela AL, Tedesco AC, Bão S, Morais PC, Lacava ZGM (2011) Preliminary biocompatibility investigation of magnetic albumin nanosphere designed as a potential versatile drug delivery system. *Int J Nanomedicine* 6:1709–1717. <https://doi.org/10.2147/IJN.S21323>
86. Fenech M (2008) The micronucleus assay determination of chromosomal level DNA damage. In: *Methods in molecular biology* (Clifton, N.J.). Springer, Cham, pp 185–216. https://doi.org/10.1007/978-1-59745-548-0_12
87. Fernández-Bertólez N, Costa C, Brandão F, Kiliç G, Duarte JAJA, Teixeira JPJP, Pásaro E, Valdiglesias V, Laffon B (2018a) Toxicological assessment of silica-coated iron oxide nanoparticles in human astrocytes. *Food Chem Toxicol* 118:13–23. <https://doi.org/10.1016/j.fct.2018.04.058>
88. Fernández-Bertólez N, Costa C, Brandão F, Kiliç G, Teixeira JP, Pásaro E, Laffon B, Valdiglesias V (2018b) Neurotoxicity assessment of oleic acid-coated iron oxide nanoparticles in SH-SY5Y cells. *Toxicology* 406–407:81–91. <https://doi.org/10.1016/j.tox.2018.06.003>
89. Fernández-Bertólez N, Costa C, Bessa MJ, Park M, Carriere M, Dussert F, Teixeira JP, Pásaro E, Laffon B, Valdiglesias V (2019a) Assessment of oxidative damage induced by iron oxide nanoparticles on different nervous system cells. *Mutat Res Toxicol Environ Mutagen* 845:402989. <https://doi.org/10.1016/j.mrgentox.2018.11.013>
90. Fernández-Bertólez N, Costa C, Brandão F, Duarte JA, Teixeira JP, Pásaro E, Valdiglesias V, Laffon B (2019b) Evaluation of cytotoxicity and genotoxicity induced by oleic acid-coated iron oxide nanoparticles in human astrocytes. *Environ Mol Mutagen* 60:816–829. <https://doi.org/10.1002/em.22323>
91. Forest V, Vergnon JM, Pourchez J (2017) Biological monitoring of inhaled nanoparticles in patients: an appealing approach to study causal link between human respiratory pathology and exposure to nanoparticles. *Chem Res Toxicol* 30:1655–1660. <https://doi.org/10.1021/acs.chemrestox.7b00192>
92. Frank JA, Zywicke H, Jordan E, Mitchell J, Lewis BK, Miller B, Bryant LH, Bulte JW (2002) Magnetic intracellular labeling of mammalian cells by combining (FDA-approved) superparamagnetic iron oxide MR contrast agents and commonly used transfection agents. *Acad Radiol* 9:S484–S487. [https://doi.org/10.1016/S1076-6332\(03\)80271-4](https://doi.org/10.1016/S1076-6332(03)80271-4)
93. Frantellizzi V, Conte M, Pontico M, Pani A, Pani R, De Vincentis G (2020) New frontiers in molecular imaging with superparamagnetic iron oxide nanoparticles (SPIONs): efficacy, toxicity, and future applications. *Nucl Med Mol Imaging* 54:65–80. <https://doi.org/10.1007/s13139-020-00635-w>
94. Fratila RM, Rivera-Fernández S, de la Fuente JM (2015) Shape matters: synthesis and biomedical applications of high aspect ratio magnetic nanomaterials. *Nanoscale* 7:8233–8260. <https://doi.org/10.1039/c5nr01100k>
95. Freitas MLL, Silva LP, Azevedo RB, Garcia VAP, Lacava LM, Grisólia CK, Lucci CM, Morais PC, Da Silva MF, Buske N, Curi R, Lacava ZGM (2002) A double-coated magnetite-based magnetic fluid evaluation by cytometry and genetic tests. *J Magn Magn Mater* 252:396–398. [https://doi.org/10.1016/S0304-8853\(02\)00655-8](https://doi.org/10.1016/S0304-8853(02)00655-8)
96. Fröhlich E, Meindl C, Roblegg E, Griesbacher A, Pieber TR (2012) Cytotoxicity of nanoparticles is influenced by size, proliferation and embryonic origin of the cells used for testing. *Nanotoxicology* 6:424–439. <https://doi.org/10.3109/17435390.2011.586478>

97. Gaharwar US, Meena R, Rajamani P (2017) Iron oxide nanoparticles induced cytotoxicity, oxidative stress and DNA damage in lymphocytes. *J Appl Toxicol* 37:1232–1244. <https://doi.org/10.1002/jat.3485>
98. Galaris D, Barbouti A, Pantopoulos K (2019) Iron homeostasis and oxidative stress: an intimate relationship. *Biochim Biophys Acta, Mol Cell Res* 1866:118535. <https://doi.org/10.1016/j.bbamcr.2019.118535>
99. Garcia GJM, Schroeter JD, Kimbell JS (2015) Olfactory deposition of inhaled nanoparticles in humans. *Inhal Toxicol* 27:1091–1099. <https://doi.org/10.3109/08958378.2015.1066904>
100. Ge Y, Zhang Y, He S, Nie F, Teng G, Gu N (2009) Fluorescence modified chitosan-coated magnetic nanoparticles for high-efficient cellular imaging. *Nanoscale Res Lett* 4:287–295. <https://doi.org/10.1007/s11671-008-9239-9>
101. Geppert M, Hohnholt M, Gaetjen L, Grunwald I, Bäumer M, Dringen R (2009) Accumulation of iron oxide nanoparticles by cultured brain astrocytes. *J Biomed Nanotechnol* 5:285–293. <https://doi.org/10.1016/j.neuint.2014.12.005>
102. Geppert M, Hohnholt MC, Thiel K, Nürnberger S, Grunwald I, Rezwani K, Dringen R (2011) Uptake of dimercaptosuccinate-coated magnetic iron oxide nanoparticles by cultured brain astrocytes. *Nanotechnology* 22:145101. <https://doi.org/10.1088/0957-4484/22/14/145101>
103. Ghosh S, Ghosh I, Chakrabarti M, Mukherjee A (2020) Genotoxicity and biocompatibility of superparamagnetic iron oxide nanoparticles: influence of surface modification on biodistribution, retention, DNA damage and oxidative stress. *Food Chem Toxicol* 136:110989. <https://doi.org/10.1016/j.fct.2019.110989>
104. Ginzburg VV, Balijepalli S (2007) Modeling the thermodynamics of the interaction of nanoparticles with cell membranes. *Nano Lett* 7:3716–3722. <https://doi.org/10.1021/nl072053l>
105. Gkagkanasiou M, Ploussi A, Gazouli M, Efstathopoulos EP (2016) USPIO-enhanced MRI neuroimaging: a review. *J Neuroimaging* 26:161–168. <https://doi.org/10.1111/jon.12318>
106. Gomaa IO, Abdel Kader MH, Salah Eldin T, Heikal OA (2011) Evaluation of in vitro mutagenicity and genotoxicity of magnetite nanoparticles. *Drug Discov Ther* 7:116–123. <https://doi.org/10.5582/ddt.2013.v7.3.116>
107. Gonzalez L, Kirsch-Volders M (2016) Biomonitoring of genotoxic effects for human exposure to nanomaterials: the challenge ahead. *Mutat Res Rev Mutat Res* 768:14–26. <https://doi.org/10.1016/j.mrrev.2016.03.002>
108. Gormley AJ, Ghandehari H (2009) Evaluation of toxicity of nanostructures in biological systems. In: *Nanotoxicity*. Wiley, Chichester, pp 115–159. <https://doi.org/10.1002/9780470747803.ch7>
109. Grand View Research Inc. (2019) Report GVR-3-68038-765-0 (2019) Magnetite nanoparticles market size, share & trends analysis report by application (bio-medical, electronics, energy, wastewater treatment), by region, and segment forecasts, 2019–2025. <https://www.grandviewresearch.com/industry-analysis/magnetite-nanoparticles-market>
110. Guichard Y, Schmit J, Darne C, Gaté L, Goutet M, Rousset D, Rastoix O, Wrobel R, Witschger O, Martin A, Fierro V, Binet S (2012) Cytotoxicity and genotoxicity of nanosized and microsized titanium dioxide and iron oxide particles in Syrian hamster embryo cells. *Ann Occup Hyg* 56:631–644. <https://doi.org/10.1093/annhyg/mes006>
111. Gul S, Khan SB, Rehman IU, Khan MA, Khan MI (2019) A comprehensive review of magnetic nanomaterials modern day theranostics. *Front Mater* 6:179. <https://doi.org/10.3389/fmats.2019.00179>
112. Han D-W, Hong SC, Lee JH, Lee J, Kim HY, Park JY, Cho LJ, Han D-W (2011) Subtle cytotoxicity and genotoxicity differences in superparamagnetic iron oxide nanoparticles coated with various functional groups. *Int J Nanomedicine* 6:3219. <https://doi.org/10.2147/IJN.S26355>
113. Hanini A, Schmitt A, Kacem K, Chau F, Ammar S, Gavard J (2011) Evaluation of iron oxide nanoparticle biocompatibility. *Int J Nanomedicine* 6:787–794. <https://doi.org/10.2147/IJN.S17574>
114. Hanot C, Choi Y, Anani T, Soundararajan D, David A (2015) Effects of iron-oxide nanoparticle surface chemistry on uptake kinetics and cytotoxicity in CHO-K1 cells. *Int J Mol Sci* 17:54. <https://doi.org/10.3390/ijms17010054>
115. Hildebrand H, Kühnel D, Potthoff A, Mackenzie K, Springer A, Schirmer K (2010) Evaluating the cytotoxicity of palladium/magnetite nanocatalysts intended for wastewater treatment. *Environ Pollut* 158:65–73. <https://doi.org/10.1016/j.envpol.2009.08.021>
116. Hoet PHM, Brüske-Hohlfeld I, Salata OV (2004) Nanoparticles – known and unknown health risks. *J Nanobiotechnol* 2:1–15. <https://doi.org/10.1186/1477-3155-2-12>
117. Hohnholt MC, Dringen R (2013) Uptake and metabolism of iron and iron oxide nanoparticles in brain astrocytes. *Biochem Soc Trans* 41:1588–1592. <https://doi.org/10.1042/bst20130114>
118. Hohnholt M, Geppert M, Dringen R (2010) Effects of iron chelators, iron salts, and iron oxide nanoparticles on the proliferation and the iron content of oligodendroglial OLN-93 cells. *Neurochem Res* 35:1259–1268. <https://doi.org/10.1007/s11064-010-0184-5>
119. Hohnholt MC, Geppert M, Dringen R (2011) Treatment with iron oxide nanoparticles induces ferritin synthesis but not oxidative stress in oligodendroglial cells. *Acta Biomater* 7:3946–3954. <https://doi.org/10.1016/j.actbio.2011.06.052>

120. Hohnholt MC, Geppert M, Luther EM, Petters C, Bulcke F, Dringen R (2013) Handling of iron oxide and silver nanoparticles by astrocytes. *Neurochem Res* 38:227–239. <https://doi.org/10.1007/s11064-012-0930-y>
121. Hoskins C, Cuschieri A, Wang L (2012) The cytotoxicity of polycationic iron oxide nanoparticles: common endpoint assays and alternative approaches for improved understanding of cellular response mechanism. *J Nanobiotechnol* 10:15. <https://doi.org/10.1186/1477-3155-10-15>
122. Hossen S, Hossain MK, Basher MK, Mia MNH, Rahman MT, Uddin MJ (2019) Smart nanocarrier-based drug delivery systems for cancer therapy and toxicity studies: a review. *J Adv Res* 15:1–18. <https://doi.org/10.1016/j.jare.2018.06.005>
123. Howarth C (2014) The contribution of astrocytes to the regulation of cerebral blood flow. *Front Neurosci* 8:1–9. <https://doi.org/10.3389/fnins.2014.00103>
124. Huang S, Li C, Cheng Z, Fan Y, Yang P, Zhang C, Yang K, Lin J (2012) Magnetic Fe₃O₄@mesoporous silica composites for drug delivery and bioadsorption. *J Colloid Interface Sci* 376:312–321. <https://doi.org/10.1016/j.jcis.2012.02.031>
125. Huang Y-WW, Cambre M, Lee H-JJ (2017) The toxicity of nanoparticles depends on multiple molecular and physicochemical mechanisms. *Int J Mol Sci* 18:2702. <https://doi.org/10.3390/ijms18122702>
126. Im H-J, England CG, Feng L, Graves SA, Hernandez R, Nickles RJ, Liu Z, Lee DS, Cho SY, Cai W (2016) Accelerated blood clearance phenomenon reduces the passive targeting of pegylated nanoparticles in peripheral arterial disease. *ACS Appl Mater Interfaces* 8:17955–17963. <https://doi.org/10.1021/acsami.6b05840>
127. Imam SZ, Lantz-McPeak SM, Cuevas E, Rosas-Hernandez H, Liachenko S, Zhang Y, Sarkar S, Ramu J, Robinson BL, Jones Y, Gough B, Paule MG, Ali SF, Binienda ZK (2015) Iron oxide nanoparticles induce dopaminergic damage: in vitro pathways and in vivo imaging reveals mechanism of neuronal damage. *Mol Neurobiol* 52:913–926. <https://doi.org/10.1007/s12035-015-9259-2>
128. Joris F, Valdepérez D, Pelaz B, Soenen SJ, Manshian BB, Parak WJ, De Smedt SC, Raemdonck K (2016) The impact of species and cell type on the nanosafety profile of iron oxide nanoparticles in neural cells. *J Nanobiotechnol* 14:69. <https://doi.org/10.1186/s12951-016-0220-y>
129. Jud C, Clift MJD, Petri-Fink A, Rothen-Rutishauser B (2013) Nanomaterials and the human lung: what is known and what must be deciphered to realise their potential advantages? *Swiss Med Wkly* 143:1–20. <https://doi.org/10.4414/smw.2013.13758>
130. Kanwar JR, Sun X, Punj V, Sriramoju B, Mohan RR, Zhou S-F, Chauhan A, Kanwar RK (2012) Nanoparticles in the treatment and diagnosis of neurological disorders: untamed dragon with fire power to heal. *Nanomed Nanotechnol Biol Med* 8:399–414. <https://doi.org/10.1016/j.nano.2011.08.006>
131. Karlsson HL, Cronholm P, Gustafsson J, Möller L (2008) Copper oxide nanoparticles are highly toxic: a comparison between metal oxide nanoparticles and carbon nanotubes. *Chem Res Toxicol* 21:1726–1732. <https://doi.org/10.1021/tx800064j>
132. Karlsson HL, Gustafsson J, Cronholm P, Möller L (2009) Size-dependent toxicity of metal oxide particles – a comparison between nano- and micrometer size. *Toxicol Lett* 188:112–118. <https://doi.org/10.1016/j.toxlet.2009.03.014>
133. Karlsson HL, Di Bucchianico S, Collins AR, Dusinska M (2015) Can the comet assay be used reliably to detect nanoparticle-induced genotoxicity? *Environ Mol Mutagen* 56:82–96. <https://doi.org/10.1002/em.21933>
134. Karmakar A, Zhang Q, Zhang Y (2014) Neurotoxicity of nanoscale materials. *J Food Drug Anal* 22:147–160. <https://doi.org/10.1016/j.jfda.2014.01.012>
135. Kaushik A, Jayant RD, Bhardwaj V, Nair M (2018) Personalized nanomedicine for CNS diseases. *Drug Discov Today* 23:1007–1015. <https://doi.org/10.1016/j.drudis.2017.11.010>
136. Kavithaa K, Paulpandi M, Padma PR, Sumathi S (2016) Induction of intrinsic apoptotic pathway and cell cycle arrest: via baicalein loaded iron oxide nanoparticles as a competent nano-mediated system for triple negative breast cancer therapy. *RSC Adv* 6:64531–64543. <https://doi.org/10.1039/c6ra11658b>
137. Kawabata H (2019) Transferrin and transferrin receptors update. *Free Radic Biol Med* 133:46–54. <https://doi.org/10.1016/j.freeradbiomed.2018.06.037>
138. Kenzaoui BH, Bernasconi CC, Guney-Ayra S, Juillerat-Jeanneret L (2012a) Induction of oxidative stress, lysosome activation and autophagy by nanoparticles in human brain-derived endothelial cells. *Biochem J* 441:813–821. <https://doi.org/10.1042/BJ20111252>
139. Kenzaoui BH, Bernasconi CC, Hofmann H, Juillerat-Jeanneret L (2012b) Evaluation of uptake and transport of ultrasmall superparamagnetic iron oxide nanoparticles by human brain-derived endothelial cells. *Nanomedicine* 7:39–53. <https://doi.org/10.2217/nmm.11.85>
140. Kermanizadeh A, Chauché C, Brown DM, Loft S, Møller P (2015) The role of intracellular redox imbalance in nanomaterial induced cellular damage and genotoxicity: a review. *Environ Mol Mutagen* 56:111–124. <https://doi.org/10.1002/em.21926>
141. Khan MI, Mohammad A, Patil G, Naqvi SAH, Chauhan LKS, Ahmad I (2012) Induction of ROS, mitochondrial damage and autophagy in lung epithelial cancer cells by iron oxide nanoparticles. *Biomaterials* 33:1477–1488. <https://doi.org/10.1016/j.biomaterials.2011.10.080>
142. Kiliç G, Costa C, Fernández-Bertólez N, Pásaro E, Teixeira JPJP, Laffon B, Valdíglesias V (2016) In vitro toxicity evaluation of silica-coated iron oxide nanoparticles in human SHSY5Y neuronal cells. *Toxicol Res (Camb)* 5:235–247. <https://doi.org/10.1039/c6tx90013e>

143. Kim JS, Yoon T-J, Yu KN, Kim BG, Park SJ, Kim HW, Lee KH, Park SB, Lee J-K, Cho MH (2006) Toxicity and tissue distribution of magnetic nanoparticles in mice. *Toxicol Sci* 89:338–347. <https://doi.org/10.1093/toxsci/kfj027>
144. Kim Y, Kong SD, Chen L-H, Pisanic TR, Jin S, Shubayev VI (2013) In vivo nanoneurotoxicity screening using oxidative stress and neuroinflammation paradigms. *Nanomed Nanotechnol Biol Med* 9:1057–1066. <https://doi.org/10.1016/j.nano.2013.05.002>
145. Kim J-H, Sanetuntikul J, Shanmugam S, Kim E (2015) Necrotic cell death caused by exposure to graphitic carbon-coated magnetic nanoparticles. *J Biomed Mater Res A* 103:2875–2887. <https://doi.org/10.1002/jbm.a.35418>
146. Könczöl M, Ebeling S, Goldenberg E, Treude F, Gminski R, Gieré R, Grobéty B, Rothen-Rutishauser B, Merfort I, Mersch-Sundermann V (2011) Cytotoxicity and genotoxicity of size-fractionated iron oxide (magnetite) in A549 human lung epithelial cells: role of ROS, JNK, and NF- κ B. *Chem Res Toxicol* 24:1460–1475. <https://doi.org/10.1021/tx200051s>
147. Könczöl M, Weiss A, Stangenberg E, Gminski R, Garcia-Käuffer M, Gieré R, Merfort I, Mersch-Sundermann V (2013) Cell-cycle changes and oxidative stress response to magnetite in A549 human lung cells. *Chem Res Toxicol* 26:693–702. <https://doi.org/10.1021/tx300503q>
148. Kong SD, Lee J, Ramachandran S, Eliceiri BP, Shubayev VI, Lal R, Jin S (2012) Magnetic targeting of nanoparticles across the intact blood-brain barrier. *J Control Release* 164:49–57. <https://doi.org/10.1016/j.jconrel.2012.09.021>
149. Kornberg T, Stueckle T, Antonini J, Rojanasakul Y, Castranova V, Yang Y, Wang L (2017) Potential toxicity and underlying mechanisms associated with pulmonary exposure to iron oxide nanoparticles: conflicting literature and unclear risk. *Nanomaterials* 7:307. <https://doi.org/10.3390/nano7100307>
150. Kráľovec K, Havelek R, Kročová E, Kučirková L, Hauschke M, Bartáček J, Palarčík J, Sedlák M (2019) Silica coated iron oxide nanoparticles-induced cytotoxicity, genotoxicity and its underlying mechanism in human HK-2 renal proximal tubule epithelial cells. *Mutat Res Genet Toxicol Environ Mutagen* 844:35–45. <https://doi.org/10.1016/j.mrgentox.2019.05.015>
151. Kratzer I, Ek J, Stolp H (2020) The molecular anatomy and functions of the choroid plexus in healthy and diseased brain. *Biochim Biophys Acta Biomembr* 1862:183430. <https://doi.org/10.1016/j.bbmem.2020.183430>
152. Kumar M, Singh G, Arora V, Mewar S, Sharma U, Jagannathan NR, Sapra S, Dinda AK, Kharbanda S, Singh H (2012) Cellular interaction of folic acid conjugated superparamagnetic iron oxide nanoparticles and its use as contrast agent for targeted magnetic imaging of tumor cells. *Int J Nanomedicine* 7:3503–3516. <https://doi.org/10.2147/IJN.S32694>
153. Kumari M, Rajak S, Singh SP, Kumari SI, Kumar PU, Murty USN, Mahboob M, Grover P, Rahman MF (2012) Repeated oral dose toxicity of iron oxide nanoparticles: biochemical and histopathological alterations in different tissues of rats. *J Nanosci Nanotechnol* 12:2149–2159. <https://doi.org/10.1166/jnn.2012.5796>
154. Kunzmann A, Andersson B, Thurnherr T, Krug H, Scheynius A, Fadeel B (2011a) Toxicology of engineered nanomaterials: focus on biocompatibility, biodistribution and biodegradation. *Biochim Biophys Acta Gen Subj* 1810:361–373. <https://doi.org/10.1016/j.bbagen.2010.04.007>
155. Kunzmann A, Andersson B, Vogt C, Feliu N, Ye F, Gabriëlsson S, Toprak MS, Buerki-Thurnherr T, Laurent S, Vahter M, Krug H, Muhammed M, Scheynius A, Fadeel B (2011b) Efficient internalization of silica-coated iron oxide nanoparticles of different sizes by primary human macrophages and dendritic cells. *Toxicol Appl Pharmacol* 253:81–93. <https://doi.org/10.1016/j.taap.2011.03.011>
156. Kwon D, Nho HW, Yoon TH (2014) X-ray and electron microscopy studies on the biodistribution and biomodification of iron oxide nanoparticles in *Daphnia magna*. *Colloids Surf B Biointerfaces* 122:384–389. <https://doi.org/10.1016/j.colsurfb.2014.07.016>
157. Lai DY (2015) Approach to using mechanism-based structure activity relationship (SAR) analysis to assess human health hazard potential of nanomaterials. *Food Chem Toxicol* 85:120–126. <https://doi.org/10.1016/j.fct.2015.06.008>
158. Lai X, Wei Y, Zhao H, Chen S, Bu X, Lu F, Qu D, Yao L, Zheng J, Zhang J (2015) The effect of Fe₂O₃ and ZnO nanoparticles on cytotoxicity and glucose metabolism in lung epithelial cells. *J Appl Toxicol* 35:651–664. <https://doi.org/10.1002/jat.3128>
159. Laurent S, Saei AA, Behzadi S, Panahifar A, Mahmoudi M (2014) Superparamagnetic iron oxide nanoparticles for delivery of therapeutic agents: opportunities and challenges. *Expert Opin Drug Deliv* 11:1449–1470. <https://doi.org/10.1517/17425247.2014.924501>
160. Lazaratos M, Karathanou K, Mainas E, Chatzigeorgias A, Pippa N, Demetzos C, Cournia Z (2020) Coating of magnetic nanoparticles affects their interactions with model cell membranes. *Biochim Biophys Acta Gen Subj* 1864:129671. <https://doi.org/10.1016/j.bbagen.2020.129671>
161. Lee H, Lee E, Kim DK, Jang NK, Jeong YY, Jon S (2006) Antibiofouling polymer-coated superparamagnetic iron oxide nanoparticles as potential magnetic resonance contrast agents for in vivo cancer imaging. *J Am Chem Soc* 128:7383–7389. <https://doi.org/10.1021/ja061529k>
162. Lee JH, Ju JE, BIL K, Pak PJ, Choi EK, Lee HS, Chung N (2014) Rod-shaped iron oxide nanoparti-

- cles are more toxic than sphere-shaped nanoparticles to murine macrophage cells. *Environ Toxicol Chem* 33:2759–2766. <https://doi.org/10.1002/etc.2735>
163. Lee SH, Lee DH, Jung H, Han Y-S, Kim T-H, Yang W (2015) Magnetic properties of SiO₂-coated iron oxide nanoparticles studied by polarized small angle neutron scattering. *Curr Appl Phys* 15:915–919. <https://doi.org/10.1016/j.cap.2015.04.003>
164. Li Y, Zhang H (2019) Fe₃O₄-based nanotheranostics for magnetic resonance imaging-synergized multifunctional cancer management. *Nanomedicine* 14:1493–1512. <https://doi.org/10.2217/nmm-2018-0346>
165. Li L, Mak KY, Shi J, Koon HK, Leung CH, Wong CM, Leung CW, Mak CSK, Chan NMM, Zhong W, Lin KW, Wu EX, Pong PWT (2012) Comparative in vitro cytotoxicity study on uncoated magnetic nanoparticles: effects on cell viability, cell morphology, and cellular uptake. *J Nanosci Nanotechnol* 12:9010–9017. <https://doi.org/10.1166/jnn.2012.6755>
166. Lin Z, Monteiro-Riviere NA, Riviere JE (2015) Pharmacokinetics of metallic nanoparticles. *Wiley Interdiscip Rev Nanomed Nanobiotechnol* 7:189–217. <https://doi.org/10.1002/wnan.1304>
167. Liu N, Tang M (2020) Toxic effects and involved molecular pathways of nanoparticles on cells and subcellular organelles. *J Appl Toxicol* 40:16–36. <https://doi.org/10.1002/jat.3817>
168. Liu D, Wu W, Ling J, Wen S, Gu N, Zhang X (2011a) Effective PEGylation of iron oxide nanoparticles for high performance in vivo cancer imaging. *Adv Funct Mater* 21:1498–1504. <https://doi.org/10.1002/adfm.201001658>
169. Liu Y, Chen Z, Wang J (2011b) Systematic evaluation of biocompatibility of magnetic Fe₃O₄ nanoparticles with six different mammalian cell lines. *J Nanopart Res* 13:199–212. <https://doi.org/10.1007/s11051-010-0019-y>
170. Liu Y, Xia Q, Liu Y, Zhang S, Cheng F, Zhong Z, Wang L, Li H, Xiao K (2014) Genotoxicity assessment of magnetic iron oxide nanoparticles with different particle sizes and surface coatings. *Nanotechnology* 25:425101. <https://doi.org/10.1088/0957-4484/25/42/425101>
171. Lochhead JJ, Yang J, Ronaldson PT, Davis TP (2020) Structure, function, and regulation of the blood-brain barrier tight junction in central nervous system disorders. *Front Physiol* 11:914. <https://doi.org/10.3389/fphys.2020.00914>
172. Loh JW, Saunders M, Lim LY (2012) Cytotoxicity of monodispersed chitosan nanoparticles against the Caco-2 cells. *Toxicol Appl Pharmacol* 262:273–282. <https://doi.org/10.1016/j.taap.2012.04.037>
173. Lojk J, Repas J, Veranić P, Bregar VB, Pavlin M (2020) Toxicity mechanisms of selected engineered nanoparticles on human neural cells in vitro. *Toxicology* 432:152364. <https://doi.org/10.1016/j.tox.2020.152364>
174. Loos C, Syrovets T, Musyanovych A, Mailänder V, Landfester K, Simmet T (2014) Amino-functionalized nanoparticles as inhibitors of mTOR and inducers of cell cycle arrest in leukemia cells. *Biomaterials* 35:1944–1953. <https://doi.org/10.1016/j.biomaterials.2013.11.056>
175. Lorenz C, Von Goetz N, Scheringer M, Wormuth M, Hungerbühler K (2011) Potential exposure of German consumers to engineered nanoparticles in cosmetics and personal care products. *Nanotoxicology* 5:12–29. <https://doi.org/10.3109/17435390.2010.484554>
176. Lovisolò D, Dionisi MA, Ruffinatti F, Distasi C (2018) Nanoparticles and potential neurotoxicity: focus on molecular mechanisms. *AIMS Mol Sci* 5:1–13. <https://doi.org/10.3934/molsci.2018.1.1>
177. Luther EM, Petters C, Bulcke F, Kaltz A, Thiel K, Bickmeyer U, Dringen R (2013) Endocytotic uptake of iron oxide nanoparticles by cultured brain microglial cells. *Acta Biomater* 9:8454–8465. <https://doi.org/10.1016/j.actbio.2013.05.022>
178. Ma Y, Chen T, Iqbal MZ, Yang F, Hampp N, Wu A, Luo L (2019) Applications of magnetic materials separation in biological nanomedicine. *Electrophoresis* 40:2011–2028. <https://doi.org/10.1002/elps.201800401>
179. MacHala L, Tuček J, Zbořil R (2011) Polymorphous transformations of nanometric iron(III) oxide: a review. *Chem Mater* 23:3255–3272. <https://doi.org/10.1021/cm200397g>
180. Magdolenova Z, Rinna A, Fjellsbø L, Dusinska M (2011) Safety assessment of nanoparticles cytotoxicity and genotoxicity of metal nanoparticles in vitro. *J Biomed Nanotechnol* 7:20–21. <https://doi.org/10.1166/jbn.2011.1180>
181. Magdolenova Z, Drlickova M, Henjum K, Rundén-Pran E, Tulinska J, Bilanicova D, Pojana G, Kazimirova A, Barancokova M, Kuricova M, Liskova A, Staruchova M, Ciampor F, Vavra I, Lorenzo Y, Collins A, Rinna A, Fjellsbø L, Volkovova K, Marcomini A, Amiry-Moghaddam M, Dusinska M (2015) Coating-dependent induction of cytotoxicity and genotoxicity of iron oxide nanoparticles. *Nanotoxicology* 9:44–56. <https://doi.org/10.3109/17435390.2013.847505>
182. Magro M, Vianello F (2019) Bare iron oxide nanoparticles: surface tunability for biomedical, sensing and environmental applications. *Nano* 9:1–20. <https://doi.org/10.3390/nano9111608>
183. Mah LJ, El-Osta A, Karagiannis TC (2010) γ H2AX: a sensitive molecular marker of DNA damage and repair. *Leukemia* 24:679–686. <https://doi.org/10.1038/leu.2010.6>
184. Mahaseth T, Kuzminov A (2017) Potentiation of hydrogen peroxide toxicity: from catalase inhibi-

- tion to stable DNA-iron complexes. *Mutat Res Rev Mutat Res* 773:274–281. <https://doi.org/10.1016/j.mrrev.2016.08.006>
185. Mahdavi M, Ahmad MB, Haron MJ, Namvar F, Nadi B, MZA R, Amin J (2013) Synthesis, surface modification and characterisation of biocompatible magnetic iron oxide nanoparticles for biomedical applications. *Molecules* 18:7533–7548. <https://doi.org/10.3390/molecules18077533>
 186. Mahler GJ, Esch MB, Tako E, Southard TL, Archer SD, Glahn RP, Shuler ML (2012) Oral exposure to polystyrene nanoparticles affects iron absorption. *Nat Nanotechnol* 7:264–271. <https://doi.org/10.1038/nnano.2012.3>
 187. Mahmoudi M, Simchi A, Imani M (2009a) Cytotoxicity of uncoated and polyvinyl alcohol coated superparamagnetic iron oxide nanoparticles. *J Phys Chem C* 113:9573–9580. <https://doi.org/10.1021/jp9001516>
 188. Mahmoudi M, Simchi A, Imani M, Milani AS, Stroeve P (2009b) An in vitro study of bare and poly(ethylene glycol)-co-fumarate-coated superparamagnetic iron oxide nanoparticles: a new toxicity identification procedure. *Nanotechnology* 20:225104. <https://doi.org/10.1088/0957-4484/20/22/225104>
 189. Maier-Hauff K, Ulrich F, Nestler D, Niehoff H, Wust P, Thiesen B, Orawa H, Budach V, Jordan A (2011) Efficacy and safety of intratumoral radiotherapy using magnetic iron-oxide nanoparticles combined with external beam radiotherapy on patients with recurrent glioblastoma multiforme. *J Neuro-Oncol* 103:317–324. <https://doi.org/10.1007/s11060-010-0389-0>
 190. Malhotra N, Lee J-S, Liman RAD, Ruallo JMS, Villaflores OB, Ger T-R, Hsiao C-D (2020) Potential toxicity of iron oxide magnetic nanoparticles: a review. *Molecules* 25:3159. <https://doi.org/10.3390/molecules25143159>
 191. Malvindi MA, De Matteis V, Galeone A, Brunetti V, Anyfantis GC, Athanassiou A, Cingolani R, Pompa PP (2014) Toxicity assessment of silica coated iron oxide nanoparticles and biocompatibility improvement by surface engineering. *PLoS One* 9:e85835. <https://doi.org/10.1371/journal.pone.0085835>
 192. Manickam V, Periyasamy M, Dhakshinamoorthy V, Panneerselvam L, Perumal E (2017) Recurrent exposure to ferric oxide nanoparticles alters myocardial oxidative stress, apoptosis and necrotic markers in male mice. *Chem Biol Interact* 278:54–64. <https://doi.org/10.1016/j.cbi.2017.10.003>
 193. Martinkova P, Brtnicky M, Kynicky J, Pohanka M (2018) Iron oxide nanoparticles: innovative tool in cancer diagnosis and therapy. *Adv Healthc Mater* 7:1700932. <https://doi.org/10.1002/adhm.201700932>
 194. Martirosyan A, Schneider YJ (2014) Engineered nanomaterials in food: implications for food safety and consumer health. *Int J Environ Res Public Health* 11:5720–5750. <https://doi.org/10.3390/ijerph110605720>
 195. Maynard AD, Warheit DB, Philbert MA (2011) The new toxicology of sophisticated materials: nanotoxicology and beyond. *Toxicol Sci* 120:S109–S129. <https://doi.org/10.1093/toxsci/ktq372>
 196. Mc Carthy DJ, Malhotra M, O'Mahony AM, Cryan JF, O'Driscoll CM (2015) Nanoparticles and the blood-brain barrier: advancing from in-vitro models towards therapeutic significance. *Pharm Res* 32:1161–1185. <https://doi.org/10.1007/s11095-014-1545-6>
 197. McBain SC, Yiu HHP, Dobson J (2008) Magnetic nanoparticles for gene and drug delivery. *Int J Nanomedicine* 3:169–180. <https://doi.org/10.2147/IJN.S1608>
 198. McDonald I, Sloan GC, Zijlstra AA, Matsunaga N, Matsuura M, Kraemer KE, Bernard-Salas J, Markwick AJ (2010) Rusty old stars: a source of the missing interstellar iron? *Astrophys J* 717:L92–L97. <https://doi.org/10.1088/2041-8205/717/2/L92>
 199. Mesárošová M, Kozics K, Bábelová A, Regendová E, Pastorek M, Vnuková D, Buliaková B, Rázga F, Gábelová A (2014) The role of reactive oxygen species in the genotoxicity of surface-modified magnetite nanoparticles. *Toxicol Lett* 226:303–313. <https://doi.org/10.1016/j.toxlet.2014.02.025>
 200. Migliore L, Uboldi C, Di Bucchianico S, Coppedè F (2015) Nanomaterials and neurodegeneration. *Environ Mol Mutagen* 56:149–170. <https://doi.org/10.1002/em.21931>
 201. Mitragotri S, Anderson DG, Chen X, Chow EK, Ho D, Kabanov AV, Karp JM, Kataoka K, Mirkin CA, Petrosko SH, Shi J, Stevens MM, Sun S, Teoh S, Venkatraman SS, Xia Y, Wang S, Gu Z, Xu C (2015) Accelerating the translation of nanomaterials in biomedicine. *ACS Nano* 9:6644–6654. <https://doi.org/10.1021/acsnano.5b03569>
 202. Mohammadinejad R, Moosavi MA, Tavakol S, Vardar DÖ, Hosseini A, Rahmati M, Dini L, Hussain S, Mandegary A, Klionsky DJ (2019) Necrotic, apoptotic and autophagic cell fates triggered by nanoparticles. *Autophagy* 15:4–33. <https://doi.org/10.1080/15548627.2018.1509171>
 203. Mosayebi J, Kiyasatfar M, Laurent S (2017) Synthesis, functionalization, and design of magnetic nanoparticles for theranostic applications. *Adv Healthc Mater* 6:1700306. <https://doi.org/10.1002/adhm.201700306>
 204. Mufti N, Atma T, Fuad A, Sutadji E (2014) Synthesis and characterization of black, red and yellow nanoparticles pigments from the iron sand. *AIP Conf Proc* 1617:165–169. <https://doi.org/10.1063/1.4897129>
 205. Mukherjee S, Madamsetty VS, Bhattacharya D, Roy Chowdhury S, Paul MK, Mukherjee A (2020) Recent advancements of nanomedicine in neurodegenerative disorders theranostics. *Adv Funct Mater* 30:2003054. <https://doi.org/10.1002/adfm.202003054>
 206. Mulens-Arias V, Rojas JM, Barber DF (2020) The intrinsic biological identities of iron oxide nanopar-

- ticles and their coatings: unexplored territory for combinatorial therapies. *Nanomaterials* 10:837. <https://doi.org/10.3390/nano10050837>
207. Murray AR, Kisin E, Inman A, Young S-H, Muhammed M, Burks T, Uheida A, Tkach A, Waltz M, Castranova V, Fadeel B, Kagan VE, Riviere JE, Monteiro-Riviere N, Shvedova AA (2013) Oxidative stress and dermal toxicity of iron oxide nanoparticles in vitro. *Cell Biochem Biophys* 67:461–476. <https://doi.org/10.1007/s12013-012-9367-9>
208. Murugan K, Choonara YE, Kumar P, Bijukumar D, du Toit LC, Pillay V (2015) Parameters and characteristics governing cellular internalization and trans-barrier trafficking of nanostructures. *Int J Nanomedicine* 10:2191–2206. <https://doi.org/10.2147/IJN.S75615>
209. Naqvi S, Samim M, Abdin MZ, Ahmed FJ, Maitra AN, Prashant CK, Dinda AK (2010) Concentration-dependent toxicity of iron oxide nanoparticles mediated by increased oxidative stress. *Int J Nanomedicine* 5:983–989. <https://doi.org/10.2147/IJN.S13244>
210. Natarajan S, Harini K, Gajula GP, Sarmiento B, Neves-Petersen MT, Thiagarajan V (2019) Multifunctional magnetic iron oxide nanoparticles: diverse synthetic approaches, surface modifications, cytotoxicity towards biomedical and industrial applications. *BMC Mater* 1:1–22. <https://doi.org/10.1186/s42833-019-0002-6>
211. Nel AE, Mädler L, Velegol D, Xia T, Hoek EMV, Somasundaran P, Klaessig F, Castranova V, Thompson M (2009) Understanding biophysicochemical interactions at the nano–bio interface. *Nat Mater* 8:543–557. <https://doi.org/10.1038/nmat2442>
212. Ni F, Jiang L, Yang R, Chen Z, Qi X, Wang J (2012) Effects of PEG length and iron oxide nanoparticles size on reduced protein adsorption and non-specific uptake by macrophage cells. *J Nanosci Nanotechnol* 12:2094–2100. <https://doi.org/10.1166/jnn.2012.5753>
213. Oberdörster G (2010) Safety assessment for nanotechnology and nanomedicine: concepts of nanotoxicology. *J Intern Med* 267:89–105. <https://doi.org/10.1111/j.1365-2796.2009.02187.x>
214. Oliveira H, Pérez-Andrés E, Thevenot J, Sandre O, Berra E, Lecommandoux S (2013) Magnetic field triggered drug release from polymersomes for cancer therapeutics. *J Control Release* 169:165–170. <https://doi.org/10.1016/j.jconrel.2013.01.013>
215. Oliveira F, Rocha S, Fernandes R (2014) Iron metabolism: from health to disease. *J Clin Lab Anal* 28:210–218. <https://doi.org/10.1002/jcla.21668>
216. Palanisamy S, Wang YM (2019) Superparamagnetic iron oxide nanoparticulate system: synthesis, targeting, drug delivery and therapy in cancer. *Dalt Trans* 48:9490–9515. <https://doi.org/10.1039/c9dt00459a>
217. Paolini A, Guarch CP, Ramos-López D, de Lapuente J, Lascialfari A, Guari Y, Larionova J, Long J, Nano R (2016) Rhamnose-coated superparamagnetic iron-oxide nanoparticles: an evaluation of their in vitro cytotoxicity, genotoxicity and carcinogenicity. *J Appl Toxicol* 36:510–520. <https://doi.org/10.1002/jat.3273>
218. Paris JL, Baeza A, Vallet-Regí M (2019) Overcoming the stability, toxicity, and biodegradation challenges of tumor stimuli-responsive inorganic nanoparticles for delivery of cancer therapeutics. *Expert Opin Drug Deliv* 16:1095–1112. <https://doi.org/10.1080/17425247.2019.1662786>
219. Park EJ, Umh HN, Kim SW, Cho MH, Kim JH, Kim Y (2014) ERK pathway is activated in bare-FeNPs-induced autophagy. *Arch Toxicol* 88:323–336. <https://doi.org/10.1007/s00204-013-1134-1>
220. Patel NC (2020) Methods to optimize CNS exposure of drug candidates. *Bioorg Med Chem Lett* 2020:127503. <https://doi.org/10.1016/j.bmcl.2020.127503>
221. Patil RM, Shete PB, Thorat ND, Otari SV, Barick KC, Prasad A, Ningthoujam RS, Tiwale BM, Pawar SH (2014) Non-aqueous to aqueous phase transfer of oleic acid coated iron oxide nanoparticles for hyperthermia application. *RSC Adv* 4:4515–4522. <https://doi.org/10.1039/c3ra44644a>
222. Patil RM, Thorat ND, Shete PB, Otari SV, Tiwale BM, Pawar SH (2016) In vitro hyperthermia with improved colloidal stability and enhanced SAR of magnetic core/shell nanostructures. *Mater Sci Eng C* 59:702–709. <https://doi.org/10.1016/j.msec.2015.10.064>
223. Patil RM, Thorat ND, Shete PB, Bedge PA, Gavde S, Joshi MG, Tofail SAM, Bohara RA (2018) Comprehensive cytotoxicity studies of superparamagnetic iron oxide nanoparticles. *Biochem Biophys Rep* 13:63–72. <https://doi.org/10.1016/j.bbrep.2017.12.002>
224. Paunovic J, Vucevic D, Radosavljevic T, Mandić-Rajčević S, Pantic I (2020) Iron-based nanoparticles and their potential toxicity: focus on oxidative stress and apoptosis. *Chem Biol Interact* 316:108935. <https://doi.org/10.1016/j.cbi.2019.108935>
225. Pedram MSZ, Shamloo A, GhafarZadeh E, Alasty A (2014) Modeling and simulation of crossing magnetic nanoparticles through blood brain barrier (BBB). In: 2014 36th annual international conference of the IEEE Engineering in Medicine and Biology Society. IEEE, pp 5280–5283. <https://doi.org/10.1109/EMBC.2014.6944817>
226. Peer WA, Baxter IR, Richards EL, Freeman JL, Murphy AS (2006) Molecular biology of metal homeostasis and detoxification. Springer, Berlin/Heidelberg. <https://doi.org/10.1007/b98249>
227. Peetla C, Labhasetwar V (2008) Biophysical characterization of nanoparticle-endothelial model cell membrane interactions. *Mol Pharm* 5:418–429. <https://doi.org/10.1021/mp700140a>
228. Pekny M, Pekna M (2014) Astrocyte reactivity and reactive astrogliosis: costs and benefits. *Physiol Rev* 94:1077–1098. <https://doi.org/10.1152/physrev.00041.2013>

229. Peng M, Li H, Luo Z, Kong J, Wan Y, Zheng L, Zhang Q, Niu H, Vermorken A, Van de Ven W, Chen C, Zhang X, Li F, Guo L, Cui Y (2015) Dextran-coated superparamagnetic nanoparticles as potential cancer drug carriers in vivo. *Nanoscale* 7:1115–11162. <https://doi.org/10.1039/C5NR01382H>
230. Pereira MC, Oliveira LCA, Murad E (2012) Iron oxide catalysts: Fenton and Fentonlike reactions – a review. *Clay Miner* 47:285–302. <https://doi.org/10.1180/claymin.2012.047.3.01>
231. Periasamy VS, Athinarayanan J, Alhazmi M, Alattia KA, Alshatwi AA (2016) Fe₃O₄ nanoparticle redox system modulation via cell-cycle progression and gene expression in human mesenchymal stem cells. *Environ Toxicol* 31:901–912. <https://doi.org/10.1002/tox.22098>
232. Petters C, Dringen R (2014) Comparison of primary and secondary rat astrocyte cultures regarding glucose and glutathione metabolism and the accumulation of iron oxide nanoparticles. *Neurochem Res* 39:46–58. <https://doi.org/10.1007/s11064-013-1189-7>
233. Petters C, Dringen R (2015) Uptake, metabolism and toxicity of iron oxide nanoparticles in cultured microglia, astrocytes and neurons. *Springerplus* 4:L32. <https://doi.org/10.1186/2193-1801-4-S1-L32>
234. Petters C, Bulcke F, Thiel K, Bickmeyer U, Dringen R (2014) Uptake of fluorescent iron oxide nanoparticles by oligodendroglial OLN-93 cells. *Neurochem Res* 39:372–383. <https://doi.org/10.1007/s11064-013-1234-6>
235. Petters C, Thiel K, Dringen R (2016) Lysosomal iron liberation is responsible for the vulnerability of brain microglial cells to iron oxide nanoparticles: comparison with neurons and astrocytes. *Nanotoxicology* 10:332–342. <https://doi.org/10.3109/17435390.2015.1071445>
236. Pettitt ME, Lead JR (2013) Minimum physicochemical characterisation requirements for nanomaterial regulation. *Environ Int* 52:41–50. <https://doi.org/10.1016/j.envint.2012.11.009>
237. Pfaller T, Colognato R, Nelissen I, Favilli F, Casals E, Ooms D, Leppens H, Ponti J, Stritzinger R, Puentes V, Boraschi D, Duschl A, Oostingh GJ (2010) The suitability of different cellular in vitro immunotoxicity and genotoxicity methods for the analysis of nanoparticle-induced events. *Nanotoxicology* 4:52–72. <https://doi.org/10.3109/17435390903374001>
238. Philpott CC, Ryu MS, Frey A, Patel S (2017) Cytosolic iron chaperones: proteins delivering iron cofactors in the cytosol of mammalian cells. *J Biol Chem* 292:12764–12771. <https://doi.org/10.1074/jbc.r117.791962>
239. Pitchaimani A, Nguyen TDT, Koirala M, Zhang Y, Aryal S (2017) Impact of cell adhesion and migration on nanoparticle uptake and cellular toxicity. *Toxicol Vitro* 43:29–39. <https://doi.org/10.1016/j.tiv.2017.05.020>
240. Podila R, Brown JM (2013) Toxicity of engineered nanomaterials: a physicochemical perspective. *J Biochem Mol Toxicol* 27:50–55. <https://doi.org/10.1002/jbt.21442>
241. Pongrac IM, Dobrivojević M, Ahmed LB, Babič M, Šlouf M, Horák D, Gajović S (2016) Improved biocompatibility and efficient labeling of neural stem cells with poly(L-lysine)-coated maghemite nanoparticles. *Beilstein J Nanotechnol* 7:926–936. <https://doi.org/10.3762/bjnano.7.84>
242. Powers KW, Brown SC, Krishna VB, Wasdo SC, Moudgil BM, Roberts SM (2006) Research strategies for safety evaluation of nanomaterials. Part VI. Characterization of nanoscale particles for toxicological evaluation. *Toxicol Sci* 90:296–303. <https://doi.org/10.1093/toxsci/kfj099>
243. Powers KW, Palazuelos M, Moudgil BM, Roberts SM (2007) Characterization of the size, shape, and state of dispersion of nanoparticles for toxicological studies. *Nanotoxicology* 1:42–51. <https://doi.org/10.1080/17435390701314902>
244. Qiao C, Yang J, Chen L, Weng J, Zhang X (2017) Intracellular accumulation and immunological responses of lipid modified magnetic iron nanoparticles in mouse antigen processing cells. *Biomater Sci* 5:1603–1611. <https://doi.org/10.1039/c7bm00244k>
245. Rajiv S, Jerobin J, Saranya V, Nainawat M, Sharma A, Makwana P, Gayathri C, Bharath L, Singh M, Kumar M, Mukherjee A, Chandrasekaran N (2015) Comparative cytotoxicity and genotoxicity of cobalt (II, III) oxide, iron (III) oxide, silicon dioxide, and aluminum oxide nanoparticles on human lymphocytes in vitro. *Hum Exp Toxicol* 35:170–183. <https://doi.org/10.1177/0960327115579208>
246. Ramesh V, Ravichandran P, Copeland CL, Gopikrishnan R, Biradar S, Goornavar V, Ramesh GT, Hall JC (2012) Magnetite induces oxidative stress and apoptosis in lung epithelial cells. *Mol Cell Biochem* 363:225–234. <https://doi.org/10.1007/s11010-011-1174-x>
247. Ramesh R, Kuroda S, Tam J, Sokolov K, Roth JA, Sokolov K, Ramesh R (2014) EGFR-targeted plasmonic magnetic nanoparticles suppress lung tumor growth by abrogating G2/M cell-cycle arrest and inducing DNA damage. *Int J Nanomedicine* 9:3825–3839. <https://doi.org/10.2147/IJN.S65990>
248. Ratner BD (1996) The engineering of biomaterials exhibiting recognition and specificity. *J Mol Recognit* 9:617–625. [https://doi.org/10.1002/\(SICI\)1099-1352\(199603/12\)9:5/6<617::AID-JMR310>3.0.CO;2-D](https://doi.org/10.1002/(SICI)1099-1352(199603/12)9:5/6<617::AID-JMR310>3.0.CO;2-D)
249. Rätty JK, Liimatainen T, Wirth T, Airene KJ, Ihalainen TO, Huhtala T, Hamerlynck E, Vihinen-Ranta M, Näränen A, Ylä-Herttuala S, Hakumäki JM (2006) Magnetic resonance imaging of viral particle biodistribution in vivo. *Gene Ther* 13:1440–1446. <https://doi.org/10.1038/sj.gt.3302828>
250. Reimer P, Balzer T (2003) Ferucarbotran (Resovist): a new clinically approved RES-specific contrast agent for contrast-enhanced MRI of the liver: properties, clinical development, and applications. *Eur*

- Radiol 13:1266–1276. <https://doi.org/10.1007/s00330-002-1721-7>
251. Remya NS, Syama S, Sabareeswaran A, Mohanan PV (2016) Toxicity, toxicokinetics and biodistribution of dextran stabilized iron oxide nanoparticles for biomedical applications. *Int J Pharm* 511:586–598. <https://doi.org/10.1016/j.ijpharm.2016.06.119>
252. Revia RA, Zhang M (2016) Magnetite nanoparticles for cancer diagnosis, treatment, and treatment monitoring: recent advances. *Mater Today* 19:157–168. <https://doi.org/10.1016/j.mattod.2015.08.022>
253. Rivet CJ, Yuan Y, Borca-Tasciuc DA, Gilbert RJ (2012) Altering iron oxide nanoparticle surface properties induce cortical neuron cytotoxicity. *Chem Res Toxicol* 25:153–161. <https://doi.org/10.1021/tx200369s>
254. Roca AG, Gutiérrez L, Gavilán H, Fortes Brolo ME, Veintemillas-Verdaguer S, MDP M (2019) Design strategies for shape-controlled magnetic iron oxide nanoparticles. *Adv Drug Deliv Rev* 138:68–104. <https://doi.org/10.1016/j.addr.2018.12.008>
255. Roiter Y, Ornatka M, Rammohan AR, Balakrishnan J, Heine DR, Minko S (2008) Interaction of nanoparticles with lipid membrane. *Nano Lett* 8:941–944. <https://doi.org/10.1021/nl080080l>
256. Rosenberg JT, Sachi-Kocher A, Davidson MW, Grant SC (2012) Intracellular SPIO labeling of microglia: high field considerations and limitations for MR microscopy. *Contrast Media Mol Imaging* 7:121–129. <https://doi.org/10.1002/cmmi.470>
257. Sadeghiani N, Barbosa LS, Silva LP, Azevedo RB, Morais PC, Lacava ZGM (2005) Genotoxicity and inflammatory investigation in mice treated with magnetite nanoparticles surface coated with polyaspartic acid. *J Magn Magn Mater* 289:466–468. <https://doi.org/10.1016/j.jmmm.2004.11.131>
258. Sahoo Y, Pizem H, Fried T, Golodnitsky D, Burstein L, Sukenik CN, Markovich G (2001) Alkyl phosphonate/phosphate coating on magnetite nanoparticles: a comparison with fatty acids. *Langmuir ACS J Surf Colloids* 17:7907–7911. <https://doi.org/10.1021/la010703>
259. Sakulkhu U, Mahmoudi M, Maurizi L, Salaklang J, Hofmann H (2014) Protein corona composition of superparamagnetic iron oxide nanoparticles with various physico-chemical properties and coatings. *Sci Rep* 4:1–9. <https://doi.org/10.1038/srep05020>
260. Sanaeifar N, Rabiee M, Abdolrahim M, Tahriri M, Vashae D, Tayebi L (2017) A novel electrochemical biosensor based on Fe₃O₄ nanoparticles-polyvinyl alcohol composite for sensitive detection of glucose. *Anal Biochem* 519:19–26. <https://doi.org/10.1016/j.ab.2016.12.006>
261. Sanganeria P, Sachar S, Chandra S, Bahadur D, Ray P, Khanna A (2015) Cellular internalization and detailed toxicity analysis of protein-immobilized iron oxide nanoparticles. *J Biomed Mater Res B Appl Biomater* 103:125–134. <https://doi.org/10.1002/jbm.b.33178>
262. Santhosh PB, Ulrich NP (2013) Multifunctional superparamagnetic iron oxide nanoparticles: promising tools in cancer theranostics. *Cancer Lett* 336:8–17. <https://doi.org/10.1016/j.canlet.2013.04.032>
263. Saraiva C, Praça C, Ferreira R, Santos T, Ferreira L, Bernardino L (2016) Nanoparticle-mediated brain drug delivery: overcoming blood–brain barrier to treat neurodegenerative diseases. *J Control Release* 235:34–47. <https://doi.org/10.1016/j.jconrel.2016.05.044>
264. Schulte P, Leso V, Niang M, Iavicoli I (2018) Biological monitoring of workers exposed to engineered nanomaterials. *Toxicol Lett* 298:112–124. <https://doi.org/10.1016/j.toxlet.2018.06.003>
265. Schütz CA, Staedler D, Crosbie-Staunton K, Movia D, Bernasconi CC, Kenzaoui BH, Prina-Mello A, Juillerat-Jeanneret L (2014) Differential stress reaction of human colon cells to oleic-acid-stabilized and unstabilized ultrasmall iron oxide nanoparticles. *Int J Nanomedicine* 9:3481–3498. <https://doi.org/10.2147/IJN.S65082>
266. Seo DY, Jin M, Ryu J-CC, Kim Y-JJ (2017) Investigation of the genetic toxicity by dextran-coated superparamagnetic iron oxide nanoparticles (SPION) in HepG2 cells using the comet assay and cytokinesis-block micronucleus assay. *Toxicol Environ Health Sci* 9:23–29. <https://doi.org/10.1007/s13530-017-0299-z>
267. Servin A, Elmer W, Mukherjee A, De la Torre-Roche R, Hamdi H, White JC, Bindraban P, Dimkpa C (2015) A review of the use of engineered nanomaterials to suppress plant disease and enhance crop yield. *J Nanopart Res* 17:1–21. <https://doi.org/10.1007/s11051-015-2907-7>
268. Shapiro HM (2003) Parameters and probes. In: *Practical flow cytometry*. Wiley, New York, pp 273–410. <https://doi.org/10.1002/0471722731>
269. Sharma G, Kodali V, Gaffrey M, Wang W, Minard KR, Karin NJ, Teeguarden JG, Thrall BD (2014a) Iron oxide nanoparticle agglomeration influences dose rates and modulates oxidative stress-mediated dose-response profiles in vitro. *Nanotoxicology* 8:663–675. <https://doi.org/10.3109/17435390.2013.822115>
270. Sharma HS, Menon PK, Lafuente JV, Aguilar ZP, Wang YA, Muresanu DF, Mössler H, Patnaik R, Sharma A (2014b) The role of functionalized magnetic iron oxide nanoparticles in the central nervous system injury and repair: new potentials for neuroprotection with cerebrolysin therapy. *J Nanosci Nanotechnol* 14:577–595. <https://doi.org/10.1166/jnn.2014.9213>
271. Shen Z, Liu T, Li Y, Lau J, Yang Z, Fan W, Zhou Z, Shi C, Ke C, Bregadze VI, Mandal SK, Liu Y, Li Z, Xue T, Zhu G, Munasinghe J, Niu G, Wu A, Chen X (2018) Fenton-reaction-acceleratable magnetic nanoparticles for ferroptosis therapy of orthotopic brain tumors. *ACS Nano* 12:11355–11365. <https://doi.org/10.1021/acsnano.8b06201>

272. Shete PB, Patil RM, Ningthoujam RS, Ghosh SJ, Pawar SH (2013) Magnetic core-shell structures for magnetic fluid hyperthermia therapy application. *New J Chem* 37:3784–3792. <https://doi.org/10.1039/c3nj00862b>
273. Shete PB, Patil RM, Thorat ND, Prasad A, Ningthoujam RS, Ghosh SJ, Pawar SH (2014) Magnetic chitosan nanocomposite for hyperthermia therapy application: preparation, characterization and in vitro experiments. *Appl Surf Sci* 288:149–157. <https://doi.org/10.1016/j.apsusc.2013.09.169>
274. Shete PB, Patil RM, Tiwale BM, Pawar SH (2015) Water dispersible oleic acid-coated Fe₃O₄ nanoparticles for biomedical applications. *J Magn Magn Mater* 377:406–410. <https://doi.org/10.1016/j.jmmm.2014.10.137>
275. Shi M, Cheng L, Zhang Z, Liu Z, Mao X (2015) Ferroferric oxide nanoparticles induce pro-survival autophagy in human blood cells by modulating the Beclin 1/Bcl-2/VPS34 complex. *Int J Nanomedicine* 10:207–216. <https://doi.org/10.2147/IJN.S72598>
276. Shim KH, Hulme J, Maeng EH, Kim M-K, SSA A (2014) Analysis of zinc oxide nanoparticles binding proteins in rat blood and brain homogenate. *Int J Nanomedicine* 9(Suppl 2):217–224. <https://doi.org/10.2147/IJN.S58204>
277. Shin S, Song I, Um S (2015) Role of physicochemical properties in nanoparticle toxicity. *Nano* 5:1351–1365. <https://doi.org/10.3390/nano5031351>
278. Shrestha B, Tang L, Romero G (2019) Nanoparticles-mediated combination therapies for cancer treatment. *Adv Ther* 2:1900076. <https://doi.org/10.1002/adtp.201900076>
279. Shukla S, Jadaun A, Arora V, Sinha RK, Biyani N, Jain VK (2015) In vitro toxicity assessment of chitosan oligosaccharide coated iron oxide nanoparticles. *Toxicol Rep* 2:27–39. <https://doi.org/10.1016/j.toxrep.2014.11.002>
280. Silva LHA, Silva JR, Ferreira GA, Silva RC, Lima ECD, Azevedo RB, Oliveira DM (2016) Labeling mesenchymal cells with DMSA-coated gold and iron oxide nanoparticles: assessment of biocompatibility and potential applications. *J Nanobiotechnol* 14:59. <https://doi.org/10.1186/s12951-016-0213-x>
281. Singamaneni S, Bliznyuk VN, Binek C, Tsymbal EY (2011) Magnetic nanoparticles: recent advances in synthesis, self-assembly and applications. *J Mater Chem* 21:16819–16845. <https://doi.org/10.1039/c1jm11845e>
282. Singh N, Jenkins GJS, Asadi R, Doak SH (2010) Potential toxicity of superparamagnetic iron oxide nanoparticles (SPION). *Nano Rev* 1:5358. <https://doi.org/10.3402/nano.v1i0.5358>
283. Singh N, Jenkins GJS, Nelson BC, Marquis BJ, Maffei TGG, Brown AP, Williams PM, Wright CJ, Doak SH (2012) The role of iron redox state in the genotoxicity of ultrafine superparamagnetic iron oxide nanoparticles. *Biomaterials* 33:163–170. <https://doi.org/10.1016/j.biomaterials.2011.09.087>
284. Singh SP, Rahman MF, Murty USN, Mahboob M, Grover P (2013) Comparative study of genotoxicity and tissue distribution of nano and micron sized iron oxide in rats after acute oral treatment. *Toxicol Appl Pharmacol* 266:56–66. <https://doi.org/10.1016/j.taap.2012.10.016>
285. Singh AV, Laux P, Luch A, Sudrik C, Wiehr S, Wild AM, Santomauro G, Bill J, Sitti M (2019) Review of emerging concepts in nanotoxicology: opportunities and challenges for safer nanomaterial design. *Toxicol Mech Methods* 29:378–387. <https://doi.org/10.1080/15376516.2019.1566425>
286. Smith JE, Wang L, Tan W (2006) Bioconjugated silica-coated nanoparticles for bioseparation and bioanalysis. *TrAC Trends Anal Chem* 25:848–855. <https://doi.org/10.1016/j.trac.2006.03.008>
287. Soares PIP, Laia CAT, Carvalho A, Pereira LCJ, Coutinho JT, Ferreira IMM, Novo CMM, Borges JP (2016) Iron oxide nanoparticles stabilized with a bilayer of oleic acid for magnetic hyperthermia and MRI applications. *Appl Surf Sci* 383:240–247. <https://doi.org/10.1016/j.apsusc.2016.04.181>
288. Soenen SJ, De Cuyper M, De Smedt SC, Braeckmans K (2012) Investigating the toxic effects of iron oxide nanoparticles. *Methods Enzymol* 509:195–224. <https://doi.org/10.1016/B978-0-12-391858-1.00011-3>
289. Soetaert F, Korangath P, Serantes D, Fiering S, Ivkov R (2020) Cancer therapy with iron oxide nanoparticles: agents of thermal and immune therapies. *Adv Drug Deliv Rev*. <https://doi.org/10.1016/j.addr.2020.06.025>
290. Song C, Sun W, Xiao Y, Shi X (2019) Ultrasmall iron oxide nanoparticles: synthesis, surface modification, assembly, and biomedical applications. *Drug Discov Today* 24:835–844. <https://doi.org/10.1016/j.drudis.2019.01.001>
291. Spandana AKM, Bhaskaran M, Karri VVSNR, Natarajan J (2020) A comprehensive review of nano drug delivery system in the treatment of CNS disorders. *J Drug Deliv Sci Technol* 57:101628. <https://doi.org/10.1016/j.jddst.2020.101628>
292. Sun C, Lee JSH, Zhang M (2008) Magnetic nanoparticles in MR imaging and drug delivery. *Adv Drug Deliv Rev* 60:1252–1265. <https://doi.org/10.1016/j.addr.2008.03.018>
293. Sun Z, Yathindranath V, Worden M, Thliveris JA, Chu S, Parkinson FE, Hegmann T, Miller D (2013) Characterization of cellular uptake and toxicity of aminosilane-coated iron oxide nanoparticles with different charges in central nervous system-relevant cell culture models. *Int J Nanomedicine* 8:961–970. <https://doi.org/10.2147/IJN.S39048>
294. Sutariya VB, Pathak V, Groshev A, Mahavir B, Naik S, Patel D, Pathak Y (2016) Introduction—biointeractions of nanomaterials. In: *Biointeractions of nanomaterials*. CRC Press, Boca Raton, pp 1–48. <https://doi.org/10.1201/b17191>
295. Suzuki H, Toyooka T, Ibuki Y (2007) Simple and easy method to evaluate uptake potential of nanopar-

- ticles in mammalian cells using a flow cytometric light scatter analysis. *Environ Sci Technol* 41:3018–3024. <https://doi.org/10.1021/es0625632>
296. Szalay B, Tátrai E, Nyíró G, Vezér T, Dura G (2012) Potential toxic effects of iron oxide nanoparticles in vivo and in vitro experiments. *J Appl Toxicol* 32:446–453. <https://doi.org/10.1002/jat.1779>
297. Tan BL, Norhaizan ME, Chan LC (2018) An intrinsic mitochondrial pathway is required for phytic acid-chitosan-iron oxide nanocomposite (Phy-CS-MNP) to induce G0/G1 cell cycle arrest and apoptosis in the human colorectal cancer (HT-29) cell line. *Pharmaceutics* 10:1–17. <https://doi.org/10.3390/pharmaceutics10040198>
298. Teleanu DM, Chircov C, Grumezescu AM, Teleanu RI (2019) Neurotoxicity of nanomaterials: an up-to-date overview. *Nanomaterials* 9:96. <https://doi.org/10.3390/nano9010096>
299. Teske S, Detweiler C (2015) The biomechanisms of metal and metal-oxide nanoparticles' interactions with cells. *Int J Environ Res Public Health* 12:1112–1134. <https://doi.org/10.3390/ijerph120201112>
300. Thakor AS, Jokerst JV, Ghanouni P, Campbell JL, Mitra E, Gambhir SS (2016) Clinically approved nanoparticle imaging agents. *J Nucl Med* 57:1833–1837. <https://doi.org/10.2967/jnumed.116.181362>
301. Thomsen LB, Linemann T, Pondman KM, Lichota J, Kim KS, Pieters RJ, Visser GM, Moos T, Visser GM, Moos T (2013) Uptake and transport of superparamagnetic iron oxide nanoparticles through human brain capillary endothelial cells. *ACS Chem Neurosci* 4:1352–1360. <https://doi.org/10.1021/cn400093z>
302. Thomsen LB, Thomsen MS, Moos T (2015) Targeted drug delivery to the brain using magnetic nanoparticles. *Ther Deliv* 6:1145–1155. <https://doi.org/10.4155/tde.15.56>
303. Thorat ND, Bohara RA, Noor MR, Dhamecha D, Soulimane T, Tofail SAM (2017) Effective cancer theranostics with polymer encapsulated superparamagnetic nanoparticles: combined effects of magnetic hyperthermia and controlled drug release. *ACS Biomater Sci Eng* 3:1332–1340. <https://doi.org/10.1021/acsbiomaterials.6b00420>
304. Tong L, Zhao M, Zhu S, Chen J (2011) Synthesis and application of superparamagnetic iron oxide nanoparticles in targeted therapy and imaging of cancer. *Front Med* 5:379–387. <https://doi.org/10.1007/s11684-011-0162-6>
305. Tong S, Zhu H, Bao G (2019) Magnetic iron oxide nanoparticles for disease detection and therapy. *Mater Today* 31:86–99. <https://doi.org/10.1016/j.mattod.2019.06.003>
306. Tran TT-DD, Van Vo T, Tran PH-LL (2015) Design of iron oxide nanoparticles decorated oleic acid and bovine serum albumin for drug delivery. *Chem Eng Res Des* 94:112–118. <https://doi.org/10.1016/j.cherd.2014.12.016>
307. Unterweger H, Subatzus D, Tietze R, Janko C, Poettler M, Stiegelschmitt A, Schuster M, Maake C, Boccaccini A, Alexiou C (2015) Hypericin-bearing magnetic iron oxide nanoparticles for selective drug delivery in photodynamic therapy. *Int J Nanomedicine* 6985. <https://doi.org/10.2147/IJN.S92336>
308. Uribe Madrid SI, Pal U, Kang YS, Kim J, Kwon H, Kim J (2015) Fabrication of Fe₃O₄@mSiO₂ core-shell composite nanoparticles for drug delivery applications. *Nanoscale Res Lett* 10:217. <https://doi.org/10.1186/s11671-015-0920-5>
309. Vakili-Ghartavol R, Momtazi-Borojeni AA, Vakili-Ghartavol Z, Aiyelabegan HT, Jaafari MR, Rezayat SM, Arbabi Bidgoli S (2020) Toxicity assessment of superparamagnetic iron oxide nanoparticles in different tissues. *Artif Cells Nanomed Biotechnol* 48:443–451. <https://doi.org/10.1080/21691401.2019.1709855>
310. Valdiglesias V, Kilic G, Costa C, Fernandez-Bertolez N, Pasaro E, Teixeira JP, Laffon B (2015) Effects of iron oxide nanoparticles: cytotoxicity, genotoxicity, developmental toxicity, and neurotoxicity. *Environ Mol Mutagen* 56:125–148. <https://doi.org/10.1002/em.21909>
311. Valdiglesias V, Fernández-Bertólez N, Kiliç G, Costa C, Costa S, Fraga S, Bessa MJ, Páraso E, Teixeira JP, Laffon B (2016) Are iron oxide nanoparticles safe? Current knowledge and future perspectives. *J Trace Elem Med Biol* 38:53–63. <https://doi.org/10.1016/j.jtemb.2016.03.017>
312. Valko M, Leibfritz D, Moncol J, Cronin MTD, Mazur M, Telser J (2007) Free radicals and antioxidants in normal physiological functions and human disease. *Int J Biochem Cell Biol* 39:44–84. <https://doi.org/10.1016/j.biocel.2006.07.001>
313. Vangijzegem T, Stanicki D, Laurent S (2019) Magnetic iron oxide nanoparticles for drug delivery: applications and characteristics. *Expert Opin Drug Deliv* 16:69–78. <https://doi.org/10.1080/17425247.2019.1554647>
314. Vasir JK, Labhasetwar V (2008) Quantification of the force of nanoparticle-cell membrane interactions and its influence on intracellular trafficking of nanoparticles. *Biomaterials* 29:4244–4252. <https://doi.org/10.1016/j.biomaterials.2008.07.020>
315. Veisheh O, Gunn JW, Zhang M (2010) Design and fabrication of magnetic nanoparticles for targeted drug delivery and imaging. *Adv Drug Deliv Rev* 62:284–304. <https://doi.org/10.1016/j.addr.2009.11.002>
316. Verma A, Stellacci F (2010) Effect of surface properties on nanoparticle-cell interactions. *Small* 6:12–21. <https://doi.org/10.1002/sml.200901158>
317. Voss L, Hsiao IL, Ebisch M, Vidmar J, Dreijack N, Böhmert L, Stock V, Braeuning A, Loeschner K, Laux P, Thünemann AF, Lampen A, Sieg H (2020) The presence of iron oxide nanoparticles in the food pigment E172. *Food Chem* 327:127000. <https://doi.org/10.1016/j.foodchem.2020.127000>
318. Wahajuddin, Arora S (2012) Superparamagnetic iron oxide nanoparticles: magnetic nanoplatforms



- as drug carriers. *Int J Nanomedicine* 7:3445–3471. <https://doi.org/10.2147/IJN.S30320>
319. Wan R, Mo Y, Feng L, Chien S, Tollerud DJ, Zhang Q (2012) DNA damage caused by metal nanoparticles: involvement of oxidative stress and activation of ATM. *Chem Res Toxicol* 25:1402–1411. <https://doi.org/10.1021/tx200513t>
 320. Wang J, Pantopoulos K (2011) Regulation of cellular iron metabolism. *Biochem J* 434:365–381. <https://doi.org/10.1042/bj20101825>
 321. Wang YXJ, Hussain SM, Krestin GP (2001) Superparamagnetic iron oxide contrast agents: physicochemical characteristics and applications in MR imaging. *Eur Radiol* 11:2319–2331. <https://doi.org/10.1007/s003300100908>
 322. Wang B, Feng WY, Wang M, Shi JW, Zhang F, Ouyang H, Zhao YL, Chai ZF, Huang YY, Xie YN, Wang HF, Wang J (2007) Transport of intranasally instilled fine Fe₂O₃ particles into the brain: micro-distribution, chemical states, and histopathological observation. *Biol Trace Elem Res* 118:233–243. <https://doi.org/10.1007/s12011-007-0028-6>
 323. Wang J, Sun W, Ali SF (2009) Nanoparticles: is neurotoxicity a concern? In: Sahu SC, Casciano DA (eds) *Nanotoxicity: from in vivo and in vitro models to health risks*. Wiley, Chichester, pp 171–182. <https://doi.org/10.1002/9780470747803.ch9>
 324. Wang J, Chen Y, Chen B, Ding J, Xia G, Gao C, Cheng J, Jin N, Zhou Y, Li X, Tang M, Wang XM (2010) Pharmacokinetic parameters and tissue distribution of magnetic Fe₃O₄ nanoparticles in mice. *Int J Nanomedicine* 5:861–866. <https://doi.org/10.2147/IJN.S13662>
 325. Wang J, Chen B, Jin N, Xia G, Chen Y, Zhou Y, Cai X, Ding J, Li X, Wang X (2011) The changes of T lymphocytes and cytokines in ICR mice fed with Fe₃O₄ magnetic nanoparticles. *Int J Nanomedicine* 6:605–610. <https://doi.org/10.2147/IJN.S16176>
 326. Wang Y, Ding L, Yao C, Li C, Xing X, Huang Y, Gu T, Wu M (2017) Toxic effects of metal oxide nanoparticles and their underlying mechanisms. *Sci China Mater* 60:93–108. <https://doi.org/10.1007/s40843-016-5157-0>
 327. Watanabe M, Yoneda M, Morohashi A, Hori Y, Okamoto D, Sato A, Kurioka D, Nittami T, Hirokawa Y, Shiraishi T, Kawai K, Kasai H, Totsuka Y (2013) Effects of Fe₃O₄ magnetic nanoparticles on A549 cells. *Int J Mol Sci* 14:15546–15560. <https://doi.org/10.3390/ijms140815546>
 328. Wei Y, Zhao M, Yang F, Mao Y, Xie H, Zhou Q (2016) Iron overload by superparamagnetic iron oxide nanoparticles is a high risk factor in cirrhosis by a systems toxicology assessment. *Sci Rep* 6:29110. <https://doi.org/10.1038/srep29110>
 329. Wei H, Bruns OT, Kaul MG, Hansen EC, Barch M, Wiśniewska A, Chen O, Chen Y, Li N, Okada S, Cordero JM, Heine M, Farrar CT, Montana DM, Adam G, Itrich H, Jasanoff A, Nielsen P, Bawendi MG (2017) Exceedingly small iron oxide nanoparticles as positive MRI contrast agents. *Proc Natl Acad Sci* 114:2325–2330. <https://doi.org/10.1073/pnas.1620145114>
 330. Wei X, Yang F, Chen D, Li J, Shi X, Li B, Zhang C (2020) Analyzing nanoparticle-induced neurotoxicity: a bibliometric analysis. *Toxicol Ind Health* 36:22–29. <https://doi.org/10.1177/0748233719900844>
 331. Weissleder R, Stark D, Engelstad B, Bacon B, Compton C, White D, Jacobs P, Lewis J (1989) Superparamagnetic iron oxide: pharmacokinetics and toxicity. *Am J Roentgenol* 152:167–173. <https://doi.org/10.2214/ajr.152.1.167>
 332. Wijnhoven SWP, Dekkers S, Hagens WI, De Jong WH (2009) Exposure to nanomaterials in consumer products. *RIVM Lett Rep*. 340370001/2009. <https://www.rivm.nl/bibliotheek/rapporten/340370003>
 333. Willmann W, Dringen R (2019) How to study the uptake and toxicity of nanoparticles in cultured brain cells: the dos and don't forgets. *Neurochem Res* 44:1330–1345. <https://doi.org/10.1007/s11064-018-2598-4>
 334. Wu J, Sun J (2011) Investigation on mechanism of growth arrest induced by iron oxide nanoparticles in PC12 cells. *J Nanosci Nanotechnol* 11:11079–11083. <https://doi.org/10.1166/jnn.2011.394>
 335. Wu W, He Q, Jiang C (2008) Magnetic iron oxide nanoparticles: synthesis and surface functionalization strategies. *Nanoscale Res Lett* 3:397–415. <https://doi.org/10.1007/s11671-008-9174-9>
 336. Wu W, Chen B, Cheng J, Wang J, Xu W, Liu L, Xia G, Wei H, Wang X, Yang M, Yang L, Zhang Y, Xu C, Li J (2010) Biocompatibility of Fe₃O₄/DNR magnetic nanoparticles in the treatment of hematologic malignancies. *Int J Nanomedicine* 5:1079–1084. <https://doi.org/10.2147/IJN.S15660>
 337. Wu J, Wang C, Sun J, Xue Y (2011) Neurotoxicity of silica nanoparticles: brain localization and dopaminergic neurons damage pathways. *ACS Nano* 5:4476–4489. <https://doi.org/10.1021/nn103530b>
 338. Wu J, Ding T, Sun J (2013) Neurotoxic potential of iron oxide nanoparticles in the rat brain striatum and hippocampus. *Neurotoxicology* 34:243–253. <https://doi.org/10.1016/j.neuro.2012.09.006>
 339. Wu Y, Lu Z, Li Y, Yang J, Zhang X (2020) Surface modification of iron oxide-based magnetic nanoparticles for cerebral theranostics: application and prospection. *Nanomaterials* 10:1–21. <https://doi.org/10.3390/nano10081441>
 340. Xia JG, Zhang S, Zhang Y, Ma M, Gu N (2009a) Maghemite nanoparticles and their protamine derivatives: cellular internalization and effects on cell-cycle progress. *J Nanosci Nanotechnol* 9:1025–1028. <https://doi.org/10.1166/jnn.2009.C078>
 341. Xia T, Kovochich M, Liong M, Meng H, Kabehie S, George S, Zink JJ, Nel AE (2009b) Polyethyleneimine coating enhances the cellular uptake of mesoporous silica nanoparticles and

- allows safe delivery of siRNA and DNA constructs. *ACS Nano* 3:3273–3286. <https://doi.org/10.1021/nm900918w>
342. Xiao M, Xiao ZJ, Yang B, Lan Z, Fang F (2020) Blood-brain barrier: more contributor to disruption of central nervous system homeostasis than victim in neurological disorders. *Front Neurosci* 14:1–17. <https://doi.org/10.3389/fnins.2020.00764>
343. Xiaoli F, Longquan S (2018) Neurotoxicity of nanomaterials. In: *Emerging nanotechnologies in dentistry*, 2nd edn. Elsevier, Amsterdam, pp 421–444
344. Xie W, Guo Z, Gao F, Gao Q, Wang D, Liaw BS, Cai Q, Sun X, Wang X, Zhao L (2018) Shape-, size- and structure-controlled synthesis and biocompatibility of iron oxide nanoparticles for magnetic theranostics. *Theranostics* 8:3284–3307. <https://doi.org/10.7150/thno.25220>
345. Xie L, Jin W, Chen H, Zhang Q (2019) Superparamagnetic iron oxide nanoparticles for cancer diagnosis and therapy. *J Biomed Nanotechnol* 15:215–416. <https://doi.org/10.1166/jbn.2019.2678>
346. Xu P, Li J, Chen B, Wang X, Cai X, Jiang H, Wang C, Zhang H (2012a) The real-time neurotoxicity analysis of Fe₃O₄ nanoparticles combined with daunorubicin for rat brain *in vivo*. *J Biomed Nanotechnol* 8:417–423. <https://doi.org/10.1166/jbn.2012.1402>
347. Xu P, Zeng GM, Huang DL, Feng CL, Hu S, Zhao MH, Lai C, Wei Z, Huang C, Xie GX, Liu ZF (2012b) Use of iron oxide nanomaterials in wastewater treatment: a review. *Sci Total Environ* 424:1–10. <https://doi.org/10.1016/j.scitotenv.2012.02.023>
348. Yameen B, Choi WIL, Vilos C, Swami A, Shi J, Farokhzad OC (2014) Insight into nanoparticle cellular uptake and intracellular targeting. *J Control Release* 190:485–499. <https://doi.org/10.1016/j.jconrel.2014.06.038>
349. Yang Z, Liu ZW, Allaker RP, Reip P, Oxford J, Ahmad Z, Ren G (2010) A review of nanoparticle functionality and toxicity on the central nervous system. *J R Soc Interface* 7:S411–S422. <https://doi.org/10.1098/rsif.2010.0158.focus>
350. Yang CY, Hsiao JK, Tai MF, Chen ST, Cheng HY, Wang JL, Liu HM (2011) Direct labeling of hMSC with SPIO: the long-term influence on toxicity, chondrogenic differentiation capacity, and intracellular distribution. *Mol Imaging Biol* 13:443–451. <https://doi.org/10.1007/s11307-010-0360-7>
351. Yang X, Ma P, Luo Q, Chen J, Gan Y, Du J, Ding S, Xi Z (2012) Intraperitoneal injection of magnetic Fe₃O₄-nanoparticle induces hepatic and renal tissue injury via oxidative stress in mice. *Int J Nanomedicine* 7:4809. <https://doi.org/10.2147/IJN.S34349>
352. Yang G, Ma W, Zhang B, Xie Q (2016) The labeling of stem cells by superparamagnetic iron oxide nanoparticles modified with PEG/PVP or PEG/PEI. *Mater Sci Eng C* 62:384–390. <https://doi.org/10.1016/j.msec.2016.01.090>
353. Yarjanli Z, Ghaedi K, Esmaili A, Rahgozar S, Zarrabi A (2017) Iron oxide nanoparticles may damage to the neural tissue through iron accumulation, oxidative stress, and protein aggregation. *BMC Neurosci* 18:51. <https://doi.org/10.1186/s12868-017-0369-9>
354. Yemisci M, Caban S, Gursoy-Ozdemir Y, Lule S, Novoa-Carballal R, Riguera R, Fernandez-Megia E, Andrieux K, Couvreur P, Capan Y, Dalkara T (2015) Systemically administered brain-targeted nanoparticles transport peptides across the blood-brain barrier and provide neuroprotection. *J Cereb Blood Flow Metab* 35:469–475. <https://doi.org/10.1038/jcbfm.2014.220>
355. Yoshioka Y, Higashisaka K, Tsunoda S, Tsutsumi Y (2014) Engineered cell manipulation for biomedical application. Springer, Tokyo. <https://doi.org/10.1007/978-4-431-55139-3>
356. Yu M, Huang S, Yu KJ, Clyne AM (2012) Dextran and polymer polyethylene glycol (PEG) coating reduce both 5 and 30 nm iron oxide nanoparticle cytotoxicity in 2D and 3D cell culture. *Int J Mol Sci* 13:5554–5570. <https://doi.org/10.3390/ijms13055554>
357. Yun J-W, Kim S-H, You J-R, Kim WH, Jang J-J, Min S-K, Kim HC, Chung DH, Jeong J, Kang B-C, Che J-H (2015) Comparative toxicity of silicon dioxide, silver and iron oxide nanoparticles after repeated oral administration to rats. *J Appl Toxicol* 35:681–693. <https://doi.org/10.1002/jat.3125>
358. Yun WS, Aryal S, Ahn YJ, Seo YJ, Key J (2020) Engineered iron oxide nanoparticles to improve regenerative effects of mesenchymal stem cells. *Biomed Eng Lett* 10:259–273. <https://doi.org/10.1007/s13534-020-00153-w>
359. Zeng H, Sanes JR (2017) Neuronal cell-type classification: challenges, opportunities and the path forward. *Nat Rev Neurosci* 18:530–546. <https://doi.org/10.1038/nrn.2017.85>
360. Zhang L, He R, Gu HC (2006) Oleic acid coating on the monodisperse magnetite nanoparticles. *Appl Surf Sci* 253:2611–2617. <https://doi.org/10.1016/j.apsusc.2006.05.023>
361. Zhang Y, Yang M, Portney NG, Cui D, Budak G, Ozbay E, Ozkan M, Ozkan CS (2008) Zeta potential: a surface electrical characteristic to probe the interaction of nanoparticles with normal and cancer human breast epithelial cells. *Biomed Microdevices* 10:321–328. <https://doi.org/10.1007/s10544-007-9139-2>
362. Zhang T, Qian L, Tang M, Xue Y, Kong L, Zhang S, Pu Y (2012a) Evaluation on cytotoxicity and genotoxicity of the L-glutamic acid coated iron oxide nanoparticles. *J Nanosci Nanotechnol* 12:2866–2873. <https://doi.org/10.1166/jnn.2012.5763>
363. Zhang XF, Mansouri S, Mbeh DA, Yahia L, Sacher E, Veres T (2012b) Nitric oxide delivery by core/shell superparamagnetic nanoparticle vehicles with

- enhanced biocompatibility. *Langmuir* 28:12879–12885. <https://doi.org/10.1021/la302357h>
364. Zhang Y, Newton B, Lewis E, Fu PP, Kafoury R, Ray PC, Yu H (2015) Cytotoxicity of organic surface coating agents used for nanoparticles synthesis and stability. *Toxicol Vitro* 29:762–768. <https://doi.org/10.1016/j.tiv.2015.01.017>
365. Zhang J, Chen N, Wang H, Gu W, Liu K, Ai P, Yan C, Ye L (2016a) Dual-targeting superparamagnetic iron oxide nanopropes with high and low target density for brain glioma imaging. *J Colloid Interface Sci* 469:86–92. <https://doi.org/10.1016/j.jcis.2016.02.004>
366. Zhang Q, Rajan SS, Tyner KM, Casey BJ, Dugard CK, Jones Y, Paredes AM, Clingman CS, Howard PC, Goering PL (2016b) Effects of iron oxide nanoparticles on biological responses and MR imaging properties in human mammary healthy and breast cancer epithelial cells. *J Biomed Mater Res B Appl Biomater* 104:1032–1042. <https://doi.org/10.1002/jbm.b.33450>
367. Zhang X, Zhang H, Liang X, Zhang J, Tao W, Zhu X, Chang D, Zeng X, Liu G, Mei L (2016c) Iron oxide nanoparticles induce autophagosome accumulation through multiple mechanisms: lysosome impairment, mitochondrial damage, and ER stress. *Mol Pharm* 13:2578–2587. <https://doi.org/10.1021/acs.molpharmaceut.6b00405>
368. Zhang Y, Wang Z, Li X, Wang LL, Yin M, Wang LL, Chen N, Fan C, Song H (2016d) Dietary iron oxide nanoparticles delay aging and ameliorate neurodegeneration in *drosophila*. *Adv Mater* 28:1387–1393. <https://doi.org/10.1002/adma.201503893>
369. Zhao S, Yu X, Qian Y, Chen W, Shen J (2020) Multifunctional magnetic iron oxide nanoparticles: an advanced platform for cancer theranostics. *Theranostics* 10:6278–6309. <https://doi.org/10.7150/thno.42564>
370. Zhu X-M, Wang Y-XJ, Cham-Fai Leung K, Lee S-F, Zhao F, Wang D-W, Lai JM, Wan C, Cheng CH, Ahuja AT (2012) Enhanced cellular uptake of aminosilane-coated superparamagnetic iron oxide nanoparticles in mammalian cell lines. *Int J Nanomedicine* 7:953–964. <https://doi.org/10.2147/IJN.S28316>
371. Zhu N, Ji H, Yu P, Niu J, Farooq M, Akram M, Udego I, Li H, Niu X (2018) Surface modification of magnetic iron oxide nanoparticles. *Nanomaterials* 8:810. <https://doi.org/10.3390/nano8100810>



Hazard Assessment of Benchmark Metal-Based Nanomaterials Through a Set of *In Vitro* Genotoxicity Assays

Nádia Vital, Mariana Pinhão, Naouale El Yamani, Elise Rundén-Pran, Henriqueta Louro , Maria Dušinská, and Maria João Silva 

Abstract

For safety assessment of nanomaterials (NMs), *in vitro* genotoxicity data based on well-designed experiments is required. Metal-based NMs are amongst the most used in consumer products. In this chapter, we report results for three metal-based NMs, titanium dioxide (NM-100), cerium dioxide (NM-212) and silver (NM-302) in V79 cells, using a set of *in vitro* genotoxicity assays covering different endpoints: the medium-throughput comet assay and its modified version (with the enzyme formamidopyrimidine DNA glycosylase, Fpg), measuring DNA strand breaks

(SBs) and oxidized purines, respectively; the micronucleus (MN) assay, assessing chromosomal damage; and the *Hprt* gene mutation test. The results generated by this test battery showed that all NMs displayed genotoxic potential. NM-100 induced DNA breaks, DNA oxidation damage and point mutations but not chromosome instability. NM-212 increased the level of DNA oxidation damage, point mutations and increased the MN frequency at the highest concentration tested. NM-302 was moderately cytotoxic and induced gene mutations, but not DNA or chromosome damage. In conclusion, the presented *in vitro* genotoxicity testing strategy allowed the identification of genotoxic effects caused by three different metal-based NMs, raising concern as to their impact on human health. The results support the use of this *in vitro* test battery for the genotoxicity assessment of NMs, reducing the use of more expensive, time-consuming and ethically demanding *in vivo* assays, in compliance with the 3 R's.

The original version of this chapter was revised: The reference citations within the text weren't updated in sequential order which has been corrected now. The correction to this chapter is available at https://doi.org/10.1007/978-3-030-88071-2_18

Maria Dušinská and Maria João Silva contributed equally to the work.

N. Vital · M. Pinhão
Department of Human Genetics, INSA – National Institute of Health Doutor Ricardo Jorge, I.P, Lisbon, Portugal

N. E. Yamani · E. Rundén-Pran · M. Dušinská (✉)
Health Effects Laboratory, Department of Environmental Chemistry, NILU – Norwegian Institute for Air Research, Kjeller, Norway
e-mail: Maria.Dusinska@nilu.no

H. Louro · M. J. Silva (✉)
Department of Human Genetics, INSA – National Institute of Health Doutor Ricardo Jorge, I.P, Lisbon, Portugal

ToxOmics – Toxicogenomics and Human Health, NOVA Medical School/Faculdade de Ciências Médicas, Universidade Nova de Lisboa, Lisbon, Portugal
e-mail: m.joao.silva@insa.min-saude.pt

Keywords

Nanomaterials · DNA damage · Genotoxicity · Mutagenicity · Silver nanorods/wires · Cerium dioxide · Titanium dioxide

14.1 Introduction

14.1.1 Genotoxicity Assessment of Nanomaterials

The technology based on manufactured nanomaterials (NMs) has been highlighted as a key enabling technology, due to its potential to improve many products and processes [1]. With the growing number, diversity, and complexity of NMs entering the market, there is a great demand for rapid and reliable ways of testing NMs safety, preferably using *in vitro* approaches, to avoid the ethical dilemmas associated with animal experimentation [2, 3].

Despite the number of studies about NM toxicity, uncertainties persist concerning their impact on human health [4]. Available data do not yet allow for general and consistent conclusions concerning their safety evaluation. Indeed, NMs continue to present unique challenges in this field related to their physicochemical properties, e.g., small size and large surface area, which determine their behavior in biological systems and, consequently, their potential toxicity [5]. Data comparison among toxicological studies are also challenged by the use of diverse cell lines, bioassays and dose metrics that affect their results [6].

Concerning genotoxicity assessment, NMs may induce DNA damage by different mechanisms leading to various types of genetic alterations. Therefore, a battery of *in vitro* tests covering different genotoxic mechanisms is best suited to establish the genotoxic potential of NMs [5, 7]. Currently recommended approaches for assessing *in vitro* genotoxicity of NMs, particularly in a regulatory context, consist of a test battery with *in vitro* mammalian assays that detect endpoints relevant for carcinogenicity: gene mutations, chromosome breakage (clastogenicity) and chromosome loss leading to aneuploidy [5, 7].

The testing strategy for NMs should include (a) at least one *in vitro* mammalian mutagenicity assay, such as the mouse lymphoma (L5178Y) thymidine kinase (TK) assay (MLA) (OECD TG 490) or the hypoxanthine guanine phosphoribosyl transferase (*Hprt*) gene mutation test (HPRT test, OECD TG 476); and (b) a chromosomal damage assay, such as the *in vitro* chromosome aberration assay (OECD TG 473) or the *in vitro* micronucleus (MN) assay (OECD TG 487) [5]. Additional tests can be considered, such as the *in vitro* comet assay, a DNA strand break assay, especially in the context of assessment of oxidative damaging effects, even though an Organisation for Economic Co-operation and Development (OECD) guideline is still lacking [5, 8].

In nanotoxicology, gene mutation assays are the recommended choice over the Ames test. The latter is considered not suitable due to the size of bacteria (comparable with NMs themselves) and the fact that the bacterial wall limits significantly the uptake of nanoparticles, because it lacks mammalian mechanisms of endocytosis, pinocytosis, and phagocytosis [3, 5, 9–11]. The HPRT mutation test in V79 cells has been successfully applied to study different NMs, including metal-based NMs such as titanium dioxide (TiO₂) [10, 12–14] and silver (Ag) [15, 16], carbon based NMs [17–20], silica NMs [21] or Nickel oxide NMs [22]. The *in vitro* cytokinesis-block MN assay has demonstrated an overall sensitivity for NM genotoxicity testing. A nanospecific requirement is that the cytochalasin B (CB) (that inhibits cytokinesis, rendering cells that have divided once in culture as binucleated) is added 6–24 h after NM exposure because it hinders cellular uptake of NMs [3, 5, 23]. The comet assay can be performed in a medium-throughput version with 12 minigels per slide, greatly increasing the testing capacity and allowing the simultaneous study of multiple NMs at different concentrations [24]. This reduces not only the effects of inter-experimental variation, but also time and costs of the experiments, while also generating large and valuable data sets [24]. The minigel approach was successfully used in previous studies with metal NMs, such as TiO₂, Ag NMs (different sizes and surface properties), cerium oxide (CeO₂), zinc oxide and iron oxide NMs [15, 16, 24–26].

14.1.2 Metal-Based Nanomaterials: Applications

Metal and metal oxide NMs, such as Ag and TiO₂, are amongst the most frequently used in multiple industrial and biomedical products [27], while other metal oxide NMs, such as CeO₂, are now starting to emerge [28].

TiO₂, the most used NM, has been extensively used in paints, food (e.g., in additive E171), cosmetic products (including sunscreens), electronics, water treatment and biomedical applications [27, 29–32]. Silver NMs are popular as consumer product additives mainly due to their well-documented antimicrobial properties [27, 33], and are widely used in biomedicine, cosmetics, environmental remediation, textiles, food, feed and food packaging materials [29, 30, 31, 34–37], among others. CeO₂ NMs or nanoceria, have been used as catalysts in the petroleum refining industry, as additives to promote combustion of diesel fuels, as electrolytes in oxide fuel cells, and to a lesser extent in environmental, and agricultural domains [28, 38–40]. They have also been considered of interest for biomedical applications due to their unique redox properties and thus for their potential protection of cells and tissues against oxidative damage [38–41].

In recognition of their economic significance, the OECD assigned multiple metal-based NMs, including TiO₂ (e.g., NM-100), Ag and CeO₂ (e.g., NM-212) a high priority for toxicological testing, within the frame of the Working Party on Manufactured NMs (WPMN) safety testing of a representative set of NMs [42–45]. These NMs were also included, through the years, in the list of the Community rolling action plan (CoRAP), from the European Chemicals Agency (ECHA), within the REACH framework, to be evaluated based on concerns with respect to substances' carcinogenic or mutagenic potential and widespread use [46–48]. These facts highlight both the relevance of metal-based NMs for industrial applications and the importance of rapidly clarifying their potential hazards.

14.1.3 Metal-Based Nanomaterials: Genotoxicity and Carcinogenicity

TiO₂ has been classified as possibly carcinogenic to humans (IARC, group 2B) [49] based on animal studies (inhalation exposure), and as potential occupational carcinogens [50]. TiO₂ NMs were also considered as suspect human carcinogens (category 2) via inhalation, by the Risk Assessment Committee of the ECHA, in the frame of Classification and Labelling Harmonized Report [51]. Very recently, The European Food Safety Authority (EFSA) has updated its safety assessment of the food additive titanium dioxide, E171, concluding that E171 can no longer be considered as safe when used as a food additive in view of the potential genotoxic effects (EFSA Panel on Food Additives and Flavourings, [52]). Moreover, many studies reported TiO₂ NMs as cyto- and genotoxic, although results remain inconsistent, as Charles et al. [51] recently summarized based on a review of TiO₂ NMs *in vitro* studies from 2010 to 2016 [51]. For example, using the comet assay approximately 63% of the studies presented positive results, while by using the MN assay only 35% showed positive results, and only two of the five studies showed positive results with the chromosomal aberration assay [51]. With regard to gene mutation assessment, particularly using the HPRT mutation test in V79 cells, TiO₂ NMs yielded both positive [12, 13] and negative [10] findings. Also, TiO₂ induced *Hprt* gene mutations in human lymphoblastoid (WL2-NS) cells [14], but not in Chinese hamster ovary (CHO-K1) cells [53].

Similarly, nanoceria *in vitro* toxicological profiles differed among studies possibly due to their characterized pre-oxidant or antioxidant properties [38, 54, 55]. For example, CeO₂ NMs were shown to induce DNA damage [24, 56, 57], oxidative damage and apoptosis [58] in A549 cells, a human epithelial alveolar cell line. In contrast, other studies reported no genotoxicity in the same cell line [4, 54]. CeO₂ NMs were found to be non-genotoxic even displaying antioxidant and antigenotoxic properties in normal human epithelial lung cell line (BEAS-2B) [54, 59, 60],

although the induction of DNA damage has also been described [57].

According to a recent review, exposure to Ag NMs led to overall positive results for genotoxicity, using different assays, mainly *in vitro* assays [61]. Indeed, Ag NMs were able to induce significant increases in micronuclei [62–69], chromosomal aberrations [70], DNA damage (as assessed by the comet assay) [15, 16, 24, 54, 62, 69–74] and gene mutation frequencies in mammalian cells [15, 16, 64, 73, 75]. Nevertheless, no genotoxic effects were also observed using the MN and chromosomal aberration assays [72, 74].

In view of the current *in vitro* genotoxicity testing recommendations and to contribute to a comprehensive knowledge basis on the toxicological effects of metal-based NMs, the present chapter presents original data on the genotoxicity of three benchmark metal-based NMs. Two metal oxides – titanium dioxide (NM-100) and cerium dioxide (NM-212) – and a rod shape silver NM (NM-302) were tested using a panel of *in vitro* genotoxicity assays, namely, the *Hprt* gene mutation test, the micronucleus and the comet assays, in the chinese hamster lung (V79) fibroblasts.

In vitro tests were performed in the same cell line (V79 Cells), to allow for better comparability of the outcomes of the three assays, thus reducing bias. This is one of the validated and recommended cell lines to establish the mutant frequency (MF) in the endogenous *Hprt* gene [76] and to perform the *in vitro* MN test [77]. Characterization of NMs in the batch dispersions and exposure media was also performed as a complement of the characterization of their primary physicochemical properties already published elsewhere [75, 78, 79].

Overall, the results showed that NM-100 is able to induce DNA breaks, DNA oxidation damage (formamidopyrimidine DNA glycosylase – or Fpg-modified comet assay) and point mutations but does not cause chromosome instability in Chinese hamster lung (V79) cells. NM-212 showed an increase in DNA oxidation damage, induction of *Hprt* gene mutations and of the MN frequency at the highest concentration tested. NM-302 was moderately cytotoxic and was able

to induce gene mutations, while it failed to produce DNA or chromosome damage.

14.2 Nanomaterials and Experimental Strategy

14.2.1 Nanomaterial Properties and Dispersion for Biological Assays

Titanium dioxide (NM-100) and cerium dioxide (NM-212) were obtained from the Joint Research Centre Repository (JRC, Ispra, Italy) and silver (NM-302) from Fraunhofer Institute (Munich, Germany). All the NMs were prepared under Good Laboratory Practices (GLP) to use also in regulatory purposes, and their primary characteristics have been reported [75, 78, 79, 80]. The physicochemical characteristics of these NMs are summarized in Table 14.1.

The standardized Nanogenotox dispersion protocol was used to disperse NM-100 and NM-212 by sonication, at a concentration of a 2.56 mg/mL stock dispersion [81]. Nano silver (NM-302) was stabilized in dispersant solution (91.4% of the total volume of NM dispersion); thus 1 mL of the NM solution was diluted in 32.6 mL of 2% bovine serum albumin (BSA) to reach a stock concentration of 2.56 mg/mL; 6 mL of this solution was dispersed by sonication.

Hydrodynamic particle size-distributions of the stock dispersions and their dilutions in the cell exposure media were determined by dynamic light scattering (DLS; Malvern Nano ZS, Malvern Inc., UK), as described previously [4]. Each size spectrum obtained was the average of 10 individual DLS measurements conducted using automatic optimization of analytical conditions and data treatment by general purpose size-analysis. The batch dispersions and their dilutions in the exposure media (3, 32 and 240 µg/mL, corresponding to low, middle, and high exposure concentrations) were analysed 10–30 min after sonication and, in the case of the dilutions, also 24 h after incubation at 37 °C, 5% CO₂ to mimic the *in vitro* tests. The polydispersity index (PDI)

Table 14.1 Key intrinsic physicochemical characteristics of the tested nanomaterials

Material code	Core material	Crystalline phase	Product Type	Morphology	Specific surface area (m ² /g, BET)	Average size (nm, TEM)	Coating
NM-100 ^a	TiO ₂	Anatase	Powder	Spherical or ellipsoidal	9	110 ± 57	–
NM-212 ^b	CeO ₂	Cerite	Powder	Cubic cerionite	27.2	33.3	Alkali metals (Ca, Na) and Zn
NM-302 ^c	Ag	Metallic	Dispersion	Nanorod/nanowires	–	50 × 3000	Tween 20/PEG

Physicochemical characteristics of NM-100, NM-102 and NM-302 obtained from ^a[78], ^b [79] and ^c [75], respectively; TEM Transmission electron microscopy, BET Brunauer-Emmett-Teller

and hydrodynamic size (Z_{av} , nm) for each NM were expressed as the mean of 10 consecutive measurements.

14.2.2 Experimental Strategy

V79 Male Chinese hamster lung fibroblast cells were purchased from the European Collection of Cell Culture (ECACC; Catalogue Number 86041102). Cells were cultured in Dulbecco's minimal essential medium (DMEM) D6046 (Sigma, Steinheim, Germany), supplemented with 10% (V/V) heat-inactivated fetal bovine serum (FBS), 1% (V/V) 100 U/mL penicillin and 100 µg/mL streptomycin and 200 mM L-glutamine (Sigma) in a humidified atmosphere (5% CO₂ at 37 °C).

Since preliminary data indicated that none of the NMs under study was strongly cytotoxic, the highest concentration of each NM selected for the *in vitro* assays was limited by its dispersibility, i.e. the maximum concentration that could be homogeneously dispersed in BSA-water (2.56 mg/mL) and by the highest percentage of the stock dispersion (10%) that could be added to the cultures without interference with the normal cell proliferation capacity, leading to a range of concentrations below 75 µg/cm². Immediately after sonication, the resulting stock was serially diluted to achieve a logarithmic range of concentrations (1, 3, 10, 30 and 75 µg/cm²), before adding it to the cells already seeded in different plates, according to the different assays, as described below. At the exposure time, cell

medium was replaced by the treatment medium and incubated at 37 °C and 5% CO₂. The experimental procedure for each assay is detailed below.

14.2.2.1 Alkaline Comet Assay and Fpg-Modified Comet Assay

A medium-throughput version of the comet assay, using 12 mini-gels placed on a standard microscopic slide, was used to test simultaneously five concentrations of three NMs in a single experiment, as previously described [24]. V79 cells were exposed to the NMs for 24 h, at concentrations ranging from 1 to 75 µg/cm², and embedded on slides (2 drops per concentration, 12 drops per slide). After lysis and electrophoresis, slides were examined under a fluorescence microscope (Leica DMI 6000 B), for comet scoring using the image analysis Comet Assay IV software (Perspective Instruments). As a measure of DNA strand breaks (SBs), the median of the % DNA in tail (50 comets per gel), and the mean from 2 independent experiments was calculated. In parallel, a modified version of the comet assay was used for DNA base oxidation detection, as previously described [24], with the addition of a post-lysis step of incubation with Fpg (kindly provided by Professor Andrew Collins, Department of Nutrition, University of Oslo, Norway). The Fpg converts oxidized purines into SBs that become detectable by the comet assay [24]. DNA oxidation lesions (net Fpg-sensitive sites) were calculated as the difference in % DNA in tail between samples with Fpg incubation and

samples without incubation. Positive controls were included, consisting of cultures exposed to hydrogen peroxide (Sigma) (100 μM , 5 min, on ice) for DNA breaks.

14.2.2.2 *In Vitro* Micronucleus Test

The cytokinesis-blocked MN assay (CBMN) was carried out according to the general principles of the OECD Test guideline No. 487 [77], and as previously described [82], with minor modifications. V79 cells cultured in 12-well plates for 24 h at 37 °C and 5% CO₂ were exposed to the dispersed NMs diluted in culture medium (1–75 $\mu\text{g}/\text{cm}^2$) for 24 h. Cytochalasin B (6 $\mu\text{g}/\text{mL}$) was then added to each culture where the NMs also remained for more 24 h. Cells were then harvested with a hypotonic shock (0.1 M KCL), followed by fixation (3:1 methanol:acetic acid) and immediately spread onto microscope slides and stained with 4% (v/v) Giemsa. A negative control, consisting of culture medium with BSA-water in the concentration found in the highest dose of the NM dispersant and the positive control Mitomycin C (MMC, 0.01 $\mu\text{g}/\text{mL}$), were included in all experiments. For each treatment condition, two replicate cultures were used; from each culture, at least two slides were prepared, coded and blind-scored under a bright field microscope. The analysis of micronuclei in 2000 binucleate cells per treatment condition was performed and the proportions of mono-, bi- and multinucleate cells were determined in a total of 2000 cells (500 per slide, 1000 per culture). The cytokinesis-blocked proliferation index (CBPI) and the replication Index (RI) were calculated [77].

14.2.2.3 *Hprt* Gene Mutation Test

The *Hprt* gene mutation test was carried out according to OECD guideline 476 [76], as described elsewhere [10], with minor modifications. Briefly, V79 cells were cultured in 100 mm Petri dishes (3×10^5 cells per dish) and incubated at 37 °C, for 24 h. Cells were exposed to the NMs for 24 h, at concentrations from 1 to 75 $\mu\text{g}/\text{cm}^2$; untreated cells were used as negative control and

cells treated for 30 min with 0.1 mM methyl methanesulfonate (MMS; Sigma), served as the positive control. After exposure, the medium was removed and the cells were washed, detached, and re-suspended in fresh medium. The cells were then seeded in 100 mm petri dishes and maintained in exponential growth. Duplicate samples were taken for analysis of mutant frequencies at 7 and 9 days after treatment, by detaching and subculturing in 100 mm diameter Petri dishes (3×10^5 cells/Petri dish, 3 dishes per sample) and grown in selective medium containing 6-thioguanine (Sigma) at 5 $\mu\text{g}/\text{mL}$ for 10 days to form colonies. Then, mutant (6-thioguanine-resistant) colonies were fixed, stained with 1% methylene blue (Sigma), and counted manually (only colonies with at least 50 cells were counted).

The frequency of surviving cells was assessed using the plating efficiency (PE) assay immediately after exposure (PE₀) and for each of the two harvests (7- and 9-day, PE₇ and PE₉, respectively). Briefly, treated and untreated cells were seeded in 6-well plates at 50 cells per well and incubated for 6 days at 37 °C to form colonies. After staining with 1% methylene blue (Sigma), the number of colonies was counted manually [10]. Absolute PE was calculated for each mutant harvest as the ratio between the number of colonies and the number of inoculated cells; relative PE (%) was calculated as the ratio between the number of colonies in exposed and in control cultures, multiplied by 100. The MF was expressed as the ratio between the number of *Hprt* mutants and the number of clonable cells, as determined by the PE at each harvest point.

14.2.3 Statistical Analysis

The statistical analyses of the results were performed using SPSS Statistics 19 (IBM). The results of the comet assay were analysed using the One-Way ANOVA test, if normality of the results was confirmed, or the non-parametric Kruskal-Wallis test, if that was not the case.

Fisher's exact test was applied to compare the frequency of micronucleated cells between NM-treated and vehicle-treated cultures. CBPI and RI data were analyzed using the Kruskal-Wallis test. The existence of a dose-response relationship either for the cytotoxicity, frequency of micronucleated cells, CBPI or % DNA in tail was explored by regression analysis. Differences with $p < 0.05$ were considered statistically significant.

14.3 Results and Discussion

Due to significant increase of NMs in commercial applications and presence in multiple consumer products, NMs are being extensively investigated for their safety [7]. Since a main concern with NMs exposure is their genotoxic potential, the study of mechanisms potentially leading to genotoxicity is crucial [7]. This calls for the adoption of well-designed *in vitro* testing strategies suitable for NMs, addressing different genotoxicity endpoints relevant for hazard assessment and regulatory purposes [10, 15, 83]. Special attention needs to be given to the mechanisms of toxicity and the use of representative reference materials to allow to correlate toxic effect of the NMs with specific physicochemical properties [15].

In the present chapter we present the evaluation of cytotoxic and genotoxic effects of three benchmark metal-based NMs: titanium dioxide (NM-100), cerium dioxide (NM-212) and silver (NM-302), using the recommended *in vitro* approach for NM genotoxicity testing [5, 7, 11, 84] concomitantly with the analysis of their secondary properties within cells. A unique feature of this study is the fact that we performed all the genotoxicity testing methods in the same cellular model, using the same concentration range (0–75 $\mu\text{g}/\text{cm}^2$) prepared from the same stock dispersion of each NM, and using the same exposure duration (24 h).

14.3.1 Characterization of the NMs in Stock Dispersions and in Exposure Media

The NMs used are considered as reference NMs and have been extensively characterized in many different EU projects, such as the Nanogenotox and NANoREG projects. To gather sound genotoxicity data, it is necessary to ensure that nanoparticles are well dispersed and for that we used the dispersion protocol generated in the frame of Nanogenotox [81]. The monodispersity of the tested NMs was analyzed by DLS, in both NM stock dispersions and culture medium. The size distribution of the batch dispersions demonstrated that a homogeneous dispersion was achieved for all the tested NMs (Table 14.2). NM-100 produced the finest dispersion followed by NM-212. The coarsest dispersion was achieved for NM-302, which is consistent with its presentation as nanowires (Table 14.2). In fact, NM-302 also presented higher hydrodynamic size in comparison to the other NMs, corresponding to a bimodal size distribution with a primary peak at 818.7 nm and a secondary peak at 5319 nm. Due to the morphological nature of this NM, there is not a good understanding of what the size-spectra in DLS analyses represent.

The DLS spectra data obtained after the dilution of the NMs in cell culture media shortly after sonication or after 24 h incubation (37 °C, 5% CO₂) is presented in Table 14.3. Dilution of stock dispersions of NM-100 and NM-212 in culture medium gave a slight increase in Z_{av} , compared with the respective stock dispersions. Although

Table 14.2 DLS measurements of mean polydispersity index (PDI) and mean size (Z_{av}) of the batch dispersions of nanomaterials in aqueous solution

Nanomaterial	PDI (mean \pm SD)	Z_{av} , nm (mean \pm SD)
Dispersion medium	0.24 \pm 0.01	4.56 \pm 0.13
NM-100	0.17 \pm 0.02	241.76 \pm 7.98
NM-212	0.19 \pm 0.08	311.41 \pm 49.14
NM-302	0.82 \pm 0.16	1446.00 \pm 204.19

SD standard deviation

Table 14.3 DLS measurements of polydispersity index (PDI) and mean size (Z_{av}) after NMs dilution in V79 cell culture medium, analyzed shortly after dilution or after 24 h incubation, to mimic cells exposure

	Concentration ($\mu\text{g/mL}$)	0 h		24 h	
		PDI	Z_{av} , nm	PDI	Z_{av} , nm
		(mean \pm SD)	(mean \pm SD)	(mean \pm SD)	(mean \pm SD)
NM-100	3	0.39 \pm 0.10	256.69 \pm 12.93	0.37 \pm 0.06	218.00 \pm 18.29
	32	0.25 \pm 0.05	379.64 \pm 59.30	0.22 \pm 0.01	260.60 \pm 2.77
	240	0.22 \pm 0.02	341.32 \pm 13.25	0.13 \pm 0.02	242.90 \pm 1.76
NM-212	3	0.71 \pm 0.16	125.49 \pm 23.71	0.30 \pm 0.030	169.37 \pm 19.43
	32	0.23 \pm 0.02	288.17 \pm 10.39	0.23 \pm 0.01	241.59 \pm 23.53
	240	0.17 \pm 0.02	293.18 \pm 18.71	0.18 \pm 0.04	258.03 \pm 14.05
NM-302	3	0.55 \pm 0.21	492.42 \pm 490.15	0.21 \pm 0.01	165.89 \pm 0.95
	32	0.73 \pm 0.06	837.30 \pm 245.07	0.23 \pm 0.01	156.00 \pm 0.84
	240	0.58 \pm 0.06	714.30 \pm 175.53	0.34 \pm 0.03	107.10 \pm 1.46

their mean hydrodynamic size was increased, a substantial number of smaller size particles were still detectable in dispersion, irrespectively of the concentrations analysed. In the case of NM-302, decreases in the size of the NM as well as in the PDI values were observed after dilution in cell medium. Following incubation for 24 h at 37 °C, 5% CO₂ to mimic cell exposure conditions, size distributions appeared to follow a tendency for lower Z in comparison to the measurements shortly after dispersion, and this may reflect the sedimentation of the largest agglomerates, as also observed in the cell culture plates.

14.3.2 Genotoxicity of TiO₂ Nanomaterial (NM-100)

The *in vitro* cyto- and genotoxicity of TiO₂ NMs have been intensively studied in recent years due to their wide applications and their possible carcinogenicity, as reviewed elsewhere [51, 85–87]. However, the results remain inconsistent [51, 86], either due to different cell types, physical properties of the particles, exposure doses, or incubation conditions, making conclusions concerning their genotoxicity unclear [13, 51].

In our study the cytotoxicity of a TiO₂ NM was measured in V79 cells by determining replicative indices – RI and CBPI in the context of the CBMN assay and the PE measured after exposure, within the HPRT test (Fig. 14.1b, c). The RI or CBPI results did not show cytotoxic effects,

whereas the PE results evidenced a cytotoxic effect at the lowest (1 $\mu\text{g}/\text{cm}^2$) and the highest (75 $\mu\text{g}/\text{cm}^2$) NM-100 concentrations. This latter result agrees with previous findings where V79 cell viability significantly decreased after 24 and 48 h exposure to 5 to 100 $\mu\text{g}/\text{mL}$ of anatase TiO₂ NMs [12]. Reduced V79 cell viability assessed with the MTT assay was also observed after 6 and 24 h exposure to 25–100 $\mu\text{g}/\text{mL}$ [13], which was corroborated also after 24 and 48 h exposure to 100 $\mu\text{g}/\text{mL}$ of anatase (<25 nm) and anatase/rutile (P25, >25 nm) TiO₂ [88]. After 72 h exposure to anatase/rutile TiO₂ NMs, V79 cell viability was reduced at the highest concentration tested (52 $\mu\text{g}/\text{cm}^2$) [89]. In contrast, no differences were observed in cells exposed to 3, 30 and 75 $\mu\text{g}/\text{cm}^2$ concentration of anatase/rutile TiO₂ NM-105 (15–60 nm) compared with controls using the PE assay [10]. El Yamani et al. [24], found no toxicity in A549 cells exposed to NM-100 (concentration range of 0.1–75 $\mu\text{g}/\text{cm}^2$) for 3 h and 24 h, as assessed by the alamarBlue® assay; likewise, no long-term effect was found with the colony forming efficiency (CFE) assay following 9–12 days of exposure. Nevertheless, it is worth noting that a decrease in CFE was observed for cells exposed to the lowest concentration tested [24]. Similarly, no cytotoxic effect was observed either in the same cell line exposed to a similar NM-100 dose range [4, 54] or in BEAS-2B cells [25, 54].

Concerning genotoxicity, NM-100 (Fig. 14.1a) induced significant increase in DNA damage

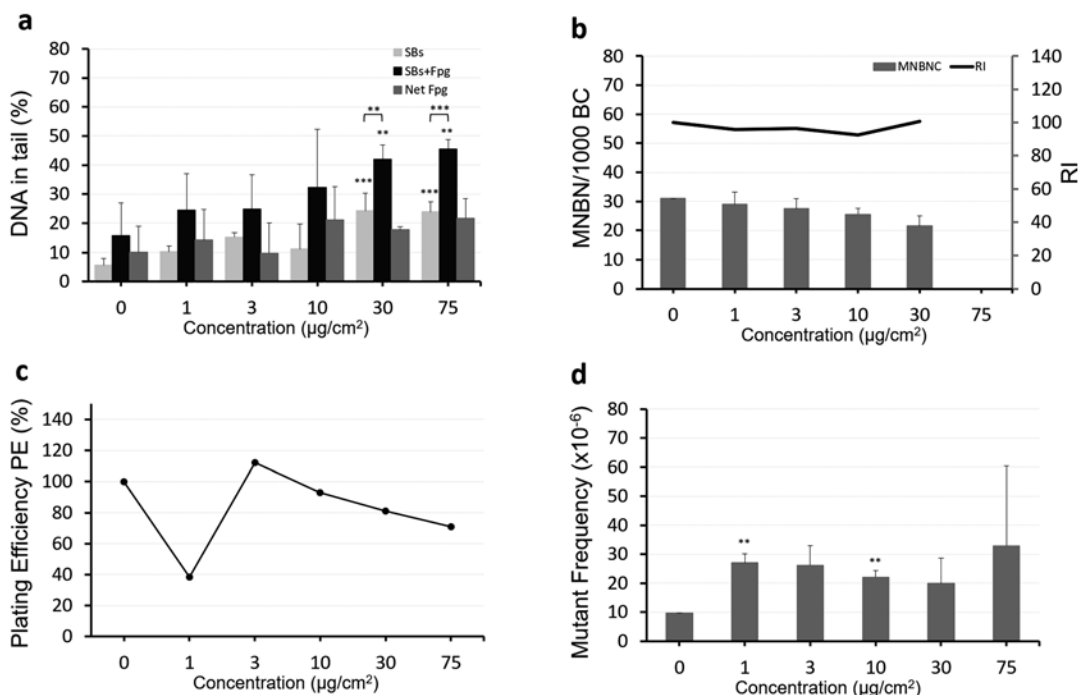


Fig. 14.1 Results obtained in V79 cells exposed for 24 hours to NM-100 using (a) the comet assay with (SBs + Fpg) and without (SBs) enzyme treatment; (b) the cytokinesis-block micronucleus assay, expressed as micronucleated binucleated cells (MNBNC) per 1000 binucleated cells (bars, primary axis) and replication index (RI; line, secondary axis); (c) the relative plating efficiency (PE %) as a measurement of cytotoxicity; and

(d) the HPRT test to measure the mutation frequency, MF ($\times 10^{-6}$), expressed as the mean \pm standard deviation ($M \pm SD$) of two independent harvests from one experiment. Data are expressed as the $M \pm SD$. *P* values indicate statistically significant differences from unexposed cells or between SBs and SBs + Fpg; **p* < 0.05; ***p* < 0.01, ****p* < 0.001. *SB* strand breaks

detected by the conventional comet assay ($p = 0.0005$, One-way Anova test) and the Fpg-modified-comet assay ($p = 0.0053$). In both cases, the two highest concentrations presented values of % DNA in tail that are significantly higher than those of the negative control ($p < 0.005$, Tukey HSD, Post-HOCs test). However, no dose-response relationship was identified using regression analysis. Furthermore, cells exposed to the two highest NM concentrations significantly raised the level of DNA damage measured by the Fpg-modified comet assay compared to the level obtained by the conventional comet assay ($p < 0.005$, Student's *t*-test), indicating the formation of DNA oxidation lesions. In contrast, NM-100 did not affect significantly the frequency of micronucleated cells (Fig. 14.1b). No data could be obtained for the highest concentration

of NM-100 tested ($75 \mu\text{g}/\text{cm}^2$) due to large amount of NMs on top of cells, interfering with scoring.

With respect to *Hprt* mutations (Fig. 14.1d), an increase of the MF relative to control was observed for all concentrations tested, reaching more than a two-fold increase at concentrations 1, 3 and $10 \mu\text{g}/\text{cm}^2$ (2.8, 2.7 and 2.3-fold increase, respectively) and a threefold increase at the highest concentration tested. However, no concentration-response relationship was detected. In agreement with our findings, Chen et al. [12] reported a concentration-dependent increase in the *Hprt* MF after 2 h treatment of V79 cells with $20 \mu\text{g}/\text{mL}$ and $100 \mu\text{g}/\text{mL}$ of TiO_2 NMs (75 nm, anatase); the top concentration induced a 2.5-fold increase in the MF [12]. Additionally, an increased % Tail DNA was

observed at that concentration, after 24 h exposure [12]. Likewise, exposure of V79 cells to smaller sized anatase TiO₂ NM (<25 nm) for 6 h led to a significant concentration-dependent increase in the level of DNA damage (25, 50, 100 µg/mL, comet assay), and in MF (50, 100 µg/mL, HPRT test), 2.98-fold higher in treated than in control cells, further indicating genotoxicity in V79 cells, after anatase TiO₂ exposure [13]. With respect to anatase/rutile TiO₂ NMs (NM-105), negative results were reported following 24 h exposure of V79-4 cells to 3, 15 and 75 µg/cm² using the HPRT test. The authors used two different dispersion procedures to address the state of agglomeration [10]. Also in V79 cells, DNA damage was observed with the comet assay after exposure to 10 and 100 µg/mL of anatase (<25 nm) and anatase/rutile (P25, >25 nm) TiO₂, for 24 h [88], while after 72 h exposure to anatase/rutile, no significant increase in MN frequency was observed in concentrations up to 250 µg/mL [89], in agreement with our findings. Using NM-100 in A549 and TK6 cells, El Yamani et al. [24] observed a concentration-dependent increase in DNA damage and DNA oxidation damage after 3 and 24 h exposure. Induction of DNA damage but not DNA oxidation damage was observed after 24 h exposure of A549 and BEAS-2B cells to NM-100, with a less pronounced effect in the latter ones [54]. Moreover, NM-100 showed to be slightly more genotoxic than NM-101 [54]. Another study reported a weak but positive induction of DNA damage following 24 h (but not 3 h) exposure to different TiO₂ NMs (NM-100, NM-101, both anatase, and NM-103, rutile) in BEAS-2B cells and NM-100 was the most genotoxic NM. In addition, increased DNA oxidation was observed for one or two concentrations of NM-100 and NM-103 (3 h exposure) and NM-101 (24 h exposure) [25]. In contrast with the mainly positive results of the comet assay, negative results have been reported for NM-100, when using the MN assay [25, 63]. For example, NM-100 was found to be the most genotoxic TiO₂ NM compared to NM-101, NM-102 and NM-103, after A549 cells exposure (3 h and 24 h) to 1–100 µg/cm², by the comet assay (and Fpg-modified version), while no effect

was observed with the MN assay [4]. Likewise, exposure of TK6 cells to anatase/rutile NM105 (21 nm) for 28 h or 48 h (3, 15 and 75 µg/cm²) failed to increase the frequency of micronucleated cells [90]. The HPRT test has also been used either alone or concomitantly with the *in vitro* MN assay and/or the comet assay to determine genotoxicity of smaller anatase TiO₂ NMs in cultured human lymphoblastoid cells (WL2-NS cells) [14] and in Chinese hamster ovary cells (CHO-K1) [53]. In the study of Wang et al. [14] TiO₂ NMs induced approximately a 2.5-fold increase in the frequency of micronucleated binucleate cells (130 µg/mL, after 6 h exposure), a three-fold increase in the % DNA in tail (65 µg/mL, after 24 h exposure), and an approximately 2.5-fold increase in the *Hprt* gene MF (130 µg/mL, after 24 h exposure) [14]. It is worth noting that cytotoxicity was observed at the highest concentration of 130 µg/mL, after 6, 24 and 48 h exposure [14]. In contrast, Wang et al. [53], reported negative results after exposure to lower concentrations (up to 40 µg/mL) of anatase TiO₂ NMs (<25 nm), in a long-term (60 days) exposure experiment, using both the comet and the HPRT assays in CHO-K1 cells [53]. Both acute (2 days) and chronic (60 days) exposures significantly increased the production of reactive oxygen species (ROS), but CHO-K1 cells appeared to adapt to the chronic exposure to TiO₂ NMs and detoxify the excess of ROS, possibly through up-regulation of super oxide dismutase (SOD), in addition to reducing particle uptake [53].

Overall, the comet assay has been the most commonly used assay to analyze genotoxicity of TiO₂ NMs due to its high sensitivity, simplicity, and speed [51, 86]. Conflicting results reported in the literature have been related either to cell type or exposure duration or to NM properties, such as crystallinity and particle size, as reported in a recent meta-analysis. Normal cells seem to be more sensitive to the genotoxicity induced by TiO₂ NMs than transformed cells [86]. In fact, both in our study and in the reviewed literature, overall positive cyto- and genotoxicity results were reported in V79 cells, while more conflicting results were observed with other cell lines, namely cancer cells, such as A549 cells.

Moreover, the meta-analysis results indicated that TiO₂ NMs were generally not able to induce MN formation, except when particles size was lower than 21 nm [86], which agrees with our findings. Interestingly, in the few studies presenting positive results for MN, low concentrations ($\leq 150 \mu\text{g/mL}$) could induce MN formation, whereas longer exposures ($> 24 \text{ h}$) and high concentrations ($> 150 \mu\text{g/mL}$) of TiO₂ NMs tended to decrease the MN frequency [86], a trend that was also observed in our study after 24 h exposure. Moreover, MN formation was influenced by size, coating, duration, and concentration of TiO₂ NMs [86]. Based on our research, and the overall findings of the literature, we conclude that the comet assay and *Hprt* gene mutation assay might be more sensitive than the *in vitro* MN assay for genotoxicity assessment of TiO₂ NMs [12, 13, 86].

14.3.3 Genotoxicity of CeO₂ Nanomaterial (NM-212)

Among the three NM tested, cerium dioxide has been the least studied regarding its toxicity, probably due to its more recent use in commercial and industrial applications. Thus, *in vitro* toxicity results are still scarce and no study was found addressing the cyto- or genotoxicity of CeO₂ NMs in V79 cells.

Concerning NM-212 cytotoxicity, a more than 30% decrease in PE (Fig. 14.2c) was observed with a single low dose ($3 \mu\text{g/cm}^2$), while no cytotoxicity was detected by the analyses of replicative and proliferation indices—RI and CBPI—from the CBMN assay (Fig. 14.2b). Therefore, our results did not show a clear toxic effect of this NM, which is in line with other studies stating no toxic effects for CeO₂ NMs [54, 59, 63]. El

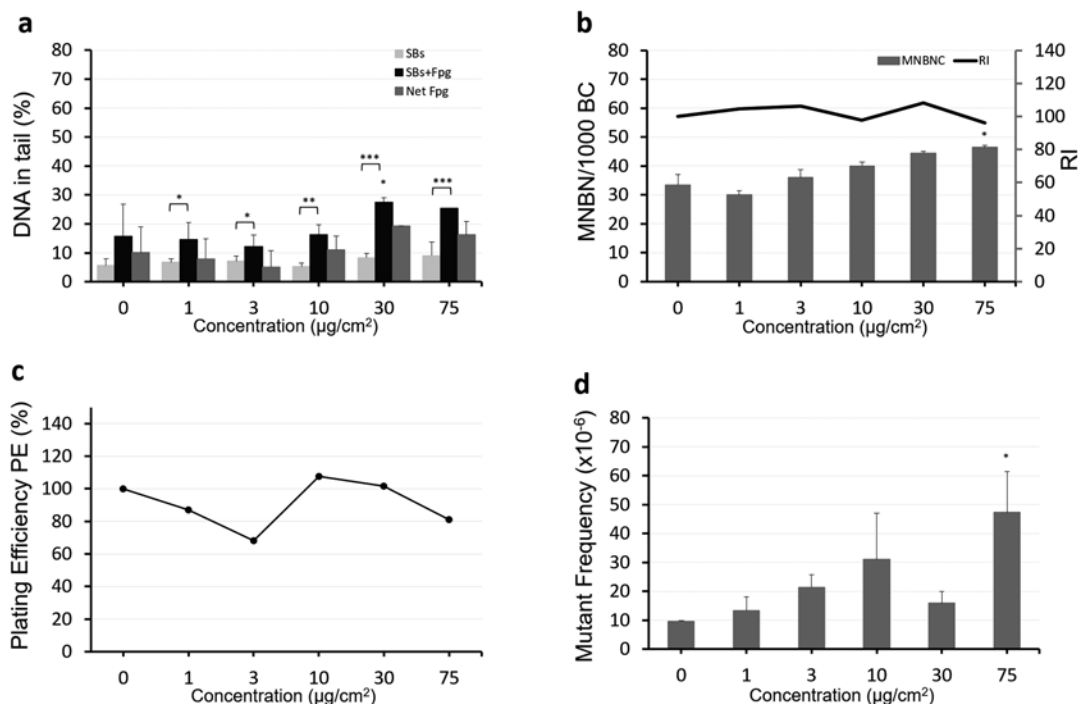


Fig. 14.2 Results obtained in V79 cells exposed for 24 h to NM-212 using (a) the comet assay with (SBs + Fpg) and without (SBs) enzyme treatment; (b) the cytokinesis-block MN assay, expressed as micronucleated binucleated cells (MNBN) per 1000 binucleated cells (bars, primary axis) and replication index (RI; line, secondary axis); (c) the relative plating efficiency (PE %) as a measurement of

cytotoxicity; and (d) the HPRT test to measure the mutation frequency, MF ($\times 10^{-6}$), expressed as the mean \pm standard deviation ($M \pm SD$) of two independent harvests from one experiment. Data are expressed as the means \pm SD. *P* values indicate statistically significant differences from unexposed cells, or between SBs and SBs + Fpg; **p* < 0.05; ***p* < 0.01, ****p* < 0.001; SB strand breaks

Yamani et al. [24] reported that A549 cells exposed to NM-212 (0.01–75 $\mu\text{g}/\text{cm}^2$), did not evidence toxicity using the alamar Blue® (3 h and 24 h exposure), and the CFE assays (9–12 days exposure), although a slight decrease in colony forming ability was observed for a low (0.3 $\mu\text{g}/\text{cm}^2$) concentration treatment [24]. Using similar assays and the same cell line, decreased cell survival (but no concentration-response) was observed (CFE assay) after 7 days exposure to high NM-212 concentrations (75 and 100 $\mu\text{g}/\text{cm}^2$) although no toxicity was detected after 24 h exposure (MTT assay) [4]. Other negative reports were also found using cell proliferation assessment in BEAS-2B and A549 cells after 24 h and 48 h exposure to the same NM [54, 63].

In contrast, some reports showed toxic effects mediated by ROS [58, 91–93], which are also controversial given that this NM is able to scavenge ROS thereby displaying antioxidant properties [55]. As an example, Mittal and Pandey [58] showed that A549 cells exposure to a smaller CeO_2 (<25 nm, cuboidal) for 24 h and 48 h resulted in concentration- and time- dependent cytotoxicity at a concentration range of 25–100 $\mu\text{g}/\text{mL}$, after NM internalization. This was accompanied by ROS generation and a decrease in cellular antioxidant status followed by apoptotic cell death [58].

Regarding the genotoxic effects of CeO_2 NM in V79 cells, NM-212 treatment (24 h) did not induce any significant increase in the level of DNA damage over the negative control, as measured with the comet assay (Fig. 14.2a). However, a 1.8-fold increase in the level of DNA oxidation lesions (Fpg-sensitive sites) was found following exposure to 30 $\mu\text{g}/\text{cm}^2$ of CeO_2 , which was not observed by the conventional comet assay. Notably, the results of the Fpg-modified comet assay were significantly increased over those of the conventional assay ($p < 0.005$, Student's t-test) for all concentrations tested, suggesting induction of DNA oxidation lesions. Additionally, our results from the CBMN assay showed an equivocal genotoxic effect following 48 h exposure to NM-212, since it induced a significant increase of micronucleated cells at the highest concentration tested ($p = 0.043$; Mann-Whitney

test; Fig. 14.2b), with no concentration-dependent increase. Contradictory results have been reported concerning the DNA damage-inducing capacity of CeO_2 NMs. A concentration-dependent increase in DNA oxidation damage (Fpg-comet assay) was observed in TK6 (0.42–42 $\mu\text{g}/\text{mL}$) and in A549 cells (30 and 75 $\mu\text{g}/\text{cm}^2$), after 3 h exposure to NM-212 [24]. Still, in TK6 cells, the increase in Fpg-sensitive sites was not maintained over the whole range of concentrations after 24 h, where DNA oxidation damage was reduced compared to 3 h exposure to the lowest concentrations (0.42–4.2 $\mu\text{g}/\text{mL}$). DNA damage (with the conventional comet assay) was observed only for the highest concentration tested [24]. Interestingly, in A549 an approximately two-fold increase in DNA oxidation damage (30 and 75 $\mu\text{g}/\text{cm}^2$) was found after 24 h compared to 3 h exposure [24]. In another study with A549 cells, increased DNA damage was observed after 6 h exposure to 25–100 $\mu\text{g}/\text{mL}$ CeO_2 NM (8–20 nm), in the standard and the Fpg-modified comet assays, the effect being more pronounced with the modified assay [58]. A positive effect was also reported after 24 h exposure to a 16–22 nm-sized CeO_2 NM (0.5–500 $\mu\text{g}/\text{mL}$), with the conventional comet assay [56]. In contrast, no genotoxicity was found following A549 cells exposure (3 h and 24 h) to NM-212, using a similar concentration range (1–100 $\mu\text{g}/\text{cm}^2$) as assessed by the standard and Fpg-modified comet assays [4]. Interestingly, an antioxidant and anti-genotoxic effect was observed following 24 h exposure to 15–160 $\mu\text{g}/\text{mL}$ of the same NM [54]. In another human epithelial lung cell line (BEAS-2B cells), NM-212 was found to be non-genotoxic (García-Rodríguez et al., [54, 63]), while smaller CeO_2 (<25 nm) displayed antioxidant and antigenotoxic properties [59, 60]. Another commercial CeO_2 NM with a smaller size and a higher specific surface area (size: 8 nm; specific surface area: 61 m^2/g) induced significant levels of DNA damage in A549 and BEAS-2B cells [57].

Very few studies on CeO_2 NMs have used the MN frequency as a biomarker of genotoxicity. Negative results have been reported in A549 cells exposed for 48 h to NM-212 using the CBMN

assay [4], and the flow cytometric MN assay in BEAS-2B cells [63]. In primary human dermal fibroblasts, the CBMN assay, in association with immunofluorescence staining of centromere protein A in micronuclei, demonstrated the genotoxic effect of a smaller (7 nm) CeO₂ NM by a clastogenic mechanism while a micro-sized (320 nm) CeO₂ material was not genotoxic [94]. Oxidative stress induction has also been observed through the measurement of catalase activity, lipid peroxidation and glutathione status. This is consistent with the implication of free radical-related mechanisms underlying the CeO₂ NM-induced clastogenic effect, possibly modulated by inhibition of cellular hydrogen peroxide release [94]. Studies using other cell types also yielded conflicting results. CeO₂ (< 25 nm) was shown to induce genotoxicity either by the comet or the MN assay in human neuroblastoma cells following 24 h exposure to 100–200 µg/mL [92]. A positive comet assay result was also obtained in skin melanoma cells after 24 h and 48 h exposure to 20–80 µg/mL [95], whereas in human lens epithelial (HLE-B3) cells, exposed to 5 and 10 µg/mL of CeO₂ NMs (~6 nm) during 24 h, no DNA damage was observed [96]. In another study transient DNA lesions (10 µg/mL) were observed following 24 h exposure of untransformed human fibroblasts to CeO₂ NM, as assessed with the comet assay [91].

Concerning the mutagenicity of NM-212, results of the HPRT mutation test (Fig. 14.2d) showed a non-significant concentration-dependent increase in MF up to 10 µg/cm² (3.2-fold increase). Notably, exposure to the highest concentration of this NM resulted in a significant 5-fold increase in the MF (higher than the observed for the positive control). To the best of our knowledge no other study has reported results for NM-212 using the HPRT test. Importantly, sub-chronic inhalation exposure to different low doses of CeO₂ NM did not induce genotoxicity in the rat hematopoietic system at the DNA, gene or chromosome levels [97].

Overall, although some authors have reported *in vitro* cyto- and genotoxic effects of CeO₂ NMs, mainly using the comet assay, conflicting results are found in the literature, and therefore there is

no general agreement about these effects [38, 55]. Again, we cannot exclude the variability of exposure conditions, e.g., cell culture medium with or without serum, as having an influence on the secondary physicochemical properties of the NMs that impacts on their toxicity. The conflicting results may be attributed also to the different CeO₂ NM primary properties, e.g., size, shape, surface area or coating, among others [55, 91, 93]. NM-212 has a cubic fluorite structure and the XPS results indicated that its surface is composed mainly of oxygen, O²⁻, and cerium, which may be present as Ce⁴⁺ (93.1%) and Ce³⁺ (6.9%) [79]. In a recent study, rod-like and octahedron-like CeO₂ NMs inhibited DNA damage by scavenging OH, but cube-like nano-CeO₂ did not eliminate OH in HepG2 cells, suggesting that cubical CeO₂ NMs are the most toxic ones [93]. An additional factor in the variability of the *in vitro* toxicological profiles of CeO₂ NMs can be possibly related to their prooxidant *versus* antioxidant properties [38, 54, 55]. Because of its multiple antioxidant enzyme-like activities, including superoxide dismutase (SOD), catalase, peroxidase-like activities, and hydroxyl radical and nitric oxide radical scavenging properties, CeO₂ NMs are expected to scavenge almost all types of ROS [55]. The pH of the medium may influence the scavenging capacity of CeO₂ NMs, causing differences in the type of free radicals removed by the NM [91]. On the other hand, the genotoxic effect of CeO₂ NMs is thought to be due to the presence of ROS and DNA oxidation damage [58, 94]. It has been postulated that the valence state of cerium influences whether CeO₂ NMs produce ROS or act as antioxidant, since the cerium atom in the CeO₂ molecule can transition between Ce³⁺ and Ce⁴⁺, thus varying the number of oxygen atoms it can bind to [39, 55, 98]. This dual mechanism of action has been proposed to be associated with cell characteristics, with prooxidant effects emerging in tumoral cells [63]. However, no prooxidant effects were observed, regardless of the conditions/cells used, in a recent study using a wide set of cell lines and different culture conditions [60]. More studies are needed to confirm the data presented here, using a battery of genotoxicity assays associated

with new approach methods to reach firm conclusions about the genotoxicity of these NMs.

14.3.4 Genotoxicity of Ag Nanomaterial (NM-302)

There has been a great increase in the application of silver NMs as antimicrobial agents in multiple end products as well as in biomedicine, Ag nowadays being one of the most popular NMs [27, 33, 34, 99]. Ag NM potential toxicity has been extensively studied and both cyto- and genotoxicity, have been reported [15, 16, 24, 54, 62–66, 70, 72, 73, 74]. Nevertheless, additional data are still required to assess its carcinogenic potential [99].

Concerning the toxicity assessment, after exposure of V79 cells for 24 h to NM-302, a

more than 30% decrease in PE (Fig. 14.3c) was observed at the lowest and highest concentrations (1 and 75 $\mu\text{g}/\text{cm}^2$) tested in the PE assay. Still, no alterations were noted in replication indices – RI and CBPI – from the CBMN assay (48 h exposure), for all tested concentrations (Fig. 14.3b). Concerning genotoxicity, in our study NM-302 did not cause significant increases in DNA damage or oxidation damage comparatively to the negative control (Fig. 14.3a). However, treatment of cells with NM-302 at 3 $\mu\text{g}/\text{cm}^2$ produced a significant increase in the level of DNA oxidation lesions over the basal level (without Fpg) ($P = 0.044$, Student's t-test), suggesting the formation of oxidised bases. No effect on micronucleated cells formation was observed after NM-302 exposure (48 h), with the CBMN assay.

Contrasting results are found in the literature concerning Ag NM cyto- and genotoxicity, which

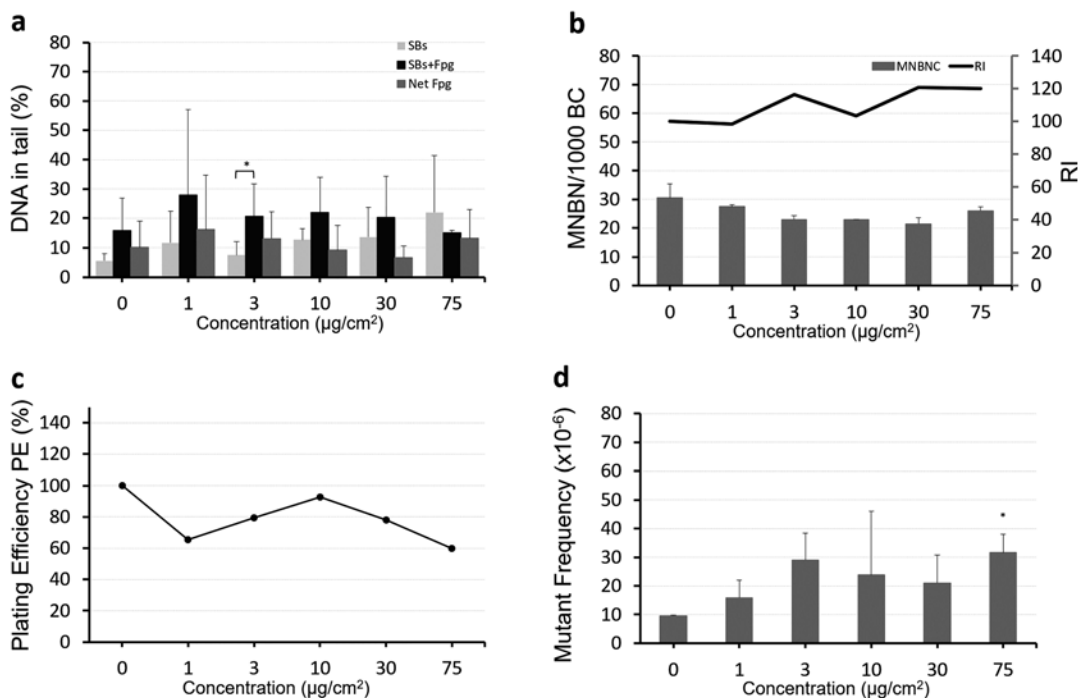


Fig. 14.3 Results obtained in V79 cells exposed for 24 h to NM-302 using (a) the comet assay with (SBs + Fpg) and without (SBs) enzyme treatment; (b) the cytokinesis-block micronucleus assay, expressed as micronucleated binucleated cells (MNBNC) in 1000 binucleated cells (bars, primary axis) and replication index (RI; line, secondary axis); (c) the plating efficiency (PE %) as a mea-

surement of cytotoxicity; and (d) the HPRT test to measure the mutation frequency, MF ($\times 10^{-6}$), expressed as the mean \pm standard deviation ($M \pm SD$) of two independent harvests from one experiment. Data are expressed as the means \pm SD. P values indicate statistically significant differences from unexposed cells, or between SBs and SBs + Fpg; $*p < 0.05$. SB strand breaks

are probably related to the different physico-chemical properties of Ag NMs, namely size, shape, charge and surface coating. The negative findings presented in this study may be related to the size of NMs, as smaller Ag NMs were found to be more cytotoxic, genotoxic and stronger inducers of ROS production compared to larger Ag NMs [15, 71, 100, 101]. In different cell lines (A549, HepG2 and HT-29), after exposure to different Ag NM sizes (20 and 200 nm), a size-related genotoxic effect was observed with the comet assay, but not with the MN assay [72]. Also in A549 cells, the genotoxicity assessment of Ag NMs differing in size (with the same shape, charge and chemical composition, including the stabilizing coating) showed strong cytotoxic and genotoxic effects for the 50 nm but not for the 200 nm NM; the latter, however, showed the strongest mutagenic potential [15]. In agreement with that observation, the highest DNA tail intensity values were found in CHO-K1 and CHO-XRS5 cells exposed to 2.5 µg/mL of 10 nm Ag NMs compared with 100 nm Ag NMs, although an opposite effect was reported using the CBMN assay [102]. Interestingly, low concentrations (<5 µg/mL) of 20 nm PVP-coated Ag NMs were more cytotoxic than 10 nm PVP-coated Ag NMs, while at higher doses (>50 µg/mL), the latter exhibited higher toxicity and induced severe DNA damage in A549 cells, as measured with the comet assay; cell cycle arrest at G2 phase and late-stage apoptosis were also observed [69]. Shape has also been shown to have a significant impact on Ag NM cyto- and genotoxicity. The silver NMs used in this study were shaped as long nanowires/nanorods (5–10 µm), which has been proposed to be a naturally toxic shape, i.e., more toxic than the analogous materials in particulate and non-fibrous forms. More precisely, in the respiratory tract inhaled biopersistent fibers may have the ability to travel through the airways and deposit inside the lungs, puncturing the tissue and producing chronic effects such as inflammation and fibrosis [103]. Limited information is currently available on the genotoxicity of silver nanorods/wires. Comparatively, exposure to Ag NM-300 K (spherical) was found to induce significant cytotoxicity and DNA damage in both

A549 and BEAS-2B, although DNA oxidation damage was detected only in A549 cells [54]. Increased MN formation without a clear direct concentration-effect relationship was observed in BEAS-2B cells [63]. In line with these findings, another study showed NM-300 K cytotoxicity in A549 cells and an induction of DNA damage in A549 or TK6 cells, independently of the exposure time (3 or 24 h), mainly due to DNA oxidation damage, as measured with the Fpg-comet assay [24].

The organic coating surrounding the silver particles may also be of importance to the cyto- and genotoxic effects, as previously stated, because it may interfere with the particles' agglomeration/aggregation status and, consequently, with their toxicity [71, 104]. Since the NM-302 is encapsulated by an organic polymer, it is unclear whether a protein corona was formed or not, and if it interfered with the results. Another aspect that could potentially cause toxicity is the liquid dispersant solution used to solubilize the nanoparticles (polyvinyl-pyrrolidone, acrylic/acrylate copolymer and polycarboxylate ether); however, V79 cells exposed to several concentrations of this dispersant solution were tested alongside the NM replicates, and neither cell viability nor DNA stability was affected (data not shown). In V79 cells, the cytotoxic effect of Ag NMs as measured by the PE assay was influenced by different charge and surface composition (negative: Ag Citrate and Ag sodium dodecyl sulfate (SDS); neutral: Ag Disperbyk-192® and Ag Tween 80®; positive: Ag Chitosan and Ag BYK-9076® [16]. Additionally, in TK6 cells, the impact of Ag NMs on the level of strand breaks and cryostasis was found to be both charge- and surface coating-dependent, with positively charged Ag NMs being the most cytostatic and genotoxic, although slight but significant increases in DNA breaks were found also in cells exposed to citrate-coated Ag [16]. For the latter, negative findings were reported using the comet assay on BEAS-2B cells exposed to citrate-coated Ag NMs of different primary particle sizes (10, 40 and 75 nm) as well as to 10 nm PVP-coated and 50 nm uncoated Ag NMs, for 4 h exposure [71]. In contrast, in BEAS-2B cells

exposed to different concentrations (2.5–240 $\mu\text{g}/\text{mL}$) of PVP-stabilized Ag NMs (42.5 ± 14.5 nm), DNA damage and intracellular ROS induction were observed using the comet assay (≥ 60.8 $\mu\text{g}/\text{mL}$), for treatments lasting 4 and 24 h, while no induction of MN or chromosome aberrations was observed [74]. Nevertheless, other studies using PVP-coated Ag NMs reported a positive CBMN assay in TK6 cells [68].

Finally, this study showed that all NM-302 concentrations, except the lowest one (1 $\mu\text{g}/\text{cm}^2$) induced at least a 2-fold increase in the *Hprt* MF, when compared to the negative control (Fig. 14.3d); a 3-fold increase was observed at concentrations of 3 and 75 $\mu\text{g}/\text{cm}^2$, suggesting a mutagenic effect of this NM. Our findings are aligned with results from previous studies performed in V79 cells. PVP-stabilized quasi-spherical Ag NMs (50 nm, 80 nm and 200 nm) induced size- dependent mutations in the *Hprt* gene of V79-4 cells after exposure to 0.21, 1.1, 5.3 and 15.9 $\mu\text{g}/\text{cm}^2$ [15]. As seen in our study, an increase of *Hprt* MF followed by a concentration-dependent decrease was observed, irrespective of the NM size. Particularly for the Ag NM 200 nm, a MF decrease was observed between 1.1 $\mu\text{g}/\text{cm}^2$ and 5.3 $\mu\text{g}/\text{cm}^2$, while in our study the number of mutants decreased in the intermediate doses (between 3 and 30 $\mu\text{g}/\text{cm}^2$). The authors suggested that this might have been due to larger genetic alterations being induced by higher NM concentrations that consequently reduced the viability of the mutant cells, resulting in an overall lower MF. These authors also showed that small (8 nm; spherical shape) Ag NMs with different charges and surface compositions (six different capping agents) induced gene mutations in V79-4 cells [16], but no reverse-concentration response was observed, attributed possibly to differences in the investigated materials. In the first study [15], PVP was applied to prevent protein binding to the surface of Ag NMs, their agglomeration and Ag dissolution; thus Ag NMs kept their primary shape and size during all exposure times in contrast to Ag NMs tested in the later study [16]. Also, the concentration-range differed in the two experiments (0.6–2.56 $\mu\text{g}/\text{cm}^2$ for the latter), way below the concentration at which the

MF started to decrease in the first study. Therefore, different ranges of tested concentrations can also explain other biological responses [16]. The capacity of two types of Ag NMs (spherical NM-300 and fibrous nanorods/wires NM- 302) to induce thymidine kinase (*Tk+/-*) mutations in L5178Y mouse lymphoma cells (MLA TK) and transformed foci in Bhas 42 cells (CTA) was also investigated [75]. Spherical NM-300 showed neither mutagenic nor carcinogenic potential, contrasting with silver nanorods/wires (NM-302), that showed a significantly increase in the number of both gene mutations and transformed foci compared with the control cells, suggesting that fibrous shape underlies the mutagenic and carcinogenic potential of nanosilver [75]. Interestingly, in the MLA TK assay, NM-302 silver nanorods/wires induced a significant increase in MF (small colonies) at all but the lowest concentration tested. An increase in large colonies was observed at 1 and 3 $\mu\text{g}/\text{cm}^3$, followed by a decrease at higher doses, increasing again at the 100 $\mu\text{g}/\text{cm}^3$ dose, i.e., displaying a trend similar to the one observed in our study. This was also observed for the NM-302 in the CTA, where a concentration-dependent increase in the number of transformed Bhas 42 cells was observed up to the 1 $\mu\text{g}/\text{cm}^2$ concentration, followed by a decrease observed at 3 $\mu\text{g}/\text{cm}^2$ and 10 $\mu\text{g}/\text{cm}^2$ [75]. Also using the MLA TK assay, cells exposure to all six types of Ag NMs (PVP- or citrate-coated 20-, 50-, and 100-nm) and ionic silver at concentration ranges of 1–60 $\mu\text{g}/\text{mL}$ and 0.4–0.65 $\mu\text{g}/\text{mL}$, respectively, led to mutagenicity influenced by size and coating, with the smallest citrate-coated Ag NM (20 nm) displaying higher mutagenic potency, only lower than the ionic Ag that displayed the highest mutagenic potency (and cytotoxicity) [64]. The same group previously detected concentration-dependent cytotoxicity and mutagenicity produced by 5 nm uncoated Ag NMs using the MLA TK assay, at doses of 3–6 $\mu\text{g}/\text{mL}$ [73]. Overall, a substantial number of studies have addressed the genotoxicity and mutagenicity of Ag NMs. Inconsistent results have been reported, and this is not surprising given the diversity of Ag NMs existent, with diverging physicochemical properties, including

surface modifications. Based on our study and comparing with the findings of the above-mentioned studies, a possible mutagenic effect of Ag NM-302 is suggested, particularly at low concentration-ranges. Further experiments to explore low concentrations for induction of potential mutagenicity (around 0.1 and 5.3 $\mu\text{g}/\text{cm}^2$) would be of interest.

14.3.5 Comparing Results Between Comet, Micronucleus and HPRT Assays

In this chapter we report data on three benchmark metal-based NMs obtained in three different genotoxicity assays: the comet assay (and its Fpg-modified version), the CBMN assay and the HPRT mutation test. An overview of the results obtained is presented in Table 14.4. Negative and positive historical values for the V79 cells were available for the HPRT test; the positive control (MMS; 0.1 mM, 30 min), induced 38.1 ± 5.23 ($\times 10^{-6}$) MF, corresponding to a significantly four-fold increase compared with the negative control, while the negative control ($9.59 \pm 0.19 \times 10^{-6}$) is in the range of historical values [10, 15, 16, 20]. No historical values were available for V79 cells either for the comet assay or for CBMN. For the comet assay, the positive control (H_2O_2) induced statistically significant DNA damage compared with the control (77.51 ± 8.02 , without Fpg; 81.63 ± 6.55 , with Fpg; 7.24 ± 15.62 net Fpg). For the CBMN assay, the positive control (MMC, 0.1 $\mu\text{g}/\text{mL}$) induced 267 MNBNC/1000 BNC and a RI = 58.1%, being significantly increased

compared to the negative control ($p = 0.043$; Mann-Whitney test). Nevertheless, for the sake of comparability within this study, criteria for a positive/negative result were established based on current recommendations [105].

As can be seen, some differences between the outcomes obtained for each NM were noted using this battery of tests. Such differences have been frequently described in the literature [4, 82, 90, 106] and can be due to distinct endpoints measured by each of the tests, reflecting differences in the mechanisms underlying the genotoxic effects, or may be related to different assay sensitivities [4, 90, 106, 107]. Our results demonstrate discrepancies particularly between the comet and MN assays results. No DNA damage was detected following exposure of cells to NM-212 or NM-302, whereas exposure to NM-100 induced DNA damage at the highest concentrations tested (30 and 75 $\mu\text{g}/\text{cm}^2$). On the other hand, the MN assay result was negative for both NM-100 and NM-302, but the frequency of micronucleated cells was increased following exposure to the highest dose of NM-212. The comet assay identifies a broad spectrum of transient primary DNA lesions, namely single- and double-strand DNA breaks, alkali-labile lesions that are converted to strand breaks under alkaline conditions, or breaks associated with incomplete excision repair sites. Such primary lesions usually arise soon after exposure to genotoxic agents and may be easily repaired by the cellular DNA repair machinery, or otherwise result in gene or chromosome alterations. On the other hand, micronuclei reflect persistent chromosome alterations. Indeed, larger DNA lesions that survive at

Table 14.4 Outcomes of the toxicological testing of the NMs in this study

NM	Comet	Fpg-Comet	CBMN	HPRT test	PE	CBPI/RI
NM-100	+	+	–	+	(+)	–
NM-212	–	(+)	(+)	(+)	(+)	–
NM-302	–	–	–	(+)	+	–

+, POSITIVE - No significant concentration-dependent effect for the endpoint analysed, ≥ 2 concentrations causing a significant effect over control; (+), EQUIVOCAL - No significant concentration-dependent effect, 1 concentration causing a significant effect; –, NEGATIVE - none of the criteria for a positive result are met according to [105]. CBPI cytokinesis-blocked proliferation index, RI replication Index, CBMN cytokinesis-block micronucleus assay

least one mitotic cycle reflect irreversibly unrepaired chromosomal damage, corresponding to clastogenic (chromosomal fragmentation) or aneugenic (changes in chromosome copy number) events. In a review of 38 studies in which both the comet and CBMN assays have been used following exposure to 66 NMs, a good overall consistency between assays was found (69%) [107]. However, a higher inconsistency was observed for TiO₂ NMs, given that 19 out of 22 TiO₂ NM analyzed induced DNA strand breakage (86%), only 7 (32%) displayed positive MN results and 9 (41%) showed consistent results between both assays [107]. Moreover, a recent review of TiO₂ NM *in vitro* genotoxic studies from 2010 to 2016, demonstrated that approximately 63% of the studies using the comet assay presented positive results, while only 35% using the MN assay showed positive results [51]. Also, according to Elespuru et al. [5], most of the studies on metal-based NMs, such as Ag, CeO₂, and to a lesser extent TiO₂ NMs, tended to yield positive results using either the Fpg method or the standard method [5].

The differences observed between assays are thought to be related to different sensitivities, measurement of different endpoints, variation in experimental conditions and different secondary properties of TiO₂ in the tested media [107]. For example, concerning Ag, both consistent and inconsistent results between assays found in the literature are, as already discussed, strongly influenced by the size, shape and coating, which might lead to different cyto- and genotoxic outcomes. Larger Ag NMs (200 nm) were found to be the most mutagenic, while small particles (50 nm) were the most cytotoxic and genotoxic [15, 75]. In the case of TiO₂, different states and sizes of agglomeration resulted in different genotoxicity responses, using the comet assay in 3 different cell lines, with larger agglomerates of dispersed TiO₂ inducing DNA damage in all cell lines, as opposed to no effect on genotoxicity with agglomerates smaller than 200 nm [84].

Also, the type and the repair capacities of the cells used, the stage of cell cycle, and the duration between exposure and analysis will contribute to the differences in sensitivity between the

MN and comet assays [108]. For TiO₂ NMs, crystallinity, particle size, cell line and exposure duration are thought to be the main variables influencing data obtained with the comet assay, while MN formation could be influenced by size, coating, exposure duration, and TiO₂ NM concentration [86]. Since we used the same cell line and exposure conditions in both assays, except for the exposure duration (24 h, for the comet assay; 48 h, for the MN assay), the differences observed between the assays are more likely to be attributable to their mechanism of action or exposure duration. Thus, these two methods provide complementary information allowing a broader interpretation of the biological effects of NMs. It is worth noting that NM overload can occur at higher NM doses, leading to erroneous data interpretation and therefore the dose-range should be carefully selected. For example, in the MN assay, a decreased number of MNBC cells was observed with the increasing concentration of TiO₂ NM-100, which might have been related to a physical interference of the NMs with the cell scoring for MN, as previously reported by others [106, 109]. As cytochalasin B was added to cells 24 h after the NM exposure, it is unlikely that interference with NM uptake occurred. This interference has been associated with negative results with this assay in other studies [3, 51, 68, 110, 111].

There were only a few studies applying both the HPRT mutation test and the comet and/or MN tests for the metal-based NMs analyzed here, and overall consistency between assays was observed [12–16, 53]. Concerning TiO₂ NMs, increased MF and % Tail DNA after 6 h [13] and 24 h exposure [12] were observed in V79 cells. Also, increased MN frequency, DNA damage level and *Hprt* gene MF were observed in WL2-NS cells [14], while following a long-term (60 days) exposure using both comet assay and HPRT test in CHO-K1 cells, no effects were observed [53]. Concerning Ag NMs, PVP-stabilized quasi-spherical Ag NMs (50 nm, 80 nm, 200 nm) induced strand breaks, DNA oxidation, inflammation and gene mutation but different cell lines were used for the different endpoints (the HPRT test was applied in V79 cells, while the other end-

points were assessed in A549 cells) [15]. In fact, the MF decreased with increasing doses, while a dose-dependent increase in DNA damage was observed [15]. Also, different Ag NMs caused DNA damage and gene mutation, in TK6 and V79 cells, respectively [16].

Overall, our results with the HPRT test showed an increase in MF for the NMs tested, particularly for the lowest concentrations (although no concentration-response was observed) suggesting that the metal-based NMs studied can be mutagenic to cells exposed to low concentrations. Additionally, the increase in MF observed for the lowest concentrations was always followed by a decrease and then by an increase at the highest dose. During the HPRT experiments we observed for all NMs that the NMs could not effectively be washed off the cells, particularly at the highest dose; thus, the true exposure period may have been longer than that initially anticipated, possibly leading to higher levels of damage than expected at the highest concentration. This issue was previously reported when performing the HPRT test (OECD 476) for different NMs [3].

14.4 Conclusions

In conclusion, differential genotoxicity potential for the tested metal-based NMs was observed in V79 cells. The results obtained generally agreed with previous results and confirm the importance of investigating the toxic potential of each NM individually, instead of assuming a common mechanism and similar genotoxic effects for a set of similar NMs, such as metallic NMs. The use of a medium throughput version of the comet assay to measure DNA damage and, particularly, the use of the enzyme Fpg allowed the detection of oxidative damage to DNA, and at the same time increased assay robustness while reducing experimental variability and time. Our preliminary results point to the *Hprt* gene mutation assay together with the Fpg comet assay, as being more sensitive to identify genotoxic effects of metal-based NMs, particularly in the case of TiO₂, as already reported [12, 13, 87]. In fact, the

results of the HPRT test, although equivocal (since no dose response could be established), contrast with the overall negative results observed, particularly, for the MN assay. Particularly for NM-100 or NM-302, the importance of using different assays was made clear, which highlights the importance of assessing different endpoints to study the genotoxicity of NMs, since no single genotoxic assay has the capacity to evaluate every type of DNA damage inducible by a NM, namely, strand breaks, aneuploidic, clastogenic and mutagenic effects [24].

Our study corroborates the usefulness of a mammalian gene mutation assay (such as the HPRT test) as a concurrent method to assess the risk of metal and metal oxide NMs. Mammalian gene mutation test and MN assay are required for safety evaluation, by ECHA, under REACH [112, 113] and by other regulatory entities such as EFSA or Scientific Committee on Consumer Safety (SCCS) for safety evaluation of NMs in food and cosmetics, respectively [9, 114]. Additionally, in the recently proposed amendment (in consultation) to specific extracts of Appendix R7-1 and R7-2 of ECHA guidance, the standard and Fpg comet assay for detection of strand breaks and DNA oxidation lesions was suggested for *in vivo* studies [115], being also recommended as an *in vitro* indicator test for cosmetics [114].

Our results support the use of this test battery as a first stage in the *in vitro* screening of NMs, provided that standardized protocols exist, including for NM preparation, and that the physicochemical characteristics of the NMs are considered.

Acknowledgments We thank Iren Elisabeth Sturtzel for her excellent help with experiments. Authors also thank Professor Andrew Collins for language corrections.

This research was co-funded by the EC FP7 NANoREG (Grant Agreement NMP4-LA-2013-310584), the EC QualityNano Research Infrastructure project (Grant Agreement No: INFRA-2010-262163), through the QualityNano Transnational Access fellowships [NILU-TAF-410 and NILU-TAF-403] attributed to N. Vital and M. J. Silva and by the Portuguese Foundation for Science and Technology through ToxOmics (UIDB/00009/2020; UIDP/00009/2020). N. Vital work is

also supported by the Portuguese Foundation for Science and Technology PhD Scholarship 2020.07168.BD.

References

- Bettencourt A, Gonçalves LM, Gramacho AC, Vieira A, Rolo D, Martins C et al (2020) Analysis of the characteristics and cytotoxicity of titanium dioxide nanomaterials following simulated *in vitro* digestion. *Nano* 10(8):1516. <https://doi.org/10.3390/nano10081516>
- Collins AR, Annangi B, Rubio L, Marcos R, Dorn M, Merker C et al (2017) High throughput toxicity screening and intracellular detection of nanomaterials. *Wiley Interdiscip Rev Nanomed Nanobiotechnol* 9(1):e1413. <https://doi.org/10.1002/wnan.1413>
- Doak SH, Manshian B, Jenkins GJS, Singh N (2012) *In vitro* genotoxicity testing strategy for nanomaterials and the adaptation of current OECD guidelines. *Mutat Res Genet Toxicol Environ Mutagen* 745(1–2):104–111. <https://doi.org/10.1016/j.mrgentox.2011.09.013>
- Louro H, Saruga A, Santos J, Pinhão M, Silva MJ (2019) Biological impact of metal nanomaterials in relation to their physicochemical characteristics. *Toxicol In Vitro* 56:172–183. <https://doi.org/10.1016/j.tiv.2019.01.018>
- Elespuru R, Pfuhrer S, Aardema MJ, Chen T, Doak SH, Doherty A et al (2018) Genotoxicity assessment of nanomaterials: recommendations on best practices, assays, and methods. *Toxicol Sci* 164(2):391–416. <https://doi.org/10.1093/toxsci/kfy100>
- Louro H, Bettencourt A, Gonçalves LM, Almeida A, Silva MJ (2015) Role of nanogenotoxicology studies in safety evaluation of NMs. In: Thomas S, Grohens Y, Ninan N (eds) *Nanotechnology applications for tissue engineering*, vol. 1, issue 1. William Andrew Publishing/Elsevier, pp 263–297. <https://doi.org/10.1016/B978-0-323-32889-0.00016-9>
- Kohl Y, Rundén-Pran E, Mariussen E, Hesler M, El Yamani N, Longhin EM, Dusinska M (2020) Genotoxicity of nanomaterials: advanced *in vitro* models and high throughput methods for human hazard assessment – a review. *Nano* 10(10):1911. <https://doi.org/10.3390/nano10101911>
- Huk A, Collins AR, El Yamani N, Porredon C, Azqueta A, De Lapuente J, Dusinska M (2015b) Critical factors to be considered when testing nanomaterials for genotoxicity with the comet assay. *Mutagenesis* 30(1):85–88. <https://doi.org/10.1093/mutage/geu077>
- EFSA Scientific Committee, Hardy A, Benford D, Halldorsson T, Jeger MJ, Knutsen HK, More S et al (2018) Guidance on risk assessment of the application of nanoscience and nanotechnologies in the food and feed chain: part 1, human and animal health. *EFSA J* 16(7):e5327. <https://doi.org/10.2903/j.efs.2018.5327>
- Kazimirova A, El Yamani N, Rubio L, García-Rodríguez A, Barancokova M, Marcos R, Dusinska M (2020) Effects of titanium dioxide nanoparticles on the *Hprt* gene mutations in V79 hamster cells. *Nano* 10(3):465. <https://doi.org/10.3390/nano10030465>
- Magdolenova Z, Collins A, Kumar A, Dhawan A, Stone V, Dusinska M (2014) Mechanisms of genotoxicity. A review of *in vitro* and *in vivo* studies with engineered nanoparticles. *Nanotoxicology* 8(3):233–278. <https://doi.org/10.3109/17435390.2013.773464>
- Chen Z, Wang Y, Ba T, Li Y, Pu J, Chen T et al (2014a) Genotoxic evaluation of titanium dioxide nanoparticles *in vivo* and *in vitro*. *Toxicol Lett* 226(3):314–319. <https://doi.org/10.1016/j.toxlet.2014.02.020>
- Jain AK, Senapati VA, Singh D, Dubey K, Maurya R, Pandey AK (2017) Impact of anatase titanium dioxide nanoparticles on mutagenic and genotoxic response in Chinese hamster lung fibroblast cells (V-79): the role of cellular uptake. *Food Chem Toxicol* 105:127–139. <https://doi.org/10.1016/j.fct.2017.04.005>
- Wang JJ, Sanderson BJS, Wang H (2007) Cytotoxicity and genotoxicity of ultrafine TiO₂ particles in cultured human lymphoblastoid cells. *Mutat Res Genet Toxicol Environ Mutagen* 628(2):99–106. <https://doi.org/10.1016/j.mrgentox.2006.12.003>
- Huk A, Izak-Nau E, Reidy B, Boyles M, Duschl A, Lynch I, Dušinska M (2014) Is the toxic potential of nanosilver dependent on its size? *Part Fibre Toxicol* 11:65. <https://doi.org/10.1186/s12989-014-0065-1>
- Huk A, Izak-Nau E, El Yamani N, Uggerud H, Vadset M, Zasonska B et al (2015a) Impact of nanosilver on various DNA lesions and *HPRT* gene mutations – effects of charge and surface coating. *Part Fibre Toxicol* 12:25. <https://doi.org/10.1186/s12989-015-0100-x>
- Asakura M, Sasaki T, Sugiyama T, Takaya M, Koda S, Nagano K et al (2010) Genotoxicity and cytotoxicity of multi-wall carbon nanotubes in cultured Chinese hamster lung cells in comparison with chrysotile a fibers. *J Occup Health* 52(3):155–166. <https://doi.org/10.1539/joh.L9150>
- Manshian BB, Jenkins GJS, Williams PM, Wright C, Barron AR, Brown AP et al (2013) Single-walled carbon nanotubes: differential genotoxic potential associated with physico-chemical properties. *Nanotoxicology* 7(2):144–156. <https://doi.org/10.3109/17435390.2011.647928>
- Mrakovcic M, Meindl C, Leitinger G, Roblegg E, Fröhlich E (2015) Carboxylated short single-walled carbon nanotubes but not plain and multi-walled short carbon nanotubes show *in vitro* genotoxicity. *Toxicol Sci* 144(1):114–127. <https://doi.org/10.1093/toxsci/kfu260>

20. Rubio L, El Yamani N, Kazimirova A, Dusinska M, Marcos R (2016a) Multi-walled carbon nanotubes (NM401) induce ROS-mediated *HPRT* mutations in Chinese hamster lung fibroblasts. *Environ Res* 146:185–190. <https://doi.org/10.1016/j.envres.2016.01.004>
21. Guichard Y, Fontana C, Chavinier E, Terzetti F, Gaté L, Binet S, Darne C (2016) Cytotoxic and genotoxic evaluation of different synthetic amorphous silica nanomaterials in the V79 cell line. *Toxicol Ind Health* 32(9):1639–1650. <https://doi.org/10.1177/0748233715572562>
22. Åkerlund E, Cappellini F, Di Bucchianico S, Islam S, Skoglund S, Derr R et al (2018) Genotoxic and mutagenic properties of Ni and NiO nanoparticles investigated by comet assay, γ -H2AX staining, *Hprt* mutation assay and ToxTracker reporter cell lines. *Environ Mol Mutagen* 59(3):211–222. <https://doi.org/10.1002/em.22163>
23. Doak SH, Griffiths SM, Manshian B, Singh N, Williams PM, Brown AP, Jenkins GJS (2009) Confounding experimental considerations in nanogenotoxicology. *Mutagenesis* 24(4):285–293. <https://doi.org/10.1093/mutage/geb010>
24. El Yamani N, Collins AR, Rundén-Pran E, Fjellsbø LM, Shaposhnikov S, Zienolddiny S, Dusinska M (2017) In vitro genotoxicity testing of four reference metal nanomaterials, titanium dioxide, zinc oxide, cerium oxide and silver: towards reliable hazard assessment. *Mutagenesis* 32(1):117–126. <https://doi.org/10.1093/mutage/gew060>
25. Di Bucchianico S, Cappellini F, Le Bihanic F, Zhang Y, Dreij K, Karlsson HL (2017) Genotoxicity of TiO₂ nanoparticles assessed by mini-gel comet assay and micronucleus scoring with flow cytometry. *Mutagenesis* 32(1):127–137. <https://doi.org/10.1093/mutage/gew030>
26. Harris G, Palosaari T, Magdolenova Z, Mennecozzi M, Gineste JM, Saavedra L et al (2015) Iron oxide nanoparticle toxicity testing using high-throughput analysis and high-content imaging. *Nanotoxicology* 9(S1):87–94. <https://doi.org/10.3109/17435390.2013.816797>
27. Vance ME, Kuiken T, Vejerano EP, McGinnis SP, Hochella MF, Hull DR (2015) Nanotechnology in the real world: redeveloping the nanomaterial consumer products inventory. *Beilstein J Nanotechnol* 6:1769–1780. <https://doi.org/10.3762/bjnano.6.181>
28. Younis A, Chu D, Li S (2016) Cerium oxide nanostructures and their applications. In: Farrukh MA (ed) *Functionalized nanomaterials* (intechopen). <https://doi.org/10.5772/65937>
29. Fytianos G, Rahdar A, Kyzas GZ (2020) Nanomaterials in cosmetics: recent updates. *Nano* 10(5):979. <https://doi.org/10.3390/nano10050979>
30. He X, Deng H, Hwang HM (2019) The current application of nanotechnology in food and agriculture. *J Food Drug Anal* 27(1):1–21. <https://doi.org/10.1016/j.jfda.2018.12.002>
31. Peters RJB, Bouwmeester H, Gottardo S, Amenta V, Arena M, Brandhoff P et al (2016) Nanomaterials for products and application in agriculture, feed and food. *Trends Food Sci Technol* 54:155–164. <https://doi.org/10.1016/j.tifs.2016.06.008>
32. Ziental D, Czarzynska-Goslinska B, Mlynarczyk DT, Glowacka-Sobotta A, Stanisz B, Goslinski T, Sobotta L (2020) Titanium dioxide nanoparticles: prospects and applications in medicine. *Nano* 10(2):387. <https://doi.org/10.3390/nano10020387>
33. Nowack B, Krug HF, Height M (2011) 120 years of nanosilver history: implications for policy makers. *Environ Sci Technol* 45:1177–1183. <https://doi.org/10.1021/es103316q>
34. Calderón-Jiménez B, Johnson ME, Montoro Bustos AR, Murphy KE, Winchester MR, Baudrit JRV (2017) Silver nanoparticles: technological advances, societal impacts, and metrological challenges. *Front Chem* 5:1–26. <https://doi.org/10.3389/fchem.2017.00006>
35. Khin MM, Nair AS, Babu VJ, Murugan R, Ramakrishna S (2012) A review on nanomaterials for environmental remediation. *Energy Environ Sci* 5(8):8075–8109. <https://doi.org/10.1039/c2ee21818f>
36. Lee SH, Jun BH (2019) Silver nanoparticles: synthesis and application for nanomedicine. *Int J Mol Sci* 20(4):865. <https://doi.org/10.3390/ijms20040865>
37. Saleem H, Zaidi SJ (2020) Sustainable use of nanomaterials in textiles and their environmental impact. *Materials* 13(22):2134. <https://doi.org/10.3390/ma13225134>
38. De Souza TAJ, Rocha TL, Franchi LP (2018) Detection of DNA damage induced by cerium dioxide nanoparticles: from models to molecular mechanism activated. In Saquib Q, Faisal M, Al-Khedhairi A, Alatar A (eds) *Cellular and molecular toxicology of nanoparticles*. Advances in experimental medicine and biology, 1048, pp 215–226. https://doi.org/10.1007/978-3-319-72041-8_13
39. Reed K, Cormack A, Kulkarni A, Mayton M, Sayle D, Klaessig F, Stadler B (2014) Exploring the properties and applications of nanocerium: is there still plenty of room at the bottom? *Environ Sci Nano* 1(5):390–405. <https://doi.org/10.1039/c4en00079j>
40. Singh K, Nayak V, Sarkar T, Singh RP (2020) Cerium oxide nanoparticles: properties, biosynthesis and biomedical application. *RSC Adv* 10(45):27194–27214. <https://doi.org/10.1039/d0ra04736h>
41. Dhall A, Self W (2018) Cerium oxide nanoparticles: a brief review of their synthesis methods and biomedical applications. *Antioxidants* 7(8):97. <https://doi.org/10.3390/antiox7080097>
42. OECD (2010) OECD series on the safety of manufactured nanomaterials, No 27. List of manufactured nanomaterials and list of endpoints for phase one of the sponsorship programme for the testing of manufactured nanomaterials: revision. ENV/JM/MONO(2010)46, OECD Publishing, Paris

43. OECD (2015) OECD Series on the Safety of Manufactured Nanomaterials, No. 45. Dossier on cerium oxide. ENV/JM/MONO(2015)8, OECD Publishing, Paris
44. OECD (2016a) Titanium dioxide: summary of the dossier. In: Series on the safety of manufactured nanomaterials. No. 73 ENV/JM/MONO, 25 OECD Environment, Health and Safety Publications, vol. 73
45. OECD (2017a) OECD series on the safety of manufactured nanomaterials, No. 83. silver nanoparticles: summary of the dossier. ENV/JM/MONO(2017)31. OECD Publishing, Paris
46. ECHA (2014) Community rolling action plan (CoRAP) update covering years 2014, 2015 and 2016. Retrieved from https://echa.europa.eu/documents/10162/13628/corap_list_2014-2016_en.pdf
47. ECHA (2018) Community rolling action plan update covering years 2016, 2017 and 2018. Retrieved from https://echa.europa.eu/documents/10162/13628/corap_update_20172019_en.pdf/6a394595-a4e5-0e10-ec66-eabdc55ce7f6
48. ECHA (2021a) Community rolling action plan (CoRAP) update covering the years 2021, 2022 and 2023. Retrieved from https://echa.europa.eu/documents/10162/9801478/corap_update_2021-2023_en.pdf/fdb46fb0-21a2-1ab7-3ce2-74dbe509a60f
49. IARC (2010) IARC Monographs on the evaluation of carcinogenic risks to humans: carbon black, titanium dioxide, and talc. Vol. 93, Lyon, France. <https://doi.org/10.1136/jcp.48.7.691-a>
50. Dankovic DA, Kuempel ED (2011) Occupational exposure to titanium dioxide National Institute for Occupational Safety and Health (ed.). NIOSH Current Intelligence Bulletin, 63. <https://stacks.cdc.gov/view/cdc/5922>
51. Charles S, Jomini S, Fessard V, Bigorgne-Vizade E, Rousselle C, Michel C (2018) Assessment of the *in vitro* genotoxicity of TiO₂ nanoparticles in a regulatory context. *Nanotoxicology* 12(4):357–374. <https://doi.org/10.1080/17435390.2018.1451567>
52. EFSA Panel on Food Additives and Flavourings, Younes M, Aquilina G, Castle L, Engel K-H, Fowler P et al (2021) Scientific opinion on the safety assessment of titanium dioxide (E171) as a food additive. *EFSA J* 19(5):e6585. <https://doi.org/10.2903/j.efsa.2021.6585>
53. Wang S, Hunter LA, Arslan Z, Wilkerson MG, Wickliffe JK (2011) Chronic exposure to nanosized, anatase titanium dioxide is not cyto- or genotoxic to Chinese hamster ovary cells. *Environ Mol Mutagen* 52(8):614–622. <https://doi.org/10.1002/em.20660>
54. García-Rodríguez A, Rubio L, Vila L, Xamena N, Velázquez A, Marcos R, Hernández A (2019a) The comet assay as a tool to detect the genotoxic potential of nanomaterials. *Nano* 9(10):1385. <https://doi.org/10.3390/nano9101385>
55. Xu C, Qu X (2014) Cerium oxide nanoparticle: a remarkably versatile rare earth nanomaterial for biological applications. *NPG Asia Materials* 6:e90. <https://doi.org/10.1038/am.2013.88>
56. De Marzi L, Monaco A, De Lapuente J, Ramos D, Borrás M, Gioacchino D et al (2013) Cytotoxicity and genotoxicity of ceria nanoparticles on different cell lines *in vitro*. *Int J Mol Sci* 14(2):3065–3077. <https://doi.org/10.3390/ijms14023065>
57. Frieke Kuper C, Gröllers-Mulderij M, Maarschalkerweerd T, Meulendijks NMM, Reus A, van Acker F et al (2015) Toxicity assessment of aggregated/agglomerated cerium oxide nanoparticles in an *in vitro* 3D airway model: the influence of mucociliary clearance. *Toxicol In Vitro* 29(2):389–397. <https://doi.org/10.1016/j.tiv.2014.10.017>
58. Mittal S, Pandey AK (2014) Cerium oxide nanoparticles induced toxicity in human lung cells: role of ROS mediated DNA damage and apoptosis. *Biomed Res Int* 2014:891934. <https://doi.org/10.1155/2014/891934>
59. Rubio L, Annangi B, Vila L, Hernández A, Marcos R (2016b) Antioxidant and anti-genotoxic properties of cerium oxide nanoparticles in a pulmonary-like cell system. *Arch Toxicol* 90(2):269–278. <https://doi.org/10.1007/s00204-015-1468-y>
60. Rubio L, Marcos R, Hernández A (2018) Nanoceria acts as antioxidant in tumoral and transformed cells. *Chem Biol Interact* 291:7–15. <https://doi.org/10.1016/j.cbi.2018.06.002>
61. Rodríguez-Garraus A, Azqueta A, Vettorazzi A, de Cerain AL (2020) Genotoxicity of silver nanoparticles. *Nano* 10(2):251. <https://doi.org/10.3390/nano10020251>
62. Butler KS, Peeler DJ, Casey BJ, Dair BJ, Elespuru RK (2015) Silver nanoparticles: correlating nanoparticle size and cellular uptake with genotoxicity. *Mutagenesis* 30(4):577–591. <https://doi.org/10.1093/mutage/gev020>
63. García-Rodríguez A, Kazantseva L, Vila L, Rubio L, Velázquez A, Ramírez MJ et al (2019b) Micronuclei detection by flow cytometry as a high-throughput approach for the genotoxicity testing of nanomaterials. *Nano* 9(12):1677. <https://doi.org/10.3390/nano9121677>
64. Guo X, Li Y, Yan J, Ingle T, Jones MY, Mei N et al (2016) Size- and coating-dependent cytotoxicity and genotoxicity of silver nanoparticles evaluated using *in vitro* standard assays. *Nanotoxicology* 10(9):1373–1384. <https://doi.org/10.1080/17435390.2016.1214764>
65. Jiang X, Foldbjerg R, Miclaus T, Wang L, Singh R, Hayashi Y et al (2013) Multi-platform genotoxicity analysis of silver nanoparticles in the model cell line CHO-K1. *Toxicol Lett* 222(1):55–63. <https://doi.org/10.1016/j.toxlet.2013.07.011>
66. Kim HR, Kim MJ, Lee SY, Oh SM, Chung KH (2011) Genotoxic effects of silver nanoparticles stimulated by oxidative stress in human normal

- bronchial epithelial (BEAS-2B) cells. *Mutat Res Genet Toxicol Environ Mutagen* 726(2):129–135. <https://doi.org/10.1016/j.mrgentox.2011.08.008>
67. Li Y, Chen DH, Yan J, Chen Y, Mittelstaedt RA, Zhang Y, Biris AS et al (2012) Genotoxicity of silver nanoparticles evaluated using the Ames test and *in vitro* micronucleus assay. *Mutat Res Genet Toxicol Environ Mutagen* 745(1–2):4–10. <https://doi.org/10.1016/j.mrgentox.2011.11.010>
68. Li Y, Doak SH, Yan J, Chen DH, Zhou M, Mittelstaedt RA et al (2017) Factors affecting the *in vitro* micronucleus assay for evaluation of nanomaterials. *Mutagenesis* 32(1):151–159. <https://doi.org/10.1093/mutage/gew040>
69. Rosário F, Hoet P, Nogueira AJA, Santos C, Oliveira H (2018) Differential pulmonary *in vitro* toxicity of two small-sized polyvinylpyrrolidone-coated silver nanoparticles. *J Toxicol Environ Health A* 81(15):675–690. <https://doi.org/10.1080/15287394.2018.1468837>
70. Hackenberg S, Scherzed A, Kessler M, Hummel S, Technau A, Froelich K et al (2011) Silver nanoparticles: evaluation of DNA damage, toxicity and functional impairment in human mesenchymal stem cells. *Toxicol Lett* 201(1):27–33. <https://doi.org/10.1016/j.toxlet.2010.12.001>
71. Gliga AR, Skoglund S, Odnevall Wallinder I, Fadeel B, Karlsson HL (2014) Size-dependent cytotoxicity of silver nanoparticles in human lung cells: the role of cellular uptake, agglomeration and Ag release. *Part Fibre Toxicol* 11:11. <https://doi.org/10.1186/1743-8977-11-11>
72. Kruszewski M, Gradzka I, Bartłomiejczyk T, Chwastowska J, Sommer S, Grzelak A et al (2013) Oxidative DNA damage corresponds to the long term survival of human cells treated with silver nanoparticles. *Toxicol Lett* 219(2):151–159. <https://doi.org/10.1016/j.toxlet.2013.03.006>
73. Mei N, Zhang Y, Chen Y, Guo X, Ding W, Ali SF et al (2012) Silver nanoparticle-induced mutations and oxidative stress in mouse lymphoma cells. *Environ Mol Mutagen* 53(6):409–419. <https://doi.org/10.1002/em.21698>
74. Nymark P, Catalán J, Suhonen S, Järventausta H, Birkedal R, Clausen PA et al (2013) Genotoxicity of polyvinylpyrrolidone-coated silver nanoparticles in BEAS 2B cells. *Toxicology* 313(1):38–48. <https://doi.org/10.1016/j.tox.2012.09.014>
75. Gábelová A, El Yamani N, Alonso TI, Buliaková B, Srančíková A, Bábelová A et al (2017) Fibrous shape underlies the mutagenic and carcinogenic potential of nanosilver while surface chemistry affects the biosafety of iron oxide nanoparticles. *Mutagenesis* 32(1):193–202. <https://doi.org/10.1093/mutage/gew045>
76. OECD (2016b) Test No. 476: *in vitro* mammalian cell gene mutation tests using the *Hprt* and *xprt* genes. OECD guideline for the testing of chemicals, Section 4. OECD Publishing, Paris
77. OECD (2016c) Test No. 487: *in vitro* mammalian cell micronucleus test. OECD Guideline for the testing of chemicals, Section 4. OECD Publishing, Paris
78. Rasmussen K, Mast J, De Temmerman P-J, Verleysen E, Waegeneers N, Steen F V, ... Mech A (2014) Titanium dioxide, NM-100, NM-101, NM-102, NM-103, NM-104, NM-105: characterisation and Physico-chemical properties. JRC repository: NM-series of representative manufactured nanomaterials. Publications Office of the European Union, Luxembourg. <https://doi.org/10.2788/79554>
79. Singh C, Friedrichs S, Ceccone G, Gibson N, Alstrup Jensen K, Levin M, ... Rasmussen K (2014) Cerium Dioxide NM-211, NM-212, NM-213, characterisation and test item preparation. JRC repository: NM-series of representative manufactured nanomaterials. EUR 26649. Publications Office of the European Union, Luxembourg (Luxembourg). <https://doi.org/10.2788/80203>
80. Nanogenotox Partners (2013) Deliverable 6: Characterisation of MNs for their clastogenic/aneugenic effects or DNA damage potentials and correlation analysis. N.J. Action 120. Retrieved from <https://vdocument.in/deliverable-6-characterisation-of-manufactured-nanogenotox-intratracheal.html>
81. Jensen AK, Kembouche Y, Christiansen E, Jacobsen NR, Wallin H, Guiot C, Spalla O, Witschger O (2011) Towards a method for detecting the potential genotoxicity of nanomaterials. Final protocol for producing suitable manufactured nanomaterial exposure media Report. The generic NANOGENOTOX dispersion protocol Standard Operation Procedure (SOP) and background documentation. Copenhagen, Denmark
82. Louro H, Pinhão M, Santos J, Tavares A, Vital N, Silva MJ (2016) Evaluation of the cytotoxic and genotoxic effects of benchmark multi-walled carbon nanotubes in relation to their physicochemical properties. *Toxicol Lett* 262:123–134. <https://doi.org/10.1016/j.toxlet.2016.09.016>
83. Dusinska M, Mariussen E, Rundén-Pran E, Hudecova AM, Elje E, Kazimirova A et al (2019) *In vitro* approaches for assessing the genotoxicity of nanomaterials. *Methods Mol Biol* 1894:83–122. https://doi.org/10.1007/978-1-4939-8916-4_6
84. Magdolenova Z, Bilaniová D, Pojana G, Fjellsbø LM, Hudecova A, Hasplova K et al (2012a) Impact of agglomeration and different dispersions of titanium dioxide nanoparticles on the human related *in vitro* cytotoxicity and genotoxicity. *J Environ Monit* 14(2):455–464. <https://doi.org/10.1039/c2em10746e>
85. Chen T, Yan J, Li Y (2014b) Genotoxicity of titanium dioxide nanoparticles. *J Food Drug Anal* 22(1):95–104. <https://doi.org/10.1016/j.jfda.2014.01.008>
86. Ling C, An H, Li L, Wang J, Lu T, Wang H et al (2021) Genotoxicity evaluation of titanium dioxide nanoparticles *in vitro*: a systematic review of the literature and meta-analysis. *Biol Trace Elem*

- Res 199:2057–2076. <https://doi.org/10.1007/s12011-020-02311-8>
87. Shi H, Magaye R, Castranova V, Zhao J (2013) Titanium dioxide nanoparticles: a review of current toxicological data. *Part Fibre Toxicol* 10:15. <https://doi.org/10.1186/1743-8977-10-15>
 88. Hamzeh M, Sunahara GI (2013) In vitro cytotoxicity and genotoxicity studies of titanium dioxide (TiO₂) nanoparticles in Chinese hamster lung fibroblast cells. *Toxicol In Vitro* 27(2):864–873. <https://doi.org/10.1016/j.tiv.2012.12.018>
 89. Roszak J, Stepnik M, Nocuń M, Ferlińska M, Smok-Pieniazek A, Grobelny J, Tomaszewska E, Wasowicz W, Cieślak M (2013) A strategy for in vitro safety testing of nanotitania-modified textile products. *J Hazard Mater* 256–257:67–75. <https://doi.org/10.1016/j.jhazmat.2013.04.022>
 90. Kazimirova A, Baranokova M, Staruchova M, Drlickova M, Volkovova K, Dusinska M (2019) Titanium dioxide nanoparticles tested for genotoxicity with the comet and micronucleus assays in vitro, ex vivo and in vivo. *Mutat Res Genet Toxicol Environ Mutagen* 843:57–65. <https://doi.org/10.1016/j.mrgentox.2019.05.001>
 91. Franchi LP, Manshian BB, de Souza TAJ, Soenen SJ, Matsubara EY, Rosolen JM, Takahashi CS (2015) Cyto- and genotoxic effects of metallic nanoparticles in untransformed human fibroblast. *Toxicol In Vitro* 29(7):1319–1331. <https://doi.org/10.1016/j.tiv.2015.05.010>
 92. Kumari M, Singh SP, Chinde S, Rahman MF, Mahboob M, Grover P (2014) Toxicity study of cerium oxide nanoparticles in human neuroblastoma cells. *Int J Toxicol* 33(2):86–97. <https://doi.org/10.1177/1091581814522305>
 93. Wang L, Ai W, Zhai Y, Li H, Zhou K, Chen H (2015) Effects of nano-CeO₂ with different nanocrystal morphologies on cytotoxicity in HepG2 cells. *Int J Environ Res Public Health* 12(9):10806–10819. <https://doi.org/10.3390/ijerph120910806>
 94. Benameur L, Auffan M, Cassien M, Liu W, Culcasi M, Rahmouni H et al (2015) DNA damage and oxidative stress induced by CeO₂ nanoparticles in human dermal fibroblasts: evidence of a clastogenic effect as a mechanism of genotoxicity. *Nanotoxicology* 9(6):696–705. <https://doi.org/10.3109/17435390.2014.968889>
 95. Ali D, Alarifi S, Alkahtani S, AlKahtane AA, Almalik A (2015) Cerium oxide nanoparticles induce oxidative stress and genotoxicity in human skin melanoma cells. *Cell Biochem Biophys* 71(3):1643–1651. <https://doi.org/10.1007/s12013-014-0386-6>
 96. Pierscionek BK, Li Y, Yasseen AA, Colhoun LM, Schachar RA, Chen W (2010) Nanoceria have no genotoxic effect on human lens epithelial cells. *Nanotechnology* 21(3):035102. <https://doi.org/10.1088/0957-4484/21/3/035102>
 97. Cordelli E, Keller J, Eleuteri P, Villani P, Ma-Hock L, Schulz M et al (2017) No genotoxicity in rat blood cells upon 3- or 6-month inhalation exposure to CeO₂ or BaSO₄ nanomaterials. *Mutagenesis* 32(1):13–22. <https://doi.org/10.1093/mutage/gew005>
 98. Xia T, Kovochich M, Liong M, Mädler L, Gilbert B, Shi H et al (2008) Comparison of the mechanism of toxicity of zinc oxide and cerium oxide nanoparticles based on dissolution and oxidative stress properties. *ACS Nano* 2(10):2121–2134. <https://doi.org/10.1021/nn800511k>. *Comparison*
 99. Hadrup N, Sharma AK, Loeschner K (2018) Toxicity of silver ions, metallic silver, and silver nanoparticle materials after in vivo dermal and mucosal surface exposure: a review. *Regul Toxicol Pharmacol* 98:257–267. <https://doi.org/10.1016/j.yrtph.2018.08.007>
 100. Foldbjerg R, Dang DA, Autrup H (2011) Cytotoxicity and genotoxicity of silver nanoparticles in the human lung cancer cell line, A549. *Arch Toxicol* 85(7):743–750. <https://doi.org/10.1007/s00204-010-0545-5>
 101. Park MVDZ, Neigh AM, Vermeulen JP, de la Fonteyne LJ, Verharen HW, Briedé JJ et al (2011) The effect of particle size on the cytotoxicity, inflammation, developmental toxicity and genotoxicity of silver nanoparticles. *Biomaterials* 32(36):9810–9817. <https://doi.org/10.1016/j.biomaterials.2011.08.085>
 102. De Souza TAJ, Franchi LP, Rosa LR, da Veiga MAMS, Takahashi CS (2016) Cytotoxicity and genotoxicity of silver nanoparticles of different sizes in CHO-K1 and CHO-XRS5 cell lines. *Mutat Res Genet Toxicol Environ Mutagen* 795:70–83. <https://doi.org/10.1016/j.mrgentox.2015.11.002>
 103. Riediker M, Zink D, Kreyling W, Oberdörster G, Elder A, Graham U et al (2019) Particle toxicology and health – where are we? *Part Fibre Toxicol* 16(1):19. <https://doi.org/10.1186/s12989-019-0302-8>
 104. Lankoff A, Arabski M, Wegierek-Ciuk A, Kruszewski M, Lisowska H, Banasik-Nowak A et al (2012) Effect of surface modification of silica nanoparticles on toxicity and cellular uptake by human peripheral blood lymphocytes *in vitro*. *Nanotoxicology* 7(3):235–250. <https://doi.org/10.3109/17435390.2011.649796>
 105. OECD (2017b) OECD series on testing & assessment, No. 238. Overview of the set of OECD genetic toxicology test guidelines and updates performed in 2014–2015. ENV/JM/MONO(2016)33/REV1. OECD Publishing, Paris
 106. Lindberg HK, Falck GCM, Suhonen S, Vippola M, Vanhala E, Catalán J et al (2009) Genotoxicity of nanomaterials: DNA damage and micronuclei induced by carbon nanotubes and graphite nanofibres in human bronchial epithelial cells in vitro. *Toxicol Lett* 186(3):166–173. <https://doi.org/10.1016/j.toxlet.2008.11.019>
 107. Karlsson HL, Di Bucchianico S, Collins AR, Dusinska M (2015) Can the comet assay be used reliably to detect nanoparticle-Induced genotoxicity? *Environ Mol Mutagen* 56(2):82–96. <https://doi.org/10.1002/em.21933>

108. Valentin-Severin I, Le Hegarat L, Lhuguenot JC, Le Bon AM, Chagnon MC (2003) Use of HepG2 cell line for direct or indirect mutagens screening: comparative investigation between comet and micronucleus assays. *Mutat Res Genet Toxicol Environ Mutagen* 536(1–2):79–90. [https://doi.org/10.1016/S1383-5718\(03\)00031-7](https://doi.org/10.1016/S1383-5718(03)00031-7)
109. Jalili P, Gueniche N, Lancelleur R, Burel A, Lavault MT, Sieg H et al (2018) Investigation of the *in vitro* genotoxicity of two rutile TiO₂ nanomaterials in human intestinal and hepatic cells and evaluation of their interference with toxicity assays. *NanoImpact* 11:69–81. <https://doi.org/10.1016/j.impact.2018.02.004>
110. Gonzalez L, Sanderson BJS, Kirsch-Volders M (2011) Adaptations of the *in vitro* MN assay for the genotoxicity assessment of nanomaterials. *Mutagenesis* 26(1):185–191. <https://doi.org/10.1093/mutage/geq088>
111. Magdolenova Z, Lorenzo Y, Collins A, Dusinska M (2012b) Can standard genotoxicity tests be applied to nanoparticles? *J Toxicol Environ Health A* 75(13–15):800–806. <https://doi.org/10.1080/15287394.2012.690326>
112. ECHA (2017a) Guidance on information requirements and chemical safety assessment. Appendix R7-1 for nanomaterials applicable to Chapter R7a Endpoint specific guidance. Version 2.0. Retrieved from https://echa.europa.eu/documents/10162/13632/appendix_r7a_nanomaterials_en.pdf
113. ECHA (2017b) Guidance on information requirements and chemical safety assessment. Chapter R7a Endpoint specific guidance. Version 6.0. Retrieved from https://echa.europa.eu/documents/10162/13632/information_requirements_r7a_en.pdf
114. SCCS (Scientific Committee on Consumer Safety) (2019) Guidance on the safety assessment of nanomaterials in cosmetics, 30–31 Oct 2019, SCCS/1611/19
115. ECHA (2021b) Guidance on information requirements and chemical safety assessment. Appendix R7-1 for nanomaterials applicable to Chapter R7a Endpoint specific guidance. Draft (internal) Version 3.0. Retrieved from https://echa.europa.eu/documents/10162/23047722/appendix_r7a_r7c_hh_v3_msc_en.pdf/6c3a1586-8e97-2522-189d-92b61f35dbf3

Part III

Towards the Risk Assessment and Regulation of Nanomaterials



Nanomaterials, a New Challenge in the Workplace

15

Ana Rita Alberto, Cristina Matos,
Gabriel Carmona-Aparicio, and Muriel Iten

Abstract

Nanomaterials are a nanotechnological product of increasing importance given the possibilities they offer to improve quality of life and support sustainable development. Safe management of nanomaterials is needed to ensure that this emerging technology has the highest levels of acceptance among different interest groups, including workers. This chapter reviews the current state that presents the different stages of risk management applied to nanomaterials, including standardisation, regulation, risk assessment and risk control. Particularly, the chapter contextualizes the development of nanotechnologies at European level and analyses the scientific evidence available on the risks derived from nanomaterials use. Furthermore, it highlights the required conditions to encourage the responsible development of nanomaterials, as well as reflects on the lack of consensus in terms of approaches and frameworks that could facilitate standardisation adoption, regulatory enforcement and industry intervention concerning nanomaterials.

A. R. Alberto (✉) · C. Matos · G. Carmona-Aparicio
M. Iten
ISQ – Instituto de Soldadura e Qualidade, Oeiras,
Portugal
e-mail: arsoares@isq.pt

Keywords

Health and safety · Nanoparticles · Risk
assessment · Risk management

15.1 Introduction

Nanotechnology is presented as one of the greatest technological revolution of our time [31]. By manipulating the materials at scales from 1 to 100 nanometers, new properties are achieved which gives nanotechnology considerable potential for its development and application in various sectors of the industry, including chemistry, pharmaceuticals, cosmetics and electronics. This is a field full of opportunities that can significantly enhance human lives by providing improvements in medicine, creating new jobs, etc. Continuously new fields of application are discovered which could also lead to improvement in the environment, such as air pollution control or wastewater treatment.

The application of Nanotechnology and the usage of synthetic or artificial nanoparticles, however, can pose a risk to health, safety and to the environment, as already highlighted by several studies found in the literature review (see [13, 57, 85]), and thus requiring a close assessment and control in its management. Nanomaterials (NMs) can be design or produced in a variety of sizes and forms, as well as with a

variety of surface modifications, or with their chemistry being changed too. Changes in these parameters may result in different nanoforms.¹ Due to differences in physicochemical parameters, nanoforms constituted by the same substance might potentially show distinct hazardous characteristics [20]. The lack of understanding regarding the mechanisms of effects of NMs makes necessary the assessment of their hazards and risks on a case by case basis [80].

Due to the numerous advantages, in the coming years, a great development of the use of nanotechnologies is expected, which will increase the number of workers exposed to nanoparticles [24]. Currently, specific regulatory occupational exposure assessments (OELs) for NMs have not been established by the EU or by any national authority and it is expected that it may take a long time before OELs have been derived for all highly diverse frequently used NMs. This is mainly due to the still existing large gaps in knowledge on particle toxicology, the high diversity of the newly developed, and used, NMs, the uncertainties about their hazardous nature and the on-going discussions on the metrics to be used for the nano-OELs e.g. mass-based or particle number based [67].

Therefore, due to the lack of uncertainties that still exist yet around of the nanomaterials, their management in the workplaces thus becomes a challenge for regulators, industry heads and occupational safety professionals. A certainty that exists is that a safe, integrated and responsible nanotechnology production and utilization strategy is necessary. In this chapter a literature review and the identification of challenges link to existing risk management framework and applications to occupational settings is performed, from both a technical and practical perspective. The aim is to understand whether the current risk management approaches are suitable for different organisations and whether it could be adapted and enhanced to make it more effective if that was necessary. This chapter summarises a set of

information regarding the risk management of NMs in the workplace, namely, the current applicable legislation, the existing standards, the available risk management tools and the great challenges associated with the lack of nanomaterials data and information.

To this end, the chapter has been structured into four sections. Section 15.2 addresses the risk management standards landscape and the regulatory aspects for nanomaterials within the European Union (EU). Section 15.3 refers to the risk Assessment process and the three phases involved: hazard characterization, Exposure Assessment and Risk evaluation. Finally, Section 15.4 covers the risk treatment based on the hierarchy of controls applied to nanomaterials: elimination and substitution; engineering controls; administrative controls and personnel protective equipment.

15.2 Risk Management Frameworks: Advances in Standardisation and Regulation

Standardisation and regulation on health and safety (H&S) management for nanotechnologies is still on going. Some aspects related to the standardisation of nanotechnologies that are still under development include aspects such as: (1) clear definition of nanotechnology and requirements for users, (2) support legal issues (e.g. exposure assessment, hazard identification, labelling, Safety Data Sheets (SDS/MSDS)); (3) promote H&S practices within organisations; and (4) define criteria for conformity assessment. According to the Scientific Committee on Emerging and Newly Identified Health Risks (SCENIHR) report [3], the relevance of standardisation and regulation can be helpful in tackling some of the following issues: (1) expand traditional standards frameworks to include nanomaterials properly; (2) reduce knowledge gaps regarding the hazardous properties of NMs, (3) adapt and recommend H&S measurement and methods applied to NMs; (4) to better assess risk control effectiveness, and (5) safeguarding robustness and consistency

¹See the definition of nanoforms in Annex VI on the Registration, Evaluation, Authorisation and Restriction of Chemicals (REACH) regulation [22].

across international standardisation bodies and users. The following subsections discuss the advancement and challenges regarding the standardisation and regulatory processes of risk management involving NMs.

15.2.1 Risk Management Standards Landscape

Technological developments, such as nanotechnologies, have to face different kind of factors and influences, internal (organizational) and external (from stakeholders), that create uncertainty about whether or not they could achieve the objectives for what they were created [50]. The effect of these risk could be managed though their identification, analysis and evaluation in order to satisfy a control criterion. To support these processes, different strategies and methodology for risk management have been presented in international standards. Particularly, the ISO 31000:2018 standard is the main reference regarding how to achieve risk management in a systematic way [47]. However, the specifics on how to respond to the uncertainties associated with nanotechnology, particularly as it is emerging technologies and which we have little information, require greater attention for its management [65].

International standards and relevant documentation, such as technical specifications, technical reports, and guidance materials, are currently being established for nanotechnologies, through the technical Committee TC-229 of the

International Standards Organization (ISO), as well as the OECD's Working Party for Manufactured Nanomaterials (WPMN) [49, 77]. At the EU level, the H&S standard development is led by the European Committee for Standardization (CEN), more precisely by the technical committee (CEN/TC) 352 on nanotechnologies and supported by "CEN/TC 137 – Assessment of workplace exposure to chemical and biological agents" and "CEN/TC 195 – Air filters for general air cleaning". The role of these bodies compasses the understanding of what effects nanotechnology might have on health and the environment, including standards focused on the areas such as vocabulary, classification, nanometrology, measurement equipment, testing and characterisation, models development; and H&S guidelines [11].

Table 15.1 shows the approximate number of published standards related to:

1. Nanotechnology concepts and vocabulary (e.g. ISO/TR 11360:2010);
2. Nanomaterials characterisation, including physico-chemical characterisation (e.g. ISO/TR 10929:2012; ISO/TR 16196:2016);
3. Hazard identification, including safety and toxicity parameters (e.g. ISO/TR 13014:2012);
4. Exposure assessment (e.g. ISO/TR 18637:2016);
5. Risk management and/or assessment frameworks (e.g. ISO/TR 12885:2018); and
6. Other aspects such as waste management, product labelling and life cycle assessment (e.g. ISO/TS 13830:2013).

Table 15.1 Published standards and guidelines on nanotechnologies by international and European standardisation and policy development bodies (as for may-2020)

Standardisation body	ISO/TC 229	CEN	OECD – WPMN	Others
Standard category				
Concepts and vocabulary	21	13	–	
Nanomaterials characterisation	60	10	5	
Risk management framework	4	3	7	1 (IEC)
Hazard identification	19	3	9	
Exposure assessment	6	13	13	
Others (Product C&L / lifecycle)	2	7	–	
Total (by may/2020)	112	49	34	

The total number of ISO standards published by this committee is 112 (May 2020), of which 54% have focused on aspects of characterization of the NMs. However, many of these published standards indirectly provide valuable information for risk management. For their part, CEN and OECD have focused on developing standards that directly respond to H&S aspects, mainly exposure assessment. A detailed list of the standards included in this analysis can be consult in <https://bit.ly/NMsStandards2020>. Current publications by OECD WPMN programme are guidance documents rather than standards. Whilst OECD does publish standards and is pioneering in the nanotechnology field, there are no relevant published standards on H&S aspects, and it is expected the publication of future standards by OECD [44].

Based on the current landscape for H&S standards for nanotechnologies, the following key aspects can be highlighted:

- **Risk assessment for nanotechnologies:** Whilst data on hazardous properties and monitoring methods is currently under development, employers are forced by labour law to manage exposure to NMs in an effective level. Considering the lack of information regarding NMs hazardous and exposure routes, risk assessment is a practical approach to undertake (e.g. control banding evaluation is one way to undertake a risk assessment that have been standardised in ISO/TS 12901–2:2014).
- **Exposure Standards:** This type of specific standards covering NMs are still limited, however they are key in supporting regulation development. Furthermore, there is a need to create standards to assess NMs when they are embedded as part of a matrix or in a nano-based product.
- **Verifying conformity with standard practices:** In order to ensure conformity with standard practices, measurement of exposures and emissions will be required. If potential NMs exposure is identified, the continuation of exposure monitoring is recommended. Nevertheless, this type of standards are not fully developed yet, since most of the available guidelines have been generated for substances in bulk form.
- **Development of standards for nanotechnology H&S control:** Conventional H&S controls (e.g. process insulation or local air extraction) can aid in the prevention of NMs inhalation exposure; nevertheless, monitoring of NMs exposures and emissions is key in supporting H&S management.
- **Material Safety Data Sheets (MSDS) and labelling:** More progress needs to be done with regards to the standardisation to support the preparation of MSDS for NMs, namely the specific content and guidance about what should considered in the different mandatory sections of the MSDS. Labelling of NMs for their utilisation by workers is also an issue of concern. Independently of the size and form of chemical substances, current H&S labelling standards mandate those particular dangerous characteristics to be identified on the labels. As a result, any NMs, or products containing them, needs to be supplied with the corresponding safety statements, pictograms, and warnings. For this reason, hazard information availability is important, including precautionary information for NMs of uncertain hazards.
- **Hazard identification:** Still development needs to be made in provide protocol or guidelines for the determination of hazard characteristics (e.g. flammability) and the ability of the nano-based products containing nano-objects to be a hazardous source. These technical specifications should also provide guidelines on the reception, preparation, and characterization of samples for testing.

Standardisation is important in helping to protect the H&S of workers. A range of international and sectorial related documents are now being developed based on the information gained by research on H&S aspects of nanotechnologies. The focus of the standard development includes, among others, facilitate the design of regulatory framework to cover nanotechnologies appropriately, support toxicology research regarding the hazardous properties of new NMs, develop risk

assessment approaches, and provide guidance on effective workplace controls to support organisations.

15.2.2 Regulatory Aspects of Nanomaterials in the EU

In the European Union, nanomaterials are covered by the same regulatory framework that ensures the safe use of all chemicals and mixtures, more precisely by REACH and CLP regulations. This means that hazardous properties of nanoforms of substances will have to be assessed and their safe use needs to be ensured.

Particularly for NMs and to provide a common basis for regulatory purposes across all areas of European Union (EU) policy, the European Commission has developed the recommendation 2011/696/EU, for a definition of the term nanomaterial [23]. Since its publication, regulatory provisions were adopted in the EU jurisdiction which explicitly address nanomaterials and contain regulatory definitions of the term “nanomaterial”. The latter were derived from the EC definition, adopting it either as a whole or in its core parts, for example in the biocidal products regulation (EU) n. 528/2010, the medical devices regulation (EU) 2017/745, the annexes of the chemicals regulation REACH (EC) n° 1907/2006 which were amended in 2018 [91].

Furthermore, in early 2019, two Science for Policy reports were published by the Joint Research Centre (JRC) [90, 91]. In one of the reports, the European Commission’s science and knowledge service aims to provide clarifications of the key concepts and terms that are used in the EU NM definition, and discusses them in a regulatory context. The second report addresses the identification of nanomaterials by measurements and discusses options and points to consider when assessing whether a particulate material is a nanomaterial or not according to the definition of nanomaterials.

As was mentioned previously, the existent EU legislation and so the generic rules set in them, independent of the context (environmental, worker and consumer protection), applies in the

same way to nanomaterials, as well as for other form of substance, although it does not refer explicitly to them. With regard to European worker protection legislation, the Framework Directive 89/391/EEC, the Chemical Agent Directive 98/24/EC, and the Carcinogen and Mutagen Directive 2004/37/EC [29] are of particular relevance whenever NMs are handled during work activities.

Regulatory decisions regarding chemical substances are commonly based on toxicological properties which in the case of nanomaterials, due to their new and specific properties, may be different when compared to those exhibited by the same substances in non-nano form. This leads to uncertainties about their safety and how to assess their risk properly. The regulatory testing of nanomaterials for safety relies on the use of standardised test guidelines that aim to ensure tests are done uniformly across different labs and deliver relevant and reliable data [89]. Through European initiatives, such as the NANoReg and Prosafe projects (see [38, 112]), and the work of the OECD WPMN, a number of existing Test Guidelines have been identified as requiring adaptation to be applicable to nanomaterials and also the need for new ones. From a regulatory point of view, the resolution of these issues becomes urgent. Taking the REACH regulation as an example, which requires information such as physicochemical, toxicological and ecotoxicological properties for the registration of nanomaterials, it has been observed a need for more test guidelines so companies can provide enough information to demonstrate the safe use of their NMs.

Further research with specific relevance for regulatory questions is needed, such as the enforcement of product labelling for the presence of NMs and indicative occupational exposure limit values establishment, contributing to reduce uncertainties with regards to the safety of NMs and for a greater availability of quality data for regulatory purpose. To this end, best practices, guidelines and assessment practices, and methods for the safety testing of nanomaterials are being developed, which will certainly contribute

to the better management of nanomaterials in the workplace.

15.3 Risk Assessment

Risk assessment is the overall process for the estimation of probabilities and expected consequences for identified risks [82]. It includes three main stages: hazard characterisation, exposure assessment, and risk evaluation. Given the many different nanomaterial types, the potential routes of exposure, nanomaterial characterization issues, limitations in research methodologies, such as time-course and dose-response issues, and inadequate *in vitro* methodologies for *in vivo* standardized and guideline toxicity testing, adequate risk assessments methods and tools for NMs are still under development [113]. The following subsections present the advancement and challenges for the different risk assessment stages for occupational settings.

15.3.1 Hazard Characterization

According Rasmussen et al. [88], the identification and characterization of NMs need more information on physicochemical properties and test methods, when compared with other chemicals in general. A degree of consensus within the scientific community has been reached in recent years, with regards to the structure of the considered properties for the characterization of NMs. These parameters has being classified in three groups [86]:

- Characterization: physical and chemical identification (e.g. composition, impurities, shape, size, size distribution, surface characteristics, etc).
- Fate: biological and environmental fate based on their solubility, hydrophobicity, dispersibility, dustiness, etc.
- (Re)activity: their reactivity, effects of their physical hazards, biological activity, etc.

In order to ensure a safe workplace with regard to the presence of chemical substances, information about their characteristics and hazards must be available to and understood by workers. Normally, information about the hazardous properties of chemicals agents present in the workplace can be obtained from material safety data sheets (MSDS), labels, European commission recommendations, occupational exposure limit values and other sources (peer reviewed data, scientific literature, relevant databases such as PubMed or ECHA, information generated by renowned institutions such as IARC, WHO, HSE, NIOSH, OSHA, ISO, etc.).

MSDSs are the first source of information on how to handle a particular product containing nanomaterials, but the information provided is still non-existent or very limited, specifically in terms of their specific hazards and risks, or incorrectly refers to “bulk material” properties rather than nano [18, 87, 101]. According to article 31 of the REACH regulation [27], the provision of MSDS for nanomaterials is mandatory only for those substances and mixtures that are classified under the CLP regulation [28] or meet the criteria established in Annex XIII of the REACH regulation as being classified as persistent, bioaccumulative and toxic (PBT) or very persistent and very bioaccumulative (vPvB substances). Nevertheless, it is a common practice by the chemical industry to provide a MSDS for non-classified substances/mixtures as well.

MSDS for NMs can be improved through a literature review which includes the latest information about the toxicological data, epidemiological studies, measurement techniques, occupational exposure values, engineering measures, and the most current regulatory requirements. In doing so, the MSDS could provide the best information as possible to the users allowing them to implement the necessary control measures to prevent or eliminate the exposure to NMs and, consequently, protect the health of workers [87].

The European Chemical Agency (ECHA), aiming to enhance the safe handling of chemicals

(including the nanomaterials) while promoting innovation and competitiveness in the EU chemical sector, introduced a dissemination tool “infocard” as a ‘first tier’ in disseminating information from ECHA’s databases. Among the various functionalities of the infocard’s user, the following stand out: highlights ECHA’s preferred substance name and main substance identifiers in one location, quickly shows the most prominent hazardous and critical properties of a substance, easy access to legislative and safe use information associated with the substance, presents key substance information and permits tracking substances through the RSS feed. This tool can therefore be an important source of information when available hazard assessments of a given nanomaterial are almost non-existent.

According to Sajid et al. [95], there is sufficient evidence that nanoparticles induce toxicity to higher organisms including human and wildlife. Jeevanandam et al. [51] concluded that toxicity of nanomaterials may depend of factors such as dose and time effect, aggregation and concentration effect, Particle size effect, particle shape effect, surface area effect, crystal structure effect, surface functionalization, pre-exposure effect. The availability of occupational and epidemiological data for chemicals, including nanomaterials, is a key aspect of risk assessment. The amount of new chemicals produced and released on the market is about a hundred thousand per year [101]. However, only a small number of them have an established exposure limit values, as an example the publication 2018 TLV and BEIs from the American Conference of Governmental Industrial Hygienists (ACGIH) presents around 700 chemicals with TLV-STEL or TLV-TWA values (short-term exposure limit and time-weighted average, over the 8-hour working day). At the nanoworld, only 56 NMs have OELs proposed values [101]. Table 15.2 presents some of the particle control values (PCV) for some of nanomaterials. This reference values include a range of particle metrics such as mass, particle number concentration and could be national exposure standards set by regulatory authorities, recommended exposure limits, exposure limits proposed by researchers, and Local

Background Particle Reference Values based upon background nanomaterial levels [79]. As it can be seen, the suggested values vary enormously, and no consensus exists between the authors.

Beyond human toxicity and eco-toxicity, NMs impose additional risks. For example, Khan [53] refer that one specific potential hazard posed by nanoparticles is their capacity to cause fire or explosion. This is because nanoparticles are almost certain to give a rise to a dust explosion hazard and that due to their large specific surface area, they may well be spontaneously flammable on exposure to air. This is particularly the case with metal nanoparticles as they oxidise easily. Additionally, Bouillard et al. [7] found that with the reduction of particle size, ignition temperature and minimum ignition energy also reduce. This indicates that a higher potential risk of inflammation and explosion is achieved when using nanopowders. In this regard, it was observed that carbon based nanopowders exhibit some propensity to explode while metallic nanopowders can be very reactive, thus delineating potential high explosion risks for facilities manufacturing such powders. However, the impacts of agglomeration on explosion severity and sensitivity for nanopowders were not fully understood through the study. This is why more research needs to be done in order to increase the understanding of NMs hazards.

Given the current limited availability of hazard data for most nanomaterials it will be challenging to establish the toxicological behaviour of specific nanomaterials with any degree of certainty. In most cases it will be necessary to refer to information that has been obtained for similar materials [41]. In this way, the use of a non-testing strategies like read-across in the hazard assessment of nanomaterials is desirable allowing, in due time and at lower costs, to perform the safety assessment of almost all nanomaterials [21]. The identification of physicochemical (PC) properties affecting the hazard potential of NMs is crucial, as it could enable to predict impacts from similar NMs and outcomes of similar assays, reducing the need for experimental (and in particular animal) testing [58, 99]. Furthermore,

Table 15.2 Particle control values of some nanomaterials

Types of nanocarbons	Proposed PCV for NMs	References
Multiwalled carbon nanotubes (MWCNT)	Occupational exposure limit (OEL) air <50 µg/m ³ for 8-hour TWA ^a during a 40-hour workweek	[84]
Carbon nanotubes (CNTs)	Proposed nanoreference values (NRV) <0.01 fibres/cm ³	[109]
Carbon nanotubes (CNTs)	Recommended exposure limit (REL) <1.0 µg/m ³ for 8-hour TWA during a 40-hour workweek	[71] ^b
Carbon nanofibers (CNFs)	Occupational exposure limit (OEL) <0.01 fibres/cm ³	[104]
Carbon nanotube group, SWCNT, DWCNT, MWCNT	Occupational exposure limit (OEL) <30 µg/m ³ for 8-hour TWA during a 40-hour workweek	[68]
TiO ₂ (10–100 nm)	Recommended exposure limit (REL) <0.3 mg/m ³ for ultrafine TiO ₂ as TWA ^a concentrations (> to 10 hours/day, during a 40-hours work week.)	[70]
TiO ₂	Occupational exposure limit (OEL) <0.3 mg/m ³ , respirable fraction.	[104]
Carbon black [CAS n. ° 1333-86-4]	ACGIH ^c : 3 mg/m ³ (TWA), for 8-hour workday and a 40-hour workweek.	[43]
Carbon black	Germany – BeKGS527: 0.2 x nano-GBP ^d density in g/cm ³ , TWA ^d , respirable — If no other relevant information is available	[43]
Carbon black	Germany – MAK: 0.3 x GBP density in g/cm ³ , TWA, respirable, 4.0, TWA, inhalable	[43]
Carbon black [CAS n. ° 1333-86-4]	OSHA ^e : Permissible exposure limits (PELS) 3 mg/m ³ 8-hour TWA	[43]
Carbon black [CAS n. ° 1333-86-4]	Recommended exposure limit (REL) 3.5 mg/m ³ (without PAHs ^g ; when PAHs are present, NIOSH considers carbon black to be a potential occupational carcinogen.	[43] [74]
Carbon black, ultrafine	Occupational exposure limit (OEL) 0.12 mg/m ³	[55]
Amorphous silicon dioxide	Occupational exposure limits (OELs) 0.3 mg/m ³ , respirable fraction, for 8-hour TWA.	[104]
Nanoclays	Occupational exposure limits (OELs) 0.3 mg/m ³ , respirable fraction, for 8-hour TWA.	[104]
Low-toxicity dust	Occupational exposure limits (OELs) 0.3 mg/m ³ , respirable fraction, 4 mg/m ³ , inhalable fraction.	[104]
Granular biopersistent particles (insoluble nanomaterials)	Benchmark exposure level (BEL): 0.066 x bulk workplace exposure limit (WEL) (µg/m ³)	[9]
Non biopersistent granular nanomaterials (1-100 nm)	Nano reference value (NVR): Applicable occupational exposure limits (OEL), workplace exposure limit (WEL) (µg/m ³)	[109]
Soluble	Benchmark exposure level (BEL): 0.5 x bulk workplace exposure limit (WEL)	[9]
Zirconium compounds	Occupational exposure limits (OELs): 5 mg/m ³ (TWA); 10 mg/m ³ , ST ^h	[1]

^aTWA Time weighted average, 8 h unless otherwise specified

^bNIOSH National Institute for Occupational Safety and Health

^cACGIH American Conference of Governmental Industrial Hygienists

^dDust of biopersistent nanomaterials without specific toxicological properties and without fibrous structures (carbon black is listed in BeKGS 527)

^eMAK Maximum Workplace Concentration, DFG Deutsche Forschungsgemeinschaft

^fOccupational Safety and Health Administration (OSHA) Permissible Exposure Limits (PELS)

^gPAH Polycyclic aromatic hydrocarbons

^hST Short Term Exposure Limit

the scientific community needs to continue developing test methods that can characterize certain behaviours of nanomaterials to support read-across strategy.

15.3.2 Exposure Assessment

Occupational exposure can be defined by the direct contact to a potentially harmful chemical,

physical or biological agent as a result of work. Concerning NMs, the primary route of entry to the human body are inhalation, however it can also occur by skin exposure, and ingestion, where the toxicity targets are the respiratory, integumentary, and gastrointestinal systems respectively. While the skin is in generally an effective barrier, the lungs and gastrointestinal tract are more defenceless [45]. In order to find the agent emission, which is defined as the transfer process of liberated NMs to the workplace air, usually expressed as a flow (particles per unit time or area) [56], similarly to other chemical agents, the first phase of NMs exposure characterisation, consists of two steps: first, a workplace survey, to have an evaluation of the processes or operations, including the way of how the agents are handled and, second, the physical form of NMs. The second phase of this exposure characterization is the quantitative evaluation, through liberated agent monitoring. It aims of obtain insights regarding inferences concerning the quantification of the occupational exposure, with the purpose of making comparisons with OELs. For the NMs, all this process should be the same, but the lack of data on workplaces studies and OELs to NMs makes comprehensive exposure assessment difficult.

15.3.2.1 Workplaces/Processes

As referred before, the emission potential of an agent, in this case NMs, it depends (among other issues) on the type of process or handling operation and its ability to release them in the workplace. The likelihood of exposure to NMs during synthesis, production and manufacturing processes is highly dependent upon the type of process and the type of equipment involved in the process. For example, Dahm et al. [14] conducted exposure assessments at six manufacturers and users of carbon nanotubes and nanofibers. This study showed that the highest exposures occurred during dry powder handling tasks including mixing and weighing operations.

In order to ensure the appropriate characterisation of the exposure route, information for workplace and process survey should include: (1)

identification of the source domain (SD) and activities related to handling nanomaterials (considering not just exposures during normal routine working but also possible accidental releases and maintenance); (2) identification of the physical form of the NMs in each stage of the work process (dry powder/suspension or liquid/embedded or bound in other materials); (3) identification of the presence of other processes in the workplace that can affect measurements or the measurement strategy employed; (4) identification of the presence or absence of ventilation, heating and air conditioning (HVAC) [25]. For the workplace exposure four SDs were identified by Schneider et al. [97] to describe the different processes: (1) During the production phase (synthesis) prior to harvesting the bulk material, point source or fugitive emission, e.g. emissions from the reactor, leaks through seals and connections, and incidental releases, can take place (SD1), in these cases, discrete nanoparticles and agglomerates will be formed; (2) During the manufacturing of products, the handling and transfer of bulk NMs powders with relatively low energy can release nanoparticles, e.g. collection, harvesting, bagging, bag dumping, bag emptying, scooping, weighing, dispersion/ compounding in composites (SD2); (3) During the application of products (sprays) or dispersion of intermediates containing nanoparticles (SD3); (4) fracturing and abrasion, or other mechanical release of NMs or materials containing NMs, of final products during further processing (SD4).

15.3.2.2 Physical Form

Exposure level to NMs will depend on their ability to be released directly from their dusty form or from the matrix where there are embedded, as well as due to their transformation and degradations characteristics. Different potential exposure scenarios will happen in function of different factors, linked to the nanoparticle reduced dimension, such as their final form in the product, dust generation (emission and dispersion) potential and solubility. The physical form to be considered is that of the material at the beginning of the process at the workstation being evaluated. Four

categories of physical forms have been identified by NRC [75] according to their increased emission potential:

1. Physically bound/ encapsulated (usually the lowest potential exposure).
2. Solid nanomaterials with nanostructures fixed to the material's surface.
3. In suspension in a liquid.
4. In the form of powder (usually highest potential exposure).

Studies on the Potential Exposure to releases in the machining of nanocomposites revealed that some NMs were often detected (96% of the experimental studies). Base matrices were also analysed, which shown the presence of matrix nanoparticles (92%), and partially embedded nanomaterials among matrix particles were often detected (76%) [34].

15.3.2.3 Quantitative Evaluation and Measuring Devices

As referred above, there is not much information about exposure assessment to NMs, and so at this time, it is not clear which units of measurement associated with exposure to nanomaterials are more important from the perspective of occupational risk prevention. Therefore, the release of airborne NMs to the workplace environments could be measure with different metrics such as mass, number and/or surface area concentration. The understanding of the behaviour of these nanomaterials, when they escape to the workplace, is still very scarce and weak, therefore no international consensus exists regarding the most appropriate metrics that must be applied for NMs environmental monitoring [42] and it is important to be aware about the workplace activities around when measurements are taken like airflows and pressure differentials generated by heating, ventilation and air conditioning systems, by air movements generated when people walk, or by doors opening and closing [78]. After the revision of the guideline limit values existing in different countries at present, the units of measurement applied are based on the quantification of nanomaterials present in the

air in the worker's breathing zone: (1) mass, expressed with $\mu\text{g}/\text{m}^3$ or mg/m^3 ; (2) number of nanoparticles/ cm^3 .

Studies refer that particle size plays an important role in determining the potential adverse effects of nanomaterials in the respiratory system: by influencing the physical, chemical, and biological nature of the material, affecting the surface-area dose of deposited particles, and enabling the deposited particles to more readily translocate to other parts of the body [69]. Nevertheless, mass concentration measurements can be a good approach when there is a correlation between the surface area of the NMs and mass concentration determined or if are available toxicity data based on mass dose for a specific NM.

Without harmonized guidance for the characterization of exposure, due to the absence of adequate instrumentation, the lack of appropriate exposure metrics and the lack of quantified exposure limits, considering that the exposure limits that exist are most often a concentration of mass, conjunction of qualitative and a quantitative assessment must be applied to establish the possible release of NMs. Due to the interest in knowing the mass concentration and number of particles and their surface area, the instrumentation used to characterize the exposure varies and is achieved through various sampling instruments designed to capture these metrics. These three metrics can be converted into each other if we are in presence of spherical particles and if the parameters related with density and size distribution are known [78]. Regarding the mentioned instruments they fall into two general categories: "direct reading" and "time-integrated". The former provides "real time" concentration values while the latter requires sampling over a period of time followed by an analysis to determine mass and/or chemical composition [10, 76]. Exposure studies involving count concentrations around the equipment/processes and for personal exposure measurements should chose the direct-reading combination handled instruments, that can afford the metrics, like particle number and size distribution (independently on the chemical

composition or morphology) based on different techniques, such as:

- Condensation Particle Counter (CPC) can measure particle number concentration but not particle size.
- Diffusion Charger (DC) measure the fraction of airborne particle surface area concentration that upon inhalation would deposit in the gas-exchange region, the number concentration, the average particle size or a combination thereof (20 nm to above 400 nm).
- Scanning Mobility Particle Sizer (SMPS) measure particles size distributions down to 10 nm and concentrations up to 1.000.000 particles/cm³ [108].
- Optical Particle Counter (OPC) assesses real-time number concentration of particles >300 nm in diameter [66].
- Electrical low-pressure impactors (ELPI) Enables the measurement of real-time particle size distribution and concentration in the size range of 6 nm–10 µm.

In order to have the NMs identification and the elemental composition, “time integrated” methods and instruments should be used. Sampling could be undertaken via open-face sampling, filtration, electrostatic or thermal precipitator, size-selective collection by cascade impaction, elutriators, personal samplers, surface sampling and wiping. Subsequent chemical and electron microscopic (EM) analyses (SEM or TEM with Energy Dispersive X-Ray Spectroscopy – EDS) and or X-ray fluorescence/ inductively coupled plasma mass spectrometry (XRF/ICP-MS), Atomic Force Microscopy (AFM) and others used on chemical laboratories, for elemental composition and particle identification [78].

Whenever possible, the measurement strategies should include sampling and laboratory analysis and the use of direct reading instruments to cover all relevant readings (e.g. particle size distribution, particle count and particle surface areas). All of these techniques have limitations in some way the first ones like lack of information on fibres (CPC, DC), the size and weight and complexity of operation (SPMS and ELPI) and

lacking real time data output (samplers and laboratory analysis) [36]. The lack of exposure-relevant documented evidence and the use of not-harmonized collected data methods and strategies are the greater disadvantage of this process.

To better understand the exposure assessment, several studies were carried out to the characterization of nanoparticle release. One key aspect of these occupational assessments is the need to distinguish the background and the specifically process NMs release. The main pathways for background characterization that are often used in exposure studies are:

- (1) Far-Field (FF) approach: The background measures are taken in a place far from the workplace where NMs are produced/handled in order to be out of the process influence, but in the same facility. If there is a divergence between the background and workplace concentrations, this implies that the NMs process emissions under investigation should be further analysed. FF background measurements should be taken at the same time as workplace measurements.
- (2) Near-Field (NF) approach: this is based on monitoring before the start of the task in the workplace. The NF background is also characterised as a “time series” approach, considering that the background concentration is assessed when the task is not occurring, and that any increases in concentration will be attributed to releases from the activity involving NMs [5].

More than 60 exposure characterization to NMs studies were done by “the National Institute for Occupational Safety and Health” (NIOSH). These studies gave NIOSH the needed information to improve an already existing technique, the “Nanoparticle Emission Assessment Technique” (NEAT 1.0), to develop the NEAT 2.0. The latter gives greater importance to integrated time, filter based sampling with elemental analysis and morphology, around breathing zone and area samples, rather than particles counters direct readings, in order to have a exposure job map [19]. NEAT

1.0 was very useful to identify the activities that leads to more nanomaterial emissions in laboratories or pilot plants but, the use of this technique in larger sites do not addresses the potential for transient or background emissions arising from normal plant operations.

Using NEAT 2.0 a quite complete perception on the overall picture of the worker exposure is given because it applies: (1) a collection of time-integrated PBZ (Personal Breathing Zone) air samples; (2) additional time-integrated air samples are collected in the PBZ for identifying task-specific exposure information during that specific task; (3) particle counters are used to supplement providing data information on peak emissions, plus (4) a collection of real-time integrated background data over the course of a full sampling period to detect background fluctuations.

It would be expensive and time consuming to carry out studies with individual exposure measurements for each chemical under every circumstance in view of the large variety of possible exposure scenarios and the amount of available data is still very scarce. When lacking relevant regulatory requirements for NMs and real time exposure data, more qualitative techniques can be implemented to characterize exposure potential. The control banding tools can be used to have an initial understanding to evaluate exposure to NMs in the workplace [97].

15.3.3 Risk Evaluation

As highlighted in the previous sections, the H&S effects of nanomaterials are currently quite unknown (e.g. there is no specific regulation, nor are there approved occupational exposure limits). However, as a potential risk factor at work, organisations still have the obligation to assess and manage NMs, as it is done with any other material introduced into the production process, considering a maximum technical approach. The complexity and level of detail required for the risk assessment depend on the hazardous substance in question and the activity being carried out; even for more complex situations, the help from experts it is recommended [4, 15].

Figure 15.1 shows the different level and kind of tools that support risk assessment based on the evaluation's aim, as well as the origin, reliability and quality of the information used. Exposure estimation can be carried out at different levels or *tiers*, starting with a more exploratory, and even pure qualitative, level to establish the least favourable scenario (Tier 1), and ending up with robust quantitative methods based on probabilistic exposure models or detailed site-specific measures (Tier 3) [78].

In recent years, several tools for assessing occupational risk have been developed. Among the Tier 1 evaluation models based on qualitative or semi-quantitative estimation from environmental concentrations, there are the Control Banding models (CB) [40]. Control banding or simplified tools are models where risk is assessed based on the severity determined through exposure parameters. These methods prioritize action on risk control, without investing excessive resources in evaluating risk in detail using quantitative exposure values. For their part, tier 2 and 3 models, based on quantitative evaluation, correspond to established measurement strategies and methodologies to proceed to obtain suitable values and, as far as possible, to compare them with the reference limit values [8]. Table 15.3 provides a summary of the most widely used nanospecific tools.

15.3.3.1 Control Banding Tools

Control banding (CB) tools calculates the severity of a task that involves NMs when information from several factors based on the physicochemical properties of the nanomaterial (surface chemistry, particle shape and diameter, and solubility), toxicological properties of the nanomaterial and the “bulk” material (carcinogenicity, toxicity to the reproduction, mutagenicity, dermal toxicity and ability to produce asthma) [96]. Probability levels are also calculated from factors such as estimated amount of nanomaterial during the task, dustiness or ability to form mists, number of workers with similar exposure, frequency and duration of the operation. When combining the severity and probability scores, a decision matrix is obtained that leads to a risk level value [16].

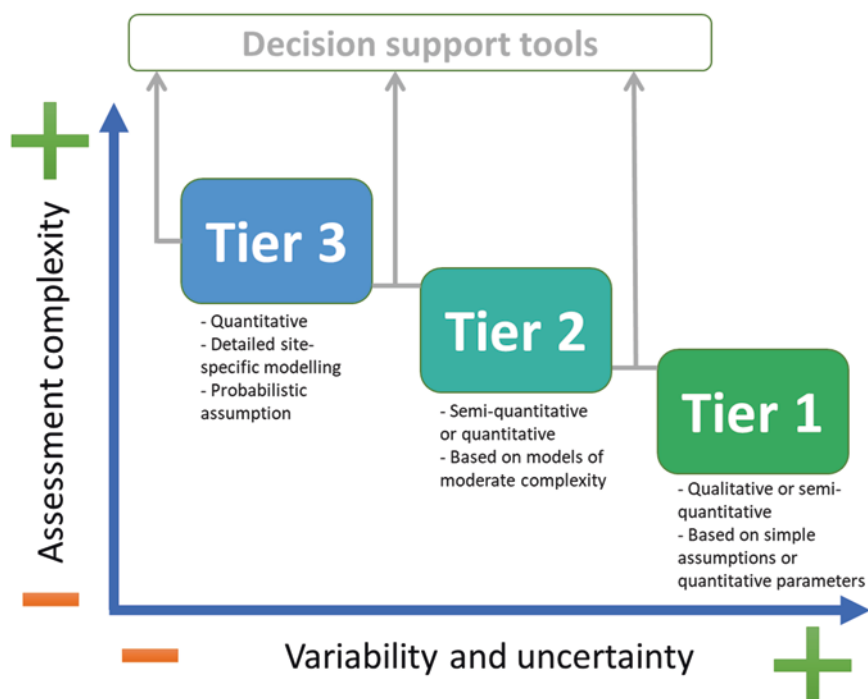


Fig. 15.1 Classification of risk evaluation tools by tiers

Table 15.3 Tiered approach tools for risk evaluation

Level	Description	Tools examples
Tier 1–2	Control banding (CB): (1) qualitative & semi-quantitative models. (2) based on the precautionary principle. (3) workplace safety only. <i>Note: There are additional CB tools that use a life-cycle approach that involve environmental and consumer aspects (also refer to as risk screening tools), however, they are out of the scope of this chapter.</i>	CB Nanotool [115], ANSES CB tool [81], Stoffenmanager Nano [110]
Tier 2–3	Occupational exposure: (1) quantitative exposure models. (2) tools based on refined information, including hazard assessment and physicochemical characterization. (3) additional tools include models to assess kinetic for human internal exposure (post-exposure risk assessment).	Nanosafar [52], ART [32], DART [37], NanoRiskCat [39], PBPK “kinetic” [105]
	RA high level models: (1) high tier quantitative models. (2) requires expertise to apply them. (3) based also in detailed information of occupational exposure, hazard assessment and physicochemical characterization.	GUIDENano [83]
	Hazard assessment: (1) determine health effects based on NMs concentrations. (2) types: In vivo (observational) and in vitro (cell) protocols. (3) in silico (computational) models. (4) it can also be applied at the kinetic level	NanoVALID – in vivo [6], EURO-NanoTox – In vitro [94], QNAR – In silico [114]
	Physicochemical characterisation: (1) protocols to characterise different physicochemical properties at each lifecycle stage	NANOREG [38]
Others	Decision support tool: (1) evaluation of models results in order to recommend courses of action. (2) determine and weigh benefits versus risks	LICARA [111], SUN DSS [64]

Table 15.4 CB tools specific for occupational exposure assessment

Tool	Target group	Comments	Inputs requirements	Number of bands		
				Hazard	Expos.	Risk
ANSES CB tool	All working environments	Scope considers solids, liquids, powders and aerosols. It also includes a risk control band.	Low	5	4	5
CB Nanotool 2.0	Laboratory-scale work	Risk levels include a recommended control approach.	High	4	4	4
NanoSafer	SMEs	It can be used for NMs in powder form. Assessment for NMs production, products containing them, and accidental emissions	Medium	4	5	5
Stoffenmanager Nano	All working environments	Scope considers insoluble NMs. It gives priority to the hazard assessment. It provides control measure recommendations.	High	5	4	3

Table 15.4 shows a comparison between the different CB tools available for occupational risk management:

CB method can provide an alternative risk assessment and management process, grouping workplaces with similar hazards and/or exposures into similar categories. Due to its relative simplicity and ease of application, CB can be an alternative/complementary tool to traditional occupational risk assessment, especially attractive for SMEs [63]. However, one of the biggest challenges in applying this tool to NMs lies in making decisions about assigning the hazard and exposure bands. Therefore, the successful implementation of this approach in any organisation still requires technicians with proven experience and competence in risk management and more specifically, in those issues directly related to the NMs used in industrial processes. Another issue associated to CB is the fact that it corresponds to a first screening for risks management. In the case when a high-risk band is selected, it will be required to refine the assessment with tier 2 or higher tier methods and also the best the effectiveness of the controls once implemented. Additionally, and depending on the role an organisation has in the NMs chain (development, manufacturing, use or disposal), we will need to use additional and more specific tools. For example, to fulfil REACH requirements, NMs producers will have to undertake a specific risk characterisation following the

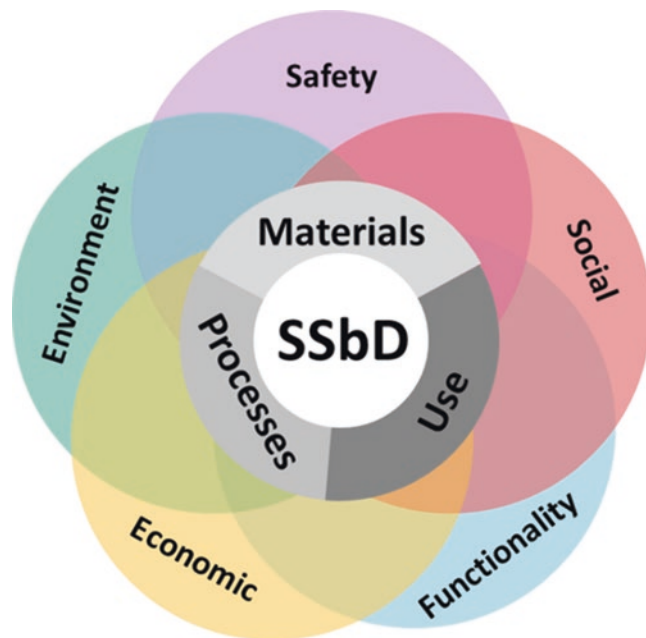
guidelines established in the ECHA R-series such as Riskofderm or Advanced REACH Tool – ART [61].

In general, the risk assessment techniques are designed to accomplish similar goals (e.g. hazard characterisation, exposure estimation, or risk valuation). Their specifications, on the other hand, differ significantly (i.e. data requirements, results, and scope of application). This makes an integration of the different tools into a unified framework difficult. Furthermore, risk assessment tools have been developed in major research projects (e.g. H2020), but most of them have not been calibrated and/or validated due to scarcity of relevant experimental data.

15.4 Risk Treatment

Due to the limited information about the health risks associated with occupational exposure to NMs, appropriate steps should be taken to minimize the risk of worker exposure through the implementation of a risk management program [69]. The application of controls aims to make sure that occupational exposure is as low as possible. This exposure should be minimized through measures such as excluding the use of certain substances, replacing them with less hazardous ones or changing the process to a safer one as far as reasonably practicable [46]. Risk assessment should help to decide the appropriate control,

Fig. 15.2 Sustainable and safe by design (SSbD) approach



taking account of necessity, practicability and cost. In all cases, selection of controls should as a minimum be based on national regulatory requirements and supplemented with additional controls, as appropriate [103].

Application of the precautionary principle does not imply that organizations should not use nanomaterials until H&S hazards are fully understood. Precautionary actions should be determined according to the assessment of possible consequences of the nanomaterials used, including the consideration of available hazard information and the concomitant uncertainties [65]. One way to incorporate precautionary principles from the design of product is through a sustainable and safe-by-design (SSbD) approach. SSbD consists on applying safety and sustainability principles and strategies on the process and products from the earlier stages of design and considering the full life cycle [100]. Particularly, the nano-specific SSbD approach is a risk management strategy in which the principal goal is to try to balance the safety of a nano-enable products, over its lifecycle, while achieving commercially viable performance and functionality [54]. There has been growing research into the knowledge and various

methods and tools that could support the implementation of a safe innovation approach, specifically in the context of nano-enable products from the several industrial sector [62]. Some examples of recent European research projects focusing on SSbD aspects include ProSafe, NanoMile, EC4SafeNano, NANoREG and NANoREG II [93]. Particularly, the latter presents the most comprehensive approach to the safer development of nanomaterials. Using the Cooper's Stage-Gate innovation methodology as the basis, their SSbD process focuses on three pillars of development (safe product, safe production and safe use) and three elements of risk assessment (uncertainty, exposure and hazard) [102]. The scope of the SSbD is shown in Fig. 15.2.

Furthermore, precautionary actions should follow the established hierarchy of controls for protecting workers, that are in general, the main approaches to risk control of hazardous materials in the workplace, focused on prevention of exposure by: (a) elimination of the hazard, (b) substitution of the hazard, (c) engineering control techniques, (d) administrative control systems and (e) use of personal protective equipment (see Fig. 15.3).

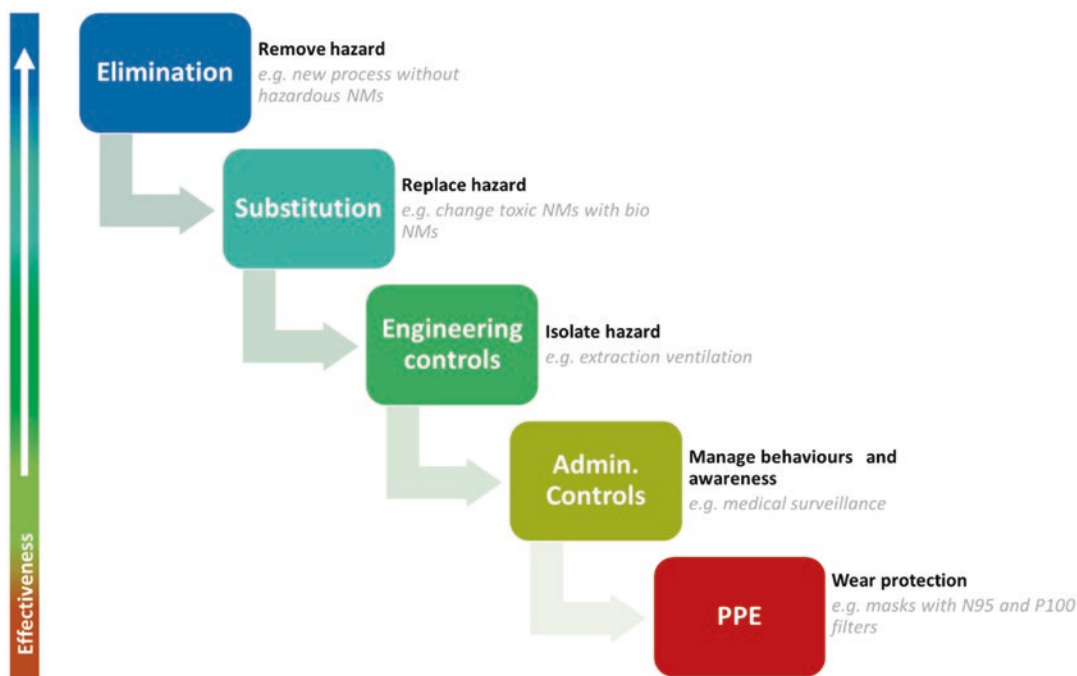


Fig. 15.3 Hierarchy of controls applied to Nanomaterials

In general, it is advisable to adopt a control as high in the control hierarchy as is technically and economically feasible. However, the decision of selecting a specific control should take into consideration the level of control required to provide a safe working environment and the efficacy of the control measures. These complementary approaches should be considered starting with the design stage of an industrial process [48]. The combination of all these control strategies should be a good approach to control the exposures. Changing the process to a less releaser of NMs, using matrices containing the NMs in order to minimize the release of NMs or modifying the NMs, for example, using coating to lower the hazardous characteristics of the NMs, are some of the measures that could be used.

15.4.1 Elimination and Substitution

The unique properties of commercial exploitation of nanoparticles are one of the reasons that hinder the application of the elimination control.

The substitution is more applicable in reducing potential toxicity, by coating with a less hazardous substance but without changing the properties [98]. Changing the NMs physical form in order to reduce the possibility of inhalation or direct contact, like encapsulate or using suspensions (see Sect. 15.3.2.2) can be another way of substitution.

15.4.2 Engineering Controls

Another level of control that can be used when the first ones could not be implemented, or the implemented ones were not successful enough is the engineering controls. These engineering controls separate workers from the source that releases NMs, or capture NMs during their manipulation, through technics such as glove boxes, or fume hoods, or laminar flow cabinets, or custom fabricated enclosures. In general, the highest risks for nanomaterials are considered to be respiratory exposure, in view of the well-known lung toxicity of particulates [69]. Control

practices for the reduction of inhalable and respirable dust in the workplace are well-known and well established. The efficiency of these methods for nanomaterials has so far been only partially evaluated, but these measures seem useful as a starting point for the development of preventive measures. Some adjustments might be needed to prevent potential exposure to nanomaterials [48]. When applying the engineering controls, they should not interfere with the workers activities (passive measures), because in this case, and if they were not properly protected from the action of workers, the controls can be easily deactivated or stopped. The type of engineering control to apply depends on the location, duration of the task, the amount and characteristics of NMs that are manipulated. Without this information, the control may not prevent exposure and sometimes could increase it [72].

Operations involving easily dispersed dry nanomaterials, deserve more attention and more stringent controls (such as enclosure) than those involving nanomaterials that are suspended in a liquid matrix or embedded in a solid. When handled, liquid nanoparticle suspensions usually offer less risk of inhalation, but if they are aerosolized by sonication or dispersed in some way the likelihood of exposure can increase significantly [35].

Nanomaterials incorporated into bulk solids may pose some risk if the solid matrix is cut, sawed, drilled, sanded, or handled in any way that creates a dust or releases the nanomaterial [17].

For air velocities prevailing in workplaces, airborne nanoparticles can be considered as having no inertia and behave in a similar way to a gas and if not fully enclosed will diffuse rapidly and will remain airborne for a long time. Because of their high diffusion velocity, these particles will readily find leakage paths in systems in which the containment is not complete [2].

Most of the engineering controls already used to remove micro-scale powders and gases are adequate to minimize occupational exposure to NMs [73]. In any case, these systems should be effective in removing the released NMs taking into account the available information about their transport and behaviour in the air [69]. Some studies showed that that a biological safety cabi-

net was more effective than a custom fume hood to control airborne exposures resulting from sanding epoxy containing CNTs [12]. In the other hand other studies show that the performance of an air-curtain hood during nanoparticle use was outstanding for the various conditions tested and avoids the difficulties found when using traditional hoods [106]. To ensure the good performance of these systems, maintenance should be planned and performed.

At the design stage of engineering controls, observance with the requirements proposed by the local authorities must be taken into account. High-Efficiency Particulate Air (HEPA) filter, preferably H14, should be effective in removing nanoparticles from the airstream. HEPA filters have been recognized as one of the most effective filtration media that can be employed as the end-of-pipe treatment to capture and eliminate transport of nanomaterials (99.97%) [107].

In the precautionary approach, it is desirable to avoid any exposure to nanomaterials, and a number of containment approaches might be considered [30]. Operations can be performed by isolating the materials in separate, ventilated rooms equipped with a system that avoids any possibility of contaminating other workplaces. Other examples of isolation are the use of closed-circuit processes, use of robotics and equipment enclosure. In certain situations, where the process is too polluting, workers can be isolated in a controlled atmosphere workstation to operate the entire process by remote control. The workers are located in booths or rooms where the air quality conditions are controlled to protect their H&S [48]. It is worth mention that when NMs are released into the atmosphere, and as aforementioned, they have the potential to cause fire or explosion when subject to an ignition source. In this case, only elimination, substitution and engineering controls could reduce these associated risks.

15.4.3 Administrative Controls

Administrative means should not be a substitute for the type of controls discussed above but they should be implemented as a complementary

action to those solutions. When engineering solutions are not completely effective or are too expensive, administrative controls become a way to mitigate exposure. These solutions include changing working methods, minimizing the time workers are exposed to NMs, limiting contaminated spaces through door control and cleaning routines in the workplace.

15.4.4 Personnel Protective Equipment

Personnel Protective Equipment (PPE) should not be the primary control and should be used to supplement the other controls, when workers are in contact with nanomaterials during activities with nanomaterial-exposure potential. In general, PPE recommendations for nanoparticle handling will be the same as for exposures to other powders, fine dusts, or aerosols.

PPE must be selected based on many reflexions, such as the toxicological effects of the nanoparticle; quantity handled and physical form (physically bound/ encapsulated, in suspension in a liquid, in the form of powder), other exposure controls in place and PPE performance requirements and limitations. PPE is suggested for performing maintenance or opening a sealed enclosure or when having evidence that any residual exposures are under control, operators should wear PPE as a precautionary measure. The workers should be communicated about the decision of use PPE and a training plan where the reasons the limitations of that decision and the properly way to use, maintain and remove of the PPE will be explained. Research is still trying to validate methods to determine the efficacy of the PPEs as a real barrier to NMs. Inhalation is the preferred entry of NMs into the human body, so respirators should be employed when workers could inhale NMs because of the lack of effective engineering controls or during activities with higher potential NMs exposure (which is the case for maintenance or emergencies). The lack of

OELs for many types of nanomaterials makes specific recommendations difficult.

N95 and P100 like the FFP2 and FFP3 filter cartridges are effective at capturing nanoparticles, but studies on the potential for face seal leakage (that is, leakage of particles through gaps between the respirator and the face) need more research addressing this issue [92]. However, the European Commission established that the level of protection of self-filtering masks against nanomaterials must be at least FFP3 with a nominal level of protection of 30 or higher [26].

Whenever exposure occurs during NMS handling tasks that provide skin contact, it is important to be aware that certain nanoparticles can cause adverse effects on the skin in specific circumstances, when crossing the skin barrier because it is compromised due to cracking or peeling, and entering the bloodstream potentially causing adverse health effects - local and systemic [60]. Workers should be informed about this ability of NMs to penetrate the skin and be stored in the skin's attachments, more so in damaged or flexed areas [59].

Protective clothing such as working clothes or disposable suits must be used and, at the end of the tasks, these must be removed and placed in specific containers, to avoid contamination of other places or workers. Polyethylene fabrics or similar are preferable [33].

Single-use gloves like disposable rubber gloves (e.g. latex), such as non-sterile medical examination gloves, should be used in order to avoid the NMs contact with the skin. Some chemicals (e.g. cleaning agents) may reduce the integrity of these kind of gloves, therefore, special care must be taken when handling these chemicals in such a way to avoid contact with them. Also, after use, these gloves should be taken off by pulling them inside out, so as to contain any raw powder or powder condensate that may have accumulated on the outside. For the same reasons eye protection must be worn in these situations (minimum of close-fitting safety glasses).

15.5 Conclusion

Due to their diversity of applications, nanotechnologies will experience an exponential expansion in the coming years and their uses promise great benefits for society. However, this growth brings additional exposure (of more workers) to a series of products with toxicological properties, in many cases unknown. In order to determine the benefits of using these advances and the risks that this entails, it is necessary to have a deeper understanding of these new materials. Many of these novel substances and elements could have the potential to be harmful for humans' health and the natural environment.

Specifically, in the H&S field and in order to adequately protect workers, it is necessary to continue the development of methods to assess the toxicity and other potentially source of hazards, as well as equipment of reasonable cost that allows monitoring exposure concentrations. Hazard identification of NMs among occupationally exposed workers in industries is one of the risk assessment, however, there is no conclusive data available on the effect of NMs in occupational contexts for many of the chemicals. The other step exposure assessment is based in air measurements that are taken in the vicinity of processes or operations using nanomaterials, either in companies or research laboratories, very little data have been published. In addition, no international consensus has been reached on any single measurement method for characterising occupational exposure. At the time there is no agreement in what testing strategies and methods of risk characterisation can be applied for nanomaterials. Precaution should be taken in controlling exposures when the extent of the hazard is not well known, as with many nanomaterials. The use of precautionary risk assessment approaches seems fairly reasonable especially considering the current lack of comprehensive and reliable toxicological and/or exposure information.

Finally, it is convenient for regulators as well as employers to strengthen research in this area

and put in place processes for risk assessment. They also need to make more efforts to facilitate the data obtained from exposure assessment at different levels (national, EU, international), which would make possible to improve toxicological studies and would also help in establishing exposure limits and determining the right index for them.

Acknowledgements ISQ acknowledges the financial support of the H2020 programme through projects PureNano (No. 821431), LightMe (No. 814552) and LightCoce (No. 814632).

Author Contributions A.R.A., C.M. and G.C.A conceived this study, led the narrative framing and wrote the chapter. M.I. provided feedback to the manuscript.

References

1. ACGIH (2008) TLVs and BEIs based on the documentation of the threshold limit values for chemical substances and physical agents & biological exposure indices. American Conference of Governmental Industrial Hygienists, Cincinnati
2. Aitken R, Creely K, Tran C (2004) Nanoparticles: an occupational hygiene review. HSE UK – Institute of Occupational Medicine, Edinburg
3. Albom A, Bridges J, De Jong W et al (2009) Risk assessment of products of nanotechnologies. Rep Sci Comm Emerg New Identified Health Risks–SCENIHR Eur Comm Health Consum DG Bruss
4. Aschberger K, Christensen FM, Rasmussen K, Jensen KA (2016) Feasibility and challenges of human health risk assessment for engineered nanomaterials. In: Engineered nanoparticles and the environment: biophysicochemical processes and toxicity. Wiley, Hoboken, pp 409–441
5. Boccuni F, Ferrante R, Tombolini F et al (2018) Workers' exposure to Nano-objects with different dimensionalities in R&D laboratories: measurement strategy and field studies. *Int J Mol Sci* 19:349
6. Bondarenko OM, Heinlaan M, Sihtmäe M et al (2016) Multilaboratory evaluation of 15 bioassays for (eco) toxicity screening and hazard ranking of engineered nanomaterials: FP7 project NANOVALID. *Nanotoxicology* 10:1229–1242
7. Bouillard J, Vignes A, Dufaud O et al (2010) Ignition and explosion risks of nanopowders. *J Hazard Mater* 181:873–880
8. Brouwer D, Boessen R, van Duuren-Stuurman B et al (2016) Evaluation of decision rules in a tiered assessment of inhalation exposure to nanomate-

- rials. *Ann Occup Hyg* 60:949–959. <https://doi.org/10.1093/annhyg/mew045>
9. BSI (2007) PD 6699–2–2007 nanotechnologies – part 2: guide to safe handling and disposal of manufactured nanomaterials. British Standards Institution, London
 10. CEN (2018) EN 17058 workplace exposure – assessment of exposure by inhalation of nano-objects and their aggregates and agglomerates. European Committee for Standardization, Brussels
 11. CEN (2020) CEN/TC 352 – nanotechnologies. https://standards.cen.eu/dyn/www/f?p=204:7:0:::FSP_ORG_ID:508478&cs=1A6FD A13EC1F6859FD3F63B18B98492ED. Accessed 20 Feb 2020
 12. Cena LG, Peters TM (2011) Characterization and control of airborne particles emitted during production of epoxy/carbon nanotube nanocomposites. *J Occup Environ Hyg* 8:86–92
 13. Chaturvedi S, Dave PN (2018) Nanomaterials: environmental, human health risk. In: *Handbook of nanomaterials for industrial applications*. Elsevier, pp 1055–1062
 14. Dahm MM, Evans DE, Schubauer-Berigan MK et al (2012) Occupational exposure assessment in carbon nanotube and nanofiber primary and secondary manufacturers. *Ann Occup Hyg* 56:542–556
 15. Dekkers S, Oomen AG, Bleeker EAJ et al (2016) Towards a nanospecific approach for risk assessment. *Regul Toxicol Pharmacol* 80:46–59. <https://doi.org/10.1016/j.yrtph.2016.05.037>
 16. Dimou K, Emond C (2017) Nanomaterials, and occupational health and safety – a literature review about control banding and a semi-quantitative method proposed for hazard assessment. *J Phys Conf Ser* 838:012020. <https://doi.org/10.1088/1742-6596/838/1/012020>
 17. Duncan TV (2015) Release of engineered nanomaterials from polymer nanocomposites: the effect of matrix degradation. *ACS Appl Mater Interfaces* 7:20–39
 18. Eastlake A, Hodson L, Geraci C, Crawford C (2012) A critical evaluation of material safety data sheets (MSDSs) for engineered nanomaterials. *J Chem Health Saf* 19:1–8
 19. Eastlake AC, Beaucham C, Martinez KF et al (2016) Refinement of the nanoparticle emission assessment technique into the nanomaterial exposure assessment technique (NEAT 2.0). *J Occup Environ Hyg* 13:708–717
 20. ECHA (2019a) Appendix for nanoforms applicable to the guidance on registration and substance identification draft (public) Version 1.0 September 2019. European Chemical Agency, Helsinki
 21. ECHA (2019b) Appendix R6–1 for nanoforms applicable to the guidance on QSARs and grouping of chemicals, Version 2.0 December 2019. European Chemical Agency, Helsinki
 22. EU Commission (2006) Regulation (EC) No 1907/2006 of the European Parliament and of the Council of 18 December 2006 concerning the Registration, Evaluation, Authorisation and Restriction of Chemicals (REACH), establishing a European Chemicals Agency, amending Directive 1999/45/EC and repealing Council Regulation (EEC) No 793/93 and Commission Regulation (EC) No 1488/94 as well as Council Directive 76/769/EEC and Commission Directives 91/155/EEC, 93/67/EEC, 93/105/EC and 2000/21/EC
 23. EU Commission (2011) Commission recommendation of 18 October 2011 on the definition of nanomaterial (2011/696/EU). *Off J Eur Communities Legis* 275:38–40
 24. EU Commission (2012) Communication from the commission to the European parliament, the council, the economic and social committee and the committee of the regions: Second Regulatory Review on Nanomaterials {SWD(2012) 288 final}
 25. EU Commission (2014a) Guidance on the protection of the health and safety of workers from the potential risks related to nanomaterials at work
 26. EU Commission (2014b) Working safely with manufactured nanomaterials – guidance for workers. Employment, Social Affairs & Inclusion, European Commission, Brussels, Belgium
 27. EU Parliament (2006) Regulation (EC) No 1907/2006 of the European Parliament and of the council of 18 December 2006 concerning the Registration, Evaluation, Authorisation and Restriction of Chemicals (REACH), establishing a European Chemicals Agency, amending Directive 1999/45/EC and repealing Council Regulation (EEC) No 793/93 and Commission Regulation (EC) No 1488/94 as well as Council Directive 76/769/EEC and Commission Directives 91/155/EEC, 93/67/EEC, 93/105/EC and 2000/21/EC
 28. EU Parliament (2008) Regulation (EC) no 1272/2008 of the European Parliament and of the council of 16 December 2008 on classification, labelling and packaging of substances and mixtures, amending and repealing Directives 67/548/EEC and 1999/45/EC, and amending Regulation (EC) no 1907/2006
 29. EUON (2020) Regulation. <https://euon.echa.europa.eu/regulation>
 30. EU-OSHA (2009) Workplace exposure to nanoparticles. European Agency for Safety and Health at Work, Bilbao, Spain
 31. Fisher E, Selin C, Wetmore J (2008) *Presenting futures*. Springer, Dordrecht
 32. Fransman W, Van Tongeren M, Cherrie JW et al (2011) Advanced Reach Tool (ART): development of the mechanistic model. *Ann Occup Hyg* 55:957–979
 33. Freeland J, Hulme J, Kinnison D et al (2012) Working safely with nanomaterials in research & development. The UK NanoSafety Partnership Group, Edinburgh
 34. Froggett SJ, Clancy SF, Boverhof DR, Canady RA (2014) A review and perspective of existing research on the release of nanomaterials from solid nanocomposites. *Part Fibre Toxicol* 11:17

35. Geraci C, Heidel D, Sayes C et al (2015) Perspectives on the design of safer nanomaterials and manufacturing processes. *J Nanopart Res* 17:366
36. Godinho da Fonseca AS (2016) Exposure characterisation and sources of nanoparticles in workplace environments. PhD thesis, Universitat de Barcelona
37. Goede HA, McNally K, Gorce J-P et al (2019) Dermal advanced REACH tool (dART) – development of a dermal exposure model for low-volatile liquids. *Ann Work Expo Health* 63:624–636
38. Gottardo S, Alessandrelli M, Amenta V et al (2017) NANoREG framework for the safety assessment of nanomaterials. European Commission Joint Research Centre, Luxembourg
39. Hansen SF, Jensen KA, Baun A (2014) NanoRiskCat: a conceptual tool for categorization and communication of exposure potentials and hazards of nanomaterials in consumer products. *J Nanopart Res* 16:2195. <https://doi.org/10.1007/s11051-013-2195-z>
40. Hristozov D, Gottardo S, Semenzin E et al (2016) Frameworks and tools for risk assessment of manufactured nanomaterials. *Environ Int* 95:36–53. <https://doi.org/10.1016/j.envint.2016.07.016>
41. HSE UK (2020) Understanding the hazards of nanomaterials. In: Health Saf Exec. <https://www.hse.gov.uk/nanotechnology/understanding-hazards-nanomaterials.htm>. Accessed 25 May 2020
42. Iavicoli I, Fontana L, Pingue P et al (2018) Assessment of occupational exposure to engineered nanomaterials in research laboratories using personal monitors. *Sci Total Environ* 627:689–702. <https://doi.org/10.1016/j.scitotenv.2018.01.260>
43. ICBA (2004) Carbon black user's guide, safety, health, & environmental information. International Carbon Black Association, Louisiana
44. IOM SAFENANO (2020) Current nanotechnology standardisation activities. <https://www.safenano.org/KnowledgeBase/Standards.aspx>. Accessed 20 Feb 2020
45. ISO (2012a) ISO/TS 12901–2 2012 nanotechnologies – occupational risk management applied to engineered nanomaterials – part 2: Use of the control banding approach. International Organization for Standardization, Geneva, Switzerland
46. ISO (2012b) ISO/TS 12901–1 2012 nanotechnologies – occupational risk management applied to engineered nanomaterials – part 1: Principles and approaches. International Organization for Standardization, Geneva, Switzerland
47. ISO (2018a) ISO 31000: 2018 risk management—principles and guidelines. International Organization for Standardization, Geneva, Switzerland
48. ISO (2018b) ISO/TR 12885:2018 nanotechnologies – health and safety practices in occupational settings. International Organization for Standardization, Geneva, Switzerland
49. ISO (2020) Technical Committees: ISO/TC 229 nanotechnologies. <https://www.iso.org/committee/381983.html>. Accessed 20 Feb 2020
50. Jalonen H (2012) The uncertainty of innovation: a systematic review of the literature. *J Manag Res* 4:1
51. Jeevanandam J, Barhoum A, Chan YS et al (2018) Review on nanoparticles and nanostructured materials: history, sources, toxicity and regulations. *Beilstein J Nanotechnol* 9:1050–1074. <https://doi.org/10.3762/bjnano.9.98>
52. Jensen KA, Saber AT, Kristensen HV et al (2013) NanoSafer vs. 1.1 – nanomaterial risk assessment using first order modeling. In: 6th International symposium on nanotechnology, occupational and environmental health, p 120
53. Khan FH (2014) Chemical hazards of nanoparticles to human and environment (a review). *Orient J Chem* 29:1399–1408
54. Kraegeloh A, Suarez-Merino B, Sluijters T, Micheletti C (2018) Implementation of safe-by-design for nanomaterial development and safe innovation: why we need a comprehensive approach. *Nano* 8:239
55. Kuempel ED, Tran CL, Castranova V, Bailer AJ (2006) Lung dosimetry and risk assessment of nanoparticles: evaluating and extending current models in rats and humans. *Inhal Toxicol* 18:717–724. <https://doi.org/10.1080/08958370600747887>
56. Kuijpers E, Bekker C, Brouwer D, le Feber M, Fransman W (2017) Understanding workers' exposure: systematic review and data-analysis of emission potential for NOAA. *J Occup Environ Hyg* 14(5): 349–359. <https://doi.org/10.1080/15459624.2016.1252843>
57. Kumar A, Kumar P, Anandan A et al (2014) Engineered nanomaterials: knowledge gaps in fate, exposure, toxicity, and future directions. *J Nanomater*
58. Lamon L, Aschberger K, Asturiol D et al (2019) Grouping of nanomaterials to read-across hazard endpoints: a review. *Nanotoxicology* 13:100–118
59. Larese Filon F, Mauro M, Adami G et al (2015) Nanoparticles skin absorption: new aspects for a safety profile evaluation. *Regul Toxicol Pharmacol* 72:310–322. <https://doi.org/10.1016/j.yrtph.2015.05.005>
60. Larese Filon F, Bello D, Cherrie JW et al (2016) Occupational dermal exposure to nanoparticles and nano-enabled products: part I – factors affecting skin absorption. *Int J Hyg Environ Health* 219:536–544. <https://doi.org/10.1016/j.ijheh.2016.05.009>
61. Lee EG, Lamb J, Savic N et al (2019) Evaluation of exposure assessment tools under REACH: part I – tier 1 tools. *Ann Work Expo Health* 63:218–229. <https://doi.org/10.1093/annweh/wxy091>
62. Leszczynski J, Puzyn T (2012) Towards efficient designing of safe nanomaterials: innovative merge of computational approaches and experimental techniques. Royal Society of Chemistry
63. Liguori B, Hansen SF, Baun A, Jensen KA (2016) Control banding tools for occupational exposure assessment of nanomaterials – ready for use in a

- regulatory context? *NanoImpact* 2:1–17. <https://doi.org/10.1016/j.impact.2016.04.002>
64. Malsch I, Subramanian V, Semenzin E et al (2015) Supporting decision-making for sustainable nanotechnology. *Environ Syst Decis* 35:54–75. <https://doi.org/10.1007/s10669-015-9539-4>
 65. Marchant GE, Sylvester DJ, Abbott KW (2008) Risk management principles for nanotechnology. *NanoEthics* 2:43–60
 66. Maynard AD, Aitken RJ (2007) Assessing exposure to airborne nanomaterials: current abilities and future requirements. *Nanotoxicology* 1:26–41. <https://doi.org/10.1080/17435390701314720>
 67. Mihalache R, Verbeek J, Graczyk H et al (2017) Occupational exposure limits for manufactured nanomaterials, a systematic review. *Nanotoxicology* 11:7–19. <https://doi.org/10.1080/17435390.2016.1262920>
 68. Nakanishi J, Morimoto Y, Ogura I et al (2015) Risk assessment of the carbon nanotube group: risk assessment of CNT. *Risk Anal* 35:1940–1956. <https://doi.org/10.1111/risa.12394>
 69. NIOSH (2009) Approaches to safe nanotechnology – managing the health and safety concerns associated with engineered nanomaterials. National Institute for Occupational Safety and Health, Washington DC
 70. NIOSH (2011) Occupational exposure to titanium dioxide. Centers for Disease Control and Prevention – National Institute for Occupational Safety and Health, Washington DC
 71. NIOSH (2013) Occupational exposure to carbon nanotubes and nanofibers. Centers for Disease Control and Prevention – National Institute for Occupational Safety and Health, Washington DC
 72. NIOSH (2014) Current strategies for engineering controls in nanomaterial production and downstream handling processes. National Institute for Occupational Safety and Health, Washington DC
 73. NIOSH (2016) Building a safety program to protect the nanotechnology workforce: a guide for small to medium-sized enterprises. National Institute for Occupational Safety and Health, Washington DC
 74. NIOSH (2017) NIOSH pocket guide to chemical hazards. National Institute for Occupational Safety and Health, Washington DC
 75. NRC (2011) Prudent practices in the laboratory: handling and management of chemical hazards, updated version. National Academies Press - National Research Council, Washington DC
 76. O’Shaughnessy PT (2013) Occupational health risk to nanoparticulate exposure. *Environ Sci Process Impacts* 15:49–62
 77. OECD (2011) Nanosafety at the OECD: the first five years 2006–2010. Organisation for Economic Co-operation and Development, Paris
 78. OECD (2015) Harmonized tiered approach to measure and assess the potential exposure to airborne emissions of engineered nano-objects and their agglomerates and aggregates at workplaces. Organisation for Economic Co-operation and Development, France, Paris
 79. OECD (2017) Strategies, techniques and sampling protocols for determining the concentrations of manufactured nanomaterials in air at the workplace. Organisation for Economic Co-operation and Development, France, Paris
 80. Osman EM (2019) Environmental and health safety considerations of nanotechnology: nano safety. *Biomed J Sci Tech Res* 19. <https://doi.org/10.26717/BJSTR.2019.19.003346>
 81. Ostiguy C, Riediker M, Triolet J et al (2010) Development of a specific control banding tool for nanomaterials: report. ANSES. French agency for food, environmental and occupational health and safety
 82. Ostrom LT, Wilhelmsen CA (2019) Risk assessment: tools, techniques, and their applications. Wiley, Cambridge
 83. Park M, Wijnhoven S (2017) GUIDEnano: a web-based guidance tool for risk assessment and mitigation of nano-enabled products. *TCDD* 3
 84. Pauluhn J (2010) Multi-walled carbon nanotubes (Baytubes®): approach for derivation of occupational exposure limit. *Regul Toxicol Pharmacol* 57:78–89. <https://doi.org/10.1016/j.yrtph.2009.12.012>
 85. Pietroiusti A, Stockmann-Juvala H, Lucaroni F, Savolainen K (2018) Nanomaterial exposure, toxicity, and impact on human health. *Wiley Interdiscip Rev Nanomed Nanobiotechnol* 10:e1513. <https://doi.org/10.1002/wnan.1513>
 86. Pośniak M (2020) Emerging chemical risks in the work environment. CRC Press, London
 87. Ramos D, Almeida L, Gomes M (2019) Application of control banding to workplace exposure to nanomaterials in the textile industry. In: Arezes PM, Baptista JS, Barroso MP et al (eds) Occupational and environmental safety and health. Springer, Berlin, pp 105–113
 88. Rasmussen K, Rauscher H, Mech A et al (2018) Physico-chemical properties of manufactured nanomaterials-characterisation and relevant methods. An outlook based on the OECD testing programme. *Regul Toxicol Pharmacol* 92:8–28
 89. Rasmussen K, Rauscher H, Kearns P et al (2019) Developing OECD test guidelines for regulatory testing of nanomaterials to ensure mutual acceptance of test data. *Regul Toxicol Pharmacol* 104:74–83
 90. Rauscher H, Mech A, Gibson N et al (2019a) Identification of nanomaterials through measurements, EUR 29942 EN. Publications Office of the European Union, Luxembourg
 91. Rauscher H, Roebben G, Mech A et al (2019b) An overview of concepts and terms used in the European Commission’s definition of nanomaterial, EUR 29647 EN. European Commission, JRC, Ispra

92. Rengasamy S, Eimer BC, Shaffer RE (2009) Comparison of nanoparticle filtration performance of NIOSH-approved and CE-marked particulate filtering Facepiece respirators. *Ann Occup Hyg* 53:117–128. <https://doi.org/10.1093/annhyg/men086>
93. Rose G, Pavlicek A, Gázsó A (2019) Safe-by-design – the early integration of safety aspects in innovation processes. *NanoTrust Doss* 50
94. Rothen-Rutishauser B, Clift MJ, Jud C et al (2012) Human epithelial cells in vitro—are they an advantageous tool to help understand the nanomaterial-biological barrier interaction? *EURO NanoTox Lett* 4:1–20
95. Sajid M, Ilyas M, Basheer C et al (2015) Impact of nanoparticles on human and environment: review of toxicity factors, exposures, control strategies, and future prospects. *Environ Sci Pollut Res* 22:4122–4143. <https://doi.org/10.1007/s11356-014-3994-1>
96. Sánchez Jiménez A, Varet J, Poland C et al (2016) A comparison of control banding tools for nanomaterials. *J Occup Environ Hyg* 13:936–949. <https://doi.org/10.1080/15459624.2016.1200191>
97. Schneider T, Brouwer DH, Koponen IK et al (2011) Conceptual model for assessment of inhalation exposure to manufactured nanoparticles. *J Expo Sci Environ Epidemiol* 21:450–463. <https://doi.org/10.1038/jes.2011.4>
98. Schulte P, Geraci C, Zumwalde R et al (2008) Occupational risk Management of Engineered Nanoparticles. *J Occup Environ Hyg* 5:239–249. <https://doi.org/10.1080/15459620801907840>
99. Sellers K, Deleebeeck NM, Messiean M et al (2015) Grouping nanomaterials: a strategy towards grouping and read-across. *Rijksinstituut voor Volksgezondheid en Milieu RIVM*
100. Semenzin E, Giubilato E, Badetti E et al (2019) Guiding the development of sustainable nano-enabled products for the conservation of works of art: proposal for a framework implementing the safe by design concept. *Environ Sci Pollut Res* 26:26146–26158
101. Silva GLE, Viana C, Domingues D, Vieira F (2019) Risk assessment and health, safety, and environmental Management of Carbon Nanomaterials. In: Clichici S, Filip A, do Nascimento GM (eds) *Nanomaterials-toxicity, human health and environment*. IntechOpen, London
102. Soeteman-Hernandez LG, Apostolova MD, Bekker C et al (2019) Safe innovation approach: towards an agile system for dealing with innovations. *Mater Today Commun* 20:100548. <https://doi.org/10.1016/j.mtcomm.2019.100548>
103. Sparrow MK (2011) *The regulatory craft: controlling risks, solving problems, and managing compliance*. Brookings Institution Press, Washington, DC
104. Stockmann-Juvala H, Taxell P, Santonen T (2014) Formulating occupational exposure limits values (OELs)(Inhalation & Dermal) – Scaffold Public Documents-SPD7. Finnish Institute of Occupational Health, Helsinki, Finland
105. Sweeney LM, MacCalman L, Haber LT et al (2015) Bayesian evaluation of a physiologically-based pharmacokinetic (PBPK) model of long-term kinetics of metal nanoparticles in rats. *Regul Toxicol Pharmacol* 73:151–163
106. Tsai S-J, Huang RF, Ellenbecker MJ (2010) Airborne nanoparticle exposures while using constant-flow, constant-velocity, and air-curtain-isolated fume hoods. *Ann Occup Hyg* 54:78–87
107. Tsai CS-J, Echevarría-Vega ME, Sotiriou GA et al (2012) Evaluation of environmental filtration control of engineered nanoparticles using the Harvard versatile engineered nanomaterial generation system (VENGES). *J Nanopart Res* 14:812. <https://doi.org/10.1007/s11051-012-0812-x>
108. TSI (2012) NanoScan SMPS nanoparticle sizer model 3910. TSI, Minnesota, US
109. van Broekhuizen P, van Veelen W, Streekstra W-H et al (2012) Exposure limits for nanoparticles: report of an International workshop on nano reference values. *Ann Occup Hyg*. <https://doi.org/10.1093/annhyg/mes043>
110. van Duuren-Stuurman B, Vink SR, Verbist KJM et al (2012) Stoffenmanager Nano Version 1.0: a web-based tool for risk prioritization of airborne manufactured nano objects. *Ann Occup Hyg*. <https://doi.org/10.1093/annhyg/mer113>
111. van Harmelen T, Zondervan-van den Beuken EK, Brouwer DH et al (2016) LICARA nanoSCAN-a tool for the self-assessment of benefits and risks of nanoproducts. *Environ Int* 91:150–160
112. van Teunenbroek T, Dijkzeul A, Baker J (2017) PROSAFE – promoting the implementation of safe by design: white paper. Dutch Ministry of Infrastructure and the Environment
113. Warheit DB (2018) Hazard and risk assessment strategies for nanoparticle exposures: how far have we come in the past 10 years? *F1000Res* 7
114. Yan X, Sedykh A, Wang W et al (2019) In silico profiling nanoparticles: predictive nanomodeling using universal nanodescriptors and various machine learning approaches. *Nanoscale* 11:8352–8362
115. Zalk DM, Paik SY, Swuste P (2009) Evaluating the control banding Nanotool: a qualitative risk assessment method for controlling nanoparticle exposures. *J Nanopart Res* 11:1685–1704. <https://doi.org/10.1007/s11051-009-9678-y>
116. Kuijpers EC, Bekker D, Brouwer M, le Feber W, Fransman (2017) Understanding workers' exposure: Systematic review and data-analysis of emission potential for NOAA. *Journal of Occupational and Environmental Hygiene* 5:349-359 10.1080/15459624.2016.1252843

Open Access This chapter is licensed under the terms of the Creative Commons Attribution 4.0 International License (<http://creativecommons.org/licenses/by/4.0/>), which permits use, sharing, adaptation, distribution and reproduction in any medium or format, as long as you give appropriate credit to the original author(s) and the source, provide a link to the Creative Commons license and indicate if changes were made.

The images or other third party material in this chapter are included in the chapter's Creative Commons license, unless indicated otherwise in a credit line to the material. If material is not included in the chapter's Creative Commons license and your intended use is not permitted by statutory regulation or exceeds the permitted use, you will need to obtain permission directly from the copyright holder.





Nanomaterials in Foods and Human Digestion: An Important Layer in the Assessment of Potential Toxic Effects

Carla Martins, Paula Alvito, and Ricardo Assunção

Abstract

The use of nanoparticles (e.g. titanium dioxide) in commercial food products to modify some properties, such as brightness and whiteness, increased in the last years and is nowadays widespread. Despite the inhalation of nanoparticles is already a topic of concern, the potential adverse health effects due to ingestion still

present gaps of knowledge. In fact, gastrointestinal tract is the first interface between the body and the external environment and consequently could represent a target organ for compounds present in food, namely nanoparticles, that could exert toxic effects. The *in vitro* digestion models used to simulate the human digestion may contribute to fill these gaps. The applicability of the *in vitro* digestion methods is discussed concerning its potential use as a tool for addressing the toxicity of ingested nanomaterials or other food contaminants, mimicking the physiological processes.

C. Martins (✉)

NOVA National School of Public Health, Public Health Research Center, Universidade NOVA de Lisboa, Lisbon, Portugal

Food and Nutrition Department, National Institute of Health Dr. Ricardo Jorge, Lisbon, Portugal

CESAM, Centre for Environmental and Marine Studies, University of Aveiro, Aveiro, Portugal

Comprehensive Health Research Center (CHRC), Universidade NOVA de Lisboa, Lisbon, Portugal
e-mail: carla.martins@insa.min-saude.pt

P. Alvito

Food and Nutrition Department, National Institute of Health Dr. Ricardo Jorge, Lisbon, Portugal

CESAM, Centre for Environmental and Marine Studies, University of Aveiro, Aveiro, Portugal

R. Assunção

Food and Nutrition Department, National Institute of Health Dr. Ricardo Jorge, Lisbon, Portugal

CESAM, Centre for Environmental and Marine Studies, University of Aveiro, Aveiro, Portugal

Comprehensive Health Research Center (CHRC), Universidade NOVA de Lisboa, Lisbon, Portugal

Keywords

In vitro digestion · Digestion models · Ingested nanomaterials · Human digestion simulation · Gastrointestinal system

16.1 General Introduction

Several challenges are posed nowadays through the development of novel foods and their by-products. The current food production system is making efforts to promote shifts to more sustainable products, guaranteeing simultaneously the food safety and nutritional quality. The inclusion of nanomaterials (NMs) in foods is one of these challenges. The increased shelf-life, flavor release and absorption of nutrients and other bio-

active components have been referred as some of the beneficial effects of the use of NMs in foods [48]. As more NMs are being included in food production systems, a need to understand the potential risks and benefits of their use for consumers' health is essential. The knowledge of NMs' fate along the gastrointestinal system with the use of *in vitro* digestion models is a major contribution for this assessment.

16.2 Inclusion of Nanomaterials in Foods

According to the Novel Food Regulation (EU) 2015/2283 and referring to Regulation (EU) 1169/2011 on the Provision of Food Information to Consumers, the term ENM (Engineered Nanomaterials) means "any intentionally produced material that has one or more dimensions of the order of 100 nm or less or that is composed of discrete functional parts, either internally or at the surface, many of which have one or more dimensions of the order of 100 nm or less, including structures, agglomerates or aggregates, which may have a size above the order of 100 nm but retain properties that are characteristic of the nanoscale" [16, 18, 19].

Dietary intake of ENM can be an important pathway of human exposure to nanoparticles (NPs) and food additives, as other forms deliberately added in food industry, are considered the primary source of ingested exposure. ENM intake by food is not yet extensively characterized in developed countries; however, it is estimated to be considerable, as revealed by a study that reported an ingestion uptake estimate of $\sim 10^{12}$ nanoparticles/person per day, consisting mainly of titanium dioxide (TiO₂), colloidal silica, and mixed silicates [7, 47]. The estimation of human daily intake of NPs has been a subject of interest in the last years. Rompelberg et al. [40] estimated the exposure of the Dutch population to TiO₂ NP through oral intake of several products (food, supplements and toothpaste). The median estimates of exposure were 1.90 $\mu\text{g}/\text{kg}$ bw/day, 0.26 $\mu\text{g}/\text{kg}$ bw/day and 0.10 $\mu\text{g}/\text{kg}$ bw/day for the

age groups of 2–6 years old, 7–69 years old and ≥ 70 years old, respectively. Also Yin et al. [55] estimated that the mean daily intake of TiO₂ particles (including nanosized particles) from seafood and surimi products ranged from 0.02 to 3.09 $\mu\text{g}/\text{kg}$ bw/day, with individuals aged 20–30 years old showing the highest exposure levels.

The progress observed during the last years in nanotechnology contributed for the increasing interest of its application in the food industry [43]. The use of nanotechnologies can be considered in every phase of food production, including the food processing and food preservation. Several applications in food industry have been reported in various dimensions such as the characteristics of foods (texture, taste, color, strength), the food additives encapsulation, the new flavors and sensations, the control of aroma release, and the stability/shelf-life of products [10]. NPs can be organic (lipid and protein NPs), inorganic (silver, titanium dioxide, or zinc oxide), or including carbon-based NPs (carbon nanofibers and carbon nanotubes) [12]. NPs can enhance some characteristics of foods such as texture or color and can also be incorporated in food packaging. Another important contribute to this area is the possibility of incorporating nanomaterials (e.g. titanium dioxide, silver nanoparticles, carbon nanotubes) that allow to mitigate food losses due to different microbial infections. [46, 52]. Additionally, the development of nanoprobes for detection of chemical (mycotoxins, pesticides, antibiotics, plasticizers, melamine) and microbiological contaminants (food spoilage) are nowadays established areas of research as pointed out by [39]. Nutraceuticals and functional antimicrobial ingredients used as encapsulated play a crucial role in the preservation and bioavailability of bioactive ingredients, food processing and storage, and also in the transport through the gastrointestinal tract. Nanoemulsions are used in flavored oils, salad dressing, personalized beverages, sweeteners, and other processed foods, to create lipid-soluble compounds that are bioactive for targeted delivery of lutein, β -carotene, vitamins A and D, and omega-3-fatty acids [38, 43].

The progress observed in nanotechnology has contributed to the transformation of food science and the food industry with increased investment and market share. As briefly explained, the broad applications of nanotechnology will contribute to a new digital improvements namely in the domains of food reliability, food safety, and shelf-life performance [26, 43]. However, there is a consensus regarding the challenges ahead in this field. The interactions of nanomaterials with the food systems need to be further estimated, thus contributing for harmonized actions at a global scale in a combined effort of food regulators, authorities, and industry [21, 26, 37, 43].

16.3 The Importance of Human Digestion for the Toxicity Assessment of Nanomaterials

Considering that ingestion is a route of human exposure to NMs, it is of utmost importance to assess the possible influence of digestion on these particles. The physiological response to specific nanomaterials in foods is understood in full when framed by the human digestive processes in more detail [4].

16.3.1 The Fate of Nanomaterials During Human Digestion

During digestion, the chemical environments are modified within the three main compartments (mouth, stomach and intestine) regarding pH, enzymes, and inorganic compounds. The transit through the gastrointestinal (GI) system may lead to several modification in the NP including dissolution, agglomeration and deagglomeration; all these may affect the intestinal absorption that is different if in presence of dissolved ions or nanoparticles, and depends on their size, shape and physicochemical properties [44].

The first step of digestion happens in the mouth and involves the mixture of food with salivary fluid, containing about 99.5% water with 0.3% of electrolytes and proteins, including amy-

lase [35]. Salivary pH values vary between fasted to fed state, from 6.2–7.4 to 7.4–7.6, respectively [50]. The transient time in mouth compartment is short. Nevertheless, there may be an impact in some types of NMs such as silver NPs for which the aggregation of 52% of nanoparticles was reported [25] and for carbohydrate NPs that may be digested by amylase [33].

After bolus formation in the oral phase, it is processed in the stomach to a semi-solid chime, by action of the gastric juice constituted by hydrochloric acid, various electrolytes, enzymes (pepsin and gastric lipase), intrinsic factor, mucus, and hormones [27]. Stomach pH vary during digestion from 1.5 to 2.0 in the fasted state to 3.0–7.0 in the fed state. The key gastric proteolytic enzyme (pepsin) and gastric lipase are activated via acid hydrolysis [42]. The physic-chemical properties of gastric environment, mainly high strong acid conditions and high ionic strength, promote modifications in NMs. For lipid NPs, the aggregation status is modified due to changes in their surface properties, such as surface charge and steric coating. The triglycerides, common components of lipid NPs, start to digest when there is enough secretion of gastric lipase in the stomach [54]. Studies in gastric fluid showed that TiO₂ NPs tended to agglomerate in the presence of gastric fluid with an effect more apparent and significant in the nanoparticle range [24]. Similar findings were reported for Ag NPs that in gastric fluid agglomerated by forming clusters with proteins [28], a process enhanced by the presence of pepsin [3].

The small intestine, where the highest percentage of chemical breakdown and absorption occur by secretions of the liver, gall bladder, pancreas, and intestinal epithelia, receives the gastric chime that is neutralized by bicarbonate raising the pH from 2 to 6.2. The degradation of food starts in the duodenum that receives about 1.2–1.5 L/day of pancreatic juice [23]. Simultaneously and gradually over the course of 3–4 h (depending of the meal ingested), the pancreatic juice, composed by a mixture of enzymes, proenzymes, protease inhibitors, sodium bicarbonate and other electrolytes, is secreted. The characteristics of NMs

when reaching the intestine encompass the influence of the different gastrointestinal tract environments, are determinant for their ability to absorption by intestinal epithelium and accordingly to the potential toxicity [33]. Small molecules are mainly absorbed at the small intestine passively through diffusion or actively through several transporter systems in the gut wall [23]. Although NPs suffer a process of agglomeration during the gastric phase, in the presence of the small intestine environment, characterized by a basic pH, presence of bile and pancreatic enzymes, the clusters are disintegrated [28]. Similar observations were reported for Ag NPs that retained their original size in intestinal fluid [53].

These findings are of utmost importance since it is known that the toxicity of a NM is the outcome of its intrinsic physicochemical properties such as size, shape, surface properties, and chemical composition, that will influence their cellular uptake [41]. Regarding the availability in the intestine and the absorption of NMs, it is crucial to understand properly the definitions of bioavailability and bioaccessibility (Fig. 16.1). Bioavailability is defined as the part of ingested compound that reaches the systematic circulation and is ultimately utilized [51] and oral bioavailability is resultant of three processes including: i) bioaccessibility (release of the compound from its matrix into digestive juice in the gastrointestinal tract); ii) intestinal transport, across the intestinal epithelium into the vena Portae; and iii) metabolism (degradation of the compound in the liver and intestine) [51]. Oral bioavailability includes bioaccessibility, which is defined as the quantity of a compound that is released from its matrix in the gastrointestinal tract, becoming available for absorption. Digestion is the chemical disintegration of food particles into absorb-

able molecules and, absorption refers to the transport of nutrients, water and electrolytes from the lumen of the small intestine into the cell, and then into the blood [51].

16.3.2 In Vitro Digestion Models

Several gastrointestinal models have been developed to better understand the effects of human digestion of nutrients, contaminants, additives, and other food components, as nanomaterials. As above mentioned, the gastrointestinal tract is a complex system with several physical and biochemical processes (*i.e.* hormonal response, gastric emptying, enzymes and fluids secretion, motility) that are dependent on the individual physiology and on the food consumed [36]. Although studies developed in humans are considered the “gold standard” for addressing diet related issues, *in vitro* methods have many advantages namely being more rapid, less expensive, and not presenting ethical constrictions. These characteristics make possible the analysis of several with a higher degree of standardization, reproducibility and in controlled conditions [9, 35].

These models may differ between each other regarding many parameters: the number of compartments and number of phases considered, the digestion fluids composition, the source of enzymes, the ratio between food and enzymes or digestive fluids, and the compartment staying time. The models may comprise a dynamic variation of these parameters along the digestion simulation, a semi-dynamic variation where only some parameters change through time, and static conditions that are maintained throughout the process.

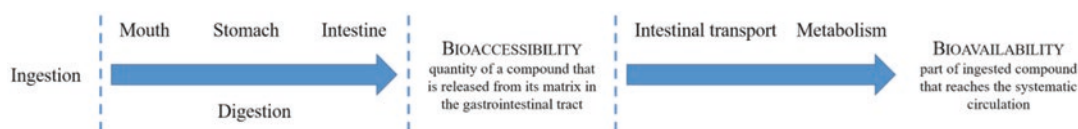


Fig. 16.1 Schematic representation of bioaccessibility and bioavailability concepts

One of the best-known dynamic models is the TNO Gastro-Intestinal Model (TIM), a multi-compartmental dynamic model from the early 1990s, that comprises the simulation of human digestion in three compartments (stomach, small intestine, large intestine). During this, the exposure conditions of meals regarding absorption of nutrients and water and secretion of digestive fluids, are modified intending to simulate the gastrointestinal tract [49]. The system is computer-controlled and the different parameters are combined in a protocol, thus allowing for reproducibility [49].

Other multi-compartmental models were also developed presenting different characteristics. The DIDGI® system was developed at INRA, focused on the stomach and the small intestine, and monitors the disintegration and the kinetics of hydrolysis of the food. The Simulator or the Human Intestinal Microbial Ecosystem (SHIME®), developed at Ghent University, is dedicated to the study of the gastrointestinal microbial ecology and physiology in healthy populational groups (adults, babies, elderlies) and also for individuals with specific disease conditions (e.g. Inflammatory Bowel Disease, pathogen infection). The Engineered Stomach and small INtestinal system (ESIN), developed at University of Auvergne (Clermont-Ferrand, France), is also dedicated to the simulation of human stomach and small intestine environment. The gastric compartment is patented and is able to reproduce the dynamic gastric emptying of liquids and solids during human digestion. The SIMGI® (SIMulator of the GastroIntestinal tract) from the Institute of Food Science Research CIAL (CSIC-UAM, Madrid, Spain) is also a computer-controlled model that simulates the human digestion process in the stomach and in the small intestine, but is also able to reproduce the microbiota responsible for metabolic bioconversions in the large intestine [11, 15]. Other dynamic models developed so far include mono-compartmental systems: Dynamic Gastric Model (DGM, Institute of Food Research, Norwich, UK), Human Gastric Simulator (HGS, University of California, Davis, USA) and the Artificial Colon (ARCOL, University of Clermont Auvergne, Clermont-Ferrand, France) [15].

Recently, with the aim of solving an existing gap between static and dynamic digestion models in what regards the human GIT physiological variations, a standardized semi-dynamic model was developed. This model is based on a previous static version, but it mimics closely the dynamic nature of gastric secretions and emptying. This model was foreseen for a broad use, comprising a wide range of foods [36].

Despite the innovation presented by dynamic and semi-dynamic digestion models, the static models are still recognized as simple, easy-to-use and reproducible [17, 32, 35]. These models that consider a constant ratio of food to enzymes and electrolytes and a constant pH for each digestive phase, are characterized as simple models and due to these characteristics have been used in several scientific fields [6]. Within the INFOGEST network [14] and considering the need for the harmonization of digestion conditions, an international consensus on fundamental digestion parameters for the static *in vitro* simulation of adult digestion was obtained and published in 2014 [35]. This method was further optimized, namely the assay for determination of pepsin enzymatic activity, and validated through an interlaboratory trial [17]. The method INFOGEST 2.0 that includes all the improvements was recently described by Brodkorb et al. [6]. The scope of application is very broad: evaluation of release of nutrients and/or food contaminants or assessment of endpoints resulting from digestion of foods by analyzing the digestion products. To perform the whole protocol, approximately 7 days should be considered, where ~5 d are needed to determine the activities of enzymes [6].

16.3.3 Application of Digestion Models to Nanomaterials

During digestion, the chemical environments are modified within the three main compartments (mouth, stomach, and intestine) regarding pH, enzymes, and inorganic compounds. These changes, as above mentioned, may induce nanoparticle modifications including dissolution,

agglomeration and deagglomeration, thus affecting the intestinal uptake [44].

During the recent years, several *in vitro* digestion models have been applied to study the potential impact of human digestion in nanomaterials properties and health effects. Table 16.1 provides examples of studies that used *in vitro* digestion models as well as the main characteristics of the models applied.

As it can be concluded from the information presented in Table 16.1, the available studies used *in vitro* digestion models with different characteristics not only regarding the digestive fluids' composition and pH in each compartment, but also regarding the static or dynamic conditions of the models.

The use of *in vitro* digestion models allowed obtaining results of the interactions of ENMs with food and GIT components and understanding their influence on nanomaterials' fate and transport, biokinetics and toxicological profile. Regarding Fe₂O₃ NP, differences in particle size, charge, and morphology were found among digested samples from the different compartments (mouth, stomach, and small intestine) [13]. This study demonstrated the influence of food matrix and the gastrointestinal environment in Fe₂O₃ NP biological properties [13]. For TiO₂ NP, the influence in mean particle diameter was also observed with increasing particle size when pH decreases (stomach), suggesting that the particles may have suffered an agglomeration or structural rearrangement under more acidic pH conditions [31]. The effect of TiO₂ NP in digestion of lipids using oil-in-water emulsions was assessed, and a reduced impact on the gastrointestinal fate and digestion of lipids was observed [31].

The use of *in vitro* digestion models has a major importance in studies where the transport through the intestinal barrier is evaluated. [1] using the model proposed by [51] concluded that the transport of silver as either total Ag or Ag NPs was limited (<0.1%), and the surface chemistry of Ag NPs and their digestion influence their dissolution properties, uptake/association with the Caco-2/HT29-MTX mono-layer. For Al NPs, [45] found no nano-specific cellular effects, either with or without *in vitro* digestion. The artificial

digestion did not cause a complete aggregation of Al in the intestinal fluid, as observed for other NPs. Nano-specific toxicity caused by Al-containing nanoparticles was not observed [45]. Bettencourt et al. [4], using the harmonized protocol proposed by Brodkorb et al. [6], reported for TiO₂ NPs that the primary size (Feret min, max and mean) and particle morphology (aspect ratio) of the anatase NM-102, rutile NM-103 and anatase/rutile NM-105 were not changed after the digestion. For the anatase/rutile NM-105, and when compared to the undigested NM, a more marked adverse outcome was shown after exposure to the digestion product [4]. The use of SIMGI® dynamic system, with more gastrointestinal compartments, made possible to go beyond the assessment of NPs effects on small intestine and assess the possible effects on microbiota. [11] reported that Ag NPs experienced several modifications in gastrointestinal fluids resulting in an exposure of intestine to forms that were structurally different from the original forms, even though not disturbing the composition and metabolic activity of human intestinal microbiota [11].

The inclusion of *in vitro* digestion models to have a more complete and accurate toxicological profile has been an achievement in the last years. These studies allowed taking a step forward in the knowledge of nanomaterials' toxicity. However, it should be emphasized the importance of using harmonized protocols so that the comparison of results obtained under these studies may be possible.

16.4 Importance of *In Vitro* Digestion for Risk Assessment

Human health risk assessment of chemicals present in foods, a fundamental scientific component of risk analysis, corresponds to a complex process of evaluating the potential incidence of an adverse health effect to humans, as a consequence of various exposure conditions. It is composed of four different and interconnected steps, that include: 1) hazard identification and 2) characterization (together usually considered as hazard assess-

Table 16.1 Main characteristics of the *in vitro* digestion models recently used for nanomaterials

Reference	NM	Type of model	Compartments	Incubation (time, temperature)	Digestive fluids	pH	Aim
[13]	Iron oxide (Fe ₂ O ₃)	Static	Mouth Stomach Intestine	2 min, 37 °C 2 hours, 37 °C 2 hours, 37 °C	Mucin, amylase, salts HCl, pepsin, salts Bile salts, lipase, salts	6.8 NR 7.0	To simulate GI digestion of nano-enabled food models, in three compartments, with characterization of ENM modifications across the GI.
[31]	Titanium Dioxide (TiO ₂)	Static	Mouth Stomach Intestine	2 min, 37 °C 2 hours, 37 °C 2 hours, 37 °C	Mucin, amylase, salts HCl, pepsin, salts Bile salts, lipase, salts	6.8 2.5 7.0	To study the impact of the TiO ₂ particles on the properties of the lipid droplets in their passage through the GIT, and also on lipid digestion.
[11]	Silver (ag)	Dynamic SIMGI®	Stomach Small intestine Ascending colon Transverse colon Descending colon	70 min; 37 °C 120 min, 37 °C Time (NR), 37 °C Time (NR), 37 °C Time (NR), 37 °C	Pepsin in 0.5 mL/min of gastric juice Pancreatic juice (5 mL/min)	5.6 to 2.0 7.0 5.6 6.3 6.8	To assess modifications in microbiota composition, microbial metabolic activity, and in ag NPs size, shape, stability, and aggregation in the SIMGI® (stomach, small intestine, ascending colon, transverse colon, and descending colon).
[1]	Silver (ag)	Static	Mouth Stomach Intestine	5 min, 37 °C 2 hours, 37 °C 2 hours, 37 °C	Saliva fluid (salts, amylase, mucin) Gastric fluid (salts, proteins, pepsin, mucin) Duodenal fluid (salts, proteins, pancreatin, lipase) + bile fluid (salts, proteins, bile)	7.0 5.0 7.0	To assess the impact of <i>in vitro</i> digestion on the uptake/association and transport of the ag NPs in/or through the intestine with a Caco-2 and HT29-MTX co-culture transwell model.
[45]	Aluminum (Al)	Static	Mouth Stomach Intestine	5 min, 37 °C 2 hours, 37 °C 2 hours, 37 °C	Mucin, amylase, salts, urea Mucin, pepsin, salts, HCl Salts, pancreatin, trypsin, bile, urea	NR 2.0 7.5	To study the molecular effects of artificially digested Al species on intestinal cells.

(continued)

Table 16.1 (continued)

Reference	NM	Type of model	Compartments	Incubation (time, temperature)	Digestive fluids	pH	Aim
[4]	Titanium Dioxide (TiO ₂)	Static	Mouth Stomach Intestine	2 min, 37 °C 2 hours, 37 °C 2 hours, 37 °C	Amylase, salts HCl, pepsin, salts Bile salts, pancreatin, salts	NR 3.0 7.0	To characterize the physicochemical properties of three types of TiO ₂ after the simulated digestion process, through comparison with the primary NMs' properties. To assess the impact of the digestive process on the NMs' cytotoxicity in two human-derived intestinal cell lines.

NR = Not referred; ENM = Engineered NanoMaterials; GIT = Gastrointestinal tract

ment) examining if, and the conditions by which, a certain chemical has the potential to induce a particular adverse health effect, as well as, the relationship between the level of exposure and the related adverse health effect (usually recognized as dose-response relationship); 3) exposure assessment, determining the frequency, magnitude and duration of the ingestion of a given chemical compound; and, 4) risk characterization, which integrates the results from the previous steps, estimating the associated degree of concern [20].

Under the context of foods and the associated risk assessment of chemical compounds potentially present in foods, the concept of bioaccessibility assumes particular importance, considering that the ingested amounts of a certain chemical present in foods does not always reflect the amount of that compound available to the body and, consequently, to produce its toxic effects on target organs [22]. Consequently, *in vitro* methods that contributes to study the effects of digestion on ingested compounds constitute an important layer adding crucial information.

The amount of a specific compound that reaches the intestine after ingestion corresponds to the highest amount of that compound that could be absorbed, and consequently, reach its target organ and, therefore, producing toxicity. Thus, the determination of the bioaccessibility of a compound contributes with important information since it corresponds to the maximum oral bioavailability, and therefore an appropriate approach to estimate the internal exposure. This maximum oral bioavailability could be easily calculated by multiplying the estimated daily intake of that specific compound by its bioaccessibility value [2, 30, 51]. Regarding the nanomaterials, despite EFSA highlighted in their guidance for the risk assessment of nanomaterials used in the food chain that it is important to follow the fate of nanomaterials in the GIT, to determine whether they reach the intestinal cells in nanometric form or if they break down during the digestive process, few studies reporting that approach are available [16, 25, 34]. Additionally, just recently a study was published aiming at developing an *in vitro* method to follow the fate of silver nanoparticles in the gastrointestinal tract. This study

highlighted the importance of considering the fate of nanomaterials in the gastrointestinal tract to accomplish an accurate risk assessment of nanomaterials [28].

Despite the inherent uncertainty associated to *in vitro* approaches, *in vitro* digestion models combined with intestinal cells (e.g. Caco-2 cells) could be of particular utility e.g. in addressing mechanistic questions, mimicking as much as possible the physiological conditions, before progressing to animal studies, innately involving higher costs and efforts.

16.5 Future Perspectives

Considering the growing inclusion of nanomaterials in foods due to the enhancement of physicochemical properties, as already described, it is fundamental an accurate risk assessment of these compounds. Although several studies became available in the last years, some gaps worth to be addressed still exist. Regarding the use of *in vitro* digestion models, the inclusion of a food matrix in the model is an aspect frequently reported as fundamental. The biologically active molecules present in food might alter the signaling pathways and consequently change the effects of NPs in a biological system [5, 8, 31, 34]. The use of a standardized food model based on dietary pattern and the adjustment of analytical conditions to real exposure scenarios are also aspects emphasized by [29, 56], respectively, to be addressed.

A more complete knowledge on the toxicological profile of nanomaterials is a major contribute not only for implementation of preventive measures aiming to protect human health, but also for the development of safer-by-design nanomaterials.

Acknowledgments R.A. was supported by FCT Individual CEEC 2018 Assistant Researcher Grant CEECIND/01570/2018. Thanks are also due to project funded by FCT/MCTES through national funds (PTDC/SAU PUB/29481/2017) and FCT/MCTES for the financial support to CESAM (UIDP/50017/2020 + UIDB/50017/2020), through national funds.

References



- Abdelkhalik A et al (2020) Impact of in vitro digestion on gastrointestinal fate and uptake of silver nanoparticles with different surface modifications. *Nanotoxicology* 14(1):111–126. <https://doi.org/10.1080/17435390.2019.1675794>
- Assunção R, Silva M, Alvito P (2016) Challenges in risk assessment of multiple mycotoxins in food. *World Mycotoxin J* 9(5):791–811. <https://doi.org/10.3920/WMJ2016.2039>
- Ault AP et al (2016) Protein corona-induced modification of silver nanoparticle aggregation in simulated gastric fluid. *Environ Sci Nano Royal Soc Chem* 3(6):1510–1520. <https://doi.org/10.1039/C6EN00278A>
- Bettencourt A et al (2020) Analysis of the characteristics and cytotoxicity of titanium dioxide nanomaterials following simulated in vitro digestion. *Nanomaterials (Basel)* 10(8):1516. <https://doi.org/10.3390/nano10081516>
- Bischoff NS et al (2020) Possible adverse effects of food additive E171 (titanium dioxide) related to particle specific human toxicity, including the immune system. *Int J Mol Sci* 22(1):207. <https://doi.org/10.3390/ijms22010207>
- Brodkorb A et al (2019) INFOGEST static in vitro simulation of gastrointestinal food digestion. *Nat Protoc*. <https://doi.org/10.1038/s41596-018-0119-1>
- Buzea C, Pacheco II, Robbie K (2007) Nanomaterials and nanoparticles: sources and toxicity. *Biointerphases* 2(4):MR17–MR71. <https://doi.org/10.1116/1.2815690>
- Cao Y, Li S, Chen J (2021) Modeling better in vitro models for the prediction of nanoparticle toxicity: a review. *Toxicol Mechanisms Methods* 31(1):1–17. <https://doi.org/10.1080/15376516.2020.1828521>
- Cardoso C et al (2015) Bioaccessibility assessment methodologies and their consequences for the risk–benefit evaluation of food. *Trends Food Sci Technol* 41(1):5–23. <https://doi.org/10.1016/j.tifs.2014.08.008>
- Cho Y-H, Jones OG (2019) Assembled protein nanoparticles in food or nutrition applications. In: Lim L-T, Rogers M (eds) *Food applications of nanotechnology*. Academic Press (Advances in Food and Nutrition Research), pp 47–84. <https://doi.org/10.1016/bs.afnr.2019.01.002>
- Cueva C et al (2019) Gastrointestinal digestion of food-use silver nanoparticles in the dynamic SIMulator of the GastroIntestinal tract (simgi®). Impact on human gut microbiota. *Food Chem Toxicol* 132(July):110657. <https://doi.org/10.1016/j.fct.2019.110657>
- De Matteis V (2017) Exposure to inorganic nanoparticles: routes of entry, immune response, biodistribution and in vitro/in vivo toxicity evaluation. *Toxics* 5(4):29. <https://doi.org/10.3390/toxics5040029>
- DeLoid GM et al (2017) An integrated methodology for assessing the impact of food matrix and gastrointestinal effects on the biokinetics and cellular toxicity of ingested engineered nanomaterials. Part Fibre Toxicol. <https://doi.org/10.1186/s12989-017-0221-5>
- Dupont D et al (2011) An international network for improving health properties of food by sharing our knowledge on the digestive process. *Food Digestion* 2(1–3):23–25. <https://doi.org/10.1007/s13228-011-0011-8>
- Dupont D et al (2019) Can dynamic in vitro digestion systems mimic the physiological reality? *Critical Rev Food Sci Nutr* 59(10):1546–1562. <https://doi.org/10.1080/10408398.2017.1421900>
- EFSA et al (2018) Guidance on risk assessment of the application of nanoscience and nanotechnologies in the food and feed chain: Part 1, human and animal health. *EFSA J* 16(7). <https://doi.org/10.2903/j.efsa.2018.5327>
- Egger L et al (2016) The harmonized INFOGEST in vitro digestion method: from knowledge to action. *Food Res Int* 88:217–225. <https://doi.org/10.1016/j.foodres.2015.12.006>
- European Commission (2011) Regulation (EU) No 1169/2011 of the European parliament and of the council of 25 October 2011. *Off J Eur Union*:25–32. <https://doi.org/10.1075/ttwia.27.04ker>
- European Commission (2015) Regulation (EU) 2015/2283 of the European Parliament and of the Council of 25 November 2015 on novel foods, amending Regulation (EU) No 1169/2011 of the European Parliament and of the Council and repealing Regulation (EC) No 258/97. *Off J Eur Union* 327(258):1–22
- FAO/WHO (1997) Food consumption and exposure assessment of chemicals. Geneva. Available at: <https://apps.who.int/iris/handle/10665/63988>
- Fayaz M et al (2021) Nano-agriculture: a novel approach in agriculture. In: *Microbiota and biofertilizers*. Springer, Cham, pp 99–122. https://doi.org/10.1007/978-3-030-48771-3_7
- González-Arias CA et al (2013) Mycotoxin bioaccessibility/absorption assessment using in vitro digestion models: a review. *World Mycotoxin J* 6(2):167–184. <https://doi.org/10.3920/WMJ2012.1521>
- Johnson LR (2018) *Gastrointestinal physiology* E-book. Elsevier Health Sciences (Mosby's Physiology Monograph) Available at: <https://books.google.pt/books?id=7yRqDwAAQBAJ>
- Jones K et al (2015) Human in vivo and in vitro studies on gastrointestinal absorption of titanium dioxide nanoparticles. *Toxicol Lett* 233(2):95–101. <https://doi.org/10.1016/j.toxlet.2014.12.005>
- Kästner C et al (2017) Monitoring the fate of small silver nanoparticles during artificial digestion. *Colloids Surfaces A Physicochem Eng Aspects* 526:76–81. <https://doi.org/10.1016/j.colsurfa.2016.08.013>
- King T et al (2017) Food safety for food security: relationship between global megatrends and developments in food safety. *Trends Food Sci Technol* 68:160–175. <https://doi.org/10.1016/j.tifs.2017.08.014>

27. Kopf-Bolanz KA et al (2012) Validation of an in vitro digestive system for studying macronutrient decomposition in humans. *J Nutr* 142(2):245–250. <https://doi.org/10.3945/jn.111.148635>
28. Laloux L et al (2020) The food matrix and the gastrointestinal fluids Alter the features of silver nanoparticles. *Small* 16(21):1907687. <https://doi.org/10.1002/sml.201907687>
29. Laux P et al (2018) Nanomaterials: certain aspects of application, risk assessment and risk communication. *Arch Toxicol* 92(1):121–141. <https://doi.org/10.1007/s00204-017-2144-1>
30. Lei B et al (2015) Human health risk assessment of multiple contaminants due to consumption of animal-based foods available in the markets of Shanghai, China. *Environ Sci Pollut Res* 22(6):4434–4446. <https://doi.org/10.1007/s11356-014-3683-0>
31. Li Q et al (2017) Potential impact of inorganic nanoparticles on macronutrient digestion: titanium dioxide nanoparticles slightly reduce lipid digestion under simulated gastrointestinal conditions. *Nanotoxicology* 11(9–10):1087–1101. <https://doi.org/10.1080/17435390.2017.1398356>
32. Lucas-González R et al (2018) In vitro digestion models suitable for foods: opportunities for new fields of application and challenges. *Food Res Int* 107(2017):423–436. <https://doi.org/10.1016/j.foodres.2018.02.055>
33. McClements DJ, Xiao H (2017) Is nano safe in foods? Establishing the factors impacting the gastrointestinal fate and toxicity of organic and inorganic food-grade nanoparticles. *Science of Food* 1(1):6. <https://doi.org/10.1038/s41538-017-0005-1>
34. McClements DJ et al (2016) The role of the food matrix and gastrointestinal tract in the assessment of biological properties of ingested engineered nanomaterials (iENMs): state of the science and knowledge gaps. *NanoImpact* 3–4:47–57. <https://doi.org/10.1016/j.impact.2016.10.002>
35. Minekus M et al (2014) A standardised static in vitro digestion method suitable for food - an international consensus. *Food Funct* 5(6):1113–1124. <https://doi.org/10.1039/c3fo60702j>
36. Mulet-Cabero A-I et al (2020) ‘A standardised semi-dynamic in vitro digestion method suitable for food – an international consensus. *Food & Function Royal Soc Chem* 11(2):1702–1720. <https://doi.org/10.1039/C9FO01293A>
37. Naseer B et al (2018) Importance and health hazards of nanoparticles used in the food industry. *Nanotechnol Rev* 7(6):623–641. <https://doi.org/10.1515/ntrev-2018-0076>
38. Pathakoti K, Manubolu M, Hwang H-M (2017) Nanostructures: current uses and future applications in food science. *J Food Drug Analysis* 25(2):245–253. <https://doi.org/10.1016/j.jfda.2017.02.004>
39. Rodrigues SM et al (2017) Nanotechnology for sustainable food production: promising opportunities and scientific challenges. *Environ Sci: Nano Royal Soc Chem* 4(4):767–781. <https://doi.org/10.1039/c6en00573j>
40. Rompelberg C et al (2016) Oral intake of added titanium dioxide and its nanofraction from food products, food supplements and toothpaste by the Dutch population. *Nanotoxicology* 10(10):1404–1414. <https://doi.org/10.1080/17435390.2016.1222457>
41. Sahu SC, Hayes AW (2017) Toxicity of nanomaterials found in human environment. *Toxicol Res Appl* 1:239784731772635. <https://doi.org/10.1177/2397847317726352>
42. Sams L et al (2015) Relevant pH and lipase for in vitro models of gastric digestion. *Food Function Royal Soc Chem* 7:30–45. <https://doi.org/10.1039/c5fo00930h>
43. Shafiq M et al (2020) An overview of the applications of nanomaterials and Nanodevices in the food industry. *Foods* 9(2):148. <https://doi.org/10.3390/foods9020148>
44. Sieg H et al (2017) Impact of an artificial digestion procedure on aluminum-containing nanomaterials. *Langmuir* 33(40):10726–10735. <https://doi.org/10.1021/acs.langmuir.7b02729>
45. Sieg H et al (2020) Cellular effects of in vitro -digested aluminum nanomaterials on human intestinal cells. *ACS Appl Nano Mat* 3(3):2246–2256. <https://doi.org/10.1021/acsanm.9b02354>
46. Singh T et al (2017) Application of nanotechnology in food science: perception and overview. *Front Microbiol* 8(AUG):1–7. <https://doi.org/10.3389/fmicb.2017.01501>
47. Sohal IS et al (2018) Ingested engineered nanomaterials: state of science in nanotoxicity testing and future research needs. *Part Fibre Toxicol* 15(1):29. <https://doi.org/10.1186/s12989-018-0265-1>
48. Szakal C et al (2014) Measurement of nanomaterials in foods: integrative consideration of challenges and future prospects. *ACS Nano* 8(4):3128–3135. <https://doi.org/10.1021/nn501108g>
49. Venema K (2015) The TNO in vitro model of the colon (TIM-2). In: Verhoeckx K et al (eds) *The impact of food bioactives on health*. Springer, Cham, pp 293–304. https://doi.org/10.1007/978-3-319-16104-4_26
50. Versantvoort C, Kamp E van de, Rompelberg C (2004) Development and applicability of an in vitro model in assessing the bioaccessibility of contaminants from food, RIVM report 320102002
51. Versantvoort CHM et al (2005) Applicability of an in vitro digestion model in assessing the bioaccessibility of mycotoxins from food. *Food Chem Toxicol* 43(1):31–40. <https://doi.org/10.1016/j.fct.2004.08.007>
52. Vilarinho F et al (2018) Nanocellulose in green food packaging. *Critical Rev Food Sci Nutr* 58(9):1526–1537. <https://doi.org/10.1080/10408398.2016.1270254>
53. Walczak AP et al (2012) Behaviour of silver nanoparticles and silver ions in an in vitro human gastrointestinal digestion model. *Nanotoxicology* 7(7):1198–1210. <https://doi.org/10.3109/17435390.2012.726382>

-
54. Wang T, Luo Y (2019) Biological fate of ingested lipid-based nanoparticles: current understanding and future directions. *Nanoscale Royal Soc Chem* 11(23):11048–11063. <https://doi.org/10.1039/C9NR03025E>
55. Yin C et al (2017) TiO₂ particles in seafood and surimi products: attention should be paid to their exposure and uptake through foods. *Chemosphere* 188:541–547. <https://doi.org/10.1016/j.chemosphere.2017.08.168>
56. Zhang Z et al (2019) Development of a standardized food model for studying the impact of food matrix effects on the gastrointestinal fate and toxicity of ingested nanomaterials. *NanoImpact* 13:13–25. <https://doi.org/10.1016/j.impact.2018.11.002>



Overview of Adverse Outcome Pathways and Current Applications on Nanomaterials

Dora Rolo, Ana Tavares, Nádía Vital,
Maria João Silva , and Henriqueta Louro 

Abstract

Nanomaterials (NMs) have important and useful applications in chemical industry, electronics, pharmaceuticals, food and others. Their rapid proliferation presents a dilemma to regulators regarding hazard identification and increased concerns for public health.

The Adverse Outcome Pathways (AOPs) are innovative central elements of a toxicological knowledge framework, developed for supporting chemical risk assessment based on mechanistic reasoning. AOPs describe a sequence of causally linked events at different levels of biological organisation, triggered by exposure to a stressor (like chemicals or NMs) leading to an adverse health effect in humans or wildlife. The integrative analysis of the cellular and molecular mechanisms of nanotoxicity towards the identification of connected adverse outcomes drives a sequential line – an AOP landscape definition. Each defined AOP

is available for crossing data, linking known and unknown landscapes, reducing the reliance on animal studies, associated costs and ethical issues. NMs have unique properties, with specific associated toxicological challenges, which may represent unknown AOP landscapes.

In this chapter, an overview of AOPs as important novel strategic tools in nanotoxicology is presented, highlighting the current applications in hazard identification and human health risk assessment.

Keywords

Nanomaterials · Adverse outcome · Risk assessment · Nanotoxicology

17.1 Introduction

Manufactured nanomaterials (NMs), as well as other advanced and emerging materials (e.g., composites incorporating NMs), can contribute to technological innovation, by improving product performance and functionality, thus presenting significant benefits to consumers [11]. However, safety evaluation of NMs has been challenging, due to the number, diversity, and complexity of these substances, and to the time and costs involved in meeting regulatory requirements that are also evolving side by side with the

D. Rolo (✉) · A. Tavares · N. Vital
Department of Human Genetics, National Institute of Health Dr. Ricardo Jorge (INSA), Lisbon, Portugal
e-mail: dora.rolo@insa.min-saude.pt

M. J. Silva · H. Louro
Department of Human Genetics, National Institute of Health Dr. Ricardo Jorge (INSA), Lisbon, Portugal
ToxOmics – Centre for Toxicogenomics and Human Health, NOVA Medical School, NOVA University, Lisbon, Portugal

development of nanotechnology [11]. Additionally, risk assessment (RA) and regulatory decision-making have been relying heavily on animal testing methods. *In vivo* methods are time consuming, costly, and ethically questionable, which make them unfeasible to generate health hazard information to all NMs and its nanoforms to meet those requirements [11, 14, 19]. All these aspects are hampering the rapid development and market uptake of nanotechnologies. This requires novel approaches to assess the safety of NMs for humans and the environment, as recognised by the scientific community and by regulators and risk assessors. This can be achieved with the use of alternatives to animal testing, which is in line with the current policy turning globally: a) refining and replacing *in vivo* studies; b) favouring more cost-effective approaches, such as novel high-throughput *in vitro* methods; c) using “omics” data and computational methods for data analysis and predictive modelling [29, 47, 49]. However, to be considered credible for use as resource in decision-making processes, these approaches should rely on mechanistic understanding of toxicological pathways [19, 65]. These methods are actually being used, but they still offer limited information on the mechanism of toxicity of a substance, and how the informations are eventually related to an Adverse Outcome (AO) observed in the organism. Therefore, scarcely any have found regulatory acceptance, like the micronucleous assay [14, 19].

Scientifically valid and reliable read-across requires a clear rationale for the grouping and the selection of analogues as to be justified by physicochemical resemblance and/or endpoint-specific considerations (e.g., biological similarity) [36]. However, identifying groups for categorization based on the biological effects proceeding from narrow changes in the NMs physicochemical characteristics has been shown to be a challenging task [11]. For example, it was shown that, within groups of closely related NMs, with chemical resemblance, different genotoxic effects are observed [30, 32]. Considering that assessing health and environmental risks of NMs with traditional animal testing approaches is ethi-

cally undesirable and too cost- and time-consuming, new approaches are needed that meet current requirements for regulatory risk assessment while reducing reliance on *in vivo* assays and enabling the implementation of safer-by-design product development [11].

In 2012, the Environmental, Health and Safety Division from the OECD initiated a program aiming to advance the Adverse Outcome Pathway (AOP), which is an analytical construct that describes a sequential string of causally associated events at different levels of biological organisation edging an ecotoxicological or adverse health effect [51]. The AOPs provides a transparent and scientifically-based framework that relates known mechanistic or predictive relationships between molecular initiating events (MIEs), key events (KEs), and adverse outcomes (AOs) considered relevant to risk assessment (RA) and/or regulatory decision-making [1, 39, 43, 46] (see Fig. 17.1).

AOPs are usually represented in an increasing order of biological organization ranging from cellular, continuing to tissue/organ, and ending to the organism level [14]. This ends up in a simplified and “linear” representation of an individual AOP, which may be an adequate basis for prediction of relevant regulatory outcomes, like acute or chronic toxicity, toxicity to reproduction, development neurotoxicity, non-genotoxic carcinogenicity, or endocrine disruption. They have been used in a predictive toxicology and animal testing reduction perspective, in environmental monitoring, drug development and mixtures’ safety assessment. The MIE describes the interaction of a stressor (e.g. chemical, or NM) with a biological target, being either specific or not [8]. KEs should be measurable and essential for the related AO, and the causal linkages between the KE, named as Key Event Relationships (KERs), should be based on research data demonstrating biological plausibility [14]. In environmental toxicology, the AO usually associated with growth inhibition, diminished survival or reproductive damage of an individual and with consequences for the whole population [8]. Evidence may be obtained from several sources including *in vivo*, *in vitro* or *in silico* studies (see Fig. 17.1).

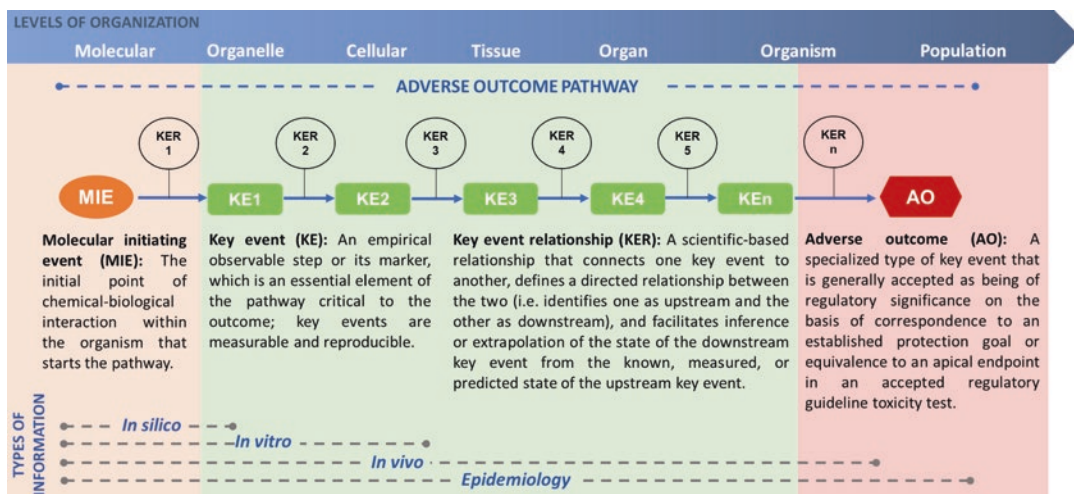


Fig. 17.1 Schematic representation of an adverse outcome pathway (AOP) and definition of terms

The assessment of AOPs and evaluation of their suitability for application in several regulatory contexts and therefore the gathering of relevant biological information relies partly on: (1) the confidence and precision with which the KEs can be measured; (2) the extend level of confidence within the KERs linked in an AOP supported by evidence; and (3) weight of evidence (WoE) for the whole hypothesised pathway, taking under consideration a variety of parameters including any uncertainties and inconsistencies [43].

17.2 AOPs Development

In 2014, Villeneuve et al. [59] have defined three operationally defined stages of an AOP development:

- Putative AOP** – Assembly of a hypothesized set of KEs and KERs, supported mainly through biological plausibility and/or statistical inference. Assembly of partial AOPs with incomplete linkage between the MIE and AO due to known gaps and uncertainties;
- Qualitative AOP** – Assembly of KEs supported by characterization of how the KEs can be measured and KERs supported by empirical evidence as well as plausibility or

statistical inference, along with qualitative evaluation of the overall AOP WoE. Characterized as formal, the information included in the descriptions is in accordance with internationally harmonized OECD guidance;

- Quantitative AOP (qAOP)** – Association of KEs supported by descriptions of how the KERs can be measured, their accuracy and precision. The quantitative assessment of KER is determined in order to understand the degree and extend of a change between two consecutive KEs.

As previously described, qAOPs are developed from qualitative AOPs but have quantitative descriptors for KE and KERs, which may be “partially” quantitative, with some, but not all, KERs with quantitative description. Both qualitative AOPs and qAOPs, can be used in hazard identification and assessment, but qAOP models are needed for dose-response assessments. Risk assessment applications combine qAOPs with chemical specific information, characterizing the concentration of an available stressor, in order to activate the MIEs [49]. An ideal qAOP should comprise several characteristics, namely: transparency, so that the model can be evaluated independently; flexibility, in order to enable the analysis of new and also already well-known

molecules; reproducibility, to ensure the consistency of the model; be user-friendly, enabling its simple interpretation and application; be publicly available; address a specific regulatory question; enable the prediction of a specific AO; and enable its integration with other mathematic models [54].

AOPs that share common MIEs, KEs or AOs are often assembled and form an AOP network [43]. As more pathways are described, connections between KEs that are common to different pathways or biological networks are identified, which is a premise for predicting AOs from MIEs [14]. Therefore, AOP networks can capture better the biological complexity and can represent a more consistent basis for toxicity prediction [14] and genotoxic modes of action [52]. Consequently, it is expected to describe KEs as discrete (modular) units independent of particular MIE, AO, or other KEs. Similarly, it is convenient to describe KERs relations without reference to other elements of the AOP, facilitating the generation of generic KE or KER descriptions that may be linked to other AOPs [43]. This approach increases consistency and efficiency in the AOP development process, since eliminates the need for AOP developers to completely re-describe biological measurements (KEs or KERs) already described by other researchers; avoids reference to other elements of the AOP; and facilitates the KE and KER descriptions update, whenever new methods or new evidence supporting KERs or KEs measuring are developed, thus facilitating the development and conceptualisation of AOP networks.

To be able to have a broad AOP landscape, the OECD developed web-based platforms, like AOP Knowledge Base tools (<https://aopkb.oecd.org/index.html>), compiling all knowledge on how stressors can induce adverse effects, and providing tools for AOP development and dissemination. To develop an AOP, the AOP-KB Portal is the main entry point of the AOP Knowledge Base, which enables search by keywords in AOP titles and KEs in the AOP Wiki (available at <https://aopwiki.org/>) and Effectopedia (available at <https://www.effectopedia.org/>) platforms. The AOP Wiki is an interactive and virtual encyclo-

paedia for AOP development. Following their development and review, the endorsed AOPs are published in the OECD Series on AOPs. The AOP-Wiki is a collaborative, international effort and is a component of the OECD-sponsored AOP Knowledge base (AOP-KB, available at <https://aopkb.oecd.org/>). AOP networks are also critical for addressing exposures to multiple stressors that results in an identical AO or individual stressors that perturb multiple MIEs as well as for understanding potential interactions between coexisting AOPs [27, 58, 59].

The “omics” technologies, such as transcriptomics, proteomics, and metabolomics have become valuable tools in toxicological research and are promising resources for the development and application of AOPs. They can be used both in the determination of MIE and KE, and in proposing biomarkers for particles toxicity screening [60]. The “omics profile” can also be used comparatively, to analyse the effect of NMs with regard to other stressors [50, 53]. Analysis of existing “big data” allows for advanced bioinformatics categorization into mechanistically meaningful results useful for classification of NMs based on the responses connected to toxicity pathways and AO [38]. Data mining and further computational linkage between AOPs and KEs facilitates the creation of connections between genomic responses and AOPs, supporting efficient development of disease-predictive assessment methods, biomarker discovery, and better understanding and descriptions of disease [38].

17.3 AOPs Associated with Nanomaterials

The AOP framework has been applied by different authors to help to structure current information on possible KE leading to a particular AO, based on scientific peer reviewed literature to facilitate the identification of data gaps and research needs, as seen in recent papers [5, 6, 18]. Highlighting the existing toxicological information is not yet enough to fully disclose the underlying mechanisms of NMs toxicity and to support the full development of AOPs of rele-

vance for NMs [19]. By definition, an AOP is chemical-agnostic, meaning that each AOP is not specific for one particular chemical/NM, enabling one AOP to be used to describe the potential actions of a group of physicochemical related stressor [49]. However, generally, AOPs constructed for chemicals may be used to describe the AOPs of relevance to NMs, but due to size-associated changes in the physicochemical and structural properties of NMs and unique interactions with biological structures that could influence their toxicity potential, special considerations may be needed to specify the NM property-mediated deviations in the pathway [19]. Recently, a systematic methodology was created for curating KEs, using a case study approach, that has the potential not only for the development of AOPs for NMs, but is also expected to aid in the application of the existing data for decision making [20].

Great progress in AOPs research has occurred since AOPs were first described, as observed by the extend of manuscripts published from 2010 to 2020, indicating an exponential growth, with more than 400 publications in 2020, based on a PubMed literature search. As of January 2021, there are 16 OECD-endorsed AOPs, 20 are at the ultimate review level of the approval process, and 48 proposals with an OECD status under development (Source: <https://aopwiki.org/>).

Several initiatives are developing NM-relevant AOPs, thus identifying NMs as potential stressors. An AOP search, in the AOP-Wiki, found listed several stressors related to NMs (nano-sized stressor) which are associated with under development AOPs (see Table 17.1), such as nanoparticles, insoluble nano-sized particles, silver nanoparticles, silica nanoparticles, UV-activated titanium dioxide nanoparticles, graphene oxide nanoparticles, carbon nanotubes, and multi-walled carbon nanotubes (MWCN), single-walled carbon nanotubes, carbon nanofibers.

These AOPs are still under development and therefore OECD does not recommend their citation as these AOPs may be subject to changes before they are formally endorsed. It seems that it is more challenging to identify or predict molec-

Table 17.1 List of Adverse Outcomes and the associated nano-sized stressors, available at AOP-KB database and AOP-Wiki on 28th September, 2020

Adverse outcomes (AO code)	AOP codes	Associated nano-sized stressor (Stressor code)
Liver fibrosis (344) and Hepatotoxicity (1294)	AOP144 and AOP 209	Nanoparticles (224) Silica nanoparticles (254)
Reproductive failure (1277)	AOP 207, AOP 208 and AOP 210	Silver nanoparticles (252); UV-activated titanium dioxide nanoparticles (253); Graphene oxide nanoparticles (255)
Pulmonary fibrosis (1458)	AOP 173 and AOP 241	Carbon nanotubes (318); Multi-walled carbon nanotubes (MWCN), single-walled carbon nanotubes, carbon nanofibers (338)
Arterial plaque progression (1443)	AOP 237	Graphene oxide nanoparticles (255); Carbon nanotubes (318); Insoluble nano-sized particles (377)

ular targets for NMs (compared with other chemical stressors) due to their specific properties. Nevertheless, to give a brief overview of the current stand concerning the association between the nano-sized stressors to those AOPs or to identify papers where the AOP framework was applied in relation to the above-mentioned stressors, a PubMed search was performed, considering the search string “(nanomaterial [MeSH]) AND (“Adverse outcome pathway” OR “Molecular initiating event” OR “Key event” OR “Adverse outcome”)”. It should be emphasized that it was not intended to be a systematic literature review approach for determination of potential KEs using nanotoxicity literature. Table 17.2 summarizes the selected publications from a PubMed search, where either KE and/or an AOP is proposed or where the AOP framework was applied in relation to the above-mentioned stressors, which are further presented in the next sections.

Table 17.2 Selected publications found in the literature search, providing mechanistic knowledge that may contribute to nanoparticles-associated AOPs

References	Tested NMs	Description of the study	<i>In vivo</i> models	<i>In vitro</i> models	Doses or concentrations	Exposure duration	MIE	KE	AO
Carbon-based nanomaterials									
Ma et al. [34]	MWCNTs-COOH	Study on the effects of CNTs on synovial cells and chondrocytes using <i>in vitro</i> and <i>in vivo</i> models, including the potential mechanism underlying CNTs induced joint degeneration	BALB/c mice	THP-1; human chondrocyte cell line (SW-1353); human Synovioocyte cell line (SW-982); HEK293/TLR4/MD2/CD14 cell line	Doses: 0.5, 1.0, 2.0 and 4.0 mg/kg bw Concentrations: 1, 10, 20, 40, 80 µg/mL	<i>In vivo</i> experiments: 6 h, 12 h, 24 h, 48 h, 2 days, 7 days and 14 days <i>In vitro</i> experiments: 24 h	Activation of the TLR-NF-κB signalling pathway triggering pro-inflammatory responses in macrophages	Priming of synovioocytes and chondrocytes by pro-inflammatory cytokines and production of enzymes, e.g., matrix metalloproteinase (MMP) members and cyclooxygenase (COX) members, involved articular cartilage degeneration.	Synovial inflammation
Huax et al. [22]	Mitsui-7 (MWCNTs)	Study on the potential capacity of a panel of CNT to induce experimental mesothelioma	Wistar rats and C57BL/6 mice	–	Long-term exposure: 6 mg/rat; Short-term exposure: 2 mg/rat and 0.2 mg/mouse	1, 7, 15 and 30 days	–	Selective recruitment and accumulation of monocytic myeloid-derived suppressor cells (M-MDSC) in the peritoneal cavity, rendering a suitable environment for tumoral cell evasion from T cell surveillance.	Mesothelioma
Labib et al. [28]	MWCNTs (NM 401, NRCWE-026, Mitsui-7)	Study on the use of toxicogenomics to establish points of departure for MWCNT-induced lung fibrosis and assessment of its relevance for human health risk assessment of MWCNTs	C57BL/6 mice	–	0, 18, 54, 162 µg/mouse (NM 401 and NRCWE-026); 0, 10, 20, 40, 80 µg/mouse (Mitsui-7)	24 h, 3 days, 28 days (NM 401 and NRCWE-026); 24 h, 7 days, 28 days, 56 days (Mitsui-7)	Cellular sensing of the substance-induced damage	KE1: Enrolment and intrusion of different immune cell types into the lung tissue, clearing the invading stressor and initiating the process of tissue repair; IL-1R1-mediated pathway is primarily involved in this process (acute inflammation); KE2: a) retention or repeated exposure and b) persistent inflammation; KE3: TH2/M2 response, secretion/activation of interleukins and growth factors; KE4: Chronic inflammation, epithelial and endothelial injury, loss of alveolar capillary Membrane integrity, and activation and proliferation of fibroblasts/myofibroblasts; KE5: Repeated cycles of preceding KEs resulting in excessive extracellular matrix (ECM) deposition.	Lung fibrosis

Nikota et al. [38]	Mitsui-7 (MWCNTs)	The study explored specifically the mechanisms underlying KE1 and KE3 of an already established AOP for lung fibrosis. Pre-existent AOP in Labib et al. [29]	C57BL/6 mice	-	162 µg/mouse	1–28 days	Cellular sensing of the MWCNTs in the lungs and the release of danger signals	KE1: Induction of inflammatory cytokines/chemokines/growth factors; infiltration of inflammatory cells into the lung tissue and acute inflammation; KE2: Retention of MWCNTs, associated with the persistence of inflammatory signals, production of ROS and lung injury; all acting in a positive feedback loop; KE3: Deregulated tissue regeneration, measured as activation of Th2 type cells and M2 type macrophages, and secretion of anti-inflammatory mediators and growth factors that play a role in progression of lung fibrosis; KE4 and 5: Activation of fibroblast/myofibroblast proliferation and uncontrolled ECM deposition leading to fibrotic lesions in the lungs.	Lung fibrosis
Wang et al. [64]	MWCNTs	Comparative <i>in vivo</i> study on the fibrogenic responses in the lungs of four genetically diverse inbred mouse strains exposed to MWCNTs. The paper also describes the utility of IL-1 β and TGF- β 1 production in transformed cell lines or BMDMs to assess key events 1 and 2 responses for predicting a lung fibrosis AOP.	C57Bl/6, Balb/c, NOD/ShiLJ, and A/J mice	THP-1 cells; BMDM cells (<i>ex vivo</i>)	2 mg/kg bw 12.5–100 µg/mL for THP-1 cells	<i>In vivo</i> experiments: 21 days <i>In vitro</i> experiments: 24 h	Lysosome damage and NLRP3 assembly	Damaged lysosomes release enzymes such as cathepsin B, which in synergy with oxidative stress (e.g., NADPH oxidase) and perturbation of K ⁺ efflux, instructs assembly of the NLRP3 inflammasome and IL-1 β production. A following key event could be the production of TGF- β 1 or PDGF-AA production in the epithelial cells, possibly followed by endothelial-mesenchymal transition (EMT) responses related with lung fibrosis.	Lung fibrosis

(continued)

Table 17.2 (continued)

References	Tested NMs	Description of the study	<i>In vivo</i> models	<i>In vitro</i> models	Doses or concentrations	Exposure duration	MIE	KE	AO
Ma et al. [35]	MWCNTs-NH ₂ , MWCNTs-PEG, MWCNTs-PEI, and MWCNTs-COO	Study on CNT-induced toxicity from the perspective of iron homeostasis and iron utilization for erythropoiesis	BALB/c mice	1774-A1, Hepa 1-6, and HepG2 cell lines	Dose: 200 µL/mouse (I.V. and I.P. injection); 50 µL/mouse (I.T. administration) Concentrations: 25, 40, 50, 100 µg/mL	2d to 2 weeks <i>In vitro</i> experiments: 24 h	–	Exposure leads to increased production of pro-inflammatory cytokines, namely IL-6, that increase hepatic hepcidin expression. Increased hepcidin level gives rise to limited dietary iron absorption and iron Release from macrophages, resulting in reduced iron concentration in serum. Hepcidin, that regulates, which leads to sequestered iron for erythroid cells and causing the reduction of serum iron levels. Under anaemia, the spleen is the organ responsible for the extramedullary erythropoiesis, associated with enlarged spleen.	Development of Anaemia of Inflammation and extramedullary erythropoiesis in spleen
Khan et al. [25]	Graphene oxide	Study on <i>in vivo</i> exposure of a marine filter-feeding bivalve to graphene oxide with the overall goal of contributing with biomarker-based information to an AOP framework	<i>C. virginica</i> (Eastern oysters)	–	0 mg/L, 2.5 mg/L and 5 mg/L	14 days	Endocytotic phagocytotic uptake; direct piercing of the plasma membrane; and/or generation of ROS at the cell surface	KE1: Excessive intracellular production of ROS that leads to polyunsaturated fatty acids (PUFAs) damage, represented by elevated malondialdehyde (MDA) levels; KE2: Lipid peroxidation and oxidative damage to other macromolecules and organelles induced by ROS; KE3: ROS associated changes in glutathione-s-transferase (GST) activities resulting in activation of cellular signalling; KE4: Cell death.	–

Metal-based nanomaterials

Kim et al. [26]	Titanium dioxide with and without photoactivation	Study aimed to investigate the toxicity of TiO ₂ NPs on the <i>C. elegans in vivo</i> model, with and without photoactivation, revealing that UV-activated TiO ₂ NPs led to significant reproductive toxicity, with the possible involvement of the Janus kinase /signal transducer and activator of transcription (and transforming growth factor beta pathways. (linked to AOP208 (https://aopwiki.org/aops/208))	<i>Caenorhabditis elegans</i>	–	0, 2, 5, 10 mg/L	24 h	–	In UV-activated TiO ₂ NPs exposed <i>C. elegans</i> : JAK/STAT pathway is suggestive of cooperation with DAF-7/TGF-β signalling in maintaining reproductive growth with UV-activated TiO ₂ NPs TiO ₂ NPs phototoxicity seems to induce up-regulation of JAK/STAT pathway target gene <i>sta-1</i> , and TGF-β pathway target gene <i>daf-7</i> , in conformity with their reproductive growth role. Possible relation between <i>sta-1</i> and <i>daf-7</i> gene and cross-talk partner for STA-1 with DAF-7/TGF-β pathway, suggesting different signalling pathways involved in TiO ₂ NPs-specific and UV-specific phototoxicity.	Reproductive toxicity
Ma et al. [36]	Silver nanoparticles (< 150 nm)	Study on the reproductive toxicity of AgNPs in zebrafish, including the underlying mechanisms involved in mitochondrial-mediated apoptosis pathway.	Zebrafish	–	0, 10, 33 and 100 µg/L	5 weeks	ROS production on gonad tissue (biochemical response)	KE at cellular level: Oxidative stress KE at organ level: Germ cell apoptosis	Impaired reproduction

(continued)

Table 17.2 (continued)

References	Tested NMs	Description of the study	<i>In vivo</i> models	<i>In vitro</i> models	Doses or concentrations	Exposure duration	MIE	KE	AO
Gomes et al. [15]	Cu-NPs (spherical) and Cu-nanowires	Study aimed to assess the effects of Cu materials varying in type, shape and history, anchoring gene expression, and population effect (reproduction)	<i>Enchytraeus crypticus</i>	-	Cu-NPs: EC20/50 (980/1760 mg Cu/kg) Cu - nanowires: (0, 100, 400, 600, 800, 1000, 1500 mg Cu/kg)	Survival and reproduction: 3 weeks; Gene expression assay: 3 and 7 days	Cu-NP; DNA damage and Notch signalling perturbation; Cu-nanowires: ROS; DNA damage; Notch signalling perturbation; alterations on the meiotic cell cycle	Multiple. <i>Cu-NP</i> : Multiple potential events at cellular level possible leading to reproduction failure (EC50); Cuticle pattern formation, senescence, lysosome organization, reduced intracellular pH; Negative regulation of neuron apoptotic process; (related to MIE notch signalling perturbation); DNA gap filling and DNA double strand repair (related to MIE DNA damage); Potential events at cellular or tissue level possible leading to epigenetic events; Protein modifications. <i>Cu-nanowires</i> : Potential events at cellular level possible leading to reproduction failure (EC20); Male gamete generation and hermaphrodite genitalia development Potential events at cellular level possible leading to reproduction failure (EC20/EC50); Cell redox homeostasis imbalance, endoplasmic reticulum dependent peroxisome organization (related to MIE ROS generation); DNA gap filling and DNA double strand repair (related to MIE DNA damage); Endocytosis; Negative regulation of neuron apoptotic process (related to MIE notch signalling perturbation); Potential events at cellular level possible leading to reproduction failure (EC50); Reduced embryogenesis (related to MIE notch signalling perturbation) Possible leading to epigenetic events; Protein modifications	Impaired reproductive system development

Jeong et al. [23]	Silver nanoparticles (uncoated, <100 nm)	Study aimed to build an AOP to link oxidative stress with reproductive toxicity following exposure to silver nanoparticles, using a Bayesian network model, supported also in previously published results. (linked to AOP207- NADPH oxidase and P38 MAPK activation leading to reproductive failure in <i>C. elegans</i> (https://aopwiki.org/aops/207))	<i>Caenorhabditis elegans</i>	-	Uptake: 5 mg/L; ROS: 0.5, 1, 2, or 3 mg/L; gene expression: 0.1, 0.5, or 1 mg/L; mitochondrial membrane potential: 0.5, 1, 2 or 3 mg/L; reproduction assay: 2 mg/L	Uptake: 0.5, 1, 3, 5 or 7 h; ROS: 4 h; gene expression: 24 h; mitochondrial membrane potential: 4 h; reproduction assay: 72 h	Potential MIE: Activation of NADPH oxidase.	MIE: Activation of NADPH oxidase; KE: ROS formation; KE: Increase oxidative stress leads to activation of PMK-1 P38 MAPK; KE: Activation of HIF-1; KE: Increased DNA damage-repair; KE: Mitochondria damaging; KE: Apoptosis.	Reproductive failure
Gomes et al. [16]	Nickel nanoparticles (20 nm)	Study aimed to investigate the mechanisms of toxicity of nickel nanoparticles and to compare them to nickel nitrate, using high-throughput profiling of gene expression.	<i>Enchytraeus crypticus</i>	-	EC20/50 (980/1760 mg Ni/kg)	3 and 7 days	ROS generation and/or increase cation transport	Proteolysis, protein damage, apoptosis, inflammatory response, interference with the nervous system and decrease in energy metabolism (shared also with nickel nitrate)	Impaired reproduction
Brand et al. [6]	Titanium dioxide	Study based on scientific peer reviewed literature, aimed at better understand whether TiO ₂ can induce AO, following oral exposure, based on the AOP framework. A compilation of two AOP possible leading to effects on the liver (fibrosis, edema and steatosis), is presented, supported in existing AOP 144 on liver fibrosis (https://aopwiki.org/aops/144) and AOP 34 on hepatic steatosis (https://aopwiki.org/aops/34)	Based on multiple <i>in vivo</i> studies in rat and mice	-	Oral exposure range: 0.2–24,000 mg/kg/bw/day (rats); 5–2500 mg/kg/bw/day (mice)	Multiple settings	Endocytotic lysosomal Uptake	Liver fibrosis; KE1: Lysosomal disruption; KE2: ROS generation (proposed by the authors); K3: Mitochondrial dysfunction; K4: Cell death/injury; K5: Increased inflammatory mediators (sub-key events KE5a Kupffer cell activation and KE5b TGF-β1 expression, proposed by the authors); K6: Leukocyte recruitment; KE7: Hepatic stellate cell activation; KE8: Extra-cellular matrix alteration/collagen accumulation. Liver steatosis: Share KE1 to KE3 with liver fibrosis pathway; KE3.1 fatty liver cells; associated event: Increased liver weight. Liver oedema: Share KE1 to KE6 with liver fibrosis pathway; KE6.1 liver inflammation; associated event: Increased liver weight	Liver fibrosis; Steatosis; Liver oedema.

(continued)

Table 17.2 (continued)

References	Tested NMs	Description of the study	<i>In vivo</i> models	<i>In vitro</i> models	Doses or concentrations	Exposure duration	MIE	KE	AO
Braakhuis et al. [5]	Titanium dioxide	Study based on scientific peer reviewed literature, aimed at evaluating the ability of TiO ₂ to induce KE in the AOPs for inhalation And oral exposure leading to tumour formation, and aimed at identifying knowledge gaps in two postulating AOP.	Based on multiple <i>in vivo</i> studies in rat and mice	–	Inhalation: 0.5–1200 mg/m ³ (rats); 0.5–5 mg/m ³ (mice); Instillation: 0.2–600 mg/kg (rats); 0.01 – 50 mg/kg (mice); Oral exposure range:0.2–24,000 mg/kg/bw/day (rats);5–2500 mg/kg/bw/day (mice)	Multiple settings	Inhalation exposure: Impaired clearance; Oral exposure: Cellular uptake in intestine	Inhalation exposure: KE1 ROS generation; KE2 oxidative stress; KE3 persistent inflammation; KE4 persistent epithelial injury; KE5 genetic damage of lung epithelial tissue; KE6 epithelial cell proliferation KE7 preneoplastic epithelial lesions Oral exposure: KE1 ROS generation; KE2 oxidative stress; KE3 persistent inflammation; KE4 persistent epithelial injury; KE5 DNA damage in Intestinal cells; KE6 epithelial cell proliferation; KE7 preneoplastic epithelial lesions	Inhalation exposure: Lung adenomas/ Carcinomas Oral exposure: Intestinal adenomas/ Carcinomas
Silicon-based nanomaterials									
Chatterjee et al. [9]	Amorphous silica nanoparticles (aSiNPs)	Study on the molecular mechanisms involved in aSiNPs-mediated hepatotoxicity with a systems toxicology approach and how it is related to the physicochemical properties of aSiNPs.	–	HepG2 cells	For total RNA extraction, quantitative real-time PCR, microarray and global gene expression experiments: 100 mg/L; 100 mg/L; For total cholesterol measurements: 10, 25, 50, 100 and 200 mg/L	All experiments: 24 h	–	aSiNPs exposures in HepG2 cells caused modulation of cholesterol and steroid biosynthesis pathways. The increased level of cholesterol biosynthesis, was observed to be proportional with the larger the surface area.	–

CNTs: Carbon nanotubes, COX: cyclooxygenase, Cu-NP: Copper nanoparticles, ECM: extracellular matrix, EMT: endothelial-mesenchymal transition, GST: glutathione-s-transferase, MDA: malondialdehyde, M-MDSC: Myeloid Derived Suppressor Cells, MMP: matrix metalloproteinase, MWCNTs: Multi-walled carbon nanotubes, PUFAs: polyunsaturated fatty acids

17.3.1 AOPs Associated with Carbon-Based NMs

Seven recent articles, all published after 2016, proposed and/or studied KEs or AOPs associated with exposure to carbon-based NMs (CNMs). Multi-walled carbon nanotubes (MWCNTs) were the vast majority of the CNMs approached in these studies, reflecting not only the higher amount of information regarding these nanofibers in the literature, but also the lack of data on KEs and/or AOPs regarding many other forms of CNMs. For instance, only one study, by Khan et al. [25], was found for CNMs using an ecotoxicological model, describing KEs following exposure to graphene oxide on cell injury and histopathological damage [25].

Several AOs identified for NMs such as lung fibrosis, lung emphysema, and lung cancer, have been shown to involve Inflammation, oxidative stress, and cytotoxicity events. The most extensively observed and reported AO following exposure to NMs is lung fibrosis, and it was the most frequently referred in the analysed studies on CNMs [19]. A putative AOP was firstly proposed by Labib et al. [28] on how inflammation and healing induced by inflammatory response could lead to disease progression, and another study on this topic by Nikota et al. [37] has further explored the mechanisms involved in pulmonary inflammation and its essentiality as a KE prior to lung fibrosis. These studies and others, contributed to the AOP 173, which describes the qualitative linkages leading to pulmonary fibrosis. This AOP is under development within the OECD Project 1.32 and is included in the OECD work plan (<https://aopwiki.org/aops/173>). Briefly, it proposes a MIE that triggers the secretion of a myriad of pro-inflammatory and pro-fibrotic mediators that signal the enrolment of pro-inflammatory leukocytes into the lungs. In the presence of repeated stimulus or persistent stressor, non-resolving inflammation and subsequent tissue injury, leads to the alveolar capillary membrane integrity loss (KE3) and activation of the T Helper type 2-cell signalling (KE4). During such activation, anti-inflammatory and pro-repair/fibrotic molecules are secreted, which produces fibroblast proliferation and myofibroblast

differentiation, and synthesis and deposition of extracellular matrix or collagen. Excessive collagen deposition results in alveolar septa thickening, decrease in total lung volume and lung fibrosis (AO) (<https://aopwiki.org/aops/173>; [19]). Reactive oxygen species (ROS) and consequently the oxidative stress have also been referred as possibly having an important role in the pro-inflammatory pathway that leads to inflammation-associated cell to tissue injury, by activating intracellular signalling pathways. These ROS can also be synthesized by pro-inflammatory cells and macrophages and in a positive feedback loop, perpetuating the toxicity cascade towards injury and ultimately lung fibrosis [18, 19]. One of the analysed studies has also approached the susceptibility of MWCNT-induced pro-fibrogenic effects in different genetic backgrounds and proposed that these NMs trigger lysosome damage (MIE), that cause the release of biological products acting synergistically with oxidative stress and perturbation of potassium efflux, leading to the assembly of the NLRP3 inflammasome and IL-1 β production, followed by TGF- β 1 production or PDGF-AA production in the epithelial cells. These results were considered by the authors as a good proof-of-principle evidence to support the development of an AOP [63]. In fact, AOP 241 - “*Latent Transforming Growth Factor beta1 activation leads to pulmonary fibrosis*”, has been also developed by Martens and colleagues, in which it is proposed that exposure to carbon nanotubes (CNTs) can also activate TGF- β 1 (MIE), leading to an increase in the differentiation of fibroblasts, induction of epithelial mesenchymal transition, accumulation of collagen, and activation of the TGF- β pathway, resulting in pulmonary fibrosis (AO) (<https://aopwiki.org/aops/241>). Interestingly, despite the common AO, AOPs 173 and 241 do not share any KE (<https://aopwiki.org/aops/173>; <https://aopwiki.org/aops/241>). Non-inflammatory mechanisms for lung fibrosis have been also proposed in the literature, with direct activation and differentiation of lung fibroblasts by high aspect ratio materials, such as CNTs, translocated to lung interstitium leading to collagen synthesis and fibrosis [19, 57].

The recruitment of inflammatory cells in AOP 173, is a shared KE with AOP 303 -

“Frustrated phagocytosis-induced lung cancer” (<https://aopwiki.org/aops/303>). AOP 303 is under development by Seidel and colleagues within the OECD Project 1.86 and is included in the OECD work plan. It proposes that HARMs, such as asbestos fibres and CNTs, because of their shape and rigidity, pose issues with the process of phagocytosis and lead to incomplete or frustrated phagocytosis (MIE), leading to the increased secretion of pro-inflammatory mediators (cytokines), and increased recruitment of inflammatory cells such as macrophages and neutrophils. The increased cytokine secretion and modification of the metabolic patterns of the immune cells results in an increased production of ROS that can lead to long lasting oxidative stress, causing increased DNA damage and mutation in epithelial cells. Increased DNA damage and consequent mutations can lead to a non-regulated cell proliferation, that can cause the accumulation of mutations in oncogenes or tumour suppressor genes, a prerequisite for cancer development (AO) (<https://aopwiki.org/aops/303>; [19]). However, there is also growing evidence that, besides inflammation, immunosuppressive responses can also contribute to carcinogenesis [22]. In this study, it was observed that CNTs have the intrinsic capacity to induce the selective, rapid and sustained accumulation of monocytic Myeloid Derived Suppressor Cells (M-MDSC), a prognostic marker of tumour progression, rendering a suitable environment for tumoral cell evasion. Moreover, the observed joint presence of M-MDSC and inflammatory neutrophils after CNTs exposure suggested that synchronized immunosuppressed and inflammatory mechanisms might contribute to the emergence of neoplastic cells and tumour progression. The authors, therefore, suggested that M-MDSC could represent a new component in an AOP leading to the development of mesothelioma [22].

Other analysed studies and AOPs have been also approaching AOs caused by inflammatory processes and oxidative stress. Ma et al. [33] observed that exposure to MWCNTs caused systemic pro-inflammatory responses leading to synovial inflammation within knee joints [33].

Another study by the same research group observed that exposure to MWCNTs increased the production of inflammatory cytokine interleukin-6 (IL-6) and the induction of hepcidin, causing a disruption in iron homeostasis, leading to the development of anaemia and extramedullary erythropoiesis in spleen [34]. AOP 210 – “Activation of c-Jun N-terminal kinase (JNK) and Forkhead box O (FOXO) and reduction of WNT pathways leading to reproductive failure: Integrated multi-OMICS approach for AOP building”, under development by Choi and colleagues, describes how oxidative stress caused by exposure to graphene oxide nanoparticles can lead to reproduction failure in *C. elegans* model (<https://aopwiki.org/aops/210>). Moreover, AOP 237 – “Secretion of inflammatory cytokines after cellular sensing of the stressor leading to plaque progression”, under development by Poulsen and colleagues, within the OECD Project 1.55 and included in the OECD work plan, describes how exposure to CNTs and graphene oxide NMs can cause an inflammatory response in pulmonary cells, that in turn can increase the levels of certain proteins in serum, which are risk factors for cardiovascular disease in humans (<https://aopwiki.org/aops/237>). Although so far a path has been traced to increase knowledge on the effects of CNMs in lung disease, such as lung fibrosis, more research is still needed in exploring intersections with other AOs and other KEs related with other tissues and organs.

17.3.2 AOPs Associated with Metal-Based NMs

Concerning metal-based NMs, only seven articles proposed key events and/or AOPs associated with nano-sized stressors such as titanium dioxide nanoparticles (TiO₂NPs, with and without UV activation), silver nanoparticles (AgNPs), copper nanoparticles (Cu-NPs), copper nanowires (Cu-nanowires), and nickel nanoparticles, all of them published after 2017. Five of the articles referred to ecotoxicological studies [15, 16, 23, 26, 35] focused on potential pathways leading to reproductive failure and two articles explored

putative AOPs based on *in vivo* studies in rats and mice to address different adverse outcomes in liver, intestine and lungs [5, 6]. In Table 17.2, are presented the main characteristics of these studies.

In ecotoxicological studies with different models, the AOP framework was applied to address reproductive failure as a possible adverse outcome following exposure to metal-based NMs nanoparticles, in different case studies. Gomes et al. [15] drafted an AOP based on a case study in the *Enchytraeus crypticus* model exposed to Cu-NPs, and Cu-nanowires in LUFA 2.2 soil. MIE, such as DNA damage followed by DNA double strand repair and DNA gap filling was found to be possibly implicated in reproduction impairment for both Cu-NPs and Cu-nanowires. Notch signalling pathway (MIE), which is involved in neurogenesis and plays a major role in the regulation of embryonic development, was also affected by both NMs possibly leading to negative regulation of neuron apoptotic processes and potentially correlated with negative effects on reproduction at the EC₅₀ [15]. Increased ROS generation was also proposed as MIE following exposure to Cu-nanowires, but not to Cu-NPs. Differentiation between materials occurred at predicted cellular processes, e.g., senescence and cuticle pattern formation for Cu-NPs, which can be caused by the contact of the NPs with the worms' tegument, and Cu-nanowires affecting reproductive system possible via hermaphrodite genitalia development and male meiosis/male gamete generation with negative effects on reproduction at the EC₂₀. Protein modifications (i.e., methylation and ubiquitination) which indicate longer-term/ epigenetic effects were found following exposure to both NMs [15]. The same group built an AOP framework based on *E. crypticus* exposed to reproduction effect concentration EC₂₀ and EC₅₀ of nickel nanoparticles and NiNO₃ in LUFA 2.2 soil, based on gene expression and organism/population data to shed lights on the mechanisms of toxicity leading to reduction in reproduction [16]. Results showed commonly affected pathways between nickel nanoparticles and NiNO₃ including increase in proteolysis, apoptosis and inflammatory response, and inter-

ference with the nervous system and no specific mechanisms for nickel nanoparticles were found. Increase in Cation transport and ROS generation were considered as potential MIE leading to those cellular responses [16]. The AOP approach is also being explored as a basis for describing and predicting reproduction toxicity following chronic exposure to silver nanoparticles in zebrafish [35] and *Caenorhabditis elegans* [23]. Ma et al. [35] found a significantly decreased fecundity after five week exposure at the highest exposure concentration of AgNPs (100 µg/L), accompanied by an increased germ cell apoptosis in adult zebrafish (three months old) gonad tissues, activated by ROS generation and accumulation, as the MIE, which lead to the induction of oxidative stress and apoptosis in the gonad tissue as key events by mitochondria-mediated apoptotic signalling pathways with activation of bax, caspase-9, and caspase-3 genes [35]. According to the authors, increased apoptosis by AgNPs exposure in reproductive organs may be a possible inner mechanism responsible for impairment of testicular and ovarian functions, which ultimately inhibit egg production and subsequent reproductive toxicity in zebrafish [35]. Jeong et al. [23] conducted a case study of building an AOP to link oxidative stress with reproductive toxicity following exposure to AgNPs, postulating that oxidative stress could be the MIE or an early KE to reproduction failure (AO), based on *Caenorhabditis elegans* model. Authors suggest that following uptake of AgNPs, the NADPH oxidase activation is the MIE leading to ROS formation and increase oxidative stress with activation of PMK-1 of p38 mitogen-activated protein kinase pathway (P38 MAPK) which in turn could lead to either DNA damage, mitochondrial damage or activation of Hypoxia-inducible factor HIF-1, all of which leading to apoptosis, and consequently to reproductive failure. ROS formation could also lead directly to mitochondrial damage [23]. The proposed AOP is under development (AOP-Wiki: <https://aopwiki.org/aops/207>) with the title AOP 207 "NADPH oxidase and P38 MAPK activation leading to reproductive failure in *C. elegans*". The same group investigated the toxicity of TiO₂NPs on the *C. elegans*, with and

without UV activation, and found that UV-activated TiO₂NPs led to significant reproductive toxicity through oxidative stress [26]. This pathway suggests the potential relation between the JAK/STAT and TGF-β pathways as KEs in the TiO₂NPs-induced reproductive toxicity, which correlated with the observation of increased gene expression of those pathways. Results from the study indicated that the JAK/STAT pathway was specific to TiO₂NPs, whereas the TGF-β pathway was specific to UV. The identification of MIEs, KEs and KERs within reproductive toxicity *via* the JAK/STAT and TGF-β pathways, is still under development [26]. In the AOP wiki, the same group proposed an AOP in which UV-activated Titanium dioxide nanoparticles are identified as a stressor (Stressor 253) in the under development AOP 208 “JAK/STAT and TGF-beta pathways activation leading to reproductive failure” (AOP-Wiki: <https://aopwiki.org/aops/208>).

More recently, based on scientific peer reviewed literature of studies that addressed the carcinogenic potential of TiO₂NPs in rodents exposed through inhalation or oral route, Braakhuis et al. applied the AOP framework to evaluate the ability of TiO₂ to induce KE in putative AOPs leading to tumour formation, and assessed the relevance of current data on rodents to humans and data gaps which need to be filled to reduce uncertainties related to the carcinogenic potential of TiO₂ [5]. The authors suggested two AOPs for these NMs, one for lung tumours after prolonged inhalation and another one for intestinal adenoma or carcinoma. The first AOP postulated identified a chain of events possibly leading to lung adenomas/ carcinomas, following chronic inhalation of TiO₂ at relatively high doses and its deposition in the lungs. Therefore, particles can accumulate in the lungs, and possible lead to impairment of the lung clearance (the MIE). This initiating event can result in a continuous recruitment of neutrophils thus promoting persistent inflammation leading to ROS generation, which can induce oxidative stress, in case the antioxidant capacity of the lungs is exceeded. Inflammation can also be induced via ROS generation and oxidative stress, after direct

deposition of TiO₂ in the lungs, acting in a positive feedback loop mechanism propagating the initial inflammatory response, which appears to be related to TiO₂ exposures at lower cumulative doses without impaired clearance. Both inflammation and oxidative stress can be constant upon chronic exposure to TiO₂ and can induce persistent epithelial injury, which can eventually lead to regenerative cell proliferation, preneoplastic epithelial lesions, and ultimately lung tumours (AO). The persistent epithelial injury could also lead to increased DNA damage in epithelial cells, and consequent mutations. This mutagenic effect may induce a cellular proliferation, which promotes the fixation of the mutations and potentially results in epithelial lung tumours (e.g., adenomas and carcinomas). Besides the indirect DNA damage pathway, the deposition of TiO₂ in the lungs might be able to induce direct DNA damage in epithelial cells, which could also contribute to tumorigenesis in the lung. Overall, according to the authors, while there is sufficient evidence that lung tumours are induced at high cumulative concentrations and that a mechanism via impaired clearance and persistent lung inflammation in rats is expected, there are yet insufficient and contradictory data on the ROS generation, the induction of oxidative stress, and the DNA-damaging potential of TiO₂ and the possible impact of particle form on lung, which should be further investigated.

The second suggested AOP related to TiO₂ proposed by the same authors and further explored by Brand et al., concerns a possible pathway leading to intestinal adenomas/ carcinomas as adverse outcomes, which is constructed based on 18 *in vivo* oral exposure studies in rodents based on several TiO₂ crystalline forms, such as food additive E171 or specific TiO₂NPs [5, 6]. Although, the Mode of Action (MoA) of possible TiO₂ carcinogenicity after oral ingestion is not completely understood, similar to the inhalation route, it is suggested that the uptake of TiO₂ by intestinal cells (MIE) might induce or promote colon tumours via persistent inflammation and/or ROS generation [5, 6]. In the cells, TiO₂ can generate ROS, which can induce oxidative stress in case the antioxidant capacity is

exceeded. Inflammation response can also be increased either following the generation of ROS and induction of oxidative stress or upon direct contact with TiO₂ in the intestine, which in turn can promote continuous increase of ROS generation in a feedback loop. Both persistent inflammation and oxidative stress can induce epithelial injury that in turn may induce indirectly DNA damage in intestinal cells or epithelial cell proliferation, both of which possibly trigger preneoplastic epithelial lesions, if damage is not repaired, and ultimately lead to intestinal adenomas/ carcinomas. Both direct DNA damage or persistent epithelial injury after intestine uptake without ROS generation or persistent inflammation is also postulated. Concerning this suggested AOP and according to the authors, compared to the inhalation route, there is less information available on each of the KEs for oral exposure to TiO₂, to support all the KE.

To increase the knowledge about whether oral exposure to TiO₂ NMs in animal studies is able to induce effects in liver at concentrations relevant for humans, recently, Brand et al., used the AOP framework to describe chains of events leading to the induction of steatosis, oedema and fibrosis in the liver. This helped to structure the available literature information from animal studies and to assess whether the associated KE and AO are likely to occur due to TiO₂ exposure, and at which dose [6]. The AOP 144 and 34 were considered and compiled in a suggested AOP which used as its core the events leading to liver fibrosis as described in the qualitative AOP 144 “Endocytic lysosomal uptake leading to liver fibrosis” Included in OECD Work Plan (<https://aopwiki.org/aops/144>), amended with information from recent research and extended by connecting to the AOP34 that describes hepatic steatosis pathway (<https://aopwiki.org/aops/34>). According to the authors, although the available data suggests that TiO₂NPs may generate ROS, promote oxidative stress and liver inflammation, it is unknown whether these events may cause irreversible adverse effects in humans [6]. Further studies are needed to allow for conclusions to whether TiO₂ leads to AOs in the liver, and, if so, under which conditions.

17.3.3 AOPs Associated with Silicon-Based NMs

Concerning silicon-based NMs, following the literature search, we obtained one paper concerning Silica nanoparticles. Nevertheless, AOP 209 (<https://aopwiki.org/aops/209>), still under development, named as “Perturbation of cholesterol and glutathione homeostasis leading to hepatotoxicity”, was associated to the nano-sized silica stressor (<https://aopwiki.org/stressors/254>). In 2016, Chatterjee et al. [9] proposed that perturbation of cholesterol biosynthesis as a function of surface area was a principal MoA of amorphous silica NPs, which necessitates a safe-by-design approach to reduce their biological applications. In this AOP the MIE is the sterol regulatory element binding transcription factor 2 (SREBF2) gene activation and repressions of glutathione synthetase (GSS) and glutathione S-transferases (GSTA1, GSTA2, GSTA3, GSTA5) genes and the KEs are cholesterol regulation disorders, through upregulated unsaturated fatty acid concentration, and glutathione homeostasis leading to oxidative stress, DNA damage and an AO as hepatotoxicity (HepG2 cell death). Other AOPs, like AOP 144, previously described at Sect. 17.3.2 associated with oral exposure to TiO₂ NMs, or AOP 237, previously described at Sect. 17.3.1, associated with carbon-based NMs, have also been described to be triggered by non-soluble stressors, although further studies are needed to confirm these observations.

In conclusion, as seen above, several efforts are currently underway to advance the development of AOPs with direct relevance for NMs. AOPs that link NM-induced AOs are now starting to emerge particularly for CNMs, metal-based NMs and silicon-based NMs. However, until now, none of them have been published in the OECD Series on AOPs. CNMs have been associated with different AO in a number of AOPs currently under development, mostly related with lung/pulmonary fibrosis. Metal-based NMs, such as silver nanoparticles or UV-activated titanium dioxide nanoparticles were found to be mainly associated to reproductive failure in lower organisms based on ecotoxicity studies, while in higher

organisms, TiO₂ has been proposed as a nano stressor in the AOP 144, leading to liver fibrosis. Silica nanoparticles were associated with liver hepatotoxicity in the AOP 209, based on lower organism models. On the other side, AOP 237 (Secretion of inflammatory cytokines after cellular sensing of the stressor leading to plaque progression) was associated with different nano-sized stressors: graphene oxide nanoparticles, carbon nanotubes and insoluble nano-sized particles.

Also noteworthy is the fact that the majority of the current efforts in the development of AOPs still rely heavily on animal studies, which have been proven to be fundamental for the construction of predictive models. Alternatives involving toxicity endpoints for the assessment of AOs, as well as strategies that enable validation and refinement of these approaches for the regulatory acceptance are needed [21]. Therefore, it is notorious that there is still a long way to go in replacing *in vivo* assays by *in vitro* and/or *in silico* methodologies in AOPs construction.

17.4 The AOP Framework for Nanomaterials Risk Assessment and Regulatory Decision-Making

The AOPs frameworks have great potential to support decision-making about NMs in different contexts, particularly in regulatory and RA. This has been recognized by different organizations involved in regulatory/policy activities. The OECD Working Party on Manufactured Nanomaterials (WPMN) recommended the use of AOP frameworks for NMs RA and reducing *in vivo* testing in its report on “Alternative Testing Strategies in RA of Manufactured NMs: Current State of Knowledge and Research Needs to Advance Their Use” [40]. Also, the WPMN launched the project “Advancing AOP Development for NM RA and Categorisation” (NanoAOP project), with the objective to contribute to the future development and application of AOPs for NM regulatory decision making, as proposed by the OECD Extended Advisory Group for Molecular Screening and

Toxicogenomics (*EAGMST*) [44–46]. Moreover, The European Food Safety Authority (EFSA), also acknowledged its relevance to use for NMs in its “Guidance on risk assessment of the application of nanoscience and nanotechnologies in the food and feed chain” [13]. However, despite the increasing awareness of this concept in the nanotoxicology community and the agnostic nature of AOPs, to date, most of the AOPs developed or under development have been constructed based on observed adverse effects induced by other chemicals than NMs [14].

There are many ways in which the AOP framework can be applied to support decision making regarding NMs, which includes: i) development of NM categories based on biological responses, ii) informing test method refinement/development, iii) developing IATA for hazard and RA and, iv) risk assessment [41–43, 47, 48, 56, 61]. Each of these applications will be briefly described in the following subsections.

17.4.1 Development of Nanomaterials Categories Based on Biological Responses

AOPs have the potential to advance grouping, categorisation and therefore data gap filling by read-across [17, 41, 43]. In current European Union (EU) chemicals legislation, grouping and read-across between chemicals is accepted for achieve information requirements for RA, as long as it is adequately justified. However, for NMs, scientifically-based grouping and read-across methods have not yet been fully established, despite several suggested science-based approaches [36]. In fact, identifying groups for categorization based on the biological effects arising from small changes in the NMs physicochemical characteristics has been shown to be a challenging task [11]. NMs toxicity has been shown to be influenced by several physicochemical properties, including dissolution rate, electronic band gap, aspect ratio, dispersibility in solution, contaminants, particle size and surface chemistry [11, 30, 31]. Moreover, traditional

read-across studies have been mainly relying on the similarities between the chemical structure of the compounds, rather than considering the complex biological processes that are activated by substance exposure [53]. Scientifically valid and robust read-across requires a clear rationale for the grouping and the selection of an analogue needs to be justified by physicochemical similarity and/or endpoint-specific considerations, such as biological similarity. The AOP framework can support grouping and categorization of NMs, since grouping is more reliable if based on at least a partially known MoA underlying an adverse effect [36]. The description of the MIE and the underlying physical interaction of the NMs with biomolecules make it possible to relate their physicochemical properties to the probability of a MIE and to identify the NMs properties of concern. This further allows to group NMs according to their ability to induce a MIE/AOP, replacing biological testing with *in silico* or *in vitro* screening [11]. Then, well-established linkages between the MIE or KEs and the AO will further support the justification for the data gap filling by read-across [41]. Projects such as the EU funded SmartNanoTox are addressing the relationships between physicochemical properties of NMs and KEs leading to pulmonary AOs. The project aims to suggest descriptors for grouping of NMs according to their toxicological MoA and to create a database of bio-nano interactions that will enable development of read-across and Quantitative Structure-Activity Relationship (QSAR) tools for the toxicity assessment of new NMs based on the AOP framework (<http://www.smartnanotox.eu>).

17.4.2 Support in the Development, Design and Validation of *In Vitro* Testing

Nowadays, regulatory toxicity testing and assessment approaches remain to a large extent based on *in vivo* testing, conducted in accordance with standardised test guidelines or protocols such as OECD Test Guidelines [41]. This classical approach is based on selected endpoints, and typ-

ically provides minimal information on the MoA, thus limiting the development and application of new *in vitro*, *in silico* and *in chemico* approaches for regulatory use [56]. Despite multiple efforts on designing and developing such alternative approaches, the sensitivity and accuracy to predict the toxicological responses at organ or organism levels still hinders their acceptance by the regulatory community [19]. Based on the understanding of the mechanisms underlying adverse health effects, AOPs are expected to improve the predictability of experimental testing (e.g., *in vivo*, *in vitro*, *in chemico*) and computational (*in silico*) approaches to support regulatory decision-making [56]. Consequently, AOPs are expected to inform on the design of an adequate testing strategy for endpoints of interest by determining and combining assays or prediction models that can address specific KEs along a particular AOP [41]. Connecting KEs in an AOP to *in vitro* and kinetic data, the correlation between the experimental results and specific events can be established. The testing strategy to establish the mechanistic understanding derived from an AOP and KEs coverage, depend on the available assays [41]. Moreover, an AOP-based testing strategy, can also support the identification and/or possible development of *in vitro* and *ex vivo* screening assays for targets related to MIEs or KE identified and thus, those who are developing alternative methods can direct resources to the development of those testing methods while decreasing the overall number of assays required for hazard identification [41]. An example of the use of AOP to develop and improve testing is the skin sensitization AOP (AOP 40 in the AOP-Wiki), one of the first AOPs officially endorsed by the OECD. The mechanistic knowledge obtained on skin sensitization has been used to develop and validate standardized *in vitro* tests targeting the KEs in the AOP, which are now published and accepted for regulatory purposes as an alternative to animal testing [11]. The framework of skin sensitization AOP was recently applied to investigate the potential mechanisms of immunotoxicity of widely used NMs as single-wall carbon nanotubes, TiO₂, and fullerene (C60), covering the first and third KEs of skin sensitiza-

tion AOP [4]. A study by Barosova et al. [2] used the proposed AOP 173 (see Sect. 17.3) on lung fibrosis that is under review by the OECD. This includes to design a testing strategy to assess the pro-inflammatory and pro-fibrotic impacts of different MWCNTs upon an advanced *in vitro* lung cell system, which comprises primary human alveolar epithelial cells, pulmonary endothelial cells, fibroblasts and optionally, alveolar macrophages [2]. This system is now being further assessed under the EU Horizon 2020 project PATROLS (<https://www.patrols-h2020.eu/>) for testing NMs.

17.4.3 Development of IATA

One of the most important purposes for AOP development is that it may be a base for the creation of Integrated Approaches to Testing and Assessment (IATA), which are science-based approaches for chemicals' hazard characterisation. It relies on an integrated analysis of known information together with the generation of new data, using a combination of different approaches, such as QSAR, read-across, *in silico*, *in chemico*, *in vitro*, *ex vivo*, *in vivo*, or omics technologies. IATA follows a strategy to answer a defined hypothesis in a specific regulatory situation, taking into consideration the acceptable level of uncertainty related to the decision context [7, 47, 56]. OECD has developed a guidance document providing an approach for the use of the AOP concept in developing IATA [41]. Based on the overall framework of IATA, and once the problem is formulated (e.g., to answer a specific regulatory question) the AOP allows, in a structured way, to: i) gather and evaluate the information available for the chemical of interest and possibly conclude on the hazard based on existing information, ii) identify whether such information is adequate for decision-making by WoE assessment and iii) to assist in determining what additional information (and therefore, which test, if any) would increase the certainty of linking an initiating event to the adverse effect(s) [41]. The application of IATA may also lead to the refine-

ment, reduction and/or replacement of conventional *in vivo* testing.

Different EU funded Projects are addressing the use of IATA to support the environmental health and safety of NMs. The GRACIOUS project (<https://www.h2020gracious.eu/>) has proposed grouping hypotheses, which have been substantiated with data generated by means of IATA. Moreover, NanoSolveIT (<https://nanosolveit.eu/>), aspires to introduce a groundbreaking *in silico* IATA, implemented through a decision support system packaged as both a stand-alone open software and via a Cloud platform. Lastly, RiskGone (<https://riskgone.wpi.edu/>) will develop regulatory-relevant guidance, addressing both human and environmental health and prioritising *in vitro* methods, based on an IATA framework.

17.4.4 Risk Assessment

Identifying health risks early and in an adequate manner is of utmost importance. For NMs, this can be achieved in terms of exposure and toxic potential by combining knowledge on nanotoxicology and general risk methodologies such as RA [50]. In general, RA of chemical substances is conducted through four steps: 1) hazard identification - the analysis of the MoA and the WoE of harmful effects on humans; 2) dose-response assessment - the mathematical relationship between exposure degree and toxic effect; 3) exposure assessment - the frequency, duration, and levels of exposure to the substance; and 4) risk characterization - conclusions on substance's risk integrating all the information acquired in the previous steps, and providing a basis for policy-making [24]. Mechanistic information has been used for decades in all steps of RA to decrease uncertainty and increase predictivity [64]. When applying the MoA to characterize human hazard or risk, it is important not only to understand the MIE and AO, but also critical KEs along the pathway [47]. Thus, once complete, an AOP provides a framework that can be used to test a hypothetical MoA [52]. A key advantage of

this framework is that measurement and confirmation of several, but not all, KEs can be sufficient evidence to confidently assign a MoA, potentially reducing testing. Overall, AOPs at any level of development (putative, qualitative, or quantitative) can be useful to support decision making. AOPs applicability for different purposes should be evaluated on a case-by-case basis, the called “fit-for- purpose”, and will depend on the level of development, the amount of available experimental and observational data, its completeness, the confidence in the underlying information, the regulatory relevance, the methods used, and the strength of information supporting the KERs [10, 19, 62, 64]. Putative or qualitative AOPs can provide a scientifically credible basis to link AOs of regulatory concern to specific pathway perturbations or biological activities [29]. As previously described in this chapter, this can be useful to guide toxicity testing strategies, inform prioritization of research by identifying knowledge gaps, aid in screening and prioritization of NMs for further toxicity testing using animal models and guide the principles of decision matrices such as IATA [19]. However, other regulatory purposes such as RA, require the ability to define the exposure conditions (in terms of dose, duration, frequency, etc.) under which an AO will be observed and/or with what probability, which will need to rely on the degree of quantitative understanding of the relationships linking KEs [29]. Therefore, well-constructed qAOPs models can represent the bridge from descriptive knowledge to the prediction of an AO in hazard and RA. These models allow gathering information on NMs categories, enable the identification and characterization of the hazard, as well as the necessary and causally-interlinked steps at molecular, cellular, and organ level that will lead to an adverse effect. It also allows to describe mathematically the relationships between these steps, the exposure doses, and the time, obtaining for each step a dose-(time)-response curve [19, 49, 50, 54]. Due to its numerous advantages, the field of qAOPs is gaining momentum. However, examples of qAOP models are still scarce, and currently there is no guidance on how to develop and evaluate

qAOP models for chemicals or NMs regulatory applications [49, 54]. Although quantification has now been pursued for a limited number of AOPs, the vast majority are still qualitative and still can be extremely valuable for many regulatory applications if providing a strong evidence base [62]. Considering the many issues associated with toxicity testing of NMs, a well-constructed qualitative AOP can help focus research, toxicity testing and regulatory efforts, prioritizing NMs that require immediate testing, and aiding in the development of targeted toxicity assays [19].

17.5 Challenges and Future Perspectives

There has been great efforts and debate in the last years on the development of the AOPs framework, and its potential applications and limitations in different contexts. Several challenges in the development and application of AOPs particularly in RA and regulatory decision-making, have been widely acknowledged for chemicals in general, and particularly for NMs. Its development and application have been overall limited by nano-specific challenges, related to limitations of current literature, particularly concerning the lack of complete understanding of the biological mechanisms of action underlying NMs-induced adverse health, the use of different exposure conditions and models. Other NMs-specific challenges are the limited consideration of NMs dispersion and dosimetry, the general lack of physicochemical characterization of NMs, and the overall data fragmentation [11, 46] which hamper the comparability among results and conclusions. The biological effects of small changes in NMs physicochemical makeup are not easily predicted with current strategies. We have previously shown that NMs with the same chemistry, but differing in primary properties may yield different biological effects [3, 31, 55]. Likewise, we reported that these secondary features may be potentially more relevant for determining toxicological outcomes [31]. In particular, processes like human digestion may modify the NMs characteristics leading to unexpected toxic-

ity in intestine cells and its impact in an AO at the intestinal level is under investigation in the INGESTnano project. Due to their specific properties, NMs do not usually present a classical dose-response relationship, and their toxicity is frequently unpredictable from chemical substance models. Furthermore, physicochemical characteristics are all interdependent and, therefore, determining the contribution of a single parameter to toxicity remains difficult [11, 14]. Such adversities could also hinder the prediction and identification of MIEs.

Particularly when addressing NMs, the development of AOPs is still at an initial qualitative phase, where the focus is on the identification of KEs, but scarce information is available about the relationship existing between them [14]. Conventionally, experimental study designs do not incorporate AOP rationale and thus, with the available toxicological data, construction of quantitative AOPs for NMs is yet a challenge [18]. Additionally, RA has been mainly based on data from animal studies, mostly in mice and rats, and from *in vitro* experiments with human or rodent cell lines, due to the current lack of human data [14], which may imply uncertainty from interspecies differences [11]. Another issue is also related with the fact that some AOs, such as inflammation and tissue injury, might be reversible, and therefore, identifying the threshold beyond which it becomes adverse would be critical for its successful implementation in NMs RA [18].

The level of complexity of AOPs in another important aspect that should be further developed. A frequent criticism is that individual AOPs are constructed as linear sequences of biological events connecting a MIE to an AO, and thus might oversimplify the complexity of biological systems and the exposures to stressors [27]. Moreover, exposure scenarios might also involve not only a single substance, but multiple combinations of compounds, triggering multiple AOPs that can form a network [27]. To fully account for the biologic processes that may influence the final outcome, most cases of RA and regulatory decision making will require more than one AOP within an interconnected network [12] to reflect

this complexity [11], and to represent a more relevant basis for toxicity prediction [14]. Moreover, specific NMs physicochemical properties make structure-based predictive models complicated, and studies focused on molecular interactions in nanotoxicology are still under development.

Despite the challenges described regarding AOP development and its application for NMs, some progress has already been made, either within the frame of the OECD NanoAOP project [44–46], or in other projects worldwide. Overcoming those challenges will contribute moving towards a larger application of AOPs for NMs RA and regulatory decision-making, which is still in its initial phase. In addition, increased transparent communication and inclusive collaboration among multiple stakeholders, including academics, policy-makers, regulators and industry, with a broad range of expertise is needed to overcome the identified challenges and to facilitate the development, adoption and use of the AOP framework for NMs decision making [11].

Acknowledgements This work was funded by national funds through the FCT – Foundation for Science and Technology, I.P., under the projects PTDC/SAU-PUB/29481/2017, PTDC/SAU-PUB/32587/2017 and UIDB/00009/2020; UIDP/00009/2020 (Centre for Toxicogenomics and Human Health – ToxOmics). NV is supported by the FCT PhD Scholarship 2020.07168. BD. The authors thank the support from all INGESTnano team members.

References

1. Ankley GT, Bennett RS, Erickson RJ, Hoff DJ et al (2010) Adverse outcome pathways: a conceptual framework to support ecotoxicology research and risk assessment. *Environ Toxicol Chem* 29(3):730–741. <https://doi.org/10.1002/etc.34>
2. Barosova H, Maione AG, Septiadi D, Sharma M et al (2020) Use of EpiAlveolar lung model to predict fibrotic potential of multiwalled carbon nanotubes. *ACS Nano* 14(4):3941–3956. <https://doi.org/10.1021/acsnano.9b06860>
3. Bettencourt A, Gonçalves LM, Gramacho AC, Vieira A et al (2020) Analysis of the characteristics and cytotoxicity of titanium dioxide nanomaterials following simulated *in vitro* digestion. *Nano* 10(8):1–18. <https://doi.org/10.3390/nano10081516>
4. Bezerra SF, Santos Rodrigues B, Silva ACG, Ávila RI et al (2021) Application of the adverse outcome



- pathway framework for investigating skin sensitization potential of nanomaterials using new approach methods. *Contact Dermatitis* 84(2):67–74. <https://doi.org/10.1111/cod.13669>
5. Braakhuis HM, Gosens I, Heringa MB, Oomen AG et al (2021) Mechanism of action of TiO₂: recommendations to reduce uncertainties related to carcinogenic potential. *Annu Rev Pharmacol Toxicol* 61(1):203–223. <https://doi.org/10.1146/annurev-pharmtox-101419-100049>
 6. Brand W, Peters RJB, Braakhuis HM, Maślankiewicz L et al (2020) Possible effects of titanium dioxide particles on human liver, intestinal tissue, spleen and kidney after oral exposure. *Nanotoxicology* 14(7):985–1007. <https://doi.org/10.1080/17435390.2020.1778809>
 7. Brockmeier EK, Hodges G, Hutchinson TH, Butler E et al (2017) The role of omics in the application of adverse outcome pathways for chemical risk assessment. *Toxicol Sci* 158(2):252–262. <https://doi.org/10.1093/toxsci/kfx097>
 8. Carusi A, Davies MR, De Grandis G, Escher BI et al (2018) Harvesting the promise of AOPs: an assessment and recommendations. *Sci Total Environ* 628–629:1542–1556. <https://doi.org/10.1016/j.scitotenv.2018.02.015>
 9. Chatterjee N, Yang J, Atluri R, Lee W et al (2016) Amorphous silica nanoparticle-induced perturbation of cholesterol homeostasis as a function of surface area highlights safe-by-design implementation: an integrated multi-OMICS analysis. *RSC Adv* 6(73):68606–68614. <https://doi.org/10.1039/c6ra06006d>
 10. Coady K, Browne P, Embry M, Hill T et al (2019) When are adverse outcome pathways and associated assays “fit for purpose” for regulatory decision-making and management of chemicals? *Integr Environ Assess Manag* 15(4):633–647. <https://doi.org/10.1002/ieam.4153>
 11. Ede JD, Lobaskin V, Vogel U, Lynch I et al (2020) Translating scientific advances in the AOP framework to decision making for nanomaterials. *Nanomaterials* 10(6):1–22. <https://doi.org/10.3390/nano10061229>
 12. Edwards SW, Tan Y-M, Villeneuve DL, Meek ME et al (2015) Adverse outcome pathways--organizing toxicological information to improve decision making. *J Pharmacol Exp Ther* 356(1):170–181. <https://doi.org/10.1124/jpet.115.228239>
 13. EFSA Scientific Committee, Hardy A, Benford D, Thorhallur Halldorsson MJJ, Knutsen HK, More S, Naegeli H, Hubert Noteborn CO, Ricci A, Rychen G, Schlatter JR, Vittorio Silano RS et al (2018) Guidance on risk assessment of the application of nanoscience and nanotechnologies in the food and feed chain: part 1, human and animal health. *EFSA J* 16(7). <https://doi.org/10.2903/j.efsa.2018.5327>
 14. Gerloff K, Landesmann B, Worth A, Munn S et al (2017) The adverse outcome pathway approach in nanotoxicology. *Computation Toxicol* 1:3–11. <https://doi.org/10.1016/j.comtox.2016.07.001>
 15. Gomes SIL, Roca CP, Pegoraro N, Trindade T et al (2018) High-throughput tool to discriminate effects of NMs (Cu-NPs, Cu-nanowires, CuNO₃, and Cu salt aged): transcriptomics in *Enchytraeus crypticus*. *Nanotoxicology* 12(4):325–340. <https://doi.org/10.1080/17435390.2018.1446559>
 16. Gomes SIL, Roca CP, Scott-Fordsmand JJ, Amorim MJB (2019) High-throughput transcriptomics: insights into the pathways involved in (nano) nickel toxicity in a key invertebrate test species. *Environ Pollut* 245:131–140. <https://doi.org/10.1016/j.envpol.2018.10.123>
 17. Halappanavar S, Vogel U, Wallin H, Yauk CL (2018) Promise and peril in nanomedicine: the challenges and needs for integrated systems biology approaches to define health risk. *Wiley Interdiscip Rev Nanomed Nanobiotechnol* 10(1):e1465. <https://doi.org/10.1002/wnan.1465>
 18. Halappanavar S, Ede JD, Shatkin JA, Krug HF (2019) A systematic process for identifying key events for advancing the development of nanomaterial relevant adverse outcome pathways. *NanoImpact* 15(July):100178. <https://doi.org/10.1016/j.impact.2019.100178>
 19. Halappanavar S, van den Brule S, Nymark P, Gaté L et al (2020a) Adverse outcome pathways as a tool for the design of testing strategies to support the safety assessment of emerging advanced materials at the nanoscale. *Part Fibre Toxicol* 17(1):16. <https://doi.org/10.1186/s12989-020-00344-4>
 20. Halappanavar S, Ede JD, Mahapatra I, Krug HF, et al. (2020b) A methodology for developing key events to advance nanomaterial-relevant adverse outcome pathways to inform risk assessment. *Nanotoxicology* 0 (0), 1–24. doi:<https://doi.org/10.1080/17435390.2020.1851419>
 21. Halappanavar S, Nymark P, Krug HF, Clift MJD, Rothen-Rutishauser B, Vogel U (2021) Non-animal strategies for toxicity assessment of nanoscale materials: role of adverse outcome pathways in the selection of endpoints. *Small* 17(15):e2007628. <https://doi.org/10.1002/smll.202007628>. Epub 2021 Feb 9
 22. Huaux F, d’Ursel de Bousies V, Parent M-A, Orsi M et al (2015) Mesothelioma response to carbon nanotubes is associated with an early and selective accumulation of immunosuppressive monocytic cells. *Part Fibre Toxicol* 13(1):46. <https://doi.org/10.1186/s12989-016-0158-0>
 23. Jeong J, Song T, Chatterjee N, Choi I et al (2018) Developing adverse outcome pathways on silver nanoparticle-induced reproductive toxicity via oxidative stress in the nematode *Caenorhabditis elegans* using a Bayesian network model. *Nanotoxicology* 12(10):1182–1197. <https://doi.org/10.1080/17435390.2018.1529835>
 24. Kang DS, Yang JH, Kim HS, Koo BK et al (2018) Application of the adverse outcome pathway framework to risk assessment for predicting carcinogenicity of chemicals. *J Cancer Prevent* 23(3):126–133. <https://doi.org/10.15430/jcp.2018.23.3.126>

25. Khan B, Adeleye AS, Burgess RM, Russo SM et al (2019) Effects of graphene oxide nanomaterial exposures on the marine bivalve, *Crassostrea virginica*. *Aquat Toxicol* 216(April):105297. <https://doi.org/10.1016/j.aquatox.2019.105297>
26. Kim H, Jeong J, Chatterjee N, Roca CP et al (2017) JAK/STAT and TGF- β activation as potential adverse outcome pathway of TiO₂NPs phototoxicity in *Caenorhabditis elegans*. *Sci Rep* 7(1):1–12. <https://doi.org/10.1038/s41598-017-17495-8>
27. Knapen D, Vergauwen L, Villeneuve DL, Ankley GT (2015) The potential of AOP networks for reproductive and developmental toxicity assay development. *Reprod Toxicol* 56:52–55. <https://doi.org/10.1016/j.reprotox.2015.04.003>
28. Labib S, Williams A, Yauk CL, Nikota JK et al (2015) Nano-risk science: application of toxicogenomics in an adverse outcome pathway framework for risk assessment of multi-walled carbon nanotubes. *Part Fibre Toxicol* 13(1):15. <https://doi.org/10.1186/s12989-016-0125-9>
29. LaLone CA, Ankley GT, Belanger SE, Embry MR et al (2017) Advancing the adverse outcome pathway framework – an international horizon scanning approach. *Environ Toxicol Chem* 36(6):1411–1421. <https://doi.org/10.1002/etc.3805>
30. Louro H (2018) Relevance of physicochemical characterization of nanomaterials for understanding nano-cellular interactions. In: *Advances in experimental medicine and biology*. https://doi.org/10.1007/978-3-319-72041-8_8
31. Louro H, Pinhão M, Santos J, Tavares A et al (2016) Evaluation of the cytotoxic and genotoxic effects of benchmark multi-walled carbon nanotubes in relation to their physicochemical properties. *Toxicol Lett*. <https://doi.org/10.1016/j.toxlet.2016.09.016>
32. Louro H, Saruga A, Santos J, Pinhão M et al (2019) Biological impact of metal nanomaterials in relation to their physicochemical characteristics. *Toxicol In Vitro*. <https://doi.org/10.1016/j.tiv.2019.01.018>
33. Ma J, Li R, Qu G, Liu H et al (2016) Carbon nanotubes stimulate synovial inflammation by inducing systemic pro-inflammatory cytokines. *Nanoscale* 8(42):18070–18086. <https://doi.org/10.1039/C6NR06041B>
34. Ma J, Li R, Liu Y, Qu G et al (2017) Carbon nanotubes disrupt iron homeostasis and induce anemia of inflammation through inflammatory pathway as a secondary effect distant to their portal-of-entry. *Small* 13(15):1603830. <https://doi.org/10.1002/smll.201603830>
35. Ma Y-B, Lu C-J, Junaid M, Jia P-P et al (2018) Potential adverse outcome pathway (AOP) of silver nanoparticles mediated reproductive toxicity in zebrafish. *Chemosphere* 207:320–328. <https://doi.org/10.1016/j.chemosphere.2018.05.019>
36. Mech A, Rasmussen K, Jantunen P, Aicher L et al (2019) Insights into possibilities for grouping and read-across for nanomaterials in EU chemicals legislation. *Nanotoxicology* 13(1):119–141. <https://doi.org/10.1080/17435390.2018.1513092>
37. Nikota J, Banville A, Goodwin LR, Wu D et al (2017) Stat-6 signaling pathway and not Interleukin-1 mediates multi-walled carbon nanotube-induced lung fibrosis in mice: insights from an adverse outcome pathway framework. *Part Fibre Toxicol* 14(1):37. <https://doi.org/10.1186/s12989-017-0218-0>
38. Nymark P, Kohonen P, Hongisto V, Grafström RC (2018) Toxic and genomic influences of inhaled nanomaterials as a basis for predicting adverse outcome. *Ann Am Thorac Soc* 15(Supplement_2):S91–S97. <https://doi.org/10.1513/AnnalsATS.201706-478MG>
39. OCDE (2018). *Environment directorate joint meeting of the chemicals committee and the working party on chemicals, pesticides and biotechnology* (233), 1–62. Available from: [https://one.oecd.org/document/ENV/JM/MONO\(2016\)12/en/pdf](https://one.oecd.org/document/ENV/JM/MONO(2016)12/en/pdf)
40. OECD (2016a) Alternative testing strategies in risk assessment of manufactured nanomaterials: current state of knowledge and research needs to advance their use. OECD Environment, Health and Safety Publications Series on the Safety of Manufactured Nanomaterials No 80 JT03408320. (80), 36
41. OECD (2016b) OECD, ‘Guidance document for the use of adverse outcome pathways in developing Integrated Approaches to Testing and Assessment (IATA),’ OECD Series on Testing & Assessment No. 260 JT03407308, OECD Publishing, Paris, 2016. *OECD Guidelines for the Testing of Chemicals*. Available from: [http://www.oecd.org/officialdocuments/publicdisplaydocumentpdf/?cote=env/jm/mono\(2016\)67&doclanguage=en](http://www.oecd.org/officialdocuments/publicdisplaydocumentpdf/?cote=env/jm/mono(2016)67&doclanguage=en)
42. OECD (2018a) *Case study on grouping and read-across for nanomaterials – genotoxicity of nano-TiO₂ Series on Testing and Assessment No. 292 JT03435966*. Available from: [http://www.oecd.org/officialdocuments/publicdisplaydocumentpdf/?cote=ENV/JM/MONO\(2018\)28&docLanguage=En](http://www.oecd.org/officialdocuments/publicdisplaydocumentpdf/?cote=ENV/JM/MONO(2018)28&docLanguage=En)
43. OECD (2018b) *OECD series on adverse outcome pathways No. 1 Users’ Handbook supplement to the Guidance Document for developing and assessing Adverse Outcome Pathways*. <https://doi.org/10.1787/5jlvm9d1g32-en>
44. OECD (2020a) *Joint meeting of the chemicals committee and the working party on chemicals, pesticides and biotechnology Advancing Adverse Outcome Pathway (AOP) Development for Nanomaterial Risk Assessment and Categorisation Part 1 : Final Project Report and Recommen.* (93)
45. OECD (2020b) *Joint meeting of the chemicals committee and the working party on chemicals, pesticides and biotechnology Advancing Adverse Outcome Pathway (AOP) Development for Nanomaterial Risk Assessment and Categorisation Part 2 : Case Study on Tissue Injury Serie.* (94)
46. OECD (2020c) *Joint meeting of the chemicals committee and the working party on chemicals, pesticides and biotechnology Advancing Adverse Outcome Pathway (AOP) Development for Nanomaterial Risk Assessment and Categorization Part3 : Workshop Report and Recommendation.* (95)

47. Patlewicz G, Simon TW, Rowlands JC, Budinsky RA et al (2015) Proposing a scientific confidence framework to help support the application of adverse outcome pathways for regulatory purposes. *Regul Toxicol Pharmacol* 71(3):463–477. <https://doi.org/10.1016/j.yrtph.2015.02.011>
48. Perkins EJ, Antczak P, Burgoon L, Falciani F et al (2015) Adverse outcome pathways for regulatory applications: examination of four case studies with different degrees of completeness and scientific confidence. *Toxicol Sci* 148(1):14–25. <https://doi.org/10.1093/toxsci/kfv181>
49. Perkins EJ, Ashauer R, Burgoon L, Conolly R et al (2019) Building and applying quantitative adverse outcome pathway models for chemical hazard and risk assessment. *Environ Toxicol Chem* 38(9):1850–1865. <https://doi.org/10.1002/etc.4505>
50. Romeo D, Salieri B, Hischer R, Nowack B et al (2020) An integrated pathway based on in vitro data for the human hazard assessment of nanomaterials. *Environ Int* 137. <https://doi.org/10.1016/j.envint.2020.105505>
51. Sachana M (2019) Adverse outcome pathways and their role in revealing biomarkers. In: *Biomarkers in toxicology*. Elsevier, pp 163–170. <https://doi.org/10.1016/B978-0-12-814655-2.00009-8>
52. Sasaki JC, Allemang A, Bryce SM, Custer L et al (2020) Application of the adverse outcome pathway framework to genotoxic modes of action. *Environ Mol Mutagen* 61(1):114–134. <https://doi.org/10.1002/em.22339>
53. Serra A, Fratello M, Cattelani L, Liampa I et al (2020) Transcriptomics in toxicogenomics, part III: data modelling for risk assessment. *Nano* 10(4):708. <https://doi.org/10.3390/nano10040708>
54. Spinu N, Cronin MTD, Enoch SJ, Madden JC et al (2020) Quantitative adverse outcome pathway (qAOP) models for toxicity prediction. *Arch Toxicol* 94(5):1497–1510. <https://doi.org/10.1007/s00204-020-02774-7>
55. Tavares AM, Louro H, Antunes S, Quarré S et al (2014) Genotoxicity evaluation of nanosized titanium dioxide, synthetic amorphous silica and multi-walled carbon nanotubes in human lymphocytes. *Toxicol In Vitro* 28(1). <https://doi.org/10.1016/j.tiv.2013.06.009>
56. Tollefsen KE, Scholz S, Cronin MT, Edwards SW et al (2014) Applying adverse outcome pathways (AOPs) to support integrated approaches to testing and assessment (IATA). *Regul Toxicol Pharmacol* 70(3):629–640. <https://doi.org/10.1016/j.yrtph.2014.09.009>
57. Vietti G, Lison D, van den Brule S (2015) Mechanisms of lung fibrosis induced by carbon nanotubes: towards an adverse outcome pathway (AOP). *Part Fibre Toxicol* 13(1):11. <https://doi.org/10.1186/s12989-016-0123-y>
58. Villeneuve DL, Crump D, Garcia-Reyero N, Hecker M et al (2014a) Adverse outcome pathway (AOP) development I: strategies and principles. *Toxicol Sci* 142(2):312–320. <https://doi.org/10.1093/toxsci/kfu199>
59. Villeneuve DL, Crump D, Garcia-Reyero N, Hecker M et al (2014b) Adverse outcome pathway development II: best practices. *Toxicol Sci* 142(2):321–330. <https://doi.org/10.1093/toxsci/kfu200>
60. Vinken M (2019) Omics-based input and output in the development and use of adverse outcome pathways. *Curr Opin Toxicol* 18:8–12. <https://doi.org/10.1016/j.cotox.2019.02.006>
61. Vinken M, Knapen D, Vergauwen L, Hengstler JG et al (2017) Adverse outcome pathways: a concise introduction for toxicologists. *Arch Toxicol* 91(11):3697–3707. <https://doi.org/10.1007/s00204-017-2020-z>
62. Vinken M, Knapen D, Vergauwen L, Hengstler JG (2018) Europe PMC funders group adverse outcome pathways: a concise introduction for toxicologists. *91(11):3697–3707*. <https://doi.org/10.1007/s00204-017-2020-z>. Adverse
63. Wang X, Liao Y-P, Telesca D, Chang CH et al (2017) The genetic heterogeneity among different mouse strains impacts the lung injury potential of multi-walled carbon nanotubes. *Small* 13(33):1700776. <https://doi.org/10.1002/sml.201700776>
64. Willett C, Fitzpatrick S, Meek B, Westmoreland C (2018) Use of adverse outcome pathways in human risk assessment and toxicology. In: *A systems biology approach to advancing adverse outcome pathways for risk assessment*. Cham, Springer International Publishing, pp 349–378. https://doi.org/10.1007/978-3-319-66084-4_17
65. Wittwehr C, Aladjov H, Ankley G, Byrne HJ et al (2017) How adverse outcome pathways can aid the development and use of computational prediction models for regulatory toxicology. *Toxicol Sci* 155(2):326–336. <https://doi.org/10.1093/toxsci/kfw207>



Correction to: Hazard Assessment of Benchmark Metal-Based Nanomaterials Through a Set of *In Vitro* Genotoxicity Assays

Nádia Vital, Mariana Pinhão, Naouale El Yamani, Elise Rundén-Pran, Henriqueta Louro , Maria Dušinská, and Maria João Silva 

Correction to:

Chapter 14 in: H. Louro, M. J. Silva (eds.), *Nanotoxicology in Safety Assessment of Nanomaterials, Advances in Experimental Medicine and Biology* 1357, https://doi.org/10.1007/978-3-030-88071-2_14

The original version of this chapter was revised: The reference citations within the text weren't updated in sequential order. It has been corrected now; the renumbered citations have been updated throughout the respective chapter

The updated version of this chapter can be found at https://doi.org/10.1007/978-3-030-88071-2_14